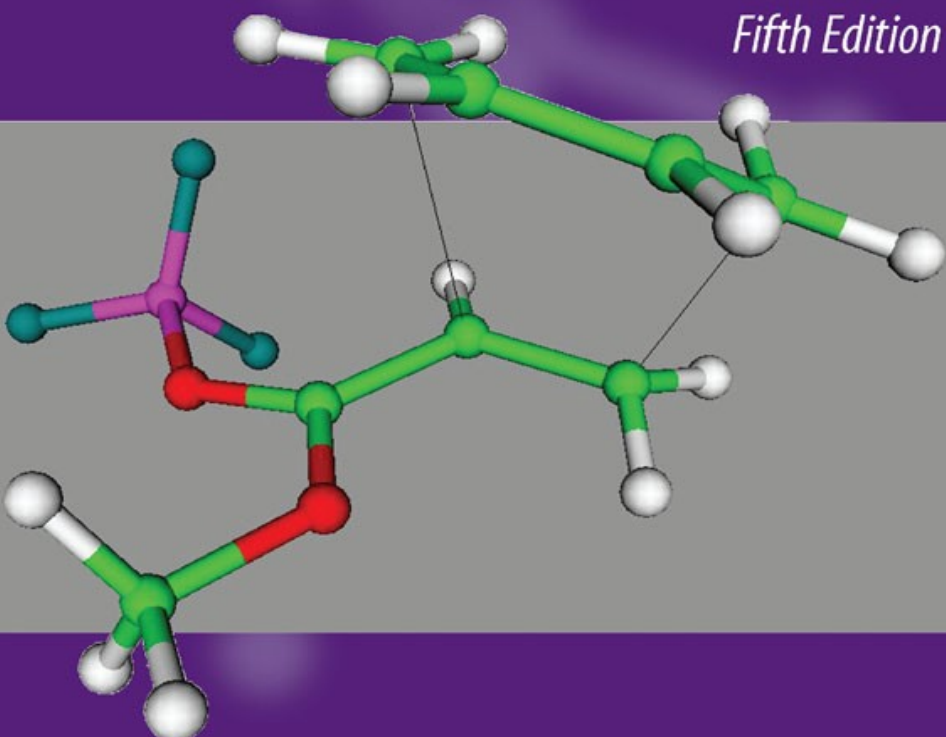


Advanced Organic Chemistry

Part A: Structure and Mechanisms

Fifth Edition



Francis A. Carey
Richard J. Sundberg

 Springer

Advanced Organic Chemistry

FIFTH
EDITION

Part A: Structure and Mechanisms

Advanced Organic Chemistry

PART A: Structure and Mechanisms

PART B: Reactions and Synthesis

Advanced Organic Chemistry

FIFTH
EDITION

Part A: Structure and Mechanisms

FRANCIS A. CAREY
and RICHARD J. SUNDBERG

*University of Virginia
Charlottesville, Virginia*



Francis A. Carey
Department of Chemistry
University of Virginia
Charlottesville, VA 22904

Richard J. Sundberg
Department of Chemistry
University of Virginia
Charlottesville, VA 22904

Library of Congress Control Number: 2006939782

ISBN-13: 978-0-387-44897-8 (hard cover) e-ISBN-13: 978-0-387-44899-3
ISBN-13: 978-0-387-68346-1 (soft cover)

Printed on acid-free paper.

©2007 Springer Science+Business Media, LLC

All rights reserved. This work may not be translated or copied in whole or in part without the written permission of the publisher (Springer Science+Business Media, LLC, 233 Spring Street, New York, NY 10013, USA), except for brief excerpts in connection with reviews or scholarly analysis. Use in connection with any form of information storage and retrieval, electronic adaptation, computer software, or by similar or dissimilar methodology now known or hereafter developed is forbidden.

The use in this publication of trade names, trademarks, service marks and similar terms, even if they are not identified as such, is not to be taken as an expression of opinion as to whether or not they are subject to proprietary rights.

9 8 7 6 5 4 3 2 (corrected 2nd printing, 2008)

springer.com

Preface

This Fifth Edition marks the beginning of the fourth decade that *Advanced Organic Chemistry* has been available. As with the previous editions, the goal of this text is to allow students to build on the foundation of introductory organic chemistry and attain a level of knowledge and understanding that will permit them to comprehend much of the material that appears in the contemporary chemical literature. There have been major developments in organic chemistry in recent years, and these have had a major influence in shaping this new edition to make it more useful to students, instructors, and other readers.

The expanding application of computational chemistry is reflected by amplified discussion of this area, especially density function theory (DFT) calculations in Chapter 1. Examples of computational studies are included in subsequent chapters that deal with specific structures, reactions and properties. Chapter 2 discusses the principles of both configuration and conformation, which were previously treated in two separate chapters. The current emphasis on enantioselectivity, including development of many enantioselective catalysts, prompted the expansion of the section on stereoselective reactions to include examples of enantioselective reactions. Chapter 3, which covers the application of thermodynamics and kinetics to organic chemistry, has been reorganized to place emphasis on structural effects on stability and reactivity. This chapter lays the groundwork for later chapters by considering stability effects on carbocations, carbanions, radicals, and carbonyl compounds.

Chapters 4 to 7 review the basic substitution, addition, and elimination mechanisms, as well as the fundamental chemistry of carbonyl compounds, including enols and enolates. A section on the control of regiochemistry and stereochemistry of aldol reactions has been added to introduce the basic concepts of this important area. A more complete treatment, with emphasis on synthetic applications, is given in Chapter 2 of Part B.

Chapter 8 deals with aromaticity and Chapter 9 with aromatic substitution, emphasizing electrophilic aromatic substitution. Chapter 10 deals with concerted pericyclic reactions, with the aromaticity of transition structures as a major theme. This part of the text should help students solidify their appreciation of aromatic stabilization as a fundamental concept in the chemistry of conjugated systems. Chapter 10 also considers

the important area of stereoselectivity of concerted pericyclic reactions. Instructors may want to consider dealing with these three chapters directly after Chapter 3, and we believe that is feasible.

Chapters 11 and 12 deal, respectively, with free radicals and with photochemistry and, accordingly, with the chemistry of molecules with unpaired electrons. The latter chapter has been substantially updated to reflect the new level of understanding that has come from ultrafast spectroscopy and computational studies.

As in the previous editions, a significant amount of specific information is provided in tables and schemes. These data and examples serve to illustrate the issues that have been addressed in the text. Instructors who want to achieve a broad coverage, but without the level of detail found in the tables and schemes, may choose to advise students to focus on the main text. In most cases, the essential points are clear from the information and examples given in the text itself.

We have made an effort to reduce the duplication between Parts A and B. In general, the discussion of basic mechanisms in Part B has been reduced by cross-referencing the corresponding discussion in Part A. We have expanded the discussion of specific reactions in Part A, especially in the area of enantioselectivity and enantiosselective catalysts.

We have made more extensive use of abbreviations than in the earlier editions. In particular, EWG and ERG are used throughout both Parts A and B to designate electron-withdrawing and electron-releasing substituents, respectively. The intent is that the use of these terms will help students generalize the effect of certain substituents such as C=O, C≡N, NO₂, and RSO₂ as electron withdrawing and R (alkyl) and RO (alkoxy) as electron releasing. Correct use of this shorthand depends on a solid understanding of the interplay between polar and resonance effects in overall substituent effects. This matter is discussed in detail in Chapter 3 and many common functional groups are classified.

Several areas have been treated as “Topics”. Some of the Topics discuss areas that are still in a formative stage, such as the efforts to develop DFT parameters as quantitative reactivity indices. Others, such as the role of carbocations in gasoline production, have practical implications.

We have also abstracted information from several published computational studies to present three-dimensional images of reactants, intermediates, transition structures, and products. This material, including exercises, is available at the publishers web site, and students who want to see how the output of computations can be applied may want to study it. The visual images may help toward an appreciation of some of the subtle effects observed in enantioselective and other stereoselective reactions. As in previous editions, each chapter has a number of problems drawn from the literature. A new feature is solutions to these problems, which are also provided at the publisher’s website at springer.com/carey-sundberg

Our goal is to present a broad and fairly detailed view of the core area of organic reactivity. We have approached this goal by extensive use of both the primary and review literature and the sources are referenced. Our hope is that the reader who works through these chapters, problems, topics, and computational studies either in an organized course or by self-study will be able to critically evaluate and use the current literature in organic chemistry in the range of fields in which is applied, including the pharmaceutical industry, agricultural chemicals, consumer products, petroleum chemistry, and biotechnology. The companion volume, Part B, deals extensively with organic synthesis and provides many more examples of specific reactions.

Acknowledgment and Personal Statement

The revision and updating of *Advanced Organic Chemistry* that appears as the Fifth Edition spanned the period September 2002 through December 2006. Each chapter was reworked and updated and some reorganization was done, as described in the Prefaces to Parts A and B. This period began at the point of conversion of library resources to electronic form. Our university library terminated paper subscriptions to the journals of the American Chemical Society and other journals that are available electronically as of the end of 2002. Shortly thereafter, an excavation mishap at an adjacent construction project led to structural damage and closure of our departmental library. It remained closed through June 2007, but thanks to the efforts of Carol Hunter, Beth Blanton-Kent, Christine Wiedman, Robert Burnett, and Wynne Stuart, I was able to maintain access to a few key print journals including the *Journal of the American Chemical Society*, *Journal of Organic Chemistry*, *Organic Letters*, *Tetrahedron*, and *Tetrahedron Letters*. These circumstances largely completed an evolution in the source for specific examples and data. In the earlier editions, these were primarily the result of direct print encounter or search of printed *Chemical Abstracts* indices. The current edition relies mainly on electronic keyword and structure searches. Neither the former nor the latter method is entirely systematic or comprehensive, so there is a considerable element of circumstance in the inclusion of specific material. There is no intent that specific examples reflect either priority of discovery or relative importance. Rather, they are interesting examples that illustrate the point in question.

Several reviewers provided many helpful corrections and suggestions, collated by Kenneth Howell and the editorial staff of Springer. Several colleagues provided valuable contributions. Carl Trindle offered suggestions and material from his course on computational chemistry. Jim Marshall reviewed and provided helpful comments on several sections. Michal Sabat, director of the Molecular Structure Laboratory, provided a number of the graphic images. My co-author, Francis A. Carey, retired in 2000 to devote his full attention to his text, *Organic Chemistry*, but continued to provide valuable comments and insights during the preparation of this edition. Various users of prior editions have provided error lists, and, hopefully, these corrections have

been made. Shirley Fuller and Cindy Knight provided assistance with many aspects of the preparation of the manuscript.

This Fifth Edition is supplemented by the *Digital Resource* that is available at springer.com/carey-sundberg. The *Digital Resource* summarizes the results of several computational studies and presents three-dimensional images, comments, and exercises based on the results. These were developed with financial support from the Teaching Technology Initiative of the University of Virginia. Technical support was provided by Michal Sabat, William Rourk, Jeffrey Hollier, and David Newman. Several students made major contributions to this effort. Sara Higgins Fitzgerald and Victoria Landry created the prototypes of many of the sites. Scott Geyer developed the dynamic representations using IRC computations. Tanmaya Patel created several sites and developed the measurement tool. I also gratefully acknowledge the cooperation of the original authors of these studies in making their output available. *Problem Responses* have been provided and I want to acknowledge the assistance of R. Bruce Martin, David Metcalf, and Daniel McCauley in helping work out some of the specific kinetic problems and in providing the attendant graphs.

It is my hope that the text, problems, and other material will assist new students to develop a knowledge and appreciation of structure, mechanism, reactions, and synthesis in organic chemistry. It is gratifying to know that some 200,000 students have used earlier editions, hopefully to their benefit.

Richard J. Sundberg
Charlottesville, Virginia
March 2007

Introduction

This volume is intended for students who have completed the equivalent of a two-semester introductory course in organic chemistry and wish to expand their understanding of *structure and reaction mechanisms* in organic chemistry. The text assumes basic knowledge of physical and inorganic chemistry at the advanced undergraduate level.

Chapter 1 begins by reviewing the familiar Lewis approach to structure and bonding. Lewis's concept of electron pair bonds, as extended by adding the ideas of hybridization and resonance, plus fundamental atomic properties such as electronegativity and polarizability provide a solid foundation for *qualitative* descriptions of trends in reactivity. In polar reactions, for example, the molecular properties of acidity, basicity, nucleophilicity, and electrophilicity can all be related to information embodied in Lewis structures. The chapter continues with the more *quantitative* descriptions of molecular structure and properties that are obtained by quantum mechanical calculations. Hückel, semiempirical, and ab initio molecular orbital (MO) calculations, as well as density functional theory (DFT) are described and illustrated with examples. This material is presented at a level sufficient for students to recognize the various methods and their ranges of application. Computational methods can often provide insight into reaction mechanisms by describing the structural features of intermediates and transition structures. Another powerful aspect of computational methods is their ability to represent electron density. Various methods of describing electron density, including graphical representations, are outlined in this chapter and applied throughout the remainder of the text. Chapter 2 explores the two structural levels of stereochemistry—*configuration* and *conformation*. Molecular conformation is important in its own right, but can also influence reactivity. The structural relationships between stereoisomers and the origin and consequences of molecular chirality are discussed. After reviewing the classical approach to resolving racemic mixtures, modern methods for chromatographic separation and kinetic resolution are described. The chapter also explores how stereochemistry affects reactivity with examples of *diastereoselective* and *enantioselective* reactions, especially those involving addition to carbonyl groups. Much of today's work in organic chemistry focuses on enantioselective reagents and catalysts. The enantioselectivity of these reagents usually involves rather small and sometimes subtle differences in intermolecular interactions. Several of the best-understood enantioselective

reactions, including hydrogenation, epoxidation of allylic alcohols, and dihydroxylation of alkenes are discussed. Chapter 3 provides examples of structure-stability relationships derived from both experimental thermodynamics and computation. Most of the chapter is about the effects of substituents on reaction rates and equilibria, how they are measured, and what they tell us about reaction mechanisms. The electronic character of the common functional groups is explored, as well as substituent effects on the stability of carbocations, carbanions, radicals, and carbonyl addition intermediates. Other topics in this chapter include the Hammett equation and related linear free-energy relationships, catalysis, and solvent effects. Understanding how thermodynamic and kinetic factors combine to influence reactivity and developing a sense of structural effects on the energy of reactants, intermediates and transition structures render the outcome of organic reactions more predictable.

Chapters 4 to 7 relate the patterns of addition, elimination, and substitution reactions to the general principles developed in Chapters 1 to 3. A relatively small number of reaction types account for a wide range of both simple and complex reactions. The fundamental properties of carbocations, carbanions, and carbonyl compounds determine the outcome of these reactions. Considerable information about reactivity trends and stereoselectivity is presented, some of it in tables and schemes. Although this material may seem overwhelming if viewed as individual pieces of information, taken in the context of the general principles it fills in details and provides a basis for recognizing the relative magnitude of various structural changes on reactivity. The student should strive to develop a sufficiently broad perspective to generate an intuitive sense of the effect of particular changes in structure.

Chapter 4 begins the discussion of specific reaction types with an examination of *nucleophilic substitution*. Key structural, kinetic, and stereochemical features of substitution reactions are described and related to reaction mechanisms. The limiting mechanisms S_N1 and S_N2 are presented, as are the “merged” and “borderline” variants. The relationship between stereochemistry and mechanism is explored and specific examples are given. Inversion is a virtually universal characteristic of the S_N2 mechanism, whereas stereochemistry becomes much more dependent on the specific circumstances for borderline and S_N1 mechanisms. The properties of carbocations, their role in nucleophilic substitution, carbocation rearrangements, and the existence and relative stability of bridged (nonclassical) carbocations are considered. The importance of carbocations in many substitution reactions requires knowledge of their structure and reactivity and the effect of substituents on stability. A fundamental characteristic of carbocations is the tendency to rearrange to more stable structures. We consider the mechanism of carbocation rearrangements, including the role of bridged ions. The case of nonclassical carbocations, in which the bridged structure is the most stable form, is also discussed.

Chapter 5 considers the relationship between mechanism and regio- and stereoselectivity. The reactivity patterns of electrophiles such as protic acids, halogens, sulfur and selenium electrophiles, mercuric ion, and borane and its derivatives are explored and compared. These reactions differ in the extent to which they proceed through discrete carbocations or bridged intermediates and this distinction can explain variations in regio- and stereochemistry. This chapter also describes the E1, E2, and E1cb mechanisms for elimination and the idea that these represent specific cases within a continuum of mechanisms. The concept of the variable mechanism can explain trends in reactivity and regiochemistry in elimination reactions. Chapter 6 focuses on the fundamental properties and reactivity of *carbon nucleophiles*, including

organometallic reagents, enolates, enols, and enamines. The mechanism of the aldol addition is discussed. The acidity of hydrocarbons and functionalized molecules is considered. Chapter 7 discusses the fundamental reactions of carbonyl groups. The reactions considered include hydration, acetal formation, condensation with nitrogen nucleophiles, and the range of substitution reactions that interconvert carboxylic acid derivatives. The relative stability and reactivity of the carboxylic acid derivatives is summarized and illustrated. The relationships described in Chapters 6 and 7 provide the broad reactivity pattern of carbonyl compounds, which has been extensively developed and is the basis of a rich synthetic methodology.

Chapter 8 discusses the concept of *aromaticity* and explores the range of its applicability, including annulenes, cyclic cations and anions, polycyclic hydrocarbons, and heterocyclic aromatic compounds. The criteria of aromaticity and some of the methods for its evaluation are illustrated. We also consider the *antiaromaticity* of cyclobutadiene and related molecules. Chapter 9 explores the mechanisms of *aromatic substitution* with an emphasis on electrophilic aromatic substitution. The general mechanism is reviewed and the details of some of the more common reactions such as nitration, halogenation, Friedel-Crafts alkylation, and acylation are explored. Patterns of position and reactant selectivity are examined. Recent experimental and computational studies that elucidate the role of aromatic radical cations generated by electron transfer in electrophilic aromatic substitution are included, and the mechanisms for nucleophilic aromatic substitution are summarized. Chapter 10 deals with *concerted pericyclic reactions*, including *cycloaddition*, *electrocyclic reactions*, and *sigmatropic rearrangements*. This chapter looks at how *orbital symmetry* influences reactivity and introduces the idea of aromaticity in transition structures. These reactions provide interesting examples of how stereochemistry and reactivity are determined by the structure of the transition state. The role of Lewis acids in accelerating Diels-Alder reactions and the use of chiral auxiliaries and catalysts to achieve enantioselectivity are explored.

Chapter 11 deals with *free radicals* and their reactions. Fundamental structural concepts such as substituent effects on bond dissociation enthalpies (BDE) and radical stability are key to understanding the mechanisms of radical reactions. The patterns of stability and reactivity are illustrated by discussion of some of the absolute rate data that are available for free radical reactions. The reaction types that are discussed include halogenation and oxygenation, as well as addition reactions of hydrogen halides, carbon radicals, and thiols. Group transfer reactions, rearrangements, and fragmentations are also discussed.

Chapter 12 ventures into the realm of *photochemistry*, where structural concepts are applied to following the path from initial excitation to the final reaction product. Although this discussion involves comparison with some familiar intermediates, especially radicals, and offers mechanisms to account for the reactions, photochemistry introduces some new concepts of *reaction dynamics*. The excited states in photochemical reactions traverse energy surfaces that have small barriers relative to most thermal reactions. Because several excited states can be involved, the mechanism of conversion between excited states is an important topic. The nature of *conical intersections*, the transition points between excited state energy surfaces is examined.

Fundamental concepts of structure and its relationship to reactivity within the context of organic chemistry are introduced in the first three chapters, and thereafter the student should try to relate the structure and reactivity of the intermediates and transition structures to these concepts. Critical consideration of bonding, stereochemistry, and substituent effects should come into play in examining each of the basic

reactions. Computational studies frequently serve to focus on particular aspects of the reaction mechanism. Many specific reactions are cited, both in the text and in schemes and tables. The purpose of this specific information is to illustrate the broad patterns of reactivity. As students study this material, the goal should be to look for the underlying relationships in the broad reactivity patterns. Organic reactions occur by a combination of a relatively few reaction types—substitution, addition, elimination, and rearrangement. Reagents can generally be classified as electrophilic, nucleophilic, or radical in character. By focusing on the fundamental character of reactants and reagents, students can develop a familiarity with organic reactivity and organize the vast amount of specific information on reactions.

Contents

Preface.....	v
Acknowledgment and Personal Statement	vii
Introduction	ix
Chapter 1. Chemical Bonding and Molecular Structure	1
Introduction	1
1.1. Description of Molecular Structure Using Valence Bond Concepts	2
1.1.1. Hybridization	4
1.1.2. The Origin of Electron-Electron Repulsion	7
1.1.3. Electronegativity and Polarity	8
1.1.4. Electronegativity Equalization.....	11
1.1.5. Differential Electronegativity of Carbon Atoms.....	12
1.1.6. Polarizability, Hardness, and Softness	14
1.1.7. Resonance and Conjugation	18
1.1.8. Hyperconjugation.....	22
1.1.9. Covalent and van der Waals Radii of Atoms	24
1.2. Molecular Orbital Theory and Methods	26
1.2.1. The Hückel MO Method	27
1.2.2. Semiempirical MO Methods	32
1.2.3. Ab Initio Methods.....	32
1.2.4. Pictorial Representation of MOs for Molecules	35
1.2.5. Qualitative Application of MO Theory to Reactivity: Perturbational MO Theory and Frontier Orbitals	41
1.2.6. Numerical Application of MO Theory.....	50
1.3. Electron Density Functionals.....	54
1.4. Representation of Electron Density Distribution	57
1.4.1. Mulliken Population Analysis	60
1.4.2. Natural Bond Orbitals and Natural Population Analysis.....	61

1.4.3. Atoms in Molecules	63
1.4.4. Comparison and Interpretation of Atomic Charge Calculations	70
1.4.5. Electrostatic Potential Surfaces.....	73
1.4.6. Relationships between Electron Density and Bond Order	76
Topic 1.1. The Origin of the Rotational (Torsional) Barrier in Ethane and Other Small Molecules.....	78
Topic 1.2. Heteroatom Hyperconjugation (Anomeric Effect) in Acyclic Molecules.....	81
Topic 1.3. Bonding in Cyclopropane and Other Small Ring Compounds	85
Topic 1.4. Representation of Electron Density by the Laplacian Function	92
Topic 1.5. Application of Density Functional Theory to Chemical Properties and Reactivity	94
T.1.5.1. DFT Formulation of Chemical Potential, Electronegativity, Hardness and Softness, and Covalent and van der Waal Radii	95
T.1.5.2. DFT Formulation of Reactivity—The Fukui Function	97
T.1.5.3. DFT Concepts of Substituent Groups Effects	100
General References	106
Problems	106
 Chapter 2. Stereochemistry, Conformation, and Stereoselectivity	119
Introduction	119
2.1. Configuration.....	119
2.1.1. Configuration at Double Bonds.....	119
2.1.2. Configuration of Cyclic Compounds	121
2.1.3. Configuration at Tetrahedral Atoms.....	122
2.1.4. Molecules with Multiple Stereogenic Centers	126
2.1.5. Other Types of Stereogenic Centers	128
2.1.6. The Relationship between Chirality and Symmetry	131
2.1.7. Configuration at Prochiral Centers.....	133
2.1.8. Resolution—The Separation of Enantiomers.....	136
2.2. Conformation.....	142
2.2.1. Conformation of Acyclic Compounds	142
2.2.2. Conformations of Cyclohexane Derivatives	152
2.2.3. Conformations of Carbocyclic Rings of Other Sizes	161
2.3. Molecular Mechanics	167
2.4. Stereoselective and Stereospecific Reactions	169
2.4.1. Examples of Stereoselective Reactions	170
2.4.2. Examples of Stereospecific Reactions	182
2.5. Enantioselective Reactions.....	189
2.5.1. Enantioselective Hydrogenation	189
2.5.2. Enantioselective Reduction of Ketones.....	193
2.5.3. Enantioselective Epoxidation of Allylic Alcohols	196
2.5.4. Enantioselective Dihydroxylation of Alkenes.....	200
2.6. Double Stereodifferentiation: Reinforcing and Competing Stereoselectivity	204

Topic 2.1. Analysis and Separation of Enantiomeric Mixtures	208
T.2.1.1. Chiral Shift Reagents and Chiral Solvating Agents.....	208
T.2.1.2. Separation of Enantiomers	211
Topic 2.2. Enzymatic Resolution and Desymmetrization.....	215
T.2.2.1. Lipases and Esterases.....	216
T.2.2.2. Proteases and Acylases	222
T.2.2.3. Epoxide Hydrolases.....	224
Topic 2.3. The Anomeric Effect in Cyclic Compounds	227
Topic 2.4. Polar Substituent Effects in Reduction of Carbonyl Compounds	234
General References.....	239
Problems	240

Chapter 3. Structural Effects on Stability and Reactivity..... **253**

Introduction.....	253
3.1. Thermodynamic Stability	254
3.1.1. Relationship between Structure and Thermodynamic Stability for Hydrocarbons	256
3.1.2. Calculation of Enthalpy of Formation and Enthalpy of Reaction	257
3.2. Chemical Kinetics	270
3.2.1. Fundamental Principles of Chemical Kinetics	270
3.2.2. Representation of Potential Energy Changes in Reactions.....	273
3.2.3. Reaction Rate Expressions	280
3.2.4. Examples of Rate Expressions	283
3.3. General Relationships between Thermodynamic Stability and Reaction Rates.....	285
3.3.1. Kinetic versus Thermodynamic Control of Product Composition.....	285
3.3.2. Correlations between Thermodynamic and Kinetic Aspects of Reactions	287
3.3.3. Curtin-Hammett Principle.....	296
3.4. Electronic Substituent Effects on Reaction Intermediates	297
3.4.1. Carbocations.....	300
3.4.2. Carbanions	307
3.4.3. Radical Intermediates	311
3.4.4. Carbonyl Addition Intermediates	319
3.5. Kinetic Isotope Effects.....	332
3.6. Linear Free-Energy Relationships for Substituent Effects.....	335
3.6.1. Numerical Expression of Linear Free-Energy Relationships	335
3.6.2. Application of Linear Free-Energy Relationships to Characterization of Reaction Mechanisms	342
3.7. Catalysis	345
3.7.1. Catalysis by Acids and Bases.....	345
3.7.2. Lewis Acid Catalysis	354

3.8. Solvent Effects	359
3.8.1. Bulk Solvent Effects	359
3.8.2. Examples of Specific Solvent Effects	362
Topic 3.1. Acidity of Hydrocarbons	368
General References	376
Problems	376
Chapter 4. Nucleophilic Substitution	389
Introduction	389
4.1. Mechanisms for Nucleophilic Substitution	389
4.1.1. Substitution by the Ionization (S_N1) Mechanism	391
4.1.2. Substitution by the Direct Displacement (S_N2) Mechanism	393
4.1.3. Detailed Mechanistic Description and Borderline Mechanisms	395
4.1.4. Relationship between Stereochemistry and Mechanism of Substitution	402
4.1.5. Substitution Reactions of Alkyldiazonium Ions	405
4.2. Structural and Solvation Effects on Reactivity	407
4.2.1. Characteristics of Nucleophilicity	407
4.2.2. Effect of Solvation on Nucleophilicity	411
4.2.3. Leaving-Group Effects	413
4.2.4. Steric and Strain Effects on Substitution and Ionization Rates	415
4.2.5. Effects of Conjugation on Reactivity	417
4.3. Neighboring-Group Participation	419
4.4. Structure and Reactions of Carbocation Intermediates	425
4.4.1. Structure and Stability of Carbocations	425
4.4.2. Direct Observation of Carbocations	436
4.4.3. Competing Reactions of Carbocations	438
4.4.4. Mechanisms of Rearrangement of Carbocations	440
4.4.5. Bridged (Nonclassical) Carbocations	447
Topic 4.1. The Role Carbocations and Carbonium Ions in Petroleum Processing	454
General References	459
Problems	459
Chapter 5. Polar Addition and Elimination Reactions	473
Introduction	475
5.1. Addition of Hydrogen Halides to Alkenes	476
5.2. Acid-Catalyzed Hydration and Related Addition Reactions	482
5.3. Addition of Halogens	485
5.4. Sulfenylation and Selenenylation	497
5.4.1. Sulfenylation	498
5.4.2. Selenenylation	500
5.5. Addition Reactions Involving Epoxides	503
5.5.1. Epoxides from Alkenes and Peroxidic Reagents	503
5.5.2. Subsequent Transformations of Epoxides	511

5.6. Electrophilic Additions Involving Metal Ions.....	515
5.6.1. Solvomercuration.....	515
5.6.2. Argentation—the Formation of Silver Complexes	520
5.7. Synthesis and Reactions of Alkylboranes	521
5.7.1. Hydroboration	522
5.7.2. Reactions of Organoboranes	526
5.7.3. Enantioselective Hydroboration	529
5.8. Comparison of Electrophilic Addition Reactions	531
5.9. Additions to Alkynes and Allenes.....	536
5.9.1. Hydrohalogenation and Hydration of Alkynes.....	538
5.9.2. Halogenation of Alkynes.....	540
5.9.3. Mercuration of Alkynes.....	544
5.9.4. Overview of Alkyne Additions	544
5.9.5. Additions to Allenes	545
5.10. Elimination Reactions	546
5.10.1. The E2, E1 and E1cb Mechanisms	548
5.10.2. Regiochemistry of Elimination Reactions	554
5.10.3. Stereochemistry of E2 Elimination Reactions	558
5.10.4. Dehydration of Alcohols	563
5.10.5. Eliminations Reactions Not Involving C—H Bonds.....	564
General References	569
Problems.....	569

Chapter 6. Carbanions and Other Carbon Nucleophiles..... **579**

Introduction	559
6.1. Acidity of Hydrocarbons	579
6.2. Carbanion Character of Organometallic Compounds	588
6.3. Carbanions Stabilized by Functional Groups.....	591
6.4. Enols and Enamines.....	601
6.5. Carbanions as Nucleophiles in S_N2 Reactions	609
6.5.1. Substitution Reactions of Organometallic Reagents.....	609
6.5.2. Substitution Reactions of Enolates.....	611
General References	619
Problems	619

**Chapter 7. Addition, Condensation and Substitution Reactions
of Carbonyl Compounds.....** **629**

Introduction.....	629
7.1. Reactivity of Carbonyl Compounds toward Addition	632
7.2. Hydration and Addition of Alcohols to Aldehydes and Ketones.....	638
7.3. Condensation Reactions of Aldehydes and Ketones with Nitrogen Nucleophiles.....	645
7.4. Substitution Reactions of Carboxylic Acid Derivatives	654
7.4.1. Ester Hydrolysis and Exchange	654
7.4.2. Aminolysis of Esters	659
7.4.3. Amide Hydrolysis	662
7.4.4. Acylation of Nucleophilic Oxygen and Nitrogen Groups.....	664

7.5. Intramolecular Catalysis of Carbonyl Substitution Reactions	668
7.6. Addition of Organometallic Reagents to Carbonyl Groups.....	676
7.6.1. Kinetics of Organometallic Addition Reactions	677
7.6.2. Stereoselectivity of Organometallic Addition Reactions.....	680
7.7. Addition of Enolates and Enols to Carbonyl Compounds: The Aldol Addition and Condensation Reactions	682
7.7.1. The General Mechanisms	682
7.7.2. Mixed Aldol Condensations with Aromatic Aldehydes.....	685
7.7.3. Control of Regiochemistry and Stereochemistry of Aldol Reactions of Ketones.....	687
7.7.4. Aldol Reactions of Other Carbonyl Compounds.....	692
General References	698
Problems	698
Chapter 8. Aromaticity	713
Introduction	713
8.1. Criteria of Aromaticity.....	715
8.1.1. The Energy Criterion for Aromaticity.....	715
8.1.2. Structural Criteria for Aromaticity	718
8.1.3. Electronic Criteria for Aromaticity	720
8.1.4. Relationship among the Energetic, Structural, and Electronic Criteria of Aromaticity	724
8.2. The Annulenes	725
8.2.1. Cyclobutadiene.....	725
8.2.2. Benzene	727
8.2.3. 1,3,5,7-Cyclooctatetraene	727
8.2.4. [10]Annulenes—1,3,5,7,9-Cyclodecapentaene Isomers.....	728
8.2.5. [12], [14], and [16]Annulenes	730
8.2.6. [18]Annulene and Larger Annulenes	733
8.2.7. Other Related Structures.....	735
8.3. Aromaticity in Charged Rings	738
8.4. Homoaromaticity	743
8.5. Fused-Ring Systems.....	745
8.6. Heteroaromatic Systems	758
General References	760
Problems	760
Chapter 9. Aromatic Substitution	771
Introduction	771
9.1. Electrophilic Aromatic Substitution Reactions	771
9.2. Structure-Reactivity Relationships for Substituted Benzenes.....	779
9.2.1. Substituent Effects on Reactivity	779
9.2.2. Mechanistic Interpretation of the Relationship between Reactivity and Selectivity	787
9.3. Reactivity of Polycyclic and Heteroaromatic Compounds	791

9.4. Specific Electrophilic Substitution Reactions	796
9.4.1. Nitration.....	796
9.4.2. Halogenation.....	800
9.4.3. Protonation and Hydrogen Exchange	804
9.4.4. Friedel-Crafts Alkylation and Related Reactions.....	805
9.4.5. Friedel-Crafts Acylation and Related Reactions	809
9.4.6. Aromatic Substitution by Diazonium Ions	813
9.4.7. Substitution of Groups Other than Hydrogen	814
9.5. Nucleophilic Aromatic Substitution.....	816
9.5.1. Nucleophilic Aromatic Substitution by the Addition-Elimination Mechanism.....	817
9.5.2. Nucleophilic Aromatic Substitution by the Elimination-Addition Mechanism.....	821
General References	824
Problems.....	824

Chapter 10. Concerted Pericyclic Reactions..... **833**

Introduction	833
10.1. Cycloaddition Reactions	834
10.2. The Diels-Alder Reaction	839
10.2.1. Stereochemistry of the Diels-Alder Reaction.....	839
10.2.2. Substituent Effects on Reactivity, Regioselectivity and Stereochemistry	843
10.2.3. Catalysis of Diels-Alder Reactions by Lewis Acids.....	848
10.2.4. Computational Characterization of Diels-Alder Transition Structures.....	851
10.2.5. Scope and Synthetic Applications of the Diels-Alder Reaction.....	860
10.2.6. Enantioselective Diels-Alder Reactions	865
10.2.7. Intramolecular Diels-Alder Reactions	868
10.3. 1,3-Dipolar Cycloaddition Reactions.....	873
10.3.1. Relative Reactivity, Regioselectivity, Stereoselectivity, and Transition Structures	874
10.3.2. Scope and Applications of 1,3-Dipolar Cycloadditions.....	884
10.3.3. Catalysis of 1,3-Dipolar Cycloaddition Reactions	886
10.4. [2 + 2] Cycloaddition Reactions	888
10.5. Electrocyclic Reactions	892
10.5.1. Overview of Electrocyclic Reactions	892
10.5.2. Orbital Symmetry Basis for the Stereospecificity of Electrocyclic Reactions.....	894
10.5.3. Examples of Electrocyclic Reactions	903
10.5.4. Electrocyclic Reactions of Charged Species	906
10.5.5. Electrocyclization of Heteroatomic Trienes	910
10.6. Sigmatropic Rearrangements	911
10.6.1. Overview of Sigmatropic Rearrangements.....	911
10.6.2. [1,3]-, [1,5]-, and [1,7]-Sigmatropic Shifts of Hydrogen and Alkyl Groups.....	912

10.6.3. Overview of [3,3]-Sigmatropic Rearrangements	919
10.6.4. [2,3]-Sigmatropic Rearrangements.....	939
Topic 10.1. Application of DFT Concepts to Reactivity and Regiochemistry of Cycloaddition Reactions	945
Problems	951
 Chapter 11. Free Radical Reactions	965
Introduction	965
11.1. Generation and Characterization of Free Radicals.....	967
11.1.1. Background	967
11.1.2. Long-Lived Free Radicals	968
11.1.3. Direct Detection of Radical Intermediates	970
11.1.4. Generation of Free Radicals	976
11.1.5. Structural and Stereochemical Properties of Free Radicals.....	980
11.1.6. Substituent Effects on Radical Stability.....	986
11.1.7. Charged Radicals	988
11.2. Characteristics of Reactions Involving Radical Intermediates	992
11.2.1. Kinetic Characteristics of Chain Reactions.....	992
11.2.2. Determination of Reaction Rates.....	995
11.2.3. Structure-Reactivity Relationships	1000
11.3. Free Radical Substitution Reactions.....	1018
11.3.1. Halogenation	1018
11.3.2. Oxygenation	1024
11.4. Free Radical Addition Reactions	1026
11.4.1. Addition of Hydrogen Halides	1026
11.4.2. Addition of Halomethanes	1029
11.4.3. Addition of Other Carbon Radicals.....	1031
11.4.4. Addition of Thiols and Thiocarboxylic Acids	1033
11.4.5. Examples of Radical Addition Reactions.....	1033
11.5. Other Types of Free Radical Reactions.....	1037
11.5.1. Halogen, Sulfur, and Selenium Group Transfer Reactions	1037
11.5.2. Intramolecular Hydrogen Atom Transfer Reactions	1040
11.5.3. Rearrangement Reactions of Free Radicals.....	1041
11.6. $S_{RN}1$ Substitution Processes	1044
11.6.1. $S_{RN}1$ Substitution Reactions of Alkyl Nitro Compounds	1045
11.6.2. $S_{RN}1$ Substitution Reactions of Aryl and Alkyl Halides	1048
Topic 11.1. Relationships between Bond and Radical Stabilization Energies.....	1052
Topic 11.2. Structure-Reactivity Relationships in Hydrogen Abstraction Reactions.....	1056
General References.....	1062
Problems	1063
 Chapter 12. Photochemistry	1073
Introduction.....	1073
12.1. General Principles	1073

12.2. Photochemistry of Alkenes, Dienes, and Polyenes	1081
12.2.1. <i>cis-trans</i> Isomerization	1081
12.2.2. Photoreactions of Other Alkenes	1091
12.2.3. Photoisomerization of 1,3-Butadiene	1096
12.2.4. Orbital Symmetry Considerations for Photochemical Reactions of Alkenes and Dienes	1097
12.2.5. Photochemical Electrocyclic Reactions	1100
12.2.6. Photochemical Cycloaddition Reactions	1109
12.2.7. Photochemical Rearrangements Reactions of 1,4-Dienes	1112
12.3. Photochemistry of Carbonyl Compounds.....	1116
12.3.1. Hydrogen Abstraction and Fragmentation Reactions	1118
12.3.2. Cycloaddition and Rearrangement Reactions of Cyclic Unsaturated Ketones.....	1125
12.3.3. Cycloaddition of Carbonyl Compounds and Alkenes	1132
12.4. Photochemistry of Aromatic Compounds	1134
Topic 12.1. Computational Interpretation of Diene and Polyene Photochemistry	1137
General References.....	1145
Problems	1146
References to Problems.....	1155
Index	1171

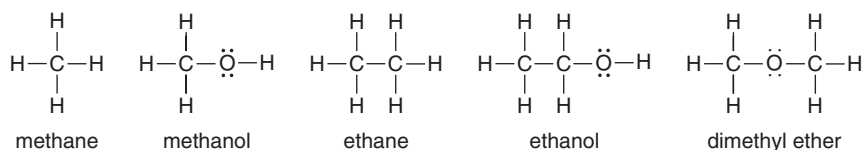
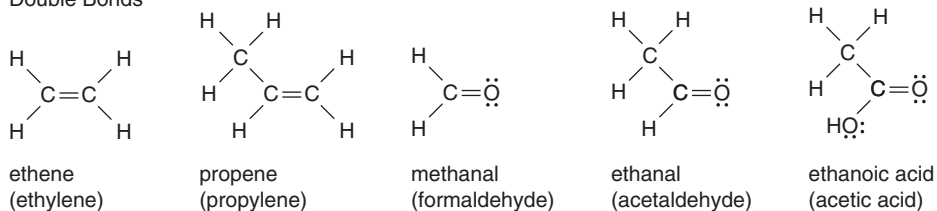
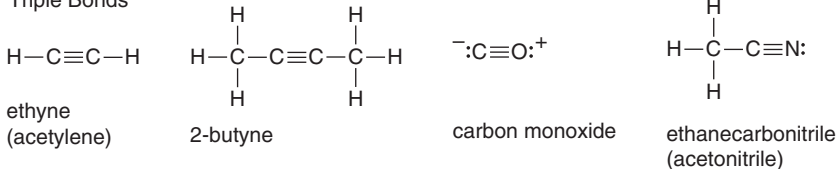
Chemical Bonding and Molecular Structure

Introduction

In this chapter we consider *molecular structure* and the concepts of *chemical bonding* that are used to interpret molecular structure. We will also begin to see how information about molecular structure and ideas about bonds can be used to interpret and predict physical properties and chemical reactivity. *Structural formulas* are a key tool for describing both structure and reactivity. At a minimum, they indicate *molecular constitution* by specifying the *connectivity* among the atoms in the molecule. Structural formulas also give a rough indication of electron distribution by representing electron pairs in bonds by lines and unshared electrons as dots, although the latter are usually omitted in printed structures. The reader is undoubtedly familiar with structural formulas for molecules such as those shown in Scheme 1.1.

In quantitative terms, molecular structure specifies the relative position of all atoms in a molecule. These data provide the bond lengths and bond angles. There are a number of experimental means for precise determination of molecular structure, primarily based on spectroscopic and diffraction methods, and structural data are available for thousands of molecules. Structural information and interpretation is also provided by *computational chemistry*. In later sections of this chapter, we describe how molecular orbital theory and density functional theory can be applied to the calculation of molecular structure and properties.

The *distribution of electrons* is another element of molecular structure that is very important for understanding chemical reactivity. It is considerably more difficult to obtain experimental data on *electron density*, but fortunately, in recent years the rapid development of both structural theory and computational methods has allowed such calculations. We make use of computational electron density data in describing molecular structure, properties, and reactivity. In this chapter, we focus on the minimum energy structure of individual molecules. In Chapter 2, we consider other elements of molecular geometry, including dynamic processes involving *conformation*, that is, the variation of molecular shape as a result of bond rotation. In Chapter 3, we discuss

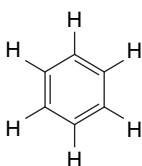
Scheme 1.1. Lewis Structures of Simple Molecules**CHAPTER 1***Chemical Bonding
and Molecular Structure***Single Bonds****Double Bonds****Triple Bonds**

how structure effects the energy of *transition structures* and *intermediates* in chemical reactions. The principal goal of this chapter is to discuss the concepts that chemists use to develop relationships between molecular structure and reactivity. These relationships have their foundation in the fundamental physical aspects of molecular structure, that is, nuclear position and electron density distribution. Structural concepts help us see, understand, and apply these relationships.

1.1. Description of Molecular Structure Using Valence Bond Concepts

Introductory courses in organic chemistry usually rely primarily on the valence bond description of molecular structure. Valence bond theory was the first structural theory applied to the empirical information about organic chemistry. During the second half of the nineteenth century, correct structural formulas were deduced for a wide variety of organic compounds. The concept of “valence” was recognized. That is, carbon almost always formed four bonds, nitrogen three, oxygen two, and the halogens one. From this information, chemists developed structural formulas such as those in Scheme 1.1. Kekulé’s structure for benzene, published in 1865, was a highlight of this period. The concept of *functional groups* was also developed. It was recognized that structural entities such as hydroxy (−OH), amino (−NH₂), carbonyl (C=O), and

carboxy (CO_2H) groups each had characteristic reactivity that was largely independent of the hydrocarbon portion of the molecule.



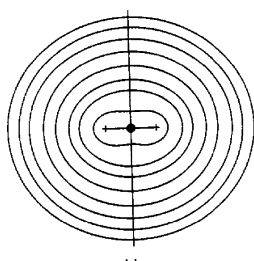
Kekulé structure
for benzene

These structural formulas were developed without detailed understanding of the nature of the *chemical bond* that is represented by the lines in the formulas. There was a key advance in the understanding of the origin of chemical bonds in 1916, when G.N. Lewis introduced the concept of electron-pair bonds and the “rule of 8” or *octet rule*, as we now know it. Lewis postulated that chemical bonds were the result of sharing of electron pairs by nuclei and that for the second-row atoms, boron through neon, the most stable structures have eight valence shell electrons.¹ Molecules with more than eight electrons at any atom are very unstable and usually dissociate, while those with fewer than eight electrons at any atom are usually highly reactive toward electron donors. The concept of bonds as electron pairs gave a fuller meaning to the traditional structural formulas, since the lines then specifically represent single, double, and triple bonds. The dots represent unshared electrons. Facility with Lewis structures as a tool for accounting for electrons, bonds, and charges is one of the fundamental skills developed in introductory organic chemistry.

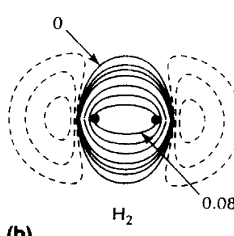
Lewis structures, however, convey relatively little information about the details of molecular structure. We need other concepts to deduce information about relative atomic positions and, especially, electron distribution. *Valence bond theory* provides one approach to deeper understanding of molecular structure. Valence bond (VB) theory has its theoretical foundation in quantum mechanics calculations that demonstrated that electrons hold nuclei together, that is, form bonds, when shared by two nuclei. This fact was established in 1927 by calculations on the hydrogen molecule.² The results showed that an energy minimum occurs at a certain internuclear distance if the electrons are free to associate with either nucleus. Electron density accumulates between the two nuclei. This can be depicted as an electron density map for the hydrogen molecule, as shown in Figure 1.1a. The area of space occupied by electrons is referred to as an *orbital*. A fundamental concept of VB theory is that there is a concentration of electron density between atoms that are bonded to one another. Figure 1.1b shows that there is *electron density depletion* relative to spherical atoms outside of the hydrogen nuclei. Nonbonding electrons are also described by orbitals, which are typically more diffuse than bonding ones. The mathematical formulation of molecular structure by VB theory is also possible. Here, we emphasize qualitative concepts that provide insight into the relationship between molecular structure and properties and reactivity.

¹. G. N. Lewis, *J. Am. Chem. Soc.*, **38**, 762 (1916).

². W. Heitler and F. London, *Z. Phys.*, **44**, 455 (1927).



(a)

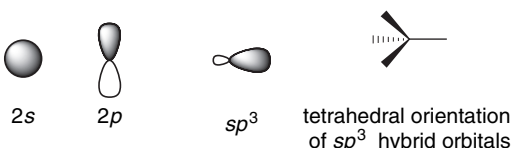


(b)

Fig. 1.1. Contour maps of (a) total electron density and (b) density difference relative to the spherical atoms for the H_2 molecule. Reproduced with permission from R. F. W. Bader, T. T. Nguyen, and Y. Tal, *Rep. Prog. Phys.*, **44**, 893 (1981).

1.1.1. Hybridization

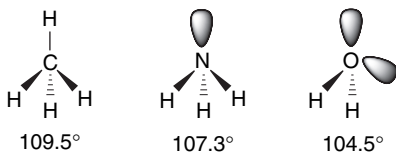
Qualitative application of VB theory to molecules containing second-row elements such as carbon, nitrogen, and oxygen involves the concept of *hybridization*, which was developed by Linus Pauling.³ The atomic orbitals of the second-row elements include the spherically symmetric $2s$ and the three $2p$ orbitals, which are oriented perpendicularly to one another. The combination of these atomic orbitals is equivalent to four sp^3 orbitals directed toward the corners of a tetrahedron. These are called sp^3 *hybrid orbitals*. In methane, for example, these orbitals overlap with hydrogen $1s$ orbitals to form σ bonds.



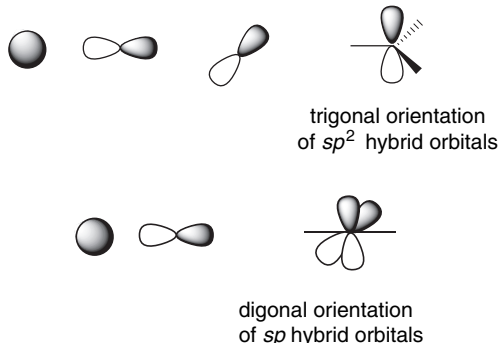
The valence bond description of methane, ammonia, and water predicts tetrahedral geometry. In methane, where the carbon valence is four, all the hybrid orbitals are involved in bonds to hydrogen. In ammonia and water, respectively, one and two nonbonding (unshared) pairs of electrons occupy the remaining orbitals. While methane

³. L. Pauling, *J. Am. Chem. Soc.*, **53**, 1367 (1931).

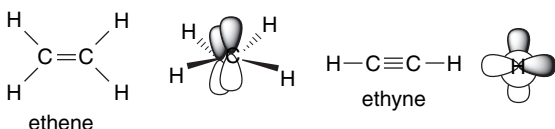
is perfectly tetrahedral, the bond angles in ammonia and water are somewhat reduced. This suggests that the electron-electron repulsions between unshared pairs are greater than for electrons in bonds to hydrogen. In other words, the unshared pairs occupy somewhat larger orbitals. This is reasonable, since these electrons are not attracted by hydrogen nuclei.



The hybridization concept can be readily applied to molecules with double and triple bonds, such as those shown in Scheme 1.1. Second-row elements are described as having sp^2 or sp orbitals, resulting from hybridization of the s orbital with two or one p orbitals, respectively. The double and triple bonds are conceived as arising from the overlap of the unhybridized p orbitals on adjacent atoms. These bonds have a nodal plane and are called π bonds. Because the overlap is not as effective as for sp^3 orbitals, these bonds are somewhat weaker than σ bonds.



The prototypical hydrocarbon examples of sp^2 and sp hybridization are ethene and ethyne, respectively. The total electron density between the carbon atoms in these molecules is the sum from the π and σ bonds. For ethene, the electron density is somewhat elliptical, because the π component is not cylindrically symmetrical. For ethyne, the combination of the two π bonds restores cylindrical symmetry. The electron density contours for ethene are depicted in Figure 1.2, which shows the highest density near the nuclei, but with net accumulation of electron density between the carbon and hydrogen atoms.



The hybridization concept also encompasses empty antibonding orbitals, which are designated by an asterisk (*). These orbitals have nodes between the bound atoms. As discussed in Section 1.1.8, σ^* and π^* orbitals can interact with filled orbitals and contribute to the ground state structure of the molecule. These empty orbitals are also

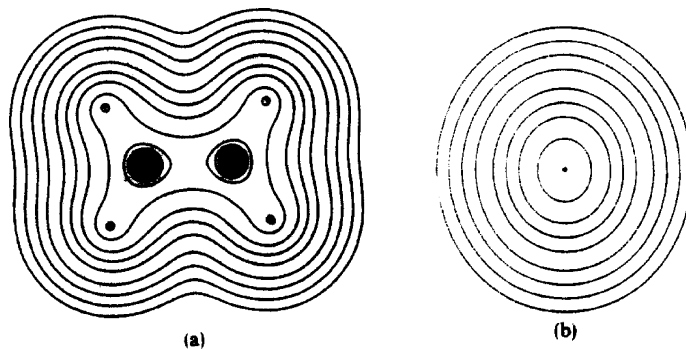
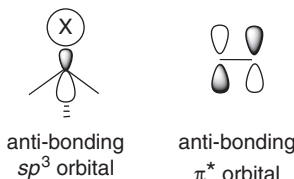
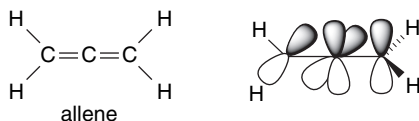


Fig. 1.2. (a) Contour map of electron density in the plane of the ethene molecule. (b) Contour map of electron density perpendicular to the plane of the ethene molecule at the midpoint of the C=C bond. Reproduced with permission from R. F. W. Bader, T. T. Nguyen-Dang, and Y. Tal, *Rep. Prog. Phys.*, **44**, 893 (1981).

of importance in terms of reactivity, particularly with electron-donating *nucleophilic* reagents, since it is the empty antibonding orbitals that interact most strongly with approaching nucleophiles.



The hybridization concept indicates some additional aspects of molecular structure. The tetrahedral, trigonal, and digonal natures of sp^3 , sp^2 , and sp carbon atoms provide an approximation of bond angles. The idea that π bonds are formed by the overlap of p orbitals puts some geometrical constraints on structure. Ethene, for example, is planar to maximize p -orbital overlap. Allene, on the other hand, must have the terminal CH₂ groups rotated by 90° to accommodate two π bonds at the central sp carbon.

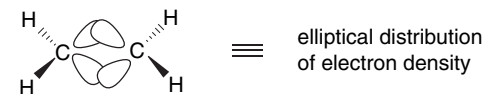


It is important to remember that hybridization is a *description* of the observed molecular geometry and electron density. Hybridization does not *cause* a molecule to have a particular shape. Rather, the molecule adopts a particular shape because it maximizes bonding interactions and minimizes electron-electron and other repulsive interactions. We use the hybridization concept to recognize similarities in structure that have their origin in fundamental forces within the molecules. The concept of hybridization helps us to see how molecular structure is influenced by the number of ligands and electrons at a particular atom.

SECTION 1.1

Description of Molecular Structure Using Valence Bond Concepts

It is worth noting at this point that a particular hybridization scheme *does not provide a unique description of molecular structure*. The same fundamental conclusions about geometry and electron density are reached if ethene and ethyne are described in terms of sp^3 hybridization. In this approach, the double bond in ethene is thought of as arising from two overlapping sp^3 orbitals. The two bonds are equivalent and are called *bent bonds*. This bonding arrangement also predicts a planar geometry and elliptical electron distribution, and in fact, this description is mathematically equivalent to the sp^2 hybridization description. Similarly, ethyne can be thought of as arising by the sharing of three sp^3 hybrid orbitals. The fundamental point is that there is a single real molecular structure defined by atomic positions and electron density. Orbitals partition the electron density in specific ways, and it is the *sum of the orbital contributions that describes the structure*.



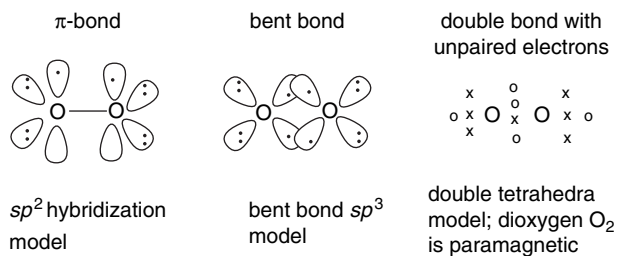
1.1.2. The Origin of Electron-Electron Repulsion

We have already assumed that electron pairs, whether in bonds or as nonbonding pairs, repel other electron pairs. This is manifested in the tetrahedral and trigonal geometry of tetravalent and trivalent carbon compounds. These geometries correspond to maximum separation of the electron-pair bonds. Part of this repulsion is electrostatic, but there is another important factor. The *Pauli exclusion principle* states that only two electrons can occupy the same point in space and that they must have opposite spin quantum numbers. Equivalent orbitals therefore maintain maximum separation, as found in the sp^3 , sp^2 , and sp hybridization for tetra-, tri-, and divalent compounds of the second-row elements. The combination of Pauli exclusion and electrostatic repulsion leads to the *valence shell electron-pair repulsion rule* (VSEPR), which states that bonds and unshared electron pairs assume the orientation that permits maximum separation.

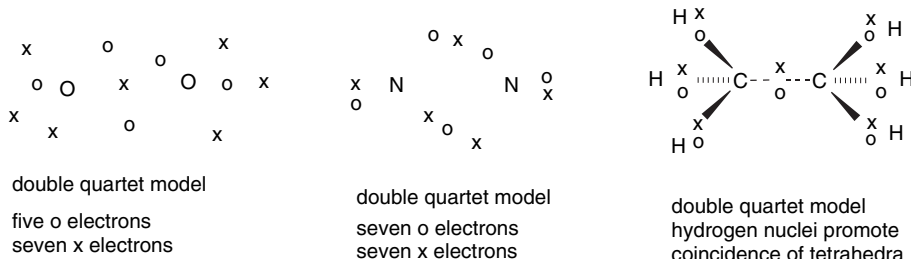
An important illustration of the importance of the Pauli exclusion principle is seen in the O_2 molecule. If we were to describe O_2 using either the sp^2 hybridization or bent bond model, we would expect a double bond with all the electrons paired. In fact, O_2 is *paramagnetic*, with two unpaired electrons, and yet it does have a double bond. If we ask how electrons would be distributed to maintain maximum separation, we arrive at two tetrahedral arrays, with the tetrahedra offset by the maximum amount.⁴ Electronic spin can be represented as x and o. The structure still has four bonding electrons between the oxygen atoms, that is, a double bond. It also obeys the octet rule for each oxygen and correctly predicts that two of the electrons are unpaired.

⁴ J. W. Linnett, *The Electronic Structure of Molecules*, Methren Co. LTD, London, 1964, pp. 37–42; R. J. Gillespie and P. L. A. Popelier, *Chemical Bonding and Molecular Geometry*, Oxford University Press, New York, 2001, pp 102–103.

This structure minimizes electron-electron repulsions and obeys the Pauli principle by maximizing the separation of electrons having the same spin.



A similar representation of N₂ with offset of the tetrahedral of electrons correctly describes the molecule as having a triple bond, but it is diamagnetic, since there are equal numbers of electrons of each spin. For ethane, all the electrons are bonding and are attracted toward the hydrogen nuclei, and the tetrahedra of electrons of opposite spin both occupy a region of space directed toward a hydrogen nucleus.



For most of the molecules and reactions we want to consider, the Pauling hybridization scheme provides an effective structural framework, and we use VB theory to describe most of the reactions and properties of organic compounds. However, we have to keep in mind that it is *neither a unique nor a complete description of electron density*, and we will find cases where we need to invoke additional ideas. In particular, we discuss *molecular orbital theory* and *density functional theory*, which are other ways of describing molecular structure and electron distribution.

1.1.3. Electronegativity and Polarity

The VB concept of electron-pair bonds recognizes that the sharing of electrons by the nuclei of two different elements is unequal. Pauling defined the concept of unequal sharing in terms of *electronegativity*,⁵ defining the term as “the power of an atom in a molecule to attract electrons to itself.” Electronegativity depends on the number of protons in the nucleus and is therefore closely associated with position in the periodic table. The metals on the left of the periodic table are the least electronegative elements, whereas the halogens on the right have the highest electronegativity in each row. Electronegativity decreases going down the periodic table for both metals and nonmetals.

The physical origin of these electronegativity trends is *nuclear screening*. As the atomic number increases from lithium to fluorine, the nuclear charge increases, as does

⁵. L. Pauling, *J. Am. Chem. Soc.*, **54**, 3570 (1932).

SECTION 1.1

Description of Molecular Structure Using Valence Bond Concepts

the number of electrons. Each successive electron “feels” a larger nuclear charge. This charge is partially screened by the additional electron density as the shell is filled. However, the screening, on average, is less effective for each electron that is added. As a result, an electron in fluorine is subject to a greater effective nuclear charge than one in an atom on the left in the periodic table. As each successive shell is filled, the electrons in the valence shell “feel” the effective nuclear charge as screened by the filled inner shells. This screening is more effective as successive shells are filled and the outer valence shell electrons are held less tightly going down the periodic table. As we discuss later, the “size” of an atom also changes in response to the nuclear charge. Going across the periodic table in any row, the atoms become *smaller* as the shell is filled because of the higher effective nuclear charge. Pauling devised a numerical scale for electronegativity, based on empirical interpretation of energies of bonds and relating specifically to electron sharing in covalent bonds, that has remained in use for many years. Several approaches have been designed to define electronegativity in terms of other atomic properties. Allred and Rochow defined electronegativity in terms of the electrostatic attraction by the effective nuclear charge Z_{eff}^6 :

$$\chi_{\text{AR}} = \frac{0.3590Z_{\text{eff}}}{r^2} + 0.744 \quad (1.1)$$

where r is the covalent radius in Å. This definition is based on the concept of nuclear screening described above. Another definition of electronegativity is based explicitly on the relation between the number of valence shell electrons, n , and the effective atomic radius r :⁷

$$V = n/r \quad (1.2)$$

As we will see shortly, covalent and atomic radii are not absolutely measurable quantities and require definition.

Mulliken found that there is a relationship between *ionization potential* (IP) and *electron affinity* (EA) and defined electronegativity χ as the average of those terms:⁸

$$\chi_{\text{abs}} = \frac{\text{IP} + \text{EA}}{2} \quad (1.3)$$

This formulation, which turns out to have a theoretical justification in density functional theory, is sometimes referred to as *absolute electronegativity* and is expressed in units of eV.

A more recent formulation of electronegativity, derived from the basic principles of atomic structure, has led to a *spectroscopic scale for electronegativity*.⁹ In this formulation, the electronegativity is defined as the average energy of a valence electron in an atom. The lower the average energy, the greater the electron-attracting power (electronegativity) of the atom. The formulation is

$$\chi_{\text{spec}} = \frac{(a\text{IP}_s + b\text{IP}_p)}{a+b} \quad (1.4)$$

⁶ A. L. Allred and E. G. Rochow, *J. Inorg. Nucl. Chem.*, **5**, 264 (1958).

⁷ Y.-R. Luo and S. W. Benson, *Acc. Chem. Res.*, **25**, 375 (1992).

⁸ R. S. Mulliken, *J. Chem. Phys.*, **2**, 782 (1934); R. S. Mulliken, *J. Chem. Phys.*, **3**, 573 (1935).

⁹ L. C. Allen, *J. Am. Chem. Soc.*, **111**, 9003 (1989); L. C. Allen, *Int. J. Quantum Chem.*, **49**, 253 (1994); J. B. Mann, T. L. Meek, and L. C. Allen, *J. Am. Chem. Soc.*, **122**, 2780 (2000).

where IP_s and IP_p are the ionization potentials of the *s* and *p* electrons and *a* and *b* are the number of *s* and *p* electrons, respectively.

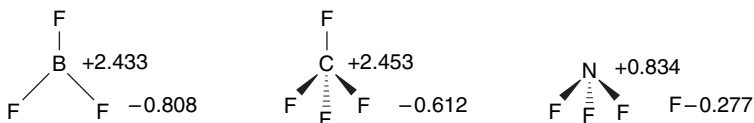
The values on this scale correlate well with the Pauling and Allred-Rochow scales. One feature of this scale is that the IP values can be measured accurately so that electronegativity becomes an *experimentally measured* quantity. When the same concepts are applied to atoms in molecules, the atom undergoes an electronegativity adjustment that can be related to the energy of its orbitals (as expressed by molecular orbital theory). The average adjusted energy of an electron is called the *energy index* (EI). The EI values of two bound atoms provide a measure of bond polarity called the *bond polarity index*¹⁰ (BPI), formulated as

$$\text{BPI}_{\text{AB}} = (\text{EI}_A - \text{EI}_A^{\text{ref}}) - (\text{EI}_B - \text{EI}_B^{\text{ref}}) \quad (1.5)$$

where EI^{ref} are parameters of A–A and B–B bonds.

These approaches, along with several others, give electronegativity scales that are in good relative agreement in assessing the electron-attracting power of the elements. Each scale is based on fundamental atomic properties. However, they are in different units and therefore not directly comparable. Table 1.1 gives the values assigned by some of the electronegativity scales. The numerical values are scaled to the original Pauling range. At this point, we wish to emphasize the broad consistency of the values, not the differences. We use the *order of the electronegativity of the elements* in a qualitative way, primarily when discussing *bond polarity*. It should be noted, however, that the concept of electronegativity has evolved from an empirical scale to one with specific physical meaning. We pursue the relationship between these scales further in Topic 1.5.3.

The most obvious consequence of differential electronegativity is that covalent bonds between different elements are *polar*. Each atom bears a partial charge reflecting the relative electronegativity of the two elements sharing the bond. These charges can be estimated, and the values found for BF_3 , CF_4 , and NF_3 are shown below.¹¹ Note that the negative charge on fluorine becomes smaller as the electronegativity of the central atom increases.



The individual polar bonds contribute to the polarity of the overall molecule. The overall molecular polarity is expressed as the dipole moment. For the three molecules shown, the overall molecular dipole moment is 0 for BF_3 (planar) and CF_4 (tetrahedral), because of the symmetry of the molecules, but NF_3 has a dipole moment of 0.235 D, since the molecule is pyramidal.¹²

¹⁰. L. C. Allen, D. A. Egolf, E. T. Knight, and C. Liang, *J. Phys. Chem.*, **94**, 5603 (1990); L. C. Allen, *Can. J. Chem.*, **70**, 631 (1992).

¹¹. R. J. Gillespie and P. L. A. Popelier, *Chemical Bonding and Molecular Geometry*, Oxford University Press, New York, 2001, p. 47.

¹². Dipole moments are frequently expressed in Debye (D) units; 1 D = 3.335641×10^{-30} C m in SI units.

Table 1.1. Electronegativity Scales^a

Atom	Original Pauling ^b	Modified Pauling ^c	Allred- Rochow ^d	Luo- Benson ^e	Mulliken ^f	Allen ^g	SECTION 1.1
H	2.1	2.20	2.20		2.17	2.30	Description of Molecular Structure Using Valence Bond Concepts
Li	1.0	0.98	0.97	0.93	0.91	0.91	
Be	1.5	1.57	1.47	1.39	1.45	1.58	
B	2.0	2.04	2.01	1.93	1.88	2.05	
C	2.5	2.55	2.50	2.45	2.45	2.54	
N	3.0	3.04	3.07	2.96	2.93	3.07	
O	3.5	3.44	3.50	3.45	3.61	3.61	
F	4.0	3.98	4.10	4.07	4.14	4.19	
Na	0.9	0.93	1.01	0.90	0.86	0.87	
Mg	1.2	1.31	1.23	1.20	1.21	1.29	
Al	1.5	1.61	1.47	1.50	1.62	1.61	
Si	1.8	1.90	1.74	1.84	2.12	1.92	
P	2.1	2.19	2.06	2.23	2.46	2.25	
S	2.5	2.58	2.44	2.65	2.64	2.59	
Cl	3.0	3.16	2.83	3.09	3.05	2.87	
Ge	1.8	2.01	2.02	1.79	2.14	1.99	
As	2.0	2.18	2.20	2.11	2.25	2.21	
Se	2.4	2.55	2.48	2.43	2.46	2.42	
Br	2.8	2.96	2.74	2.77	2.83	2.69	
Sn	1.8	1.96	1.72	1.64	2.12	1.82	
I	2.5	2.66	2.21	2.47	2.57	2.36	

a. All numerical values are scaled to the original Pauling scale.

b. L. Pauling, *The Nature of the Chemical Bond*, 3rd Edition, Cornell University Press, Ithaca, NY, 1960.

c. A. L. Allred, *J. Inorg. Nucl. Chem.*, **17**, 215 (1961).

d. A. L. Allred and E.G. Rochow, *J. Inorg. Nucl. Chem.*, **5**, 264 (1958).

e. Y. R. Luo and S.W. Benson, *Acc. Chem. Res.*, **25**, 375 (1992).

f. D. Bergman and J. Hinze, *Angew. Chem. Int. Ed. Engl.*, **35**, 150 (1996).

g. L. C. Allen, *Int. J. Quantum Chem.*, **49**, 253 (1994).

1.1.4. Electronegativity Equalization

The concept of *electronegativity equalization* was introduced by R. T. Sanderson.¹³ The idea is implicit in the concept of a molecule as consisting of nuclei embedded in an electronic cloud and leads to the conclusion that the electron density will reach an equilibrium state in which there is no net force on the electrons. The idea of electronegativity equalization finds a theoretical foundation in *density functional theory* (see Section 1.3). Several numerical schemes have been developed for the assignment of charges based on the idea that electronegativity equalization must be achieved. Sanderson's initial approach averaged all atoms of a single element, e.g., carbon, in a molecule and did not distinguish among them. This limitation was addressed by Hercules and co-workers,¹⁴ who assigned electronegativity values called SR' values to specific groups within a molecule. For example, the methyl and ethyl groups, respectively, were derived from the number of C and H atoms in the group:

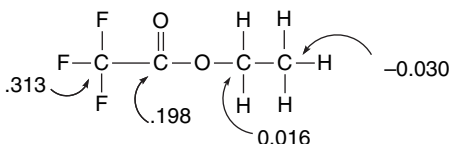
$$\text{SR'}_{\text{CH}_3} = (\text{SR}_C \times \text{SR}_H^3)^{1/4} \quad (1.6)$$

$$\text{SR'}_{\text{C}_2\text{H}_5} = [(\text{SR}_C \times \text{SR}_H^2)(\text{SR}_C \times \text{SR}_H^3)^{1/4}]^{1/4} \quad (1.7)$$

¹³. R. T. Sanderson, *Chemical Bonds and Bond Energies*, Academic Press, New York, 1976; R. T. Sanderson, *Polar Covalence*, Academic Press, New York, 1983.

¹⁴. J. C. Carver, R. C. Gray, and D. M. Hercules, *J. Am. Chem. Soc.*, **96**, 6851 (1974).

This approach was extended by M. Sastry to a variety of organic compounds.¹⁵ For example, the charges calculated for the carbon atoms in $\text{CF}_3\text{CO}_2\text{C}_2\text{H}_5$ are as shown below. We see that the carbon of the methyl group carries a small negative charge, whereas the carbons bound to more electronegative elements are positive.



The calculated charge on carbon for a number of organic molecules showed good correlation with the core atomic binding energies, as measured by X-ray photoemission spectroscopy. We discuss other methods of assigning charges to atoms based on computational chemistry in Section 1.4. We also find that all these methods are in some sense arbitrary divisions of molecules. The concept of electronegativity equalization is important, however. It tells us that electron density shifts in response to bonding between atoms of different electronegativity. This is the basis of *polar substituent effects*. Furthermore, as the data above for ethyl trifluoroacetate suggest, a highly electronegative substituent induces a net positive charge on carbon, as in the CF_3 and $\text{C}=\text{O}$ carbons in ethyl trifluoroacetate. Electronegativity differences are the origin of *polar bonds*, but electronegativity equalization suggests that there will also be an *inductive effect*, that is, the propagation of changes in electron distribution to adjacent atoms.

1.1.5. Differential Electronegativity of Carbon Atoms

Although carbon is assigned a single numerical value in the Pauling electronegativity scale, its effective electronegativity depends on its hybridization. The qualitative relationship is that carbon electronegativity toward other bound atoms increases with the extent of *s* character in the bond, i.e., $sp^3 < sp^2 < sp$. Based on the atomic radii approach, the carbon atoms in methane, benzene, ethene, and ethyne have electronegativity in the ratio 1:1.08:1.15:1.28. A scale based on bond polarity measures gives values of 2.14, 2.34, and 2.52 for sp^3 , sp^2 , and sp carbons, respectively.¹⁶ A scale based on NMR coupling constants gives values of 1.07 for methyl, 1.61 for ethenyl, and 3.37 for ethynyl.¹⁷ If we use the density functional theory definition of electronegativity (see Topic 1.5.1) the values assigned to methyl, ethyl, ethenyl, and ethynyl are 5.12, 4.42, 5.18, and 8.21, respectively.¹⁸ Note that by this measure methyl is significantly more electronegative than ethyl. With an *atoms in molecules* approach (see Section 1.4.3), the numbers assigned are methyl 6.84; ethenyl 7.10, and ethynyl 8.23.¹⁹ Table 1.2 converts each of these scales to a relative scale with methyl equal to 1. Note that the various definitions *do not* reach a numerical consensus on the relative electronegativity of sp^3 , sp^2 , and sp carbon, although the order is consistent. We are

¹⁵ M. Sastry, *J. Electron Spectros.*, **85**, 167 (1997).

¹⁶ N. Inamoto and S. Masuda, *Chem. Lett.*, 1003, 1007 (1982).

¹⁷ S. Marriott, W. F. Reynolds, R. W. Taft, and R. D. Topsom, *J. Org. Chem.*, **49**, 959 (1984).

¹⁸ F. De Proft, W. Langenaeker, and P. Geerlings, *J. Phys. Chem.*, **97**, 1826, (1995).

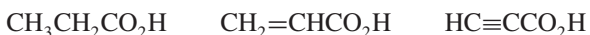
¹⁹ S. Hati and D. Datta, *J. Comput. Chem.*, **13**, 912 (1992).

Table 1.2. Ratio of Electronegativity for Carbon of Different Hybridization

Comparison	Methyl	Ethenyl	Ethyneyl
Atomic radii	1.0	1.15	1.28
Bond polarity	1.0	1.09	1.18
NMR coupling	1.0	1.50	3.15
Density function theory	1.0	1.01	1.60
Atoms in molecules	1.0	1.04	1.20

not so concerned with the precise number, but rather with the trend of increasing electronegativity $sp^3 < sp^2 < sp$. It is also important to note that the range of carbon electronegativities is close to that of hydrogen. While sp^3 carbon and hydrogen are similar in electronegativity, sp^2 and sp carbon are more electronegative than hydrogen.

If we compare the pK_a values of propanoic acid (4.87), propenoic acid (4.25), and propynoic acid (1.84), we get some indication that the hybridization of carbon does exert a substantial polar effect. The acidity increases with the electronegativity of the carbon group.



Orbitals of different hybridization on the same carbon are also thought of as having different electronegativities. For example, in strained hydrocarbons such as cyclopropane the C–H bonds are more acidic than normal. This is attributed to the additional *s* character of the C–H bonds, which compensates for the added *p* character of the strained C–C bonds.²⁰

It is also possible to assign electronegativity values to groups. For alkyl groups the numbers are: CH_3 , 2.52; C_2H_5 , 2.46; $(\text{CH}_3)_2\text{CH}$, 2.41; $(\text{CH}_3)_3\text{C}$, 2.38; C_6H_5 , 2.55, $\text{CH}_2=\text{CH}$, 2.55; $\text{HC}\equiv\text{C}$, 2.79.²¹ The order is in accord with the general trend that *more-substituted alkyl groups are slightly better electron donors than methyl groups*. The increased electronegativity of sp^2 and sp carbons is also evident. These values are based on bond energy data by a relationship first explored by Pauling and subsequently developed by many other investigators. The original Pauling expression is

$$D[A - B] = 1/2(D[A - A] + D[B - B]) + 23(\Delta\chi)^2 \quad (1.8)$$

where $\Delta\chi$ is the difference in electronegativity of A and B.

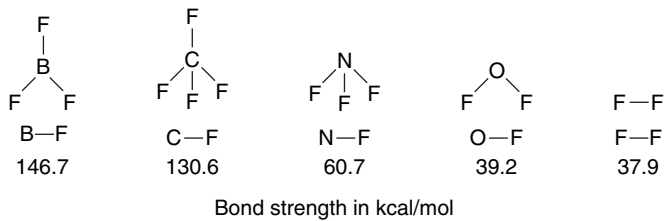
Thus the bond strength (in kcal/mol) can be approximated as the average of the two corresponding homonuclear bonds and an increment that increases with the difference in electronegativity. For any bond, application of this equation suggests a “covalent” and “polar” term. The results for the series CH_3F , CH_3OH , CH_3NH_2 , and CH_3CH_3 is shown below.

²⁰. J. N. Shoolery, *J. Chem. Phys.*, **31**, 1427 (1959); N. Muller and D. E. Pritchard, *J. Chem. Phys.*, **31**, 1471 (1959); K. B. Wiberg, R. F. W. Bader, and C. D. H. Lau, *J. Am. Chem. Soc.*, **109**, 1001 (1987).

²¹. N. Matsunaga, D. W. Rogers, and A. A. Zavitsas, *J. Org. Chem.*, **68**, 3158 (2003).

	D(A–A)	χ	$(\Delta\chi)^2$	Covalent	Polar	% Covalent	% Polar
CH ₃	89.8	2.525					
-F	38.0	3.938	1.189	63.90	27.35	70	30
-OH	56.1	3.500	0.987	72.95	22.70	76	24
-NH ₂	61.1	3.071	0.749	75.45	17.23	81	19
-CH ₃	89.8	2.525	0.000	89.8	0.0	100	0

An important qualitative result emerges from these numbers. *Bond strength is increased by electronegativity differences.* This is illustrated, for example, by the strength of the bonds of fluorine with the other second-row elements.



1.1.6. Polarizability, Hardness, and Softness

The interaction of valence shell electrons with the nucleus and intervening filled shells also affects the *polarizability* of the valence shell electrons. Polarizability can be described in terms of *hardness* and *softness*. A relatively large atom or ion with a small effective nuclear charge is relatively easily distorted (polarized) by an external charge and is called *soft*. A more compact electron distribution resulting from a higher net nuclear charge and less effective screening is called *hard*. The hard-soft-acid-base (HSAB) theory of stability and reactivity, introduced by Pearson,²² has been extensively applied to qualitative reactivity trends,²³ and has been theoretically justified.²⁴ The qualitative expression of HSAB is that hard-hard and soft-soft reaction partners are preferred to hard-soft combinations. As for electronegativity, numerical scales of hardness and softness have been devised. One definition, like the Mulliken definition of absolute electronegativity, is based on ionization potential and electron affinity:

$$\text{Hardness} = \eta = \frac{1}{2}(\text{IP} - \text{EA}) \quad \text{and} \quad \text{Softness} = \sigma = \frac{1}{\eta} \sim 2(\text{IP} - \text{EA}) \quad (1.9)$$

Hardness increases with electronegativity and with positive charge. Thus, for the halogens the order is F⁻ > Cl⁻ > Br⁻ > I⁻, and for second-row anions, F⁻ > HO⁻ > H₂N⁻ > H₃C⁻. For cations, hardness decreases with size and increases with positive charge, so that H⁺ > Li⁺ > Na⁺ > K⁺. The proton, lacking any electrons, is infinitely hard. In solution it does not exist as an independent entity but contributes to the hardness of some protonated species. Metal ion hardness increases with oxidation state as the electron cloud contracts with the removal of each successive electron. All these as

²². R. G. Pearson and J. Songstad, *J. Am. Chem. Soc.*, **89**, 1827 (1967); R. G. Pearson, *J. Chem. Educ.*, **45**, 581, 643 (1968).

²³. R. G. Pearson, *Inorg. Chim. Acta*, **240**, 93 (1995).

²⁴. P. K. Chattaraj, H. Lee, and R. G. Parr, *J. Am. Chem. Soc.*, **113**, 1855 (1991).

SECTION 1.1

Description of Molecular Structure Using Valence Bond Concepts

well as other hardness/softness relationships are consistent with the idea that hardness and softness are manifestations of the influence of nuclear charge on polarizability.

For polyatomic molecules and ions, hardness and softness are closely related to the HOMO and LUMO energies, which are analogous to the IP and EA values for atoms. The larger the HOMO-LUMO gap, the greater the hardness. Numerically, hardness is approximately equal to half the energy gap, as defined above for atoms. In general, chemical reactivity increases as LUMO energies are lower and HOMO energies are higher. The implication is that softer chemical species, those with smaller HOMO-LUMO gaps, tend to be more reactive than harder ones. In qualitative terms, this can be described as the ability of nucleophiles or bases to donate electrons more readily to electrophiles or acids and begin the process of bond formation. Interactions between harder chemical entities are more likely to be dominated by electrostatic interactions. Table 1.3 gives hardness values for some atoms and small molecules and ions. Note some of the trends for cations and anions. The smaller Li^+ , Mg^{2+} , and Na^+ ions are harder than the heavier ions such as Cu^+ , Hg^{2+} , and Pd^{2+} . The hydride ion is quite hard, second only to fluoride. The increasing hardness in the series $\text{CH}_3^- < \text{NH}_2^- < \text{OH}^- < \text{F}^-$ is of considerable importance and, in particular, correlates with nucleophilicity, which is in the order $\text{CH}_3^- > \text{NH}_2^- > \text{OH}^- > \text{F}^-$.

Figure 1.3 shows the IP-EA gap (2η) for several neutral atoms and radicals. Note that there is a correlation with electronegativity and position in the periodic table. The halogen anions and radicals become progressively softer from fluorine to iodine. Across the second row, softness decreases from carbon to fluorine. The cyanide ion is a relatively soft species.

The HSAB theory provides a useful precept for understanding Lewis acid-base interactions in that hard acids prefer hard bases and soft acids prefer soft bases. The principle can be applied to chemical equilibria in the form of the *principle of maximum hardness*,²⁵ which states that “molecules arrange themselves so as to

Table 1.3. Hardness of Some Atoms, Acids, and Bases^a

Atom	η	Cations	η	Anions	η
H	6.4	H^+		H^-	6.8
Li	2.4	Li^+	35.1	F^-	7.0
C	5.0	Mg^{2+}	32.5	Cl^-	4.7
N	7.3	Na^+	21.1	Br^-	4.2
O	6.1	Ca^{2+}	19.7	I^-	3.7
F	7.0	Al^{3+}	45.8	CH_3^-	4.0
Na	2.3	Cu^+	6.3	NH_2^-	5.3
Si	3.4	Cu^{2+}	8.3	OH^-	5.6
P	4.9	Fe^{2+}	7.3	SH^-	4.1
S	4.1	Fe^{3+}	13.1	CN^-	5.3
Cl	4.7	Hg^{2+}	7.7		
		Pb^{2+}	8.5		
		Pd^{2+}	6.8		

a. From R. G. Parr and R. G. Pearson, *J. Am. Chem. Soc.*, **105**, 7512 (1983).

²⁵. R. G. Pearson, *Acc. Chem. Res.*, **26**, 250 (1993); R. G. Parr and Z. Zhou, *Acc. Chem. Res.*, **26**, 256 (1993); R. G. Pearson, *J. Org. Chem.*, **54**, 1423 (1989); R. G. Parr and J. L. Gazquez, *J. Phys. Chem.*, **97**, 3939 (1993).

CHAPTER 1

*Chemical Bonding
and Molecular Structure*

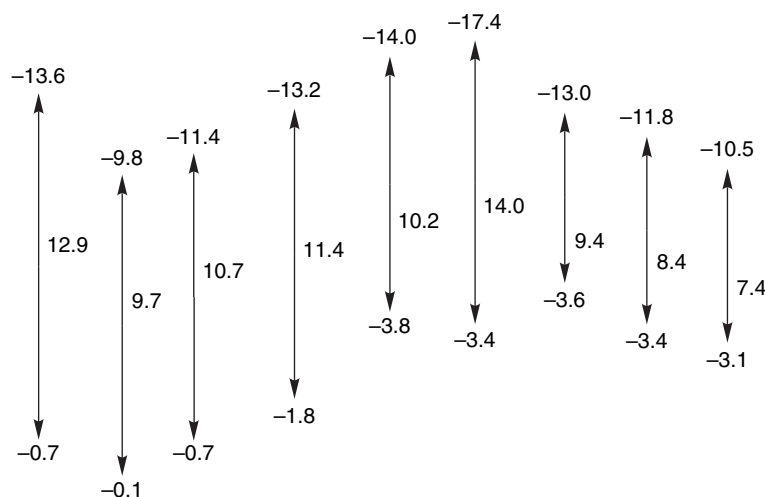


Fig. 1.3. Ionization (IP) and electron affinity (EA) gaps in eV for neutral atoms and radicals. Adapted from R. G. Pearson, *J. Am. Chem. Soc.*, **110**, 7684 (1988).

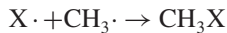
be as hard as possible." Expressed in terms of reaction energetics, ΔE is usually negative for



The hard-hard interactions are dominated by electrostatic attraction, whereas soft-soft interactions are dominated by mutual polarization.²⁶ Electronegativity and hardness determine the extent of electron transfer between two molecular fragments in a reaction. This can be approximated numerically by the expression

$$\Delta N = \frac{\chi_x - \chi_y}{2(\eta_x + \eta_y)} \quad (1.10)$$

where χ is absolute electronegativity and η is hardness for the reacting species. For example, we can calculate the degree of electron transfer for each of the four halogen atoms reacting with the methyl radical to form the corresponding methyl halide.



X·	χ_x	η_x	ΔN	$\eta_{\text{CH}_3\text{X}}$
F·	10.4	7.0	0.23	9.4
Cl·	8.3	4.7	0.17	7.5
Br·	7.6	4.2	0.14	5.8
I·	6.8	3.7	0.10	4.7

²⁶ R. G. Pearson, *J. Am. Chem. Soc.*, **85**, 3533 (1963); T. L. Ho, *Hard and Soft Acids and Bases in Organic Chemistry*, Academic Press, New York, 1977; W. B. Jensen, *The Lewis Acid-Base Concept*, Wiley-Interscience, New York, 1980, Chap. 8.

SECTION 1.1

Description of Molecular Structure Using Valence Bond Concepts

According to this analysis, the C–X bond is successively both more polar and harder in the order I < Br < Cl < F. This result is in agreement with both the properties and reactivities of the methyl halides. When bonds are compared, reacting pairs of greater hardness result in a larger net charge transfer, which adds an increment to the exothermicity of bond formation. That is, bonds formed between two hard atoms or groups are stronger than those between two soft atoms or groups.²⁷ This is an example of a general relationship that recognizes that there is an increment to bond strength resulting from added ionic character.²⁸

Polarizability measures the response of an ion or molecule to an electric field and is expressed in units of volume, typically 10^{-24} cm^3 or \AA^3 . Polarizability increases with atomic or ionic radius; it depends on the effectiveness of nuclear screening and increases as each valence shell is filled. Table 1.4 gives the polarizability values for the second-row atoms and some ions, molecules, and hydrocarbons. Methane is the least polarizable hydrocarbon and polarity increases with size. Polarizability is also affected by hybridization, with ethane > ethene > ethyne and propane > propene > propyne.

It should be noted that polarizability is *directional*, as illustrated in Scheme 1.2 for the methyl halides and halogenated benzenes.

Polarizability is related to the *refractive index* (*n*) of organic molecules, which was one of the first physical properties to be carefully studied and related to molecular structure.²⁹ As early as the 1880s, it was recognized that the value of the refractive index can be calculated as the sum of atomic components. Values for various groups were established and revised.³⁰ It was noted that some compounds, in particular compounds with conjugated bonds, had higher (“exalted”) polarizability. Polarizability is also directly related to the dipole moment *induced by an electric field*. The greater the polarizability of a molecule, the larger the induced dipole.

Table 1.4. Polarizability of Some Atoms, Ions, and Molecules^a

Atoms		Ions		Molecules		Hydrocarbons	
H	0.67			H ₂ O	1.45	CH ₄	2.59
Li	24.3			N ₂	1.74	C ₂ H ₆	4.47
Be	5.6			CO	1.95	CH ₂ =CH ₂	4.25
B	3.0			NH ₃	2.81	HC≡CH	3.93
C	1.8			CO ₂	2.91	C ₃ H ₈	6.29
N	1.1			BF ₃	3.31	CH ₃ CH=CH ₂	6.26
O	0.8					CH ₃ C≡CH	6.18
F	0.06	F ⁻	1.2			<i>n</i> -C ₄ H ₁₀	8.20
Ne	1.4	Na ⁺	0.9			<i>i</i> -C ₄ H ₁₀	8.14
Cl	2.2	Cl ⁻	3			<i>n</i> -C ₅ H ₁₂	9.99
Ar	3.6	K ⁺	2.3			Neopentane	10.20
Br	3.1	Br ⁻	4.5			<i>n</i> -C ₆ H ₁₄	11.9
Kr	4.8					Cyclohexane	10.9
I	5.3	I ⁻	7			C ₆ H ₆	10.3
Xe	6.9						

a. T. M. Miller, in *Handbook of Chemistry and Physics*, 83rd Edition, pp. 10-163–10-177, 2002.

b. A. Dalgano, *Adv. Phys.*, **11**, 281 (1962), as quoted by R. J. W. Le Fevre, *Adv. Phys. Org. Chem.*, **3**, 1 (1965).

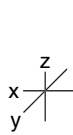
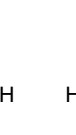
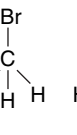
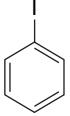
²⁷ P. K. Chattaraj, A. Cedillo, R. G. Parr, and E.M. Arnett, *J. Org. Chem.*, **60**, 4707 (1995).

²⁸ P. R. Reddy, T. V. R. Rao, and R. Viswanath, *J. Am. Chem. Soc.*, **111**, 2914 (1989).

²⁹ R. J. W. Le Fevre, *Adv. Phys. Org. Chem.*, **3**, 1 (1965).

³⁰ K. von Auwers, *Chem. Ber.*, **68**, 1635 (1935); A. I. Vogel, *J. Chem. Soc.*, 1842 (1948); J. W. Brühl, *Liebigs Ann. Chem.*, **235**, 1 (1986); J. W. Brühl, *Liebigs Ann. Chem.*, **236**, 233 (1986).

Scheme 1.2. Molecular Polarizability^a

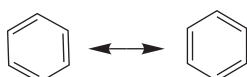
				
x	1.026	.411	.499	.657
y	1.026	.411	.499	.657
z	1.026	.509	.656	.872
				
x	1.12	1.255	1.301	1.588
y	.736	.821	.892	.996
z	1.12	1.478	1.683	1.971

a. From R J. W. Le Fevre, *Adv. Phys. Org. Chem.*, 3, 1 (1965).

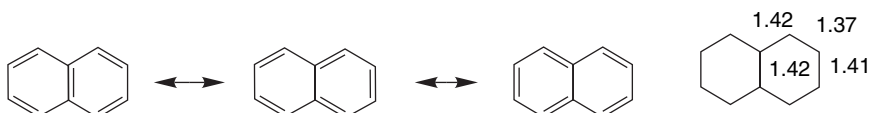
The concepts of electronegativity, polarizability, hardness, and softness are all interrelated. For the kind of qualitative applications we make in discussing reactivity, the concept that initial interactions between reacting molecules can be dominated by either partial electron transfer and bond formation (soft reactants) or by electrostatic interaction (hard reactants) is an important generalization.

1.1.7. Resonance and Conjugation

Qualitative application of VB theory makes use of the concept of *resonance* to relate structural formulas to the description of molecular structure and electron distribution. The case of benzene is a familiar and striking example. Two equivalent Lewis structures can be drawn, but the actual structure is the average of these two *resonance structures*. The double-headed arrow is used to specify a resonance relationship.



What structural information does this symbolism convey? Resonance structures imply that the true molecular structure is a weighted average of the individual structures. In the case of benzene, since the two structures are equivalent, each contributes equally. The *resonance hybrid* structure for benzene indicates hexagonal geometry and that the bond lengths are intermediate between a double and a single bond, since a bond order of 1.5 results from the average of the two structures. The actual structure of benzene is in accord with these expectations. It is perfectly hexagonal in shape and the carbon-carbon bond length is 1.40 Å. On the other hand, naphthalene, with three neutral resonance structures, shows bond length variation in accord with the predicted 1.67 and 1.33 bond orders.



SECTION 1.1

Description of Molecular Structure Using Valence Bond Concepts

Another important property of benzene is its thermodynamic stability, which is greater than expected for either of the two resonance structures. It is much more stable than noncyclic polyenes of similar structure, such as 1,3,5-hexatriene. What is the origin of this additional stability, which is often called *resonance stabilization or resonance energy*? The resonance structures imply that the π electron density in benzene is equally distributed between the sets of adjacent carbon atoms. This is not the case in acyclic polyenes. The electrons are evenly spread over the benzene ring, but in the polyene they are more concentrated between alternating pairs of carbon atoms. Average electron-electron repulsion is reduced in benzene. The difference in energy is called the *delocalization energy*. The resonance structures for benzene describe a particularly favorable bonding arrangement that leads to greater thermodynamic stability. In keeping with our emphasis on structural theory as a means of describing molecular properties, resonance *describes, but does not cause*, the extra stability.

Figure 1.4 shows electron density contours for benzene and 1,3,5-hexatriene. Note that the contours show completely uniform electron density distribution in benzene, but significant concentration between atoms 1,2; 3,4; and 5,6 in hexatriene, as was argued qualitatively above.

Resonance is a very useful concept and can be applied to many other molecules. Resonance is associated with delocalization of electrons and is a feature of *conjugated systems*, which have alternating double bonds that permit overlap between adjacent π bonds. This permits delocalization of electron density and usually leads to stabilization of the molecule. We will give some additional examples shortly.

We can summarize the applicability of the concept of resonance as follows:

1. When alternative Lewis structures can be written for a molecule and they differ only in the assignment of electrons among the nuclei, with nuclear positions being constant, then the molecule is not completely represented by a single Lewis structure, but has weighted properties of all the alternative Lewis structures.
2. Resonance structures are restricted to the maximum number of valence electrons that is appropriate for each atom: two for hydrogen and eight for second-row elements.

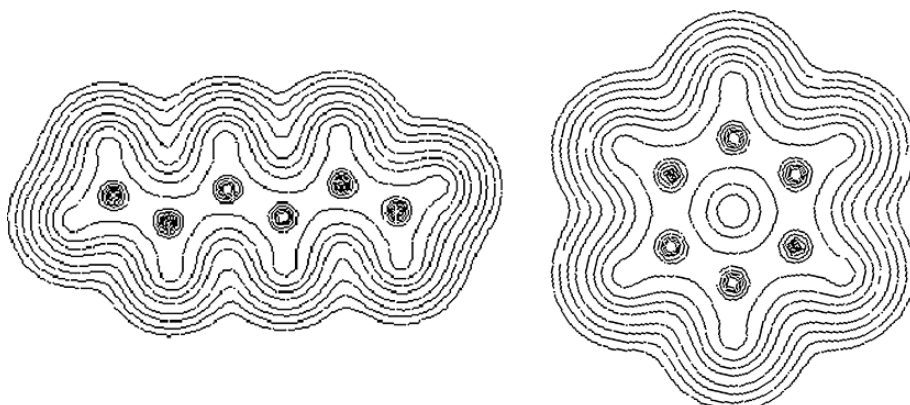
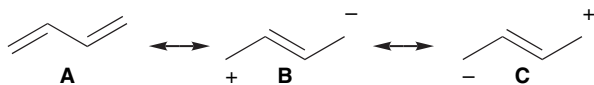


Fig. 1.4. Contour maps of electron density for 1,3,5-hexatriene and benzene in the planes of the molecules. Electron density was calculated at the HF/6-311G level. Electron density plots were created by applying the AIM2000 program; F.Biegler-Koenig, J.Shoenbohm and D.Dayles, *J. Compt. Chem.*, **22**, 545-559 (2001).

3. The more stable Lewis structures make the largest contribution to the weighted composite structure. Structures that have the following features are more stable and make the largest contribution: (a) maximum number of bonds, (b) minimum separation of opposite charges, and (c) charge distribution that is consistent with relative electronegativity.

Resonance structures are used to convey the structural and electron distribution consequences of conjugation and delocalization. Let us look specifically at 1,3-butadiene, 1,3,5-hexatriene, prop-2-enal (acrolein), methoxyethene (methyl vinyl ether), and ethenamine (vinylamine) to illustrate how resonance can help us understand electron distribution and reactivity. The hybridization picture for 1,3-butadiene suggests that there can be overlap of the p orbitals. Thermodynamic analysis (see Section 3.1.2.3) indicates that there is a net stabilization of about 3–4 kcal/mol, relative to two isolated double bonds. The electron density profile in Figure 1.5 shows some enhancement of π -electron density between C(2) and C(3).

Resonance structures portray increased electron density between C(2) and C(3), but only in structures that have fewer bonds and unfavorable charge separation.



In the diagram above there are two identical structures having opposite charge distributions and there is no net separation of charge. The importance of resonance structures to the composite structure increases with the stability of the individual structures, so structures **B** and **C** are less important than **A**, as they have separation of charge and only one rather than two π bonds. By applying resonance criteria 3a and 3b, we conclude that these two structures contribute less stabilization to butadiene than the two equivalent benzene resonance structures. Therefore, we expect the enhancement of electron density between C(2) and C(3) to be small.

For propenal (acrolein), one uncharged and two charged structures analogous to 1,3-butadiene can be drawn. In this case, the two charged structures are not equivalent.

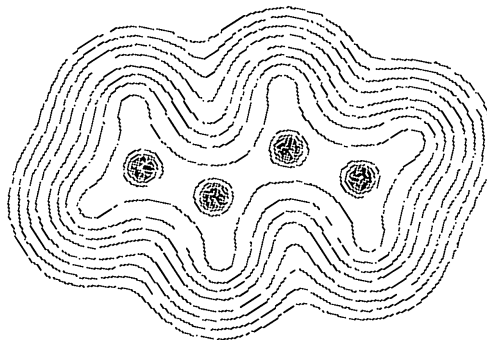
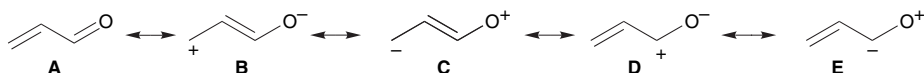
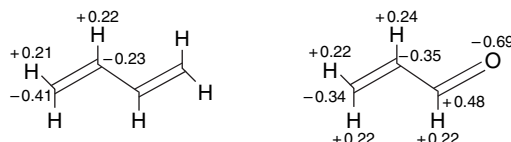


Fig. 1.5. Contour map of electron density for 1,3-butadiene in the plane of the molecule. Electron density was calculated at the HF/6-311G level. Electron density plots were created by applying the AIM2000 program; F.Biegler-Koenig, J.Shoenbohm and D.Dayles, *J. Compt. Chem.*, **22**, 545–559 (2001).

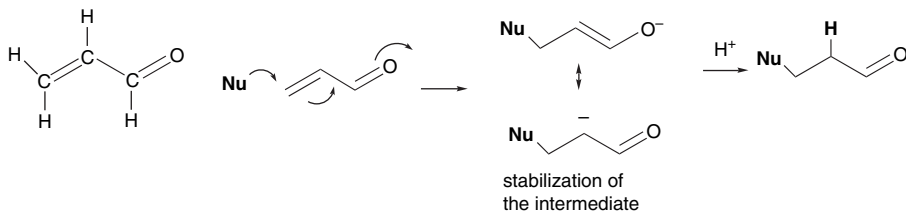
Structure **B** is a better structure than **C** because it places the negative charge on a more electronegative element, oxygen (resonance criteria 3c). Structure **D** accounts for the polarity of the C=O bond. The real molecular structure should then reflect the character of **A** > **B** ~ **D** > **C** ~ **E**. The composite structure can be qualitatively depicted by indicating weak partial bonding between C(1) and C(2) and partial positive charges at C(1) and C(3).



The electronic distributions for butadiene and propenal have been calculated using molecular orbital methods and are shown below.³¹ Butadiene shows significantly greater negative charge at the terminal carbons. In propenal there is a large charge distortion at the carbonyl group and a decrease in the electron density at the terminal carbon C(3).

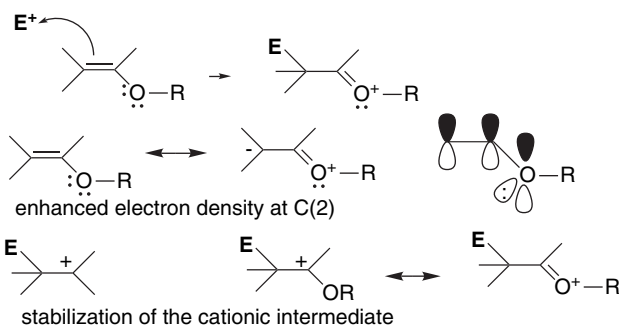


The chemical reactivity of propenal is representative of α, β -unsaturated carbonyl compounds. The conjugation between a carbon-carbon double bond and a carbonyl group leads to characteristic reactivity, which includes reduced reactivity of the carbon-carbon double bond toward electrophiles and enhanced susceptibility to the addition of nucleophilic reagents at the β carbon. The anion formed by addition is a delocalized enolate, with the negative charge shared by oxygen and carbon. The topic of nucleophilic addition to enals and enones is considered further in Section 2.6, Part B.



Methoxyethene (methyl vinyl ether) is the prototype of another important class of compounds, the *vinyl ethers*, which have an alkoxy substituent attached directly to a double bond. Such compounds have important applications in synthesis, and the characteristic reactivity is toward electrophilic attack at the β -carbon.

³¹ M. A. McAllister and T. T. Tidwell, *J. Org. Chem.*, **59**, 4506 (1994).



Why does an alkoxy group enhance reactivity and direct the electrophile to the β position? A resonance structure can be drawn that shows an oxygen unshared pair in conjugation with the double bond. More importantly, the same conjugation strongly stabilizes the cation formed by electrophilic attack. This conjugation provides an additional covalent bond in the intermediate and is strongly stabilizing (resonance criterion 3a). Taking the ethyl cation for comparison, there is a stabilization of nearly 30 kcal, according to PM3 MO semiempirical computations (see Section 1.2.2).³² Stabilization relative to the methyl cation is as follows:

CH_3^+	CH_3CH_2^+	$\text{CH}_3\text{CH}=\text{O}^+\text{R}$	$\text{CH}_3\text{CH}=\text{N}^+\text{H}_2$
0	29.0 kcal/mol	57.6 kcal/mol	80.2 kcal/mol

Vinyl amines (also called enamines) are even more reactive than vinyl ethers toward electrophiles. The qualitative nature of the conjugation is the same as in vinyl ethers, both for the neutral vinyl amine and for the cationic intermediate. However, nitrogen is an even better electron donor than oxygen, so the stabilizing effect is stronger. The stabilization for the cation is calculated to be around 80 kcal/mol relative to the methyl cation.

These molecules, propenal, methoxyethene, and etheneamine, show how we can apply VB theory and resonance to questions of reactivity. We looked at how structure and conjugation affect *electron density* and *bond formation* in both the reactant and the intermediate. When VB theory indicates that the particular disposition of function groups will change the electron distribution relative to an unsubstituted molecule, we can expect to see those differences reflected in altered reactivity. For propenal, the *electron withdrawal* by the formyl group causes decreased reactivity toward electrophiles and increased reactivity toward nucleophiles. For methoxyethene and etheneamine, the *electron release* of the substituents is reflected by increased reactivity toward electrophiles with strong *selectivity* for the β -carbon.

1.1.8. Hyperconjugation

All the examples of resonance cited in the previous section dealt with conjugation through π bonds. VB theory also incorporates the concept of hyperconjugation, which is the idea that there can be electronic interactions between σ and σ^* bonds and between σ and π^* bonds. In alkenes such as propene or 2-methylpropene, the electron-releasing effect of the methyl substituents can be represented by hyperconjugated

³² A. M. El-Nahas and T. Clark, *J. Org. Chem.*, **60**, 8023 (1995).

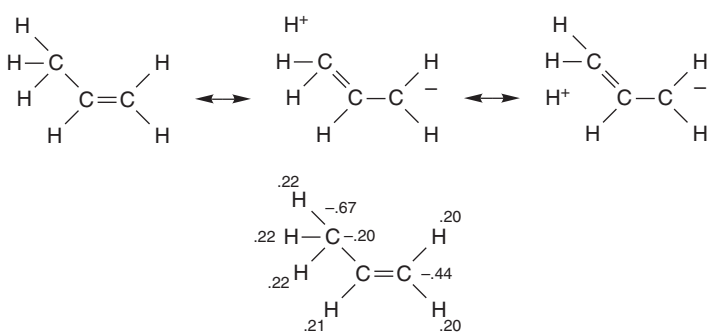
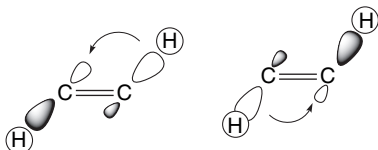


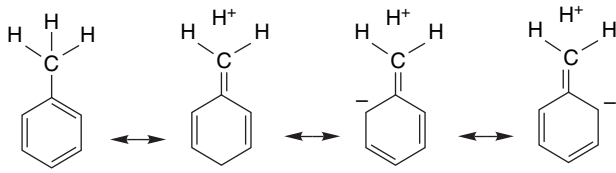
Fig. 1.6. Electron density distribution for propene.

(no-bond) resonance structures. The implication of these resonance structures is that some electron density is transferred from the C–H σ bond to the empty π^* orbital. This is in accord with the calculated electron density distribution for propene shown in Figure 1.6. Carbon-1, which is negatively charged in the resonance structure, has a higher electron density than carbon-2, even though the latter carries the methyl substituent.

There is also hyperconjugation *across* the double bond. Indeed, this interaction may be even stronger because the double bond is shorter than a corresponding single bond, permitting better orbital overlap.³³ Because these resonance structures show equivalent compensating charge transfer, there is no net charge separation, but structural features, such as bond length, and spectroscopic properties are affected.



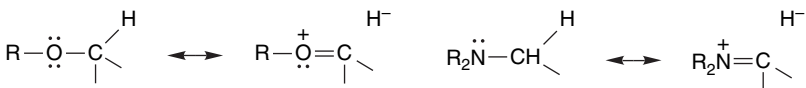
Hyperconjugation also can describe the electron-releasing effect of alkyl groups on aromatic rings.



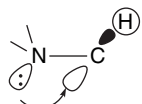
While part of the electron-releasing effect of alkyl groups toward double bonds and aromatic rings can be attributed to the electronegativity difference between sp^3 and sp^2 carbon, the fact that the β -carbon of alkenes and the *ortho* and *para* positions of aromatic rings are selectively affected indicates a resonance component.

³³ I. V. Alabugin and T. A. Zeidan, *J. Am. Chem. Soc.*, **124**, 3175 (2002).

Heteroatoms with unshared electron pairs can also interact with adjacent σ^* bonds. For example, oxygen and nitrogen substituents substantially weaken an adjacent (geminal) C–H bond.



This interaction is readily apparent in spectroscopic properties of amines. The C–H bond that is antiperiplanar to a nitrogen unshared electron pair is lengthened and weakened.³⁴ Absorptions for C–H bonds that are *anti* to nitrogen nonbonded pairs are shifted in both IR and NMR spectra. The C–H vibration is at higher frequency (lower bond energy) and the ¹H signal is at higher field (increased electron density), as implied by the resonance structures. There is a *stereochemical* component in hyperconjugation. The optimal alignment is for the σ C–H bond that donates electrons to be aligned with the σ^* orbital. The heteroatom bond-weakening effect is at a maximum when the electron pair is antiperiplanar to the C–H bond, since this is the optimal alignment for the overlap of the n and σ^* orbitals (see Topic 1.2 for further discussion).



Population of σ^* orbital
weakens anti C–H bond

1.1.9. Covalent and van der Waals Radii of Atoms

Covalent and van der Waals radii are other fundamental properties of atoms in molecules that are influenced by nuclear charge and electron distribution. A glance at a molecular model or graphic suggests that most atoms have several different dimensions. There is the distance between each bound atom and also a dimension in any direction in which the atom is not bonded to another atom. The former distance, divided between the two bonded atoms, is called the *covalent radius*. The nonbonded dimension of an atom or group in a molecule is called the *van der Waals radius*. This is the distance at which nonbonded atoms begin to experience mutual repulsion. Just short of this distance, the interatomic forces are weakly attractive and are referred to as *dispersion* or *London* forces and are attributed to mutual *polarization* of atoms.

There are several definitions and values assigned to covalent radii. Pauling created an early scale using bond lengths in simple homonuclear compounds as the starting point. An extended version of this scale is listed as “covalent” in Table 1.5. A related, but more comprehensive, approach is to examine structural data to determine covalent radii that best correlate with observed bond distances. This approach was developed by Slater.³⁵ An extensive tabulation of bond lengths derived from structural data was published in 1987.³⁶ These values are labeled “structural” in Table 1.5. A set of

³⁴ A. Pross, L. Radom, and N. V. Riggs, *J. Am. Chem. Soc.*, **102**, 2253 (1980).

³⁵ J. C. Slater, *J. Chem. Phys.*, **39**, 3199 (1964); J. C. Slater, *Quantum Theory of Molecules and Solids*, McGraw-Hill, New York, 1965, Vol. 2.

³⁶ F. H. Allen, O. Kennard, D. G. Watson, L. Brammer, A. G. Opron and R. Taylor, *J. Chem. Soc., Perkin Trans. 2*, Supplement S1–S19 (1987).

Table 1.5. Covalent Radii in Å

	Covalent ^a	Structural ^b	Alcock ^c	Carbon ^d	SECTION 1.1
H	0.37	0.25	0.30	0.327	<i>Description of Molecular Structure Using Valence Bond Concepts</i>
Li	1.34	1.45		1.219	
Be	0.90	1.05	1.06	0.911	
B	0.82	0.85	0.83	0.793	
C (<i>sp</i> ³)	0.77	0.70	0.77	0.766	
C (<i>sp</i> ²)	0.67				
C (<i>sp</i>)	0.60				
N	0.75	0.65	0.70	0.699	
O	0.73	0.60	0.66	0.658	
F	0.71	0.50	0.62	0.633	
Al	1.18	1.25	1.18	1.199	
Si	1.11	1.10	1.09	1.123	
P	1.06	1.00	1.09	1.110	
S	1.02	1.00	1.05	1.071	
Cl	0.99	1.00	1.02	1.039	
Se	1.19	1.15	1.20	1.201	
Br	1.14	1.15	1.20	1.201	
I	1.33	1.4	1.40	1.397	

a. L. E. Sutton, ed., *Tables of Interatomic Distances and Configuration in Molecules and Ions*, Suppl., 1956–1959, Chemical Society Special Publication No. 18, 1965.

b. J. C. Slater, *J. Chem. Phys.*, **39**, 3199 (1964).

c. N. W. Alcock, *Bonding and Structure*, Ellis Horwood, Chichester, 1990.

d. C. H. Suresh and N. Koga, *J. Phys. Chem. A*, **105**, 5940 (2001).

numbers that may be particularly appropriate for organic compounds was introduced by Alcock, who examined carbon compounds and subtracted the carbon covalent radii to obtain the covalent radii of the bound atoms.³⁷ This definition was subsequently applied to a larger number of compounds using computational bond length data.³⁸ These values are listed as “carbon” in Table 1.5. The covalent radii given for *sp*³, *sp*², and *sp* carbon are half of the corresponding C–C bond lengths of 1.55, 1.34, and 1.20 Å. Note that the covalent radii shorten somewhat going to the right in the periodic table. This trend reflects the greater nuclear charge and the harder character of the atoms on the right and is caused by the same electronic shielding effect that leads to decreased polarizability, as discussed in Section 1.1.6. Covalent radii, of course, increase going down the periodic table.

Van der Waals radii also require definition. There is no point at which an atom ends; rather the electron density simply decreases to an infinitesimal value as the distance from the nucleus increases. There are several approaches to assigning van der Waals radii. A set of numbers originally suggested by Pauling was refined and extended by Bondi.³⁹ These values were developed from nonbonded contacts in crystal structures and other experimental measures of minimum intermolecular contact. A new set of data of this type, derived from a much larger structural database, was compiled somewhat more recently.⁴⁰ The latter values were derived from a search of nearly 30,000 crystal structures. Table 1.6 gives both sets of radii.

³⁷. N. W. Alcock, *Bonding and Structure*, Ellis Horwood, Chichester, 1990.

³⁸. C. H. Suresh and N. Koga, *J. Phys. Chem. A*, **105**, 5940 (2001).

³⁹. A. Bondi, *J. Phys. Chem.*, **68**, 441 (1964).

⁴⁰. R. S. Rowland and R. Taylor, *J. Phys. Chem.*, **100**, 7384 (1996).

Table 1.6. Van der Waals Radii in Å

	Bondi ^a	Structural ^b
H	1.20	1.09
C	1.70	1.75
N	1.55	1.61
O	1.52	1.56
F	1.47	1.44
S	1.80	1.79
Cl	1.75	1.74
Br	1.85	1.85
I	1.98	2.00

a. A. Bondi, *J. Phys. Chem.*, **68**, 441 (1964).b. R. S. Rowland and R. Taylor, *J. Phys. Chem.*, **100**, 7384 (1996).

Van der Waals dimensions are especially significant in attempts to specify the “size” of molecules, for example, in computational programs that attempt to “fit” molecules into biological receptor sites. In the next chapter, we discuss the effects of van der Waals interactions on molecular shape (conformation). These effects can be quantified by various *force fields* that compute the repulsive energy that molecules experience as *nonbonded repulsion*.

1.2. Molecular Orbital Theory and Methods

Molecular orbital (MO) theory is an alternative way of describing molecular structure and electron density. The fundamental premise of MO theory is that the orbitals used to describe the molecule are not necessarily associated with particular bonds between the atoms but can encompass all the atoms of the molecule. The properties of the molecule are described by the sum of the contributions of all orbitals having electrons. There are also empty orbitals, which are usually at positive (i.e., antibonding) energies. The theoretical foundation of MO theory lies in quantum mechanics and, in particular, the Schrödinger equation, which relates the total energy of the molecule to a wave function describing the electronic configuration:

$$E = \int \psi H \psi d\tau \quad \text{when} \quad \int \psi^2 d\tau = 1 \quad (1.11)$$

where H is a Hamiltonian operator.

The individual MOs are described as linear combinations of the atomic orbitals $\{\varphi_x\}$ (LCAO):

$$\psi_p = c_{1p}\varphi_1 + c_{2p}\varphi_2 + c_{3p}\varphi_3 \dots c_{np}\varphi_n \quad (1.12)$$

The atomic orbitals that are used constitute the *basis set* and a minimum basis set for compounds of second-row elements is made up of the $2s$, $2p_x$, $2p_y$, and $2p_z$ orbitals of each atom, along with the $1s$ orbitals of the hydrogen atoms. In MO calculations, an initial molecular structure and a set of approximate MOs are chosen and the molecular energy is calculated. Iterative cycles of calculation of a self-consistent electrical field (SCF) and geometry optimization are then repeated until a minimization

SECTION 1.2

Molecular Orbital Theory and Methods

of total energy is reached. It is not possible to carry out these calculations exactly, so various approximations are made and/or parameters introduced. Particular sets of approximations and parameters characterize the various MO methods. We discuss some of these methods shortly.

The output of an MO calculation includes atomic positions and the fractional contribution of each basis set orbital to each MO, that is, the values of c_{kp} . The energy of each MO is calculated, and the total binding energy of the molecule is the sum of the binding energies of the filled MOs:

$$E = \sum f_{ii} + h_{ii} \quad (1.13)$$

The electronic charge at any particular atom can be calculated by the equation

$$q_r = \sum n_j c_{jr}^2 \quad (1.14)$$

where c_{jr} is the contribution of the atom to each occupied orbital. Thus, MO calculations give us information about molecular structure (from the nuclear positions), energy (from the total binding energy), and electron density (from the atomic populations).

The extent of approximation and parameterization varies with the different MO methods. As computer power has expanded, it has become possible to do MO calculations on larger molecules and with larger basis sets and fewer approximations and parameters. The accuracy with which calculations can predict structure, energy, and electron density has improved as better means of dealing with the various approximations have been developed. In the succeeding sections, we discuss three kinds of MO calculations: (1) the Hückel MO method, (2) semiempirical methods, and (3) ab initio methods, and give examples of the application of each of these approaches.

1.2.1. The Hückel MO Method

The Hückel MO (HMO) method was very important in introducing the concepts of MO theory into organic chemistry. The range of molecules that the method can treat is quite limited and the approximations are severe, but it does provide insight into a number of issues concerning structure and reactivity. Furthermore, the mathematical formulation is simple enough that it can be used to illustrate the nature of the calculations. The HMO method is restricted to planar conjugated systems such as polyenes and aromatic compounds. The primary simplification is that only the $2p_z$ orbitals are included in the construction of the HMOs. The justification is that many of the properties of conjugated molecules are governed by the π orbitals that arise from the p_z atomic orbitals. A further approximation of the HMO calculations is that only adjacent p_z orbitals interact. This allows construction of mathematical formulations for the π MOs for such systems as linear and branched-chain polyenes, cyclic polyenes, and fused-ring polyenes. For conjugated linear polyenes such as 1,3,5-hexatriene, the energy levels are given by the equation

$$E = \alpha + m_j \beta \quad (1.15)$$

where $m_j = 2 \cos(j\pi/n + 1)$ for $j = 1, 2, 3, \dots, n$, with n being the number of carbon atoms in the conjugated polyene.

The quantity α is called the *Coulomb integral*; it represents the binding of an electron in a $2p_z$ orbital and is considered to be constant for all sp^2 carbon atoms. The

quantity β is called the *resonance integral* and represents the energy of an electron distributed over two or more overlapping $2p_z$ orbitals. For linear polyenes, this equation generates a set of HMOs distributed symmetrically relative to the energy α associated with an isolated $2p_z$ orbital. The contribution of each atomic orbital to each HMO is described by a coefficient:

$$C_{rj} = \left(\frac{2}{n+1} \right)^{1/2} \sin \left(\frac{rj\pi}{n+1} \right) \quad (1.16)$$

Figure 1.7 gives the resulting HMOs for $n = 2$ to $n = 7$. Table 1.7 gives the coefficients for the HMOs of 1,3,5-hexatriene. From these coefficients, the overall shape of the orbitals can be deduced and, in particular, the location of nodes is determined. Nodes represent an antibonding contribution to the total energy of a particular orbital. Orbitals with more nodes than bonding interactions are *antibonding* and are above the reference α energy level. The spacing between orbitals decreases with the length of the polyene chain, and as a result, the gap between the HOMO and LUMO decreases as the conjugated chain lengthens.

These coefficients give rise to the pictorial representation of the 1,3,5-hexatriene molecular orbitals shown in Figure 1.8. Note in particular the increase in the energy of the orbital as the number of nodes goes from 0 to 5. The magnitude of each atomic coefficient indicates the relative contribution at that atom to the MO. In ψ_1 , for example, the central atoms C(3) and C(4) have larger coefficients than the terminal atoms C(1) and C(6), whereas for ψ_3 the terminal carbons have the largest coefficients.

The equation for the HMOs of completely conjugated monocyclic polyenes is

$$E = \alpha + m_j \beta \quad (1.17)$$

where $m_j = 2 \cos(2j\pi/n)$ for $j = 0, \pm 1, \pm 2, \dots, (n-1)/2$ for $n = \text{odd}$ and $(n/2)$ for $n = \text{even}$. This gives rise to the HMO diagrams shown in Figure 1.9 for cyclic polyenes with $n = 3$ to $n = 7$. Table 1.8 gives the atomic coefficients for benzene, $n = 6$, and Figure 1.10 gives pictorial representations of the MOs.

There is an easy way to remember the pattern of MOs for monocyclic systems. Figure 1.11 shows Frost's circle.⁴¹ A polygon corresponding to the ring is inscribed

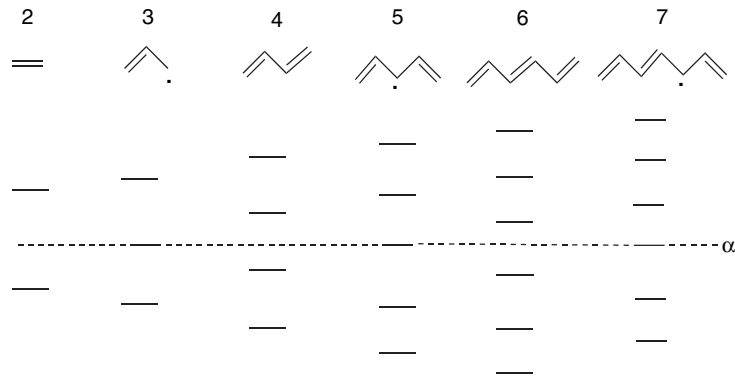


Fig. 1.7. HMO orbital diagram for polyenes $n = 2$ to $n = 7$.

⁴¹ A. A. Frost and B. Musulin, *J. Chem. Phys.*, **21**, 572 (1953).

Table 1.7. Energy Levels and Atomic Coefficients for HMOs of 1,3,5-Hexatriene

π orbital m_j	c_1	c_2	c_3	c_4	c_5	c_6	SECTION 1.2
Ψ_1	1.802	0.2319	0.4179	0.5211	0.5211	0.4179	0.2319
Ψ_2	1.247	0.4179	0.5211	0.2319	-0.2319	-0.5211	-0.4179
Ψ_3	0.445	0.5211	0.2319	-0.4179	-0.4179	0.2319	0.5211
Ψ_4	-0.445	0.5211	-0.2319	-0.4179	0.4179	0.2319	-0.5211
Ψ_5	-1.247	0.4179	-0.5211	0.2319	0.2319	-0.5211	0.4179
Ψ_6	-1.802	0.2319	-0.4179	0.5211	-0.5211	0.4179	-0.2319

in a circle with one point of the polygon at the bottom. The MO pattern corresponds to each point of contact of the polygon and circle. If the circle is given a radius of 2β , the point of contact gives the coefficient of β in the expression for the energy of the MO. Compilations of HMO energy levels and atomic coefficients are available for a number of conjugated systems.⁴²

What do we learn about molecules such as 1,3,5-hexatriene and benzene from the HMO description of the π orbitals?

1. *The frontier MOs are identified and described.* The frontier orbitals are the *highest occupied MO* (HOMO) and the *lowest unoccupied MO* (LUMO). These orbitals are intimately involved in chemical reactivity, because they are the most available to electrophiles and nucleophiles, respectively. From the atomic coefficients, which can be represented graphically, we see the symmetry and relative atomic contribution

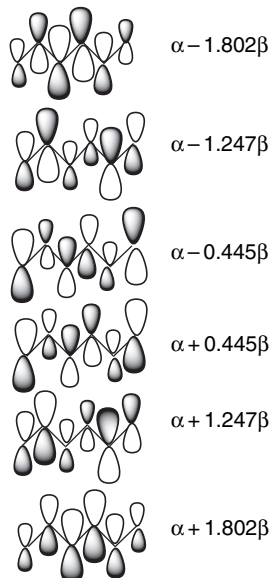


Fig. 1.8. π Molecular orbitals for 1,3,5-hexatriene.

⁴². E. Heilbronner and P. A. Straub, *Hückel Molecular Orbitals*, Springer Verlag, New York, 1966; C. A. Coulson, A. Streitwieser, Jr., and J. I. Brauman, *Dictionary of π -Electron Calculations*, W H. Freeman, San Francisco, 1965.

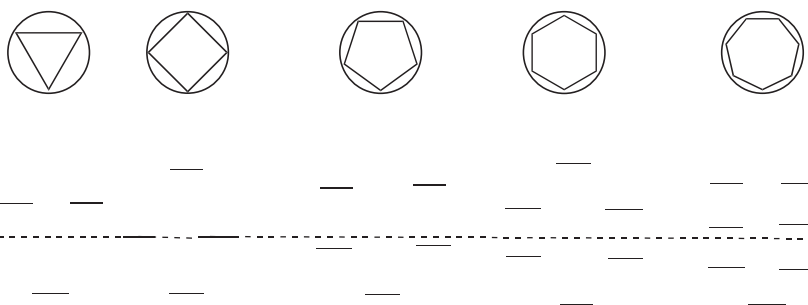


Fig. 1.9. HMO energy levels for cyclic polyene $n = 3$ to $n = 7$.

of the orbitals. Reaction is facilitated by large overlap of interacting orbitals, so we expect reactions to involve atoms with large orbital coefficients.

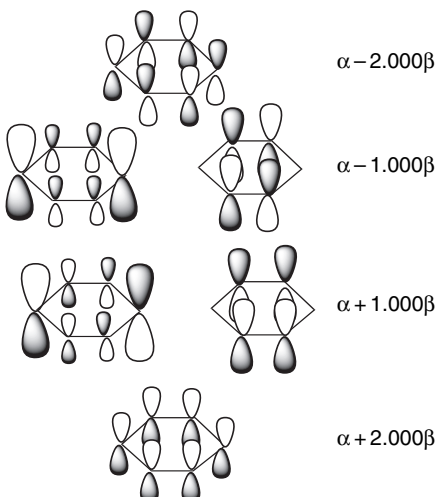
2. The HOMO-LUMO gap is approximated. Remember that for atoms, radicals, and ions, hardness and softness are defined in relation to the electron affinity (EA) and ionization potential (IP) (see Section 1.1.6). The energies of the HOMO and LUMO are indicators of the IP and EA, respectively, of the molecules. The HOMO-LUMO gap is an indicator of the reactivity of the molecules in terms of hardness or softness. The smaller the gap, the softer the molecule.

3. The overall stabilization of the molecule as the result of conjugation is estimated. Remember from the resonance concept in VB theory that conjugation is generally associated with additional stabilization (see Section 1.1.7). In HMO theory this stabilization is expressed as the difference between the energy of the conjugated system and the same number of isolated double bonds. The energy of an isolated double bond in the HMO method is equal to $2\alpha + 2\beta$, so for 1,3,5-hexatriene, a stabilization of 0.988β is computed. For benzene, the computed stabilization is 2β :

$$\begin{aligned} \text{Three isolated double bonds} &= 3(2\alpha + 2\beta) = 6\alpha + 6\beta \\ \text{Hexatriene} &= 2(\alpha + 1.802\beta) + 2(\alpha + 1.247\beta) + 2(\alpha + 0.445\beta) = 6\alpha + 6.988\beta \\ \text{Stabilization} &= (6\alpha + 6.988\beta) - (6\alpha + 6\beta) = 0.988\beta \\ \text{Benzene} &= 2(\alpha + 2\beta) + 2(\alpha + \beta) + 2(\alpha + \beta) = 6\alpha + 8\beta \\ \text{Stabilization} &= (6\alpha + 8\beta) - (6\alpha + 6\beta) = 2.0\beta \end{aligned}$$

Let us consider the significance of this stabilization, which is sometimes called the *delocalization energy* (DE). The stabilization results from the removal of the restriction that the π electrons be localized between two particular atoms. Comparison of the DE of 1,3,5-hexatriene and benzene would suggest that the triene is stabilized by almost half the extent of benzene, but *thermodynamic comparisons do*

Table 1.8. Energy Levels and Coefficients for HMOs of Benzene

Fig. 1.10. π Molecular orbitals for benzene.

not support this result (see Section 3.1.1). Relative to three ethene double bonds, 1,3,5-hexatriene is stabilized by about 8 kcal,⁴³ whereas for benzene the stabilization is around 30 kcal/mol. Furthermore, the HMO DE for polycyclic aromatic hydrocarbons such as anthracene and phenanthrene continues to increase with molecular size. This is contrary to chemical reactivity and thermodynamic data, which suggest that on a per atom basis, benzene represents the optimum in stabilization. Thus, the absolute value of the DE does not seem to be a reliable indicator of stabilization.

On the other hand, the *difference in stabilization* between acyclic and cyclic polyenes turns out to be a very useful indicator of the extra stabilization associated with cyclic systems. This extra stabilization or *aromaticity* is well represented by the difference in the DE of the cyclic compound and the polyene having the same number of conjugated double bonds.⁴⁴ For 1,3,5-hexatriene and benzene, this difference is 1.012β . For comparison of molecules of different sizes, the total stabilization energy is divided by the number of π electrons.⁴⁵ We will see in Chapter 9 that this value gives a very useful estimate of the stability of cyclic conjugated systems.

For monocyclic conjugated polyenes, high stabilization is found for systems with $(4n + 2)$ π electrons but not for systems with $(4n)$ π electrons. The relationship is formulated as *Hückel's rule*, which states that completely conjugated planar hydrocarbons are strongly stabilized (aromatic) when they have $(4n + 2)$ π electrons. Benzene (6π electrons) is aromatic but cyclobutadiene (4π electrons) and cyclooctatetraene (8π electrons) are not.

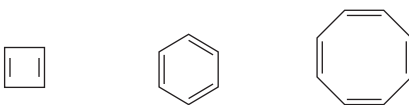


Fig. 1.11. Frost's circle mnemonic for HMOs of cyclic polyenes.

⁴³ W. Fang and D. W. Rogers, *J. Org. Chem.*, **57**, 2294 (1992).

⁴⁴ M. J. S. Dewar and C. de Llano, *J. Am. Chem. Soc.*, **91**, 789 (1969).

⁴⁵ B. A. Hess, Jr., and L. J. Schaad, Jr., *J. Am. Chem. Soc.*, **93**, 305, 2413 (1971).



Hückel's rule also pertains to charged cyclic conjugated systems. The cyclopropenyl (2 π electrons), cyclopentadienyl anion (6 π electrons), and cycloheptatrienyl (tropylium) cation (6 π electrons) are examples of stabilized systems. We say much more about the relationship between MO configuration and aromaticity in Chapter 9.



1.2.2. Semiempirical MO Methods

Beginning in the 1960s, various more elaborate MO methods were developed and applied to organic molecules. Among those that are historically significant are extended Hückel theory (EHT),⁴⁶ complete neglect of differential overlap (CNDO),⁴⁷ and modified neglect of differential overlap (MNDO).⁴⁸ In contrast to HMO theory, these methods include all the valence shell electrons in the calculation. Each of these methods incorporates various approximations and parameters. The parameters are assigned values based on maximizing the agreement for a set of small molecules. The CNDO findings were calibrated with higher-level computational results, while MNDO was calibrated to experimental stability data. These parameters are then employed for computations on more complex molecules. The output provides molecular geometry, atomic coefficients, and orbital energies. Each method had both strengths and limitations with respect to the range of molecules and properties that could be adequately described. At the present time, the leading semiempirical methods, called AM1⁴⁹ and PM3,⁵⁰ are incorporated into various MO computational programs and are widely employed in the interpretation of structure and reactivity. In Section 1.2.6, we illustrate some of the problems that can be addressed using these methods.

1.2.3. Ab Initio Methods

Ab initio computations are based on iterative calculations of a self-consistent electronic field (SCF), as is the case in the semiempirical methods just described, but do not use experimental data to calibrate quantities that appear in the calculations. These methods are much more computationally demanding than semiempirical methods, but their reliability and range of applicability has improved greatly as more powerful computers have permitted more sophisticated approaches and have enabled handling of more complex molecules. The computations are carried out by successive series of calculations minimizing the energy of the electron distribution and the molecular geometry. The cycle of the calculations is repeated until there is no further improvement (convergence).

- ⁴⁶. R. Hoffmann, *J. Chem. Phys.*, **39**, 1397 (1963).
- ⁴⁷. J. A. Pople and G. A. Segal, *J. Chem. Phys.*, **44**, 3289 (1966).
- ⁴⁸. M. J. S. Dewar and W. Thiel, *J. Am. Chem. Soc.*, **99**, 4907 (1977).
- ⁴⁹. M. J. S. Dewar, E. G. Zoebisch, E. F. Healy, and J. P. Stewart. *J. Am. Chem. Soc.*, **109**, 3902 (1985).
- ⁵⁰. J. P. Stewart, *J. Comput. Chem.*, **10**, 209, 221 (1989).

SECTION 1.2

Molecular Orbital Theory and Methods

Specific ab initio methods are characterized by the form of the wave function and the nature of the basis set functions that are used. The most common form of the wave function is the single determinant of molecular orbitals expressed as a linear combination of basis functions, as is the case with semiempirical calculations. We describe alternatives later in this section. Early calculations were often done with Slater functions, designated STO for Slater-type orbitals. Currently most computations are done with Gaussian basis functions, designated by GTOs. A fairly accurate representation of a single STO requires three or more GTOs. This is illustrated in Figure 1.12, which compares the forms for one, two, and three GTOs. At the present time most basis sets use a six-Gaussian representation, usually designated 6G. The weighting coefficients for the N components of a STO-NG representation are not changed in the course of a SCF calculation.

A basis set is a collection of basis functions. For carbon, nitrogen, and oxygen compounds, a minimum basis set is composed of a 1s function for each hydrogen and 1s, 2s, and three 2p functions for each of the second-row atoms. More extensive and flexible sets of basis functions are in wide use. These basis sets may have two or more components in the outer shell, which are called *split-valence* sets. Basis sets may include *p* functions on hydrogen and/or *d* and *f* functions on the other atoms. These are called *polarization functions*. The basis sets may also include *diffuse functions*, which extend farther from the nuclear center. Split-valence bases allow description of tighter or looser electron distributions on atoms in differing environments. Polarization permits changes in orbital shapes and shifts in the center of charge. Diffuse functions allow improved description of the outer reaches of the electron distribution.

Pople developed a system of abbreviations that indicates the composition of the basis sets used in ab initio calculations. The series of digits that follows the designation 3G or 6G indicates the number of Gaussian functions used for each successive shell. The combination of Gaussian functions serves to improve the relationship between electron distribution and distance from the nucleus. Polarization functions incorporate additional orbitals, such as *p* for hydrogen and *d* and/or *f* for second-row atoms. This permits changes in orbital shapes and separation of the centers of charge. The inclusion of *d* and *f* orbitals is indicated by the asterisk (*). One asterisk signifies *d* orbitals on second-row elements; two asterisks means that *p* orbitals on hydrogen are also included. If diffuse orbitals are used they are designated by a plus sign (+), and the

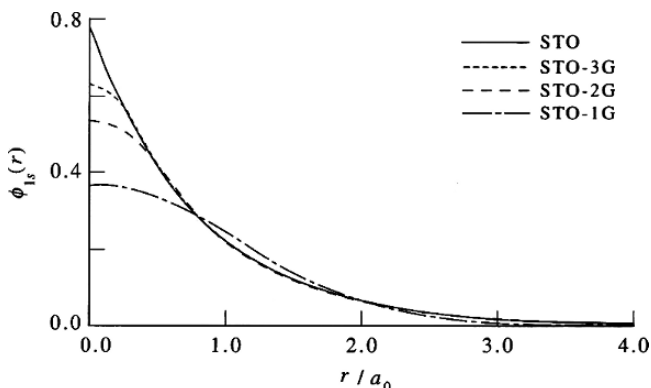


Fig. 1.12. Comparison of electron distribution for STO, G, 2G, and 3G expressions of orbitals.

designation double plus (++) means that diffuse orbitals are present on both hydrogen and the second-row elements. Split-valence sets are indicated by a sequence defining the number of Gaussians in each component. Split-valence orbitals are designated by primes, so that a system of three Gaussian orbitals would be designated by single, double, and triple primes ('', "", and ""). For example 6-311 + G(*d, p*) conveys the following information:

- 6: Core basis functions are represented as a single STO-6G expression.
- 311: The valence set is described by three sets of STO-NG functions; each set includes an *s* orbital and three *p* orbitals. In the 6-311+G(*d*) basis there are three such sets. One is composed of three Gaussians (STO-3G expression of one *s*-type and three *p*-type forms) and the other two are represented by a single Gaussian (STO-1G) representation of the *s-p* manifold. The collection of components of the split-valence representation can be designated by a series of primes.
- +: A STO-1G diffuse *s-p* manifold is included in the basis set for each nonhydrogen atom; ++ implies that diffuse functions are also included for the hydrogen atoms.
- *p*: A set of *p* functions placed on each nonhydrogen atom and specifies the composition.
- *d*: A set of STO-1G *d*-functions is placed on each nonhydrogen atom for which *d* functions are not used in the ground state configuration. If *d* functions are so used, polarization is effected by a manifold of *f* functions.

The composition of several basis sets is given in Table 1.9.

An important distinguishing feature among ab initio calculations is the extent to which they deal with *electron correlation*. Correlation is defined as the difference between the exact energy of a molecular system and the best energy obtainable by a SCF calculation in which the wave function is represented by a single determinant. In single-determinant calculations, we consider that each electron experiences an averaged electrostatic repulsion defined by the total charge distribution, a *mean field* approximation. These are called *Hartree-Fock* (HF) calculations. Correlation corrections arise from fluctuations of the charge distribution. Correlation energies can be estimated by including effects of admixtures of excited states into the Hartree-Fock determinant.

Table 1.9. Abbreviations Describing Gaussian Basis Sets^a

Designation	H	C	Functions on second-row atoms
3-21G	2	9	1s'; 2s', 3 2p'; 2s'', 3 2p''
3-21+G	2	13	1s'; 2s', 3 2p'; 2s'', 3 2p''; 2s+, 3 2p+
6-31G* or 6-31G(<i>d</i>)	2	15	1s; 2s', 3 2p'; 2s'', 3 2p''; 5 3d
6-31G** or 6-31(<i>d,p</i>)	5	18	1s; 2s', 3 2p'; 2s'', 3 2p''; 2s'''; 3 2p'''
6-31+G* or 6-31+(<i>d</i>)	3	19	1s; 2s', 3 2p'; 2s'', 3 2p''; 5 3d; 2s+, 3 2p+
6-311G** or 6-311(<i>d,p</i>)	6	18	1s; 2s', 3 2p'; 2s'', 3 2p''; 2s'''
6-311G(<i>df,p</i>)	6	25	1s; 2s', 3 2p'; 2s'', 3 2p'; 2s'''
6-311G(3df,3pd)	17	35	1s; 2s', 3 2p'; 2s'', 3 2p''; 2s'''

a. From E. Lewars, *Computational Chemistry*, Kluwer Academic Publishers, Boston, 2003, pp. 225–229.

This may be accomplished by perturbation methods such as *Moeller-Plesset* (MP)⁵¹ or by including excited state determinants in the wave equation as in *configurational interaction* (CISD)⁵² calculations. The excited states have electrons in different orbitals and reduced electron-electron repulsions.

The output of ab initio calculations is analogous to that from HMO and semiempirical methods. The atomic coordinates at the minimum energy are computed. The individual MOs are assigned energies and atomic orbital contributions. The total molecular energy is calculated by summation over the occupied orbitals. Several schemes for apportioning charge among atoms are also available in these programs. These methods are discussed in Section 1.4. In Section 1.2.6, we illustrate some of the applications of ab initio calculations. In the material in the remainder of the book, we frequently include the results of computational studies, generally indicating the type of calculation that is used. The convention is to list the treatment of correlation, e.g., HF, MP2, CISDT, followed by the basis set used. Many studies do calculations at several levels. For example, geometry can be minimized with one basis set and then energy computed with a more demanding correlation calculation or basis set. This is indicated by giving the basis set used for the energy calculation followed by parallel lines (//) and the basis set used for the geometry calculation. In general, we give the designation of the computation used for the energy calculation. The information in Scheme 1.3 provides basic information about the nature of the calculation and describes the characteristics of some of the most frequently used methods.

1.2.4. Pictorial Representation of MOs for Molecules

The VB description of molecules provides very useful generalizations about molecular structure and properties. Approximate molecular geometry arises from hybridization concepts, and qualitative information about electron distribution can be deduced by applying the concepts of polarity and resonance. In this section we consider how we can arrive at similar impressions about molecules by using the underlying principles of MO theory in a qualitative way. To begin, it is important to remember some fundamental relationships of quantum mechanics that are incorporated into MO theory. The *Aufbau principle* and the *Pauli exclusion principle*, tell us that electrons occupy the MOs of lowest energy and that any MO can have only two electrons, one of each spin. The MOs must also conform to molecular symmetry. Any element of symmetry that is present in a molecule must also be present in *all the corresponding MOs*. Each MO must be either *symmetric* or *antisymmetric* with respect to each element of molecular symmetry. To illustrate, the π MOs of *s-cis*-1,3-butadiene in Figure 1.13 can be classified with respect to the plane of symmetry that dissects the molecule between C(2) and C(3). The symmetric orbitals are identical (exact reflections) with respect to this plane, whereas the antisymmetric orbitals are identical in shape but

⁵¹. W. J. Hehre, L. Radom, P. v. R. Schleyer, and J. A. Pople, *Ab Initio Molecular Orbital Theory*, Wiley-Interscience, New York, 1986, pp. 38–40; A. Bondi, *J. Phys. Chem.*, **68**, 441 (1964); R. S. Rowland and R. Taylor, *J. Phys. Chem.*, **100**, 7384 (1996); M. J. S. Dewar and C. de Llano, *J. Am. Chem. Soc.*, **91**, 789 (1969); R. Hoffmann, *J. Chem. Phys.*, **39**, 1397 (1963); J. A. Pople and G. A. Segal, *J. Chem. Phys.*, **44**, 3289 (1966); M. J. S. Dewar and W. Thiel, *J. Am. Chem. Soc.*, **99**, 4907 (1977); M. J. S. Dewar, E. G. Zoebisch, E. F. Healy, and J. P. Stewart, *J. Am. Chem. Soc.*, **109**, 3902 (1985); J. P. Stewart, *J. Comput. Chem.*, **10**, 209, 221 (1989); J. A. Pople, M. Head-Gordon, and K. Raghavachari, *J. Phys. Chem.*, **87**, 5968 (1987).

⁵². J. A. Pople, M. Head-Gordon, and K. Raghavachari, *J. Phys. Chem.*, **87**, 5968 (1987).

Scheme 1.3. Characteristics of ab Initio MO Methods

STO-3G. STO-3G is a minimum basis set consisting of 1s orbitals for hydrogen and 2s and 2p orbitals for second-row elements, described by Gaussian functions.

Split-Valence Gaussian Orbitals. (3-21G, 4-31G, 6-31G) Split-valence orbitals are described by two or more Gaussian functions. Also in this category are Dunning-Huzinaga orbitals.

Polarized Orbitals. These basis sets add further orbitals, such as p for hydrogen and d for carbon that allow for change of shape and separation of centers of charge. Numbers in front of the d, f designations indicate inclusion of multiple orbitals of each type. For example, 6-311(2df, 2pd) orbitals have two d functions and one f function on second-row elements and two p functions and one d function on hydrogen.

Diffuse Basis Sets. (6-31+G*, 6-31++G*) Diffuse basis sets include expanded orbitals that are used for molecules with relatively loosely bound electrons, such as anions and excited states. 6-31+G* have diffuse p orbitals on second-row elements. 6-31++G* orbitals have diffuse orbitals on both second-row elements and hydrogen.

Correlation Calculations

MP2, MP4. MP (Moeller-Plesset) calculations treat correlation by a perturbation method based on adding excited state character. MP2 includes a contribution from the interaction of doubly excited states with the ground state. MP4 includes, single, double, and quadruple excited states in the calculation.

CISD. CISD (configuration interaction, single double) are LCAO expressions that treat configuration interactions by including one or two excited states. The designations CISDT and CISDTQ expand this to three and four excitations, respectively.

CAS-SCF. CAS-SCF (complete active space self-consistent field) calculations select the chemically most significant electrons and orbitals and apply configuration interactions to this set.

Composite Calculations

G1, G2, G2(MP2), and G3 are composite computations using the 6-311G** basis set and MP2/6-31G* geometry optimization. The protocols are designed for efficient calculation of energies and electronic properties. The G2 method calculates electron correlation at the MP4 level, while G2(MP2) correlation calculations are at the MP2 level. A scaling factor derived from a series of calibration molecules is applied to energies.

CBS. CBS protocols include CBS-4, CBS-Q, and CBS-APNO. The objectives are the same as for G1 and G2. The final energy calculation (for CBS-Q) is at the MP4(SQD)/6-31G(d, p) level, with a correction for higher-order correlation. A scaling factor is applied for energy calculations.

References to Scheme 1.3

STO-3G: W. J. Hehre, R. F. Stewart, and J. A. Pople, *J. Phys. Chem.*, **51**, 2657 (1969).

3-21G, 4-21G, and 6-31G: R. Ditchfield, W. J. Hehre, and J. A. Pople, *J. Chem. Phys.*, **54**, 724 (1971); W. J. Hehre and W. A. Lathan, *J. Chem. Phys.*, **56**, 5255 (1972); W. J. Hehre, R. Ditchfield, and J. A. Pople, *J. Chem. Phys.*, **56**, 2257 (1972); M. M. Franci, W. J. Pietro, W. J. Hehre, J. S. Binkley, M. S. Gordon, D. J. DeFrees, and J. A. Pople, *J. Chem. Phys.*, **77**, 3654 (1982).

Dunning-Huzinaga Orbitals: T. H. Dunning, Jr., and P. J. Hay, in *Modern Theoretical Chemistry*, Vol. 3, H. F. Schaefer, ed., Plenum Publishing, New York, 1977, pp 1–27.

MP: J. S. Binkley and J. A. Pople, *Int. J. Quantum Chem.*, **9**, 229 (1975).

G1, G2, G3: J. A. Pople, M. Head-Gordon, D. J. Fox, K. Raghavachari, and L. A. Curtiss, *J. Chem. Phys.*, **90**, 5622 (1989); L. A. Curtiss, C. Jones, G. W. Trucks, K. Raghavachari, and J. A. Pople, *J. Chem. Phys.*, **93**, 2537 (1990); L. A. Curtiss, K. Raghavachari, G. W. Trucks, and J. A. Pople, *J. Chem. Phys.*, **94**, 7221 (1991); L. A. Curtiss, K. Raghavachari, and J. A. Pople, *J. Chem. Phys.*, **98**, 1293 (1993); M. Head-Gordon, *J. Chem. Phys.*, **100**, 13213 (1996); L. A. Curtiss and K. Raghavachari, *Theor. Chem. Acc.*, **108**, 61 (2002).

CBS-Q: J. W. Ochterski, G. A. Petersson, and J. A. Montgomery, *J. Chem. Phys.*, **104**, 2598 (1996); G. A. Petersson, *Computational Thermochemistry*, ACS Symposium Series, Vol. 677, pp 237–266 (1998).

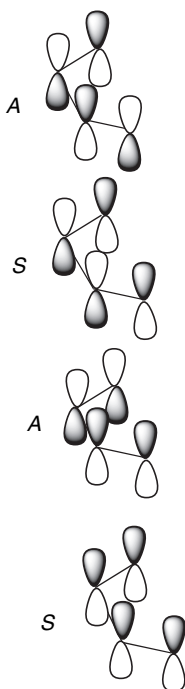


Fig. 1.13. Symmetry characteristics of butadiene HMOs with respect to a plane bisecting the molecule in the *s-cis* conformation perpendicular to the plane of the molecule.

change phase at all locations. Although these formal symmetry restrictions can ignore nonconjugated substituents, the symmetry pattern of the MOs must conform to the symmetry of the conjugated system.

What do the MOs of other small molecules look like? Let us consider methane. A convenient frame of reference is a cube with the four hydrogens at alternate corners and the carbon at the center. This orientation of the molecule reveals that methane possesses three twofold symmetry axes, one each along the x , y , and z axes. There are also planes of symmetry diagonally across the cube. Because of this molecular symmetry, the MOs of methane must possess symmetry with respect of these same axes. There are two possibilities: the orbital may be unchanged by 180° rotation about the axis (symmetric), or it may be transformed into an orbital of identical shape but opposite phase by the symmetry operation (antisymmetric). The minimum basis set orbitals are the hydrogen $1s$ and the carbon $2s$, $2p_x$, $2p_y$, and $2p_z$ atomic orbitals. The combinations that are either symmetric or antisymmetric with respect to the diagonal planes of symmetry are shown in Figure 1.14. These give rise to four bonding MOs. One has no nodes and bonds between all the atoms. The other three consist of two boomerang-shaped lobes, with a node at carbon corresponding to the node in the basis set p orbital.

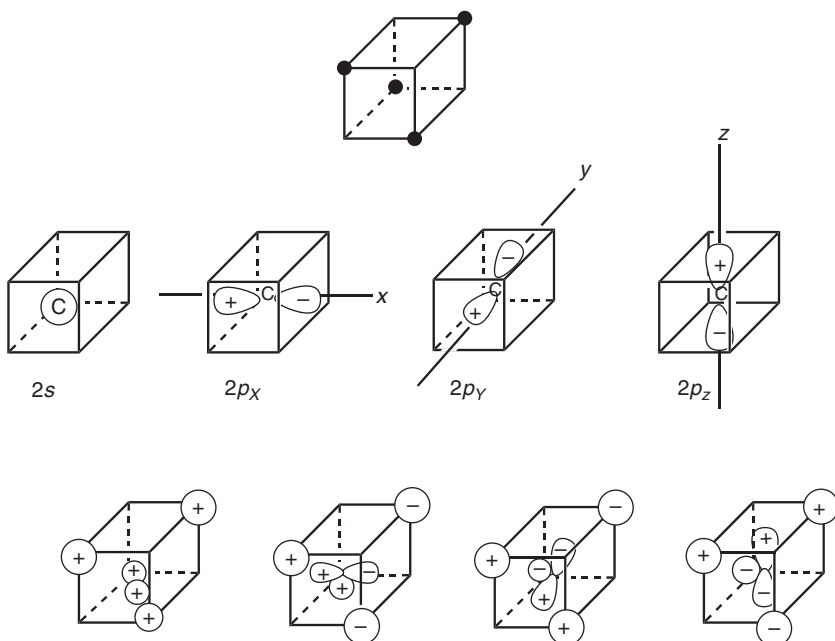


Fig. 1.14. Combinations of atomic orbitals leading to the methane molecular orbitals.

The carbon $2s$ orbital is symmetric with respect to each axis but the three $2p$ orbitals are each antisymmetric to two of the axes and symmetric with respect to one. The combinations that give rise to molecular orbitals that meet these symmetry requirements are shown in the lower part of Figure 1.14. The bonding combination of the carbon $2s$ orbital with the four $1s$ hydrogen orbitals leads to a molecular orbital that encompasses the entire molecule and has no nodes. Each of the MOs derived from a carbon $2p$ orbital has a node at carbon. The three combinations are equivalent, but higher in energy than the MO with no nodes. The four antibonding orbitals arise from similar combinations, but with the carbon and hydrogen orbitals having opposite phases in the region of overlap. Thus the molecular orbital diagram arising from these considerations shows one bonding MO with no nodes and three degenerate (having the same energy) MOs with one node. The diagram is given in Figure 1.15.

There is experimental support for this MO pattern. The ESCA spectrum of methane is illustrated in Figure 1.16. It shows two peaks for valence electrons at 12.7 and 23.0 eV, in addition to the band for the core electron at 291.0 eV.⁵³ Each band

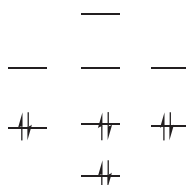


Fig. 1.15. Molecular orbital diagram for methane.

⁵³ U. Gelius, in *Electron Spectroscopy*, D. A. Shirley, ed., American Elsevier, New York, 1972, pp. 311–344.

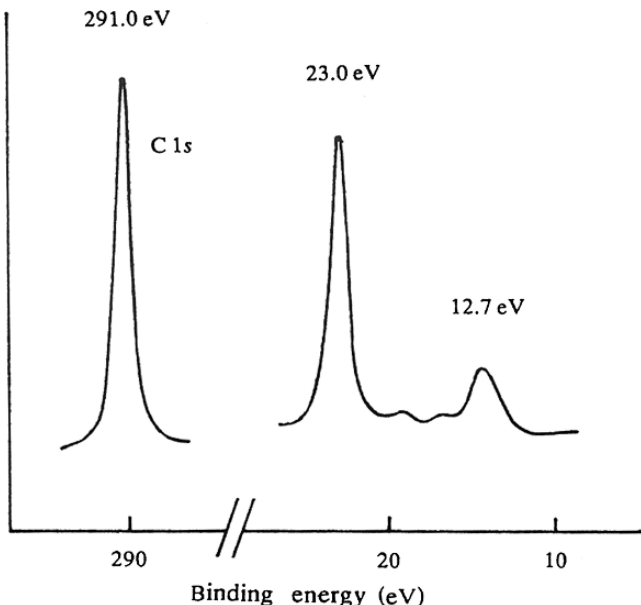
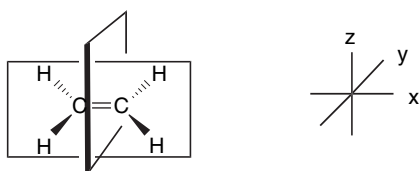


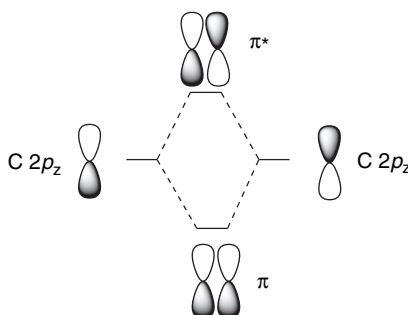
Fig. 1.16. ESCA spectrum of methane.

corresponds to the binding energy for the removal of a particular electron, not the successive removal of one, two, and three electrons. The presence of two bands in the valence region is consistent with the existence of two different molecular orbitals in methane.

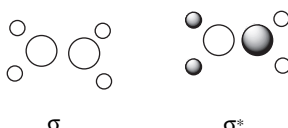
The construction of the MOs of ethene is similar to the process used for methane, but the total number of atomic orbitals is greater: twelve instead of eight. We must first define the symmetry of ethene, which is known from experiment to be a planar molecule.



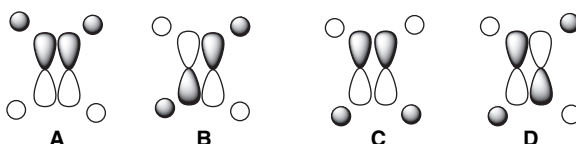
This geometry possesses three important elements of symmetry, the molecular plane and two planes that bisect the molecule. All MOs must be either symmetric or antisymmetric with respect to each of these symmetry planes. With the axes defined as in the diagram above, the orbitals arising from carbon $2p_z$ have a node in the molecular plane. These are the π and π^* orbitals. Because the two p_z atomic orbitals are perpendicular (orthogonal) to all the other atomic orbitals and the other orbitals lie in the nodal plane of the p_z orbitals, there is no interaction of the p_z with the other C and H atomic orbitals. The π orbital is symmetric with respect to both the $x-z$ plane and the $y-z$ plane. It is antisymmetric with respect to the molecular ($x-y$) plane. On the other hand, π^* is antisymmetric with respect to the $y-z$ plane.



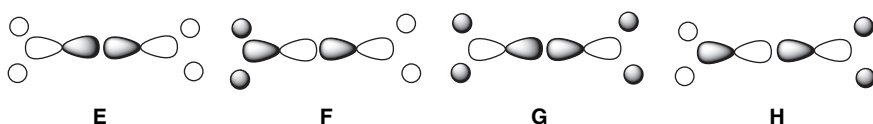
The orbitals that remain are the four hydrogen 1s, two carbon 1s, and four carbon 2p orbitals. All lie in the molecular plane. The combinations using the carbon 2s and hydrogen 1s orbitals can take only two forms that meet the molecular symmetry requirements. One, σ , is bonding between all atoms, whereas σ^* is antibonding between all nearest-neighbor atoms. No other combination corresponds to the symmetry of the ethene molecule.



Let us next consider the interaction of $2p_y$ with the four hydrogen 1s orbitals. There are four possibilities that conform to the molecular symmetry.



Orbital **A** is bonding between all nearest-neighbor atoms, whereas **B** is bonding within the CH_2 units but antibonding with respect to the two carbons. The orbital labeled **C** is C–C bonding but antibonding with respect to the hydrogens. Finally, orbital **D** is antibonding with respect to all nearest-neighbor atoms. Similarly, the $2p_x$ orbitals must be considered. Again, four possible combinations arise. Note that the nature of the overlap of the $2p_x$ orbitals is different from the $2p_y$ case, so the two sets of MOs have different energies.



The final problem in construction of a qualitative MO diagram for ethene is the relative placement of the orbitals. There are some useful guidelines. The relationship between the relative energy and the number of nodes has already been mentioned. The more nodes, the higher the energy of the orbital. Since π -type interactions are normally weaker than σ -type, we expect the separation between σ and σ^* to be greater than between π and π^* . Within the sets

ABCD and **EFGH** we can order **A** < **B** < **C** < **D** and **E** < **F** < **G** < **H** on the basis that C–H bonding interactions outweigh C–C antibonding interactions arising from weaker *p*-*p* overlaps. Placement of the set **ABCD** in relation to **EFGH** is not qualitatively obvious. Calculations give the results shown in Figure 1.17.⁵⁴ Pictorial representations of the orbitals are given in Figure 1.18.

The kinds of qualitative considerations that we used to construct the ethene MO diagram do not give any indication of how much each atomic orbital contributes to the individual MOs. This information is obtained from the coefficients provided by the MO calculation. Without these coefficients we cannot specify the shapes of the MOs very precisely. However, the qualitative ideas do permit conclusions about the *symmetry* of the orbitals. As will be seen in Chapter 10, just knowing the symmetry of the MOs provides very useful insight into many chemical reactions.

1.2.5. Qualitative Application of MO Theory to Reactivity: Perturbational MO Theory and Frontier Orbitals

The construction of MO diagrams under the guidance of the general principles and symmetry restrictions that we have outlined can lead to useful insights into molecular structure. Now we want to consider how these concepts can be related to reactivity. In valence bond terminology, structure is related to reactivity in terms of the electronic nature of the substituents. The impact of polar and resonance effects on the electron

<i>D</i>	—	0.892
σ^*	—	0.845
<i>H</i>	—	0.640
<i>G</i>	—	0.621
<i>C</i>	—	0.587
π^*	—	0.243
π	—	-0.371
<i>B</i>	—	-0.506
<i>F</i>	—	-0.562
<i>A</i>	—	-0.644
<i>E</i>	—	-0.782
σ	—	-1.01

Fig. 1.17. Ethene molecular orbital energy levels. Energies are in atomic units. From W. L. Jorgensen and L. Salem, *The Organic Chemists Book of Orbitals*, Academic Press, New York, 1973.

⁵⁴ W. L. Jorgensen and L. Salem, *The Organic Chemist's Book of Orbitals*, Academic Press, New York, 1973.

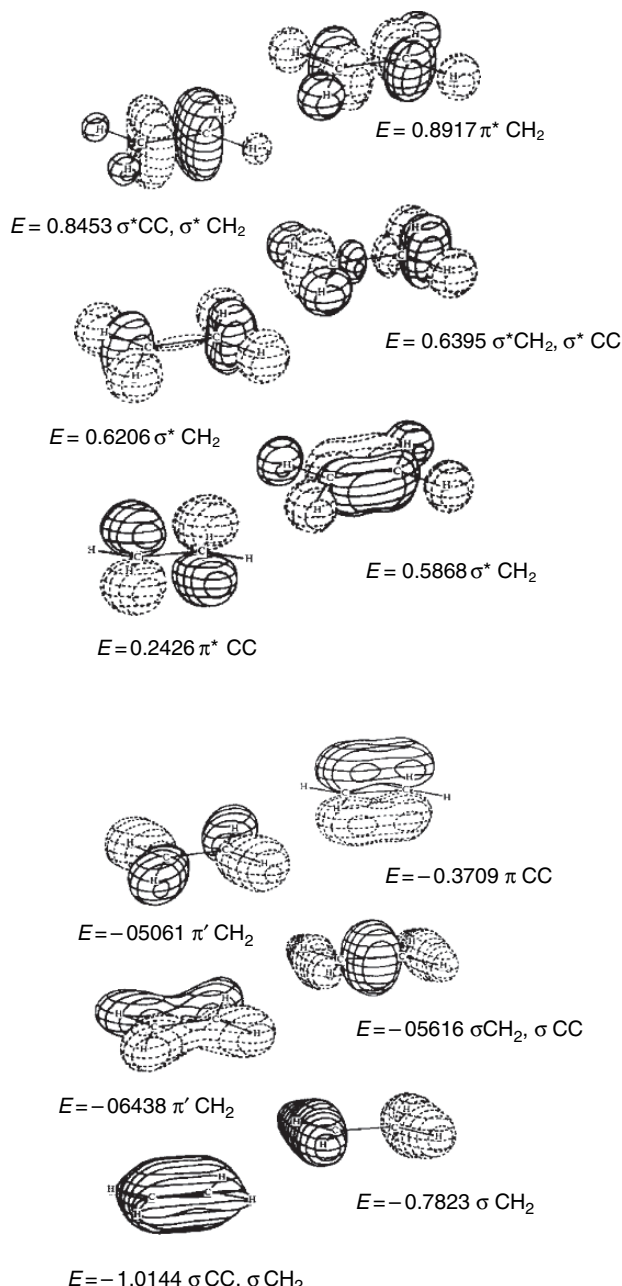


Fig. 1.18. Pictorial representation of ethene MOs. Reproduced with permission from W. L. Jorgensen and L. Salem, *The Organic Chemist's Book of Orbitals*, Academic Press, New York, 1973.

distribution and stability of reactants, transition structures, intermediates, and products is assessed and used to predict changes in reactivity. In MO theory, reactivity is related to the relative energies and shapes of the orbitals that are involved as the reactants are transformed into products. Reactions that can take place through relatively stable

SECTION 1.2

Molecular Orbital Theory and Methods

intermediates and transition structures are more favorable than reactions that involve less stable ones. The *symmetry of the molecular orbitals* is a particularly important feature of many analyses of reactivity based on MO theory. The shapes of orbitals also affect the energy of reaction processes. Orbital shapes are defined by the atomic coefficients. The strongest interactions (bonding when the interacting orbitals have the same phase) occur when the orbitals have high coefficients on those atoms that undergo bond formation.

The qualitative description of reactivity in molecular orbital terms begins with a basic understanding of the MOs of the reacting systems. At this point we have developed a familiarity with the MOs of ethene and conjugated unsaturated systems from the discussion of HMO theory and the construction of the ethene MOs from atomic orbitals. To apply these ideas to new systems, we have to be able to understand how a change in structure will affect the MOs. One approach is called *perturbation molecular orbital theory* or PMO for short.⁵⁵ The system under analysis is compared to another related system for which the MO pattern is known. In PMO theory, the MO characteristics of the new system are deduced by analyzing how the change in structure affects the MO pattern. The type of changes that can be handled in a qualitative way include substitution of atoms by other elements, with the resulting change in electronegativity, as well as changes in connectivity that alter the pattern of direct orbital overlap. The fundamental thesis of PMO theory is that the resulting changes in the MO energies are relatively small and can be treated as adjustments (perturbations) on the original MO system.

Another aspect of qualitative application of MO theory is the analysis of interactions of the orbitals in reacting molecules. As molecules approach one another and reaction proceeds there is a mutual perturbation of the orbitals. This process continues until the reaction is complete and the product (or intermediate in a multistep reaction) is formed. The concept of *frontier orbital control* proposes that the most important interactions are between a particular pair of orbitals.⁵⁶ These orbitals are the highest filled orbital of one reactant (the HOMO) and the lowest unfilled (LUMO) orbital of the other reactant. We concentrate attention on these two orbitals because they are the closest in energy. A basic postulate of PMO theory is that *interactions are strongest between orbitals that are close in energy*. Frontier orbital theory proposes that these strong initial interactions guide the course of the reaction as it proceeds to completion. A further general feature of MO theory is that only MOs of matching symmetry can interact and lead to bond formation. Thus, analysis of a prospective reaction path focuses attention on the *relative energy and symmetry* of the frontier orbitals.

These ideas can be illustrated by looking at some simple cases. Let us consider the fact that the double bonds of ethene and formaldehyde have quite different chemical reactivities. Formaldehyde reacts readily with nucleophiles, whereas ethene does not. The π bond in ethene is more reactive toward electrophiles than the formaldehyde C=O π bond. We have already described the ethene MOs in Figures 1.17 and 1.18. How do those of formaldehyde differ? In the first place, the higher atomic number of

⁵⁵. C. A. Coulson and H. C. Longuet-Higgins, *Proc. R. Soc. London Ser. A*, **192**, 16 (1947); L. Salem, *J. Am. Chem. Soc.*, **90**, 543, 553 (1968); M. J. S. Dewar and R. C. Dougherty, *The PMO Theory of Organic Chemistry*, Plenum Press, New York, 1975; G. Klopman, *Chemical Reactivity and Reaction Paths*, Wiley-Interscience, New York, 1974, Chap. 4.

⁵⁶. K. Fukui, *Acc. Chem. Res.*, **4**, 57 (1971); I. Fleming, *Frontier Orbital and Organic Chemical Reactions*, Wiley, New York, 1976; L. Salem, *Electrons in Chemical Reactions*, Wiley, New York, 1982, Chap. 6.



π^* — LUMO 0.2426 LUMO — π^* 0.2467

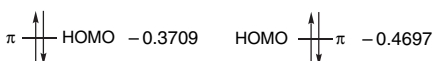


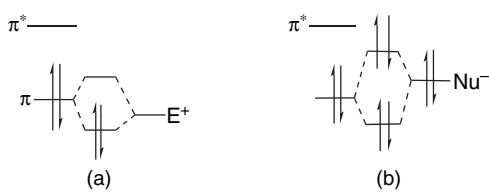
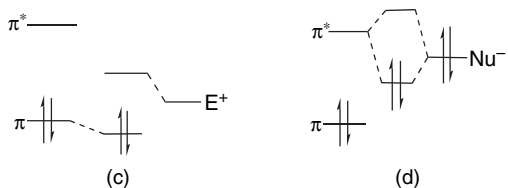
Fig. 1.19. Relative energy of the π and π^* orbitals in ethene and formaldehyde. Energies values in au are from W. L. Jorgensen and L. Salem, *The Organic Chemists Book of Orbitals*, Academic Press, New York, 1973.

oxygen provides two additional electrons, so that in place of the CH_2 group of ethene, the oxygen of formaldehyde has two pairs of nonbonding electrons. This introduces an additional aspect to the reactivity of formaldehyde. The oxygen atom can form a bond with a proton or a Lewis acid, which increases the effective electronegativity of the oxygen.

Another key change has to do with the frontier orbitals, the π (HOMO) and π^* (LUMO) orbitals. These are illustrated in Figure 1.19. One significant difference between the two molecules is the lower energy of the π and π^* orbitals in formaldehyde. These are lower in energy than the corresponding ethene orbitals because they are derived in part from the lower-lying (more electronegative) $2p_z$ orbital of oxygen. Because of its lower energy, the π^* orbital is a better acceptor of electrons from the HOMO of any attacking nucleophile than is the LUMO of ethene. We also see why ethene is more reactive to electrophiles than formaldehyde. In electrophilic attack, the HOMO acts as an electron donor to the approaching electrophile. In this case, because the HOMO of ethene lies higher in energy than the HOMO of formaldehyde, the electrons are more easily attracted by the approaching electrophile. The unequal electronegativities of the oxygen and carbon atoms also distort electron distribution in the π molecular orbital. In contrast to the symmetrical distribution in ethene, the formaldehyde π MO has a higher atomic coefficient at oxygen. This results in a net positive charge on the carbon atom, which is favorable for an approach by a nucleophile. One method of charge assignment (see Section 1.4.1) estimates that the π orbital has about 1.2 electrons associated with oxygen and 0.8 electrons associated with carbon, placing a positive charge of $+0.2e$ on carbon. This is balanced by a greater density of the LUMO on the carbon atom.

One principle of PMO theory is that the degree of perturbation is a function of the degree of overlap of the orbitals. Thus in the qualitative application of MO theory, it is important to consider the shape of the orbitals (as indicated quantitatively by their atomic coefficients) and the proximity that can be achieved by the orbitals within the limits of the geometry of the reacting molecules. Secondly, the strength of an interaction depends on the relative energy of the orbitals. The closer in energy, the greater the mutual perturbation of the orbitals. This principle, if used in conjunction with reliable estimates of relative orbital energies, can be of value in predicting the relative importance of various possible interactions.

Let us illustrate these ideas by returning to the comparisons of the reactivity of ethene and formaldehyde toward a nucleophilic species and an electrophilic species.

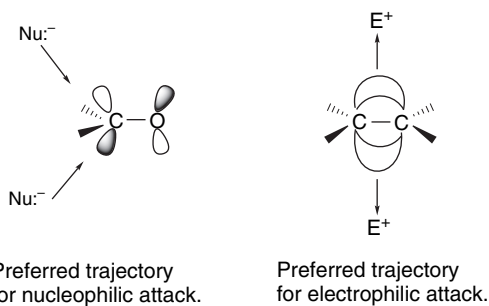
Interaction of ethene frontier orbitals with E^+ and Nu^- Interaction of formaldehyde frontier orbitals with E^+ and Nu^- Fig. 1.20. PMO description of interaction of ethylene and formaldehyde with an electrophile (E^+) and a nucleophile (Nu^-).

The perturbations that arise as a nucleophile and an electrophile approach are sketched in Figure 1.20.

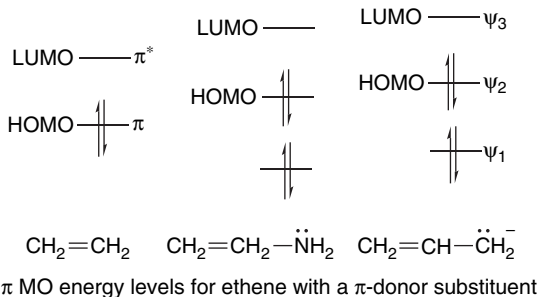
The electrophilic species E^+ must have a low-lying empty orbital. The strongest interaction will be with the ethene π orbital and this leads to a stabilizing effect on the complex since the electrons are located in an orbital that is stabilized (Figure 1.20a). The same electrophilic species would lie further from the π orbital of formaldehyde since the formaldehyde orbitals are shifted to lower energy. As a result the mutual interaction with the formaldehyde HOMO will be weaker than in the case of ethene (Figure 1.20c). The conclusion is that an electrophile will undergo a greater stabilizing attraction on approaching ethene than it will on approaching formaldehyde. In the case of Nu^- , a strong bonding interaction with π^* of formaldehyde is possible (Figure 1.20d). In the case of ethene, the strongest interaction is with the HOMO of the nucleophile, but this is a destabilizing interaction since both orbitals are filled and the lowering of one orbital is canceled by the raising of the other (Figure 1.20b). Thus we conclude that a nucleophile with a high-lying HOMO will interact more favorably with formaldehyde than with ethene.

The representations of nucleophilic attack on formaldehyde as involving the carbonyl LUMO and electrophilic attack on ethene as involving the HOMO also make a prediction about the trajectory of the approach of the reagents. The highest LUMO density is on carbon and it is oriented somewhat away from the oxygen. On the other hand, the ethene HOMO is the π orbital, which has maximum density at the midpoint above and below the molecular plane. Calculations of the preferred direction of attack of electrophilic and nucleophilic reagents are in accord with this representation, as shown below.⁵⁷

⁵⁷. H. B. Bürgi, J. D. Dunitz, J. M. Lehn, and G. Wipff, *Tetrahedron*, **30**, 1563 (1974); H. B. Bürgi, J. M. Lehn, and G. Wipff, *J. Am. Chem. Soc.*, **96**, 1956 (1974); K. N. Houk, M. N. Paddon-Row, N. G. Rondan, Y.D. Wu, F. K. Brown, D. C. Spellmeyer, J. T. Metz, Y. Li, and R. J. Loncarich, *Science*, **231**, 1108 (1986).



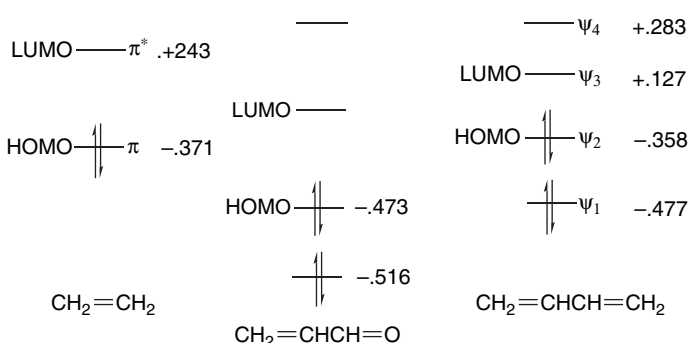
The ideas of PMO theory can also be used to describe substituent effects. Let us consider, for example, the effect of a π -donor substituent and a π -acceptor substituent on the MO levels and reactivity of substituted ethenes. We can take the amino group as an example of a π -donor substituent. The nitrogen atom adds one additional $2p_z$ orbital and two electrons to the π system. The overall shape of the π orbitals for ethenamine is very similar to those of an allyl anion. The highest charge density is on the terminal atoms, i.e., the nitrogen atom and the β -carbon, because the HOMO has a node at the center carbon. The HOMO in ethenamine resembles ψ_2 of the allyl anion and is higher in energy than the HOMO of ethene. It is not as high as the allyl ψ_2 because ethenamine is neutral rather than anionic and because of the greater electronegativity of the nitrogen atom. Thus we expect ethenamine, with its higher-energy HOMO, to be more reactive toward electrophiles than ethene. Furthermore, the HOMO has the highest coefficient on the terminal atoms so we expect an electrophile to become bonded to the β -carbon or nitrogen, but not to the α -carbon. The LUMO corresponds to the higher-energy ψ_3 of the allyl anion, so we expect ethenamine to be even less reactive toward nucleophiles than is ethene.



An example of a π -acceptor group is the formyl group as in propenal (acrolein).



In this case, the π MOs resemble those of butadiene. Relative to butadiene, however, the propenal orbitals lie somewhat lower in energy because of the more electronegative oxygen atom. This factor also increases the electron density at oxygen at the expense of carbon.



π MO energy levels in au for ethylene with a π -acceptor substituent. From Ref 54.

The LUMO, which is the frontier orbital in reactions with nucleophiles, has a larger coefficient on the β -carbon atom, whereas the two occupied orbitals are distorted in such a way as to have larger coefficients on the oxygen. The overall effect is that the LUMO is relatively low lying and has a high coefficient on the β -carbon atom. Frontier orbital theory therefore predicts that nucleophiles will react preferentially at the β -carbon atom.

MO orbital calculations at the HF/6-31G** level have been done on both propenal and ethenamine. The resulting MOs were used to calculate charge distributions. Figure 1.21 gives the electron densities calculated for butadiene, propenal, and aminoethyene.⁵⁸ We see that the C(3) in propenal has a less negative charge than the terminal carbons in butadiene. On the other hand, C(2), the β -carbon in ethenamine, is more negative.

The MO approach gives the same qualitative picture of the substituent effect as described by resonance structures. The amino group is pictured by resonance as an electron donor, indicating a buildup of electron density at the β -carbon, whereas the formyl group is an electron acceptor and diminishes electron density at the β -carbon.



The chemical reactivity of these two substituted ethenes is in agreement with the MO and resonance descriptions. Amino-substituted alkenes, known as enamines, are very reactive toward electrophilic species and it is the β -carbon that is the site of attack. For example, enamines are protonated on the β -carbon. Propenal is an electrophilic alkene, as predicted, and the nucleophile attacks the β -carbon.

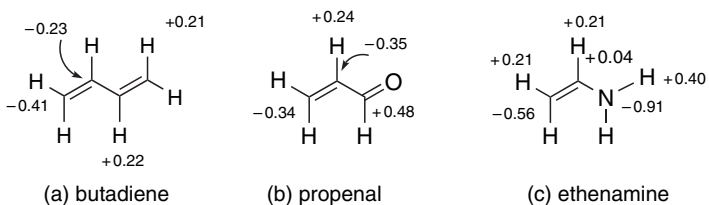
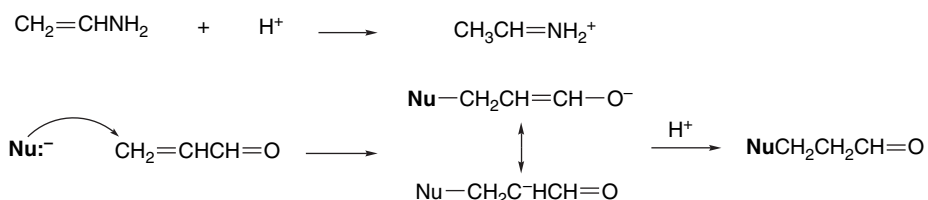
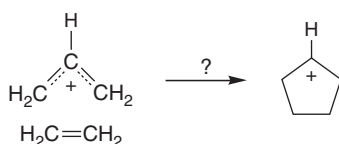


Fig. 1.21. Charge distribution in butadiene, acrolein, and aminoethylene based on HF/6-31G* calculations. From *J. Org. Chem.*, **59**, 4506 (1994).

⁵⁸ M. A. McAllister and T. T. Tidwell, *J. Org. Chem.*, **59**, 4506 (1994).



Frontier orbital theory also provides the framework for analysis of the effect that the orbital symmetry has on reactivity. One of the basic tenets of PMO theory is that the symmetries of two orbitals must match to permit a strong interaction between them. This symmetry requirement, used in the context of frontier orbital theory, can be a very powerful tool for predicting reactivity. As an example, let us examine the approach of an allyl cation and an ethene molecule and ask whether the following reaction is likely to occur:



The positively charged allyl cation would be the electron acceptor in any initial interaction with ethene. Therefore to consider this reaction in terms of frontier orbital theory, the question we have to ask is: "Do the ethene HOMO and allyl cation LUMO interact favorably as the reactants approach one another?" The orbitals that are involved are shown in Figure 1.22. If we assume that a symmetrical approach is necessary to simultaneously form the two new bonds, we see that the symmetries of the two orbitals do not match. Any bonding interaction developing at one end is canceled by an antibonding interaction at the other end. The conclusion drawn from this analysis is that this particular reaction process is not favorable. We would need to consider other modes of approach to examine the problem more thoroughly, but this analysis

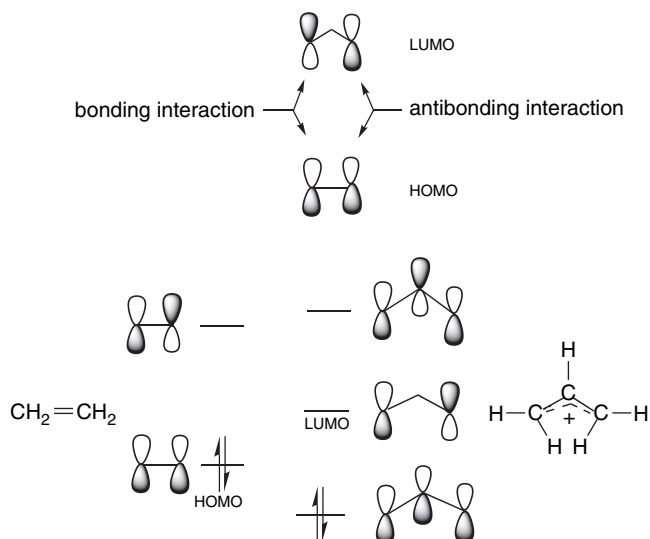


Fig. 1.22. MOs for ethene and allyl cation.

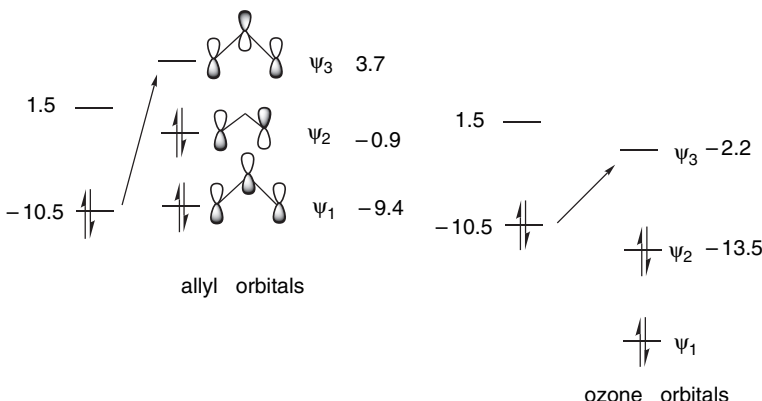
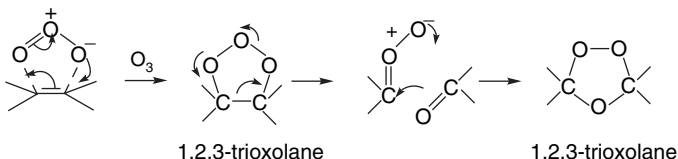


Fig. 1.23. Comparison of FMO interactions of ethene with an allyl anion and ozone.

indicates that simultaneous (concerted) bond formation between ethene and an allyl cation to form a cyclopentyl cation will not occur.

Another case where orbital symmetry provides a useful insight is ozonolysis, which proceeds through a 1,2,3-trioxolane intermediate to a 1,2,4-trioxolane (ozonide) product.



Each step in this reaction sequence is a *concerted reaction* and therefore requires matching of orbital symmetry. The first step is a *cycloaddition reaction*, the second is a *cycloreversion*, and the third is another cycloaddition.⁵⁹ Furthermore, because of the electronegative character of O₃ relative to a C=C double bond, we anticipate that O₃ will furnish the LUMO and the alkene the HOMO. The π orbitals of ozone are analogous to those of an allyl anion, although much lower in energy, and contain four π electrons. We see that concerted bond formation is possible. Because of the large shift in the placement of the orbitals, the strongest interaction is between the ethene HOMO and the O₃ LUMO. The approximate energies (eV) shown in Figure 1.23 are from CNDO calculations.⁶⁰

In contrast to the reaction of ethene with ozone, which is very fast, the reaction with an allyl anion itself is not observed, even though the reaction does meet the symmetry requirement.



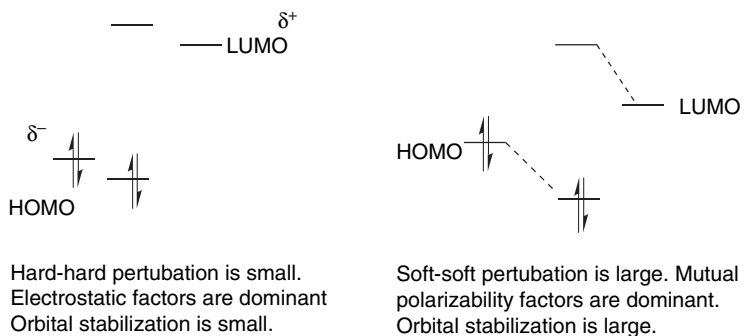
A major factor is the absence of an electrophilic component, that is, a species with a low-lying LUMO. The energy of ψ₃ for of allyl anion lies well above the π orbital of ethene.⁶¹

⁵⁹. R. C. Kuczkowski, *Chem. Soc. Rev.*, **21**, 79 (1992).

⁶⁰. K. N. Houk, J. Sims, C. R. Watts, and L. J. Luskus, *J. Am. Chem. Soc.*, **95**, 7301 (1973).

⁶¹. R. R. Sauers, *Tetrahedron Lett.*, **37**, 7679 (1996).

The concepts of PMO and frontier orbital theory can be related to the characteristics of hard-hard and soft-soft reactions. Recall that hard-hard reactions are governed by electrostatic attractions, whereas soft-soft reactions are characterized by partial bond formation. The hard-hard case in general applies to situations in which there is a large separation between the HOMO and LUMO orbitals. Under these conditions the stabilization of the orbitals is small and the electrostatic terms are dominant. In soft-soft reactions, the HOMO and LUMO are close together, and the perturbational stabilization is large.



1.2.6. Numerical Application of MO Theory

Molecular orbital computations are currently used extensively for calculation of a range of molecular properties. The energy minimization process can provide detailed information about the most stable structure of the molecule. The total binding energy can be related to thermodynamic definitions of molecular energy. The calculations also provide the total electron density distribution, and properties that depend on electron distribution, such as dipole moments, can be obtained. The spatial distribution of orbitals, especially the HOMO and LUMO, provides the basis for reactivity assessment. We illustrate some of these applications below. In Chapter 3 we show how MO calculations can be applied to intermediates and transition structures and thus help define reaction mechanisms. Numerical calculation of spectroscopic features including electronic, vibrational, and rotational energy levels, as well as NMR spectra is also possible.

Most MO calculations pertain to the *gas phase*. The effect of solvent can be probed by examining the effect of the dielectric constant on the structure and energy of molecules. The most common treatment of solvation effects is by one of several *continuum models*, which describe the change in energy as a result of *macroscopic solvation effects*. They describe averaged effects of the solvent, rather than specific interactions. The calculations require information about the shape of the molecule and its charge distribution, which are available from the MO computation. The molecule is represented as a surface reflecting van der Waal radii and point charges corresponding to charge separation. The solvent is characterized by a dielectric constant chosen to correspond to the solvent of interest. The calculations take into account electrostatic, polarization, and repulsive interactions with the solvent. A commonly used procedure is the polarizable continuum model (PCM).⁶² The application of a solvation model

⁶². J. Tomasi and M. Persico, *Chem. Rev.*, **94**, 2027 (1994); V. Barone, M. Cossi, and J. Tomasi, *J. Phys. Chem.*, **107**, 3210 (1997).

can adjust the relative energy of molecules. Species with substantial charge separation will be stabilized most strongly.

Current ab initio methods give computed molecular structures that are in excellent agreement with experimental results. Quite good agreement is obtained using relatively small basis sets, without the need for correlation corrections. Scheme 1.4 compares the bond lengths for some small compounds calculated at the MP2/6-31G* level with experimental values.

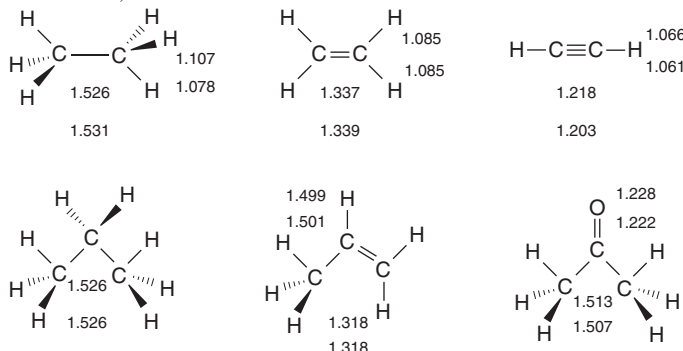
Quite good energy comparisons can also be obtained. The MO calculations pertain to a rigid molecule at 0 K, so corrections for zero-point energy and temperature effects must be made for comparison with thermodynamic data (see Section 3.1). The various computational methods differ in their scope of application and reliability. All give good results for most small hydrocarbons. A particularly challenging area is small ring compounds and other strained molecules. Table 1.10 gives some data comparing agreement for some small hydrocarbons and also for some strained molecules.

A common numerical application of MO calculations is to compare the stability of related compounds. For example, in the discussion of both resonance and qualitative MO theory, we stated that “stabilization” results from attachment of conjugating substituents to double bonds. We might ask, “How much stabilization?” One way to answer this question is to compare the total energy of the two compounds, but since they are not isomers, simple numerical comparison is not feasible. We discuss various ways to make the comparison, and some of the pitfalls, in Chapter 3, but one method is to use *isodesmic reactions*. These are hypothetical reactions in which *the number of each kind of bond is the same on each side of the equation*. For the case of substituents on double bonds the isodesmic reaction below estimates the added stabilization, since it is balanced with respect to bond types. Any extra stabilization owing to substituents will appear as an energy difference.



Scheme 1.4. Comparison of Computed and Experimental Bond Lengths^a

(Upper number is MP2/6-31G* computed bond length. Lower number is experimental value.)



a. From E. Lewars, *Computational Chemistry*, Kluwer Academic Publishers, Boston 2003, pp. 255–260.

Table 1.10. Comparison of Differences in kcal/mol between Computed and Experimental ΔH_f for Some Hydrocarbons

	MNDO ^a	AM1 ^b	PM3 ^c	HF/6-31G* ^a	G2 ^d
Methane	5.9	9.0	4.9	-0.5	0.7
Ethane	0.3	2.6	2.1	0.9	-0.2
Butane	0.7	-0.7	1.3	-0.8	-0.6
Pentane	0.7	-2.8	0.6	-0.5	
Cyclopentane	-11.9	-10.4	-5.6	4.0	-0.4
Cyclohexane	-5.3	-9.0	-1.5	3.1	3.9
Cyclopropane					-1.6
Cyclobutane					-1.5
Bicyclo[1.1.0]butane					-1.5
Bicyclo[2.2.1]heptane	2.1	-2.0	-1.3	8.8	
Bicyclo[2.2.2]octane	-2.2	-11.9	-3.7	10.7	
Ethene	3.1	4.0	4.2	-2.4	0.3
Allene	-1.6	0.6	1.5	-6.8	0.0 ^e
1,3-Butadiene	2.7	3.6	5.0	-2.9	0.5 ^f
Benzene	1.5	2.2	3.6		4.0 ^g

a. M. J. S. Dewar, E. G. Zoebisch, E. F. Healy, and J. J. P. Stewart, *J. Am. Chem. Soc.*, **107**, 3902 (1985).b. M. J. S. Dewar and D. M. Storch, *J. Am. Chem. Soc.*, **107**, 3898 (1985).c. J. J. P. Stewart, *J. Comput. Chem.*, **10**, 221 (1989).d. J. A. Pople, M. Head-Gordon, D. J. Fox, K. Raghavachari, and L. A. Curtiss, *J. Chem. Phys.*, **90**, 5622 (1989); L. A. Curtiss, K. Raghavachari, G. W. Trucks, and J. A. Pople, *J. Chem. Phys.*, **94**, 7221 (1991); L. A. Curtiss, K. Raghavachari, P. C. Redfern, and J. Pople, *J. Phys. Chem.*, **106**, 1063 (1997).e. D. W. Rogers and F. W. McLafferty, *J. Phys. Chem.*, **99**, 1375 (1993).f. M. N. Glukhovtsev and S. Laiter, *Theor. Chim. Acta*, **92**, 327 (1995).g. A. Nicolaides and L. Radom, *J. Phys. Chem.*, **98**, 3092 (1994).

The results using HF/4-31G⁶³ and HF/6-31G**⁶⁴ for some common substituents are given below. They indicate that both electron-donating groups, such as amino and methoxy, and electron-withdrawing groups, such as formyl and cyano, have a stabilizing effect on double bonds. This is consistent with the implication of resonance that there is a stabilizing interaction as a result of electron delocalization.

Stabilization (kcal/mol)		
Substituent	HF/4-31G	HF/6-31G**
CH ₃	3.2	3.05
NH ₂	11.2	7.20
OH	6.6	6.43
OCH ₃	6.1	
F		0.99
Cl		-0.54
CH=O	4.5	
CN	2.4	
CF ₃	-2.5	

The dipole moments of molecules depend on both the molecular dimensions and the electron distribution. For example, Z-1,2-dichloroethene has a dipole moment of 1.90 D, whereas, owing to its symmetrical structure, the *E* isomer has no molecular dipole.

⁶³. A. Greenberg and T. A. Stevenson, *J. Am. Chem. Soc.*, **107**, 3488 (1985).⁶⁴. K. B. Wiberg and K. E. Laidig, *J. Org. Chem.*, **57**, 5092 (1992).

Table 1.11. Comparison of Computed and Experimental Molecular Dipoles^a

	HF/6-31G*	MP2/6-31G*	Experimental
CH ₃ C≡CH	0.64	0.66	0.75
CH ₃ OCH ₃	1.48	1.60	1.30
CH ₃ OH	1.87	1.95	1.70
CH ₃ Cl	2.25	2.21	1.87
(CH ₃) ₂ SO	4.50	4.63	3.96

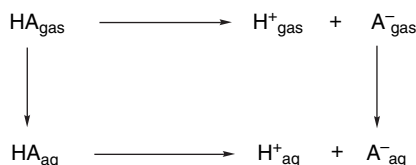
a. From E. Lewars, *Computational Chemistry*, Kluwer Academic Publishers, Boston, 2003, pp 296–300.

SECTION 1.2
Molecular Orbital Theory and Methods



MO calculations of molecular dipoles involves summing the electron distribution in the filled orbitals. Although calculating the order correctly, both HF/6-31G* and MP2/6-31G* calculations seem to overestimate the dipole moments of small polar molecules (Table 1.11).

MO calculations can also be applied to reactions. The effect of substituents on the acidity (pK_a) of carboxylic acids is a well-studied area experimentally. Shields and co-workers used several of the ab initio protocols to calculate the aqueous acidity of some substituted carboxylic acids relative to acetic acid,⁶⁵ which represented quite a challenging test of theory. The dissociation of a carboxylic acid involves formation of ions, and solvation is a major component of the free energy change. Furthermore, solvation introduces both enthalpy and entropy components. The calculations were approached using a thermodynamic cycle that includes the energies of solvation of the neutral acids and the anion. Since the calculation is relative to acetic acid, the energy of solvation of the proton cancels out.



Calculated Solvation Energies CPCM/HF/6-31+G(d) (kcal/mol)

X-CO ₂ H	HA	Exp	A ⁻	Experimental
H	-8.23		-77.10	
CH ₃	-7.86	-6.69	-77.58	-77
ClCH ₂	-10.61		-70.57	
NCH ₂	-14.52		-69.99	
(CH ₃) ₃ C	-6.70		-72.42	

⁶⁵ A. M. Toth, M. D. Liptak, D. L. Phillips, and G. C. Shields, *J. Chem. Phys.*, **114**, 4595 (2001).

Table 1.12. Calculated pK_a Relative to Acetic Acid^a

CHAPTER 1 <i>Chemical Bonding and Molecular Structure</i>	X-CO ₂ H	CBS-4	CBS-QB3	G-2	G2(MP2)	G3	Experimental
	H	2.46	3.10	3.83	3.88	4.02	3.75
	CH ₃ ^b	[4.75]	[4.75]	[4.75]	[4.75]	[4.75]	4.75
	ClCH ₂	3.30	2.92	3.37	3.37	3.18	2.85
	NCH ₂	1.38	1.90	2.31	2.32	1.90	2.45
	(CH ₃) ₃ C	5.08	4.75	6.28	6.24	6.20	5.03

a. CPCM/HF/6-31+G(d) continuum solvent model

b. Reference standard.

The differences in ionization energies are only a small fraction (1–5 kcal/mol) of the total gas phase ionization energies (325–350 kcal/mol), and the solvation terms for the anions are quite large (70–80 kcal/mol). The results from CBS-4, CBS-QB3, G2, G2(MP), and G3, along with the experimental results are shown in Table 1.12. The calculation reproduces the electron-withdrawing and acid-strengthening effect of substituents such as Cl and CN and the acid-weakening effect of the *t*-butyl group. The mean errors ranged between 0.4 and 1.2 kcal/mol for the various methods.

1.3. Electron Density Functionals

Another means of calculating molecular properties is based on *density functional theory* (DFT),⁶⁶ which focuses on the total electron density of a molecule. The introduction of efficient versions of density functional theory in the 1990s profoundly altered computational chemistry. Computational study of medium-sized organic and organometallic systems is currently dominated by density functional methods. DFT methods are founded on a theorem by Hohenberg and Kohn that states that the exact energy for a ground state system is defined entirely by the electron density and the functional of that density that links it to the energy.⁶⁷ This means that the density functional contains all the information on electron correlation. The invention of useful approximations to the functional has made DFT powerful and popular.

DFT calculations describe the electron density ρ at a point in a particular field, designated $n(\mathbf{r})$. The external potential operating on this field, symbolized by $v(\mathbf{r})$, is generated by the atomic nuclei. The electron distribution is specified by $\rho(\mathbf{r})$, which is the measure of electron density per unit volume at any point \mathbf{r} . Integration over space provides the information needed to describe the structure and electron distribution of molecules. The calculation involves the construction of an expression for the electron density. The energy of the system is expressed by the Kohn-sham equation.⁶⁸

$$E = T + v_{en} + J_{ee} + v_{xc} \quad (1.18)$$

where T is the kinetic energy, v_{en} and J_{ee} are electrostatic electron-nuclear and electron-electron interactions, respectively, and v_{xc} are electron correlation and exchange effects.

The energy function F contains terms for kinetic energy, electrostatic interactions, and exchange and correlation energy:

⁶⁶. R. G. Parr and W. Yang, *Density Functional Theory of Atoms and Molecules*, Oxford University Press, Oxford, 1989; W. Kohn, A. D. Becke, and R. G. Parr, *J. Phys. Chem.*, **100**, 12974 (1996).

⁶⁷. P. Hohenberg and W. Kohn, *Phys. Rev. A*, **136**, 864 (1964); M. Levy, *Proc. Natl. Acad. Sci. USA*, **76**, 6062 (1979).

⁶⁸. W. Kohn and L. J. Shan *Phys. Rev. A*, **140**, 1133 (1965).

$$F[n(\mathbf{r})] = T_s[n(\mathbf{r})] + 1/2 \int \frac{n(\mathbf{r})n(\mathbf{r}')}{|r - r'|} dr dr' + E_{xc}[n(\mathbf{r})] \quad (1.19)$$

The energy of the system is given by integration:

$$E = \sum_i^0 \varepsilon_i - \frac{1}{2} \int \frac{n(\mathbf{r})n(\mathbf{r}')}{|r - r'|} dr dr' - \int \nu_{xc}(\mathbf{r})n(\mathbf{r})dr + E_{xc}[n(\mathbf{r})] \quad (1.20)$$

In principle, these equations provide an exact description of the energy, but the value $E_{xc}[n(\mathbf{r})]$ is not known. Although $E_{xc}[n(\mathbf{r})]$ cannot be formulated exactly, Kohn and Sham developed equations that isolate this term:

$$\begin{aligned} h_i^{KS} \chi_i &= \varepsilon_i \chi_i \\ h_i^{KS} &= -\frac{1}{2} \nabla_i^2 - \sum \frac{Z_A}{|r_i - R_A|} + \int \frac{\rho(r')}{|r_i - r'|} dr' + V_{xc}[\rho] \end{aligned}$$

Various approximations have been developed and calibrated by comparison with experimental data and MO calculations. The strategy used is to collect the terms that can be calculated exactly and parameterize the remaining terms. Parameters in the proposed functionals are generally selected by optimizing the method's description of properties of a training set of molecular data. The methods used most frequently in organic chemistry were developed by A. D. Becke.⁶⁹ Lee, Yang, and Parr⁷⁰ (LYP) developed a correlation functional by a fit to exact helium atom results. Combining such “pure DFT” functionals with the Hartree-Fock form of the exchange is the basis for the hybrid methods. Becke’s hybrid exchange functional called “B3,” combined with the LYP correlation functional, is the most widely applied of the many possible choices of exchange and correlation functionals. This is called the B3LYP method. Much of the mechanics for solution of the Kohn-Sham equations is analogous to what is used for solution of the SCF (Hartree-Fock) equations and employs the same basis sets. That is, a guess is made at the orbitals; an approximation to the Kohn-Sham Hamiltonian h_i^{KS} is then reconstructed using the guess. Revised orbitals are recovered from the Kohn-Sham equations, the Hamiltonian is reconstructed, and the process continued until it converges.

DFT computations can be done with less computer time than the most advanced ab initio MO methods. As a result, there has been extensive use of B3LYP and other DFT methods in organic chemistry. As with MO calculations, the minimum energy geometry and total energy are calculated. Other properties that depend on electronic distribution, such as molecular dipoles, can also be calculated.

A number of DFT methods and basis sets have been evaluated for their ability to calculate bond distances in hydrocarbons.⁷¹ With the use of the B3LYP functionals, the commonly employed basis sets such as 6-31G* and 6-31G** gave excellent correlations with experimental values but overestimated C–H bond lengths by about 0.1 Å, while C–C bond lengths generally were within 0.01 Å. Because of the systematic variation, it is possible to apply a scaling factor that predicts C–H bond lengths with high accuracy. Ground state geometries have also been calculated (B3LYP) for molecules such as formaldehyde, acetaldehyde, and acetone.

⁶⁹. A. D. Becke, *Phys. Rev. A*, **38**, 3098 (1988); A. D. Becke, *J. Chem. Phys.*, **96**, 2155 (1992); A. D. Becke, *J. Chem. Phys.*, **97**, 9173 (1992); A. D. Becke, *J. Chem. Phys.*, **98**, 5648 (1993).

⁷⁰. C. Lee, W. Yang and R. G. Parr, *Phys. Rev. B*, **37**, 785 (1988).

⁷¹. A Neugebauer and G. Häflinger, *Theochem*, **578**, 229 (2002).

Bond Distances in Carbonyl Compounds

CHAPTER 1

Chemical Bonding
and Molecular Structure

Basis set	CH ₂ =O	CH ₃ CH=O	(CH ₃) ₂ C=O				
	C—H	C=O	C—H	C=O	C—C	C=O	C—C
Experiment	1.108	1.206	1.106	1.213	1.504	1.222	1.507
311 + +G** ^a	1.105	1.201	1.109	1.205	1.502	1.211	1.514
aug-CCPVDZ ^b	1.114	1.207					

a. W. O. George, B. F. Jones, R. Lewis, and J. M. Price, *J. Molec. Struct.*, **550/551**, 281 (2000).

b. B. J. Wang, B. G. Johnson, R. J. Boyd, and L. A. Eriksson, *J. Phys. Chem.*, **100**, 6317 (1996).

In Chapter 3, we compare the results of DFT calculations on the relative thermodynamic stability of hydrocarbons with those from MO methods. There is some indication that B3LYP calculations tend to underestimate the stability of hydrocarbons as the size of the molecule increases. For example, with the 6-311 + +G(3df, 2p) basis set, the error calculated for propane (−1.5 kcal/mol), hexane (−9.3), and octane (−14.0) increased systematically.⁷² Similarly, when the effect of successive substitution of methyl groups on ethane on the C–C bond energy was examined, the error increased from 8.7 kcal/mol for ethane to 21.1 kcal/mol for 2,2,3,3-tetramethylbutane (addition of six methyl groups, B3LYP/6-311 + +G(d, p)). The trend for the MP2/6-311 + +G (d, p) was in the same direction, but those were considerably closer to the experimental value.⁷³ The difficulty is attributed to underestimation of the C–C bond strength. As we study reactions, we will encounter a number of cases where DFT calculations have provided informative descriptions of both intermediates and transition structures.⁷⁴ In these cases, there is presumably cancellation of these kinds of systematic errors, because the comparisons that are made among reactants, intermediates, and product compare systems of similar size. Use of isodesmic reaction schemes should also address this problem.

DFT calculations have been used to compute the gas phase acidity of hydrocarbons and compare them with experimental values, as shown in Table 1.13. The

Table 1.13. Gas Phase Enthalpy of Ionization of Hydrocarbons in kcal/mol by B3LYP/6-311++G Computation**

Compound	ΔH_{calc}	ΔH_{exp}
CH ₄ ^a	416.8	416.7
C ₂ H ₆ ^a	419.4	420.1
CH ₃ CH ₂ CH ₃ (<i>pri</i>) ^a	416.5	419.4
CH ₃ CH ₂ CH ₃ (<i>sec</i>) ^a	414.4	415.6
(CH ₃) ₃ CH (<i>tert</i>) ^a	410.2	413.1
Cyclopropane ^b	411.5	411.5
Bicyclo[1.1.0]butane ^b	396.7	399.2
Bicyclo[1.1.1]pentane ^b	407.7	—
Cubane ^b	406.7	404.0
CH ₂ =CH ₂ ^a	405.8	407.5
HC≡CH ^a	375.4	378.8

a. P. Burk and K. Sillar, *Theochem*, **535**, 49 (2001).

b. I. Alkorta and J. Elguero, *Tetrahedron*, **53**, 9741 (1997).

⁷². L. A. Curtiss, K. Ragahavachari, P. C. Redfern and J. A. Pople, *J. Chem. Phys.*, **112**, 7374 (2000).

⁷³. C. E. Check and T. M. Gilbert, *J. Org. Chem.*, **70**, 9828 (2005).

⁷⁴. T. Ziegler, *Chem. Rev.*, **91**, 651 (1991).

Table 1.14. Gas Phase Ionization Energies in kcal/mol for Some Strong Acids^a

Acid	DFT	Experimental	DFT
H ₂ SO ₄	306	302.2	CISO ₃ H
FSO ₃ H	295.9	299.8	HClO ₄
CF ₃ SO ₃ H	297.7	299.5	HBF ₄
CH ₃ SO ₃ H	317.0	315.0	H ₂ S ₂ O ₇
CF ₃ CO ₃ H	316.0	316.3	HSbF ₆

a. From B3LYP/6-311 + G** computations. Ref. 75.

SECTION 1.4
Representation of
Electron Density
Distribution

agreement with experimental values is quite good. The large differences associated with hybridization changes are well reproduced. The increased acidity of strained hydrocarbons such as cyclopropane, bicyclo[1.1.1]butane, and cubane is also reproduced. For acyclic alkanes, the acidity order is *tert*-H > *sec*-H > *pri*-H, but methane is more acidic than ethane. We discuss the issue of hydrocarbon acidity further in Topic 3.1.

DFT computations can be extended to considerably larger molecules than advanced ab initio methods and are being used extensively in the prediction and calculation of molecular properties. A recent study, for example, examined the energy required for ionization of very strong acids in the gas phase.⁷⁵ Good correlations with experimental values were observed and predictions were made for several cases that have not been measured experimentally, as shown in Table 1.14.

Apart from its computational application, the fundamental premises of DFT lead to a theoretical foundation for important chemical concepts such as electronegativity and hardness-softness. The electron density distribution should also be capable of describing the structure, properties, and reactivity of a molecule. We explore this aspect of DFT in Topic 1.5.

1.4. Representation of Electron Density Distribution

The total electron density distribution is a physical property of molecules. It can be approached experimentally by a number of methods. Electron density of solids can be derived from X-ray crystallographic data.⁷⁶ However, specialized high-precision measurements are needed to obtain information that is relevant to understanding chemical reactivity. Gas phase electron diffraction can also provide electron density data.⁷⁷ The electron density is usually depicted as a comparison of the observed electron density with that predicted by spherical models of the atoms and is called *deformation electron density*. For example, Figure 1.24 is the result of a high-precision determination of the electron density in the plane of the benzene ring.⁷⁸ It shows an accumulation of electron density in the region between adjacent atoms and depletion of electron density in the center and immediately outside of the ring. Figure 1.25

⁷⁵. I. A. Koppel, P. Burk, I. Koppel, I. Leito, T. Sonoda, and M. Mishima, *J. Am. Chem. Soc.*, **122**, 5114 (2000).

⁷⁶. P. Coppens, *X-ray Charge Densities and Chemical Bonding*, Oxford University Press, Oxford, 1997.

⁷⁷. S. Shibata and F. Hirota, in *Stereochemical Applications of Gas-Phase Electron Diffraction*, I. Hargittai and M. Hargittai, eds., VCH Publishers, New York, 1988, Chap. 4.

⁷⁸. H.-B. Burgi, S. C. Capelli, A. E. Goeta, J. A. K. Howard, M. A. Sparkman, and D. S. Yufit, *Chem. Eur. J.*, **8**, 3512 (2002).

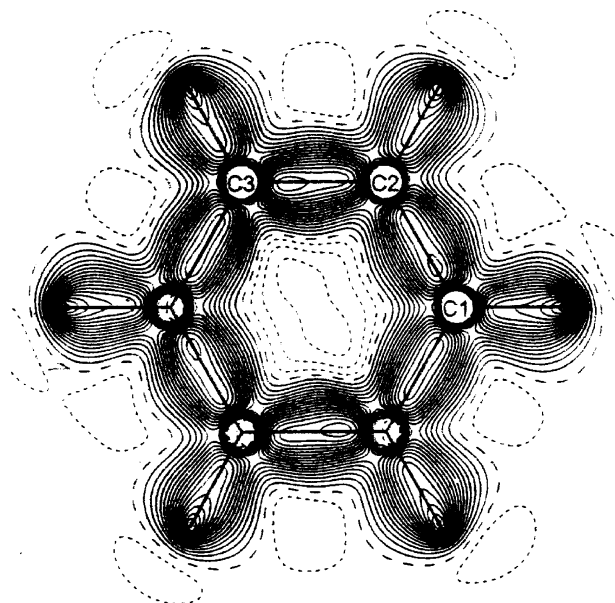


Fig. 1.24. Deformation electron density in the molecular plane of benzene. Contours at $0.05e\text{\AA}^{-3}$ intervals. Positive contours are solid; negative contours are dashed. From *Chem. Eur. J.*, **8**, 3512 (2002).

shows electron density difference maps for benzene in and perpendicular to the molecular plane. The latter representation shows the ellipsoidal distribution owing to the π bond. These experimental electron density distributions are consistent with our concept of bonding. Electron density accumulates between the carbon-carbon and carbon-hydrogen bond pairs and constitutes both the σ and π bonds. The density above and below the ring is ellipsoid, owing to the π component of the bonding.

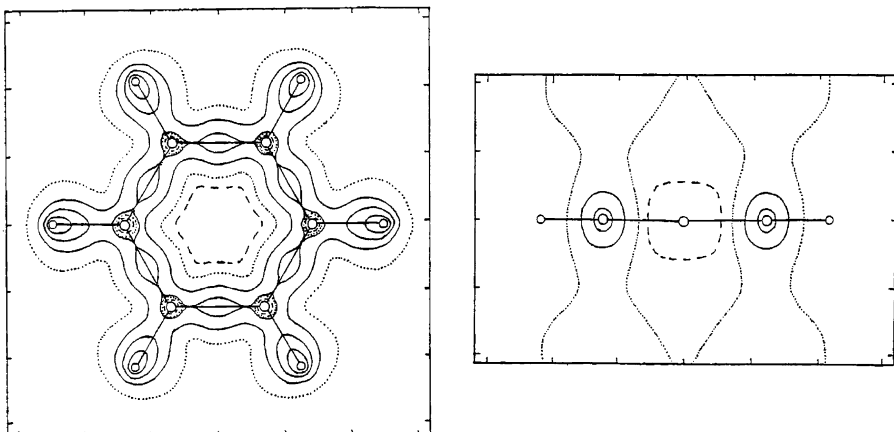


Fig. 1.25. Deformation electron density maps for benzene. (a) In the plane of the ring. (b) Perpendicular to the ring and intersecting a C–C bond. The positive contours (solid lines) are in steps of $0.2e\text{\AA}^{-3}$ and negative contours (dashed lines) in steps of $0.1e\text{\AA}^{-3}$. From S. Shibata and F. Hirota, in *Stereochemical Applications of Gas-Phase Electron Diffraction*, I. Hargittai and M. Hargittai, eds., VCH Publishers, Weinheim, 1988, Chap. 4.

Figure 1.26 presents data for formaldehyde. Panel (a) is the theoretical electron density in the molecular plane. It shows the expected higher electron density around oxygen. The hydrogen atoms are represented by the small peaks extending from the large carbon peak. The electron density associated with the C–H bonds is represented by the ridge connecting the hydrogens to carbon. Panels (b) and (c) are difference maps. Panel (b) shows the accumulation of electron density in the C–H bonding regions and that corresponding to the oxygen unshared electrons. Panel (c) shows the net accumulation of electron density between the carbon and oxygen atoms, corresponding to the σ and π bonds. The electron density is shifted toward the oxygen.

These experimental electron density distributions are in accord with the VB, MO, and DFT descriptions of chemical bonding, but are not easily applied to the determination of the relatively small differences caused by substituent effects that are of primary interest in interpreting reactivity. As a result, most efforts to describe electron density distribution rely on theoretical computations. The various computational approaches to molecular structure should all arrive at the same “correct” *total electron distribution*, although it might be partitioned among orbitals differently. The issue we discuss in this section is how to interpret information about electron density in a way that is chemically informative, which includes efforts to partition the total electron density among atoms. These efforts require a definition (model) of the atoms, since there is no inherent property of molecules that partitions the total electron density among individual atoms.

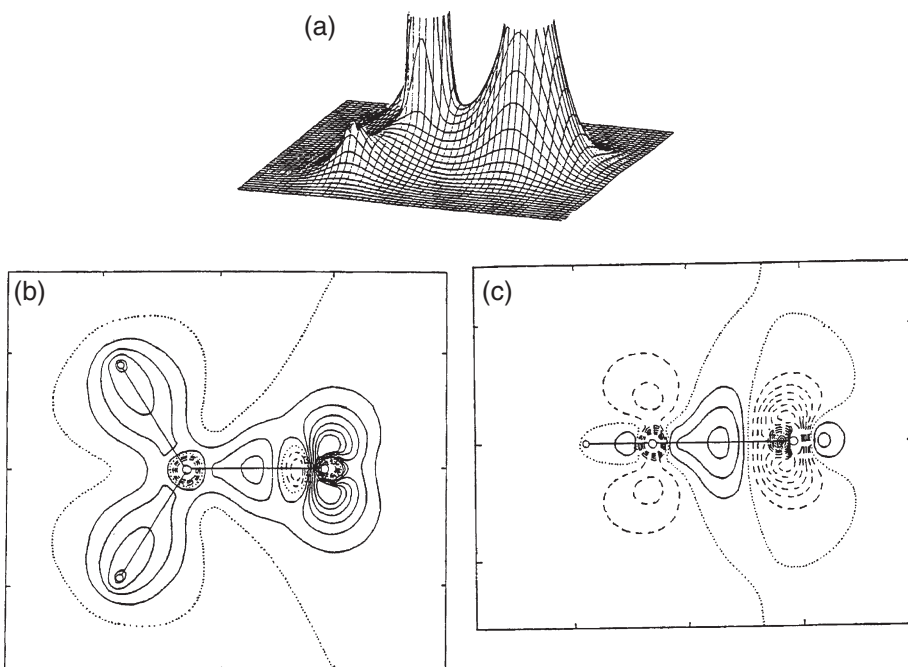
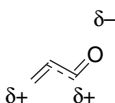


Fig. 1.26. Comparison of electron density of formaldehyde with a spherical atom model: (a) total electron density in the molecular plane; (b) the electron density difference in the molecular plane; (c) the electron density difference in a plane perpendicular to the molecular plane. The contours in (b) and (c) are in steps of $0.2e\text{\AA}^{-3}$. The solid contours are positive and the dashed contours are negative. From S. Shibata and F. Hirota, in *Stereochemical Applications of Gas-Phase Electron Diffraction*, I. Hargittai and M. Hargittai, eds., VCH Publishers, Weinheim, 1988, Chap. 4.

Qualitative VB theory uses resonance structures and bond polarity relationships to arrive at an indication of relative charge distribution. For example, in propenal the combination of a preferred resonance structure and the higher electronegativity of oxygen relative to carbon leads to the expectation that there will be a net negative charge on oxygen and compensating positive charges on C(1) and C(3) (see p. 21). How much the hydrogen atoms might be affected is not clear. As a first approximation, they are unaffected, since they lie in the nodal plane of the conjugated π system, but because the electronegativity of the individual carbons is affected, there are second-order adjustments.



Numerical expression of atomic charge density in qualitative VB terminology can be obtained by use of the electronegativity equalization schemes discussed in Section 1.1.4. The results depend on assumptions made about relative electronegativity of the atoms and groups. The results are normally in agreement with chemical intuition, but not much use is made of such analyses at the present time. MO calculations give the total electron density distribution as the sum of the electrons in all the filled molecular orbitals. The charge distribution for individual atoms must be extracted from the numerical data. Several approaches to the goal of numerical representation of electron distribution have been developed.⁷⁹

1.4.1. Mulliken Population Analysis

In MO calculations, the total electron density is represented as the sum of all populated MOs. The electron density at any atom can be obtained by summing the electron density associated with the basis set orbitals for each atom. Electron density shared by two or more atoms, as indicated by the overlap integral, is partitioned equally among them. This is called a *Mulliken population analysis*.⁸⁰

$$P = \sum_{\mu=1}^{N_{\text{occ}}} c_{\mu\mu} c_{\nu\nu} X_\mu X_\nu \quad (1.21)$$

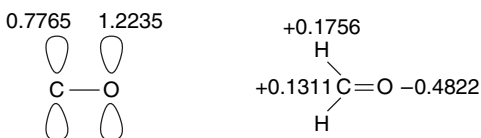
$$P_A = \sum c_{\mu\mu} c_{\nu\nu} X_\mu X_\nu \text{ for } \mu, \nu \text{ on } A \quad (1.22)$$

The Mulliken population analysis, and all other schemes, depend on the definition used to assign charges to atoms. For example, the π orbital in formaldehyde has two electrons, and according to HF/3-21G calculations they are assigned as shown at the left below. When all the basis set orbitals are considered, the charge distribution is as shown on the right.⁸¹ Output from typical MO calculations can provide this kind of atomic charge distribution. No great significance can be attached to the specific numbers, since they are dependent on the particular basis set that is used. The qualitative trends in redistribution

⁷⁹. S. M. Bachrach, *Rev. Comput. Chem.*, **5**, 171 (1994).

⁸⁰. R. S. Mulliken, *J. Chem. Phys.*, **36**, 3428 (1962).

⁸¹. W. J. Hehre, L. Radom, P. v. R. Schleyer, and J. A. Pople, *Ab Initio Molecular Orbital Theory*, Wiley-Interscience, New York, 1986, pp. 118–121; A. Szabo and N. S. Ostlund, *Modern Quantum Chemistry: Introduction to Advanced Electronic Structure Theory*, Macmillan, New York, 1982.



1.4.2. Natural Bond Orbitals and Natural Population Analysis

Another approach for assignment of atomic charges, known as the *natural population analysis* (NPA) method, developed by F. Weinhold and collaborators,⁸² involves formulating a series of hybrid orbitals at each atom. *Natural bond orbitals* (NBO) describe the molecule by a series of localized bonding orbitals corresponding to a Lewis structure. Another set of orbitals describes combinations in which electron density is transferred from filled to antibonding orbitals. These interactions correspond to *hyperconjugation* in VB terminology. The total energy of the molecule is given by the sum of these two components:

$$E = E_{\sigma,\sigma} + E_{\sigma,\sigma^*} \quad (1.23)$$

Typically the E_{σ,σ^*} term accounts for only a small percentage of the total binding energy; however, as it represents a perturbation on the localized structure, it may be particularly informative at the level of chemical structure and reactivity. The charges found by NPA are illustrated below by the methyl derivatives of the second-row elements. Note that the hydrogens are assigned quite substantial positive charges ($\sim 0.2e$), even in methane and ethane. The total positive charge on the hydrogen *decreases* somewhat as the substituent becomes more electronegative. The carbon atom shows a greater shift of electron density to the substituent as electronegativity increases, but remains slightly negative, even for fluoromethane. The protocol for the NPA method is incorporated into MO computations and is used frequently to represent electron distribution.

NPA Populations for CH₃-X(6-31G*)^a

X	δC	δH_3^b	δX
H	-0.867	+0.650	+0.217
Li	-1.380	+0.576	+0.805
BeH	-1.429	+0.689	+0.740
BH ₂	-1.045	+0.712	+0.333
CH ₃	-0.634	+0.643	0.000
NH ₂	-0.408	+0.586	-0.178
OH	-0.225	+0.547	-0.322
F	-0.086	+0.513	-0.427

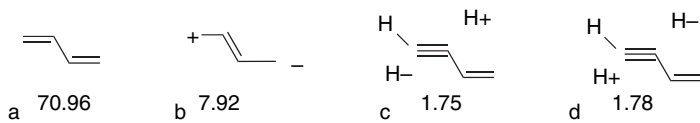
a. From A. E. Reed, R. B. Weinstock and F. Weinhold, *J. Chem. Phys.*, **83**, 735 (1985).

b. Total charge on the three hydrogens of the methyl group.

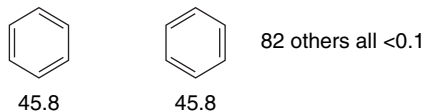
⁸². A. E. Reed, R. B. Weinstock, and F. Weinhold, *J. Chem. Phys.*, **83**, 735 (1985); A. E. Reed, L. A. Curtiss, and F. Weinhold, *Chem. Rev.*, **88**, 899 (1988); F. Weinhold and J. Carpenter, in R. Naaman and Z Vager, eds., *The Structure of Small Molecules and Ions*, Plenum Press, New York, 1988.

Scheme 1.5. Relative Weight of NBO Resonance Structures^a

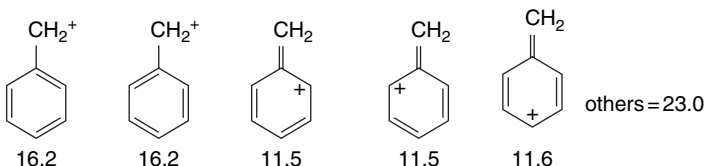
Butadiene



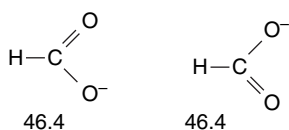
Benzene



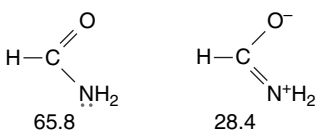
Benzyl Cation



Formate Anion



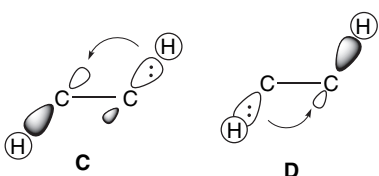
Formamide



a. E. D. Glendening and F. Weinhold, *J. Comput. Chem.*, **19**, 593, 610 (1998).

The NPA electron distribution can be related to the VB concept of resonance structures. The orbitals corresponding to localized structures and those representing delocalization can be weighted. For example, Scheme 1.5 shows the relative weighting of the most important resonance structures for 1,3-butadiene, benzene, the benzyl cation, formamide, and the formate anion. These molecules are commonly used examples of the effect of conjugation and resonance on structure and reactivity.

Resonance structure **b** is commonly used to describe delocalization of π electrons in butadiene. Resonance structures **c** and **d** describe hyperconjugation. The structures represent electron transfer between *anti* hydrogens by σ - σ^* interactions. Note that the hydrogen atoms act as both electron donors and acceptors. As the two hydrogens are in very similar chemical environments, we expect little net transfer of charge, but the delocalization affects such properties as NMR spin coupling constants. We will see in Topic 1.1 that this kind of delocalization is also important for hydrogens bonded to sp^3 carbon atoms.



The NBO resonance structures for benzyl cation reveals the importance of charge delocalization to the *ortho* and *para* positions. The resonance structures shown for formate ion and formamide represent the important cases of carboxylate anions and amides and coincide with the qualitative ideas about the relative importance of resonance structures discussed on pp. 19–20.

1.4.3. Atoms in Molecules

Chemists have long thought of a molecule as the sum of its constituent atoms and groups. The homologous hydrocarbons, for example, have closely related properties, many of which can be quantitatively expressed as the sum of contributions from the CH₃, CH₂, CH, and C groups in the molecule. The association of properties with constituent atoms is also inherent in the concept of functional groups and its implication that a particular combination of atoms, such as a hydroxy group, has properties that are largely independent of the remainder of the molecule. There is now a vast amount of both experimental and computational data on nuclear positions and electron distribution in molecules. The question is whether these data can be interpreted as being the sum of atomic properties and, if so, how one would go about “dividing” a molecule into its constituent atoms.

R. F. W. Bader and associates at Canada’s McMaster University have derived a means of describing the electron distribution associated with specific atoms in a molecule, called the *atoms in molecules* (AIM) method.⁸³ The foundation of this approach is derived from quantum mechanics and principles of physics. It uses the methods of topology to identify atoms within molecules. The electron density of a molecule is depicted by a series of contours. *Bond paths* are the paths of maximum electron density between any two atoms. The *critical point* is a point on the bond path where the electron density is a maximum or a minimum with respect to dislocation in any direction. The bond critical point is defined by the equation

$$\nabla \rho(\mathbf{r}) \cdot \overline{N}(\mathbf{r}) = 0 \quad (1.24)$$

The critical point is the point at which the gradient vector field for the charge density is zero, that is, either a maximum or minimum along \overline{N} . The condition $\nabla \rho(\mathbf{r}) \cdot \overline{N}(\mathbf{r}) = 0$ applied to other paths between two atoms defines a unique surface that can represent the boundary of the atoms within the molecule. The electron density within these boundaries then gives the atomic charge. The combination of electron density contours, bond paths, and critical points defines the *molecular graph*. This analysis can be applied to electron density calculated by either MO or DFT methods. For a very simple molecule such as H₂, the bond path is a straight line between the nuclei. The

⁸³ R. F. W. Bader, *Atoms in Molecules: A Quantum Theory*, Oxford University Press, Oxford, 1990. For an introductory discussion of the AIM method for describing electron density, see C. F. Matta and R. J. Gillespie, *J. Chem. Ed.*, **79**, 1141 (2002).

electron density accumulates between the two nuclei, relative to electron distribution in spherical atoms, as indicated earlier in Figure 1.1. Although there is an electron density minimum on the bond path midway between the two hydrogens, this minimum is a maximum with respect to displacement perpendicular to the bond path.

Bond paths are generally *not* linear in more complex molecules. They are particularly strongly curved in strained molecules, such as those containing small rings. Figure 1.27 gives the molecular graphs for ethane, propane, butane, pentane, and hexane, showing subdivision of the molecule into methyl and methylene groups. Note that the CH₂ units become increasingly similar as the chain is lengthened. Bader's work gives a theoretical foundation to the concept that the properties of a molecule are the sum of the properties of the constituent atoms or groups.

The total electron density graphs for molecules such as methyl cation, ethane, and ethene show strong peaks around the nuclear positions. Figure 1.28a illustrates the electron density $\rho(\mathbf{r})$ for the methyl cation, and Figure 1.28b gives the corresponding gradients, showing the surfaces that partition the ion into C and H atoms. Note that there are peaks in the electron density corresponding to the nuclear positions. The existence of bonds is indicated by the ridge of electron density between the C and H atoms. The arrow in Figure 1.28a indicates the location of the bond critical point, which occurs at a *saddle point*, that is, the electron density is at a minimum along the bond path, but a maximum with respect to any other direction. Figure 1.28b shows the gradient and the zero flux surface that divides the ion into C and H atoms. The dots show the location of the bond critical points.

The electron density can also be characterized by its *ellipticity*, the extent to which it deviates from cylindrical symmetry, reflecting the contribution of π orbitals. While the C≡C bond in ethyne is cylindrically symmetrical, the C–C bonds in ethene and benzene have greater extension in the direction of the π component.⁸⁴ Ellipticity is defined by

$$E = \lambda_1/\lambda_2 - 1 \quad (1.25)$$

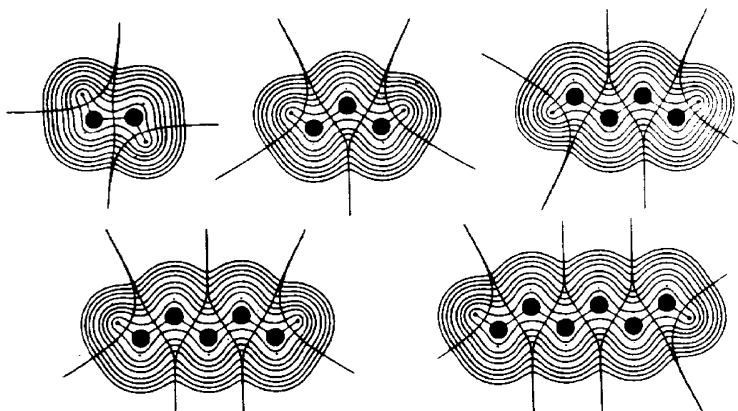


Fig. 1.27. Molecular graphs for ethane, propane, butane, pentane, and hexane. Reproduced with permission from R. F. W. Bader, in *The Chemistry of Alkanes and Cycloalkanes*, S. Patai and Z. Rappoport, eds., John Wiley & Sons, New York, 1992, Chap. 1.

⁸⁴ R. F. W. Bader, T. S. Slee, D. Cremer, and E. Kraka, *J. Am. Chem. Soc.*, **105**, 5061 (1983); D. Cremer and E. Kraka, *J. Am. Chem. Soc.*, **107**, 3800 (1985).

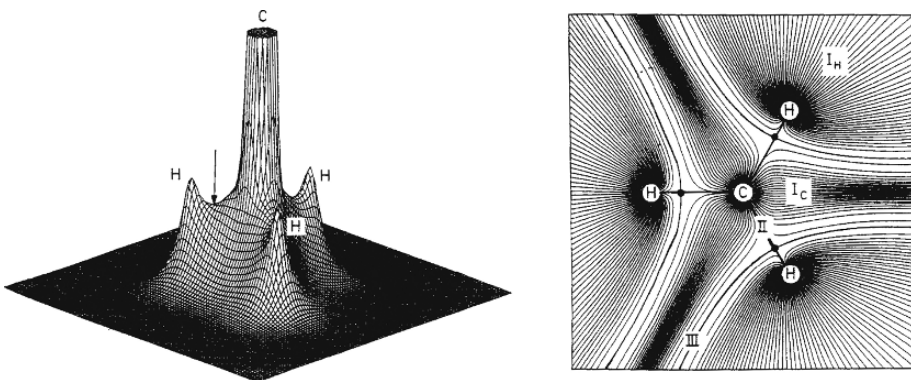
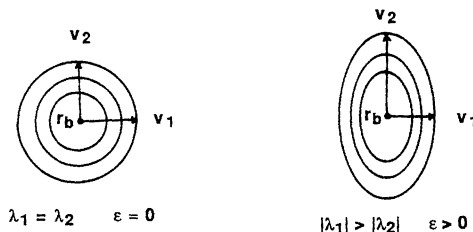


Fig. 1.28. (a) Electron density of the methyl cation in the plane of the atoms (truncated at C); (b) gradient vector field $\bar{V}p(\mathbf{r})$ of the electron density distribution terminating at H (I_H), C (I_C); the bond path and critical point (II); and the zero flux surfaces (III) partitioning the ion into C and H atoms. From E. Kraka and D. Cremer, in *Theoretical Models of Chemical Bonding*, Part 2, Z. B. Maksic, ed., Springer Verlag, Berlin, 1990, pp. 459, 461.

where λ_1 and λ_2 are vectors to a specified electron density in the two dimensions perpendicular to the bond path at the bond critical point.



The ellipticity of the electron density in benzene is 0.23, while that in ethene is 0.45 using HF/6-31G* electron density. Ellipticity can provide structural insight as an indicator of π character. For example, the ellipticity of the C(2)–C(3) bond in 1,3-butadiene is about one-seventh that of the 1,2-bond, indicating a modest contribution from the π bond. Bond ellipticity can also indicate delocalization through hyperconjugation. For example, the C(2)–C(3) bond in propene has an ellipticity of 0.03, reflecting the $\sigma - \pi^*$ interactions in the molecule (see pp. 22–23).

We would expect the electron density to respond to the electronegativity of the atoms forming the bond. This relationship has been examined for the hydrogen compounds of the second-row elements. Table 1.15 gives the AIM radius for each of the second-row elements in its compound with hydrogen. Note that the bond critical point moves closer to the hydrogen as the other element becomes more electronegative. That is, the *hydrogen gets smaller* as electron density shifts to the more electronegative element. The charge density at the bond critical point, $p_{(c)}$, rises rapidly at first, but then levels off going toward the right in the periodic table. The initial increase reflects the increasing covalent character of the bond. The bonds to Li and Be are largely ionic in character, whereas the other bonds have increasing covalent character.

These relationships are depicted in Figure 1.29. Note that the hydrogen changes from hydridelike character in LiH to the much diminished electron density in H–F. There is steadily greater sharing of electron density from Li to C, as indicated by the

Table 1.15. Charge Density and Its Location at Bond Critical Points for Hydrogen Compounds of the Second-Row Elements (6-31G^{})^a**

Compound	rX (au)	rH (au)	$\rho_{(c)}$
LiH	1.358	1.656	0.0369
BeH ₂	1.069	1.416	0.0978
BH ₃	0.946	1.275	0.1871
CH ₄	1.252	0.801	0.2842
NH ₃	1.421	0.492	0.3495
OH ₂	1.460	0.352	0.3759
FH	1.454	0.279	0.3779

a. K. E. Edgecombe and R. J. Boyd, *Int. J. Quantum Chem.*, **29**, 959 (1986).

increased prominence of the nonspherical valence (shared) electron density. Beginning at N, the electron density associated with unshared electron pairs becomes a prominent feature.

Although not so dramatic in character, the same trends can be seen in carbon atoms of different hybridization. The “size” of hydrogen shrinks as the electronegativity of carbon increases in the sequence $sp^3 < sp^2 < sp$ (Figure 1.30).

Wiberg and co-workers looked at how electron density changes as substituents on methane change from very electropositive (e.g., lithium) to very electronegative (e.g., fluorine).⁸⁵ This is a question of fundamental relevance to reactivity, since we know that compounds such as methyl lithium are powerful bases and nucleophiles, whereas the methyl halides are electrophilic in character. The results illustrate how fundamental characteristics of reactivity can be related to electron density. Table 1.16 gives the methyl group “radius” and $\rho_{(c)}$, the electron density at the bond critical point for several substituted methanes.

Going across the second row, X = Li, BeH, CH₃, F, we see that the bond critical point moves closer to C as the C “shrinks” in response to the more electronegative substituents. This is particularly evident in the value of R , which gives the ratio of the

Table 1.16. Bond Critical Points, Charge Density, and Bond Angles for Substituted Methanes^a

X	rC	rX	R	$\rho_{(c)}C-X$	$\angle H-C-X^\circ$
Li	1.2988	0.7025	0.541	0.0422	112.6
BeH	1.1421	0.5566	0.487	0.1030	112.1
CH ₃	0.7637	0.7637	1.000	0.2528	111.2
H	0.6605	0.4233	1.560	0.2855	109.5
CN	0.6263	0.8421	1.344	0.2685	109.8
O ⁻	0.4417	0.8781	1.988	0.3343	116.5
O-Li	0.4425	0.9181	2.075	0.2872	112.5
F	0.4316	0.9331	2.162	0.2371	109.1
CF ₃	0.6708	0.8286	1.235	0.2871	109.4
NH ₃ ⁺	0.4793	1.0278	2.144	0.2210	108.1
N ₂ ⁺	0.4574	1.0522	2.301	0.1720	105.0

NOTE: rC and rX are distances to bond critical point in Å. R is the ratio at these distances. $\rho_{(c)}$ is the electron density at the bond critical point and $\angle H-C-X$ is the bond angle.

a. K. B. Wiberg and C. M. Breneman, *J. Am. Chem. Soc.*, **112**, 8765 (1990).

⁸⁵. K. B. Wiberg and C. M. Breneman, *J. Am. Chem. Soc.*, **112**, 8765 (1990).

SECTION 1.4

Representation of
Electron Density
Distribution

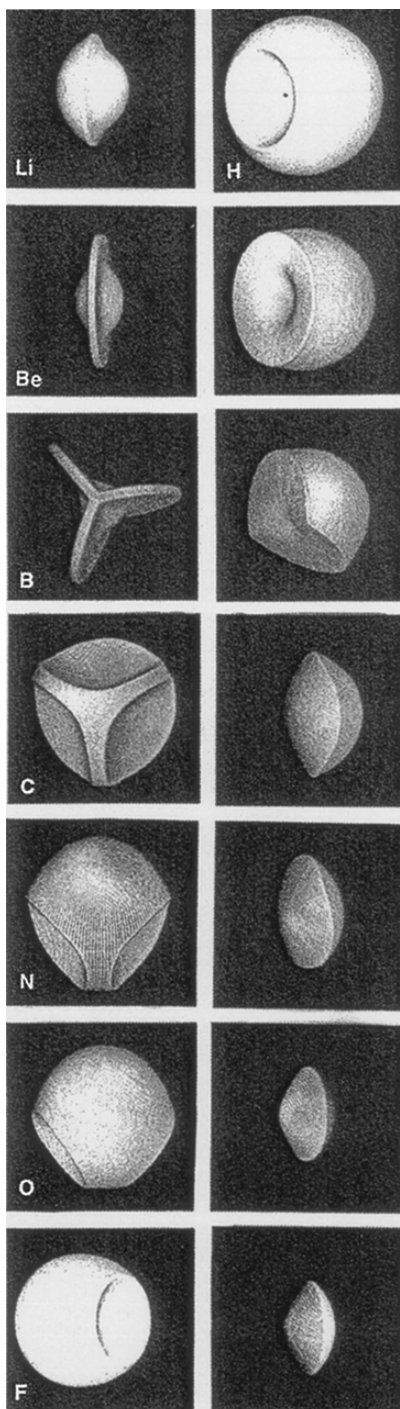


Fig. 1.29. Representation of the atoms in the second-row hydrides. The hydrides of Li, Be, and B consist primarily of a core of decreasing radius and a small, but increasing, shared density. The form of the atoms changes markedly at methane. No core is visible on the C atom, and the H atoms are reduced in size and lie on the convex interatomic surface. The increasing polarity of the remaining molecules is reflected in the decreasing size of the H atom and the increasing convexity of the interatomic surface. Reproduced from R. F. W. Bader, *Angew. Chem. Int. Ed. Engl.*, **33**, 620 (1994), by permission of Wiley-VCH.

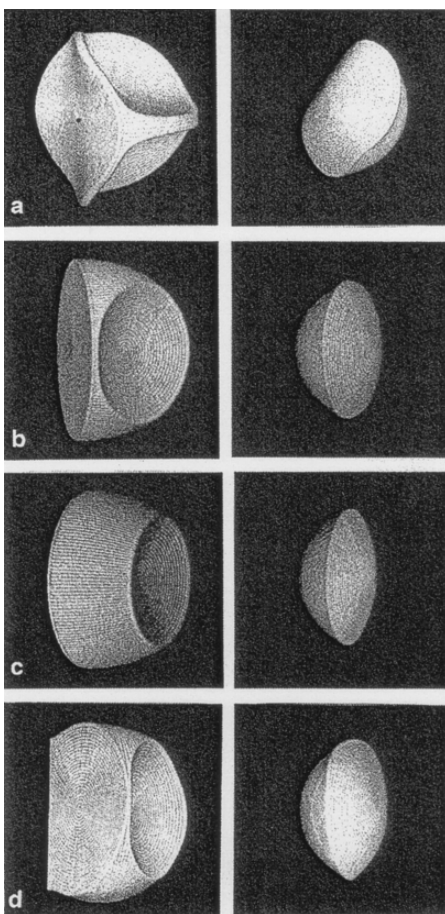
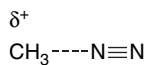


Fig. 1.30. The carbon and hydrogen atoms in: (a) ethane, (b) ethene, (c) ethyne, and (d) benzene. Note that the hydrogen is largest in ethane and smallest in ethyne. Reproduced from *Angew. Chem. Int. Ed. Engl.*, **33**, 620 (1994), by permission of Wiley-VCH.

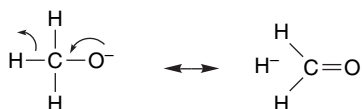
C radius to the radius of the substituent X in the $C-X$ bond. The charge density $\rho_{(c)}$ is very low for the largely ionic $C-Li$ bond. It is also worth noting that there is a trend in bond angles: they become smaller as the substituent becomes more electronegative. This can be attributed to the $C-X$ bond having more p character as the substituent becomes more electronegative. The net atomic charges are shown in Table 1.17.

The methyldiazonium ion $[CH_3-N\equiv N]^+$ is interesting. Later (Section 4.1.5) we will learn that $N\equiv N$ is a very reactive leaving group and indeed it is the best there is, at least of those routinely used in solution chemistry. The computed structure of $[CH_3-N\equiv N]^+$ shows a weak bond (low value of ρ) and a high net positive charge (+0.840) on the methyl group. This structural information suggests that $[CH_3-N\equiv N]^+$ is a methyl cation weakly bound to N_2 , and poised to release N_2 .



There is a remarkable difference in the stability of methyl and ethyldiazonium ions.⁸⁶ The affinity of CH_3^+ for N_2 (C–N bond strength) based on thermodynamic data is 45 ± 7 kcal/mol. Computational results give values of 43.5 ± 1 kcal/mol. The ethyldiazonium ion is much less stable and the computed bond strength is only 11.5 kcal/mol, some 32 kcal/mol less than for methyldiazonium ion. Two aspects of this comparison are worth remembering for future reference: (1) The very unstable methyldiazonium ion is the *most stable* of the alkyl diazonium ions by a considerable margin. Later (Section 11.2.1, Part B) we will examine aryl diazonium ions and find that they are substantially more stable. (2) The indication that because it is better able to disperse the positive charge, an ethyl group binds nitrogen even more weakly than a methyl group presages the major differences in carbocation stability (methyl < *pri* < *sec* < *tert*) that we explore in Chapters 3 and 4.

The methoxide ion CH_3O^- is another important and familiar reagent. We know it to be a strong base and a good nucleophile. These characteristics are consistent with the high charge density on oxygen. Less well appreciated is the reactivity of methoxide as a hydride donor. We see that potential chemical reactivity reflected in the high negative charge on hydrogen in the methoxide ion given in Table 1.17.



The AIM method provides a means of visualizing the subdivision of molecules into atoms. However, its definition of atoms differs from that used for the MPA and NPA methods, and it gives distinctly different numerical values for atomic charges. The distortion of charge toward the more electronegative atom is greater than in the MPA and NPA methods. The magnitude of these charge distributions often overwhelm resonance contributions in the opposite direction. Another feature of AIM charges is that they assign small negative charge to hydrogen and positive charge to carbon in hydrocarbons. This is the reverse of the case for MPA and NPA charges and is also counter to the electronegativity scales, which assign slightly greater electronegativity to carbon than hydrogen.

Table 1.17. Net AIM Charges for Methyl Derivatives

X	δC	δX	δH_3^a
Li	-0.506	+0.903	-0.397
BeH	-0.669	+0.876	-0.207
CH_3	+0.237	0	-0.237
CN	+0.343	-0.362	+0.018
O^-	+1.206	-1.475	-0.732
F	+0.867	-0.743	-0.123
NH_3^+	+0.504	+0.337	+0.159
N_2^+	+0.390	+0.160	+0.450

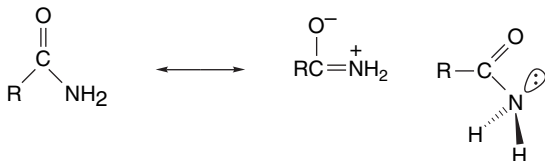
^a. δC = total electron density for carbon in the methyl group; δX = total electron density for substituent X; δH = net electron density on the three hydrogens in the methyl group. From K. B. Wiberg and C. M. Breneman, *J. Am. Chem. Soc.*, **112**, 8765 (1990).

⁸⁶. R. Glaser, G. S.-C. Choy, and M. K. Hall, *J. Am. Chem. Soc.*, **113**, 1109 (1991).

1.4.4. Comparison and Interpretation of Atomic Charge Calculations

While the total electron density is a real physical property that can be measured or calculated, atomic charge distribution is not a physically observable quantity. Rather, the values depend on the definition and procedures used to define atoms and assign charges. Moreover, with some methods, the charge found is dependent on the basis set orbitals that are used. For these reasons, the actual numerical values of charge should not be taken literally, but useful information about the trends in electron distribution within a molecule and qualitative comparisons can be made.⁸⁷ For example, Table 1.18 gives the total charge on carbon and oxygen in formaldehyde using several different basis sets by the MPA, NPA, and AIM methods. Each of the methods shows the expected shift of electron density from carbon to oxygen, but the shift is considerably more pronounced for the AIM analysis.

Atomic charges have been used to analyze the nature of the interaction between the nitrogen and carbon groups in amides. In VB language this interaction is described in terms of resonance. These resonance structures account for the most characteristic properties of amides. Amides are quite polar and react with protons and Lewis acids at oxygen, but not at nitrogen. The partial C=N double bond character also accounts for the observed rotational barrier of about 18 kcal/mol.



There has been a NPA analysis of the delocalization in amides.⁸⁸ Both the planar and rotated forms of formamide and its =S, =Se, and =Te analogs were studied by NPA and natural resonance theory. HF/6-31+G*, MP2/6-31+G*, and B3LYP/6-31+G* calculations were employed. At the MP2/6-31+G* level, the transfer of charge noted on going from the planar to rotated form of formamide was +0.105 at N, -0.088 at O, and -0.033 at C. This charge transfer is consistent with the resonance formulation. The shifts were in the same direction but somewhat larger for the heavier elements,

Table 1.18. Atomic Populations in Formaldehyde Calculated Using Various Methods and Basis Sets^a

Basis set	Oxygen population			Carbon population		
	MPA	NPA	AIM	MPA	NPA	AIM
STO-3G	8.188	8.187	8.935	5.925	5.833	4.999
4-31G	8.485	8.534	8.994	5.824	5.778	5.069
3-21G	8.482	8.496	8.935	5.869	5.782	5.124
6-31G*	8.416	8.578	9.295	5.865	5.668	4.742
6-31G**	8.432	8.577	9.270	5.755	5.676	4.701
6-311+G**	8.298	8.563	9.240	5.892	5.606	4.755

^a From S. M. Bachrach, *Rev. Comp. Chem.*, **5**, 171 (1994).

⁸⁷ S. M. Bachrach, *Rev. Comp. Chem.*, **5**, 171 (1994).

⁸⁸ E. D. Glendening and J. A. Hrabal, II, *J. Am. Chem. Soc.*, **119**, 12940 (1997).

Table 1.19. AIM Charge Distribution and Bond Order in Planar and 90° Formamide^a

A. Charge Distribution			90°			
	Planar			90°		
	σ	π	Total	σ	π	Total
O	5.682	1.710	9.394	5.736	1.604	9.344
N	4.626	1.850	8.476	4.852	1.370	8.222
C	1.632	1.710	4.020	1.854	0.390	4.240

B. Bond Order			90°			
	Planar			90°		
C=O	0.668	0.458	1.127	0.677	0.571	1.248
C—N	0.655	0.229	0.884	0.844	0.046	0.891

^a K. B. Wiberg and K. E. Laidig, *J. Am. Chem. Soc.*, **109**, 5935 (1987). K. B. Wiberg and C. M. Breneman, *J. Am. Chem. Soc.*, **114**, 831 (1992).

evidently reflecting the increasing ability of S, Se, and Te to accept electron density by *polarization*. As indicated earlier in Scheme 1.3, formamide shows a considerable contribution from the dipolar resonance structure when analyzed by natural resonance theory. At the MP2/6-31G+* level, the weightings of the two dominant structures are 58.6 and 28.6%. The C=N bond order is 1.34 and the C=O bond order is 1.72. The specific numbers depend on the computational method, but this analysis corresponds closely to the traditional description of amide resonance.

An AIM electron distribution analysis was also performed by comparing the planar structure with a 90° rotated structure that would preclude resonance. The charges, π , and total bond orders are given in Table 1.19. Although the O charge does not change much, the C—N bond order does, consistent with the resonance formulation. The charge buildup on oxygen suggested by the dipolar resonance structure is largely neutralized by a compensating shift of σ electron density from carbon to nitrogen.

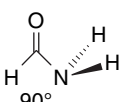
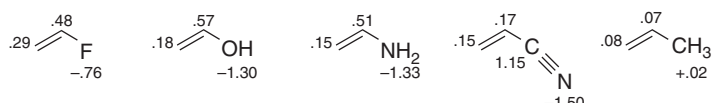


Table 1.20 gives data by which we can compare the output of several methods of charge assignment for substituted ethenes. If we compare ethene and ethenamine as an example of a double bond with an electron-releasing group (ERG) substituent, we see evidence of the conjugation (resonance) effects discussed on p. 22. The MPA and NPA methods show an increase in negative charge at the terminal CH₂ group, as indicated by resonance. There is a smaller, although still negative, charge on this carbon in the compounds with electron-withdrawing groups (EWG), e.g., CH=O, CF₃, CN, and NO₂. The AIM charges present a quite different picture, with *inductive effects* resulting from differences in electronegativity playing a dominant role. The shift of electron density to more electronegative atoms overwhelms other factors. Compare, for example, the fluoro, hydroxy, amino, cyano, and methyl substituents. The dominant factor in the charge distribution here is accumulation of negative charge on the more electronegative atoms. Note that the calculated charge at the terminal C is the same for NH₂ and CN substituents, which have opposing influences on reactivity.

Table 1.20. Calculated Atomic Charges for Substituted Alkenes^a

XY_n	C(1)	H(1)	C(2)	H(2)	X(3)	Y(3)	MPA			NPA			AIM			
							C(1)	H(1)	C(2)	H(2)	X(3)	Y(3)	C(1)	H(1)	C(2)	
H	-0.25	+0.12			-0.42	+0.21					+0.08	-0.04				
CH_3	-0.29	+0.12	-0.09	+0.13	-0.36	+0.12	-0.44	+0.20	-0.20	+0.21	-0.67	+0.22	+0.08	-0.05	+0.02	
CF_3	-0.25	+0.16	-0.26	+0.17	+1.11	-0.37	-0.35	+0.23	-0.36	+0.23	+1.27	-0.42	+0.12	0.00	+0.07	
CH=O	-0.26	+0.16	-0.19	+0.17	+0.37	-0.34	+0.22	-0.35	+0.24	+0.48	+0.48	+0.05	0.00	+0.05	+0.02	
CN	-0.23	+0.16	-0.12	+0.19	+0.27	-0.45	-0.31	+0.23	-0.35	+0.26	+0.30	-0.35	+0.15	+0.01	+0.17	+1.30
NO_2	-0.24	+0.19	+0.03	+0.25	+0.55	-0.46	-0.32	+0.24	-0.14	+0.25	+0.64	-0.46	+0.17	+0.04	+0.38	+1.15
NH_2	-0.36	+0.12	+0.14	+0.14	-0.71	+0.28	-0.56	+0.21	+0.04	+0.21	-0.91	+0.40	+0.15	-0.05	+0.51	-1.50
OH	-0.39	+0.12	+0.26	+0.20	-0.61	+0.35	-0.59	+0.22	+0.22	+0.20	-0.77	+0.50	+0.18	-0.04	+0.57	-0.40
F	-0.36	+0.14	+0.30	+0.14	-0.37	-0.55	+0.23	+0.31	+0.19	-0.40	+0.29	-0.01	+0.48	+0.01	-0.01	+0.63
																-0.7

a. M. A. McAllister and T. T. Tidwell, *J. Org. Chem.*, **59**, 4506 (1994). The calculations are at the HF6-31G** level. Hydrogens at each carbon atom are averaged.



AIM charges on substituted ethenes.

There are, as indicated at the beginning of this section, not necessarily “right” and “wrong” charge densities, since they are determined by the definitions of the models that are used, not by a physical measurement. That circumstance should be kept in mind when using atomic charge densities in evaluating structural and reactivity features. We encounter all three (MPA, NPA, AIM) of the methods for charge assignment in specific circumstances. The MPA and NPA methods, which are based on orbital occupancy partitions, seem to parallel qualitative VB conceptions more closely. In Table 1.20, for example, C(1) is less negative with the EWG cyano and nitro groups than with propene. For the ERG amino and hydroxy, the carbon is more negative. The AIM charges minimize these resonance effects by compensating adjustments in the σ electron distribution. The tendency of the AIM charges to emphasize polar effects can be seen in nitroethene and cyanoethene. The AIM charges are more positive at C(2) than at C(1). These characteristic shifts of charge toward the more electronegative element are due, at least in part, to an inherent tendency of the AIM analysis to derive larger sizes for the more electronegative elements.⁸⁹

1.4.5. Electrostatic Potential Surfaces

While atomic charges must be assigned on the basis of definitions that depend on the method, the *electrostatic potential surface* (EPS) of a molecule is both a theoretically meaningful and an experimentally determinable quantity. The mathematical operation in constructing the electronic potential surface involves sampling a number of points external to the van der Waals radii of atoms in the molecule. A positive charge is attracted to regions of high electron density (negative potential) and repelled in regions of low electron density (positive potential). The calculations then give a contour map or color representation of the molecule’s charge distribution. Several approaches have been developed, one of which is called CHELPG.⁹⁰

Figure 1.31 shows electrostatic potential maps for the planar (conjugated) forms butadiene, ethenamine, and propenal.⁹¹ The diagrams on the left are in the plane of the molecule, and those on the right are perpendicular to the plane of the molecule and depict effects on the π orbital. Solid and dashed lines represent positive and negative potentials, respectively. The electrostatic potential for butadiene is positive at all locations in the plane of the molecule. For propenal (b) the potential becomes negative in the area of the oxygen unshared electron pairs. For ethenamine there is a negative potential external to the CH₂ group. There are regions of negative potential above and below the molecular plane in butadiene, reflecting the π electron density. This area is greatly diminished and shifted toward oxygen in propenal. For ethenamine the negative potential is expanded on C(2) and also includes the plane of the molecule. This is consistent with an increase in the electron density at C(2). Table 1.21 gives

^{89.} C. L. Perrin, *J. Am. Chem. Soc.*, **113**, 2865 (1991).

^{90.} A. C. M. Breneman and K. B. Wiberg, *J. Comput. Chem.*, **11**, 361 (1990).

^{91.} K. B. Wiberg, R. E. Rosenberg, and P. R. Rablen, *J. Am. Chem. Soc.*, **113**, 2890 (1991).

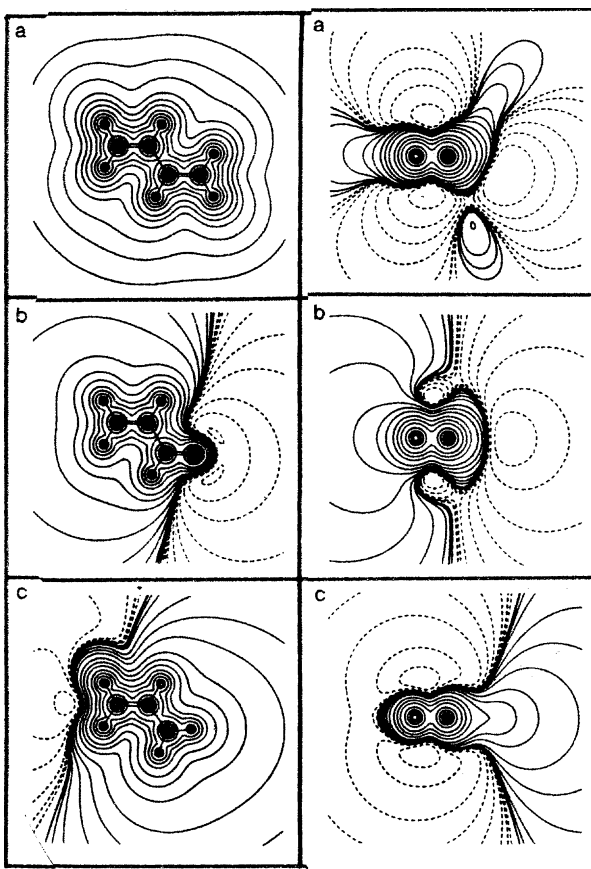


Fig. 1.31. Electrostatic potential contours for: (a) butadiene, (b) propenal, and (c) ethenamine. Solid lines are positive potential and dashed lines are negative. Left. In the plane of the molecule. Right. In the plane of the π electrons. Reproduced from *J. Am. Chem. Soc.*, 113, 2890 (1991), by permission of the American Chemical Society.

the effective atomic charges derived from electrostatic potential at the CH_2 , CH , and a substituent group comparable to propenal.

These charges are in accord with the resonance (pp. 20–22) and qualitative MO (pp. 46–48) descriptions of electron density in these molecules. The $\text{CH}_2=\text{CH}-$ bond in ethenamine is seen to be strongly polarized, with the π -donor effect of the nitrogen unshared pair increasing electron density at C(2), while the polar effect makes C(1) substantially positive. The effects on the double bond in propenal are much less

Table 1.21. Atomic Charges for Butadiene, Propenal, and Ethenamine Derived from Electrostatic Potentials

X	CH_2	CH	X	
$-\text{CH}=\text{CH}_2$	-0.097	+0.097	$\text{CH} + 0.097$	$\text{CH}_2 - 0.097$
$-\text{CH}=\text{O}$	+0.024	-0.065	$\text{CH} + 0.579$	$\text{O} - 0.538$
$-\text{NH}_2$	-0.292	+0.438	$\text{N} - 0.950$	$\text{H} + 0.178$

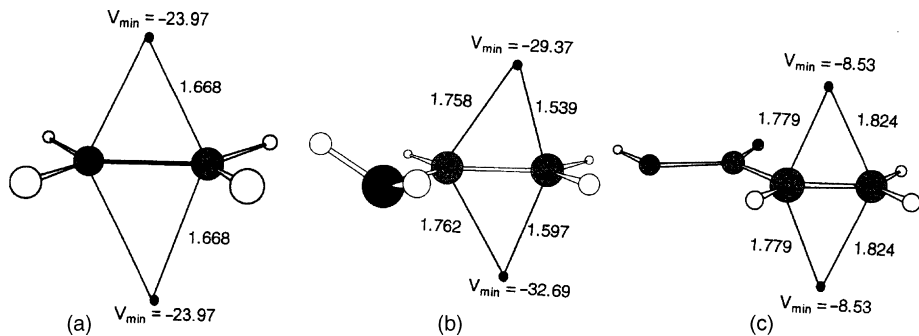


Fig. 1.32. Location and magnitude of points of most negative potential for: (a) ethene, (b) ethenamine, and (c) propenoic acid. Potentials are in kcal/mol. From *J. Org. Chem.*, **66**, 6883 (2001).

dramatic. Most of the charge separation is in the formyl group. However, the charge at the terminal CH_2 changes from slightly negative to slightly positive.

The effect of substituents on ethene on the location and magnitude of the most negative potential has been calculated (HF/6-31G**).⁹² Figure 1.32 compares the position and magnitude for ethene, ethenamine, and propenoic acid, which has an electron-withdrawing carbonyl group comparable to propenal. Table 1.22 gives the same data for several other substituted ethenes.

The V_{neg} data give an order of $\text{NH}_2 > \text{OH}, \text{OCH}_3 > \text{CH}_3 > \text{CH}_2=\text{CH} > \text{HC}\equiv\text{C} > \text{F} > \text{CO}_2\text{H} > \text{CH}=\text{O} > \text{NO}_2$. This corresponds well with substituent effects that are discussed in Chapter 3. Note that the order $\text{CH}_3 > \text{CH}_2=\text{CH} > \text{HC}\equiv\text{C}$ reflects the electronegativity differences of the carbon substituents. The location of the point of most negative potential (cp) also shifts with substituents. It is closer to the terminal carbon C(2) for electron-releasing groups, but slightly closer to C(1) for electron-withdrawing groups. The cp is closer to the molecular plane for electron-releasing groups. This information can be translated into predictions about reactivity toward electrophiles. Donor substituents both increase the negative potential and move it toward C(2), consistent with preferred attack by the electrophile at the more electron-rich carbon (Markovnikov's rule, see Chapter 5). Electron-withdrawing groups such

Table 1.22. Magnitude and Location of Most Negative Potential in Substituted Ethenes

Substituent	V_{neg}	C(1)-cp	C(2)-cp
NH_2	-33.07	1.758	1.539
OH	-26.54	1.795	1.606
CH_3O	-25.98	1.790	1.628
CH_3	-25.04	1.696	1.618
H	-23.97	1.668	1.669
$\text{CH}_2=\text{CH}$	-21.90	1.724	1.682
$\text{HC}\equiv\text{C}$	-15.94	1.769	1.773
F	-13.99	1.850	1.689
HO_2C	-8.53	1.779	1.824
$\text{HC}=\text{O}$	-5.08	1.790	1.839
O_2N	+5.90	2.205	2.223

⁹² C. H. Suresh, N. Koga, and S. R. Gadre, *J. Org. Chem.*, **66**, 6883 (2001).

as CH=O and NO₂ decrease the negative potential (in fact it is positive for NO₂) and increase the distance from the double bond. This results in a weaker attraction to the approaching electrophile and reduced reactivity.

1.4.6. Relationships between Electron Density and Bond Order

We would expect there to be a relationship between the electron density among nuclei and the bond length. There is a correlation between bond length and bond order. Bonds get shorter as bond order increases. Pauling defined an empirical relationship for bond order in terms of bond length for C–C, C=C, and C≡C bond lengths.⁹³ For carbon, the parameter a is 0.3:

$$n_{\text{BOND}} = \exp\left(\frac{r_0 - r}{a}\right) \quad (1.26)$$

The concept of a bond order or bond index can be particularly useful in the description of transition structures, where bonds are being broken and formed and the bond order can provide a measure of the extent of reaction at different bonds. It has been suggested that the parameter in the Pauling relationship (1.26) should be 0.6 for bond orders < 1.⁹⁴

MO calculations can define bond order in terms of atomic populations. Mayer developed a relationship for the bond order that is related to the Mulliken population analysis⁹⁵:

$$B_{AB} = \sum_{\lambda \in A} \sum_{\omega \in B} (PS)_{\omega\lambda} (PS)_{\lambda\omega} \quad (1.27)$$

Wiberg applied a similar expression to CNDO calculations, where S = 1, to give the bond index, BI⁹⁶:

$$\text{BI}_{AB} = \sum_{\lambda \in A} \sum_{\omega \in B} P_{\omega\lambda} P_{\lambda\omega} \quad (1.28)$$

In these treatments, the sum of the bond order for the second-row elements closely approximates the valence number, 4 for carbon, 3 for nitrogen, and 2 for oxygen. As with the Mulliken population analysis, the Mayer-Wiberg bond orders are basis-set dependent.

The NPA orbital method of Weinhold (Section 1.4.2) lends itself to a description of the bond order. When the NPAs have occupancy near 2.0, they correspond to single bonds, but when delocalization is present, the occupancy (and bond order) deviates, reflecting the other contributing resonance structures. There have also been efforts to define bond orders in the context of AIM. There is a nearly linear relationship between the $\rho_{(c)}$, and the bond length for the four characteristic bond orders for carbon 1, 1.5 (aromatic), 2, and 3.⁹⁷

⁹³. L. Pauling, *J. Am. Chem. Soc.*, **69**, 542 (1947).

⁹⁴. Ref. 30 in K. N. Houk, S. N. Gustafson, and K. A. Black, *J. Am. Chem. Soc.*, **114**, 8565 (1992).

⁹⁵. I. Mayer, *Chem. Phys. Lett.*, **97**, 270 (1983).

⁹⁶. K. B. Wiberg, *Tetrahedron*, **24**, 1083 (1968).

⁹⁷. R. F. W. Bader, T. T. Nguyen-Dang, and Y. Tal, *Rep. Prog. Phys.*, **44**, 893 (1981); For 6-31G* values see X. Fadera, M. A. Austen, and R. F. W. Bader, *J. Phys. Chem. A*, **103**, 304 (1999).

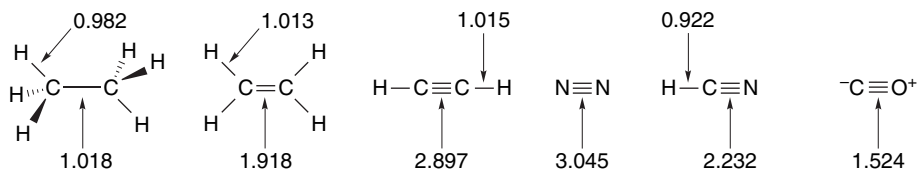
	r (au)	ρ (au)
C_2H_6	2.906	0.241
C_6H_6	2.646	0.291
C_2H_4	2.468	0.329
C_2H_2	2.207	0.368

This linear relationship exists for a variety of other C–C bonds, including those in strained ring molecules and even in carbocations.⁹⁸ There is also a high-precision correlation ($r = -0.998$) for a series of bond lengths in aromatic compounds having differing bond orders,⁹⁹ but it does not appear to hold for C–O or C–N bonds.¹⁰⁰

Bond order in the AIM context has also been defined as:¹⁰¹

$$\rho_{AB} = 2 \sum_i \langle i/i \rangle_A \langle i/i \rangle_B \quad (1.29)$$

For hydrocarbons, this treatment gives bond orders closely corresponding to the Lewis structures, but there is a reduction of the bond order for polar bonds, owing to the ionic portion of the bond.



Chapter Summary

In this chapter we have reviewed the basic concepts of chemical bonding and their relationship to molecular structure. We have also introduced the two major computational approaches based on both molecular orbital (MO) and density functional theory (DFT) methods. These computational methods are powerful complements to experimental methods for describing molecular structure and properties. The orbital and electron density representations these computations provide can help interpret structure, properties, and reactivity. We must, however, remember to distinguish between the parts of this information that represent physically measurable properties (e.g., molecular dimensions and total electron distribution) and those that depend on definition (e.g., individual orbital shapes, atomic charge assignments). Our goal is to grasp the fundamental structural consequences of nuclear positions and electron distribution. Three key concepts, *electronegativity*, *delocalization*, and *polarizability*, allow us to make qualitative judgments about structure and translate them into a first approximation of expected properties and reactivity.

⁹⁸. R. F. W. Bader, T. H. Tang, Y. Tal, and F. W. Biegler-König, *J. Am. Chem. Soc.*, **104**, 946 (1982).

⁹⁹. S. T. Howard and T. M. Krygowski, *Can. J. Chem.*, **75**, 1174 (1997).

¹⁰⁰. S. T. Howard and O. Lamacque, *J. Phys. Org. Chem.*, **16**, 133 (2003).

¹⁰¹. J. Cioslowski and S. T. Mixon, *J. Am. Chem. Soc.*, **113**, 4142 (1991).

Topic 1.1. The Origin of the Rotational (Torsional) Barrier in Ethane and Other Small Molecules

One of the most general structural features of saturated hydrocarbons is the preference for staggered versus eclipsed conformations. This preference is seen with the simplest hydrocarbon with a carbon-carbon bond—ethane. The staggered conformation is more stable than the eclipsed by 2.9 kcal/mol, as shown in Figure 1.33.¹⁰²

The preference for the staggered conformation continues in larger acyclic and also cyclic hydrocarbons, and is a fundamental factor in the conformation of saturated hydrocarbons (see Section 2.2.1). The origin of this important structural feature has been the subject of ongoing analysis.¹⁰³ We consider here the structural origin of the energy barrier. A first step in doing so is to decide if the barrier is the result of a destabilizing factor(s) in the eclipsed conformation or a stabilizing factor(s) in the staggered one. One destabilizing factor that can be ruled out is van der Waals repulsions. The van der Waals radii of the hydrogens are too small to make contact, even in the eclipsed conformation. However, there is a repulsion between the bonding electrons. This includes both electrostatic and quantum mechanical effects (exchange repulsion) resulting from the Pauli exclusion principle, which requires that occupied orbitals maintain maximum separation (see Section 1.1.2). There is also a contribution from nuclear-nuclear repulsion, since the hydrogen nuclei are closer together in the eclipsed conformation. The main candidate for a stabilizing interaction is σ delocalization (hyperconjugation). The staggered conformation optimizes the alignment of the σ and σ^* orbitals on adjacent carbon atoms.

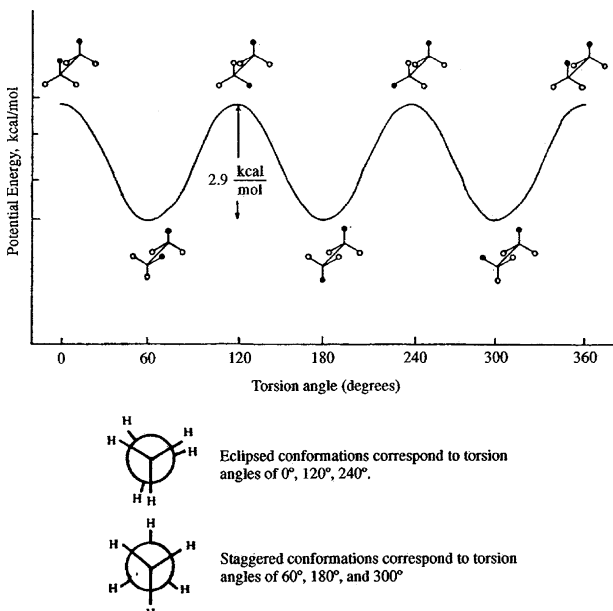


Fig. 1.33. Potential energy as a function of rotation angle for ethane.

¹⁰². K. S. Pitzer, *Disc. Faraday Soc.*, **10**, 66 (1951); S. Weiss and G. E. Leroi, *J. Chem. Phys.*, **48**, 962 (1968); E. Hirota, S. Saito, and Y. Endo, *J. Chem. Phys.*, **71**, 1183 (1979).

¹⁰³. R. M. Pitzer, *Acc. Chem. Res.*, **16**, 207 (1983).

The Origin of the Rotational (Torsional) Barrier in Ethane and Other Small Molecules

The repulsive electronic interactions were emphasized in early efforts to understand the origin of the rotational barrier.¹⁰⁴ In particular the π character of the π_z , π_y , π'_z , and π'_y (see Figure 1.34) was emphasized.¹⁰⁵ The repulsive interactions among these orbitals are maximized in the eclipsed conformation.

Efforts have been made to dissect the contributing factors within an MO framework. The NPA method was applied to ethane. Hyperconjugation was found to contribute nearly 5 kcal/mol of stabilization to the staggered conformation, whereas electron-electron repulsion destabilized the eclipsed conformation by 2 kcal/mol.¹⁰⁶ These two factors, which favor the staggered conformation, are partially canceled by other effects. The problem is complicated by adjustments in bond lengths and bond angles that minimize repulsive interactions. These deformations affect the shapes and energies of the orbitals. When the effects of molecular relaxation are incorporated into

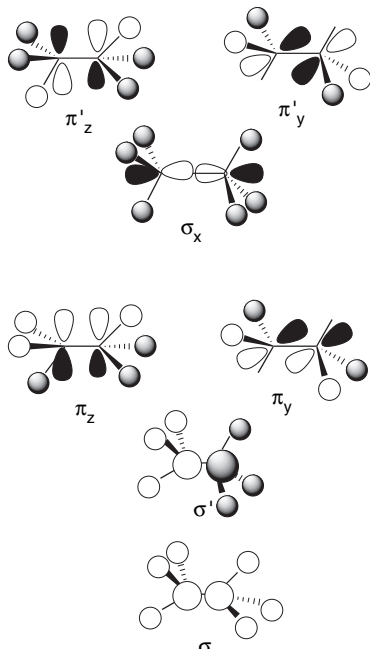


Fig. 1.34. Molecular orbitals of ethane revealing π character of π_z , π_y , π'_z , and π'_y orbitals. Only filled orbitals are shown.

¹⁰⁴. J. P. Lowe, *J. Am. Chem. Soc.*, **92**, 3799 (1970); J. P. Lowe, *Science*, **179**, 527 (1973).

¹⁰⁵. E. T. Knight and L. C. Allen, *J. Am. Chem. Soc.*, **117**, 4401 (1995).

¹⁰⁶. J. K. Badenhoop and F. Weinhold, *Int. J. Quantum Chem.*, **72**, 269 (1999).

the analysis, the conclusion reached is that delocalization (hyperconjugation) is the principal factor favoring the staggered conformation.¹⁰⁷

When methyl groups are added, as in butane, two additional conformations are possible. There are two staggered conformations, called *anti* and *gauche*, and two eclipsed conformations, one with methyl-methyl eclipsing and the other with two hydrogen-methyl alignments. In the methyl-methyl eclipsed conformation, van der Waals repulsions come into play. The barrier for this conformation increases to about 6 kcal/mol, as shown in Figure 1.35. We pursue the conformation of hydrocarbons further in Section 2.2.1.

Changing the atom bound to a methyl group from carbon to nitrogen to oxygen, as in going from ethane to methylamine to methanol, which results in shorter bonds, produces a regular *decrease* in the rotational barrier from 2.9 to 2.0 to 1.1 kcal/mol, respectively. The NPA analysis was applied to a dissection of these barriers.¹⁰⁸ The contributions to differences in energy between the eclipsed and staggered conformations were calculated for four factors. These are effects on the localized bonds (E_{Lewis}), hyperconjugation (E_{deloc}), van der Waals repulsions (E_{steric}), and exchange ($E_{2\times 2}$). The dominant stabilizing terms are the ΔE_{deloc} and $\Delta E_{2\times 2}$, representing hyperconjugation and exchange, respectively, but

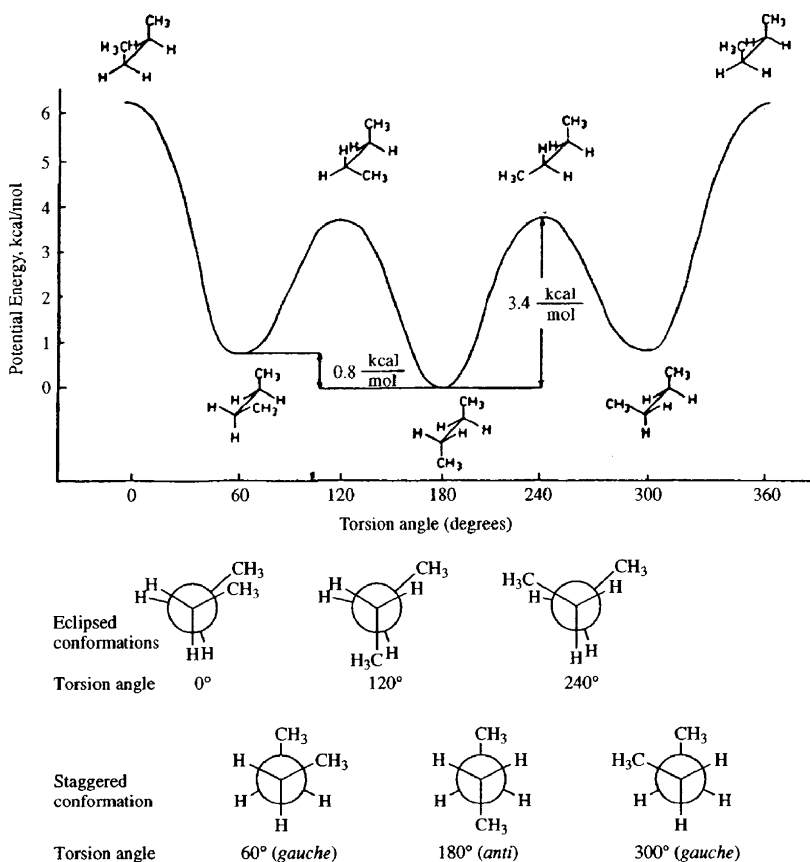


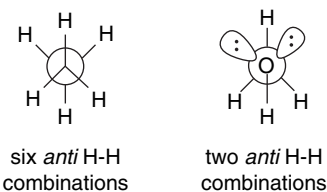
Fig. 1.35. Potential energy diagram for rotation about the C(2)–C(3) bond in butane.

¹⁰⁷. V. Popovits and L. Goodman, *Nature*, **411**, 565 (2001); F. Weinhold, *Angew. Chem. Int. Ed. Engl.*, **42**, 4188 (2003).

¹⁰⁸. J. K. Badenhoop and F. Weinhold, *Int. J. Quantum Chem.*, **72**, 269 (1999).

	CH ₃ CH ₃	CH ₃ NH ₂	CH ₃ OH
ΔE_{Lewis}	-1.423	-0.766	-0.440
ΔE_{deloc}	+4.953	+2.920	+1.467
ΔE_{steric}	-0.827	-0.488	-1.287
$\Delta E_{2 \times 2}$	+2.009	+1.483	+0.475
ΔE_{total}	+4.712	+3.149	+0.215

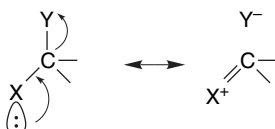
The methanol rotational barrier was further explored, using the approach described above for ethane.¹⁰⁹ The effect of changes in molecular structure that accompany rotation were included. The approach taken was to systematically compare the effect on the rotational barrier of each specific interaction, e.g., hyperconjugation and exchange repulsion, and to determine the effect on molecular geometry, i.e., bond lengths and angles. The analysis of electrostatic forces (nuclear-nuclear, electron-electron, and nuclear-electron) showed that it was the nuclear-electron forces that are most important in favoring the staggered conformation, whereas the other two actually favor the eclipsed conformation. The structural response to the eclipsed conformation is to lengthen the C–O bond, destabilizing the molecule. The more favorable nuclear-electron interaction in the staggered conformation is primarily a manifestation of hyperconjugation. In comparison with ethane, a major difference is the number of hyperconjugative interactions. The oxygen atom does not have any antibonding orbitals associated with its unshared electron pairs and these orbitals cannot act as acceptors. The oxygen unshared electrons function only as donors to the adjacent *anti* C–H bonds. The total number of hyperconjugative interactions is reduced from six in ethane to two in methanol.



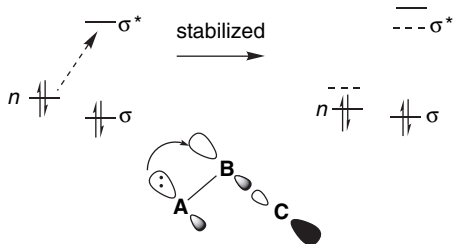
Topic 1.2. Heteroatom Hyperconjugation (Anomeric Effect) in Acyclic Molecules

It is expected that hyperconjugation would be enhanced in certain systems containing heteroatoms. If one atom with an unshared electron pair is a particularly good electron donor and another a good σ^* acceptor, the $n \rightarrow \sigma^*$ contribution should be enhanced. This is represented by a charged, “no-bond” resonance structure.

¹⁰⁹. V. Pophristic and L. Goodman, *J. Phys. Chem. A*, **106**, 1642 (2002).



Heteroatom hyperconjugation can also be expressed in MO terms. The n , σ , and σ^* orbitals are involved, as depicted below. If the A atom is the donor and C the acceptor, the MO perturbation indicates a stabilization of the A n orbital by partial population of the B–C σ^* orbital.



This stereoelectronic interaction has a preference for an *anti* relationship between the donor electron pair and the acceptor σ^* orbital. Such interactions were first recognized in carbohydrate chemistry, where the term *anomeric effect* originated. We use the more general term *heteroatom hyperconjugation* in the discussion here. The $n \rightarrow \sigma^*$ interaction should be quite general, applying to all carbon atoms having two heteroatom substituents. Such compounds are generally found to be stabilized, as indicated by the results from an HF/3-21G level calculations given in Table 1.23.

A study of the extent of hyperconjugation in disubstituted methanes using B3LYP/6-31G** calculations and NPA analysis found that σ^* acceptor capacity increases with electronegativity, i.e., in the order C < N < O < F for the second row.¹¹⁰ However, acceptor σ^* capacity also increases going down the periodic table for the halogens, F < Cl < Br < I. The electronegativity trend is readily understood, but the trend with size had not been widely recognized. The effect is attributed to the lower energy of the σ^* orbitals with the heavier elements. Donor ability also appears to increase going down the periodic table. This trend indicates that *softness* (polarizability) is a factor in hyperconjugation. The stabilizations for substituted methylamines according to these B3LYP/6-31G** calculations are as follows:

Table 1.23. Calculated Stabilization in kcal/mol for Disubstituted Methanes^a

X(donor)	Y(acceptor)	NH ₂	OH	F
NH ₂	10.6	12.7	17.6	
OH		17.4	16.2	
F			13.9	

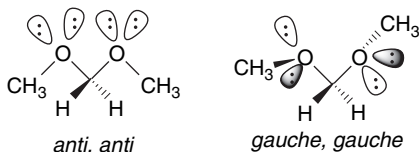
a. P. v. R. Schleyer, E. D. Jemmis, and G. W. Spitznagel, *J. Am. Chem. Soc.*, **107**, 6393 (1985).

¹¹⁰ I. V. Alabugin and T. A. Zeidan, *J. Am. Chem. Soc.*, **124**, 3175 (2002).

$\text{H}_2\text{N}-\text{CH}_2-\text{X} \leftrightarrow \text{H}_2\text{N}^+=\text{CH}_2 \text{ X}^-$	
X	kcal/mol
H	8.07
F	20.49
Cl	22.55
Br	29.87

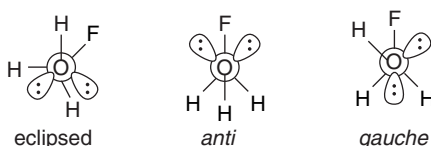
Heteroatom hyperconjugation favors the *anti* alignment of the interacting orbitals. One way to estimate the magnitude of the stabilization is to compare the conformations of individual molecules that are or are not properly aligned for hyperconjugation. Hyperconjugative stabilization is expected to have at least three interrelated consequences: (1) altered bond lengths; (2) enhanced polarity, as represented by the charged resonance structure; and (3) an energetic preference for the conformation that optimizes hyperconjugation. These issues have been examined for many small molecules, and we illustrate the analysis by considering a few, such as dimethoxymethane, fluoromethanol, fluoromethylamine, and diaminomethane.

Dimethoxymethane prefers a conformation that allows alignment of an unshared pair on each oxygen (donor) with a C–O σ^* orbital on the other. This condition is met in the conformation labeled *gauche, gauche*. In contrast, the extended hydrocarbon-like *anti, anti* conformation does not permit this alignment.



Calculations using the 6-31* basis set found the *gauche, gauche* conformation to be about 5 kcal/mol more stable than the *anti, anti*.¹¹¹ Later MP2/6-311++G** and B3LYP/6-31G** calculations found the *gauche, gauche* arrangement to be about 7 kcal/mol more stable than *anti, anti*. There are two other conformations that have intermediate (3–4 kcal/mol) energies.¹¹² Dissecting these conformational preferences to give an energy for the anomeric effect is complicated, but there is general agreement that in the case of dimethoxymethane it accounts for several kcal/mol of stabilization.

Fluoromethanol also shows a preference for the *gauche* conformation. At the HF/6-31G** level it is 4.8 kcal/mol more stable than the *anti* conformation and 2.4 kcal/mol more stable than the eclipsed conformation.¹¹³ Only the *gauche* conformation aligns an unshared pair *anti* to the C–F bond.



NPA analysis was used to isolate the $n \rightarrow \sigma^*$ component and placed a value of 18 kcal/mol on the heteroatom hyperconjugation. This is about 11 kcal/mol higher than

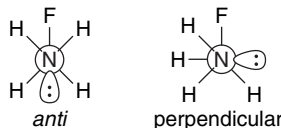
¹¹¹ K. B. Wiberg and M. A. Murcko, *J. Am. Chem. Soc.*, **111**, 4821 (1989).

¹¹² J. R. Kneisler and N. L. Allinger, *J. Comput. Chem.* **17**, 757 (1996).

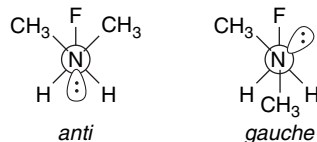
¹¹³ U. Salzner and P. v. R. Schleyer, *J. Am. Chem. Soc.*, **115**, 10231 (1993).

the same component in the *anti* and eclipsed conformations, so other factors must contribute to reducing the total energy difference.

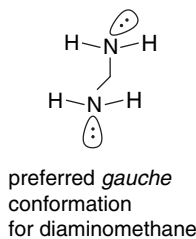
Another molecule that has received attention is fluoromethylamine. From MP2/6-31G** calculations the *anti* arrangement of the nitrogen unshared pair and the C–F bond is found to be the most stable conformation by 7.5 kcal/mol.¹¹⁴ Some of the structural effects expected for hyperconjugation, such as lengthening of the C–F bond are seen, but are not dramatic.¹¹⁵



Experimental structural data (electron diffraction) is available for *N*-fluoromethyl-*N,N*-dimethylamine.¹¹⁶ The only conformation observed is the *anti* arrangement of the unshared pair and C–F bond. MP2/6-311G(2d,p) calculations suggest that the *gauche* alignment is about 5 kcal/mol less stable.



Diaminomethane would also be expected to be stabilized by an anomeric effect. Overall, there is a rather small preference for the *gauche*, *gauche* conformation, but NPA analysis suggests that there is an $n \rightarrow \sigma^*$ component of 5–6 kcal/mol that is offset by other factors.¹¹⁷



We should conclude by emphasizing that the *stabilization of these compounds does not mean that they are unreactive*. In fact, α -halo ethers and α -halo amines are highly reactive toward solvolysis. The hyperconjugation that is manifested in net stabilization *weakens* the carbon-halogen bond and the molecules dissociate readily in polar solvents. Methoxymethyl chloride is at least 10^{14} times as reactive a methyl

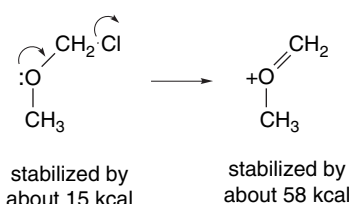
¹¹⁴. J. J. Irwin, T. K. Ha, and J. Dunitz, *Helv. Chim. Acta*, **73**, 1805 (1990).

¹¹⁵. K. B. Wiberg and P. R. Rablen, *J. Am. Chem. Soc.*, **115**, 614 (1993).

¹¹⁶. D. Christen, H. G. Mack, S. Rudiger, and H. Oberhammer, *J. Am. Chem. Soc.*, **118**, 3720 (1996).

¹¹⁷. L. Carballeira and I. Perez-Juste, *J. Comput. Chem.* **22**, 135 (2001).

chloride toward solvolysis in ethanol,¹¹⁸ owing to the fact that the cationic intermediate is stabilized even more, 57.6 kcal/mol, according to the computational results on p. 22.

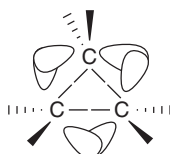


As indicated at the beginning of this section, heteroatom hyperconjugation was first recognized in carbohydrates. The anomeric effect has been particularly well studied in cyclic systems, such as found in carbohydrates. We return to the anomeric effect in cyclic systems in Topic 2.3.

Topic 1.3. Bonding in Cyclopropane and Other Small Ring Compounds

Molecules such as cyclopropane that are forced by geometry to have nonideal bond angles are said to be *strained*. This means that the bonds are not as strong as those in comparable molecules having ideal bond angles and results in both lower thermodynamic stability and increased reactivity. The increased reactivity has at least two components. (1) Typically, reactions lead to a less strained product and partial relief of strain lowers the energy barrier. (2) Strained molecules require orbital rehybridization, which results in electrons being in higher energy orbitals, so they are more reactive.¹¹⁹ There have been many experimental and computational studies aimed at understanding how strain affects structure and reactivity.

The simplest VB description of cyclopropane is in terms of bent bonds. If the carbons are considered to be sp^3 hybrid, in accordance with their tetravalent character, the bonding orbitals are not directed along the internuclear axis. The overlap is poorer and the bonds are “bent” and weaker.



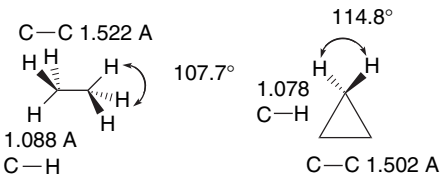
The overlap can be improved somewhat by adjustment of hybridization. Increased p character in the C–C bonds reduces the interorbital angle and improves overlap, which means that the C–H bonds must have increased s character. Compared to ethane or propane, cyclopropane has slightly shorter C–C and C–H distances and an open CH₂ bond angle,¹²⁰ which is consistent with rehybridization. The C–H bonds in cyclopropane are significantly stronger than those in unstrained hydrocarbons, owing

¹¹⁸. P. Ballinger, P. B. de la Mare, G. Kohnstam, and B. M. Prestt, *J. Chem. Soc.*, 3641 (1955).

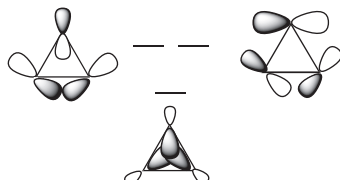
¹¹⁹. A. Sella, H. Basch, and S. Hoz, *J. Am. Chem. Soc.*, **118**, 416 (1996).

¹²⁰. J. Gauss, D. Cremer, and J. F. Stanton, *J. Phys. Chem. A*, **104**, 1319 (2000).

to the greater *s* character in the carbon orbital. Proponents of VB description argue that the properties of cyclopropane are well described by the bent bond idea and that no other special characteristics are needed to explain bonding in cyclopropane.¹²¹ There is, however, an unresolved issue. Cyclopropane has a total strain energy of 27.5 kcal/mol. This is only slightly greater than that for cyclobutane (26.5 kcal/mol), which suggests that there might be some special stabilizing feature present in cyclopropane.



In MO terms, cyclopropane can be described as being formed from three sp^2 -hybridized methylene groups. The carbon-carbon bonds in the plane of the ring are then considered to be derived from six unhybridized carbon $2p$ orbitals. This leads to a delocalized molecular orbital with maximum overlap *inside* the ring and two other degenerate orbitals that have maximum density *outside* the ring. According to this picture, the orbital derived from lobes pointing to the center of the ring should be particularly stable, since it provides for delocalization of the electrons in this orbital.



MOs for cyclopropane derived from C $2p$ orbitals

Schleyer and co-workers made an effort to dissect the total bonding energy of cyclopropane into its stabilizing and destabilizing components.¹²² Using C–H bond energies to estimate the strain in the three-membered ring relative to cyclohexane, they arrived at a value of 40.4 kcal/mol for total strain. The stronger C–H bonds (108 kcal/mol), contribute 8.0 kcal/mol of stabilization, relative to cyclohexane. Using estimates of other components of the strain, such as eclipsing, they arrived at a value of 11.3 kcal/mol as the stabilization owing to σ delocalization. The concept of σ delocalization is also supported by the NMR spectrum and other molecular properties that are indicative of a ring current. (See Section 8.1.3 for a discussion of ring current as an indicator of electron delocalization.) The Laplacian representation (see Topic 1.4) of the electron density for cyclopropane shown in Figure 1.36 shows a peak at the center of the ring that is not seen in cyclobutane.¹²³ The larger cross-ring distances in cyclobutane would be expected to reduce overlap of orbitals directed toward the center of the ring.

¹²¹ J. G. Hamilton and W. E. Palke, *J. Am. Chem. Soc.*, **115**, 4159 (1993); P. Karadakov, J. Gerratt, D. L. Cooper, and M. Raimondi, *J. Am. Chem. Soc.*, **116**, 7714 (1994); P. B. Karadakov, J. Gerratt, D. L. Cooper, and M. Raimondi, *Theochem*, **341**, 13 (1995).

¹²² K. Exner and P. v. R. Schleyer, *J. Phys. Chem. A*, **105**, 3407 (2001).

¹²³ D. Cremer and J. Gauss, *J. Am. Chem. Soc.*, **108**, 7467 (1986).

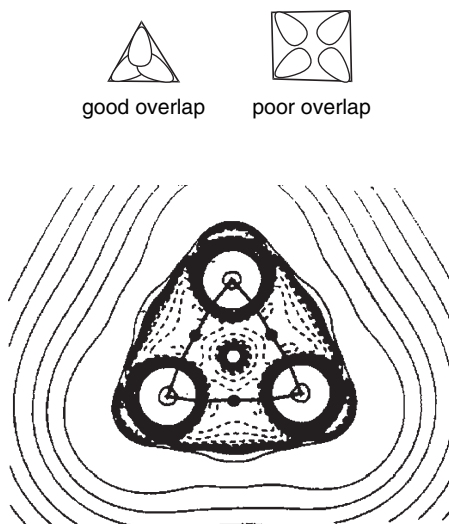
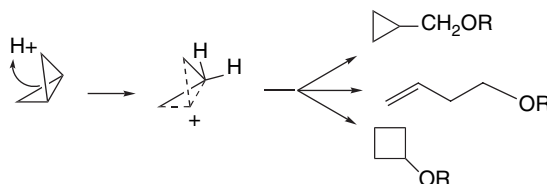


Fig. 1.36. Contours of the Laplacian for cyclopropane in the plane of the rings. Dots are bond critical points. Reproduced with permission from R. F. W. Bader, in *Chemistry of Alkanes and Cycloalkanes*, S. Patai and Z. Rappoport, eds., John Wiley & Sons, New York, 1992, Chap. 1.

Bicyclo[1.1.0]butane, bicyclo[1.1.1]pentane, [1.1.1]propellane, and spiro[2.2]pentane are other molecules where strain and rehybridization affect molecular properties. The molecules show enhanced reactivity that can be attributed to characteristics of the rehybridized orbitals. The structures are shown in Scheme 1.6, which also shows calculated AIM charge distributions and strain energy.

The strain in bicyclo[1.1.0]butane results in decreased stability and enhanced reactivity.¹²⁴ The strain energy is 63.9 kcal/mol; the central bond is nearly pure *p* in character,¹²⁵ and it is associated with a relatively high HOMO.¹²⁶ These structural features are reflected in enhanced reactivity toward electrophiles. In acid-catalyzed reactions, protonation gives the bicyclobutonium cation (see Section 4.4.5) and leads to a characteristic set of products.



¹²⁴ S. Hoz, in *The Chemistry of the Cyclopropyl Group*, Part 2, S. Patai and Z. Rappoport, eds., Wiley, Chichester, 1987, pp 1121–1192; M. Christl, *Adv. Strain Org. Chem.*, **4**, 163 (1995).

¹²⁵ J. M. Schulman and G. J. Fisanick, *J. Am. Chem. Soc.*, **92**, 6653 (1970); R. D. Bertrand, D. M. Grant, E. L. Allred, J. C. Hinshaw, and A. B. Strong, *J. Am. Chem. Soc.*, **94**, 997 (1972); D. R. Whitman and J. F. Chiang, *J. Am. Chem. Soc.*, **94**, 1126 (1972); H. Finkelmeier and W. Lüttke, *J. Am. Chem. Soc.*, **100**, 6261 (1978).

¹²⁶ K. B. Wiberg, G. B. Ellison, and K. S. Peters, *J. Am. Chem. Soc.*, **99**, 3941 (1977).

Scheme 1.6. AIM Charge Distribution and Strain Energy (kcal/mol) for Cyclic Hydrocarbons**Monocyclic**

Charge:	C -0.010 H +0.005	C +0.06 H -0.03	C +0.08 H -0.04	C +0.08 H -0.04
Strain:	27.5	26.5	6.2	0

Bicyclic

		C(5) -0.03 H(5) +0.002		C(2) -0.059 H(2) -0.030
	C(2) +0.072 H(2) -0.002 C(1) -0.12 H(1) +0.054 63.9		C(2) +0.082 H(2) -0.025 C(1) +0.030 H(1) -0.028 51.8	
	C(2) +0.043 H(2) -0.030 C(1) +0.036 H(1) -0.011 68.0			C(2) +0.061 H(2) -0.40 C(1) +0.101 H(1) -0.044 7.4

Propellanes

	C(2) +0.026 H(2) +0.023 C(1) -0.107 98		C(7) +0.042 H(7) +0.013 C(2) +0.099 H(2) -0.020 C(1) -0.152 105		C(2) +0.051 H(2) -0.023 C(1) =-0.016 89

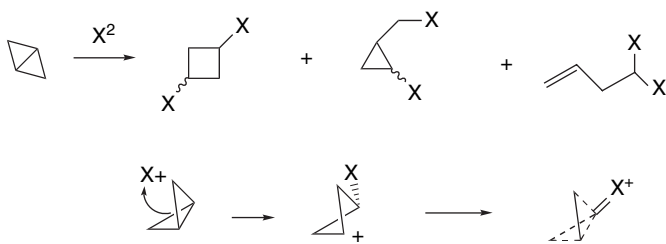
Others

	C(2) =+ 0.003 H(2) =+ 0.007 C(1) =-0.072 63.2		C(1) =-0.111 H(1) =+ 0.111 140		C(1) =+ 0.003 H(1) =-0.003 154.7

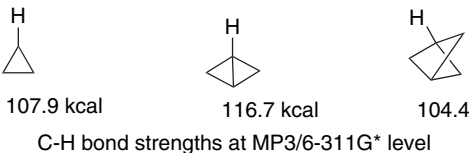
a. R. F. W. Bader in *The Chemistry of Alkanes and Cycloalkanes*, S. Patai and Z. Rappoport, eds., John Wiley & Sons, New York, 1992, p. 51.

Bicyclo[1.1.0]butane also reacts with the halogens. With I₂, the main product is 1,3-diiodocyclobutane (5:1 *cis:trans*). With Br₂ and Cl₂, cyclopropylcarbinyl and butenyl products are also formed.¹²⁷ The initial attack occurs from the *endo* face of the molecule and the precise character of the intermediate appears to be dependent on the halogen.

¹²⁷. K. B. Wiberg, G. M. Lampman, R. P. Ciula, D. S. Connor, P. Schertler, and J. Lavanish, *Tetrahedron*, **21**, 2749 (1968); K. B. Wiberg and G. J. Szeimies, *J. Am. Chem. Soc.*, **92**, 571 (1970).



The bridgehead C–H bond in tricyclo[1.1.1]pentane is not quite as strong as the C–H bond in cyclopropane. A value of 104.4 kcal/mol is calculated at the MP3/6-31G* level.¹²⁸ The total strain energy is 68 kcal/mol.



The alignment of the two bridgehead bonds is such that there is strong interaction between them. As a result of this interaction, there is hyperconjugation between the two bridgehead substituents. For example, the ^{19}F chemical shifts are effected by $\sigma \rightarrow \sigma^*$ donation to the C–F σ^* orbital.¹²⁹

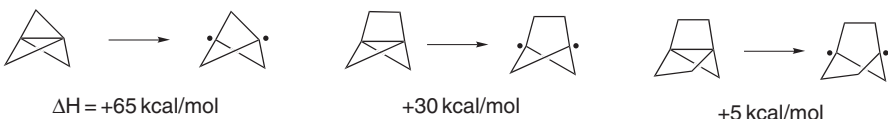


[1.1.1]Propellane has a very unusual shape. All four bonds at the bridgehead carbons are directed toward the same side of the nucleus.¹³⁰ There have been many computational studies of the [1.1.1]propellane molecule. One of the main objectives has been to understand the nature of the bridgehead-bridgehead bond and the extension of the orbital external to the molecule. The distance between the bridgehead carbons in [1.1.1]propellane is calculated to be 1.59 Å. The molecule has been subjected to AIM analysis. The $\rho_{(c)}$ value for the bridgehead-bridgehead bond is $0.173 a_0^{-3}$, which indicates a bond order of about 0.7.¹³¹ There is a low-temperature X-ray crystal structure of [1.1.1]propellane. Although it is not of high resolution, it does confirm the length of the bridgehead bond as 1.60 Å.¹³² Higher-resolution structures of related tetracyclic compounds give a similar distance and also show electron density external to the bridgehead carbons.¹³³

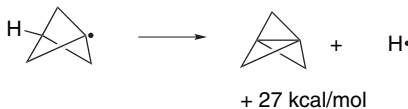


- ^{128.} K. B. Wiberg, C. M. Hadad, S. Sieber, and P. v. R. Schleyer, *J. Am. Chem. Soc.*, **114**, 5820 (1992).
- ^{129.} W. Adcock and A. N. Abeywickrema, *J. Org. Chem.*, **47**, 2957 (1982); J. A. Koppel, M. Mishima, L. M. Stock, R. W. Taft, and R. D. Topsom, *J. Phys. Org. Chem.*, **6**, 685 (1993).
- ^{130.} L. Hedberg and K. Hedberg, *J. Am. Chem. Soc.*, **107**, 7257 (1985).
- ^{131.} K. B. Wiberg, R. F. W. Bader, and C. D. H. Lau, *J. Am. Chem. Soc.*, **109**, 985 (1987); W. Adcock, M. J. Brunger, C. I. Clark, I. E. McCarthy, M. T. Michalewicz, W. von Niessen, E. Weigold, and D. A. Winkler, *J. Am. Chem. Soc.*, **119**, 2896 (1997).
- ^{132.} P. Seiler, *Helv. Chim. Acta*, **73**, 1574 (1990).
- ^{133.} P. Seiler, J. Belzner, U. Bunz, and G. Szeimies, *Helv. Chim. Acta*, **71**, 2100 (1988).

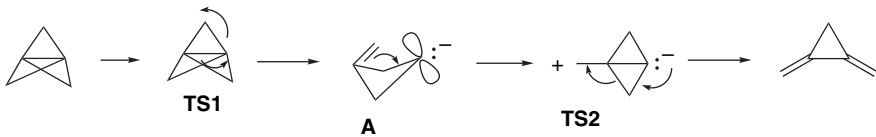
Surprisingly, [1.1.1]propellane is somewhat more stable to thermal decomposition than the next larger propellane, [2.1.1]propellane, indicating a reversal in the trend of increased reactivity with increased strain. To understand this observation, it is important to recognize that the energy of *both the reactant and intermediate* influence the rate of unimolecular reactions that lead to decomposition. In the case of propellanes, homolytic rupture of the central bond is expected to be the initial step in decomposition. This bond rupture is very endothermic for [1.1.1]propellane. Because relatively less strain is released in the case of [1.1.1]propellane than in the [2.1.1]- and [2.2.1]-homologs, [1.1.1]propellane is kinetically most stable.¹³⁴



Another manifestation of the relatively small release of strain associated with breaking the central bond comes from MP4/6-31G* calculations on the energy of the reverse ring closure.¹³⁵



The thermal decomposition of [1.1.1]propellane has been studied both experimentally and by computation.¹³⁶ The initial product is 1,2-dimethylenecyclopropane, and the E_a is 39.7 kcal/mol. The mechanism of the reactions has been studied using both MO and DFT calculations. The process appears to be close to a concerted process, which is represented in Figure 1.37. DFT computations suggest that structure A is an intermediate,¹³⁷ slightly more stable than TS1 and TS2. The corresponding MO calculations [CCSD(T)/6-311G(2d,p)] do not find a minimum. However, both methods agree that A, TS1, and TS2 are all close in energy. Note that this reaction is *heterolytic* and that the diradical is not an intermediate. This implies that there is a smaller barrier for the observed reaction than for homolytic rupture of the central bond. The calculated E_a is substantially less than the bond energy assigned to the bridgehead bond, which implies that bond making proceeds concurrently with bond breaking, as expected for a concerted process.



Visual models, additional information and exercises on Thermal Rearrangement of [1.1.1]Propellane can be found in the Digital Resource available at: Springer.com/carey-sundberg.

¹³⁴. K. B. Wiberg, *Angew. Chem. Int. Ed. Engl.*, **25**, 312 (1985).

¹³⁵. W. Adcock, G. T. Binmore, A. R. Krstic, J. C. Walton and J. Wilkie, *J. Am. Chem. Soc.*, **117**, 2758 (1995).

¹³⁶. O. Jarosch, R. Walsh, and G. Szeimies, *J. Am. Chem. Soc.*, **122**, 8490 (2000).

¹³⁷. Both B3LYP/6-311G(d,p) and B3PW91/D95(d,p) computations were done and the latter were in closer agreement with the CCSD(T)/6-311G(2d,p) results.

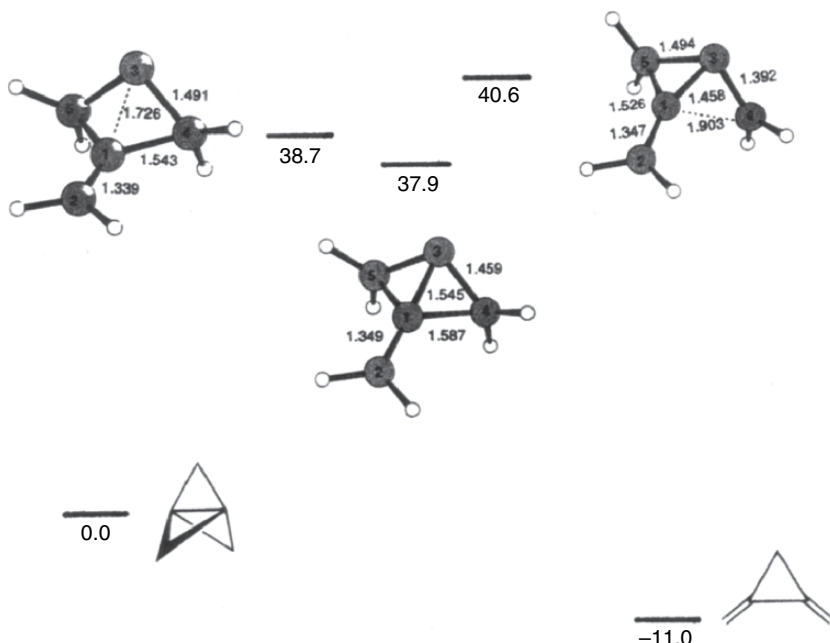
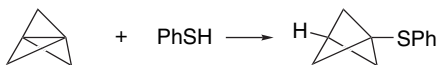
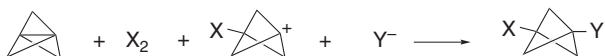


Fig. 1.37. DFT (B3PW91/D95(*d,p*) representation of the thermal isomerization of [1.1.1]propellane to 1,2-dimethylenecyclopropane. Adapted from O. Jarosch, R. Walsh, and G. Szeimies, *J. Am. Chem. Soc.*, **122**, 8490 (2000).

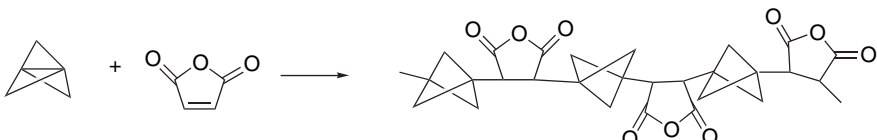
Both radicals and electrophiles react at the bridgehead bond of [1.1.1]propellane. The reactivity toward radicals is comparable to that of alkenes, with rates in the range of 10^6 to $10^8\text{ M}^{-1}\text{s}^{-1}$, depending on the particular radical.¹³⁸ For example, [1.1.1]propellane reacts with thiophenol at room temperature.¹³⁹



Reaction with the halogens breaks the bridgehead bond and leads to 1,3-dihalobicyclo[1.1.1]butanes. When halide salts are included, mixed dihalides are formed, suggesting an ionic mechanism.¹⁴⁰



[1.1.1]Propellane and maleic anhydride copolymerize to an alternating copolymer.¹⁴¹



Each of these reactions indicates the high reactivity of the bridgehead-bridgehead bond.

¹³⁸. P. F. McGarry and J. C. Scaiano, *Can. J. Chem.*, **76**, 1474 (1998).

¹³⁹. K. B. Wiberg and S. T. Waddell, *J. Am. Chem. Soc.*, **112**, 2194 (1990).

¹⁴⁰. I. R. Milne and D. K. Taylor, *J. Org. Chem.*, **63**, 3769 (1998).

¹⁴¹. J. M. Gosau and A.-D. Schlüter, *Chem. Ber.*, **123**, 2449 (1990).

Topic 1.4. Representation of Electron Density by the Laplacian Function

Electron distribution in molecules can be usefully represented by the *Laplacian* of the electron density. The Laplacian is defined by the equation

$$\nabla^2\rho = \frac{\partial^2\rho}{\partial x^2} + \frac{\partial^2\rho}{\partial y^2} + \frac{\partial^2\rho}{\partial z^2} \quad (1.30)$$

which is a measure of the curvature of the electron density. The negative of $\nabla^2\rho$, called L , depicts regions of electron concentration as maxima and regions of electron depletion as minima. The Laplacian function can distinguish these regions more easily than the total electron density contours. It also depicts the concentric shells corresponding to the principal quantum numbers. Figure 1.38 shows the L functions for water, ammonia, and methane. The diagrams show concentration of valence shell electron density in the region of bonds. The water and ammonia molecules also show maxima corresponding to the nonbonding electrons.

Figure 1.39 shows L for ethane, ethene, and ethyne.¹⁴² Note the regions of bonding associated with the two shells of carbon between the two carbons and between carbon and hydrogen. Figure 1.40 shows a perspective view of ethene indicating the saddle point between the carbon atoms. The ridge with a saddle point corresponds to electron density in the nodal plane of the π bond.

Figure 1.41 compares the Laplacian of the experimental electron density from a low-temperature crystallographic study of ethane with the computed L using the 6-311G** basis set.¹⁴³ This serves to make a connection between computed and experimental electron density.

The electron density for small molecules corresponds to expectations based on electronegativity. Figure 1.42 gives $L(\mathbf{r})$ for N₂ (a), CO (b), and H₂C=O (c, d). The diagram for nitrogen shows the concentric shells and accumulation of electron density between the nitrogen nuclei. The distribution, of course, is symmetrical. For C≡O there is a substantial shift of electron density toward carbon, reflecting the polar character of the C≡O bond. Figure 1.42c is $L(\mathbf{r})$ in the molecular plane of formaldehyde. In

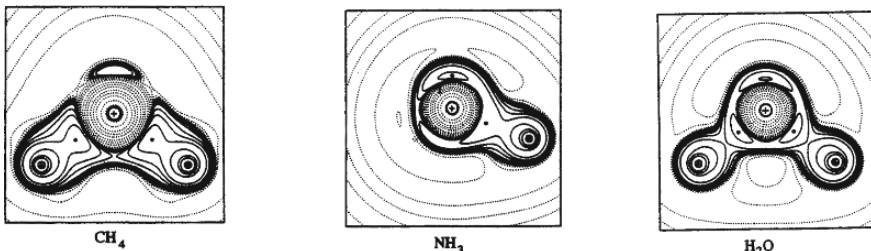


Fig. 1.38. Contour maps of L for methane, ammonia, and water. For water, the contours are in the plane of the molecule. For ammonia and methane the contours are in the plane that bisects the molecule with a hydrogen above and below the plane. Reproduced with permission from R. J. Gillespie and P. L. A. Popelier, *Chemical Bonding and Molecular Geometry*, Oxford University Press, Oxford, 2001, p. 172.

¹⁴² R. F. W. Bader, S. Johnson, T.-H. Tang and P. L. A. Popelier *J. Phys. Chem.*, **100**, 15398 (1996).

¹⁴³ V. G. Tsirelson, *Can. J. Chem.*, **74**, 1171 (1996).

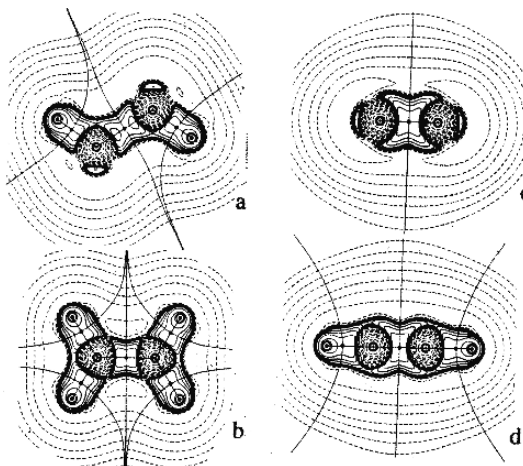


Fig. 1.39. Contour maps of $L(r)$ for: (a) ethane in a plane bisecting anti-hydrogens; (b) ethene in the molecular plane; (c) ethene perpendicular to the molecular plane, and (d) ethyne. The solid lines depict the zero-flux surfaces of the C and H atoms. From *J. Phys. Chem.* **100**, 15398 (1996).

addition to the C–H bonds, the contours indicate the electron density associated with the unshared pairs on oxygen. Figure 1.42d, shows L perpendicular to the plane of the molecule and is influenced by the π component of the C=O bond. It shows greater electron density around oxygen, which is consistent with the expectation that carbon would have a partial positive charge.

These diagrams can help to visualize the electron density associated with these prototypical molecules. We see that most electron density is closely associated with

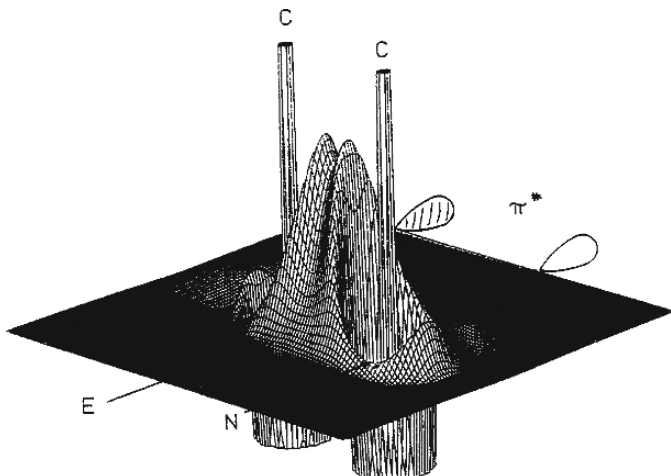


Fig. 1.40. Perspective of Laplacian $-\nabla^2 \rho_c(r)$ of ethene in a plane perpendicular to the molecular plane. From E. Kraka and D. Cremer in *The Concept of the Chemical Bond*, Z. B. Maksic, ed., Springer-Verlag 1990, p. 533.

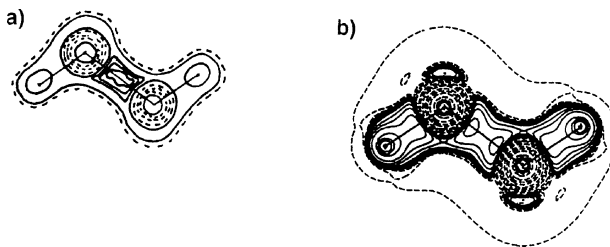


Fig. 1.41. Comparison of experimental (a) and theoretical (b) Laplacian of the electron density of ethane. From *Can. J. Chem.*, **74**, 1171 (1996).

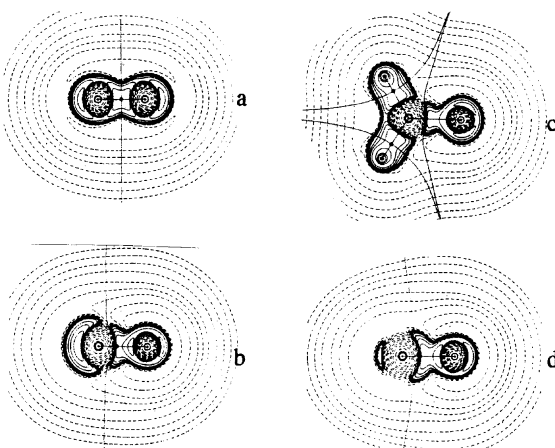


Fig. 1.42. Contour plots of $L(\mathbf{r})$ for N_2 (a), CO (b), and $H_2C=O$ in (c) and perpendicular to (d) the plane of the molecule. From *J. Phys. Chem.*, **100**, 15398 (1996).

the nuclei, but that regions of increased electron density corresponding to chemical bonds can be recognized. Most of the electron density diagrams that are available are the results of computation. Where experimental data are available, there is excellent correspondence with the computational data.

Topic 1.5. Application of Density Functional Theory to Chemical Properties and Reactivity

The qualitative ideas of valence bond (VB) theory provide a basis for understanding the relationships between structure and reactivity. Molecular orbital (MO) theory offers insight into the origin of the stability associated with delocalization and also the importance of symmetry. As a central premise of density functional theory (DFT) is that the electron density distribution determines molecular properties, there has been an effort to apply DFT to numerical evaluation of the qualitative concepts such as electronegativity, polarizability, hardness, and softness. The sections that follow explore the relationship of these concepts to the description of electron density provided by DFT.

DFT suggests quantitative expressions and interrelation of certain properties such as electronegativity and polarizability, and the related concepts of hardness and softness introduced in Sections 1.1.3 through 1.1.6.¹⁴⁴ DFT calls the escaping tendency of an electron from a particular field its *chemical potential*,¹⁴⁵ μ , defined by

$$\mu = (\partial E / \partial N)_v \quad (1.31)$$

which is the slope of a curve for the energy of the system as a function of the change in the number of electrons.

A stable system, such as a molecule, attains a common chemical potential among its components. That is, there is no net force to transfer electron density from one point to another. The idea that chemical potential is equivalent throughout a molecule, and specifically between bonded atoms, accords with the concept of *electronegativity equalization* (see Section 1.1.4).¹⁴⁶ Chemical potential is related to electrophilicity and nucleophilicity. A system with an attraction toward electrons is electrophilic, whereas a system that can donate electrons is nucleophilic. Chemical potential is considered to be the opposite of absolute (Mulliken) electronegativity and can be approximated by

$$\mu = -\frac{IP + EA}{2} \quad (1.32)$$

which is negative of the Mulliken absolute electronegativity:

$$\chi = \frac{IP + EA}{2} \quad (1.33)$$

Since μ is the slope of electronic energy as a function of the change in the number of electrons, the Mulliken equation gives the energy for the +1 (IP) and -1 (EA) ionization states. This is illustrated in Figure 1.43, which shows that $(IP + EA)/2$ is the average slope over the three points and should approximate the slope at the midpoint, where $N = 0$.¹⁴⁷

The Luo-Benson expression for electronegativity¹⁴⁸

$$V = n/r \quad (1.34)$$

which relates electronegativity to the number of valence shell electrons n and the atomic radius r is both theoretically related¹⁴⁹ and empirically correlated¹⁵⁰ with the Mulliken

- ¹⁴⁴. P. W. Chattaraj and R. G. Parr, *Structure and Bonding*, **80**, 11 (1993); G.-H. Liu and R. G. Parr, *J. Am. Chem. Soc.*, **117**, 3179 (1995).
- ¹⁴⁵. R. G. Parr, R. A. Donnelly, M. Levy, and W. E. Palke, *J. Chem. Phys.*, **68**, 3801 (1978).
- ¹⁴⁶. R. T. Sanderson, *J. Am. Chem. Soc.*, **105**, 2259 (1983); R. T. Sanderson, *Polar Covalence*, Academic Press, New York, 1983.
- ¹⁴⁷. R. G. Pearson, *Chemical Hardness*, Wiley-VCH, Weinheim, 1977, p. 33; see also R. P. Iczkowski and J. L. Margrave, *J. Am. Chem. Soc.*, **83**, 3547 (1961).
- ¹⁴⁸. Y. R. Luo and S. W. Benson, *J. Phys. Chem.*, **92**, 5255 (1988); Y.-R. Luo and S. W. Benson, *J. Am. Chem. Soc.*, **111**, 2480 (1989); Y. R. Luo and S. W. Benson, *J. Phys. Chem.*, **94**, 914 (1990); Y. R. Luo and S. W. Benson, *Acc. Chem. Res.*, **25**, 375 (1992).
- ¹⁴⁹. P. Politzer, R. G. Parr, and D. R. Murphy, *J. Chem. Phys.*, **79**, 3859 (1983).
- ¹⁵⁰. Y. R. Luo and P. D. Pacey, *J. Am. Chem. Soc.*, **113**, 1465 (1991).

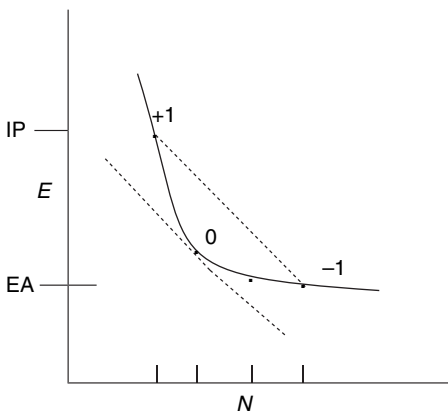


Fig. 1.43. Diagram showing that $(EA + IP)/2$ provides an approximation of the slope of E for the neutral atoms. Adapted from R. G. Pearson, *Chemical Hardness*, Wiley-VCH, Weinheim, 1997, p. 33.

absolute electronegativity $(IP + EA)/2$. The principle of maximum hardness¹⁵¹ (p. 16) can be derived as a consequence of DFT, as can the concepts of hardness and softness.¹⁵²

In DFT, hardness is defined as

$$2\eta = (\partial\mu/\partial N)_v \quad (1.35)$$

which is the curvature of the plot of E versus N and is approximated by

$$\eta \cong (IP - EA)/2 \quad (1.36)$$

and softness, $S = 1/\eta$ is

$$(\partial N/\partial\mu)_v \cong 2/(IP - EA) \quad (1.37)$$

There is a linear correlation between the empirical electronegativity (Pauling scale) and hardness and the absolute electronegativity (Mulliken electronegativity) for the nontransition metals¹⁵³:

$$\chi = 0.44\eta + 0.044\chi_{abs} + 0.04 \quad (1.38)$$

This correlation is illustrated in Figure 1.44. Polarizability is related to softness. Expressed as $\alpha^{1/3}$, it is proportional to softness, approximated by $2/(IP - EA)$.¹⁵⁴

DFT also suggests explicit definitions of covalent and van der Waals radii. The covalent radius in the AIM context is defined by the location of the bond critical point

- ¹⁵¹. R. G. Parr and P. K. Chattaraj, *J. Am. Chem. Soc.*, **113**, 1854 (1991); T. K. Ghanty and S. K. Ghosh, *J. Phys. Chem.*, **100**, 12295 (1996).
- ¹⁵². P. K. Chattaraj, H. Lee, and R. G. Parr, *J. Am. Chem. Soc.*, **113**, 1855 (1991).
- ¹⁵³. R. G. Pearson, *Chemical Hardness*, Wiley-VCH, Weinheim, Germany, 1997, p. 44; J. K. Nagle, *J. Am. Chem. Soc.*, **112**, 4741 (1990).
- ¹⁵⁴. T. K. Ghanty and S. K. Ghosh, *J. Phys. Chem.*, **97**, 4951 (1993); S. Hati and D. Datta, *J. Phys. Chem.*, **98**, 10451 (1994).

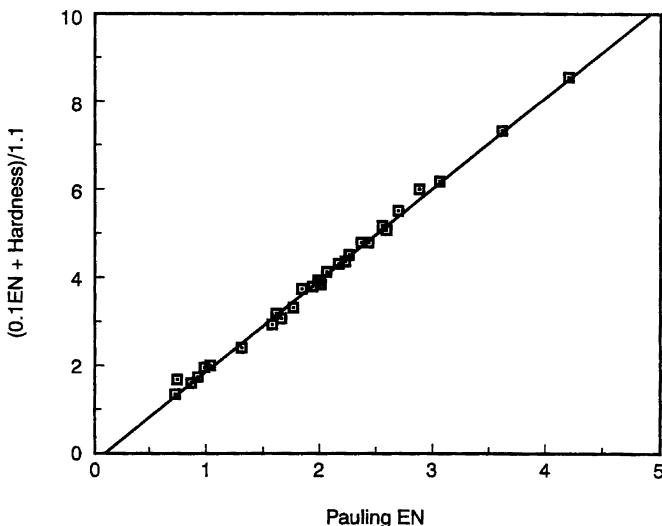


Fig. 1.44. Correlation between empirical (Pauling) electronegativity, (χ_{Pauling}), hardness (η), and absolute (Mulliken) electronegativity (χ_{abs}). From R. G. Pearson, *Chemical Hardness*, Wiley-VCH, Weinheim, 1997, p. 54.

and depends on the other element in the bond. The covalent radii of atoms can also be defined theoretically within DFT,¹⁵⁵ and are equated with the distance at which the chemical potential equals the total electrostatic potential calculated for the atom. This is the point at which the electrostatic potential crosses from negative to positive and where the sum of the kinetic energy and exchange and correlation functionals is zero. Using the approximation $-(\text{IP} + \text{EA})/2 = \mu$, one finds φ_r , the distance at which this equality holds¹⁵⁶:

$$\text{at } r_c V_c = \mu \cong -\frac{\text{IP} + \text{EA}}{2} \quad (1.39)$$

The values derived in this way are shown in Table 1.24.

The AIM treatment defines van der Waals radii in terms of a particular electron density contour. It has been suggested that the 0.002 au contour provides a good representative of the van der Waals dimension of a molecule.¹⁵⁷

T.1.5.2. DFT Formulation of Reactivity—The Fukui Function

The electron density $\rho(\mathbf{r})$ can provide information about the *reactivity* of a molecule. MO theory can assess reactivity in terms of frontier orbitals and, in particular, the energy, atomic distribution and symmetry of the HOMO and LUMO. DFT provides a representation of total electron distribution and extracts indicators of reactivity. The

¹⁵⁵ P. Ganguly, *J. Am. Chem. Soc.*, **115**, 9287 (1993).

¹⁵⁶ P. Politzer, R. G. Parr, and D. R. Murphy, *J. Chem. Phys.*, **79**, 3859 (1983).

¹⁵⁷ R. F. W. Bader, W. H. Henneker, and P. D. Cade, *J. Chem. Phys.* **46**, 3341 (1967); R. F. W. Bader and H. J. T. Preston, *Theor. Chim. Acta*, **17**, 384 (1970).

Table 1.24. Covalent Radii from DFT

Atom	Covalent radius (au) ^a
Li	1.357
B	1.091
C	0.912
N	0.814
O	0.765
F	0.671
Na	1.463
Al	1.487
Si	1.296
P	1.185
S	1.120
Cl	0.999
Se	1.209
Br	1.116
I	1.299

a. P. Politzer, R. G. Parr, and D. R. Murphy, *J. Chem. Phys.*, **79**, 3859 (1983); M. K. Harbola, R. G. Parr, and C. Lee, *J. Chem. Phys.*, **94**, 6055 (1991).

responsiveness of this electron distribution to a perturbing external field, e.g., an approaching reagent, must be evaluated. This responsiveness is described by the *Fukui function*,¹⁵⁸ which is a reactivity indicator is defined by

$$f(\mathbf{r}) = [n(\mathbf{r})/N] \left[\frac{\delta\mu}{\delta\nu(\mathbf{r})} \right]_N = \left(\frac{\partial\rho(\mathbf{r})}{\partial N} \right)_{\nu(\mathbf{r})} \quad (1.40)$$

where N is the change in the number of electrons in the system.

Fukui functions are defined for electrophilic (f^-), nucleophilic (f^+), and radical (f°) reactions by comparing the electron density $\rho(\mathbf{r})$, with one fewer electron, one more electron, and the average of the two¹⁵⁹:

$$f^-(\mathbf{r}) = \rho_N(\mathbf{r}) - \rho_{N-1}(\mathbf{r}) \quad (1.41)$$

$$f^+(\mathbf{r}) = \rho_{N+1}(\mathbf{r}) - \rho_N(\mathbf{r}) \quad (1.42)$$

$$f^\circ(\mathbf{r}) = \frac{\rho_{N+1}(\mathbf{r}) - \rho_{N-1}(\mathbf{r})}{2} \quad (1.43)$$

The Fukui function describes interactions between two molecules in terms of the electron transfer between them. The extent of electron transfer is related to chemical potential (and electronegativity) and hardness (and polarizability).

$$\Delta N = \frac{|\mu_B^\circ - \mu_A^\circ|}{\eta_B^\circ + \eta_A^\circ} \quad (1.44)$$

The responsiveness of the electron density to interaction with another field is nonuniform over the molecule. The electron density can be further partitioned among

¹⁵⁸. R. G. Parr and W. Yang, *J. Am. Chem. Soc.*, **106**, 4049 (1984).

¹⁵⁹. C. Lee, W. Yang, and R. G. Parr, *Theochem*, **40**, 305 (1988).

the atoms of a molecule by *condensed Fukui* functions. These calculations must use a scheme, such as Mulliken population analysis (see Section 1.4.1) for dividing the electron density among the atoms. The condensed Fukui functions identify regions of space that are electron-rich (f^-) and electron-poor (f^+).¹⁶⁰ Reactivity at individual atoms can also be expressed as *local softness*, which is the product of the Fukui function and global softness S .¹⁶¹ As with the Fukui function, these are defined for electrophilic, nucleophilic, and radical reactants.

$$s^- = [\rho_{(N)} - \rho_{(N-1)}]S \quad (1.45)$$

$$s^+ = [\rho_{(N+1)} - \rho_{(N)}]S \quad (1.46)$$

and

$$s^\circ = \frac{1}{2}[\rho_{(N+1)} - \rho_{(N-1)}]S \quad (1.47)$$

The idea that *frontier orbitals* control reactivity introduced in the context of MO theory has an equivalent in DFT. The electron density distribution should have regions of differing susceptibility to approach by nucleophiles and electrophiles. Reactivity should correspond to the ease of distortion of electron density by approaching reagents. This response to changes in electron distribution is expressed in terms of the Fukui function, which describes the ease of displacement of electron density in response to a shift in the external field. Since the electron distribution should respond differently to interaction with electron acceptors (electrophiles) or electron donors (nucleophiles), there should be separate f^+ and f^- functions. Reaction is most likely to occur at locations where there is the best match (overlap) of the f^+ function of the electrophile and the f^- function of the nucleophile.¹⁶² For example, the f^+ and f^- functions for formaldehyde have been calculated and are shown in Figure 1.45.¹⁶³ The f^+ function, describing interaction with a nucleophile, has a shape similar to the π^* MO. It has a higher concentration on carbon than on oxygen and the maximum value is perpendicular to the molecular plane. The f^- function is similar in distribution to the nonbonding (n) electron pairs of oxygen. This treatment, then, leads to predictions about the reactivity toward nucleophiles and electrophiles that are parallel to those developed from MO theory (see p. 45). A distinction to be made is that in the MO formulation the result arises on the basis of a particular orbital combination—the HOMO and LUMO. The DFT formulation, in contrast, comes from the total electron density. Methods are now being developed to compute Fukui functions and other descriptors of reactivity derived from total electron density.

DFT can evaluate properties and mutual reactivity from the electron distribution. These relationships between qualitative concepts in chemistry, such as electronegativity and polarizability, suggest that DFT does incorporate fundamental relationships between molecular properties and structure. At this point, we want to emphasize the conceptual relationships between the electron density and electronegativity and polarizability. We can expect electrophiles to attack positions with relatively high electron density and polarizability. Nucleophiles should attack positions of relatively

¹⁶⁰ Y. Li and J. N. S. Evans, *J. Am. Chem. Soc.*, **117**, 7756 (1995).

¹⁶¹ W. Yang and W. J. Mortier, *J. Am. Chem. Soc.*, **108**, 5708 (1986).

¹⁶² R. F. Nalewajski, *Top. Catal.*, **11/12**, 469 (2000).

¹⁶³ A. Michalak, F. De Proft, P. Geerlings, and R. F. Nalewajski, *J. Phys. Chem. A*, **103**, 762 (1999); F. Gilardoni, J. Weber, H. Chermette, and T. R. Ward, *J. Phys. Chem. A*, **102**, 3607 (1998).

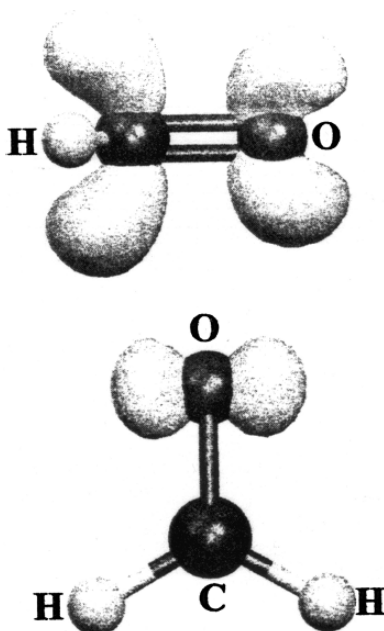


Fig. 1.45. Fukui function f^+ and f^- isosurfaces for $\text{CH}_2=\text{O}$ (0.001 au). Reproduced with permission from F. Gilardoni, J. Weber, H. Chermette, and T. R. Ward, *J. Phys. Chem. A*, **102**, 3607 (1998).

low electron density. The hard-soft concept also states that *reactant and reagent should match* with respect to these properties. The methods for exploiting this potential are currently under development.

T.1.5.3. DFT Concepts of Substituent Groups Effects

The interpretation and correlation of information about organic compounds depends on the concept of *substituent effects*, which is the idea that a particular group of atoms will affect structure and reactivity in a predictable way. This is a long-standing and fundamental concept in organic chemistry. Recent developments, particularly in DFT, have provided new theoretical foundations and interpretations. Substituents groups can be classified as electron-releasing (ERG) or electron-withdrawing (EWG). There is an approximate ordering of such groups that is related in a general way to electronegativity. We discuss substituent effects in detail in Chapter 3, but here we want to introduce some broad concepts concerning the ways that substituents affect structure and reactivity.

Traditionally, the focus has been on polar and resonance effects, based on VB ideas about structure, and the emphasis is on partial charges arising from polar bonds and resonance/hyperconjugation. However, in MO theory, we use the idea of *perturbations*. The question asked is, “How does a substituent affect the energy and shapes of the orbitals, with particular attention to the HOMO and LUMO, the *frontier orbitals*. Ultimately, substituents affect structure and reactivity by changing the electron density distribution. From the concept of electronegativity, we know that bonds have dipoles,

which influence interactions with approaching reagents and thus affect reactivity. We also discussed the concept of *polarizability*, which refers to the ease of distortion of the electron density distribution of an atom or an ion and can be described as *hardness* or *softness*. Since chemical reactions involve the reorganization of electrons by breaking and forming bonds, polarizability also has a major influence on reactivity.

There have been a number of efforts to assign numerical values to electronegativity of substituent groups, analogous to the numbers assigned to atoms (see Section 1.1.3). These have been based on structural parameters, charge distribution, thermodynamic relationships and on MO computations.¹⁶⁴ More recently, DFT descriptions of electron density have developed and these, too, have been applied to organic functional groups. DFT suggests quantitative expressions of some of the qualitative concepts such as electronegativity, polarizability, hardness, and softness.¹⁶⁵ DFT describes a molecule as an electron density distribution, in which the nuclei are embedded, that is subject to interaction with external electrical fields, such as that of an approaching reagent. Several methods are currently being explored to find correlations and predictions based on DFT concepts that were introduced in Section 1.3.

De Proft, Langenaeker, and Geerlings applied the DFT definitions of electronegativity, hardness, and softness to calculate group values, which are shown in Table 1.25. These values reveal some interesting comparisons. The electronegativity values calculated for C₂H₅, CH₂=CH, and HC≡C are in accord with the relationship with hybridization discussed in Section 1.1.5. The methyl group is significantly more electronegative and harder than the ethyl group. This is consistent with the difference noted between methyl and ethyl diazonium ions in Section 1.4.3. Typical EWGs such as CH=O, C≡N, and NO₂ show high electronegativity. Hardness values are more difficult to relate to familiar substituent effects. The acetyl, carboxamide, and nitro groups, for example, are among the softer substituents. This presumably reflects the electron density of the unshared electron pairs on oxygen in these groups.

AIM results from methyl compounds were also used to develop a group electronegativity scale. Boyd and Edgecombe defined a quantity F_A in terms of r_H , the location of the bond critical point to hydrogen, N_A the number of valence electrons of the atom A, and $\rho_{(c)}$, the electron density at the bond critical point¹⁶⁶:

$$F_n = r_H/N_A \rho(r_c) r_{AH} \quad (1.48)$$

These were then scaled to give numerical comparability with the Pauling electronegativity scale.¹⁶⁷ In another approach, the charge on the methyl group was taken as the indicator of the electronegativity of the group X and the results were scaled to the Pauling atomic electronegativity scale.¹⁶⁸ It was also noted that the electronegativity value correlated with the position of the bond critical point relative to the bond length:

$$r_c/R = 0.785 - 0.042\chi_x^0 \quad (1.49)$$

As the group becomes more electronegative, the critical point shifts toward the substituent. Table 1.26 compares two of the traditional empirical electronegativity

¹⁶⁴. A. R. Cherkasov, V. I. Galkin, E. M. Zueva, and R. A. Cherkasov, *Russian Chem. Rev.* (Engl. Transl.), **67**, 375 (1998).

¹⁶⁵. P. W. Chattaraj and R. G. Parr, *Struct. Bonding*, **80** 11 (1993); G.-H. Liu and R. G. Parr, *J. Am. Chem. Soc.*, **117**, 3179 (1995).

¹⁶⁶. R. J. Boyd and K. E. Edgecombe, *J. Am. Chem. Soc.*, **110**, 4182 (1988).

¹⁶⁷. R. J. Boyd and S. L. Boyd, *J. Am. Chem. Soc.*, **114**, 1652 (1992).

¹⁶⁸. S. Hati and D. Datta, *J. Comput. Chem.*, **13**, 912 (1992).

Table 1.25. Properties of Substituent Groups^a

CHAPTER 1
*Chemical Bonding
and Molecular Structure*

Group	χ (eV)	η (eV)	$S(10^{-2} \text{ eV}^{-1})$
CH_3	5.12	5.34	9.36
CH_3CH_2	4.42	4.96	10.07
$\text{CH}_2=\text{CH}$	5.18	4.96	10.07
$\text{HC}\equiv\text{C}$	8.21	5.77	8.67
$\text{HC}=\text{O}$	4.55	4.88	10.25
$\text{CH}_3\text{C}=\text{O}$	4.29	4.34	11.51
CO_2H	5.86	4.71	10.61
CO_2CH_3	5.48		
CONH_2	4.67	4.42	11.32
CN	8.63	5.07	9.86
NH_2	6.16	6.04	8.28
NO_2	7.84	4.89	10.22
OH	6.95	5.69	8.79
CH_3O	5.73	4.39	10.28
F	10.01	7.00	7.14
CH_2F	4.97	5.31	9.41
CHF_2	5.25	5.42	9.22
CF_3	6.30	5.53	9.05
SH	5.69	3.96	12.62
CH_3S	4.99	3.71	13.49
Cl	7.65	4.59	10.89
CH_2Cl	4.89	4.71	10.61
CHCl_2	5.12	4.38	11.42
CCl_3	5.53	4.10	12.21

a. F. De Proft, W. Langemaeker, and P. Geerlings, *J. Phys. Chem.*, **97**, 1826 (1993).

scales with these two sets calculated on a theoretical basis. Figure 1.46 is a plot that provides an indication of the scatter in the numerical values in comparison with an empirical scale.

The broad significance of the correlation shown in Figure 1.46 is to cross-validate the theoretical and empirical views of functional groups that have developed in organic chemistry. The two theoretical scales are based entirely on measures of electron density. As to more specific insights, with reference to Table 1.26, we see the orders $\text{CCl}_3 > \text{CHCl}_2 > \text{CH}_2\text{Cl}$ in electronegativity. This accords with the expectation for cumulative effects and is consistent with polar effects, as observed, for example, in the acidities of the corresponding carboxylic acids shown in Table 1.27. Note from Table 1.25 that the hardness and softness of the fluoro and chloro groups differ. Each additional fluoro substituent makes the group harder, but each chlorine makes it softer. This difference reflects the greater polarizability of the chlorine atoms.

If we compare the F, NO_2 , CN, and CF_3 substituents, representing familiar EWGs, we see that they are in the upper range of group electronegativity in Table 1.25 (10.01, 7.84, 8.63, and 6.30, respectively). With the exception of F, however, these substituents are not particularly hard.

The values for ethyl, vinyl, and ethynyl are noteworthy. Quite high electronegativity and hardness are assigned to the ethynyl group. This is in reasonable accord with the empirical values in Table 1.25. The methyl group also deserves notice. We will see in other contexts that the methyl group is harder than other primary alkyl groups. The theoretical treatments suggest this to be the case. It is not clear that the empirical scales reflect much difference between a methyl and ethyl group. This may be because

Table 1.26. Empirical and Theoretical Electronegativity Scales for Some Functional Groups

Group	Wells ^a	Inamoto and Masuda ^b	Boyd and Boyd ^c	Hati and Datta ^d
CH ₃	2.3	2.47	2.55	2.09
CH ₂ Cl	2.75	2.54	2.61	
CHCl ₂	2.8	2.60	2.66	
CCl ₃	3.0	2.67	2.70	
CF ₃	3.35	2.99	2.71	2.49
CH ₂ = CH	3.0	2.79	2.58	2.18
HC≡C	3.3	3.07	2.66	2.56
Ph	3.0	2.72	2.58	
N≡C	3.3	3.21	2.69	3.61
H	2.28	2.18		2.20
NH ₂	3.35	2.99	3.12	2.96
N ⁺ H ₃	3.8	3.71	3.21	3.52
N≡N ⁺		3.71		4.06
NO ₂	3.4	3.42	3.22	3.44
OH	3.7	3.47	3.55	3.49
F	3.95		3.95	3.75
Cl	3.03		3.05	2.68
Br	2.80		2.75	
I	2.28			

a. P. R. Wells, *Prog. Phys. Org. Chem.*, **6**, 111 (1968).b. N. Inamoto and S. Masuda, *Chem. Lett.*, 1003 (1982).c. R. J. Boyd and S. L. Boyd, *J. Am. Chem. Soc.*, **114**, 1652 (1992).d. S. Hati and D. Datta, *J. Comput. Chem.*, **13**, 912 (1992).

the theoretical results pertain to isolated molecules, whereas the empirical values are derived from measurements in solution. The smaller size of the methyl group makes it less polarizable than larger alkyl groups. This difference is maximized in the gas phase, where there are no compensating solvent effects.

Let us now consider a few simple but important systems that can illustrate the application of these ideas. We know that the acidity of the hydrides of the second-row elements increases sharply going to the right in the periodic table. The same trend is true for the third row and in each case the third-row compound is more acidic than its second-row counterpart. This is illustrated by the gas phase ionization enthalpy data in Table 1.28.

The gas phase data from both the second- and third-row compounds can be correlated by an expression that contains terms both for electronegativity (χ) and hardness (μ). The sign is negative for hardness:

$$\Delta G_{\text{acid}} = 311.805 - 18.118\chi + 33.771\mu \quad (1.50)$$

Table 1.27. Gas Phase and Aqueous pK_a Values

	pK _a		pK _a
FCH ₂ CO ₂ H	2.59	ClCH ₂ CO ₂ H	2.87
CHF ₂ CO ₂ H	NA	CHCl ₂ CO ₂ H	1.35
CF ₃ CO ₂ H	0.52	CCl ₃ CO ₂ H	0.66

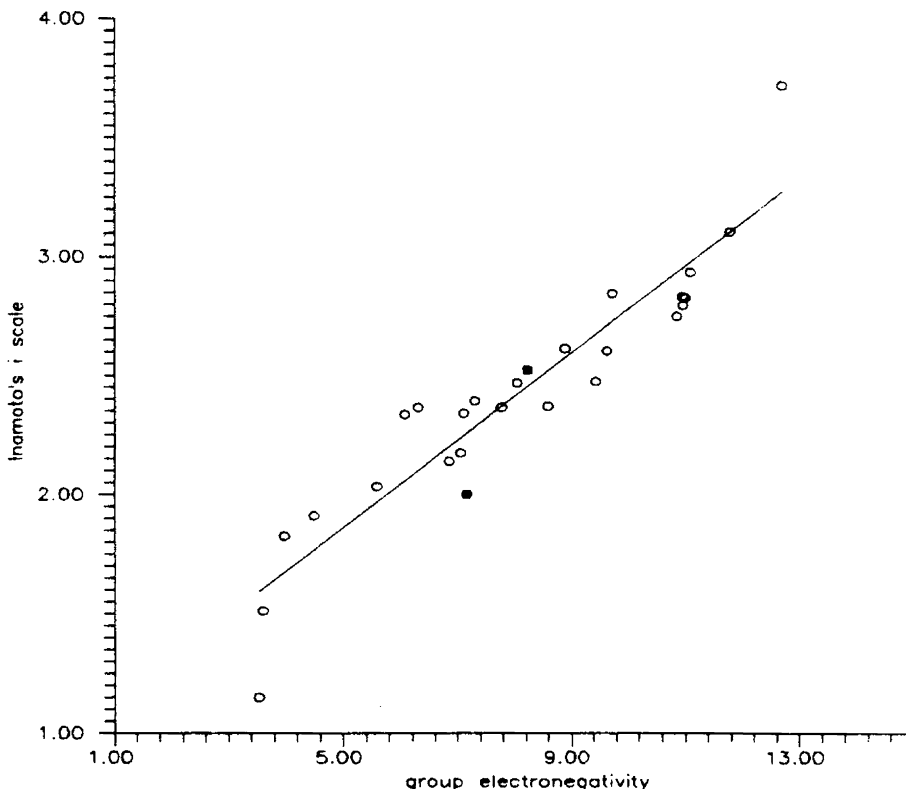


Fig. 1.46. Correlation between AIM electronegativity χ (in eV) with Inamoto i empirical group electronegativity scale. Correlation coefficient is 0.938. Reproduced with permission from S. Hati and D. Datta, *J. Comput. Chem.*, **13**, 912 (1992).

The implication is that both increased electronegativity and polarizability (or softness) contribute to acidity. The increasing acidity can be interpreted in terms of the ability of the anion to accommodate the negative charge left by the removal of a proton. The more electronegative and the more polarizable (softer) the anion, the better it can accept the additional charge. There is a related trend going down the periodic table, i.e., HI > HBr > HCl > HF. The order reflects the increasing bond strength from HI to HF, which is probably due to a combination of overlap and electronegativity effects.

Turning to an analogous group of organic compounds, we know that the order of acidity of alcohols in aqueous media is $\text{CH}_3\text{OH} > \text{CH}_3\text{CH}_2\text{OH} > (\text{CH}_3)_2\text{CHOH} >$

Table 1.28. Gas Phase and Aqueous pK Values^a

Second row	ΔH	pK	Third row	ΔH	pK
CH_4	416.8	48	SiH_4	372.4	
NH_3	403.7	38	PH_3	369.0	29
H_2O	390.8	15.7	H_2S	351.3	7.0
HF	371.4	3.2	HCl	333.4	-7

a. F. De Proft, W. Langenaeker, and P. Geerlings, *Int J. Quantum Chem.*, **55**, 459 (1995).

$(\text{CH}_3)_3\text{COH}$, but the order is exactly the opposite in the gas phase.¹⁶⁹ The reverse order in the gas phase attracted a good deal of interest when it was discovered, since it is contrary to the general expectation that more highly substituted alkyl groups are better electron donors than methyl and primary groups. Both qualitative¹⁷⁰ and quantitative¹⁷¹ treatments have identified polarizability, the ability to accept additional charge, as the major factor in the gas phase order. Note also that the order is predicted by the HSAB relationship since the softer (more substituted) alkoxides should bind a hard proton more weakly than the harder primary alkoxides.

Another study examined the acidity of some halogenated alcohols. The gas phase acidity order is $\text{ClCH}_2\text{OH} > \text{BrCH}_2\text{OH} > \text{FCH}_2\text{OH} > \text{CH}_3\text{OH}$. The same $\text{Cl} > \text{Br} > \text{F}$ order also holds for the di- and trihalogenated alcohols.¹⁷² The order reflects competing effects of electronegativity and polarizability. The electronegativity order $\text{F} > \text{Cl} > \text{Br}$ is reflected in the size of the bond dipole. The polarizability order $\text{Br} > \text{Cl} > \text{F}$ indicates the ability to disperse the negative charge. The overall trend is largely dominated by the polarizability order. These results focus attention on the importance of polarizability, especially in the gas phase, where there is no solvation to stabilize the anion. The intrinsic ability of the substituent group to accommodate negative charge becomes very important.

The role of substituents has been investigated especially thoroughly for substituted acetic and benzoic acids. Quantitative data are readily available from $\text{p}K_a$ measurements in aqueous solution. Considerable data on gas phase acidity are also available.¹⁷³ EWG substituents increase both solution and gas phase acidity. In the gas phase, branched alkyl groups slightly enhance acidity. In aqueous solution, there is a weak trend in the opposite direction, which is believed to be due to poorer solvation of the more branched anions. Geerling and co-workers have applied DFT concepts to substituent effects on acetic acids.¹⁷⁴ The Fukui functions and softness descriptors were calculated using electron density and Mulliken population analysis (see Topic 1.5.2). The relative correlation of these quantities with both solution and gas phase acidity was then examined. In both cases, the best correlations were with the Mulliken charge. In the case of gas phase data, the correlations were improved somewhat by inclusion of a second parameter for group softness. The picture that emerges is consistent with the qualitative concepts of HSAB. The reactions in question are hard-hard interactions, the transfer of a proton (hard) to an oxygen base (also hard). The reactions are largely controlled by electrostatic relationships, as modeled by the Mulliken charges. The involvement of softness in the gas phase analysis suggests that polarizability makes a secondary contribution to anionic stability in the gas phase.

¹⁶⁹ J. I. Brauman and L. K. Blair, *J. Am. Chem. Soc.*, **92**, 5986 (1976).

¹⁷⁰ W. M. Schubert, R. B. Murphy, and J. Robins, *Tetrahedron*, **17**, 199 (1962); J. E. Huheey, *J. Org. Chem.*, **36**, 204 (1971).

¹⁷¹ F. De Proft, W. Langenaeker, and P. Geerlings, *Tetrahedron*, **51**, 4021 (1995); P. Pérez, *J. Phys. Chem. A*, **105**, 6182 (2001).

¹⁷² S. Damoun, W. Langenaeker, G. Van de Woude, and P. Geerlings, *J. Phys. Chem.*, **99**, 12151 (1995).

¹⁷³ C. Jin Feng, R. D. Topsom, A. D. Headley, I. Koppel, M. Mishima, R. W. Taft, and S. Veji, *Theochem*, **45**, 141 (1988).

¹⁷⁴ F. De Proft, S. Amira, K. Choho, and P. Geerlings, *J. Phys. Chem.*, **98**, 5227 (1994).

- T. A. Albright, J. K. Burdett, and M. H. Whangbo, *Orbital Interactions in Chemistry*, John Wiley & Sons, New York, 1985.

R. F. W. Bader, *Atoms in Molecules: A Quantum Theory*, Clarendon Press, Oxford, 1990.

W. T. Borden, *Modern Molecular Orbital Theory for Organic Chemists*, Prentice-Hall, Englewood Cliffs, NY, 1975.

I. Fleming, *Frontier Orbital and Organic Chemical Reactions*, John Wiley & Sons, New York, 1976.

W. J. Hehre, L. Radom, P. v. R. Schleyer, and J. Pople, *Ab Initio Molecular Orbital Theory*, Wiley-Interscience, New York, 1986.

F. Jensen, *Introduction to Computational Chemistry*, John Wiley & Sons, Chichester, 1999.

W. Koch and M. C. Holthausen, *A Chemist's Guide to Density Functional Theory*, Wiley-VCH, Chichester, 2000.

E. Lewars, *Computational Chemistry*, Kluwer Academic Publishers, Boston, 2003.

R. G. Parr and W. Yang, *Density Functional Theory of Atoms and Molecules*, Oxford University Press, Oxford, 1989.

L. Salem, *Electrons in Chemical Reactions*, John Wiley & Sons, New York, 1982.

P. v. R. Schleyer, ed., *Encyclopedia of Computational Chemistry*, John Wiley & Sons, New York, 1998.

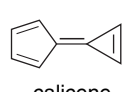
H. E. Zimmerman, *Quantum Mechanics for Organic Chemists*, Academic Press, New York, 1975.

Problems

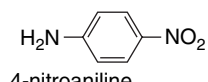
(References for these problems will be found on page 1155.)

- 1.1. Suggest an explanation for the following observations:

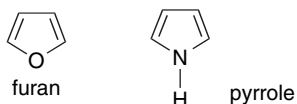
 - Although the hydrocarbon calicene has so far defied synthesis, but it has been suggested that it is a 111-carbon cluster with a $\text{C}_{56}\text{D}_{55}$ core.



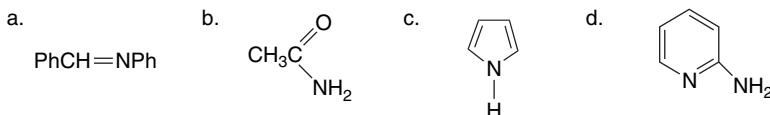
- b. The measured dipole moment of 4-nitroaniline (6.2 D) is larger than the value calculated using standard group dipoles (5.2 D).



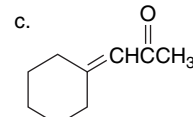
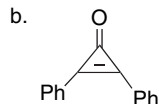
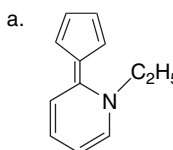
- c. The dipole moments of furan and pyrrole are in opposite directions.



- 1.2. Predict the preferred site of protonation for each of the following molecules and explain the basis of your prediction.

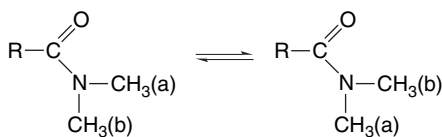


- 1.3. What physical properties, such as absorption spectra, bond lengths, dipole moment, etc., could be examined to obtain evidence of resonance interactions in the following molecules. What deviation from “normal” physical properties would you expect?



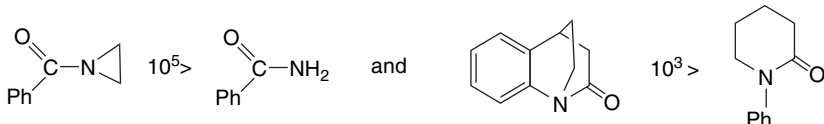
- 1.4. Consider each of the following physical characteristics of certain amides.

- a. Carboxamides have rotational barriers on the order of 20 kcal/mol for the process:



Develop a structural explanation for the barrier both in resonance and MO terminology.

- b. The gas phase rotational barrier of *N,N*-dimethylformamide is about 19.4 kcal/mol, which is about 1.5 kcal/mol less than in solution. Is this change consistent with the explanation you presented in part (a)? Explain.
 c. Account for the substantial differences in relative rates of alkaline hydrolysis for the following pairs of carboxamides.



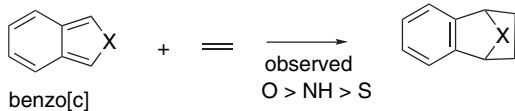
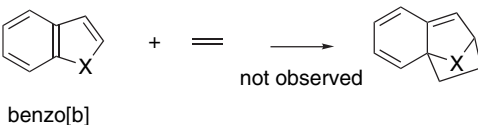
- 1.5. The AM1 semiempirical MO method was used to calculate structure, HOMO-LUMO orbital coefficients, and charge distribution for several substituted cyclopropenones. The results for 2-phenylcyclopropenone, 2-phenyl-3-methylcyclopropenone, and 2,3-diphenylcyclopropenone are given in Table 1.P5a. Based on this information, make predictions about the following reactions:

- What will be the site of protonation of a cyclopropenone?
- What will be the site of reaction of a cyclopropenone with a hard nucleophile, such as -OH ?
- Is an alkyl or aryl substituent most effective in promoting reaction with a soft nucleophile?

Table 1.P5a. Orbital Coefficients and Energies

R	LUMO Coefficients				HOMO coefficients				Energy(kcal/mol)	
	C(1)	C(2)	C(3)	O	C(1)	C(2)	C(3)	O	HOMO	LUMO
C(2)=Ph	-0.088	0.445	-0.494	0.074	-0.058	-0.240	-0.444	0.275	-9.54	-0.82
C(3)=H										
C(2)=Ph	-0.079	0.439	-0.501	0.066	0.071	-0.298	-0.436	0.290	-9.29	-0.76
C(3)=CH ₃										
C(2)=Ph	0.000	0.455	-0.455	0.000	-0.084	-0.348	-0.348	.270	-8.90	-1.14
C(3)=Ph										
Charges	C(1)	C(2)	C(3)	O						
C(2)=Ph	0.28	-0.11	-0.19	-0.27						
C(3)=H										
C(2)=Ph	0.28	-0.11	-0.14	-0.27						
C(3)=CH ₃										
C(2)=Ph	0.28	-0.11	-0.11	-0.27						
C(3)=Ph										

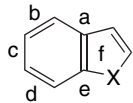
1.6. It is observed that benzo[c] derivatives of furan, pyrrole, and thiophene are less stable and much more reactive than the corresponding benzo[b] derivatives. The differences are apparent for example in [4 + 2] cycloadditions, which are facile with the benzo[c] but not the benzo[b] derivatives. Some MO properties from AM1 calculations are given in Tables 1.P6a, 1.P6b and 1.P6c. What features of the results are in accord with the experimental observations? Do you find any features of the results than run counter to the observations.

**Table 1.P6a. Enthalpy of Reactants and Transition Structures**

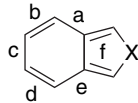
	O	NH	S
ΔH_f (kcal/mol)			
Benzo[b]	20.8	55.2	42.4
Benzo[c]	27.9	61.7	49.4
ΔH_f for 4 + 2 TS			
Benzo[b]	75.7	115.3	110.8
Benzo[c]	64.5	104.8	102.4
ΔH^\ddagger for 4 + 2 TS			
Benzo[b]	38.4	43.6	51.9
Benzo[c]	20.1	26.6	36.5

Table 1.P6b. Bond Orders in Carbocyclic Rings

Benzo[b]heterocycles



Benzo[c]heterocycles

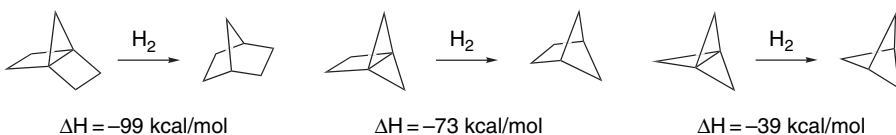


	O	NH	S		O	NH	S
a	1.34	1.30	1.30	a	1.12	1.16	1.15
b	1.46	1.50	1.51	b	1.71	1.66	1.67
c	1.37	1.33	1.32	c	1.15	1.19	1.18
d	1.45	1.50	1.51	d	1.71	1.66	1.67
e	1.45	1.28	1.30	e	1.12	1.16	1.15
f	1.30	1.27	1.32	f	1.14	1.20	1.20

Table 1.P6c. Orbital Energies in ev

	O	NH	S
HOMO:benzo[b]	-9.010	-8.403	-8.430
HOMO:benzo[c]	-8.263	-7.796	-8.340
LUMO:benzo[b]	-0.063	0.300	-0.166
LUMO:benzo[c]	-0.396	0.142	-0.592

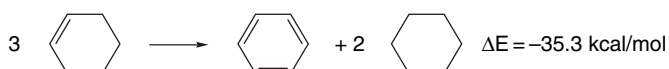
- 1.7. The propellanes are highly reactive in comparison with unstrained hydrocarbons and readily undergo reactions that result in the rupture of the central bond. For example, it has been suggested that the polymerization of propellanes occurs by initial dissociation of the center bond. Perhaps surprisingly, it has been found that [1.1.1]propellane is considerably *less reactive* than either [2.2.1]propellane or [2.1.1]propellane. Use the computational enthalpy data below to estimate the energy required to break the center bond in each of the three propellanes. Assume that the bridgehead C–H bonds in each of the bicycloalkanes has a bond enthalpy of -104 kcal/mol . How might the results explain the relative reactivity of the propellanes.



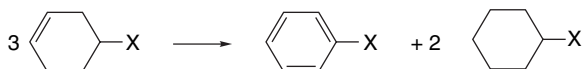
- 1.8. Examine the heats of hydrogenation shown for unsaturated eight-membered ring hydrocarbons. (a) Discuss the differences among the different compounds in comparison with the standard ΔH_{H_2} for an unstrained *cis* double bond, which is 27.4 kcal/mol . (b) Assigning a strain energy of 9.3 kcal/mol to cyclooctane, calculate the relative strain of each of the other compounds. (c) What role does conjugation play in relation to the observed ΔH_{H_2} ? (d) What conclusion do these data permit as to whether cyclooctatetraene is stabilized or destabilized by cyclic conjugation.

Compound	ΔH_{H_2} (kcal/mol)
Z, Z, Z, Z-1,3,5,7-Cyclooctatetraene	97.06
Z, Z, Z-1,3,5-Cyclooctatriene	76.39
Z, Z, Z-1,3,6-Cyclooctatriene	79.91
Z, Z-1,3-Cyclooctadiene	48.96
Z, Z-1,4-Cyclooctadiene	52.09
Z, Z-1,5-Cyclooctadiene	53.68
Z-Cyclooctene	22.98
E-Cyclooctene	32.24

- 1.9. An isodesmic reaction suitable for calculating the resonance stabilization of benzene relative to cyclohexene is



A similar calculation can be done with substituent groups in place. The results for several substituents by G3(MP2) computations are as follows:



X	ΔE (kcal/mol)
H	-35.3
CH_3	-35.8
CH_3CH_2	-36.1
$\text{CH}_2=\text{CH}$	-38.1
$\text{HC}\equiv\text{C}$	-37.3
H_2N	-39.5

How do the calculated effects of substituents compare with the qualitative expectations on the basis of resonance concepts? How do the calculated stabilizations for the individual substituents compare with those calculated for double bonds and given on p. 52.

- 1.10. The explanation of substituent effects on the acidity of substituted carboxylic acids usually focuses on two factors: (a) The ability of the substituent to stabilize the negative charge; and (b) the effect of solvation on the anion. However, there will also be substituent effects on the stability and solvation of the undissociated acid. The studies described on p. XXX resulted in the following values for the gas phase energy (in hartrees) of the acids and anions and the resulting ΔG for gas phase ionization. Using this information and the solvation energies on p. 53,

analyze the relative importance of intrinsic anion stabilization and solvation on the observed acidity.

X	Acid, E_{gas}	Anion, E_{gas}	ΔG (kcal/mol)
H	-189.551612	-189.005818	342.49
CH_3	-228.792813	-228.241528	345.94
ClCH_2	-687.945725	-687.414262	333.50
NCCH_2	-320.909115	-320.386960	327.66
$(\text{CH}_3)_3\text{C}$	-346.481196	-345.936639	341.71

- 1.11. Cyclic amines such as piperidine and its derivatives show substantial differences in the properties of the axial C(2) and C(6) bonds. The axial C–H bonds are *weaker* than the equatorial C–H bonds, as indicated by a shifted C–H stretching frequency in the IR spectrum. The axial hydrogens also appear at higher field in $^1\text{H-NMR}$ spectra. Axial C(2) and C(6) methyl groups *lower* the ionization potential of the unshared pair of electrons on nitrogen more than equatorial C(2) and C(6) methyl groups. Discuss the structural basis of these effects in MO terminology.
- 1.12. Construct a qualitative MO diagram for the following systems and discuss how the π MOs are modified by addition of the substituent.
- vinyl fluoride, compared to ethene
 - propenal, compared to ethene
 - acrylonitrile, compared to ethene
 - propene, compared to ethene
 - benzyl cation, compared to benzene
 - fluorobenzene, compared to benzene
- 1.13. Given below are the ΔE for some isodesmic reactions. Also given are the AIM and NPA charges at the carbon atoms of the double bond. Provide an explanation for these results in terms of both resonance structure and MO terminology.
- Draw resonance structures and qualitative MO diagrams that indicate the stabilizing interaction.
 - Explain the order of stabilization $\text{N} > \text{O} > \text{F}$ in both resonance and MO terminology.
 - Interpret the AIM and NPA charges in relationship to the ideas presented in (a) and (b).



X	ΔE	$\delta\text{C}(1)^a$	$\delta\text{C}(2)^a$	$\delta\text{C}(1)^b$	$\delta\text{C}(2)^b$
H	0	+0.08	+0.08	-0.25	-0.25
CH_3	-3.05	+0.02	+0.08	-0.09	-0.29
NH_2	-7.20	+0.51	+0.15	+0.14	-0.36
OH	-6.43	+0.58	+0.18	+0.26	-0.39
F	-0.99	+0.48	+0.29	+0.30	-0.36

- a. AIM charges
b. NPA charges

- 1.14. In the Hückel MO treatment, orbitals on nonadjacent atoms are assumed to have no interaction. The concept of *homoconjugation* suggests that such orbitals may interact, especially in rigid structures in which the orbitals are directed toward one another. Consider, e.g., norbornadiene, (bicyclo[2.2.1]hepta-2,5-diene).



- Construct an MO diagram according to HMO theory and assign orbital energies.
- Construct the qualitative MO diagram that would result from significant overlap between the C(3) and C(5) and C(2) and C(6) orbitals.
- The ionization potentials (IP) of some 2-substituted norbornadienes are given below. The two IP values pertain to the π system. Use PMO theory to analyze the effect these substituents have on the IP. Use a qualitative MO diagram to show how the substituents interact with the two double bonds and how this affects the IP. Discuss the effect the substituents have on the IP.

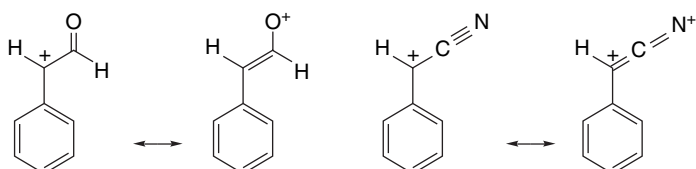
X	IP ₁	IP ₂
H	8.69	9.55
CH ₃ O	8.05	9.27
CN	9.26	10.12

- 1.15. a. Sketch the nodal properties of the Hückel HOMO orbital of the pentadienyl cation.
 b. The orbital coefficients of two of the π MOs of pentadienyl are given below. Specify which is of lower energy; classify each orbital as bonding, nonbonding, or antibonding; and specify whether each orbital is S or A with respect to a plane bisecting the molecule perpendicular to the plane of the structure.

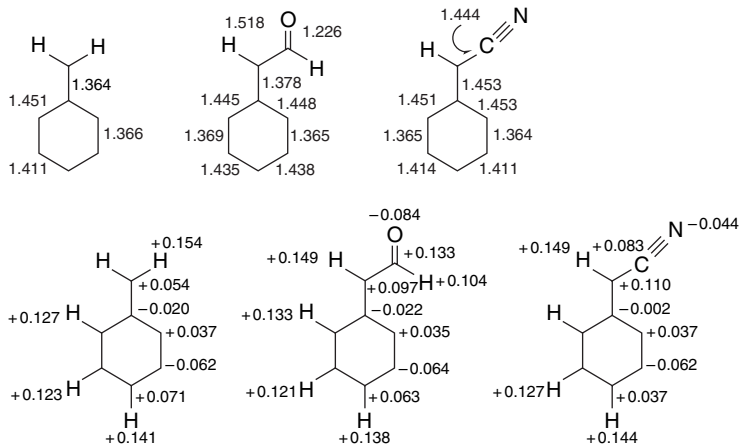
$$\psi_x = 0.50\varphi_1 + 0.50\varphi_2 - 0.50\varphi_4 - 0.50\varphi_5$$

$$\psi_y = 0.58\varphi_1 - 0.58\varphi_3 + 0.58\varphi_5$$

- 1.16. There has been discussion as to whether unsaturated EWGs such as formyl or cyano stabilize or destabilize carbocations.



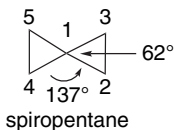
The diagrams below give STO-3G bond lengths and Mulliken charge densities for the benzyl cation and for its α -formyl and α -cyano derivatives. Analyze the effect of the substituents on the carbocation.



- 1.17 a. Calculate the HMO energy levels and atomic orbital coefficients for 1,3-butadiene.
 b. Estimate the delocalization energy, in units of β , of the cyclobutadienyl dication $C_4H_4^{2+}$ from HMO theory.
 c. Estimate, in units of β , the energy associated with the longest-wavelength UV-VIS absorption of 1,3,5,7-octatetraene. Does it appear at a longer or shorter wavelength than the corresponding absorption in 1,3,5-hexatriene?
- 1.18. Spiropentane has unusual strain and hybridization. Consider the following facets of its structure.
- The strain energy of spiropentane (62.5 kcal/mol) is considerably more than twice that of cyclopropane (27.5 kcal/mol). Suggest an explanation.
 - The structure of spiropentane has been determined by X-ray crystallography. The endocyclic angles at the spiro carbon are about 62° , and the bond angles between C–C bonds in the adjacent rings are about 137° . How would you relate the strain to the hybridization of each carbon in spirocyclopentane based on these bond angles?
 - The fractional s character in a C–C bond can be estimated from ^{13}C – ^{13}C coupling constants using the equation

$$J_{Ci-Cj} = K(s_i)(s_j)$$

where K is a constant = 550 Hz and s is the fractional s character of each atom. In spiropentane, the J for coupling between C(1) and C(3) is 20.2 Hz. The J between C(2) and C(3) is about 7.5 Hz. Calculate the s character of the C(1)–C(3) and C(2)–C(3) bonds.



- 1.19. Predict whether the following gas phase reactions will be thermodynamically favorable or unfavorable. Explain your answer.

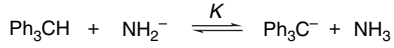


- 1.20. For each reaction, predict which compound would react faster (k) or give the more complete (K) reaction. Explain the basis for your prediction.

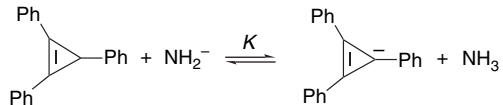
a.



b.



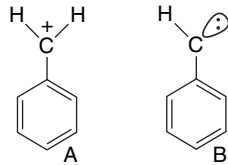
OR



c.



- 1.21. Computational comparison of the structures of the benzyl cation (**A**) and singlet phenyl carbene (**B**) indicate a much greater degree of double-bond character for the exocyclic bond in **A** than in **B**. Provide a rationale for this difference, both in VB and MO terminology.



- 1.22. Interesting stability and structural trends have been found with MP2/6-31G* calculations on substituted imines. The data below give the ΔE for the isodesmic reaction:



The data suggest that ΔE increases with χ_{XY} , the group electronegativity of the substituent. The $\text{X}-\text{N}=\text{CH}_2$ bond angle also decreases with χ_{AB} . The NPA

charges on the various atoms are given at the right of the table below. Discuss these trends, with particular attention to the interaction between the unshared electron pair on nitrogen and the C=N bond with the substituents.

Substituent	χ_{XY}	ΔE	$XN = CH_2 (\circ)$	$\delta(X)^a$	$\delta(Y)^b$	$\delta(N)$	$\delta(C)$	$\delta(H)av$
H	2.20	+4.1	110	+0.36	—	-0.66	-0.04	+0.17
CH_3	2.55	0.0	116	-0.44	+0.20(H_2)	-0.47	-0.06	+0.17
$CH=O$	2.66	-3.6	114	+0.65	-0.63 (=O)	-0.63	+0.07	+0.20
CN	2.69	-4.8	117	+0.47	-0.39 (N)	-0.55	+0.07	+0.20
CF_3	2.71	-4.7	118	+1.41	-0.42(F) ₃	-0.59	+0.03	+0.20
NO_2	3.22	-10.0	111	+0.77	-0.44(O) ₂	-0.38	+0.04	+0.22
NH_2^c	3.12	-12.4	117	-0.71	+0.38(H_2)	-0.26	-0.15	+0.18
OH	3.55	-20.5	110	-0.64	+0.51 (H)	-0.14	-0.13	+0.20
F	4.00	-29.0	108	-0.31	—	0.00	-0.12	+0.22
H_3Si	1.90	+13.2	120	+1.29	-0.24(H_3)	-0.92	+0.03	+0.16

a. The charge on atom X.

b. The average charge on each atom Y.

c. The nitrogen in pyramidal in the lowest energy structure.

1.23. Table 1.P23a shows NPA charges for planar and twisted (C–N rotation) for formamide, 3-aminoacrolein and squaramide. Table 1.P23b gives computed ^{17}O chemical shifts for the planar and twisted forms. Figures 1.P23A–F are maps showing the potential for interaction with a particle of charge $+0.5e$. The barriers

Table 1.P23a. NPA Charges

	Planar	Twisted
Formamide		
O	-0.710	-0.620
C	+0.690	+0.695
N	-0.875	-0.929
NH_2	-0.080	-0.182
CH	+0.789	+0.812
3-Aminoacrolein		
O	-0.665	-0.625
C(1)	+0.512	+0.506
C(2)	-0.456	-0.351
C(3)	+0.198	+0.144
N	-0.832	-0.884
NH_2	-0.060	-0.149
Squaramide		
O(1)	-0.655	-0.609
C(1)	+0.519	+0.530
O(2)	-0.631	-0.626
C(2)	+0.554	+0.548
C(3)	+0.162	+0.088
C(4)	+0.258	+0.348
N(3)	-0.819	-0.851
NH_2	-0.001	-0.095
O(4)	-0.711	-0.687

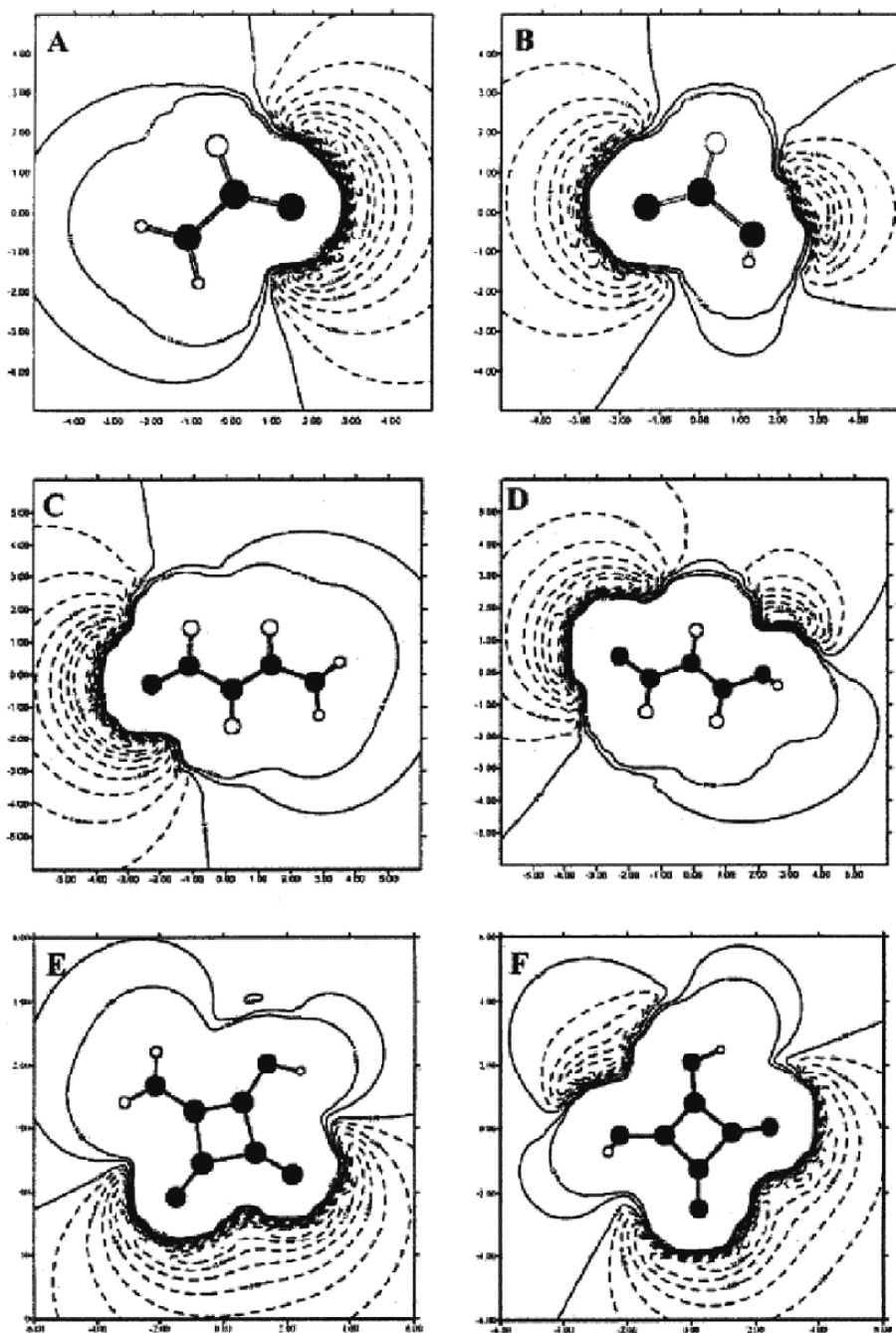
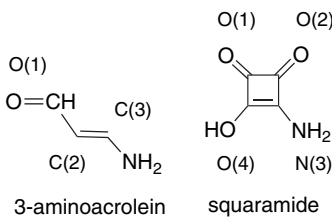


Fig. 1.P23. Molecular interaction potential maps for planar (left) and twisted (right) conformations of formamide, 3-aminoacrolein and squaramide.

Table 1.P23b. Calculated ^{17}O Chemical Shifts in ppm

	Planar	Twisted	Δ
Formamide	390	602	212
3-Aminoacrolein	568	630	62
Squaramide O(1)	446	526	80

to rotation of the three molecules are 14.9, 8.8, and 9.9 kcal/mol, respectively. On the basis of these data, discuss the extent of resonance interaction in each compound.



Stereochemistry, Conformation, and Stereoselectivity

Introduction

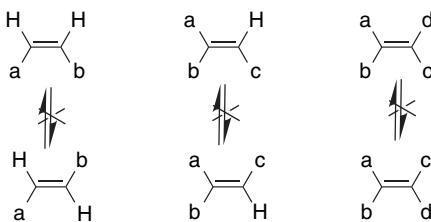
In the discussion of the structural features of carbon compounds in the Chapter 1, we emphasized some fundamental principles of molecular geometry. Except in strained rings, sp^3 carbon is nearly tetrahedral in shape. Double bonds involving sp^2 carbon are trigonal and planar and have a large barrier to rotation. The sp hybridization, e.g., in alkynes, leads to a linear (digonal) geometry. *Stereochemistry* in its broadest sense describes how the atoms of a molecule are arranged in three-dimensional space. In particular, *stereoisomers* are molecules that have identical connectivity (constitution) but differ in three-dimensional structure. Stereoisomers differ from one another in *configuration* at one or more atoms. *Conformations* are the various shapes that are available to molecules by single-bond rotations and other changes that do not involve bond breaking. Usually, conformational processes have relatively low energy requirements. The stereochemical features of a molecule, both configuration and conformation, can influence its reactivity. After discussing configuration and conformation, we consider *stereoselectivity*, the preference of a reaction for a particular stereoisomeric product.

2.1. Configuration

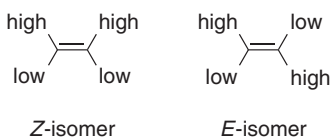
2.1.1. Configuration at Double Bonds

The sp^2 hybridization in the carbon atoms in a double bond and the resulting π bond favor a planar arrangement of the two carbon atoms and the four immediate

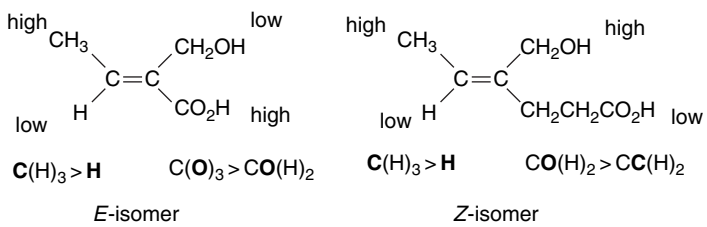
ligand atoms. When the substituents at the two carbons are nonidentical, two structurally distinct molecules exist.



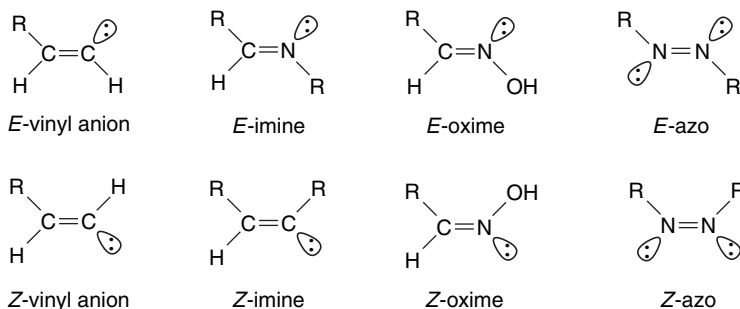
Owing to the high barrier to rotation in most alkenes ($> 50 \text{ kcal/mol}$), these structures are not easily interconverted and the compounds exist as two isomers (stereoisomers) having different physical and chemical properties. There are two common ways of naming such compounds. If there is only one substituent at each carbon, the compounds can be called *cis* and *trans*. The isomer with both substituents on the same side of the double bond is the *cis* isomer, whereas the one with substituents on opposite sides is the *trans* isomer. If there is more than one substituent at either carbon, these designations can become ambiguous. There is an unambiguous system that can be applied to all compounds, no matter how many or how complex the substituents might be: the isomers are designated *Z* (for together) or *E* (for opposite). This system is based on the *Cahn-Ingold-Prelog priority rules*, which assign priority in the order of decreasing atomic number. If two substituent atoms have the same atomic number (e.g., two carbon substituents), the atomic numbers of successive atoms in the groups are compared until a difference is found. Multiple bonds, such as in a carbonyl group, are counted as two (or three for a triple bond) atoms. It is the *first difference* that determines priority. When priority has been assigned, the isomer with the higher-priority groups at each carbon on the same side of the double bond is called the *Z*-isomer. The isomer with the higher-priority substituents on opposite sides is the *E*-isomer.



Example 2.1

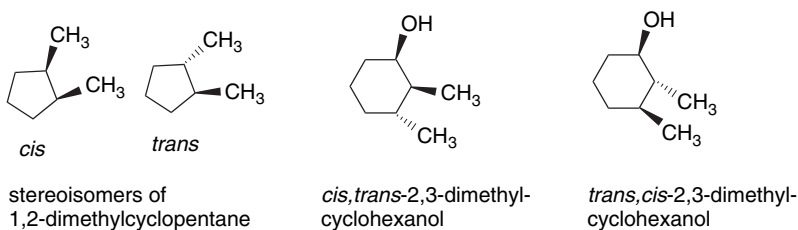


Certain atoms have an unshared electron pair rather than a substituent. Electron pairs are assigned the lowest priority in the Cahn-Ingold-Prelog convention, so assignment the Z- or E-configuration to compounds such as imines and oximes follows the same rules with R or H >:.

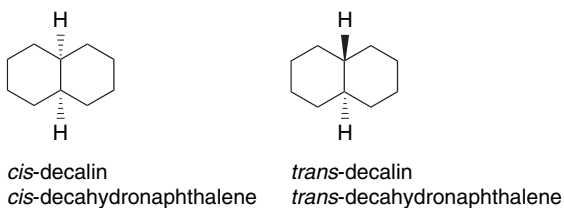


2.1.2. Configuration of Cyclic Compounds

Just as substituents can be on the same or opposite side of a double bond, they can be on the same or opposite side in cyclic compounds. The two arrangements are different *configurations* and cannot be interchanged without breaking and reforming at least one bond. Here the terms *cis* (for the same side) and *trans* (for the opposite side) are unambiguous and have been adopted as the designation of configuration. The stereochemistry is specified *relative to the group that takes precedence in the naming of the molecule*, as illustrated for 2,3-dimethylcyclohexanol.

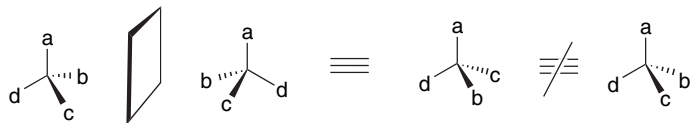


Stereoisomers also arise when two rings share a common bond. In the *cis* isomer both branches of the fused ring are on the same side. In the *trans* isomer they are on opposite sides.



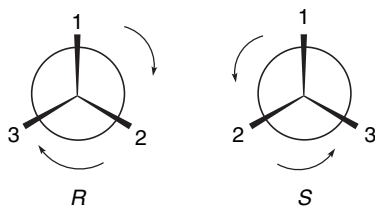
2.1.3. Configuration at Tetrahedral Atoms

Carbon and other atoms with sp^3 hybridization have approximately tetrahedral geometry. With the exception of small deviations in bond angles, each of the substituents is in a geometrically equivalent position. Nevertheless, there is an important stereochemical feature associated with tetrahedral centers. If all four substituents are different, they can be arranged in two different ways. The two different arrangements are mirror images of one another, but they cannot be superimposed.

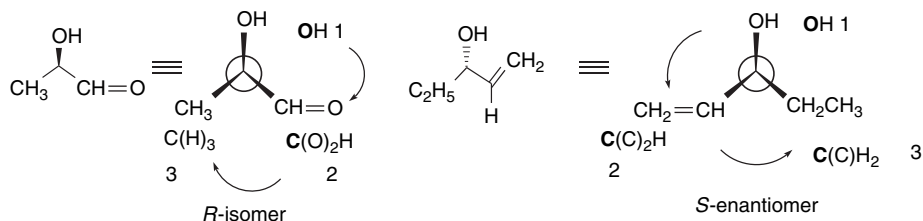


Any object that cannot be superimposed on its mirror image is called *chiral*, that is, it has the property of being right-handed or left-handed. Molecules (or other objects) that are not chiral are described as being *achiral*, which is the opposite of chiral. Tetrahedral atoms with four nonidentical substituents, then, give rise to two stereoisomers. Such atoms are called *stereogenic centers*, sometimes shortened to *stereocenters*. An older term applied specifically to carbon is *asymmetric carbon*.

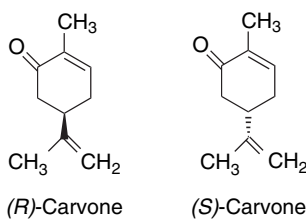
The chirality (or handedness) at stereogenic centers is specified by application of the Cahn-Ingold-Prelog priority rules, as described for double bonds. The four nonidentical ligand atoms are assigned a decreasing priority $1 > 2 > 3 > 4$. The molecule is then viewed opposite from the lowest-priority group, that is, the group is placed behind the stereocenter and away from the viewer. Two arrangements are possible for the other three substituents. The groups can decrease in priority in either a clockwise or a counterclockwise direction. The clockwise direction configuration is assigned *R* (for *rectus*) and the counterclockwise direction is assigned *S* (for *sinistre*).



Example 2.2



The two nonsuperimposable mirror image molecules are called an *enantiomeric pair* and each is the *enantiomer* of the other. The separated enantiomers have identical properties with respect to achiral environments. They have the same solubility, physical, and spectroscopic properties and the same chemical reactivity toward achiral reagents. However, they have different properties in chiral environments. The enantiomers react at different rates toward chiral reagents and respond differently to chiral catalysts. Usually enantiomers cause differing physiological responses, since biological receptors are chiral. For example, the odor of the *R*- (spearmint oil) and *S*- (caraway seed oil) enantiomers of carvone are quite different.



The activity of enantiomeric forms of pharmaceuticals is often distinctly different.

Enantiomers also differ in a specific physical property, namely the rotation of plane polarized light. The two enantiomers rotate the light in equal, but opposite directions. The property of rotating plane polarized light is called *optical activity*, and the magnitude of rotation can be measured by instruments called polarimeters. The observed rotation, known as α , depends on the conditions of measurement, including concentration, path length, solvent, and the wavelength of the light used. The rotation that is characteristic of an enantiomer is called the *specific rotation* and is symbolized by $[\alpha]_{589}$, where the subscript designates the wavelength of the light. The observed rotation α at any wavelength is related to $[\alpha]$, by the equation

$$[\alpha]_\lambda = \frac{100\alpha}{cl} \quad (2.1)$$

where c is the concentration in g/100 mL and l is the path length in decimeters.

Depending on how it was obtained, a sample of a chiral compound can contain only one enantiomer or it can be a mixture of both. Enantiomerically pure materials are referred to as *homochiral* or *enantiopure*. The 1:1 mixture of enantiomers has zero net rotation (because the rotations caused by the two enantiomers precisely cancel each other) and is called a *racemic mixture* or *racemate*. A racemic mixture has its own characteristic properties in the solid state. It differs in melting point and solubility from the pure enantiomers, owing to the fact that the racemic mixture can adopt a different crystalline structure from that of the pure enantiomers. For example, Figure 2.1 shows the differing intermolecular hydrogen-bonding and crystal-packing arrangements in $(+/-)$ and $(-)$ 2,5-diazabicyclo[2.2.2]octa-3,6-dione.¹

The composition of a mixture of enantiomers is given by the *enantiomeric excess*, abbreviated e.e., which is the percentage excess of the major enantiomer over the minor enantiomer:

$$\text{e.e.} = \% \text{ Major} - \% \text{ Minor} \quad (2.2)$$

¹. M.-J. Birelle, J. Gabard, M. Leclercq, J.-M. Lehn, M. Cesario, C. Pascard, M. Cheve, and G. Dutruc-Rosset, *Tetrahedron Lett.*, **35**, 8157 (1994).

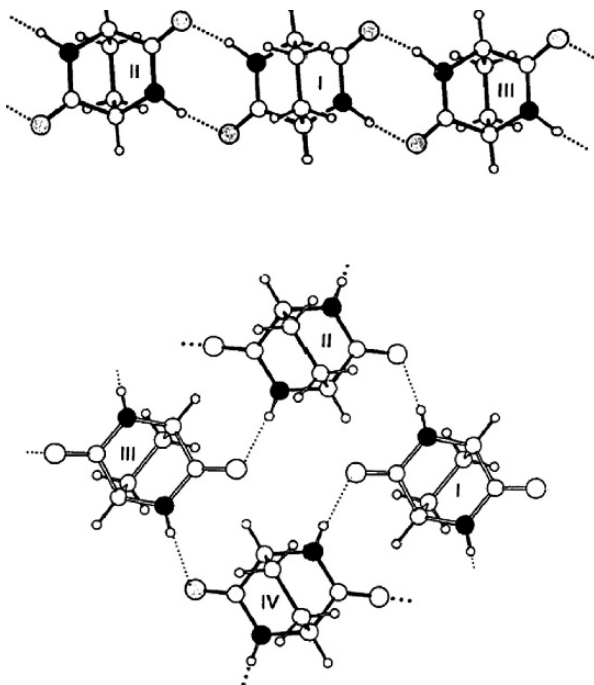


Fig. 2.1. Alternative hydrogen-bonding and crystal-packing arrangements for racemic (top) and (–) (bottom) forms of 2,5-diazabicyclo[2.2.2]octane-3,6-dione. Reproduced from *Tetrahedron Lett.*, **35**, 8157 (1994), by permission of Elsevier.

Alternatively, e.e. can be expressed in terms of the mole fraction of each enantiomer:

$$\text{e.e.} = (\text{Mole fraction}_{\text{major}} - \text{Mole fraction}_{\text{minor}}) \times 100 \quad (2.3)$$

The *optical purity*, an older term, is numerically identical. It represents the observed rotation, relative to the rotation of the pure enantiomer. Since the two enantiomers cancel each other out, the observed rotation is the product of (% Major – % Minor) × [α]_λ. If [α]_λ is known, measurement of α allows the optical purity and enantiomeric excess to be determined:

$$\text{e.e.} = \frac{\alpha_{\text{obs}} \times 100}{[\alpha]_{\lambda}} \quad (2.4)$$

There are several other ways of measuring e.e., including NMR spectroscopy, chromatography, and capillary electrophoresis (see Topic 2.1).

Measurement of rotation as a function of wavelength is useful in structural studies aimed at determining the configuration of a chiral molecule. This technique is called *optical rotatory dispersion* (ORD),² and the resulting plot of rotation against wavelength is called an ORD curve. The shape of the ORD curve is determined by the

². P. Crabbe, *Top. Stereochem.* **1**, 93 (1967); C. Djerassi, *Optical Rotatory Dispersion*, McGraw-Hill, New York, 1960; P. Crabbe, *Optical Rotatory Dispersion and Circular Dichroism in Organic Chemistry*, Holden Day, San Francisco, 1965; E. Charney, *The Molecular Basis of Optical Activity. Optical Rotatory Dispersion and Circular Dichroism*, Wiley, New York, 1979.

configuration of the molecule and its absorption spectrum. In many cases, the ORD curve can be used to determine the configuration of a molecule by comparison with similar molecules of known configuration. Figure 2.2 shows the UV, ORD, and CD spectra of an enantiomerically pure sulfonium ion salt.³

Chiral substances also show differential absorption of circularly polarized light. This is called *circular dichroism* (CD) and is quantitatively expressed as the molecular ellipticity θ , where ϵ_L and ϵ_R are the extinction coefficients of left and right circularly polarized light:

$$\theta = 3330(\epsilon_L - \epsilon_R) \quad (2.5)$$

Molecular ellipticity is analogous to specific rotation in that two enantiomers have exactly opposite values at every wavelength. Two enantiomers also show CD spectra having opposite signs. A compound with several absorption bands may show both positive and negative bands. Figure 2.3 illustrates the CD curves for both enantiomers of 2-amino-1-phenyl-1-propanone.⁴

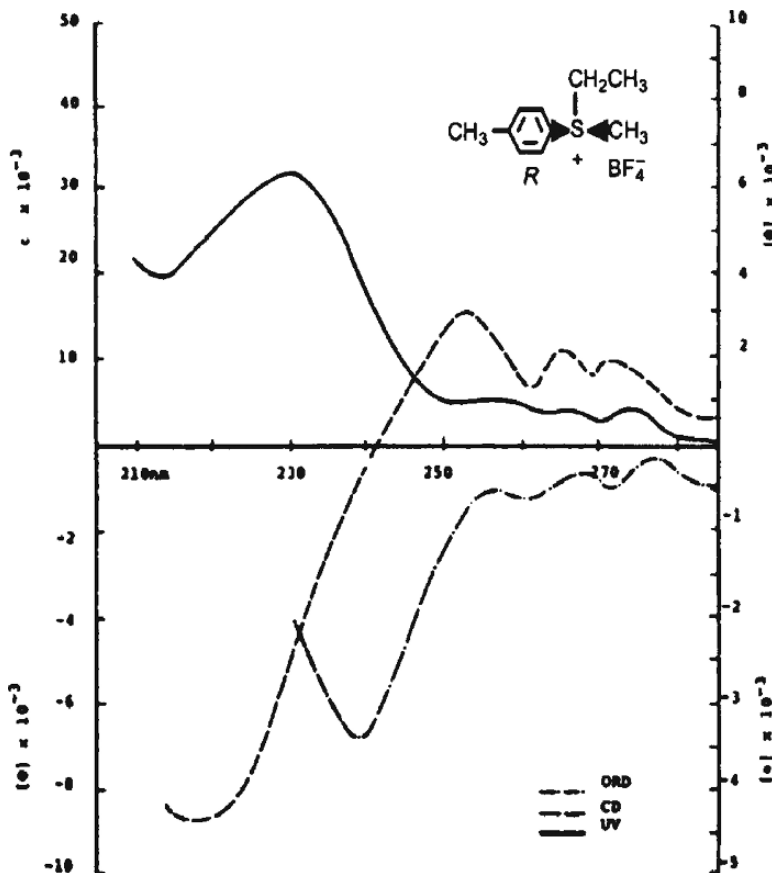


Fig. 2.2. UV absorption, ORD, and CD curves of (*R*)-ethyl methyl *p*-tolyl sulfonium tetrafluoroborate. Reproduced from *J. Org. Chem.*, **41**, 3099 (1976), by permission of the American Chemical Society.

³. K. K. Andersen, R. L. Caret, and D. L. Ladd, *J. Org. Chem.*, **41**, 3096 (1976).

⁴. J.-P. Wolf and H. Pfander, *Helv. Chim. Acta*, **69**, 1498 (1986).

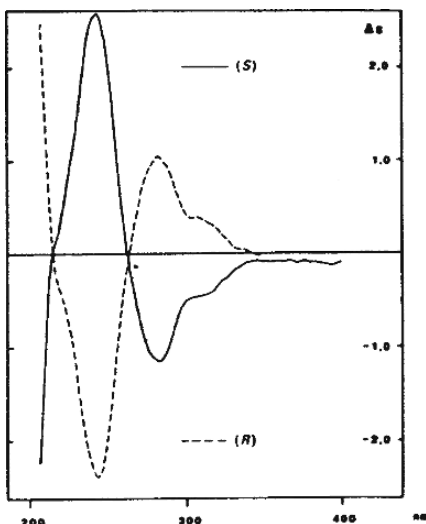


Fig. 2.3. CD spectra of (*S*)- and (*R*)-2-amino-1-phenyl-1-propanone hydrochloride. Reproduced from *Helv. Chim. Acta*, **69**, 1498 (1986), by permission of Wiley-VCH.

2.1.4. Molecules with Multiple Stereogenic Centers

Molecules can have several stereogenic centers, including double bonds with *Z* or *E* configurations and asymmetrically substituted tetrahedral atoms. The maximum number of stereoisomers that can be generated from *n* stereogenic centers is 2^n . There are several ways of representing molecules with multiple stereogenic centers. At the present time, the most common method in organic chemistry is to depict the molecule in an extended conformation with the longest chain aligned horizontally. The substituents then point in or out and up or down at each tetrahedral site of substitution, as represented by wedged and dashed bonds. The four possible stereoisomers of 2,3,4-trihydroxybutanal are shown in this way in Figure 2.4. The configuration at each center is specified as *R* or *S*. The isomers can also be characterized as *syn* or *anti*. Two

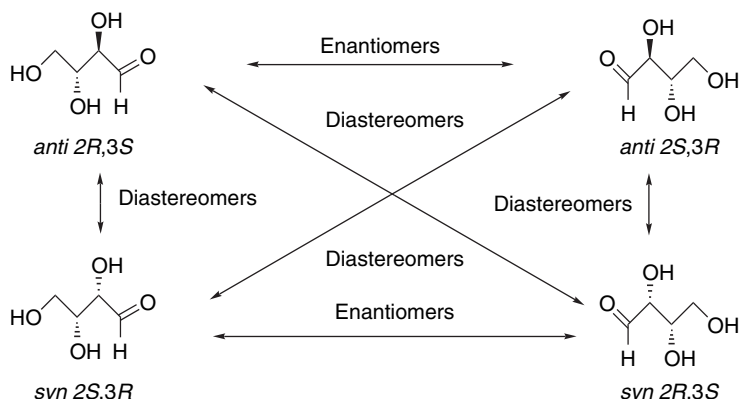
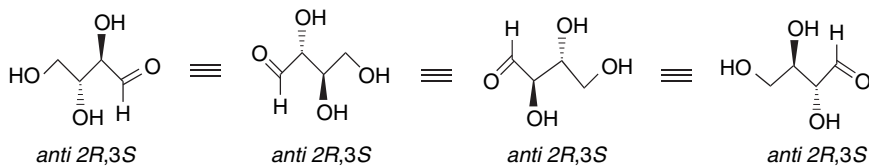


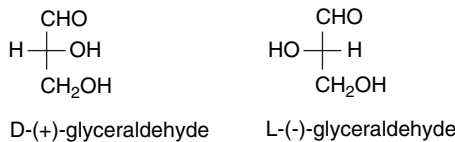
Fig. 2.4. Extended chain representation of all stereoisomers of 2,3,4-trihydroxybutanal.

adjacent substituents pointed in the same direction (in or out) are *syn*, whereas those pointed in opposite directions are *anti*.

For molecules with more than one stereogenic center, the *enantiomeric pair must have the opposite configuration at each center*. The two enantiomeric relationships are shown in Figure 2.4. There are four other pairings that do not fulfill this requirement, but the structures are still stereoisomeric. Molecules that are stereoisomeric but are not enantiomeric are called *diastereomers*, and four of these relationships are pointed out in Figure 2.4. Molecules that are diastereomeric have the same *constitution* (connectivity) but differ in *configuration* at one or more of the stereogenic centers. The positions in two diastereomers that have different configurations are called *epimeric*. For example, the *anti*-*2R,3S* and *syn*-*2R,3S* stereoisomers have the same configuration at C(2), but are epimeric at C(3). There is nothing unique about the way in which the molecules in Figure 2.4 are positioned, except for the conventional depiction of the extended chain horizontally. For example, the three other representations below also depict the *anti*-*2R,3S* stereoisomer.



Another means of representing molecules with several stereocenters is by *Fischer projection formulas*. The main chain of the molecule is aligned vertically, with (by convention) the most oxidized end of the chain at the top. The substituents that are shown horizontally project toward the viewer. Thus the vertical carbon-carbon bonds point away from the viewer at all carbon atoms. Fischer projection formulas represent a *completely eclipsed conformation* of the vertical chain. Because the horizontal bonds project from the plane of the paper, any reorientation of the structures must not change this feature. *Fischer projection formulas may be reoriented only in the plane of the paper*. Fischer projection formulas use an alternative system for specifying chirality. The chirality of the highest-numbered chiral center (the one most distant from the oxidized terminus, that is, the one closest to the bottom in the conventional orientation), is specified as D or L, depending on whether it is like the D- or L-enantiomer of glyceraldehyde, which is the reference compound. In the conventional orientation, D-substituents are to the right and L-substituents are to the left.



The *relative configuration* of adjacent substituents in a Fischer projection formula are designated *erythro* if they are on the same side and *threo* if they are on the opposite side. The stereochemistry of adjacent stereocenters can also be usefully represented

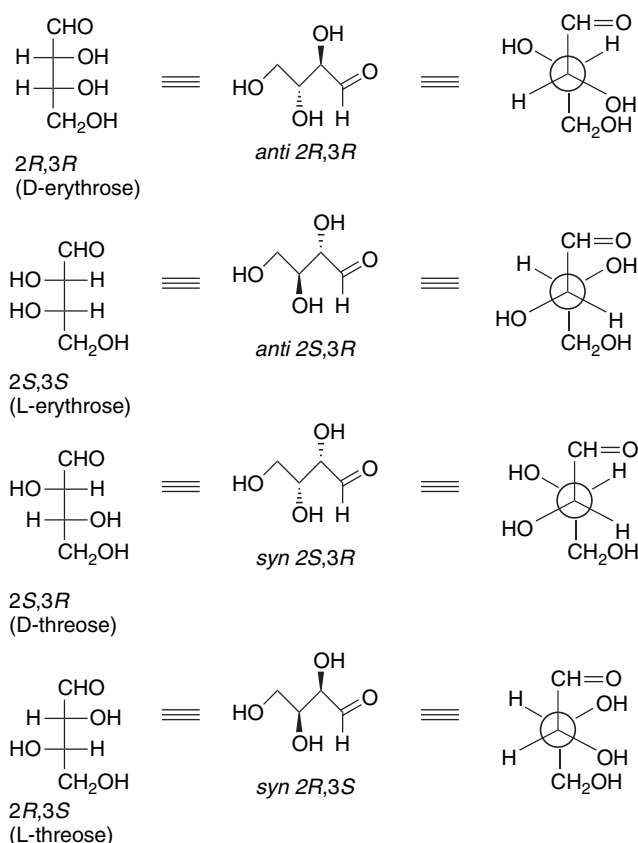


Fig. 2.5. Fischer, extended, and Newman projection representations of the stereoisomers of 2,3,4-trihydroxybutanal.

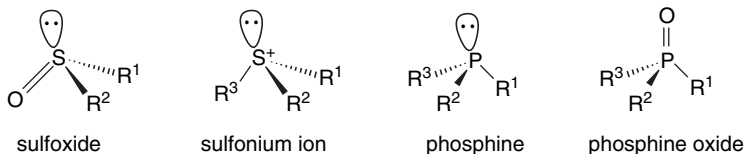
by *Newman projection formulas*. Figure 2.5 shows 2,3,4-trihydroxybutanal (now also with its carbohydrate names, erythrose and threose) as Fischer projection formulas as well as extended and Newman representations.

Because the Fischer projection formulas represent an eclipsed conformation of the carbon chain, the relative orientation of two adjacent substituents is opposite from the extended staggered representation. Adjacent substituents that are *anti* in an extended representation are on the same side of a Fischer projection formula, whereas adjacent substituents that are *syn* in an extended representation are on opposite sides in a Fischer projection. As with extended representations, an enantiomeric pair represented by Fischer projection formulas has the opposite configuration at *all stereogenic centers* (depicted as left or right.)

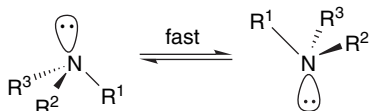
2.1.5. Other Types of Stereogenic Centers

Although asymmetrically substituted carbon atoms are by far the most common type of stereogenic center in organic compounds, several other kinds of stereogenic centers are encountered. Tetravalent nitrogen (ammonium) and phosphorus (phosphonium) ions are obvious extensions. Phosphine oxides are also tetrahedral and are chiral if all three substituents (in addition to the oxygen) are different. Not quite

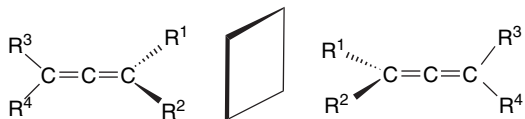
so evident are the cases of *trivalent* sulfur and phosphorus compounds, including sulfonium salts, sulfoxides, and phosphines. The heteroatom in these structures is approximately tetrahedral, with an electron pair occupying one of the tetrahedral positions. Because there is a relatively high energy barrier to inversion of these tetrahedral molecules, they can be obtained as pure enantiomers.



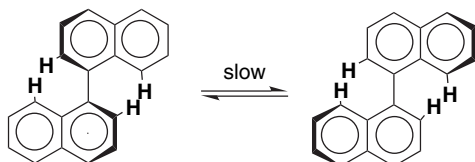
Trivalent nitrogen compounds are also approximately tetrahedral in shape. In this case, however, the barrier to inversion is small and the compounds cannot be separated as pure enantiomers at normal temperatures.



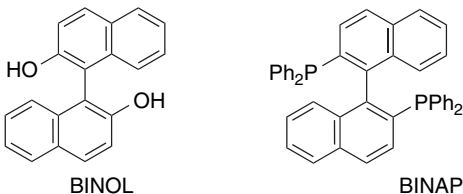
Allenes (see p. 6 for a discussion of bonding in allenes) can be chiral. An allene having nonidentical substituents at both sp^2 carbons gives nonsuperimposable mirror images.



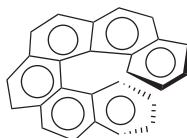
Molecules with shapes analogous to screws are also chiral, since they can be right-handed or left-handed. There are several kinds of molecules in which steric factors impose a screwlike shape. A very important case is 1, 1'-binaphthyl compounds. Steric interactions between the 2 and 8' hydrogens prevent these molecules from being planar, and as a result, there are two nonsuperimposable mirror image forms.



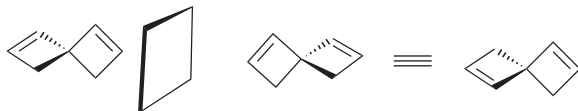
A particularly important example is the 2,2'-diol, which is called BINOL. Another important type includes 1,1'-binaphthyl diphosphines, such as BINAP.⁵ BINOL and BINAP are useful chiral ligands in organometallic compounds that serve as catalysts for hydrogenations and other reactions. In Section 2.5.1.1, we discuss how compounds such as BINOL and BINAP have been used to develop *enantioselective hydrogenation catalysts*.



A spectacular example of screw-shaped chirality is hexahelicene, in which the six fused benzene rings cannot be planar and give rise to right-handed and left-handed enantiomers. The specific rotation $[\alpha]_{589}$ is about 3700.⁶ Hexahelicene can be racemized by heating. The increased molecular vibration allows the two terminal rings to slip past one another. The activation energy required is 36.2 kcal/mol.⁷

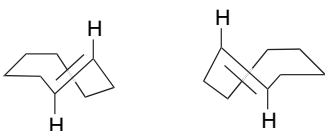


Many *spiro* compounds are chiral. In *spiro* structures, two rings share a common atom. If neither ring contains a plane of symmetry, *spiro* compounds are chiral. An example is *S*-(+)-*spiro*[3,3]hepta-1,5-diene.⁸

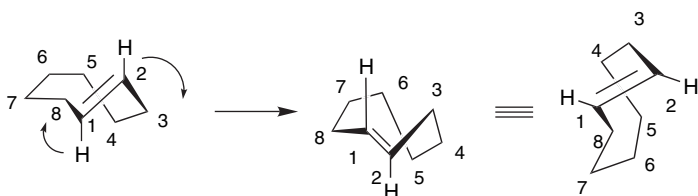


The *E*-cycloalkenes are also chiral. *E*-cyclooctene is a good example. Examination of the structures below using molecular models demonstrates that the two mirror images cannot be superimposed.

- ⁵. A. Noyori and H. Takaya, *Acc. Chem. Res.*, **23**, 345 (1990).
- ⁶. M. S. Newman and D. Lednicer, *J. Am. Chem. Soc.*, **78**, 4765 (1956).
- ⁷. R. H. Martin and M. J. Marchant, *Tetrahedron*, **30**, 347 (1974).
- ⁸. L. A. Hulshof, M. A. McKervey, and H. Wynberg, *J. Am. Chem. Soc.*, **96**, 3906 (1974).

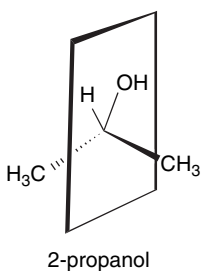


E-cyclooctene is subject to thermal racemization. The molecular motion allows the double bond to slip through the ring, giving the enantiomer. The larger and more flexible the ring, the easier the process. The rates of racemization have been measured for *E*-cyclooctene, *E*-cyclononene, and *E*-cyclodecene. For *E*-cyclooctene the half-life is 1 h at 183.9°C. The activation energy is 35.6 kcal/mol. *E*-cyclononene, racemizes much more rapidly. The half-life is 4 min at 0°C, with an activation energy of about 20 kcal/mol. *E*-cyclodecene racemizes immediately on release from the chiral platinum complex used for its preparation.⁹



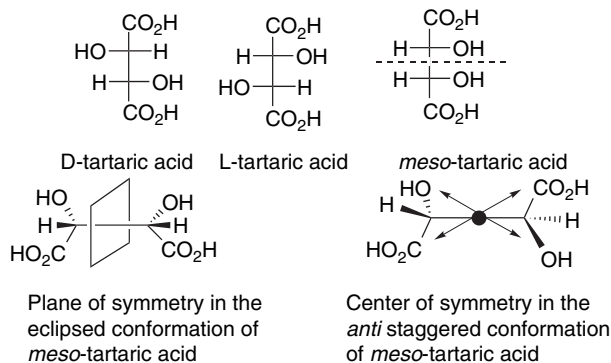
2.1.6. The Relationship between Chirality and Symmetry

Molecules that possess certain elements of symmetry are not chiral, because the element of symmetry ensures that the mirror image forms are superimposable. The most common example is a *plane of symmetry*, which divides a molecule into two halves that have identical placement of substituents on both sides of the plane. A trivial example can be found at any tetrahedral atom with two identical substituents, as, for example, in 2-propanol. The plane subdivides the 2-H and 2-OH groups and the two methyl groups are identical.

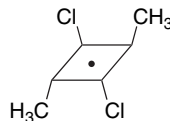


⁹. A. C. Cope and B. A. Pawson, *J. Am. Chem. Soc.*, **87**, 3649 (1965); A. C. Cope, K. Banholzer, H. Keller, B. A. Pawson, J. J. Whang, and H. J. S. Winkler, *J. Am. Chem. Soc.*, **87**, 3644 (1965).

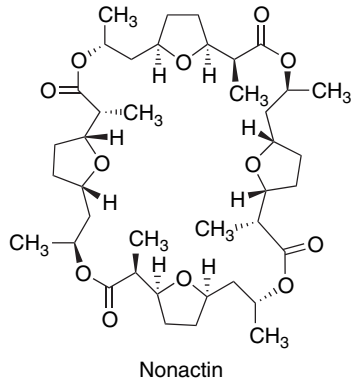
More elaborate molecules can also have a plane of symmetry. For example, there are only three stereoisomers of tartaric acid (2,3-dihydroxybutanedioic acid). Two of these are chiral but the third is achiral. In the achiral stereoisomer, the substituents are located with respect to each other in such a way as to generate a plane of symmetry. Compounds that contain two or more stereogenic centers but have a plane of symmetry are called *meso forms*. Because they are achiral, they do not rotate plane polarized light. Note that the Fischer projection structure of *meso*-tartaric acid reveals the plane of symmetry.



A less common element of symmetry is a *center of symmetry*, which is a point in a molecule through which a line oriented in any direction encounters the same environment (structure) when projected in the opposite direction. For example, *trans, trans, cis*-2,4-dichloro-1,3-dimethylcyclobutane has a center of symmetry, but no plane of symmetry. It is achiral.

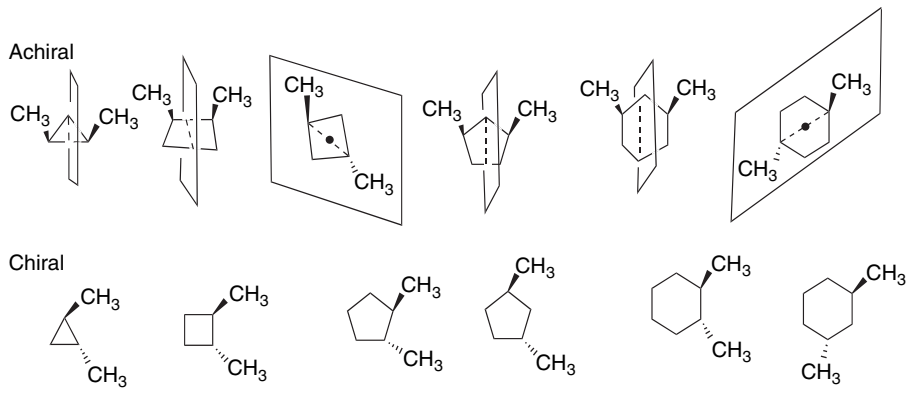


Another very striking example is the antibiotic nonactin. Work out problem 2.15 to establish the nature of the of symmetry in nonactin.



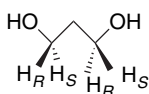
Various di- and polysubstituted cyclic compounds provide other examples of molecules having elements of symmetry. Since chirality depends on *configuration*, not *conformation*, cyclic molecules can be represented as planar structures to facilitate recognition of symmetry elements. These planar structures clearly convey the *cis* and *trans* relationships between substituents. Scheme 2.1 gives some examples of both chiral and achiral dimethylcycloalkanes. Note that in several of the compounds there is both a center and a plane of symmetry. Either element of symmetry ensures that the molecule is achiral.

Scheme 2.1. Chiral and Achiral Disubstituted Cycloalkanes

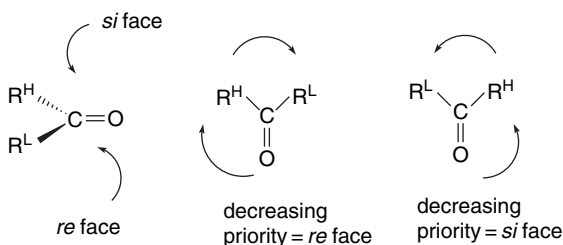


2.1.7. Configuration at Prochiral Centers

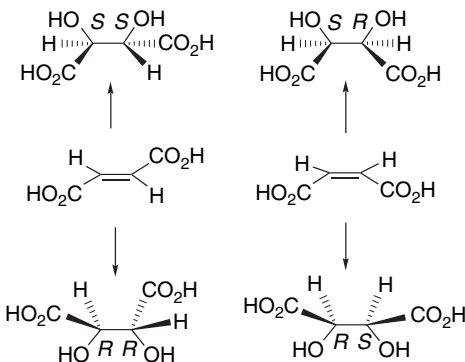
Prochiral centers have two identical ligands, such as two hydrogens, and are achiral. In many situations, however, these identical ligands are *topologically nonequivalent* or *heterotopic*. This occurs when the other two substituents are different. If either of the identical groups is replaced by a different ligand, a stereogenic center is created. The two positions are called *enantiotopic*. The position, which if assigned a higher priority, gives an *R* configuration is called pro-*R*. The position, which if assigned a higher priority, gives an *S* configuration is called pro-*S*. Propane-1,3-diol is an example of a prochiral molecule. The C(1) and C(3) positions are prochiral, but the C(2) is not, because its two hydroxymethyl ligands are identical.



Unsymmetrically substituted carbonyl groups are prochiral centers, since addition of a fourth ligand generates a stereogenic center. These are designated by determining the Cahn-Ingold-Prelog priority order. The carbonyl group is said to have an *re* face and an *si* face.



Achiral reagents do not distinguish between the two faces, but chiral reagents do and give unequal amounts of enantiomeric products. Other trigonal centers, including carbon-carbon double bonds, present two prochiral faces. For example, *E*- and *Z*-butenedioic acid (maleic and fumaric acid) generate different stereoisomers when subjected to *syn*-dihydroxylation. If the reagent that is used is chiral, the *E*-isomer will generate different amounts of the *R,R* and *S,S* products. The *S,R* and *R,S* forms generated from the *Z*-isomer are *meso* forms and will be achiral, even if they are formed using a chiral reagent.



The concept of heterotopic centers and faces can be extended to diastereotopic groups. If one of two equivalent ligands in a molecule is replaced by a test group, the ligands are diastereotopic when the resulting molecules are diastereomers. Similarly, if a transformation at opposite faces of a trigonal center generates two different diastereomers, the faces are diastereotopic. There is an important difference between enantiotopic and diastereotopic centers. Two identical ligands at enantiotopic centers are in *chemically equivalent environments*. They respond identically to probes, including chemical reagents, that are achiral. They respond differently to chiral probes, including chiral reagents. Diastereotopic centers are *topologically nonequivalent*. That is, their environments in the molecule are different and they respond differently to achiral, as well as to chiral probes and reagents. As a consequence of this nonequivalence, diastereotopic protons, as an example, have different chemical shifts and are distinguishable in NMR spectra. Enantiotopic protons do not show separate NMR signals. Two diastereotopic protons give rise to a more complex NMR pattern. Because of their chemical shift difference, they show a geminal coupling. An example of this effect can be seen in the proton NMR spectra of 1-phenyl-2-butanol, as shown in

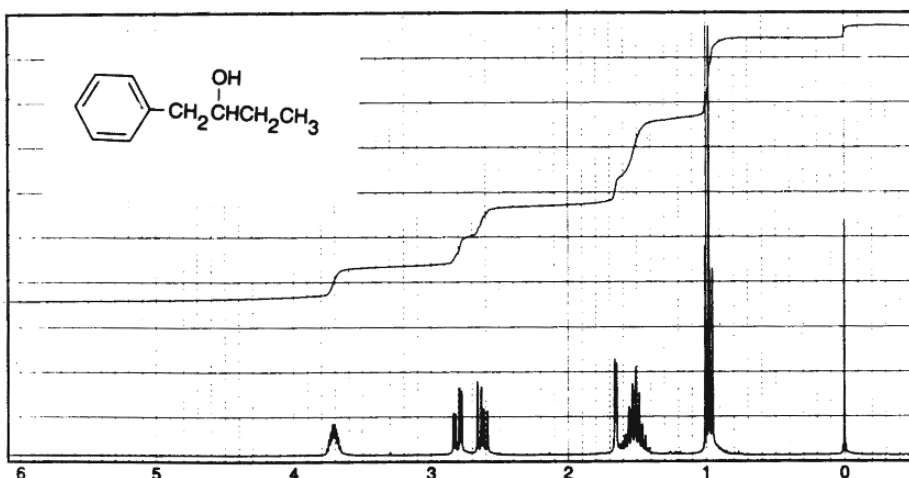
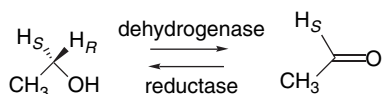


Fig. 2.6. NMR spectrum of 1-phenyl-2-butanol showing the diastereotopic nature of C(1) protons. Reproduced from Aldrich Library of ^{13}C and ^1H NMR Spectra, Vol. 2, 1993, p. 386.

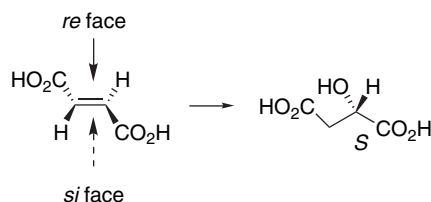
Figure 2.6. The C(1) CH_2 group appears as a quartet near 2.8 ppm with further coupling to the C(2) proton. The C(1) hydrogens are diastereotopic. The C(3) hydrogens are also diastereotopic, but their nonidentity is not obvious in the multiplet at about 1.6 ppm.

Because biological reactions involve chiral enzymes, enantiotopic groups and faces typically show different reactivity. For example, the two methylene hydrogens in ethanol are enantiotopic. Enzymes that oxidize ethanol, called *alcohol dehydrogenases*, selectively remove the pro-*R* hydrogen. This can be demonstrated by using a deuterated analog of ethanol in the reaction.



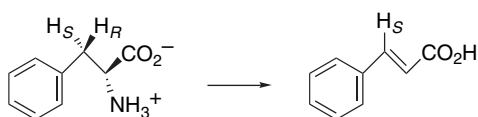
Conversely, *reductases* selectively reduce acetaldehyde from the *re* face.

Fumaric acid is converted to L-malic acid (*S*-2-hydroxybutanedioic acid) by the enzyme *fumarase*. The hydroxy group is added stereospecifically from the *si* face of the double bond.



Enzymes also distinguish between diastereotopic groups and faces. For example, L-phenylalanine is converted to cinnamic acid by the enzyme *phenylalanine ammonia*

lyase. The reaction occurs by an *anti* elimination involving the amino group and the 3-*pro-R* hydrogen.

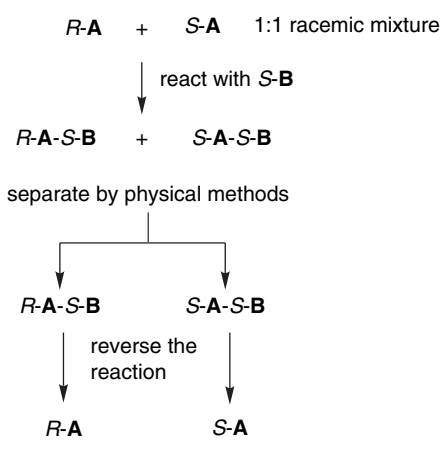


2.1.8. Resolution—The Separation of Enantiomers

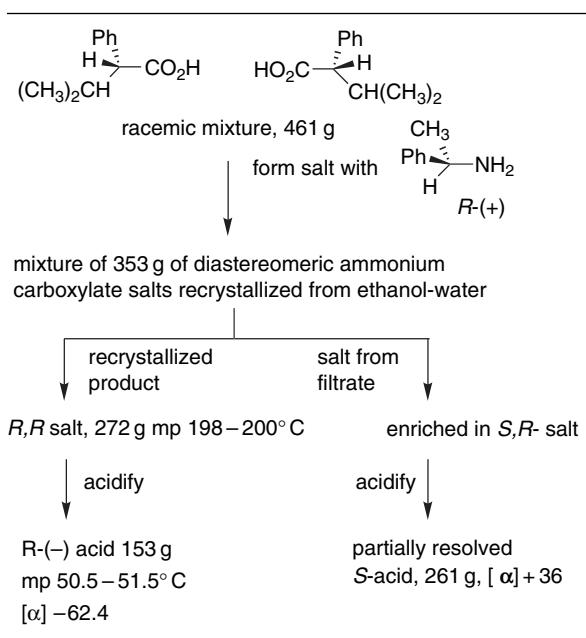
Since all living cells and organisms involve reactions of enantiomerically pure materials such as carbohydrates, proteins, and DNA, most naturally occurring chiral compounds exist in enantiomerically pure form. Chemical reactions, however, often produce racemic mixtures. This is *always* the case if only racemic and/or achiral reactants, reagents, catalysts, and solvents are used. The products of chemical reactions can be enantiomerically enriched or enantiopure only if chiral starting materials, reagents, catalysts or solvents are used. (See Section 2.5 for a discussion of enantioselective reactions.) Racemic mixtures can be separated into the two enantiomeric forms. The process of separating a racemic mixture into its enantiomers is called *resolution*, and it can be accomplished in several different ways.

Historically, the usual method was to use an existing enantiomerically pure compound, often a naturally occurring material, as a *resolving agent*. When a racemic mixture of **A** (*R,S*-**A**) reacts with a pure enantiomer (*S*-**B**), the two products are *diastereomeric*, namely *R,S*-**AB** and *S,S*-**AB**. As diastereomers have differing physical properties, they can be separated by such means as crystallization or chromatography. When the diastereomers have been separated, the original reaction can be reversed to obtain enantiomerically pure (or enriched) samples. The concept is summarized in Scheme 2.2. Scheme 2.3 describes an actual resolution.

Scheme 2.2. Conceptual Representation of Resolution through Separation of Diastereomeric Derivatives



Scheme 2.3. Resolution of 3-Methyl-2-Phenylbutanoic Acid^a



* a. C. Aaron, D. Dull, J. L. Schmiegel, D. Jaeger, Y. Ohahi, and H. S. Mosher, *J. Org. Chem.*, **32**, 2797 (1967).

Another means of resolution is to use a chiral material in a physical separation. Currently, many resolutions are done using medium- or high-pressure chromatography with chiral column-packing materials. Resolution by chromatography depends upon differential adsorption of the enantiomers by the chiral stationary phase. Differential adsorption occurs because of the different “fit” of the two enantiomers to the chiral adsorbent. Figure 2.7 shows such a separation. Topic 2.1 provides additional detail on several types of chiral stationary phases.

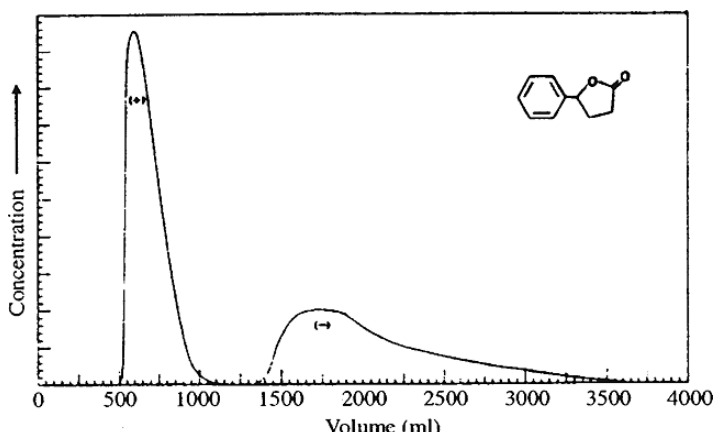
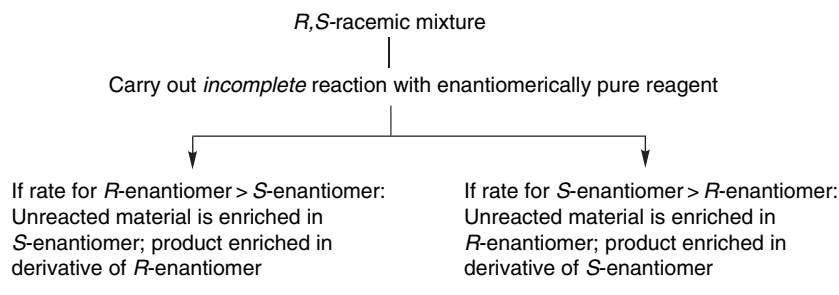


Fig. 2.7. Preparative chromatographic resolution of 5 g of γ -phenyl- γ -butyrolactone on 480 g of cellulose triacetate (column 5 cm \times 60 cm). Reproduced from *Helv. Chim. Acta*, **70**, 1569 (1987), by permission of Wiley-VCH.

Scheme 2.4. Conceptual Basis of Kinetic Resolution

Another means of resolution depends on the difference in rates of reaction of two enantiomers with a chiral reagent. The rates of reaction of each enantiomer with a single enantiomer of a chiral reagent are different because the transition structures and intermediates (*R*-substrate...*R*-reagent) and (*S*-substrate...*R*-reagent) are *diastereomeric*. *Kinetic resolution* is the term used to describe the separation of enantiomers on the basis of differential reaction rates with an enantiomerically pure reagent. Scheme 2.4 summarizes the conceptual basis of kinetic resolution.

Because the separation is based on differential rates of reaction, the degree of resolution that can be achieved depends on both the *magnitude of the rate difference and the extent of reaction*. The greater the difference in the two rates, the higher the enantiomeric purity of both the reacted and unreacted enantiomer. The extent of enantiomeric purity can be controlled by controlling the degree of conversion. As the extent of conversion increases, the enantiomeric purity of the *unreacted enantiomer increases*.¹⁰ The relationship between the relative rate of reaction, extent of conversion, and enantiomeric purity of the unreacted enantiomer is shown graphically in Figure 2.8.

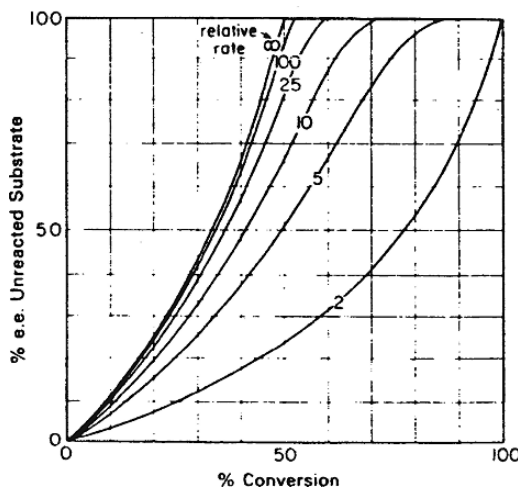


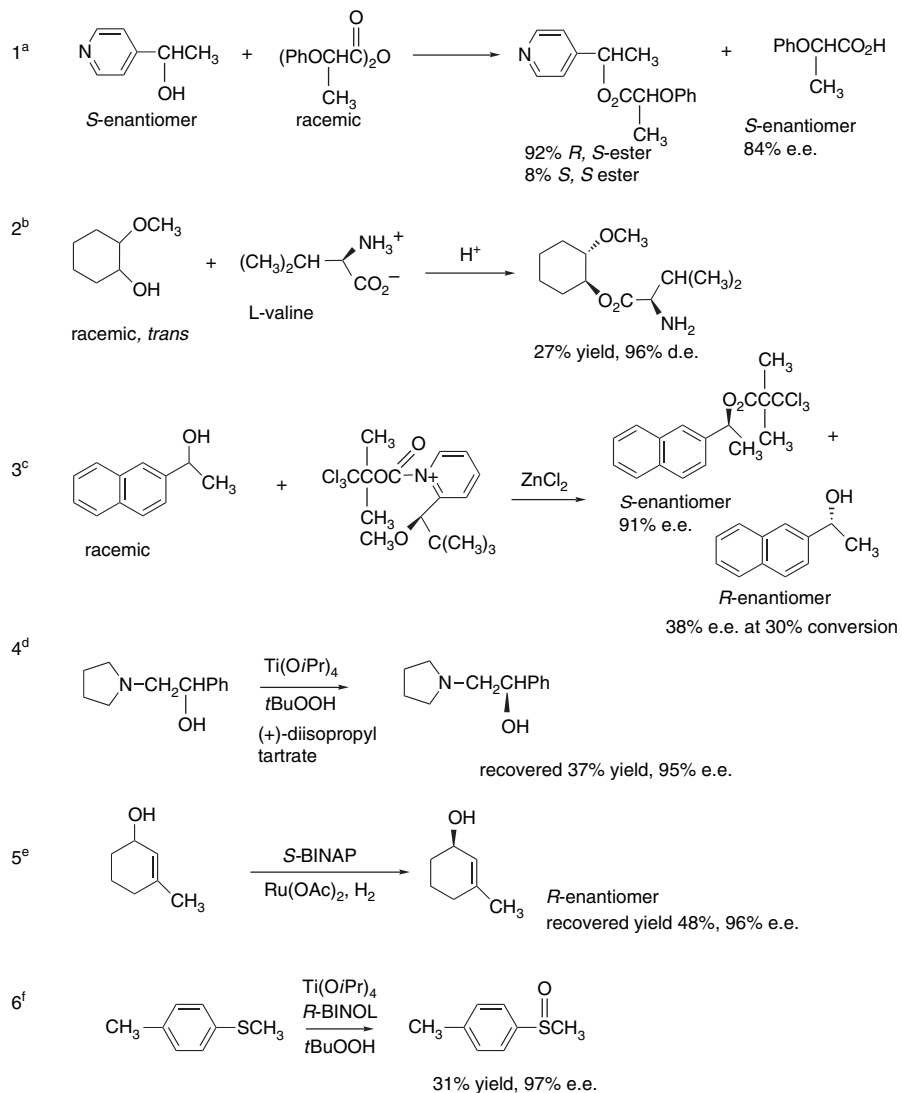
Fig. 2.8. Dependence of enantiomeric excess on relative rate of reaction and extent of conversion with a chiral reagent in kinetic resolution. Reproduced from *J. Am. Chem. Soc.*, **103**, 6237 (1981), by permission of the American Chemical Society.

¹⁰ V. S. Martin, S. S. Woodard, T. Katsuki, Y. Yamada, M. Ikeda, and K. B. Sharpless, *J. Am. Chem. Soc.*, **103**, 6237 (1981).

Of course, the high conversion required for high enantiomeric purity when the relative reactivity difference is low has a serious drawback. The *yield of the unreacted substrate is low* if the overall conversion is high. Relative reactivity differences of < 10 can achieve high enantiomeric purity only at the expense of low yield.

Scheme 2.5 gives some specific examples of kinetic resolution procedures. Entries 1 to 3 in Scheme 2.5 are acylation reactions in which esters are formed. Either the

Scheme 2.5. Examples of Kinetic Resolution



a. U. Salz and C. Rüchardt, *Chem. Ber.*, **117**, 3457 (1984).

b. P. Stead, H. Marley, M. Mahmoudian, G. Webb, D. Noble, Y. T. Ip, E. Piga, S. Roberts, and M. J. Dawson, *Tetrahedron: Asymmetry*, **7**, 2247 (1996).

c. E. Vedejs and X. Chen, *J. Am. Chem. Soc.*, **118**, 1809 (1996).

d. S. Miyano, L. D. Lu, S. M. Viti, and K. B. Sharpless, *J. Org. Chem.*, **48**, 3608 (1983).

e. M. Kitmura, I. Kasahara, K. Manabe, R. Noyori, and H. Takaya, *J. Org. Chem.*, **53**, 708 (1988).

f. N. Komatsu, M. Hashizuma, T. Sugita, and S. Uemura, *J. Org. Chem.*, **58**, 7624 (1993).

alcohol or the acylation reagent is enantiopure. The enantioselectivity is a result of differential interactions in the TS (transition structure) and the reactions are carried to partial conversion to achieve kinetic resolution. These reactions presumably proceed via the typical addition-elimination mechanism for acylation (see Section 7.4) and do not have the benefit of any particular organizing center such as a metal ion. The observed enantioselectivities are quite high, and presumably depend primarily on steric differences in the diastereomeric TSs. Entries 4 and 5 involve enantioselective catalysts. Entry 4, is an oxidative cleavage that involves a complex of Ti(IV) with the chiral ligand, diisopropyl tartrate. It is sufficiently selective to achieve 95% e.e. at the point of about 67% completion. The other enantiomer is destroyed by the oxidation. Entry 5 uses a hydrogenation reaction with the chiral BINAP ligand (see p. 130 for structure). The *S*-enantiomer is preferentially hydrogenated and the *R*-enantiomer is obtained in high e.e. In both of these examples, the reactant coordinates to the metal center through the hydroxy group prior to reaction. The relatively high e.e. that is observed in each case reflects the high degree of order and discrimination provided by the chiral ligands at the metal center. Entry 6 is the oxidative formation of a sulfoxide, using BINOL (see p. 130) as a chiral ligand and again involves a metal center in a chiral environment. We discuss enantioselective catalysis further in Section 2.5.

Enzymes constitute a particularly important group of enantioselective catalysts,¹¹ as they are highly efficient and selective and can carry out a variety of transformations. Enzyme-catalyzed reactions can be used to resolve organic compounds. Because the enzymes are derived from L-amino acids, they are chiral and usually one enantiomer of a reactant (substrate) is much more reactive than the other. The interaction with each enantiomer is diastereomeric in comparison with the interaction of the enzyme with the other enantiomer. Since enzymatic catalysis is usually based on a specific fit to an “active site,” the degree of selectivity between the two enantiomers is often very high. For enzymatic resolutions, the enantioselectivity can be formulated in terms of two reactants in competition for a single type of catalytic site.¹² Enzymatic reactions can be described by *Michaelis-Menten kinetics*, where the key parameters are the equilibrium constant for binding at the active site, K , and the rate constant, k , of the enzymatic reaction. The rates for the two enantiomers are given by

$$v_R = k_R[R]/K_R \text{ and } v_S = k_S[S]/K_S \quad (2.6)$$

In a resolution with the initial concentrations being equal, $[S] = [R]$ the enantiomeric selectivity ratio E is the relative rate given by

$$E = \frac{k_S/K_S}{k_R/K_R} \quad (2.7)$$

Figure 2.9 shows the relationship between the e.e. of unreacted material and product as a function of the extent of conversion and the value of E .

The most generally useful enzymes catalyze hydrolysis of esters and amides (esterases, lipases, peptidases, acylases) or interconvert alcohols with ketones and aldehydes (oxido-reductases). Purified enzymes can be used or the reaction can be done by incubating the reactant with an organism (e.g., a yeast) that produces an

¹¹. J. B. Jones, *Tetrahedron*, **42**, 3351 (1986); J. B. Jones, in *Asymmetric Synthesis*, J. D. Morrison, ed., Vol. 5, Academic Press, Chap. 9; G. M. Whitesides and C.-H. Wong, *Angew. Chem. Int. Ed. Engl.*, **24**, 617 (1985).

¹². C.-S. Chen, Y. Fujimoto, G. Girdaukas, and C. J. Sih, *J. Am. Chem. Soc.*, **104**, 7294 (1982).

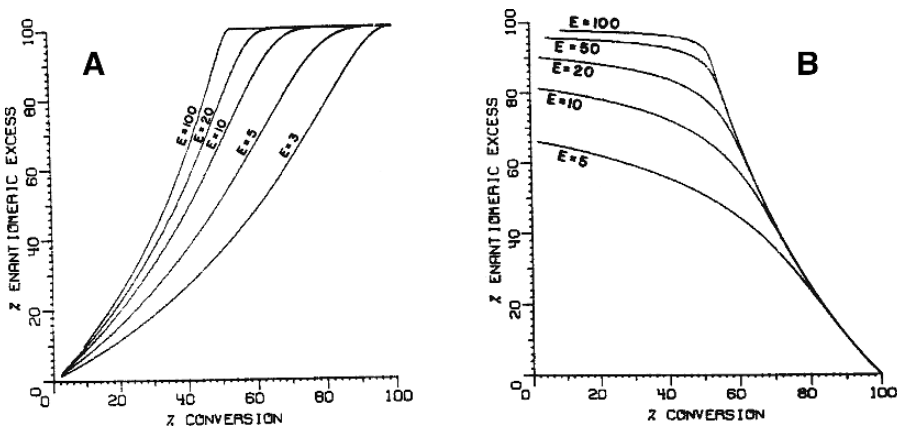
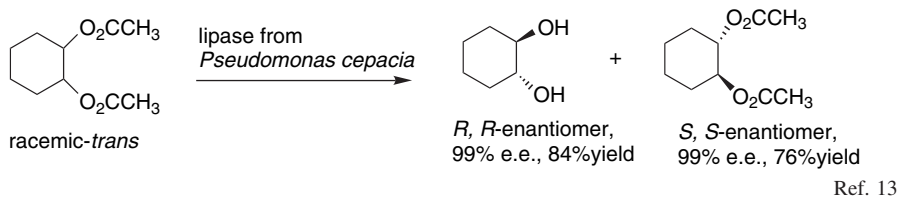
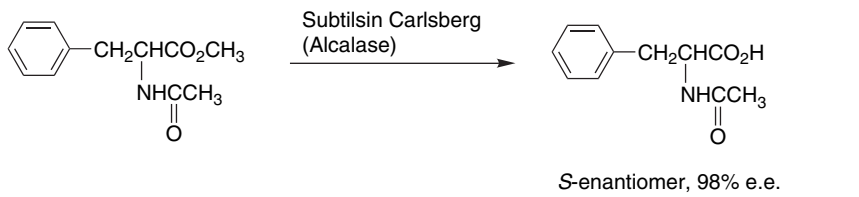


Fig. 2.9. Plots of enantiomeric excess as a function of extent of conversion for various values of E : (A) unreacted starting material; (B) product. Reproduced from *J. Am. Chem. Soc.*, **104**, 7294 (1982), by permission of the American Chemical Society.

appropriate enzyme during fermentation. Two examples are shown below. The main restriction on enzymatic resolution is the relatively limited range of reactions and substrates to which it is applicable. Enzymes usually have high substrate specificity, that is, they show optimal reactivity for compounds that are similar in structure to the natural substrate. Topic 2.2 gives further information about the application of enzymatic resolution.



Ref. 13



Ref. 14

¹³ G. Caron and R. J. Kazlauskas, *J. Org. Chem.*, **56**, 7251 (1991).

¹⁴ J. M. Roper and D. P. Bauer, *Synthesis*, 1041 (1983).

2.2. Conformation

CHAPTER 2

Stereochemistry,
Conformation,
and Stereoselectivity

The structural aspects of stereochemistry discussed in the previous section are the consequences of *configuration*, the geometric arrangement fixed by the chemical bonds within the molecule. Now, we want to look at another level of molecular structure, *conformation*. Conformations are the different shapes that a molecule can attain without breaking any covalent bonds. They differ from one another as the result of rotation at one or more single bond. The energy barrier for rotation of carbon-carbon single bonds is normally small, less than 5 kcal/mol, but processes that involve several coordinated rotations can have higher energy requirements. *Conformational analysis* is the process of relating conformation to the properties and reactivity of molecules.

2.2.1. Conformation of Acyclic Compounds

Ethane is a good molecule with which to begin. The two methyl groups in ethane can rotate with respect to one another. There are two unique conformations, called *staggered* and *eclipsed*. The eclipsed conformation represents the maximum energy and the staggered is the minimum. The difference between the two is 2.88 kcal/mol, as shown in Figure 2.10. As a result, any individual molecule is likely to be in the

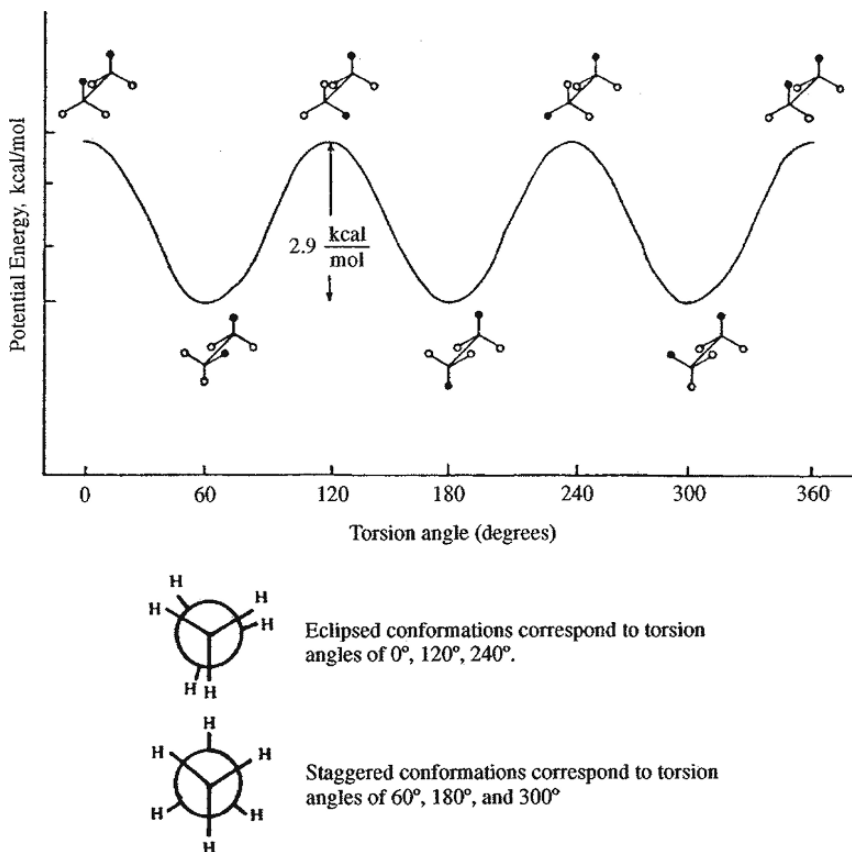
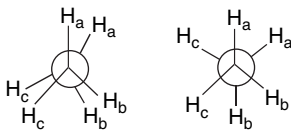
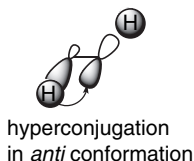


Fig. 2.10. Potential energy as a function of torsion angle for ethane.



Shortly, we will learn that for some hydrocarbon molecules, van der Waals repulsions are a major factor in conformational preferences and energy barriers, but that is not the case for ethane. Careful analysis of the van der Waals radii show that the hydrogens do not come close enough to account for the barrier to rotation.¹⁵ Furthermore, the barrier of just under 3 kcal is applicable to more highly substituted single bonds. The barrier becomes significantly larger only when additional steric components are added, so the barrier must be an intrinsic property of the bond and not directly dependent on substituent size. The barrier to rotation is called the *torsional barrier*. There are analogous (although smaller) barriers to rotation about C–N and C–O bonds. Topic 1.3 probes further into the origin of the torsional barrier in small molecules. The conclusion reached is that the main factor responsible for the torsional barrier is σ - σ^* delocalization (hyperconjugation), which favors the staggered conformation.



The interplay between the torsional barrier and nonbonded (van der Waals) interactions can be illustrated by examining the conformations of *n*-butane. The relationship between energy and the torsion angle for rotation about the C(2)–C(3) bond is presented in Figure 2.11. The potential energy diagram of *n*-butane resembles that of ethane in having three maxima and three minima, but differs in that one of the minima is lower than the other two and one of the maxima is of higher energy than the other two. The minima correspond to staggered conformations. Of these, the *anti* is lower in energy than the two *gauche* conformations. The energy difference between the *anti* and *gauche* conformations in *n*-butane is about 0.6 kcal/mol.¹⁶ The maxima correspond to eclipsed conformations, with the highest-energy conformation being the one with the two methyl groups eclipsed with each other.

The rotational profile of *n*-butane can be understood as a superimposition of van der Waals repulsion on the ethane rotational energy profile. The two *gauche* conformations are raised in energy relative to the *anti* by an energy increment resulting from the van der Waals repulsion between the two methyl groups of 0.6 kcal/mol. The

¹⁵. E. Eliel and S. H. Wilen, *Stereochemistry of Organic Compounds*, Wiley, New York, 1994, p. 599.

¹⁶. G. J. Szasz, N. Sheppard, and D. H. Rank, *J. Chem. Phys.*, **16**, 704 (1948); P. B. Woller and E. W. Garbisch, Jr., *J. Am. Chem. Soc.*, **94**, 5310 (1972).

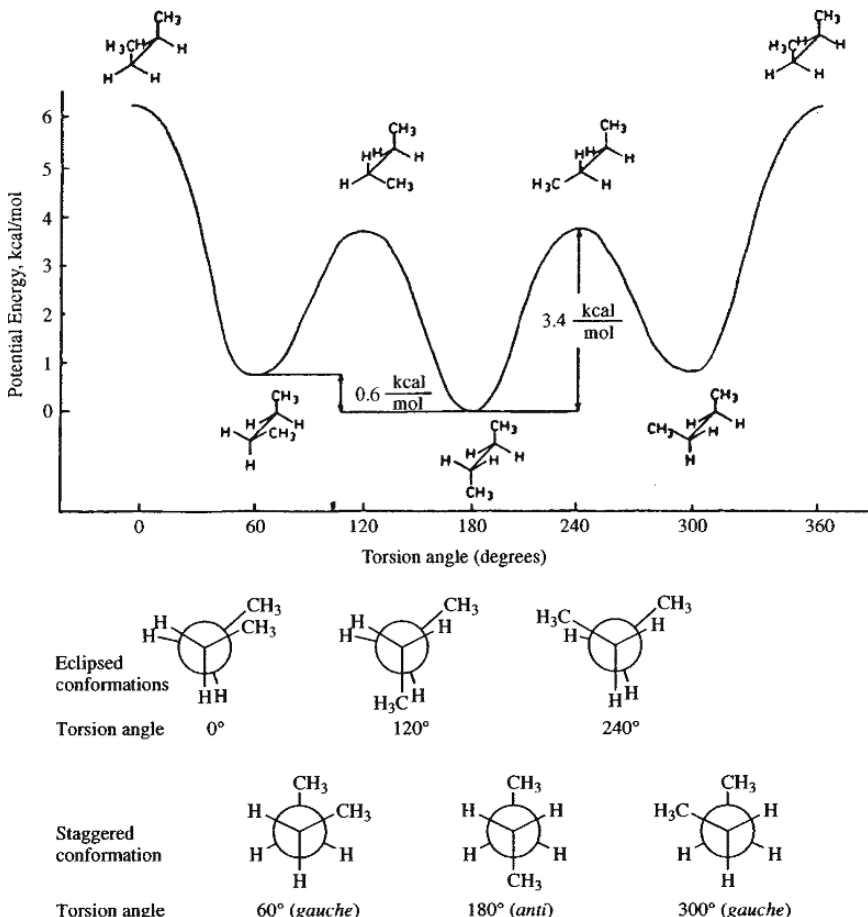


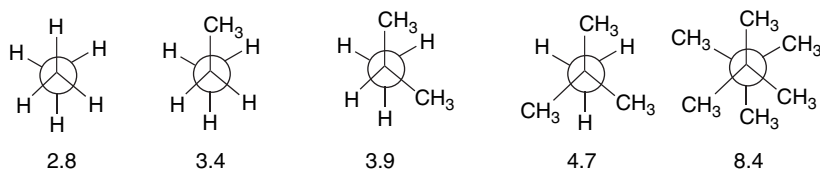
Fig. 2.11. Potential energy diagram for rotation about the C(2)–C(3) bond in *n*-butane.

eclipsed conformations all incorporate 2.8 kcal/mol of torsional strain relative to the staggered conformations, just as in ethane. The methyl-methyl eclipsed conformation is further strained by the van der Waals repulsion between the methyl groups. The van der Waals repulsion between methyl and hydrogen is smaller in the other eclipsed conformations. The methyl/methyl eclipsed barrier is not known precisely, but the range in experimental and theoretical values is between 4.0 and 6.6 kcal/mol, with the most recent values being at the low end of the range.¹⁷

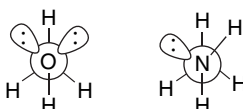
The conformation of other simple hydrocarbons can be interpreted by extensions of the principles illustrated in the analysis of rotational barriers in ethane and *n*-butane. The staggered conformations correspond to torsional minima and the eclipsed conformations to torsional maxima. Of the staggered conformations, *anti* forms are more stable than *gauche*. Substitution of a methyl group for hydrogen on one of the carbon atoms produces an increase of 0.4–0.6 kcal/mol in the height of the rotational energy barrier. The barrier in ethane is 2.88 kcal/mol. In propane, the barrier is 3.4 kcal/mol, corresponding to an increase of 0.5 kcal/mol for methyl-hydrogen eclipsing. When

¹⁷ N. L. Allinger, R. S. Grev, B. F. Yates, and H. F. Schaefer, III, *J. Am. Chem. Soc.*, **112**, 114 (1990); W. A. Herrebout, B. J. van der Veken, A. Wang, and J. R. Durig, *J. Phys. Chem.*, **99**, 578 (1995).

two methyl-hydrogen eclipsing interactions occur, as in 2-methylpropane, the barrier is raised to 3.9 kcal/mol. The increase in going to 2,2-dimethylpropane, in which the barrier is 4.7 kcal/mol, is 1.8 kcal/mol for the total of three methyl-hydrogen eclipsing interactions. For 2,2,3,3-tetramethylbutane, in which there are three methyl-methyl interactions, the barrier is 8.4 kcal/mol. Rotational barriers in kcal/mol are shown below.



The magnitudes of the barriers to rotation of many small organic molecules have been measured.¹⁸ The experimental techniques used to study rotational processes include microwave spectroscopy, electron diffraction, ultrasonic absorption, and infrared spectroscopy.¹⁹ Some representative barriers are listed in Table 2.1. As with ethane, the barriers in methylamine and methanol appear to be dominated by *hyperconjugative stabilization* of the *anti* conformation. The barrier decreases ($2.9 \rightarrow 2.0 \rightarrow 1.1$) in proportion to the number of anti H–H arrangements ($3 \rightarrow 2 \rightarrow 1$). (See Topic 1.1 for further discussion.)²⁰



The conformation of simple alkenes can be considered by beginning with propene. There are two families of conformations available to terminal alkenes: *eclipsed* and *bisected* conformations, as shown below for propene. The eclipsed conformation is preferred by about 2 kcal/mol and represents a barrier to rotation of the methyl group.^{21,22} A simple way to relate the propene rotational barrier to that of ethane is to regard the π bond as a “banana bond” (see p. 7). The bisected conformation of propene is then seen to correspond to the eclipsed conformation of ethane, while the more stable eclipsed conformation corresponds to the staggered conformation of ethane.²³

- ¹⁸. For reviews, see (a) J. P. Lowe, *Prog. Phys. Org. Chem.*, **6**, 1 (1968); (b) J. E. Andersen, in *The Chemistry of Alkenes and Cycloalkens*, S. Patai and Z. Rappoport, eds., Wiley, Chichester, 1992, Chap. 3II. D.
- ¹⁹. Methods for determination of rotational barriers are discussed in Ref. 18a and by E. Wyn-Jones and R. A. Pethrick, *Top. Stereochem.*, **5**, 205 (1969).
- ²⁰. J. K. Badenhoop and F. Weinhold, *Int. J. Quantum Chem.*, **72**, 269 (1999); V. Pophristic and L. Goodman, *J. Phys. Chem. A*, **106**, 1642 (2002).
- ²¹. J. R. Durig, G. A. Guirgis, and S. Bell, *J. Phys. Chem.*, **93**, 3487 (1989).
- ²². Detailed analysis of the rotation shows that it is coupled with vibrational processes. L. Goodman, T. Kundu, and J. Leszczynski, *J. Phys. Chem.*, **100**, 2770 (1996).
- ²³. K.-T. Lu, F. Weinhold, and J. C. Weisshaar, *J. Chem. Phys.*, **102**, 6787 (1995).

Table 2.1. Rotational Barriers of Compounds of Type $\text{CH}_3 - \text{X}^a$

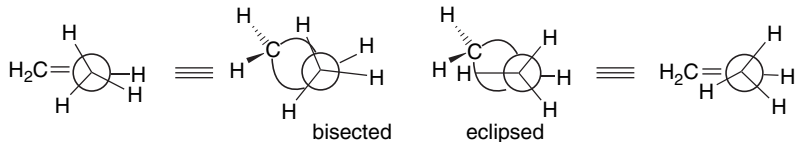
Alkanes ^a	Barrier (kcal/mol)	Heteroatom compounds	Barrier (kcal/mol)
$\text{CH}_3 - \text{CH}_3$	2.9	$\text{CH}_3 - \text{NH}_2^c$	2.0
$\text{CH}_3 - \text{CH}_2\text{CH}_3$	3.4	$\text{CH}_3 - \text{NHCH}_3^c$	3.0
$\text{CH}_3 - \text{CH}(\text{CH}_3)_2$	3.9	$\text{CH}_3 - \text{N}(\text{CH}_3)_2^c$	4.4
$\text{CH}_3 - \text{C}(\text{CH}_3)_3$	4.7	$\text{CH}_3 - \text{OH}^d$	1.1
$(\text{CH}_3)_3\text{C} - \text{C}(\text{CH}_3)_3$	8.4 ^b	$\text{CH}_3 - \text{OCH}_3^d$	4.6

a. Taken from the compilation of J. P. Lowe, *Prog. Phys. Org. Chem.*, **6**, 1 (1968).

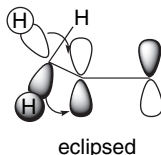
b. Footnote 9, J. E. Andersen, A. de Meijere, S. I. Kozhushkov, L. Lunazzi, and A. Mazzanti, *J. Org. Chem.*, **68**, 8494 (2003).

c. M. L. Senent and Y. G. Meyers, *J. Chem. Phys.*, **105**, 2789 (1996).

d. V. Popovits, L. Goodman, and N. Guchhait, *J. Phys. Chem. A*, **101**, 4290 (1997).



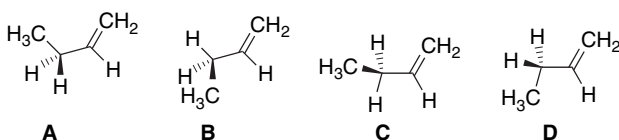
The conformation of propene is influenced by hyperconjugation. The methyl substituent has an overall stabilizing effect (2.7 kcal) on the double bond, as can be concluded from the less negative heat of hydrogenation compared to ethene (see Section 3.1.1). This stabilization arises from $\sigma-\pi^*$ interactions. The major effect is a transfer of electron density from the methyl σ C–H bonds to the empty π^* orbital.



Computational approaches can provide an indication of the magnitude of the interaction. A “block-localized” wave function calculation estimates a stabilization of about 5.4 kcal/mol at the 6-31G** level.²⁴ The computation also shows a shortening of the C(2)–C(3) single bond as the result of the $\sigma-\pi^*$ delocalization. Because the extent of hyperconjugation differs between the two unique conformers, this factor contributes to the energy difference between them. The energy difference between the eclipsed and bisected conformations has been broken into components, as described for ethane in Topic 1.3. The hyperconjugation component is the major factor. At the MP2/6-311(3d,2p) level of computation, the $\text{CH}_3 - \text{C} =$ bond length is 1.4952 Å, versus 1.5042 Å in the staggered conformation. The corresponding difference in energy is the largest component of the energy barrier and results from adjustments in the bond length in response to the rotation.²⁵

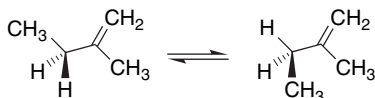
²⁴. The block-localized calculations are conceptually similar to NBO analysis (see Section 1.4.2) in that they compare a calculation in which the orbitals are strictly localized with the unrestricted calculation to estimate the effect of delocalization. Y. Mo and S. D. Peyerimhoff, *J. Chem. Phys.*, **109**, 1687 (1998).

²⁵. T. Kundu, L. Goodman, and J. Leszczynski, *J. Chem. Phys.*, **103**, 1523 (1995).

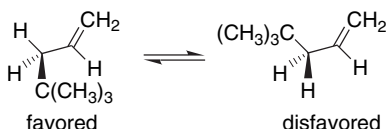


Conformations **A** and **B** are of the eclipsed type, whereas **C** and **D** are bisected. It has been determined by microwave spectroscopy that the eclipsed conformations are more stable than the bisected ones and that **B** is about 0.15 kcal more stable than **A**.²⁶ MO calculations at the HF/6-31G* level found relative energies of 0.00, -0.25, 1.75, and 1.74 kcal/mol, respectively, for **A**, **B**, **C**, and **D**.²⁷ More recently, experimental far-IR spectroscopy and MP2/6-31G++(3df,3pd) computations indicate a difference of about 0.2 kcal (favoring **B**).²⁸

Further substitution can introduce van der Waals repulsions that influence conformational equilibria. For example, methyl substitution at C(2), as in 2-methyl-1-butene, introduces a methyl-methyl *gauche* interaction in the conformation analogous to **B**, with the result that in 2-methyl-1-butene the two eclipsed conformations are of approximately equal energy.²⁹



Increasing the size of the group at C(3) increases the preference for the eclipsed conformation analogous to **B** at the expense of **A**. 4,4-Dimethyl-1-pentene exists mainly in the hydrogen-eclipsed conformation.



This interaction is an example of *1,3-allylic strain*.³⁰ This type of steric strain arises in eclipsed conformations when substituents on the double bond and the C(3) group, which are coplanar, are large enough to create a nonbonded repulsion. The conformation of alkenes is an important facet with regard to the stereoselectivity of addition

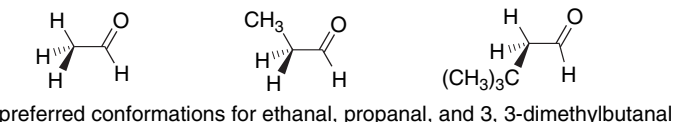
- ²⁶. S. Kondo, E. Hirota, and Y. Morino, *J. Mol. Spectrosc.*, **28**, 471 (1968).
- ²⁷. W. J. Hehre, J. A. Pople, and A. J. P. Devaqueut, *J. Am. Chem. Soc.*, **98**, 664 (1976).
- ²⁸. S. Bell, B. R. Drew, G. A. Guirgis, and J. R. During, *J. Mol. Struct.*, **553**, 199 (2000).
- ²⁹. T. Shimanouchi, Y. Abe, and K. Kuchitsu, *J. Mol. Struct.*, **2**, 82 (1968).
- ³⁰. R. W. Hoffmann, *Chem. Rev.*, **89**, 1841 (1989).

reactions of alkenes. Allylic strain and other conformational factors contribute to the relative energy of competing TSs, and can lead to a preference for a particular stereoisomeric product.

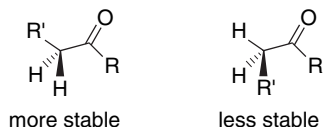
The preferred conformations of carbonyl compounds, like 1-alkenes, are eclipsed rather than bisected, as shown below for ethanal and propanal. The barrier for methyl group rotation in ethanal is 1.17 kcal/mol.³¹ Detailed analysis has indicated that small adjustments in molecular geometry, including σ -bond lengthening, must be taken into account to quantitatively analyze the barrier.³² The total barrier can be dissected into nuclear-nuclear, electron-electron, nuclear-electron, and kinetic energy (Δt), as described in Topic 1.3 for ethane. MP2/6-311+G (3df,2p) calculations lead to the contributions tabulated below. The total barrier found by this computational approach is very close to the experimental value. Contributions to the ethanal energy barrier in kcal/mol are shown below.

ΔV_{nn}	-10.621
ΔV_{ee}	-5.492
ΔV_{ne}	+18.260
Δt	-0.938
A total	+1.209

In propanal, it is the methyl group, rather than the hydrogen, that is eclipsed with the carbonyl group in the most stable conformation. The difference in the two eclipsed conformations has been determined by microwave spectroscopy to be 0.9 kcal/mol.³³ A number of other aldehydes have been studied by NMR and found to have similar rotameric compositions.³⁴ When the alkyl substituent becomes too sterically demanding, the hydrogen-eclipsed conformation becomes more stable. This is the case with 3,3-dimethylbutanal.



Ketones also favor eclipsed conformations. The preference is for the rotamer in which the alkyl group, rather than a hydrogen, is eclipsed with the carbonyl group because this conformation allows the two alkyl groups to be *anti* rather than *gauche* with respect to the other carbonyl substituent.



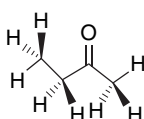
³¹ I. Kleiner, J. T. Hougen, R. D. Suenram, F. J. Lovas, and M. Godefroid *J. Mol. Spectros.*, 153, 578 (1992); S. P. Belov, M. Y. Tretyakov, I. Kleiner, and J. T. Hougen, *J. Mol. Spectros.*, 160, 61 (1993).

³². L. Goodman, T. Kundu, and J. Leszczynski, *J. Am. Chem. Soc.*, **117**, 2082 (1995).

^{33.} S. S. Butcher and E. B. Wilson, Jr., *J. Chem. Phys.*, **40**, 1671 (1964).

³⁴. G. J. Karabatsos and N. Hsi, *J. Am. Chem. Soc.*, **87**, 2864 (1965).

The conformational profile for 2-butanone has been developed from analysis of its infrared spectrum.³⁵ The dominant conformation is *anti* with a C(1)H and the C(4) methyl group eclipsed with the carbonyl.



The C(3)–C(4) rotational barrier is 2.48 kcal/mol, similar to the ethane barrier, while the C(1)–C(2) rotational barrier is 0.67 kcal/mol. Figure 2.12 shows the rotational potential energy diagram for 2-butanone as calculated at the HF/6-31G level. The preferred conformation of 3-methyl-2-butanone is similar.³⁶

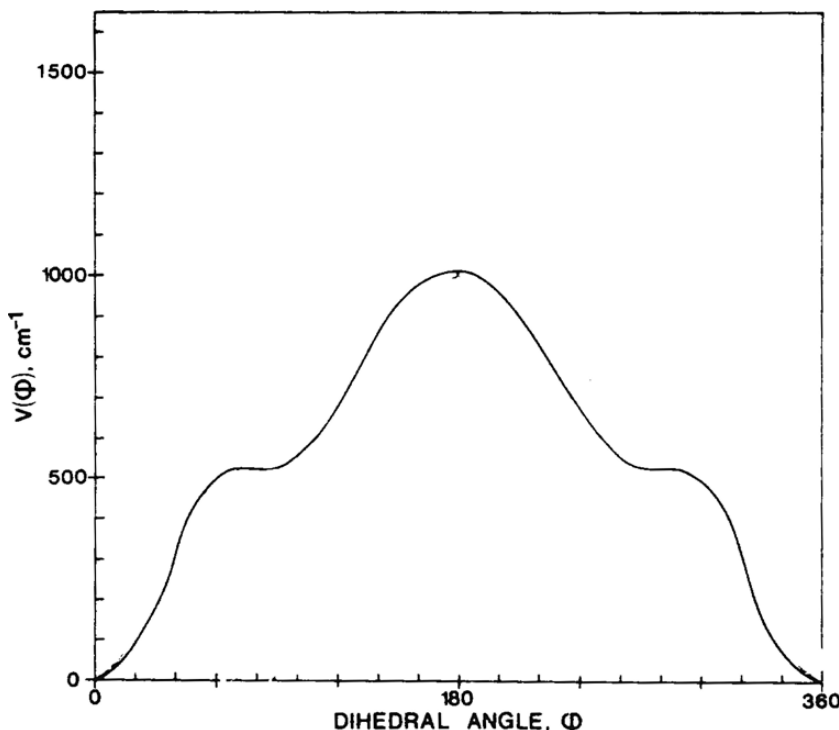
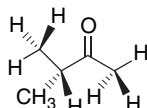


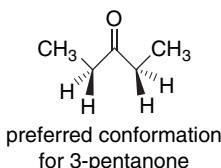
Fig. 2.12. Calculated potential energy diagram (HF/6-31G) for rotation about C(2)–C(3) bond of 2-butanone. Reproduced from *Can. J. Chem.* **69**, 1827 (1991), by permission of the National Research Council Press.

³⁵ J. R. Durig, F. S. Feng, A. Y. Wang, and H. V. Phan, *Can. J. Chem.*, **69**, 1827 (1991).

³⁶ T. Sakurai, M. Ishiyama, H. Takeuchi, K. Takeshita, K. Fukushi, and S. Konaka, *J. Mol. Struct.*, **213**, 245 (1989); J. R. Durig, S. Shen, C. Zeng, and G. A. Guirgis, *Can. J. Anal. Sci. Spectrosc.* **48**, 106 (2003).

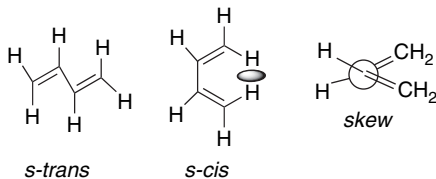


Moreover, electron diffraction studies of 3-pentanone indicate the methyl-eclipsed conformation shown below to be the most stable rotamer.³⁷



The pattern, then, is that methyl and unbranched alkyl groups prefer to be eclipsed with the carbonyl group.

1,3-Dienes adopt conformations in which the double bonds are coplanar, so as to permit optimum π -orbital overlap and electron delocalization. The two alternative planar conformations for 1,3-butadiene are referred to as *s-trans* and *s-cis*. In addition to the two planar conformations, there is a third conformation, referred to as the *skew* conformation, which is cisoid but not planar. Various types of structural studies have shown that the *s-trans* conformation is the most stable one for 1,3-butadiene.³⁸ A small amount of the skew conformation is also present in equilibrium with the major conformer.³⁹ The planar *s-cis* conformation incorporates a van der Waals repulsion between the hydrogens on C(1) and C(4), which is relieved in the skew conformation.



The barrier for conversion of the skew conformation to the *s-trans* is 3.9 kcal/mol. The energy maximum presumably refers to the conformation in which the two π bonds are mutually perpendicular. The height of this barrier gives an approximation of the stabilization provided by conjugation in the planar *s-trans* conformation. Various MO calculations find the *s-trans* conformation to be 2–5 kcal/mol lower in energy than either the planar or skew cisoid conformations.⁴⁰ Most high-level MO calculations

³⁷ C. Romers and J. E. G. Creutzberg, *Rec. Trav. Chim.*, **75**, 331 (1956).

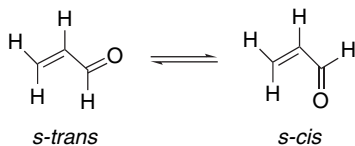
³⁸ A. Almenningen, O. Bastiansen, and M. Traetteburg, *Acta Chem. Scand.*, **12**, 1221 (1958); K. K. Kuchitsu, T. Fukuyama, and Y. Morino, *J. Mol. Struct.*, **1**, 643 (1967); R. L. Lipnick and E. W. Garbisch, Jr., *J. Am. Chem. Soc.*, **95**, 6370 (1973).

³⁹ K. B. Wiberg and R. E. Rosenburg, *J. Am. Chem. Soc.*, **112**, 1509 (1990).

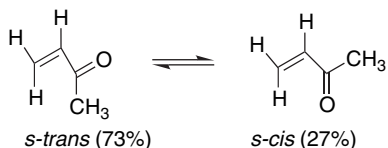
⁴⁰ A. J. P. Devaquet, R. E. Townshend, and W. J. Hehre, *J. Am. Chem. Soc.*, **98**, 4068 (1976); K. B. Wiberg, P. R. Rablen, and M. Marquez, *J. Am. Chem. Soc.*, **114**, 8654 (1992); M. Head-Gordon and J. A. Pople, *J. Phys. Chem.*, **97**, 1147 (1993).

favor the skew conformation over the planar *s-cis*, but the energy differences found are quite small.^{39,41}

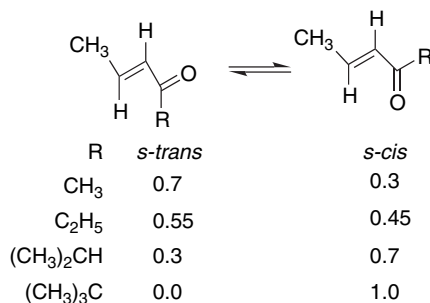
The case of α,β -unsaturated carbonyl compounds is analogous to that of 1,3-dienes, in that conjugation favors coplanarity of the C=C—C=O system. The rotamers that are important are the *s-trans* and *s-cis* conformations. Microwave data indicate that the *s-trans* form is the only conformation present in detectable amounts in 2-propenal (acrolein).⁴²



The equilibrium distribution of *s-trans* and *s-cis* conformations of substituted α,β -unsaturated ketones depends on the extent of van der Waals interaction between the C(1) and the C(4) substituents.⁴³ Methyl vinyl ketone has the minimal unfavorable van der Waals repulsions and exists predominantly as the *s-trans* conformer.



When larger alkyl groups are substituted for methyl, the ratio of the *s-cis* form progressively increases as the size of the alkyl group increases.⁴⁴



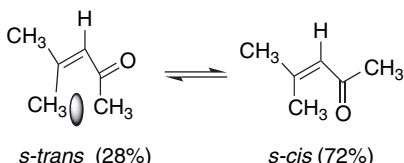
An unfavorable methyl-methyl interaction destabilizes the *s-trans* conformation of 4-methylpent-3-en-2-one (mesityl oxide) relative to the *s-cis* conformation, and the equilibrium favors the *s-cis* form.

⁴¹ J. Breulet, T. J. Lee, and H. F. Schaefer, III, *J. Am. Chem. Soc.*, **106**, 6250 (1984); D. Feller and E. R. Davidson, *Theor. Chim. Acta*, **68**, 57 (1985).

⁴² E. A. Cherniak and C. C. Costain, *J. Chem. Phys.* **45**, 104 (1966).

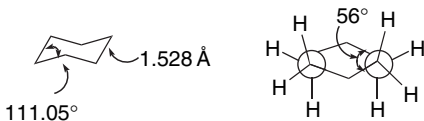
⁴³ G. Montaudo, V. Librando, S. Caccamese, and P. Maravigna, *J. Am. Chem. Soc.*, **95**, 6365 (1973).

⁴⁴ A. Bienvenue, *J. Am. Chem. Soc.*, **95**, 7345 (1973).



2.2.2. Conformations of Cyclohexane Derivatives

The conformational analysis of six-membered ring compounds is particularly well developed. Cyclohexane and its derivatives lend themselves to thorough analysis because they are characterized by a small number of energy minima. The most stable conformations are separated by barriers that are somewhat higher and more easily measured than rotational barriers in acyclic compounds or other ring systems. The most stable conformation of cyclohexane is the chair. Electron diffraction studies in the gas phase reveal a slight flattening of the chair, compared with the geometry obtained using tetrahedral molecular models. The torsion angles are 55.9° , compared with 60° for the “ideal” chair conformation, and the axial C–H bonds are not perfectly parallel, but are oriented outward by about 7° . The C–C bonds are 1.528 \AA , the C–H bonds are 1.119 \AA , and the C–C–C angles are 111.05° .⁴⁵

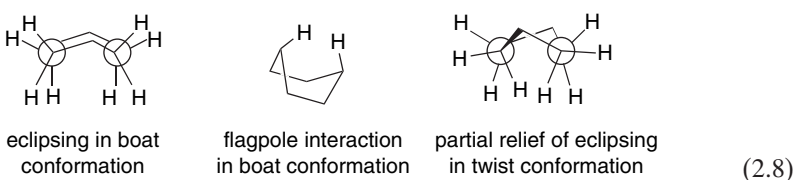


Two nonchair conformations of cyclohexane that have normal bond angles and bond lengths are the *twist* and the *boat*,⁴⁶ both of which are less stable than the chair. A direct measurement of the chair-twist energy difference has been made using low-temperature IR spectroscopy.⁴⁷ The chair was determined to be 5.5 kcal/mol lower in energy than the twist. The twist and the boat conformations are more flexible than the chair, but are destabilized by torsional strain, as the bonds along the “sides” of the boat are eclipsed. In addition, the boat conformation is further destabilized by a van der Waals repulsion between the “flagpole” hydrogens. Both this van der Waals repulsion and the torsional strain are somewhat reduced in the twist conformation.

⁴⁵ H. J. Geise, H. R. Buys, and F. C. Mijlhoff, *J. Mol. Struct.*, **9**, 447 (1971).

⁴⁶ For a review of nonchair conformations of six-membered rings, see G. M. Kellie and F. G. Riddell, *Top. Stereochem.* **8**, 225 (1974).

⁴⁷ M. Squillacote, R. S. Sheridan, O. L. Chapman, and F. A. L. Anet, *J. Am. Chem. Soc.*, **97**, 3244 (1975).



Interconversion of chair forms is known as *conformational inversion*, and occurs by rotation about the carbon-carbon bonds. For cyclohexane, the first-order rate constant for ring inversion is $10^4\text{--}10^5 \text{ sec}^{-1}$ at 27°C . The enthalpy of activation is 10.8 kcal/mol.⁴⁸ Calculation of the geometry of the transition state by *molecular mechanics* (see Section 2.3) suggests a half-twist form lying 12.0 kcal/mol above the chair. According to this analysis, the half-twist form incorporates 0.2 kcal/mol of strain from bond length deformation, 2.0 kcal/mol of bond angle strain, 4.4 kcal/mol of van der Waals stain, and 5.4 kcal/mol of torsional strain.⁴⁹ Figure 2.13 presents a two-dimensional energy diagram illustrating the process of conformational inversion in cyclohexane. The boat form is not shown in the diagram because the chair forms can interconvert without passing through the boat. The boat lies 1–2 kcal/mol above the twist conformation and is a transition state for interconversion of twist forms.⁵⁰

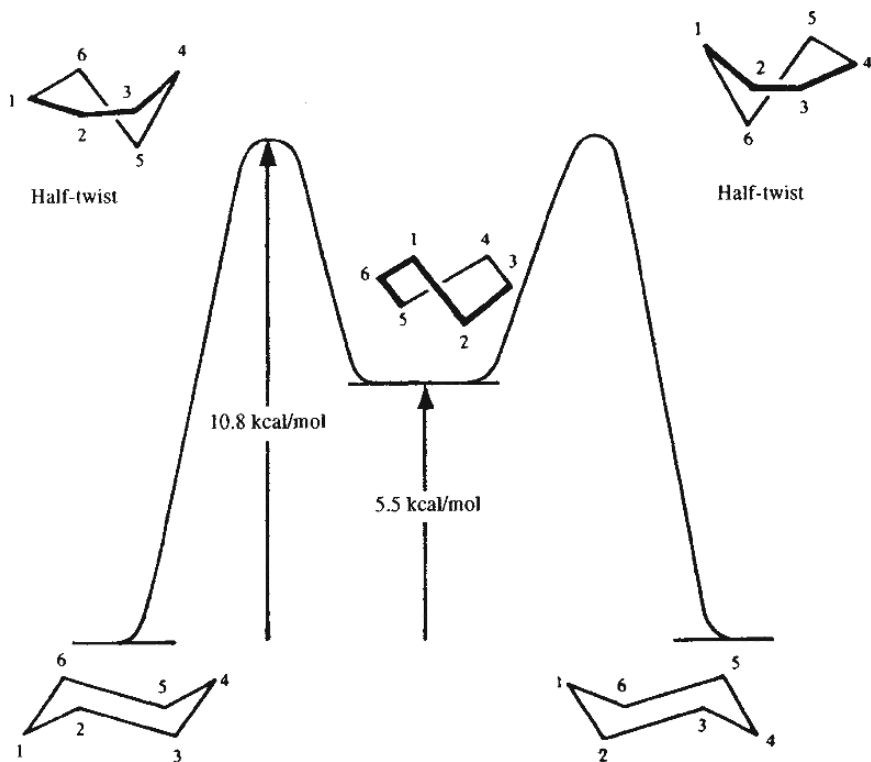


Fig. 2.13. Energy diagram for ring inversion of cyclohexane.

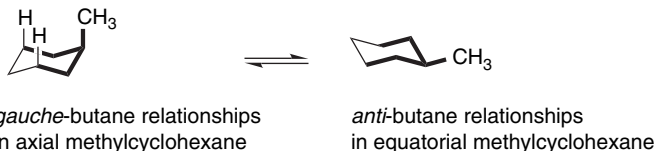
- ⁴⁸. F. A. L. Anet and A. J. R. Bourn, *J. Am. Chem. Soc.*, **89**, 760 (1967).
⁴⁹. N. L. Allinger, M. A. Miller, F. A. van Catledge, and J. A. Hirsch, *J. Am. Chem. Soc.*, **89**, 4345 (1967); N. L. Allinger, *J. Am. Chem. Soc.*, **99**, 8127 (1997).
⁵⁰. N. Leventis, S. B. Hanna, and C. Sotiriou-Leventis, *J. Chem. Educ.*, **74**, 813 (1997); R. R. Sauers, *J. Chem. Educ.*, **77**, 332 (2000).

Visual models, additional information and exercises on Cyclohexane Conformations can be found in the Digital Resource available at: Springer.com/carey-sundberg.

Substitution on a cyclohexane ring does not greatly affect the rate of conformational inversion, but does change the equilibrium distribution between alternative chair forms. All substituents that are axial in one chair conformation become equatorial on ring inversion, and vice versa. For methylcyclohexane, ΔG for the equilibrium is -1.8 kcal/mol , corresponding to a composition with 95% of the equatorial methyl conformation.



Two factors contribute to the preference for the equatorial conformation. The equatorial methyl conformation corresponds to an *anti* arrangement with respect to the C(2)–C(3) and C(6)–C(5) bonds, whereas the axial methyl group is in a *gauche* relationship to these bonds. We saw earlier that the *gauche* conformation of *n*-butane is 0.5–0.6 kcal/mol higher in energy than the *anti* conformation. In addition, there is a van der Waals repulsion between the axial methyl group and the axial hydrogens at C(3) and C(5). Interactions of this type are called *1,3-diaxial interactions*.



Energy differences between conformations of substituted cyclohexanes can be measured by several methods, as can the kinetics of the ring inversion processes. NMR spectroscopy is especially valuable for both thermodynamic and kinetic studies.⁵¹ Depending on the rate of the process, the difference in chemical shift between the two sites and the field strength of the spectrometer, the observed spectrum will be either a weighted average spectrum (rapid site exchange, $k > 10^5 \text{ sec}^{-1}$) or a superposition of the spectra of the two conformers reflecting the equilibrium composition (slow site exchange, $k < 10^3 \text{ sec}^{-1}$). At intermediate rates of exchange, broadened spectra are observed. Analysis of the temperature dependence of the spectra can provide the activation parameters for the conformational process. Figure 2.14 illustrates the change in appearance of a simple spectrum.

For substituted cyclohexanes, the slow-exchange condition is met at temperatures below about -50°C . Data for the half-life for conformational equilibration of

⁵¹ G. Binsch, *Top. Stereochem.*, **3**, 97 (1968); F. G. Riddell, *Nucl. Magn. Reson.*, **12**, 246 (1983); J. Sandstrom, *Dynamic NMR Spectroscopy*, Academic Press, New York, 1982; J. L. Marshall, *Nuclear Magnetic Resonance*, Verlag Chemie, Deerfield Beach, FL, 1983; M. Oki, *Applications of Dynamic NMR to Organic Chemistry*, VCH Publishers, Deerfield Beach, FL, 1985; Y. Takeuchi and A. P. Marchand, eds., *Applications of NMR Spectroscopy in Stereochemistry and Conformational Analysis*, VCH Publishers, Deerfield Beach, FL, 1986.

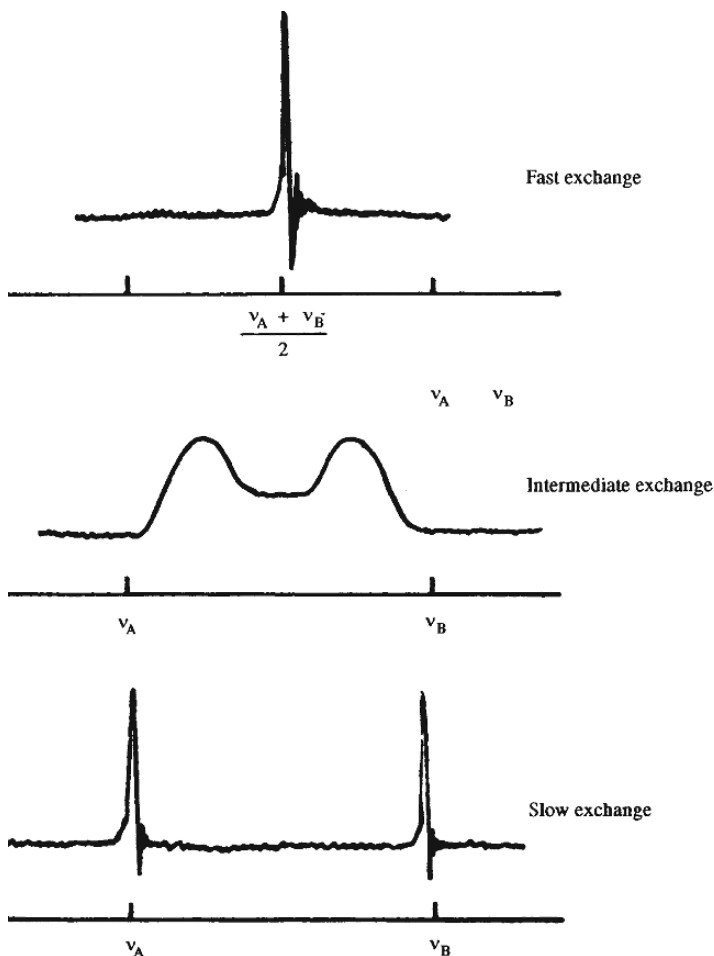


Fig. 2.14. Appearance of NMR spectra for system undergoing site exchange at various rates.

chlorocyclohexane as a function of temperature is shown below. From these data, it can be seen that conformationally pure solutions of equatorial chlorocyclohexane can be maintained at low temperature.⁵²

**Half-Life for Conformation Inversion
for Chlorocyclohexane at Various
Temperatures**

Temperature (°C)	Half-Life
25	1.3×10^{-5} s
-60	2.5×10^{-2} s
-120	23 min
-160	22 yr

⁵² F. R. Jensen and C. H. Bushweller, *J. Am. Chem. Soc.*, **91**, 3223 (1969).

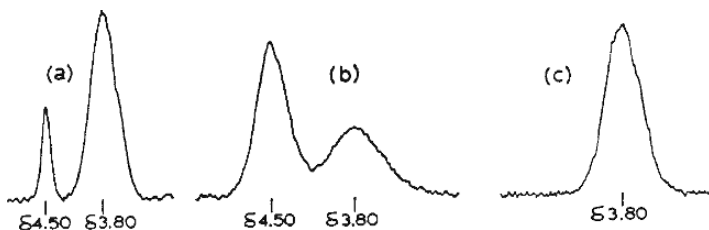
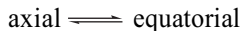


Fig. 2.15. 60-MHz ^1H -NMR spectrum for the C(1)H in chlorocyclohexane: (a) axial-equatorial equilibrium at -115°C ; (b) axial-enriched mixture at -150°C ; (c) pure equatorial conformer at -150°C . Reproduced from *J. Am. Chem. Soc.*, **91**, 3223 (1969), by permission of the American Chemical Society.

Crystallization of chlorocyclohexane at low temperature provided crystals containing only the equatorial isomer. When the solid is dissolved at -150°C , the NMR spectrum of the solution exhibits only the signal characteristic of the equatorial conformer. When the solution is warmed to -115° , the conformation equilibrium is reestablished. The appearance of the 60-MHz spectrum of the H-C-Cl hydrogen is shown in Figure 2.15.

The free-energy difference between conformers is referred to as the *conformational free energy*. For substituted cyclohexanes it is conventional to specify the value of $-\Delta G_c$ for the equilibrium:



As ΔG_c is negative when the equatorial conformation is more stable than the axial, the value of $-\Delta G_c$ is positive for groups that favor the equatorial position. The larger the $-\Delta G_c$, the greater the preference for the equatorial position.

The case of iodocyclohexane provides an example of the use of NMR spectroscopy to determine the conformational equilibrium constant and the value of $-\Delta G_c$. At -80°C , the NMR shows two distinct peaks in the area of the CHI signal as shown in Figure 2.16.⁵³ The multiplet at higher field is a triplet of triplets with coupling constants of 3.5 and 12 Hz. This pattern is characteristic of a hydrogen in an axial position with two axial-axial couplings and two axial-equatorial couplings. The broader peak at lower field is characteristic of a proton at an equatorial position and reflects the four equatorial-equatorial couplings of such a proton. The relative area of the two peaks is 3.4:1 in favor of the conformer with the axial hydrogen. This corresponds to a $-\Delta G_c$ value of 0.47 kcal/mol for the iodo substituent.

Another method for measuring conformational free energies involves establishing an equilibrium between diastereomers differing only in the orientation of the designated substituent group. The equilibrium constant can then be determined and used to calculate the free-energy difference between the isomers. For example, *cis*- and *trans*-*t*-butylcyclohexanol can be equilibrated using a nickel catalyst in refluxing benzene to give a mixture containing 28% *cis*-4-*t*-butylcyclohexanol and 72% *trans*-*t*-butylcyclohexanol.⁵⁴

⁵³. F. R. Jensen, C. H. Bushweller, and B. H. Beck, *J. Am. Chem. Soc.*, **91**, 334 (1969).

⁵⁴. E. L. Eliel and S. H. Schroeter, *J. Am. Chem. Soc.*, **87**, 5031 (1965).

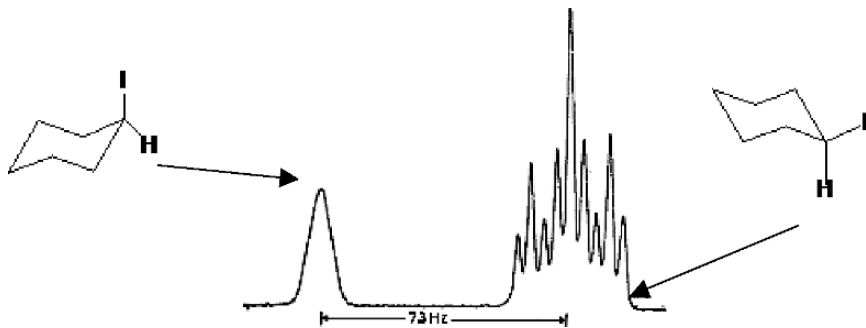
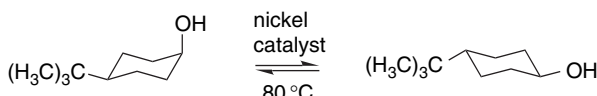


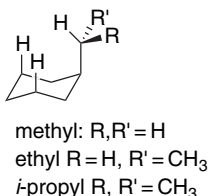
Fig. 2.16. NMR spectrum of iodocyclohexane at -80°C . Only the low field CHI signal is shown (100 MHz). Reproduced from *J. Am. Chem. Soc.*, **91**, 344 (1969), by permission of the American Chemical Society.



Assuming that only conformations that have the *t*-butyl group equatorial are significant, the free-energy change for the equilibration is equal to the free-energy difference between an axial and equatorial hydroxy group. The equilibrium constant leads to a value of $-\Delta G_c = 0.7 \text{ kcal/mol}$ for the hydroxy substituent. This approach also assumes that the *t*-butyl group does not distort the ring or interact directly with the hydroxy group.

There are several other methods available for determining conformational free energies.⁵⁵ Values for many substituents in addition to those listed in Table 2.2 have been compiled.⁵⁶

The methyl, ethyl, and isopropyl groups have similar conformational energies, with isopropyl being only slightly greater than methyl and ethyl. The similar values for the three substituents reflects the fact that rotation about the bond between the substituent and the ring allows each group to adopt a conformation that minimizes the effect of the additional methyl substituent in the ethyl and isopropyl groups.



A *t*-butyl substituent in the axial orientation experiences a strong van der Waals repulsion with the *syn*-axial hydrogens that cannot be relieved by rotation about the bond to the ring. As a result, the $-\Delta G_c$ value for *t*-butyl group is much larger than for the other alkyl groups. A value of about 5 kcal/mol has been calculated by molecular

⁵⁵ F. R. Jensen and C. H. Bushweller, *Adv. Alicyclic Chem.*, **3**, 139 (1971).

⁵⁶ E. L. Eliel, S. H. Wilen, and L. N. Mander *Stereochemistry of Organic Compounds*, Wiley, New York, 1993, pp. 696–697.

Table 2.2. Conformational Free Energies ($-\Delta G_c$) for Some Substituent Groups^a

Substituent	$-\Delta G_c$	Substituent	$-\Delta G_c$
F	0.26 ^b	C ₆ H ₅	2.9 ^e
Cl	0.53 ^b	CN	0.2 ^b
I	0.47 ^b	CH ₃ CO ₂	0.71 ^b
CH ₃	1.8 ^c	HO ₂ C	1.35 ^d
CH ₃ CH ₂	1.8 ^c	C ₂ H ₅ O ₂ C	1.1–1.2 ^d
(CH ₃) ₂ CH	2.1 ^c	HO (aprotic solvent)	0.52 ^d
(CH ₃) ₃ C	>4.7 ^d	HO (protic solvent)	0.87 ^d
CH ₂ =CH	1.7 ^c	CH ₃ O	0.60 ^d
HC≡C	0.5 ^f	O ₂ N	1.16 ^b

a. For a more extensive compilation see E. L. Eliel, S. H. Wilen, and L. N. Mander *Stereochemistry of Organic Compounds*, Wiley, New York, 1993, pp. 696–697.

b. F. R. Jensen and C. H. Bushweller, *Adv. Alicyclic Chem.*, **3**, 140 (1971).

c. N. L. Allinger and L. A. Freiburg, *J. Org. Chem.*, **31**, 804 (1966).

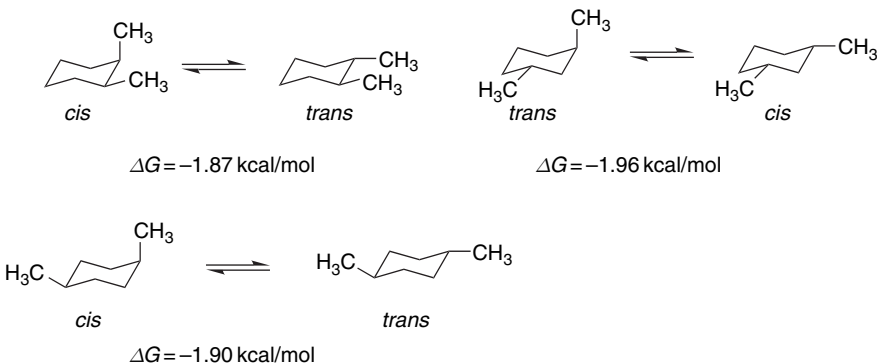
d. J. A. Hirsch, *Top. Stereochem.*, **1**, 199 (1967).

e. E. L. Eliel and M. Manoharan, *J. Org. Chem.*, **46**, 1959 (1981).

mechanics.⁵⁷ Experimental attempts to measure the $-\Delta G_c$ value for *t*-butyl have provided only a lower limit, because very little of the axial conformation is present and the energy difference is similar to that between the chair and twist forms of the cyclohexane ring.

The strong preference for a *t*-butyl group to occupy the equatorial position makes it a useful group for the study of *conformationally biased systems*. A *t*-butyl substituent ensures that the conformational equilibrium lies heavily to the side having the *t*-butyl group equatorial but does not stop the process of conformational inversion. It should be emphasized that “conformationally biased” is not synonymous with “conformationally locked.” Because ring inversion can still occur, it is incorrect to think of the systems being “locked” in a single conformation.

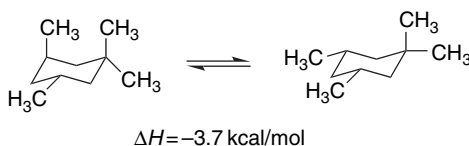
When two or more substituents are present on a cyclohexane ring, the interactions between the substituents must be included in the analysis. The dimethylcyclohexanes provide a case in which a straightforward interpretation is in good agreement with the experimental data. The ΔG of the equilibrium for the *cis* \rightleftharpoons *trans* isomerization is given for 1,2-, 1,3-, and 1,4-dimethylcyclohexane.⁴⁹



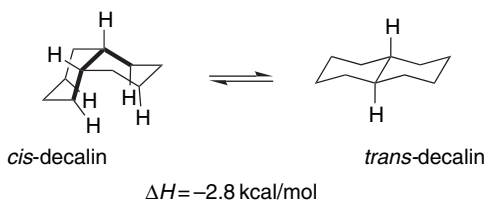
⁵⁷ N. L. Allinger, J. A. Hirsch, M. A. Miller, I. J. Tyminski, and F. A. VanCatledge, *J. Am. Chem. Soc.*, **90**, 1199 (1968); B. van de Graf, J. M. A. Baas, and B. M. Wepster, *Recl. Trav. Chim. Pays-Bas*, **97**, 268 (1978); J. M. A. Baas, A. van Veen, and B. M. Wepster, *Recl. Trav. Chim. Pays-Bas*, **99**, 228 (1980); S. Antunez and E. Juaristi, *J. Org. Chem.*, **61**, 6465 (1996).

The more stable diastereomer in each case is the one in which both methyl groups are equatorial. The ΔG difference favoring the diequatorial isomer is about the same for each case (about 1.9 kcal/mol) and is very close to the $-\Delta G_c$ value of the methyl group (1.8 kcal/mol). This implies that there are no important interactions present that are not also present in methylcyclohexane. This is reasonable since in each case the axial methyl group interacts only with the 3,5-diaxial hydrogens, just as in methylcyclohexane. Moreover, both of the 1,2-dimethyl isomers have similar *gauche* interactions between the two methyl groups.

Conformations in which there is a 1,3-diaxial interaction between substituent groups *larger than hydrogen* are destabilized by van der Waals repulsion. Equilibration of *cis*- and *trans*-1,1,3,5-tetramethylcyclohexane, for example, results in a mixture favoring the *cis* isomer by 3.7 kcal/mol.⁵⁸ This provides a value for a 1,3-diaxial methyl-methyl interaction that is 1.9 kcal/mol higher than the 1,3-methyl-hydrogen interaction.



The decalin (decahydronaphthalene) ring provides another important system for the study of conformational effects in cyclohexane rings. Equilibration of the *cis* and *trans* isomers favors the *trans* isomer by about 2.8 kcal/mol. Note that this represents a change in configuration, not conformation. The energy difference can be analyzed by noting that the *cis* isomer has an inter-ring *gauche*-butane interaction that is not present in the *trans* isomer. There are also cross-ring interactions between the axial hydrogens on the concave surface of the molecule.

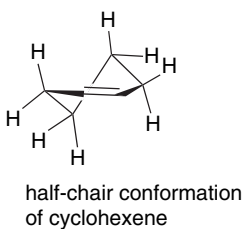


There is an important difference between the *cis*- and *trans*-decalin systems with respect to their conformational flexibility. Owing to the nature of its ring fusion, *trans*-decalin is incapable of chair-chair inversion; *cis*-decalin is conformationally mobile and undergoes ring inversion at a rate only slightly slower than cyclohexane ($\Delta G^\ddagger = 12.3\text{--}12.4 \text{ kcal/mol}$).⁵⁹ The *trans*-decalin system is a “conformationally locked” system and can be used to compare properties and reactivity of groups in axial or equatorial environments.

⁵⁸. N. L. Allinger and M. A. Miller, *J. Am. Chem. Soc.*, **83**, 2145 (1961).

⁵⁹. F. R. Jensen and B. H. Beck, *Tetrahedron Lett.*, 4523 (1966); D. K. Dalling, D. M. Grant, and L. F. Johnson, *J. Am. Chem. Soc.*, **93**, 367 (1971); B. E. Mann, *J. Magn. Resonance*, **21**, 17 (1976).

The effect of introducing sp^2 -hybridized atoms into acyclic molecules was discussed in Section 2.2.1, and it was noted that torsional barriers in 1-alkenes and aldehydes are somewhat smaller than in alkanes. Similar effects are seen when sp^2 centers are incorporated into six-membered rings. Whereas the energy barrier for ring inversion in cyclohexane is 10.3 kcal/mol, it is reduced to 7.7 kcal/mol in methylenecyclohexane⁶⁰ and to 4.9 kcal/mol in cyclohexanone.⁶¹ The conformation of cyclohexene is described as a half-chair. Structural parameters determined on the basis of electron diffraction and microwave spectroscopy reveal that the double bond can be accommodated into the ring without serious distortion. The C(1)–C(2) bond length is 1.335 Å, and the C(1)–C(2)–C(3) bond angle is 123°.⁶² The substituents at C(3) and C(6) are tilted from the usual axial and equatorial directions and are referred to as *pseudoaxial* and *pseudoequatorial*.



There have been both experimental and theoretical studies of the conformational process. According to NMR studies, the E_a for ring inversion is 5.3 kcal/mol.⁶³ An IR study gave a significantly higher barrier of about 10 kcal/mol.⁶⁴ A more recent theoretical study using both MO and DFT calculations found the barrier to be about 5.5–6.0 kcal/mol.⁶⁵ The preference for equatorial orientation of a methyl group in cyclohexene is less than in cyclohexane, because of the ring distortion and the removal of one 1,3-diaxial interaction. A value of 1 kcal/mol has been suggested for the $-\Delta G_c$ value for a methyl group in 4-methylcyclohexene.⁶⁶

Alkylidenecyclohexanes bearing alkyl groups of moderate size at C(2) tend to adopt the conformation with the alkyl group axial, in order to relieve unfavorable interactions with the alkylidene group. This results from van der Waals repulsion between the alkyl group in the equatorial position and *cis* substituents on the exocyclic

⁶⁰ J. T. Gerig, *J. Am. Chem. Soc.*, **90**, 1065 (1968).

⁶¹ F. R. Jensen and B. H. Beck, *J. Am. Chem. Soc.*, **90**, 1066 (1968).

⁶² J. F. Chiang and S. H. Bauer, *J. Am. Chem. Soc.*, **91**, 1898 (1969); L. H. Scharpen, J. E. Wollrab, and D. P. Ames, *J. Chem. Phys.*, **49**, 2368 (1968).

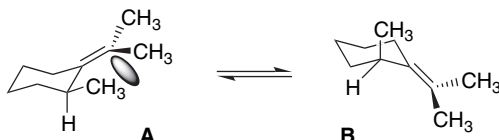
⁶³ F. A. L. Anet and M. Z. Haq, *J. Am. Chem. Soc.*, **87**, 3147 (1965).

⁶⁴ V. E. Rivera-Gaines, S. J. Leibowitz, and J. Laane, *J. Am. Chem. Soc.*, **113**, 9735 (1991).

⁶⁵ S. V. Shishkina, O. V. Shiskin, and J. Leszczynski, *Chem. Phys. Lett.*, **354**, 428 (2002).

⁶⁶ B. Rickborn and S.-Y. Lwo, *J. Org. Chem.*, **30**, 2212 (1965).

double bond, and is an example of 1,3-allylic strain.⁶⁷ The repulsive energy is small for methylenecyclohexanes, but molecular mechanics calculations indicate that the axial conformation **B** is 2.6 kcal/mol more stable than **A** with an exocyclic isopropylidene group.⁶⁸



An alkyl group at C(2) of a cyclohexanone ring is more stable in the equatorial than in the axial orientation. The equatorial orientation is eclipsed with the carbonyl group and corresponds to the more stable conformation of open-chain ketones (see p. 148). This conformation also avoids 3,5-diaxial interactions with *syn*-diaxial hydrogens. Conformational free energies ($-\Delta G_c$) for 2-alkyl substituents in cyclohexanones have been determined by equilibration studies. The value for the methyl group is similar to cyclohexanes, whereas the values for ethyl and isopropyl are somewhat smaller. This is attributed to a compensating repulsive steric interaction with the carbonyl oxygen for the larger substituents.⁶⁹



The $-\Delta G_c$ of an alkyl group at C(3) of cyclohexanone is less than that of a alkyl group in cyclohexane because of reduced 1,3-diaxial interactions. A C(3) methyl group in cyclohexanone has a $-\Delta G_c$ of 1.3–1.4 kcal/mol.⁵⁴

2.2.3. Conformations of Carbocyclic Rings of Other Sizes

The most important structural features that influence the conformation and reactivity of cycloalkanes differ depending on whether small (cyclopropane and cyclobutane), common (cyclopentane, cyclohexane, and cycloheptane), medium (cyclooctane through cycloundecane), or large (cyclododecane and up) rings are

⁶⁷ F. Johnson, *Chem. Rev.*, **68**, 375 (1968); R. W. Hoffmann, *Chem. Rev.*, **89**, 1841 (1989).

⁶⁸ N. L. Allinger, J. A. Hirsch, M. A. Miller, and I. J. Tyminski, *J. Am. Chem. Soc.*, **90**, 5773 (1968); P. W. Rabideau, ed., *The Conformational Analysis of Cyclohexenes, Cyclohexadiene and Related Hydroaromatic Compounds*, VCH Publishers, Weinheim, 1989.

⁶⁹ N. L. Allinger and H. M. Blatter, *J. Am. Chem. Soc.*, **83**, 994 (1961); B. Rickborn, *J. Am. Chem. Soc.*, **84**, 2414 (1962); E. L. Eliel, N. L. Allinger, S. J. Angyal, and G. A. Morrison, *Conformational Analysis*, Interscience, New York, 1965, pp. 113–114.

Table 2.3. Strain Energies for Cycloalkanes^a

Cycloalkane	Strain energy (kcal/mol)
Cyclopropane	28.1 ^b
Cyclobutane	26.3
Cyclopentane	7.3
Cyclohexane	1.4
Cycloheptane	7.6
Cyclooctane	11.9
Cyclononane	15.5
Cyclodecane	16.4
Cyclododecane	11.8

a. Values taken from E. M. Engler, J. D. Andose, and P. v. R. Schleyer, *J. Am. Chem. Soc.*, **95**, 8005 (1973).

b. P. v. R. Schleyer, J. E. Williams, and K. R. Blanchard, *J. Am. Chem. Soc.*, **92**, 2377 (1970).

considered. The small rings are dominated by angle and torsional strain. The common rings are relatively unstrained and their conformations are most influenced by torsional factors. Medium rings exhibit conformational equilibria and chemical properties indicating that cross-ring van der Waals repulsions play an important role. Large rings become increasingly flexible and possess a large number of low-energy conformations. The combination of all types of strain for a given ring results in a total *strain energy* for that ring. Table 2.3 presents data on the strain energies of cycloalkanes up to cyclodecane.

The cyclopropane ring is planar and the question of conformation does not arise. The C–C bond lengths are slightly shorter than normal, at 1.50 Å, and the H–C–H angle of 115° is opened somewhat from the tetrahedral angle.⁷⁰ These structural features and the relatively high reactivity of cyclopropane rings are explained by the concept of “bent bonds,” in which the electron density is displaced from the internuclear axis (see Topic 1.3).

Cyclobutane adopts a puckered conformation in which substituents can occupy axial-like or equatorial-like positions.⁷¹ 1,3-Disubstituted cyclobutanes show small energy preferences for the *cis* isomer, which places both substituents in equatorial-like positions.⁷² The energy differences and the barrier to inversion are both smaller than in cyclohexane.



There is minimal angle strain in cyclopentane, but considerable torsional strain is present. Cyclopentane is nonplanar and the two minimum energy geometries are the envelope and the half-chair.⁷³ In the envelope conformation, one carbon atom is

⁷⁰. O. Bastiansen, F. N. Fritsch, and K. Hedberg, *Acta Crystallogr.*, **17**, 538 (1964).

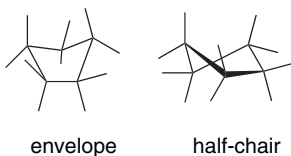
⁷¹. A. Almenningen, O. Bastiansen, and P. N. Skancke, *Acta Chem. Scand.*, **15**, 711 (1961).

⁷². (a) K. B. Wiberg and G. M. Lampman, *J. Am. Chem. Soc.*, **88**, 4429 (1966);

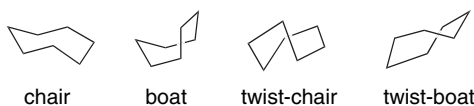
(b) N. L. Allinger and L. A. Tushaus, *J. Org. Chem.*, **30**, 1945 (1965).

⁷³. A. C. Legon, *Chem. Rev.*, **80**, 231 (1980); B. Fuchs, *Top. Stereochem.*, **10**, 1 (1978).

displaced from the plane of the other four. In the half-chair conformation, three carbons are coplanar, with one of the remaining two being above the plane and the other below. The planar portions of both conformations have torsional strain owing to C–H and C–C bond eclipsing. The energy differences between the conformers are small and there is rapid interconversion of conformers.⁷⁴ All of the carbon atoms move rapidly through planar and nonplanar positions, owing to a process called *pseudorotation*.



As ring size increases, there are progressively more conformations that have to be considered. For cycloheptane, four conformations have been calculated to be particularly stable.⁷⁵ NMR investigations indicate that the twist-chair is the most stable.⁷⁶ Various derivatives adopt mainly twist-chair conformations.⁷⁷ The individual twist-chair conformations interconvert rapidly by pseudorotation.⁷⁸ The most recent MM4 and CCSD/6-311++G** computations (see Section 2.3) indicate the following relative energies.⁷⁹ Figure 2.17 shows the conformations.



	MM4	CCSD/6-311++G**
Twist-chair	0	0
Chair	1.4	0.9
Boat	3.8	3.3
Twist-boat	3.5	3.3

Relative energy in kcal/mol

- ⁷⁴. W. J. Adams, H. J. Geise, and L. S. Bartell, *J. Am. Chem. Soc.*, **92**, 5013 (1970); J. B. Lambert, J. J. Papay, S. A. Khan, K. A. Kappauf, and E. S. Magyar, *J. Am. Chem. Soc.*, **96**, 6112 (1974).
- ⁷⁵. J. B. Hendrickson, *J. Am. Chem. Soc.*, **89**, 7036 (1967); D. F. Bocian and H. L. Strauss, *J. Am. Chem. Soc.*, **99**, 2866 (1977); P. M Iavanov and E. Osawa, *J. Comput. Chem.*, **5**, 307 (1984).
- ⁷⁶. J. B. Hendrickson, R. K. Boeckman, Jr., J. D. Glickson, and E. Grunwald, *J. Am. Chem. Soc.*, **95**, 494 (1973).
- ⁷⁷. F. H. Allen, J. A. K. Howard, and N. A. Pitchard, *Acta Crystallog.*, **B49**, 910 (1993).
- ⁷⁸. D. F. Bocian, H. M. Pickett, T. C. Rounds, and H. L. Strauss, *J. Am. Chem. Soc.*, **97**, 687 (1975).
- ⁷⁹. K. B. Wiberg, *J. Org. Chem.*, **68**, 9322 (2003).

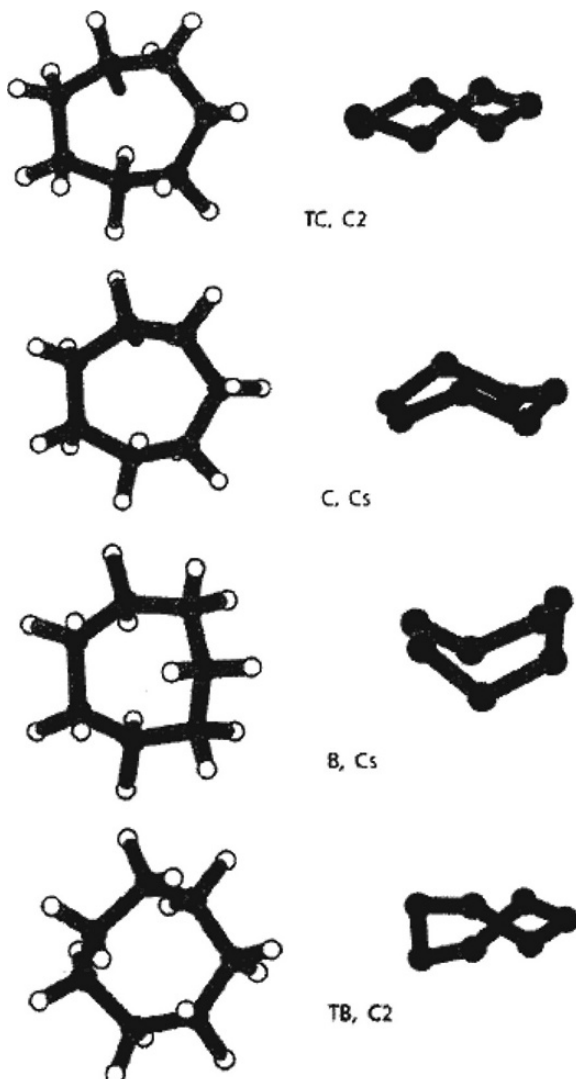


Fig. 2.17. The four most favorable conformations of cycloheptane.
Reproduced from *J. Org. Chem.*, **68**, 9322 (2003), by permission
of the American Chemical Society.

For cyclooctane, a total of 11 conformations have been suggested for consideration and their relative energies calculated. According to MM⁸⁰ and CCSDT/6-311++G**⁷⁹ computations, there are five other conformations that are energy minima, of which the boat-chair is calculated to be the most stable. This result is in agreement with analyses of the temperature dependence of the ¹⁹F NMR spectra of fluorocyclooctanes.⁸¹ The activation energy for interconversion of conformers is 5–8 kcal/mol.

⁸⁰. I. Kolossvary and W. C. Guida, *J. Am. Chem. Soc.*, **115**, 2107 (1993).

⁸¹. J. E. Anderson, E. S. Glazer, D. L. Griffith, R. Knorr, and J. D. Roberts, *J. Am. Chem. Soc.*, **91**, 1386 (1969); see also F. A. Anet and M. St. Jacques, *J. Am. Chem. Soc.*, **88**, 2585, 2586 (1966).

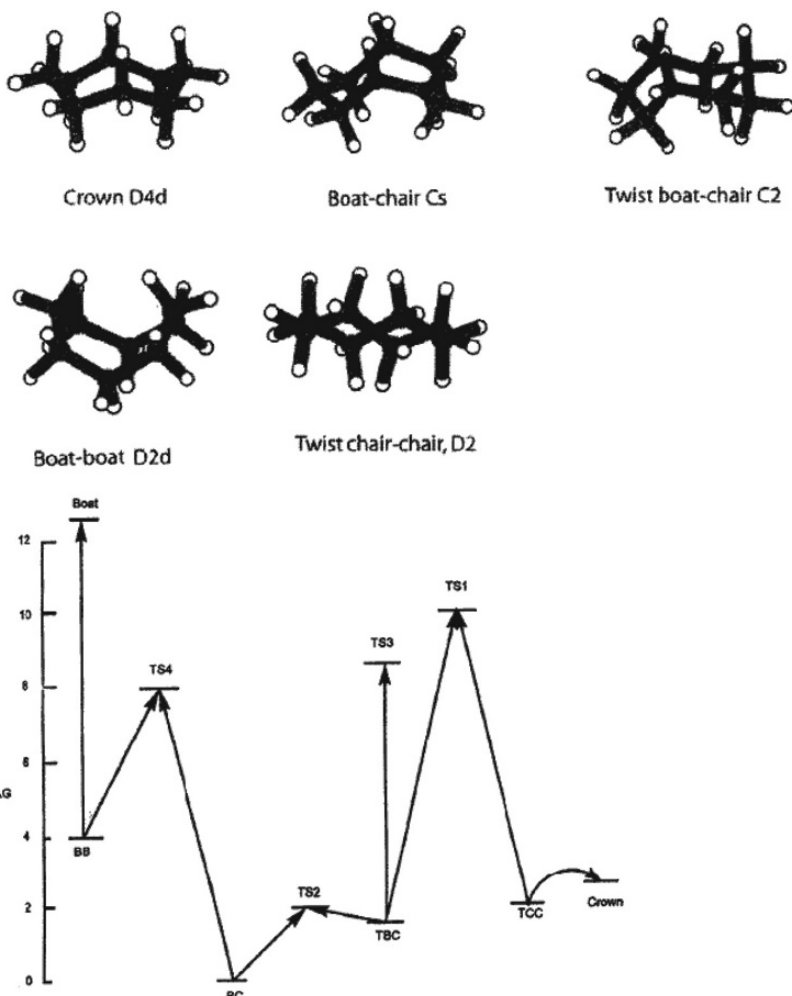


Fig. 2.18. Structures of the low-energy conformations of cyclooctane and the energy barriers separating them. Reproduced from *J. Org. Chem.*, **68**, 9322 (2003), by permission of the American Chemical Society.

Figure 2.18 illustrates the low-energy conformations and the barriers separating them. The crown and twist-chair-twist conformations are quite similar.

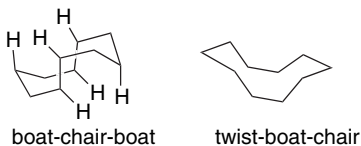
The number of conformations rapidly increases with ring size. For cyclodecane there are 18 conformers that are found as minima in MM3 calculations.⁸² The lowest four are within 1 kcal/mol of one another. Low-temperature NMR studies indicate that the boat-chair-boat is the lowest in energy,⁸³ and studies of cyclodecane derivatives by X-ray crystallography showed that the boat-chair-boat conformation is adopted in the solid state.⁸⁴ As was indicated in Table 2.3, cyclodecane is significantly more

⁸². N. Weinberg and S. Wolfe, *J. Am. Chem. Soc.*, **116**, 9860 (1994).

⁸³. D. M. Pawar, S. V. Smith, H. L. Mark, R. M. Odom, and E. A. Noe, *J. Am. Chem. Soc.*, **120**, 10715 (1998).

⁸⁴. J. D. Dunitz, in *Perspectives in Structural Chemistry*, Vol II, J. D. Dunitz and J. A. Ibers, eds., Wiley, New York, 1968, pp. 1–70.

strained than cyclohexane. Examination of the boat-chair-boat conformation reveals that the source of most of this strain is the close van der Waals contacts between two sets of three hydrogens on either side of the molecule, as indicated in the drawing below. Distortion of the molecule to twist forms relieves this interaction but introduces torsional strain.



The conformational possibilities for larger rings quickly become very large, but an interesting simplifying concept has emerged. The diamond lattice, which consists of a continuous array of chair cyclohexane rings, is the most stable arrangement for a large array of sp^3 carbon atoms. There are both theoretical and experimental results that show that complex polycyclic saturated hydrocarbons are most stable in diamond-type structures. Adamantane is a familiar example of this type of structure.



It might be anticipated that large flexible rings would adopt similar structures incorporating the chair cyclohexane conformation. Conformations for C_{10} through C_{24} cycloalkanes corresponding to diamond lattice sections have been identified by systematic topological analysis using models and molecular mechanics computations.⁸⁵ This type of relationship is illustrated in Figure 2.19 for cyclodecane. Molecular

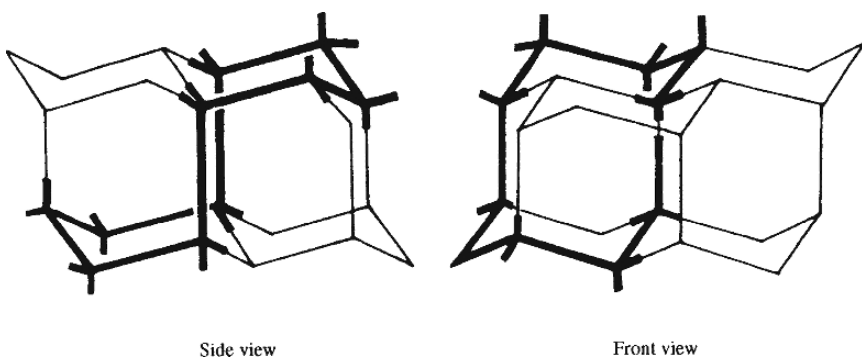


Fig. 2.19. Equivalent diamond lattice conformations of cyclodecane (boat-chair-boat).

⁸⁵. J. Dale, *J. Chem. Soc.*, 93 (1963); M. Saunders, *Tetrahedron*, **23**, 2105 (1967); J. Dale, *Top. Stereochem.*, **9**, 199 (1976).

mechanics computations indicate that this is indeed the minimum energy conformation for cyclododecane.^{80,86}

As the ring size increases, the number of possible conformations increases further so that many alternative diamond lattice conformations are available.⁸⁷

2.3. Molecular Mechanics

The analysis of molecular conformation can be systematically and quantitatively approached through molecular mechanics.⁸⁸ A molecule adopts the geometry that minimizes its total strain energy. The minimum energy geometry is strained (destabilized) to the extent that its structural parameters deviate from their ideal values. The energy for a particular kind of distortion is a function of the amount of distortion and the opposing force. The total strain energy is the sum of several contributions:

$$E_{\text{strain}} = E(r) + E(\theta) + E(\varphi) + E(d) \quad (2.9)$$

where $E(r)$ is the energy associated with stretching or compression of bonds, $E(\theta)$ is the energy of bond angle distortion, $E(\varphi)$ is the torsional strain, and $E(d)$ are the energy increments that result from nonbonded interactions between atoms.

Molecular mechanics calculations involve summation of the force fields for each type of strain. The original mathematical expressions for the force fields were derived from classical mechanical potential energy functions. The energy required to stretch a bond or to bend a bond angle increases as the square of the distortion:

$$\text{Bond stretching : } E(r) = 0.5k_r(r - r_0)^2 \quad (2.10)$$

where k_r is the stretching force constant, r the bond length, and r_0 the normal bond length.

$$\text{Bond angle bending : } E(\theta) = 0.5k_\theta(\Delta\theta)^2 \quad (2.11)$$

where k_θ is the bending force constant and $\Delta\theta$ is the deviation of the bond angle from its normal value. The torsional strain is a sinusoidal function of the torsion angle. Torsional strain results from the barrier to rotation about single bonds, as described for ethane on p. 142–143. For molecules with a threefold barrier such as ethane, the form of the torsional barrier is:

$$E(\varphi) = 0.5V_0(1 + \cos 3\varphi) \quad (2.12)$$

where V_0 is the rotational energy barrier and φ is the torsional angle. For hydrocarbons, V_0 can be taken as being equal to the ethane barrier (2.9 kcal/mol).

Nonbonded interaction energies, which may be attractive or repulsive, are the most difficult contributions to evaluate. When two uncharged atoms approach each other, the interaction between them is very small at large distances, becomes slightly

⁸⁶ M. Saunders, *J. Comput. Chem.*, **12**, 645 (1991).

⁸⁷ M. Saunders, *J. Am. Chem. Soc.*, **109**, 3150 (1987); V. L. Shannon, H. L. Strauss, R. G. Snyder, C. A. Elliger, and W. L. Mattice, *J. Am. Chem. Soc.*, **111**, 1947 (1989); M. Saunders, K. N. Houk, Y. D. Wu, W. C. Still, M. Lipton, G. Chang, and W. C. Guida, *J. Am. Chem. Soc.*, **112**, 1419 (1990).

⁸⁸ For general reviews see: W. Gans, A. Amann, and J. C. A. Boeyens, *Fundamental Principles of Molecular Modeling*, Plenum Press, New York, 1996; A. K. Rappe and C. J. Casewitt, *Molecular Mechanics Across Chemistry*, University Science Books, Sausalito, CA, 1997; J. C. A. Boeyens and P. Comba, *Coordn. Chem. Rev.*, **212**, 3 (2001).

attractive as the separation approaches the sum of their van der Waals radii, but then becomes strongly repulsive as the separation becomes less than the sum of their van der Waal radii. The attractive interaction results from a mutual polarization of the electrons of the atoms. Such attractive forces are called *London forces* or *dispersion forces* and are relatively weak interactions. London forces vary inversely with the sixth power of internuclear distance and become negligible as internuclear separation increases. At distances smaller than the sum of the van der Waals radii, the much stronger electron-electron repulsive forces are dominant. Electrostatic forces must take into account bond dipoles and their orientation. Bond dipoles also have a polarizing effect on adjacent groups.⁸⁹

The separation of the total strain energy into component elements of bond length strain, bond angle strain, torsional strain, and nonbonded interactions is useful for analysis of structural and steric effects on equilibria and reactivity. Minimization of the total strain energy of a molecule, expressed by a parameterized equation for each of the force fields, can be accomplished by iterative computation. The quantitative application of molecular mechanics for calculation of minimum energy geometries, heats of formation, and strain energies has been developed to a high level of reliability. The method has been refined to the point that geometries of saturated hydrocarbons can be calculated to an accuracy of 0.005 Å in bond length and 1° in bond angle.⁹⁰ Similar accuracy can be obtained for unsaturated hydrocarbons⁹¹ and molecules with oxygen functional groups.⁹² Molecular mechanics calculations can also be applied to unstable reactive intermediates such as carbocations.⁹³

The molecular mechanics computations can be done using commercially available programs. The parameters used in the programs determine the range of applicability and reliability of the results. Several systems of parameters and equations for carrying out the calculations have been developed. The most frequently used methods in organic chemistry are those developed by N. L. Allinger and co-workers and is frequently referred to as MM (molecular mechanics) calculations.⁹⁴ The most recent version is called MM4.⁹⁵ The computations involve iterations to locate an energy minimum. Precautions must be taken to establish that a true (“global”) minimum, as opposed to a local minimum energy, has been achieved. This can be accomplished by using a number of different initial geometries and comparing the structures and energies of the minima that are located. In addition to comparing the relative energy of various conformations of an individual molecule, MM computations can be used to calculate total molecular energy (enthalpy of formation) to a high level of accuracy. Heats of formation for most hydrocarbons are accurate to ±0.5 kcal/mol. This application of MM is discussed further in Section 3.1.2.4.

- ⁸⁹. L. Dosen-Micovic, D. Jeremic, and N. L. Allinger, *J. Am. Chem. Soc.*, **105**, 1716, 1723 (1983); B. Mannfors, K. Palmo, and S. Krimm, *J. Mol. Struct.*, **556**, 1 (2000).
- ⁹⁰. N. L. Allinger, Y. H. Yuh, and J.-H. Lii, *J. Am. Chem. Soc.*, **111**, 8551 (1989); N. L. Allinger, K. Chen, and J.-H. Lii, *J. Comput. Chem.*, **17**, 642 (1996).
- ⁹¹. N. Nevins, K. Chen, and N. L. Allinger, *J. Comput. Chem.*, **17**, 669 (1996); N. Nevins, J.-H. Lii, and N. L. Allinger, *J. Comput. Chem.*, **17**, 695 (1996); N. Nevins and N. L. Allinger, *J. Comput. Chem.*, **17**, 730 (1996).
- ⁹². C. H. Langley, J. H. Lii, and N. L. Allinger, *J. Comput. Chem.*, **22**, 1396, 1426, 1451 (2001).
- ⁹³. B. Reindl, T. Clark, and P. v. R. Schleyer, *J. Comput. Chem.*, **17**, 1406 (1996); B. Reindl and P. v. R. Schleyer, *J. Comput. Chem.*, **18**, 28 (1997); B. Reindl, T. Clark, and P. v. R. Schleyer, *J. Comput. Chem.*, **18**, 533 (1997); B. Reindl, T. Clark, and P. v. R. Schleyer, *J. Phys. Chem. A*, **102**, 8953 (1998).
- ⁹⁴. N. L. Allinger, Y. H. Yuh and J.-H. Lii, *J. Am. Chem. Soc.*, **111**, 8551 (1989).
- ⁹⁵. N. L. Allinger, K. S. Chen, and J. H. Lii, *J. Comput. Chem.*, **17**, 642 (1996).

Molecular mechanics can also be used in connection with MO or DFT calculations in computations on transition structures. Because transition structures have partial bonds that vary from case to case, no general set of parameters is applicable. One approach is to apply MO or DFT calculations to the reacting portion of the molecule to obtain structural information. This portion of the structure can then be incorporated into an MM computation involving the remainder of the molecule.⁹⁶ It is also possible to use several levels of computations. For example, high-level MO or DFT calculations can be applied to the reaction core, intermediate level calculations to the part of the system immediately adjacent to the reaction core, and MM calculations for the remainder of the molecule.⁹⁷ Two examples of these approaches are given in Section 2.5.4, where large catalytic molecules have been examined using combined approaches.

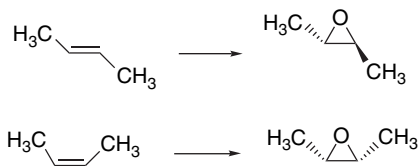
2.4. Stereoselective and Stereospecific Reactions

In this section we discuss relationships between reactivity and stereochemistry. Many reactions can produce two or more stereoisomeric products. If a reaction shows a preference for one of the stereoisomers, it is *stereoselective*. Throughout the sections on individual reactions in Parts A and B, we discuss the stereoselectivity associated with particular reactions. In this chapter, we use a few examples to illustrate the fundamental concepts of stereoselectivity.

Stereoselectivity is intimately related to the mechanism of the reaction. Some reactions are *stereospecific*, that is reactions in which *stereoisomeric reactants each provide stereoisomeric products*. For example, the S_N2 substitution reaction results in an inversion of the configuration. It is a stereospecific reaction. The *R*-reactant gives the *S*-product and the *S*-reactant gives the *R*-product (assuming the priority order remains unchanged).



As another example, epoxidation of *E*-2-butene gives *trans*-2,3-dimethyloxirane, whereas *Z*-2-butene gives *cis*-2,3-dimethyloxirane.



⁹⁶ J. E. Eksterowicz and K. N. Houk, *Chem. Rev.*, **93**, 2439 (1993); F. Maseras and K. Morokuma, *J. Comput. Chem.*, **16**, 1170 (1995).

⁹⁷ M. Svensson, S. Humbel, R. D. J. Froese, T. Matsubara, S. Sieber, and K. Morokuma, *J. Phys. Chem.*, **100**, 19357 (1996).

We discuss several examples to illustrate how reactant structure and mechanism can lead to stereoselectivity, including stereospecificity. We also consider *enantioselective* and *enantiospecific* reactions, which are reactions that favor one enantiomer of a reaction product.

2.4.1. Examples of Stereoselective Reactions

Scheme 2.6 gives some examples of the types of stereoselective reactions that are discussed. The first three examples in the scheme are catalytic hydrogenations. Usually such reactions favor *syn* addition of hydrogen from the less hindered face of the double bond; that is, both hydrogens are added to the same face of the π bond. The second entry illustrates another aspect of catalytic hydrogenation: the tendency of hydroxy groups to be *syn*-directive, that is, to favor addition from the same side that is occupied by the hydroxy group. These features are believed to be related to the interaction of the alkene with the catalytic surface during hydrogenation and are discussed further in Section 2.4.1.1. As can be seen from the variable degree of stereoselectivity in Entries 1 and 2, as well as the exception in Entry 3, *catalytic hydrogenation is not always highly stereoselective*.

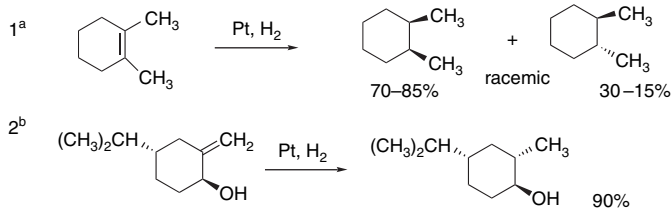
Entries 4 through 6 are examples of stereoselective reduction of cyclic ketones. Comparing entries 4 and 5 shows that stereoselectivity can be controlled by the choice of reagents. As we discuss further in Section 2.4.1.2, some hydride donors, e.g., NaBH_4 , approach from the axial direction to give equatorial alcohol. More bulky reducing agents favor the equatorial approach and give axial alcohol. Entry 6 illustrates the tendency of reagents to attack the norbornane ring from the *exo* direction. Entry 7 is an example of diastereoselective addition of a Grignard reagent adjacent to a stereocenter. This is an example of *1,2-asymmetric induction*, in which the configuration at the adjacent stereocenter establishes a preference for the direction of addition to the carbonyl group. This kind of reaction has been studied extensively and is discussed in Section 2.4.1.3. One of the issues that must be considered in this case is the conformation of the reactant. Although the preferred conformation of ring compounds is often evident, the flexibility of acyclic compounds introduces additional variables. Entry 8 is another example in which the configuration of the α -oxy substituent controls the direction of addition of hydride to the carbonyl group.

2.4.1.1. Substituent Directing Effects in Heterogeneous and Homogeneous Hydrogenation The hydrogenation of carbon-carbon double bonds is a very general reaction. Except for very sterically hindered cases, the reaction usually proceeds rapidly and cleanly. Hydrogenation can be carried out using either finely dispersed metal (heterogeneous) or soluble (homogeneous) metal complexes. The heterogeneous catalysts are transition metals, particularly platinum, palladium, rhodium, ruthenium, and nickel. The metals are used as finely dispersed solids or adsorbed on inert supports such as charcoal or alumina. Homogeneous catalysts are usually complexes of rhodium, ruthenium, or iridium. Phosphine ligands are common in these catalytic complexes. Depending upon the conditions and the catalyst, other functional groups may also be subject to catalytic hydrogenation, but for now we focus on double bonds.



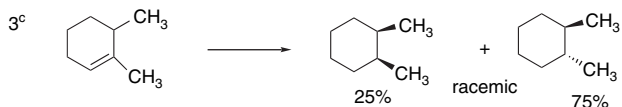
Scheme 2.6. Examples of Stereoselective Reactions**SECTION 2.4***Stereoselective and
Stereospecific Reactions***A. Catalytic Hydrogenation.** (See section 2.4.1.1)

Unfunctionalized alkene usually reacts by preferential *syn* delivery of hydrogen from the less hindered face of the double bond. The degree of stereoselectivity is dependent on the reactant structure, catalysts and reaction conditions. Donor functional groups, particularly hydroxy and amino can be *syn* directive.

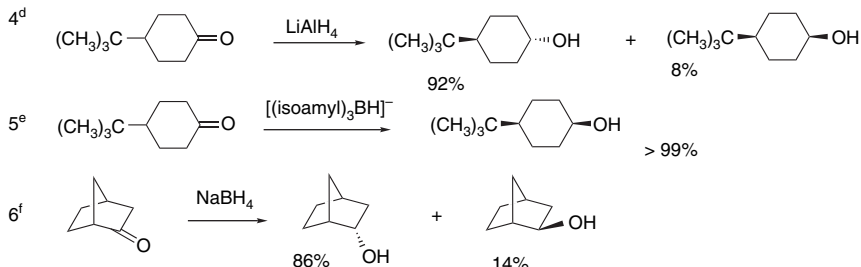


(The same article also sites other examples with low stereoselectivity.)

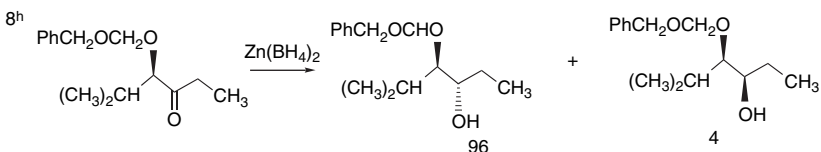
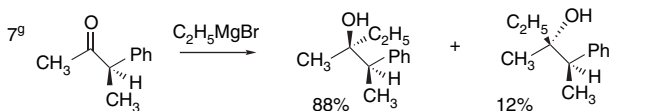
A representative exception.

**B. Hydride Reduction of Cyclic Ketones** (see Section 2.4.1.2)

Unhindered cyclohexanones normally react with NaBH_4 and LiAlH_4 by preferential reagent approach from the axial direction forming mainly the equatorial alcohol. The presence of axial substituents or use of more sterically demanding reagents, such as alkylborohydrides leads to selective equatorial approach and formation of axial alcohols. Bicyclic ketones are generally reduced by hydride approach from the less hindered face of the carbonyl group.

**C. Nucleophilic Addition to Acyclic Ketones** (see Section 2.4.1.3)

Adjacent stereocenters influence the mode of addition of nucleophiles such as hydrides and organometallic reagents to acyclic ketones. The Felkin-Ahn transition state provides a predictive model that is general when steric effects are dominant. Other factors must be considered when polar or chelating substituents are present.



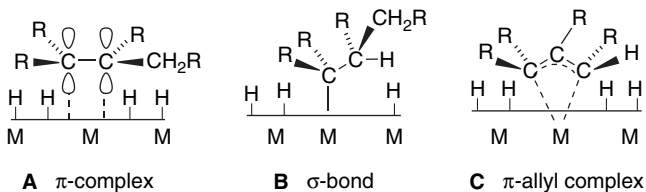
(Continued)

CHAPTER 2

Stereochemistry,
Conformation,
and Stereoselectivity

- a. C. A. Brown, *J. Am. Chem. Soc.*, **91**, 5901 (1969).
- b. M. C. Dart and H. B. Henbest, *J. Chem. Soc.*, 3563 (1960).
- c. S. Siegel and G. V. Smith, *J. Am. Chem. Soc.*, **82**, 6082, 6087 (1960).
- d. H. C. Brown and W. C. Dickason, *J. Am. Chem. Soc.*, **92**, 709 (1970).
- e. S. Krishnamurthy and H. C. Brown, *J. Am. Chem. Soc.*, **98**, 3383 (1976).
- f. H. C. Brown and J. Muzzio, *J. Am. Chem. Soc.*, **88**, 2811 (1966).
- g. O. Arjona, R. Perez-Ossorio, A. Perez-Rubalcaba, and M. L. Quiroga, *J. Chem. Soc., Perkin Trans. 2*, 597 (1981); C. Alvarez-Ibarra, O. Arjona P. Perez-Ossorio, A. Perez-Rubalcaba, M. L. Quiroga, and M. J. Santesmases, *J. Chem. Soc., Perkin Trans. 2*, 1645 (1983).
- h. G. J. McGarvey and M. Kimura, *J. Org. Chem.*, **47**, 5420 (1982).

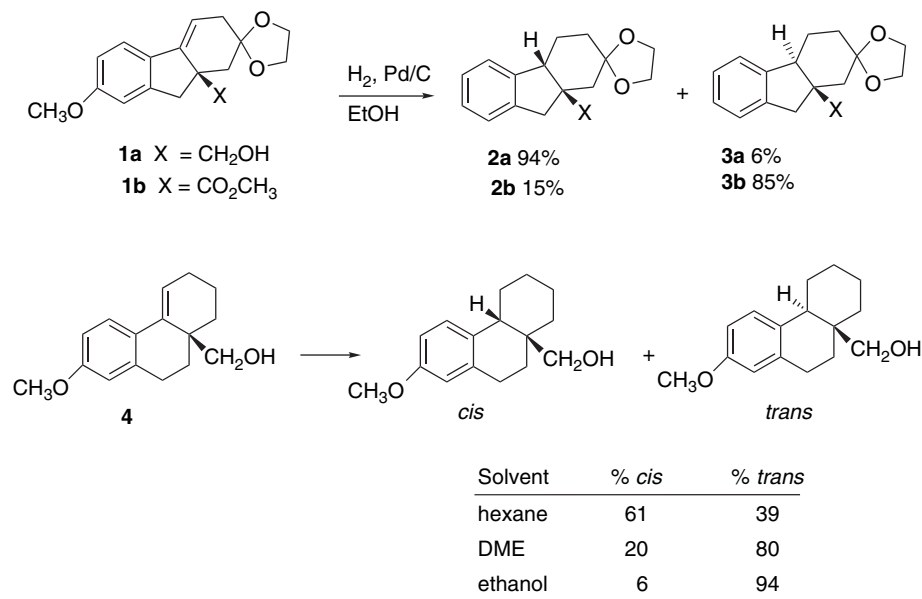
The mechanistic description of heterogeneous hydrogenation is somewhat vague, partly because the reactive sites on the metal surface are not as precisely described as small molecule reagents in solution. As understanding of the chemistry of homogeneous hydrogenation catalysts has developed, it has become possible to extrapolate those mechanistic concepts to heterogeneous catalysts. It is known that hydrogen is adsorbed onto the metal surface, forming metal-hydrogen bonds similar to those found in transition metal hydride complexes. Alkenes are also adsorbed on the catalyst surface and at least three types of intermediates have been implicated in hydrogenation. The initially formed intermediate is pictured as attached at both carbon atoms of the double bond by π -type bonding, as shown in **A**. The bonding involves the alkene π and π^* orbitals interacting with acceptor and donor orbitals of the metal. A hydrogen can be added to the adsorbed group, leading to **B**, which involves a carbon-metal σ bond. This species can react with another hydrogen to give the alkane. Alkanes have little affinity for the catalyst surface, so this reaction is effectively irreversible. A third intermediate species, shown as **C**, accounts for double-bond isomerization and the exchange of hydrogen that sometimes accompanies hydrogenation. This intermediate is equivalent to an allyl group bound to the metal surface by π bonds. It can be formed from adsorbed alkene by abstraction of an allylic hydrogen atom by the metal. Formation of the allyl species is reversible and can lead to alkene isomerization. Analogous reactions take place at single metal ions in homogeneous catalysis. A major uncertainty in heterogeneous catalysis is whether there are cooperative interactions involving several metal centers.



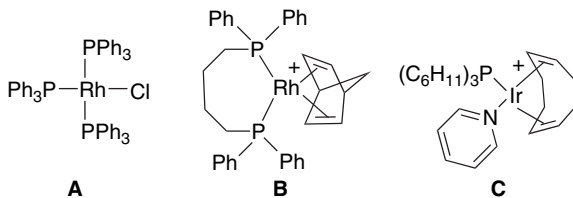
In most cases, both hydrogen atoms are added to the same side of the reactant (*syn* addition). If hydrogenation occurs by addition of hydrogen in two steps, as implied by the mechanism above, the intermediate must remain bonded to the metal surface in such a way that the stereochemical relationship is maintained. Adsorption to the catalyst surface normally involves the less sterically congested face of the double bond, and as a result, hydrogen is added from the less hindered face of the molecule. There are many cases of hydrogenations where hydrogen addition is not entirely *syn* and independent corroboration of the stereochemistry is normally necessary.

The facial stereoselectivity of hydrogenation is affected by the presence of polar functional groups that can influence the mode of adsorption to the catalyst surface. For

instance, there are many examples where the presence of a hydroxy group results in the hydrogen being introduced from the same side of the molecule occupied by the hydroxy group. This *syn*-directive effect suggests that the hydroxy group interacts with the catalyst surface. This behavior can be illustrated with the alcohol **1a** and the ester **1b**.⁹⁸ Although the overall shapes of the two molecules are similar, the alcohol gives mainly the product with a *cis* ring juncture (**2a**), whereas the ester gives mainly a product with *trans* stereochemistry (**3b**). The stereoselectivity of hydroxy-directed hydrogenation is a function of solvent and catalyst as indicated for alcohol **4**.⁹⁹ The *cis* isomer is the main product in hexane. In ethanol, the competing interaction of the solvent molecules evidently swamps out the directive effect of the hydroxymethyl group in **4** and the *trans* product is formed.



Substituent directive effects are also observed with soluble (homogeneous) hydrogenation catalysts. A number of transition metal complexes function as homogeneous hydrogenation catalysts. Three important examples are shown below.

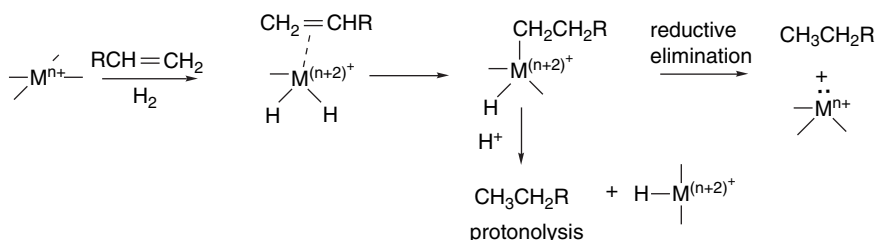


⁹⁸ H. W. Thompson, *J. Org. Chem.*, **36**, 2577 (1971).

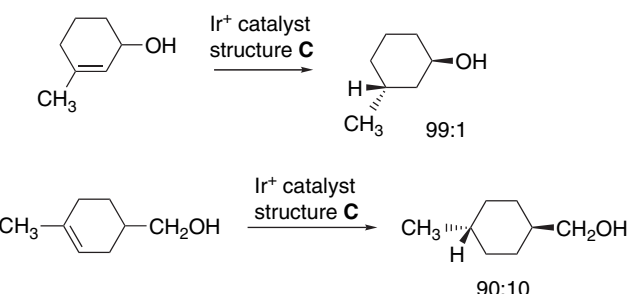
⁹⁹ H. W. Thompson, E. McPherson, and B. L. Lences, *J. Org. Chem.*, **41**, 2903 (1976).

Compound **A** is known as Wilkinson's catalyst and was one of the first of the homogeneous catalysts to be developed.¹⁰⁰ The cationic rhodium complex **B** is a useful catalyst for hydrogenations that involve a chelated structure between the reactant and the catalyst, such as allylic alcohols.¹⁰¹ The catalyst is activated by the hydrogenation of the norbornadiene ligand, which opens two binding sites at the catalytic metal. The iridium complex **C** (Crabtree catalyst) functions in a similar manner.¹⁰² The cyclooctadiene ligand is removed on exposure to hydrogen, providing two open positions. The Rh^+ and Ir^+ metal centers in these catalysts have eight electrons in their valence shells and are able to accommodate up to five additional donor pairs. We will encounter other examples of homogeneous catalysts in Section 2.5.1.1 when we discuss enantioselective hydrogenation.

The mechanism of homogeneous catalysis involves the same steps as heterogeneous catalysis. An initial π complex is formed with the reactant. Metal-hydride bonds then react with the complexed alkene to form a C–H bond and σ bond between the metal and alkyl group. There can be variation in the timing of formation of the M–H bonds. The metal carbon bond can be broken by either *reductive elimination* or *protonolysis*. Note that reductive elimination changes the metal oxidation state, whereas protonolysis does not. The catalytic cycle proceeds by addition of alkene and hydrogen.



As in heterogeneous hydrogenation, substituents can affect the stereoselectivity of the reduction by forming an additional bond to the metal center. This requires that there be sufficient ligand positions to accommodate binding by the substituent. Stereoselective hydrogenation based on substituent directive effects is particularly prevalent for cyclic compounds. The iridium catalyst $[\text{Ir}(\text{cod})_2\text{py}(\text{PCy}_3)]^+\text{PF}_6^-$ (structure **C** above) has been used frequently. Cyclohexenols and cyclohexenylmethanols exhibit good stereoselectivity, with delivery of the hydrogen *syn* to the hydroxy group.¹⁰³



¹⁰⁰ J. A. Osborn, F. H. Jardine, J. F. Young, and G. Wilkinson, *J. Chem. Soc. A*, 1711 (1966).

¹⁰¹ J. M. Brown, B. A. Chaloner, A. G. Kent, B. A. Murrer, P. N. Nicholson, D. Parker, and P. J. Sidebottom, *J. Organomet. Chem.*, **216**, 263 (1981); D. A. Evans and M. M. Morrissey, *J. Am. Chem. Soc.*, **106**, 3866 (1984).

¹⁰² R. H. Crabtree, H. Felkin, and G. E. Morris, *J. Organomet. Chem.*, **141**, 205 (1977).

¹⁰³ R. M. Crabtree and M. W. Davis, *J. Org. Chem.*, **51**, 2655 (1986).

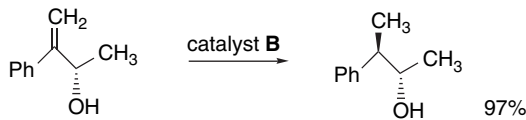
In contrast to the results seen with heterogeneous catalysts, the methoxy, ester, and acetyl groups are also strongly directive in the 4-methylcyclohex-3-enyl system. The effect of amido substituents is greater than the ester substituent.¹⁰⁴ This result indicates that the carbonyl oxygen is a strong donor group toward the Ir⁺ catalyst, whereas carbonyl groups are not effective as directing groups with the heterogeneous catalysts.

X	directed	nondirected	ref.
—CO ₂ CH ₃	95	1.7	a
—COCH ₃	99.2	0.8	a
—OCH ₃	>99.9	0.1	a
	>99	<1	b
—CH ₂ CO ₂ CH ₃	50	50	b

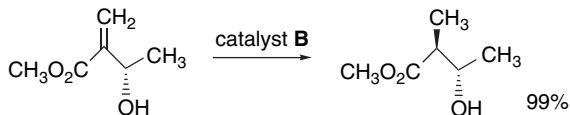
a. R. M. Crabtree and M.W. Davis, *J. Org. Chem.*, **51**, 2685 (1986).

b. A. G. Schultz and P. J. McCloskey, *J. Org. Chem.*, **50**, 5905 (1985).

The flexibility of acyclic systems adds another element to the analysis of substituent directive effects. Some of the best examples of stereoselective reductions involve allylic alcohols and the rhodium catalyst **B**.

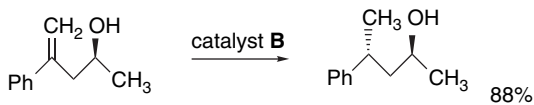


Ref. 105



Ref. 106

Stereoselectivity is also observed for homoallylic alcohols.



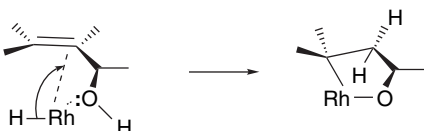
Ref. 105

¹⁰⁴. A. G. Schultz and P. J. McCloskey, *J. Org. Chem.*, **50**, 5905 (1985).

¹⁰⁵. J. M. Brown and R. G. Naik, *J. Chem. Soc. Chem. Commun.*, 348 (1982).

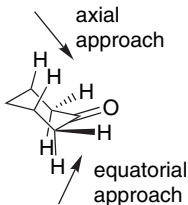
¹⁰⁶. J. M. Brown and I. Cutting, *J. Chem. Soc., Chem. Commun.*, 578 (1985).

The stereoselectivity for allylic and homoallylic alcohols is attributed to a chelated complex with delivery of the hydrogen *syn* with respect to the hydroxy group.¹⁰⁷



The general principles that emerge from these examples are the following: (1) The choice of catalyst must be appropriate. In particular, it must have sufficient exchangeable coordination sites to accommodate the directive group and still support the hydrogenation mechanism. (2) The structure of the reactant determines the nature of the coordination and the degree and direction of stereoselectivity. For cyclic systems, this usually results in *syn* delivery of hydrogen. For acyclic systems, the conformation of the coordinated reagent will control stereoselectivity. (3) In the examples cited above, the phosphine ligands were not explicitly considered, but their presence is crucial to the stability and reactivity of the metal center. When we consider enantioselective hydrogenation in Section 2.5.1.1, we will see that chiral phosphine ligands can also be used to establish a chiral environment at the metal center.

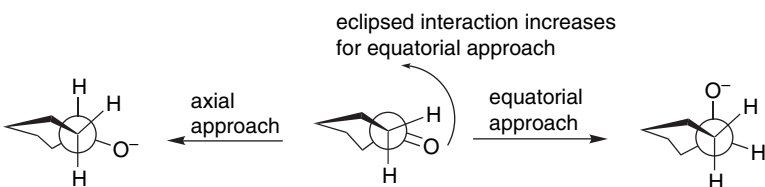
2.4.1.2. Hydride Reduction of Cyclic Ketones Section B of Scheme 2.6 gives some examples of hydride reduction of cyclic ketones. The stereoselectivity of nucleophilic additions to cyclic ketones has been studied extensively. The stereoselectivity in cyclohexanones is determined by the preference for approach of reactants from the axial or equatorial direction. The chair conformation of cyclohexanone places the carbonyl group in an unsymmetrical environment. The axial face has C(2, 6) – H_{eq} bonds that are nearly eclipsed with the C=O bond and the C(3,5)-dialixial hydrogens point toward the trajectory for reagent approach. In contrast, the equatorial face has axial C–H bonds at an angle of roughly 120° to the carbonyl plane. There is more steric bulk, including the 3,5-axial hydrogens, on the axial face. Remember also that the reagent interaction is with the LUMO and that the optimal trajectory is at an angle somewhat greater than 90° to the carbonyl plane.



It is observed that small nucleophiles prefer to approach the carbonyl group of cyclohexanone from the axial direction, even though this is a more sterically

¹⁰⁷ J. M. Brown, *Angew. Chem. Int. Ed. Engl.*, **26**, 190 (1987).

congested approach.¹⁰⁸ For example, NaBH_4 and LiAlH_4 deliver hydride by axial approach to form mainly the equatorial alcohol. How do the differences in the C–C bonds (on the axial side) as opposed to the C–H bonds (on the equatorial side) influence the stereoselectivity of cyclohexanone reduction? Torsional effects are believed to play a major role in the preference for axial approach. In the reactant conformation, the carbonyl group is almost eclipsed by the equatorial C(2) and C(6) C–H bonds. This torsional strain is relieved by axial attack, whereas equatorial approach increases strain because the oxygen atom must move through a fully eclipsed arrangement.¹⁰⁹



The stereoselectivity can be reversed by using more sterically demanding reagents. More bulky reducing agents usually approach the cyclohexanone carbonyl from the equatorial direction. This is called *steric approach control* and is the result of van der Waals repulsions with the 3,5-axial hydrogens. Alkylborohydride reagents are used instead of NaBH_4 , and alkoxy derivatives can be used in place of LiAlH_4 . The bulkier nucleophiles encounter the 3,5-axial hydrogens on the axial approach trajectory and therefore prefer the equatorial approach.¹¹⁰ A large amount of data has been accumulated on the stereoselectivity of reduction of cyclic ketones.¹¹¹ Table 2.4 compares the stereochemistry of reduction of several ketones by hydride donors of increasing steric bulk. The trends in the data illustrate the increasing importance of steric approach control as both the hydride reagent and the ketone become more highly substituted. For example, the axial methyl group in 3,3,5-trimethylcyclohexanone favors an equatorial approach. The alkyl-substituted borohydrides have especially high selectivity for the less hindered direction of approach.

The factors controlling the direction of reagent approach have also been studied in norbornan-2-ones. The stereochemistry of a number of reactions of the parent system and the 7,7-dimethyl derivative have been examined.¹¹² Some of the results are included in Table 2.4. These compounds reveal a reversal of the preferred direction of attack with the introduction of the 7,7-dimethyl substituents. In the parent system the *exo* direction of attack is preferred because the single CH_2 group at C(7) offers less steric resistance than the $-\text{CH}_2\text{CH}_2-$ unit on the *endo* side of the molecule. The *endo*

¹⁰⁸ B. W. Gung, *Tetrahedron*, **52**, 5263 (1996).

¹⁰⁹ M. Cherest, H. Felkin, and N. Prudent, *Tetrahedron Lett.*, 2199 (1968); M. Cherest and H. Felkin, *Tetrahedron Lett.*, 2205 (1968); Y. D. Wu and K. N. Houk, *J. Am. Chem. Soc.*, **109**, 906, 908 (1987); Y. D. Wu, K. N. Houk, and M. N. Paddon-Row, *Angew. Chem. Int. Ed. Engl.*, **31**, 1019 (1992).

¹¹⁰ W. G. Dauben, G. Fonken, and D. S. Noyce, *J. Am. Chem. Soc.*, **78**, 2579 (1956); H. C. Brown and W. C. Dickason, *J. Am. Chem. Soc.*, **92**, 709 (1970); D. C. Wigfield, *Tetrahedron*, **35**, 449 (1979); T. Wipke and P. Gund, *J. Am. Chem. Soc.*, **98**, 8107 (1976).

¹¹¹ D. C. Wigfield, *Tetrahedron*, **35**, 449 (1979); D. C. Wigfield and D. J. Phelps, *J. Org. Chem.*, **41**, 2396 (1976).

¹¹² H. C. Brown, J. H. Kawakami, and K.-T. Liu *J. Am. Chem. Soc.*, **95**, 2209 (1973).

Table 2.4. Stereoselectivity of Hydride Reducing Agents toward Cyclic Ketones^a

Reductant	% equat.	% equat.	% equat.	% exo	% endo
NaBH ₄	20 ^b	25 ^c	58 ^c	86 ^d	86 ^d
LiAlH ₄	8	24	83	89	92
LiAl(OMe) ₃ H	9	69		98	99
LiAl(O- <i>t</i> -Bu) ₃ H	9 ^e	36 ^f	95	94 ^f	94 ^f
LiBH(<i>s</i> -Bu) ₃	93 ^g	98 ^g	99.8 ^g	99.6 ^g	99.6 ^g
LiBH(siam) ^h	>99 ⁱ	>99 ⁱ	>99 ⁱ	NR ⁱ	

a. Except where noted otherwise, the data are those given by H. C. Brown and W. C. Dickason, *J. Am. Chem. Soc.*, **92**, 709 (1970). Data for many other cyclic ketones and reducing agents are given by A. V. Kamernitzky and A. A. Akhrem, *Tetrahedron*, **18**, 705 (1962) and W. T. Wipke and P. Gund, *J. Am. Chem. Soc.*, **98**, 8107 (1976).

b. P. T. Lansbury and R. E. MacLeay, *J. Org. Chem.*, **28**, 1940 (1963).

c. B. Rickborn and W. T. Wuesthoff, *J. Am. Chem. Soc.*, **92**, 6894 (1970).

d. H. C. Brown and J. Muzzio, *J. Am. Chem. Soc.*, **88**, 2811 (1966).

e. J. Klein, E. Dunkelblum, E. L. Eliel, and Y. Senda, *Tetrahedron Lett.*, 6127 (1968).

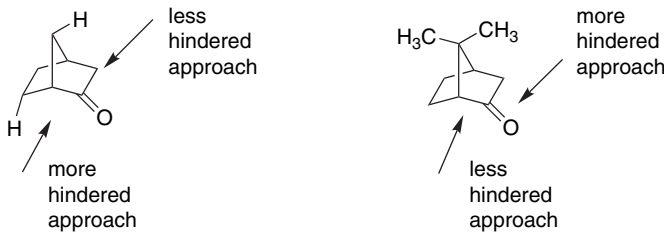
f. E. C. Ashby, J. P. Sevenair, and F. R. Dobbs, *J. Org. Chem.*, **36**, 197 (1971).

g. H. C. Brown and S. Krishnamurthy, *J. Am. Chem. Soc.*, **94**, 7159 (1972).

h. (siam) is an abbreviation for 1,2-dimethylpropyl.

i. S. Krishnamurthy and H. C. Brown, *J. Am. Chem. Soc.*, **98**, 3383 (1976).

hydrogens are in a relationship to the reaction site that is similar to the 1,3-diaxial interaction in a chair cyclohexane ring. When a *syn*-7-methyl group is present, the relative steric bulk of the two bridges is reversed.¹¹³

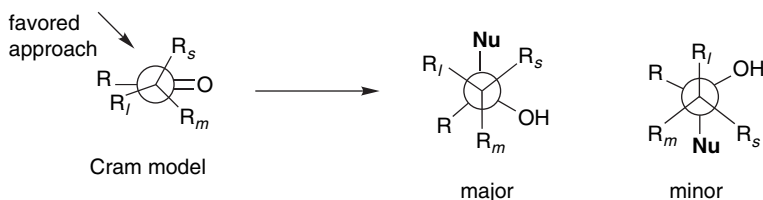


This relatively straightforward combination of torsional and steric effects as the source of stereoselectivity becomes more complicated when *polar* substituents are introduced into the picture. Polar effects are discussed in Topic 2.4.

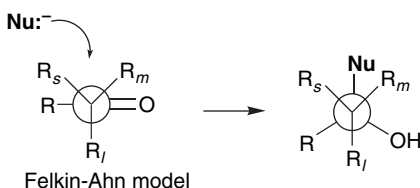
2.4.1.3. Stereoselective Nucleophilic Additions to Acyclic Carbonyl Groups The stereochemistry of nucleophilic addition to acyclic aldehydes and ketones is influenced by nearby substituents. A particularly important case occurs when there is a stereogenic center adjacent to the carbonyl group. As a result of the adjacent substituent, two diastereomers can be formed, depending on the direction of the approach of the nucleophile. The stereoselectivity of addition can be predicted on the basis of a conformational model of the TS. The addition reaction has been studied with several kinds

¹¹³. H. C. Brown and J. Muzzio, *J. Am. Chem. Soc.*, **88**, 2811 (1966).

of nucleophiles; we use data from hydride addition and organometallic compounds in our discussion. The initial data were analyzed some time ago by D. J. Cram and co-workers,¹¹⁴ who observed that the *major* product was correctly predicted by a model in which the largest α group was eclipsed with the other carbonyl substituent. This empirical relationship became known as *Cram's rule*.



As chemists considered the origin of this diastereoselectivity, the reactant conformation that is considered to be the most important one has changed. The currently preferred *Felkin-Ahn model* places the largest substituent perpendicular to the carbonyl group.¹¹⁵ The major product results from the nucleophile approaching opposite to the largest substituent. This is the same product as predicted by the Cram model, although the interpretation is different.



The Felkin-Ahn model invokes a combination of steric and stereoelectronic effects to account for the observed stereoselectivity. An approach from the direction of the smallest substituent minimizes steric interaction with the groups R_l (largest group) and R_m (medium group). Another key idea is that the nucleophile approaches from above or below the carbonyl group on a trajectory that makes an angle of about 107° to the plane of the carbonyl group.¹¹⁶ This reflects the fact that the primary interaction of the approaching nucleophile is with the antibonding LUMO. However, it is also proposed that there is a stereoelectronic (hyperconjugation) effect, which involves the interaction between the approaching nucleophile and the LUMO of the carbonyl group. This orbital, which accepts the electrons of the incoming nucleophile, is stabilized when the R_l group is perpendicular to the plane of the carbonyl group.¹¹⁷ This conformation permits a stabilizing interaction between the developing bond to the nucleophile and the antibonding σ^* orbital associated with the $C - R_l$ bond. Because this is a $\sigma \rightarrow \sigma^*$ interaction, it should increase in importance with the electron-acceptor capacity of X.

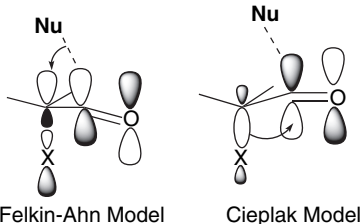
¹¹⁴ D. J. Cram and F. A. Abd Elhafez, *J. Am. Chem. Soc.*, **74**, 5828 (1952).

¹¹⁵ M. Cherest, H. Felkin, and N. Prudent, *Tetrahedron Lett.*, 4199 (1968).

¹¹⁶ H. B. Burgi, J. D. Dunitz, and E. Shefter, *J. Am. Chem. Soc.*, **95**, 5065 (1973).

¹¹⁷ N. T. Ahn, *Top. Current Chem.*, **88**, 145 (1980).

The *Cieplak model* emphasizes an alternative interaction, between the σ orbital of the C–X bond and the antibonding orbital to the nucleophile.¹¹⁸ In this case, a better donor X should be the most stabilizing. Li and le Noble pointed out that *both of these hyperconjugative interactions will be present in the transition structure.*¹¹⁹ There is also general agreement that addition of reactive nucleophiles have *early transition states*, which would suggest that substituent effects might best be examined in the *reactant*.



One broad generalization is that when steric interactions are dominant the Felkin-Ahn model is predictive. Thus *steric approach control*, the idea that the approaching nucleophile will approach the carbonyl group from the least hindered direction, is the first guiding principle.¹²⁰

The TS model emphasizing steric effects must be elaborated when there is a polar substituent in the vicinity of the carbonyl group. At least three additional factors may then be involved. There are stereoelectronic effects associated with heteroatom substituents. Electronegative substituents such as halogen are assigned to the 1 position in the Felkin-Ahn TS on the basis of presumed stronger stereoelectronic interactions with the C=O bond. According to this analysis, the σ^* bond to the halogen stabilizes the TS. An *anti*-periplanar arrangement maximizes this interaction. It is likely that there are also electrostatic effects involved in controlling nucleophilic addition reactions, since compounds such as decalones,¹²¹ norbornan-7-ones,¹²² and adamantanones,¹²³ which have remote substituents that cannot directly interact with the reaction site, nevertheless influence the stereoselectivity. It remains a point for discussion as to whether these substituent effects are electrostatic in nature or are transmitted by hyperconjugation. (See Topic 2.4 for further discussion.)

It should also be emphasized that the *metal counterions* associated with the nucleophiles are active participants in carbonyl addition reactions. There are strong interactions between the carbonyl oxygen and the metal ions in the TSs and intermediates. This effect can be recognized, for example, in the reactivity of borohydrides, where the Li^+ , Ca^{2+} , and Zn^{2+} salts are more reactive than the standard NaBH_4 reagent because of the greater Lewis acid strength of these cations.

The examples just discussed pertain to substituents that are on the carbon adjacent to the carbonyl center and the stereoselectivity is referred to as 1,2-asymmetric

¹¹⁸. A. S. Cieplak, *J. Am. Chem. Soc.*, **103**, 4540 (1981).

¹¹⁹. H. Li and W. J. le Noble, *Recl. Trav. Chim. Pays-Bas*, **111**, 199 (1992).

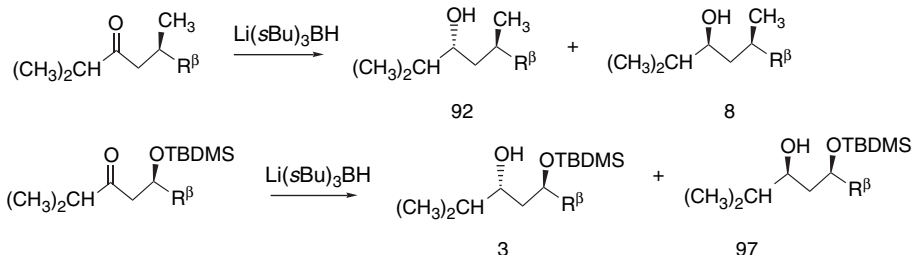
¹²⁰. W. G. Dauben, G. J. Fonken, and D. S. Noyce, *J. Am. Chem. Soc.*, **78**, 2579 (1956); H. C. Brown and H. R. Deck, *J. Am. Chem. Soc.*, **87**, 5620 (1965).

¹²¹. Y.-D. Wu, J. A. Tucker, and K. N. Houk, *J. Am. Chem. Soc.*, **113**, 5018 (1991).

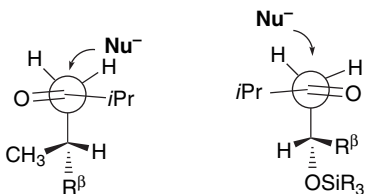
¹²². G. Mehta and F. A. Khan, *J. Am. Chem. Soc.*, **112**, 6140 (1990); H. Li, G. Mehta, S. Padma, and W. J. le Noble, *J. Org. Chem.*, **56**, 2006 (1991); G. Mehta, F. A. Khan, B. Ganguly, and J. Chandrasekhan, *J. Chem. Soc., Perkin Trans.*, **2**, 2275 (1994).

¹²³. C. K. Cheung, L. T. Tseng, M.-H. Lin, S. Srivastava, and W. J. Le Noble, *J. Am. Chem. Soc.*, **108**, 1598 (1986); J. M. Hahn and W. J. Le Noble, *J. Am. Chem. Soc.*, **114**, 1916 (1992).

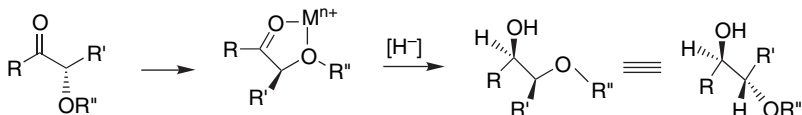
induction. More remote substituents can also affect the stereoselectivity of addition to the carbonyl group. For example, both β -methyl and β -siloxy substituents result in highly stereoselective reductions in ketones by trialkylborohydrides, but their directive effects are opposite.¹²⁴ This is a case of 1,3-asymmetric induction.



These results are attributed to alternative conformations of the reactant, with hydride attack being *anti* to the largest alkyl substituent in the methyl case and *anti* to the siloxy group in that case. The corresponding TSs are both of the Felkin-Ahn type in the sense that the large substituent is aligned perpendicularly with respect to the carbonyl group. In the methyl case, the favored TS minimizes the steric interaction of the isopropyl group with the β substituents. In the siloxy case, the favored TS has a stabilizing arrangement of the C=O and C–O dipoles and also avoids a steric interaction between the isopropyl group and R $^\beta$.



Another factor that affects stereoselectivity of carbonyl addition reactions is *chelation*.¹²⁵ If an α or β substituent can form a chelate with a metal ion involving the carbonyl oxygen, the stereoselectivity is usually governed by the chelated conformation. Complexation between a donor substituent, the carbonyl oxygen, and the Lewis acid can establish a preferred conformation for the reactant, which then controls reduction. Usually hydride is delivered from the less sterically hindered face of the chelate.



For example, α -hydroxy¹²⁶ and α -alkoxyketones¹²⁷ are reduced to *anti* 1,2-diols by Zn(BH₄)₂ via chelated TSs. This stereoselectivity is consistent with the preference for

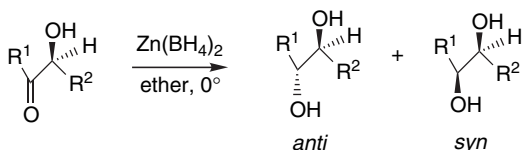
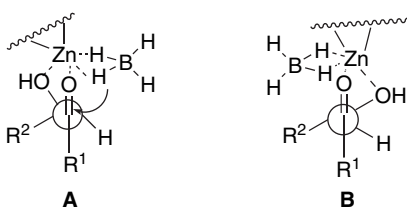
¹²⁴ D. A. Evans, M. J. Dart, and J. L. Duffy, *Tetrahedron Lett.*, **35**, 8541 (1994).

¹²⁵ D. J. Cram and K. R. Kopecky, *J. Am. Chem. Soc.*, **81**, 2748 (1959); D. J. Cram and D. R. Wilson, *J. Am. Chem. Soc.*, **85**, 1245 (1963).

¹²⁶ T. Nakata, T. Tanaka, and T. Oishi, *Tetrahedron Lett.*, **24**, 2653 (1983).

¹²⁷ G. J. McGarvey and M. Kimura, *J. Org. Chem.*, **47**, 5420 (1982).

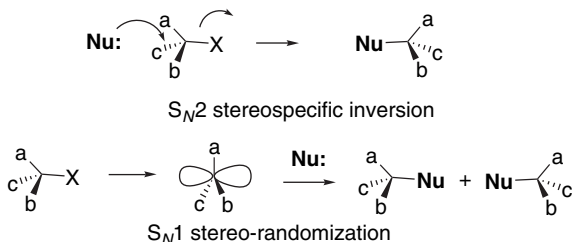
TS **A** over **B**. The stereoselectivity increases with the bulk of substituent R². LiAlH₄ shows a similar trend, but with reduced selectivity.



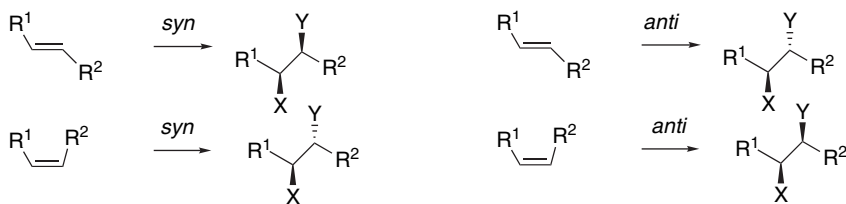
R ¹	R ²	Zn(BH ₄) ₂ <i>anti : syn</i>	LiAlH ₄ <i>anti : syn</i>
n-C ₅ H ₁₁	CH ₃	77:23	64:36
CH ₃	n-C ₅ H ₁₁	85:15	70:30
i-C ₃ H ₇	CH ₃	85:15	58:42
CH ₃	i-C ₃ H ₇	96:4	73:27
Ph	CH ₃	98:2	87:13
CH ₃	Ph	90:10	80:20

2.4.2. Examples of Stereospecific Reactions

In stereospecific reactions the configuration of the product is directly related to the configuration of the reactant and is determined by the reaction mechanism. Stereoisomeric reactants give different, usually stereoisomeric, products. The reaction mechanism determines the stereochemical relationship between the reactants and products. For any given reaction, stereospecificity may be lost or altered if there is a change in the mechanism. For example, the S_N2 reaction occurs with stereospecific inversion. However, when the mechanism shifts to S_N1 because of a change in reactants or reaction conditions, stereospecificity is lost.

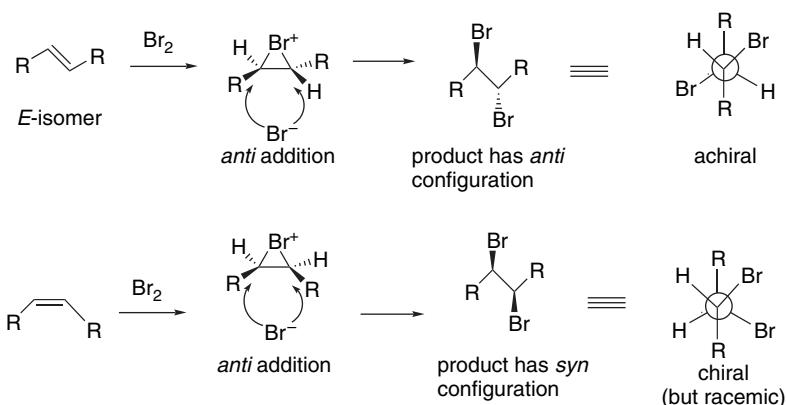


Another familiar and important example is *syn* and *anti* addition to double bonds. There are many examples of stereospecific reactions involving additions to carbon–carbon double bonds. Addition can be *anti* or *syn*, depending on the mechanism. If the mechanism specifies *syn* or *anti* addition, different products will be obtained from the *E*- and *Z*-isomers.

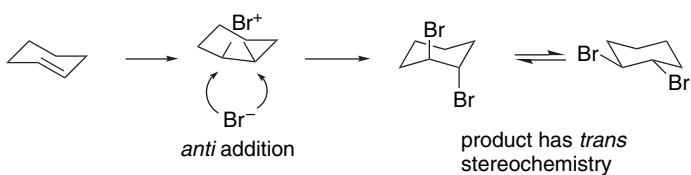


The examples in Scheme 2.7 include bromination, epoxidation and dihydroxylation, and hydroboration-oxidation of alkenes.

2.4.2.1. Bromination of Alkenes The bromination of substituted alkenes provides a number of examples of stereospecific reactions. These can be illustrated by considering the *Z*- and *E*-stereoisomers of disubstituted alkenes. The addition of bromine is usually stereospecifically *anti* for unconjugated disubstituted alkenes and therefore the *Z*- and *E*-alkenes lead to *diastereomeric products*. When both substituents on the alkene are identical, as in 2-butene, the product from the *Z*-alkene is chiral, whereas the product from the *E*-alkene is the achiral *meso* form (see p. 132).

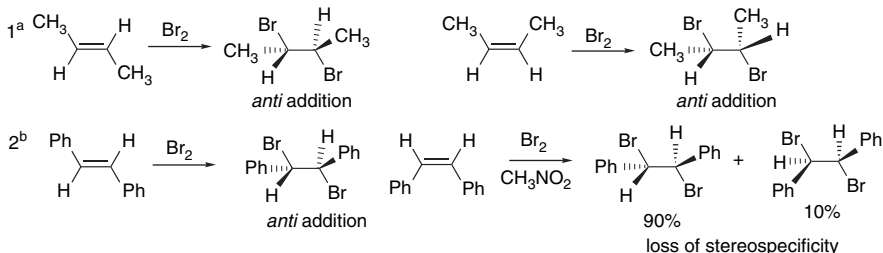


The preference for *anti* addition is also evident from the formation of the *trans* product from cyclic alkenes.

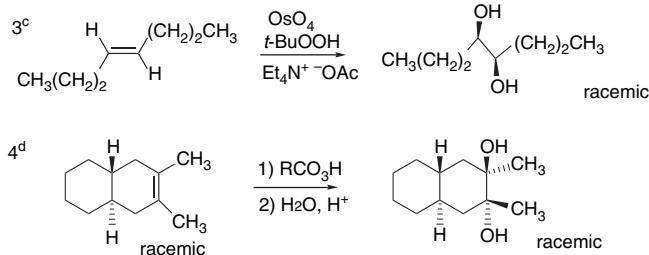


Scheme 2.7. Examples of Stereospecific Reactions**A. Bromination of Alkenes** (see Section 2.4.2.1 for additional discussion)

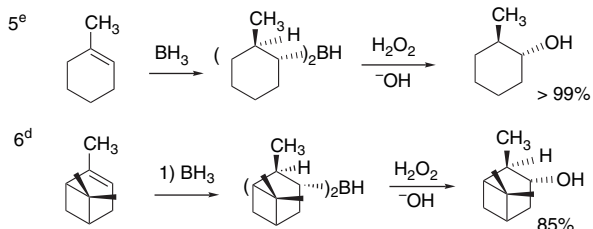
Bromination of simple alkenes normally proceeds via a bromonium ion and is stereospecifically *anti*. Exceptions occur when the bromonium ion is in equilibrium with a corresponding carbocation.

**B. Dihydroxylation and Epoxidation-Hydrolysis of Alkenes** (see Section 2.4.2.2 for additional discussion)

Dihydroxylation of epoxides can be carried out with *syn* stereospecificity using OsO_4 as the active oxidant. The reaction occurs by a cycloaddition mechanism. Epoxidation is also a stereospecific *syn* addition. Ring opening of epoxides by hydrolysis also leads to diols. This is usually an *anti* addition with inversion of configuration at the site of nucleophilic attack, leading to overall *anti* dihydroxylation.

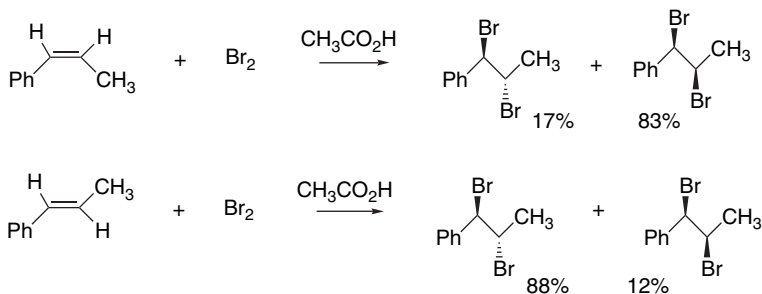
**C. Hydroboration-Oxidation** (see Section 2.4.2.3 for additional discussion)

Hydroboration-oxidation occurs by *syn* addition. The reagents are borane or an alkyl or dialkyl derivative, followed by oxidation, usually with H_2O_2 and -OH . The oxidation occurs with *retention of configuration of the alkyl group*. The regioselectivity favors addition of the boron at the less-substituted carbon of the double bond. As a result, the reaction sequence provides a stereospecific *syn*, *anti*-Markovnikov hydration of alkenes.

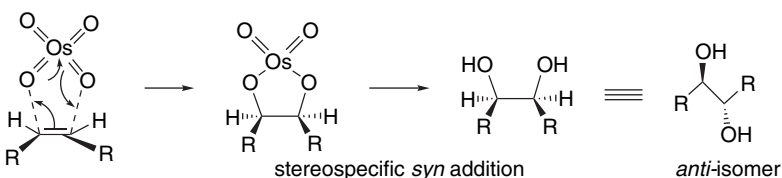


- a. J. H. Rolston and K. Yates, *J. Am. Chem. Soc.*, **91**, 1469, 1477 (1969).
- b. R. E. Buckles, J. M. Bader, and R. L. Thurmaier, *J. Org. Chem.*, **27**, 4523 (1962).
- c. K. Akashi, R. E. Palermo, and K. B. Sharpless, *J. Org. Chem.*, **43**, 2063 (1978).
- d. B. Rickborn and D. K. Murphy, *J. Org. Chem.*, **34**, 3209 (1969).
- e. H. C. Brown and G. Zweifel, *J. Am. Chem. Soc.*, **83**, 2544 (1961).
- f. G. Zweifel and H. C. Brown, *Org. Synth.*, **52**, 59 (1972).

The mechanism of bromination is discussed more fully in Section 5.3, but the fundamental cause of the stereospecificity is the involvement of the positively charged bromonium ion intermediate. The bromonium ion is opened by an *anti* approach of the bromide, leading to net *anti* addition. Entry 1 in Scheme 2.7 illustrates this behavior. Stereospecific products are obtained from the *E*- and *Z*-isomers, both as the result of *anti* addition. Stereospecificity is diminished or lost when the bromonium ion is not the *only intermediate in the reaction*. Entry 2 in Scheme 2.7 shows this behavior for *cis*-stilbene in nitromethane, where most of the product is the result of *syn* addition. The addition is *anti* in less polar solvents such as cyclohexane or carbon tetrachloride. The loss of *anti* stereospecificity is the result of a change in mechanism. The polar solvent permits formation of a carbocation intermediate. If the bromonium ion can open to a carbocation, a mixture of *syn* and *anti* products is formed. In the stilbene case, the more stable *anti* product is formed. Some loss of stereospecificity is also observed with 1-phenylpropene, where the phenyl group provides stabilization of an open carbocation intermediate.¹²⁸ Part of the product from both isomers is the result of *syn* addition.

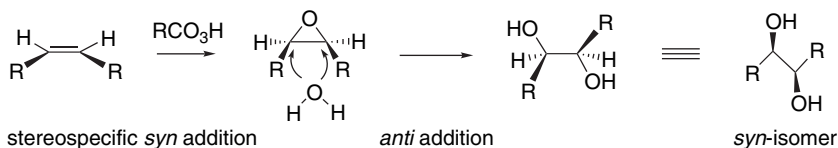


2.4.2.2. Epoxidation and Dihydroxylation of Alkenes There are several ways to convert alkenes to diols. Some of these methods proceed by *syn* addition, but others lead to *anti* addition. An important example of *syn* addition is osmium tetroxide-catalyzed dihydroxylation. This reaction is best carried out using a catalytic amount of OsO₄, under conditions where it is reoxidized by a stoichiometric oxidant. Currently, the most common oxidants are *t*-butyl hydroperoxide, potassium ferricyanide, or an amine oxide. The two oxygens are added from the same side of the double bond. The key step in the reaction mechanism is a [3 + 2] cycloaddition that ensures the *syn* addition.

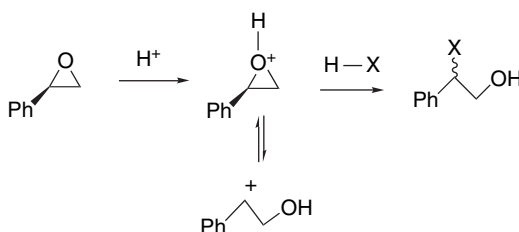


¹²⁸ R. C. Fahey and H.-J. Schneider, *J. Am. Chem. Soc.*, **90**, 4429 (1968).

Alkenes can be converted to diols with overall *anti* addition by a two-step sequence involving epoxidation and hydrolysis. The epoxidation is a *syn* addition that occurs as a single step. When epoxidation is followed by hydrolytic ring opening, the configuration of the diols is determined by the configuration of the alkene, usually with net *anti* dihydroxylation. The hydrolysis reaction proceeds by back-side epoxide ring opening.



Nucleophilic ring opening of epoxides usually occurs with *anti* stereochemistry, with nucleophilic attack at the less substituted carbon.¹²⁹ On the other hand, the acid-catalyzed epoxidation-hydrolysis sequence is not always stereospecific. In the case of (*S*)-1-phenyloxirane (styrene oxide), the acid-catalyzed ring opening is regioselective and proceeds through the more stable (benzylic) carbocation; there is extensive racemization because of the involvement of a carbocation.¹³⁰



The ring opening of β -methylstyrene oxide also leads to extensive stereorandomization at the benzylic position.¹³¹

As summarized in Scheme 2.8, these reactions provide access to three different overall stereochemical outcomes for alkene dihydroxylation, *syn* addition, *anti* addition, or stereorandom addition, depending on the reaction mechanism. In Section 2.5.4 we will discuss enantioselective catalyst for alkene dihydroxylation. These reactions provide further means of controlling the stereochemistry of the reaction.

2.4.2.3. Hydroboration-Oxidation Hydroboration is a stereospecific *syn* addition. Hydroboration is covered in further detail in Section 5.7. The reaction occurs by an electrophilic attack by borane or alkylborane on the double bond with a concerted shift of hydrogen.

¹²⁹ R. E. Parker and N. S. Isaacs, *Chem. Rev.*, **59**, 737 (1959).

¹³⁰ G. Berti, F. Bottari, P. L. Ferrarini, and B. Macchia, *J. Org. Chem.*, **30**, 4091 (1965); B. Lin and D. L. Whalen, *J. Org. Chem.*, **59**, 1638 (1994).

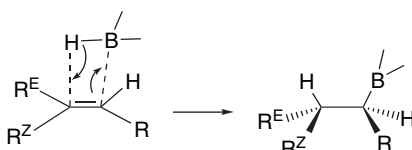
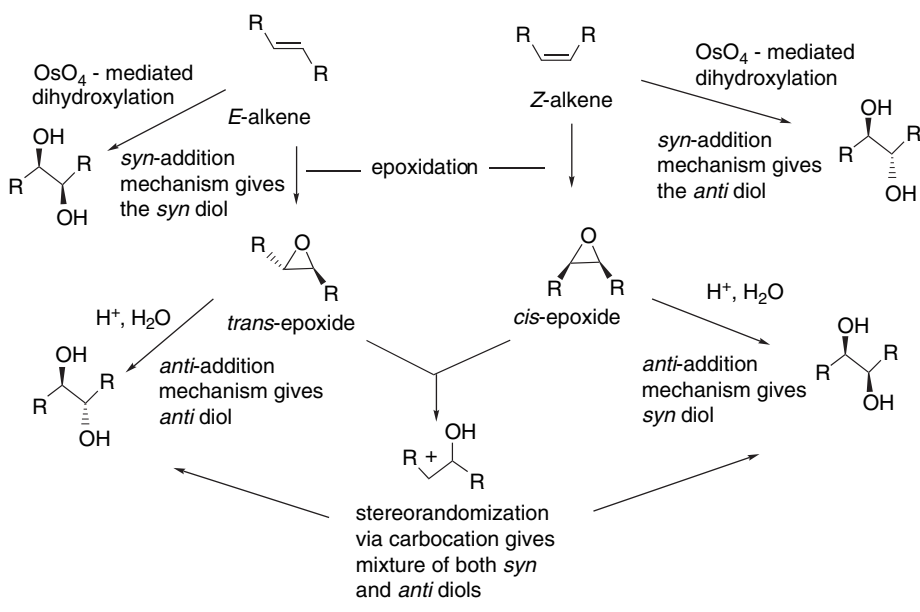
¹³¹ R. S. Mohan and D. L. Whalen, *J. Org. Chem.*, **58**, 2663 (1993).

Scheme 2.8. Summary of Stereochemistry of Alkene Dihydroxylation by OsO₄-Catalysis and Epoxide Ring Opening

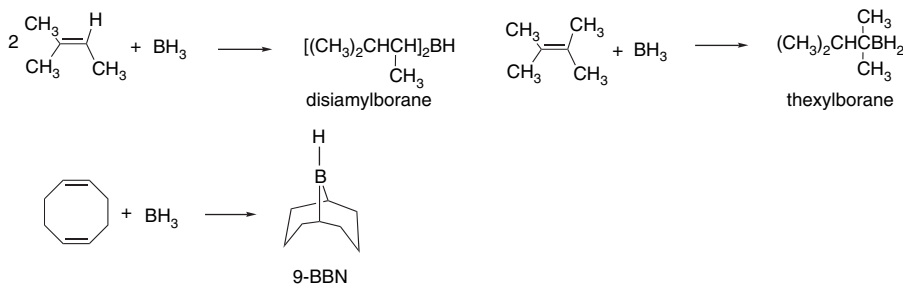
187

SECTION 2.4

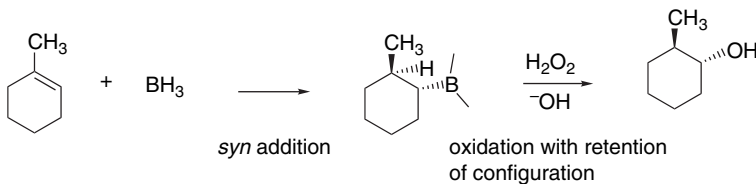
Stereoselective and
Stereospecific Reactions



When the reaction is done with borane it is usually carried to the trialkylborane stage, but by controlling the stoichiometry the dialkyl or monoalkylborane can be obtained, especially from highly substituted alkenes such as 2-methyl-2-butene or 2,3-dimethylbutene. The resulting dialkyl and monoalkyl boranes are known as disiamylborane and thexyloborane. Another useful dialkyl borane is 9-borabicyclo[3.3.1]nonane, known as 9-BBN.



When hydroboration is done in a synthetic context it is usually followed by a secondary reaction, most frequently oxidation by hydrogen peroxide and a base, which gives the corresponding alcohol *with retention of configuration*. The stereospecificity is very high. The regioselectivity is also usually excellent for the addition of the borane at the less substituted carbon of the double bond. This is illustrated in Entry 5 of Scheme 2.7, where 1-methylcyclohexene gives *trans*-2-methylcyclohexanol as a result of *syn* addition, followed by oxidation with retention of configuration. The stereospecificity is higher than 99% and none of the *cis* isomer is detected.



There is also an element of stereoselectivity associated with the hydroboration. The borane approaches from the less hindered face of the alkene. For 3-methylcyclohexene, a mixture of products is formed because the 3-methyl substituent has only weak influence on the regiochemistry and the steric approach. This stereoselectivity is accentuated by use of the larger dialkyl and alkyl boranes, as is illustrated by the data for 7,7-dimethylnorbornene in Table 2.5. All of the stereoselectivity and regioselectivity elements are illustrated by Entry 6 in Scheme 2.7. The boron adds at the less substituted end of the double bond and *anti* to the larger dimethyl bridge. Note that this forces the C(2) methyl into proximity of the larger bridge. After oxidation, the hydrogen and hydroxy that were added are *syn*.

Each of the stereoselective reactions that were considered in Section 2.4 are discussed in more detail when the reaction is encountered in subsequent chapters. The key point for the present is that *reaction mechanism determines stereochemical outcome*. Knowledge about the mechanism allows the prediction of stereochemistry, and conversely, information about stereochemistry provides insight into the mechanism. As we consider additional reactions, we will explore other examples of the relationships between mechanism and stereochemistry.

Table 2.5. Stereoselectivity of Hydroboration

Reagent	3-Methylcyclohexene ^a				Norbornene ^b		7,7-Dimethyl-norbornene ^b	
	<i>cis</i> -2	<i>trans</i> -2	<i>cis</i> -3	<i>trans</i> -3 ^a	<i>exo</i>	<i>endo</i> ^b	<i>exo</i>	<i>endo</i> ^c
B_2H_6	16	34	18	32	99.5	0.5	22	78
Disiamylborane	18	30	27	25	87	13		
9-BBN	0	20	40	40	99.5	0.5	3	97

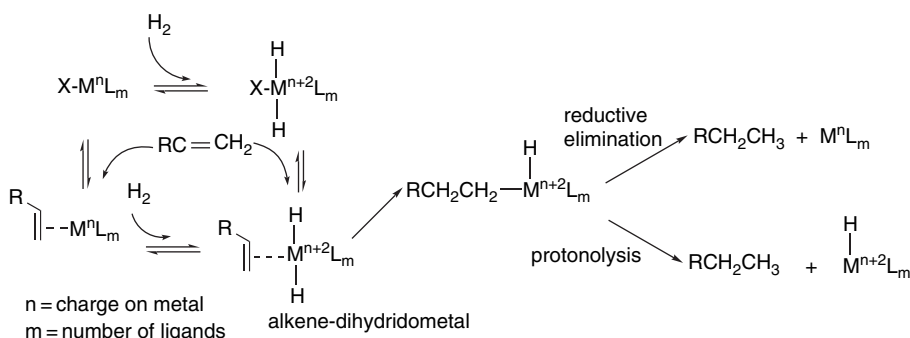
a. H. C. Brown, R. Liotta, and L. Brener, *J. Am. Chem. Soc.*, **99**, 3427 (1977).

b. H. C. Brown, J. H. Kawakami, and K.-T. Liu, *J. Am. Chem. Soc.*, **95**, 2209 (1973).

Enantioselective reactions are a particular case of stereoselective reactions that show a preference for one of a pair of enantiomers. As noted in Section 2.1.8, no reaction can produce an excess of one enantiomer unless there is at least one chiral component involved. *Enantiospecific reactions* are a special case of stereoselective reactions in which the mechanism ensures that the configuration of reactant, reagent, or catalyst determines that of the product. A simple example is S_N2 substitution, where the back-side displacement mechanism dictates inversion of configuration. In the next several subsections, we discuss examples of enantioselective and enantiospecific reactions.

2.5.1. Enantioselective Hydrogenation

Most catalytic hydrogenations are carried out under heterogeneous conditions using finely dispersed transition metals as catalysts. Such reactions take place on the catalyst surface (heterogeneous hydrogenation) and are not normally enantioselective, although they may be stereoselective (see Section 2.4.1.1). In addition, certain soluble transition metal complexes are active hydrogenation catalysts.¹³² Many of these catalysts include phosphine ligands, which serve both to provide a stable soluble complex and to adjust the reactivity of the metal center. Hydrogenation by homogeneous catalysts is believed to take place through a π complex of the unsaturated compound. The metals also react with molecular hydrogen and form metal hydrides. The addition of hydrogen to the metal can occur before or after complexation of the alkene. An alkylmetal intermediate is formed by transfer of hydrogen from the metal to the carbon. This intermediate can break down to alkane by reductive elimination or in some cases by reaction with a proton source.

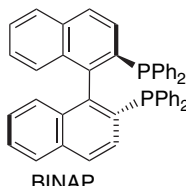


The process of homogeneous catalytic hydrogenation can be made enantioselective by establishing a chiral environment at the catalytic metal center. Most of the successful cases of enantioselective hydrogenation involve reactants having a potential

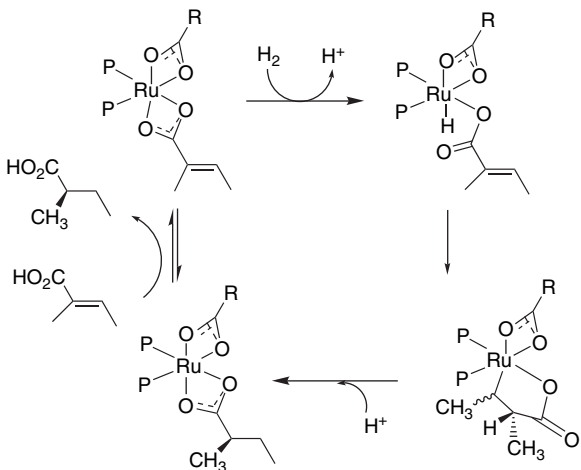
¹³² A. J. Birch and D. H. Williamson, *Org. Reactions*, **24**, 1 (1976); B. R. James, *Homogeneous Hydrogenation*, Wiley, New York, 1973; B. R. James, in *Comprehensive Organometallic Chemistry*, G. Wilkinson, F. G. A. Stone, and E. W. Abel, eds., Pergamon Press, Oxford, 1982, Vol. 8, Chap. 51; P. A. Chaloner, M. A. Esteruelas, F. Joo, L. A. Oro, *Homogeneous Hydrogenation*, Kluwer Academic, Dordrecht, 1994.

coordinating group. For example, α , β -unsaturated acids and esters, as well as allylic alcohols, are among the reactants that give good results. The reason for this is that the functional group can complex with the metal center, increasing the overall degree of structural organization. Scheme 2.9 provides some examples of enantioselective hydrogenations. Entries 1 and 2 involve acrylic acid derivatives with rhodium catalysts containing chiral phosphine ligands. Entry 3 involves an unsaturated diester. The reactants in Entries 4 and 5 are α -amido acrylic acids.

A number of chiral ligands have been explored in order to develop enantioselective hydrogenation catalysts.¹³³ Some of the most successful catalysts are derived from chiral 1, 1'-binaphthylidiphosphines such as BINAP.¹³⁴ These ligands are chiral by virtue of the sterically restricted rotation of the two naphthyl rings (see Section 2.1.5). Scheme 2.10 gives the structures and common names of some other important chiral diphosphine ligands.



α , β -Unsaturated acids can be reduced enantioselectively with ruthenium and rhodium catalysts having chiral phosphine ligands. The mechanism of such reactions using Ru(BINAP)(O₂CCH₃)₂ is consistent with the idea that coordination of the carboxy group establishes the geometry at the metal ion.¹³⁵ The configuration of the product is established by the hydride transfer from ruthenium to the α -carbon that occurs on formation of the alkyl-metal intermediate. The second hydrogen is introduced by protonolysis.



¹³³. B. Bosnich and M. D. Fryzuk, *Top. Stereochem.*, **12**, 119 (1981); W. S. Knowles, W. S. Chrisopfel, K. E. Koenig, and C. F. Hobbs, *Adv. Chem. Ser.*, **196**, 325 (1982); W. S. Knowles, *Acc. Chem. Res.*, **16**, 106 (1983).

¹³⁴. R. Noyori and H. Takaya, *Acc. Chem. Res.*, **23**, 345 (1990).

¹³⁵. M. T. Ashby and J. T. Halpern, *J. Am. Chem. Soc.*, **113**, 589 (1991).

A. Acrylic acid and esters.

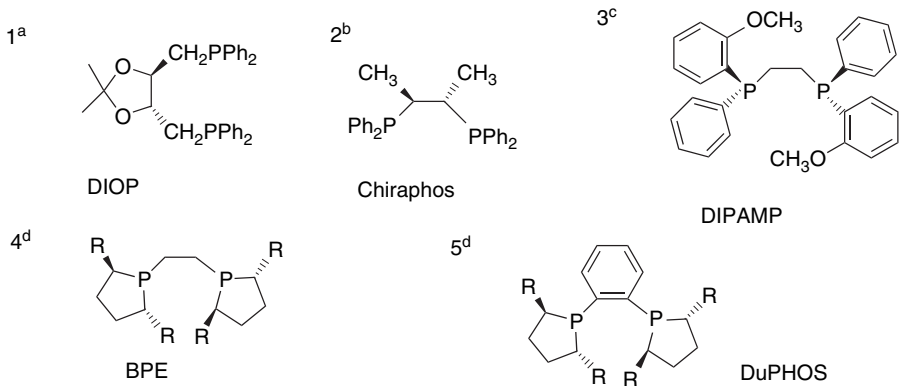
	Reactant	Catalyst	Product	e.e.
1 ^a				96%
2 ^b				99%
3 ^c				88%

B. α -Amidoacrylic acids.

4 ^d				94%
5 ^e				100%

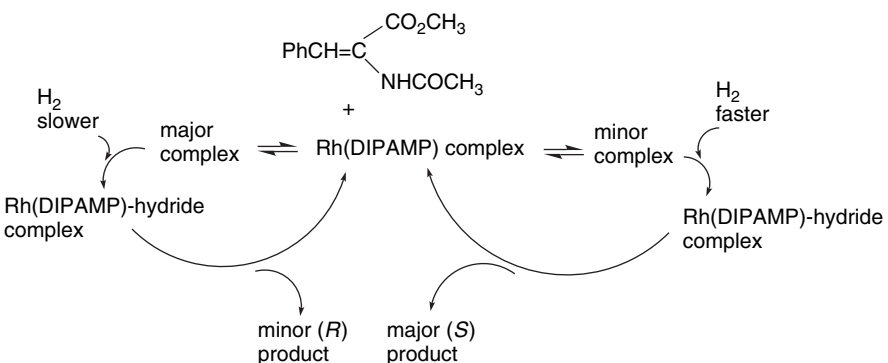
a. T. Chiba, A. Miyashita, H. Nohira, and H. Takaya, *Tetrahedron Lett.*, **32**, 4745 (1991).b. M. J. Burk, F. Bienewald, M. Harris, and A. Zanotti-Gerosa, *Angew. Chem. Int. Ed. Engl.*, **37**, 1931 (1998).c. W. C. Chrisopf and B. D. Vineyard, *J. Am. Chem. Soc.*, **101**, 4406 (1979).d. B. D. Vineyard, W. S. Knowles, M. J. Sabacky, G. L. Bachman, and D. J. Weinkauf, *J. Am. Chem. Soc.*, **99**, 5946 (1977).e. A. Miyashita, H. Takaya, T. Souchi, and R. Noyori, *Tetrahedron*, **40**, 1245 (1984).

Scheme 2.10. Some Chiral Diphosphine Ligands Used in Enantioselective Hydrogenation



- a. H. B. Kagan and T.-P. Dang, *J. Am. Chem. Soc.*, **94**, 6429 (1972).
 b. M. D. Fryzuk and B. Bosnich, *J. Am. Chem. Soc.*, **100**, 5491 (1978).
 c. W. S. Knowles, *Acc. Chem. Res.*, **16**, 106 (1983).
 d. M. J. Burk, J. E. Feaster, W. A. Nugent, and R. L. Harlow, *J. Am. Chem. Soc.*, **115**, 10125 (1993).

An especially important case is the enantioselective hydrogenation of α -amidoacrylic acids, which leads to α -aminoacids.¹³⁶ A particularly detailed study was carried out on the mechanism of reduction of methyl Z- α -acetamidocinnamate by a rhodium catalyst with the chiral diphosphine ligand DIPAMP.¹³⁷ It was concluded that the reactant can bind reversibly to the catalyst to give either of two complexes. Addition of hydrogen at rhodium then leads to a reactive rhodium hydride intermediate and eventually to product. Interestingly, the addition of hydrogen occurs most rapidly in the *minor isomeric complex* and the enantioselectivity is due to this kinetic preference. The major isomer evidently encounters greater steric repulsions if hydrogenation proceeds and is therefore less reactive.¹³⁸



¹³⁶ J. M. Brown, *Chem. Soc. Rev.*, **22**, 25 (1993). A. Pfaltz and J. M. Brown in *Stereoselective Synthesis*, G. Helmchen, R. W. Hoffmann, J. Mulzer and E. Schauman, eds., Thieme, New York, 1996, Part D, Sec. 2.5.1.2; U. Nagel and J. Albrecht, *Top. Catal.*, **5**, 3 (1998).

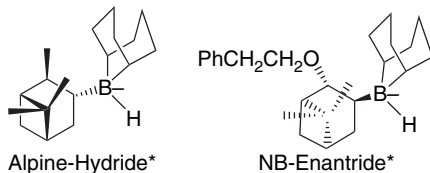
¹³⁷ C. R. Landis and J. Halpern, *J. Am. Chem. Soc.*, **109**, 1746 (1987).

¹³⁸ S. Feldgus and C. R. Landis, *J. Am. Chem. Soc.*, **122**, 12714 (2000).

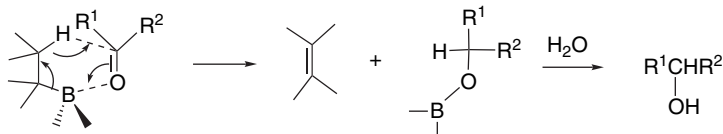
These examples illustrate the factors that are usually involved in successful enantioselective hydrogenation. The first requirement is that the metal center have the necessary reactivity toward both molecular hydrogen and the reactant alkene. The metal center must retain this reactivity in the presence of the chiral ligands. Furthermore, because most of the ligands are bidentate, there must be sufficient coordination sites to accommodate the ligand, as well as hydrogen and the reactant. In particular, there must be at least one remaining coordination site for the functional group. As we can see from the detailed mechanisms of the α -amido acrylates, the Rh center proceeds through a hexacoordinate dihydride intermediate to a pentacoordinate σ -alkyl intermediate. The reductive elimination frees two coordination sites (including the dissociation of the product). This coordinatively unsaturated complex can then proceed through the catalytic cycle by addition of reactant and hydrogen.

2.5.2. Enantioselective Reduction of Ketones

Hydride reducing agents convert ketones to secondary alcohols. Unsymmetrical ketones lead to chiral secondary alcohols. The common hydride reducing agents NaBH_4 and LiAlH_4 are achiral and can only produce racemic alcohol. Let us look at some cases where the reaction can be enantioselective. A number of alkylborohydride derivatives with chiral substituents have been prepared. These reagents are generally derived from naturally occurring terpenes.¹³⁹ Two examples of the alkylborohydride group have the trade names Alpine-Hydride[®] and NB-Enantride[®].¹⁴⁰ NB-Enantride achieves 76% e.e. in the reduction of 2-butanone.¹⁴¹



Trialkylboranes and dialkylchloroboranes are also useful for reduction of aldehydes and ketones.¹⁴² These reactions involve the coordination of the carbonyl oxygen to boron and transfer of a β -hydrogen through a cyclic TS.



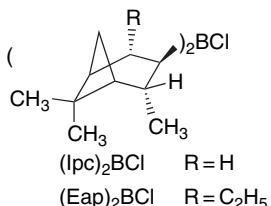
¹³⁹. M. M. Midland, *Chem. Rev.*, **89**, 1553 (1989).

¹⁴⁰. Alpine-Hydride and NB-Enantride are trade names of the Sigma Aldrich Corporation.

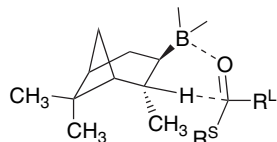
¹⁴¹. M. M. Midland, A. Kazubski, and R. E. Woodling, *J. Org. Chem.*, **56**, 1068 (1991).

¹⁴². M. M. Midland and S. A. Zderic, *J. Am. Chem. Soc.*, **104**, 525 (1982).

When the borane is chiral, these reactions can be enantioselective. The most highly developed of the chiral boranes are derived from α -pinene. The dialkylborane is known as diisopinocampheylborane, Ipc_2BH . Both enantiomers are available.¹⁴³ The corresponding *B*-alkyl and chloroborane derivatives act as enantioselective reductants toward ketones. For example the BBN derivative of isopinocampheylborane is enantioselective in the reduction of acetophenone.¹⁴⁴ The degree of enantioselectivity of alkylchloroboranes depends on the alkyl substituent, increasing from methyl (14% e.e. *S*), ethyl (33% e.e. *S*) through isopropyl (81% e.e. *S*), but then completely reversing with the *t*-butyl derivative (96% e.e. *R*).¹⁴⁵ Di-(isopinocampheyl)chloroborane,¹⁴⁶ $(\text{Ipc})_2\text{BCl}$, and *t*-butylisopinocampheylchloroborane¹⁴⁷ achieve high enantioselectivity for aryl and hindered dialkyl ketones. Diiso-2-ethylapopinocampheylchloroborane, $(\text{Eap})_2\text{BCl}$, shows good enantioselectivity toward an even wider range of ketones.¹⁴⁸ Table 2.6 gives some typical results for enantioselective reduction of ketones.



In most cases, the enantioselectivity can be predicted by a model that places the smaller carbonyl substituent toward the isopinocampheyl methyl group.¹⁴⁹



The origin of the enantioselectivity has been examined using semiempirical (AM1) computations.^{145c} The main differences in stability arise at the stage of formation of the borane-ketone complex, where the boron changes from sp^2 to sp^3 hybridization. The boron substituents introduce additional steric compressions.

An even more efficient approach to enantioselective reduction of ketones is to use a chiral catalyst. One of the most successful is the oxazaborolidine **D**, which is

- ^{143.} H. C. Brown, P. K. Jadhav, and A. K. Mandal, *Tetrahedron*, **37**, 3547 (1981); H. C. Brown and P. K. Jadhav, in *Asymmetric Synthesis*, J. D. Morrison, ed., Academic Press, New York, 1983, Chap. 1.
- ^{144.} M. M. Midland, S. Greer, A. Tramontano, and S. A. Zderic, *J. Am. Chem. Soc.*, **101**, 2352 (1979).
- ^{145.} (a) M. M. Rogic, *J. Org. Chem.*, **61**, 1341 (1996); (b) M. M. Rogic, P. V. Ramachandran, H. Zinnen, L. D. Brown, and M. Zheng, *Tetrahedron: Asymmetry*, **8**, 1287 (1997); (c) M. M. Rogic, *J. Org. Chem.*, **65**, 6868 (2000).
- ^{146.} H. C. Brown, J. Chandrasekharan, and P. V. Ramachandran, *J. Am. Chem. Soc.*, **110**, 1539 (1988); M. Zhao, A. O. King, R. D. Larsen, T. R. Verhoeven, and P. J. Reider, *Tetrahedron Lett.*, **38**, 2641 (1997).
- ^{147.} H. C. Brown, M. Srebnik, and P. V. Ramachandran, *J. Org. Chem.*, **54**, 1577 (1989).
- ^{148.} H. C. Brown, P. V. Ramachandran, A. V. Teodorovic, and S. Swaminathan, *Tetrahedron Lett.*, **32**, 6691 (1991).
- ^{149.} M. M. Midland and J. L. McLoughlin, *J. Org. Chem.*, **49**, 1316 (1984).

Table 2.6. Enantioselective Reduction of Ketones

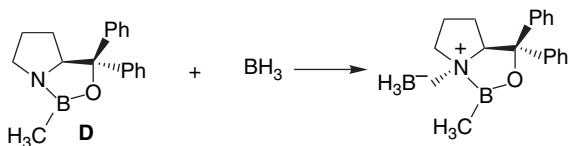
Reagent	Ketone	% e.e.	Configuration
Alpine-Borane ^{®a}	3-Methyl-2-butanone	62	S
NB-Enantride ^{®b}	2-Octanone	79	S
Eapine-Hydride ^c	2-Octanone	78	S
(Ipc) ₂ BCl ^d	2-Acetyl naphthalene	94	S
(Ipc)(<i>t</i> -Bu)BCl ^e	Acetophenone	96	R
(Ipc) ₂ BCl ^f	2,2-Dimethylcyclohexanone	91	S
(Eap) ₂ BCl ^g	3-Methyl-2-butanone	95	R

SECTION 2.5
Enantioselective Reactions

NOTE: © Trademark of Sigma Aldrich Corporation.

- a. H. C. Brown and G. G. Pai, *J. Org. Chem.*, **50**, 1384 (1985).
- b. M. M. Midland and A. Kazubski, *J. Org. Chem.*, **47**, 2495 (1982).
- c. P. Ramachandran, R. Veeraghavan, H. C. Brown, and S. Swaminathan, *Tetrahedron: Asymmetry*, **1**, 433 (1990).
- d. M. Zhao, A. O. King, R. D. Larsen, T. R. Verhoeven, and P. J. Reider, *Tetrahedron Lett.*, **38**, 2641 (1997).
- e. H. C. Brown, M. Srebnik, and P. V. Ramachandran, *J. Org. Chem.*, **54**, 1577 (1989).
- f. H. C. Brown, J. Chandrasekharan, and P. V. Ramachandran, *J. Am. Chem. Soc.*, **110**, 1539 (1988).
- g. H. C. Brown, P. V. Ramachandran, A. V. Teodorovic, and S. Swaminathan, *Tetrahedron Lett.*, **32**, 6691 (1991).

derived from the amino acid proline.¹⁵⁰ The enantiomer is also available. An adduct of borane and **D** is the active reductant. This adduct can be prepared, stored, and used as a stoichiometric reagent, if so desired.¹⁵¹



A catalytic amount (5–20 mol %) of this reagent, along with additional BH_3 as the reductant, can reduce ketones such as acetophenone and pinacolone in > 95% e.e. There are experimental data indicating that the steric demand of the boron substituent influences enantioselectivity.¹⁵² The enantioselectivity and reactivity of these catalysts can be modified by changes in substituent groups to optimize selectivity toward a particular ketone.¹⁵³

Computational studies have explored the mechanism and origin of the enantioselectivity of these reactions. Based on semiempirical MO calculations (MNDO), it has

¹⁵⁰ E. J. Corey, R. K. Bakshi, S. Shibata, C.-P. Chen, and V. K. Singh, *J. Am. Chem. Soc.*, **109**, 7925 (1987); E. J. Corey and C. J. Helal, *Angew. Chem. Int. Ed. Engl.*, **37**, 1987 (1998).

¹⁵¹ D. J. Mahre, A. S. Thompson, A. W. Douglas, K. Hoogsteen, J. D. Carroll, E. G. Corley, and E. J. J. Grabowski, *J. Org. Chem.*, **58**, 2880 (1993).

¹⁵² E. J. Corey and R. K. Bakshi, *Tetrahedron Lett.*, **31**, 611 (1990); T. K. Jones, J. J. Mohan, L. C. Xavier, T. J. Blacklock, D. J. Mathre, P. Sohar, E. T. T. Jones, R. A. Reamer, F. E. Roberts, and E. J. J. Grabowski, *J. Org. Chem.*, **56**, 763 (1991).

¹⁵³ A. W. Douglas, D. M. Tschaen, R. A. Reamer, and Y.-J. Shi, *Tetrahedron: Asymmetry*, **7**, 1303 (1996).

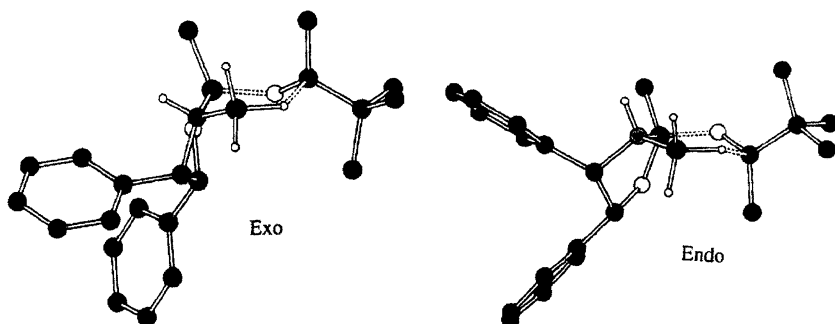
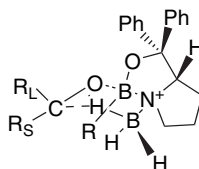
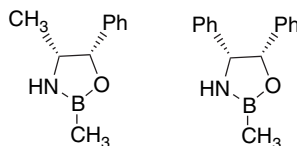


Fig. 2.20. Optimized (HF/3-21G) structures of the *exo* and *endo* transition states for reduction of *t*-butyl methyl ketone by a model catalyst. The *exo* structure is favored by 2.1 kcal, in accord with an experimental e.e. of 88%. Reproduced from *J. Am. Chem. Soc.*, **116**, 8516 (1994), by permission of the American Chemical Society.

been suggested that the enantioselectivity in these reductions arises from a chair-like TS in which the governing steric interaction is the one with the alkyl substituent on boron.¹⁵⁴



There also have been ab initio studies of the transition structure using several model catalysts and calculations at the HF/3-21G, HF/6-31G(*d*), and MP2/6-31G(*d*) levels.¹⁵⁵ The enantioselectivity is attributed to the preference for an *exo* rather than an *endo* approach of the ketone, as shown in Figure 2.20.



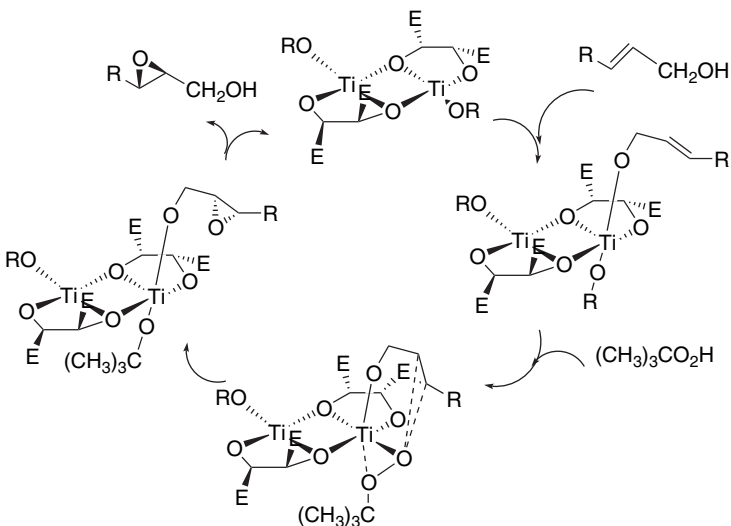
2.5.3. Enantioselective Epoxidation of Allylic Alcohols

Certain transition metal complexes catalyze oxidation of allylic alcohols to the corresponding epoxides. The most useful procedures involve *t*-butyl hydroperoxide as

¹⁵⁴. D. K. Jones, D. C. Liotta, I. Shinkai, and D. J. Mathre, *J. Org. Chem.*, **58**, 799 (1993); L. P. Linney, C. R. Self, and T. H. Williams, *J. Chem. Soc., Chem. Commun.* 1651 (1994).

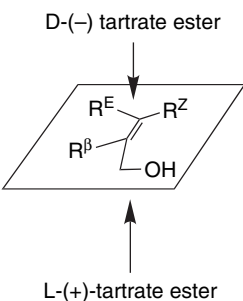
¹⁵⁵. G. J. Quallich, J. F. Blake, and T. M. Woodall, *J. Am. Chem. Soc.*, **116**, 8516 (1994).

the stoichiometric oxidant in combination with titanium catalysts. When enantiomerically pure tartrate esters are included in the system, the reaction is highly enantioselective and is known as *Sharpless asymmetric epoxidation*.¹⁵⁶ Either the (+) or (-) tartrate ester can be used, so either enantiomer of the desired product can be obtained. The allylic hydroxy group serves to coordinate the reactant to titanium. The mechanism involves exchange of the allylic alcohol and *t*-butyl hydroperoxide for another ligand at the titanium atom. In the TS an oxygen atom from the peroxide is transferred to the double bond.¹⁵⁷ The electrophilic metal polarizes the weak O–O bond of the hydroperoxide to effect the transfer of oxygen to the alkene π bond. Both kinetic data and consideration of the energetics of the monomeric and dimeric complexes suggest that the active catalyst is dimeric.¹⁵⁸



The orientation of the reactants is governed by the chirality of the tartrate ester.¹⁵⁹ The enantioselectivity can be predicted in terms of the model shown below.¹⁶⁰

- ^{156.} R. A. Johnson and K. B. Sharpless, in *Catalytic Asymmetric Synthesis*, I. Ojima, ed., VCH Publishers, New York, 1993, pp. 103–158.
- ^{157.} M. G. Finn and K. B. Sharpless in *Asymmetric Synthesis*, Vol. 5, J. D. Morrison, ed., Academic Press, New York, 1985, Chap 8; B. H. McKee, T. H. Kalantar, and K. B. Sharpless, *J. Org. Chem.*, **56**, 6966 (1991); For an alternative description of the origin of enantioselectivity, see E. J. Corey, *J. Org. Chem.*, **55**, 1693 (1990).
- ^{158.} M. G. Finn and K. B. Sharpless, *J. Am. Chem. Soc.*, **113**, 113 (1991).
- ^{159.} V. S. Martin, S. S. Woodard, T. Katsuki, Y. Yamada, M. Ikeda, and K. B. Sharpless, *J. Am. Chem. Soc.*, **103**, 6237 (1981); K. B. Sharpless, S. S. Woodard, and M. G. Finn, *Pure Appl. Chem.*, **55**, 1823 (1983); M. G. Finn, and K. B. Sharpless, *J. Am. Chem. Soc.*, **113**, 113 (1991); B. H. McKee, T. H. Kalantar, and K. B. Sharpless, *J. Org. Chem.*, **56**, 6966 (1991).
- ^{160.} M. G. Finn and K. B. Sharpless in *Asymmetric Synthesis*, J. D. Morrison, ed., Vol 5, Academic Press, New York, 1985, Chap. 5.



There has been a DFT (BLYP/HW3) study of the TS and its relationship to the enantioselectivity of the reaction.¹⁶¹ The strategy used was to build up the model by successively adding components. First the titanium coordination sphere, including the allylic alcohol and peroxide group, was modeled (Figure 2.21a). The diol ligand and allylic alcohol were added to the coordination sphere (Figure 2.21b). Then the steric bulk associated with the hydroperoxide was added (Figure 2.21c). Finally the tartrate esters were added (using formyl groups as surrogates; Figure 2.21d). This led successively to TS models of increasingly detailed structure. The energies of the added components were minimized to identify the most stable structure at each step. The key features of the final TS model are the following: (1) The peroxide-titanium interaction has a spiro rather than planar arrangement in the TS for oxygen transfer. (2) The breaking O–O bond is nearly perpendicular to the plane of the C=C bond to meet the stereoelectronic requirement for electrophilic attack. (3) The orientation of the alkyl group of the peroxide plays a key role in the enantioselectivity, which is consistent with the experimental observation that less bulky hydroperoxides give much lower enantioselectivity. (4) This steric effect leads to an arrangement in which the C–O bond of the allylic alcohol bisects the O–Ti–O bonds in the favored TS. (5) The tartrate ester groups at the catalytically active titanium center are in equatorial positions and do not coordinate to titanium, which implies a conformation flip of the diolate ring as part of the activation process, since the ester groups are in axial positions in the dimeric catalyst. (6) This conformation of the tartrate ligands places one of the ester groups in a position that blocks one mode of approach and determines the enantioselectivity.

Visual models, additional information and exercises on the Sharpless Epoxidation can be found in the Digital Resource available at: Springer.com/carey-sundberg.

As with enantioselective hydrogenation, we see that several factors are involved in the high efficacy of the $Ti(OiPr)_4$ -tartrate epoxidation catalysts. The metal ion has two essential functions. One is the assembly of the reactants, the allylic alcohol, and the hydroperoxide. The second is its Lewis acid character, which assists in the rupture of the O–O bond in the coordinated peroxide. In addition to providing the reactive oxidant, the *t*-butyl hydroperoxide contributes to enantioselectivity through its steric bulk. Finally, the tartrate ligands establish a chiral environment that leads to a preference for one of the diastereomeric TSs and results in enantioselectivity.

¹⁶¹ Y.-D. Wu and D. K. W. Lai, *J. Am. Chem. Soc.*, **117**, 11327 (1995).

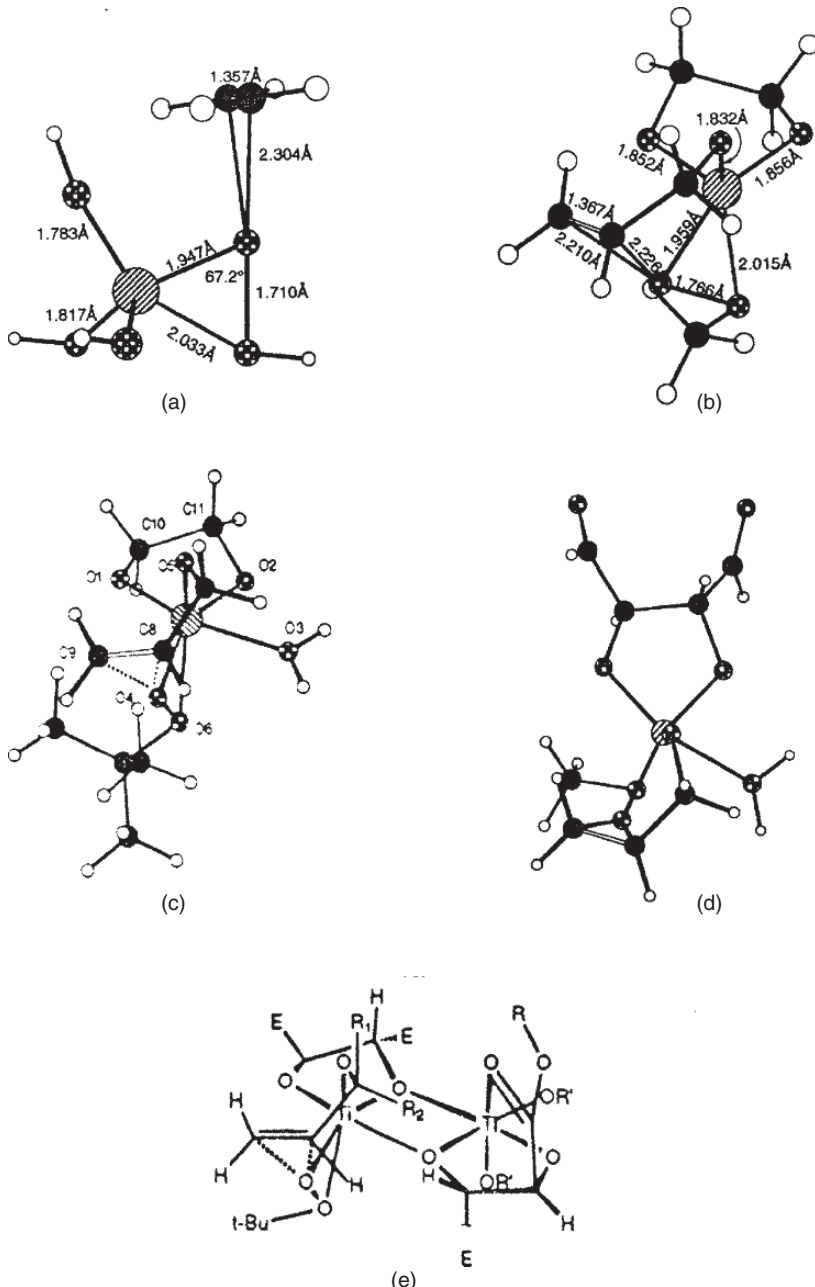
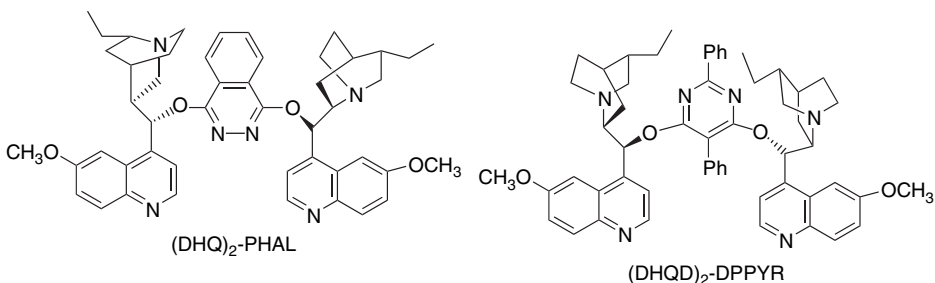


Fig. 2.21. Successive models of the transition structures for Sharpless epoxidation: (a) the hexacoordinate Ti core with hydroxide and hydroperoxide ligand and a coordinated alkene; (b) Ti with methylhydroperoxide, allyl alcohol, and ethanediol as ligands; (c) monomeric catalytic center incorporating *t*-butylhydroperoxide as oxidant; (d) monomeric catalytic center with formyl groups added; (e) representation of the active dimeric catalyst. Reproduced from *J. Am. Chem. Soc.*, **117**, 11327 (1995), by permission of the American Chemical Society.

2.5.4. Enantioselective Dihydroxylation of Alkenes

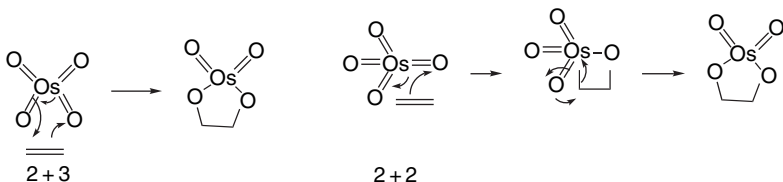
Osmium tetroxide is a stereospecific oxidant that produces diols from alkenes by a *syn*-addition.¹⁶² Currently, the reaction is carried out using a catalytic amount of OsO₄, with a stoichiometric oxidant such as *t*-butyl hydroperoxide,¹⁶³ potassium ferricyanide,¹⁶⁴ or morpholine-*N*-oxide.¹⁶⁵ Osmium tetroxide oxidations can be highly enantioselective in the presence of chiral ligands. The most highly developed ligands are derived from the cinchona alkaloids dihydroquinine (DHQ) and dihydroquinidine (DHQD).¹⁶⁶ The most effective ligands are dimeric derivatives of these alkaloids such as (DHQ)₂-PHAL and (DHQD)₂-DDPYR,¹⁶⁷ in which the alkaloid units are linked by heterocyclic ethers. These ligands not only induce high enantioselectivity, but they also *accelerate the reaction*.¹⁶⁸ Optimization of the reaction conditions permits rapid and predictable dihydroxylation of many types of alkenes.¹⁶⁹ The premixed catalysts are available commercially and are referred to by the trade names AD-mix™.



From extensive studies, a consensus has been reached about some aspects of the catalytic mechanism and enantioselectivity: (1) The amine ligands, in particular the quinuclidine nitrogen, are important in activating and stabilizing the osmium intermediate.¹⁷⁰ (2) From the kinetics of the reaction, it is also evident that the *binding of the*

162. M. Schroeder, *Chem. Rev.*, **80**, 187 (1980).
 163. K. B. Sharpless and K. Akashi, *J. Am. Chem. Soc.*, **98**, 1986 (1976); K. Akashi, R. E. Palermo, and K. B. Sharpless, *J. Org. Chem.*, **43**, 2063 (1978).
 164. M. Minato, K. Yamamoto and J. Tsuji, *J. Org. Chem.*, **55**, 766 (1990); K. B. Sharpless, W. Amberg, Y. L. Bennani, G. A. Crispino, J. Hartung, K.-S. Jeong, H.-L. Kwong, K. Morikawa, Z.-M. Wang, D. Xu, and X.-L. Zhang, *J. Org. Chem.*, **57**, 2768 (1992); J. Eames, H. J. Mitchell, A. Nelson, P. O'Brien, S. Warren, and P. Wyatt, *Tetrahedron Lett.*, **36**, 1719 (1995).
 165. V. VanRheenen, R. C. Kelly, and D. Y. Cha, *Tetrahedron Lett.*, 1973 (1976).
 166. H. C. Kolb, M. S. Van Nieuwenhze, and K. B. Sharpless, *Chem. Rev.*, **94**, 2483 (1994).
 167. G. A. Crispino, K.-S. Jeong, H. C. Kolb, Z.-M. Wang, D. Xu, and K. B. Sharpless, *J. Org. Chem.*, **58**, 3785 (1993); G. A. Crispino, A. Makita, Z.-M. Wang, and K. B. Sharpless, *Tetrahedron Lett.*, **35**, 543 (1994); K. B. Sharpless, W. Amberg, Y. L. Bennani, G. A. Crispino, J. Hartung, K. S. Jeong, H.-C. Kwong, K. Morikawa, Z. M. Wang, D. Xu, and X. L. Zhang, *J. Org. Chem.*, **57**, 2768 (1992); W. Amberg, Y. L. Bennani, R. K. Chadha, G. A. Crispino, W. D. Davis, J. Hartung, K. S. Jeong, Y. Ogino, T. Shibata, and K. B. Sharpless, *J. Org. Chem.*, **58**, 844 (1993); H. Becker, S. B. King, M. Taniguchi, K. P. M. Vanhessche, and K. B. Sharpless, *J. Org. Chem.*, **60**, 3940 (1995).
 168. P. G. Anderson and K. B. Sharpless, *J. Am. Chem. Soc.*, **115**, 7047 (1993).
 169. H.-L. Kwong, C. Sorato, Y. Ogino, H. Chen, and K. B. Sharpless, *Tetrahedron Lett.*, **31**, 2999 (1990); T. Gobel and K. B. Sharpless, *Angew. Chem. Int. Ed. Engl.*, **32**, 1329 (1993).
 170. D. W. Nelson, A. Gypser, P. T. Ho, H. C. Kolb, T. Kondo, H.-L. Kwong, D. V. McGrath, A. E. Rubin, P.-O. Norrby, K. P. Gable, and K. B. Sharpless, *J. Am. Chem. Soc.*, **119**, 1840 (1997).

reactant is a distinct step in the mechanism and that there are *attractive interactions* between the catalyst ligands and the reactant.¹⁷¹ The ligands do not function only by steric exclusion, but contribute to the net stabilization of the TS. (3) The aromatic linker groups determine the size of the binding pocket; the ethyl groups on the quinuclidine ring have differing orientations in the DHQD and DHQ catalysts and are a more integral part of the pocket in the DHQD system. (4) The concerted [2 + 3]cycloaddition mechanism for the actual oxidation step is energetically preferable to an alternative two-step mechanism involving [2 + 2]cycloaddition.¹⁷²



Within these general terms, the interpretation and prediction of enantioselectivity depends on the binding of the particular reactant in the catalyst pocket. A wide range

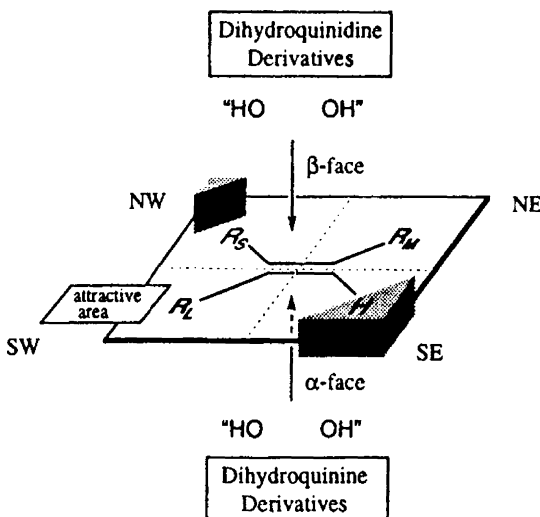


Fig. 2.22. Predictive schematic model for enantioselectivity of AD-mix dihydroxylation catalysts. Reproduced from *Chem. Rev.*, **94**, 2483 (1994), by permission of the American Chemical Society.

- ¹⁷¹ H. C. Kolb, M. S. Van Nieuwenhze, and K. B. Sharpless, *Chem. Rev.*, **94**, 2483 (1994); E. J. Corey and M. C. Noe, *J. Am. Chem. Soc.*, **118**, 319 (1996); E. J. Corey and M. C. Noe, *J. Am. Chem. Soc.*, **118**, 11038 (1996); P.-O. Norrby, H. Becker, and K. B. Sharpless, *J. Am. Chem. Soc.*, **118**, 35 (1996). H. C. Kolb, P. G. Andersson, and K. B. Sharpless, *J. Am. Chem. Soc.*, **116**, 1278 (1994); B. B. Lohray and V. Bhushan, *Tetrahedron Lett.*, **33**, 5113 (1992).
- ¹⁷² S. Dapprich, G. Ujaque, F. Maseras, A. Lledos, D. G. Musaev, and K. Morokuma, *J. Am. Chem. Soc.*, **118**, 11660 (1996); U. Pidun, C. Boehme, and G. Frenking, *Angew. Chem. Int. Ed. Engl.*, **35**, 2817 (1996); M. Torrent, L. Deng, M. Duran, M. Sola, and T. Ziegler, *Organometallics*, **16**, 13 (1997).

of reactants have been examined, and an empirical model for predicting orientation has been developed from the data.¹⁷³ This model is shown in Figure 2.22. Note that the DHQD and DHQ ligands have opposite enantioselectivity because they are of opposite absolute configuration.

There have been several efforts aimed at theoretical modeling and analysis of the enantioselectivity of osmium-catalyzed dihydroxylation. The system is too large to be amenable to ab initio approaches, but combinations of quantum chemical (either MO or DFT) and molecular mechanics make the systems tractable. A hybrid investigation based on DFT (B3LYP/6-31G) computation and MM3 was applied to the (DHQD)₂PYDZ catalyst (PYDZ = 3, 5-pyridazinyl).¹⁷⁴ This study examined a number of possible orientations of styrene within the complex and computed their relative energy. The energies were obtained by combining DFT calculations on the reaction core of OsO₄ and the double bond, with MM3 calculations on the remainder of the molecule. Two orientations were found to be very close in energy and these were 2.5–10 kcal/mol more favorable than all the others examined. Both led to the observed enantioselectivity. The two preferred TS structures are shown in Figure 2.23.

Most of the differences in energy among the various orientations are due to differences in the MM portion of the calculation, pointing to nonbonded interactions as the primary determinant of the binding mode. Specifically, attractive interaction with quinoline ring A ($\pi - \pi$ stacking, 6.1 kcal/mol), quinoline ring B (2.3 kcal/mol), and a perpendicular binding interaction with the pyridazine ring (1.3 kcal/mol) offset the energy required to fit the reactant molecule to the catalytic site. This is consistent with the view that there is an *attractive interaction with the ligand system*.

Norrby, Houk, and co-workers approached the problem by deriving a molecular mechanics type of force field from quantum chemical calculations.¹⁷⁵ This model, too, suggests that there are two possible bonding arrangements and that either might be preferred, depending on the reactant structure. This model was able

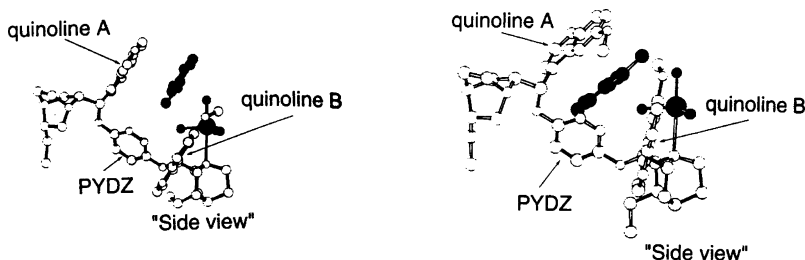


Fig. 2.23. Two most favored orientations of styrene for enantioselective dihydroxylation by (DHQD)PYDZ catalyst. The bridging structure is 3,5-pyridazinyl. Reproduced from *J. Am. Chem. Soc.*, **121**, 1317 (1999), by permission of the American Chemical Society.

¹⁷³. H. C. Kolb, P. G. Andersson, and K. B. Sharpless, *J. Am. Chem. Soc.*, **116**, 1278 (1994).

¹⁷⁴. G. Ujaque, F. Maseras, and A. Lledos, *J. Am. Chem. Soc.*, **121**, 1317 (1999).

¹⁷⁵. P.-O. Norrby, T. Rasmussen, J. Haller, T. Strassner, and K. N. Houk, *J. Am. Chem. Soc.*, **121**, 10186 (1999).

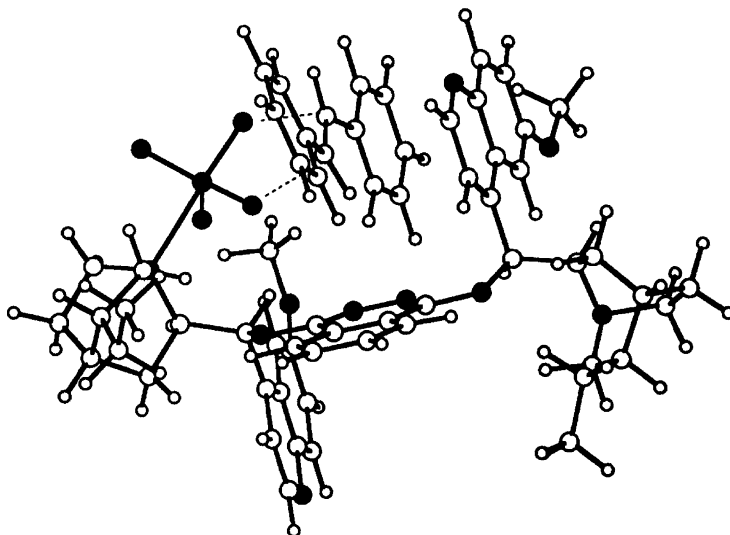


Fig. 2.24. Preferred orientation of stilbene with the (DHQD)2PHAL catalyst. Reproduced from *J. Am. Chem. Soc.*, **121**, 10186 (1999), by permission of the American Chemical Society.

to predict the observed enantioselectivity for several styrene derivatives with the PHAL linker. Figure 2.24 shows the optimum TS for the reaction with stilbene. A noteworthy feature of this model is that it uses *both* the binding modes identified for styrene.

Visual models, additional information and exercises on Enantioselective Dihydroxylation can be found in the Digital Resource available at: Springer.com/carey-sundberg.

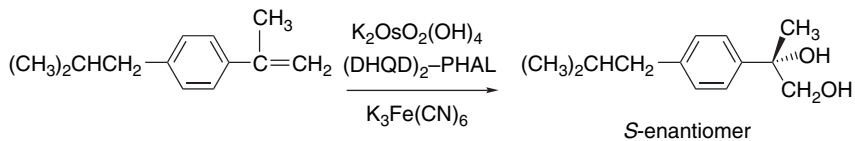
The cases we have considered involve aryl rings as the governing structural feature for enantioselectivity. The AD systems also show excellent enantioselectivity toward functionalized alkenes, especially allylic and homoallylic systems with oxygen substituents.¹⁷⁶ In these systems, another important structural variable comes into play, that is, the conformation of the allylic substituent and its possible interaction with the reaction site.¹⁷⁷

The asymmetric dihydroxylation has been applied in many synthetic sequences and is discussed further in Part B, Chapter 12. For example the dihydroxylation was the starting point for enantioselective synthesis of *S*-ibuprofen and a similar route was used to prepare *S*-naproxen, which contains a methoxynaphthalene ring.¹⁷⁸ Ibuprofen and naproxen are examples of the NSAID class of analgesic and anti-inflammatory agents.

¹⁷⁶. J. K. Cha and N. S. Kim, *Chem. Rev.*, **95**, 1761 (1995); For additional recent example see: A. Bayer and J. S. Svendsen, *Eur. J. Org. Chem.*, 1769 (2001); L. F. Tietze and J. Gorlitzer, *Synthesis*, 877 (1997).

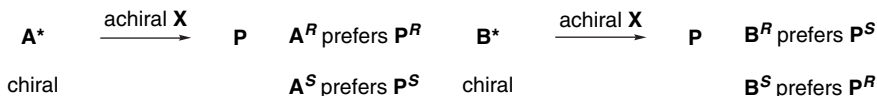
¹⁷⁷. E. Vedejs, W. H. Dent, III, D. M. Gapinski, and C. K. McClure, *J. Am. Chem. Soc.*, **109**, 5437 (1987).

¹⁷⁸. H. Ishibashi, M. Maeki, J. Yagi, M. Ohba, and T. Kanai, *Tetrahedron*, **55**, 6075 (1999).



2.6. Double Stereodifferentiation: Reinforcing and Competing Stereoselectivity

Up to this point, we have considered cases in which there is a single major influence on the stereo- or enantioselectivity of a reaction. We saw examples of reactant control of facial selectivity, such as 1,2- and 1,3-asymmetric induction in carbonyl addition reactions. In the preceding section, we considered several examples in which the chirality of the catalyst controls the stereochemistry of achiral reagents. Now let us consider cases where there may be two or more independent influences on stereoselectivity, known as *double stereodifferentiation*.¹⁷⁹ For example, if a reaction were to occur between two carbonyl compounds, each having an α -stereocenter, one carbonyl compound would have an inherent preference for *R* or *S* product. The other would have also have an inherent preference. These preferences would be expressed even toward achiral reagents.



If A^* and B^* were then to react with one another to create a product with a new chiral center, there would be a two (enantiomeric) matched pairs and two (enantiomeric) mismatched pairs.



In the matched cases the preference of one compound is reinforced by the other. In the mismatched case, they are competing. The concept of matched and mismatched TSs

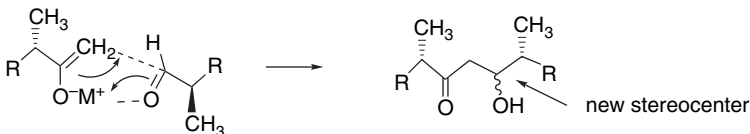
¹⁷⁹ C. H. Heathcock and C. T. White, *J. Am. Chem. Soc.*, **101**, 7076 (1979); S. Masamune, W. Choy, J. S. Petersen, and L. R. Sita, *Angew. Chem. Int. Ed. Engl.*, **24**, 1 (1985).

can be expressed in terms of the free-energy differences resulting from the individual preferences $\Delta\Delta G^*_1$ and $\Delta\Delta G^*_2$ plus any incremental change resulting from the combination ΔG^*_{12} .

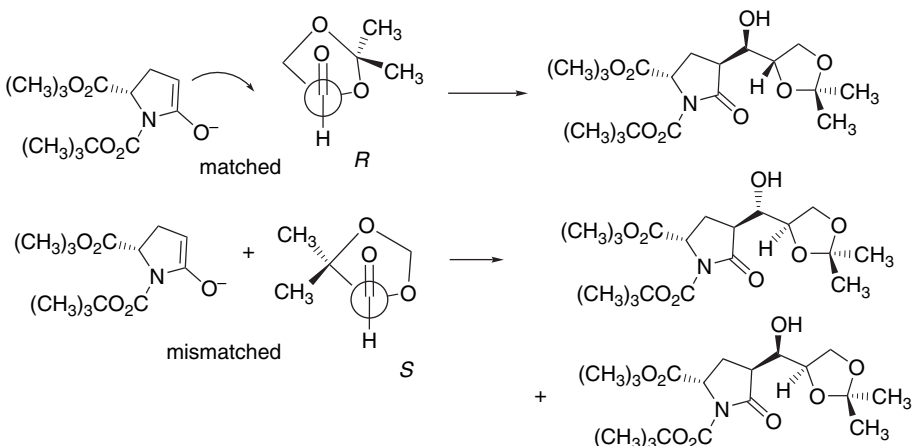
$$\Delta G^*_{\text{matched}} = \Delta\Delta G^*_1 + \Delta\Delta G^*_2 + \Delta G^*_{12}$$

$$\Delta G^*_{\text{mismatched}} = \Delta\Delta G^*_1 - \Delta\Delta G^*_2 + \Delta G^*_{12}$$

An example of such a situation is an aldol addition reaction in which one carbonyl compound acts as the nucleophile and the other as the electrophile.

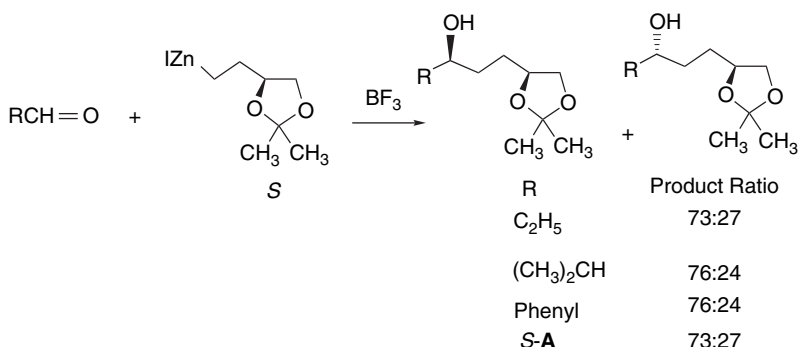


In fact, this case has been extensively studied and we consider it in more detail in Part B, Chapter 2. An example is the condensation of the enolate of a derivative of pyroglutamic acid and a protected form of glyceraldehyde. In the case of the (*R*)-aldehyde a single enantiomer is formed, whereas with the (*S*)-aldehyde a 1:1 mixture of two diastereomers is formed, along with a small amount of a third diastereomer.¹⁸⁰ The facial preference of the enolate is determined by the steric effect of the *t*-butoxycarbonyl group, whereas in the aldehyde the Felkin-Ahn TS prefers an approach *anti* to the α -oxygen.

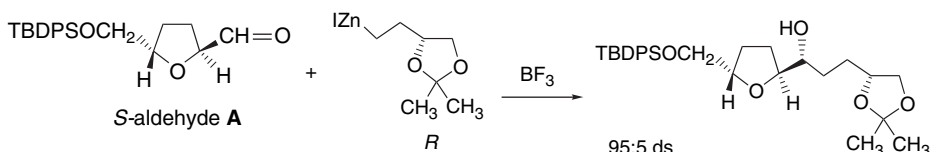


Another example involves addition of an organozinc reagent to a tetrahydrofuran aldehyde. With achiral aldehydes, only a small preference for formation of one enantiomer is seen.

¹⁸⁰ P. B. Hitchcock, B. A. Starkmann, and D. W. Young, *Tetrahedron Lett.*, **42**, 2381 (2001).

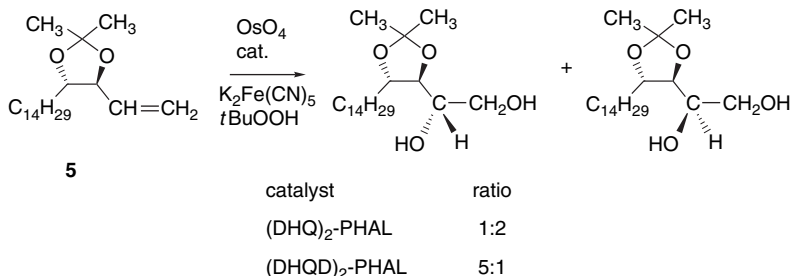


When a chiral aldehyde is used, the matched combination gives a 95:5 stereoselectivity.¹⁸¹



In this case, it is the stereocenter in the aldehyde that has the dominant influence on the diastereoselectivity.

In the analysis of multiple stereochemical influences, it is useful to classify the stereoselectivity as *substrate (reactant) controlled* or *reagent controlled*. For example, in the dihydroxylation of the chiral alkene **5**, the product is determined primarily by the choice of hydroxylation catalyst, although there is some improvement in the diastereoselectivity with one pair.¹⁸² This is a case of *reagent-controlled* stereoselection.

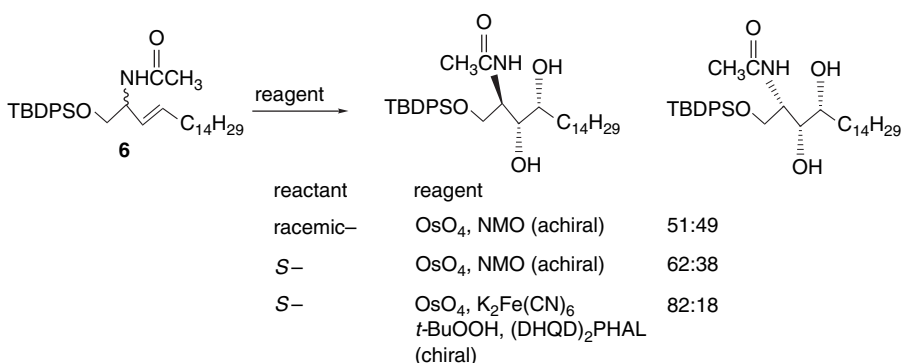


Similarly with the internal alkene **6**, the use of racemic reactant and achiral catalyst gives racemic product. Use of enantiopure *reactant* causes a modest degree of diastereoselectivity to arise from the stereocenter in the reactant. However, when a chiral catalyst is used this is reinforced by the *reagent-control*.¹⁸³

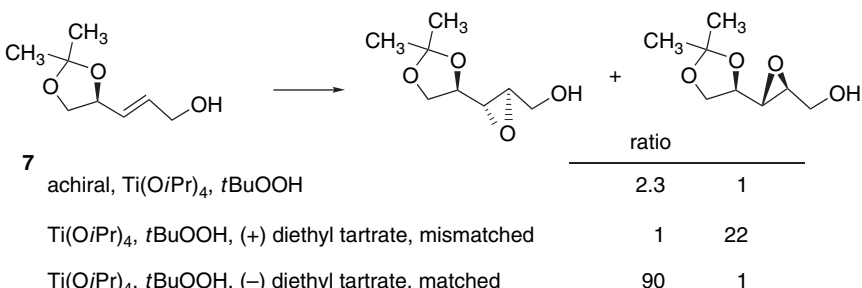
¹⁸¹. U. Koert, H. Wagner, and U. Pindun, *Chem. Ber.*, **127**, 1447 (1994).

¹⁸². R. A. Fernandes and P. Kumar, *Tetrahedron Lett.*, **41**, 10309 (2001).

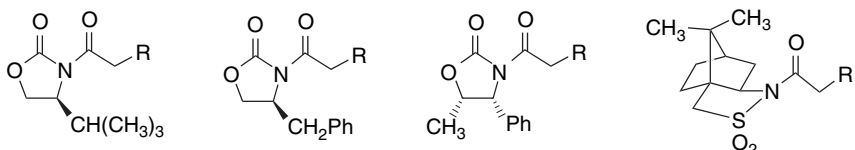
¹⁸³. C. Martin, W. Prunck, M. Bortolussi, and R. Bloch, *Tetrahedron: Asymmetry*, **11**, 1585 (2000).



Another example of reagent control can be found in the Sharpless epoxidation of **7**. With achiral reagents in the absence of a tartrate ligand, there is weak stereoselection. The tartrate-based catalysts control the enantioselectivity, although there is a noticeable difference between the matched and mismatched pairs.



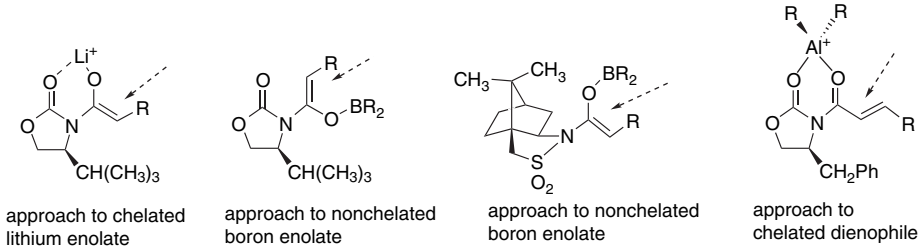
An important strategy for achieving *substrate control* is the use of *chiral auxiliaries*, which are structures incorporated into reactants for the purpose of influencing the stereochemistry. Two of the most widely used systems are oxazolidinones¹⁸⁴ derived from amino acids and sultams¹⁸⁵ derived from camphorsulfonic acid. These groups are most often used as carboxylic acid amides. They can control facial stereoselectivity in reactions such as enolate alkylation, aldol addition, and Diels-Alder cycloadditions, among others. The substituents on the chiral auxiliary determine the preferred direction of approach.



¹⁸⁴ D. J. Ager, I. Prakash and D. R. Schaad, *Chem. Rev.*, **96**, 835 (1996).

¹⁸⁵ W. Oppolzer, J. Blagg, I. Rodriguez, and E. Walther, *J. Am. Chem. Soc.*, **112**, 2767 (1990).

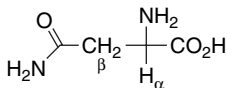
Depending upon the particular system, there may or may not be chelation between a metal cation or Lewis acid and the auxiliary. A change from a chelated to a nonchelated structure can lead to a change in the direction of approach. The configuration at the α -carbon can be controlled in this way. We will see many examples of the implementation of this strategy in subsequent chapters.



Topic 2.1. Analysis and Separation of Enantiomeric Mixtures

2.1.1. Chiral Shift Reagents and Chiral Solvating Agents

There are several techniques for determination of the enantiomeric purity of a chiral compound. As discussed in Section 2.1.3, the measured rotation can provide this information if the specific rotation $[\alpha]$ is known. However, polarimetry is not very sensitive, especially if $[\alpha]$ is relatively low. Several other methods for determining enantiomeric purity have been developed. One of the most frequently used in organic chemistry involves NMR spectroscopy with *chiral shift reagents*, which are complexes of a lanthanide metal and a chiral ligand. The reagents also have labile ligand positions that can accommodate the substance being analyzed. The lanthanides have strong affinity for oxygen and nitrogen functional groups that act as Lewis bases. The lanthanides also have the property of inducing large chemical shifts without excessive broadening of the lines.¹⁸⁶ Shift reagents can be used with both ^1H and ^{13}C NMR spectra. For small organic molecules the most frequently used shift reagents are $\text{Eu}[\text{tfc}]_3$ and $\text{Eu}[\text{nfc}]_3$ (see Scheme 2.11).¹⁸⁷ The scheme also shows some chiral shift reagents that have proven successful for analysis of amino acids and oligopeptides. Figure 2.25 shows a comparison of the NMR spectrum of asparagine with and without the chiral shift reagent.

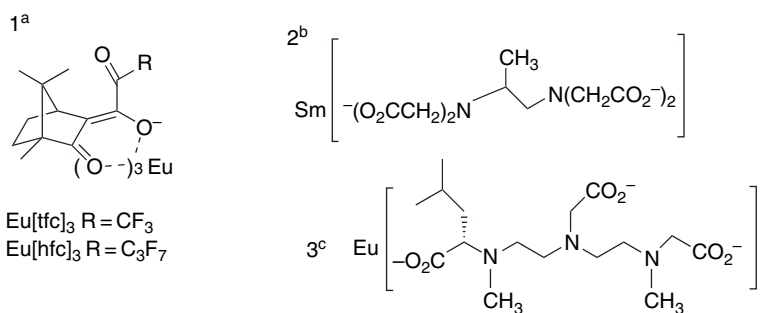


There are also several reagents that can be used to derivatize alcohols, amines, or carboxylic acids to give diastereomeric compounds. The diastereomers then give distinct NMR spectra that can be used to determine the enantiomeric ratio. Typically these compounds have at least an aryl substituent, which leads to strong shifts of signals owing to the anisotropic shielding of aromatic rings. Examples of such compounds are given in Scheme 2.12.

¹⁸⁶ D. Parker, *Chem. Rev.*, **91**, 1441 (1991); R. Rothchild, *Enantiomer*, **5**, 457 (2000).

¹⁸⁷ H. L. Goering, J. N. Eikenberry, G. S. Koermer, and C. J. Lattimer, *J. Am. Chem. Soc.*, **96**, 1493 (1974).

Scheme 2.11. Chiral Shift Reagents



- a. H. L. Goering, J. Eikenberry, G. Koerner, and C. J. Lattimer, *J. Am. Chem. Soc.*, **96**, 1493 (1974).
 b. A. Inamoto, K. Ogasawara, K. Omata, K. Kabuto, and Y. Sasaki, *Org. Lett.*, **2**, 3543 (2000).
 c. M. Watanabe, T. Hasegawa, H. Miyake, and Y. Kojima, *Chem. Lett.*, 4 (2001).

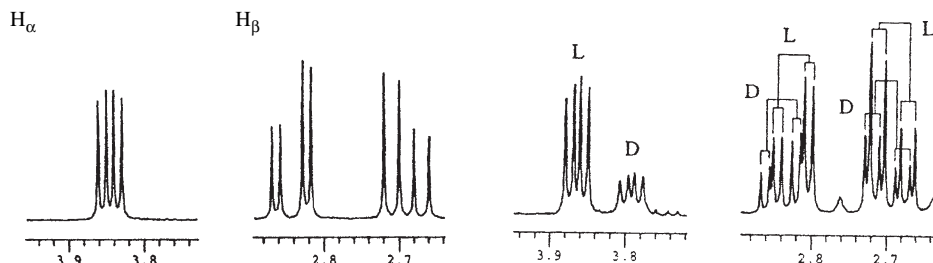
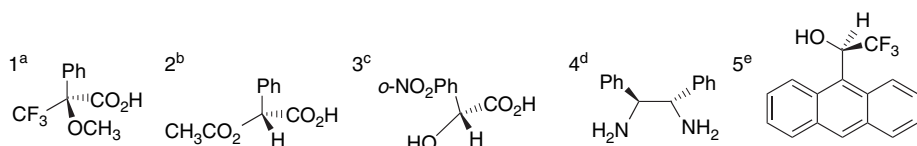


Fig. 2.25. NMR spectrum of 1:2 D:L asparagine mixture with NMR chiral shift reagent: (a) without shift reagent; (b) with shift reagent. Reproduced from *Org. Lett.*, **2**, 3543 (2000), by permission of the American Chemical Society.

Scheme 2.12. Chiral Derivatizing and Solvating Agents



- a. J. A. Dale, D. L. Dull, and H. S. Mosher, *J. Org. Chem.*, **34**, 2543 (1969); J. A. Dale and H. S. Mosher, *J. Am. Chem. Soc.*, **95**, 512 (1973).
 b. D. Parker, *J. Chem. Soc., Perkin Trans. 2*, 83 (1983).
 c. M. A. Haiza, A. Sanyal, and J. K. Snyder, *Chirality*, **9**, 556 (1997).
 d. R. Fulwood and D. Parker, *Tetrahedron: Asymmetry*, **3**, 25 (1992); R. Fulwood and D. Parker, *J. Chem. Soc., Perkin Trans. 2*, 57 (1994).
 e. W. H. Pirkle and S. D. Beare, *J. Am. Chem. Soc.*, **91**, 5150 (1969); W. H. Pirkle and D. J. Hoover, *Top. Stereochem.*, **13**, 263 (1982).

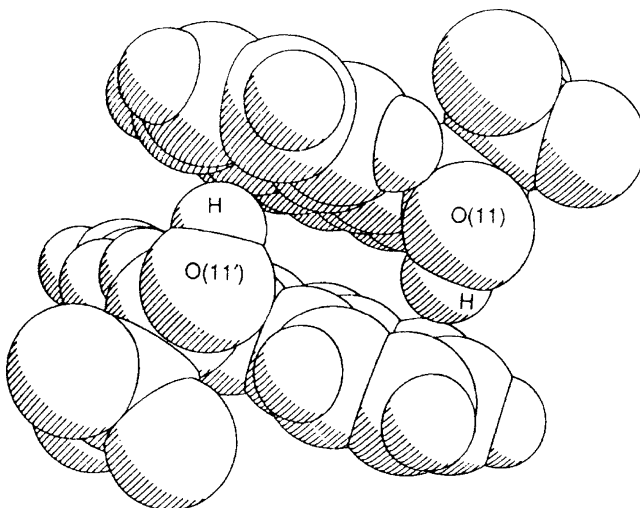
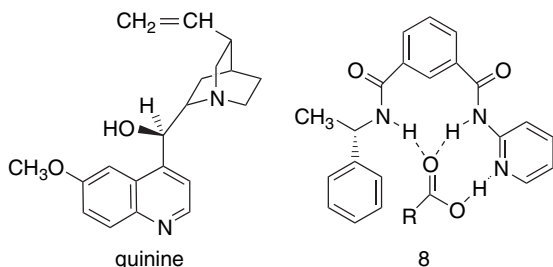


Fig. 2.26. Space-filling model of crystallographic structure of *S*-enantiomer 2,2,2-trifluoro-1-(9-anthryl)ethanol showing hydrogen bonding to the A-ring of anthracene. Reproduced from *J. Chem. Soc., Chem. Commun.*, 765 (1991), by permission of the Royal Society of Chemistry.

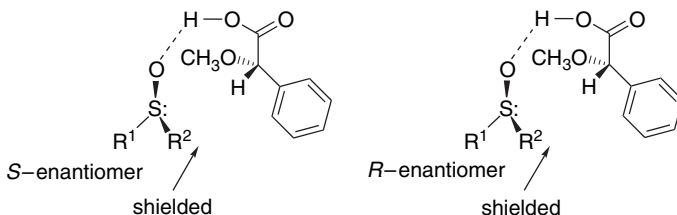
Chemical shifts sufficient for analysis can sometimes be achieved without the need for covalent bonding. If solvation is strong enough, the chiral additive induces sufficiently different chemical shifts in the two enantiomeric complexes to permit analysis. One such compound is called the *Pirkle alcohol* (Entry 5 in Scheme 2.12).¹⁸⁸ The structurally important features of this compound are the trifluoroethanol group, which provides a strong hydrogen bond acceptor, and the anthracene ring, which generates anisotropic shielding. In some cases, there may also be π - π stacking interactions. The structure of the compound has been determined in both the crystalline state and solution. Figure 2.26 shows an intermolecular hydrogen bond between the hydroxy group and the anthracene ring for the *S*-enantiomer.¹⁸⁹

Various amines and amides that can serve as hydrogen bond donors are used as chiral solvating agents for carboxylic acids and alcohols. One example is 1,2-diphenylethane-1,2-diamine (Entry 4 in Scheme 2.12).¹⁹⁰ The alkaloid quinine also shows enantioselective solvation with certain alcohols.¹⁹¹ It is also possible to design molecules to act as chiral receptors, such as structure **8**, which incorporates a binding environment for the carboxylic acid group and gives good NMR resolution of chiral and prochiral carboxylic acids.¹⁹²

- ¹⁸⁸. W. H. Pirkle and S. D. Beare, *J. Am. Chem. Soc.*, **91**, 5150 (1969); W. H. Pirkle and D. J. Hoover, *Top. Stereochem.*, **13**, 263 (1982).
- ¹⁸⁹. H. S. Rzepa, M. L. Webb, A. M. Z. Slawin, and D. J. Williams, *J. Chem. Soc., Chem. Commun.*, 765 (1991); M. L. Webb and H. S. Rzepa, *Chirality*, **6**, 245 (1994).
- ¹⁹⁰. R. Fulwood and D. Parker, *Tetrahedron: Asymmetry*, **3**, 25 (1992); R. Fulwood and D. Parker, *J. Chem. Soc., Perkin Trans.*, **2**, 57 (1994); S. E. Yoo and S. I. Kim, *Bull. Kor. Chem. Soc.*, **17**, 673 (1996).
- ¹⁹¹. C. Rosini, G. Uccello-Barretta, D. Pini, C. Abete, and P. Salvadori, *J. Org. Chem.*, **53**, 4579 (1988).
- ¹⁹². T. Stork and G. Helmchen, *Rec. Trav. Chim. Pays-Bas*, **114**, 253 (1995).



Sulfoxides form hydrogen-bonded complexes with α -methoxyphenylacetic acid, which results in differential shielding of the two substituents.¹⁹³



T.2.1.2 Separation of Enantiomers

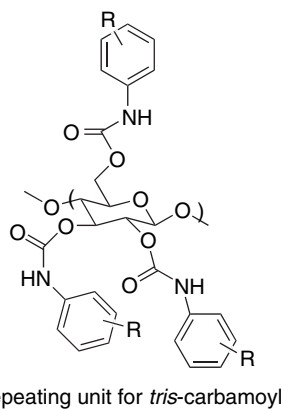
The classical method for separating enantiomers is to form diastereomeric compounds using a stoichiometric amount of a *resolving agent*. This method was described in Section 2.1.8. In this section, we discuss methods of resolution based on physical separations, including chromatography with chiral packing materials and capillary electrophoresis.

T.2.1.2.1. Separation by Chromatography. Chromatography is an important means of separating enantiomers on both an analytical and preparative scale. These separations are based on use of a *chiral stationary phase* (CSP). Chromatographic separations result from differential interactions of the enantiomers with the solid column packing material. The differential adsorption arises from the diastereomeric nature of the interaction between the enantiomers and the CSP. Hydrogen bonding and aromatic π - π interactions often contribute to the binding.

One important type of chiral packing material is derivatized polysaccharides, which provide a chiral lattice, but separation is improved by the addition of structural features that enhance selectivity. One group of compounds includes aryl esters and carbamates, which are called Chiralcel (also spelled Chiracel)¹⁹⁴; two of the most important examples are the 4-methylbenzoyl ester, called Chiralcel OJ, and the 3,5-dimethylphenyl carbamate, called Chiralcel OD. There is a related series of materials derived from amylose rather than cellulose, which have the trade name Chiraldex.

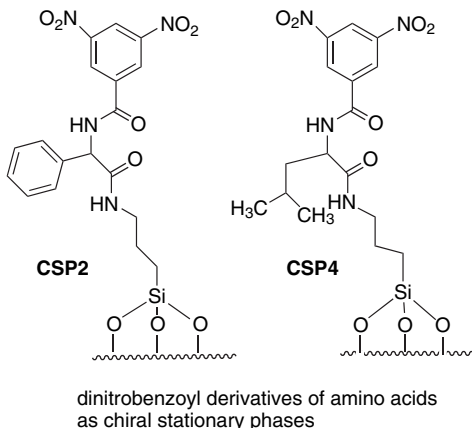
¹⁹³ P. H. Buist, D. Marecak, H. L. Holland, and F. M. Brown, *Tetrahedron: Asymmetry*, **6**, 7 (1995).

¹⁹⁴ Y. Okamoto and E. Yashima, *Angew. Chem.*, **37**, 1021 (1998).



Related materials can be prepared in which the polysaccharides are linked to a silica support by covalently bound tether groups. For example, silica derivatized by 3-aminopropyl groups can be linked to polysaccharides using diisocyanates.¹⁹⁵ These materials seem to adopt organized structural patterns on the surface, and this factor is believed to contribute to their resolving power. The precise structural basis of the chiral recognition and discrimination of derivatized polysaccharides has not been elucidated, but it appears that in addition to polar interactions, π - π stacking is important for aromatic compounds.¹⁹⁶

Other types of CSPs, known as *brush type*, have been constructed synthetically. A chiral structure, usually an amide, is linked to silica by a tether molecule. This approach has the potential for design of the chiral recognition elements. The ability to synthetically manipulate the structures also permits investigation of the role of specific structural elements in chiral selectivity. Several synthetic CSPs were developed by W. H. Pirkle and co-workers at the University of Illinois. An important example is the 3,5-dinitrobenzoyl (3,5-DNB) derivative of *R*-phenylglycine, which is attached to silica by aminopropyl tethers (**CSP 2**). The 3,5-DNB derivatives of several other amino acids (e.g., **CSP 4**) and diamines have also been explored.¹⁹⁷

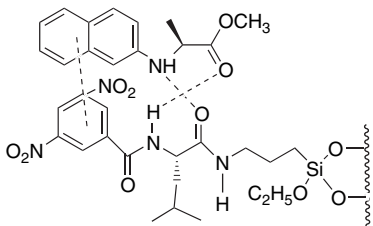


¹⁹⁵ E. Yashima, H. Fukaya, and Y. Okamoto, *J. Chromatogr. A*, **677**, 11 (1994).

¹⁹⁶ C. Yamamoto, E. Yashima, and Y. Okamoto, *Bull. Chem. Soc. Jpn.*, **72**, 1815 (1999).

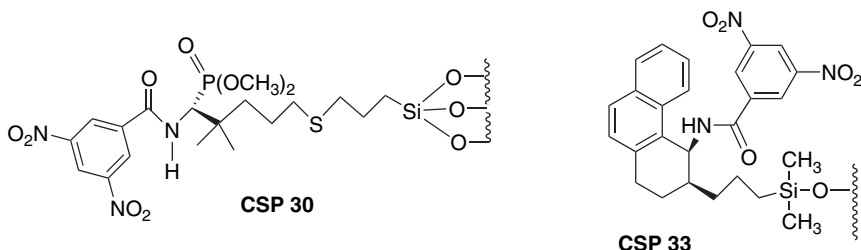
¹⁹⁷ C. J. Welch, *J. Chromatogr. A*, **666**, 3 (1994); C. J. Welch, *Adv. Chromatogr.*, **35**, 171 (1995).

These materials generally show good resolving power toward compounds that have aromatic rings and polar groups. A combination of π - π interactions and hydrogen bonding is believed to be the basis of chiral recognition.¹⁹⁸ The relative electronic character of the aromatic rings is important. Complementary donor-acceptor capacity enhances selectivity.¹⁹⁹



suggested recognition mechanism for
resolution of *N*-(2-naphthyl)amino acids
on dinitrobenzoylamino acid CSP

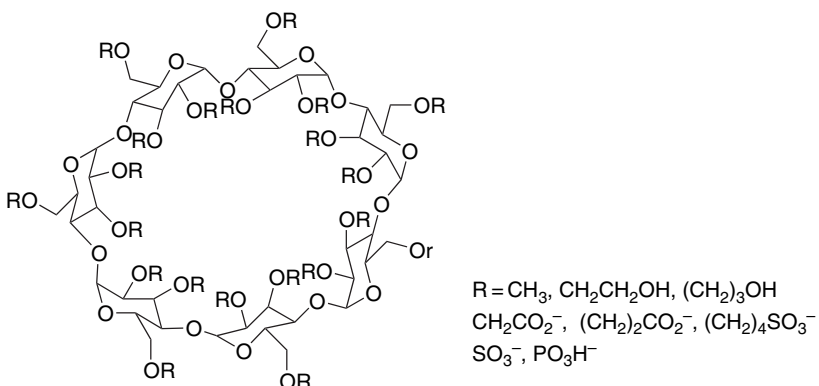
Several variations of these CSPs have been developed, such as the phosphonate ester **CSP 30** and the tetrahydrophenanthryl amide **CSP 33**. These compounds are used in pharmaceutical studies. The former CSP is a good resolving agent for the β -adrenergic blocker class of compounds, such as propanolol,²⁰⁰ whereas the latter is a good CSP for separation of NSAIDs, such as naproxen and ibuprofen.²⁰¹



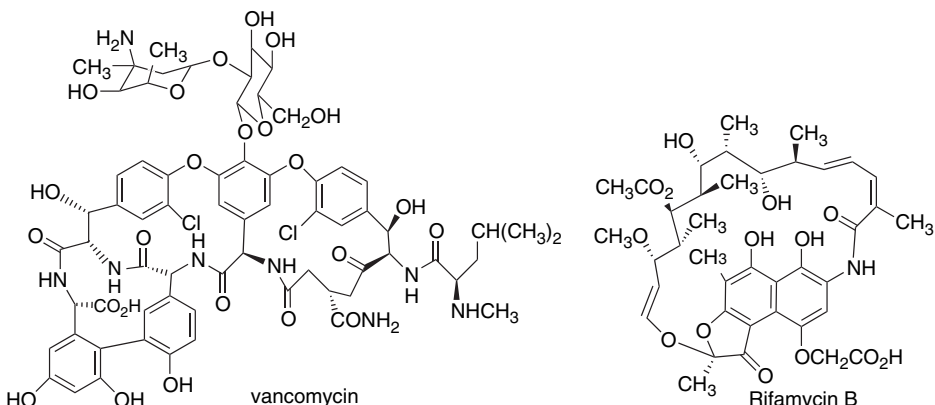
T.2.1.2.2. Resolution by Capillary Electrophoresis. Another methodology that has been adapted to analysis of enantiomers is *capillary electrophoresis*.²⁰² The principle of electrophoretic separation is differential migration of a charged molecule in a

- ^{198.} W. H. Pirkle and T. C. Pochapsky, *J. Am. Chem. Soc.*, **108**, 5627 (1986); W. H. Pirkle and T. C. Pochapsky, *J. Am. Chem. Soc.*, **109**, 5975 (1987); W. H. Pirkle, J. A. Burke, III, and S. R. Wilson, *J. Am. Chem. Soc.*, **111**, 9222 (1989); M. H. Hyun, J.-J. Ryoo, and W. H. Pirkle, *J. Chromatogr. A*, **886**, 47 (2000).
- ^{199.} W. H. Pirkle, T. C. Pochapsky, G. S. Mahler, D. E. Corey, D. S. Reno, and D. M. Alessi, *J. Org. Chem.*, **51**, 4991 (1986).
- ^{200.} W. H. Pirkle and J. A. Burke, *Chirality*, **1**, 57 (1989).
- ^{201.} W. H. Pirkle, C. J. Welch, and B. Lamm, *J. Org. Chem.*, **57**, 3854 (1992).
- ^{202.} A. Rizzi, *Electrophoresis*, **22**, 3079 (2001); G. Gubitz and M. G. Schmid, *J. Chromatogr. A*, **792**, 179 (1997).

polymer matrix under the influence of an electric field. Gel electrophoresis, a very important bioanalytical technique, is done in a polyacrylamide gel and depends on molecular size and charge differences to achieve differential migration. This method is primarily applied to macromolecules, such as polypeptides and oligonucleotides. Capillary electrophoresis (CE) has been developed as a technique for analysis of small chiral molecules, especially drugs. The most widely applied method of analysis is *capillary zone electrophoresis*, in which a *chiral selector* is added to the electrolyte buffer. The difference in binding between the chiral selector and the two enantiomers being analyzed then determines the rate of migration. Among the most commonly used chiral selectors are cyclodextrins, which are cyclic oligosaccharides. The cyclodextrins can be modified to incorporate polar, anionic, or cationic groups.



Macrocyclic antibiotics such as vancomycin and rifamycin B are also used as chiral selectors.



Another approach to chiral electrophoresis involves covalent attachment of the chiral selector to either the capillary wall or the packing material.²⁰³ For open columns, where the packing material is attached to the capillary wall, a completely methylated β -cyclodextrin is linked to the surface through a polysiloxane (Chirasil-Dex 1). The packed columns use silica bound to the methylated cyclodextrin (Chirasil-Dex 2).

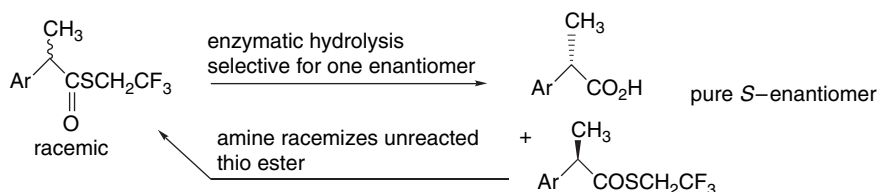
²⁰³. V. Schurig and D. Wistuba, *Electrophoresis*, **20**, 2313 (1999).

The strength of CE as an analytical tool is the very high degree of enantioselection that can be achieved, along with high speed and sensitivity. It is more difficult to use CE on a preparative scale, although successful separation has been reported on the milligram scale.²⁰⁴

We have seen that in each of these means of enantiomeric separation, chiral recognition depends upon a combination of intermolecular forces, including electrostatic attractions, hydrogen bonding, and π - π stacking. These differential interactions then lead to distinctions between the properties of the two enantiomers, such as chemical shifts in NMR methods or relative mobility in chiral chromatography and electrophoresis. There is much current interest in both the analysis of these interactions and manipulation of structure to increase selectivity.

Topic 2.2. Enzymatic Resolution and Desymmetrization

Enzymatic resolution is based on the ability of enzymes (catalytic proteins) to distinguish between *R*- and *S*-enantiomers or between enantiotopic pro-*R* and pro-*S* groups in prochiral compounds.²⁰⁵ The selective conversion of pro-*R* and pro-*S* groups is often called *desymmetrization* or *asymmetrization*.²⁰⁶ Note that in contrast to enzymatic resolution, which can at best provide half the racemic product as resolved material, prochiral compounds can be completely converted to a single enantiomer, provided that the selectivity is high enough. Complete conversion of a racemic mixture to a single enantiomeric product can sometimes be accomplished by coupling an enzymatic resolution with another reaction (chemical or enzymatic) that racemizes the reactant. This is called *dynamic resolution*,²⁰⁷ and it has been accomplished for several α -arylpropanoic acids via the thioesters, using an amine to catalyze racemization.²⁰⁸ Trifluoroethyl thioesters are advantageous because of their enhanced rate of exchange and racemization.



The criterion for a successful enzymatic resolution is that one enantiomer be a preferred substrate for the enzyme. Generally speaking, the enantioselectivity is quite high, since enzyme-catalyzed reactions typically involve a specific fit of the reactant (substrate) into the catalytically active site. The same necessity for a substrate fit, however, is the primary limitation on enzymatic resolution. The compound to be

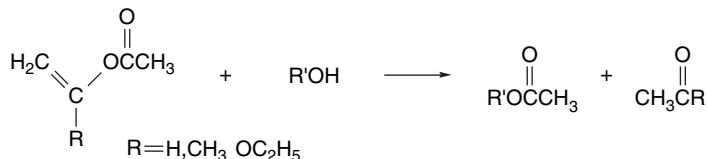
- ²⁰⁴ F. Glukhovskiy and G. Vigh, *Electrophoresis*, **21**, 2010 (2000); A. M. Stalcup, R. M. C. Sutton, J. V. Rodrigo, S. R. Gratz, E. G. Yanes, and P. Painuly, *Analyst*, **125**, 1719 (2000).
- ²⁰⁵ C. J. Sih and S. H. Wu, *Top. Stereochem.*, **19**, 63 (1989).
- ²⁰⁶ E. Schoffers, A. Golebiowski, and C. R. Johnson, *Tetrahedron*, **52**, 3769 (1996).
- ²⁰⁷ S. Caddick and K. Jenkins, *Chem. Soc. Rev.*, **25**, 447 (1996); H. Stecher and K. Faber, *Synthesis*, 1 (1997).
- ²⁰⁸ L. S. Chang, S. W. Tsai, and J. Kuo, *Biotechnol Bioeng.*, **64**, 120 (1999); C. Y. Chen, Y. S. Chang, S. A. Lin H.-I. Wen, Y.-C. Cheng, and S.-W. Tsai, *J. Org. Chem.*, **67**, 3323 (2002); P.-J. Um and D. G. Dueckhammer, *J. Am. Chem. Soc.*, **120**, 5605 (1998)..

resolved must be an acceptable substrate for the enzyme. If not, there will be no reaction with either enantiomer. The types of reactions that are suitable for enzymatic resolutions are somewhat limited. The most versatile enzymes—*esterases* and *lipases*—catalyze formation or hydrolysis of esters. There are also enzymes that catalyze amide formation and hydrolysis, which can be broadly categorized as *acylases* or *amidases*. We also discuss *epoxide hydrolases*, which open epoxide rings. Another important family is the *oxido-reductases*, which interconvert alcohols and carbonyl compound by oxidation and reduction.

T.2.2.1. Lipases and Esterases

The most widely applied enzymes for resolution are lipases and esterases, which can catalyze either the hydrolysis or the formation of esters.²⁰⁹ The natural function of these enzymes is to catalyze hydrolysis of fatty acid esters of glycerol. There are a number of such enzymes that are commercially available. A very important property of these esterases and lipases is that they can accept a fairly wide variety of molecules as substrates. They are also adaptable for use in organic solvents, which further enhances their practical utility.²¹⁰

The esterases and lipases are members of a still larger group of enzymes that catalyze acyl transfer, either in the direction of solvolysis or by acylation of the substrate. Both types of enzymes are called *hydrolases*. In water, hydrolysis occurs, but in the presence of alcohols, transesterification can occur. Reactions in the acylation direction are done in the presence of acyl donors. Esters of enols such as vinyl acetate or isopropenyl acetate are often used as sources of the acyl group. These enol esters are more reactive than alkyl esters, and the enol that is displaced on acyl transfer is converted to acetaldehyde or acetone. To avoid side products arising from these carbonyl compounds, one can use 1-ethoxyvinyl esters, which give ethyl acetate as the by-product.²¹¹



The esterases, lipases, and other enzymes that catalyze acyl transfer reactions share a common mechanism. The active site in these enzymes involves a *catalytic triad* consisting of the imidazole ring from a histidine, the hydroxy group of a serine, and a carboxy group from an aspartic acid.²¹² The three moieties, working together, effect transfer of an acyl group to the serine. In solvolysis, this acyl group is then transferred to the solvent, whereas in acylation it is transferred to the substrate. The mechanism is outlined in Figure 2.27. We discuss the catalytic mechanisms of these triads in more detail in Section 7.5.

- ^{209.} P. Andersch, M. Berger, J. Hermann, K. Laumen, M. Lobell, R. Seemayer, C. Waldinger, and M. P. Schneider, *Meth. Enzymol.*, **286**, 406 (1997).
- ^{210.} A. M. Klibanov, *Acc. Chem. Res.*, **23**, 114 (1990); G. Carrea and S. Riva, *Angew. Chem. Int. Ed. Engl.*, **39**, 2227 (2000).
- ^{211.} Y. Kita, Y. Takebe, K. Murata, T. Naka, and S. Akai, *J. Org. Chem.*, **65**, 83 (2000).
- ^{212.} R. J. Kazlauskas and H. K. Weber, *Curr. Opinion Chem. Biol.*, **2**, 121 (1998).

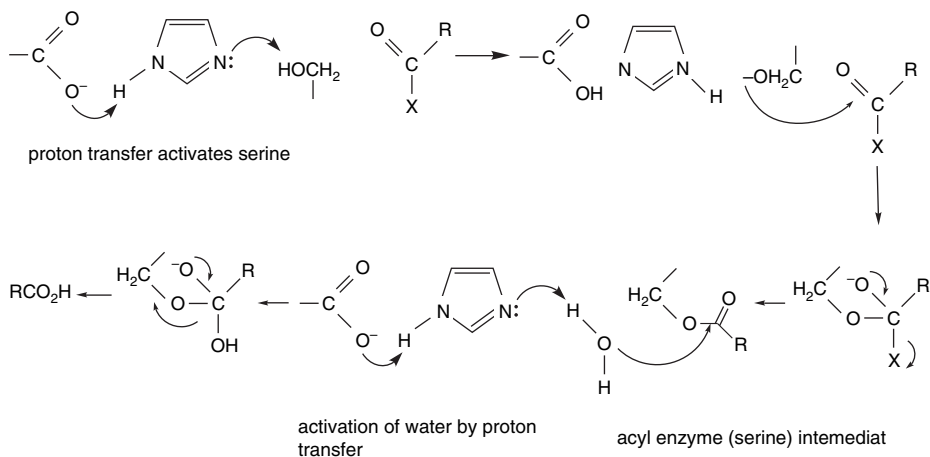


Fig. 2.27. Mechanism for carboxylate-histidine-serine triad catalysis of acyl transfer.

The most commonly used of the hydrolytic enzymes is *pig liver esterase* (PLE). The natural function of this enzyme to hydrolyze esters during digestion and it has fairly broad range of substrate reactivity. It has been used to resolve chiral alcohols and esters by acylation or hydrolysis, respectively. *Meso*-derivatives of succinic and glutaric acid diesters are generally good substrates for PLE and are good examples of substrates for desymmetrization. A predictive model for the stereoselectivity of PLE was developed by analysis of many cases.²¹³ The model pictures two hydrophobic pockets, one larger (H_L) and one smaller (H_S) and two polar pockets, one front (P_F) and one back (P_B). These pockets are specifically located in relation to the catalytic serine, and the fit of the substrate then determines the enantioselectivity. Alkyl and aryl groups fit into either the H_L or H_S sites based on size. The P_F site can accommodate moderately polar groups, such as the ester substituent in diesters, whereas the P_B site accepts more polar groups, including hydroxy and carbonyl groups, and excludes nonpolar groups. This model successfully correlates and predicts the results for a variety of esters and diesters. For example, Figure 2.28 shows the fit of an α -sulfinyl ester into the catalytic site.²¹⁴

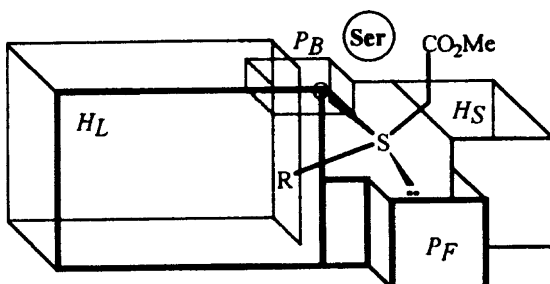


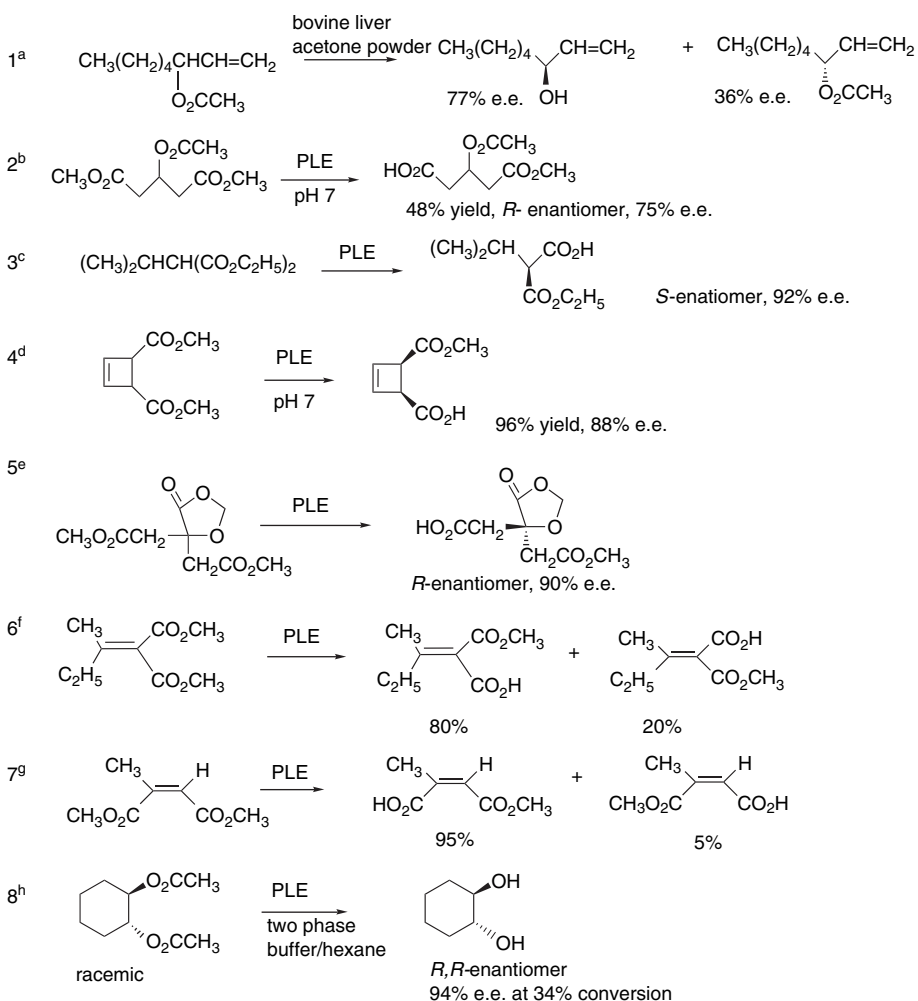
Fig. 2.28. Accommodation of preferred *S*-enantiomer of α -sulfinylacetate esters in the Jones model of a PLE active site. Reproduced from *Tetrahedron: Asymmetry*, **11**, 911 (2000), by permission of Elsevier.

²¹³ E. J. Toone, M. J. Werth, and J. B. Jones, *J. Am. Chem. Soc.*, **112**, 4946 (1990); L. Provencher, H. Wynn, J. B. Jones, and A. Krawczyk, *Tetrahedron: Asymmetry*, **4**, 2025 (1993); L. Provencher and J. B. Jones, *J. Org. Chem.*, **59**, 2729 (1994).

²¹⁴ P. Kielbasinski, *Tetrahedron Asymmetry* **11**, 911 (2000).

Scheme 2.13 shows a few examples of resolutions and desymmetrizations using esterases. Entry 1 shows the partial resolution of a chiral ester using a crude enzyme source. The enantioselectivity is only moderate. Entries 2 to 5 are examples of desymmetrization, in which prochiral ester groups are selectively hydrolyzed. Entries 6 and 7 are examples of selective hydrolysis of unsaturated esters that lead to isomeric monoesters. These cases are examples of diastereoselectivity. In Entry 8, the *R,R*-enantiomer of a racemic diester is selectively hydrolyzed. In all these cases, the

Scheme 2.13. Representative Resolutions and Desymmetrizations Using Esterases



- a. D. Basavaiah and S. B. Raju, *Tetrahedron*, **50**, 4137 (1994).
- b. B. Loubinoux, J.-L. Sinnes, A. C. O'Sullivan, and T. Winkler, *Tetrahedron*, **51**, 3549 (1995).
- c. B. Klotz-Berendes, W. Kleemis, U. Jegelka, H. J. Schaefer, and S. Kotila, *Tetrahedron: Asymmetry*, **8**, 1821 (1997).
- d. I. Harvey and D. H. G. Crout, *Tetrahedron: Asymmetry*, **4**, 807 (1993).
- e. R. Chenevert, B. T. Ngatcha, Y. S. Rose, and D. Goupil, *Tetrahedron: Asymmetry*, **9**, 4325 (1998).
- f. T. Schirmeister and H. H. Otto, *J. Org. Chem.*, **58**, 4819 (1993).
- g. R. Schmid, V. Partali, T. Anthonsen, H. W. Anthonsen, and L. Kvittingen, *Tetrahedron Lett.*, **42**, 8543 (2001).
- h. G. Caron and R. J. Kazlauskas, *J. Org. Chem.*, **56**, 7251 (1991).

Lipases are another important group of hydrolases. The most commonly used example is porcine pancreatic lipase (PPL). Lipases tend to function best at or above the solubility limit of the hydrophobic substrate. In the presence of water, the substrate forms an insoluble phase (micelles); the concentration at which this occurs is called the *critical micellar concentration*. The enzyme is activated by a conformational change that occurs in the presence of the micelles and results in the opening of the active site. Lipases work best in solvents that can accommodate this activation process.²¹⁵ PPL is often used as a relatively crude preparation called “pancreatin” or “steapsin.” The active site in PPL has not been as precisely described as the one for PLE. There are currently two different models, but they sometimes make contradictory predictions.²¹⁶ It has been suggested that the dominant factors in binding are the hydrophobic and polar pockets (sites B and C in Figure 2.29), but that the relative location of the catalytic site is somewhat flexible and can accommodate to the location of the hydrolyzable substituent.²¹⁷

A more refined model of stereoselectivity has been proposed on the basis of the X-ray structure of PPL²¹⁸ and the stereoselectivity toward several aryl-substituted diols. This model proposes an important π - π stacking interaction between the aryl

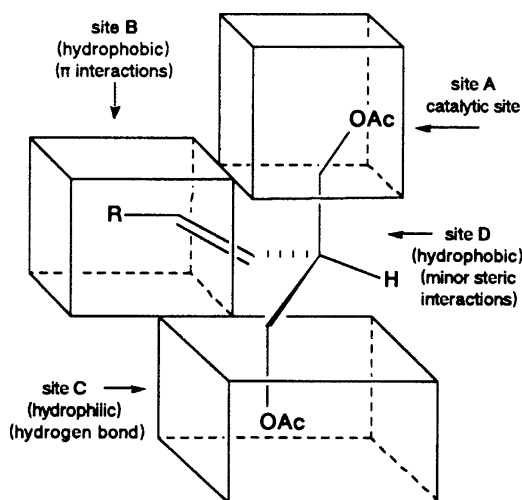


Fig. 2.29. Preferred accommodation of 2-*E*-alkenyl-1,3-propanediol diacetates in an active site model for PPL. Reproduced from *J. Org. Chem.*, **57**, 1540 (1992), by permission of the American Chemistry Society.

- ²¹⁵ B. Rubin, *Nature Struct. Biol.*, **1**, 568 (1994); R. D. Schmid and R. Verger, *Angew. Chem. Int. Ed. Engl.*, **37**, 1609 (1998).
- ²¹⁶ J. Ehrler and D. Seebach, *Liebigs Ann. Chem.*, 379 (1990); P. G. Hultin and J. B. Jones, *Tetrahedron Lett.*, **33**, 1399 (1992); Z. Wimmer, *Tetrahedron*, **48**, 8431 (1992).
- ²¹⁷ A. Basak, G. Bhattacharya, and M. H. Bdour, *Tetrahedron*, **54**, 6529 (1998). A. Basak, K. R. Rudra, H. M. Bdour, and J. Dasgupta, *Biorg. Med. Chem. Lett.*, **11**, 305 (2001); A. Basak, K. R. Rudra, S. C. Ghosh, and G. Bhattacharya, *Ind. J. Chem. B.*, **40**, 974 (2001).
- ²¹⁸ J. Hermoso, D. Pignol, B. Kerfleuc, I. Crenon, C. Chapus, and J. C. Fontecilla-Camps, *J. Biol. Chem.*, **271**, 18007 (1996); J. Hermoso, D. Pignol, S. Penel, M. Roith, C. Chapus, and J. C. Fontecilla-Camps, *EMBO J.*, **16**, 5531 (1997).

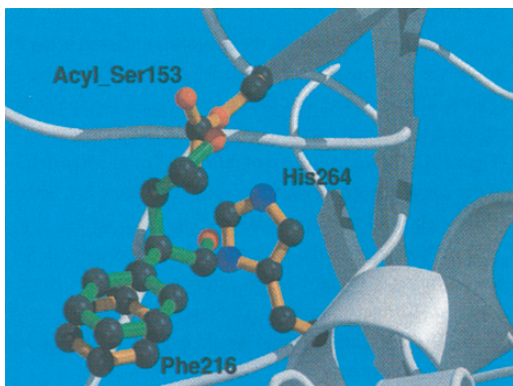
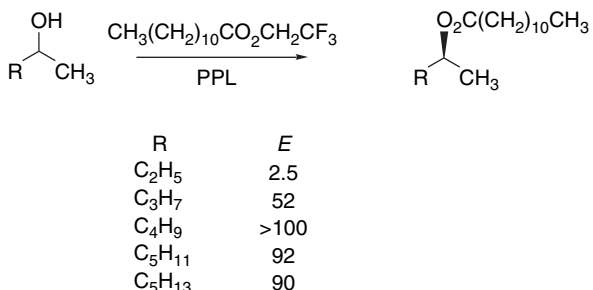


Fig. 2.30. Active site model of PPL showing the binding of 2-phenylpentane-1,4-diol in an active site. Note the $\pi - \pi$ -stacking with Phe-216 and placement of the C(4) hydroxyl near the acyl serine-153 residue. Reproduced from *Tetrahedron*, **55**, 14961 (1999), by permission of Elsevier. (See also color insert.)

group and a phenylalanine residue near the active site.²¹⁹ Based on the detailed protein structure, this model is consistent with the model proposed by Guanti et al.²²⁰ The model (Figure 2.30) suggests a hydrophilic site and a rather selective hydrophobic site. The D site is considered to be quite flexible, whereas the B site is particularly favorable for unsaturated groups.

The enantioselectivity of PPL depends on discrimination in binding of the substrate. In the case of acylation of simple secondary alcohols, there is poor discrimination for 2-butanol, but 2-hexanol exhibits the maximal *E* value, and larger alcohols show good enantioselectivity.²²¹ (The definition of *E* is given on p. 140.)



Two other lipases of microbial origin are also used frequently in organic chemistry. A lipase from *Pseudomonas cepacia* (formerly identified as *Pseudomonas fluorescens*) is often referred to as *lipase PS*. The binding site for this enzyme is narrower than those of the other commonly used lipases, and it often has excellent

²¹⁹ I. Borreguero, J. V. Sinisterra, A. Rumbero, J. A. Hermoso, M. Martinez-Ripoll, and A. R. Alcantara, *Tetrahedron*, **55**, 14961 (1999).

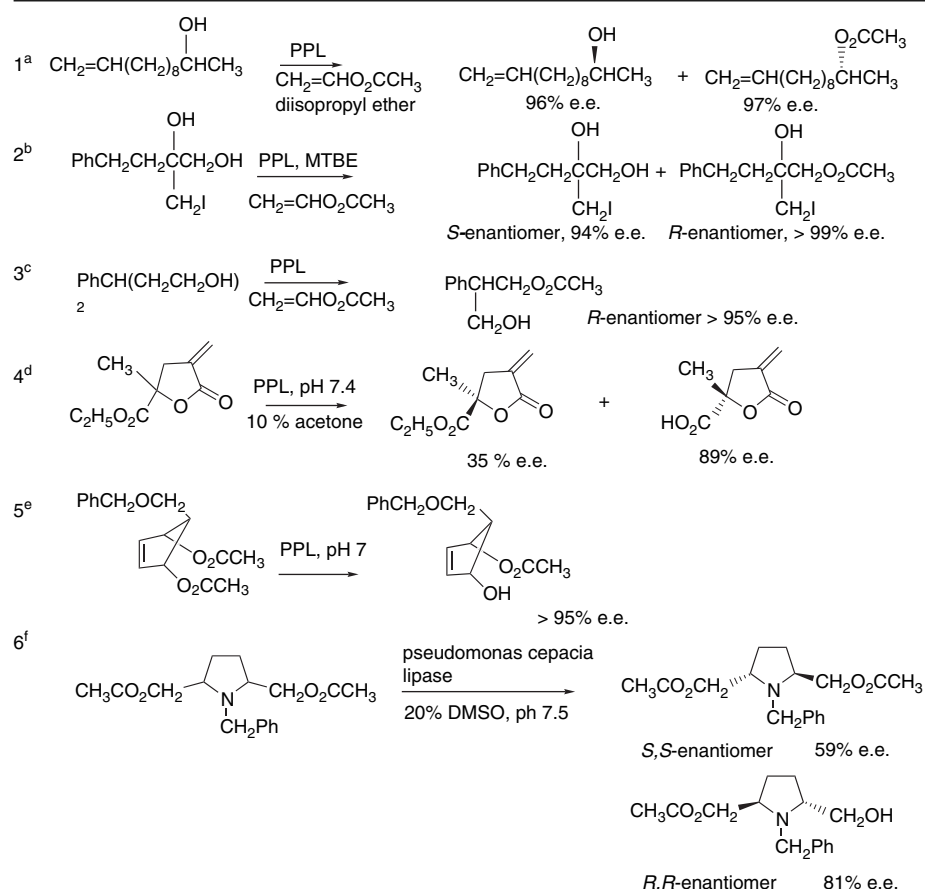
²²⁰ G. Guanti, L. Banfi, and E. Narisano, *J. Org. Chem.*, **57**, 1540 (1992).

²²¹ B. Morgan, A. C. Oehschlager, and T. M. Stokes, *Tetrahedron*, **47**, 1611 (1991).

selectivity. Lipases from *Candida rugosa* (formerly *Candida cylindracea*), *C. antartica*, and *C. lipolytica* are also used frequently.²²² Like the esterases, lipases can act as hydrolysis catalysts toward esters or as acylation catalysts toward alcohols. Unlike PLE, the lipases have a specific type of natural substrate, namely triacyl glycerides. They are somewhat more selective in terms of substrate than PLE. Generally, neither α,α -disubstituted carboxylates nor esters of tertiary alcohols are accepted as substrates. As with PLE, either kinetic resolution or desymmetrization of prochiral reactants can be achieved. The enantioselectivity of lipases depends upon discrimination between the enantiomeric substrates at the active site. A large hydrophobic site acts as the receptor for the largest nonpolar substituent.

Some examples of some lipase-catalyzed reactions are given in Scheme 2.14. The first three examples in Scheme 2.14 are acylations. Entries 1 and 2 are enantioselective

Scheme 2.14. Representative Resolutions Using Various Lipases



a. A. Sharma, S. Sankaranarayanan, and S. Chattopadhyay, *J. Org. Chem.*, **61**, 1814 (1996).

b. S.-T. Chen and J.-M. Fang, *J. Org. Chem.*, **62**, 4349 (1997).

c. A. Rumbero, I. Borreguero, J. V. Sinisterra, and A. R. Alcantara, *Tetrahedron*, **55**, 14947 (1999).

d. G. Pitacco, A. Sessanta, O. Santi, and E. Valentini, *Tetrahedron: Asymmetry*, **11**, 3263 (2000).

e. I. C. Cotterill, P. B. Cox, A. F. Drake, D. M. LeGrand, E. J. Hutchinson, R. Latouche, R. B. Pettman, R. J. Pryce, S. M. Roberts, G. Ryback, V. Sik, and J. O. Williams, *J. Chem. Soc., Perkin Trans. 1*, 3071 (1991).

f. Y. Kawanami, H. Moriya, Y. Goto, K. Tsukao, and M. Hashimoto, *Tetrahedron*, **52**, 565 (1996).

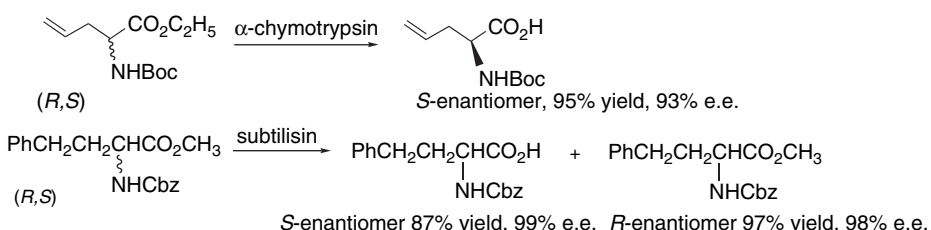
²²² F. Theil, *Chem. Rev.*, **95**, 2203 (1995).

acylations of a chiral secondary alcohol. Entry 3 is a desymmetrization of a 3-phenylpentane-1,5-diol. Entry 4 is a resolution of an ester group attached to a methylene- γ -lactone. Entries 5 and 6 are desymmetrizations of diesters.

T.2.2.2. Proteases and Acylases

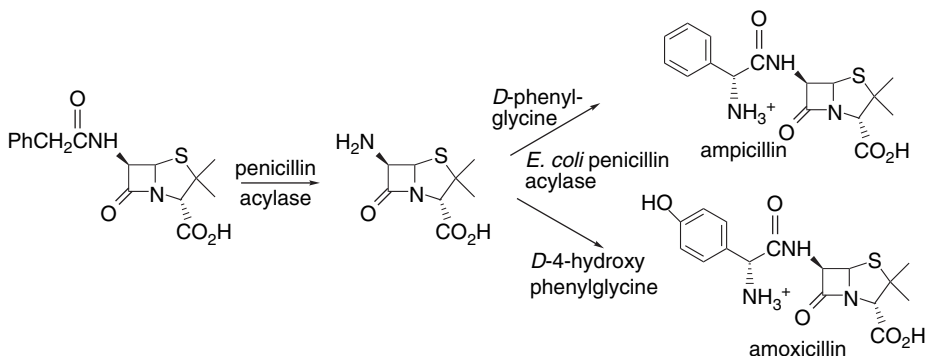
Proteases and *acylases* have the capacity to catalyze hydrolysis and formation of amide bonds. Proteases find extensive application in analytical biochemistry.²²³ The proteases are used to break down large proteins into polypeptides. Various proteases exhibit selectivity for particular sequences in peptides and proteins. Many of the proteases are digestive enzymes and in general they have much more stringent structural requirements for substrates than esterases and lipases. For example, chymotrypsin is selective for hydrolysis at the carboxy group of aromatic amino acids, while trypsin cleaves at the carboxy group of the basic (protonated) amino acids lysine and arginine. The proteases, like the esterases and lipases, function on the basis of a catalytic triad involving a serine, histidine, and aspartic acid.²²⁴ They can catalyze formation and hydrolysis of esters as well as amides.²²⁵

Considerable attention has also been given to enantioselective enzymatic hydrolysis of esters of α -amino acids. This is of particular importance as a means of preparing enantiopure samples of unusual (non-proteinaceous) α -amino acids.²²⁶ The readily available proteases α -chymotrypsin (from bovine pancreas) and subtilisin (from *Bacillus licheniformis*) selectively hydrolyze the L-esters, leaving D-esters unreacted. These enzymatic hydrolysis reactions can be applied to *N*-protected amino acid esters, such as those containing *t*-Boc²²⁷ and Cbz²²⁸ protecting groups.



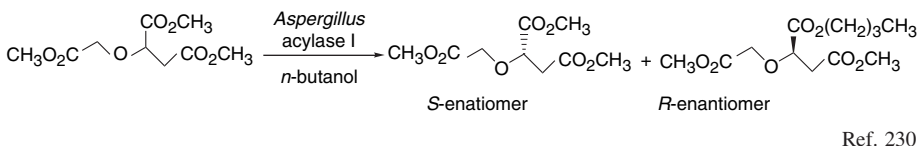
Much of the interest in acylases originated from work with the penicillins. Structurally modified penicillins can be obtained by acylation of 6-aminopenicillanic acid. For example, the semisynthetic penicillins such as amoxicillin and ampicillin are obtained using enzymatic acylation.²²⁹ Acylases are used both to remove the phenyl-acetyl group from the major natural penicillin, penicillin G, and to introduce the modified acyl substituent.

- ²²³ A. J. Barrett, N. D. Rawlings, and J. F. Woessner, eds., *Handbook of Proteolytic Enzymes*, 2nd Edition, Elsevier, 2004.
- ²²⁴ L. Polgar in *Mechanisms of Protease Action*, CRC Press, Boca Raton, FL, Chap. 3, 1989; J. J. Perona and C. S. Craik, *Protein Sci.*, 4 337 (1995).
- ²²⁵ K. Watanabe and S. Uejii, *J. Chem. Soc., Perkin Trans. 1*, 1386 (2001); T. Ke, C. R. Westcott, and A. M. Klibanov, *J. Am. Chem. Soc.*, **118**, 3366 (1996).
- ²²⁶ T. Miyazawa, *Amino Acids*, **16**, 191 (1999).
- ²²⁷ B. Schricker, K. Thirring, and H. Berner, *Biorg. Med. Chem. Lett.*, **2**, 387 (1992).
- ²²⁸ S.-T. Chen, S.-Y. Chen, S.-C. Hsiao, and K.-T. Wang, *Biotechnol. Lett.*, **13**, 773 (1991).
- ²²⁹ A. Bruggink, E. C. Roos, and E. de Vroom, *Org. Process Res. Dev.*, **2**, 128 (1998).

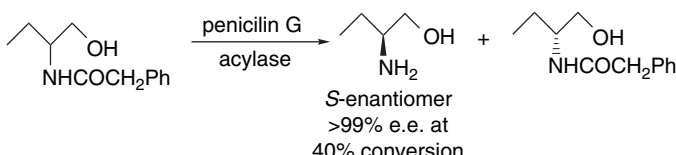


Similar reactions are used in preparation of the related cephalosporin antibiotics.

A related group of acylases catalyzes amide formation and hydrolysis. *Aspergillus* is one source of such enzymes. One class of substrates is made up of di- and triesters with α -heteroatom substituents. Such substrates show selectivity for the carboxy group that is α to the heteroatom, which is the position analogous to the amide bond in peptides.

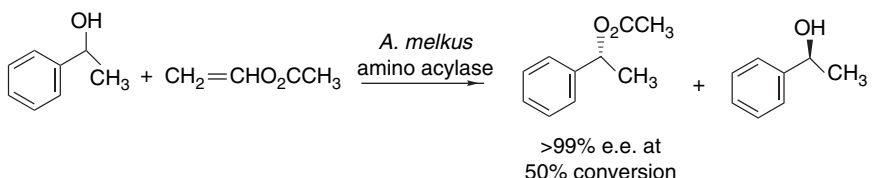


Ref. 230



Ref. 231

Acylases can be used to catalyze esterification of alcohols. These reactions are usually carried out by using vinyl esters. The selectivity (*E*) values for such reactions can be quite high.



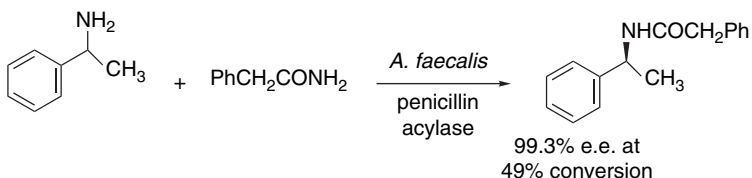
Ref. 232

²³⁰ A. Liljeblad, R. Aksela, and L. T. Kanerva, *Tetrahedron: Asymmetry*, **12**, 2059 (2001).

²³¹ N. W. Fadnavis, M. Sharfuddin, and S. K. Vadivel, *Tetrahedron: Asymmetry*, **10**, 4495 (1999).

²³² M. Bakker, A. S. Spruijt, F. van Rantwijk, and R. A. Sheldon, *Tetrahedron: Asymmetry*, **11**, 1801 (2000).

Enantioselective acylation of amines is generally more challenging and less explored, although good results have been reported in some cases. A number of 1-phenylethylamines and 4-phenylbutane-2-amine were resolved using an acylase from *Alcaligenes faecalis*.



Ref. 233

T.2.2.3. Epoxide Hydrolases

Epoxide hydrolases (EH) catalyze the hydrolytic ring opening of epoxides to diols. The natural function of the epoxide hydrolases seems to be to detoxify epoxides, and they have a fairly broad range of acceptable substrates. The epoxide hydrolases use a catalytic triad active site, reminiscent of the lipases and esterases. In the hydrolases, however, an aspartate carboxylate, rather than a serine hydroxy, functions as the nucleophile to open the epoxide ring. The glycol monoester intermediate is then hydrolyzed, as shown in Figure 2.31. According to this mechanism, and as has been experimentally confirmed, the oxygen that is introduced into the diol originates in the aspartate carboxylate group.²³⁴

There are several forms of EHs that have been used to effect enantioselective opening of epoxides. One commonly used form is isolated as a crude microsomal preparation from rodent livers. EH can also be isolated from bacteria, fungi, and yeasts.²³⁵ The structure of the EH from *Agrobacterium radiobacter* AD1 has been solved by X-ray crystallography.²³⁶ In this enzyme, the catalytic triad involves His-275, Asp-107, and Tyr-152 and/or Tyr-215. The tyrosine functions as a general acid

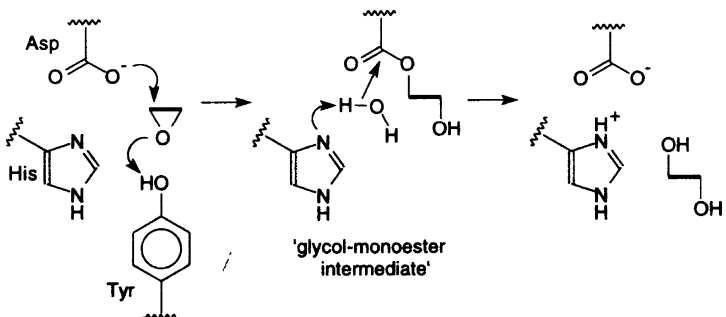


Fig. 2.31. Proposed mechanism of microsomal epoxide hydrolase.

- ²³³ D. T. Guranda, L. M. van Langen, F. van Rantwijk, R. A. Sheldon, and V. K. Svedas, *Tetrahedron: Asymmetry*, **12**, 1645 (2001).
- ²³⁴ G. M. Lacourciere and R. N. Armstrong, *J. Am. Chem. Soc.*, **115**, 10466 (1993); B. Borhan, A. D. Jones, F. Pinot, D. F. Grant, M. J. Kurth, and B. D. Hammock, *J. Biol. Chem.*, **270**, 26923 (1995).
- ²³⁵ C. A. G. M. Weijers and J. A. M. de Bont, *J. Mol. Catal. B, Enzymes*, **6**, 199 (1999).
- ²³⁶ M. Nardini, I. S. Ridder, H. J. Rozeboom, K. H. Kalk, R. Rink, D. B. Janssen, and B. W. Dijkstra, *J. Biol. Chem.*, **274**, 14579 (1999); M. Nardini, R. B. Rink, D. B. Janssen, and B. W. Djikstra, *J. Mol. Catal. B, Enzymatic*, **11**, Spec. Issue, 1035 (2001).

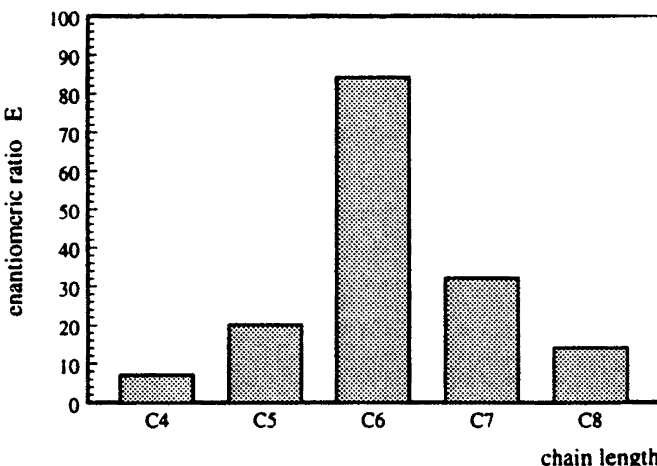


Fig. 2.32. Effect of chain length on enantioselectivity ratio E for unbranched monosubstituted epoxides. Reproduced from *Tetrahedron: Asymmetry*, **9**, 467 (1998), by permission of Elsevier.

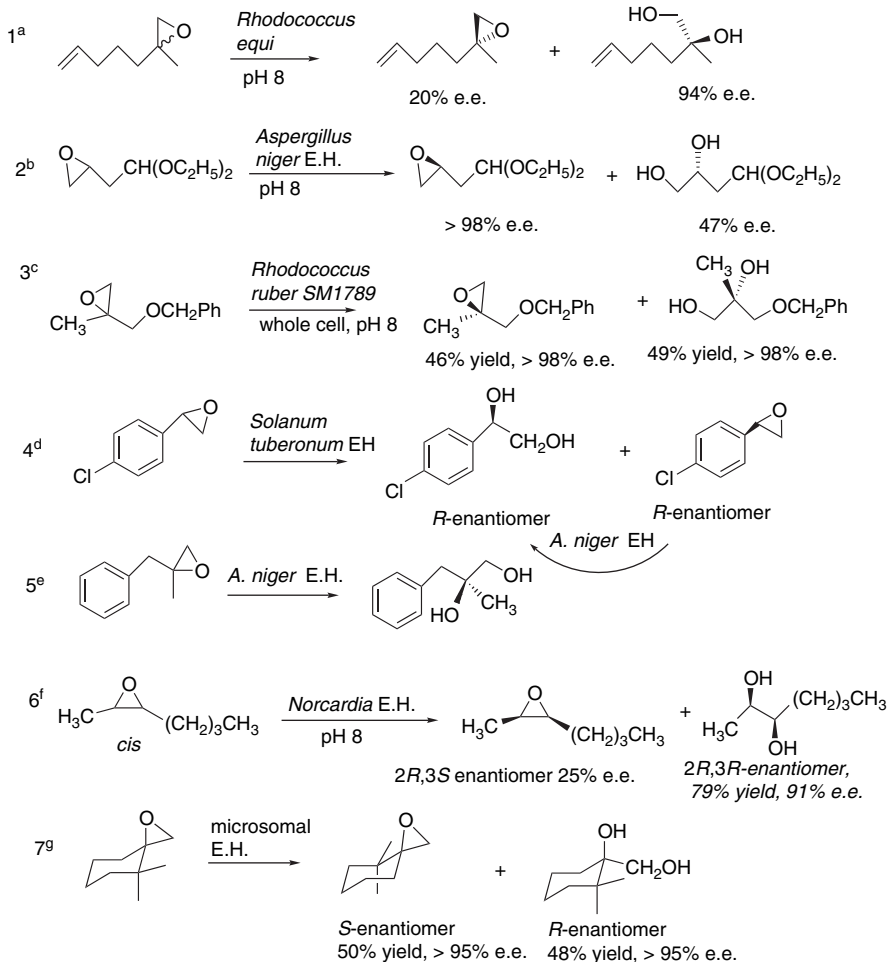
catalyst. A crystal structure has also been determined for the *Aspergillus niger* EH.²³⁷ The essential amino acids in these and other EHs have been identified by site-specific mutagenesis experiments.²³⁸

One of the more extensively investigated EHs is from the fungus *Aspergillus niger*.²³⁹ The best studied of the yeast EH is from *Rhodotorula glutina*,²⁴⁰ which can open a variety of mono-, di-, and even trisubstituted epoxides. The E values for simple monosubstituted epoxides show a sharp maximum in selectivity for the hexyl substituent, as can be seen in Figure 2.32. This indicates that there is a preferential size for binding of the hydrophobic groups.

Scheme 2.15 gives some examples of the use of epoxide hydrolases in organic synthesis. Entries 1 to 3 are kinetic resolutions. Note that in Entry 1 the hydrolytic product is obtained in high e.e., whereas in Entry 2 it is the epoxide that has the highest e.e. In the first case, the reaction was stopped at 18% conversion, whereas in the second case hydrolysis was carried to 70% completion. The example in Entry 3 has a very high E (> 100) and both the unreacted epoxide and diol are obtained with high e.e. at 50% conversion. Entry 4 shows successive use of two separate EH reactions having complementary enantioselectivity to achieve nearly complete

- ²³⁷ J. Y. Zou, B. M. Halberg, T. Bergfors, F. Oesch, M. Arnold, S. L. Mowbray, and T. A. Jones, *Structure with Folding and Design*, **8**, 111 (2000).
- ²³⁸ H. F. Tzeng, L. T. Laughlin, and R. N. Armstrong, *Biochemistry*, **37**, 2905 (1998); R. Rink, J. H. L. Spelberg, R. J. Pieters, J. Kingma, M. Nardini, R. M. Kellogg, B. K. Dijkstra, and D. B. Janssen, *J. Am. Chem. Soc.*, **121**, 7417 (1999); R. Rink, J. Kingma, J. H. L. Spelberg, and D. B. Janssen, *Biochemistry*, **39**, 5600 (2000).
- ²³⁹ S. Pedragosa-Moreau, A. Archelas, and R. Furstoss, *J. Org. Chem.*, **58**, 5533 (1993); S. Pedragosa-Moreau, C. Morisseau, J. Zylber, A. Archelas, J. Baratti, and R. Furstoss, *J. Org. Chem.*, **61**, 7402 (1996); S. Pedragosa-Moreau, A. Archelas, and R. Furstoss, *Tetrahedron*, **52**, 4593 (1996).
- ²⁴⁰ C. A. G. M. Weijers, *Tetrahedron: Asymmetry*, **8**, 639 (1997); C. A. G. M. Weijers, A. L. Botes, M. S. van Dyk, and J. A. M. de Bont, *Tetrahedron: Asymmetry*, **9**, 467 (1998).

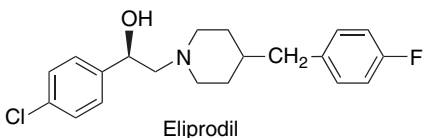
Scheme 2.15. Representative Enantioselective Enzymatic Epoxide Openings



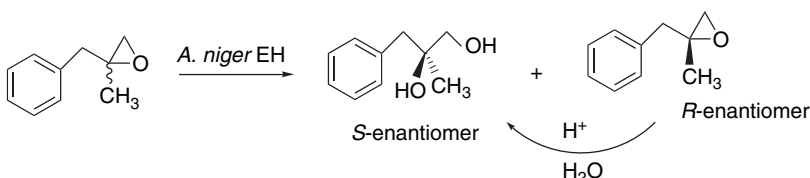
- a. W. Kroutil, I. Osprian, M. Mischitz, and K. Faber, *Synthesis*, 156 (1997).
 b. C. Guerard, F. Alphand, A. Archelas, C. Demuyncck, L. Hecquet, R. Furstoss, and J. Bolte, *Eur. J. Org. Chem.*, 3399 (1999).
 c. A. Steinreiber, H. Hellstrom, S. F. Mayer, R. V. A. Orru, and K. Faber, *Synlett*, 111 (2001).
 d. K. B. Manoj, A. Archelas, J. Baratti, and R. Furstoss, *Tetrahedron*, **57**, 695 (2001).
 e. R. V. A. Orru, I. Osprian, W. Kroutil, and K. Faber, *Synthesis*, 1259 (1998).
 f. W. Kroutil, M. Mischitz, and K. Faber, *J. Chem. Soc., Perkin Trans. 1*, 3629 (1997).
 g. G. Bellucci, C. Chiappe, G. Ingrosso, and C. Rosini, *Tetrahedron: Asymmetry*, **6**, 1911 (1995).

conversion of 4-chlorophenylloxirane to the *R*-enantiomer, which is used to prepare the drug Eliprodil.²⁴¹ This compound is a glutamate antagonist that has promising neuroprotective activity in the treatment of stroke. First, an EH from *Solanum tuberosum* that hydrolyzes the *S*-enantiomer was used, leaving the *R*-enantiomer unchanged. When the reaction is complete, *Aspergillus niger* EH converts the *R*-enantiomer to the *R*-3-diol, which can be converted to the *R*-epoxide by chemical means.

²⁴¹ K. M. Manoj, A. Archelas, J. Baratti, and P. Furstoss, *Tetrahedron*, **57**, 695 (2001).



Entry 5 is an interesting example that entails both enzymatic and hydrolytic epoxide conversion. In the first step, an enzymatic hydrolysis proceeds with *retention* of the configuration at the tertiary center. This reaction is selective for the *S*-epoxide. The remaining *R*-epoxide is then subjected to acid-catalyzed hydrolysis, which proceeds with *inversion* at the center of chirality (see p. 186). The combined reactions give an overall product yield of 94%, having 94% e.e.²⁴²



Entry 6 is one of several examples demonstrating enantioselectivity for both the *cis* and *trans* isomers of heptane-2,3-epoxide. Entry 7 shows the kinetic resolution of an exocyclic cyclohexane epoxide. The two stereoisomeric monomethyl analogs were only partially resolved and the 3-methyl isomer showed no enantioselectivity. This shows that the steric or hydrophobic effect of the dimethyl substituents is critical for selective binding.

Topic 2.3. The Anomeric Effect in Cyclic Compounds

The incorporation of heteroatoms into rings can result in stereoelectronic effects that significantly affect conformation and, ultimately, reactivity. It is known from many examples in carbohydrate chemistry that pyranose (six-membered oxygen-containing rings) sugars substituted with an electron-withdrawing group such as halogen or alkoxy at C(2) are often more stable when the substituent has an axial rather than an equatorial orientation. This tendency is not limited to carbohydrates but carries over to simpler ring systems such as 2-substituted tetrahydropyrans. The phenomenon is known as the *anomeric effect*, since it involves a substituent at the anomeric position in carbohydrate pyranose rings.²⁴³ Scheme 2.16 lists several compounds that exhibit the anomeric effect, along with some measured equilibrium compositions. In Entries 1 to 3, the

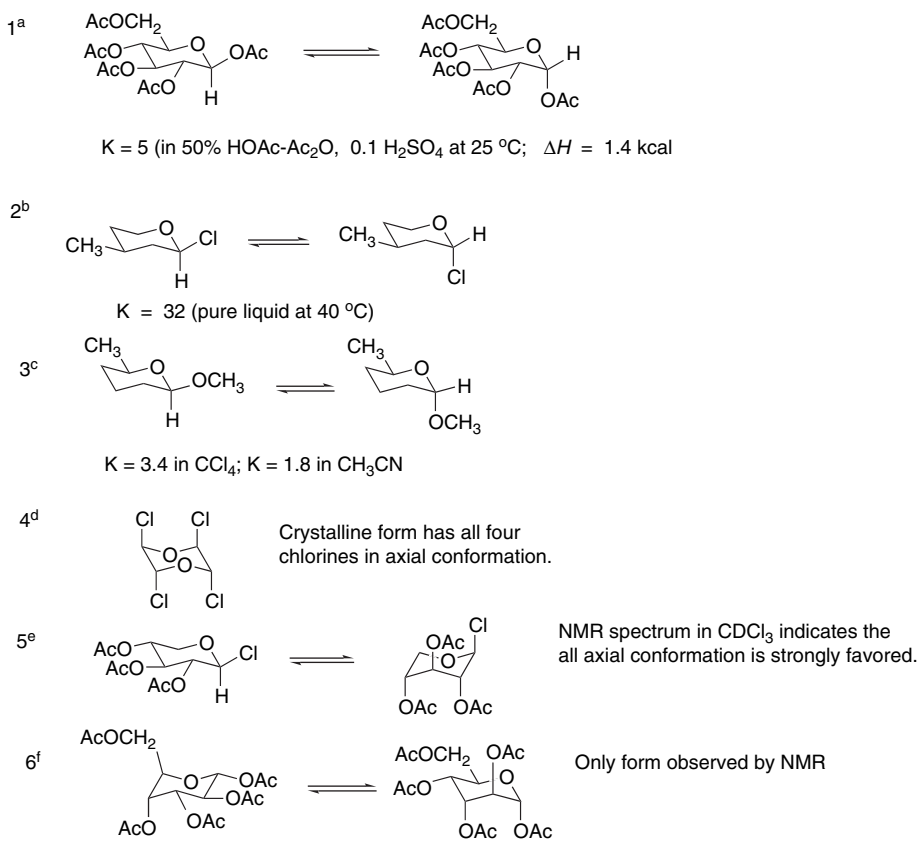
²⁴² R. V. Orru, I. Osprian, W. Kroutil, and K. Faber, *Synthesis*, 1259 (1998).

²⁴³ For reviews, see R. U. Lemieux, *Pure Appl. Chem.* **25**, 527 (1971); W. A. Szarek and D. Horton, eds., *Anomeric Effects*, ACS Symposium Series, No. 87, American Chemical Society, Washington, DC, 1979; A. J. Kirby, *The Anomeric Effect and Related Stereoelectronic Effects at Oxygen*, Springer-Verlag, Berlin, 1983; P. Deslongchamps, *Stereoelectronic Effects in Organic Chemistry*, Pergamon Press, Oxford, 1983; M. L. Sinot, *Adv. Phys. Org. Chem.*, **24**, 113 (1988); P. R. Graczyk and M. Mikolajczyk, *Top. Stereochem.*, **21**, 159 (1994); E. Juraisti and G. Cuevas, *The Anomeric Effect*, CRC Press, Boca Raton, FL, 1995; C. J. Cramer, *Theochem*, **370**, 135 (1996).

Scheme 2.16. Cyclic Compounds that Exhibit the Anomeric Effect

CHAPTER 2

Stereochemistry,
Conformation,
and Stereoselectivity



- a. W. A. Bonner, *J. Am. Chem. Soc.*, **73**, 2659 (1951).
 b. C. B. Anderson and D. T. Tepp, *J. Org. Chem.*, **32**, 607 (1967).

- c. E. L. Eliel and C. A. Giza, *J. Org. Chem.*, **33**, 3754 (1968).
 d. E. W. M. Rutten, N. Nibbering, C. H. MacGillavry, and C. Romers, *Rec. Trav. Chim. Pays-Bas*, **87**, 888 (1968).
 e. C. V. Holland, D. Horton, and J. S. Jewell, *J. Org. Chem.*, **32**, 1818 (1967).
 f. B. Coxon, *Carbohydrate Res.*, **1**, 357 (1966).

equilibria are between diastereoisomers and involve reversible dissociation of the 2-substituent. In all cases, the more stable isomer is written on the right. The magnitude of the anomeric effect depends on the nature of the substituent and decreases with increasing dielectric constant of the medium.²⁴⁴ The effect of the substituent can be seen by comparing the related 2-chloro- and 2-methoxy substituted tetrahydropyrans in Entries 2 and 3. The 2-chloro compound exhibits a significantly greater preference for the axial orientation than the 2-methoxy. Entry 3 also provides data relative to the effect of solvent polarity, where it is observed that the equilibrium constant is larger in carbon tetrachloride ($\epsilon = 2.2$) than in acetonitrile ($\epsilon = 37.5$).

Compounds in which conformational, rather than configurational, equilibria are influenced by the anomeric effect are depicted in Entries 4 to 6. X-ray diffraction studies have unambiguously established that all the chlorine atoms of *trans*, *cis*, *trans*-2,3,5,6-tetrachloro-1,4-dioxane occupy axial sites in the crystal (Entry 4). Each chlorine

²⁴⁴ K. B. Wiberg and M. Marquez, *J. Am. Chem. Soc.*, **116**, 2197 (1994).

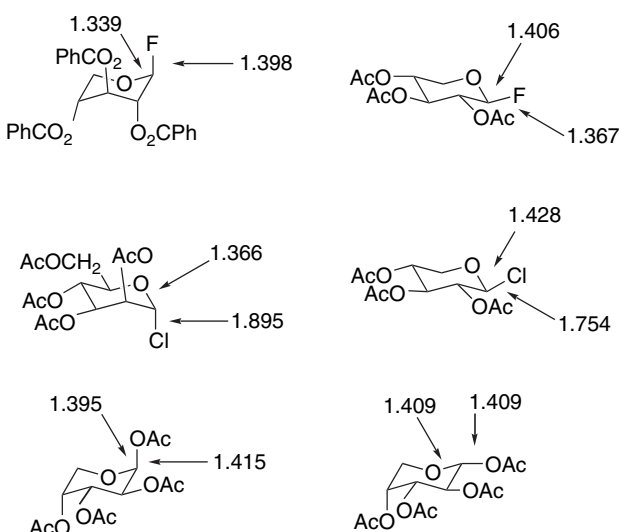
in the molecule is bonded to an anomeric carbon and is subject to the anomeric effect. Equally striking is the observation that all the substituents of the tri-*O*-acetyl- β -D-xylopyranosyl chloride shown in Entry 5 are in the axial orientation *in solution*. Here, no special crystal packing forces can favor the preferred conformation. The anomeric effect of a single chlorine is sufficient to drive the equilibrium in favor of the conformation that puts the three acetoxy groups in axial positions.

Changes in bond lengths are also frequently observed in connection with the anomeric effect. The exocyclic bond is shortened and the ring C–O bond to the anomeric center is lengthened. Scheme 2.17 shows some comparisons.

In 2-alkoxytetrahydropyran derivatives there is a correlation between the length of the exocyclic C–O bond and the nature of the oxygen substituent. Figure 2.33 shows bond length data for a series of monocyclic and bicyclic 2-aryloxytetrahydropyran derivatives. The more electron withdrawing the group, the longer the bond to the exocyclic oxygen and the shorter the ring C–O bond. This indicates that the extent of the anomeric effect *increases with the electron-accepting capacity of the exocyclic oxygen*.²⁴⁵

Several structural factors have been considered as possible causes of the anomeric effect. In localized valence bond terminology, there is a larger dipole-dipole repulsion between the polar bonds at the anomeric carbon in the equatorial conformation.²⁴⁶ This dipole-dipole interaction is reduced in the axial conformation and this factor contributes to the solvent dependence of the anomeric effect. The preference for the axial orientation is highest in nonpolar solvent effects, where the effect of dipolar

Scheme 2.17. Bond Distances in Å at Anomeric Carbons^a



a. From H. Paulsen, P. Luger, and F. P. Heiker, *Anomeric Effect: Origin and Consequences*, W. A. Szarek and D. Horton, eds., ACS Symposium Series No. 87, American Chemical Society, 1979, Chap. 5.

²⁴⁵ A. J. Briggs, R. Glenn, P. G. Jones, A. J. Kirby, and P. Ramaswamy, *J. Am. Chem. Soc.* **106**, 6200 (1984).

²⁴⁶ J. T. Edward, *Chem. Ind. (London)*, 1102 (1955).

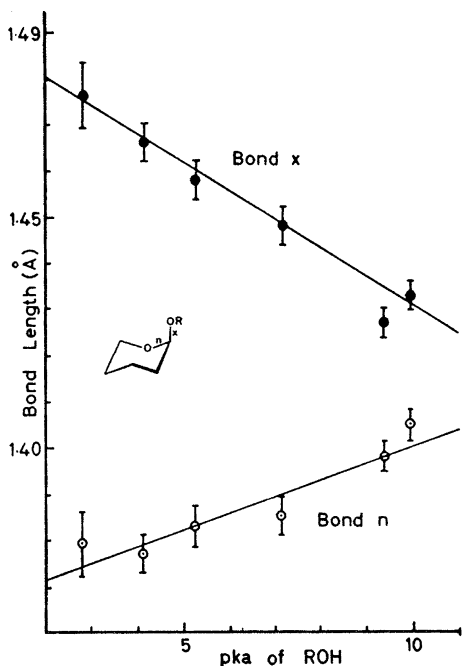
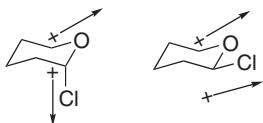


Fig. 2.33. Relationship between pK_a of alkoxy substituents and bond lengths in anomeric systems. The points represented are (left to right) 2,4-dinitrophenyl, 3,5-dinitrophenyl, 2,5-dinitrophenyl, 4-nitrophenyl*, 4-chlorophenyl*, and phenyl*. For the groups marked with an asterisk, the data are from a bicyclic structure. Reproduced from *J. Am. Chem. Soc.*, **106**, 6200 (1984), by permission of the American Chemical Society.

interactions would be strongest. For example, Table 2.7 shows the solvent dependence of 2-methoxytetrahydropyran.²⁴⁷



In general, electrostatic interactions alone do not seem to be sufficient to account for the magnitude of the anomeric effect and do not directly explain the bond length changes that are observed.²⁴⁸ These factors led to the proposal that the anomeric effect is, at least in part, due to $\sigma \rightarrow \sigma^*$ hyperconjugation effects.²⁴⁹ From the molecular orbital viewpoint, the anomeric effect is expressed as resulting from an interaction

²⁴⁷ R. U. Lemieux, A. A. Pavia, J. C. Martin, and K. A. Watanabe, *Can. J. Chem.*, **47**, 4427 (1969).

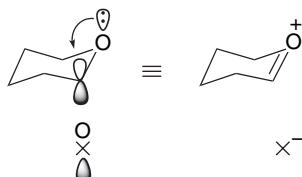
²⁴⁸ C. Altona, C. Knobler, and C. Romers, *Acta Cryst.*, **16**, 1217 (1963); C. Altona and C. Romers, *Acta Cryst.*, **16**, 1225 (1963).

²⁴⁹ C. Romers, C. Altona, H. R. Buys, and E. Havinga, *Top. Stereochem.*, **4**, 39 (1969).

Table 2.7. Solvent Dependence of Conformational Equilibrium for 2-Methoxytetrahydropyran

Solvent	Dielectric constant	% Axial conformer
CCl ₄	2.2	83
Benzene	2.3	82
Chloroform	4.7	71
Acetone	20.7	72
Methanol	32.6	69
Acetonitrile	37.5	68
Water	78.5	52

between the lone-pair electrons on the pyran oxygen and the σ^* orbital associated with the bond to the electronegative substituent.²⁵⁰ When the C–X bond is axial, an interaction between an occupied *p*-type orbital on oxygen (unshared electrons) and the antibonding σ^* orbital of the C–X combination is possible. This interaction permits delocalization of the unshared electrons and would be expected to shorten and strengthen the C–O bond while lengthening and weakening the C–X bond, as is observed. These are the same structural factors identified in Topic 1.2, where the effect of hyperconjugation on conformation of acyclic compounds is discussed.



There have been various studies aimed at determining the energy differences associated with the anomeric effect. Temperature-dependent ¹³C-NMR chemical shift studies of 2-methoxytetrahydropyran determined ΔG values ranging from 0.5 to 0.8 kcal/mol, depending on the solvent.²⁵¹ Wiberg and Marquez measured a difference of 1.2 kcal/mol between the axial and equatorial methoxy group in the conformationally biased 3,5-dimethyltetrahydropyran ring.²⁴⁴ The energy difference decreased in more-polar solvents; the equatorial isomer is preferred in water.

There have also been a number of computational investigations into the nature of the anomeric effect. The axial-equatorial conformational equilibria for 2-fluoro and 2-chlorotetrahydropyran have been investigated with several MO calculations, including the MP2/6-31G* level. The MP2/6-31G* calculations give values of 3.47 and 2.84 kcal/mol, respectively, for the energy favoring the axial conformer.²⁵² Solvent effects were also explored computationally and show the usual trend of reduced stability for the axial conformation as solvent polarity increases. Salzner and Schleyer applied

²⁵⁰ S. Wolfe, A. Rauk, L. M. Tel, and I. G. Csizmaida, *J. Chem. Soc. B*, 136 (1971); S. O. David, O. Eisenstein, W. J. Hehre, L. Salem, and R. Hoffmann, *J. Am. Chem. Soc.* **95**, 306 (1973); F. A. Van-Catledge, *J. Am. Chem. Soc.*, **96**, 5693 (1974).

²⁵¹ H. Booth, J. M. Dixon, and S. A. Readshaw, *Tetrahedron*, **48**, 6151 (1992).

²⁵² I. Tvaroska and J. P. Carver, *J. Phys. Chem.*, **98**, 6452 (1994).

Table 2.8. Calculated Energy Differences for Tetrahydropyrans (kcal/mol)

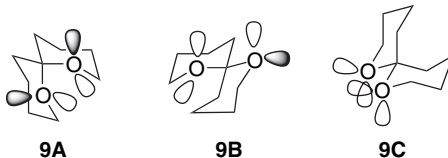
Substituent	ΔE_{total}	ΔE_{local}	ΔE_{deloc}
F	2.8	-1.2	4.0
CH_3O	1.5	-0.3	1.8
HO	1.3	-0.5	1.8
H_2N	-2.8	-6.4	3.6
H_3N^+	-3.0	-15	12
Cl	2.5	-5.4	7.9

an NBO analysis (see Section 1.4.2) to separate steric, polar, and other localized effects from the delocalization components of the anomeric effect.²⁵³ Using MP2/6-31G* level calculations, they arrived at the results in Table 2.8.

According to this analysis, the $\sigma \rightarrow \sigma^*(\Delta E_{\text{deloc}})$ interaction is stabilizing for all substituents. However, opposing electrostatic and steric effects (ΔE_{local}) are larger for the NH_2 and NH_3^+ groups. Cortes and co-workers carried out a similar analysis for 1,3-dioxanes using B3LYP/6-31G(*d,p*) computations.²⁵⁴ The results are shown in Table 2.9.

The B3LYP computations arrive at much larger values than found for the tetrahydropyrans, especially for the Cl and H_3N^+ substituents, although there are also large compensating localization effects. These theoretical efforts provide support for $\sigma \rightarrow \sigma^*$ delocalization as a component of the anomeric effect, although leaving uncertainty as to the relative energies that are involved.

In bicyclic systems such as **9**, the dominant conformation is the one with the maximum anomeric effect. In the case of **9**, only conformation **9A** provides the preferred *anti*-periplanar geometry for both oxygens.²⁵⁵ Anti periplanar relationships are indicated by the shaded oxygen orbitals. Other effects, such as torsional strain and nonbonded repulsion contribute to the conformational equilibrium, of course.

**Table 2.9. Calculated Energy Differences in 1,3-Dioxanes (kcal/mol)**

Substituent	ΔE_{total}	ΔE_{local}	ΔE_{deloc}
F	4.0	1.66	2.34
CH_3O	2.30	5.17	2.87
HO	-0.98	2.06	3.04
H_2N	1.75	6.01	-4.26
H_3N^+	-1.32	-52.67	51.36
Cl	6.79	-12.69	19.45

²⁵³ U. Salzner and P. v. R. Schleyer, *J. Org. Chem.*, **59**, 2138 (1994).

²⁵⁴ F. Cortes, J. Tenorio, O. Collera and G. Cuevas, *J. Org. Chem.*, **66**, 2918 (2001).

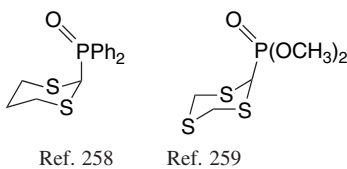
²⁵⁵ P. Deslongchamps, D. D. Rowan, N. Pothier, G. Sauve, J. K. Saunders *Can. J. Chem.*, **59**, 1132 (1981).

The Anomeric Effect in Cyclic Compounds

Anomeric effects are also observed for elements in the heavier rows of the periodic table. For example, *trans*-2,3-dichloro-1,4-dithiane exists in the diaxial conformation.²⁵⁶



Tetravalent phosphorus groups prefer axial orientations in 1,3-dithianes and 1,3,5-trithianes. NMR studies have indicated a preference of about 1 kcal for the diphenylphosphoryl group. When combined with the conformational energy in a cyclohexane ring, this suggests an anomeric effect of around 3 kcal.²⁵⁷



Ref. 258

Ref. 259

The anomeric effect is not limited to six-membered ring compounds. In five-membered rings the anomeric effect can affect both ring and substituent conformation. The 1,3-dioxole ring adopts a puckered conformation as a result of an anomeric effect.²⁶⁰ Similar effects are observed, although attenuated, in 1,3-benzodioxoles.²⁶¹



The anomeric effect is also believed to be an important factor in the conformation of ribonucleosides. The anomeric effect with the exocyclic nitrogen is stronger when the heterocyclic base is in the pseudoaxial position. Steric factors, on the other hand, favor the pseudoequatorial conformation. By analysis of the pH-dependent conformational equilibria, a contribution from the anomeric effect of as much as 5.6 kcal for adenosine and 9.0 kcal for guanosine has been suggested.²⁶²

^{256.} H. T. Kalff and C. Romers, *Acta Cryst.*, **18**, 164 (1965).

^{257.} E. Juaristi, N. A. Lopez-Nunez, R. S. Glass, A. Petsom, R. O. Hutchins, and J. P. Stercho, *J. Org. Chem.*, **51**, 1357 (1986).

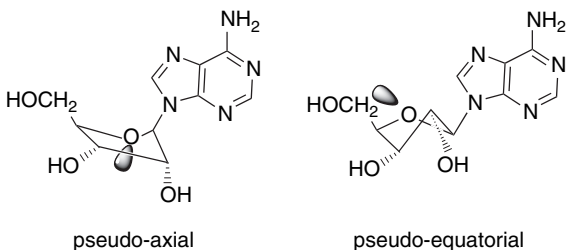
^{258.} E. Juaristi, L. Valle, C. Mora-Uzeta, B. A. Valenzuela, P. Joseph-Nathan, and M. Fredrich, *J. Org. Chem.*, **47**, 5038 (1982).

^{259.} M. Mikolajczyk, M. Balczewski, K. Wroblewski, J. Karolak-Wojciechowska, A.J. Miller, M. W. Wieczorek, M. Y. Antipin, and Y. T. Struchkov, *Tetrahedron*, **40**, 4885 (1984).

^{260.} D. Suarez, T. L. Sordo, and J. A. Sordo, *J. Am. Chem. Soc.*, **118**, 9850 (1996).

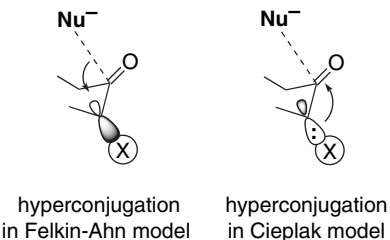
^{261.} S. Sakurai, N. Meinander, K. Morris, and J. Laane, *J. Am. Chem. Soc.*, **121**, 5056 (1999).

^{262.} J. Plavec, C. Thibaudeau, and J. Chattopadhyaya, *Pure Appl. Chem.*, **68**, 2137 (1996); I. Luyten, C. Thibaudeau, and J. Chattopadhyaya, *J. Org. Chem.*, **62**, 8800 (1997).



Topic 2.4. Polar Substituent Effects in Reduction of Carbonyl Compounds

The stereoselectivity of hydride reduction was discussed in terms of steric approach and torsional effects in Section 2.4.1.2. Two additional factors have to be considered when polar substituents are present. The polar substituents enhance the importance of hyperconjugation involving σ and σ^* orbitals. Polar substituents also introduce bond dipoles and the potential for electrostatic interactions. Both the hyperconjugative and dipolar interactions depend on the equatorial or axial orientation of the substituent. There are two contrasting views of the nature of the hyperconjugative effects. One is the *Felkin-Ahn model*, which emphasizes stabilization of the developing negative charge in the forming bond by interaction with the σ^* orbital of the substituent. The preferred alignment for this interaction is with an axial position and the strength of the interaction should increase with the electron-accepting capacity of the substituent.²⁶³ The Cieplak model²⁶⁴ emphasizes an alternative interaction in which the σ orbital of the C–X bond acts as a donor to the developing antibonding orbital.²⁶⁵ It has been pointed out that both of these interactions can be present, since they are not mutually exclusive, although one should dominate.²⁶⁶ Moreover, hydride reductions involve *early transition states*. The electronic effects of substituents on the reactant should be more prominent than effects on the TS.



There have been computational efforts to understand the factors controlling axial and equatorial approaches. A B3LYP/6-31G* calculation of the TS for addition of lithium hydride to cyclohexanone is depicted in Figure 2.34.²⁶⁷ The axial approach is

^{263.} N. T. Ahn, *Top. Current Chem.*, **88**, 145 (1980).

²⁶⁴ A. S. Cieplak, *J. Am. Chem. Soc.*, **103**, 4540 (1981).

²⁶⁵ Both the Felkin-Ahn and Cieplak models are also applied to alkyl substituents.

²⁶⁶ H. Li and W. J. le Noble, *Recl. Trav. Chim. Pays-Bas.*, **111**, 199 (1992).

²⁶⁷ T. Senju, and S. Tomoda, *Chem. Lett.*, 431 (1997).

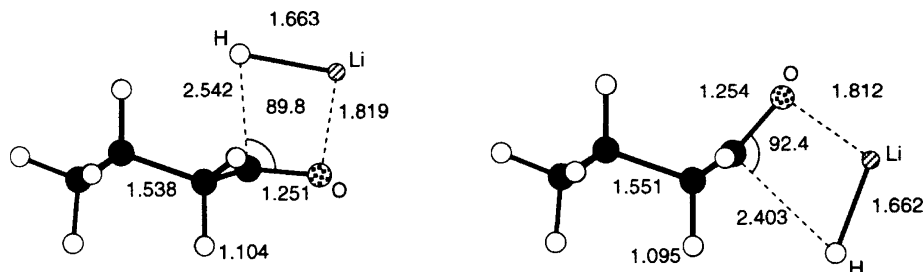
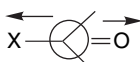


Fig. 2.34. B3LYP/6-31G* transition structures for axial and equatorial addition of LiH to cyclohexanone. Reproduced from *Chem. Lett.*, 431 (1997).

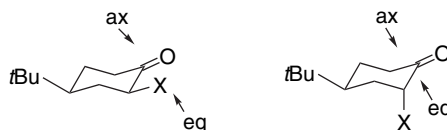
found to be 1.7 kcal more stable, in good agreement with the experimental ratio of 9:1. About half of the energy difference between the two TSs can be attributed to the torsional effect (see p. 177). An NBO analysis was applied to search for hyperconjugative interactions. The Felkin-Ahn interactions were minimal. The Cieplak effect was evident, but was similar in both the axial and equatorial approach TSs, raising doubts that it could determine the stereoselectivity.

Polar substituents may also affect stereoselectivity through an electrostatic effect that depends on the size and orientation of the bond dipole. These are relatively easy to determine for the ground state molecule but may be altered somewhat in the TS. The dipole from an electronegative substituent prefers to be oriented *anti* to the carbonyl substituent.



Rosenberg and co-workers approached the problem of separating the hyperconjugative and electrostatic interactions by examining the product ratios for NaBH₄ reduction of both axially and equatorially oriented substituents in 4-*t*-butylcyclohexanones.²⁶⁸ The product ratios were used to calculate the energy difference, $\Delta\Delta G$ (kcal/mol), for axial and equatorial approach. The results are given in Table 2.10.

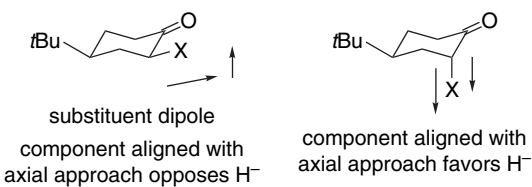
Table 2.10. Percent Axial and Equatorial Approach in Reduction of 2-Substituted 4-*t*-Butylcyclohexanones



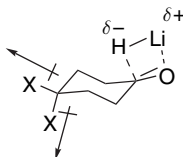
Substituent	% Equatorial	% Axial	$\Delta\Delta G$ (kcal/mol)	% Equatorial	% Axial	$\Delta\Delta G$ (kcal/mol)
H	9	91	0	9	91	0
CH ₃	11	89	0.12	5	95	-0.35
OCH ₃	67	33	1.64	8	92	-0.08
F	40	60	1.04	9	91	0
Cl	34	66	0.90	0.9	99.1	-1.30
Br	29	71	0.77	1.4	98.6	1.05

²⁶⁸ R. E. Rosenberg, R. L. Abel, M. D. Drake, D. J. Fox, A. K. Ignatz, D. M. Kwiat, K. M. Schaal, and P. R. Virkle, *J. Org. Chem.*, **66**, 1694 (2001).

The equatorial substituents all shift the ratio toward an increased equatorial approach in the order $\text{CH}_3\text{O} >> \text{F} > \text{Cl} > \text{Br} >> \text{CH}_3$. All axial substituents except F, which has no effect, favor increasing axial attack in the order $\text{F} < \text{CH}_3\text{O} < \text{CH}_3 << \text{Br} < \text{Cl}$. These results can be at least partially explained in terms of an electrostatic interaction between the dipole of the substituent and the approaching nucleophile. In the case of the equatorial substituents, the fraction of the dipole that is *opposed* to an approaching negative charge in the TS increases in the order Cl (0.28) < F (0.43) < OCH_3 (0.98), which agrees with the substituent effect. The dipole for axial substituents *favors axial attack*. Here, the fractional alignment of the dipoles is OCH_3 (0.49) < Cl (0.97) < F (0.98). There is an inherent preference for an axial approach in the case of the *trans* (axial) substituents, which is reinforced by Cl and Br but not by F or OCH_3 . In these cases some other factor(s) must be operating.



The role of orientation of substituent dipoles is also considered to be a major factor in 3- and 4-substituted cyclohexanones. Shi and Boyd used an AIM analysis to examine stereoselectivity in 3- and 4-substituted cyclohexanones.²⁶⁹ Little difference in charge depletion was found for the two faces of the cyclohexanone ring. Addition TSs for LiH, similar to those in Figure 2.34, were studied. Energies and charge distributions were obtained from HF/6-31G(d) and MP2/6-31G(d) calculations. Polar F and Cl substituents at C(4) reduce the TS barrier, which is in accord with experimental results. The effect for axial substituents was larger than for equatorial, so that the axial substituents are predicted to have a greater preference for axial approach. The authors suggest that the effect has its origins in the C–X bond dipoles. The axial dipole has a larger component perpendicular to the carbonyl group and favors axial approach by the hydride.

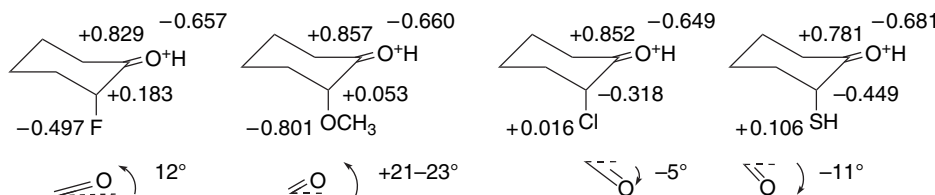


Another computational study²⁷⁰ examined how cyclohexanone substituent electronic effects respond to Lewis acid complexation. The metal cation was modeled by a H^+ (which represents the hard extreme of a Lewis acid). It was found that the complexation amplifies the effect of the α -donor substituents. The computations indicate that the electron-donor substituents cause pyramidalization at the carbonyl carbon and that this then controls the direction of nucleophile approach. The results

²⁶⁹ Z. Shi and R. J. Boyd, *J. Am. Chem. Soc.*, **115**, 9614 (1993).

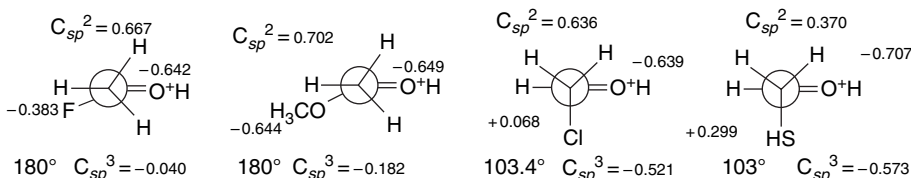
²⁷⁰ V. K. Yadav, D. A. Jeyaraj, and R. Balamurugan, *Tetrahedron*, **56**, 7581 (2000).

are summarized below. According to NPA charge analysis, the Cl and SH substituents are significant σ donors and lead to movement of oxygen to the equatorial direction, favoring axial approach by the nucleophile. The oxygen and fluoro substituents have the opposite effects and favor equatorial approach. Experimental data are available for the SH, Cl, and OCH_3 substituents and are in accord with these predictions. Looking at the data in Table 2.10, we see that axial OCH_3 and F have little effect, whereas Cl and Br favor axial approach. These results are in agreement with the better donor capacity attributed to third-row elements in the discussion of heteroatom hyperconjugation (Topic 1.2). This study concludes that the substituents effects operate in the *ground state molecule and are accentuated by coordination of a cation at oxygen.*



Angle quoted is change in pyramidalization upon protonation.

Yadav and co-workers also reported calculations aimed at comparing the relative donor ability of some heteroatom substituents.²⁶⁹ The preferred orientation of the substituent with respect to a carbonyl group was examined using substituted acetaldehydes as the model. The calculations were done at the MP2/6-31G(*d*) level and charges were assigned by the NPA method. According to these results, methoxy and fluoro substituents are poor σ donors and maintain a dihedral angle of 180° with respect to the carbonyl, presumably reflecting the strong opposing polarity of the C=O and C–F (or C–O) bonds. This orientation was also found for the protonated carbonyl group. On the other hand, when the carbonyl group is protonated, Cl and SH substituents assume nearly perpendicular angles that maximize hyperconjugation. They become positively charged, reflecting $\sigma \rightarrow \pi^*$ electron donation (Cieplak model).



In contrast to the case of cyclic ketones, there is not much experimental data for polar α -substituents for acyclic ketones. Moreover, in some cases, such as α -methoxy, chelation effects are the dominant factor.

Electronic effects have been examined using *endo,endo*-disubstituted norbornan-7-ones. The *endo* substituents are located so that there are no direct steric interactions with the reaction site. The amount of *anti* versus *syn* approach by NaBH_4 has been determined,²⁷¹ and the results are given in Table 2.11

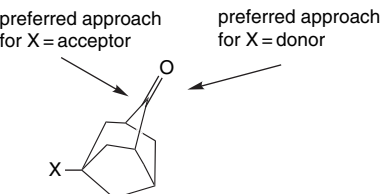
²⁷¹ G. Mehta, F. A. Khan, *J. Am. Chem. Soc.*, **112**, 6140 (1990); H. Li, G. Mehta, S. Padma, and W. J. le Noble, *J. Org. Chem.*, **56**, 2006 (1991); G. Mehta, F. A. Khan, B. Ganguly, and J. Chandrasekhan, *J. Chem. Soc., Perkin Trans. 2*, 2275 (1994).

Table 2.11. Stereoselectivity in NaBH_4 Addition to Norbornan-7-ones

Substituent	% syn	% anti
CH_3	45	55
C_2H_5	20	80
$\text{CH}_2=\text{CH}$	36	64
CH_3OCH_2	40	60
$\text{CH}_3\text{O}_2\text{C}$	84	16

The trend in the data is that electron-donor substituents favor *anti* addition, whereas acceptor substituents favor *syn* addition. A particularly intriguing point is that the 2,3-diethyl compound is more *anti* selective than the 2,3-dimethyl derivative. This is puzzling for any interpretation that equates the electronic effects of the methyl and ethyl groups. Two explanations have been put forward for the overall trend in the data. According to an orbital interaction (hyperconjugation) model, electron-withdrawing substituents decrease the stabilization of the LUMO (Cieplak model) and favor *syn* addition. An electrostatic argument focuses on the opposite direction of the dipole resulting from electron-releasing and electron-withdrawing substituents.²⁷² The dipoles of the electron-withdrawing groups will facilitate *syn* approach. Several levels of theory have been applied to these results.²⁷³ Most recently, Yadav examined the effect using B3LYP/6-31G*-level calculations on both the neutral and the protonated ketones.²⁷⁴ The *anti*-periplanar orbital stabilization found for the diethyl compound was about 0.5 kcal/mol higher than for the dimethyl derivative. In this model, the resulting greater pyramidalization of the reactant accounts for the enhanced selectivity.

Adamantanone is another ketone where interesting stereoselectivity is noted. Reduction by hydride donors is preferentially *syn* to acceptor substituents at C(5) and *anti* to donor substituents.²⁷⁵ These effects are observed even for differentially substituted phenyl groups.²⁷⁶ As the substituents are quite remote from the reaction center, steric effects are unlikely to be a factor.



²⁷². G. Mehta, F. A. Khan, and W. Adcock, *J. Chem. Soc. Perkin Trans.*, **2**, 2189 (1995).

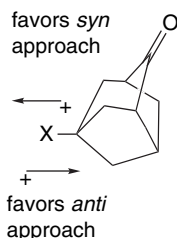
²⁷³. M. N. Paddon-Row, Y.-D. Wu, and K. N. Houk, *J. Am. Chem. Soc.*, **114**, 10638 (1992); R. Ganguly, J. Chandrasekhan, F. A. Khan, and G. Mehta, *J. Org. Chem.*, **58**, 1734 (1993); G. M. Keseru, Z. Kovari, and G. Naray-Szabo, *J. Chem. Soc. Perkin Trans.*, **2**, 2231 (1996).

²⁷⁴. V. K. Yadav, *J. Org. Chem.*, **66**, 2501 (2001); V. K. Yadav and R. Balmurugan, *J. Chem. Soc. Perkin Trans.*, **2**, 1 (2001).

²⁷⁵. C. K. Cheung, L. T. Tseng, M.-H. Lin, S. Srivastava and W. J. Le Noble, *J. Am. Chem. Soc.*, **108**, 1598 (1986); J. M. Hahn and W. J. Le Noble, *J. Am. Chem. Soc.*, **114**, 1916 (1992).

²⁷⁶. I. H. Song and W. J. Le Noble, *J. Org. Chem.*, **59**, 58 (1994).

These effects are attributed to differences in the σ -donor character of the C–C bonds resulting from the substituent (Cieplak model). Electron-attracting groups diminish the donor capacity and promote *syn* addition. An alternative explanation invokes a direct electrostatic effect arising from the C–X bond dipole.²⁷⁷



The arguments supporting the various substituent effects on stereoselectivity in cyclic ketones have been discussed by some of the major participants in the field in a series of review articles in the 1999 issue of *Chemical Reviews*.²⁷⁸ While many of the details are still subject to discussion, several general points are clear. (1) For cyclohexanones, in the absence of steric effects, the preferred mode of attack by small hydride reducing agents is from the axial direction. Torsional effects are a major contributing factor to this preference. (2) When steric factors are introduced, either by adding substituents to the ketone or using bulkier reducing agents, equatorial approach is favored. Steric approach control is generally the dominant factor for bicyclic ketones. (3) In bicyclic ketones, electron donor substituents favor an *anti* mode of addition and acceptor substituents favor a *syn* approach.

The issues that remain under discussion are: (1) the relative importance of the acceptor (Felkin-Ahn) or donor (Cieplak) hyperconjugation capacity of α substituents; (2) the relative importance of electrostatic effects; and (3) the role of reactant pyramidalization in transmitting the substituent effects. Arguments have been offered regarding the importance of electrostatic effects in all the systems we have discussed. Consideration of electrostatic effects appears to be important in the analysis of stereoselective reduction of cyclic ketones. Orbital interactions (hyperconjugation) are also involved, but whether they are primarily ground state (e.g., reactant pyramidalization) or transition state (e.g., orbital stabilization) effects is uncertain.

General References

- D. Ager and M. B. East, *Asymmetric Synthetic Methodology*, CRC Press, Boca Raton, FL, 1996.
- R. S. Atkinson, *Stereoselective Synthesis*, John Wiley & Sons, New York, 1995.
- J. Dale, *Stereochemistry and Conformational Analysis*, Verlag Chemie, New York, 1978.
- E. L. Eliel, N. L. Allinger, S. J. Angyal, and G. A. Morrison, *Conformational Analysis*, Wiley-Interscience, New York, 1965.
- E. L. Eliel, S. H. Wilen, and L. N. Mander, *Stereochemistry of Organic Compounds*, John Wiley & Sons, New York, 1993.
- E. Juaristi and G. Cuevas, *The Anomeric Effect*, CRC Press, Boca Raton, FL, 1995.
- A. J. Kirby, *Stereoelectronic Effects*, Oxford University Press, Oxford, 1996.

²⁷⁷ W. Adcock, J. Cotton, and N. A. Trout, *J. Org. Chem.*, **59**, 1867 (1994).

²⁷⁸ B. W. Gung and W. G. le Noble, eds., Thematic Issue on Diastereoselection, *Chemical Reviews*, **99**, No. 5, 1999.

Problems

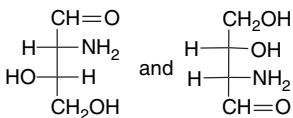
CHAPTER 2

Stereochemistry,
Conformation,
and Stereoselectivity

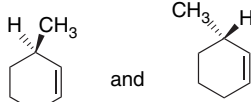
(References for these problems will be found on page 1156.)

- 2.1. Indicate whether the following pairs of compounds are identical, enantiomers, diastereomers, or structural isomers.

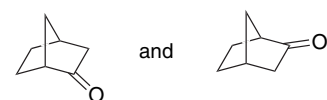
a.



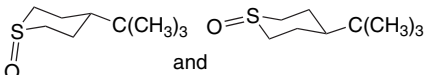
b.



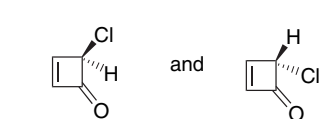
c.



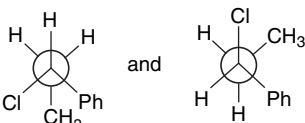
d.



e.

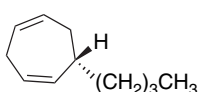


f.

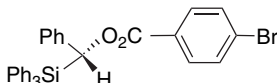


- 2.2. Use the sequence rule to specify the configuration of the stereogenic center in each of the following molecules.

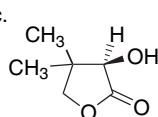
a.



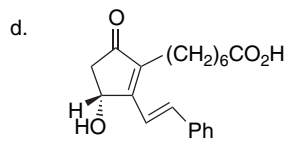
b.



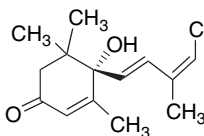
c.



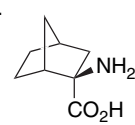
d.



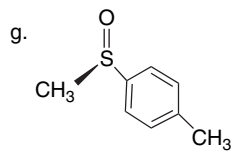
e.



f.



g.



- 2.3. Draw structural formulas for each of the following compounds, clearly showing all aspects of the stereochemistry.

a. *E*-3,7-dimethyl-2,6-octadien-1-ol (geraniol)b. *R*-4-methyl-4-phenylcyclohex-2-enonec. L-*erythro*-2-(methylamino)-1-phenylpropan-1-ol [(-)-ephedrine]d. 7*R*,8*S*-7,8-epoxy-2-methyloctadecane (dispalure, a pheromone of the female gypsy moth)

- e. methyl 1*S*-cyano-2*R*-phenylcyclopropanecarboxylate
 f. *Z*-2-methyl-2-buten-1-ol
 g. *E*-(3-methyl-2-pentenylidene)triphenylphosphorane

2.4. Draw the structures of the product(s) described for each reaction. Specify all aspects of the stereochemistry.

- stereospecific *anti* addition of bromine to *cis*- and *trans*-cinnamic acid.
- methanolysis of *S*-3-bromooctane with 6% racemization.
- stereospecific *syn* thermal elimination of acetic acid from 1*R*,2*S*-diphenylpropyl acetate
- stereoselective epoxidation of bicyclo[2.2.1]hept-2-ene proceeding 94% from the *exo* face.

2.5. The preferred conformation of 1-methyl-1-phenylcyclohexane has the phenyl group in the axial orientation ($\Delta G = -0.32 \text{ kcal/mol}$) even though its conformational free energy (2.9 kcal/mol) is greater than that of methyl (1.8 kcal/mol). Explain.

2.6. The computed (HF/6-31G*) rotational profiles for acetone (2-propanone), 2-butanone, and 3-methyl-2-butanone are given in Figure 2.6P. Draw Newman projections corresponding to each clear maximum and minimum in the curves for each compound. Analyze the factors that stabilize/destabilize each conformation and discuss the differences among them.

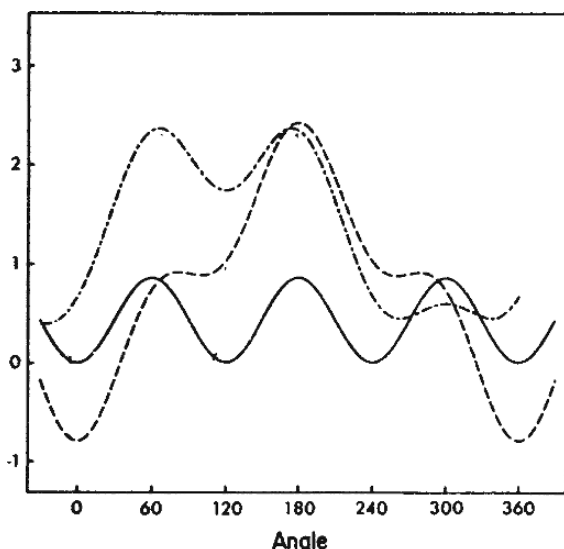
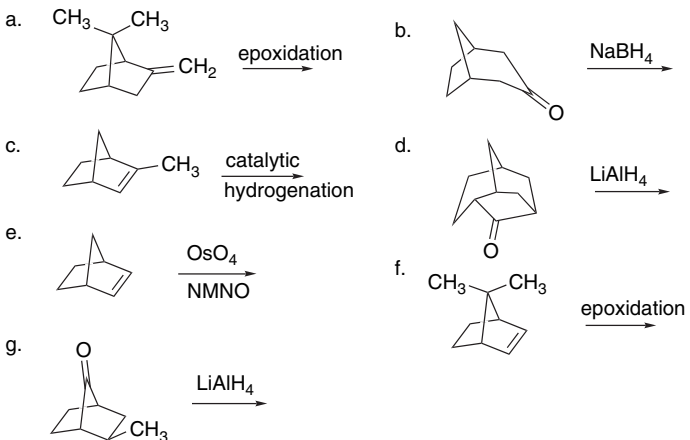
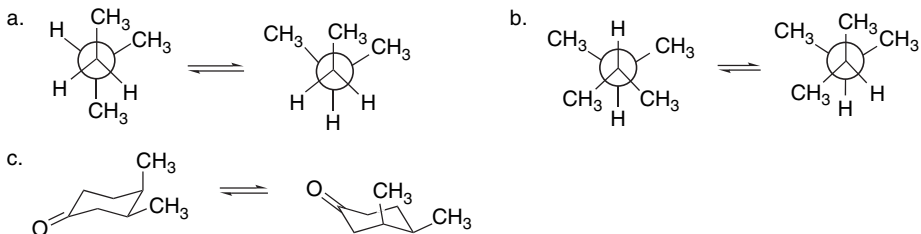


Fig. 2.6P. Rotational profile for acetone (A, solid line), 2-butanone (B, dashed line), and 3-methyl-2-butanone (C, dot-dashed line). Reproduced by permission of the American Chemical Society.

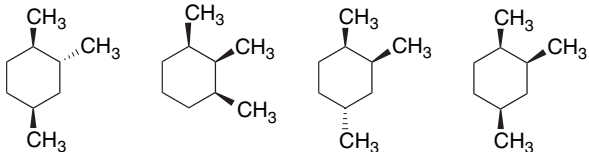
2.7. Predict the stereochemical outcome of the following reactions:



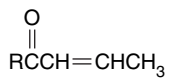
2.8. Estimate ΔH for each of the following conformational equilibria.



2.9. Estimate the free-energy difference between the stable and unstable chair conformations of the following trimethylcyclohexanes.

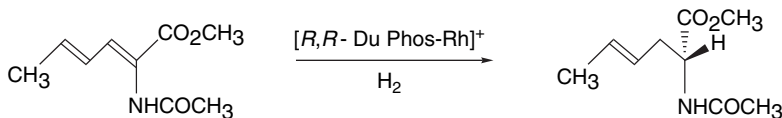


2.10. Predict the preferred conformation of the stereoisomeric *E*-enones **10-A**. How would you expect the conformational equilibrium to change as R becomes progressively larger?

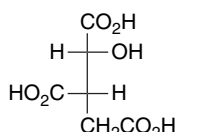


10-A

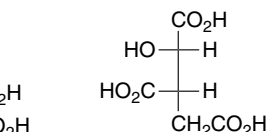
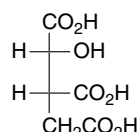
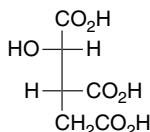
- 2.11. 1,2-Diphenyl-1-propanol can be prepared by hydride reduction of 1,2-diphenyl-1-propanone or by addition of phenylmagnesium bromide to 2-phenylpropanal. Predict the stereochemistry of the major product in each case.
- 2.12. What is the basis of the *chemoselectivity* observed between the two different double bonds in the following reaction?



- 2.13. Assign configuration, using the sequence rule, to each stereocenter in the stereoisomers citric acids shown below and convert the Fischer projections to extended chain representations.



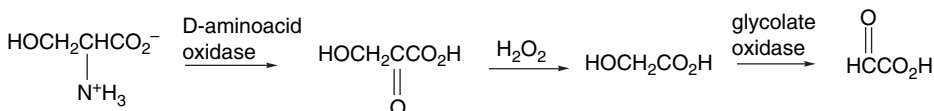
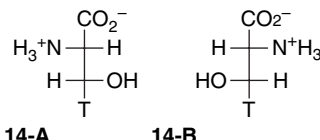
isocitric acids



alloisocitric acids

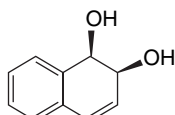
- 2.14. The following questions illustrate how stereochemical considerations can be used to elucidate aspects of biological mechanisms and reactions.

- a. A mixture of ^3H -labeled **14-A** and **14-B** was carried through the reaction sequence shown:

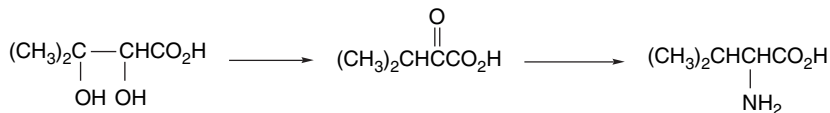


D-amino acid oxidase will oxidize only serine having *R* configuration at C(2). Glycolate oxidase will remove only the *pro-R* hydrogen of glycolic acid. Does the product ($\text{O}=\text{CHCO}_2\text{H}$) contain tritium? Explain your reasoning.

- b. Enzymatic oxidation of naphthalene by bacteria proceeds by way of the intermediate *cis*-diol shown. Which prochiral face of C(1) and C(2) of naphthalene is hydroxylated in this process?

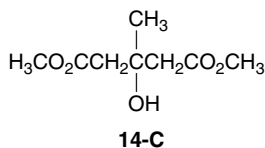


- c. The biosynthesis of valine by bacteria involves the following sequence:

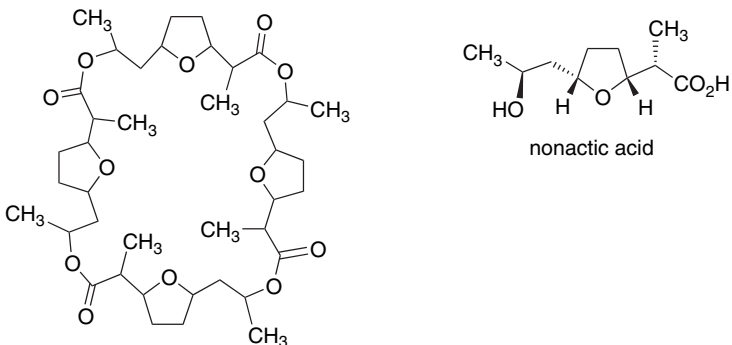


The stereochemistry of the reaction has been examined using the starting diol in which each methyl group was separately replaced by CD_3 . The diol- d_3 of the $2R,3R$ configuration produces $2S,3S$ -valine- d_3 , whereas the $2R,3S$ diol- d_3 produces $2S,3R$ -valine- d_3 . From this information deduce whether the C(2) and C(3) hydroxy are replaced with inversion or retention of configuration. Show the basis for your conclusion.

- d. A synthesis of the important biosynthetic intermediate mevalonic acid starts with the enzymatic hydrolysis of the diester **14-C** by pig liver esterase. The *pro-R* ester group is selectively hydrolyzed. Draw a three-dimensional structure of the product.



- 2.15. The structure of nonactin is shown below without any specification of stereochemistry. It is isolated as a pure substance from natural sources and gives no indication of being a mixture of stereoisomers. Although it is not optically active, it does not appear to be a racemic mixture, because it does not yield separate peaks on chiral HPLC columns. When completely hydrolyzed, it yields racemic nonactic acid. Deduce the stereochemical structure of nonactin from this information.



- 2.16. (a) The signals for the benzylic hydrogens in the ^1H NMR spectra of the *cis* and *trans* isomers of 1-benzyl-2,6-dimethylpiperidine have distinctly different appearances, as shown in Figure 2.16Pa. Answer the following questions about these spectra: (a) Which isomer corresponds to which spectrum and why do they have the appearances they do? (b) Only one isomer shows a multiplet corresponding to ring C–H hydrogens adjacent to nitrogen near 3 ppm. Why are these signals not visible in the other partial spectrum? (b) The partial ^1H NMR spectra corresponding to each benzyl ether of the diastereomeric 2,6-dimethylcyclohexanols are shown in Figure 2.16Pb. Assign the stereochemistry of each isomer.

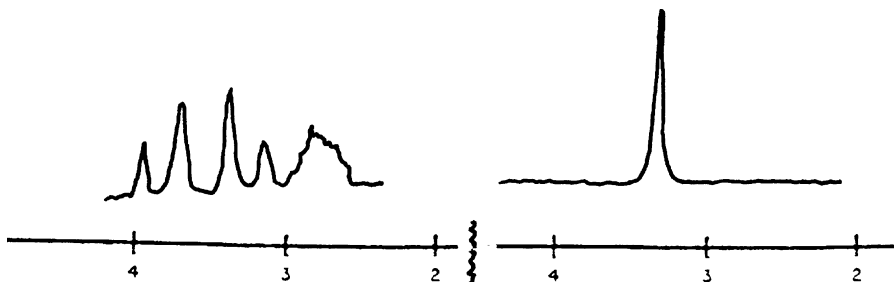


Fig. 2.16Pa. Partial ^1H NMR spectra of *cis* and *trans* isomers of 1-benzyl-2,6-dimethylpiperidine.
Reproduced by permission of Elsevier.

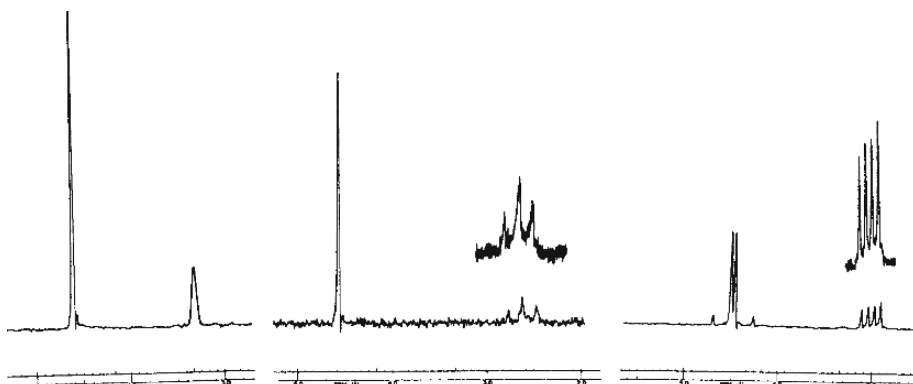


Fig. 2.16Pb. Partial ^1H NMR spectra of three stereoisomeric benzyl ethers of 2,6-dimethylcyclohexanol.
Reproduced by permission of the American Chemical Society.

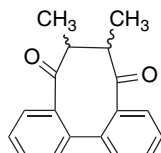
- 2.17. The *trans:cis* ratio of equilibrium for 4-*t*-butylcyclohexanol has been determined in several solvents near 80°C. From the data, calculate the conformational free energy, $-\Delta G_c$, for the hydroxy group in each solvent. What correlation do you find between the observed conformational equilibria and properties of the solvent?

Solvent	<i>trans</i> (%)	<i>cis</i> (%)
Cyclohexane	70.0	30.0
Benzene	72.5	27.5
1,2-Dimethoxyethane	71.0	29.0
Tetrahydrofuran	72.5	27.5
<i>t</i> -Butyl alcohol	77.5	22.5
<i>i</i> -Propyl alcohol	79.0	21.0

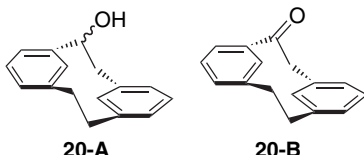
- 2.18. *Trans*-3-alkyl-2-chlorocyclohexanones (alkyl=methyl, ethyl, isopropyl) exist with the substituents in the diequatorial conformation. In contrast, the corresponding *E*-O-methyloximes exist in the diaxial conformation. Explain the preference for the diaxial conformation of the oxime ethers.

- 2.19. The two stereoisomers (**19-A** and **19-B**) of the structure shown below have distinctly different NMR spectra. Isomer **19-A** shows single signals for the methyl

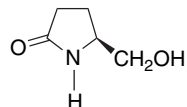
(doublet at 1.25) and methine (broad quartet at 2.94 ppm). Isomer **19-B** shows two methyl peaks (doublets at 1.03 and 1.22 ppm) and two quartets (2.68 and 3.47 ppm) for the methine hydrogens. Both spectra are temperature dependent. For isomer **19-A**, at -40°C the methyl doublet splits into two doublets of unequal intensity (1.38 and 1.22 ppm in the ratio of 9:5). The methine signal also splits into two broad signals at 3.07 and 2.89 ppm, also in the ratio of 9:5. For isomer **19-B**, pairs of doublets and quartets become single signals (still doublet and quartet, respectively) at 95°C . The spectrum shows no change on going to -40°C . Assign the stereochemistry of **19-A** and **19-B** and explain how the characteristics of the spectra are related to the stereochemistry.

**19-A**

- 2.20. Compound **20-A** can be resolved to give an enantiomerically pure substance with $[\alpha]_D = -124$. Oxidation gives an enantiomerically pure ketone **20-B**, $[\alpha]_D = -439$. Heating **20-A** establishes an equilibrium with a stereoisomer with $[\alpha]_D = +22$. Oxidation of this compound gives the enantiomer of **20-B**. Heating either enantiomer of **20-B** leads to racemization with $\Delta G^\ddagger = 25 \text{ kcal/mol}$. Deduce the stereochemical relationship between these compounds.



- 2.21. When partially resolved samples of *S*-5-(hydroxymethyl)pyrrolidin-2-one are allowed to react with benzaldehyde in the presence of an acid catalyst, two products **21-A** ($\text{C}_{12}\text{H}_{13}\text{NO}_2$) and **21-B** ($\text{C}_{24}\text{H}_{26}\text{N}_2\text{O}_4$) are formed. The ratio of **21-A:21-B** depends on the enantiomeric purity of the starting material. When it is enantiomerically pure, only **21-A** is formed, but if it is racemic only **21-B** is formed. Partially resolved samples give **21-A** and **21-B** in a ratio corresponding to the e.e. The rotation of **21-A** is $[\alpha]D = +269.6$, but **21-B** is not optically active. Develop an explanation for these observations including likely structures for **21-A** and **21-B**. Assign the configuration of all the stereogenic centers in the products you propose.

*S*-5-(hydroxymethyl)-
pyrrolidinone

2.22. Figure 2.22Pa,b shows energy as a function of rotation for a series of 2-substituted acetaldehydes, with $\theta = 0^\circ$ in the *syn* conformation and $\theta = 180^\circ$ in the *anti* conformation. The calculations were done by the PM3 method. Figure 2.P22a represents the isolated molecule, while Figure 2.P22b represents an elliptical solvent cavity with a dielectric constant of 4.7, approximating CHCl_3 . The Table 2.22P gives the calculated rotational barriers. Discuss the following aspects of the data. (a) Rationalize the $\text{Br} > \text{Cl} > \text{F}$ order of preference for *anti* conformation in the gas phase; (b) Why does the polar medium shift the equilibrium to favor more of the *syn* conformation?

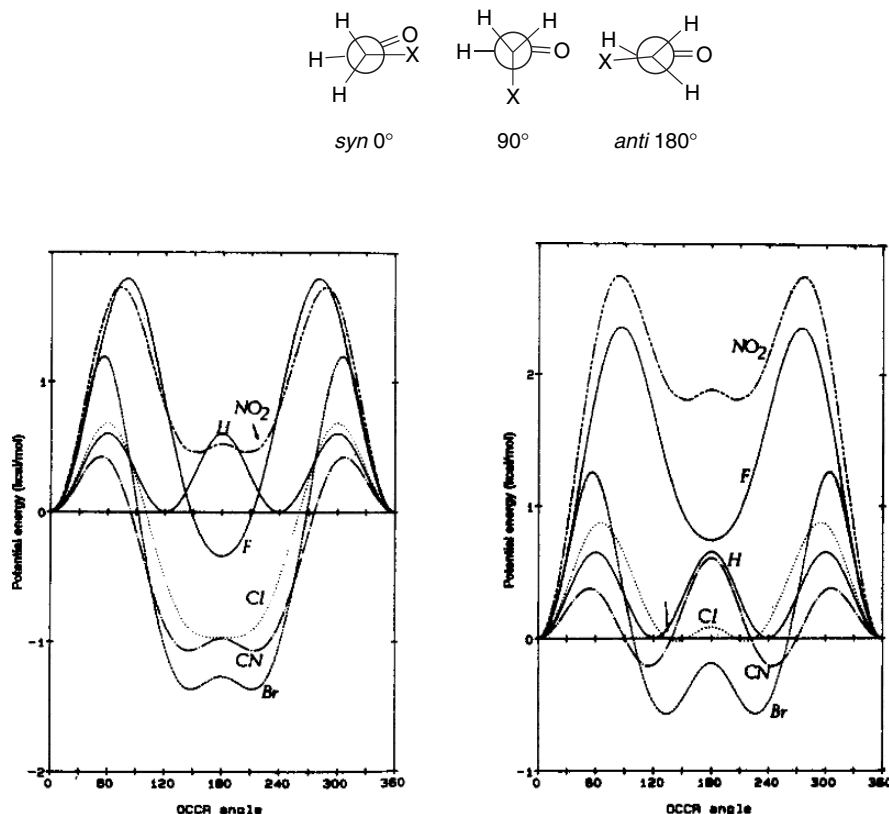


Fig. 2.22P. (a) Rotational profile of the isolated molecules. (b) Rotational profile in solvent cavity with dielectric constant 4.7. Reproduced by permission of Elsevier.

2.23. Provide a mechanistic explanation, including proposed transition structure(s), to account for the stereoselectivity observed in the following reactions:

a.

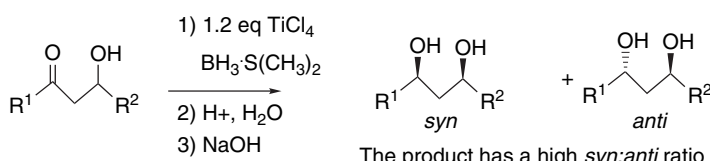
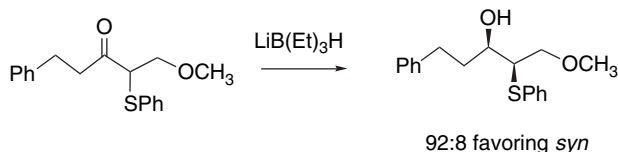


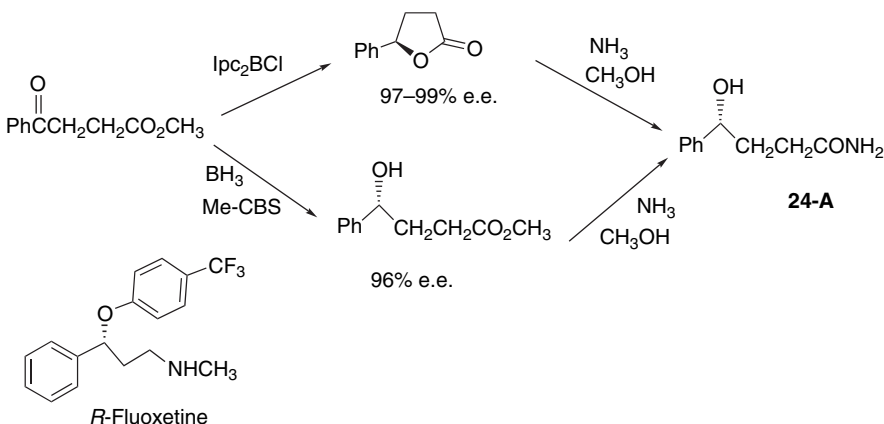
Table 2.22P. Energy Difference between *syn* and *anti* Conformations

Substituent	$E_{syn} - E_{anti}$ (kcal/mol)	$\varepsilon = 4.7$
	Vacuum	
H	+0.60	+0.65
F	-0.34	+0.74
Cl	-0.97	-0.02
Br	-1.36	-0.57
CN	-1.07	-0.21
NO ₂	+0.46	+1.85

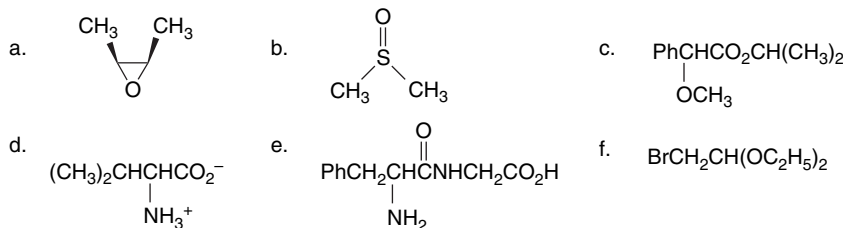
b.



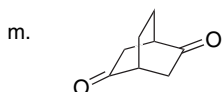
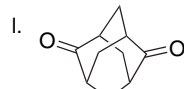
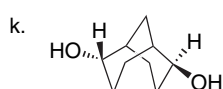
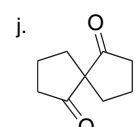
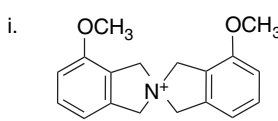
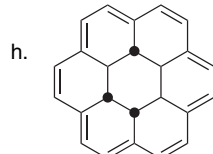
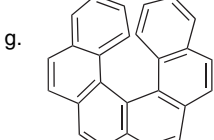
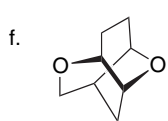
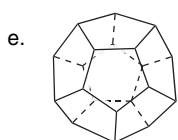
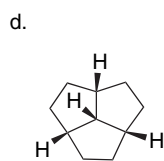
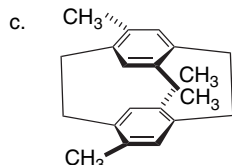
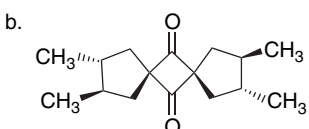
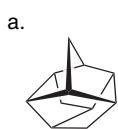
- 2.24. Either oxaborazolidine-catalysis (Me-CBS) or (Ipc)₂BCl reductions can be used to prepare **24-A** a precursor of Fluoxetine (Prozac®) in good yield and high e.e. Suggest transition structures that account for the observed enantioselectivity.



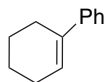
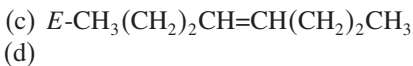
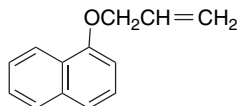
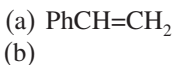
- 2.25 Some of the compounds shown below contain enantiotopic or diastereotopic atoms or groups. Which possess this characteristic? For those that do, indicate the atoms or groups that are diastereotopic and assign the groups as *pro-R* and *pro-S*.



2.26. Indicate which of the following structures are chiral. For each molecule that is achiral, indicate an element of symmetry that is present in the molecule.



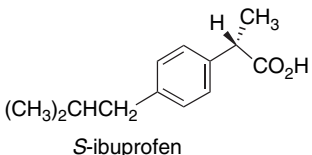
2.27. Predict the absolute configuration of the diols obtained from each of the following alkenes using either a dihydroquinidine or a dihydroquinine type dihydroxylation catalysts.



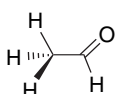
2.28. Based on the standard transition state models, predict the absolute configuration of the products of the following reactions:

- Reduction of 1-phenyl-1-propanone by $\text{BH}_3\text{-THF}$ using the oxaborazolidine catalyst derived from (*S*)- α , α -diphenylpyrrolidine-2-methanol.
- Reduction of 1,1,1-trifluorodec-3-yn-one by (*S*)-Alpine borane.
- Sharpless asymmetric epoxidation of *E*-hex-2-en-1-ol using (+)-diethyl tartrate.

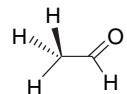
- 2.29. Ibuprofen, an example of an NSAID, is the active ingredient in several popular over-the-counter analgesics. In the United States, it is sold in racemic form, even though only the *S*-enantiomer is pharmacologically active. Suggest methods that might be used to obtain or prepare ibuprofen in enantiomerically pure form, based on processes and reactions discussed in chapter 2.



- 2.30. Ab initio MO calculations (HF/4-31G) indicate that the eclipsed conformation of acetaldehyde is about 1.1 kcal more stable than the staggered conformation. Provide an explanation of this effect in terms of MO theory. Construct a qualitative MO diagram and point out the significant differences that favor the eclipsed conformation. Identify the interactions that are stabilizing and those that are destabilizing. Identify other factors that need to be considered to analyze the origin of the rotational barrier.

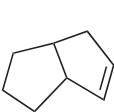


$E = 152.685 \text{ au}$
eclipsed



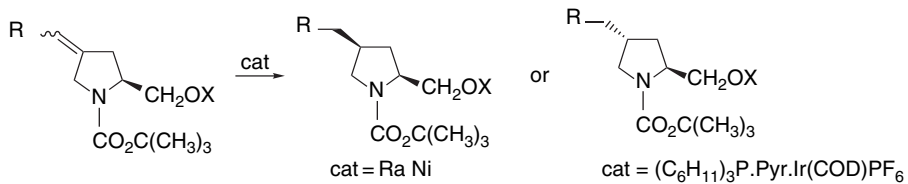
$E = 152.683 \text{ au}$
staggered

- 2.31. Treatment of alkylphosphoryl dichlorides with 1 equiv. of *L*-proline ethyl ester in the presence of 1-methylimidazole (acting as an acid-scavenger) leads to formation of a monophosphoramidate with low (< 20% diastereoselectivity). Addition of 0.25 equiv. of 4-nitrophenol then gives a 4-nitrophenylphosphoramidate with high (98%) diastereoselectivity, which in turn can be treated with methanol to isolate the methyl 4-nitrophenylphosphonate ester in high enantiomeric purity. This constitutes a kinetic resolution process. Write a mechanistic scheme that accounts for this series of transformations.
- 2.32. Use an appropriate computation program to compare the TS energies for hydroboration of the following alkenes by $(\text{CH}_3)_2\text{BH}$. Predict the *exo:endo* ratio for each compound. What factor might complicate the interpretation of the *exo:endo* ratio?



- 2.33. 9-BBN exhibits a high degree of stereoselectivity toward 1,3-dimethyl cycloalkenes such as 1,3-dimethylcyclopentene and 1,3-dimethylcyclohexene, giving exclusively the *trans, trans*-2,6-dimethyl cycloalkanols. Offer an explanation.
- 2.34. Diastereoselective reduction of a number of 4-alkyleneprolinols has been accomplished. With a silyl protecting group in place, using Raney nickel, the

cis isomers are formed in ratio of about 15:1. When the unprotected alcohols are used with the Crabtree catalyst, quite high selectivity for the *trans* isomer is found. Explain these results.



R	X = <i>t</i> -Butyldimethylsilyl	X = H
C_2H_5	13:1	>40:1
Ph	15:1	>40:1
CH_3O_2C	15:1	16:1

Structural Effects on Stability and Reactivity

Introduction

The concepts of *stability* and *reactivity* are fundamental to understanding chemistry. In this chapter we consider first the *thermodynamic* definition of chemical stability. We then consider *chemical kinetics* (Section 3.2) and how it can provide information about reactivity. We also explore how structure influences stability and reactivity. We want to learn how to make predictions about reactivity based on the structure of the reactants and intermediates. We begin by reviewing the principles of thermodynamics and kinetics, which provide the basis for understanding the relationship of structure to stability and reactivity.

Reactions are usefully described in terms of potential energy diagrams such as shown in Figure 3.1, which identify the potential energy changes associated with the reacting molecules as they proceed to products. The diagram plots the free energy of the system as a function of the progress of the reaction. For each individual step in the reaction there is a *transition state* representing the highest energy arrangement of the molecules for that step. The successive *intermediates* are the molecules that are formed and then react further in the course of the overall reaction. The energies of the transition states relative to the reactants determine the rate of reaction. The energy difference between the reactants and products is ΔG , the free-energy change associated with the reaction. The free energy of a chemical reaction is defined by the equation

$$\Delta G = \Delta H - T\Delta S \quad (3.1)$$

where ΔH is the *enthalpy change* and ΔS is the *entropy change* for the reaction. The enthalpy term is a measure of the stability of the molecule and is determined by the strength of the chemical bonds in the structure. The entropy term specifies the change

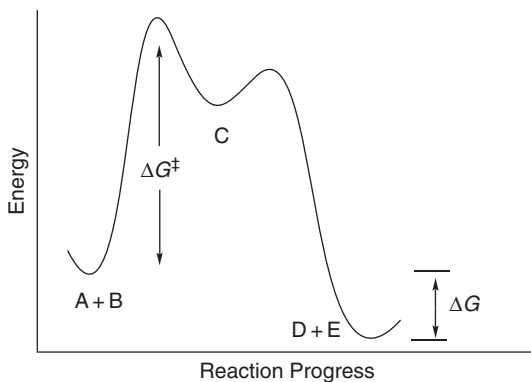


Fig. 3.1. Reaction potential energy profile showing transition states and intermediate for a reaction $A + B \rightarrow C \rightarrow D + E$.

in the order (probability) associated with the reaction. The *free energy* of the reaction, ΔG , determines the position of the equilibrium for the reaction:

$$\Delta G = -RT \ln K \quad (3.2)$$

where K is the equilibrium constant for the reaction:

$$K = \frac{[D][E]}{[A][B]}$$

The energy required to proceed from reactants to products is ΔG^\ddagger , *the free energy of activation*, which is the energy at the transition state relative to the reactants. We develop the theoretical foundation for these ideas about reaction rates in Section 3.2. We first focus attention on the methods for evaluating the inherent thermodynamic stability of representative molecules. In Section 3.3, we consider general concepts that interrelate the thermodynamic and kinetic aspects of reactivity. In Section 3.4, we consider how substituents affect the stability of important intermediates, such as carbocations, carbanions, radicals, and carbonyl addition (tetrahedral) intermediates. In Section 3.5, we examine quantitative treatments of substituent effects. In the final sections of the chapter we consider catalysis and the effect of the solvent medium on reaction rates and mechanisms.

3.1. Thermodynamic Stability

Thermodynamic data provide an unambiguous measure of the stability of a particular compound under specified conditions. The thermodynamic measure of molecular stability is ΔH_f° , the *standard enthalpy of formation*, which gives the enthalpy of the compound relative to the reference state of its constituent elements under standard conditions of 1 atm and 298 K. For each element a particular form is assigned an enthalpy (potential energy content) of 0. For example, for hydrogen, nitrogen, oxygen, and fluorine, the gaseous diatomic molecules are the reference states. For carbon, 0 energy is assigned to graphite ($C_{(g)}$), which consists entirely of sp^2

carbon atoms. The ΔH_f° of compounds can be measured directly or indirectly. The ΔH_f° in kcal/mol of HF, H_2O , NH_3 , and CH_4 are found to be as follows:

	ΔH_f°
$1/2 \text{H}_2 + 1/2 \text{F}_2 \longrightarrow \text{HF}$	-136.9
$\text{H}_2 + 1/2 \text{O}_2 \longrightarrow \text{H}_2\text{O}$	-68.3
$3/2 \text{H}_2 + 1/2 \text{N}_2 \longrightarrow \text{NH}_3$	-11.0
$2\text{H}_2 + \text{C}_{(g)} \longrightarrow \text{CH}_4$	-17.8

The ΔH_f° of a given compound is a physical constant and is independent of the process by which the compound is formed. Therefore, ΔH_f° values are additive and can be calculated precisely for balanced chemical equations if all the necessary data are available. For example, it might be experimentally impossible to measure the ΔH_f° of methane directly by calorimetry, but it can be calculated as the sum of the enthalpy for an equivalent reaction sequence, e.g.:

ΔH° (kcal/mol)		
$\text{C}_{(g)} + 1/2 \text{O}_2 \longrightarrow \text{:C}\equiv\text{O}:+$	-26.4	
$\text{:C}\equiv\text{O}:+ + 3\text{H}_2 \longrightarrow \text{CH}_4 + \text{H}_2\text{O}$	-59.7	
$\text{H}_2\text{O} \longrightarrow \text{H}_2 + 1/2 \text{O}_2$	+68.3	
$\text{C}_{(g)} + 2\text{H}_2 \longrightarrow \text{CH}_4$	-17.8	

The ΔH_f° for many compounds has been determined experimentally and the data tabulated.¹ In the sections that follow, we discuss approaches to computing ΔH_f° when the experimental data are not available. It is important to note that direct comparison of the ΔH_f° values for nonisomeric compounds is not meaningful. The ΔH_f° for methane through hydrogen fluoride, for example, gives us no comparative information on stability, because the reference points are the individual elements. Other information is needed to examine relative stability. For example, as is discussed in the next section, it is possible to assign *bond energies* to the bonds in CH_4 , NH_3 , H_2O , and HF. This is the energy required to break a C–H, N–H, O–H, or H–F bond. These numbers do begin to provide some basis for comparison of the properties of nonisomeric compounds, as we now see that the X–H bonds become stronger as we go from C to F in the second-row compounds with hydrogen.

Compound	X–H bond energy (kcal/mol)
CH_4	105.0
NH_3	108.2
H_2O	119.3
HF	136.4

¹. J. B. Pedley, R. D. Naylor, and S. P. Kirby, *Thermochemical Data of Organic Compounds*, 2nd Edition, Chapman and Hall, London, 1986; H. Y. Afeefy, J. F. Liebman, and S. E. Stein, in *NIST Chemistry Webbook*, NIST Standard Reference Database Number 69, P. J. Linstrom and W. G. Mallard, eds., 2001 (<http://webbook.nist.gov>).

3.1.1. Relationship between Structure and Thermodynamic Stability for Hydrocarbons

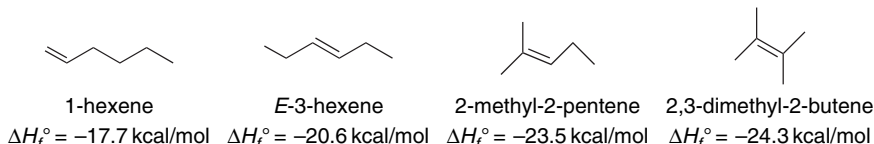
Extensive thermodynamic data are available for the major classes of hydrocarbons. Table 3.1 gives data for the C₄–C₆ and C₈ alkanes and the C₄–C₆ alkenes, and several general relationships become apparent. One is that *chain branching increases the stability of alkanes*. This relationship is clear, for example, in the data for the C₆ alkanes, with a total enthalpy difference of nearly 4 kcal/mol between the straight-chain hexane and the tetra-substituted 2,2-dimethylbutane. There is a similar range of 4.5 kcal/mol between the least stable (octane) and most stable

Table 3.1. Standard Enthalpy of Formation of Some Hydrocarbons (in kcal/mol)^a

Alkanes (liquid)			
C ₄		C ₈	
Butane	−35.0	Octane	−59.8
2-Methylpropane	−36.7	2-Methylheptane	−60.9
		3-Methylheptane	−60.3
C ₅		4-Methylheptane	−60.1
Pentane	−41.5	2,2-Dimethylhexane	−62.6
2-Methylbutane	−42.7	2,3-Dimethylhexane	−60.4
2,2-Dimethylpropane	−45.5	2,4-Dimethylhexane	−61.4
		2,5-Dimethylhexane	−62.2
C ₆		3,4-Dimethylhexane	−60.2
Hexane	−47.5	3,3-Dimethylhexane	−61.5
2-Methylpentane	−48.9	2,2,3-Trimethylpentane	−61.4
3-Methylpentane	−48.4	2,2,4-Trimethylpentane	−62.0
2,3-Dimethylbutane	−49.6	2,3,4-Trimethylpentane	−60.9
2,2-Dimethylbutane	−51.1	2,3,3-Trimethylpentane	−60.6
		3-Ethyl-2-methylpentane	−59.7
		3-Ethyl-3-methylpentane	−60.4
		2,2,3,3-Tetramethylbutane	−64.3
B. Alkenes (liquid)			
C ₄		C ₆	
1-Butene	−4.90	1-Hexene	−17.7
E-2-Butene	−7.89	E-2-Hexene	−20.4
Z-2-Butene	−7.10	Z-2-Hexene	−20.1
2-Methylpropene	−8.96	E-3-Hexene	−20.6
		Z-3-Hexene	−18.9
C ₅		2-Methyl-1-pentene	−21.5
1-Pentene	−11.2	3-Methyl-1-pentene	−18.7
E-2-Pentene	−13.9	4-Methyl-1-pentene	−19.1
Z-2-Pentene	−12.8	2-Methyl-2-pentene	−23.5
2-Methyl-1-butene	−12.3	3-Methyl-2-pentene	−22.6
3-Methyl-1-butene	−16.4	E-3-Methyl-2-pentene	−22.6
		Z-3-Methyl-2-pentene	−22.6
		E-4-Methyl-2-pentene	−21.9
		Z-4-Methyl-2-pentene	−20.8
		2,3-Dimethyl-1-butene	−22.3
		3,3-Dimethyl-1-butene	−20.9
		2-Ethyl-1-butene	−20.8
		3,3-Dimethyl-1-butene	−20.9
		2,3-Dimethyl-2-butene	−24.3

a. From *Thermochemical Data of Organic Compounds*, 2nd Edition, J. B. Pedley, R. O. Naylor, and S. P. Kirby, Chapman and Hall, London, 1986.

(2,2,3,3-tetramethylbutane) of the C₈ isomers. For alkenes, substitution on the double bond is stabilizing. There is a range of nearly 7 kcal/mol for the C₆H₁₂ isomers. The data for C₆ alkenes, for example show:



These relationships are a result of the stabilizing effect of branching and double-bond substitution and hold quite generally, except when branching or substitution results in van der Waals repulsions (see Section 2.3), which have a destabilizing effect.

3.1.2. Calculation of Enthalpy of Formation and Enthalpy of Reaction

In Chapter 1, we introduced various concepts of structure and the idea that the properties of molecules are derived from the combination of the properties of the atoms. One of the qualitative conclusions from these considerations is that the properties of CH₃, CH₂, CH, and C groups in hydrocarbons are expected to be similar from molecule to molecule, as long as they are not perturbed by a nearby functional group. Several methods for the calculation of thermodynamic data based on summation of group properties have been developed and are discussed in the next two sections.

3.1.2.1. Calculations of Enthalpy of Reaction Based on Summation of Bond Energies. The computation of molecular energy by MO or DFT methods gives the *total binding energy* of a molecule. This is a very large number, since it includes all the electron-nuclei forces in the atoms, not just the additional attractive forces of the bonding electrons. The total energy can be converted to an energy representing all bonding between atoms by subtracting the energy of the individual atoms. This difference in energy is called the *energy of atomization*. This quantity still represents an energy that is far larger than the change involved in chemical reactions, which is of primary interest to chemists. The focus of chemical reactivity is on the bonds that are being formed and broken in the reaction. Useful relationships between structure and reactivity can be developed by focusing on *bond dissociation energies* (BDE). The most completely developed information pertains to *homolytic bond dissociation*,² which is the energy required to break a specific bond in a molecule with one electron going to each of the atoms. From the general bond energies in Part A of Table 3.2 we can discern several trends. One is that C–C bonds are considerably stronger than the other homonuclear bonds for the second-row elements (compare with O–O and N–N bonds). We can also note that the bonds in the dihalogens are relatively weak, with a somewhat irregular trend with respect to position in the periodic table: F₂ < Cl₂ > Br₂ > I₂. The bonds to hydrogen are also slightly irregular: N < C < O < F. For the hydrogen halides, there is a sharp drop going down the periodic table.

It is known that the immediate molecular environment significantly affects the bond energy, as is illustrated by the data in Part B of Table 3.2. For hydrocarbons the C–H bond dissociation energy depends on the degree of substitution and hybridization

². For a discussion of the measurement and application of bond dissociation energies, see S. J. Blanksby and G. B. Ellison, *Acc. Chem. Res.*, **36**, 255 (2003).

Table 3.2. Bond Energies (in kcal/mol)

A. Some Generalized Bond Energies ^a					
C–C	81	C–H	98	C=C	145
N–N	65	N–H	92	C≡C	198
O–O	34	O–H	105	N≡N	225
F–F	38	F–H	136	C=O	173
Cl–Cl	57	Cl–H	102	C–O	79
Br–Br	45	Br–H	87	C–N	66
I–I	36	I–H	71		

B. Some Specific Bond Dissociation Energies ^b					
CH ₃ –H	105.0	H ₃ C–CH ₃	90.2	H ₃ C–F	110.0
CH ₃ CH ₂ –H	100.5	H ₅ C ₂ –CH ₃	88.5	H ₃ C–Cl	83.7
(CH ₃) ₂ CH–H	98.1	(CH ₃) ₂ CH–CH ₃	88.2	H ₃ C–Br	70.3
(CH ₃) ₃ C–H	95.7	H ₅ C ₂ –C ₂ H ₅	86.8	H ₃ C–I	57.1
H ₂ C=CH–H	111.2	(CH ₃) ₂ CH–CH(CH ₃) ₂	84.1	CH ₃ CH ₂ –F	113.1
HC≡C–H	132.8	H ₂ C=CHCH ₂ –CH ₃	75.9	CH ₃ CH ₂ –Cl	84.2
H ₂ C=CHCH ₂ –H	88.2	H ₂ C=CH–CH=CH ₂	116.9	CH ₃ CH ₂ –Br	70.0
Ph–H	112.9	H ₂ C=CH ₂	174.1	CH ₃ CH ₂ –I	55.8
PhCH ₂ –H	88.5	HC≡CH	229.5	(CH ₃) ₂ CH–F	115.4
HC≡CHCH ₂ –H	88.9	Ph–CH ₃	102.0	(CH ₃) ₂ CH–Cl	84.6
H ₂ N–H	108.2	PhCH ₂ –CH ₃	76.4	(CH ₃) ₂ CH–Br	71.5
CH ₃ NH–H	101.6			(CH ₃) ₂ CH–I	56.1
CH ₃ O–H	104.2			H ₃ C–OH	92.0

a. From Table 1, G. J. Janz, *Thermodynamic Properties of Organic Compounds*, Academic Press, New York, 1967.

b. Y. R. Luo, *Handbook of Bond Dissociation Energies in Organic Compounds*, CRC Press, Boca Raton, FL, 2002

of the carbon atom. Primary, secondary, and tertiary sp^3 C–H, sp^2 C–H, and sp C–H bonds have characteristic values that are significantly different from one another. The variation in bond strengths is related to the stability of the resulting radicals. For C–H bonds, for example, the decrease in bond strength methane > *pri* > *sec* > *tert* reflects the increasing stability of the more highly substituted carbon radicals. The extra strength of the C–H bond to sp^2 and sp carbons, as reflected by ethene, ethyne, and benzene, is due in part to the poor stability of ethenyl, ethynyl, and phenyl radicals. The relatively weak primary C–H bonds in propene and methylbenzene reflect conjugative stabilization of the resulting allyl and benzyl radicals (see Section 3.4.3).

A direct approach to estimation of the ΔH for a reaction is to apply the fundamental thermodynamic relationship,

$$\Delta H = \Delta H_f^\circ_{\text{reactants}} - \Delta H_f^\circ_{\text{products}} \quad (3.3)$$

This equation is exact, but can be applied only if the thermodynamic data pertaining to the actual reaction conditions are available. Thermodynamic manipulations can be used to account for changes in temperature or pressure, but solvation energies are often uncertain (see Section 3.8). The relationship in Equation (3.3) can be approximated by

$$\Delta H = \text{BDE}_{\text{bonds formed}} - \text{BDE}_{\text{bonds broken}} \quad (3.4)$$

For example, data from Table 3.2 can be used to calculate the ΔH for reaction of each of the halogens with ethane. The strong trend in exothermicity of F₂ > Cl₂ > Br₂ > I₂ is evident:

X	Break		Form		ΔH
	CH ₃ CH ₂ –H	X ₂	CH ₃ CH ₂ –X	H–X	
F	100.5	38	113.1	109	-83.6
Cl	100.5	57	84.2	102	-28.7
Br	100.5	45	70.0	87	-11.5
I	100.5	36	55.8	71	+9.7

While bonds of similar type, e.g., C–C, C–O, C–Cl, are of approximately the same strength, the precise value depends on both hybridization and the degree of substitution. For instance, as can be seen in Table 3.2, there is a range from 105.0 to 95.7 kcal/mol for the C–H bonds in methane, ethane, propane (C(2)–H), and isobutane (C(2)–H). The differences between C–H bonds for sp^3 , sp^2 , and sp carbon is even greater, as can be seen from the significantly different C–H BDE values for ethane, ethene, ethyne, and benzene. Similarly, C–C bonds between sp^2 carbons are considerably stronger than those between two sp^3 carbons, as is indicated by the C(2)–C(3) BDE of 116.9 kcal/mol for 1,3-butadiene. For estimation of reaction enthalpy using Equation (3.4), the most appropriate BDE must be chosen.

3.1.2.2. Relationships between Bond Energies and Electronegativity and Hardness. In his efforts to correlate important chemical properties, Pauling recognized that the difference in electronegativity between two bonded atoms contributes to bond strength. He proposed the empirical relationship

$$\text{BDE}_{AB} = 1/2(\text{BDE}_{AA} + \text{BDE}_{BB}) + 23(\Delta\chi)^2 \quad (3.5)$$

where $\Delta\chi$ is the difference in electronegativity of the two atoms. A related expression is

$$\text{BDE}_{AB} = (\text{BDE}_{AA} \times \text{BDE}_{BB})^{1/2} + 30(\Delta\chi)^2 \quad (3.6)$$

Both relationships propose that BDE is a function of the strength of the two homonuclear bonds and an increment for electronegativity differences.³ Although the quantitative reliability of the relationships in Equations (3.5) and (3.6) is limited, the equations do indicate that there is an increment to bond strength that is related to electronegativity differences. Subsequently, many investigators have probed the accuracy, scope, and theoretical foundation of these relationships and have suggested other formulations that improve the accuracy.⁴ A refinement of the empirical relationship that includes a term for polarizability gives the equation

$$\text{BDE}_{AB} = [\text{BDE}_{AA} \times \text{BDE}_{BB}]^{1/2} + |2.883(\Delta\chi)|^{[\alpha(A)+\alpha(B)]} \quad (3.7)$$

where α are polarizability parameters for each element.⁵ The polarizability parameters particularly improve the relationship for third-row atoms and other highly polarizable groups.

³. L. Pauling, *J. Am. Chem. Soc.*, **54**, 3570 (1932); L. Pauling, *The Nature of the Chemical Bond*, 3rd Edition, Cornell University Press, Ithaca, NY, 1960, Chap. 3.

⁴. R. R. Reddy, T. V. R. Rao, and R. Viswanath, *J. Am. Chem. Soc.*, **111**, 2914 (1989).

⁵. J. W. Ochterski, G. A. Petersson, and K. B. Wiberg, *J. Am. Chem. Soc.*, **117**, 11299 (1995).

The original Pauling equation was reexamined recently by Zavitsas and co-workers.⁶ The equation was shown to give quite good agreement with thermochemical data. Furthermore, it permitted assignment of electronegativity and *stabilization energy* to important radicals. The stabilization energy SE is assigned as

$$SE = 1/2(BDE_{[CH_3-CH_3]} - BDE_{[X-X]}) \quad (3.8)$$

Some values are given in Table 3.3. For future reference, note the order of radical stabilization: alkyl > alkenyl > alkynyl and allyl > benzyl > tertiary > secondary > primary. In Section 3.4.3, we discuss the structural basis of these relationships.

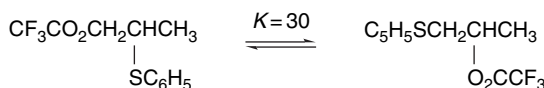
Another idea underlying the nature of bond formation is the concept of *electronegativity equalization*⁷ or *electronegativity equilibration*⁸ (see Section 1.1.4). This concept states that electron density flows from the less electronegative partner in a bond (making it more positive and therefore more electronegative) to the more electronegative atom (making it more negative and therefore less electronegative) until both atoms have the same effective electronegativity. At that point, there is no net attractive force on the electrons in the bond. This intuitively compelling idea has a theoretical foundation in DFT, which states that the electronic chemical potential μ is uniform throughout a molecule. It is observed that the apparent bond strength for several series of compounds increases in the order $CH_3 - X < pri - X < sec - X, tert - X$.⁹ The differences *increase* with the electronegativity of the substituent X. These electronegativity relationships lead to some qualitative trends. For alkyl groups with electronegative substituents, such as halogens, oxygen, or nitrogen, the trend is *tert* > *sec* > *pri* > CH_3 . On the other hand, for organometallics, alanes, and boranes, the order is reversed. Compounds that can readily interconvert can isomerize in response to these stability relationships.¹⁰

**Table 3.3. Group Electronegativity and Stabilization Energies (in kcal/mol)
Based on the Pauling Equation^a**

Group	X	SE	Group	X	SE
CH_3	2.525	0.0	HO	3.500	
C_2H_5	2.462	1.2	CH_3O	3.439	26.0
<i>i</i> – C_3H_7	2.411	1.4	PhO	3.376	43.1
<i>t</i> – C_4H_9	2.378	3.7	CH_3NH	3.018	13.5
$CH_2=CHCH_2$	2.488	14.3	$(CH_3)_3Si$	1.838	5.9
$PhCH_2$	2.506	11.7	F	3.938	25.9
Ph	–13.1		Cl	3.174	15.9
$CH_2=CH$	–11.6				
$HC\equiv C$	–32.1				
$CH_3C=O$	7.9				

a. N. Matsunaga, D. W. Rogers, and A. A. Zavitsas, *J. Org. Chem.*, **68**, 3158 (2003).

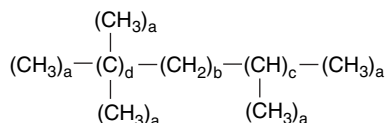
- ⁶. N. Matsunaga, D. W. Rogers, and A. A. Zavitsas, *J. Org. Chem.*, **68**, 3158 (2003).
- ⁷. S. G. Bratsch, *J. Chem. Educ.*, **61**, 588 (1984); R. T. Sanderson, *Polar Covalence*, Academic Press, New York, 1983.
- ⁸. D. W. Smith, *J. Chem. Educ.*, **67**, 559 (1990).
- ⁹. Y. R. Luo and S. W. Benson, *J. Phys. Chem.*, **92**, 5255 (1988); Y. R. Luo and S. W. Benson, *Acc. Chem. Res.*, **25**, 375 (1992); N. Laurencelle and P. D. Pacey, *J. Am. Chem. Soc.*, **115**, 625 (1993).
- ¹⁰. J. N. Harvey and H. G. Viehe, *J. Prakt. Chem. Chem. Zeitung*, **337**, 253 (1995).



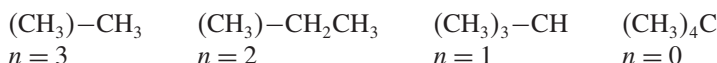
Isomer with the more electronegative substituent on the more highly substituted site is the more stable compound.

These treatments of bond energies illustrate that there are fundamental relationships between bond strengths and atomic properties such as electronegativity and polarizability. The crucial point is that bond strength *is increased by electronegativity differences in a given row of the periodic table* as a result of an increment that is due to electrostatic attraction.

3.1.2.3. Calculation of ΔH_f Using Transferable Group Equivalents. The idea that the properties of molecules are the sum of its component atoms and groups has led to the development of schemes by which thermodynamic properties can be calculated as the sum of contributions from all structural units.¹¹ The most highly developed is that of S. W. Benson and co-workers.¹² The molecule is divided into its component groups. For example, isoctane (which incidentally is the standard for 100 in octane ratings) consists of five C–(C)(H)₃ (a), one C–(C)₂(H)₂ (b), one C–(C)₃(H) (c), and one C–(C)₄ (d), as labeled on the structure.



The four groups designated above are sufficient to describe all alkanes. Finer distinctions can be made if these groups are subdivided further, depending on the number of hydrogens on the adjacent carbon. For example, a CH₃ group might be found in four different environments:



Modified increments are also assigned to carbons adjacent to double or triple bonds or benzene rings. The enthalpy of formation of a molecule can then be calculated as the sum of the contributions of the component groups. The main limitation of this method is that it does not explicitly consider long-range nonbonded interactions. The group equivalents refer to *strain-free molecules*. Further refinement can be incorporated by taking account of nonbonded interactions. For example, *gauche* interactions can be counted and applied as a correction to the sum of group equivalents.¹³

¹¹. For a discussion of the pioneering efforts in this field, see J. D. Cox and G. Pilcher, *Thermochemistry of Organic and Organometallic Compounds*, Academic Press, New York, 1970, Chap. 7.

¹². N. Cohen and S. W. Benson, *Chem. Rev.*, **93**, 2419 (1993).

¹³. N. Cohen and S. W. Benson, *The Chemistry of Alkanes and Cycloalkanes*, S. Patai and Z. Rappoport, eds., Wiley, 1992, Chap. 6; S. W. Benson and N. Cohen, in *Computational Thermodynamics*, K. K. Irikura and D. J. Frurip, eds., *ACS Symposium Series*, **677**, 20 (1996).

CHAPTER 3

Structural Effects on Stability and Reactivity

5 C-(C)(H ₃) _a	-10.00	-50.00
1 C(C) ₂ (H ₂) _b	-5.00	-5.00
1 C(C) ₃ (H) _c	-2.40	-2.40
1 3C(C) ₄	-0.10	-0.10
3 <i>gauche</i> correction	-0.80	+2.40
Calculated value		-55.10

Group equivalent methods can be extended to functionalized compounds by assigning the enthalpy components of the substituent groups.¹⁴

Various other methods for making calculations based on bond dissociation energies more precise have been developed. A method developed by G. Leroy and co-workers is based on extensive thermochemical data, as well as energies calculated by MO methods.¹⁵ The heat of atomization of unstrained hydrocarbons is equated to the number of C–C and primary, secondary and tertiary C–H bonds. The heat of atomization is given by

$$\Delta H_{\text{atom}} = N_{\text{cc}}(E_{\text{cc}}) + N_{\text{pri}}(E_{\text{C-H}_{\text{pri}}}) + N_{\text{sec}}(E_{\text{C-H}_{\text{sec}}}) + N_{\text{tert}}(E_{\text{CH}_{\text{tert}}}) \quad (3.9)$$

For stable compounds with known ΔH_{atom} the stabilization (or destabilization) is then the difference between ΔH_{atom} and the calculated sum of standard bond energies:

$$\text{SE} = \Delta H_{\text{atom}} - \sum \text{BE}_{\text{standard}} \quad (3.10)$$

Leroy and co-workers developed an extensive series of standard bond energy terms. Terms for specific substituent effects were also assigned, e.g., the $\Delta(\text{C}_d-\text{C})$ and $\Delta(\text{C}-\text{H})^0$ terms are adjustments for bonds between double bonds and having oxygen substituents, respectively. Comparison of the sum of the standard BE with the actual ΔH_{atom} gives the extra stabilization present in the compound. Calculations for butadiene stabilization (conjugation) and dimethoxymethane (anomeric effect) are given below.

	Butadiene		Dimethoxymethane	
Bond energies:	2E(C=C)	2(137.23)	Bond energies	4E(C–O)
	4E(C _d –H) ₂	4(100.30)		2E(C–H) _s
	2E(C _d –H) ₁	2(99.78)		4Δ(C–H) _s ⁰
	E(C–C)	85.44		4(–2.05)
	2Δ(C _d ^c –C)	2(3.88)		6E(C–H) _p ⁰
	ΣN _{AB} B _{AB} =	968.42 kcal/mol ⁻¹		6(95.87)
ΔH _{atom}		971.5	ΣN _{AB} B _{AB} =	1128.72 kcal/mol ⁻¹
	SE	3.08 kcal/mol	ΔH _{atom}	1133.06
			SE	4.34 kcal/mol

The enthalpy change of a homolytic bond dissociation is expressed as the difference in stabilization of the products and reactants. A virtue of this approach is

¹⁴. J. B. Pedley, R. D. Naylor, and S. P. Kirby, *Thermochemical Data of Organic Compounds*, 2nd Edition, Chapman and Hall, London, 1986, Chap. 2.

¹⁵. G. Leroy, M. Sana, and C. Wilante, *J. Mol. Structure: Theochem.*, **234**, 303 (1991).

that it recognizes that there may be special stabilization, e.g., conjugation and anomeric effects, in the reactants as well as in the dissociated radicals.

$$\text{BDE} = \sum_{\text{R-Z}} \text{BE}_{\text{standard}} - \sum_{\text{R}\cdot} \text{BE}_{\text{standard}} - \sum_{\text{Z}\cdot} \text{BE} + \text{SE}_{\text{R-Z}} - \text{SE}_{\text{R}\cdot} - \text{SE}_{\text{Z}\cdot} \quad (3.11)$$

Table 3.4 gives some representative results.

According to this analysis, the weakening of the C–H bonds in isobutane and toluene is largely due to the stabilization of the resulting radicals. However, even though trichloromethyl radicals are quite stable, there is also considerable stabilization in the starting material chloroform, and the C–H bond in chloroform is not weakened as much as that in isobutane. More is said about separating structural effects in reactant and intermediate radicals in Topic 11.1.

The calculation of ΔH_f° is now usually done by computational chemistry, but the success of the group equivalent approaches makes an important point. The properties of groups are very similar from molecule to molecule, similar enough to make additivity schemes workable. However, *specific interactions*, e.g., nonbonded interactions, that depend on the detailed structure of the molecule are not accounted for. Whenever interactions that are not accounted for by the group equivalents exist, there will be a discrepancy between the calculated and actual properties of the molecule. Analyses such as that of Leroy can provide valuable insights and concepts. In particular, they provide a means for recognizing stabilization effects present in reactants, as demonstrated by the calculations for 1,3-butadiene and dimethoxymethane.

3.1.2.4. Calculation of Enthalpy of Formation by Molecular Mechanics. Molecular mechanics (MM) is a systematic approach to the calculation of molecular energy based on the summation of bond properties and nonbonding (e.g., van der Waals) interactions (review Section 2.4). MM provides a means for analyzing the energy differences between molecules and among various geometries of a particular molecule.¹⁶ Several systems of parameters and equations for carrying out the calculations have been developed. The method most frequently used in organic chemistry is the one developed by N. L. Allinger and co-workers.¹⁷ In the most recent version of MM calculations

**Table 3.4. Calculation of the C–X Bond Dissociation Energies
(in kcal/mol; 298.15 K)**

R–X	$\Delta \Sigma N_{AB} E_{AB}$	$\text{SE}_0(\text{R}-\text{X})$	$\text{SE}_0(\text{R}\cdot)$	BDE(R–X)
Et–H	99.8	0	0	100.3
t-Bu–H	96.8	0.8	3.7	93.9
Et–Cl	83.3	0	-0.5	83.8
t-Bu–Cl	85.6	0	3.7	81.9
C ₆ H ₅ CH ₂ –H	99.8	-1.0	11.6	87.1
(t-Bu) ₂ CH–H	98.2	-6.0	-5.9	98.2
Cl ₃ C–H	93.9	-16.3	-18.0	95.7

¹⁶ F. H. Westheimer, in *Steric Effects in Organic Chemistry*, M. S. Newman, ed., Wiley, New York, 1956, Chap. 12; J. E. Williams, P. J. Stang, and P. v. R. Schleyer, *Annu. Rev. Phys. Chem.*, **19**, 531 (1968); D. B. Boyd and K. P. Lipkowitz, *J. Chem. Educ.*, **59**, 269 (1982); P. J. Cox, *J. Chem. Ed.*, **59**, 275 (1982); N. L. Allinger, *Adv. Phys. Org. Chem.*, **13**, 1 (1976); E. Osawa and H. Musso, *Top. Stereochem.*, **13**, 117 (1982); U. Burkett and N. L. Allinger, *Molecular Mechanics*, ACS Monograph 177, American Chemical Society, Washington, DC, 1982.

¹⁷ N. L. Allinger, Y. H. Yuh, and J. -H. Li, *J. Am. Chem. Soc.*, **111**, 8551 (1989).

for organic molecules, known as MM4,¹⁸ the computations involve iterations to locate an energy minimum. Precautions must be taken to establish that a true (“global”) minimum, as opposed to a local minimum energy, is found. This can be accomplished by using a number of different initial geometries and comparing the structures of the minima that are located. As with the group equivalent approach, MM calculations of ΔH_f° are grounded in experimental measurements of a limited number of molecules that were used to optimize the parameters. The original parameters pertained to hydrocarbons, but as the method has developed, the parameters have been extended to many functional groups. MM calculations specifically take molecular geometry into account, including nonbonded and dipolar interactions. Van der Waals interactions are described in terms of energy functions and parameters that describe the interaction of the approaching atoms. Polar interactions are modeled as electrostatic interactions.

Heats of formation are calculated as a sum of the bond energies and other stabilizing and destabilizing (e.g., strain) increments for the structure. MM4 calculations include terms for contributions of higher-energy conformations.¹⁹ For a set of hydrocarbons ranging from methane and ethane to adamantane and bicyclo[2.2.2]octane, the heats of formation are calculated with a standard deviation of 0.353 kcal/mol. The MM4 system has also been applied to alkenes,²⁰ aldehydes,²¹ and ketones.²²

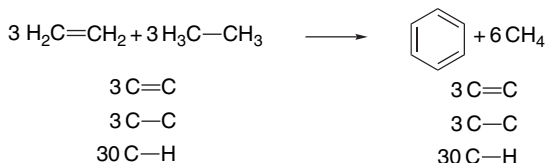
3.1.2.5. Thermodynamic Data from MO and DFT Computations. MO and DFT calculations provide another approach to obtaining thermodynamic data. The accuracy with which the various computational methods reproduce molecular energies varies. Of the semiempirical methods only MINDO,²³ MNDO²⁴, AM1,²⁵ and PM3²⁶ provide reliable estimates of energies and the range of applicability is open to some discussion.²⁷ Among the ab initio methods the level of accuracy generally increases with larger basis sets and treatment of correlation effects. G1, G2, and G3 computations can achieve a level of accuracy that permits comparison of energy data among related molecules. DFT calculations have also been applied to various compounds.²⁸ Users of computational thermochemical data must critically assess the reliability of the method being applied in the *particular case* under study.

A large series of compounds, including hydrocarbon derivatives, was studied at the G2 and G2(MP2,SVP) levels and compared with results from the B3LYP method.²⁹ Another group carried out a similar comparison on a smaller set of molecules.³⁰

- ¹⁸ N. L. Allinger, K. Chen, and J. -H. Lii, *J. Comput. Chem.*, **17**, 642 (1996).
- ¹⁹ N. L. Allinger, L. R. Schmitz, I. Motoc, C. Bender, and J. Labanowski, *J. Phys. Org. Chem.*, **3**, 732 (1990); N. L. Allinger, L. R. Schmitz, I. Motoc, C. Bender, and J. Labanowski, *J. Am. Chem. Soc.*, **114**, 2880 (1992).
- ²⁰ N. Nevins, K. Chen, and N. L. Allinger, *J. Comput. Chem.*, **17**, 695 (1996).
- ²¹ C. H. Langley, J. H. Lii, and N. L. Allinger, *J. Comput. Chem.*, **22**, 1396 (2001).
- ²² C. H. Langley, J. H. Lii, and N. L. Allinger, *J. Comput. Chem.*, **22**, 1426, 1451, 1476 (2001).
- ²³ R. C. Bingham, M. J. S. Dewar, and D. H. Lo, *J. Am. Chem. Soc.*, **97**, 1294 (1975).
- ²⁴ M. J. S. Dewar and G. P. Ford, *J. Am. Chem. Soc.*, **101**, 5558 (1979).
- ²⁵ M. J. S. Dewar, E. G. Zoebisch, E. F. Healy, and J. J. P. Stewart, *J. Am. Chem. Soc.*, **107**, 3902 (1985).
- ²⁶ J. J. P. Stewart, *J. Comput. Chem.*, **10**, 221 (1989).
- ²⁷ J. A. Pople, *J. Am. Chem. Soc.*, **97**, 5307 (1975); T. A. Halgren, D. A. Kleier, J. H. Hall, Jr., L. D. Brown, and W. L. Lipscomb, *J. Am. Chem. Soc.*, **100**, 6595 (1978); M. J. S. Dewar and D. M. Storch, *J. Am. Chem. Soc.*, **107**, 3898 (1985).
- ²⁸ K. Raghavachari, B. B. Stefanov, and L. A. Curtiss, *Molec. Phys.*, **91**, 555 (1997); B. S. Jursic, *Theochem*, **391**, 75 (1997); B. S. Jursic, *Theochem*, **417**, 99 (1997); J. Andzelm, J. Baker, A. Scheiner, and M. Wrinn, *Int. J. Quantum Chem.*, **56**, 733 (1995).
- ²⁹ L. A. Curtiss, K. Raghavachari, P. C. Redfern, and J. A. Pople, *J. Chem. Phys.*, **106**, 1063 (1997).
- ³⁰ J.-W. Pan, D. W. Rogers, and F. J. McLafferty, *Theochem*, **468**, 59 (1999).

Table 3.5 includes the B3LYP/6–311 + G(3df,2p) results for some small hydrocarbons. MO and DFT calculations pertain to molecules at 0 K without any molecular motion. In order to make comparisons with thermodynamic data at 298 K, corrections for both zero-point energy (ZPE) and the difference in thermal energy must be made. The corrections are normally incorporated into calculations intended for thermochemical comparisons. The corrections are based on calculation of the vibrations and rotations that contribute to ZPE and thermal energy. Table 3.5 gives a comparison of some calculated ΔH_f with experimental values for some simple hydrocarbons. The absolute errors are small for methods such as G2, CBS-Q, and CBS-QB. There are some indications that B3LYP calculations tend to underestimate the stability of hydrocarbons as the size of the molecule increases. For example, using the 6-311 + +G(3df, 2p) basis set, the error increased systematically from propane (-1.5 kcal/mol) to hexane (-9.3) and octane (-14.0).³¹ Similarly, the effect of successively adding methyl groups to ethane resulted in an error of 21.1 kcal/mol for 2,2,3,3-tetramethylbutane.³²

MO methods can also be used to calculate *heats of reaction* by comparing the heats of formation of reactants and products. The *total energy* calculated for even a small hydrocarbon, relative to the separate nuclei and electrons, is enormous (typically 50,000 and 100,000 kcal/mol for C₂ and C₄ compounds, respectively) relative to the energy of reaction. Sometimes the energy is tabulated as the *energy of atomization*, corresponding to the difference in total energy of the molecule and that of the separate atom, which is the energy required to break all the bonds. These values, too, are very large in comparison with the heat of reaction. The energy differences that are of principal chemical interest, such as ΔH for a reaction, are likely to be in the range of 0–30 kcal/mol. A very small error relative to the total energy in an MO calculation becomes a very large error in a calculated ΔH . Fortunately, the absolute errors for compounds of similar structure are likely to be comparable and tend to cancel in calculation of the *energy differences* between related molecules. Calculation of heats of formation and heats of reaction is frequently done on the basis of *isodesmic reactions*,³³ in order to provide for maximum cancellation of errors in total binding energies. An isodesmic reaction is defined as a process in which the number of formal bonds of each type is kept constant; that is, there are the same number of C–H, C=C, C=O, etc., bonds on each side of the equation.³⁴ For example, an isodesmic reaction to evaluate the stability of benzene would be:



The comparison can be further refined by use of *homodesmotic reactions* in which there is matching not only of bond types, but also of hybridization. Thus in the reaction

³¹ L. A. Curtiss, K. Raghavachari, P. C. Redfern, and J. A. Pople, *J. Chem. Phys.*, **112**, 7374 (2000).

³² C. E. Check and T. M. Gilbert, *J. Org. Chem.*, **70**, 9828 (2005).

³³ W. J. Hehre, R. Ditchfield, L. Radom, and J. A. Pople, *J. Am. Chem. Soc.*, **92**, 4796 (1970).

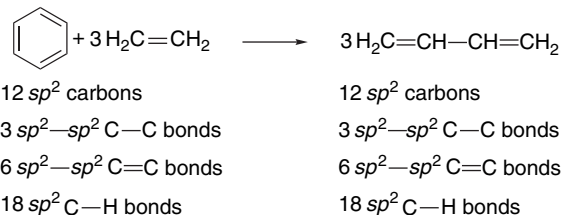
³⁴ D. A. Ponomarev and V. V. Takhistov, *J. Chem. Ed.*, **74**, 201 (1997).

Table 3.5. Comparison of Differences between Calculated and Experimental ΔH_f in kcal/mol for some Hydrocarbons.^a

Hydrocarbon	MNDO ^a	AM1 ^b	PM3 ^c	HF/3-21G ^a	HF/6-31G ^a	G2 ^d	CBS-Q ^e	CBS-QB3 ^f	MP4/QCI ^g	B3LYP/6-311+G(3df,2p) ^h
Methane	5.9	9.0	4.9	-0.9	-0.5	0.7	-0.2	-0.4	-0.6	-1.6
Ethane	0.3	2.6	2.1	0.2	0.9	-0.2	-0.6	-0.6	-0.7	0.0
Butane	0.7	-0.7	-2.8	-0.8	-0.8	0.6				-0.8
Pentane	0.7	-2.8	5.1	3.5	-0.5	-0.5				
Cyclopropane	-1.5	-18.7	0.2	-10.6	-2.4	-2.4	-1.7			-0.6
Cyclobutane	-12.0	-10.5	-10.5	-5.6	-10.5	-10.5	-3.4	-3.4		
Cyclopentane	-5.3	-9.0	-9.0	-1.5	-1.5	-9.1	-0.1	-0.1		
Cyclohexane	3.1	4.0	4.0	4.2	-1.6	-2.4	0.3	-1.0	0.0	-0.5
Ethene	-1.6	0.6	0.6	1.5	-2.5	-6.8	0.0 ⁱ	1.3	0.0	-2.4
Alene	2.7	3.6	5.0	-4.7	-2.9	0.5 ^j	0.7	0.7		-1.5 ^d
1,3-Butadiene										-4.0 ^d
Benzene										
Bicyclo[2.2.1]heptane	2.1	-2.0	-1.3	2.2	3.6	4.0 ^k	1.5			
Bicyclo[2.2.2]octane	-2.2	-11.9	-11.9	-3.7	8.8					
					10.7					

- a. M. J. S. Dewar, E. G. Zoebisch, E.F. Healy, and J. J. P. Stewart, *J. Am. Chem. Soc.*, **107**, 3902 (1985).
 b. M. J. S. Dewar and D. M. Storch, *J. Am. Chem. Soc.*, **107**, 3898 (1985).
 c. J. J. P. Stewart, *J. Comput. Chem.*, **10**, 221 (1989).
 d. J. A. Pople, M. Head-Gordon, D. J. Fox, K. Raghavachari, and L. A. Curtiss, *J. Chem. Phys.*, **90**, 5622 (1989); L. A. Curtiss, K. Raghavachari, G. W. Trucks, and J. A. Pople, *J. Phys. Chem.*, **94**, 7221 (1991); L. A. Curtiss, K. Raghavachari, P. C. Redfern, and J. Pople, *J. Chem. Phys.*, **106**, 1063 (1997).
 e. L. A. Curtiss, K. Raghavachari, P. C. Redfern, and B. B. Stefanov, *J. Chem. Phys.*, **108**, 692 (1998).
 f. M. Saey, M. F. Reyniers, G. B. Marin, V. Van Speybroeck, and M. Waroquier, *J. Phys. Chem. A*, **107**, 9147 (2003).
 g. M. Sana and M. T. Nguyen, *Chem. Phys. Lett.*, **196**, 390 (1992).
 h. J.-W. Pan, D. W. Rogers, and F. J. McLafferty, *Theochem*, **468**, 59 (1999).
 i. D. W. Rogers and F. J. McLafferty, *J. Phys. Chem.*, **99**, 1375 (1993).
 j. M. N. Glikhovskiy and S. Laier, *Theor. Chim. Acta*, **92**, 327 (1995).
 k. A. Nicolaides and L. Radom, *J. Phys. Chem.*, **98**, 3092 (1994).

below, the number of sp^3 , sp^2 , and sp C–H bonds and the hybridization types of the C–C bonds are balanced.³⁵



Further refinements are possible. For example, in evaluating cyclic compounds, use of matching ring sizes can be specified so as to cancel errors resulting from ring strain.³⁶ Although the reaction may not correspond to any real chemical process, the calculation can test the reliability of the computation methods because of the additivity of ΔH_f° data.

The accuracy of the computational ΔH can be judged by comparison with ΔH obtained by summation of tabulated ΔH_f° for reactants and products. Table 3.6 compares some ΔH_f° values calculated at the G2 level of theory from atomization energies and isodesmic reactions. For molecules of this size, the use of isodesmic reactions can usually achieve ΔH_f° data within 0.5 kcal/mol.³⁷ A study of a series of hydrocarbons, including somewhat larger molecules, comparing G2 and G3 calculations is also available.³⁸

For larger molecules that are outside the range of ab initio calculations, the semiempirical methods can be used. For example, the AM1 and PM3 methods have been used for a series of polycyclic aromatic hydrocarbons. Some results are shown in Table 3.7. The average errors were 9.1 kcal/mol for AM1 and 5.9 for PM3. Both methods can be internally calibrated by least-squares correlations, which improve the average error to 1.3 kcal/mol for AM1 and 2.1 for PM3.

Table 3.6. Comparison of Differences from Experimental ΔH_f° in kcal/mol for G2 Calculations Using Atomization Energy versus Isodesmic Reactions^a

	ΔH_f° (exp)	G2 (atomization)	G2 (isodesmic)
Propane	−25.0	0.4	0.1
Cyclopropane	66.0	−2.9	−1.6
Butane	−30.0	0.4	0.2
Cyclobutane	37.4	−2.9	−1.5
Bicyclo[1.1.0]butane	51.9	−3.0	−1.5
Cyclopentane	−18.3	−1.1	−0.4
Benzene	19.7	−3.9	−0.8

a. K. Raghavachari, B. Stefanov, and L. A. Curtiss, *J. Chem. Phys.*, **106**, 6764 (1997).

³⁵ P. George, M. Trachtman, C. W. Bock, and A. M. Brett, *Tetrahedron*, **32**, 317 (1976).

³⁶ P. v. R. Schleyer, P. K. Freeman, H. Jiao, and B. Goldfuss, *Angew. Chem. Int. Ed. Engl.*, **34**, 337 (1995); M. K. Cyranski, P. v. R. Schleyer, T. M. Krygowski, H. Jiao, and G. Hohlneicher, *Tetrahedron*, **59**, 1657 (2003).

³⁷ K. Raghavachari, B. B. Stefanov, and L. A. Curtiss, *J. Chem. Phys.*, **106**, 6764 (2000).

³⁸ R. Notario, O. Castano, J. -L. M. Abboud, R. Gomperts, L. M. Frutos, and R. Palmeiro, *J. Org. Chem.*, **64**, 9011 (1999); R. Notario, O. Castano, R. Gomperts, L. M. Frutos, and R. Palmeiro, *J. Org. Chem.*, **65**, 4298 (2000).

Table 3.7. Comparison of Experimental ΔH_f° (kcal/mol) and Semiempirical Values for Polycyclic Aromatic Hydrocarbons

Molecule ^a	Experimental ΔH_f°	AM1 ^b	PM3 ^c
Benzene	20.0	22.0	23.5
Naphthalene	36.0	40.6	40.7
Phenanthrene	49.7	57.4	55.0
Anthracene	55.2	62.5	61.7
Pyrene	54.0	67.4	64.1
Triphenylene	66.5	75.5	68.3
Chrysene	66.0	76.2	70.9
Benz[a]anthracene	70.3	78.3	74.5
Benzo[c]phenanthrene	69.6	81.2	77.6
Perylene	78.4	89.3	82.0
Tetracene	72.3	86.9	84.3

a. For structures of the polycyclic aromatic hydrocarbons, see Scheme 8.2, p. 746.

b. W. C. Herndon, P. C. Nowak, D. A. Connor, and P. Lin, *J. Am. Chem. Soc.*, **114**, 41 (1992).c. D. M. Camaioli, S. T. Autrey, T. B. Salinas, and J. A. Franz, *J. Am. Chem. Soc.*, **118**, 2013 (1996)

Any set of computed energies can be used for calculation of reaction enthalpies by comparing the energy of reactants and products. Table 3.8 gives some data for hydrogenation, hydrogenolysis, and isomerization reactions at several levels of theory, including data for small ring compounds, which represent a particularly challenging test of the accuracy of the computational methods.

The relative merits of various computational methods have been discussed in the literature.³⁹ In general, the ab initio types of calculations are more reliable but

Table 3.8. Comparison of Calculated and Observed ΔH for Some Reactions^a

Reaction	HF/6-31G*	MP2/6-311G*	B3LYP/6-31G*	Observed
$\text{CH}_2=\text{CH}_2 + \text{H}_2 \rightarrow \text{C}_2\text{H}_6$	-36.0	-32.2	-31.7	-30.8
$\text{CH}_2=\text{CHCH}=\text{CH}_2 + 2\text{H}_2 \rightarrow \text{C}_4\text{H}_{10}$	-62.5	-55.6	-52.4	-53.3
 + 3H ₂ → C ₆ H ₁₂	-53.8	-41.1	-38.1	-44.0
C ₂ H ₆ + H ₂ → 2CH ₄	-18.8	-10.4	-16.5	-15.5
 + H ₂ → C ₃ H ₈	-41.8	-35.6	-38.6	-35.9
 → CH ₂ =CHCH ₃	-8.9	-6.2	-10.5	-8.5
 + H ₂ → C ₄ H ₁₀	-40.3	-34.1	-37.3	-35.9
 + H ₂ → 	-53.2	-44.0	-47.0	-44.4
 → CH ₂ =CHCH=CH ₂	-20.9	-22.4	-31.9	-26.2

a. In kcal/mol; K. B. Wiberg and J. W. Ochlerski, *J. Comput. Chem.*, **18**, 108 (1997).

³⁹ J. A. Pople, *J. Am. Chem. Soc.*, **97**, 5306 (1975); W. J. Hehre, *J. Am. Chem. Soc.*, **97**, 5308 (1975); T. A. Halgren, D. A. Kleier, J. H. Hall, Jr., L. D. Brown, and W. N. Lipscomb, *J. Am. Chem. Soc.*, **100**, 6595 (1978); M. J. S. Dewar and G. P. Ford, *J. Am. Chem. Soc.*, **101**, 5558 (1979); W. J. Hehre, *Acc. Chem. Res.*, **9**, 399 (1976); M. J. S. Dewar, E.G. Zoebisch, E. F. Healy, and J. J. P. Stewart,

the semiempirical calculations are much faster in terms of computer time. The time requirement for an ab initio calculation increases rapidly as the number of atoms in the molecule increases. The C₈ hydrocarbons represent the current practical limit for high-level ab initio computations. DFT computations are faster than ab initio computations and the amount of computer time required does not increase as rapidly with molecular size. The choice of basis set orbitals influences the outcome, and often several basis sets are checked to determine which are adequate. A choice of computational method is normally made on the basis of evidence that the method is suitable for the problem at hand and the availability of appropriate computer programs and machine time. Results should be subjected to critical evaluation by comparison with experimental data or checked by representative calculations using higher-level methods.

3.1.2.6. Limitations on Enthalpy Data for Predicting Reactivity. Whether ΔH for a projected reaction is based on tabulated thermochemical data, bond energy, equivalent group additivity, or on MO or DFT computations, fundamental issues that prevent a final conclusion about a reaction's feasibility remain. In the first place, most reactions of interest occur in solution, and the enthalpy, entropy, and free energy associated with any reaction depend strongly on the solvent medium. There is only a limited amount of tabulated thermochemical data that are directly suitable for the treatment of reactions in organic solvents.⁴⁰ MO and DFT calculations usually refer to the isolated (gas phase) molecule. Estimates of solvation effects on reactants, products, intermediates, and transition states must be made in order to apply either experimental or computational thermochemical data to reactions occurring in solution. There may be substantial differences between solvation energies of reactants, transition states, intermediates, and products. If so, these solvation differences become a major factor in determining reactivity.

An even more fundamental limitation is that ΔH data give no information about the *rate of a chemical reaction*. It is the energy of the transition state relative to the reactants that determines the reaction rate. To be in a position to make judgments on reactivity, we have to see how structure is related to *reactivity*. To do this, we need information about the energy of transition states and intermediates, but because transition states are transitory, we have no physical means of determining their structure. We can, however, determine their energy relative to reactants on the basis of reaction kinetics. We address this topic in the next sections by first examining the principles of chemical kinetics. We can also obtain information about transition states and intermediates by studying the effect of substituents on the rate of reaction. In Section 3.4, we look at how key intermediates such as carbocations, carbanions, and radicals respond to substituents.

Theoretical descriptions of molecules have been applied to the structure of transition states and unobservable intermediates. By applying MO or DFT methods, structures can be calculated for successive geometries that gradually transform the reactants into products. Exploration of a range of potential geometries and calculation of the energy of the resulting ensembles can, in principle, locate and describe

J. Am. Chem. Soc., **107**, 3902 (1985); J. N. Levine, *Quantum Chemistry*, 3rd Edition, Allyn and Bacon, 1983, pp. 507–512; W. Hehre, L. Radom, P. v. R. Schleyer, and J. A. Pople, *Ab Initio Molecular Orbital Calculations*, John Wiley & Sons, 1986, Chap. 6; B. H. Besler, K. M. Merz, Jr., and P. Kollman, *J. Comput. Chem.*, **11**, 431 (1990); M. Sana and M. T. Nguyen, *Chem. Phys. Lett.*, **196**, 390 (1992).

⁴⁰ Guthrie has explored the use of a group equivalent scheme to compute ΔG_f for aqueous solutions. J. P. Guthrie, *Can. J. Chem.*, **70**, 1042 (1992).

the minimum energy pathway. To the extent that the calculations accurately reflect the molecular reality, this provides a structural description of the reaction path and transition state. Thus we can refer to the *transition structure*, that is, the structural description of the reacting ensemble at the transition state.⁴¹ We use the abbreviation TS to refer to transition structures. We use the term *transition state* in the context of energetic analysis where there is no explicit consideration of the structure. In Section 3.7 we focus attention on another aspect of reactivity—the use of catalysts to accelerate reaction.

3.2. Chemical Kinetics

3.2.1. Fundamental Principles of Chemical Kinetics

Thermodynamic data give us a means of quantitatively expressing *stability*. Now we need to explore the relationship between *structure* and *reactivity*. The quantitative description of reactivity is called *chemical kinetics*. A fundamental thermodynamic equation relates the equilibrium constant for a reaction to the free-energy change associated with the reaction:

$$\Delta G = -RT \ln K \quad (3.12)$$

The free energy contains both enthalpy and entropy terms:

$$\Delta G = \Delta H - T\Delta S \quad (3.13)$$

Thus we see that thermodynamic stability, as measured by free energy, places a limit on the *extent of a chemical reaction*. However, it does not directly determine the rate of the reaction.

The nature of the *rate constants* k_r for individual steps in a chemical reaction can be discussed in terms of *transition state theory*, which is a general approach for analyzing the energetic and entropic components of a reaction process. In transition state theory, a reaction is assumed to involve the attainment of an *activated complex* that goes on to product at an extremely rapid rate. The rate of decomposition of the activated complex has been calculated from the assumptions of the theory to be about $6 \times 10^{12} \text{ s}^{-1}$ at room temperature. The observed rate constant k_r is given by the expression⁴²

$$k_r = \frac{\kappa k_B T}{h} (e^{-\Delta H^\ddagger / RT}) (e^{\Delta S^\ddagger / R}) \quad (3.14)$$

⁴¹ Although the terms *transition state* and *transition structure* are often used interchangeably, if the transition state is taken as defined by transition state theory, it may differ in structure from the maximum energy obtained by computation; K. N. Houk, Y. Li, and J. D. Evanseck, *Angew. Chem. Int. Ed. Engl.*, **31**, 682 (1992).

⁴² For a more complete development of these relationships, see M. Boudart, *Kinetics of Chemical Processes*, Prentice-Hall, Englewood Cliffs, NJ, 1968, pp. 35–46; or I. Amdur and G. G. Hammes, *Chemical Kinetics: Principles and Selected Topics*, McGraw-Hill, New York, 1966, pp. 43–58; J. W. Moore and R. G. Pearson, *Kinetics and Mechanism*, Wiley, New York, 1981, pp. 159–169; M. M. Kreevoy and D. G. Truhlar, in C. F. Bernasconi, *Investigation of Rates and Mechanisms of Reaction: Techniques of Organic Chemistry*, 4th Edition, Vol. VI, Part 1, Interscience, New York, 1986.

in which κ is the transmission coefficient, which is usually taken to be 1, k_B is Boltzmann's constant, h is Planck's constant, R is the gas constant, and T is the absolute temperature. If the activated complex is considered to be in equilibrium with its component molecules, the attainment of the transition state (TS) can be treated as being analogous to a bimolecular reaction:

$$K^\ddagger = \frac{[TS]}{[A][B]} \quad (3.15)$$

The position of this equilibrium is related to the free energy required for attainment of the transition state. The symbol (\ddagger) is used to specify that it is a transition state or “activated complex” that is under discussion:

$$\Delta G^\ddagger = -RT \ln K^\ddagger \quad (3.16)$$

The free energy ΔG^\ddagger is called the *free energy of activation*. The rate of a reaction step is then given by

$$\text{Rate} = \frac{\kappa k_B T}{h} [TS] \quad (3.17)$$

$$\text{Rate} = \frac{\kappa k_B T}{h} e^{-\Delta G^\ddagger / RT} [A][B] \quad (3.18)$$

Comparison with the form of the expression for the rate of any single reaction step reveals that the magnitude of ΔG^\ddagger is the factor that determines the magnitude of k_r at any given temperature:

$$\text{Rate} = k_r [A][B] \quad (3.19)$$

The temperature dependence of reaction rates permits evaluation of the enthalpy and entropy components of the free energy of activation. The terms in Equation (3.14) can be rearranged to examine the temperature dependence:

$$k_r = \frac{\kappa k_B T}{h} \left(e^{-\Delta H^\ddagger / RT} \right) \left(e^{\Delta S^\ddagger / R} \right) \quad (3.20)$$

The term $(\kappa k_B T/h)e^{\Delta S^\ddagger / R}$ varies only slightly with T compared to $e^{-\Delta H^\ddagger / RT}$ because of the exponential nature of the latter. To a good approximation, then:

$$\frac{k_r}{T} = C e^{-\Delta H^\ddagger / RT} \quad (3.21)$$

$$\ln \frac{k_r}{T} = \frac{-\Delta H^\ddagger}{RT} + C' \quad (3.22)$$

A plot of $\ln(k_r/T)$ versus $1/T$ is a straight line, and its slope is $-\Delta H^\ddagger / R$. After ΔH^\ddagger is determined in this manner, ΔS^\ddagger is available from the relationship

$$\Delta S^\ddagger = \frac{\Delta H^\ddagger}{T} + R \ln \frac{hk_r}{\kappa k_B T} \quad (3.23)$$

which can be obtained by rearranging Equation (3.14).

The temperature dependence of reactions is frequently expressed in terms of the Arrhenius equation:

$$k_r = A e^{-E_a/RT} \quad \text{or} \quad \ln k_r = -E_a/RT + \ln A \quad (3.24)$$

The E_a can be determined experimentally by measuring the reaction rate at several temperatures over as wide a range as practical. A plot of $\ln k_r$ against $1/T$ then gives a line of slope equal to $-E_a/R$. The value of E_a incorporates the ΔH term and the value of A reflects the entropy term. At constant pressure, E_a and ΔH are related by the expression

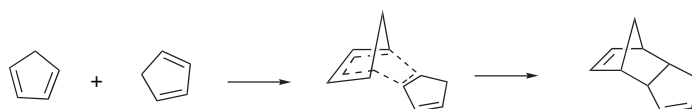
$$\Delta H^\ddagger = E_a - RT \quad (3.25)$$

and ΔS^\ddagger is related to A by

$$\Delta S^\ddagger = R[\ln(h/k_B T) + \ln A - 1] \quad (3.26)$$

The magnitude of ΔH^\ddagger and ΔS^\ddagger reflect transition state structure. Atomic positions in the transition state do not correspond to their positions in the ground state. In particular, the reacting bonds are partially formed or partially broken. The energy required for bond reorganization is reflected in the higher energy content of the activated complex and corresponds to the enthalpy of activation ΔH^\ddagger . The entropy of activation, ΔS^\ddagger , is a measure of the degree of organization resulting from the formation of the activated complex. If translational, vibrational, or rotational degrees of freedom are lost in going to the transition state, there is a decrease in the total entropy of the system. Conversely, an increase of translational, vibrational, or rotational degrees of freedom results in a positive entropy of activation. For reactions in solution, the organization of solvent contributes to the entropy of activation.

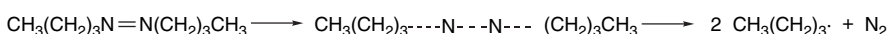
Wide variation in enthalpy and entropy of activation for different reaction systems is possible, as illustrated by the following two reactions.



$$\Delta H^\ddagger = 15.5 \text{ kcal/mol}$$

$$\Delta S^\ddagger = -34 \text{ eu}$$

Ref. 43



$$\Delta H^\ddagger = 52 \text{ kcal/mol}$$

$$\Delta S^\ddagger = +19 \text{ eu}$$

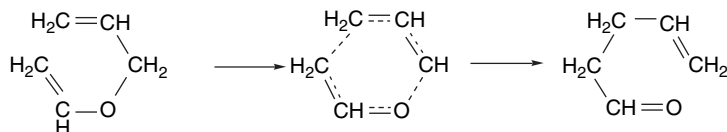
Ref. 44

The relatively low ΔH^\ddagger term for the dimerization of cyclopentadiene is characteristic of concerted reactions (see Chapter 10), in which bond making accompanies

⁴³ A. Wassermann, *Monatsch. Chem.*, **83**, 543 (1952).

⁴⁴ A. U. Blackham and N. L. Eatough, *J. Am. Chem. Soc.*, **84**, 2922 (1962).

bond breaking. It differs markedly from ΔH^\ddagger for the thermal decomposition of 1,1'-azobutane, in which the rate-determining step is a homolytic cleavage of a C–N bond, with little new bond making to compensate for the energy cost of the bond breaking. The entropy of activation, on the other hand, is more favorable in the 1,1'-azobutane decomposition, since a translational degree of freedom is being gained in the TS as the molecular fragments separate. The dimerization of cyclopentadiene is accompanied by a very negative entropy of activation because of the loss of translational and rotational degrees of freedom in formation of the highly ordered cyclic TS. The two reacting molecules must attain a specific orientation to permit the bonding interactions that occur as the TS is approached. Unimolecular reactions that take place by way of cyclic transition states also typically have negative entropies of activation because of the loss of rotational degrees of freedom associated with the highly ordered TS. For example, thermal isomerization of vinyl allyl ether to 4-pentenal has $\Delta S^\ddagger = -8 \text{ cal/mol-deg}^{-1}$.⁴⁵



It is important to remember that the enthalpy and entropy of activation reflect the response of the *reacting system as a whole* to formation of the activated complex. As a result, the interpretation of these parameters is more complicated for reactions taking place in solution than for gas phase reactions. This is particularly true for processes involving formation or destruction of charged species. The solvolysis of *t*-butyl chloride in 80% aqueous ethanol, for example, has as its rate-determining step unimolecular ionization of the carbon-chlorine bond to form chloride and *t*-butyl cations. One might think that this ionization would lead to a positive entropy of activation, since two independent particles are being generated. In fact, the entropy of activation is $-6.6 \text{ cal/mol-deg}^{-1}$. Owing to its polar character, the TS requires a greater ordering of solvent molecules than the nonpolar reactant.⁴⁶ Reactions that generate charged species usually exhibit negative entropies of activation in solution. The reverse is true for reactions in which charged reactants lead to a neutral transition state.

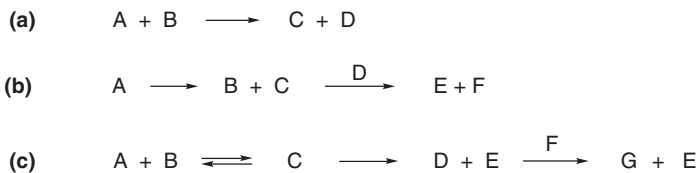
3.2.2. Representation of Potential Energy Changes in Reactions

3.2.2.1. Reaction Energy Profiles. It is often useful to describe reactions in terms of an energy profile that traces the potential energy of the reacting ensemble of molecules as they proceed from reactants to products, such as shown in Figure 3.1 (page 254). Thermodynamic stability establishes the relative energy of the reactants and the products, but does not provide any information about the intervening stages of the process. It is these intervening stages that determine how fast (or slow) a reaction will be. If a large ΔG^\ddagger is required, the reaction will be slow. Reactions often proceed through a sequence of steps involving formation of a series of intermediates that eventually lead to the products. Interpretation of the kinetic characteristics of a reaction can provide information about the intervening steps by providing information about *intermediates*

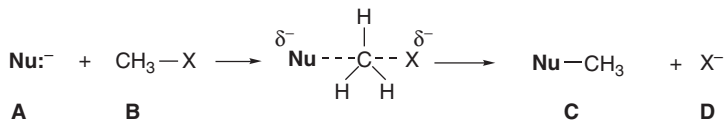
⁴⁵. F. W. Schuler and G. W. Murphy, *J. Am. Chem. Soc.*, **72**, 3155 (1950).

⁴⁶. E. Grunwald and S. Winstein, *J. Am. Chem. Soc.*, **70**, 846 (1948).

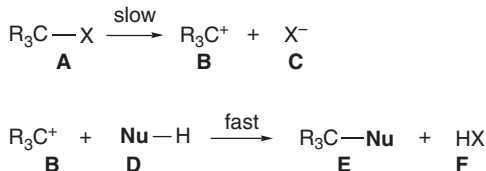
that exist along the reaction pathway. The sequence of reaction steps and intermediates involved in the overall transformation is the *reaction mechanism*. Reactants, intermediates, and products correspond to energy minima on the energy diagram and are separated by *activated complexes or transition states*, which are the molecular arrangements having the maximum energy for each successive step of the reaction mechanism. Figure 3.2 gives reaction energy diagrams for hypothetical reactions that proceed in one, two, or three steps through zero, one, or two intermediates. For the example in Figure 3.2, these are:



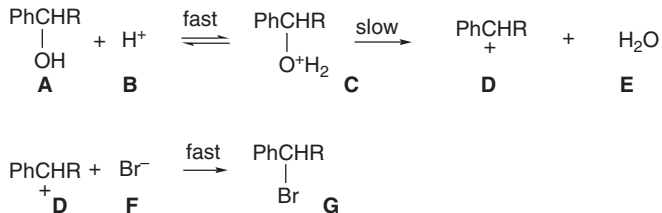
The diagram in (a), for example, might correspond to an S_N2 displacement reaction.



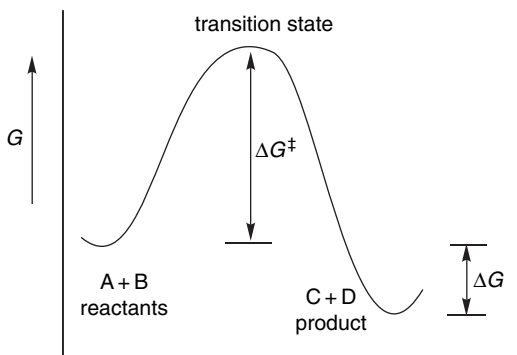
The diagram in (b) could pertain to an S_N1 reaction with a solvent **D** proceeding through a carbocation intermediate (**B**).



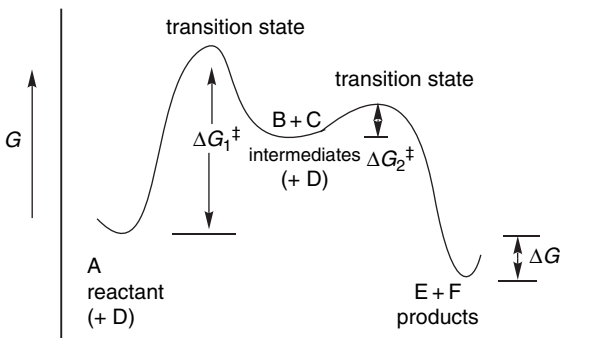
The diagram in (c) might apply to an acid-catalyzed ionization mechanism, such as might occur in a reaction of a secondary benzylic alcohol with HBr.



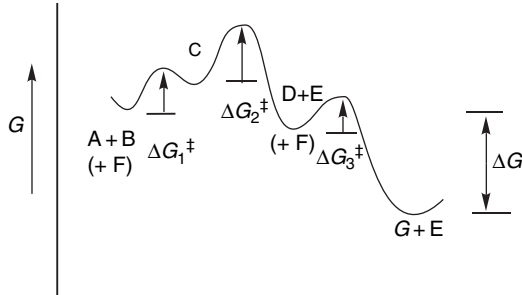
Such diagrams make clear the difference between an intermediate and a transition state. An intermediate lies in a depression on the potential energy curve. Thus, it has a finite lifetime, which depends on the depth of the depression. A shallow depression implies a low activation energy for the subsequent step, and therefore a short lifetime. The deeper the depression, the longer the lifetime of the intermediate. The situation at a transition state is quite different. This arrangement has only fleeting existence and represents an energy maximum on the reaction path.



(a) Energy diagram for a single-step reaction.



(b) Energy diagram for a two-step reaction.



(c) Energy diagram for a three-step reaction.

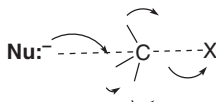
Fig. 3.2. Reaction energy profiles for one-, two-, and three-step reactions showing successive transition states and intermediates.

There is one path between reactants and products that has a lower energy maximum than any other and is the pathway that the reaction will follow. *The curve in a potential energy plot represents this lowest energy pathway.* It corresponds to a path across an energy surface describing energy as a function of the spatial arrangement of the atoms involved in the reaction. The progress of the reaction is called the *reaction coordinate*, and is a measure of the structural changes taking place as reaction occurs. The principle of microscopic reversibility arises directly from transition state theory. *The same pathway that is traveled in the forward direction of a*

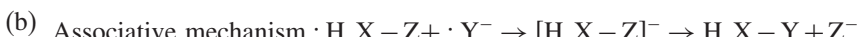
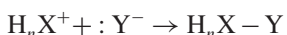
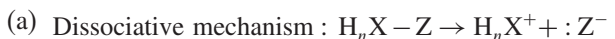
reaction will be traveled in the reverse direction, because it affords the lowest energy barrier for either process. Thus, information about the nature of a transition state or intermediate deduced by a study of a forward reaction is applicable to the reverse process occurring under the same conditions.

The overall rate of the reaction is controlled by the *rate-determining step*—the step that has the highest energy requirement and is the bottleneck for the overall process. In general, steps that occur after the rate-determining step do not enter into the overall rate equation for the reaction. In the example illustrated in Figure 3.2b, the first step is rate determining and the overall rate of the reaction would be given by the rate expression for the first step. In example (c), the second step is rate-determining.

3.2.2.2. Reaction Energy Diagrams with Two or More Dimensions. The reaction energy diagrams in Figure 3.2 depict reaction progress in terms of rupture and formation of the affected bonds. The reaction coordinate dimension represents the extent of completion of the bond-breaking/bond-making process. For example, in the S_N2 reaction shown in Figure 3.2a, the reaction coordinate corresponds to the trajectory for approach of the nucleophile and departure of the leaving group, but also implicitly includes the inversion of the carbon atom. The reaction coordinate can be expressed in terms of the Nu—C bond order, which begins as 0 at the left and proceeds to 1 when the reaction is complete.



Many reactions can usefully be described in terms of two-dimensional energy diagrams in which change in two different bonds are represented. For example, a nucleophilic substitution reaction at some element X (e.g., silicon) might occur by any of three general mechanisms:



The two-step mechanisms [(a) and (b)] represent paths along the edge of the two-dimensional reaction energy diagram, differing in the order of the two steps (Figure 3.3). The single-step (concerted) mechanism involves a more or less diagonal path with simultaneous bond breaking and bond making, as indicated by path C in Figure 3.3. These two-dimensional diagrams are often referred to as Albery-More

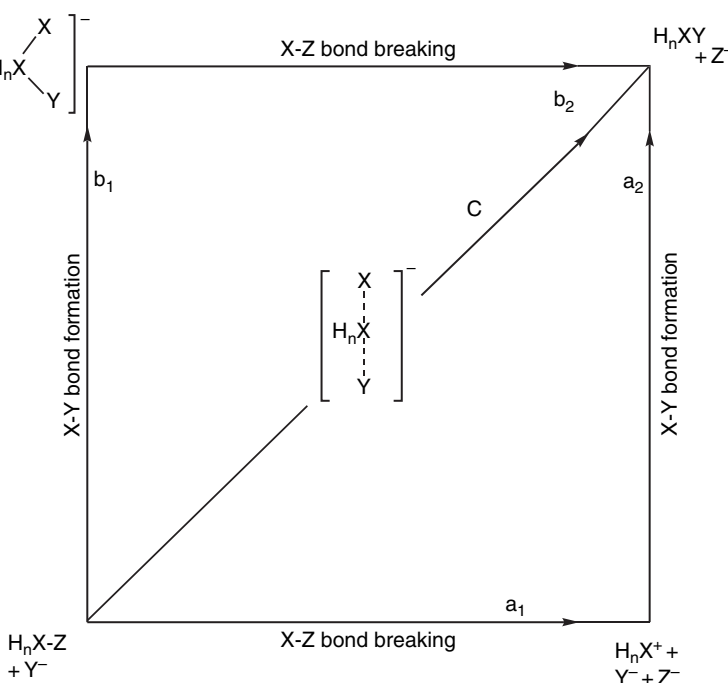
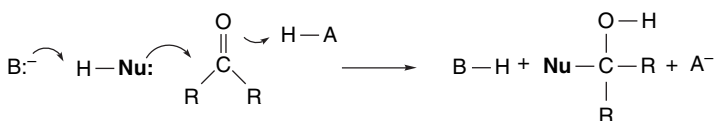


Fig. 3.3. Two-dimensional reaction energy diagram showing (a) dissociative, (b) associative, and (c) concerted mechanisms for a substitution reaction.

O’Ferrall-Jencks diagrams.⁴⁷ Energy is not explicitly shown in such diagrams, but it is a third dimension. We use such diagrams in the discussions of several reaction types, including elimination reactions (Section 5.10.1) and carbonyl addition reactions (Section 7.1). When the energy dimension is added, the diagram takes the form of a contour plot as shown in Figure 3.4. The preferred reaction pathway is over the lowest barrier.

Reactions involving changes at three bonds require a reaction cube and those with more bonding changes require cubes within cubes.⁴⁸ Figure 3.5 is a general representation of a reaction cube, and Figure 3.6 shows the cube corresponding to a reaction involving deprotonation of a nucleophile and protonation of a carbonyl oxygen in a carbonyl addition reaction.



Diagrams such as these can summarize the conclusions of kinetic and other studies of reaction mechanisms. Whether the diagram is in one, two, or three dimensions, it can specify the sequence of steps in the overall reaction.

⁴⁷ W. J. Albery, *Prog. React. Kinetics*, **4**, 353 (1967); R. A. More O’Ferrall, *J. Chem. Soc. B*, 274 (1970); W. P. Jencks, *Chem. Rev.*, **72**, 705 (1972).

⁴⁸ E. Grunwald, *J. Am. Chem. Soc.*, **107**, 4715 (1985); P. H. Scudder, *J. Org. Chem.*, **55**, 4238 (1990); J. P. Guthrie, *J. Am. Chem. Soc.*, **118**, 12878 (1996).

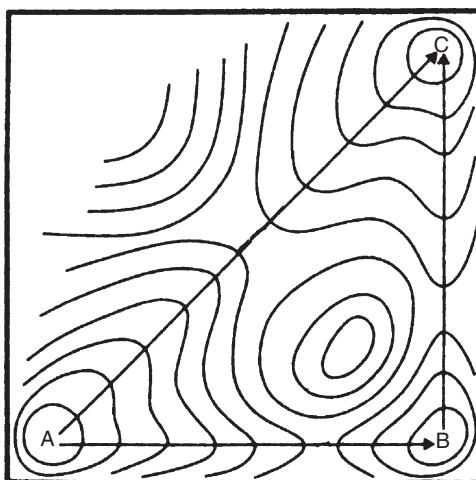


Fig. 3.4. Two-dimensional energy diagram showing energy contours for stepwise ($A \rightarrow B \rightarrow C$) and concerted ($A \rightarrow C$) reaction pathways.

3.2.2.3. Computation of Reaction Potential Energy Surfaces. As transition states cannot be observed, there is no experimental means of establishing their structure. Computational methods can be applied for descriptions of intermediates and transition structures. Structural attributes such as bond lengths, bond orders, electron density distribution, and orbital occupancy can be found for transition structures and intermediates, as was described in Sections 3.1.2.5 for stable molecules. The evaluation of a

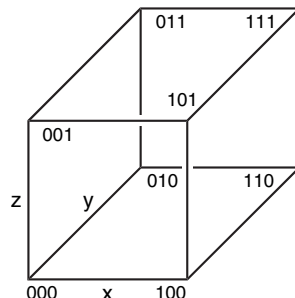


Fig. 3.5. Three-dimensional reaction coordinate diagram: x , y , and z are the three edge coordinates; [0,0,0] is the starting point; [1,1,1] is the product; [1,0,0], [0,1,0], and [0,0,1] are the corner intermediates corresponding to reaction along only one edge coordinate; and [1,1,0], [1,0,1], and [0,1,1] are the corner intermediates corresponding to the reaction along two edge coordinates. Reproduced with permission from *Can. J. Chem.*, **74**, 1283 (1996).

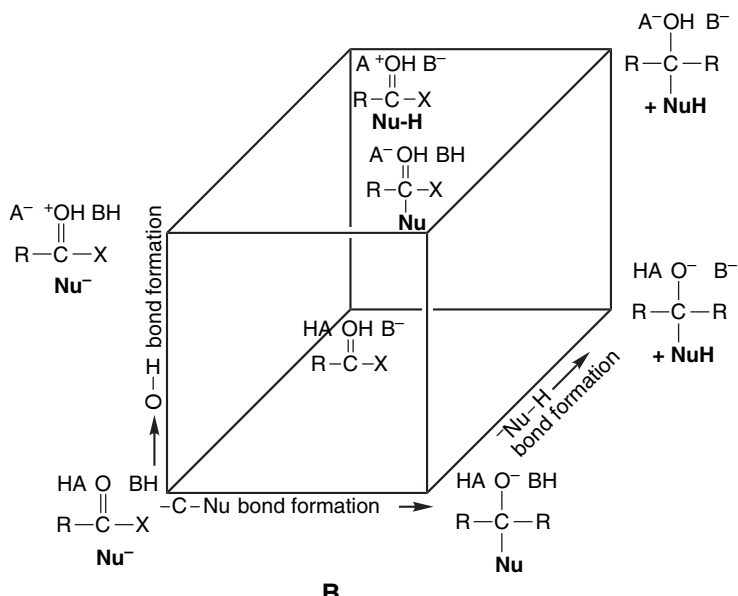


Fig. 3.6. Reaction progress cube showing possible intermediates for nucleophilic addition to a carbonyl group involving HA , B^- , and Nu-H . Adapted from *J. Org. Chem.*, **55**, 4238 (1990).

reaction mechanism typically involves the comparison of the energy of potential TSs. The expectation is that the reaction will proceed through the lowest energy TS, so if this can be reliably computed, the reaction mechanism can be defined. In the evaluation of stereoselectivity, for example, a comparison of the energies of the alternative TSs can predict the product ratio.

A very large number of structural variations can be conceived, but the structures of interest are the transition structures and intermediates that connect the reactants and products. The mathematics involved in characterizing a potential energy surface involves evaluation of energy gradients as a function of structural change. A *transition state is a minimum in energy with respect to all changes in molecular dimensions except along the reaction coordinate, where it is a maximum on the energy surface*. The transition state is a *saddle point*; that is, it is an energy minimum relative to change in any coordinate except in the direction of reaction. It is an energy maximum relative to that motion so the force constant is negative because there is no barrier to movement in that direction. A property of transition structures is that they have a *single imaginary vibrational frequency*, corresponding to the structural change in the direction of the reaction process. Because there are ordinarily many possible structural variations, the potential energy surface is a multidimensional hypersurface,⁴⁹ which can be described mathematically in terms of all the dimensions being explored. Because the reaction coordinate corresponds to the lowest-energy path, it can be located mathematically by minimization of the energy in all dimensions except that corresponding to the progress of the reaction. The computed minimum-energy path is called the *intrinsic reaction coordinate*.⁵⁰

⁴⁹. P. N. Skancke, *Acta Chem. Scand.*, **47**, 629 (1993).

⁵⁰. K. Fukui, *J. Phys. Chem.*, **74**, 4161 (1970); S. Kato and K. Fukui, *J. Am. Chem. Soc.*, **98**, 6395 (1976).

The calculation of the properties of transition structures is more problematic than for stable molecules because TSs involve bond breaking. Thus computations based on the concept of electron pairing may not be applicable, especially for species with radical character. Nevertheless, computational studies have provided insight into many reactions and we frequently use the results of these studies, as well as experimental work, in developing the details of reaction mechanisms.

3.2.3. Reaction Rate Expressions

Experimental kinetic data can provide detailed insight into reaction mechanisms. The rate of a given reaction can be determined by following the disappearance of a reactant or the appearance of a product. The extent of reaction is often measured spectroscopically, because spectroscopic techniques provide a rapid, continuous means of monitoring changes in concentration. Numerous other methods are available and may be preferable in certain cases. For example, continuous pH measurement or acid-base titration can be used to follow the course of reactions that consume or generate an acid or a base. Conductance measurements provide a means for determining the rate of reactions that generate ionic species; polarimetry can be used to follow reactions involving optically active materials. In general, any property that can be measured and quantitatively related to the concentration of a reactant or a product can be used to determine a reaction rate.

The goal of a kinetic study is to establish the quantitative relationship between the concentration of reactants and catalysts and the observed rate of the reaction. Typically, such a study involves rate measurements at enough different concentrations of each reactant to determine the *kinetic order* with respect to each reactant. A complete investigation allows the reaction to be described by a *rate expression* or *rate law*, which is an algebraic formula containing one or more *rate constants*, as well as terms for the concentration of all reactant species that are involved in the rate-determining and prior steps. Each concentration has an exponent called the *order of the reaction* with respect to that component. The overall kinetic order of the reaction is the sum of all the exponents in the rate expression. The mathematical form of the rate expression for a reaction depends on the order of the reaction. Using $[A_0]$, $[B_0]$, $[C_0]$, etc, for the initial ($t = 0, t_0$) concentrations and $[A]$, $[B]$, $[C]$, etc, as the reactant concentrations at time t , give the following expressions⁵¹:

FIRST ORDER: Rate = $k[A]$

$$\ln \frac{[A_0]}{[A]} = kt \quad \text{or} \quad [A] = [A_0] e^{-kt} \quad (3.27)$$

SECOND ORDER/ONE REACTANT: Rate = $k[A]^2$

$$kt = \frac{1}{A} - \frac{1}{A_0} \quad (3.28)$$

SECOND ORDER/TWO REACTANTS: Rate = $k[A][B]$

$$kt = \frac{1}{[B_0] - [A_0]} \ln \frac{[A_0][B]}{[B_0][A]} \quad (3.29)$$

⁵¹. J. W. Moore and R. G. Pearson, *Kinetics and Mechanism*, 3rd Edition, John Wiley & Sons, New York, 1981, Chap. 2.

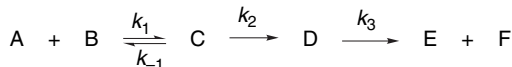
$$kt = \frac{1}{2} \left(\frac{1}{[A]^2} - \frac{1}{[A_o]^2} \right) \quad (3.30)$$

$$kt = \frac{2}{(2[B_o] - [A_o])} \left(\frac{1}{[A]} - \frac{1}{[A_o]} \right) + \frac{2}{(2[B_o] - [A_o])^2} \ln \frac{[B_o][A]}{[A_o][B]} \quad (3.31)$$

Integrated expressions applicable to other systems are available.⁵²

The kinetic data available for a particular reaction are examined to determine if they fit a simple kinetic expression. For example, for a first-order reaction, a plot of $\log [A]$ versus t yields a straight line with a slope of $-k/2.303$. For second-order reactions, a plot of $1/[A]$ versus t is linear with a slope of k . Figure 3.7 shows such plots. Alternatively, the value of k can be calculated from the integrated expression over a sufficient time range. If the value of k remains constant, the data are consistent with that rate expression.

Many organic reactions consist of a series of steps involving several intermediates. The overall rate expression then depends on the relative magnitude of the rate constants for the individual steps. The relationship between a kinetic expression and a reaction mechanism can be appreciated by considering the several individual steps that constitute the overall reaction mechanism. The expression for the rate of any *single step* in a reaction mechanism contains a term for the concentration for each reacting species. Thus, for the reaction sequence:



the rates for the successive steps are:

$$\text{STEP 1: } \frac{d[C]}{dt} = k_1[\text{A}][\text{B}] - k_{-1}[\text{C}]$$

$$\text{STEP 2: } \frac{d[\text{D}]}{dt} = k_2[\text{C}]$$

$$\text{STEP 3: } \frac{d[\text{E}]}{dt} = \frac{d[\text{F}]}{dt} = k_3[\text{D}]$$

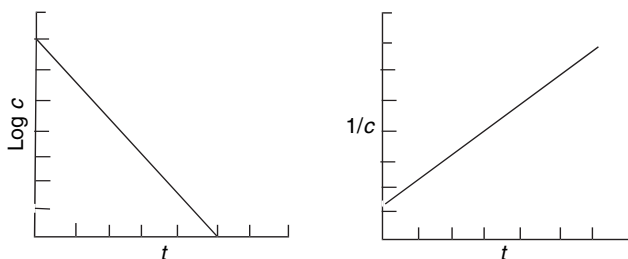


Fig. 3.7. Linear plots of $\log c$ versus t for a first-order reaction (a) and $1/c$ versus t for a second-order reaction.

⁵² C. Capellos and B. N. J. Bielski, *Kinetic Systems*, Wiley-Interscience, New York, 1972.

If we specify that the first step is a very rapid but unfavorable equilibrium, and that $k_2 \ll k_3$, then the second step is rate determining. Under these circumstances, the overall rate of the reaction will depend on the rate of the second step. In the reaction under consideration, the final step follows the rate-determining step and does not affect the rate of the overall reaction; k_3 does not appear in the overall rate expression. The rate of the reaction is governed by the second step, which is the bottleneck in the process. The rate of this step is equal to k_2 multiplied by the molar concentration of intermediate C, which is small and may not be measurable. It is therefore necessary to express the rate in terms of the concentration of reactants. In the case under consideration, this can be done by recognizing that [C] is related to [A] and [B] by an equilibrium constant:

$$K = \frac{[C]}{[A][B]}$$

Furthermore, K is related to k_1 and k_{-1} by the requirement that no net change in composition occur at equilibrium

$$k_{-1}[C] = k_1[A][B]$$

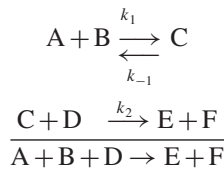
$$[C] = \frac{k_1}{k_{-1}}[A][B]$$

The rate of Step 2 can therefore be written in terms of [A] and [B]:

$$\frac{d[D]}{dt} = k_2[C] = k_2 \frac{k_1}{k_{-1}}[A][B] = k_{\text{obs}}[A][B]$$

Experimentally, it would be observed that the reaction rate would be proportional to both [A] and [B]. The reaction will be first order in each reactant and second order overall.

A useful approach that is often used in analysis and simplification of kinetic expressions is the *steady state approximation*, which can be illustrated by a hypothetical reaction scheme:



If C is a reactive, unstable species, its concentration will never be very large. It must be consumed at a rate that closely approximates the rate at which it is formed. Under these conditions, it is a valid approximation to set the rate of formation of C equal to its rate of destruction:

$$k_1[A][B] = k_2[C][D] + k_{-1}[C]$$

Rearrangement of this equation provides an expression for [C]:

$$\frac{k_1[A][B]}{(k_2[D] + k_{-1})} = [C]$$

By substituting into the rate for the second step, we obtain the following expression:

283

$$\text{Rate} = k_2[\text{C}][\text{D}] = k_2 \frac{k_1[\text{A}][\text{B}]}{(k_2[\text{D}] + k_{-1})} [\text{D}]$$

SECTION 3.2

Chemical Kinetics

If $k_2[\text{D}]$ is much greater than k_{-1} , the rate expression simplifies to

$$\text{Rate} = \frac{k_2 k_1 [\text{A}][\text{B}][\text{D}]}{k_2[\text{D}]} = k_1[\text{A}][\text{B}]$$

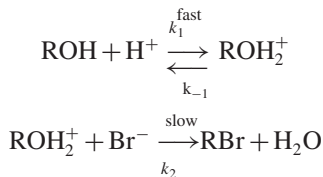
On the other hand, if $k_2[\text{D}]$ is much less than k_{-1} , the observed rate expression becomes

$$\text{Rate} = \frac{k_1 k_2 [\text{A}][\text{B}][\text{D}]}{k_{-1}}$$

The first situation corresponds to the first step being rate determining; in the second case, it is the second step, with the first step being a preequilibrium.

3.2.4. Examples of Rate Expressions

The normal course of a kinetic investigation involves the postulation of likely mechanisms and comparison of the observed rate expression with those expected for the various mechanisms. Those mechanisms that are incompatible with the observed kinetics can be eliminated as possibilities. One common kind of reaction involves proton transfer occurring as a rapid equilibrium preceding the rate-determining step, for example, in the reaction of an alcohol with hydrobromic acid to give an alkyl bromide:

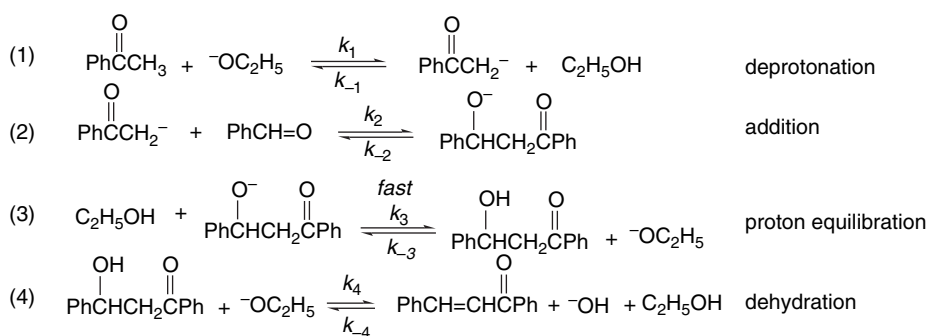


The overall rate being measured is that of Step 2, but there may be no means of directly measuring $[\text{ROH}_2^+]$. The concentration of the protonated intermediate ROH_2^+ can be expressed in terms of the concentration of the starting material by taking into consideration the equilibrium constant, which relates $[\text{ROH}]$, $[\text{Br}^-]$, and $[\text{H}^+]$:

$$\begin{aligned} K &= \frac{[\text{ROH}_2^+]}{[\text{ROH}][\text{H}^+]} \\ [\text{ROH}_2^+] &= K[\text{ROH}][\text{H}^+] \\ \text{Rate} &= k_2 K[\text{ROH}][\text{H}^+][\text{Br}^-] = k_{\text{obs}}[\text{ROH}][\text{H}^+][\text{Br}^-] \end{aligned}$$

To illustrate the development of a kinetic expression from a postulated reaction mechanism, let us consider the base-catalyzed reaction of benzaldehyde and acetophenone. Based on general knowledge of base-catalyzed reactions of carbonyl compounds, a reasonable sequence of steps can be written, but the relative rates of the steps is an open question. Furthermore, it is known that reactions of this type

are reversible, so the potential reversibility of each step must be taken into account. A completely reversible mechanism is as follows:



Because proton transfer reactions between oxygen atoms are usually very fast, Step 3 can be assumed to be a rapid equilibrium. With the above mechanism assumed, let us examine the rate expression that would result, depending upon which of the steps is rate determining. If Step 1 is rate controlling the rate expression would be

$$\text{Rate} = k_1[\text{PhCOCH}_3][\text{OC}_2\text{H}_5]$$

Under these conditions the concentration of the second reactant, benzaldehyde, would not enter into the rate expression. If Step 1 is an equilibrium and Step 2 is rate controlling, we obtain the rate expression

$$\text{Rate} = k_2[\text{PhCOCH}_2^-][\text{PhCHO}]$$

which on substituting in terms of the prior equilibrium gives

$$\text{Rate} = k_2 K_1 [\text{PhCOCH}_3][\text{OC}_2\text{H}_5][\text{PhCHO}]$$

since

$$[\text{PhCOCH}_2^-] = K_1 [\text{PhCOCH}_3][\text{OC}_2\text{H}_5]$$

where K_1 is the equilibrium constant for the deprotonation in the first step. If the final step is rate controlling the rate is

$$\text{Rate} = k_4[\text{PhCHCH}_2\text{COPh}][\text{OC}_2\text{H}_5]$$

The concentration of the intermediate $\text{PhCHOHCH}_2\text{COPh}$ (I) can be expressed in terms of the three prior equilibria. Using I for the intermediate and I^- for its conjugate base and neglecting $[\text{EtOH}]$, since it is the solvent and will remain constant, gives the following relationships:

$$K_3 = \frac{[\text{I}][\text{OC}_2\text{H}_5]}{[\text{I}^-]} \quad \text{and} \quad [\text{I}] = K_3 \frac{[\text{I}^-]}{[\text{OC}_2\text{H}_5]}$$

Substituting for $[\text{PhCOCH}_2^-]$ from the equilibrium expression for Step 1 gives

285

$$[\mathbf{I}] = \frac{K_3 K_2 [\text{PhCHO}]}{[-\text{OEt}]} K_1 [\text{PhCOCH}_3] [-\text{OEt}] = K' [\text{PhCHO}] [\text{PhCOCH}_3]$$

This provides the final rate expression:

$$\text{Rate} = k_{\text{obs}} [-\text{OC}_2\text{H}_5] [\text{PhCHO}] [\text{PhCOCH}_3]$$

Note that the form of this third-order kinetic expression is identical to that in the case where the second step was rate determining and would not distinguish between the two possibilities.

Experimental studies of this base-catalyzed condensation have revealed that it is third order, indicating that either the second or fourth step must be rate determining. Studies on the intermediate **I** obtained by an alternative synthesis have shown that k_4 is about four times as large as k_3 so that about 80% of **I** goes on to product. These reactions are faster than the overall reaction under the same conditions, so the second step must be rate controlling.⁵³

These examples illustrate the relationship between kinetic results and the determination of the reaction mechanism. Kinetic results can exclude from consideration all mechanisms that require a rate law different from the observed one. It is often true, however, that related mechanisms give rise to identical predicted rate expressions. In that case, the mechanisms are *kinetically equivalent* and a choice between them is not possible solely on the basis of kinetic data. A further limitation on the information that kinetic studies provide should also be recognized. Although the data can give the *composition* of the activated complex for the rate-determining and preceding steps, it provides no information about the *structure* of the activated complex or any intermediates. Sometimes the structure can be inferred from related chemical experience, but it is never established solely by kinetic data.

SECTION 3.3

*General Relationships
between Thermodynamic
Stability and Reaction
Rates*

3.3. General Relationships between Thermodynamic Stability and Reaction Rates

We have considered the fundamental principles of thermodynamics and reaction kinetics. Now we would like to search for relationships between stability, as defined by thermodynamics, and reactivity, which is described by kinetics. Reaction potential energy diagrams are key tools in making these connections.

3.3.1. Kinetic versus Thermodynamic Control of Product Composition

Product composition at the end of the reaction may be governed by the equilibrium thermodynamics of the system. When this is true, the product composition is governed by *thermodynamic control* and the stability difference between the competing products, as given by the free-energy difference, determines the product composition. Alternatively, product composition may be governed by competing rates of formation of

⁵³. E. Coombs and D. P. Evans, *J. Chem. Soc.*, 1295 (1940); D. S. Noyce, W. A. Pryor, and A. H. Bottini, *J. Am. Chem. Soc.*, **77**, 1402 (1955).

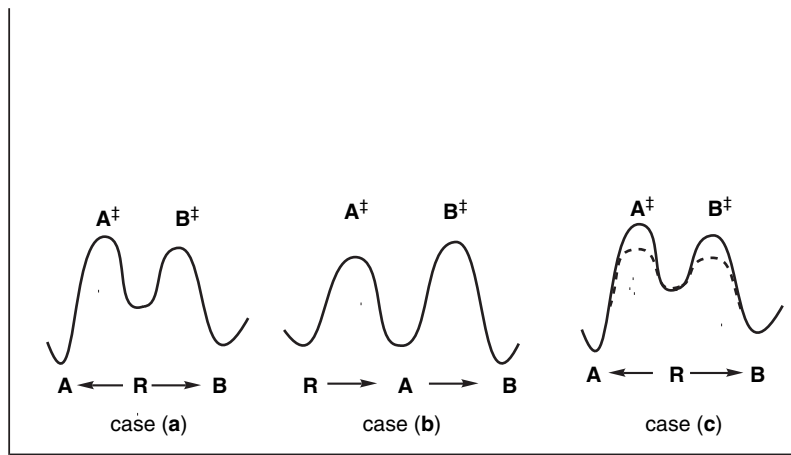


Fig. 3.8. Examples of reactions under kinetic and thermodynamic control. (a) $\Delta G_A^\ddagger < \Delta G_B^\ddagger$; (b) $\Delta G_A^\ddagger < \Delta G_B^\ddagger$; (c) alternative mechanism for product equilibrium.

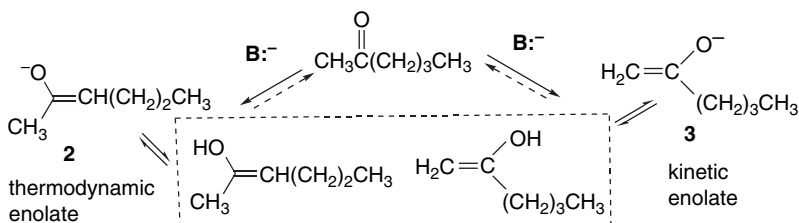
products, which is called *kinetic control*. Let us consider cases (a) to (c) in Figure 3.8. In case (a), the ΔG^\ddagger 's for formation of the competing transition states A^\ddagger and B^\ddagger from the reactant R are substantially less than the ΔG^\ddagger 's for formation of A and B, respectively. If the latter two ΔG^\ddagger 's are sufficiently large that the competitively formed products A and B do not return to R, the ratio of the products A and B at the end of the reaction will not depend on their relative stabilities, but only on the *relative rates of formation*. The formation of A and B is effectively irreversible in these circumstances. The reaction energy profile in case (a) corresponds to this situation and is a case of kinetic control. The relative amounts of products A and B depend on the relative activation barriers ΔG_A^\ddagger and ΔG_B^\ddagger and not on the relative stability of products A and B. The diagram shows $\Delta G_B^\ddagger < \Delta G_A^\ddagger$, so the major product will be B, even though it is less stable than A.

Case (b) represents a situation of two successive reactions. The lowest ΔG^\ddagger is that for formation of A^\ddagger from R. But, the ΔG^\ddagger for formation of B^\ddagger from A is not much larger. The system in (b) might be governed by either kinetic or thermodynamic factors. Conversion of R to A will be only slightly faster than conversion of A to B. If the reaction conditions are carefully adjusted it will be possible for A to accumulate and not proceed to the more stable product B. Under such conditions, A will be the dominant product and the reaction will be under kinetic control. Under somewhat more energetic conditions, for example, at a higher temperature, A will be transformed into B. Under these conditions the reaction will be under thermodynamic control. A and B will equilibrate and the product ratio will depend on the equilibrium constant determined by ΔG for the reaction $A \rightleftharpoons B$.

In case (c), the solid reaction energy profile represents the same situation of kinetic control as shown in (a), with product B (which is thermodynamically less stable) being formed because $\Delta G_B^\ddagger < \Delta G_A^\ddagger$. The dashed energy profile represents a different set of conditions for the same transformation, such as addition of a catalyst or change of solvent, that substantially reduces the energy of A^\ddagger and B^\ddagger such that interconversion of A and B is fast. This will result in formation of the more stable product A, even though the barrier to formation of B remains lower. Under these circumstances, the reaction is under *thermodynamic control*.

Thus, whenever competing or successive reaction products can come to equilibrium, the product composition will reflect relative stability and be subject to thermodynamic control. If product composition is governed by competing rates, the reaction is under kinetic control. A given reaction may be subject to either thermodynamic or kinetic control, depending on the conditions.

The idea of kinetic versus thermodynamic control can be illustrated by a brief discussion of the formation of enolate anions from unsymmetrical ketones. This is a very important matter for synthesis and is discussed more fully in Chapter 6 and in Section 1.1.2 in Part B. Most ketones can give rise to more than one enolate. Many studies have shown that the ratio among the possible enolates that are formed depends on the reaction conditions.⁵⁴ This can be illustrated for the case of 2-hexanone. If the base chosen is a strong, sterically hindered one, such as lithium diisopropylamide, and the solvent is aprotic, the major enolate formed is **3** in the diagram below. If a protic solvent or a weaker base (one comparable in basicity to the ketone enolate) is used, the dominant enolate is **2**. Under these latter conditions, equilibration can occur by reversible formation of the enol. Enolate **3** is the kinetic enolate, but **2** is thermodynamically favored.



The structural and mechanistic basis for the relationships between kinetic versus thermodynamic control and the reaction conditions is as follows. The α -hydrogens of the methyl group are less sterically hindered than the α -hydrogens of the butyl group. As a result, removal of a methyl hydrogen as a proton is faster than removal of a butyl hydrogen. This effect is magnified when the base is sterically bulky and is particularly sensitive to the steric environment of the competing hydrogens. If the base is very strong, the enolate will not be reconverted to the ketone because the enolate is too weak a base to regain the proton. These conditions correspond to (a) in Figure 3.8 and represent a case of kinetic control. If a weaker base is used or if the solvent is protic, protons can be transferred reversibly between the isomeric enolates and the base (because the base strengths of the enolate and the base are comparable). Under these conditions the more stable enolate will be dominant because the enolates are in equilibrium. The more substituted enolate **2** is the more stable of the pair, just as more substituted alkenes are more stable than terminal alkenes. This corresponds to case (c) in Figure 3.8, and product (enolate) equilibration occurs through rapid proton exchange. In protic solvents this exchange can occur through the enols.

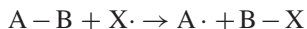
3.3.2. Correlations between Thermodynamic and Kinetic Aspects of Reactions

Is there any inherent relationship between the free energy of a reaction, ΔG , and the rate of reaction, which is governed by ΔG^\ddagger ? Are more exothermic reactions

⁵⁴ J. d'Angelo, *Tetrahedron*, **32**, 2979 (1976); H. O. House, *Modern Synthetic Reactions*, 2nd Edition, W. A. Benjamin, Menlo Park, CA, 1972.

faster? These questions raise the issue of a relationship between the thermodynamic and kinetic aspects of reactivity. It turns out that there frequently are such relationships *in series of closely related reactions*, although there is no fundamental requirement that this be the case. The next several sections discuss examples of such relationships.

3.3.2.1. Bell-Evans-Polyani Relationship. The Bell-Evans-Polyani formula deals with the relationship between reaction rate and exothermicity for a series of related single-step reactions.⁵⁵ Evans and Polyani pointed out that for a series of homolytic atom transfer reactions of the general type

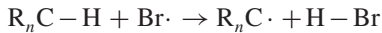


there was a relationship between the activation energy and the reaction enthalpy, which can be expressed as

$$E_a = E_0 + \alpha \Delta H \quad (3.32)$$

where E_0 is the activation energy of the reference reaction and ΔH is the enthalpy of each reaction in the series. In terms of reaction energy diagrams, this indicates that for reactions having similar energy profiles, the height of the barrier will decrease as the reaction becomes more exothermic (and vice versa), as illustrated in Figure 3.9.

This relationship can be explored, for example, by considering the rates of hydrogen abstraction reactions. For example, the E_a for hydrogen abstraction from simple hydrocarbons⁵⁶ shown below can be compared with the ΔH of the reaction, as derived from the bond energy data in Table 3.2. The plot is shown in Figure 3.10.



Alkane	E_a	ΔH
CH ₃ -H	18.3	+18.0
C ₂ H ₅ -H	13.4	+13.5
(CH ₃) ₂ CH-H	10.2	+11.1
C ₂ H ₅ CH(CH ₃)-H	10.2	+11.3
(CH ₃) ₃ C-H	7.5	+8.7

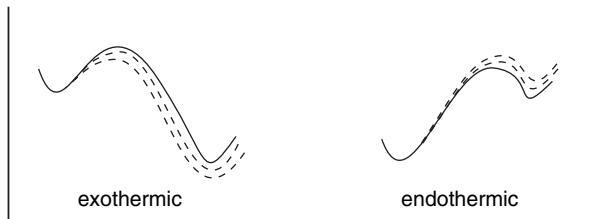


Fig. 3.9. Energy profiles for series of related reactions illustrating the Bell-Evans-Polyani relationship.

⁵⁵ M. G. Evans and M. Polanyi, *Trans. Faraday Soc.*, **34**, 11 (1938).

⁵⁶ G. C. Fettis and A. F. Trotman-Dickenson, *J. Am. Chem. Soc.*, **81**, 5260 (1959).

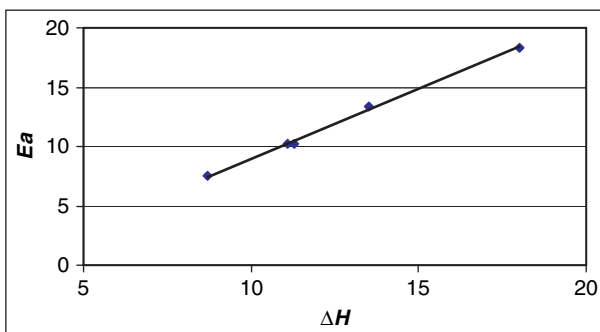


Fig. 3.10. Plot of E_a for abstraction of hydrogen from alkanes by bromine atom versus ΔH .

Another example of data of this type pertains to the reaction of *t*-butoxy radicals with hydrocarbons.⁵⁷ The *t*-butoxy radical is more reactive and less selective than bromine atoms and the E_a are quite low. There is a correlation corresponding to Equation (3.32), with $\alpha = 0.3$ for hydrocarbons with C–H bond strengths greater than ~90 kcal/mol. For weaker bonds, the E_a levels off at about 2 kcal/mol. We say more about the relationship between E_a for hydrogen abstraction and the enthalpy of the reaction in Topic 11.2.

Hydrocarbon	BDE (kcal/mol)	E_a (kcal/mol)
Triphenylmethane	81	1.9
Diphenylmethane	84	2.4
3-Phenylpropene	82	2.5
Toluene	90	3.5
Cyclopentane	97	3.5
Cyclohexane	99	4.4
<i>t</i> -Butylbenzene	101	6.1

3.3.2.2. Hammond's Postulate. Because the rates of chemical reactions are controlled by ΔG^\ddagger , information about the structure of TSs is crucial to understanding reaction mechanisms. However, because TSs have only transitory existence, it is not possible to make experimental measurements that provide direct information about their structure. Hammond pointed out the circumstances under which it is valid to relate transition state structure to the structure of reactants, intermediates, or products.⁵⁸ His statement is known as *Hammond's postulate*. Discussing individual steps in a reaction mechanism, Hammond's postulate states: “*If two states, as, for example, a transition state and an unstable intermediate, occur consecutively during a reaction process and have nearly the same energy content, their interconversion will involve only a small reorganization of molecular structure.*”

This statement can be discussed with reference to potential energy diagrams. Case (a) in Figure 3.11 represents a very exothermic step with a low activation energy. It follows from Hammond's postulate that in this step, the TS will resemble the reactant, because the two are close in energy and interconverted by a small structural

⁵⁷. M. Finn, R. Fridline, N. K. Suleman, C. J. Wohl, and J. M. Tanko, *J. Am. Chem. Soc.*, **126**, 7578 (2004).

⁵⁸. G. S. Hammond, *J. Am. Chem. Soc.*, **77**, 334 (1955).

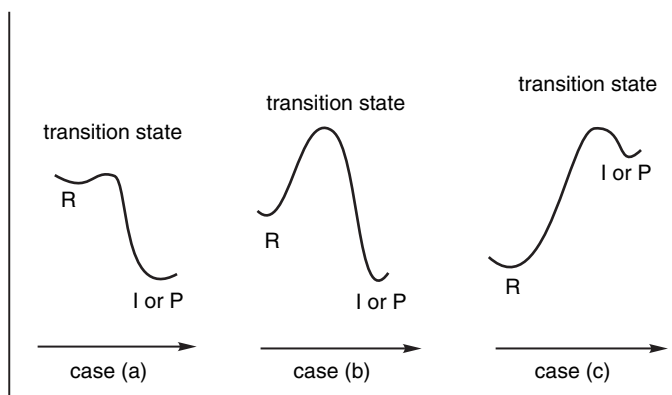
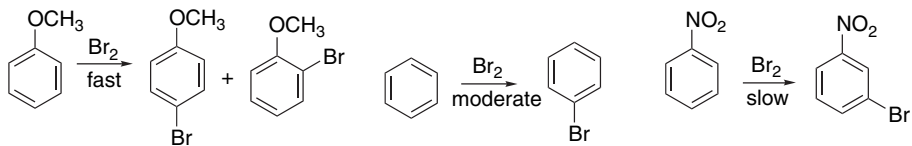


Fig. 3.11. Reaction energy diagram illustrating Hammond's postulate: (a) early transition structure resembles reactant, (b) midpoint transition structure resembles neither reactant or product, (c) late transition structure resembles intermediate or product.

change. This is depicted in the potential energy diagram as a small displacement toward product along the reaction coordinate. This means that comparisons between closely related series of reactants should depend primarily on *structural features present in the reactant*. Case (b) describes a step in which the energy of the TS is a good deal higher than either the reactant or the product. In this case, neither the reactant nor the product is a good model of the TS. Independent information is needed to postulate the characteristics of the TS. Comparison among a series of reactants should focus primarily on TS structure. Case (c) illustrates an endothermic step, such as might occur in the formation of an unstable intermediate. In this case the energy of the TS is similar to that of the intermediate and the TS should be similar in structure to the intermediate. Structural and substituent effects can best be interpreted in terms of their effect on the stability of the intermediate.

The significance of the concept incorporated in Hammond's postulate is that in appropriate cases it permits discussion of TS structure in terms of the reactants, intermediates, or products in a multistep reaction sequence. The postulate indicates that the cases where such comparison is appropriate are those in which the TS energy is close to that of the reactant, intermediate, or product. Chemists sometimes speak of an “early” or “late” TS. An “early” TS is reactant-like, whereas a “late” TS is intermediate- (or product-) like.

Electrophilic aromatic substitution is a situation in which it is useful to discuss TS structure in terms of a reaction intermediate. The *ortho*, *para*, and *meta* directing effects of aromatic substituents were among the first structure-reactivity relationships to be developed in organic chemistry. Certain functional groups activate aromatic rings toward substitution and direct the entering electrophile to the *ortho* and *para* positions, whereas others are deactivating and lead to substitution in the *meta* position. The bromination of methoxybenzene (anisole), benzene, and nitrobenzene can serve as examples for discussion.



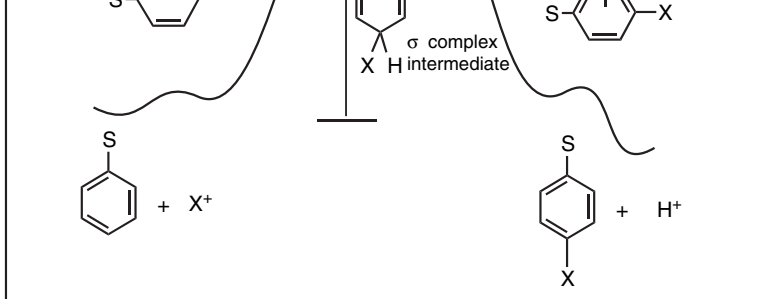
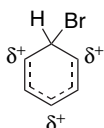


Fig. 3.12. Potential energy diagram for electrophilic aromatic substitution.

It can be demonstrated that the reactions are kinetically controlled; that is, there is no isomerization among the *ortho*, *meta*, and *para* products after they are formed. It is therefore the ΔG^\ddagger values that hold the key to the connection between the rate effects and the substituent-directing effects. However, to discuss the effect of substituents on ΔG^\ddagger , we must know something about the reaction mechanism and the nature of the competing TS. Electrophilic aromatic substitution is dealt with in detail in Chapter 9. Evidence presented there indicates that electrophilic aromatic substitution involves a distinct intermediate and two less well-defined states. The potential energy diagram in Figure 3.12 is believed to be a good representation of the energy changes that occur during bromination. By application of the Hammond postulate, we conclude that that the rate-determining step involves formation of a TS that closely resembles the intermediate, which is called the “ σ complex.” It is therefore appropriate to discuss the effect of substituents on the TS in terms of the structure of this intermediate.

Because the product composition is kinetically controlled, the isomer ratio is governed by the relative magnitudes of ΔG_o^\ddagger , ΔG_m^\ddagger , and ΔG_p^\ddagger , the energies of activation for the *ortho*, *meta*, and *para* transition states, respectively. Figure 3.13 shows a qualitative comparison of these ΔG^\ddagger values. At the TS, a positive charge is present on the benzene ring, primarily at positions 2, 4, and 6 in relation to the entering bromine.



The electron-releasing methoxy group interacts directly to delocalize the charge and stabilize the intermediates leading to *o*- and *p*-bromination, but does not stabilize the intermediate leading to *m*-substitution product.

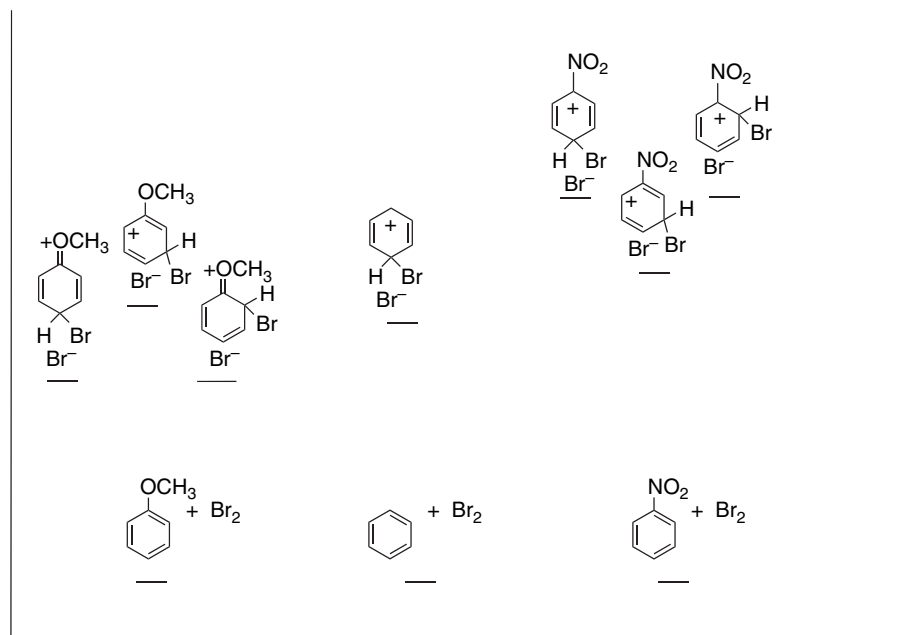
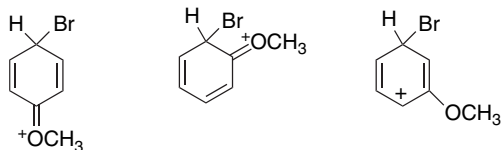
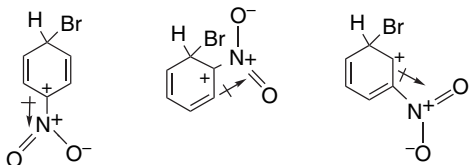


Fig. 3.13. Relative energies of intermediates for bromination of methoxybenzene, benzene, and nitrobenzene indicating the effect of substituents on energy of intermediates.



The *o*- and *p*-intermediates are therefore stabilized relative to benzene but the *m*-intermediate is not, as is illustrated in Figure 3.13. As a result, methoxybenzene reacts faster than benzene and the product is mainly the *o*- and *p*-isomers.

In the case of nitrobenzene, the electron-withdrawing nitro group cannot stabilize the positive charge in the σ -complex intermediate. In fact, it strongly destabilizes the intermediate as a result of an unfavorable polar interaction. This destabilization is greatest in the *o*- and *p*-intermediates, which place a partial positive charge on the nitro-substituted carbon. The *meta*-TS is also destabilized relative to benzene, but not as much as the *ortho*- and *para*-TS. As a result nitrobenzene is less reactive than benzene and the product is mainly the *meta*-isomer



The substituent effects in aromatic electrophilic substitution are dominated by *resonance effects*. In other systems, stereoelectronic or steric effects might be more

important. Whatever the nature of the substituent effects, the Hammond postulate recognizes that structural discussion of transition states in terms of reactants, intermediates, or products is valid only when their structures and energies are similar.

3.3.2.3. The Marcus Equation. The *Marcus equation* provides a means for numerical evaluation of the relationship between ΔG° and ΔG^\ddagger . The Marcus equation proposes that for a single-step reaction process there is a relationship involving the net exo- or endothermicity of the reaction and an energy associated with the activation process called the *intrinsic barrier*.⁵⁹ The Marcus equation proposes that for a series of related reactions, there is a predictable relationship between ΔG^\ddagger and ΔG° , the free energy of reaction. The energies of the reactants, transition state, and products can be described by intersecting parabolic potential energy functions. The relationship can be expressed by the following equation:

$$\Delta G^\ddagger = \tilde{G}[1 + (\Delta G^\circ/4\tilde{G})]^2 \quad (3.33)$$

where \tilde{G} is the intrinsic barrier of the reaction and ΔG° and ΔG^\ddagger are free energy and energy of activation for the reaction under consideration.

The Marcus equation (3.33), like the Bell-Evans-Polyani relationship, indicates that for a related series of reactions, the activation energy (and therefore the rate) is related to the net free-energy change. It is based on assumption of a parabolic shape of the potential energy curve and breaks down at certain limits. The range of the equation can be extended by other formulations of the shape of the potential energy functions.⁶⁰ Figure 3.14 plots a series of reaction energy profiles with $\tilde{G} = 25$ kcal and ΔG° varying

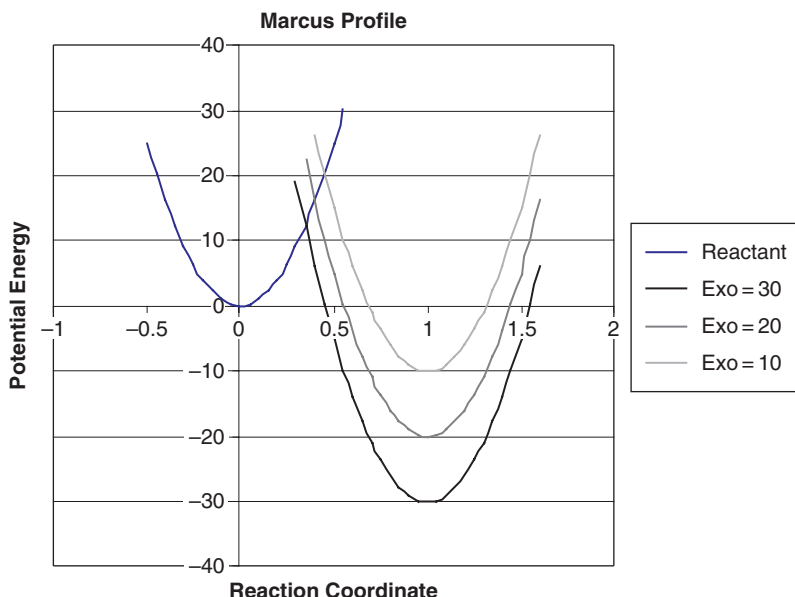


Fig. 3.14. Marcus equation plots for a hypothetical reaction series with an intrinsic barrier of 25 kcal/mol and exothermicities of 10, 20, and 30 kcal/mol.

⁵⁹ R. A. Marcus, *J. Phys. Chem.*, **72**, 891 (1968); R. A. Marcus, *J. Am. Chem. Soc.*, **91**, 7224 (1969).

⁶⁰ E. S. Lewis, C. S. Shen, and R. A. More O'Ferrall, *J. Chem. Soc., Perkin Trans.*, **2**, 1084 (1981).

from 0 to -30 kcal/mol , and it illustrates that we can indeed expect a correlation between reaction exothermicity (or endothermicity) and rate. The Marcus equation makes another prediction that is quite surprising—that the barrier will increase again for very exothermic reactions. This is called the *inverted region*. This aspect of Marcus theory is not widely applied in organic chemistry, but is of considerable importance in electron transfer reactions.

The Marcus equation can be modified to Equation (3.34) to take account of other energy changes, for example, the desolvation and electrostatic interactions that are involved in bringing together the ensemble of reacting molecules. These energies contribute to the observed activation energy. Similarly, there may be residual interactions in the product ensemble that differ from the independent molecules.⁶¹ Guthrie proposed the following equations:

$$\Delta G_{\text{corr}} = \tilde{G} \left(1 + \frac{\Delta G^{\circ}_{\text{corr}}}{4\tilde{G}} \right)^2 \quad (3.34)$$

$$\Delta G^{\ddagger}_{\text{corr}} = \Delta G^{\ddagger}_{\text{obs}} - W_R \quad (3.35)$$

$$\Delta G^{\circ}_{\text{corr}} = \Delta G^{\circ}_{\text{obs}} + W_R - W_P \quad (3.36)$$

where W_R is work to bring reactants together and W_P is work to bring products together. In this formulation, the assignment of W_R and W_P terms, which includes solvation, requires careful consideration. Figure 3.15 shows a reaction energy diagram including the W_R and W_P terms.

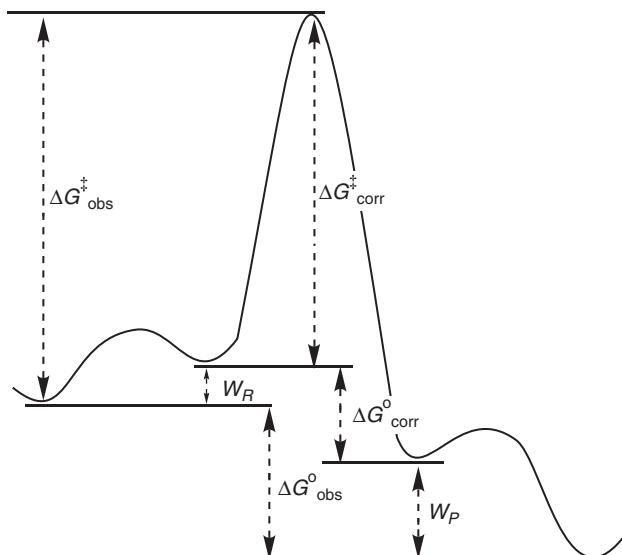
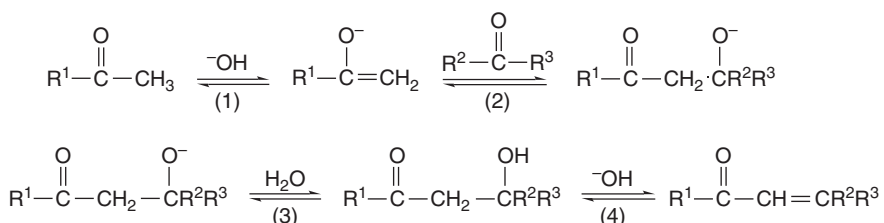


Fig. 3.15. Model for a reaction, $A + B \rightleftharpoons A, B \rightleftharpoons C, D \rightleftharpoons C + D$ used in applying the Marcus theory. The reactants come together in an encounter complex (A, B) at a free-energy cost W_R and react within this complex to form (C, D), the encounter complex of products, which then separate, releasing free energy W_P . The Marcus theory applies to reactions within the encounter complex where $\Delta G^{\ddagger}_{\text{corr}}$ is determined by $\Delta G^{\circ}_{\text{corr}}$ and the intrinsic barrier \tilde{G} . Reproduced from *Can. J. Chem.*, **74**, 1283 (1996), by permission from National Research Council Press.

⁶¹ J. P. Guthrie, *Can. J. Chem.*, **74**, 1283 (1996).

With these two relationships, if reliable values of W_R and W_P can be determined and \tilde{G} established for a reaction series, the activation barriers can be calculated from the thermodynamic data that provide ΔG° . Relationships of this kind have been shown to occur in many different organic reactions, so the principles appear to have considerable generality. For example, Guthrie investigated both the addition (Step 2) and elimination (Step 4) parts of the aldol condensation reaction (see p. 283–285).⁶² Steps (1) and (3) are proton transfers that are fast under the reaction conditions.



A series of acceptors [$\text{CH}_2=\text{O}$, $\text{CH}_3\text{CH}=\text{O}$, $\text{PhCH}=\text{O}$, $(\text{CH}_3)_2\text{C}=\text{O}$] and a series of enolates ($-\text{CH}_2\text{CH}=\text{O}$, $-\text{CH}_2\text{COCH}_3$, $-\text{CH}_2\text{COPh}$) were examined and good correlations of both the addition and elimination steps were found, as shown in Figure 3.16. The potential value of the Marcus equation is the ability it provides to make predictions of reaction rates based on equilibrium data (which can be obtained from computation as well as experiment).

The Bell-Evans-Polanyi relationship, Hammond's postulate, and the Marcus equation are all approaches to analyzing, understanding, and predicting relationships between the thermodynamics and kinetics of a series of closely related reactions. This is an important issue in organic chemistry, where series of reactions differing only in peripheral substituents are common. Each of these approaches provides a sound basis for the intuitive expectation that substituents that favor a reaction in a thermodynamic

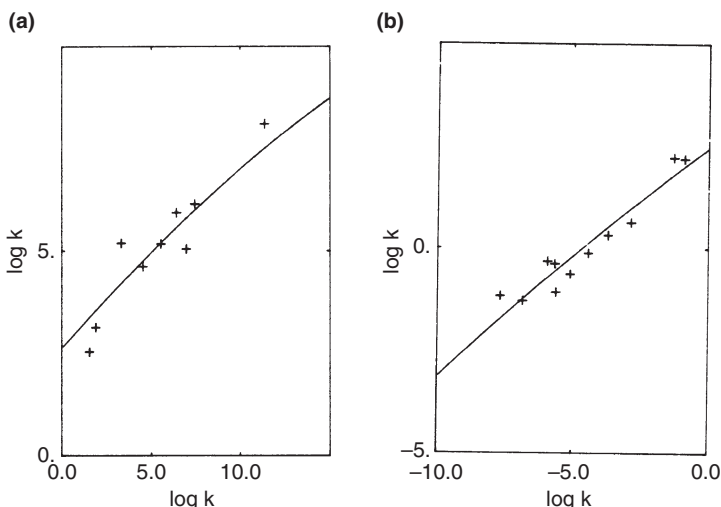


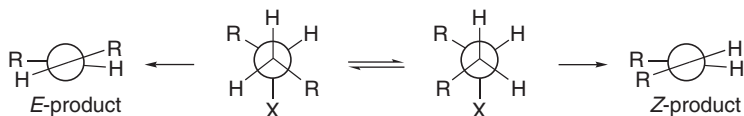
Fig. 3.16. Marcus correlations for (a) addition and (b) elimination steps of an aldol reaction. The values of the intrinsic barrier \tilde{G} are (a) 13.8 ± 0.8 kcal/mol and (b) 14.1 ± 0.5 kcal/mol. Adapted from *J. Am. Chem. Soc.*, **113**, 7249 (1991).

⁶² J. P. Guthrie, *J. Am. Chem. Soc.*, **113**, 7249 (1991).

sense will also do so in a kinetic sense. Each of these approaches pertains to series of reactions that proceed by *similar mechanisms*, because they are based upon a series of closely related reaction energy profiles. If substituents have a strong enough effect to change the mechanism, for example, a change in the rate-determining step, the relationships cannot be expected to hold.

3.3.3. Curtin-Hammett Principle.

In Chapter 2, we discussed conformational equilibria of organic molecules. At this point, let us consider how conformational equilibria can affect chemical reactivity. Under what circumstances can the position of the conformational equilibrium for a reactant determine which of two competing reaction paths will be followed? A potential energy diagram is shown in Figure 3.17. It pertains to a situation where one conformation of a reactant would be expected to give product A and another product B. This might occur, for example, in a stereospecific *anti* elimination.



In most cases, the energy of activation for a chemical reaction is greater than that for a conformational equilibration, as is illustrated in the Figure 3.17. If this is the case, ΔG_a^\ddagger and $\Delta G_b^\ddagger \gg \Delta G_c$. The conformers of the reactant are in equilibrium and are interconverted at a rate much faster than the competing reactions occur.

According to transition state theory,

$$k_r = \frac{\kappa k_B T}{h} e^{\Delta G_c^\ddagger / RT} \quad \text{and} \quad K_c = e^{\Delta G_c / RT} \quad (3.37)$$

$$\text{Product ratio} = \frac{(\kappa k_B T / h) e^{-\Delta G_a^\ddagger / RT} e^{+\Delta G_c / RT}}{(\kappa k_B T / h) e^{-\Delta G_b^\ddagger / RT}} \quad (3.38)$$

$$= e^{(-\Delta G_a^\ddagger + \Delta G_b^\ddagger + \Delta G_c) / RT} \quad (3.39)$$

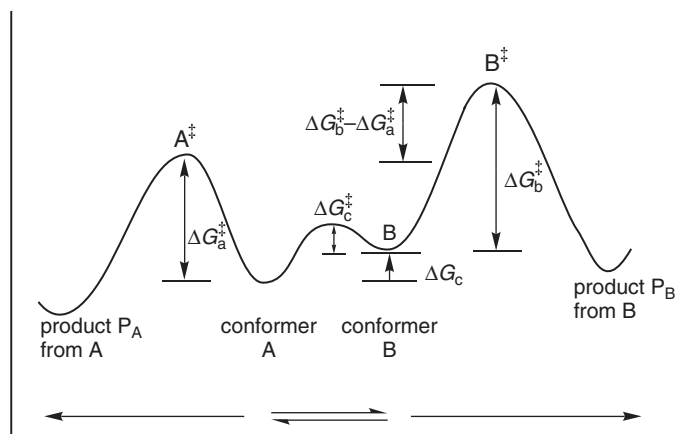


Fig. 3.17. Reaction potential energy diagram illustrating the Curtin-Hammett principle.

$$\Delta G_b^\ddagger - \Delta G_a^\ddagger + \Delta G_c = G_b^\ddagger - G_a^\ddagger \quad (3.40)$$

The product ratio is therefore not determined by ΔG_c but by the relative energy of the two transition states A^\ddagger and B^\ddagger . The conclusion that the ratio of products formed from conformational isomers is not determined by the conformational equilibrium ratio is known as the *Curtin-Hammett principle*.⁶³ Although the rate of the formation of the products is dependent upon the relative concentration of the two conformers, because ΔG_b^\ddagger is decreased relative to ΔG_a^\ddagger to the extent of the difference in the two conformational energies, the conformational preequilibrium is established rapidly, relative to the two competing product-forming steps.⁶⁴ The position of the conformational equilibrium cannot control the product ratio. The reaction can proceed through a minor conformation if it is the one that provides access to the lowest-energy transition state.

The same arguments can be applied to other energetically facile interconversions of two potential reactants. For example, some organic molecules can undergo rapid proton shifts (tautomerism) and the chemical reactivity of the two isomers may be quite different. However, it is not valid to deduce the ratio of two tautomers on the basis of subsequent reactions that have activation energies greater than that of the tautomerism. Just as in the case of conformational isomerism, the ratio of products formed in subsequent reactions is not controlled by the position of the facile equilibrium, but by the E_a of the competing steps.

SECTION 3.4

Electronic Substituent Effects on Reaction Intermediates

3.4. Electronic Substituent Effects on Reaction Intermediates

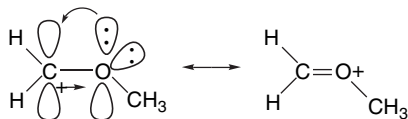
It is often observed that the introduction of substituents changes the rate of organic reactions, even if the substituent is not directly involved in the reaction. Changes that affect the ΔG^\ddagger for the rate-determining, or preceding, steps will cause a change in the observed reaction rate. The difference can result from energy changes in the reactant(s) or transition state, or both. Shifts in product composition can result from changes in the relative ΔG^\ddagger of competing reaction paths. In the broadest terms, there are three kinds of substituent effects, resulting from electronic, steric, and structure-specific interactions. *Steric effects* have their origin in nonbonding interactions. *Structure-specific interactions* include, for example, intramolecular hydrogen bonding and neighboring-group participation that depend on location of the substituents that are involved. In this section, we focus on *electronic effects*. Electronic substituent effects can be further subdivided. Substituents can operate by delocalization of electrons by *resonance* or *hyperconjugation*, including $\sigma - \sigma^*$ and $\sigma - \pi^*$, as well as $\pi - \pi^*$ delocalization. Resonance and hyperconjugation operate through specific orbital interactions and therefore impose particular *stereochemical* requirements; that is, interacting orbitals must be correctly aligned. *Polar effects* are electrostatic and include both the effect of proximate charges owing to bond dipoles and the effects of more distant centers of charge. Polar effects also may have a geometric component. For example, the orientation of a particular bond dipole determines how it interacts with a developing charge at a reaction center elsewhere in the molecule. Polar effects are

⁶³. D. Y. Curtin, *Rec. Chem. Prog.*, **15**, 111 (1954); E. L. Eliel, *Stereochemistry of Carbon Compounds*, McGraw-Hill, New York, 1962, pp. 151–152, 237–238.

⁶⁴. For a more complete discussion of the relationship between conformational equilibria and reactivity, see J. I. Seeman, *Chem. Rev.*, **83**, 83 (1983).

sometimes subdivided into *inductive* and *field effects*. Effects attributed to proximate electronic changes owing to bond dipoles are called inductive effects and those that are due to dipole interaction through space are called field effects. *Polarizability effects*, which result from distortion of electronic distribution of a group, provide another mechanism of substituent interaction, and can be particularly important in the gas phase.

The broad classification of substituents into electron-releasing groups (ERGs) and electron-withdrawing groups (EWGs) is useful. However, to achieve further refinement, we must make two additional distinctions. *The electronic effects of substituents resulting from delocalization and polar interactions are not necessarily in the same direction.* A methoxy substituent on a carbocation is a good example. The oxygen atom is strongly stabilizing by resonance because it permits a π bond to form between oxygen and carbon, thereby delocalizing the positive charge. However, the C–O bond dipole is destabilizing, since it increases the positive charge at carbon. In this case the resonance stabilizing effect is dominant and the carbocation is strongly stabilized (see p. 21–22).



We also have to recognize that the relative importance of delocalization and polar effects depends on the nature of the charge that develops in the TS or the intermediate. The delocalization effects of most substituents are in opposite directions, depending on whether a negative or a positive charge is involved, but there are exceptions. Phenyl and vinyl groups can stabilize either negative or positive charges by delocalization. In Section 3.6, we discuss *linear free-energy relationships*, which permit the quantitative description of substituent effects. At this point, however, we want to make a qualitative assessment. Scheme 3.1 lists a number of common substituent groups and indicates whether the group is an ERG or an EWG substituent. The effects of substituents are shown separately for resonance and polar interactions. In the discussions of substituent effects in future chapters, we frequently make reference to the electronic effects of ERG and EWG substituents.

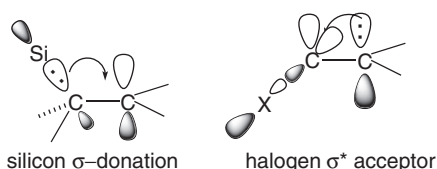
We can quickly note some of the general features of the various types of substituents. Alkyl groups are electron releasing by virtue of σ delocalization (hyperconjugation) and small polar effects. The π and π^* orbitals of vinyl, phenyl, and ethynyl groups allow them to delocalize both positive and negative charges. Because of the greater electronegativity of sp^2 and especially sp carbon, relative to sp^3 carbon, the unsaturated groups are weakly electron attracting from the polar perspective. (See p. 12–13 to review carbon electronegativity trends.) Oxygen and nitrogen substituents having unshared electron pairs are strong electron donors by resonance. Alkoxy, acyloxy, amino, and acylamido are common examples of this kind of group. On the other hand, because of the higher electronegativity of oxygen and nitrogen relative to carbon, they are EWGs through polar interactions. This is especially true of the acyloxy and acylamido groups because of the dipole associated with the carbonyl group. All the various carbonyl functional groups are EWG through both resonance and polar contributions. The C=O bond dipole and the higher electronegativity of the carbonyl carbon both contribute to the latter effect.

The halogens are an interesting group. They act as electron donors by resonance involving the unshared pairs, but this is opposed by a polar effect resulting from their

Scheme 3.1. Classification of Substituent Groups

Substituent	Resonance	Polar	SECTION 3.4 <i>Electronic Substituent Effects on Reaction Intermediates</i>
<u>Alkyl</u> CH ₃ , C ₂ H ₅ , (CH ₃) ₃ C, etc.	ERG	ERG (small)	
<u>Vinyl and aryl</u> CH ₂ =CH, C ₆ H ₅ , etc.	ERG or EWG	EWG (small)	
<u>Ethyneyl</u> HC≡C, etc.	ERG or EWG	EWG	
<u>Alkoxy, Acyloxy, Amino, Acylamido</u> RO, RCO ₂ , R ₂ N, RCONH, etc	ERG	EWG	
<u>Carbonyl</u> HC=O, RC=O, ROC=O, R ₂ NC=O, etc.	EWG	EWG	
<u>Halogens</u> F, Cl, Br, I	ERG	EWG	
<u>Polyhaloalkyl</u> CF ₃ , CCl ₃ , etc.	EWG	EWG	
<u>Other Nitrogen Groups</u> CN, NO ₂ , R ₃ N ⁺ , etc.	EWG	EWG	
<u>Sulfur Groups</u> RS RSO RSO ₂	ERG ERG EWG	EWG EWG EWG	
<u>Silyl Groups</u> R ₃ Si	ERG	ERG	

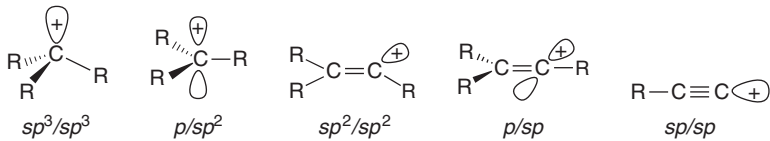
higher electronegativity. Moreover, the resonance and polar effects both weaken going down the periodic table. Resonance weakens because of longer bonds and poorer orbital overlap with carbon, whereas the polar effect decreases as the electronegativity diminishes. As a result, the halogens often exhibit unusual trends resulting from a changing balance between the resonance and polar effects. Halogen substituent effects are also affected by polarizability, which increases from fluorine to iodine. When halogen is placed on a carbon, as in trifluoromethyl or trichloromethyl, the groups are EWG by both polar and resonance mechanisms. The resonance component is associated with σ^* orbitals. The sulfur substituents RS, RSO, and RSO₂ show a shift from being resonance donors to strong polar acceptors, as the sulfur unshared pairs are involved in bonding to oxygen. Trialkylsilyl groups are slightly better ERGs than alkyl, since the silicon is less electronegative than carbon. Trialkylsilyl groups are very good electron donors by hyperconjugation.



There are many types of reaction intermediates that are involved in organic reactions. In this section we consider substituent effects on four important examples—carbocations, carbanions, radicals, and carbonyl addition (tetrahedral) intermediates—which illustrate how substituent effects can affect reactivity. Carbocation and carbanions are intermediates with positive and negative charge, respectively, and we will see that they have essentially opposite responses to most substituent groups. We also discuss substituent effects on neutral radical intermediates, where we might not, at first glance, expect to see strong electronic effects, since there is no net charge on the intermediate. The fourth case to be considered is the important class of carbonyl addition reactions, where substituent effects in the *reactant* often have the dominant effect on reaction rates.

3.4.1. Carbocations

Carbocations have a vacant orbital that bears a positive charge. Within the standard hybridization framework, there are five possible hybridization types if all the electrons are paired.

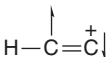


The approximate relative energies of these structures are illustrated in Figure 3.18. For trivalent carbon, the preferred hybridization is for the positive charge to be located in an unhybridized *p* orbital. Similarly, the *p/sp* hybridization is preferred for alkenyl carbocations. These hybridizations place the charge in a less electronegative *p*

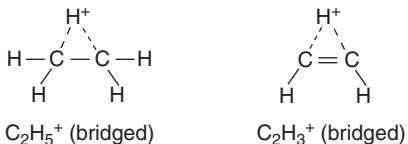
	MP4(SDQ)/6-31G**	MP2/6-31G*
$\text{HC}\equiv\text{C}^+$		+ 55.3
CH_3^+	0.0 Reference	
C_6H_5^+		-26.5
C_2H_3^+ (bridged)		-25.6
CH_3CH_2^+ (bridged)	-33.8	-40.8
CH_3CH_2^+ (open)	-39.0	-34.4
$\text{CH}_2=\text{C}^+\text{CH}_3$	-42.9	-46.5
$\text{CH}_2=\text{CHCH}_2^+$	-54.5	-60.0
$(\text{CH}_3)_2\text{C}^+\text{H}$	-58.5	-58.9
$\text{C}_6\text{H}_5\text{CH}_2^+$		-74.5
$(\text{CH}_3)_3\text{C}^+$		-75.0

Fig. 3.18. Gas phase carbocation stabilities relative to methyl cations in kcal/mol. Data from Y. Apeloig and T. Müller, in *Dicoordinated Carbocations*, Z. Rapoport and P. J. Stang, eds., John Wiley & Sons, New York, 1997, Chap.2.

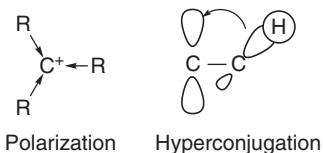
orbital. The sp^3/sp^3 and sp^2/sp^2 arrangements are not energy minima, but lie at least 20–30 kcal above the p/sp^2 and p/sp arrangements.⁶⁵ The very high relative energy of terminal ethynyl carbocations reflects the fact that the positive charge is associated with a more electronegative sp orbital if the triple bond is retained. Various MO computations indicate that the ethynyl cation adopts an alternative electronic configuration which places the positive charge in a π orbital, but the cation is nevertheless very unstable.⁶⁶



Certain carbocations, especially in the gas phase, appear to be *bridged*. This is true for ethyl and vinyl cations. More will be said about bridging in Section 4.4.



The carbocation stability order $\text{CH}_3 < pri < sec < tert$ is due to the electron-releasing effect of alkyl substituents. The electron release is a combination of a polar effect that is due to the greater electronegativity of the sp^2 carbon and a hyperconjugative effect through which the electrons in σ C–H and C–C bonds of the alkyl group are delocalized to the empty p orbital. The delocalization has a stereoelectronic aspect, since alignment of a C–H (or C–C) bond with the empty p orbital maximizes electron delocalization. Gas phase experimental⁶⁷ and computational⁶⁸ data (Figure 3.18) indicate that the stabilization energies are as follows (relative to methyl in kcal/mol): $\text{CH}_3^+(0, 0)$; $\text{CH}_3\text{CH}_2^+(40, 41)$, $(\text{CH}_3)_2\text{CH}^+(60, 59)$; $(\text{CH}_3)_3\text{C}^+(85, 75)$.

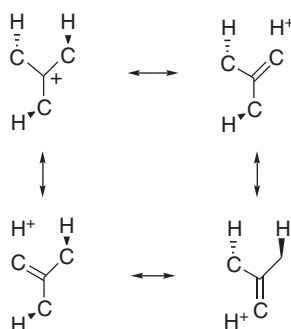


⁶⁵ Y. Apeloig and T. Müller in *Dicoordinated Carbocations*, Z. Rappoport and P. J. Stang, eds., John Wiley & Sons, New York, 1997, Chap. 2; J. Abboud, I. Alkorta, J. Z. Davalos, P. Muller, and E. Quintanilla, *Adv. Phys. Org. Chem.*, **37**, 57 (2002).

⁶⁶ L. A. Curtiss and J. A. Pople, *J. Chem. Phys.*, **91**, 2420 (1989); W. Koch and G. Frenking, *J. Chem. Phys.*, **93**, 8021 (1990); K. Hashimoto, S. Iwata, and Y. Osamura, *Phys. Chem. Lett.*, **174**, 649 (1990).

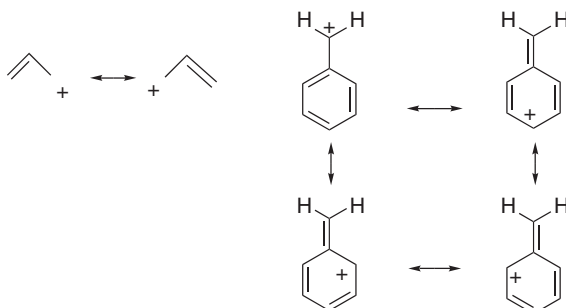
⁶⁷ D. H. Aue, in *Dicoordinated Carbocations*, Z. Rappoport and P. J. Stang, eds., John Wiley & Sons, New York, 1997, Chap. 3; D. H. Aue and M. T. Bowers, in *Gas Phase Ion Chemistry*, M. T. Bowers, ed., Academic Press, New York, 1979.

⁶⁸ Y. Apeloig and T. Müller, in *Dicoordinated Carbocations*, Z. Rappoport and P. J. Stang, eds., John Wiley & Sons, New York, 1997, Chap. 2.



Resonance Representation of Hyperconjugation

Carbocations that are adjacent to π bonds, as in allylic and benzylic carbocations, are strongly stabilized by delocalization. The stabilization in the gas phase is about 60 kcal/mol for the allyl cation and 75 kcal/mol for benzyl ions, relative to the methyl cation.⁶⁷



Resonance representation of allylic and benzylic stabilization

Total resonance stabilization has been calculated at the MP2/6-31G* level for a number of conjugated ions, as shown in Table 3.9. One general trend seen in this data is a decrease of the effect of successive phenyl rings in the benzyl, diphenylmethyl, and triphenylmethyl series. Two factors are involved. The effect of resonance stabilization is decreased because the successive rings must be twisted from planarity. This factor and related steric repulsions attenuate the effect of each successive phenyl group relative to methyl (see Column B). In the allyl series a 1-phenyl substituent adds 39.4 kcal of stabilization, while a 2-phenyl group adds only 11.4.⁶⁹

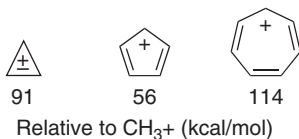
Table 3.9. Stabilization Energy in kcal/mol for Delocalized Carbocations

Carbocation	Resonance stabilization	Stabilization relative to CH_3^+
$\text{C}_6\text{H}_5\text{CH}_2^+$	76.4	75.4
$\text{CH}_2=\text{CHCH}_2^+$	53.2	
$(\text{C}_6\text{H}_5)_2\text{CH}^+$	102.7	91.6
$(\text{C}_6\text{H}_5)_3\text{C}^+$	124.8	102.2
$\text{C}_6\text{H}_5\text{C}^+\text{HCH}=\text{CH}_2$	92.6	
$\text{CH}_2=\text{C}-\underset{\text{C}_6\text{H}_5}{\text{CH}_2}^+$	64.6	

a. B. Reindl, T. Clark and P. v. P. Schleyer, *J. Phys. Chem. A*, **102**, 8953 (1998).

⁶⁹. B. Reindl, T. Clark, and P. v. R. Schleyer, *J. Phys. Chem. A.*, **102**, 8953 (1998).

When the vacant *p* orbital is part of a completely conjugated cyclic system, there can be further stabilization resulting from aromaticity. (See Section 8.3 for further discussion.) The cyclopropenyl cation and the cycloheptatrienyl cation fit into this category. When cyclic conjugation is antiaromatic, as in the cyclopentadienyl cation, there is net stabilization relative to a methyl cation, but significantly less than for the aromatic analogs.⁷⁰



Carbocation stability in the gas phase can be measured by mass spectrometry and reported as *hydride affinity*, which is the enthalpy of the reaction:

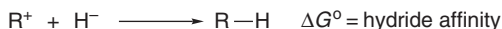


Table 3.10 gives values for the hydride affinity for some carbocations. There is good agreement with the theoretical results shown in Figure 3.18 and the data in Table 3.10.

Substituents such as oxygen and nitrogen that have nonbonding electrons are very strongly stabilizing toward carbocations. This is true both for ether-type oxygen and carbonyl-type oxygen (in acylium ions). Even fluorine and the other halogens are

Table 3.10. Hydride Affinity of Some Carbocations

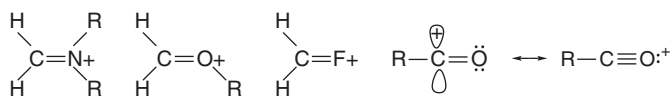
Hydride affinity (kcal/mol)			
	Gas ^a		Gas ^a
CH_3^+	314	$\text{CH}_2=\text{CHCH}_2^+$	256
CH_3CH_2^+ (bridged)	270	$\text{CH}_2=\text{CHCC}^+\text{HCH}_3$	239
$(\text{CH}_3)_2\text{CH}^+$	252	$\text{CH}_2=\text{CHC}^+(\text{CH}_3)_2$	230
$(\text{CH}_3)_3\text{C}^+$	237	$\text{CH}_3\text{CH}=\text{CHC}^+\text{HCH}_3$	228
$\text{CH}_2=\text{CH}^+$ (bridged)	288		284
	223 ^b		239
	258 ^b		225
	200 ^b		220 ^b

a. From D. H. Aue in *Dicoordinate Carbocations*, Z. Rappoport and P. J. Stand, eds., John Wiley & Sons, New York, 1997, Chap. 3.

b. From D. H. Aue and M. T. Bowers, in *Gas Phase Ion Chemistry*, M. T. Bowers, ed., Academic Press, New York, 1979.

⁷⁰. Y. Mo, H. Jiao, Z. Lin, and P. v. R. Schleyer, *Chem. Phys. Lett.*, **289**, 383 (1998).

stabilizing by delocalization (but we discuss the opposing polar effect of the halogens below).



The stabilizing effect of delocalization can be seen even with certain functional groups that are normally considered to be electron withdrawing. For example, computations indicate that cyano and carbonyl groups have a stabilizing resonance effect. This is opposed by a polar effect, so the net effect is destabilizing, but the resonance component is stabilizing.



Resonance stabilization of carbocations by electron pair donation

Table 3.11 shows some gas phase stabilization energies computed by various methods. Columns A and B refer to stabilization of substituted methyl (methylium) carbocations, whereas columns C and D are referenced to ethylium ions. Because these values refer to the gas phase, where there is no solvation, the absolute stabilization energies are substantially larger than those found in solution studies. Nevertheless, the results provide a good indication of the relative effect of the various substituents on carbocation stability. Note that of all the substituents included, only NO_2 is strongly destabilizing. The data for F, Cl, CN, and $\text{CH}=\text{O}$ indicate small stabilization, reflecting the compensating polar (destabilizing) and delocalization (stabilizing) effects mentioned earlier.

The most wide-ranging and internally consistent computational comparison of substituent effects on carbocation was reported by a group working in The

Table 3.11. Calculated Substituent Stabilization on Carbocations (in kcal/mol)

Substituent	CH_3^+		CH_3CH_2^+	
	PM3 ^a	MP2/6-31G** ^b	MP2/6-311+G(d,p) ^c	B3LYP/6-311+G(d,p) ^c
NH_2	80.2			
CH_3O	57.6			
OH	51.4			
Ph	56.3			
$\text{CH}_2=\text{CH}$	43.3	66.1	30.9	37.3
CH_3	29.0	41.5	17.1	23.4
F	5.5		6.0	7.1
Cl			9.7	10.6
CN	5.0	4.3		
$\text{CH}=\text{O}$	1.7	0.2		
NO_2	-30.8	-22.3		

a. A. M. El-Nahas and T. Clark, *J. Org. Chem.*, **60**, 8023 (1995).

b. X. Creary, X.Y. Wang, and Z. Jiang, *J. Am. Chem. Soc.*, **117**, 3044 (1995).

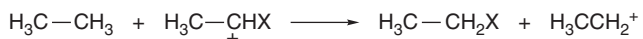
c. K. van Alem, E. J. R. Sudholter, and H. Zuilhof, *J. Phys. Chem. A*, **102**, 10860 (1998).

Table 3.12. Computed Substituent (De)Stabilization of Carbocation (in kcal/mol)^a

X	Ethyl	Vinyl	X	Ethyl	Vinyl	SECTION 3.4
H	0.00	0.00	C≡N	-16.02	-11.71	<i>Electronic Substituent Effects on Reaction Intermediates</i>
CH ₃	18.63	25.89	CH=O	-10.25	-4.51	
CH ₂ OH	15.30	21.69	CO ₂ H	-8.41	-5.92	
CH ₂ CN	-2.10	4.76	H ₂ N	64.96	53.69	
CH ₂ Cl	5.59	12.90	HO	37.43	25.92	
CH ₂ CF ₃	3.62	9.63	O ₂ N	-23.09	-25.44	
CH ₂ F	4.98	10.89	F	6.95	-9.25	
CF ₃	-23.56	-16.41	Cl	9.83	11.17	
CH ₂ =CH	31.98	25.64	Br	9.52	12.70	
HC≡C	18.17	25.64	I	13.32	20.53	
C ₆ H ₅	36.77	54.10				
c-C ₃ H ₅	42.97	47.06				

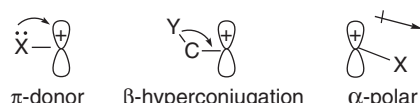
a. K. van Alem, G. Lodder, and H. Zuilhof, *J. Phys. Chem.*, **106**, 10681 (2002).

Netherlands.⁷¹ This study compared MP2/6-311++G(*d,p*), CBS-Q, and B3LYP/6-311+G(*d,p*) calculations and found that the CBS-Q method gave the best correlation with experimental data. There was also good correlation with MP2 and B3LYP results, which could be used to obtain “CBS-Q-like” results when the CBS-Q method was not applicable. Table 3.12 gives some of the computed stabilization (+) and destabilization (−) relative to ethyl and vinyl cations found using isodesmic reactions:



The results show substantial destabilization for CF₃, CN, CH=O, CO₂H, and NO₂ groups.

The relative stability, charge distribution, and bond orders obtained by the calculation identified three main factors in carbocation stabilization as π-donation, β-hyperconjugation, and the α-polar effects.



The π-donor and β-hyperconjugation effects are present for both alkyl and vinyl carbocations. The vinyl carbocations exhibit somewhat larger stabilizations because they are inherently less stable. The vinyl cations also appear to be more sensitive to the α-polar effect. Note that the F, OH, and NH₂ substituents are less stabilizing of vinyl cations than of alkyl cations. This is believed to be due to the greater sensitivity to the polar effect of the more electronegative *sp* carbon in the vinyl cations. The NPA and bond order characterizations of the carbocations are shown in Table 3.13. The values give the charge associated with the cationic carbon and the bond order between the cationic carbon and the substituent X.

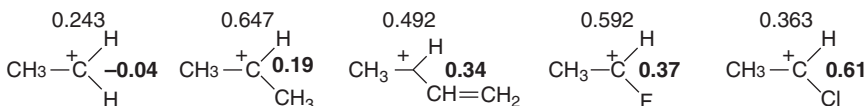
⁷¹. K. van Alem, G. Lodder, and H. Zuilhof, *J. Phys. Chem. A.*, **106**, 10681 (2002).

Table 3.13. NPA and Bond Order Characterizations of Substituted Carbocations

X	C(+)		C ⁺ -X Bond Order	
	Alkyl	Vinyl	Alkyl	Vinyl
CH ₃	0.647	0.585	0.19	0.20
CH ₂ OH	0.702	0.568	0.15	0.17
CH ₂ CN	0.633	0.598	0.15	0.18
CH ₂ Cl	0.719	0.585	0.18	0.16
CH ₂ F	0.659	0.577	0.14	0.15
CH ₂ CF ₃	0.612	0.601	0.13	0.18
CF ₃	0.666	0.618	-0.07	-0.06
CH ₂ =CH	0.492	0.440	0.34	0.27
HC≡C	0.542	0.704	0.28	0.29
C ₆ H ₅	0.420	0.383	0.40	0.29
c-C ₃ H ₅	0.558	0.525	0.46	0.42
C≡N	0.602	0.572	0.13	0.15
HC=O	0.664	0.656	0.02	-0.03
HO ₂ C	0.650	0.587	-0.02	-0.02
H ₂ N	0.531	0.394	0.55	0.47
HO	0.242	0.125	0.76	0.67
O ₂ N	0.499	0.424	0.02	0.04
F	0.592	0.524	0.37	0.39
Cl	0.363	0.274	0.61	0.60
Br	0.284	0.205	0.67	0.65
I	0.193	0.123	0.74	0.68

a. K. van Alem, G. Lodder, and H. Zuilhof, *J. Phys. Chem. A*, **106**, 10681 (2002).

Except for π -donor substituents, most of the positive charge resides on the cationic carbon. The strongest effect is seen for the halogens, where there is a sharp drop in the positive charge in the order F > Cl > Br > I. Note from the NPA charge at the cationic carbon that F is more effective than CH₃ in delocalizing the positive charge. However, the net stabilization is much less because the polar effect of the σ C—F bond is strongly destabilizing.⁷² The resonance effect is also indicated by increased bond order to the substituent (shown in bold).



Charge on trivalent carbon (upper) and bond order (bold) on carbocation

One feature of the charge distributions in carbocations that deserves attention is the greater positive charge calculated for the trigonal carbon in 2-propyl cation than for ethyl cation. This tendency for more substituted alkyl carbocations to be *more positive* has been found in other calculations⁷³ and is consistent with the relative ¹³C chemical shifts observed in NMR.⁷⁴ How does this relationship accord with the very strong *stabilizing* influence on alkyl groups on carbocations? Levy⁷⁵ has argued that

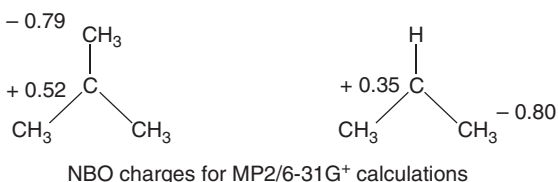
⁷². K. van Alem, E. J. R. Sudhölder, and H. Zuilhof, *J. Phys. Chem. A*, **102**, 10860 (1998).

⁷³. R. Hoffmann, *J. Chem. Phys.*, **40**, 2480 (1964).

⁷⁴. G. A. Olah and A. M. White, *J. Am. Chem. Soc.*, **91**, 5801 (1969).

⁷⁵. J. B. Levy, *Struct. Chem.*, **10**, 121 (1999).

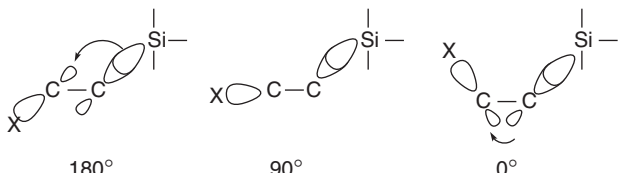
the alternating (+) and (−) charges found in tertiary cations provide the source of the stabilization. The hydrogens bear most of the positive charge according to NPA charge assignment.



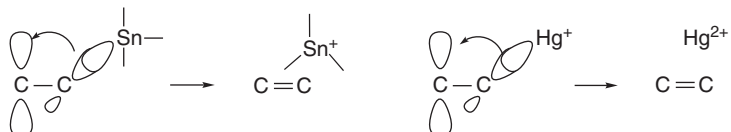
Silicon substitution β to a carbocation is very stabilizing by hyperconjugation.⁷⁶



This stabilization has been shown to be primarily a delocalization effect by demonstrating a strong dependence on the dihedral angle between the Si–C bond and the empty *p* orbital of the carbocation. Kinetic rate enhancements of about 1012, 0, and 104 were found for compounds with angles of 180°, 90°, and 0°, respectively. This is consistent with a hyperconjugation mechanism and with analyses of orbital overlap that show considerably stronger overlap for the *anti* (180°) than *syn* (0°) orientations.⁷⁷

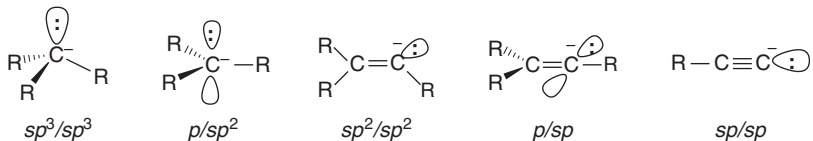


This β-stabilization is even stronger for less electronegative elements such as tin and mercury. In effect, the electron release is complete and elimination occurs. We discuss this kind of reaction further in Section 5.10.5.



3.4.2. Carbanions

Carbanions have negative charge on carbon and, as with carbocations, there are several conceivable hybridization schemes.



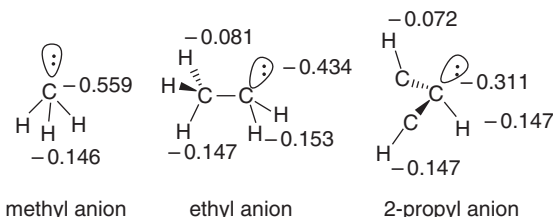
⁷⁶. J. B. Lambert, *Tetrahedron*, **46**, 2677 (1996); J. B. Lambert, Y. Zhao, R. W. Emblidge, L. A. Salvador, X. Liu, J. -H. So, and E. C. Chelius, *Acc. Chem. Res.*, **32**, 183 (1999).

⁷⁷. A. J. Green, Y. -I. Kuan, and J. M. White, *J. Org. Chem.*, **60**, 2734 (1995).

Because the nonbonding orbital is occupied, stability increases with *s* character, the converse of the situation for carbocations. The order of stability of carbanions is $sp^3 < sp^2 < sp$. The relative stability of gas phase carbanions can be assessed by the energy of their reaction with a proton, which is called *proton affinity*. The proton affinities of the prototypical hydrocarbons methane, ethene, and ethyne have been calculated at the MP4/6-31+G* level.⁷⁸ The order is consistent with the electronegativity trends discussed in Section 1.1.5, and the larger gap between *sp* and *sp*², as compared to *sp*² and *sp*³, is also evident. The relative acidity of the hydrogen in terminal alkynes is one of the most characteristic features of this group of compounds.

Proton affinity (kcal/mol)		
$R^- + H^+ \longrightarrow R - H$		
CH ₄	H ₂ C=CH ₂	HC≡CH
419.4	408.7	375.1

The order of gas phase carbanion stability has been calculated as Et < Me ~ iso-Pr < tert-Bu by both MP2/6-31 + G(*d,p*) and B3LYP/6-31 + G(*d,p*) calculations.⁷⁹ Experimental values in the same order have been recorded.⁸⁰ The *pri* < *sec* < *tert* order reflects the ability of the larger groups to disperse the negative charge (polarizability). The Et < Me order indicates that electron donation by CH₃ (relative to H) slightly destabilizes the ethyl carbanion. However, a larger *tert*-butyl substituent (in the neopentyl anion) has a net stabilizing effect that is evidently due to polarizability. Note that the effect of substitution is *very much smaller* than for carbocations. The range between primary and tertiary carbanions is only about 10 kcal/mol, compared to about 75 kcal/mol for carbocations. The alkyl anions are calculated to be pyramidal, in agreement with the *sp*³ hybridization model. The bond angles at the trivalent carbon are as follows: CH₃⁻ : 109.4°; CH₃CH₂⁻ : 111.0°; (CH₃)₂CH⁻ : 109.1°, and (CH₃)₃C⁻ : 109.6°.⁸¹ AIM charges were also calculated (B3LYP/6-311 + G**), as shown below, and indicate some σ -delocalization to the β -hydrogens. Note in particular that in the ethyl and 2-propyl anions the *anti* hydrogens are more negative than the *gauche*. Note also the considerable reduction in the charge at carbon as the anion becomes larger. These trends are in accord with dispersal of the negative charge by both hyperconjugation and polarization. Table 3.14 compares proton affinities calculated by several methods with experimental values.



⁷⁸. W. H. Saunders, Jr., and J. E. Van Verth, *J. Org. Chem.*, **60**, 3452 (1995).

⁷⁹. R. R. Sauers, *Tetrahedron*, **55**, 10013 (1999).

⁸⁰. C. H. DePuy, S. Gronert, S. E. Barlow, V. M. Bierbaum, and R. Damrauer, *J. Am. Chem. Soc.*, **111**, 1968 (1989).

⁸¹. P. Burk and K. Sillar, *Theochem*, **535**, 49 (2001).

Table 3.14. Computational and Experimental Proton Affinities for Small Hydrocarbons (in kcal/mol)

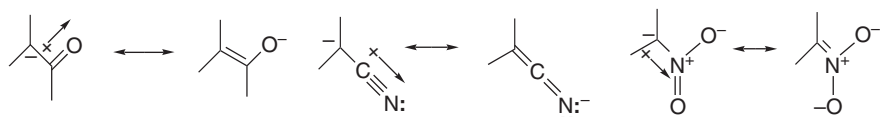
Group	MP2/6–31+G(<i>d,p</i>) ^a	B3LYP/6–311G(3df,2dp) ^a	G2 ^b	Experimental ^c
CH ₃ ⁻	419.0	414.5	418.4	415–421.5
CH ₃ CH ₂ ⁻	421.8	417.0	420.6	420.1
(CH ₃) ₂ CH ⁻	419.6	413.4	418.3	419.4
(CH ₃) ₃ C ⁻	412.1	406.9	412.2	413.1
<i>c</i> –(CH ₂) ₂ CH ⁻	415.5	411.3		409–413.5

a. R. R. Sauers, *Tetrahedron*, **55**, 10013 (1999).b. P. Burk and K. Sillar, *Theochem*, **535**, 49 (2001).

c. Range of values includes quoted error ranges.

SECTION 3.4
Electronic Substituent Effects on Reaction Intermediates

Electron-withdrawing groups such as carbonyl, cyano, and nitro strongly stabilize carbanions as the result of complementary resonance and polar effects. Table 3.15 gives some computed stabilization energies for various substituent groups.



The stabilization by substituents such as F and OH is presumably due to polar effects. Note that there is considerable discrepancy between the semiempirical and ab initio results, as the former indicate much greater substituent stabilization for the second-row elements C through F. The large stabilizing effect for BH₂ is due to the capacity of the –BH₂ group to accept two electrons. The effect of the heavier substituents, Cl through SiH₃, is primarily due to polarizability. Very large stabilizations owing to delocalization are seen for the conjugated substituents CH₂=CH through NO₂.

Third- and fourth-row substituents such as sulfenyl, sulfinyl, sulfonyl, phosphinyl, and selenenyl stabilize carbanions. Because these substituents have tetrahedral

Table 3.15. Calculated Stabilization Energies for Methyl Anions (in kcal/mol)

Substituent	AM1 ^a	AM1 _(H₂O) ^a	PM ^a	PM _(H₂O) ^a	MP2/6–31G ^{*b}	MP4SDQ/6–31G ^{*b}	QCISD(T)/6–31G ^{*b}
F	19.4	14.4	24.6	21.0	9.09	10.52	10.23
OH	15.9	12.0	19.4	16.4	5.15	5.58	5.70
NH ₂	20.1	13.3	20.9	15.1	–0.67	–0.74	0.46
CH ₃	14.5	4.6	14.7	5.7	3.14	3.32	2.99
BH ₂					57.34	56.83	57.90
Cl					18.13	19.48	19.36
SH					20.98	20.45	20.53
PH ₂					23.45	22.37	22.25
SiH ₃					25.27	24.78	24.79
CH=CH ₂	45.5	29.4	33.0	31.4			
CH=O	62.7			60.3			
CN	55.0	41.2	59.4	49.3			
NO ₂	85.8	69.7	91.9	72.5			
Li					8.95	17.83	24.39
Na					5.04	16.99	21.92

a. M. El-Nahas, *J. Chem. Res. (Synop.)*, 310 (1996).b. A. M. El-Nahas and P. v. R. Schleyer, *J. Comput. Chem.*, **15**, 596 (1994).

hybridization, the question arises as to whether the stabilization is through delocalization, polar, or polarization effects. The α substituents increase acidity in the order $\text{Se} > \text{S} > \text{O}$ and $\text{Br} > \text{Cl} > \text{F}$, which indicates that some factor apart from electronegativity (bond polarity) must contribute to the stabilization. The stabilization has been described both in terms of polarization and *d* orbital participation for the larger elements. The latter effect, as expressed in resonance terminology, implies shortening of the C–X bond. G2 calculations show very slight shortening for the C–PH₂ and C–SH bonds, but the halogens do not show such a trend.⁸² Polarization appears to be the main mechanism for carbanion stabilization by the heavier elements.⁸³

Another computational approach to assessing carbanion stabilization by substituents entails calculation of proton affinity. Table 3.16 gives the results of G2 and MP4/6-31G* computations. The energy given is the energy required to remove a proton from the methyl group. The strong stabilization of the π -electron acceptors, such as BH₂, CH=O, NO₂, and CN, is evident. The second-row elements are in the order of electronegativity F > OH > NH₂, but the effects are comparatively small. The stabilization by third- and fourth-row elements (S, P, Se) are reproduced, and the halogen order, F < Cl < Br, also suggests that polarization is more important than dipolar stabilization.

These computational studies provide a description of carbanion stabilization effects that is consistent with that developed from a range of experimental observations. The strongest effects come from conjugating EWG substituents that can delocalize the negative charge. Carbon atom hybridization is also a very strong effect. The effect of saturated oxygen and nitrogen substituents is relatively small and seems to be O > N, suggesting a polar effect. This may be opposed by electron-electron repulsion arising from the unshared electrons on nitrogen and oxygen.

Table 3.16. Gas Phase Proton Affinity of Substituted Methanes (in kcal/mol)

Compound	G2 ^a	MP4/6-31G* ^b
CH ₃ NH ₂	418.8	
CH ₃ OH	414.6	417.7 ^b
CH ₃ OCH ₃	412.8	
CH ₃ PH ₂	393.9	
CH ₃ SH	397.6	403.1 ^b
CH ₃ SeH		399.3 ^b
CH ₃ F	410.4	412.6 ^b
CH ₃ Cl	398.2	404.5 ^b
CH ₃ Br	393.5	400.3 ^b
CH ₃ BH ₂	363.0	
CH ₃ CH=O	368.1	367.1 ^c
CH ₃ CH=CH ₂		392.5 ^c
CH ₃ NO ₂	358.4	
CH ₃ CN	375.0	375.9 ^c

a. P. M. Mayer and L. Radom, *J. Phys. Chem. A*, **102**, 4918 (1998).

b. J. E. Van Verth and W. H. Saunders, Jr., *J. Org. Chem.*, **62**, 5743 (1997).

c. W. H. Saunders, Jr., and J. E. Van Verth, *J. Org. Chem.*, **60**, 3452 (1995).

⁸². P. M. Mayer and L. A. Radom, *J. Phys. Chem. A*, **102**, 4918 (1998).

⁸³. P. Speers, K. E. Laidig, and A. Streitwieser, *J. Am. Chem. Soc.*, **116**, 9257 (1994).

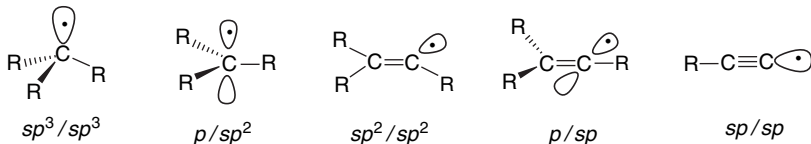
There is also a good deal of information available on carbanion stability in solution.⁸⁴ These data are derived from equilibrium measurements analogous to acid dissociation constants, in which the extent of deprotonation of hydrocarbons by strong base is determined:



Only a few hydrocarbon derivatives can be directly measured in aqueous solution, but extensive studies have been done in other solvents, in particular DMSO. We consider this solution data in Chapter 6.

3.4.3. Radical Intermediates

Carbon radicals have an unpaired electron in a nonbonding orbital. The possible hybridization schemes are shown below.



The methyl radical is close to planarity.⁸⁵ Experimental⁸⁶ and computational⁸⁷ results indicate that simple alkyl radicals are shallow pyramids with low barriers for inversion, which is consistent with p/sp^2 hybridization. The ethenyl radical is bent with a C–C–H bond angle of 137° .⁸⁸ High-level MO calculations arrive at a similar structure.⁸⁹ This geometry indicates sp^2/sp^2 hybridization. The alkenyl radicals can readily invert through the linear p/sp radical as a transition structure.⁹⁰ A major structural effect in alkyl (beyond methyl) and alkenyl radicals is a marked weakening of the β -C–H bonds, which occurs by interaction of the β -C–H and the SOMO (singly occupied molecular orbital). According to both computational (CBS-4) and thermodynamic cycles, the strength of the β -C–H bond is only 30–35 kcal/mol.⁹¹ This leads to one of the characteristic bimolecular reactions of alkyl radicals—disproportionation to an alkane and an alkene. Similar values pertain to β -C–H bonds in vinyl radicals.



- ⁸⁴. E. Bunzel and J. M. Dust, *Carbanion Chemistry*, Oxford University Press, Oxford, 2003.
- ⁸⁵. M. Karplus and G. K. Fraenkel, *J. Chem. Phys.*, **35**, 1312 (1961); L. Andrews and G. C. Pimentel, *J. Chem. Phys.*, **47**, 3637 (1967); E. Hirota, *J. Phys. Chem.*, **87**, 3375 (1983).
- ⁸⁶. M. Karplus and G. K. Fraenkel, *J. Chem. Phys.*, **35**, 1312 (1961); L. Andrews and G. C. Pimentel, *J. Chem. Phys.*, **47**, 3637 (1967); E. Hirota, *J. Phys. Chem.*, **87**, 3375 (1983); T. J. Sears, P. M. Johnson, P. Jin, and S. Oatis, *J. Phys. Chem.*, **104**, 781 (1996).
- ⁸⁷. F. M. Bickelhaupt, T. Ziegler, and P. v. R. Schleyer, *Organometallics*, **15**, 1477 (1996); M. N. Paddon-Row and K. N. Houk, *J. Phys. Chem.*, **89**, 3771 (1985); J. Pacansky, W. Koch, and M. D. Miller, *J. Am. Chem. Soc.*, **113**, 317 (1991); H. H. Suter and T. K. Ha, *Chem. Phys.*, **154**, 227 (1991); A. L. L. East and P. R. Bunker, *Chem. Phys. Lett.*, **282**, 49 (1998).
- ⁸⁸. J. H. Wang, H. -C. Chang, and Y. -T. Chen, *Chem. Phys.*, **206**, 43 (1996).
- ⁸⁹. L. A. Curtiss and J. A. Pople, *J. Chem. Phys.*, **88**, 7405 (1988); K. A. Peterson and T. H. Dunning, *J. Chem. Phys.*, **106**, 4119 (1997).
- ⁹⁰. P. R. Jenkins, M. C. R. Symons, S. E. Booth, and C. J. Swain, *Tetrahedron Lett.*, **33**, 3543 (1992).
- ⁹¹. X. -M. Zhang, *J. Org. Chem.*, **63**, 1872 (1998).

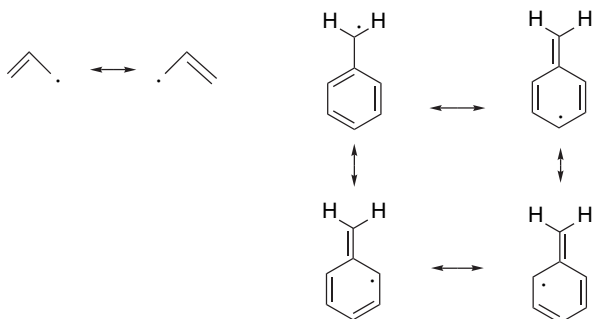
A good place to begin discussion of substituent effects on radicals is by considering the most common measure of radical stability. Radical stabilization is often defined by comparing C–H bond dissociation energies (BDE). For substituted methanes, the energy of the reaction should reflect any stabilizing features in the radical $\text{X}-\text{CH}_2\cdot$.



The BDEs are usually tabulated as the enthalpy change for the reaction at 298 K. The values can be determined experimentally⁹² or calculated theoretically. Table 3.2 B (p. 258) gives some C–H BDE for important C–H bonds. The BDEs become smaller in the order $\text{CH}_3 > \text{pri} > \text{sec} > \text{tert}$. The relatively low enthalpies of the dissociation for forming allyl and benzyl radicals by removal of hydrogen from propene and toluene, respectively, is due to the stabilization of these radicals by delocalization. On the other hand the C–H bond to sp^2 (ethene, benzene) and sp (ethyne) carbon are substantially stronger than bonds to sp^3 carbon. The BDEs correlate with the ease of formation of the corresponding radicals.⁹³ The reactivity of C–H groups toward radicals that abstract hydrogen is $\text{pri} < \text{sec} < \text{tert}$. Vinyl and phenyl substituents at a reaction site weaken the C–H bond and enhance reactivity. On the other hand, hydrogen abstraction from an sp^2 (vinyl or aryl) C–H bond or from a sp carbon in a terminal alkyne is difficult because of the increased strength of the corresponding C–H bonds.

The trend of reactivity $\text{tert} > \text{sec} > \text{pri}$ is consistently observed in various hydrogen atom abstraction reactions, but the range of reactivity is determined by the nature of the reacting radical. The relative reactivity of *pri*, *sec*, and *tert* positions toward hydrogen abstraction by methyl radicals is 1:4.8:61.⁹⁴ An allylic or benzylic hydrogen is more reactive toward a methyl radical by a factor of about 9, compared to an unsubstituted C–H. The relative reactivity toward the *t*-butoxy radical is *pri*: 1, *sec*: 10, *tert*: 50.⁹⁵ In the gas phase, the bromine atom is much more selective, with relative reactivities of *pri*: 1, *sec*: 250, *tert*: 6300.⁹⁶ Data for other types of radicals have been obtained and tabulated.⁹⁶

The stabilizing effects of vinyl groups (in allylic radicals) and phenyl groups (in benzyl radicals) are large and can be described in resonance terminology.



⁹² J. Berkowitz, G. B. Ellison, and D. Gutman, *J. Phys. Chem.*, **98**, 2744 (1994).

⁹³ J. A. Kerr, *Chem. Rev.*, **66**, 465 (1966).

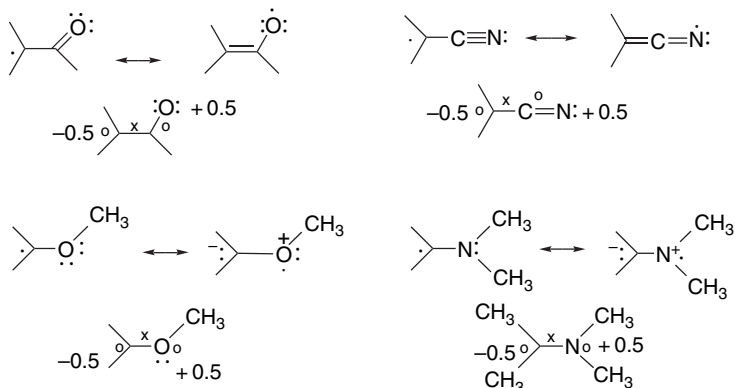
⁹⁴ W. A. Pryor, D. L. Fuller, and J. P. Stanley, *J. Am. Chem. Soc.*, **94**, 1632 (1972).

⁹⁵ C. Walling and B. B. Jacknow, *J. Am. Chem. Soc.*, **82**, 6108 (1960).

⁹⁶ A. F. Trotman-Dickenson, *Adv. Free Radical Chem.*, **1**, 1 (1965).

For the vinyl substituent, the stabilization can be expressed in terms of simple Hückel MO (HMO) theory. The interaction of a p orbital with an adjacent vinyl group creates the allyl radical. In HMO calculations, the resulting orbitals have energies of $\alpha + 1.4\beta$, α , and $\alpha - 1.4\beta$. Thus the interaction of the p orbital with both the π and π^* orbitals leaves it at the same energy level, but the π and π^* levels are transformed to ψ_1 and ψ_3 of the allyl radical. There is a net stabilization of 0.8β for the two electrons in the more stable ψ_1 orbital. One measure of the stabilization energy is the barrier to rotation at a terminal methylene group. A value of 16.8 kcal/mol has been calculated.⁹⁷ The experimental barrier is 15.7 kcal/mol. Another measure of the stabilization is the lowering of the C–H BDE for the allylic bond in propene, which indicates a stabilization of 13.4 kcal/mol.⁹⁸

For radicals, nearly all functional groups are stabilizing. Both EWGs such as carbonyl and cyano and ERGs such as methoxy and dimethylamino have a stabilizing effect on a radical intermediate at an adjacent carbon. The stabilizing role of functional groups can be expressed in resonance terms. Resonance structures depict these interactions as delocalization of the unpaired electron into the substituent group. For unsaturated substituents, the resonance is analogous to the allyl radical. For donor substituents, a dipolar structure is involved. Linnett structures with three-electron bonds are also descriptive of the effect of donor substituents, and imply a degree of charge separation.



The radical-stabilizing effect of both types of substituents also can be described in MO terms. In this case, the issue is how the unpaired electron in a p orbital interacts with the orbitals of the adjacent substituent, such as vinyl, carbonyl, or methoxy. Figure 3.19 presents a qualitative description of the situation. For unsaturated EWG substituents such as carbonyl, the orbitals are similar to an allyl system, but the energies are lower because of the lower energy of the π and π^* orbitals of the carbonyl group. In the case of an π -electron acceptor there is a lowering of both the ψ_1 orbital and the SOMO containing the unpaired electron, that is, the radical is stabilized. The radical also is more *electrophilic* because the SOMO is lowered in energy. For an electron donor substituent, the strongest interaction is between the unpaired electron in the p orbital and a nonbonding pair on the electron donor. This interaction results in lowering the energy of the orbital occupied by the electron pair, while raising the energy of the

⁹⁷ D. A. Hrovat and W. T. Borden, *J. Phys. Chem.*, **98**, 10460 (1994).

⁹⁸ W. R. Roth, F. Bauer, A. Beitat, T. Ebbrecht, and M. Wustefel, *Chem. Ber.*, **124**, 1453 (1991).

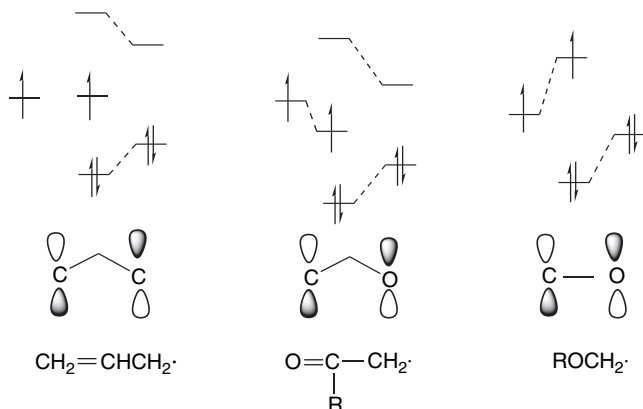


Fig. 3.19. PMO representation of p -orbital interactions with (a) $\text{C}=\text{C}$, (b) $\text{C}=\text{O}$, and (c) OR substituents. The form of the resulting SOMO is shown at the bottom.

orbital occupied by the single electron. The net effect is stabilizing, since there are two electrons in the stabilized orbital and only one in the destabilized one. The radical center is now more *nucleophilic* because the energy of the SOMO is raised.

Substituent effects on radicals can be expressed as *radical stabilization energies* (RSE). Table 3.17 gives some RSEs determined by one such approach developed by Leroy,^{99,100} which can be defined as the difference between the observed enthalpy of atomization ΔH_a and the sum of standard bond energies.

$$\text{RSE} = \Delta H_a - \Sigma \text{BE}$$

The ΔH_a can be obtained from thermodynamic data or calculated theoretically.¹⁰¹ These RSE values are generally consistent with chemical experience. For example, the low stability attributed to aryl and vinyl radicals, as opposed to the high stability of benzyl and allyl radicals, is consistent with their respective reactivities. The somewhat less familiar stability of aminoalkyl and acyl radicals is reproduced. The need for care is illustrated by the value for $\text{Cl}_3\text{C}\cdot$, which implies considerable *destabilization*. Chemical experience (see Section 11.4.2) shows that $\text{CCl}_3\cdot$ is a quite accessible species, although it appears in Table 3.17 as one of the most destabilized radicals. The C–H BDE for $\text{H}-\text{CCl}_3$ is intermediate between those for *pri* and *tert* C–H bonds. The apparent “destabilization” of $\text{CCl}_3\cdot$ is due to a “destabilization” that is also present in the reactant $\text{Cl}_3\text{C}-\text{H}$. Similarly, the acetyl radical is listed as destabilized, but it, too, is an accessible species. We return to this issue in Topic 11.1. Schemes for assignment of RSE that depend on the definition of standard bond energy terms are subject to the particular definitions that are used. These systems, however, are valuable in providing a basis for comparing substituent effects on a qualitative basis. These approaches can be

^{99.} G. Leroy, D. Peeters, and C. Wilante, *Theochem*, **5**, 217 (1982); G. Leroy, *Theochem*, **5**, 77 (1988).

^{100.} Other approaches to radical stabilization energies: C. Ruchardt and H. D. Beckhaus, *Top. Curr. Chem.*, **130**, 1 (1985); F. M. Welle, H.-D. Beckhaus, and C. Ruchardt, *J. Org. Chem.*, **62**, 552 (1997); F. G. Bordwell and X.-M. Zhang, *Acc. Chem. Res.*, **26**, 510 (1993); F. G. Bordwell, X.-M. Zhang, and R. Filler, *J. Org. Chem.*, **58**, 6067 (1993).

^{101.} J. Espinosa-Garcia and G. Leroy, *Recent Devel. Phys. Chem.*, **2**, 787 (1998).

Table 3.17. Thermochemical Stabilization Energies for Some Substituted Radicals (in kcal/mol)

	RSE ^a		RSE ^a
CH ₃ [.]	-1.67	CH ₃ (OH)CH [.]	2.15
CH ₃ CH ₂ [.]	2.11	(NC)FCH [.]	-2.79
NCCH ₂ [.]	6.50	F ₂ CH [.]	-4.11
NH ₂ CH ₂ [.]	3.92	(CH ₃) ₃ C [.]	4.35
CH ₃ NHCH ₂ [.]	12.18	CH ₃ ·C(CN) ₂	3.92
(CH ₃) ₂ NCH ₂ [.]	14.72	CH ₃ ·C(OH) ₂	0.15
HOCH ₂ [.]	3.13	CH ₃ ·C(CN)(OH)	2.26
CH ₃ OCH ₂ [.]	3.64	CF ₃ [.]	-4.17
FCH ₂ [.]	-1.89	CCl ₃ [.]	-13.79
(CH ₃) ₂ CH [.]	2.57	CH ₂ =CH—CH ₂ [.]	13.28
(NC) ₂ CH [.]	5.17	C ₆ H ₅ —CH ₂ [.]	12.08
(HO) ₂ CH [.]	-2.05	CH ₂ =CH [.]	-6.16
		HC≡C [.]	-15.57
		C ₆ H ₅ [.]	-10.27
		C ₅ H ₅ [.]	19.24
		CH ₃ C ⁺ O	7.10

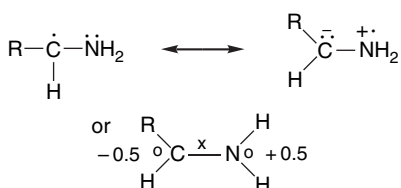
a. Stabilization energy as defined by G. Leroy, D. Peeters, and C. Wilante, *Theochem*, **5**, 217 (1982).

SECTION 3.4

Electronic Substituent Effects on Reaction Intermediates

illustrated by considering the effects on two types of compounds that exhibit significant radical stabilization, namely amines and compounds with captodative stabilization.

The CH bond dissociation energies of amines are particularly interesting and significant. The radical can be stabilized by interaction with the nitrogen unshared pair.

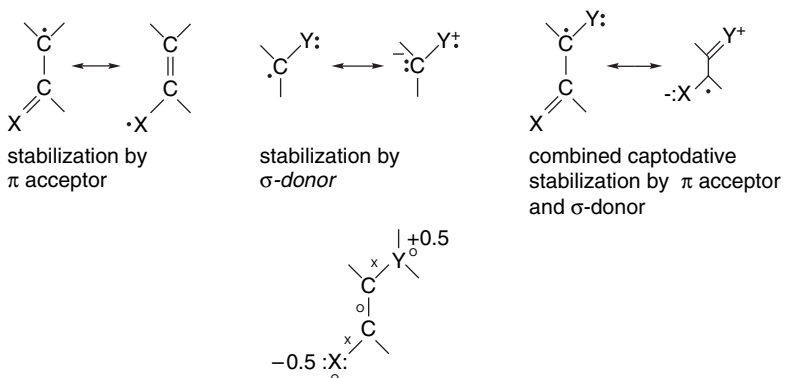


However, the same interaction—hyperconjugation—is present in the parent amine, as revealed by spectroscopic features of the C—H bond (see Section 1.1.8). Recent direct measurements have been made for (CH₃)₃N and (CH₃CH₂)₃N, as well as the pyrrolidine and piperidine, among others.¹⁰² The results obtained are shown below. The recommended value for the RSE for the aminomethyl radical is 13 ± 1 kcal/mol. Similar results were obtained using G2(MP2) calculations with isodesmic reactions. Pyrrolidine, the five-membered cyclic amine, has a slightly larger RSE because there is some relief of eclipsing interactions in the radical.

¹⁰² (a) D. D. M. Wayner, K. B. Clark, A. Rauk, D. Yu, and D. A. Armstrong, *J. Am. Chem. Soc.*, **119**, 8925 (1997); (b) J. Lalevee, X. Allonas, and J.-P. Fouassier, *J. Am. Chem. Soc.*, **124**, 9613 (2002).

	<i>pri</i>	BDE	RSE	<i>sec</i>	BDE	RSE	<i>tert</i>	BDE	RSE
H ₂ NCH ₂ —H		93.9	12.2	(CH ₃) ₂ NH	87.0	12.7	(CH ₃) ₃ N	92.5	12.4
H ₂ NCH ₂ —H CH ₃		90.0	13.1	CH ₂ NH	90.0	14.8	Et ₃ N	91.0	13.8
H ₂ NC(CH ₃) ₂ —H		88.9	12.2	CH ₂ NH	92.0	12.9	Bu ₃ N	91.0	13.8

Captodative radicals have both electron donor and electron acceptor substituents at the radical center. The separate stabilizing effects of these substituents appear to have the ability to be synergistic. A Linnett structure gives a similar representation.



The Leroy analysis has been applied to captodative systems.¹⁰³ Table 3.18 shows the radical RSE calculated for some captodative radicals. An interesting aspect of the data is the failure of cyano groups to provide captodative stabilization. A significant consequence of the captodative effect is that the C—H bond of α -amino derivatives of acids, esters, aldehydes, and ketones are expected to be very significantly weakened,

Table 3.18. Stabilization Energy for Some Captodative Radicals (in kcal/mol)^a

HO—·CH—CN	-3.40
HO—·CH—CH=O	7.10
HO—·CH—CO ₂ H	5.01
HO—·CH—NO ₂	0.03
H ₂ N—·CH—CN	0.25
H ₂ N—·CH—CH=O	6.86
H ₂ N—·CH—CO ₂ H	7.72
H ₂ N—·CH—NO ₂	3.97

a. From G. Leroy, J. P. Dewispelaere, H. Benkادou, D. R. Temsamani, and C. Wilante, *Bull. Soc. Chim. Belg.*, **103**, 367 (1994); G. Leroy, M. Sana, and C. Wilante, *Theochem*, **234**, 303 (1991).

¹⁰³ G. Leroy, J. P. Dewispelaere, H. Benkادou, D. R. Temsamani, and C. Wilante, *Bull. Soc. Chim. Belg.*, **103**, 367 (1994); G. Leroy, M. Sana, and C. Wilante, *Theochem*, **234**, 303 (1991).

falling in the range 75–80 kcal, which is weaker than either allylic or benzylic bonds. Because of the prevalence of such bonds in peptides and proteins, the strength of the C–H bonds of α -amido carboxamides is of substantial biological interest.¹⁰⁴

The stabilization provided by various functional groups contributes to reduced BDEs for bonds to the stabilized radical center. Computational methods can be used to assess these effects. The BDE can be calculated by comparing the total energy of the dissociated radicals with the reactant. Differences in bond dissociation energies relative to methane (Δ BDE) can be taken as a measure of the stabilizing effect of the substituent on the radical. Some computed Δ BDE values are given in Table 3.19 and compared with experimental values. As an example of the substituent effect on BDEs, it can be seen that the primary C–H bonds in acetonitrile (12 kcal/mol) and acetone (11 kcal/mol) are significantly weaker than a primary C–H bond in methane. The data show that both electron-releasing and electron-withdrawing functional groups stabilize radicals. The strong bond-weakening effect of amino substituents is noteworthy, both in its size and the apparent underestimation of this effect by the computations. A recent reevaluation of the Δ BDE for amines arrived at a value of 13 ± 1 kcal/mol, which is in better agreement with the calculations.^{102b}

Theoretical calculations on radical stability entail some issues that are not present in diamagnetic molecules. These complications originate from the need to account for the singly occupied orbital. A comparison assessed the ability of a range of computational methods to reproduce radical stabilization energies.¹⁰⁵ A variant of the CBS-Q method called CBS-RAD was found adequate for calculation of geometry and energy of the $\text{FCH}_2\cdot$, $\text{CH}_2=\text{CF}\cdot$, and $\text{NCCH}_2\cdot$ radicals. This method, along with others,

Table 3.19. Substituent Stabilization Relative to the Methyl Radical (in kcal/mol)

Substituent	Δ BDE ^a	AUMP2 ^b	B3LYP/6-31+G ^c	G3(MP2)RAD ^d	CBS-RAD ^d
H	0.0	0.0	0.0	0.0	0.0
CH_3	7	3.2	4.8	3.4	3.8
$\text{CH}_2=\text{CH}$	19	12.6	18.8	16.9	17.6
C_6H_5	17				
HC=O		9.5		8.3	9.6
$\text{CH}_3\text{C=O}$	11		9.2		
$\text{C}_6\text{H}_5\text{C=O}$	12				
$\text{CO}_2\text{C}_2\text{H}_5$	10			5.1	6.0
CN	12	6.7	10.4	7.6	8.9
NO_2	7			2.8	3.3
F	3	5.0		3.0	3.3
CH_3O	12	8.9(OH)	9.8	7.4	8.2
NH_2	22	11.1	13.3	10.6	11.6
$(\text{CH}_3)_2\text{N}$	21				

a. F. G. Bordwell, X. -M. Zhang, and M. S. Almajjar, *J. Am. Chem. Soc.*, **114**, 7623 (1992); F. G. Bordwell and X. -M. Zhang, *Acc. Chem. Res.*, **26**, 570 (1993).

b. M. Lehd and F. Jensen, *J. Org. Chem.*, **56**, 884 (1991).

c. B. S. Jursic, J. W. Timberlake, and P. S. Engel, *Tetrahedron Lett.*, **37**, 6473 (1996).

d. D. J. Henry, C. J. Parkinson, P. M. Mayer, and L. Radom, *J. Phys. Chem. A*, **105**, 6750 (2001).

¹⁰⁴. P. E. M. Siegbahn, M. R. A. Blomberg, and R. H. Crabtree, *Theoretical Chem. Acc.*, **97**, 289 (1997); P. A. Frey, *Annu. Rev. Biochem.*, **70**, 121 (2001); G. Sawyers, *FEMS Microbiological Rev.*, **22**, 543 (1998).

¹⁰⁵. P. M. Mayer, C. J. Parkinson, D. M. Smith, and L. Radom, *J. Chem. Phys.*, **108**, 604 (1998).

was then applied to a wider range of radicals. G3(MP2), AUMPQ, and B3LYP/6-31+G methods are also satisfactory. Some of these data are included in Table 3.19.

Table 3.20 provides some other comparisons. The first column gives experimental BDEs derived from thermodynamic data. The other columns give ΔH calculated for the dissociative reaction, using various computational methods:



The computations that do not include electron correlation (HF) lead to large errors, but the other current methods that are applicable to molecules of this size perform satisfactorily.

Comparison of the thermochemical, kinetic, and computational evaluation of radical substituent effects provides a consistent picture. Delocalization, as in allylic and benzylic systems, provides ~ 15 kcal/mol of stabilization. Conjugated EWGs such as acyl and cyano provide significant stabilization, usually in the range of 5–10 kcal/mol. Oxygen and especially nitrogen groups provide stabilization as well. In contrast, the sp^2 and sp C–H bonds directly on vinyl, aryl, and alkynyl carbons are difficult to break, and the corresponding radicals are considered to be destabilized. An interesting contrast to these are acyl radicals, which are relatively easily formed from aldehydes by hydrogen atom abstraction (see Section 11.4.3). Stabilization results from conjugation with the oxygen electrons. These radicals are isoelectronic with NO and like NO, a Linnett-type structure can be drawn for acyl radicals. Showing a bond order of 2.5.



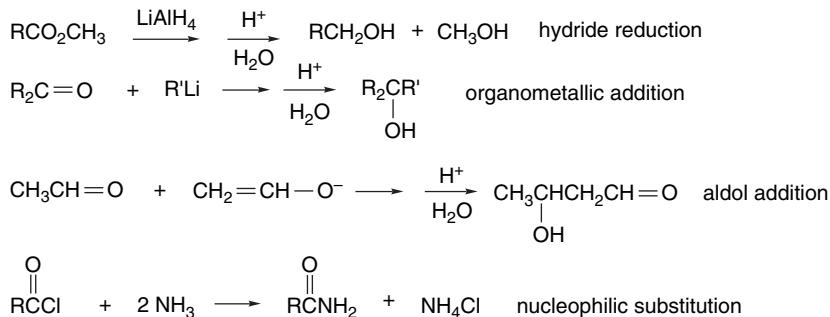
Table 3.20. Comparison of Experimental and Calculated C–H Bond Dissociation Energies for Hydrocarbons and Representative Derivatives (in kcal/mol)

Compound	Experimental		Theoretical BDE					
	BDE (av.) ^a	HF/6-31G(d,p)	MP2/6-31G(d,p)	CBS-4 ^b	CBS ^b	G2(MP2) ^b	G2 ^b	B3LYP/6-31G(d,p)
H–H	104.2	79.5	95.8			104.0		106.4
CH ₃ –H	104.8	79.4	100.3	103.6	103.3	104.0	104.0	105.8
CH ₃ CH ₂ –H	101.1	76.8	98.9	99.9	100.0	100.0	100.9	101.1
(CH ₃) ₂ CH–H	97.6	74.5	95.3	97.0	97.4	98.4	98.5	97.1
CH ₃) ₃ C–H	96.5	72.7	93.7					94.0
CH ₃ =CHCH ₂ –H	84.9	85.0	87.5		87.3			
FCH ₂ –H	101.7	77.8	96.0			99.1		
ClCH ₂ –H	101.5	76.6	95.0			99.7		
HOCH ₂ –H	96.2	74.1	92.3	95.6	95.3	96.2	96.2	95.2
H ₂ NCH ₂ –H	92.2	67.5	85.0	91.8	91.9	93.1	93.1	87.7
HSCH ₂ –H	94.1	74.9	93.1			96.3		
NCCH ₂ –H	93.4	69.8	96.2			93.8		
O=CHCH ₂ –H	94.2	67.3	93.5			93.4		
CH ₃ COCH ₂ –H	95.1	69.4	94.4			94.0		
HO ₂ CCH ₂ –H	96.0	73.7	95.2			97.2		
CH ₃ SO ₂ CH ₂ –H	99.0	80.8	101.2			103.4		
Cl ₃ C–H	95.6	71.8	89.4			92.0		

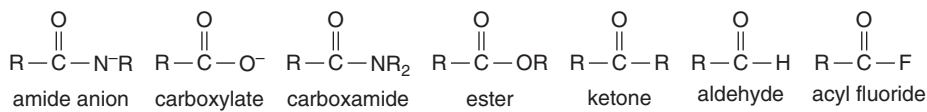
a. H.-G. Korth and W. Sicking, *J. Chem. Soc., Perkin Trans.*, **2**, 715 (1997).

b. J. W. Ochterski, G.A. Petersson, and K. B. Wiberg, *J. Am. Chem. Soc.*, **117**, 11299 (1995).

Addition of nucleophiles to carbonyl groups constitutes a very important class of reactions. A wide variety of reactions fall into this category, including hydride reductions, organometallic additions, aldol additions, and the nucleophilic substitution (including, e.g., hydrolysis, esterification, and aminolysis) reactions of carboxylic acid derivatives. We focus attention on the latter group of reactions at this point, because they are familiar from introductory organic chemistry and illustrate important substituent effects on carbonyl group reactivity. Nucleophilic substitution reactions of carboxylic acid derivatives also serve to emphasize the point that substituents can influence reaction rates through effects on reactants as well as on transition states and intermediates.

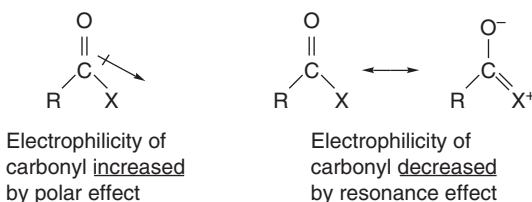


The major classes of carbonyl compounds include aldehydes, ketones, carboxamides, esters, carboxylic acids and anhydrides, and carbonyl halides (acyl halides). These groups differ in the identity of the substituent X on the carbonyl group. At this point we concentrate on these examples, but a number of other carbonyl derivatives have important roles in synthetic and/or biological reactions. These other compounds include acyl cyanides, acyl azides, *N*-acylimidazoles, *O*-aryl esters, and thioesters. The carbonyl compounds are arranged below in the order of the increasing reactivity toward nucleophilic addition.



Carbonyl Derivatives: Order of increasing reactivity toward nucleophilic addition

At this point we want to consider the relative reactivity of carboxylic acid derivatives and other carbonyl compounds in general terms. We return to the subject in more detail in Chapter 7. Let us first examine some of the salient structural features of the carbonyl compounds. The strong polarity of the C=O bond is the origin of its reactivity toward nucleophiles. The bond dipole of the C–X bond would be expected increase carbonyl reactivity as the group X becomes more electronegative. There is another powerful effect exerted by the group X, which is resonance electron donation.



Substituents with unshared electrons allow electron delocalization, which stabilizes the compound and increases the negative charge on oxygen. This resonance effect stabilizes the carbonyl compound and decreases the reactivity of the carbonyl group toward nucleophiles. The order of electron donation by resonance is $\text{RN}^- > \text{O}^- > \text{NR}_2 > \text{OR} \sim \text{OH} > \text{F}$. The trends in the resonance and polar effects of these substituents are *reinforcing* and lead to the overall reactivity trends shown above. The amido group is the strongest resonance donor and weakest polar acceptor, whereas the fluorine is the weakest π donor and strongest σ acceptor.

There have been several attempts to analyze these substituent effects using computational approaches. For example, the isodesmic reaction



yields the results shown in Table 3.21.¹⁰⁶ In this formulation, the total stabilization includes both the differences between the C–X and the C–C bond strength and the resonance stabilization of the substituent. Remember (Section 3.1.2.2) that the C–X bond strength increases because of electronegativity differences. An indication of the extent of the π conjugation can be obtained from the C–X π bond orders shown in Figure 3.20. The $\text{C}=\text{X}^+$ bond order decreases in the series $\text{NH}_2(0.28) > \text{OCH}_3(0.22) > \text{F}(0.13)$. These values can be contrasted to those for $\text{C}\equiv\text{N}$ and CH_3 , where there is minimal π delocalization and the π bond orders are around 0.04. Figure 3.20 also shows the atomic charges, as determined by the AIM method.

It is also desirable to separate the resonance component of the total stabilization energy. Wiberg addressed the issue by comparing total stabilization with the rotational barrier, which should be a measure of the resonance contribution.¹⁰⁷ The resonance component for F was assumed to be zero. This analysis provides the order $\text{NH}_2 > \text{OH}$ for the π stabilization but $\text{OH} > \text{NH}_2$ for the σ component, as shown in Table 3.22.

Table 3.21. Carbonyl Substituent Stabilization as Estimated by Isodesmic Replacement by Methyl (in kcal/mol)^a

Substituent	ΔH_{exp}	HF/6-31G*	MP2/6-31G*	MP3/6-311++G**
NH_2	19.6	20.6	21.2	18.3
OH	23.4	25.5	26.8	22.3
F	17.9	19.0	21.1	16.4
SiH_3		-13.0	-12.0	-12.6
PH_2		-6.2	-3.5	-3.9
SH	4.5	4.3	7.3	5.5
Cl	6.6	2.9	7.9	6.7
CN		-11.8	-9.3	-11.0
CF_3		-11.9	-11.0	-12.4

a. Data from K. B. Wiberg, C. M. Hadad, P. R. Rablen, and J. Ciosowski, *J. Am. Chem. Soc.*, **114**, 8644 (1992).

¹⁰⁶ K. B. Wiberg, C. M. Hadad, P. R. Rablen, and J. Ciosowski, *J. Am. Chem. Soc.*, **114**, 8644 (1992).

¹⁰⁷ K. B. Wiberg, *Acc. Chem. Res.*, **32**, 922 (1999); K. B. Wiberg, *J. Chem. Educ.*, **73**, 1089 (1996).

(a) Charge density

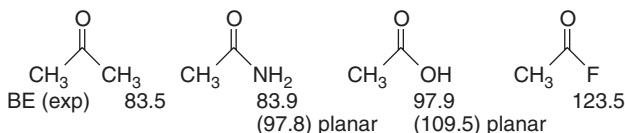
$\begin{array}{c} -1.17 \\ \text{O} \\ \\ +0.19 \end{array}$	$\begin{array}{c} -1.08 \\ \text{O} \\ \\ +0.14 \end{array}$	$\begin{array}{c} -1.21 \\ \text{O} \\ \\ +0.07 \end{array}$	$\begin{array}{c} -1.21 \\ \text{O} \\ \\ +0.07 \end{array}$
$\text{H}_3\text{C}-\text{C}-\text{F}$	$\text{H}_3\text{C}-\text{C}-\text{CF}_3$	$\text{H}_3\text{C}-\text{C}-\text{OH}$	$\text{H}_3\text{C}-\text{C}-\text{NH}_2$
+1.64	+1.080	+1.63	+1.57

(b) π -Bond order

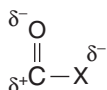
$\begin{array}{c} 0.56 \\ \text{O} \\ \\ \text{H}_3\text{C}-\text{C}-\text{F} \end{array}$	$\begin{array}{c} 0.61 \\ \text{O} \\ \\ \text{H}_3\text{C}-\text{C}-\text{Cl} \end{array}$	$\begin{array}{c} 0.64 \\ \text{O} \\ \\ \text{H}_3\text{C}-\text{C}-\text{CN} \end{array}$	$\begin{array}{c} 0.63 \\ \text{O} \\ \\ \text{H}_3\text{C}-\text{C}-\text{CH}_3 \end{array}$	$\begin{array}{c} 0.53 \\ \text{O} \\ \\ \text{H}_3\text{C}-\text{C}-\text{OH} \end{array}$	$\begin{array}{c} 0.52 \\ \text{O} \\ \\ \text{H}_3\text{C}-\text{C}-\text{NH}_2 \end{array}$
0.13	0.14	0.04	0.04	0.21	0.28

Fig. 3.20. Charge density (a) and bond orders (b) for carbonyl derivatives.

The bond energies of the $\text{O}=\text{C}-\text{X}$ bonds increase sharply with electronegativity. For NH_2 and OH there are different values for perpendicular and planar structures, reflecting the resonance contribution to the planar form.



The increasing $\text{C}-\text{X}$ bond strength (apart from resonance) is attributed to the electrostatic attraction associated with the difference in electronegativity. This is accentuated by the already existing $\text{C}=\text{O}$ charge separation and leads to a favorable juxtaposition of positive and negative charge.¹⁰⁸



There have been several attempts¹⁰⁹ to assign relative importance to the polar (including electrostatic) and resonance components of the stabilization carboxylate

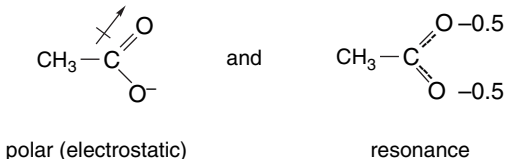
Table 3.22. Separation of the Resonance Component of the Stabilization Energy

	Total SE	ΔH_{rot}	ΔH_{σ}
F	16.7	—	16.7
OH	27.7	11.5	16.2
NH ₂	19.3	13.9	5.4
Cl	6.8	—	6.8
SH	6.1	8.1	-2.0
PH ₂	-3.9	0	-3.9
SiH ₃	-12.7	0	-12.7

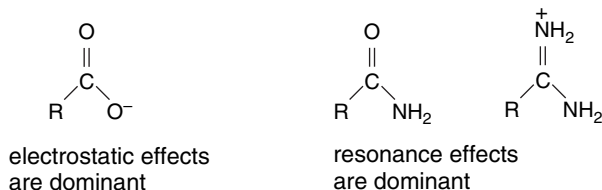
¹⁰⁸ J. B. Levy, *Struct. Chem.*, **10**, 121 (1999).

¹⁰⁹ P. C. Hiberty and C. P. Byrman, *J. Am. Chem. Soc.*, **117**, 9875 (1995); R. W. Taft, I. A. Koppel, R. D. Topsom, and F. Anvia, *J. Am. Chem. Soc.*, **112**, 2047 (1990); M. R. F. Siggel, A. Streitwieser, Jr., and T. D. Thomas, *J. Am. Chem. Soc.*, **110**, 8022 (1988).

anions. In a comparison of the acidity of acetic acid (pK 4.7) with that of alcohols (pK 16–18), the issue is the relative importance of the C=O bond dipole and resonance in stabilizing the carboxylate anion. These approaches have led to estimates ranging from 50 to 80% of the stabilization being polar in origin.



Rablen¹¹⁰ investigated carbonyl substituent effects by using a series of isodesmic reactions designed to separate resonance and polar effects. He found the oxygen π contributions to be about 6 kcal/mol, as opposed to about 14 kcal/mol for nitrogen. The order of the polar effect is F > O > N > C, whereas that for the resonance effect is N > O > F. His analysis suggests that the stabilization in acetate (O⁻ donor) is about one-third resonance and two-thirds electrostatic. On the other hand, in amides and amidines, the order is reversed, roughly two-thirds resonance and one-third electrostatic.



A physical property that reflects the electronic character of the carbonyl substituent is the ^{17}O NMR chemical shift. Although the relation of the chemical shift to electronic properties is complex, there is a correlation with the resonance electron-donating ability of the substituent. The π -donor substituents cause large downfield shifts in the order Cl ≪ F < OCH₃ < NH₂. Nonconjugating substituents, such as cyano, trifluoromethyl, and methyl, have much smaller effects (Table 3.23).

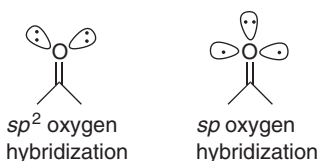
Table 3.23. ^{17}O Chemical Shifts for $\text{CH}_3\text{COX}^{\text{a}}$

X	^{17}O
CN	603 ^b
CF ₃	592
H	592
CH ₃	571
Cl	502
F	374
CH ₃ O	361
NH ₂	313

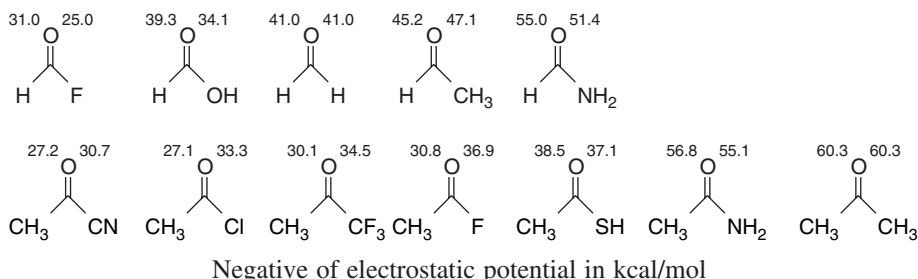
a. H. Dahm and P. A. Carrupt, *Magn. Reson. Chem.*, **35**, 577 (1997).

b. J.-C. Zhuo, *Molecules*, **4**, 320 (1999).

¹¹⁰ P. R. Rablen, *J. Am. Chem. Soc.*, **122**, 357 (2000).

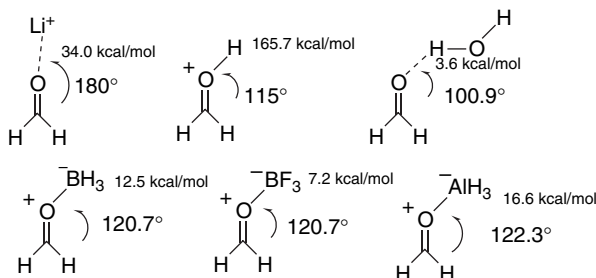


Wiberg and co-workers calculated the electrostatic potential at the carbonyl oxygen for several derivatives at the MP2/6-31+G* level.¹¹¹ The most negative electrostatic potential is found at angles somewhat greater than 120°, but generally corresponding with the trigonal *sp*² hybridization model.



Note that the unsymmetrical compounds have somewhat different potentials *syn* and *anti* to the substituent. The qualitative order found for the formyl series F < OH < H < CH₃ < NH₂ suggests a mixture of σ polar effects and π-electron donation. The acetyl series also included CN, Cl, and SH. It is interesting that the fluoride is calculated to have a more negative potential at oxygen than the chloride. This indicates a resonance contribution that attenuates the σ polar effect.

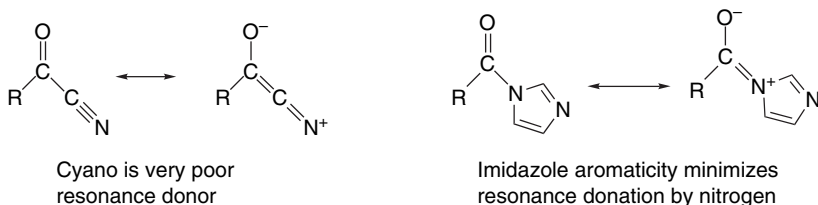
The reactivity of carbonyl groups is strongly influenced by interactions between protons or Lewis acids and the carbonyl oxygen unshared electrons. Wiberg and co-workers computationally probed the interaction of the carbonyl oxygen with Li⁺, H⁺, and water (hydrogen bonding). Whereas Li⁺ prefers a linear structure, indicating that the attraction is primarily electrostatic rather than directional bonding, both protonation and hydrogen bonding favored the trigonal geometry. The same was true for the Lewis acids, BH₃, BF₃, and AlH₃. The bonding energy was also calculated. Note the wide range of bond strengths from hydrogen bonding (3.6 kcal/mol) to formation of a very strong bond by protonation (165.7 kcal/mol). The calculated bond strengths for the Lewis acids is much smaller.



¹¹¹ K. B. Wiberg, M. Marquez, and H. Castejon, *J. Org. Chem.*, **59**, 6817 (1994).

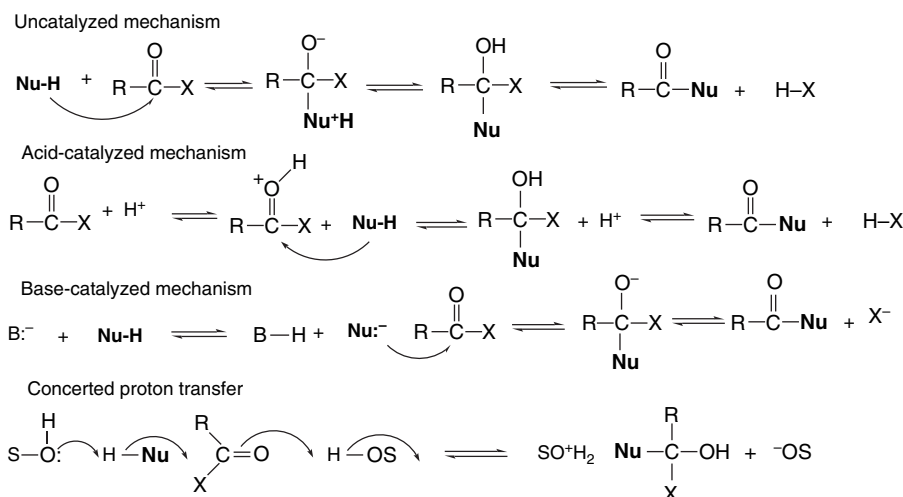
Other workers examined hydrogen bonding of HF with carbonyl compounds. There is good correlation between the strength of the hydrogen bond (1–8 kcal/mol) and the electrostatic potential at the carbonyl oxygen.¹¹² Thus one important factor in carbonyl group reactivity is the potential for interaction with protons and Lewis acids, including metal ions.

We can summarize the structural effects of the substituents at the carbonyl group in terms of the resonance and polar contributions. While there may be variation in the relative weighting assigned to the polar and resonance components, the general trends are clear. Electron pair donors interact with the carbonyl group by resonance and the order of electron donation is $\text{C}^- > \text{HN}^- > \text{O}^- > \text{H}_2\text{N} > \text{RO} > \text{F}$. The polar effect owing to substituent electronegativity is in the opposite direction, with $\text{F} > \text{RO} > \text{H}_2\text{N}$. These effects are *reinforcing* and increase carbonyl electrophilicity in the order $\text{C}^- < \text{HN}^- < \text{O}^- < \text{H}_2\text{N} < \text{RO} < \text{F}$. The consequences of these resonance and polar effects on the carbonyl group can be observed in various ground state, i.e., reactant, properties. Groups such as cyano and imidazolide that have very weak resonance stabilization are dominated by the polar effect of the substituent and are quite reactive toward nucleophiles.



Let us now examine how substituent effects in *reactants* influence the rates of nucleophilic additions to carbonyl groups. The most common mechanism for substitution reactions at carbon centers is by an *addition-elimination mechanism*. The adduct formed by the nucleophilic addition step is tetrahedral and has sp^3 hybridization. This adduct may be the product (as in hydride reduction) or an intermediate (as in nucleophilic substitution). For carboxylic acid derivatives, all of the steps can be reversible, but often one direction will be strongly favored by product stability. The addition step can be acid-catalyzed or base-catalyzed or can occur without specific catalysis. In protic solvents, proton transfer reactions can be an integral part of the mechanism. Solvent molecules, the nucleophile, and the carbonyl compound can interact in a concerted addition reaction that includes proton transfer. The overall rate of reaction depends on the reactivity of the nucleophile and the position of the equilibria involving intermediates. We therefore have to consider how the substituent might affect the energy of the tetrahedral intermediate.

¹¹² P. Bobadova-Parvanova and B. Galabov, *J. Phys. Chem. A.*, **102**, 1815 (1998); J. A. Platts, *Phys. Chem. Phys.*, **2**, 3115 (2000).



Some time ago, J. P. Guthrie derived an energy profile pertaining to the hydrolysis of methyl acetate under acidic, neutral, and basic conditions from kinetic data.¹¹³ These reaction profiles are shown in Figure 3.21. This reaction can serve to introduce the issues of relative reactivity in carbonyl addition reactions. The diagram shows that the reaction is nearly energetically neutral in acidic solution, but becomes exothermic in neutral and basic solutions because of the additional stabilization associated with the carboxylate group. The activation barrier is highest for the neutral reaction. The activation barrier is lowered in acidic solution as a result of the enhanced reactivity of the protonated carbonyl (acid-catalyzed mechanism). The activation barrier for the basic hydrolysis is reduced because hydroxide ion is a more powerful nucleophile than water (base-catalyzed mechanism).

The energy relationships among reactants, transition states, intermediates, and products have been further explored for the base-catalyzed hydrolysis of methyl acetate.¹¹⁴ The relative energies of the species shown in Figure 3.22 were calculated using

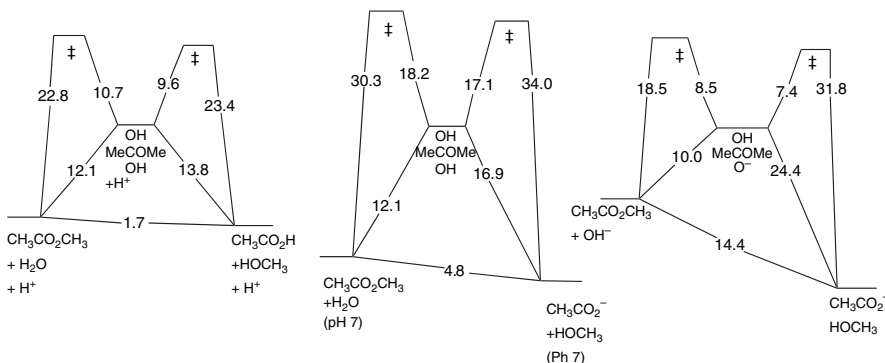


Fig. 3.21. Comparative reaction energy profiles for acidic, neutral, and basic hydrolysis of methyl acetate in water. Adapted from *J. Am. Chem. Soc.*, **95**, 6999 (1973), by permission of the American Chemical Society.

¹¹³ J. P. Guthrie, *J. Am. Chem. Soc.*, **95**, 6999 (1973).

¹¹⁴ C.-G. Zhan, D. W. Landry, and R. L. Ornstein, *J. Am. Chem. Soc.*, **122**, 1522 (2000).

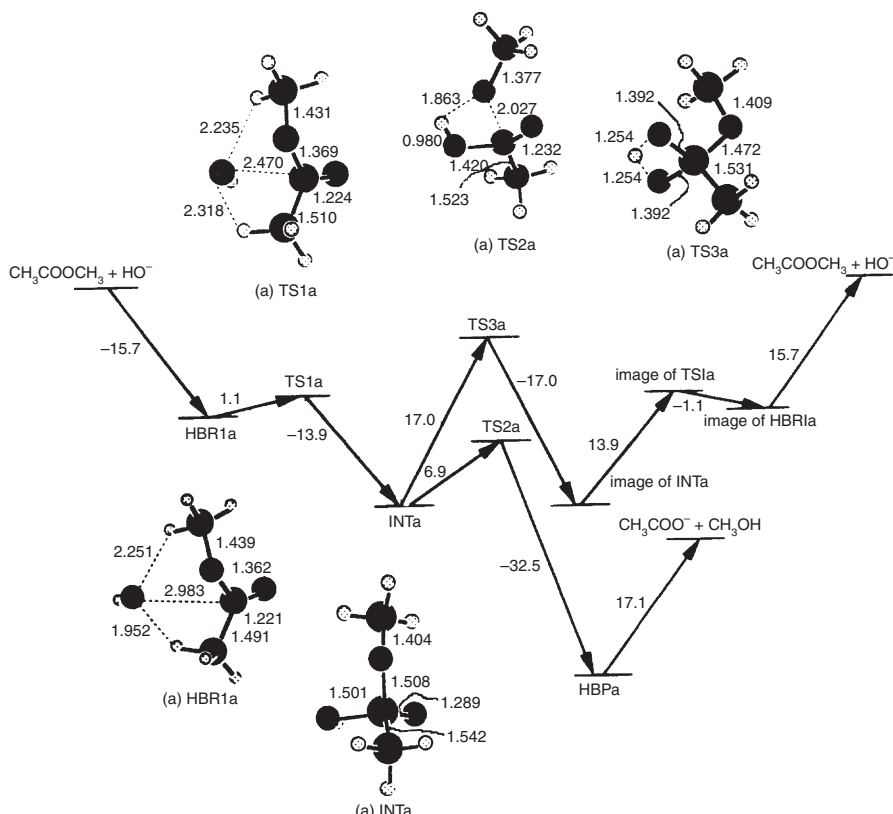
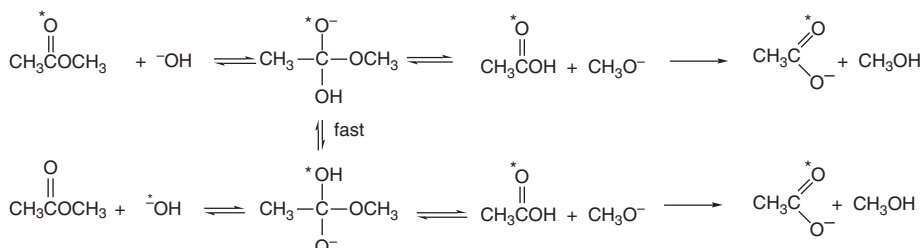


Fig. 3.22. Energy profiles (in kcal/mol) and structures of intermediates and transition states for competing hydrolysis and carbonyl oxygen exchange for methyl acetate and hydroxide ion in the gas phase. Adapted from *J. Am. Chem. Soc.*, **122**, 1522 (2000), by permission of the American Chemical Society.

several MO and DFT computations. The values quoted are for BLYP/6-31++G(*d,p*) level calculations and refer to the gas phase. These energy values describe both the hydrolysis reaction and the carbonyl oxygen exchange reaction, both of which occur through the same tetrahedral addition intermediate. **HBR1a** is a complex between $\text{^{\circ}}\text{OH}$ and the reactant. **TS1a** and **INTa** are the TS and tetrahedral intermediate, respectively, resulting from hydroxide addition. **TS2a** is the TS leading to methoxide elimination, which results in the stable complex of methanol and acetate ion. **TS3a** is the TS for proton transfer between the two oxygens, which leads to oxygen exchange via an intermediate that is structurally identical to **TS1a**.



This theoretical examination of carbonyl addition reactions serves to emphasize the enormous role that solvation effects play. As indicated in Figure 3.22 and other studies, gas phase addition of hydroxide ion to esters is calculated to be *exothermic* and to encounter only a very small barrier at **TS1a** and **TS2a**.¹¹⁵ The major contribution to the activation barrier (18.5 kcal/mol) that is observed in solution is the energy of desolvation of the hydroxide ion.¹¹⁶ We return to a discussion of solvation effects on carbonyl additions is Section 3.8.

A similar comparison of the gas phase and solution phase reaction of *N,N*-dimethylacetamide was conducted.¹¹⁷ Energies were calculated at the MP2/6-31+G** level. Solution phase calculations were done using a continuum solvent model. The results are summarized in Figure 3.23 and, as with the ester reaction, the addition is calculated to be exothermic in the gas phase, but to have a barrier in solution. Interestingly, the HF/6-31+G** energy values are somewhat closer to the experimental values than the MP2/6-31+G** results. The solution value is 24.6 kcal/mol.¹¹⁸

Similar energy profiles for the other classes of carbonyl compounds would allow us to make broad comparisons in reactivity. Unfortunately, the reactivity covers a very

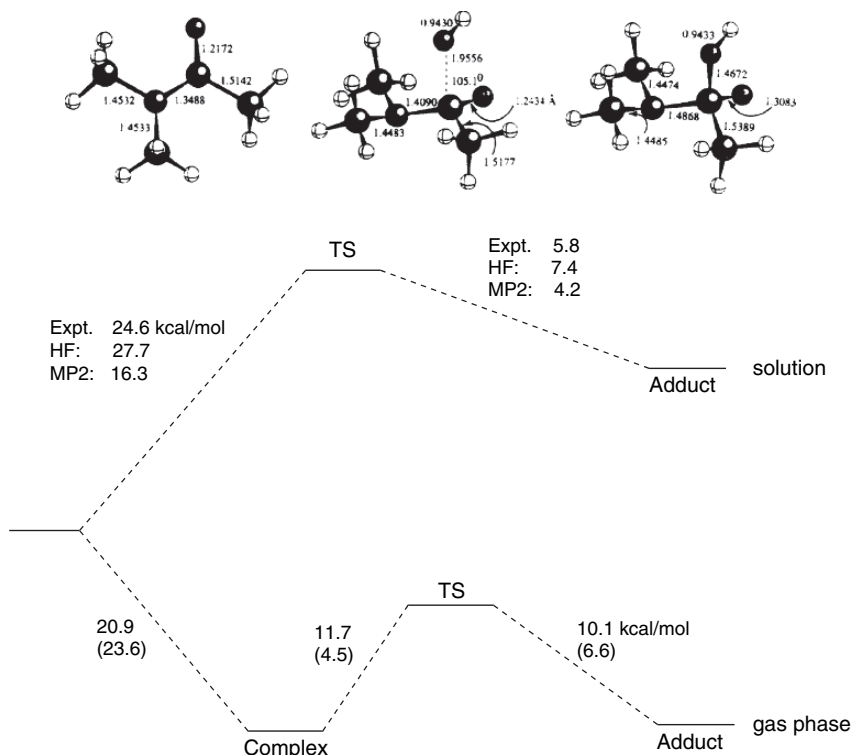


Fig. 3.23. Gas phase and solution reaction energy profiles for addition of hydroxide ion to *N,N*-dimethylacetamide. MP2 values are in parentheses Adapted from *Theochem*, **429**, 41 (1998), by permission of Elsevier.

¹¹⁵ K. Hori, *J. Chem. Soc., Perkin Trans.*, **2**, 1629 (1992); I. Lee, D. Lee, and C. K. Kim, *J. Phys. Chem. A*, **101**, 879 (1997); F. Hæfner, C.-H. Hu, T. Brink, and T. Norin, *Theochem*, **459**, 85 (1999).

¹¹⁶ M. J. S. Dewar and D. M. Storch, *J. Chem. Soc., Chem. Commun.*, 94 (1985); J. P. Guthrie, *Can. J. Chem.*, **68**, 1643 (1990).

¹¹⁷ Y.-J. Zheng and R. L. Ornstein, *Theochem*, **429**, 41 (1998).

¹¹⁸ J. P. Guthrie, *J. Am. Chem. Soc.*, **96**, 3608 (1974).

wide range and it is not easy to make direct experimental comparisons. In Scheme 3.2 some available kinetic data are provided that allow at least a qualitative comparison of the reactivity of the most common derivatives. The ratio of reaction toward hydroxide is anhydride > ester > amide, reflecting the expected trend and is dominated by the resonance effect. Acyl chlorides are even more reactive, judging by a comparison of methanolysis and hydrolysis. The data for esters give the nucleophilicity order as $\text{-OH} > \text{NH}_3 > \text{H}_2\text{O}$, as expected.

A more extensive and precise set of data has been developed that includes aldehydes and ketones (but not acyl halides), which pertains to the equilibrium constant for hydration.¹¹⁹

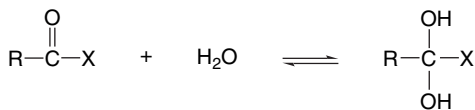


Table 3.24 shows the values for equilibrium constants for nucleophilic addition of both water and hydroxide ion. We can see the following trends in these data: For aldehydes and ketones, the addition is disfavored in the order Ph > alkyl > H. The order $\text{NH}_2 < \text{OR} < \text{CH}_3 < \text{H}$ is indicated by the K_{hydr} values of $10^{-13.8}$, $10^{-6.6}$, $10^{0.03}$, and $10^{3.36}$ for *N,N*-dimethylformamide, methyl formate, acetaldehyde, and formaldehyde,

Scheme 3.2. Relative Reactivity Data for Some Carboxylic Acid Derivatives

	$\text{CH}_3-\overset{\text{O}}{\underset{\parallel}{\text{C}}}-\text{Cl}$	$(\text{CH}_3\overset{\text{O}}{\underset{\parallel}{\text{C}}})_2\text{O}$	$\text{CH}_3-\overset{\text{O}}{\underset{\parallel}{\text{C}}}-\text{OR}'$	$\text{CH}_3-\overset{\text{O}}{\underset{\parallel}{\text{C}}}-\text{N}(\text{CH}_3)_2$
Hydrolysis (-OH)		$8.9 \times 10^2 \text{ M}^{-1} \text{ s}^{-1}$ at 25°C (a)	$2.2 \times 10^{-2} \text{ M}^{-1} \text{ s}^{-1}$ at 0°C $E_a = 18.5$ (b)	$1.8 \times 10^{-5} \text{ M}^{-1} \text{ s}^{-1}$ $E_a = 24.1$ (c)
Hydrolysis (H_2O)		$2.4 \times 10^{-3} \text{ s}^{-1}$ at 25°C (a)	$3 \times 10^{-10} \text{ s}^{-1}$ at 0°C $E_a = 30.2$ kcal(b)	
Methanolysis (CH_3OH)	$1 \times 10^{-1} \text{ s}^{-1}$ at 0°C (d)			
Aminolysis (NH_3)			$2.8 \times 10^{-7} \text{ M}^{-1} \text{ s}^{-1}$ in 10 M H_2O in dioxane (e) $3.7 \times 10^{-7} \text{ M}^{-1} \text{ s}^{-1}$ in 5 M $\text{HOCH}_2\text{CH}_2\text{OH}$ in dioxane (f)	

- a. C. Castro and E. A. Castro, *J. Org. Chem.*, **46**, 2939 (1981); J. F. Kirsch and W. P. Jencks, *J. Am. Chem. Soc.*, **86**, 837 (1964).
- b. J. P. Guthrie, *J. Am. Chem. Soc.*, **95**, 6999 (1973).
- c. J. P. Guthrie, *J. Am. Chem. Soc.*, **96**, 3608 (1974).
- d. T. W. Bentley, G. Llewelyn, and J. A. McAlister, *J. Org. Chem.*, **61**, 7927 (1996).
- e. F. H. Wetzel, J. G. Miller, and A. R. Day, *J. Am. Chem. Soc.*, **75**, 1150 (1953).
- f. E. M. Arnett, J. G. Miller, and A. R. Day, *J. Am. Chem. Soc.*, **72**, 5635 (1950).

¹¹⁹ J. P. Guthrie, *J. Am. Chem. Soc.*, **122**, 5529 (2000).

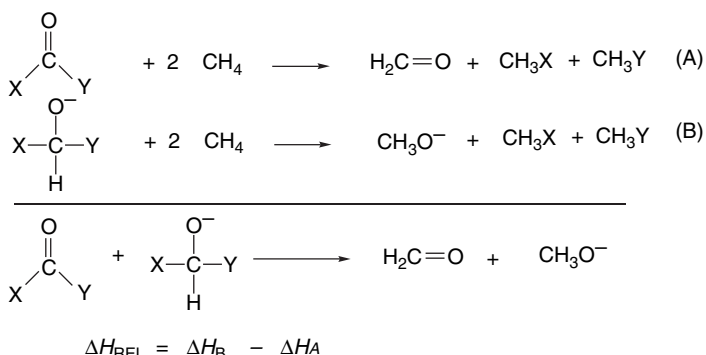
Table 3.24. Equilibrium Constants for Hydration and Hydroxide Addition for Selected Carbonyl Compounds

Compounds ^a	$\log K_{\text{H}_2\text{O}}$	$\log K_{-\text{OH}}$
$\text{CH}_2=\text{O}$	3.36	6.51
$\text{CH}_3\text{CH}=\text{O}$	0.03	4.68
$(\text{CH}_3)_2\text{CHCH}=\text{O}$	-0.21	2.99
$\text{PhCH}=\text{O}$	-2.10	2.5
$(\text{CH}_3)_2\text{C}=\text{O}$	-2.85	2.04
HCO_2CH_3	-6.6	1.58
$\text{CH}_3\text{CO}_2\text{CH}_3$	-8.2	-0.82
$(\text{CH}_3)_2\text{CHCO}_2\text{CH}_3$	-10.42	-1.05
$\text{CF}_3\text{CO}_2\text{CH}_3$	-0.9	5.53
HCOSC_2H_5	-3.5	2.1
$\text{CH}_3\text{COSC}_2\text{H}_5$	-8.2	-0.92
$\text{CF}_3\text{COSC}_2\text{H}_5$	-2.8	3.77
$\text{HCON}(\text{CH}_3)_2$	-13.8	-3.75
$\text{CH}_3\text{CON}(\text{CH}_3)_2$	-14.2	-4.75
$\text{CF}_3\text{CON}(\text{CH}_3)_2$	-9.2	-0.13

a. Data from J. P. Guthrie, *J. Am. Chem. Soc.*, **122**, 5529 (2000).

respectively. The hydroxide addition is in the same order but lies much further toward the adduct: $10^{-3.75}$, $10^{-0.82}$, $10^{4.68}$, and $10^{6.5}$, respectively, as expected for the stronger nucleophile. These data give a good indication of the overall reactivity of carbonyl compounds toward a prototypical nucleophilic addition, but incorporate structural effects pertaining to both the reactant and tetrahedral adduct. For example, the 100-fold difference between benzaldehyde and 2-methylpropanal presumably reflects the extra conjugative stabilization of the aromatic aldehyde. Similarly, the 10^7 and 10^5 difference between the ethyl esters and *N,N*-dimethylamides of acetic acid and trifluoroacetic acid, respectively, are due to the polar effect of the trifluoromethyl group. Note, however, that the differences are only slightly smaller ($10^{6.5}$ and $10^{4.5}$) in the anionic hydroxide adducts.

What can we say about substituent effects on the tetrahedral adducts? These have been assessed by comparing hydride affinity of the various derivatives, relative to formaldehyde,¹²⁰ using the isodesmic reaction sequence shown below.



¹²⁰ R. E. Rosenberg, *J. Am. Chem. Soc.*, **117**, 10358 (1995).

The effect of the same substituents on the adduct was evaluated by another isodesmic reaction:



This analysis permits assignment of hydride affinity to the carbonyl compounds relative to formaldehyde. The stabilization of the carbonyl compound by X relative to H is shown in Table 3.25 as $\Delta\text{C=O}$. The stabilization of the hydride adduct is shown as ΔCHO^- . The difference, the hydride affinity relative to $\text{CH}_2=\text{O}$, is listed as ΔHA . The resonance donors NH_2 and CH_3O have the largest stabilizing effect on the carbonyl starting material, but F also has a very significant stabilizing effect. The stabilization of the tetrahedral adduct is in the order of bond strength $\text{F} > \text{CH}_3\text{O} > \text{NH}_2 > \text{CH}_3$. The difference between the two values places the overall substituent effect for reactivity toward hydride in the order $\text{F} > \text{H} > \text{CH}_3 > \text{OCH}_3 > \text{NH}_2$, in excellent agreement with experimental data. The polar EWGs CN and CF_3 strongly favor hydride addition by strong stabilization of the anionic tetrahedral adduct. As a result, they have the largest overall effect on the stability of the hydride adduct, followed by fluoro and formyl.

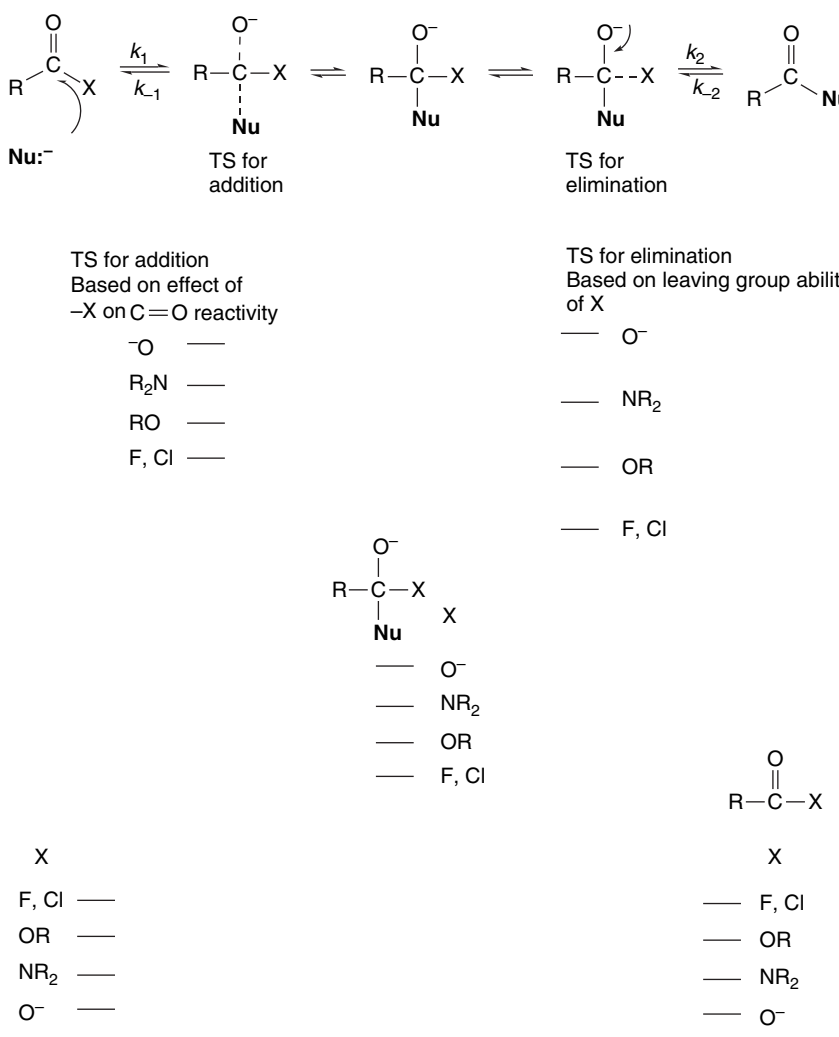
The stability relationships for carbonyl substitution reactions by an anionic nucleophile are summarized in Scheme 3.3. The simplest substitution reactions consist of two reversible steps, the formation of the tetrahedral intermediate and the subsequent elimination of the original substituent. As we discuss in Chapter 7, the mechanism is frequently more complex, often involving proton transfers. However, the stability effects of the carbonyl groups can be illustrated in terms of the simple two-step mechanisms. The stability order of reactants and products is $\text{F}, \text{Cl} < \text{OR} < \text{NR}_2 < \text{O}^-$. The order of stability of the *anionic* tetrahedral intermediates is $\text{F} > \text{RO} > \text{RN}_2 > \text{O}^-$. The diagram clearly indicates that the reactivity order will be $\text{F} > \text{RO} > \text{R}_2\text{N} > \text{O}^-$. Note also that the relative rates for the two possible fates of the tetrahedral intermediate (forward or reverse) are determined by the ease with which either X^- or Nu^- departs from the tetrahedral intermediate. This order will be $\text{F}^- > \text{RO}^- > \text{NH}_2^- > \text{O}^{2-}$, so we expect substitution on acyl fluorides (and other acyl halides) to be fast and irreversible. On the other hand, nucleophilic substitution on carboxylate anions, which is at the other end of the reactivity range, is nearly impossible. (We will see in Section 7.2.2.2 in Part B that organolithium compounds are strong enough nucleophiles to achieve addition with carboxylate groups, at least in the presence of Li^+ .) The relative stability

Table 3.25. Substituent Effects on Hydride Affinity of XYC=O by an Isodesmic Reaction Sequence (in kcal/mol by G2(MP2) Calculations)^a

X	Y	$\Delta\text{C=O}$	ΔHCO^-	ΔHA
H	H	0	0	0
H	CH_3	11.1	9.6	1.5
H	NH_2	31.5	21.8	9.7
H	CH_3O	32.8	29.0	3.8
H	F	26.1	38.2	-12.1
H	CH=O	3.1	19.0	-15.9
H	CF_3	-3.0	23.3	-26.3
H	CN	-2.4	25.9	-28.3

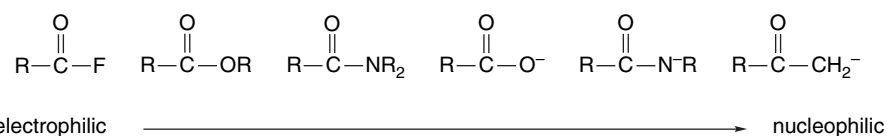
a. R. E. Rosenberg, *J. Am. Chem. Soc.*, **117**, 10358 (1993).

Scheme 3.3. Summary of Substituent Effects on Carbonyl Substitution Reactions



of the carboxylate starting material and the double negative charge on the tetrahedral intermediate make the activation energy for the first step very high. Even if the intermediate is formed, the prospective leaving group O^{2-} is very difficult to eliminate, so $k_{-1} > k_2$ and no substitution is observed.

Perhaps it is worth noting in summary that the series can be extended to include $\text{X}=\text{NH}^-$ and $\text{X}=\text{CH}_2^-$. These analogs would be expected to be even less reactive than carboxylate toward nucleophilic addition. The latter species is an *enolate*. We will learn in Section 7.7 that enolates are reactive nucleophiles. Carboxylate and amide anions also are nucleophilic. Even amides are somewhat nucleophilic. Going across the periodic table from F to CH_2^- , the carbonyl substituent **X** transforms the carbonyl group from an electrophile to part of an nucleophilic structure in the anionic structures by increasing electron donation.



3.5. Kinetic Isotope Effects

A special type of substituent effect that has proved very valuable in the study of reaction mechanisms is the replacement of an atom by one of its isotopes. Isotopic substitution most often involves replacing protium by deuterium (or tritium), but is applicable to nuclei other than hydrogen. The quantitative differences are largest, however, for hydrogen because its isotopes have the largest relative mass differences. Isotopic substitution usually has no effect on the qualitative chemical reactivity of the substrate, but it often has an easily measured effect on the rate, which is called a *kinetic isotope effect (KIE)*. Let us consider how this modification of the rate arises. Initially, the discussion concerns *primary kinetic isotope effects*, those in which a bond to the isotopically substituted atom is broken in the rate-determining step. We use C–H bonds as the specific case for discussion but the same concepts apply for other elements.

Any C–H bond has characteristic vibrations that impart some energy, called the *zero-point energy*, to the molecule. The energy associated with these vibrations is related to the mass of the vibrating atoms. Owing to the greater mass of deuterium, the vibrations associated with a C–D bond contribute less to the zero-point energy than the corresponding C–H bond. For this reason, substitution of protium by deuterium lowers the zero-point energy of a molecule. For a reaction involving cleavage of a bond to hydrogen (or deuterium), a vibrational degree of freedom in the normal molecule is converted to a translational degree of freedom as the bond is broken. The energy difference that is due to this vibration disappears at the transition state. The transition state has the same energy for the protonated and deuterated species. Because the deuterated molecule has the lower zero-point energy, it has a higher activation energy to reach the transition state, as illustrated in Figure 3.24.

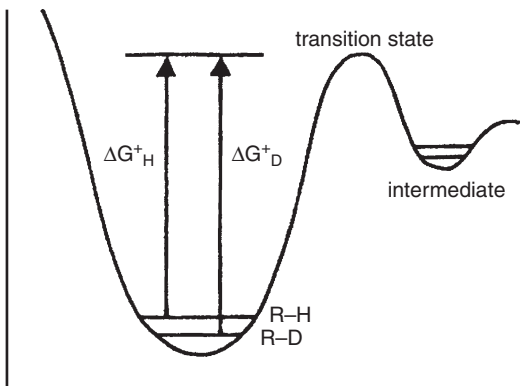
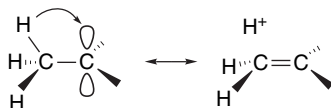


Fig. 3.24. Differing zero-point energies of protium- and deuterium-substituted molecules as the cause of primary kinetic isotope effects.

Just how large the rate difference is depends on the nature of the TSs. The maximum effect occurs when the hydrogen being transferred is bound about equally to two other atoms at the TS. The calculated maximum for the isotope effect k_H/k_D involving C–H bonds is about 7 at room temperature.¹²¹ When bond breaking is more or less than half complete at the TS, the isotope effect is smaller and can be close to 1 if the TS is very reactant-like or very product-like. Primary isotope effects can provide two very useful pieces of information about a reaction mechanism. First, the existence of a substantial isotope effect, i.e., $k_H/k_D > 2$, is strong evidence that the bond to that particular hydrogen is being broken in the rate-determining step. Second, the magnitude of the isotope effect provides a qualitative indication of where the TS lies with regard to product and reactant. A relatively low primary isotope effect implies that the bond to hydrogen is either only slightly or nearly completely broken at the TS. That is, the TS must occur quite close to reactant or to product. An isotope effect near the theoretical maximum is good evidence that the TS involves strong bonding of the hydrogen to both its new and old bonding partner.

Isotope effects may also be observed when the substituted hydrogen atom is not directly involved in the reaction. Such effects, known as *secondary kinetic isotope effects*, are smaller than primary effects and are usually in the range of $k_H/k_D = 0.7 - 1.5$. They may be normal ($k_H/k_D > 1$) or inverse ($k_H/k_D < 1$), and are also classified as α or β , etc., depending on the location of the isotopic substitution relative to the reaction site. Secondary isotope effects result from a tightening or loosening of a C–H bond at the TS. The strength of the bond may change because of a hybridization change or a change in the extent of hyperconjugation, for example. If an sp^3 carbon is converted to sp^2 as reaction occurs, a hydrogen bound to the carbon will experience decreased resistance to C–H bending. The freeing of the vibration for a C–H bond is greater than that for a C–D bond because the former is slightly longer, and the vibration has a larger amplitude. This will result in a normal isotope effect. Entry 5 in Scheme 3.4 is an example of such a reaction that proceeds through a carbocation intermediate. An inverse isotope effect will occur if coordination at the reaction center increases in the TS. The bending vibration will become more restricted. Entry 4 in Scheme 3.4 exemplifies a case involving conversion of a tricoordinate carbonyl group to a tetravalent cyanohydrin. In this case the secondary isotope effect is 0.73.

Secondary isotope effects at the β -position have been especially thoroughly studied in nucleophilic substitution reactions. When carbocations are involved as intermediates, substantial β -isotope effects are observed because the hyperconjugative stabilization by the β -hydrogens weakens the C–H bond.¹²² The observed secondary isotope effects are normal, as would be predicted since the bond is weakened.



Detailed analysis of isotope effects reveals that there are many other factors that can contribute to the overall effect in addition to the dominant change in bond vibrations. There is not a sharp numerical division between primary and secondary effects,

¹²¹ K. B. Wiberg, *Chem. Rev.*, **55**, 713 (1955); F. H. Westheimer, *Chem. Rev.*, **61**, 265 (1961).

¹²² V. J. Shiner, W. E. Buddenbaum, B. L. Murr, and G. Lamaty, *J. Am. Chem. Soc.*, **90**, 809 (1968); A. J. Kresge and R. J. Preto, *J. Am. Chem. Soc.*, **89**, 5510 (1967); G. J. Karabatsos, G. C. Sonnichsen, C. G. Papaioannou, S. E. Scheppelle, and R. L. Shone, *J. Am. Chem. Soc.*, **89**, 463 (1967); D. D. Sunko and W. J. Hehre, *Prog. Phys. Org. Chem.*, **14**, 205 (1983).

Scheme 3.4. Some Representative Kinetic Isotope Effects

	Reaction	k_H/k_D (°C)
A. Primary kinetic isotope effects		
1 ^b	$\text{PhCH}_2-\text{H}^* + \text{Br}\cdot \longrightarrow \text{Ph}-\text{CH}_2\cdot + \text{H}^*\text{--Br}$	4.6 (77)
2 ^c	$(\text{CH}_3)_2\text{C}-\overset{\text{O}}{\underset{\text{H}^*}{\text{C}}}-\text{C}(\text{CH}_3)_2 + \text{OH}^- \longrightarrow (\text{CH}_3)_2\text{C}-\overset{\text{O}^-}{\underset{\text{H}^*}{\text{C}}}-\text{C}=\text{C}(\text{CH}_3)_2$	6.1 (25)
3 ^d	$\begin{array}{c} \text{H}^* \\ \\ \text{Cyclopentyl-N}^+(\text{CH}_3)_3 \end{array} + \text{OH}^- \longrightarrow \text{Cyclopentene} + (\text{CH}_3)_3\text{N}$	4.0 (191)
B. Secondary kinetic isotope effects		
4 ^e	$\text{CH}_3\text{O}-\text{C}_6\text{H}_4-\text{CH}^*=\text{O} + \text{HCN} \longrightarrow \text{CH}_3\text{O}-\text{C}_6\text{H}_4-\overset{\text{H}^*}{\underset{\text{C}}{\text{C}}}(\text{OH})-\text{C}\equiv\text{N}$	0.73 (25)
5 ^f	$\text{CH}_3-\text{C}_6\text{H}_4-\overset{\text{H}^*}{\underset{\text{H}^*}{\text{C}}}\text{Cl} \xrightarrow[\text{CF}_3\text{CH}_2\text{OH}]{\text{H}_2\text{O}} \text{CH}_3-\text{C}_6\text{H}_4-\overset{\text{H}^*}{\underset{\text{H}^*}{\text{C}}}\text{OH}$	1.30 (25)
6 ^g	$\text{Bicyclo[2.2.1]hept-2-ene-5,6-diene} \longrightarrow \text{Bicyclo[2.2.1]hept-2-ene} + \text{CH}_2^*=\text{CH}_2^*$	1.37 (50)

a. Temperature of measurement is indicated in parentheses.

b. K. B. Wiberg and L. H. Slaugh, *J. Am. Chem. Soc.*, **80**, 3033 (1958).c. R. A. Lynch, S. P. Vincenti, Y. T. Lin, L. D. Smucker, and S. C. Subba Rao, *J. Am. Chem. Soc.*, **94**, 8351 (1972).d. W. H. Saunders, Jr., and T. A. Ashe, *J. Am. Chem. Soc.*, **91**, 473 (1969).e. L. do Amaral, H. G. Bull, and E. H. Cordes, *J. Am. Chem. Soc.*, **94**, 7579 (1972).f. V. J. Shiner, Jr., M. W. Rapp, and H. R. Pinnick, Jr., *J. Am. Chem. Soc.*, **92**, 232 (1970).g. M. Taagepera and E. R. Thornton, *J. Am. Chem. Soc.*, **94**, 1168 (1972).

especially in the range between 1 and 2. For these reasons, isotope effects are usually used in conjunction with other criteria in the description of reaction mechanisms.¹²³

A new method for determining KIE using compounds of natural isotopic abundance has been developed.¹²⁴ This method makes experimental data more readily available. The method is based on the principle that as the reaction proceeds, the amount of the slower reacting isotope, e.g., ²H or ¹³C, is enriched in the remaining reactant. For example, an isotope effect of 1.05 leads to ~25% enrichment of the less reactive isotope at 99% conversion. The extent of enrichment can be measured by ²H

¹²³. For more complete discussion of isotope effects see: W. H. Saunders, in *Investigation of Rates and Mechanisms of Reactions*, E. S. Lewis, ed., *Techniques of Organic Chemistry*, 3rd Edition, Vol. VI, Part 1, John Wiley & Sons, New York, 1974, pp. 211–255; L. Melander and W. H. Saunders, Jr., *Reaction Rates of Isotopic Molecules*, Wiley, New York, 1980; W. H. Saunders, in *Investigation of Rates and Mechanisms of Reactions*, C. F. Bernasconi, ed., *Techniques of Organic Chemistry*, 4th Edition, Vol. VI, Part 1, Interscience, New York, 1986, Chap. VIII.

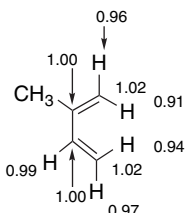
¹²⁴. D. A. Singleton and A. A. Thomas, *J. Am. Chem. Soc.*, **117**, 9357 (1995).

or ^{13}C NMR spectroscopy. The ratio of enrichment is related to the fraction of reaction completed and allows calculation of the KIE.

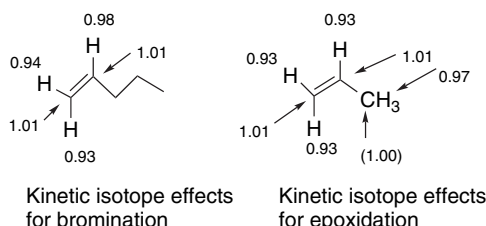
$$\text{KIE} = \frac{\ln(1 - F)}{\ln[(1 - F)R/R_0]} \quad (3.41)$$

where F is the fractional completion and R/R_0 is the isotopic enrichment.

The method can be simultaneously applied to each atom of interest. An atom that is expected to have a negligible KIE is selected as an internal standard. For example, with the methyl group as the internal standard, the KIE for every other position in isoprene was determined for the Diels-Alder reaction with maleic anhydride. This method is especially useful for the measurement of carbon isotope effects, where normal methods require synthesis of isotopic labeled reactants.



The experimental KIE can be compared with KIEs calculated from transition structures on the basis of the vibrational frequencies associated with specific bonds. This information is available from computed transition structures,¹²⁵ and the comparison can provide a direct experimental means of evaluating the computed transition structures.¹²⁶ The method has also been used to measure KIE in reactions such as the bromination of pentene¹²⁷ and epoxidation of propene.¹²⁸ Those transition structures that are inconsistent with the observed KIE can be excluded.



3.6. Linear Free-Energy Relationships for Substituent Effects

3.6.1. Numerical Expression of Linear Free-Energy Relationships

Many important relationships between substituent groups and chemical properties have been developed. For example, in Section 1.2.5 (p. 53), we discussed the effect

¹²⁵ M. Saunders, K. E. Laidig, and M. Wolfsberg, *J. Am. Chem. Soc.*, **111**, 8989 (1989).

¹²⁶ J. E. Baldwin, V. P. Reddy, B. A. Hess, Jr., and L. J. Schaad, *J. Am. Chem. Soc.*, **110**, 8554 (1988); K. N. Houk, S. M. Gustafson, and K. A. Black, *J. Am. Chem. Soc.*, **114**, 8565 (1992); J. W. Storer, L. Raimondi, and K. N. Houk, *J. Am. Chem. Soc.*, **116**, 9675 (1994).

¹²⁷ S. R. Merrigan and D. A. Singleton, *Org. Lett.*, **1**, 327 (1997).

¹²⁸ D. A. Singleton, S. R. Merrigan, J. Liu, and K. N. Houk, *J. Am. Chem. Soc.*, **119**, 3385 (1997).

of substituent groups on the acid strength of acetic acid derivatives. It was noted in particular that the presence of groups more electronegative than hydrogen increases the acid strength relative to acetic acid. In Section 3.4, we dealt with substituent effects on carbocation, carbanion, radical, and carbonyl addition intermediates. In many cases, structure-reactivity relationships can be expressed quantitatively in ways that are useful both for interpretation of reaction mechanisms and for prediction of reaction rates and equilibria. The most widely applied of these relationships is the *Hammett equation*, which correlates rates and equilibria for many reactions of compounds containing substituted phenyl groups. It was noted in the 1930s that there is a linear relationship between the acid strengths of substituted benzoic acids and the rates of many other chemical reactions, e.g., the rates of hydrolysis of substituted ethyl benzoates. The correlation is illustrated graphically in Figure 3.25, which shows $\log k/k_0$, where k_0 is the rate constant for hydrolysis of ethyl benzoate and k is the rate constant for the substituted esters plotted against $\log K/K_0$, where K and K_0 are the corresponding acid dissociation constants.

Analogous plots for many other reactions of aromatic compounds show a similar linear correlation with the acid dissociation constants of the corresponding benzoic acids, but with a range of both positive and negative slopes. Neither the principles of thermodynamics nor transition state theory require that there be such linear relationships. In fact, many reaction series fail to show linear correlations. Insight into the significance of the correlations can be gained by considering the relationship between the correlation equation and the free-energy changes involved in the two processes. The line in Figure 3.25 defines an equation in which m is the slope of the line:

$$m \log \frac{K}{K_0} = \log \frac{k}{k_0} \quad (3.42)$$

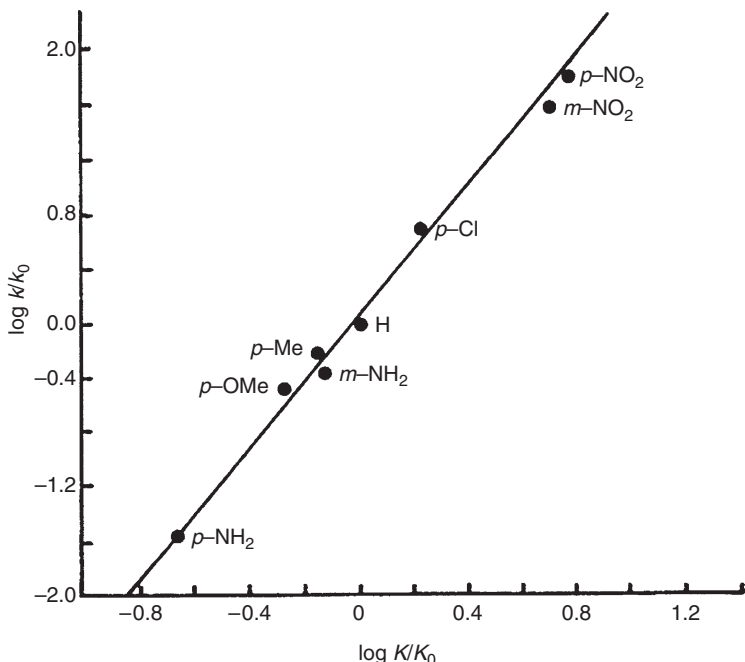


Fig. 3.25. Correlation of acid dissociation constants of benzoic acids with rates of basic hydrolysis of ethyl benzoates.

$$\begin{aligned} m(\log K - \log K_0) &= \log k - \log k_0 \\ m(-\Delta G/2.3RT + \Delta G_0/2.3RT) &= \Delta G^\ddagger/2.3RT + \Delta G_0^\ddagger/2.3RT \\ m(-\Delta G + \Delta G_0) &= -\Delta G^\ddagger + \Delta G_0^\ddagger \\ m\Delta\Delta G &= \Delta\Delta G^\ddagger \end{aligned} \quad (3.43)$$

SECTION 3.6

Linear Free-Energy Relationships for Substituent Effects

The linear correlation therefore indicates that the change in ΔG^\ddagger on introduction of a series of substituent groups is *directly proportional* to the change in the ΔG of ionization that is caused by the same series of substituents on benzoic acid. The correlations arising from such direct proportionality in free-energy changes are called *linear free-energy relationships*.¹²⁹

Since ΔG and ΔG^\ddagger are combinations of enthalpy and entropy terms, a linear free-energy relationship between two reaction series can result from one of three circumstances: (1) ΔH is constant and the ΔS terms are proportional for the series; (2) ΔS is constant and the ΔH terms are proportional; or (3) ΔH and ΔS are linearly related. Dissection of the free-energy changes into enthalpy and entropy components has often shown the third case to be true.

The Hammett linear free-energy relationship is expressed in the following equations for equilibria and rate data, respectively:

$$\log \frac{K}{K_0} = \sigma\rho \quad (3.44)$$

$$\log \frac{k}{k_0} = \sigma\rho \quad (3.45)$$

The numerical values of the terms σ and ρ are defined by selection of the reference reaction, the ionization of benzoic acids. This reaction is assigned the *reaction constant* $\rho = 1$. The *substituent constant*, σ , can then be determined for a series of substituent groups by measurement of the acid dissociation constant of the substituted benzoic acids. The σ values are then used in the correlation of other reaction series, and the ρ values of the reactions are thereby determined. The relationship between Equations (3.44) and (3.45) is evident when the Hammett equation is expressed in terms of free energy. For the standard reaction $\log[K/K_0] = \sigma\rho$:

$$-\Delta G/2.3RT + \Delta G_0/2.3RT = \sigma\rho = \sigma \quad (3.46)$$

since $\rho = 1$ for the standard reaction. Substituting into Eq. (3.42):

$$\begin{aligned} m\sigma &= -\Delta G^\ddagger/2.3RT + \Delta G^\ddagger/2.3RT \\ m\sigma &= \log k - \log k_0 \\ m\sigma &= \log \frac{k}{k_0} \end{aligned} \quad (3.47)$$

¹²⁹ A. Williams, *Free-Energy Relationships in Organic and Bio-Organic Chemistry*, Royal Society of Chemistry, Cambridge, UK, 2003.

The value of σ reflects the effect the substituent group has on the ΔG of ionization of the substituted benzoic acid, and several factors contribute. A substituent group can affect electron density on the benzene ring by both resonance and polar effects. These changes in charge distribution affect the relative energy of the reactant and product and cause a shift in the equilibrium for the reaction. In the case of a reaction rate, the relative effect on the reactant and the TS determine the change in ΔG^\ddagger .

The effect of substituents is illustrated in Figure 3.26. Because substituent effects are a combination of resonance and polar effects, individual substituents may have both electron-donating and electron-withdrawing components (see Scheme 3.1). For example, the methoxy group is a π donor but a σ acceptor. As resonance effects are generally dominant in aromatic systems, the overall effect of a methoxy group is electron release (in the *ortho* and *para* positions). For other groups, such as NO_2 and CN , the resonance and polar effects are reinforcing. The main polar effect seems to be electrostatic¹³⁰ (through space) and is sometimes referred to as a *field effect*, to distinguish it from an *inductive effect* (through bonds).

The Hammett equation in the form Equation (3.44) or (3.45) is free of complications owing to steric effects because it is applied only to *meta* and *para* substituents. The geometry of the benzene ring ensures that groups in these positions cannot interact sterically with the site of reaction. The σ values for many substituents have been determined, and some are shown in Table 3.26. Substituent constants are available for a much wider range of substituents.¹³¹ The σ value for any substituent reflects the interaction of the substituent with the reacting site by a combination of resonance and polar interactions. Table 3.26 lists some related substituent constants such as σ^+ , σ^- , σ_f , and σ_R . We discuss these shortly. Table 3.27 shows a number of ρ values. The ρ value reflects the sensitivity of the particular reaction to substituent effects. The examples that follow illustrate some of the ways in which the Hammett equation can be used.

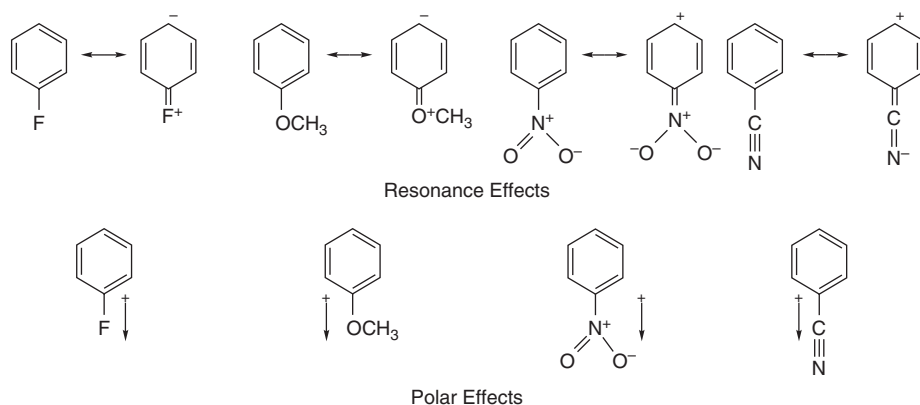


Fig. 3.26. Resonance and polar effects of representative substituents.

¹³⁰ K. Bowden and E. J. Grubbs, *Chem. Soc. Rev.*, **25**, 171 (1996).

¹³¹ C. Hansch, A. Leo, and R. W. Taft, *Chem. Rev.*, **91**, 165 (1991); J. Shorter, *Aust. J. Chem.*, **48**, 1453 (1995); J. Shorter, *Pure Appl. Chem.*, **66**, 2451 (1994); J. Shorter, *Aust. J. Chem.*, **51**, 525 (1988); J. Shorter, *Pure Appl. Chem.*, **69**, 2497 (1997).

Table 3.26. Substituent Constants^a

Substituent	Structure	σ_m	σ_p	σ^+	σ^-	σ_I	σ_R	SECTION 3.6
Acetamido	CH ₃ CONH	0.21	0.00	-0.60	0.46	0.28	-0.35	Linear Free-Energy Relationships for Substituent Effects
Acetoxy	CH ₃ CO ₂	0.37	0.45	0.19		0.38	-0.23	
Acetyl	CH ₃ CO	0.38	0.50		0.84	0.30	0.20	
Amino	NH ₂	-0.16	-0.66	-1.30	-0.15	0.17	-0.80	
Bromo	Br	0.37	0.23	0.15	0.25	0.47	-0.25	
t-Butyl	(CH ₃) ₃ C	-0.10	-0.20	-0.26	-0.13	-0.01	-0.18	
Carboxy	HO ₂ C	0.37	0.45	0.42	0.77	0.30	0.11	
Chloro	Cl	0.37	0.23	0.11	0.19	0.47	-0.25	
Cyano	N≡C	0.56	0.66	0.66	1.00	0.57	0.08	
Diazonium	N ⁺ ≡N	1.76	1.91		3.43			
Dimethylamino	(CH ₃) ₂ N	-0.16	-0.83	-1.70	-0.12	0.13	-0.88	
Ethoxy	C ₂ H ₅ O	0.10	-0.24	-0.81	-0.28	0.28	-0.57	
Ethenyl	CH ₂ =CH	-0.06	0.04	-0.16		0.11	-0.15	
Ethyl	C ₂ H ₅	-0.07	-0.15	-0.30	-0.19	-0.01	-0.14	
Ethynyl	HC≡C	0.21	0.23	0.18	0.53	0.29	-0.04	
Fluoro	F	0.34	0.06	-0.07	-0.03	0.54	-0.48	
Hydrogen	H	0.0	0.0	0.0	0.0	0.0	0.0	
Hydroxy	HO	0.12	-0.37	-0.92	-0.37	0.24	-0.62	
Methanesulfonyl	CH ₃ SO ₂	0.60	0.72		1.13	0.59	0.11	
Methoxy	CH ₃ O	0.12	-0.27	-0.78	-0.26	0.30	-0.58	
Methoxycarbonyl	CH ₃ OCO	0.37	0.45	0.49	0.74	0.32	0.11	
Methyl	CH ₃	-0.07	-0.17	-0.31	-0.17	-0.01	-0.16	
Methylthio	CH ₃ S	0.15	0.00	-0.60	0.06	0.30		
Nitro	NO ₂	0.71	0.78	0.79	1.27	0.67	0.10	
Phenyl	C ₆ H ₅	0.06	0.01	-0.18	0.02	0.12	-0.11	
Trifluoromethyl	CF ₃	0.43	0.54	0.61	0.65	0.40	0.11	
Trimethylammonio	(CH ₃) ₃ N ⁺	0.88	0.82	0.41	0.77	1.07	-0.11	
Trimethylsilyl	(CH ₃) ₃ Si	-0.04	-0.07	0.02		-0.11	0.12	

a. Values of σ_m , σ_p , σ^+ , and σ^- are from C. Hansch, A. Leo, and R. W. Taft, *Chem. Rev.*, **91**, 165 (1991); Values of σ_I and σ_R are from M. Charton, *Prog. Phys. Org. Chem.*, **13**, 119 (1981).

Example 3.2 The pK_a of *p*-chlorobenzoic acid is 3.98; that of benzoic acid is 4.19. Calculate σ for *p*-Cl.

$$\begin{aligned}\sigma &= \log \frac{K_{\text{p-Cl}}}{K_{\text{H}}} = \log K_{\text{p-Cl}} - \log K_{\text{H}} \\ &= -\log K_{\text{H}} - (\log K_{\text{p-Cl}}) \\ &= \text{p}K_{\text{oH}} - \text{p}K \sigma_{\text{p-Cl}} \\ &= 4.19 - 3.98 = 0.21\end{aligned}$$

Example 3.3 The ρ value for alkaline hydrolysis of methyl esters of substituted benzoic acids is 2.38, and the rate constant for hydrolysis of methyl benzoate under the conditions of interest is $2 \times 10^{-4} \text{ M}^{-1} \text{ s}^{-1}$. Calculate the rate constant for the hydrolysis of methyl *m*-nitrobenzoate.

$$\log \frac{k_{\text{m-NO}_2}}{k_{\text{H}}} = \sigma_{\text{m-NO}_2}(\rho) = (0.71)(2.38) = 1.69$$

Table 3.27. Reaction Constants^a

	Reaction	ρ
ArCO ₂ H	\rightleftharpoons	ArCO ₂ ⁻ + H ⁺ , water
ArCO ₂ H	\rightleftharpoons	ArCO ₂ ⁻ + H ⁺ , ethanol
ArCH ₂ CO ₂ H	\rightleftharpoons	ArCH ₂ CO ₂ ⁻ + H ⁺ , water
ArCH ₂ CH ₂ CO ₂ H	\rightleftharpoons	ArCH ₂ CH ₂ CO ₂ ⁻ + H ⁺ , water
ArOH	\rightleftharpoons	ArO ⁻ + H ⁺ , water
ArNH ₃ ⁺	\rightleftharpoons	ArNH ₂ + H ⁺ , water
ArCH ₂ NH ₃ ⁺	\rightleftharpoons	ArCH ₂ NH ₂ + H ⁺ , water
ArCO ₂ C ₂ H ₅ + OH ⁻	\longrightarrow	ArCO ₂ ⁻ + C ₂ H ₅ OH
ArCH ₂ CO ₂ C ₂ H ₅ + OH ⁻	\longrightarrow	ArCH ₂ CO ₂ ⁻ + C ₂ H ₅ OH
ArCH ₂ Cl + H ₂ O	\longrightarrow	ArCH ₂ OH + HCl
ArC(CH ₃) ₂ Cl + H ₂ O	\longrightarrow	ArC(CH ₃) ₂ OH + HCl
ArNH ₂ + PhCOCl	\longrightarrow	ArNHCOPh + HCl

a. From R. P. Wells, *Linear Free Energy Relationships*, Academic Press, New York, 1968, pp. 12–13.

$$\frac{k_{m-\text{NO}_2}}{k_{\text{H}}} = 49$$

$$k_{m-\text{NO}_2} = 98 \times 10^{-4} M^{-1} \text{s}^{-1}$$

Example 3.4 Using data in Tables 3.26 and 3.27, calculate how much faster than *p*-nitrobenzyl chloride *p*-bromobenzyl chloride will hydrolyze in water.

$$\log \frac{k_{\text{p-Br}}}{k_{\text{H}}} = (-1.31)(0.23), \quad \log \frac{k_{\text{p-NO}_2}}{k_{\text{H}}} = (-1.31)(0.78)$$

$$\log k_{\text{Br}} - \log k_{\text{H}} = 0.30, \quad \log k_{\text{NO}_2} - \log k_{\text{H}} = -1.02$$

$$\log k_{\text{Br}} + 0.30 = \log k_{\text{H}}, \quad \log k_{\text{NO}_2} + 1.02 = \log k_{\text{H}}$$

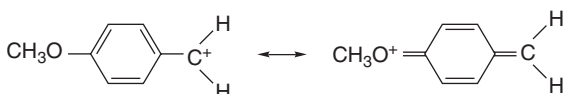
$$\log k_{\text{Br}} + 0.30 = \log k_{\text{NO}_2} + 1.02$$

$$\log k_{\text{Br}} - \log k_{\text{NO}_2} = 0.72$$

$$\log \frac{k_{\text{Br}}}{k_{\text{NO}_2}} = 0.72$$

$$\frac{k_{\text{Br}}}{k_{\text{NO}_2}} = 5.25$$

As we mentioned earlier, not all reaction series can be correlated by a Hammett equation. An underlying reason for the inability of Hammett σ_m and σ_p values to correlate all reaction series is that the substituent effects used to assign σ are a mixture of resonance and polar components. When direct resonance interaction with a reaction site is possible, the extent of the resonance increases and the substituent constants appropriate to the “normal” mix of resonance and polar effects fail. There have been various attempts to develop sets of σ values that take extra resonance interactions into account. In addition to the σ_m and σ_p values used with the classical Hammett equation Table 3.27 lists substituent constants σ^+ and σ^- . These are substituent constant sets that reflect enhanced resonance participation. The σ^+ values are used for reactions in which there is direct resonance interaction between an electron donor substituent and a cationic reaction center, whereas the σ^- set pertains to reactions in which there is a direct resonance interaction between an electron acceptor and an anionic reaction site. In these cases, the resonance component of the substituent effect is particularly important.



Direct resonance interaction with cationic center



Direct resonance interaction with anionic center

One approach to correct for the added resonance interaction is a modification of the Hammett equation known as the Yukawa-Tsuno equation¹³²:

$$\log \frac{k}{k_0} = \rho(\sigma^\circ + r\Delta\bar{\sigma}_{R^+}) \quad (3.48)$$

where $\bar{\sigma}_{R^+} = \sigma^+ - \sigma^\circ$

The additional parameter r is adjusted from reaction to reaction to optimize the correlation. It reflects the extent of the additional resonance contribution. A large r corresponds to a reaction with a large resonance component, whereas when r goes to zero, the equation is identical to the original Hammett equation. When there is direct conjugation with an electron-rich reaction center, an equation analogous to Equation (3.48) can be employed, but σ^- is used instead of σ^+ .

A more ambitious goal is to completely separate resonance and polar effects by using independent substituent constants to account for them. The resulting equation, called a *dual-substituent-parameter equation*, takes the form

$$\log \frac{K}{K_0} \quad \text{or} \quad \log \frac{k}{k_0} = \sigma_I \rho_I + \sigma_R \rho_R \quad (3.49)$$

where ρ_I and ρ_R are the reaction constants that reflect the sensitivity of the system to polar and resonance effects. The σ_I values have been defined from studies in reaction systems where no resonance component should be present.¹³³

¹³² Y. Tsuno and M. Fujio, *Chem. Soc. Rev.*, **25**, 129 (1996).

¹³³ M. Charton, *Prog. Phys. Org. Chem.*, **13**, 119 (1981).

In general, the dissection of substituent effects need not be limited to the resonance and polar components that are of special prominence in reactions of aromatic compounds. Any type of substituent interaction with a reaction center might be indicated by a substituent constant characteristic of the particular type of interaction and a reaction parameter indicating the sensitivity of the reaction series to that particular type of interaction. For example, it has been suggested that electronegativity and polarizability can be treated as substituent effects that are separate from polar and resonance effects.¹³⁴ This gives rise to the equation

$$\log \frac{k}{k_0} = \sigma_F \rho_F + \sigma_R \rho_R + \sigma_\chi \rho_\chi + \sigma_\alpha \rho_\alpha \quad (3.50)$$

where σ_F is the polar, σ_R is the resonance, σ_χ is the electronegativity, and σ_α is the polarizability substituent constant. In general, we emphasize the resonance and polar components in our discussion of substituent effects.

The Hammett substituent constants in Table 3.26 provide a more quantitative interpretation of substituent effects than was given in Scheme 3.1, where substituents were simply listed as EWG or ERG with respect to resonance and polar components. The values of σ_R and σ_I provide comparative evaluations of the separate resonance and polar effects. By comparing σ_R and σ_I , individual substituents can be separated into four quadrants, as in Scheme 3.5. Alkyl groups are electron releasing by both resonance and polar effects. Substituents such as alkoxy, hydroxy, and amino, which can act as resonance donors, have negative σ_p and σ^+ values, but when polar effects are dominant these substituents act as EWGs, as illustrated by the positive σ_m and σ_I values. A third group of substituents act as EWGs by both resonance and polar interactions. This group includes the carbonyl substituents, such as in aldehydes, ketones, esters, and amides, as well as cyano, nitro, and sulfonyl substituents. Of the common groups, only trialkylsilyl substituents are electron withdrawing by resonance and electron donating by polar effects, and both effects are weak.

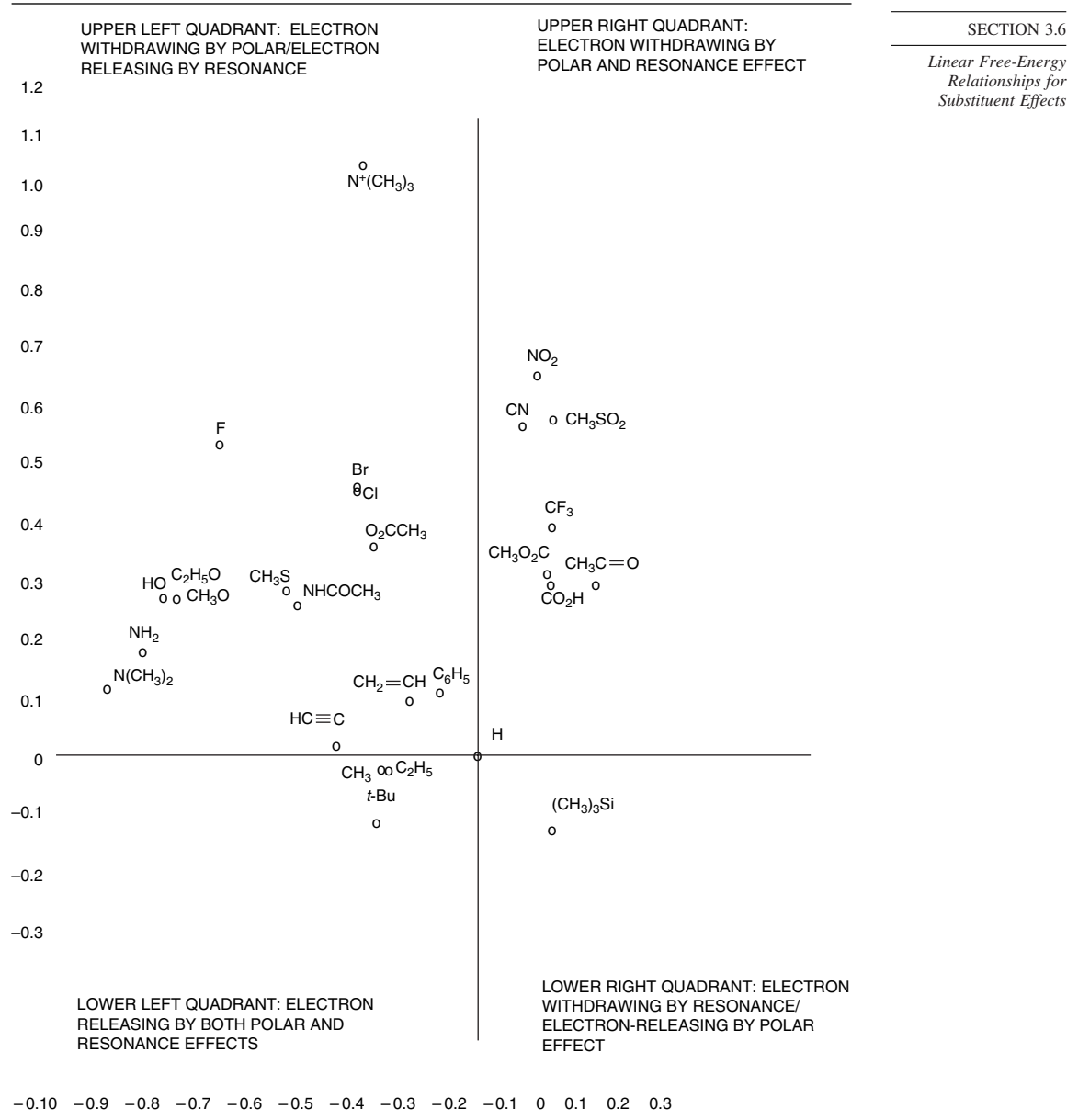
3.6.2. Application of Linear Free-Energy Relationships to Characterization of Reaction Mechanisms

Let us now consider how linear free-energy relationships can provide insight into reaction mechanisms. The choice of benzoic acid ionization as the reference reaction for the Hammett equation leads to $\sigma > 0$ for EWGs and $\sigma < 0$ for ERGs, since EWGs favor the ionization of the acid and ERGs have the opposite effect. Further inspection of the Hammett equation shows that ρ will be positive for all reactions that are favored by ERGs and negative for all reactions that are favored by EWGs. If the rates of a reaction series show a satisfactory correlation, both the sign and magnitude of ρ provide information about the TSs and intermediates for the reaction. In Example 3.3 (p. 340), the ρ value for hydrolysis of substituted methyl benzoates is +2.38. This indicates that EWGs facilitate the reaction and that the reaction is *more sensitive* ($\rho > 1$) to substituent effects than the ionization of benzoic acids. The observation that the reaction is favored by EWGs is in agreement with the mechanism for ester hydrolysis discussed in Section 3.4.4. The tetrahedral intermediate is negatively charged. Its formation should therefore be favored by substituents that stabilize the developing charge. There is also a ground state effect working in the same direction. EWG substituents make

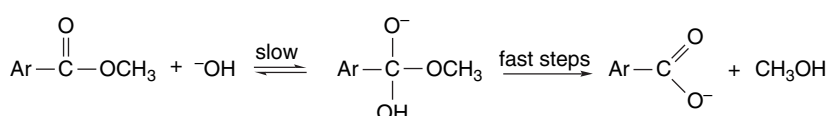
¹³⁴ R. W. Taft and R. D. Topsom, *Prog. Phys. Org. Chem.*, **16**, 1 (1987).

Scheme 3.5. Relationship between σ_I and σ_R Substituent Constants

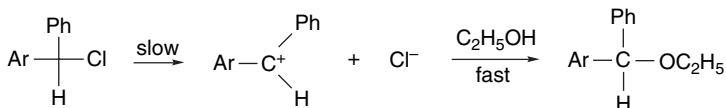
343



the carbonyl group more electrophilic and favor the addition of hydroxide ion in the rate-determining step.



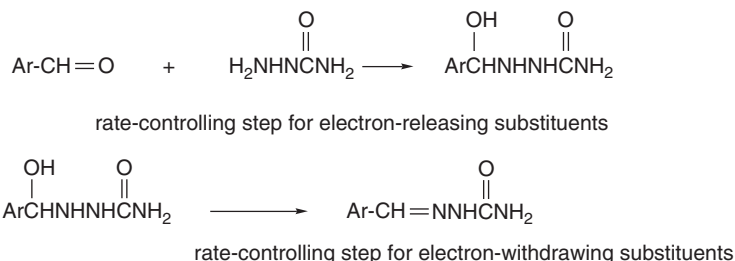
The solvolysis of diarylmethyl chlorides in ethanol correlates with σ^+ and shows a ρ value of -4.2 , indicating that ERGs strongly facilitate the reaction.¹³⁵ This ρ value is consistent with a mechanism involving carbocation formation as the rate-determining step. ERGs facilitate the ionization by a stabilizing interaction with the electron-deficient carbocation that develops as ionization proceeds.



The large ρ shows that the reaction is very sensitive to substituent effects and implies that there is a relatively large redistribution of charge in going to the TS.

The magnitudes of substituent effects differ in solution and the gas phase. In general, substituent effects are much stronger in the latter because there is no “leveling effect” from solvation. For example, in the ionization of benzoic acids, the substituent effects in terms of ΔH are about 11 times larger in the gas phase than in the aqueous phase.¹³⁴ The relative importance of direct resonance interactions seems to be greater in aqueous solution. For example, the ρ_p value of NH_2 increases from -0.17 in the gas phase to -0.39 in benzene and -0.66 in water. This indicates that the charge separation implied by the resonance structures is facilitated by solvation.

Not all reactions can be described by the Hammett equations or the multiparameter variants. There can be several reasons for this. One possibility is a change in mechanism as substituents vary. In a multistep reaction, for example, one step may be rate determining for EWGs, but a different step may become rate limiting for ERG substituents. The rate of semicarbazone formation of benzaldehydes, for example, shows a nonlinear Hammett plot with ρ of about 3.5 for ERGs, but ρ near -0.25 for EWGs.¹³⁶ The change in ρ is believed to be the result of a change in the rate-limiting step.



Any reaction that undergoes a major change in mechanism or TS structure over the substituent series would be expected to give a nonlinear Hammett plot.

The development of linear free-energy relationships in aliphatic molecules is complicated because steric and conformation factors come into play along with electronic effects. A number of successful treatments of aliphatic systems have been developed by separating electronic effects from steric effects. We do not discuss these methods in the present work, but there are reviews available that can be consulted for information about this area.¹³⁷

¹³⁵. S. Nishida, *J. Org. Chem.*, **32**, 2692 (1967).

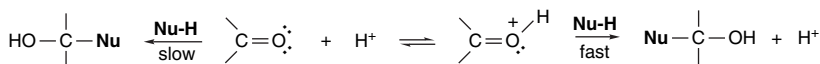
¹³⁶. D. S. Noyce, A. T. Bottini and S. G. Smith, *J. Org. Chem.*, **23**, 752 (1958).

¹³⁷. M. Charton, *Prog. Phys. Org. Chem.*, **10**, 81 (1973); S. Ehrenson, R. T. C. Brownlee, and R. W. Taft, *Prog. Phys. Org. Chem.*, **10**, 1 (1973).

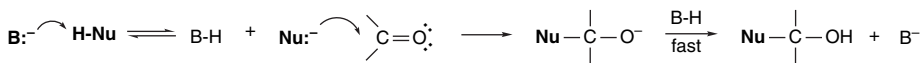
Many chemical reactions involve a *catalyst*. A very general definition of a catalyst is *a substance that makes a reaction path available with a lower energy of activation*. Strictly speaking, a catalyst is not consumed by the reaction, but organic chemists frequently speak of acid-catalyzed or base-catalyzed mechanisms that do lead to overall consumption of the acid or base. Better phrases under these circumstances would be *acid promoted* or *base promoted*. Catalysts can also be described as electrophilic or nucleophilic, depending on the catalyst's electronic nature. Catalysis by Lewis acids and Lewis bases can be classified as electrophilic and nucleophilic, respectively. In free-radical reactions, the *initiator* often plays a key role. An initiator is a substance that can easily generate radical intermediates. Radical reactions often occur by chain mechanisms, and the role of the initiator is to provide the free radicals that start the chain reaction. In this section we discuss some fundamental examples of catalysis with emphasis on proton transfer (Brønsted acid/base) and Lewis acid catalysis.

3.7.1. Catalysis by Acids and Bases

A detailed understanding of reaction mechanisms requires knowledge of the role catalysts play in the reaction. Catalysts do not affect the position of equilibrium of a reaction, which is determined by ΔG° and is independent of the path (mechanism) of the transformation. Catalysts function by increasing the rate of one or more steps in the reaction mechanism by providing a reaction path having a lower E_a . The most general family of catalytic processes are those that involve transfer of a proton. Many reactions are strongly catalyzed by proton donors (Brønsted acids) or proton acceptors (Brønsted bases). Catalysis occurs when the conjugate acid or conjugate base of the reactant is more reactive than the neutral species. As we discussed briefly in Section 3.4.4, reactions involving nucleophilic attack at carbonyl groups are often accelerated by acids or bases. Acid catalysis occurs when the conjugate acid of the carbonyl compound, which is much more electrophilic than the neutral molecule, is the kinetically dominant reactant. Base-catalyzed additions occur as a result of deprotonation of the nucleophile, generating a more reactive anion.



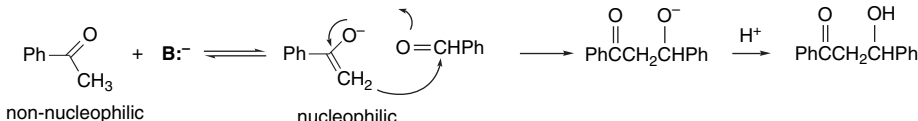
acid catalysis of carbonyl addition by reactant protonation



base catalysis of carbonyl addition by deprotonation of the nucleophile

Many important organic reactions involve carbanions as nucleophiles. The properties of carbanions were introduced in Section 3.4.2, and their reactivity is discussed in more detail in Chapter 6. Most C–H bonds are very weakly acidic and have no tendency to ionize spontaneously to form carbanions. Reactions that involve carbanion intermediates are therefore usually carried out in the presence of a base that can generate the reactive carbanion intermediate. Base-catalyzed addition reactions of carbonyl compounds provide many examples of this type of reaction. The reaction

between acetophenone and benzaldehyde that was considered in Section 3.2.4, for example, requires a basic catalyst and the kinetics of the reaction show that the rate is proportional to the base concentration. The reason for this is that the neutral acetophenone molecule is not nucleophilic and does not react with benzaldehyde. The much more nucleophilic enolate (carbanion) formed by deprotonation is the reactive nucleophile.



3.7.1.1. Specific and General Acid/Base Catalysis. The effect that acid and base catalysts have on reaction rates can be quantitatively studied by kinetic techniques. It is possible to recognize two distinct types of catalysis by acids and bases. The term *specific acid catalysis* is used when the reaction rate is dependent on the *equilibrium protonation* of a reactant. This type of catalysis is independent of the structure of the various proton donors present in solution. Specific acid catalysis is governed by the *hydrogen ion concentration* (pH) of the solution. For example, for a reaction in a series of aqueous buffer systems, the rate of the reaction is a function of the pH, but not of the concentration or identity of the acidic and basic components of the buffers. The kinetic expression for such a reaction includes a term for hydrogen ion concentration, $[H^+]$, but not for any other proton donor. In *general acid catalysis* the nature and concentration of proton donors present in solution affect the reaction rate. The kinetic expression for such reactions include terms for each of the proton donors. The terms *specific base catalysis* and *general base catalysis* apply in the same way to base-catalyzed reactions.

SPECIFIC ACID CATALYSIS:

$$\text{Rate} = k[H^+][X][Y]$$

where $[X][Y]$ are the concentration of the reactants.

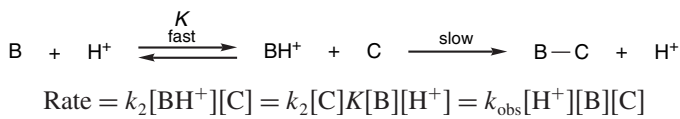
GENERAL ACID CATALYSIS:

$$\text{Rate} = k_1[H^+][X][Y] + k_2[HA^2][X][Y] + k_3[HA^3][X][Y] + \cdots + k_n[HA^n][X][Y]$$

where HA^2, HA^3, \dots, HA^n are all kinetically significant proton donors.

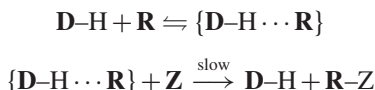
The experimental detection of general acid catalysis is done by rate measurements at constant pH but differing buffer concentration or composition. The observation of a change in rate is evidence of general acid catalysis. If the rate remains constant, the reaction is dependent only on $[H^+]$ and exhibits specific acid catalysis. Similarly, reactions that are general base catalyzed show a dependence of the rate on the concentration and identity of the basic constituents of the buffer system.

Specific acid catalysis is observed when a reaction proceeds through a protonated intermediate that is in equilibrium with its conjugate base. Since the position of this equilibrium is a function of the concentration of solvated protons, only a single acid-dependent term appears in the kinetic expression. For example, in a two-step reaction involving a rate-determining reaction of one reactant with the conjugate acid of a second, the kinetic expression is

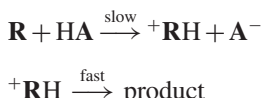


In the actual experiments, since buffers are used to control pH, the points are extrapolated to zero buffer concentration by making measurements at several buffer concentrations (but at the same pH). Such plots are linear if the reaction is subject to specific acid base catalysis.

Several situations can lead to the observation of general acid catalysis. General acid catalysis can occur as a result of hydrogen bonding between the reactant **R** and a proton donor **D**-H to form a reactive complex $\{\text{D}-\text{H} \cdots \text{R}\}$, which then undergoes reaction with a reactant **Z**:

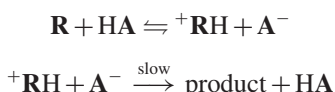


Under these circumstances, a distinct contribution to the overall rate is found for each potential hydrogen bond donor **D**-H. General acid catalysis is also observed when a rate-determining proton transfer occurs from acids other than the solvated proton:



Each acid HA^1 , HA^2 , etc., makes a contribution to the overall rate of the reaction.

General acid catalysis is also observed if a prior equilibrium between the reactant and the acid is followed by rate-controlling proton transfer. Each individual conjugate base A^- appears in the overall rate expression:



Note that specific acid catalysis describes a situation where the reactant is in *equilibrium* with regard to proton transfer and proton transfer is not rate-determining. On the other hand, each case that leads to general acid catalysis *involves proton transfer in the rate-determining step*. Because of these differences, the study of rates as a function of pH and buffer concentrations can permit conclusions about the nature of proton transfer processes and their relationship to the rate-determining step in a reaction.

The details of proton transfer processes can also be probed by examination of *solvent isotope effects* by comparing the rates of a reaction in H_2O versus D_2O . The solvent isotope effect can be either normal or inverse, depending on the nature of the proton transfer process. D_3O^+ is a stronger acid than H_3O^+ . As a result, reactants in D_2O solution are somewhat more extensively protonated than in H_2O at identical acid concentrations. A reaction that involves a rapid equilibrium protonation proceeds *faster* in D_2O than in H_2O because of the higher concentration of the protonated reactant. On the other hand, if proton transfer is part of the rate-determining step, the reaction will be *faster* in H_2O than in D_2O because of the normal primary kinetic isotope effect of the type of reaction.

3.7.1.2. Brønsted Catalysis Law. As might be expected, there is a relationship between the effectiveness of general acid catalysts and the acidic strength of a proton donor, as measured by its acid dissociation constant K_a . The stronger acids are more effective catalysts. This relationship is expressed by the *Brønsted catalysis law*:

$$\log k_{\text{cat}} = \alpha \log K + b \quad (3.51)$$

An analogous equation holds for catalysis by bases. This equation requires that the E_a for the catalytic step for a series of acids be directly proportional to ΔG of dissociation for the same series of acids. The proportionality constant α is an indication of the sensitivity of the catalytic step to structural changes, relative to the effect of the same structural changes on acid dissociation. It is often found that a single proportionality constant α is restricted to only structurally similar acids and that linear relationships having α values of different magnitude apply to each type of acid.

Figure 3.27 is plot of the Brønsted relationship for hydrolysis of a vinyl ether. The plot shows that the effectiveness of the various carboxylic acids as catalysts is related to their dissociation constants. In this particular case, the value of α is 0.79.¹³⁸

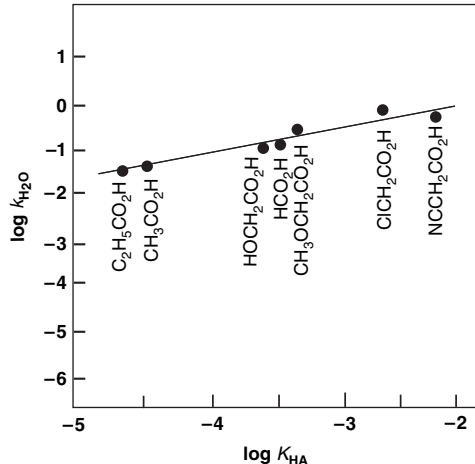
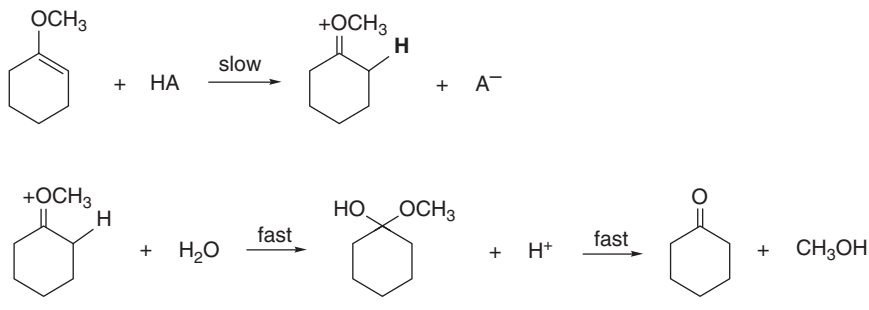
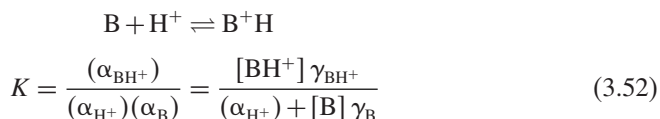


Fig. 3.27. Brønsted relation for the hydrolysis of cyclohexyl methyl ether. Adapted from *J. Am. Chem. Soc.*, **93**, 413 (1971), by permission of the American Chemical Society.

¹³⁸ A. J. Kresge, H. L. Chen, Y. Chiang, E. Murrill, M. A. Payne, and D. S. Sagatys, *J. Am. Chem. Soc.*, **93**, 413 (1971).

Since α relates the sensitivity of the proton transfer process to that of dissociation of the acid, it is sometimes suggested that the value of α can be used as an indicator of TS structure. The closer α approaches unity, the greater the degree of proton transfer in the TS. There are limits to the generality of this interpretation, however.¹³⁹

3.7.1.3. Acidity Functions. Some organic reactions require acid concentrations considerably higher than can be accurately measured on the pH scale, which applies to relatively dilute aqueous solutions. For example, concentrated acidic solutions can have formal proton concentrations of 10M or more, but these formal concentrations are not a suitable measure of the *activity* of protons in such solutions. For this reason, *acidity functions* have been developed to measure the proton-donating strength of concentrated acidic solutions. The activity of the hydrogen ion (solvated proton) can be related to the extent of protonation of a series of bases by the equilibrium expression for the protonation reaction:



where γ is the activity coefficient for the base and its conjugate acid. A common measure of acidity is referred to as h_0 and is defined by measuring the extent of protonation of a series of bases for which K is measured. The relative concentration of the base and its conjugate acid then defines h_0 for any particular acidic solution:

$$h_0 = \frac{[\text{BH}^+] \gamma_{\text{BH}^+}}{K[\text{B}] \gamma_{\text{B}}} \quad (3.53)$$

The quantity H_0 defined as $-\log h_0$ is commonly tabulated and it corresponds to the pH of very concentrated acidic solutions. The H_0 values are established by making measurements in increasingly acidic solutions with a series of successively weaker bases. The series is begun by measuring a reference base in aqueous solution where $H_0 \sim \text{pH}$. This base can then be used to find the H_0 of a somewhat more acidic solution. The K of a somewhat weaker base is then determined in the more acidic solution. This second base can then be used to extend H_0 into a still more acidic solution. The process is continued by using a series of bases to establish H_0 for successively more acidic solutions.¹⁴⁰ The assumption involved in this procedure is that the ratio of the activity coefficients for the series of base cations does not change from solvent to solvent, that is,

$$\frac{\gamma_{\text{B}_1} [\text{H}^+]}{\gamma_{\text{B}_1}} = \frac{\gamma_{\text{B}_2} [\text{H}^+]}{\gamma_{\text{B}_2}} = \frac{\gamma_{\text{B}_3} [\text{H}^+]}{\gamma_{\text{B}_3}} = \dots \quad (3.54)$$

¹³⁹. A. J. Kresge, *J. Am. Chem. Soc.*, **92**, 3210 (1970); R. A. Marcus, *J. Am. Chem. Soc.*, **91**, 7224 (1969); F. G. Bordwell and W. J. Boyle, Jr., *J. Am. Chem. Soc.*, **94**, 3907 (1972); D. A. Jencks and W. P. Jencks, *J. Am. Chem. Soc.*, **99**, 7948 (1977); A. Pross, *J. Org. Chem.*, **49**, 1811 (1984).

¹⁴⁰. For reviews and discussion of acidity functions, see E. M. Arnett, *Prog. Phys. Org. Chem.*, **1**, 223 (1963); C. H. Rochester, *Acidity Functions*, Academic Press, New York, 1970; R. A. Cox and K. Yates, *Can. J. Chem.*, **61**, 225 (1983); C. D. Johnson and B. Stratton, *J. Org. Chem.*, **51**, 4100 (1986).

Table 3.28. H_0 as a Function of Composition of Aqueous Sulfuric Acid^a

% H ₂ SO ₄	H_0	%H ₂ SO ₄	H_0
5	0.24	55	-3.91
10	-0.31	60	-4.46
15	-0.66	65	-5.04
20	-1.01	70	-5.80
25	-1.37	75	-6.56
30	-1.72	80	-7.34
35	-2.06	85	-8.14
40	-2.41	90	-8.92
45	-2.85	95	-9.85
50	-3.38	98	-10.41

a. From J. Jorgenson and D. R. Hartter, *J. Am. Chem. Soc.*, **85**, 878 (1963).

Not surprisingly, the results often reveal a dependence on the particular type of base used, so no universal H_0 scale can be established. Nevertheless, this technique provides a very useful measure of the relative hydrogen ion activity of concentrated acid solutions that can be used in the study of reactions that proceed only at high acid concentrations. Table 3.28 gives H_0 values for some water-sulfuric acid mixtures.

3.7.1.4. pH-Rate Profiles. pH-Rate profiles are a useful tool for analysis of acid and base catalysis.¹⁴¹ The rate of the reaction is measured as a function of the pH. Reactions are typically studied under pseudo-first-order conditions so that the rates are first order in the reactant at each pH:

$$\text{Rate} = k_{\text{obs}}[\text{R}]$$

Observed pH rate profiles typically consist of several regions including segments with linear dependence on [H⁺] or [OH⁻], pH-independent, and curved transitions between linear areas. The occurrence of [H⁺] (or [OH⁻]) in the rate expression indicates either that a protonated (or deprotonated) form of the reactant is involved (preequilibrium) or that H⁺ (or OH⁻) is involved in the rate-determining step. Figure 3.28 shows some pH dependencies that may be components of a specific profile. Curves (a) and (b) show linear dependence on [H⁺] and [OH⁻] that is due to specific acid and base catalysis, respectively. The horizontal portion of the profile corresponds to a reaction that does not involve acid or base catalysis. Usually the slope of the linear part of the curve is -1(H⁺) or +1(OH⁻) because there is only one protonation (or deprotonation) step.

The rate expressions for (a) and (b), respectively, would be:

$$(a) \text{Rate} = k_{\text{H}^+}[\text{R}][\text{H}^+] + k_{\text{H}_2\text{O}}[\text{R}]$$

$$(b) \text{Rate} = k_{-\text{OH}}[\text{R}][-\text{OH}] + k_{\text{H}_2\text{O}}[\text{R}]$$

where k_{H^+} , $k_{-\text{OH}}$, and $k_{\text{H}_2\text{O}}$ are the rate constants for the acid-catalyzed, base-catalyzed, and uncatalyzed reactions, respectively.

For cases (c) and (d), the rates level off at high [H⁺] and [OH⁻], respectively. This circumstance occurs if the reactant is completely protonated (or deprotonated) so

¹⁴¹ J. M. Loudon, *J. Chem. Educ.*, **68**, 973 (1991).

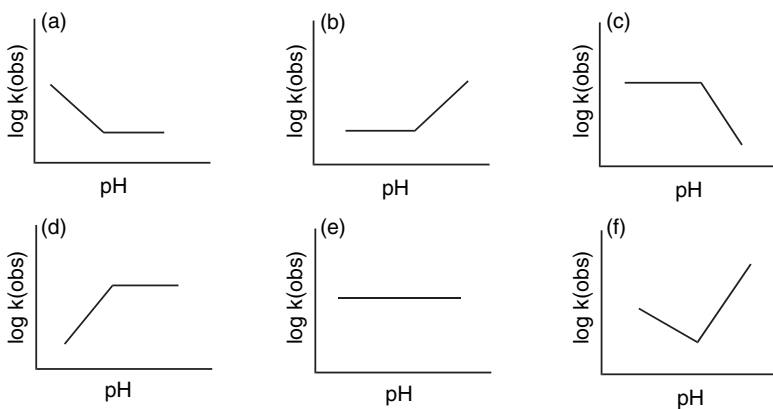


Fig. 3.28. Schematic components of pH rate profiles: (a) acid catalyzed with uncatalyzed component, (b) base catalyzed with uncatalyzed component, (c) acid catalyzed with saturation, (d) base catalyzed with saturation, (e) uncatalyzed reaction, (f) reaction subjected to both acid and base catalysis. Adapted from *J. Chem. Soc., Perkin Trans.*, **2**, 365 (2000).

that further increase in $[H^+]$ or $[^-OH]$ causes no further change in the rate. The form of the corresponding rate equations is

$$k_{obs} = \frac{K_{H^+}[H^+]K_a}{K_a + [H^+]} \quad (3.55)$$

where K_a is the acid dissociation constant of R.

For base catalysis with saturation, the form is

$$k_{obs} = \frac{k_{^-OH} K_w}{K_a + [H^+]} \quad (3.56)$$

The curve in (f) would be observed for a reaction that is catalyzed by both acid and base, for which the rate expression is

$$\text{Rate} = k_{H^+}[H^+][R] + k_{^-OH}[^-OH][R] + k_{H_2O}[R] \quad (3.57)$$

In general, there may be a change in mechanism or a change in the rate-limiting step across the range of pH. This results in a pH-rate profile that combines components from the profiles in (a)–(e) of Figure 3.28. There are useful conclusions that can be drawn by inspection of pH profiles. (1) The number of terms in the overall rate expression is one more than the number of upward bends in the profile. (2) upward bends signal a transition to a different mechanism. Each upward bend represents a new mechanism becoming a significant component of the total reaction. For example, in the case of a reaction catalyzed by both acid and base (and also involving an uncatalyzed component), the upward bend in the acidic region corresponds to the acid-catalyzed component and the upward bend in the basic region is the base-catalyzed component, as illustrated in Figure 3.29.

$$k_{obs} = k_{H^+}[H^+] + k_{^-OH}[^-OH] + k_{H_2O} = k_{H^+}[H^+] + k_{^-OH}\frac{K_w}{[H^+]} + k_{H_2O} \quad (3.58)$$

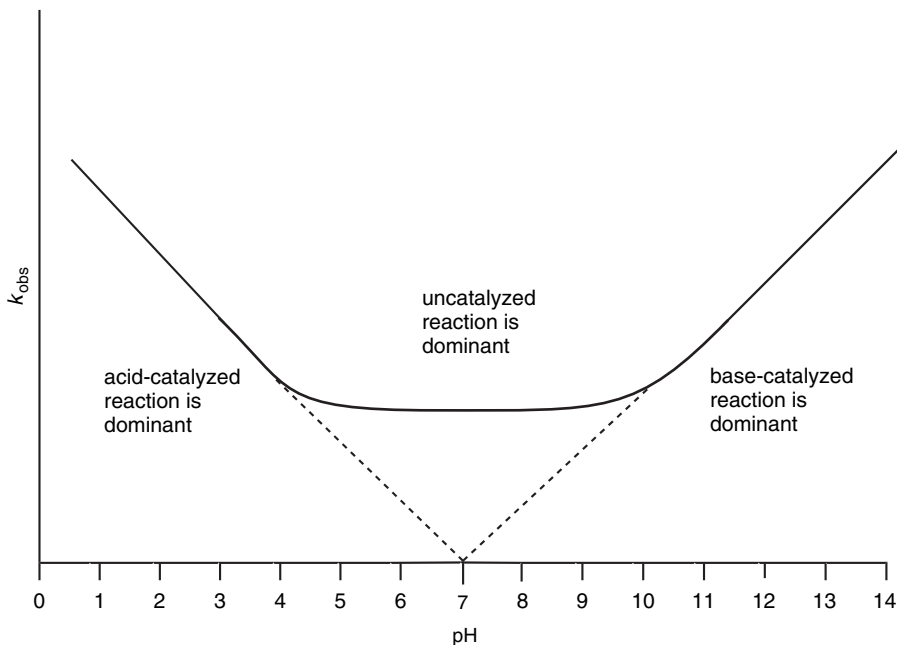
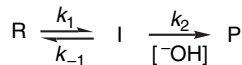
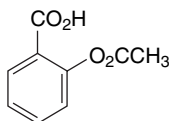


Fig. 3.29. pH-rate profile showing upward bends corresponding to the change from uncatalyzed to acid-catalyzed and base-catalyzed mechanisms.

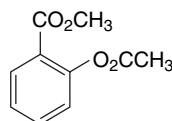
Downward bends in pH profiles occur when there is a change in the rate-limiting step. For example, if there is an unfavorable equilibrium between the reactant and an unstable intermediate, which then undergoes a base-catalyzed reaction, there will be a downward bend. The rate of the equilibrium is pH independent. At low $[\text{OH}^-]$, the rate-limiting step will be governed by k_2 . The rate will increase as $[\text{OH}^-]$ increases until it is no longer rate limiting. At that point k_1 becomes the rate-limiting step, $[\text{OH}^-]$ no longer affects the observed rate, and the curve bends downward:



We can illustrate the interpretation of pH rate profiles by considering the pH rate profile for the hydrolysis of aspirin. The pH rate profile and that of its methyl ester are shown in Figure 3.30. The methyl ester is a classic case in which there are both acid- and base-catalyzed regions and an uncatalyzed region as described by Equation (3.58). These features are characteristic of the normal ester hydrolysis mechanism outlined on pp. 325–326. Under the reaction conditions, only the more reactive *O*-aryl ester group is hydrolyzed. Aspirin, however, shows a region between pH 2 and pH 9 that reveals one downward and two upward bends. Thus there must be a fourth variant of the mechanism (since there are a total of three upward bends).



aspirin



aspirin methyl ester

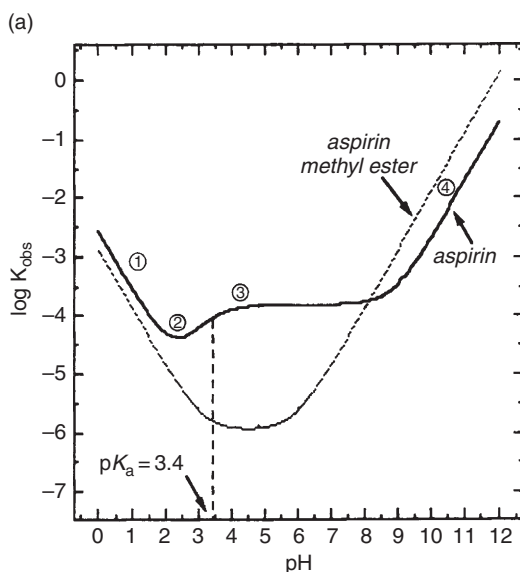
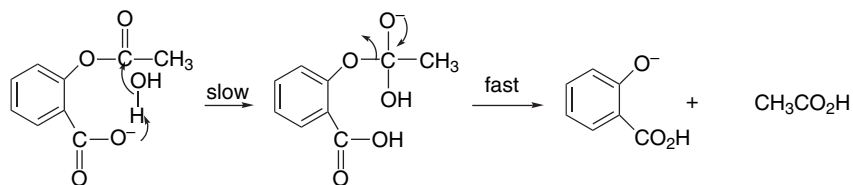


Fig. 3.30. pH rate profile of aspirin and its methyl ester.
Reproduced from *J. Chem. Educ.*, **68**, 973 (1991).

The fact that there is a downward bend in the curve at about pH 5 suggests that the CO_2^- group in aspirin, which is absent from the methyl ester, might be involved in the reaction. The CO_2^- group becomes protonated in this region, which might account for the decreased rate below pH 5. This would require the addition of a fourth term to the rate curve where $[\text{As}^-]$ is the carboxylate anion of aspirin. The concentration of $[\text{As}^-]$ is governed by the acid dissociation constant K_{as} . This leads to the expression

$$k_{\text{obs}} = k_{\text{H}^+} [\text{H}^+] + \frac{k_{\text{H}_2\text{O}} [\text{H}^+]}{K_{\text{as}} + [\text{H}^+]} + \frac{k_i K_{\text{as}}}{K_{\text{as}} + [\text{H}^+]} + \frac{k_{-\text{OH}} K_{\text{w}}}{[\text{H}^+]}$$

In the region pH 5 to pH 8 $[\text{As}^-]$ is constant, since it is completely deprotonated above pH 5, and the rate is pH independent in this region. Thus the pH-rate profile for aspirin identifies four distinct regions as the pH increases. Regions 1 and 4 correspond to reactions involving a H^+ and $-\text{OH}$ in the rate-determining transition state and are the normal acid- and base-catalyzed mechanisms for ester hydrolysis. Region 2 corresponds to the uncatalyzed reaction and Region 3 is the fourth mechanism, which involves the anion of aspirin or a kinetically equivalent species. Based on other studies, this mechanism has been interpreted as a carboxylate-assisted deprotonation of water leading to rate-determining formation of the tetrahedral intermediate.¹⁴² (See Section 7.5 for discussion of the evidence for this mechanism.)

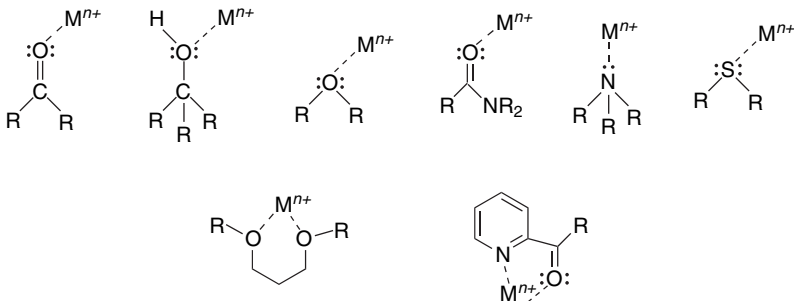


¹⁴² A. P. Fresht and A. J. Kirby, *J. Am. Chem. Soc.*, **89**, 4857 (1967).

3.7.2. Lewis Acid Catalysis

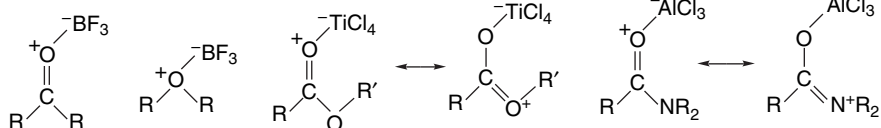
Lewis acids act as electron pair acceptors. The proton is an important special case, but many other compounds catalyze organic reactions by acting as electron pair acceptors. The most important Lewis acids in organic reactions are metal cations and covalent compounds of metals. Metal cations that function as Lewis acids include the alkali metal monocations Li^+ , Na^+ , K^+ , di- and trivalent ions such as Mg^{2+} , Ca^{2+} , Zn^{2+} , Sc^{3+} , and Bi^{3+} ; transition metal cations and complexes; and lanthanide cations, such as Ce^{3+} and Yb^{3+} . Neutral electrophilic covalent molecules can also act as Lewis acids. The most commonly employed of the covalent compounds include boron trifluoride, aluminum trichloride, titanium tetrachloride, and tin(IV)tetrachloride. Various other derivatives of boron, aluminum, titanium, and tin also are Lewis acid catalysts.

The catalytic activity of metal cations originates in the formation of a donor-acceptor complex between the cation and the reactant, which acts as a Lewis base. As a result of the complexation, the donor atom becomes effectively more electronegative. All functional groups that have unshared electron pairs are potential electron donors, but especially prominent in reaction chemistry are carbonyl oxygens (sp^2), hydroxy or ether (sp^3) oxygen, as well as similar nitrogen- and sulfur-containing functional groups. For oxygen and nitrogen functional groups, the catalysis generally correlates with hardness, so the smaller and more positively charged ions have the strongest effects. Halogen substituents can act as electron donors to strong Lewis acids. The presence of two potential donor atoms in a favorable geometric relationship permits formation of “bidentate” chelate structures and may lead to particularly strong complexes.



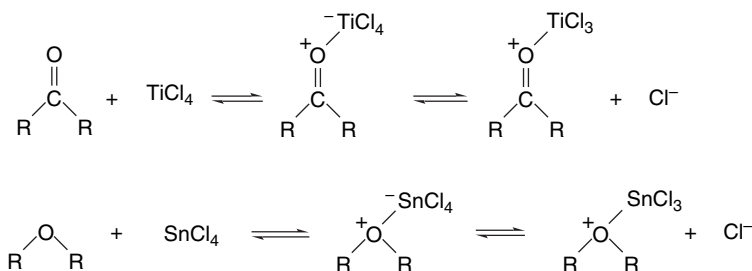
There is a partial transfer of charge to the metal ion from the donor atom, which increases the effective electronegativity of the donor atom. The Lewis acid complexes of carbonyl groups, for example, are more reactive to nucleophilic attack. Hydroxy groups complexed to metal cations are stronger acids and better leaving groups than an uncomplexed hydroxy. Ether or sulfide groups complexed with metal ions are better leaving groups.

Neutral compounds such as boron trifluoride and aluminum trichloride form Lewis acid-base complexes by accepting an electron pair from the donor molecule. The same functional groups that act as electron pair donors to metal cations can form complexes with boron trifluoride, aluminum trichloride, titanium tetrachloride, and related compounds. In this case the complex is formed between two neutral species, it too is neutral, but there is a formal positive charge on the donor atom and a formal negative charge on the acceptor atom.



Complexes of carbonyl oxygen with trivalent boron and aluminum compounds tend to adopt a geometry consistent with directional interaction with one of the oxygen lone pairs. Thus the C–O–M bonds tend to be in the trigonal (120° – 140°) range and the boron or aluminum is usually close to the carbonyl plane.¹⁴³ The structural specificity that is built into Lewis acid complexes can be used to advantage to achieve stereoselectivity in catalysis. For example, use of chiral ligands in conjunction with Lewis acids is frequently the basis for enantioselective catalysts.

Titanium(IV) tetrachloride and tin(IV) tetrachloride can form complexes that are similar to those formed by metal ions and those formed by neutral Lewis acids. Complexation can occur with displacement of a chloride from the metal coordination sphere or by an increase in the coordination number at the Lewis acid.



For example, the crystal structure of the adduct of titanium tetrachloride and the ester formed from ethyl 2-hydroxypropanoate (ethyl lactate) and acrylic acid has been determined.¹⁴⁴ It is a chelate with the oxygen donor atoms incorporated into the titanium coordination sphere along with the four chloride anions, as shown in Figure 3.31.

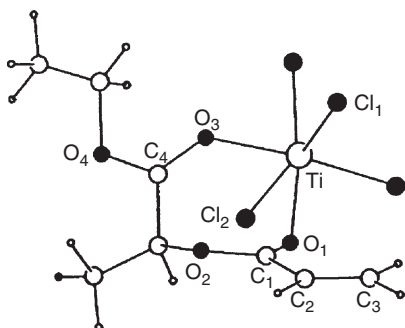
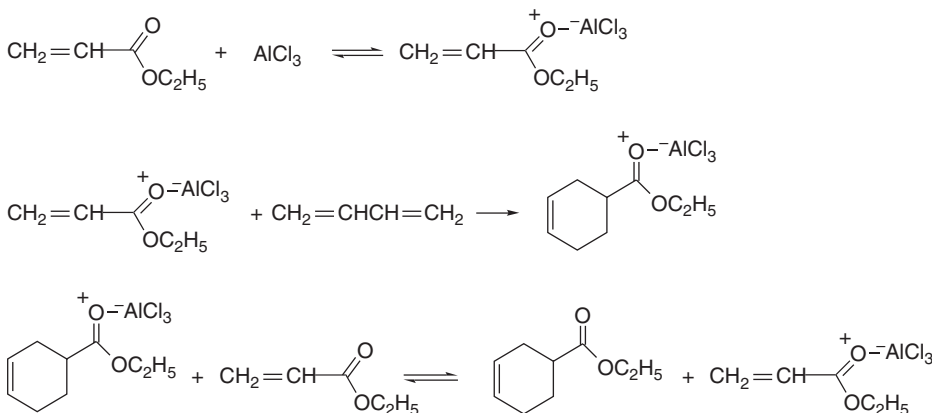


Fig. 3.31. TiCl_4 complex of ethyl lactate.
Reproduced from *Angew. Chem. Int. Ed. Engl.*, **29**, 112, by permission of Wiley-VCH.

¹⁴³ S. Shambayati, W. E. Crowe, and S. L. Schreiber, *Angew. Chem. Int. Ed. Engl.*, **29**, 256 (1990).

¹⁴⁴ T. Poll, J. O. Melter, and G. Helmchen, *Angew. Chem. Int. Ed. Engl.*, **24**, 112 (1985).

Diels-Alder addition reactions are accelerated by catalytic amounts of a Lewis acid. The complexed ester (ethyl acrylate in the example given) is substantially more reactive than the uncomplexed molecule, and the reaction proceeds through the complex. The reactive complex is regenerated by exchange of the Lewis acid from the adduct. The reaction is accelerated because the dienophile becomes more electrophilic. In MO terminology, the LUMO energy is lowered, resulting in stronger interaction with the diene HOMO.



The strength of the complexation depends on both of the donor atom and the metal ion. The solvent is also an important factor because solvent molecules that are electron donors can compete for the Lewis acid. Qualitative predictions about the strength of donor-acceptor complexation can be made on the basis of the hard-soft-acid-base (HSAB) concept (see Section 1.1.6). The better matched the donor and acceptor, the stronger the complexation. Scheme 3.6 gives an approximate ordering of hardness and softness for some neutral and ionic Lewis acids and bases.

There are more structural variables to consider in catalysis by Lewis acids than in the case of catalysis by protons. In addition to the hard-soft relationship, steric, geometric, and stereoelectronic factors can come into play. This makes the development of an absolute scale of “Lewis acid strength” difficult, since the complexation strength depends on the specific characteristics of the base. There are also variations in the strength of the donor-acceptor bonds. Bond strengths calculated for complexes such as H₃N⁺-BF₃⁻ (22.0 kcal/mol) and (CH₃)₃N⁺-BH₃⁻ (41.1 kcal/mol) are substantially

Scheme 3.6. Relative Hardness and Softness

	Lewis acids		Lewis bases	
	Cationic	Neutral	Neutral	Anionic
Hard	H ⁺	BF ₃ , AlCl ₃	H ₂ O	F ⁻ , SO ₄ ²⁻
	Li ⁺ , Mg ²⁺ , Ca ²⁺	R ₃ B	Alcohols	Cl ⁻
	Na ⁺		Ketones, ethers	Br ⁻
	Zn ²⁺ , Cu ²⁺		Amines	N ₃ ⁻
	Pd ²⁺ , Hg ²⁺ , Ag ⁺		Sulfides	CN ⁻
	RS ⁺ , RSe ⁺			I ⁻
Soft	I ⁺			S ²⁻

Table 3.29. Relative Lewis Acidity^a

Acid	ΔH (kcal/mol) ^b	π^* (eV) ^c	NMR $\Delta\delta$ ^d	Relative acidity
BCl_3	-6.6	-2.52	1.35	1.00
AlCl_3	-25.6	-2.31	1.23	0.91
$\text{C}_2\text{H}_5\text{AlCl}_2$	-20.0	-2.03	1.15	0.80
BF_3	+4.1	-1.93	1.17	0.76
$(\text{C}_2\text{H}_5)_2\text{AlCl}$	-5.6	-1.82	0.91	0.71
$(\text{C}_2\text{H}_5)_3\text{Al}$	-10.1	-1.68	0.63	0.63
SnCl_4	+10.0	-1.58	0.87	0.61

SECTION 3.7
Catalysis

a. P. Laszlo and M. Teston, *J. Am. Chem. Soc.*, **112**, 8750 (1990).

b. As found by MNDO calculation

c. LUMO π energy in eV.

d. Change of chemical shift of H(3) in butenal.

less than for covalent bonds between similar elements (see also Section 3.4.4). Some Lewis acid-base complexes have weak bonds that are primarily electrostatic in nature (e.g., $\text{CH}_3\text{CN}^+ - \text{BF}_3^-$, 9.1 kcal/mol).¹⁴⁵

There have been several efforts to develop measures of Lewis acid strength. One indication of Lewis acid strength of a number of compounds commonly used in synthesis is shown in Table 3.29. The relative acidity values given are derived from the LUMO level of the π^* orbital of the compound, with the BCl_3 complex defined as 1.00 and the uncomplexed but-2-enal LUMO energy taken as 0.¹⁴⁶ These values correlate with ${}^1\text{H-NMR}$ chemical shift of the H(3) proton of butenal.¹⁴⁷ In contrast, the calculated (MNDO) bond strengths (ΔH) do not correlate with the acid strength.

In another study, the ${}^{13}\text{C}$ chemical shift for acetone in complexes with various Lewis acids was determined (Table 3.30).¹⁴⁸ One general trend that can be noted is the increasing shift with the formal oxidation state of the metal.

A quite broad range of Lewis acid strengths was evaluated by comparing their effect on the shift of the fluorescence of complexes with *N*-methylacridone.¹⁴⁹ The shifts also correlated with the capacity of the Lewis acid to facilitate the reduction of

Table 3.30. ${}^{13}\text{C}$ Chemical Shifts in Lewis Acid Complexes of Acetone

Lewis Acid	${}^{13}\text{C}$ Chemical Shift
-	210
MgCl_2	221
ZnCl_2	227
$\text{Sc}(\text{O}_3\text{SCF}_3)_3$	239
AlCl_3	245
SbF_5	250

¹⁴⁵ V. Jonas, G. Frenking, and M. T. Reetz, *J. Am. Chem. Soc.*, **116**, 8741 (1994).

¹⁴⁶ P. Laszlo and M. Teston, *J. Am. Chem. Soc.*, **112**, 8750 (1990).

¹⁴⁷ R. F. Childs, D. L. Mulholland, and A. Nixon, *Can. J. Chem.*, **60**, 801 (1982).

¹⁴⁸ D. H. Barich, J. B. Nicholas, T. Xu, and J. F. Haw, *J. Am. Chem. Soc.*, **120**, 12342 (1998).

¹⁴⁹ S. Fukuzumi and K. Ohkubo, *J. Am. Chem. Soc.*, **124**, 10270 (2002).

Table 3.31. Wavelength and Energy Shift in N-Methylacridone-Lewis Acid Complexes

Lewis acid	λ_{max} (nm)	$h\nu_{\text{fl}}$ (eV)
$\text{Fe}(\text{ClO}_4)_3$	478	2.59
$\text{Sc}(\text{O}_3\text{SCF}_3)_3$	474	2.62
$\text{Fe}(\text{ClO}_4)_2$	471	2.63
$\text{Cu}(\text{ClO}_4)_2$	471	2.63
$\text{Yb}(\text{O}_3\text{SCF}_3)_3$	460	2.70
$\text{La}(\text{O}_3\text{SCF}_3)_3$	458	2.71
$\text{Zn}(\text{O}_3\text{SCF}_3)_3$	456	2.72
Ph_3SnCl	455	2.72
Bu_2SnCl_2	453	2.72
$\text{Mg}(\text{ClO}_4)_2$	451	2.75
LiClO_4	442	2.81
NaClO_4	437	2.84
Uncomplexed	432	2.87

O_2 to O_2^- , which is again a measure of the ability to stabilize anionic charge. The fluorescence shifts are given in Table 3.31 and the correlation is shown in Figure 3.32. The orders $\text{Li}^+ > \text{Na}^+$ and $\text{Mg}^{2+} > \text{Ca}^{2+} > \text{Sr}^{2+} > \text{Ba}^{2+}$ show that Lewis acidity decreases with the size of the cation. According to this scale, the tin halides are comparable in acidity to Mg^{2+} . The strong Lewis acidity of Sc^{3+} , Y^{3+} , and the lanthanides, such as La^{3+} and Yb^{3+} , has been exploited in various synthetic applications.

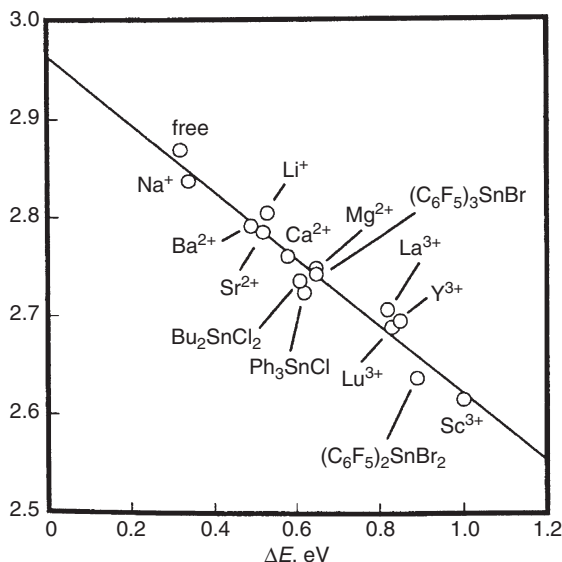


Fig. 3.32. Correlation between fluorescence shift and shift in oxidation energy for several Lewis acids. Reproduced from *J. Am. Chem. Soc.*, **124**, 10270 (2002), by permission of the American Chemical Society.

3.8.1. Bulk Solvent Effects

SECTION 3.8

Solvent Effects

Since most organic reactions are done in solution, it is important to recognize some of the ways that solvents affect the course and rates of reactions. Some of the more common solvents can be roughly classified as in Table 3.32 on the basis of their structure and dielectric constants. There are important differences between *protic solvents*, those which contain hydrogens that form hydrogen bonds and can exchange rapidly (such as those bonded to oxygen, nitrogen, or sulfur), and *aprotic solvents*, in which all hydrogen is bound to carbon. Similarly, *polar solvents*, those that have high dielectric constants, have effects on reaction rates that are different from nonpolar solvent media.

When discussing solvent effects, it is important to distinguish between the macroscopic effects and those that depend upon details of structure. Macroscopic properties refer to properties of the bulk solvent. One example is the dielectric constant, which is a measure of the ability of the solvent to increase the capacitance of a condenser. Dielectric constants increase with molecular dipole moment and polarizability because of the ability of both the permanent and induced molecular dipole to align with the external electric field. An important property of solvent molecules is the response to changes in charge distribution as reaction occurs. The dielectric constant of a solvent is a good indicator of its ability to accommodate separation of charge. It is not the only factor, however, since, being a macroscopic property, it conveys little information about the ability of the solvent molecules to interact with the solute molecules and ions at close range. These direct solute-solvent interactions depend on the specific structures of the molecules.

Solvents that fall into the nonpolar aprotic class are not very effective at stabilizing the development of charge separation. These molecules have small dipole moments and do not have hydrogens capable of forming hydrogen bonds. Reactions that involve charge separation in the TS therefore proceed more slowly in this class of solvents than in protic or polar aprotic solvents. The reverse is true for reactions in which species having opposite charges come together in the TS. In this case the TS is less highly charged than the individual reactants and reaction is favored by weaker solvation that

Table 3.32. Dielectric Constants (ϵ) and Molecular Dipole Moment (μ) of Some Common Solvents

Nonpolar	Aprotic solvents				Protic solvents			
	ϵ	μ	Polar	ϵ	μ		ϵ	μ
Hexane	1.9	0	Pyridine	12	2.21	Acetic acid	6.1	1.7
CCl ₄	2.2	0	Acetone	21	2.88	CF ₃ CO ₂ H	8.6	
Dioxane	2.2	0	HMPA	30		<i>t</i> -Butanol	12.5	1.7
Benzene	2.3	0	Nitromethane	36	3.46	Ammonia	(22)	1.47
Diethyl ether	4.3	1.15	DMF	37	3.82	Ethanol	24.5	1.69
Chloroform	4.8	1.04	Acetonitrile	38	3.92	Methanol	32.7	1.7
THF	7.6	1.75	DMSO	47	3.96	Water	78	1.85

a. Dielectric constants (ϵ) and dipole moments (μ) in debye units from the compilation of solvent properties in J. A. Riddick and W. B. Bunger, eds., *Organic Solvents*, Vol. II of *Techniques of Organic Chemistry*, 3rd Edition, Wiley-Interscience, New York, 1970.

Scheme 3.7. Effect of Solvent Polarity on Reactions of Various Charge Types

1.	Neutralization of charge. $\delta^- \quad \delta^+$ $A^- + B^- \rightarrow A\cdots B \rightarrow A - B$	Favored by nonpolar solvent
2.	Separation of charge. $\delta^- \quad \delta^+$ $A - B \rightarrow A\cdots B \rightarrow A^- + B^-$	Favored by polar solvent
3.	Neutral reactants and products. $A + B \rightarrow A\cdots B \rightarrow A - B$	Relatively insensitive to solvent polarity
4.	Relative concentration of charge. $\delta^+ \quad \delta^+$ $[A - B]^+ \rightarrow A\cdots B \rightarrow A + B^+$	Slightly favored by polar solvent
5.	Relative dispersal of charge. $\delta^+ \quad \delta^+$ $A^+ + B \rightarrow A\cdots B \rightarrow [A - B]^+$	Slightly favored by nonpolar solvent

leaves the oppositely charged reactants in a more reactive state. Arguing along these lines, the broad relationships between reactivity and solvent type shown in Scheme 3.7 can be deduced.

Many empirical measures of solvent polarity have been developed.¹⁵⁰ One of the most useful is based on shifts in the absorption spectrum of a reference dye. The position of absorption bands is sensitive to solvent polarity because the electronic distribution, and therefore the polarity, of the excited state is different from that of the ground state. The shift in the absorption maxima reflects the effect of solvent on the energy gap between the ground state and excited state molecules. An empirical solvent polarity measure called $E_T(30)$ is based on this concept.¹⁵¹ Some values for common solvents are given in Table 3.33 along with the dielectric constants for the solvents. It can be seen that a quite different order of polarity is given by these two quantities.

Table 3.33. $E_T(30)$, an Empirical Measure of Solvent Polarity, Compared with Dielectric Constant^a

	$E_T(30)$	ϵ		$E_T(30)$	ϵ
Water	63.1	78	DMF	43.8	37
Trifluoroethanol	59.5		Acetone	42.2	21
Methanol	55.5	32.7	Dichloromethane	41.1	8.9
80:20 Ethanol-water	53.7		Chloroform	39.1	4.8
Ethanol	51.9	24.5	Ethyl acetate	38.1	6.0
Acetic acid	51.2	6.1	THF	37.4	7.6
2-Propanol	48.6	19.9	Diethyl ether	34.6	4.3
Acetonitrile	46.7	38	Benzene	34.5	2.3
DMSO	45.0	47			

From C. Reichardt, *Angew. Chem. Int. Ed. Engl.*, **18**, 98 (1979)

¹⁵⁰. C. Reichardt, *Angew. Chem. Int. Ed. Engl.*, **18**, 98 (1979); C. Reichardt, *Solvent Effects in Organic Chemistry*, Verlag Chemie, Weinheim, 1990; J. Catalan, V. Lopez, P. Perez, R. Martin-Villamil, and J. G. Rodriguez, *Liebigs Ann.*, 241 (1995); C. Laurance, P. Nicolet, M. T. Dalati, J. L. M. Abboud, and R. Notario, *J. Phys. Chem.*, **98**, 5807 (1994).

¹⁵¹. C. Reichardt and K. Dimroth, *Fortschr. Chem. Forsch.*, **11**, 1 (1968); C. Reichardt, *Justus Liebigs Ann. Chem.*, **752**, 64 (1971).

As a specific example of a solvent effect, let us consider how the solvent affects the solvolysis of *t*-butyl chloride. Much evidence, which is discussed in detail in Chapter 4, indicates that the rate-determining step of the reaction is ionization of the carbon-chlorine bond to give a carbocation and the chloride ion. The TS reflects some of the charge separation that occurs in the ionization:



Figure 3.33 is a schematic interpretation of the solvation changes that take place during the ionization of *t*-butyl chloride, with S representing surrounding solvent molecules. With the neutral slightly polar reactant, there is only weak solvation. As charge separation develops in the TS, solvent molecules align with the most favorable orientation of the dipoles. The charged ions are strongly solvated.

The bulk dielectric constant may be a poor indicator of the ability of solvent molecules to facilitate the charge separation in the TS. The fact that the carbon and chlorine remain partially bonded at the TS prevents the solvent molecules from actually intervening between the developing centers of charge. Instead, the solvent molecules must stabilize the charge development by acting around the periphery of the activated complex. The nature of this interaction depends upon the detailed structure of the activated complex and solvent. The ability of solvents to stabilize the TS of *t*-butyl chloride ionization has been measured by comparing the rate of the reaction in the different solvent mixtures. The solvents were then assigned Y values, with the reference solvent taken as 80:20 ethanol-water. The Y value of other solvents is defined by the equation

$$\log \frac{k_{\text{solvent}}}{k_{\text{80\% ethanol}}} = Y \quad (3.59)$$

Table 3.34 lists the Y values for some alcohol-water mixtures and for some other solvents. The Y value reflects primarily the ionization power of the solvent. It is largest for polar solvents such as water and formic acid and becomes progressively smaller and eventually negative as the solvent becomes less polar and contains more (or larger) nonpolar alkyl groups. Note that among the solvents listed there is a spread of more than 10^6 in the measured rate of reaction between *t*-butyl alcohol ($Y = -3.2$) and water ($Y = +3.49$). This large range of reaction rates demonstrates how important solvent effects can be.

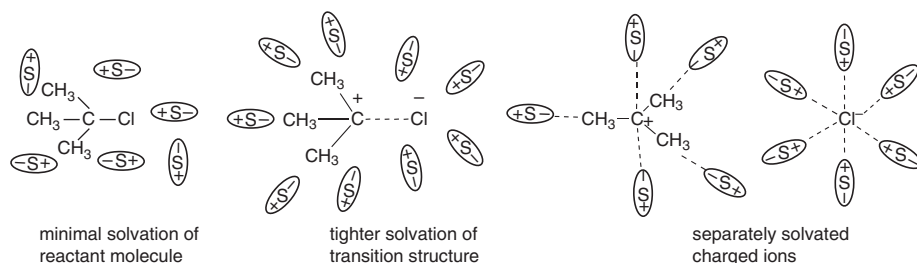


Fig. 3.33. Schematic representation of solvation changes during ionization of *t*-butyl chloride.

Table 3.34. *Y* Values for Some Solvent Systems.^a

CHAPTER 3
*Structural Effects on
 Stability and Reactivity*

Ethanol-water	<i>Y</i>	Methanol-water	<i>Y</i>	Other solvents	<i>Y</i>
100:0	-2.03	100:0	-1.09	Acetic acid	-1.64
80:20	0.00	80:20	0.38	Formic acid	2.05
50:50	1.65	50:50	1.97	<i>t</i> -Butyl alcohol	-3.2
20:80	3.05	10:90	3.28	90:10 acetone:water	-1.85
0:100	3.49			90:10 dioxane:water	-2.03

a. From A. H. Fainberg and S. Winstein, *J. Am. Chem. Soc.*, **78**, 2770 (1956).

Several other treatments of solvent effects on solvolysis rates have been developed.¹⁵² The equations typically include several terms related to: (a) macroscopic nonspecific solvent properties, such as the dipole moment and dielectric constant; (b) empirical polarity criteria, such as $E_T(30)$; (c) solvent electrophilicity and nucleophilicity parameters; and (d) terms related to solvent *cohesivity*. The last term accounts for the difference in work required to disrupt structure within the solvent, when, for example, there is expansion in volume between reactants and the TS.

3.8.2. Examples of Specific Solvent Effects

The electrostatic solvent effects discussed in the preceding paragraphs are not the only possible modes of interaction of solvent with reactants and TS. Specific structural effects may cause either the reactants or the TS to be particularly strongly solvated. Figure 3.34 shows how such solvation can affect the relative energies of the ground state and the TS and cause rate variations from solvent to solvent. Unfortunately, no

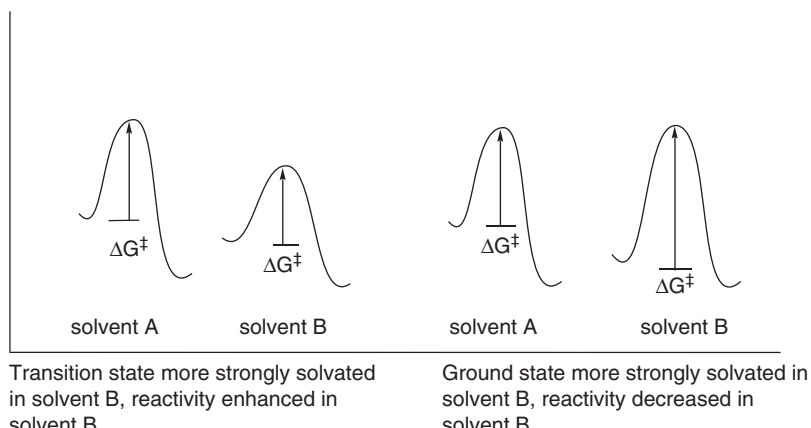


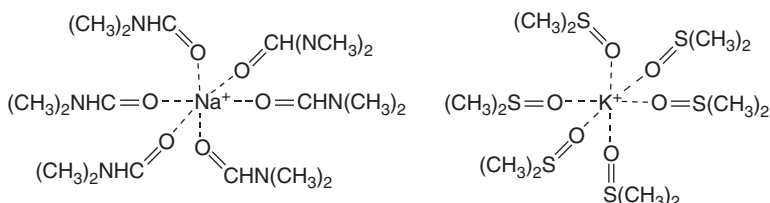
Fig. 3.34. Reaction energy profiles showing effect on E_a of (a) preferred solvation of the transition state and (b) preferred solvation of reactants.

¹⁵² G. F. Dvorko, A. J. Vasil'kevich, E. A. Ponomareva, and J. V. Koschii, *Russ. J. Gen. Chem.*, **70**, 724 (2000); I. A. Koppel and V. Palm, *Advances in Linear Free Energy Relationships*, N. B. Chapman and J. Shorter, eds., Plenum Press, New York, 1972, Chap. 5.; M. H. Abraham, R. W. Taft, and M. J. Kamlet, *J. Org. Chem.*, **46**, 3053 (1981); M. H. Abraham, R. M. Doherty, M. J. Kamlet, J. M. Harris, and R. W. Taft, *J. Chem. Soc., Perkin Trans.*, **2**, 913 (1987); M. R. C. Goncalves, A. M. N. Simoes, and L. M. P. C. Albuquerque, *J. Chem. Soc., Perkin Trans.*, **2**, 1379 (1990).

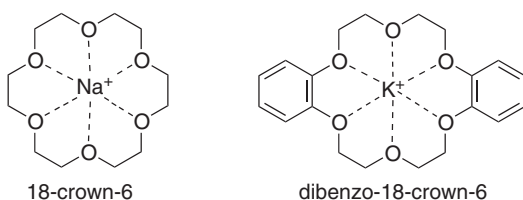
general theory for quantitatively predicting such specific effects has been developed to date. Nevertheless, there are many cases where specific interactions with solvent molecules strongly influence the outcome and/or the rate of reactions.

3.8.2.1. Enhanced Nucleophilicity in Polar Aprotic Solvents. An important example of solvent effects is the enhanced nucleophilicity of many anions in polar aprotic solvents as compared with protic solvents.¹⁵³ In protic solvents, anions are strongly solvated by hydrogen bonding. This is particularly true for hard anions that have a high concentration of charge on oxygen such as alkoxide ions. Hydrogen-bonding decreases the ability of the nucleophile to act as an electron donor. Stated another way, the energy required to disrupt hydrogen bonding adds to the activation energy of the reaction.

In polar aprotic solvents, no hydrogens suitable for hydrogen bonding are present. As a result, the electrons of the anion are more available for reaction. The anion is at a higher energy level because of the small stabilization by the solvent. The polarity of the aprotic solvents is also important for the solubility of ionic compounds. Dissolved ionic compounds are likely to be present as ion pairs or larger aggregates in which the reactivity of the anion is diminished by the electrostatic interaction with the cation. Energy must be expended against this electrostatic attraction to permit the anion to react as a nucleophile. Metal cations such as K^+ and Na^+ are strongly solvated by polar aprotic solvents such as DMSO and DMF. The oxygen atoms in these molecules act as electron donors toward the cations. The dissolved salts are dissociated, and as a result the anions are more reactive because they are poorly solvated and not associated with cations.

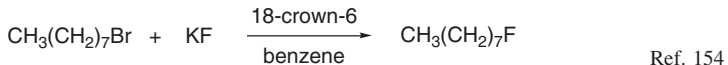


3.8.2.2. Crown Ether and Phase Transfer Catalysts Particularly striking examples of the effect of specific solvation occur with the *crown ethers*. These macrocyclic polyethers specifically solvate cations such as Na^+ and K^+ .



¹⁵³ A. J. Parker, *Q. Rev. Chem. Soc.*, **16**, 163 (1962); C. D. Ritchie, in *Solute-Solvent Interactions*, J. F. Coetzee and C. D. Ritchie, eds., Marcel Dekker, New York, 1969, Chap. 4; E. Bunzel and H. Wilson, *Adv. Phys. Org. Chem.*, **14**, 133 (1977).

When added to nonpolar solvents, the crown ethers increase the solubility of ionic materials. For example, in the presence of 18-crown-6, potassium fluoride is soluble in benzene and acts as a reactive nucleophile:



In the absence of the polyether, potassium fluoride is insoluble in benzene and unreactive toward alkyl halides. Similar enhancement of solubility and reactivity of other salts is observed in the presence of crown ethers. The solubility and reactivity enhancement results because the ionic compound is dissociated to a tightly complexed cation and a “naked” anion. Figure 3.35 shows the tight coordination that can be achieved with a typical crown ether. The complexed cation, because it is surrounded by the nonpolar crown ether, has high solubility in the nonpolar media. To maintain electroneutrality the anion is also transported into the solvent. The cation is shielded from close interaction with the anion because of the surrounding crown ether molecule. As a result, the anion is unsolvated and at a relatively high energy and therefore highly reactive.

A related solvation phenomenon is the basis for *phase transfer catalysis*.¹⁵⁵ The catalysts here are salts in which one of the ions (usually the cation) has large nonpolar substituent groups that confer good solubility in organic solvents. The most common examples are tetraalkylammonium and tetraalkylphosphonium ions. In two-phase systems consisting of water and a nonpolar organic solvent, these cations are extracted into the organic phase and, as a result of electrostatic forces, anions are transferred to the organic phase. The anions are weakly solvated and display high reactivity. Reactions are carried out between a salt containing the desired nucleophilic anion and

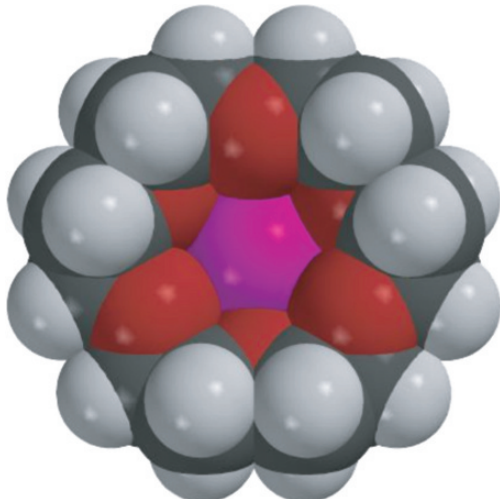
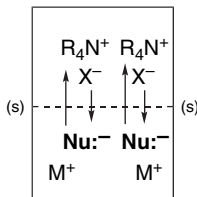


Fig. 3.35. Space-filling molecular model depicting a metal cation complexed by 18-crown-6. (See also color insert.)

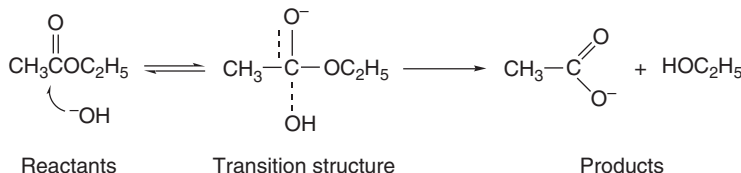
¹⁵⁴ C. Liotta and H. P. Harris, *J. Am. Chem. Soc.*, **96**, 2250 (1974).

¹⁵⁵ C. M. Starks, C. L. Liotta, and M. Halpern, *Phase Transfer Catalysis: Fundamentals: Applications and Industrial Perspectives*, Chapman and Hall, New York, 1994.

an organic reactant, typically in a hydrocarbon or nonpolar halogenated solvent. The addition of phase transfer catalysts causes migration of the anion into the organic phase and, because of its high nucleophilicity, reaction occurs under exceptionally mild conditions.



3.8.2.3. Differential Solvation of Reactants and Transition States. It should always be kept in mind that solvent effects can modify the energy of both the reactants and the transition state. It is the *difference* in the solvation that is the basis for changes in activation energies and reaction rates. Thus, although it is common to discuss solvent effects solely in terms of reactant solvation or transition state solvation, this is an oversimplification. A case that illustrates this point is the base-promoted hydrolysis of esters by hydroxide ion.



The reaction is faster in DMSO-water than in ethanol-water. Reactant solvation can be separated from transition state solvation by calorimetric measurement of the heat of solution of the reactants in each solvent system. The data in Figure 3.36 compare the energies of the reactants and TS for ethyl acetate and hydroxide ion reacting in aqueous ethanol versus aqueous DMSO. It can be seen that both the reactants and the TS are more strongly solvated in the ethanol-water medium.¹⁵⁶ The enhancement

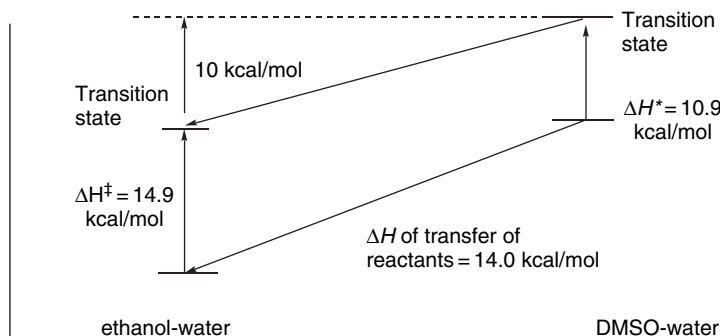
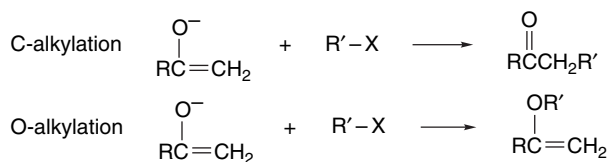


Fig. 3.36. Comparative reactant and transition state solvation in the reaction of ethyl acetate with hydroxide ion in ethanol/water and DMSO. Data from *J. Am. Chem. Soc.*, **94**, 71 (1972).

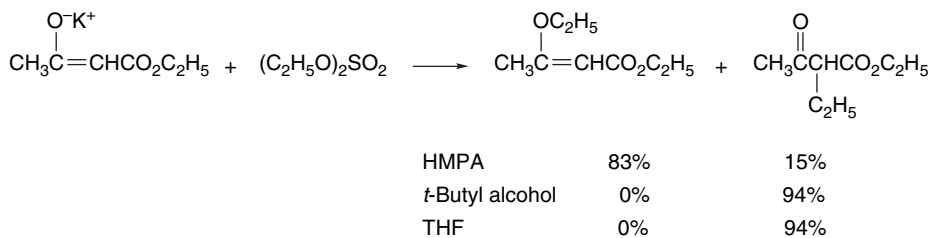
¹⁵⁶ P. Haberfield, J. Friedman, and M. F. Pinkson, *J. Am. Chem. Soc.*, **94**, 71 (1972).

in reaction rate comes from the fact that the difference is greater for the small hard hydroxide ion than for the larger anionic species present at the transition state.¹¹⁶ It is generally true that solvation forces are strongest for the small, hard anions and decrease with size and softness.

3.8.2.4. Oxygen versus Carbon Alkylation in Ambident Enolate Anions. Enolate anions are *ambident nucleophiles*. Alkylation of an enolate can occur at either carbon or oxygen. Since most of the negative charge of an enolate is on the oxygen atom, it might be supposed that O-alkylation would dominate. A number of factors other than charge density affect the C/O-alkylation ratio and it is normally possible to establish reaction conditions that favor alkylation on carbon.



O-Alkylation is most pronounced when the enolate is least solvated. When the potassium salt of ethyl acetoacetate is treated with ethyl sulfate in the polar aprotic solvent HMPA, the major product (83%) results from O-alkylation. In THF, where ion clustering occurs, all of the product is C-alkylated. In *t*-butyl alcohol, where the acetoacetate anion is hydrogen bonded by solvent, again only C-alkylation is observed.¹⁵⁷



Higher C/O ratios are observed with alkyl halides than with alkyl sulfonates and sulfates. The highest C/O-alkylation ratios are given by alkyl iodides. For ethylation of potassium ethyl acetoacetate in HMPA the product compositions shown below were obtained.¹⁵⁸

¹⁵⁷ A. L. Kurts, A. Masias, N. K. Genkina, I. P. Beletskaya, and O. A. Reutov, *Dokl. Akad. Nauk. SSSR* (Engl. Transl.), **187**, 595 (1969).

¹⁵⁸ A. L. Kurts, N. K. Genkina, A. Masias, I. P. Beletskaya, and O. A. Reutov, *Tetrahedron*, **27**, 4777 (1971).

$\text{CH}_3\text{C}=\text{CHCO}_2\text{C}_2\text{H}_5 + \text{C}_2\text{H}_5\text{X} \longrightarrow \text{CH}_3\text{C}(\text{OC}_2\text{H}_5)=\text{CHCO}_2\text{C}_2\text{H}_5 + \text{CH}_3\overset{\text{O}}{\underset{\text{C}_2\text{H}_5}{\text{C}}}(\text{CHCO}_2\text{C}_2\text{H}_5)$			
X = OTs	88%	11%	(plus 1% dialkyl)
X = Cl	60%	32%	(plus 8% dialkyl)
X = Br	39%	38%	(plus 23% dialkyl)
X = I	13%	71%	(plus 16% dialkyl)

Leaving-group effects on the ratio of C- to O-alkylation can be correlated by the HSAB rationale.¹⁵⁹ Of the two nucleophilic sites in an enolate ion, oxygen is harder than carbon. Nucleophilic substitution reactions of the S_N2 type proceed best when the nucleophile and leaving group are either both hard or both soft.¹⁶⁰ Consequently, ethyl iodide, with the soft leaving group iodide, reacts preferentially with the softer carbon site rather than the harder oxygen. Oxygen-leaving groups, such as sulfonate and sulfate, are harder and react preferentially at the hard oxygen site of the enolate. The hard-hard combination is favored by an early transition state where the electrostatic attraction is the most important factor. The soft-soft combination is favored by a later transition state where partial bond formation is the dominant factor. The C-alkylation product is more stable than the O-alkylation product (because the bond energy of C=O + C-C is greater than C=C + C-O), as illustrated in Figure 3.37.

Similar effects are also seen with enolates of simple ketones. For isopropyl phenyl ketone, the inclusion of one equivalent of 12-crown-4 in a DME solution of the lithium enolate changes the C:O ratio from 1.2:1 to 1:3, using methyl sulfate as the alkylating agent.¹⁶¹ The crown ether selectively solvates the Li⁺ ion, leaving the anion in a more

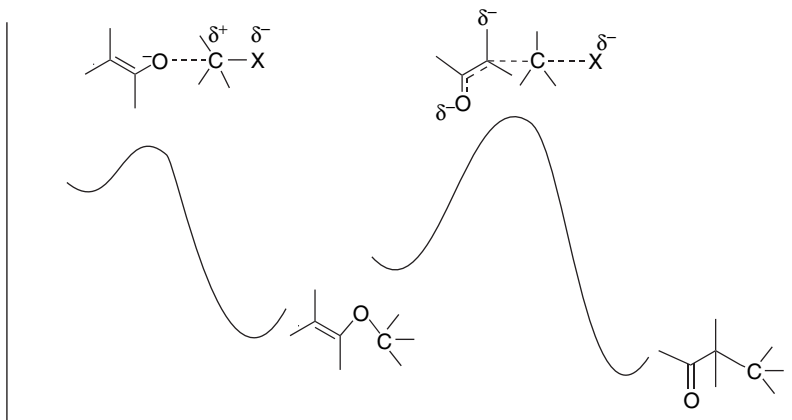


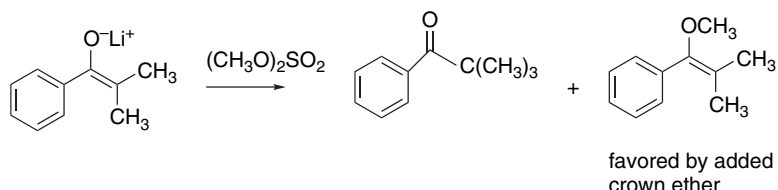
Fig. 3.37. Differential reaction energy profiles for O versus C alkylation of enolates. (a) O-Alkylation is characterized by an early transition state, weak O-solvation, high anion reactivity, and relatively large electrostatic effects. (b) C-Alkylation is characterized by a later transition state with more C-C bond formation and more diffuse charge distribution.

¹⁵⁹ T. -L. Ho, *Hard and Soft Acids and Bases Principle in Organic Chemistry*, Academic Press, New York (1977).

¹⁶⁰ R. G. Pearson and J. Songstad, *J. Am. Chem. Soc.*, **89**, 1827 (1967).

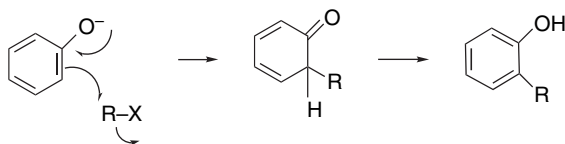
¹⁶¹ L. M. Jackman and B. C. Lange, *J. Am. Chem. Soc.*, **103**, 4494 (1981).

reactive state. With methyl iodide as the alkylating agent, C-alkylation is strongly favored with or without 12-crown-4.

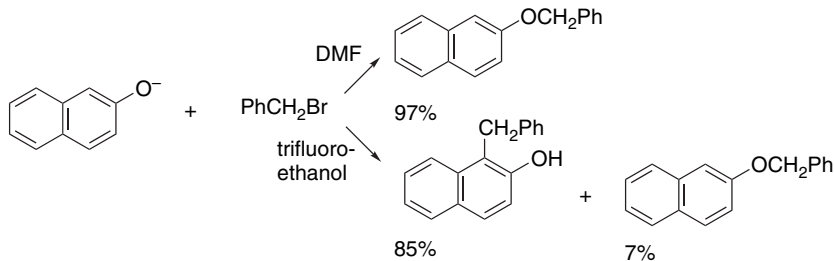


To summarize, the amount of O-alkylation is maximized by use of an alkyl sulfate or alkyl sulfonate in a polar aprotic solvent. The amount of C-alkylation is maximized by using an alkyl halide in a less polar or protic solvent. The majority of synthetic operations involving ketone enolates are carried out in THF or DME using an alkyl bromide or alkyl iodide and C-alkylation is favored.

Phenoxyde ions are a special case related to enolate anions and have a strong preference for O-alkylation because C-alkylation disrupts aromatic conjugation.

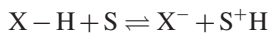


Phenoxyde undergoes O-alkylation in solvents such as DMSO, DMF, ethers, and alcohols. However, in water and trifluoroethanol there is extensive C-alkylation.¹⁶² These latter solvents form particularly strong hydrogen bonds with the oxygen atom of the phenolate anion. This strong solvation decreases the reactivity at oxygen and favors C-alkylation.



Topic 3.1. Acidity of Hydrocarbons

One of the fundamental properties of compounds containing hydrogen is their ability to act as proton donors, that is, as *Brønsted acids*.



¹⁶². N. Kornblum, P. J. Berrigan, and W. J. LeNoble, *J. Am. Chem. Soc.*, **85**, 1141 (1963); N. Kornblum, R. Seltzer, and P. Haberfield, *J. Am. Chem. Soc.*, **85**, 1148 (1963).

The concept of acidity was discussed earlier in relation to aqueous solutions and the acidity of carboxylic acids and alcohols (see p. 321–322). The acidity of such compounds can be measured and expressed as the pK_a .

$$pK_a = -\log K \text{ where } K = \frac{[S^+H][X^-]}{[HX][S]}$$

Determination of the acidity of hydrocarbons is more difficult. As most are very weak acids, very strong bases are required to cause deprotonation. Water and alcohols are far more acidic than most hydrocarbons and are unsuitable solvents for generation of hydrocarbon anions. A strong base deprotonates the solvent rather than the hydrocarbon. For synthetic purposes, aprotic solvents such as ether, THF, and dimethoxyethane are used, but for equilibrium measurements solvents that promote dissociation of ion pairs and ion clusters are preferred. Weakly acidic solvents such as dimethyl sulfoxide (DMSO), dimethylformamide (DMF), and cyclohexylamine are used in the preparation of moderately basic carbanions. The high polarity and cation-solvating ability of DMSO and DMF facilitate dissociation of ion pairs so that the equilibrium data obtained refer to the free ions, rather than to ion aggregates.

The basicity of a base-solvent system can be specified by a basicity constant H_- . The H_- is a measure of solution basicity, analogous to the acidity function H_0 (see Section 3.7.1.3). The value of H_- approximates the pH of strongly basic solutions. The larger the value of H_- , the greater the proton-abtracting ability of the medium. Use of a series of overlapping indicators permits assignment of H_- values to base-solvent systems, and allows pK 's to be determined over a range of 0–30 pK units. Table 3.35 presents H_- values for some solvent-base systems.

The acidity of a hydrocarbon can be determined in an analogous way.¹⁶³ If the electronic spectra of the neutral and anionic forms are sufficiently different, the concentrations of each can be determined directly, and the position of the equilibrium constant is related to pK by the equation

$$pK_{R-H} = H_- + \log \frac{[R-H]}{[R^-]}$$

A measurement of the ratio $[RH] : [R^-]$ at a known H_- yields the pK . If the electronic spectrum of the hydrocarbon and its anion are not sufficiently different, an indicator is

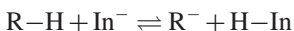
Table 3.35. Values of H_- for Some Solvent-Base Systems

Solvent	H_-^a
5M KOH	15.5
10M KOH	17.0
1M KOH	18.5
0.01M NaOMe in 1:1 DMSO-MeOH	15.0
0.01M NaOMe in 10:1 DMSO-MeOH	18.0
0.01M NaOEt in 20:1 DMSO-MeOH	21.0

a. From J. R. Jones, *The Ionization of Carbon Acids*, Academic Press, New York, 1973, Chap. 6.

¹⁶³ D. Dolman and R. Stewart, *Can. J. Chem.*, **45**, 911 (1967); E. C. Steiner and J. M. Gilbert, *J. Am. Chem. Soc.*, **87**, 382 (1965); K. Bowden and R. Stewart, *Tetrahedron*, **21**, 261 (1965).

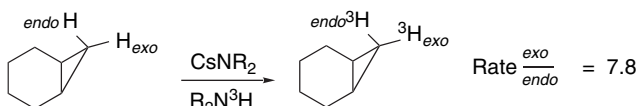
used and its spectrum is monitored. Equilibrium is established between the indicator and hydrocarbon in the basic medium. The relationship



then provides a way to relate the concentrations that are not directly measured—[RH] and [R⁻]—to quantities that are—[HIn] and [In⁻].

The p*K* values are influenced by the solvent and other conditions of the measurement. The extent of ion pairing is a function of the ability of the solvent to solvate the ionic species. Ion pairing is greatest in nonpolar solvents such as ethers. In dipolar aprotic solvents, especially DMSO, ion pairing is much less likely to be significant.¹⁶⁴ The identity of the cation present can also have a significant effect if ion pairs are present. Owing to these factors, the numerical p*K* values are not absolute and are specific to the solvent. Nevertheless, they provide a useful measure of relative acidity. The two solvents that have been used for most quantitative measurements on weak carbon acids are cyclohexylamine and DMSO. Some of these values are given in Table 3.36. It is not expected that the values will be numerically identical with aqueous p*K_a*, but for most compounds the same relative order of acidity is observed for hydrocarbons of similar structural type.

A number of hydrocarbons have been studied in cyclohexylamine using cesium cyclohexylamide as the base. For many of the compounds studied, spectroscopic measurements were used to determine the relative extent of deprotonation of two hydrocarbons and thus establish relative acidity.¹⁶⁵ For other hydrocarbons, the acidity was derived by kinetic measurements. Such studies are usually done by observing the rate of isotopic exchange (deuterium or tritium) at the site of interest. The rate of hydrocarbon exchange can be measured using ³H NMR spectroscopy.¹⁶⁶ The course of exchange can be followed by the appearance of the ³H NMR signal corresponding to the hydrogen undergoing exchange. For example, the rates of exchange of both the *exo* and *endo* hydrogens in norcarane can be followed.

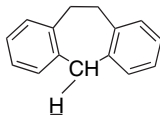
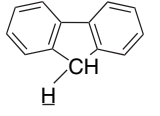
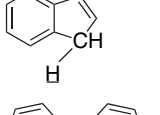
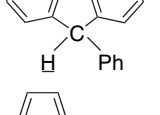
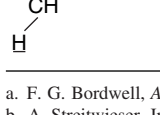


It has been found that there is often a correlation between the rate of proton abstraction (kinetic acidity) and the thermodynamic stability of the carbanion (thermodynamic acidity). Owing to this relationship, kinetic measurements can be used to construct orders of hydrocarbon acidities. These kinetic measurements have the advantage of not requiring the presence of a measurable concentration of the carbanion at any time; instead, the relative ease of carbanion formation is judged from the rate

- ¹⁶⁴. E. M. Arnett, T. C. Moriarity, L. E. Small, J. P. Rudolph, and R. P. Quirk, *J. Am. Chem. Soc.*, **95**, 1492 (1973); T. E. Hogen-Esch and J. Smid, *J. Am. Chem. Soc.*, **88**, 307 (1966).
- ¹⁶⁵. A. Streitwieser, Jr., J. R. Murdoch, G. Hafelinger, and C. J. Chang, *J. Am. Chem. Soc.*, **95**, 4248 (1973); A. Streitwieser, Jr., E. Ciuffarin, and J. H. Hammons, *J. Am. Chem. Soc.*, **89**, 63 (1967); A. Streitwieser, Jr., E. Juaristi, and L. L. Nebenzahl, in *Comprehensive Carbanion Chemistry*, Part A, E. Bunzel and T. Durst, eds., Elsevier, New York, 1980, Chap. 7.
- ¹⁶⁶. R. E. Dixon, P. G. Williams, M. Saljoughian, M. A. Long, and A. Streitwieser, *Magn. Res. Chem.*, **29**, 509 (1991).

Table 3.36. Acidity of Some Hydrocarbons

TOPIC 3.1
Acidity of Hydrocarbons

Hydrocarbon	$K^+(DMSO)^a$	$Cs^+(cyclohexylamine)^b$	$Cs^+(THF)^c$
PhCH ₂ -H	43	41.2	40.9
Ph ₂ CH-H	32.4	33.4	33.3
Ph ₃ C-H	30.6	31.4	31.3
		31.2	
	22.6	22.7	22.9
	20.1	19.9	22.9
	17.9	18.5	18.2
	18.1	16.6 ^{d,e}	

a. F. G. Bordwell, *Acc. Chem. Res.*, **21**, 456, 463 (1988).

b. A. Streitwieser, Jr., J. R. Murdoch, G. Hafelinger, and C. J. Chang, *J. Am. Chem. Soc.*, **95**, 4248 (1973); A. Streitwieser, Jr., and F. Guibe, *J. Am. Chem. Soc.*, **100**, 4532 (1978).

c. M. J. Kaufman, S. Gronert, and A. Streitwieser, Jr., *J. Am. Chem. Soc.*, **110**, 2829 (1988); A. Streitwieser, J. C. Ciula, J. A. Krom, and G. Thiele, *J. Org. Chem.*, **56**, 1074 (1991).

d. A. Streitwieser, Jr., and L. L. Nebenzahl, *J. Am. Chem. Soc.*, **98**, 2188 (1976).

e. The pK of cyclopentadiene in water is 16.0.

at which exchange occurs. This method is applicable to very weak acids, for which no suitable base will generate a measurable carbanion concentration. This method was used to extend the scale to hydrocarbons such as toluene, for which the exchange rate, but not equilibrium data, can be obtained.¹⁶⁷

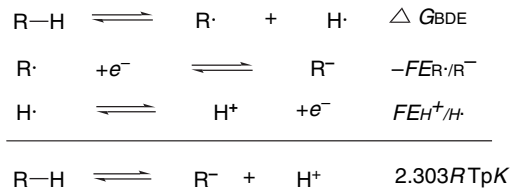
For synthetic purposes, carbanions are usually generated in ether solvents, often THF or dimethoxyethane. There are relatively few quantitative data available on hydrocarbon acidity in such solvents. Table 3.36 contains several entries for Cs⁺ salts in THF. The numerical values are scaled with reference to the pK of fluorene of 22.9.¹⁶⁸

¹⁶⁷. A. Streitwieser, Jr., M. R. Granger, F. Mares, and R. A. Wolf, *J. Am. Chem. Soc.*, **95**, 4257 (1973).

¹⁶⁸. M. J. Kaufman, S. Gronert, and A. Streitwieser, Jr., *J. Am. Chem. Soc.*, **110**, 2829 (1988); A. Streitwieser, Jr., J. C. Ciula, J. A. Krom, and G. Thiele, *J. Org. Chem.*, **56**, 1074 (1991).

Allylic conjugation stabilizes carbanions and pK values of 43 (in cyclohexylamine)¹⁶⁹ and 47–48 (in THF-HMPA)¹⁷⁰ have been determined for propene. On the basis of exchange rates with cesium cyclohexylamide, cyclohexene and cycloheptene have been found to have pK values of about 45 in cyclohexylamine.¹⁷¹ The hydrogens on the sp^2 carbons in benzene and ethylene are more acidic than the hydrogens in saturated hydrocarbons. A pK of 43 has been estimated for benzene on the basis of extrapolation from a series of fluorobenzenes.¹⁷² Electrochemical measurements have been used to establish a lower limit of about 46 for the pK of ethylene.¹⁷⁰

For saturated hydrocarbons, exchange is too slow and reference points are so uncertain that direct determination of pK values by exchange measurements is not feasible. The most useful approach to obtain pK data for such hydrocarbons involves making a measurement of the electrochemical potential for the one electron reduction of the hydrocarbon radical. From this value and known C–H bond dissociation energies, pK values can be calculated.



Early application of these methods gave estimates of the pK of toluene of about 45 and propene of about 48. Methane was estimated to have a pK in the range of 52–62.¹⁷⁰ More recent electrochemical measurements in DMF provided the results in Table 3.37.¹⁷³ These measurements put the pK of methane at about 48, with benzylic and allylic stabilization leading to values of 39 and 38 for propene and toluene, respectively. The electrochemical values that overlap with the pK_{DMSO} scale for compounds such as diphenylmethane and triphenylmethane are in reasonable agreement.

Most of the hydrocarbons included in Tables 3.36 and 3.37 illustrate the effect of *anion stabilization*. Cyclopentadiene is the most striking example. The pK is similar to that of alcohols. The high relative acidity of cyclopentadiene is due to the *aromatic*

Table 3.37. pK Values for Weakly Acidic Hydrocarbons Based on Reduction Potentials in DMF^a

	pK		pK
CH_3-H	48	$\text{CH}_2=\text{CHCH}_2-\text{H}$	38
$\text{CH}_3\text{CH}_2-\text{H}$	51	$\text{CH}_2=\text{CHC}(\text{CH}_3)-\text{H}$	38
$(\text{CH}_3)_2\text{CH}-\text{H}$	50	$\text{HC}\equiv\text{CCH}_2-\text{H}$	38
$(\text{CH}_3)_3\text{C}-\text{H}$	49	PhCH_2-H	39
cyclopentane	49	$\text{Ph}_2\text{CH}-\text{H}$	31
cyclohexane	49	$\text{Ph}_3\text{C}-\text{H}$	29

a. K. Daasbjerg, *Acta Chem. Scand.*, **49**, 578 (1995).

¹⁶⁹ D. W. Boerth and A. Streitwieser, Jr., *J. Am. Chem. Soc.*, **103**, 6443 (1981).

¹⁷⁰ B. Jaun, J. Schwarz, and R. Breslow, *J. Am. Chem. Soc.*, **102**, 5741 (1980).

¹⁷¹ A. Streitwieser, Jr., and D. W. Boerth, *J. Am. Chem. Soc.*, **100**, 755 (1978).

¹⁷² A. Streitwieser, Jr., P. J. Scannon, and H. M. Niemeyer, *J. Am. Chem. Soc.*, **94**, 7936 (1972).

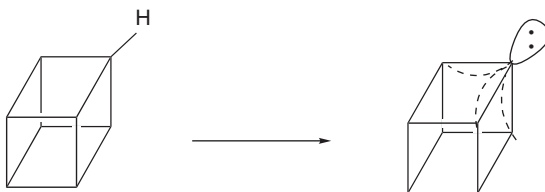
¹⁷³ K. Daasbjerg, *Acta Chem. Scand.*, **49**, 878 (1995).

stabilization of the anion. Indene and fluorene derivatives also benefit from stabilization of the cyclopentadienide rings that are incorporated into their structures. The much greater acidity of fluorene relative to dibenzocycloheptatriene (Table 3.36) reflects the aromatic stabilization of the cyclopentadienide ring in the anion of fluorene. Toluene, diphenylmethane, and triphenylmethane anions are also stabilized by delocalization of the negative charge. Note, however, that the third phenyl substituent has only a small effect on the acidity of triphenylmethane, which presumably reflects steric problems that preclude optimal alignment of the rings in the carbanion.

Another factor that influences hydrocarbon acidity is hybridization at the carbon atom. Acidity increases sharply in the order $sp^3\text{C}-\text{H} < sp^2\text{C}-\text{H} < sp\text{C}-\text{H}$. Terminal alkynes are among the most acidic of the hydrocarbons. For example, in DMSO, phenylacetylene is found to have a pK near 26.5.¹⁷⁴ In cyclohexylamine, the value is 23.2.¹⁷⁵ An estimate of the pK in aqueous solution of 20 is based on a Brønsted relationship.¹⁷⁶ The relatively high acidity of alkynes is associated with the high s character of the C–H bond. The s character is 50%, as opposed to 25% in sp^3 bonds. The electrons in orbitals with high s character experience decreased shielding of the nuclear charge. The carbon is therefore effectively more electronegative, as viewed from the proton sharing an sp hybrid orbital, and hydrogens on sp carbons exhibit greater acidity. This same effect accounts for the relatively high acidity of the hydrocarbons on cyclopropane and other strained rings that have increased s character in the C–H bonds.¹⁷⁷ There is a correlation between the coupling constant $J^{1\text{H}}-\text{C}^{13}$ and acidity, because the $J^{1\text{H}}-\text{C}^{13}$ coupling constant is related to hybridization.¹⁷⁸ The relationship between hybridization and acidity may not be as straightforward as suggested by the correlations for alkynes, alkenes, cyclopropane, and alkanes. Sauers tabulated % s character for 28 hydrocarbons and found relatively poor correlation with % s character.¹⁷⁹

Cubane has had an interesting place in the discussion of the correlation between C–H acidity and carbon hybridization. Its kinetic acidity was measured by the ^3H exchange NMR technique and found to be about 6.6×10^4 as reactive as benzene.¹⁸⁰ An experimental gas phase measurement of the proton affinity (PA) as 404 kcal/mol is available.¹⁸¹ (See Tables 3.14 and 3.38 for comparable data on other hydrocarbons.) Both of these values indicate that cubane is somewhat more acidic than expected on the basis of the carbon hybridization. There appears to be unusual hybridization of the anion in this case. An AIM analysis suggests that the C–C bond paths in the anion are *less than* 90° , suggesting that the bonds bend inward toward the center of the ring. Sauers also noted an *increase* in s character on going from the hydrocarbon to the anion.¹⁷⁹ Of the 28 deprotonations he examined, only cyclopropane and bicyclo[1.1.1]pentane also showed increased s character in the anion.

- ¹⁷⁴ F. G. Bordwell and W. S. Matthews, *J. Am. Chem. Soc.*, **96**, 1214 (1974).
- ¹⁷⁵ A. Streitwieser, Jr., and D. M. E. Reuben, *J. Am. Chem. Soc.*, **93**, 1794 (1971).
- ¹⁷⁶ D. B. Dahlberg, M. A. Kuzemko, Y. Chiang, A. J. Kresge, and M. F. Powell, *J. Am. Chem. Soc.*, **105**, 5387 (1983).
- ¹⁷⁷ A. Streitwieser, Jr., R. A. Caldwell, and W. R. Young, *J. Am. Chem. Soc.*, **91**, 529 (1969); G. L. Closs and R. B. Larrabee, *Tetrahedron Lett.*, 287 (1965); M. Randic and Z. Mossic, *Chem. Rev.*, **72**, 43 (1972).
- ¹⁷⁸ M. A. Battiste and J. M. Coxon, *The Chemistry of the Cyclopropyl Group*, Z. Rapoport, ed., John Wiley & Sons, New York, 1987, pp. 255–305.
- ¹⁷⁹ R. R. Sauers, *Tetrahedron*, **55**, 10013 (1999).
- ¹⁸⁰ A. Streitwieser, L. Xie, P. Speers, and P. G. Williams, *Magn. Res. Chem.*, **36**, S509 (1996).
- ¹⁸¹ M. Hare, T. Emrick, P. E. Eaton, and S. R. Kass, *J. Am. Chem. Soc.*, **119**, 237 (1997).



As we discussed in Section 3.4.2, measurements in the gas phase, which eliminate the effect of solvation, show structural trends that parallel measurements in solution but with larger absolute energy differences. Table 3.38 gives ΔH of gas phase proton dissociation data for some key hydrocarbons. These data show a correspondence with the hybridization and delocalization effects observed in solution. The very large heterolytic dissociation energies reflect both the inherent instability of the carbanions and also the electrostatic attraction between the oppositely charged carbanion and proton that separate.

There have been several studies aimed at using computations to examine hydrocarbon acidity. The proton affinity values for a number of hydrocarbons were calculated by both ab initio and DFT methods.¹⁷⁹ Some of the results are shown in Table 3.39.

Alkorta and Elguero found that there is good correlation between PAs calculated by B3LYP/6-311 + +G** computations and available gas phase experimental measurements.¹⁸² There was also good correlation with solution pK values. Based on these correlations, they made the interesting prediction that the as yet unknown hydrocarbon tetrahedrane would be comparable to water in acidity.

Knowledge of the structure of carbanions is important to understanding the stereochemistry, stability, and reactivity. Theoretical calculations at the ab initio level (HF/4-31G) indicate a pyramidal geometry at carbon in the methyl and ethyl anions. The optimum H–C–H angle in these two carbanions was calculated to be 97°–100°. An interesting effect is observed in that the PA (basicity) of methyl anion decreases in a regular manner as the H–C–H angle is decreased.¹⁸³ This increase in acidity with decreasing internuclear angle has a parallel in small-ring compounds, in which the acidity of hydrogens is substantially greater than in compounds having tetrahedral geometry at carbon. Pyramidal geometry at carbanions can also be predicted on the

Table 3.38. Enthalpy of Proton Dissociation for Some Hydrocarbons (Gas Phase)

Hydrocarbon	Enthalpy (kcal/mol)
Methane	418.8
Ethene	407.5
Cyclopropane	411.5
Benzene	400.8
Toluene	381.0

a. S. T. Graul and R. R. Squires, *J. Am. Chem. Soc.*, **112**, 2517 (1990).

¹⁸² I. Alkorta and J. Elguero, *Tetrahedron*, **53**, 9741 (1997).

¹⁸³ A. Streitwieser, Jr., and P. H. Owens, *Tetrahedron Lett.*, 5221 (1973); A. Steitwieser, Jr., P. H. Owens, R. A. Wolf, and J. E. Williams, Jr., *J. Am. Chem. Soc.*, **96**, 5448 (1974); E. D. Jemmis, V. Buss, P. v. R. Schleyer, and L. C. Allen, *J. Am. Chem. Soc.*, **98**, 6483 (1976).

Table 3.39. Computed Proton Affinity for Some Hydrocarbons in kcal/mol^a

Hydrocarbon	MP2/6-31+G(d,p)	B3LYP/6-311++G(2d,p)	Experimental	TOPIC 3.1
CH ₃ -H	419.0	414.5	417±2	Acidity of Hydrocarbons
CH ₃ CH ₂ -H	421.9	417.0	420-421	
(CH ₃) ₃ C-H	412.1	406.8	413.1	
Cyclopropane	419.6	413.3	411.5	
Cyclobutane	415.5	411.5	417.4	
Cyclopentane	414.0	409.1	416.1	
Bicyclo[1.1.1]-pentane-H(1)	409.4	407.5	411±3.5	
Bicyclo[2.2.1]-heptane-H(1)	411.3	409.0		
Cubane	407.6	406.5	404±3	

a. R. R. Sauers, *Tetrahedron*, **55**, 10013 (1999).

basis of qualitative considerations of the orbital occupied by the unshared electron pair. In a planar carbanion, the lone pair occupies a *p* orbital. In a pyramidal geometry, the orbital has substantial *s* character. Since the electron pair has lower energy in an orbital with some *s* character, it would be predicted that a pyramidal geometry would be favored.

An effort has been made to dissect the substituent effects in carbanions into their component parts. The energy of the anion was calculated before and after allowing first electronic and then nuclear relaxation. This might be expected to roughly correspond to polar and resonance components, since the nuclear relaxation established the optimal geometry for delocalization (although there may be partial delocalization in the unrelaxed anion). The results are summarized in Table 3.40. Most of the energy change was found at the electronic relaxation stage, but substituents such as formyl and nitro, for which resonance delocalization is expected to be important, showed the largest effect of nuclear relaxation. Interestingly, the cyano group showed only a small nuclear relaxation component, suggesting that its anion-stabilizing effect is mainly of polar origin.

Tupitsyn and co-workers examined several series of hydrocarbons in an effort to confirm the importance of delocalization and hybridization changes as the major factors

Table 3.40. Electronic and Nuclear Relaxation Components of Carbanion Stabilization^a

Substituent	Electronic (kcal/mol)	Nuclear (kcal/mol)
H	67.8	0
NH ₂	61.9	1.0
OH	60.2	1.8
F	61.4	1.6
Cl	59.7	2.6
CH=O	64.5	5.9
C≡N	62.6	1.2
NO ₂	59.5	10.6
CH ₃ S	65.9	0.7
CH ₃ SO	62.6	2.7
CH ₃ SO ₂	60.0	1.4

a. F. Tupitsyn, A. S. Popov, and N. N. Zatsepina, *Russ. J. Gen. Chem.*, **68**, 1314 (1998).

in C–H acidity.¹⁸⁴ Acidity was estimated by using AM1 computations, calibrated to experimental deprotonation energies. For small-ring, bicyclic, and cage compounds, a correlation was found for the ΔE for deprotonation and the ^1H – ^{13}C coupling constant:

$$\Delta E_{\text{deprot}} = 1870(\text{kJ}) - 0.93 J_{\text{H}-\text{C}}$$

A similar correlation pertains to cyclic alkenes and dienes in which the deprotonation is from an sp^2 carbon:

$$\Delta E_{\text{deprot}} = 1867(\text{kJ}) - 1.05 J_{\text{H}-\text{C}}$$

These correlations suggest that the dominant factor for these compounds is the hybridization of the C–H undergoing deprotonation. For hydrocarbons for which delocalization is expected to be the major factor, e.g., toluene and diphenylmethane, a different kind of correlation was found:

$$\Delta E_{\text{deprot}} = 1640(\text{kJ}) - 0.70 \Delta E_{\text{relax}}$$

where ΔE_{relax} is the stabilization found when the carbanion constrained to the geometry of the original structure is allowed to relax to the minimum energy structure. These results support the idea that C–H acidity depends primarily on hybridization and anion stabilization. In addition to the hydrocarbons that show correlations with one of the two factors, some hydrocarbons are correlated by equations that contain terms both terms.

General References

- C. F. Bernasconi, ed., *Investigation of Rates and Mechanisms: Techniques of Chemistry*, 4th ed. Vol. VI, Part 1, John Wiley & Sons, New York, 1986.
- B. K. Carpenter, *Determination of Organic Reaction Mechanisms*, Wiley-Interscience, New York, 1984.
- K. A. Connors, *Chemical Kinetics*, VCH Publishers, New York, 1990.
- J. D. Cox and G. Pilcher, *Thermochemistry of Organic and Organometallic Compounds*, Academic Press, London, 1970.
- G. G. Hammes, *Principles of Chemical Kinetics*, Academic Press, New York, 1978.
- J. Hine, *Structural Effects on Equilibria in Organic Chemistry*, Wiley-Interscience, New York, 1984.
- C. D. Johnson, *The Hammett Equation*, Cambridge University Press, Cambridge, 1973.
- L. Melander and W. H. Saunders, Jr., *Reaction Rates of Isotopic Molecules*, New York, 1980.
- M. J. Pilling and P. Seakins, *Reaction Kinetics*, 2nd ed. Oxford University Press, Oxford, 1995.
- C. Reichardt, *Solvents and Solvent Effects in Organic Chemistry*, Wiley-VCH, Weinheim, 2003.

Problems

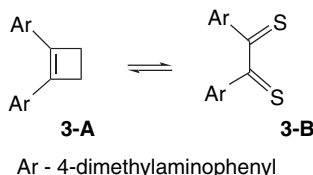
(References for these problems will be found on page 1158.)

3.1. Use thermochemical relationships to obtain the requested information.

- a. The ΔH_f of cyclohexane, cyclohexene, and benzene are, respectively, –29.5, –1.1, and +18.9 kcal/mol. Use this information to estimate the resonance stabilization of benzene.

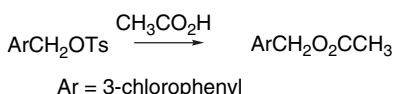
¹⁸⁴ I. F. Tupitsyn, A. S. Popov, and N. N. Satsepina, *Russian J. Gen. Chem.*, **67**, 379 (1997).

- b. Calculate ΔH for the air oxidation of benzaldehyde to benzoic acid, given that the ΔH_f of benzaldehyde and benzoic acid are -8.8 and -70.1 kcal/mol, respectively.
- c. Using the appropriate heats of formation from Table 3.1, calculate the heat of hydrogenation ΔH_{H_2} for 2-methyl-1-pentene.
- 3.2. Addition of methylmagnesium bromide to 2-methylcyclohexanone, followed by iodine-catalyzed dehydration of the resulting alcohol gave three alkenes in the ratio A:B:C = 3:31:66. Each alkene gave a mixture of *cis*- and *trans*-1,2-dimethylcyclohexane upon catalytic hydrogenation. When the alkene mixture was heated with a small amount of sulfuric acid, the ratio of A:B:C changed to 0.0:15:85. Assign structures to A, B, and C.
- 3.3. Measurement of the equilibrium constant for the interconversion of the dithiete **3-A** and the dithione **3-B** at several temperatures gave the data below. Calculate ΔG , ΔH , and ΔS .



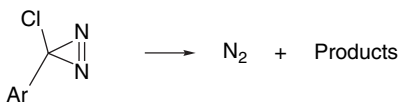
Temperature ($^{\circ}\text{C}$)	K
-2.9	16.9
11.8	11.0
18.1	8.4
21.9	7.9
29.3	6.5
32.0	6.1
34.9	5.7
37.2	5.3
42.5	4.6

- 3.4 a. Calculate the activation parameters (ΔH^{\ddagger} and ΔS^{\ddagger}) at 40°C for the acetolysis of 3-chlorobenzyl tosylate from the data given below:



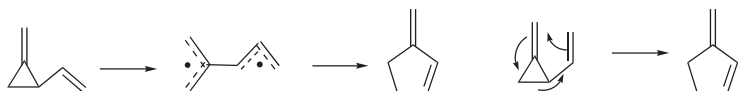
Temperature ($^{\circ}\text{C}$)	$k \times 10^5 \text{ s}^{-1}$
25.0	0.0136
40.0	0.085
50.1	0.272
58.8	0.726

- b. Calculate the activation parameters (E_a , ΔH^\ddagger , and ΔS^\ddagger) at 100°C from the data given for the reaction below.



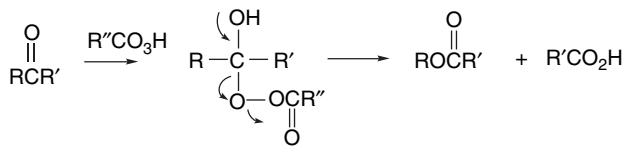
Temperature (°C)	$k \times 10^4 \text{ s}^{-1}$
60.0	0.30
70.0	0.97
75.0	1.79
80.0	3.09
90.0	8.92
95.0	15.90

- 3.5. 2-Vinylmethylenecyclopropane rearranges thermally to 3-methylene-cyclopentene. In the gas phase, the E_a is 26.0 kcal/mol, which is close to the estimated energy required for rupture of the C(2)–C(3) bond. Two possible mechanisms for this rearrangement are:

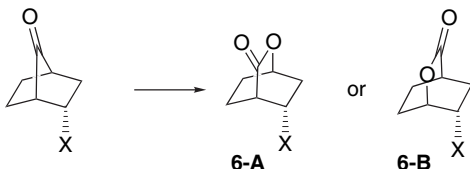


- a. Sketch qualitative reaction energy profiles for each process, based on the information given.
 b. How might an isotopic labeling experiment distinguish between these mechanisms?

- 3.6. The Baeyer–Villiger oxidation of ketones to esters (or lactones) occurs by the following mechanism:



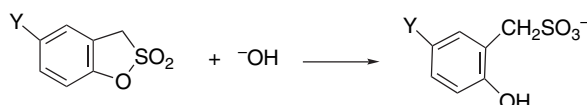
For *endo*-substituted bicyclo[2.2.1]heptan-7-ones, the product ratios shown below are observed. Account for the effect of the substituents.



X	6A:6B
CN	100:0
CO ₂ CH ₃	77:23
Ph	51:49
p-NO ₂ Ph	75:25
p-FPh	52:48
p-CH ₃ OPh	39:61

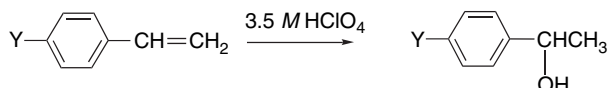
3.7

- a. Create Hammett plots versus σ and σ^- for the reaction shown below from the data given. Determine the value of ρ and compare the correlation with the two sets of substituent constants.



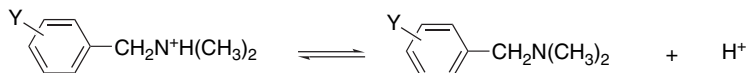
Y	$k M^{-1} s^{-1}$
H	37.4
CH ₃ O	21.3
CH ₃	24.0
Br	95.1
NO ₂	1430

- b. The pseudo-first order rate constants for acid-catalyzed hydration of substituted styrenes in 3.5M HClO₄ at 25°C are given. Plot the data against σ and σ^+ and determine ρ and ρ^+ . Interpret the significance of the results.



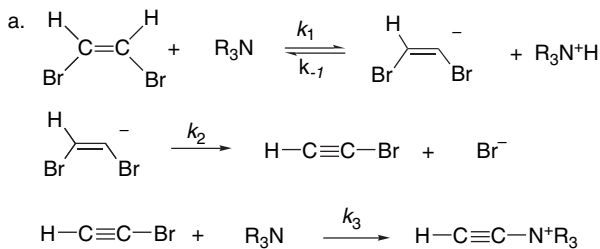
Y	$k \times 10^8 \text{ s}^{-1}$
4-CH ₃ O	488,000
4-CH ₃	16,400
H	811
4-Cl	318
4-NO ₂	1.44

- c. The acidity of a series of substituted benzylidimethylammonium ions has been measured. Determine whether these data are correlated by the Hammett equation using σ and σ^+ . What is the value of ρ ? What interpretation do you put on its sign and magnitude?

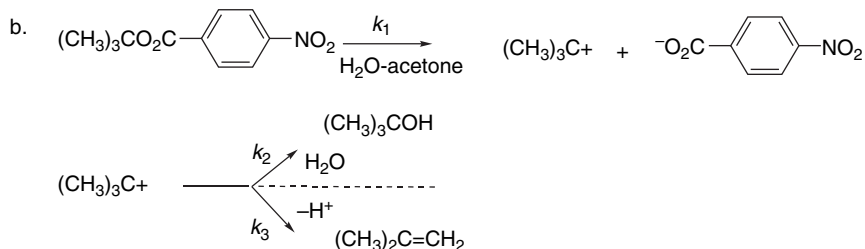


Y	pK _a
4-CH ₃ O	9.32
3-CH ₃ O	9.04
4-CH ₃	9.22
4-F	8.94
H	9.03
3-NO ₂	8.19
4-NO ₂	8.14
4-Cl	8.83
3-Cl	8.67

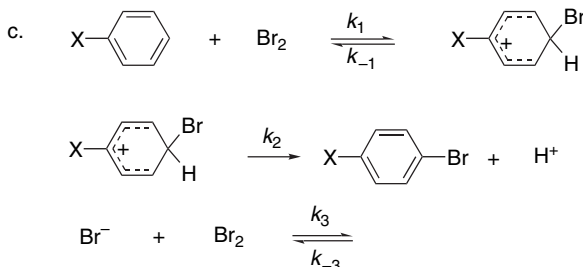
- 3.8. Write the rate law that would apply to the rate of product formation for each of the following reaction mechanisms.



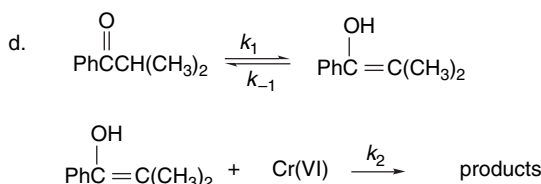
where the second step is rate-determining and the first step is an equilibrium



where the competing product-forming steps are faster than the first step



assuming that the σ complex is a steady state intermediate and that the final step is a rapid equilibrium that converts some of the initial Br₂ to unreactive Br⁻. What is the form of the rate expression if the intermediate of the first step goes on to product much faster than it reverts to starting material and if the equilibrium constant for Br⁻ formation is large.

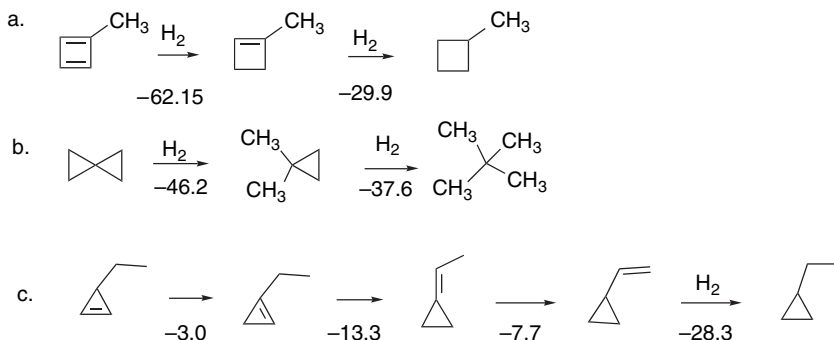


making no assumptions about the relative magnitude of k_1 , k_{-1} , or k_2 .

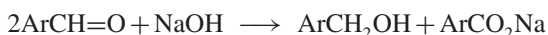
- 3.9. One method of estimating “aromatic stabilization” is to compare the heats of hydrogenation of cyclic conjugated systems with an acyclic molecule having the same number of conjugated bonds and π electrons. The table below gives the AM1 calculated heat of hydrogenation for various cyclic conjugated systems and for the corresponding polyene [ΔH_{H_2} (ref.)] For example, for benzene the comparison would be with 1,3,5-hexatriene. Calculate the aromatic stabilization or antiaromatic destabilization for each system. What conclusions do you draw? Relate your conclusions to HMO theory in Chapter 1. How does this computation deal with “strain?”

System	ΔH_{H_2} (ref.)	ΔH_{H_2} (cyclic system)
Cyclopropenyl cation	-13.3	10.6
Cyclopropenyl anion	4.7	-59.6
Cyclobutadiene	-50.7	-101.9
Cyclopentadienyl cation	-19.4	-72.9
Cyclopentadienyl anion	-0.3	-2.9
Benzene	-72.2	-45.0
Cycloheptatrienyl cation	-31.4	-23.9
Cycloheptatrienyl anion	-11.4	-26.4

- 3.10. A number of experimentally inaccessible ΔH values have been computed at the G2(MP2) level and are given below in kcal/mol. Taking for comparison ΔH_{H_2} of ethene as -32.4 kcal/mol , of 1-butene as -30.3 kcal/mol , and of cyclopropane to propane as -38.6 kcal/mol , indicate what factors lead to the observed differences in each step of the sequences shown.



- 3.11. The Cannizzaro reaction is a disproportionation that takes place in strongly basic solution and converts aromatic aldehydes to the corresponding benzyl alcohol and sodium benzoate.

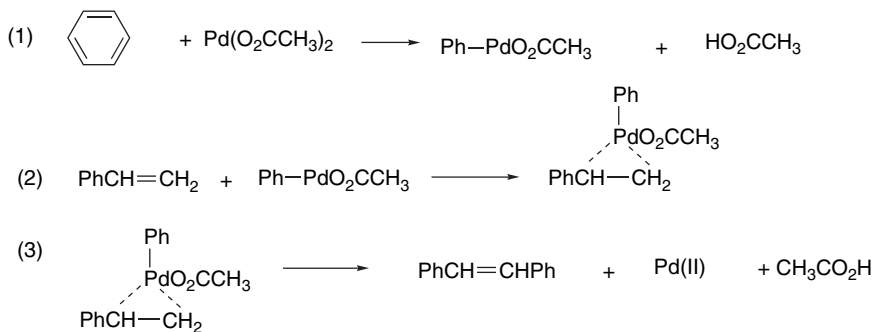


Several mechanisms, all of which involve a hydride transfer as a key step, have been postulated. On the basis of the following information, formulate one or more mechanisms that would be consistent with all the data provided. Indicate the significance of each observation with respect to the mechanism(s) you postulate.

- When the reaction is carried out in D_2O , the benzyl alcohol contains no deuterium in the methylene group.
- When the reaction is carried out in $H_2^{18}O$, both the benzyl alcohol and sodium benzoate contain ^{18}O .
- The overall reaction rate is given by the expression

$$\text{Rate} = k_{\text{obs}}[\text{PhCH=O}]^2[-\text{OH}]$$

- The rates of substituted benzaldehydes are correlated by a Hammett LFER with $\rho = +3.76$.
- The solvent isotope effect $k_{D_2O}/k_{H_2O} = 1.90$
- A mechanism for alkene arylation catalyzed by Pd(II) is outlined below. The isotope effect k_H/k_D was found to be 5 when benzene- d_6 was used. There was no isotope effect when styrene- $\beta-d_2$ was used. Which steps in the reaction mechanism could be rate determining, given this information on isotope effects?



- Comparison of the gas phase acidity of substituted benzoic acids with pK_a values in aqueous solutions reveals some interesting comparisons.
 - The trend in acidity as a function of substituent is the same for both gas phase and aqueous solution, but the substituent effects are much stronger in the gas phase. (The $\Delta\Delta G$ for any give substituent is about 10 times larger in the gas phase.)
 - Whereas acetic and benzoic acid are of comparable acidity in water, benzoic acid is considerably more acidic in the gas phase. (pK_a values are 4.75 and 4.19, respectively; and ΔG of ionization is 8.6 kcal/mol more positive for acetic acid.)
 - While the substituent effect in the gas phase is nearly entirely an enthalpy effect, it is found that in solution, the substituent effect is largely due to changes in ΔS .

Discuss how difference between the gas phase and solution can cause these effects.

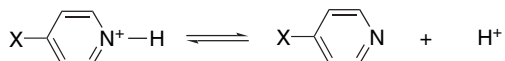
- It has been found that the ^{13}C chemical shift of aromatic ring carbons are a good indicator of the intrinsic electron-releasing or electron-withdrawing capacity of substituents, without any perturbation from approaching reagents. Such perturbation is always present when substituent effects are measured on the basis of

reactivity. The changes in chemical shifts of C(4) in some substituted benzenes are given below. Plot these against σ , σ^+ , and σ^- . What conclusions do you draw from these plots in regard to the mix of resonance and polar components in each of the σ values?

X	$\Delta\delta^a$	X	$\Delta\delta^a$
NH ₂	-9.86	CF ₃	3.29
CH ₃ O	-7.75	CN	3.80
F	-4.49	CH ₃ CO	4.18
Cl	-2.05	CH ₃ O ₂ C	4.12
Br	-1.62	CH ₃ SO ₂	4.64
CH ₃	-2.89	NO ₂	5.53

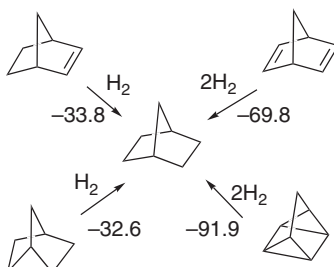
a. $\delta\Delta$ is the change in chemical shift in ppm relative to benzene in CCl₄ solution.

- 3.15. The ionization constants (pK_a) of 4-substituted pyridines have been measured, as have the ΔH of ionization at 25°C. Calculate ΔS for each ionization. Compare the contribution of ΔH and ΔS to the free energy of ionization. Test the data for linear free-energy correlations. Are the LFER dominated by the ΔH or ΔS term?



X	pK_a	ΔH (kcal/mol)	X	pK_a	ΔH (kcal/mol)
H	5.21	4.8	Cl	3.83	3.6
NH ₂	9.12	11.3	Br	3.75	3.5
CH ₃ O	6.58	6.8	CN	1.86	1.3
CH ₃	6.03	6.1			

- 3.16 a. Norbornene, norbornadiene, nortricyclane, and quadricyclane can all be hydrogenated to norbornane. The heats of hydrogenation are given in the chart. These data allow calculation of ΔH_f for the other derivatives and the results are given as Exp. in the table. The table also gives ΔH_f values calculated for each compound by MM and three semiempirical MO methods. Compare the accuracy of the semiempirical methods in predicting the experimental heats of formation.



Heats of Hydrogenation in kcal/mol

Calculated Enthalpies of Formation of Norbornane Analogs^a

Compound	MM ^b	MNDO	AM1	PM3	Exp.
Norbornadiene	55.5(30.9)	62.7	67.7	58.8	57.4
Norbornene	19.5(22.7)	25.3	26.0	22.0	21.4
Norbornane	-12.8(18.1)	-10.4	-14.4	-13.7	-12.4
Nortricyclane	19.5(52.6)	27.1	33.8	26.0	20.2
Quadricyclane	79.4(108.1)	79.1	104.4	86.3	79.5

a. In kcal/mol.

b. The calculated strain energies are given in parentheses.

- b. Subsequently, the same compounds were computed by ab initio and DFT methods. Isodesmic reactions were used to compare the ΔH_f of the compounds (except for G3(MP2), where atomization energies were used). Compare the ab initio and DFT results with the semiempirical results from Part (a).

Calculated Enthalpies of Formation of Norbornane Analogs^a

Compound	G2	G2(MP)	G2(MP2, SVP)G3(MP2)	B3LYP
Norbornadiene	56.3	57.0	56.0	56.0
Norbornene	18.5	19.1	18.0	18.5
Norbornane	-14.1	-13.6	-14.7	-13.8
Nortricyclane	16.2	16.9	15.5	16.9
Quadricyclane	79.2	80.1	80.1	80.4

a. In kcal/mol.

- c. Heats of hydrogenation have also been calculated from the semiempirical data. Since the heats of hydrogenation include the ΔH_f of H_2 , which is zero, they can be calculated as follows:

$$\Delta H_{H_2} = \Delta H_{f\text{product}} - \Delta H_{f\text{reactant}}$$

This leads to the calculated ΔH_{H_2} shown below. The ΔH_{H_2} can also be calculated on a strain compensation basis:

$$\Delta H_{H_2} = \Delta H_{f\text{product}} - \Delta H_{f\text{reactant}} + \text{strain relief}$$

The calculated values are included in the table. Compare the calculated and experimental results.

Calculated Heats of Hydrogenation of Norbornane Analogs^a

Compound	MM ^b	MNDO	AM1	PM3	Exp.
Norbornadiene	-68.3(1.5)	-73.1(-3.3)	-82.1(-12.3)	-72.5(-2.7)	-69.8
Norbornene	-32.3(1.5)	-35.7(-1.9)	-40.4(-6.6)	-35.7(-1.9)	-33.8
Nortricyclane	-32.3(0.3)	-37.5(-4.9)	-48.2(-15.6)	-33.7(-1.1)	-32.6
Quadricyclane	-92.2(-0.3)	-89.5(2.4)	-118.8(-26.9)	-100.0(-8.1)	-91.9

a. The numbers in parenthesis are the difference with the experimental value on a strain-compensated basis.

- 3.17. The second-order rate constants for the reaction of a number of amines with benzyl chloride are tabulated below. Calculate ΔH^\ddagger and ΔS^\ddagger from the data.

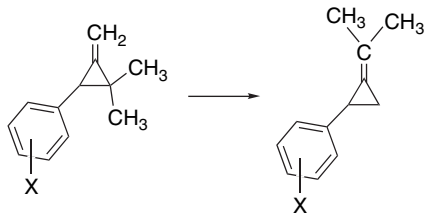
Rate Constants for the Reaction of Tertiary Amines with Benzyl Chloride

Amine	Rate constants $10^5 k_2(M^{-1} s^{-1})$								
	20° C	24° C	30° C	40° C	50° C	60° C	70° C	80° C	90° C
(CH ₃) ₃ N	38.2	50.2	72.8						
(C ₂ H ₅) ₃ N				1.67	3.07	4.54	7.49		
(C ₃ H ₇) ₃ N				0.354	0.633	1.05	1.76	3.04	
(C ₄ H ₉) ₃ N				0.471	0.844	1.24	1.94	3.22	
(C ₆ H ₁₃) ₃ N				0.290	0.566	0.860	1.54	2.62	
(C ₈ H ₁₇) ₃ N				0.336	0.570	0.912	1.60	2.73	
PhN(CH ₃) ₂						0.135	0.233	0.384	0.698
Pyridine				0.168	0.337	0.910	1.55	2.63	
Quinoline					0.051	0.105	0.226	0.457	0.820

- 3.18. Some data are given below for both gas phase (ΔG) and DMSO (pK) acidity of substituted toluenes, phenylacetonitriles, and phenylmalononitriles that illustrate the strongly acidifying effect of the cyano substituent. For each series, plot ΔG versus pK. Do the plots show any evidence of a solvent attenuation effect; that is, do the substituent effects appear to be weaker in DMSO than in the gas phase?

Group	σ	Toluenes		Phenylacetonitriles		Phenylmalononitriles	
		ΔG_{gas}	pK	ΔG_{gas}	pK	ΔG_{gas}	pK
H	0.0	373.7	43.0	344.1	21.9	314.3	4.24
4-NO ₂	0.78	345.2	20.4	323.3	12.3	299.5	-1.8
3-NO ₂	0.71	355.7	33.5	330.9	18.1	303.0	1.7
4-CN	0.66	353.6	30.7	327.9	16.0		
3-CN	0.56			332.3	18.7	304.4	2.2
4-SO ₂ CF ₃	0.96	340.7	24.1				
4-SO ₂ Ph		352.1	29.8				
4-SO ₂ CH ₃	0.72	359.3					
4-PhCO	0.43	353.5	26.8				
4-CH ₃ CO	0.50	354.9					
4-CF ₃ CO	0.80	344.1					
4-CH ₃ O ₂ C	0.45	355.4					
4-(CH ₃) ₂ NCO	0.36	367.0					
4-CF ₃	0.54			332.9	18.1		
3-CF ₃	0.43			335.3	19.2		
4-Cl	0.23			338.5	20.5	309.0	3.14
3-Cl	0.37			337.5	19.5	308.8	2.7
4-F	0.06			342.4	22.2		
3-F	0.34			344.0	20.0		
4-CH ₃ O	-0.27			345.0	23.8	315.4	5.68
3-CH ₃ O	0.12			342.8			
4-CH ₃	-0.17			345.0	22.9	315.7	4.85
3-CH ₃	-0.07			344.2			
4-(CH ₃) ₂ N	-0.83			346.6	24.6		

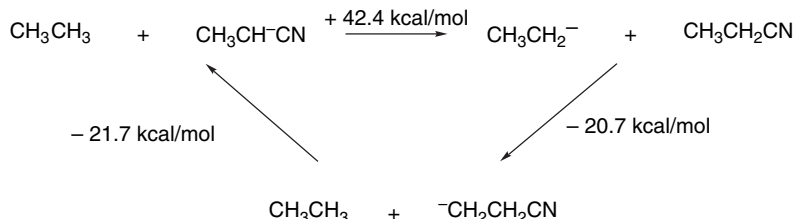
- 3.19. The rate of thermal rearrangement of 3-aryl-2,2-dimethylmethylenecyclopropanes has been studied as a function of aryl substituents. Some of the data are given below. Examine the rate data for correlation with the Hammett σ -substituent constants. What conclusion do you draw about the mechanism?



Substituent	$10^4 \text{ } k \text{ s}^{-1}$	Substituent	$10^4 \text{ } k \text{ s}^{-1}$
4-(CH ₃) ₂ N	28.2 ^a	3-CH ₃ O	3.40
4-CH ₂ =CH	16.7 ^a	3-Cl	3.30
4-NO ₂	13.5 ^a	3-F	3.17
4-CN	10.28	3-CF ₃	3.08
4-Ph	10.3 ^a	4-F	2.98
4-CH ₃ S	9.53	3-NO ₂	2.76 ^a
4-CO ₂ CH ₃	8.09	3-CN	2.69
4-CH ₃ O	6.16		
4-(CH ₃) ₃ Si	5.24		
4-Br	4.88		
4-(CH ₃) ₃ C	4.78		
4-Cl	4.75		
4-CH ₃	4.65		
4-CF ₃	4.25		
3-(CH ₃) ₃ Si	3.87		
3-CH ₃	3.82		
H	3.58		

a. Calculated from relative rate at 80° C in benzene.

- 3.20. The series of isodesmic reactions shown below has been calculated at the MP2/aug-cc-PVDZ level. The results are in good agreement with experimental gas phase proton affinity data.

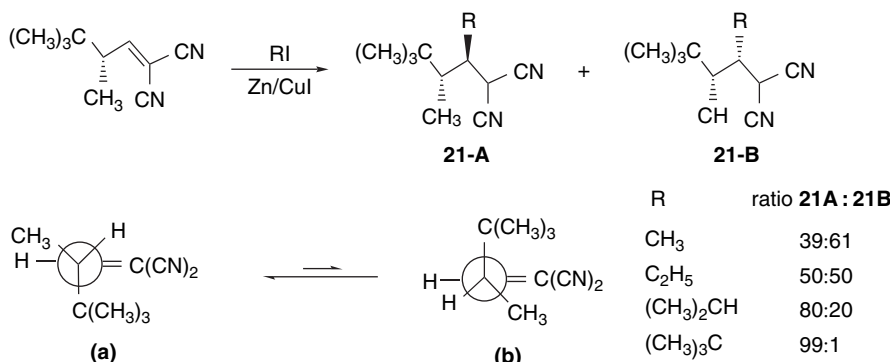


Data are also available for the pK_a of mono-, di-, and tri-cyanomethane. These data suggest substantially less cumulative drop-off as compared to an acetyl substituent. The first acetyl group causes a substantially *larger* increase in acidity, whereas the second acetyl has a *smaller* effect.

CH_4	CH_3CN	$\text{CH}_2(\text{CN})_2$	$\text{CH}(\text{CN})_3$	$\begin{array}{c} \text{O} \\ \parallel \\ \text{CH}_3\text{CCH}_3 \end{array}$	$\begin{array}{c} \text{O} \\ \parallel \\ \text{CH}_3\text{CCH}_2\text{CCH}_3 \end{array}$	
pK	49.6	29.4	11.7	-5.1	19.3	8.9

β -Cyano substituents also have a quite strong acidifying effect. A value of 29 ± 6 kcal/mol has been estimated, as compared to 42 kcal/mol for α -cyano. Structural computations find a shortening of the C(α)-CN bond in α -cyanoethyl anion but a lengthening of the C(β)-CN bond in the β -cyanoethyl anion. What structural features of the CN might contribute to its anion stabilizing capacity, as compared with other EWG substituents such as acetyl.

- 3.21. The diastereoselectivity of alkyl radical addition to substituted alkylidene malononitriles is a function of the size of the attacking radical when there is a bulky substituent at the γ -carbon. Conformational analysis of the reactant indicates that it prefers conformation **a** over **b** by 3.0 kcal/mol. Suggest a TS structure, showing reactant conformation and reagent trajectory that is in accord with these results. Use the Curtin-Hammett principle (p. 296) to construct a reaction energy diagram that illustrates the product composition in terms of TS energy.



- 3.22. In the interpretation of substituent effects, consideration must be given as to whether the effect is primarily on the reactant or the product. Some data pertaining to the changes in some substituted benzoic acids, derived from PM3 computations, are given below. The calculated $\delta\Delta H$ for ionization in the gas phase is given, as are the charges of the H, CO_2H , and CO_2^- groups and the energy of the anion HOMO. Construct correlation plots of $\delta\Delta H$ with each of the structural properties and also against the values of σ_m and σ_p from Table 3.26. What conclusions do you draw about the effects of substituents on H, CO_2H , and CO_2^- , and how would these results be reflected in relative acidity?

Substituent	$\delta\Delta H$	$q\text{H}$	$q\text{CO}_2\text{H}$	$q\text{CO}_2^-$	$\text{HOMO}_{(\text{anion})}$ (eV)
H	0	0.229	-0.0503	-1.237	-4.4549
4-F	-3.68	0.231	-0.0436	-1.229	-4.6395
3-F	-4.02	0.231	-0.0415	-1.224	-4.6487

(Continued)

Substituent	$\delta\Delta H$	qH	qCO_2H	qCO_2^-	$HOMO_{(anion)}$ (eV)
4-Cl	-3.11	0.230	-0.0460	-1.227	-4.6383
3-Cl	-3.10	0.230	-0.0440	-1.226	-4.6323
4-CN	-7.95	0.232	-0.0385	-1.215	-4.8765
3-CN	-7.49	0.232	-0.0368	-1.217	-4.8451
4-NO ₂	-12.98	0.234	-0.0297	-1.199	-5.1198
3-NO ₂	-11.14	0.235	-0.0277	-1.207	-5.0247
4-CH ₃	+0.44	0.228	-0.0519	-1.237	-4.4563
3-CH ₃	+0.22	0.228	-0.0514	-1.237	-4.4585
4-OCH ₃	+0.15	0.228	-0.0520	-1.237	-4.5000
3-OCH ₃	-0.36	0.228	-0.0490	-1.230	-4.5047

- 3.23. From the kinetic data below, calculate ΔH^* and ΔS^* for each nucleophilic substitution reaction with *n*-butyl tosylate in methanol and DMSO. What trends do you note in ΔH^* and how would you explain them? What trends do you note in ΔS^* and how would you explain them?

Nucleophile	Solvent	Second-order rate constants (in $\text{mol}^{-1} \text{s}^{-1} \times 10^4$) at °C			
		k_{20}	k_{30}	k_{40}	k_{50}
Cl ⁻	DMSO	5.06	16.7	50.4	
	MeOH	0.00550	0.0226	0.0852	
N ₃ ⁻	DMSO	16.1	48.3	135	
	MeOH	0.152	0.514	1.66	
Br ⁻	DMSO	1.75	5.69	17.8	
	MeOH	0.0191	0.0721	0.250	
SCN ⁻	DMSO	0.115	0.365	1.11	
	MeOH	0.0512	0.165	0.481	
I ⁻	DMSO		1.75	5.50	16.0
	MeOH	0.0767	0.275	0.956	

- 3.24. Use the computed values of H_{298} (in Hartrees) from the reference set below to construct homo desmotic reactions and calculate the stabilization or destabilization (strain) of the following molecules.

- 1,3,5,7-Cyclooctatetraene, $H_{298} = -308.96286$
- Bicyclo[1.1.0]butane, $H_{298} = -155.62203$
- Tetracyclo[3.2.0.0^{4,9}0^{6,8}]heptane (Quadricyclane), $H_{298} = -567.74092$

Reference Data^a

CH ₄	-40.40707	CH ₂ =CH ₂	-78.41192	c-C ₃ H ₆	-116.37701
C ₂ H ₆	-79.62641	CH ₃ CH=CH ₂	-117.63998	c-C ₄ H ₈	-156.85340
C ₃ H ₈	-118.85022	CH ₂ =C=CH ₂	-116.41308	C ₆ H ₆	-231.77508
C ₄ H ₁₀	-158.07430	(CH ₃) ₂ C=CH ₂	-156.86995		
i-C ₄ H ₁₀	-158.07751	CH ₂ =CHCH=CH ₂	-155.65855		

a. L. A. Curtiss, K. Raghavachari, P. C. Refern, and J. A. Pople, *J. Chem. Phys.*, **106**, 1063 (1997)

Nucleophilic Substitution

Introduction

Nucleophilic substitution at tetravalent (sp^3) carbon is a fundamental reaction of broad synthetic utility and has been the subject of detailed mechanistic study. An interpretation that laid the basis for current understanding was developed in England by C. K. Ingold and E. D. Hughes in the 1930s.¹ Organic chemists have continued to study substitution reactions; much detailed information about these reactions is available and a broad mechanistic interpretation of nucleophilic substitution has been developed from the accumulated data. At the same time, the area of nucleophilic substitution also illustrates the fact that while a broad conceptual framework can outline the general features to be expected for a given system, finer details reveal distinctive aspects that are characteristic of specific systems. As the chapter unfolds, the reader will come to appreciate both the breadth of the general concepts and the special characteristics of some of the individual systems.

4.1. Mechanisms for Nucleophilic Substitution

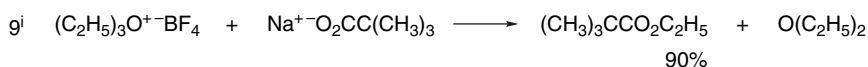
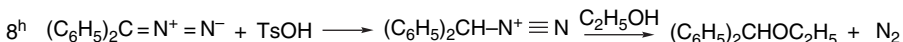
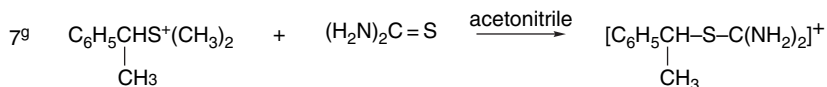
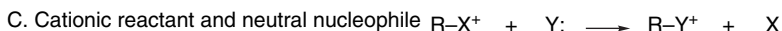
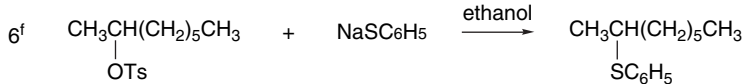
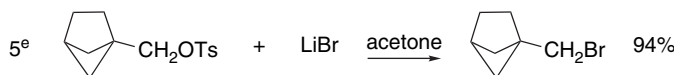
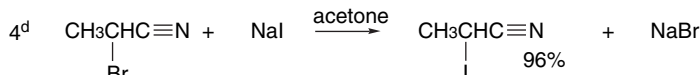
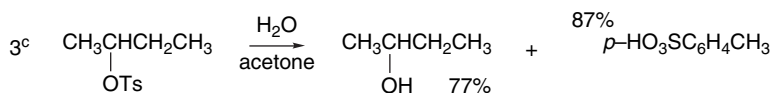
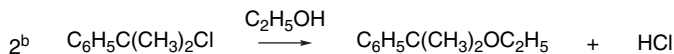
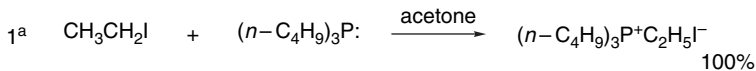
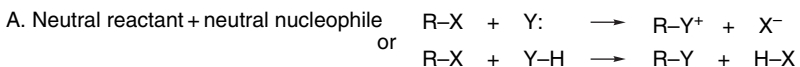
Nucleophilic substitution reactions may involve several different combinations of charged and uncharged species as reactants. The equations in Scheme 4.1 illustrate the four most common charge types. The most common reactants are neutral halides or sulfonates, as illustrated in Parts A and B of the scheme. These compounds can react with either neutral or anionic nucleophiles. When the nucleophile is the solvent, as in Entries 2 and 3, the reaction is called a *solvolytic*. Reactions with anionic nucleophiles, as in Entries 4 to 6, are used to introduce a variety of substituents such as cyanide and azide. Entries 7 and 10 show reactions that involve sulfonium ions, in which a neutral sulfide is the leaving group. Entry 8 involves generation of the diphenylmethyl diazonium ion by protonation of diphenyldiazomethane. In this reaction, the leaving

¹ C. K. Ingold, *Structure and Mechanism in Organic Chemistry*, 2nd Edition, Cornell University Press, Ithaca, NY, 1969.

group is molecular nitrogen. Alkyl diazonium ions can also be generated by nitrosation of primary amines (see Section 4.1.5). Entry 9 is a reaction of an oxonium ion. These ions are much more reactive than sulfonium ions and are usually generated by some *in situ* process.

The reactions illustrated in Scheme 4.1 show the relationship of reactants and products in nucleophilic substitution reactions, but say nothing about mechanism. In

Scheme 4.1. Representative Nucleophilic Substitution Reactions



a. S. A. Buckler and W. A. Henderson, *J. Am. Chem. Soc.*, **82**, 5795 (1960).

b. R. L. Buckson and S. G. Smith, *J. Org. Chem.*, **32**, 634 (1967).

c. J. D. Roberts, W. Bennett, R. E. McMahon, and E. W. Holroyd, *J. Am. Chem. Soc.*, **74**, 4283 (1952).

d. M. S. Newman and R. D. Closson, *J. Am. Chem. Soc.*, **66**, 1553 (1944).

e. K. B. Wiberg and B. R. Lowry, *J. Am. Chem. Soc.*, **85**, 3188 (1963).

f. H. L. Goering, D. L. Towns, and B. Dittmar, *J. Org. Chem.*, **27**, 736 (1962).

g. H. M. R. Hoffmann and E. D. Hughes, *J. Chem. Soc.*, 1259 (1964).

h. J. D. Roberts and W. Watanabe, *J. Am. Chem. Soc.*, **72**, 4869 (1950).

i. D. J. Raber and P. Gariano, *Tetrahedron Lett.*, 4741 (1971).

j. E. J. Corey and M. Jautelat, *Tetrahedron Lett.*, 5787 (1968).

order to develop an understanding of the mechanisms of such reactions, we begin by reviewing the limiting cases as defined by Hughes and Ingold, namely the *ionization mechanism* (S_N1 , substitution-nucleophilic-unimolecular) and the *direct displacement mechanism* (S_N2 , substitution-nucleophilic-bimolecular). We will find that in addition to these limiting cases, there are related mechanisms that have aspects of both ionization and direct displacement.

4.1.1. Substitution by the Ionization (S_N1) Mechanism

The ionization mechanism for nucleophilic substitution proceeds by rate-determining heterolytic dissociation of the reactant to a tricoordinate *carbocation*² and the *leaving group*. This dissociation is followed by rapid combination of the electrophilic carbocation with a Lewis base (*nucleophile*) present in the medium. A potential energy diagram representing this process for a neutral reactant and anionic nucleophile is shown in Figure 4.1.

The ionization mechanism has several distinguishing features. The ionization step is rate determining and the reaction exhibits first-order kinetics, with the rate of decomposition of the reactant being *independent of the concentration and identity of the nucleophile*. The symbol assigned to this mechanism is S_N1 , for *substitution, nucleophilic, unimolecular*:

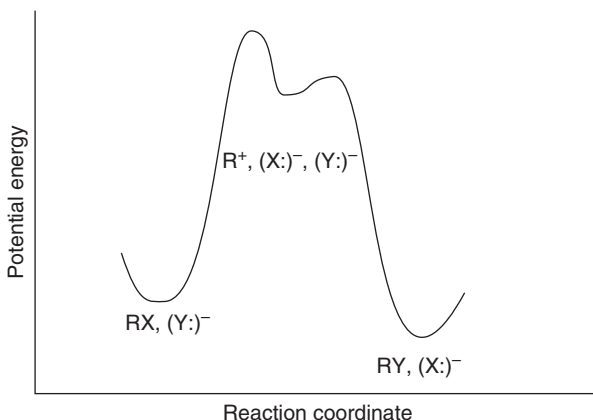
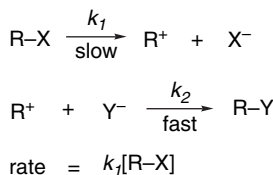


Fig. 4.1. Reaction energy profile for nucleophilic substitution by the ionization (S_N1) mechanism.

². Tricoordinate carbocations were originally called *carbonium ions*. The terms methyl cation, butyl cation, etc., are used to describe the corresponding tricoordinate cations. *Chemical Abstracts* uses as specific names methylum, ethylum, 1-methylethylum, and 1,1-dimethylethylum to describe the methyl, ethyl, 2-propyl, and *t*-butyl cations, respectively. We use *carbocation* as a generic term for carbon cations. The term *carbonium ion* is now used for pentavalent positively charged carbon species.

As the rate-determining step is endothermic with a late TS, application of *Hammond's postulate* (Section 3.3.2.2) indicates that the TS should resemble the product of the first step, the carbocation intermediate. Ionization is facilitated by factors that lower the energy of the carbocation or raise the energy of the reactant. The rate of ionization depends primarily on reactant structure, including the identity of the leaving group, and the solvent's ionizing power. The most important electronic effects are stabilization of the carbocation by electron release, the ability of the leaving group to accept the electron pair from the covalent bond that is broken, and the capacity of the solvent to stabilize the charge separation that develops in the TS. Steric effects are also significant because of the change in coordination that occurs on ionization. The substituents are spread apart as ionization proceeds, so steric compression in the reactant favors ionization. On the other hand, geometrical constraints that preclude planarity of the carbocation are unfavorable and increase the energy required for ionization.

The ionization process is very sensitive to solvent effects, which are dependent on the charge type of the reactants. These relationships follow the general pattern for solvent effects discussed in Section 3.8.1. Ionization of a neutral substrate results in charge separation, and solvent polarity has a greater effect at the TS than for the reactants. Polar solvents lower the energy of the TS more than solvents of lower polarity. In contrast, ionization of cationic substrates, such as trialkylsulfonium ions, leads to dispersal of charge in the TS and reaction rates are moderately retarded by more polar solvents because the reactants are more strongly solvated than the TS. These relationships are illustrated in Figure 4.2.

Stereochemical information can add detail to the mechanistic picture of the S_N1 substitution reaction. The ionization step results in formation of a carbocation intermediate that is planar because of its sp^2 hybridization. If the carbocation is sufficiently long-lived under the reaction conditions to diffuse away from the leaving group, it becomes symmetrically solvated and gives racemic product. If this condition is not met, the solvation is dissymmetric and product can be obtained with net retention or inversion of configuration, even though an achiral carbocation is formed. The extent of inversion or retention depends on the specific reaction. It is frequently observed that there is net *inversion of configuration*. The stereochemistry can be interpreted in terms of three different stages of the ionization process. The contact ion pair represents

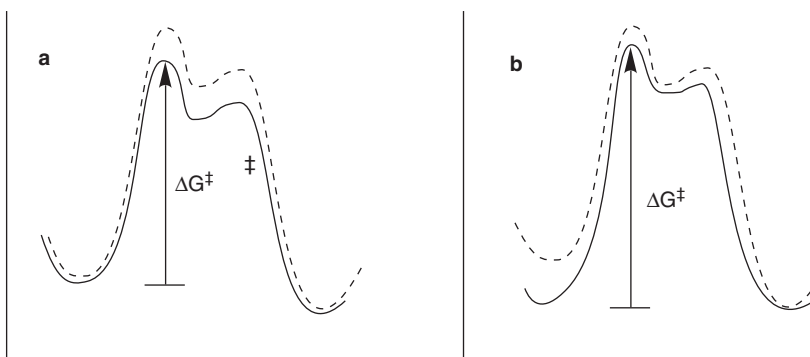
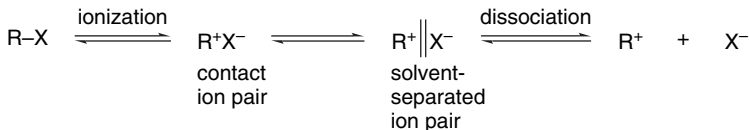


Fig. 4.2. Solid line: polar solvent; dashed line: nonpolar solvent. (a) Solvent effects on $R-X \rightarrow R^+ + X^-$. Polar solvents increase the rate by stabilization of the $R^{\delta+} \cdots X^{\delta-}$ transition state. (b) Solvent effect on $R-X^+ \rightarrow R^+ + X$. Polar solvents decrease the rate because stabilization of $R \cdots X^{\delta+}$ transition state is less than for the more polar reactant.

a very close association between the cation and anion formed in the ionization step. The solvent-separated ion pair retains an association between the two ions, but with intervening solvent molecules. Only at the dissociation stage are the ions independent and the carbocation symmetrically solvated. The tendency toward net inversion is believed to be due to electrostatic shielding of one face of the carbocation by the anion in the ion pair. The importance of ion pairs is discussed further in Sections 4.1.3 and 4.1.4.



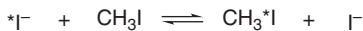
According to the ionization mechanism, if the same carbocation can be generated from more than one precursor, its subsequent reactions should be independent of its origin. But, as in the case of stereochemistry, this expectation must be tempered by the fact that ionization initially produces an ion pair. If the subsequent reaction takes place from this ion pair, rather than from the completely dissociated and symmetrically solvated ion, the leaving group can influence the outcome of the reaction.

4.1.2. Substitution by the Direct Displacement (S_N2) Mechanism

The direct displacement mechanism is concerted and proceeds through a single rate-determining TS. According to this mechanism, the reactant is attacked by a nucleophile from the side opposite the leaving group, with bond making occurring simultaneously with bond breaking between the carbon atom and the leaving group. The TS has trigonal bipyramidal geometry with a pentacoordinate carbon. These reactions exhibit second-order kinetics with terms for both the reactant and nucleophile:

$$\text{rate} = k[\text{R-X}][\text{Nu :}]$$

The mechanistic designation is S_N2 for *substitution, nucleophilic, bimolecular*. A reaction energy diagram for direct displacement is given in Figure 4.3. A symmetric diagram such as the one in the figure would correspond, for example, to exchange of iodide by an S_N2 mechanism.



The frontier molecular orbital approach provides a description of the bonding interactions that occur in the S_N2 process. The frontier orbitals are a filled nonbonding orbital on the nucleophile Y: and the σ^* antibonding orbital associated with the carbon undergoing substitution and the leaving group X. This antibonding orbital has a large lobe on carbon directed away from the C–X bond.³ Back-side approach by the nucleophile is favored because the strongest initial interaction is between the filled orbital on the nucleophile and the antibonding σ^* orbital. As the transition state is approached, the orbital at the substitution site has p character. The MO picture predicts that the reaction will proceed with inversion of configuration, because the development

³. L. Salem, *Chem. Brit.*, **5**, 449 (1969); L. Salem, *Electrons in Chemical Reactions: First Principles*, Wiley, New York, 1982, pp. 164–165.

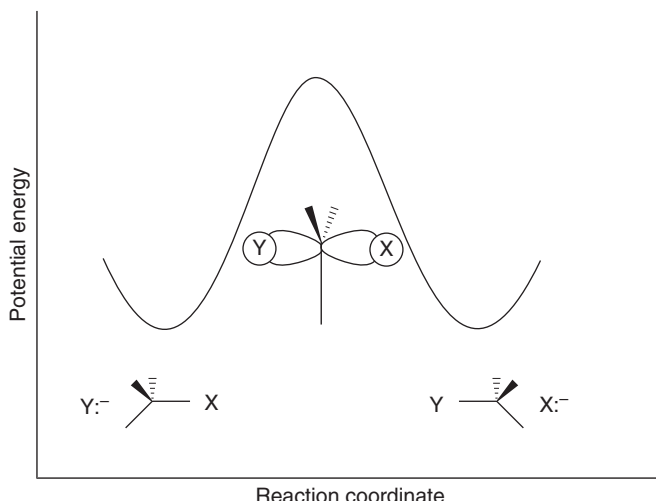
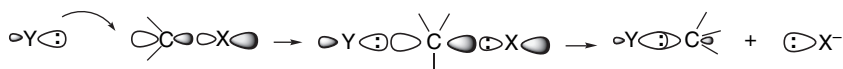
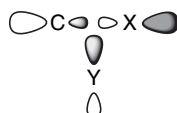


Fig. 4.3. Reaction energy profile for nucleophilic substitution by the direct displacement (S_N2) mechanism.

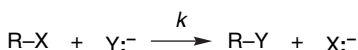
of the TS is accompanied by rehybridization of the carbon to the trigonal bipyramidal geometry. As the reaction proceeds on to product, sp^3 hybridization is reestablished in the product with inversion of configuration.



Front-side approach is disfavored because the density of the σ^* orbital is less in the region between the carbon and the leaving group and, as there is a nodal surface between the atoms, a front-side approach would involve both a bonding and an antibonding interaction with the σ^* orbital.



The direct displacement (S_N2) mechanism has both kinetic and stereochemical consequences. S_N2 reactions exhibit second-order kinetics—first order in both reactant and nucleophile. Because the nucleophile is intimately involved in the rate-determining step, not only does the rate depend on its concentration, but the nature of the nucleophile is very important in determining the rate of the reaction. This is in sharp contrast to the ionization mechanism, in which the identity and concentration of the nucleophile do not affect the rate of the reaction.



$$\text{rate} = -\frac{d[\text{R-X}]}{dt} = -\frac{d[\text{Y}^-]}{dt} = k[\text{R-X}][\text{Y}^-]$$

Owing to the fact that the degree of coordination increases at the reacting carbon atom, the rates of S_N2 reactions are very sensitive to the steric bulk of the substituents.

The optimum reactant from a steric point of view is $\text{CH}_3\text{-X}$, because it provides the minimum hindrance to approach of the nucleophile. Each replacement of hydrogen by an alkyl group decreases the rate of reaction. As in the case of the ionization mechanism, the better the leaving group is able to accommodate an electron pair, the faster the reaction. Leaving group ability is determined primarily by the C–X bond strength and secondarily by the relative stability of the anion (see Section 4.2.3). However, since the nucleophile assists in the departure of the leaving group, the leaving group effect on rate is less pronounced than in the ionization mechanism.

Two of the key observable characteristics of S_N1 and S_N2 mechanisms are kinetics and stereochemistry. These features provide important evidence for ascertaining whether a particular reaction follows an ionization (S_N1) or direct displacement (S_N2) mechanism. Both kinds of observations have limits, however. Many nucleophilic substitutions are carried out under conditions in which the nucleophile is present in large excess. When this is the case, the concentration of the nucleophile is essentially constant during the reaction and the observed kinetics become *pseudo first order*. This is true, for example, when the solvent is the nucleophile (*solvolytic*). In this case, the kinetics of the reaction provides no evidence as to whether the S_N1 or S_N2 mechanism is operating. Stereochemistry also sometimes fails to provide a clear-cut distinction between the two limiting mechanisms. Many substitutions proceed with partial inversion of configuration rather than the complete racemization or inversion implied by the limiting mechanisms. Some reactions exhibit inversion of configuration, but other features of the reaction suggest that an ionization mechanism must operate. Other systems exhibit “borderline” behavior that makes it difficult to distinguish between the ionization and direct displacement mechanism. The reactants most likely to exhibit borderline behavior are secondary alkyl and primary and secondary benzylic systems. In the next section, we examine the characteristics of these borderline systems in more detail.

4.1.3. Detailed Mechanistic Description and Borderline Mechanisms

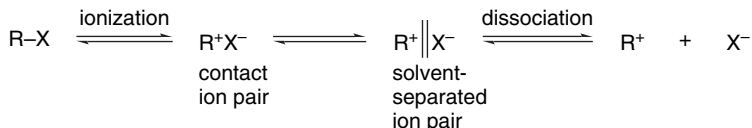
The ionization and direct displacement mechanisms can be viewed as the limits of a mechanistic continuum. At the S_N1 limit, there is *no covalent interaction* between the reactant and the nucleophile in the TS for cleavage of the bond to the leaving group. At the S_N2 limit, the bond-formation to the nucleophile is *concerted* with the bond-breaking step. In between these two limiting cases lies the borderline area in which the degree of covalent interaction with the nucleophile is intermediate between the two limiting cases. The concept of ion pairs was introduced by Saul Winstein, who proposed that there are two distinct types of ion pairs involved in substitution reactions.⁴ The role of ion pairs is a crucial factor in detailed interpretation of nucleophilic substitution mechanisms.⁵

Winstein concluded that two intermediates preceding the dissociated carbocation were required to reconcile data on kinetics and stereochemistry of solvolysis reactions. The process of ionization initially generates a carbocation and counterion in immediate

⁴. S. Winstein, E. Clippinger, A. H. Fainberg, R. Heck, and G. C. Robinson, *J. Am. Chem. Soc.*, **78**, 328 (1956); S. Winstein, B. Appel, R. Baker, and A. Diaz, *Chem. Soc. Spec. Publ.*, No. 19, 109 (1965).

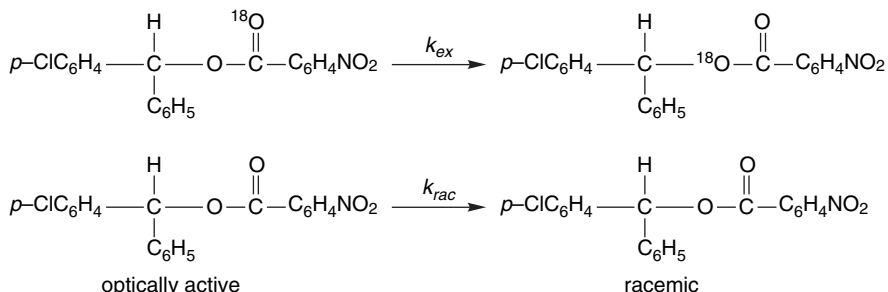
⁵. J. M. Harris, *Prog. Phys. Org. Chem.*, **11**, 89 (1984); D. J. Raber, J. M. Harris, and P. v. R. Schleyer, in *Ion Pairs*, M. Szwarc, ed., John Wiley & Sons, New York, 1974, Chap. 3; T. W. Bentley and P. v. R. Schleyer, *Adv. Phys. Org. Chem.*, **14**, 1 (1977); J. P. Richard, *Adv. Carbocation Chem.*, **1**, 121 (1989); P. E. Dietze, *Adv. Carbocation Chem.*, **2**, 179 (1995).

proximity to one another. This species, called a contact ion pair (or intimate ion pair), can proceed to a solvent-separated ion pair in which one or more solvent molecules are inserted between the carbocation and leaving group, but in which the ions are kept together by the electrostatic attraction. The “free carbocation,” characterized by symmetrical solvation, is formed by diffusion from the anion, a process known as *dissociation*.



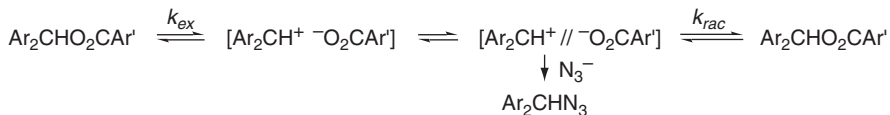
Attack by a nucleophile or the solvent can occur at each stage. Nucleophilic attack on the contact ion pair is expected to occur with inversion of configuration, since the leaving group will shield the front side of the carbocation. At the solvent-separated ion pair stage, the nucleophile can approach from either face, particularly in the case where the solvent is the nucleophile. However, the anionic leaving group may shield the front side and favor attack by external nucleophiles from the back side. Reactions through dissociated carbocations should occur with complete *racemization*. According to this interpretation, the identity and stereochemistry of the reaction products are determined by the extent to which reaction with the nucleophile occurs on the un-ionized reactant, the contact ion pair, the solvent-separated ion pair, or the dissociated carbocation.

Many specific experiments support this general scheme. For example, in 80% aqueous acetone, the rate constant for racemization of *p*-chlorobenzhydryl *p*-nitrobenzoate and the rate of exchange of the ^{18}O in the carbonyl oxygen can be compared with the rate of racemization.⁶ At 100 °C, $k_{\text{ex}}/k_{\text{rac}} = 2.3$.

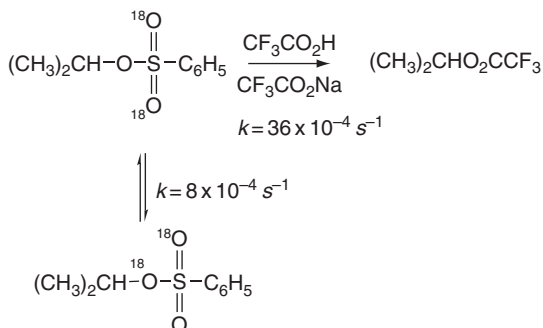


If it is assumed that ionization results in complete randomization of the ^{18}O label in the carboxylate ion, k_{ex} is a measure of the rate of ionization with ion pair return and k_{rac} is a measure of the extent of racemization associated with ionization. The fact that the rate of isotopic exchange exceeds that of racemization indicates that ion pair collapse occurs with predominant retention of configuration. This is called *internal return*. When a better nucleophile is added to the system (0.14 M NaN_3), k_{ex} is found to be unchanged, but no racemization of reactant is observed. Instead, the intermediate that can racemize is captured by azide ion and converted to substitution product with inversion of configuration. This must mean that the contact ion pair returns to the

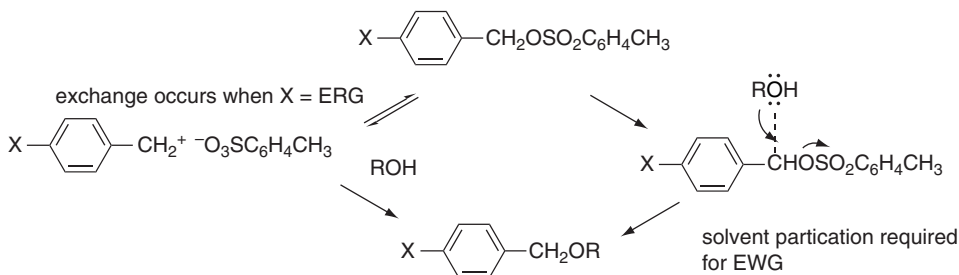
⁶ H. L. Goering and J. F. Levy, *J. Am. Chem. Soc.*, **86**, 120 (1964).



Several other cases have been studied in which isotopic labeling reveals that the bond between the leaving group and carbon is able to break without net substitution. A particularly significant case involves secondary alkyl sulfonates, which frequently exhibit borderline behavior. During solvolysis of isopropyl benzenesulfonate in trifluoroacetic acid (TFA), it has been found that exchange among the sulfonate oxygens occurs at about one-fifth the rate of solvolysis,⁷ which implies that about one-fifth of the ion pairs recombine rather than react with the nucleophile. A similar experiment in acetic acid indicated about 75% internal return.



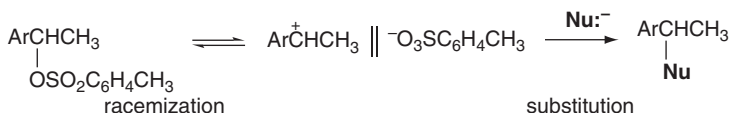
A study of the exchange reaction of benzyl tosylates during solvolysis in several solvents showed that with electron-releasing group (ERG) substituents, e.g., *p*-methylbenzyl tosylate, the degree of exchange is quite high, implying reversible formation of a primary benzyl carbocation. For an electron-withdrawing group (EWG), such as *m*-Cl, the amount of exchange was negligible, indicating that reaction occurred only by displacement involving the solvent. When an EWG is present, the carbocation is too unstable to be formed by ionization. This study also demonstrated that there was no exchange with added “external” tosylate anion, proving that isotopic exchange occurred only at the ion pair stage.⁸



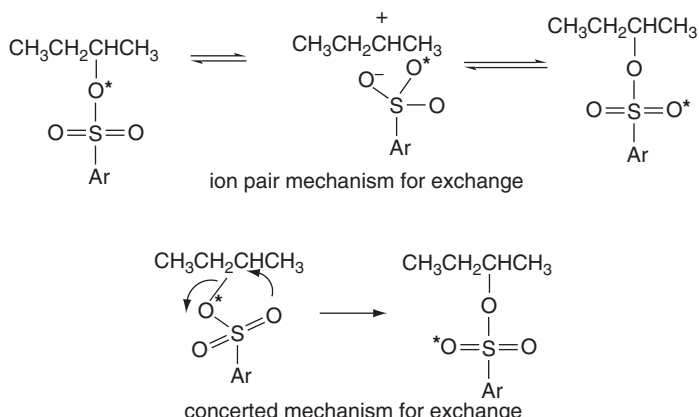
⁷. C. Paradisi and J. F. Bunnett, *J. Am. Chem. Soc.*, **107**, 8223 (1985).

⁸. Y. Tsuji, S. H. Kim, Y. Saek, K. Yatsugi, M. Fuji, and Y. Tsuno, *Tetrahedron Lett.*, **36**, 1465 (1995).

The ion pair return phenomenon can also be demonstrated by comparing the rate of racemization of reactant with the rate of product formation. For a number of systems, including 1-arylethyl tosylates,⁹ the rate of decrease of optical rotation is greater than the rate of product formation, which indicates the existence of an intermediate that can re-form racemic reactant. The solvent-separated ion pair is the most likely intermediate to play this role.



Racemization, however, does not always accompany isotopic scrambling. In the case of 2-butyl 4-bromobenzenesulfonate, isotopic scrambling occurs in trifluoroethanol solution without any racemization. Isotopic scrambling probably involves a contact ion pair in which the sulfonate can rotate with respect to the carbocation without migrating to its other face. The unlikely alternative is a concerted mechanism, which avoids a carbocation intermediate but requires a front-side displacement.¹⁰



The idea that ion pairs are key participants in nucleophilic substitution is widely accepted. The energy barriers separating the contact, solvent-separated, and dissociated ions are thought to be quite small. The reaction energy profile in Figure 4.4 depicts the three ion pair species as being roughly equivalent in energy and separated by small barriers.

The gradation from S_N1 to S_N2 mechanisms can be summarized in terms of the shape of the potential energy diagrams for the reactions, as illustrated in Figure 4.5. Curves A and C represent the S_N1 and S_N2 limiting mechanisms. The gradation from the S_N1 to the S_N2 mechanism involves greater and greater nucleophilic participation by the solvent or nucleophile at the transition state.¹¹ An ion pair with strong nucleophilic participation represents a mechanistic variation between the

⁹ A. D. Allen, V. M. Kanagasabapathy, and T. T. Tidwell, *J. Am. Chem. Soc.*, **107**, 4513 (1985).

¹⁰ P. E. Dietze and M. Wojciechowski, *J. Am. Chem. Soc.*, **112**, 5240 (1990).

¹¹ T. W. Bentley and P. v. R. Schleyer, *Adv. Phys. Org. Chem.*, **14**, 1 (1977).

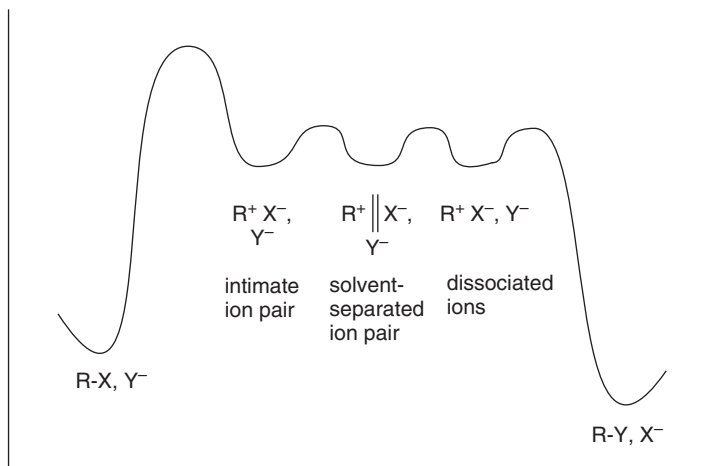
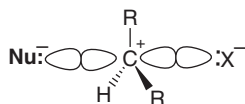


Fig. 4.4. Schematic relationship between reactants, ion pairs, and products in substitution proceeding through ion pairs.

S_N1 and S_N2 processes. This mechanism is represented by curve B and designated S_N2 (intermediate). It pictures a carbocation-like TS, but one that nevertheless requires back-side nucleophilic participation and therefore exhibits second-order kinetics.



Jencks¹² emphasized that the gradation from the S_N1 to the S_N2 mechanism is related to the stability and lifetime of the carbocation intermediate, as illustrated in Figure 4.6. In the S_N1 (lim) mechanism, the carbocation intermediate has a significant lifetime and is equilibrated with solvent prior to capture by a nucleophile. The reaction

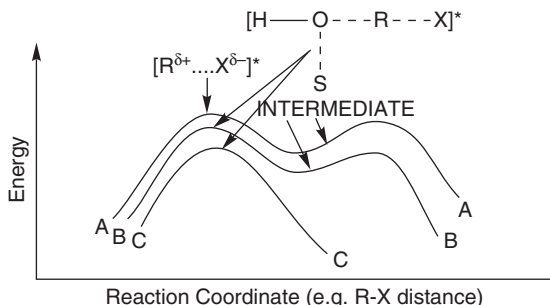


Fig. 4.5. Reaction energy profiles for substitution mechanisms. A is the S_N1 mechanism. B is the S_N2 mechanism with an intermediate ion pair or pentacoordinate species. C is the classical S_N2 mechanism. Reproduced from T. W. Bentley and P. v. R. Schleyer, *Adv. Phys. Org. Chem.*, **14**, 1 (1977), by permission of Academic Press.

¹² W. P. Jencks, *Acc. Chem. Res.*, **13**, 161 (1980).

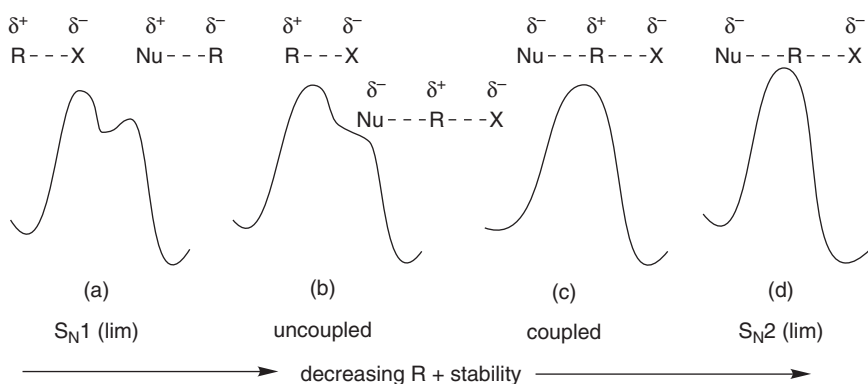
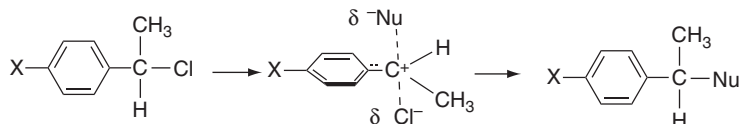


Fig. 4.6. Reaction energy profiles showing decreasing carbocation stability in change from $S_N1\text{(lim)}$ to $S_N2\text{(lim)}$ mechanisms.

is clearly stepwise and the energy minimum in which the carbocation intermediate resides is evident. As the stability of the carbocation decreases, its lifetime becomes shorter. The barrier to capture by a nucleophile becomes less and eventually disappears. This is described as the “uncoupled” mechanism. Ionization proceeds without nucleophilic participation but the carbocation does not exist as a free intermediate. Such reactions exhibit S_N1 kinetics, since there is no nucleophilic participation in the ionization. At still lesser carbocation stability, the lifetime of the ion pair is so short that it always returns to the reactant unless a nucleophile is present to capture it as it is formed. This type of reaction exhibits second-order kinetics, since the nucleophile must be present for reaction to occur. Jencks describes this as the “coupled” substitution process. Finally, when the stability of the (potential) carbocation is so low that it cannot form, the direct displacement mechanism [$S_N2\text{(lim)}$] operates. The continuum corresponds to decreasing carbocation character at the TS proceeding from $S_N1\text{(lim)}$ to $S_N2\text{(lim)}$ mechanisms. The degree of positive charge decreases from a full positive charge at a $S_N1\text{(lim)}$ to the possibility of net negative charge on carbon at the $S_N2\text{(lim)}$.

The reaction of azide ion with substituted 1-phenylethyl chlorides is an example of a coupled displacement. Although it exhibits second-order kinetics, the reaction has a substantially positive ρ value, indicative of an electron deficiency at the TS.¹³ The physical description of this type of activated complex is called the “exploded” S_N2 TS.



For many secondary sulfonates, nucleophilic substitution seems to be best explained by a coupled mechanism, with a high degree of carbocation character at the TS. The bonds to both the nucleophile and the leaving group are relatively weak, and the carbon has a substantial positive charge. However, the carbocation per se has no lifetime, because bond rupture and formation occur concurrently.¹⁴

¹³. J. P. Richard and W. P. Jencks, *J. Am. Chem. Soc.*, **106**, 1383 (1984).

¹⁴. B. L. Knier and W. P. Jencks, *J. Am. Chem. Soc.*, **102**, 6789 (1980); M. R. Skoog and W. P. Jencks, *J. Am. Chem. Soc.*, **106**, 7597 (1984).

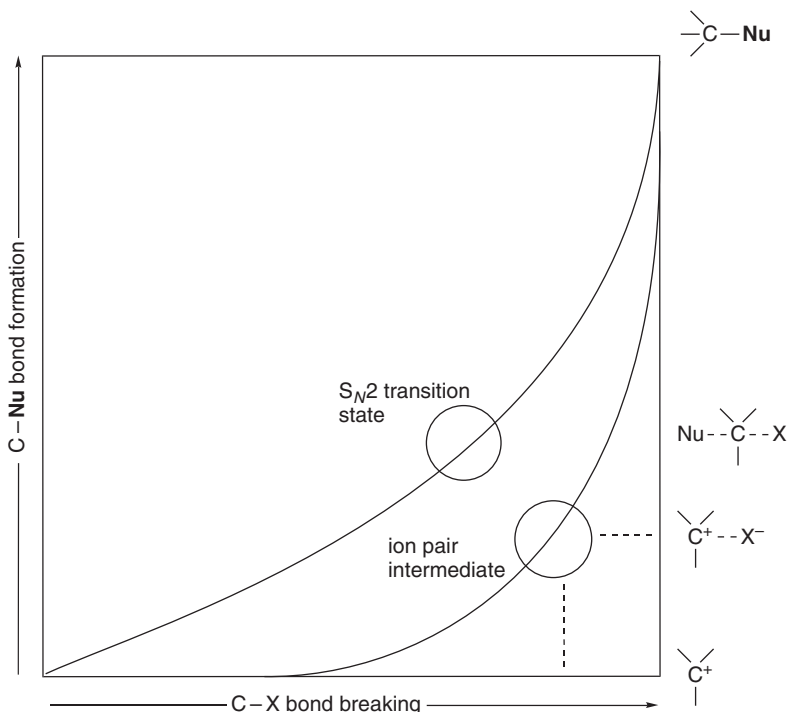


Fig. 4.7. Two-dimensional reaction energy diagram showing concerted, ion pair intermediate, and stepwise mechanisms for nucleophilic substitution.

Figure 4.7 summarizes these ideas using a two-dimensional energy diagram.¹⁵ The S_N2(lim) mechanism corresponds to the concerted pathway through the middle of the diagram. It is favored by high-energy carbocation intermediates that require nucleophilic participation. The S_N1(lim) mechanism is the path along the edge of the diagram corresponding to separate bond-breaking and bond-forming steps. An ion pair intermediate mechanism implies a true intermediate, with the nucleophile present in the TS, but at which bond formation has not progressed. The “exploded transition state” mechanism describes a very similar structure, but one that is a transition state, not an intermediate.¹⁶

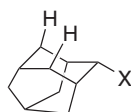
The importance of solvent participation in the borderline mechanisms should be noted. Solvent participation is minimized by high electronegativity and hardness, which reduce the Lewis basicity and polarizability of the solvent molecules. Trifluoroacetic acid and polyfluoro alcohols are among the least nucleophilic of the solvents commonly used in solvolysis studies.¹⁷ These solvents are used to define the characteristics of reactions proceeding with little nucleophilic solvent participation. Solvent nucleophilicity increases with the electron-donating capacity of the molecule. The order trifluoroacetic acid (TFA) < trifluoroethanol (TFE) < acetic acid < water < ethanol gives a qualitative indication of the trend in solvent nucleophilicity. More is said about solvent nucleophilicity in Section 4.2.1.

¹⁵. R. A. More O’Ferrall, *J. Chem. Soc. B*, 274 (1970).

¹⁶. For discussion of the borderline mechanisms, see J. P. Richard, *Adv. Carbocation Chem.*, **1**, 121 (1989); P. E. Dietze, *Adv. Carbocation Chem.*, **2**, 179 (1995).

¹⁷. T. W. Bentley, C. T. Bowen, D. H. Morten, and P. v. R. Schleyer, *J. Am. Chem. Soc.*, **103**, 5466 (1981).

Reactant structure also influences the degree of nucleophilic solvent participation. Solvation is minimized by steric hindrance and the 2-adamantyl system is regarded as being a secondary reactant that cannot accommodate significant back-side nucleophilic participation.



The 2-adamantyl system is used as a model reactant for defining the characteristics of ionization without solvent participation. The degree of nucleophilic participation in other reactions can then be estimated by comparison with the 2-adamantyl system.¹⁸

4.1.4. Relationship between Stereochemistry and Mechanism of Substitution

Studies of the stereochemistry are a powerful tool for investigation of nucleophilic substitution reactions. Direct displacement reactions by the $S_N2(\text{lim})$ mechanism are expected to result in complete inversion of configuration. The stereochemical outcome of the ionization mechanism is less predictable, because it depends on whether reaction occurs via an ion pair intermediate or through a completely dissociated ion. Borderline mechanisms may also show variable stereochemistry, depending upon the lifetime of the intermediates and the extent of ion pair recombination.

Scheme 4.2 presents data on some representative nucleophilic substitution processes. Entry 1 shows the use of 1-butyl-1-*d*,*p*-bromobenzenesulfonate (Bs, brosylate) to demonstrate that primary systems react with inversion, even under solvolysis conditions in formic acid. The observation of inversion indicates a concerted mechanism, even in this weakly nucleophilic solvent. The primary benzyl system in

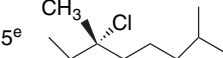
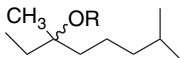
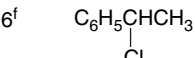
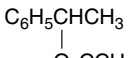
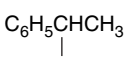
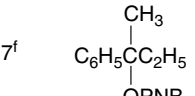
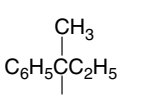
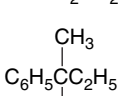
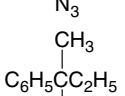
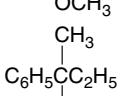
Scheme 4.2. Stereochemistry of Nucleophilic Substitution Reactions

	Reactant ^a	Conditions	Product	Stereochemistry
1 ^b	$\text{CH}_3\text{CH}_2\text{CH}_2\text{CHDOBs}$	HCO_2H 99°C	$\text{CH}_3\text{CH}_2\text{CH}_2\text{CHDO}_2\text{CH}$	$99 \pm 6\%$ inv.
2 ^c	$\text{C}_6\text{H}_5\text{CHDOTs}$	$\text{CH}_3\text{CO}_2\text{H}$ 25°C	$\text{C}_6\text{H}_5\text{CHDO}_2\text{CCH}_3$	$82 \pm 1\%$ inv.
3 ^c	$\begin{matrix} \text{CH}_3\text{CH}(\text{CH}_2)_5\text{CH}_3 \\ \\ \text{OTs} \end{matrix}$	$\text{Et}_4\text{N}^+ - \text{O}_2\text{CCH}_3$ acetone, 56°C	$\begin{matrix} \text{CH}_3\text{CH}(\text{CH}_2)_5\text{CH}_3 \\ \\ \text{O}_2\text{CCH}_3 \end{matrix}$	100% inv.
4 ^d	$\begin{matrix} \text{CH}_3\text{CH}(\text{CH}_2)_5\text{CH}_3 \\ \\ \text{OTs} \end{matrix}$	75 % aq. dioxane 65°C	$\begin{matrix} \text{CH}_3\text{CH}(\text{CH}_2)_5\text{CH}_3 \\ \\ \text{OH} \end{matrix}$	77% inv.
		75 % aq. dioxane $0.06\text{ M NaN}_3, 65^\circ\text{C}$	$\begin{matrix} \text{CH}_3\text{CH}(\text{CH}_2)_5\text{CH}_3 \\ \\ \text{OH} \end{matrix}$ 22%	100% inv.
			$\begin{matrix} \text{CH}_3\text{CH}(\text{CH}_2)_5\text{CH}_3 \\ \\ \text{N}_3 \end{matrix}$ 78%	100% inv.

(Continued)

¹⁸. F. L. Schadt, T. W. Bentley, and P. v. R. Schleyer, *J. Am. Chem. Soc.*, **98**, 7667 (1976).

Scheme 4.2. (Continued)

		SECTION 4.1	
		Mechanisms for Nucleophilic Substitution	
5 ^e			
		CH ₃ OH, DTBP, 25°C	78% inv.
		C ₂ H ₅ OH, DTBP, 40°C	55% inv.
		HCO ₂ H, DTBP, 0°C	42% inv.
		CF ₃ CH ₂ OH, DTBP, 25°C	13% ret.
		t-BuOH, 20% H ₂ O, 25°C dioxane, 20% H ₂ O, 25°C	49% inv. 98% inv.
6 ^f		K ⁺ -O ₂ CCH ₃ , CH ₃ CO ₂ H, 50°C	 15% inv.
		Et ₄ N ⁺ -O ₂ CCH ₃ 50% acetone	 65% inv.
7 ^f		K ⁺ -O ₂ CCH ₃ , CH ₃ CO ₂ H, 23°C	 5±2% inv.
		NaN ₃ in CH ₃ OH, 65°C	 56±1% inv.
		90% aq, acetone	 14% inv.
			 38% ret.

a. Abbreviations: OBs = *p*-bromobenzenesulfonate; OTs = *p*-toluenesulfonate; OPMB = *p*-nitrobenzoate; DTBP = 2,6-di-*t*-butylpyridine.

b. A. Streitwieser, Jr., *J. Am. Chem. Soc.*, **77**, 1117 (1955).

c. A. Streitwieser, Jr., T. D. Walsh, and J. R. Wolfe, *J. Am. Chem. Soc.*, **87**, 3682 (1965).

d. H. Weiner and R. A. Sneed, *J. Am. Chem. Soc.*, **87**, 287 (1965).

e. P. Muller and J. C. Rosier, *J. Chem. Soc., Perkin Trans.*, **2**, 2232 (2000).

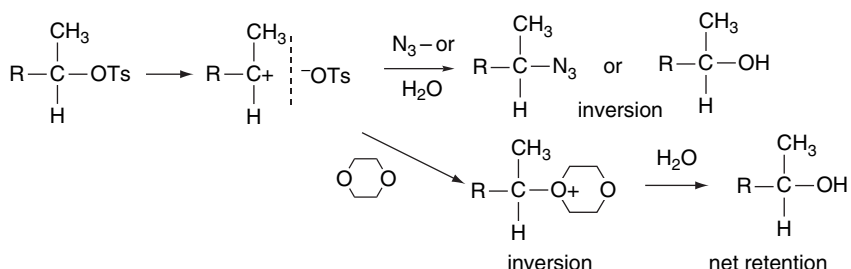
f. J. Steigman and L. P. Hammett, *J. Am. Chem. Soc.*, **59**, 2536 (1937).

g. L. H. Sommer and F. A. Carey, *J. Org. Chem.*, **32**, 800 (1967).

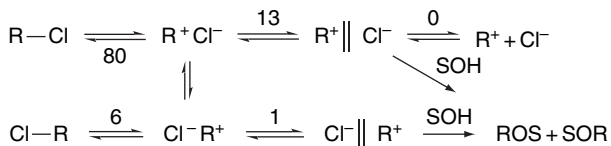
h. H. L. Goering and S. Chang, *Tetrahedron Lett.* 3607 (1965).

Entry 2 exhibits high, but not complete, inversion for acetolysis, which is attributed to competing racemization of the reactant by ionization and internal return. Entry 3 shows that reaction of a secondary 2-octyl system with the moderately good nucleophile acetate ion occurs with complete inversion. The results cited in Entry 4 serve to illustrate the importance of solvation of ion pair intermediates in reactions of secondary tosylates. The data show that partial racemization occurs in aqueous dioxane but that an added nucleophile (azide ion) results in complete inversion in the products resulting from reaction with both azide ion and water. The alcohol of retained configuration is attributed to an intermediate oxonium ion resulting from reaction of the ion pair

with the dioxane solvent, which would react with water to give product of retained configuration. When azide ion is present, dioxane does not effectively compete for the ion pair intermediate and all of the alcohol arises from the inversion mechanism.¹⁹



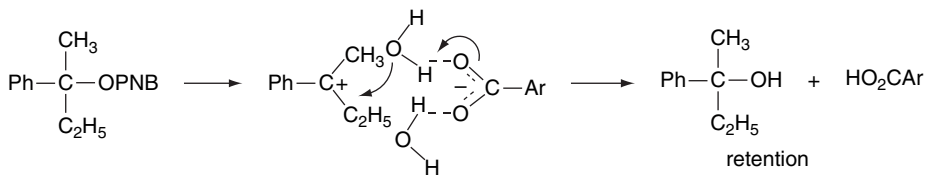
Entry 5 shows data for a tertiary chloride in several solvents. The results range from nearly complete inversion in aqueous dioxane to slight net retention in TFE. These results indicate that the tertiary carbocation formed does not achieve symmetrical solvation but, instead, the stereochemistry is controlled by the immediate solvation shell. Stabilization of a carbocation intermediate by benzylic conjugation, as in the 1-phenylethyl system shown in Entry 6, leads to substitution with extensive racemization. A thorough analysis of the data concerning stereochemical, kinetic, and isotope effects on solvolysis reactions of 1-phenylethyl chloride in several solvent systems has been carried out.²⁰ The system was analyzed in terms of the fate of the contact ion pair and solvent-separated ion pair intermediates. From this analysis, it was estimated that for every 100 molecules of 1-phenylethyl chloride that undergo ionization, 80 return to starting material of retained configuration, 7 return to inverted starting material, and 13 go on to the solvent-separated ion pair in 97:3 TFE-H₂O. A change to a more nucleophilic solvent mix (60% ethanol-water) increased the portion that solvolyzes to 28%.



The results in Entry 7 show that even for the tertiary benzylic substrate 2-phenyl-2-butyl *p*-nitrobenzoate, the expectation of complete racemization is not realized. In moderately nucleophilic media, such as potassium acetate in acetic acid, this ideal is almost achieved, with just a slight excess of inversion. The presence of the better nucleophile azide ion, however, leads to product with a significant (56%) degree of inversion. This result is attributed to nucleophilic attack on an ion pair prior to symmetrical solvation. More surprising is the observation of net retention of configuration in the hydrolysis of 2-phenyl-2-butyl *p*-nitrobenzoate in 90% aqueous acetone. It is possible that this is the result of preferential solvent collapse from the front side at the solvent-separated ion pair stage. The bulky tertiary system may hinder solvation from the rear side. It is also possible that hydrogen bonding between a water

¹⁹. H. Weiner and R. A. Sneed, *J. Am. Chem. Soc.*, **87**, 292 (1965).

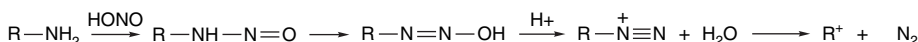
²⁰ V. J. Shiner, Jr., S. R. Hartshorn, and P. C. Vogel, *J. Org. Chem.*, **38**, 3604 (1973).



This selection of stereochemical results points out the relative rarity of the idealized S_N1 (lim) stereochemistry of complete racemization. On the other hand, the predicted inversion of the S_N2 mechanism is consistently observed, and inversion also characterizes the ion pair mechanisms with nucleophile participation. Occasionally net retention is observed. The most likely cause of retention is a double-displacement mechanism, such as proposed for Entry 4, or selective front-side solvation, as in Entry 7c.

4.1.5. Substitution Reactions of Alkyldiazonium Ions

One of the most reactive leaving groups that is easily available for study is molecular nitrogen in alkyl diazonium ions. These intermediates are generated by diazotization of primary amines. Alkyl diazonium ions rapidly decompose to a carbocation and molecular nitrogen. Nucleophilic substitution reactions that occur under diazotization conditions often differ significantly in stereochemistry, as compared with halide or sulfonate solvolysis. Recall the structural description of the alkyl diazonium ions in Section 1.4.3. The nitrogen is a very reactive leaving group and is only weakly bonded to the reacting carbon.



In contrast to an ionization process from a neutral substrate, which initially generates a contact ion pair, deamination reactions generate a cation that does not have a closely associated anion. Furthermore, since the leaving group is very reactive, nucleophilic participation is not needed for bond cleavage. The leaving group, molecular nitrogen, is quite hard, and has no electrostatic attraction to the carbocation. As a result, the carbocations generated by diazonium ion decomposition frequently exhibit rather different behavior from those generated from halides or sulfonates under solvolytic conditions.²¹

Table 4.1 shows the stereochemistry of substitution for five representative systems. Displacement at the primary 1-butyl system occurs mainly by inversion (Entry 1). However, there is also extensive formation of a rearranged product, 2-butanol (not shown in the table). Similarly, the 2-butyl diazonium ion gives 28% inversion in the unarranged product, but the main product is *t*-butanol (Entry 2). These results indicate competition between concerted rearrangement and dissociation. Several secondary diazonium ions were observed to give alcohol with predominant

²¹ C. J. Collins, *Acc. Chem. Res.*, **4**, 315 (1971); A. Streitwieser, Jr., *J. Org. Chem.*, **22**, 861 (1957); E. H. White, K. W. Field, W. H. Hendrickson, P. Dzadzic, D. F. Roswell, S. Paik, and R. W. Mullen, *J. Am. Chem. Soc.*, **114**, 8023 (1992).

Table 4.1. Stereochemistry of Deamination in Acetic Acid

	Amine	Stereochemistry
1 ^a	CH ₃ CH ₂ CH ₂ CHDNH ₂	69% inv
2 ^b	CH ₃ CH(CH ₂ CH ₃)NH ₂	28% inv
3 ^c	PhCH ₂ CH ₂ CH(CH ₃)NH ₂	65% ret
4 ^d	C ₆ H ₅ —CH(CH ₂ CH ₃)NH ₂	10% ret
5 ^e	CH ₃ C ₆ H ₅ —C(CH ₂ CH ₃) NH ₂	24% ret

a. D Brosch and W. Kirmse, *J. Org. Chem.*, **56**, 908 (1991).

b. K Banert, M. Bunse, T. Engberts, K.-R. Gassen, A. W. Kurimoto, and W. Kirmse, *Recl. Trav. Chim. Pas-Bas*, **105**, 272 (1986).

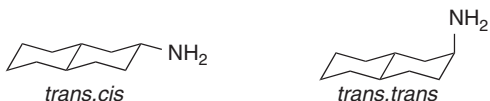
c. N Ileby, M. Kuzma, L. R. Heggvik, K. Sorbye, and A. Fiksdahl, *Tetrahedron: Asymmetry*, **8**, 2193 (1997).

d. R. Huisgen and C. Ruchardt, *Justus Liebigs Ann. Chem.*, **601**, 21 (1956).

e. E. H. White and J. E. Stuber, *J. Am. Chem. Soc.*, **85**, 2168 (1963).

retention when the reaction was done in acetic acid²² (Entry 3). However, the acetate esters formed in these reactions is largely racemic. Small net retention was seen in the deamination of 1-phenylpropylamine (Entry 4). The tertiary benzylic amine, 2-phenyl-2-butylamine, reacts with 24% net retention (Entry 5). These results indicate that the composition of the product is determined by collapse of the solvent shell. Considerable solvent dependence has been observed in deamination reactions.²³ Water favors formation of a carbocation with extensive racemization, whereas less polar solvents, including acetic acid, lead to more extensive inversion as the result of solvent participation.

An analysis of the stereochemistry of deamination has also been done using 4-*t*-butylcyclohexylamines and the conformationally rigid 2-decalylamines. The results are summarized in Table 4.2.



In solvent systems containing low concentrations of water in acetic acid, dioxane, or sulfolane, the alcohol is formed by capture of water with net retention of configuration. This result has been explained as involving a solvent-separated ion pair that

²². N. Ileby, M. Kuzma, L. R. Heggvik, K. Sorbye, and A. Fiksdahl, *Tetrahedron: Asymmetry*, **8**, 2193 (1997).

²³. W. Kirmse and R. Siegfried, *J. Am. Chem. Soc.*, **105**, 950 (1983); K. Banert, M. Bunse, T. Engbert, K.-R. Gassen, A. W. Kurimoto, and W. Kirmse, *Recl. Trav. Chim. Pays-Bas*, **105**, 272 (1986).

Table 4.2. Product Stereochemistry for Deamination of Stereoisomeric Amines

SECTION 4.2
Structural and Solvation Effects on Reactivity

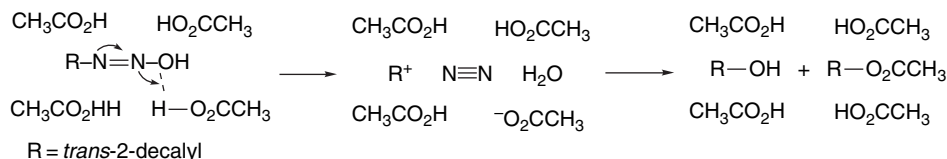
	Product composition ^a			
	Alcohol		Ester	
	Retention	Inversion	Retention	Inversion
Cis-4-t-Butylcyclohexylamine (axial) ^b	33	8	25	33
Trans-4-t-Butylcyclohexylamine (equatorial) ^b	43	2	43	12
Trans,trans-2-Decylamine (axial) ^c	26	2	32	40
Trans,cis-2-Decylamine (equatorial) ^c	18	1	55	26

a. Composition of the total of alcohol and acetate ester. Considerable alkene is also formed.

b. H. Maskill and M. C. Whiting, *J. Chem. Soc., Perkin Trans. 2*, 1462 (1976).

c. T. Cohen, A. D. Botelho, and E. Jamnkowski, *J. Org. Chem.*, **45**, 2839 (1980).

arises by concerted proton transfer and nitrogen elimination.²⁴ The water molecule formed in the elimination step is captured preferentially from the front side, leading to net retention of configuration for the alcohol. For the ester product, the extent of retention and inversion is more balanced, although it varies among the four systems.



It is clear from the data in Table 4.2 that the two pairs of stereoisomeric cyclic amines *do not form the same intermediate*. The collapse of the ions to product is evidently so fast that there is not time for relaxation of the initially formed intermediates to reach a common structure. Generally speaking, we can expect similar behavior for all alkyl diazonium ion decompositions. The low activation energy for dissociation and the neutral and hard character of the leaving group result in a carbocation that is free of direct interaction with the leaving group. Product composition and stereochemistry is determined by the details of the collapse of the solvent shell.

4.2. Structural and Solvation Effects on Reactivity

4.2.1. Characteristics of Nucleophilicity

The term *nucleophilicity* refers to the capacity of a Lewis base to participate in a nucleophilic substitution reaction and is contrasted with *basicity*, which is defined by the position of an equilibrium reaction with a proton donor, usually water. Nucleophilicity is used to describe trends in the rates of substitution reactions that are attributable to properties of the nucleophile. The relative nucleophilicity of a given species may be different toward various reactants and there is not an absolute scale of nucleophilicity. Nevertheless, we can gain some impression of the structural features

²⁴ (a) H. Maskill and M. C. Whiting, *J. Chem. Soc., Perkin Trans. 2*, 1462 (1976); (b) T. Cohen, A. D. Botelho, and E. Jankowski, *J. Org. Chem.*, **45**, 2839 (1970).

that govern nucleophilicity and the relationship between nucleophilicity and basicity.²⁵ As we will see in Section 4.4.3, there is often competition between displacement (nucleophilicity) and elimination (proton removal, basicity). We want to understand how the structure of the reactant and nucleophile (base) affect this competition.

The factors that influence nucleophilicity are best assessed in the context of the limiting S_N2 mechanism, since it is here that the properties of the nucleophile are most important. The rate of an S_N2 reaction is directly related to the effectiveness of the nucleophile in displacing the leaving group. In contrast, relative nucleophilicity has no effect on the rate of an S_N1 reaction. Several properties can influence nucleophilicity. Those considered to be most significant are: (1) the solvation energy of the nucleophile; (2) the strength of the bond being formed to carbon; (3) the electronegativity of the attacking atom; (4) the polarizability of the attacking atom; and (5) the steric bulk of the nucleophile.²⁶ Let us consider each how each of these factors affect nucleophilicity.

1. Strong solvation lowers the energy of an anionic nucleophile relative to the TS, in which the charge is more diffuse, and results in an increased E_a . Viewed from another perspective, the solvation shell must be disrupted to attain the TS and this desolvation contributes to the activation energy.
2. Because the S_N2 process is concerted, the strength of the partially formed new bond is reflected in the TS. A stronger bond between the nucleophilic atom and carbon results in a more stable TS and a reduced activation energy.
3. A more electronegative atom binds its electrons more tightly than a less electronegative one. The S_N2 process requires donation of electron density to an antibonding orbital of the reactant, and high electronegativity is unfavorable.
4. Polarizability describes the ease of distortion of the electron density of the nucleophile. Again, because the S_N2 process requires bond formation by an electron pair from the nucleophile, the more easily distorted the attacking atom, the better its nucleophilicity.
5. A sterically congested nucleophile is less reactive than a less hindered one because of nonbonded repulsions that develop in the TS. The trigonal bipyramidal geometry of the S_N2 transition state is sterically more demanding than the tetrahedral reactant so steric interactions increase as the TS is approached.

Empirical measures of nucleophilicity are obtained by comparing relative rates of reaction of a standard reactant with various nucleophiles. One measure of nucleophilicity is the *nucleophilic constant (n)*, originally defined by Swain and Scott.²⁷ Taking methanolysis of methyl iodide as the standard reaction, they defined n as

$$n_{\text{CH}_3\text{I}} = \log(k_{\text{nuc}}/k_{\text{CH}_3\text{OH}}) \text{ in CH}_3\text{OH}, 25^\circ\text{C}$$

Table 4.3 lists the nucleophilic constants for a number of species according to this definition.

It is apparent from Table 4.3 that nucleophilicity toward methyl iodide does not correlate directly with aqueous basicity. Azide ion, phenoxide ion, and bromide are all

²⁵. For general reviews of nucleophilicity see R. F. Hudson, in *Chemical Reactivity and Reaction Paths*, G. Klopman, ed., John Wiley & Sons, New York, 1974, Chap. 5; J. M. Harris and S. P. McManus, eds., *Nucleophilicity*, Vol. 215, Advances in Chemistry Series, American Chemical Society, Washington, DC, 1987.

²⁶. A. Streitwieser, Jr., *Solvolytic Displacement Reactions*, McGraw-Hill, New York, 1962; J. F. Bunnett, *Annu. Rev. Phys. Chem.*, **14**, 271 (1963).

²⁷. C. G. Swain and C. B. Scott, *J. Am. Chem. Soc.*, **75**, 141 (1953).

Table 4.3. Nucleophilicity Constants for Various Nucleophiles^a

Nucleophile	$n_{\text{CH}_3\text{I}}$	Conjugate acid $\text{p}K_a$
CH_3OH	0.0	-1.7
NO_3^-	1.5	-1.3
F^-	2.7	3.45
CH_3CO_2^-	4.3	4.8
Cl^-	4.4	-5.7
$(\text{CH}_3)_2\text{S}$	5.3	
NH_3	5.5	9.25
N_3^-	5.8	4.74
$\text{C}_6\text{H}_5\text{O}^-$	5.8	9.89
Br^-	5.8	-7.7
CH_3O^-	6.3	15.7
HO^-	6.5	15.7
NH_2OH	6.6	5.8
NH_2NH_2	6.6	7.9
$(\text{CH}_3\text{CH}_2)_3\text{N}$	6.7	10.7
CN^-	6.7	9.3
$(\text{CH}_3\text{CH}_2)_3\text{As}$	7.1	
I^-	7.4	-10.7
HO_2^-	7.8	
$(\text{CH}_3\text{CH}_2)_3\text{P}$	8.7	8.7
$\text{C}_6\text{H}_5\text{S}^-$	9.9	6.5
$\text{C}_6\text{H}_5\text{Se}^-$	10.7	
$(\text{C}_6\text{H}_5)_3\text{Sn}^-$	11.5	

a. Data from R. G. Pearson and J. Songstad, *J. Am. Chem. Soc.*, **89**, 1827 (1967); R. G. Pearson, H. Sobel, and J. Songstad, *J. Am. Chem. Soc.*, **90**, 319 (1968); P. L. Bock and G. M. Whitesides, *J. Am. Chem. Soc.*, **96**, 2826 (1974).

SECTION 4.2

Structural and Solvation
Effects on Reactivity

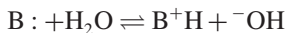
equivalent in nucleophilicity, but differ greatly in basicity. Conversely, azide ion and acetate ion are nearly identical in basicity, but azide ion is 70 times (1.5 log units) more nucleophilic. Among neutral nucleophiles, while triethylamine is *100 times more basic* than triethylphosphine (p*K*_a of the conjugate acid is 10.7 versus 8.7), the phosphine is more nucleophilic (*n* is 8.7 versus 6.7), by a factor of 100 in the opposite direction. Correlation with basicity is better if the attacking atom is the same. Thus for the series of oxygen nucleophiles $\text{CH}_3\text{O}^- > \text{C}_6\text{H}_5\text{O}^- > \text{CH}_3\text{CO}_2^- > \text{NO}_3^-$, nucleophilicity parallels basicity.

Nucleophilicity usually decreases going across a row in the periodic table. For example, $\text{H}_2\text{N}^- > \text{HO}^- > \text{F}^-$ or $\text{C}_6\text{H}_5\text{S}^- > \text{Cl}^-$. Nucleophilicity increases going down the periodic table, as, e.g., $\text{I}^- > \text{Br}^- > \text{Cl}^- > \text{F}^-$ and $\text{C}_6\text{H}_5\text{Se}^- > \text{C}_6\text{H}_5\text{S}^- > \text{C}_6\text{H}_5\text{O}^-$. Three factors work together to determine this order. Electronegativity decreases going down the periodic table. Probably more important is the greater polarizability and weaker solvation of the heavier ions, which have a more diffuse electron distribution. The bond strength effect is in the opposite direction, but is overwhelmed by electronegativity and polarizability.

There is clearly a conceptual relationship between the properties called nucleophilicity and basicity. Both describe processes involving formation of a new bond to an electrophile by donation of an electron pair. The p*K*_a values in Table 4.3 refer to basicity toward a proton. There are many reactions in which a given chemical species might act either as a nucleophile or as a base. It is therefore of great interest to be

able to predict whether a chemical species Y^- will act as a nucleophile or as a base under a given set of conditions. Scheme 4.3 lists some examples.

Basicity is a measure of the ability of a substance to attract protons and refers to an *equilibrium* with respect to a proton transfer from solvent:



These equilibrium constants provide a measure of *thermodynamic basicity*, but we also need to have some concept of *kinetic basicity*. For the reactions in Scheme 4.3, for example, it is important to be able to generalize about the rates of competing reactions. The most useful qualitative approach for making predictions is the hard-soft-acid-base (HSAB) concept²⁸ (see Section 1.1.6), which proposes that reactions occur most readily between species that are matched in hardness and softness. Hard nucleophiles prefer hard electrophiles, whereas soft nucleophiles prefer soft electrophiles.

The HSAB concept can be applied to the problem of competition between nucleophilic substitution and deprotonation as well as to the reaction of anions with alkyl halides. The sp^3 carbon is a soft electrophile, whereas the proton is a hard electrophile. Thus, according to HSAB theory, a soft anion will act primarily as a nucleophile, giving the substitution product, whereas a hard anion is more likely to remove a proton, giving the elimination product. Softness correlates with high polarizability and low electronegativity. The soft nucleophile–soft electrophile combination is associated with a late TS, where the strength of the newly forming bond contributes significantly to the structure and stability of the TS. Species in Table 4.3 that exhibit high nucleophilicity toward methyl iodide include CN^- , I^- , and $\text{C}_6\text{H}_5\text{S}^-$. These are soft species. Hardness

Scheme 4.3. Examples of Competition between Nucleophilicity and Basicity

$\text{S}_{\text{N}}1$ Substitution	Y^- acts as a nucleophile	$\text{Y}^- + \text{R}_2\text{C}^+\text{CHR}'_2 \longrightarrow \text{R}_2\text{CCH}\text{Y}$
<i>versus</i>		
E1 Elimination	Y^- acts as a base	$\text{Y}^- + \text{R}_2\text{C}^+\text{CHR}'_2 \longrightarrow \text{R}_2\text{C}=\text{CR}'_2 + \text{H}-\text{Y}$
$\text{S}_{\text{N}}2$ Substitution	Y^- acts as a nucleophile	$\text{Y}^- + \text{RCH}_2\text{CH}_2\text{X} \longrightarrow \text{RCH}_2\text{CH}_2\text{Y} + \text{X}^-$
<i>versus</i>		
E2 Elimination	Y^- acts as a base	$\text{Y}^- + \text{RCH}_2\text{CH}_2\text{X} \longrightarrow \text{RCH}=\text{CH}_2 + \text{H}-\text{Y}$
Nucleophilic addition to a carbonyl group	Y^- acts as a nucleophile	$\text{Y}^- + \text{RCH}_2\text{CR}' \longrightarrow \text{RCH}_2\text{CR}'\text{Y}$
Enolate formation	Y^- acts as a base	$\text{Y}^- + \text{RCH}_2\text{CR}' \longrightarrow \text{RCH}=\text{CR}'\text{Y}^- + \text{H}-\text{Y}$

²⁸ R. G. Pearson and J. Songstad, *J. Am. Chem. Soc.*, **89**, 1827 (1967); R. G. Pearson, *J. Chem. Ed.*, **45**, 581, 643 (1968); T. L. Ho, *Chem. Rev.*, **75**, 1 (1975).

Table 4.4. Hardness and Softness of Some Common Ions and Molecules

	Bases (Nucleophiles)	Acids (Electrophiles)	SECTION 4.2 <i>Structural and Solvation Effects on Reactivity</i>
Soft	RSH, RS ⁻ , I ⁻ , R ₃ P ^-C≡N, ^-C≡O ⁺ , RCH=CHR benzene	I ₂ , Br ₂ , RS—X, RSe—X, RCH ₂ —X Cu(I), Ag(I), Pd(II), Pt(II), Hg(II) zero-valent metal complexes	
Intermediate	Br ⁻ , N ₃ ⁻ , ArNH ₂ pyridine	Cu(II), Zn (II), Sn(II) R ₃ C ⁺ , R ₃ B	
Hard	NH ₃ , RNH ₂ H ₂ O, HO ⁻ , ROH, RO ⁻ , RCO ₂ ⁻ , Cl ⁻ F ⁻ , NO ₃ ⁻	H—X, Li ⁺ , Na ⁺ , R ₃ Si—X Mg(II), Ca(II), Al(III), Sn(IV), Ti(IV) H ⁺	

reflects a high charge density and is associated with more electronegative elements. The hard nucleophile–hard electrophile combination implies an early TS with electrostatic attraction being more important than bond formation. For hard bases, the reaction pathway is chosen early on the reaction coordinate and primarily on the basis of charge distribution. Examples of hard bases from Table 4.3 are F⁻ and CH₃O⁻. Table 4.4 classifies some representative chemical species with respect to softness and hardness. Numerical values of hardness were presented in Table 1.3.

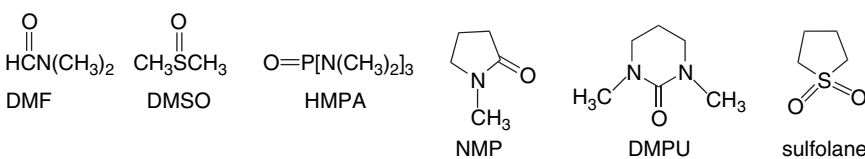
Nucleophilicity is also correlated with oxidation potential for comparisons between nucleophiles involving the same element.²⁹ Good nucleophilicity correlates with ease of oxidation, as would be expected from the electron-donating function of the nucleophile in S_N2 reactions. HSAB considerations also suggest that nucleophilicity would be associated with species having relatively high-energy electrons. Remember that soft species have relatively high-lying HOMOs, which implies ease of oxidation.

4.2.2. Effect of Solvation on Nucleophilicity

The nucleophilicity of anions is very dependent on the degree of solvation. Many of the data that form the basis for quantitative measurement of nucleophilicity are for reactions in hydroxylic solvents. In protic hydrogen-bonding solvents, anions are subject to strong interactions with solvent. Hard nucleophiles are more strongly solvated by protic solvents than soft nucleophiles, and this difference contributes to the greater nucleophilicity of soft anions in such solvents. Nucleophilic substitution reactions of anionic nucleophiles usually occur more rapidly in polar aprotic solvents than they do in protic solvents, owing to the fact that anions are weakly solvated in such solvents (see Section 3.8). Nucleophilicity is also affected by the solvation of the cations in solution. Hard cations are strongly solvated in polar aprotic solvents such as *N,N*-dimethylformamide (DMF), dimethyl sulfoxide (DMSO), hexamethylphosphoric triamide (HMPA), *N*-methylpyrrolidone (NMP), *N,N*-dimethylpropyleneurea

²⁹. M. E. Niyazymbetov and D. H. Evans, *J. Chem. Soc., Perkin Trans. 2*, 1333 (1993); M. E. Niyazymbetov, Z. Rongfeng, and D. H. Evans, *J. Chem. Soc., Perkin Trans. 2*, 1957 (1996).

(DMPU), and sulfolane.³⁰ As a result, the anions are dissociated from the cations, which enhances their nucleophilicity.



In the absence of the solvation by protic solvents, the relative nucleophilicity of anions changes. Hard nucleophiles increase in reactivity more than soft nucleophiles. As a result, the relative reactivity order changes. In methanol, for example, the relative reactivity order is $\text{N}_3^- > \text{I}^- > \text{CN}^- > \text{Br}^- > \text{Cl}^-$. In DMSO the order becomes $\text{CN}^- > \text{N}_3^- > \text{Cl}^- > \text{Br}^- > \text{I}^-$.³¹ The reactivity order in methanol is dominated by solvation and the more weakly solvated N_3^- and I^- ions are the most reactive nucleophiles. The iodide ion is large and very polarizable. The anionic charge on the azide ion is dispersed by delocalization. When the effect of solvation is diminished in DMSO, other factors become more important, including the strength of the bond being formed, which accounts for the reversed order of the halides in the two series. There is also evidence that S_N2 TSs are better solvated in aprotic dipolar solvents than in protic solvents.

In interpreting many aspects of substitution reactions, particularly solvolysis, it is important to be able to characterize the nucleophilicity of the solvent. Assessment of solvent nucleophilicity can be done by comparing rates of a standard substitution process in various solvents. One such procedure is based on the Winstein-Grunwald equation³²:

$$\log(k/k_0) = lN + mY$$

where N and Y are measures of the solvent nucleophilicity and ionizing power, respectively. The variable parameters l and m are characteristic of specific reactions. The value of N , the indicator of solvent nucleophilicity, can be determined by specifying a standard reactant for which l is assigned the value 1.00 and a standard solvent for which N is assigned the value 0.00. The parameters were originally assigned for solvolysis of *t*-butyl chloride. The scale has also been assigned for 2-adamantyl tosylate, in which nucleophilic participation of the solvent is considered to be negligible. Ethanol-water in the ratio 80:20 is taken as the standard solvent. The resulting solvent characteristics are called N_{Tos} and Y_{Tos} . Some representative values for solvents that are frequently used in solvolysis studies are given in Table 4.5. We see that nucleophilicity decreases from ethanol to water to trifluoroethanol to trifluoroacetic acid as the substituent becomes successively more electron withdrawing. Note that the considerable difference between acetic acid and formic acid appears entirely in

³⁰ T. F. Magnera, G. Caldwell, J. Sunner, S. Ikuta, and P. Kebarle, *J. Am. Chem. Soc.*, **106**, 6140 (1984); T. Mitsuhashi, G. Yamamoto, and H. Hirota, *Bull. Chem. Soc. Jpn.*, **67**, 831 (1994); K. Okamoto, *Adv. Carbocation Chem.*, **1**, 171 (1989).

³¹ R. L. Fuchs and L. L. Cole, *J. Am. Chem. Soc.*, **95**, 3194 (1973); R. Alexander, E. C. F. Ko, A. J. Parker, and T. J. Broxton, *J. Am. Chem. Soc.*, **90**, 5049 (1968); D. Landini, A. Maia, and F. Montanari, *J. Am. Chem. Soc.*, **100**, 2796 (1978).

³² S. Winstein, E. Grunwald, and H. W. Jones, *J. Am. Chem. Soc.*, **73**, 2700 (1951); F. L. Schadt, T. W. Bentley, and P. v. R. Schleyer, *J. Am. Chem. Soc.*, **98**, 7667 (1976).

Table 4.5. Solvent Nucleophilicity and Ionization Parameters^a

Solvent	<i>t</i> -Butyl chloride		2-Adamantyl tosylate	
	<i>N</i>	<i>Y</i>	<i>N</i> _{Tos}	<i>Y</i> _{Tos}
Ethanol	+0.09	-2.03	0.00	-1.75
Methanol	+0.01	-1.09	-0.04	-0.92
50% Aqueousethanol	-0.20	1.66	-0.09	1.29
Water	-0.26	3.49		
Acetic acid	-2.05	-1.64	-2.35	-0.61
Formic acid	-2.05	2.05	-2.35	3.04
Trifluoroethanol	-2.78	1.05	-3.0	1.80
97% (CF ₃) ₂ CHOH-H ₂ O	-3.93	2.46	-4.27	3.61
Trifluoroacetic acid	-4.74	1.84	-5.56	4.57

a. From F. L. Schadt, T. W. Bentley, and P. v. R. Schleyer, *J. Am. Chem. Soc.*, **98**, 7667 (1976).

the *Y* terms, which have to do with ionizing power and results from the more polar character of formic acid. The nucleophilicity parameters of formic acid and acetic acid are the same, as might be expected, because the nucleophilicity is associated with the carboxy group.

4.2.3. Leaving-Group Effects

The nature of the leaving group influences the rate of nucleophilic substitution proceeding by either the direct displacement or ionization mechanism. Since the leaving group departs with the pair of electrons from the covalent bond to the reacting carbon atom, a correlation with both bond strength and anion stability is expected. Provided the reaction series consists of structurally similar leaving groups, such relationships are observed. For example, a linear free-energy relationship (*Hammett equation*) has been demonstrated for the rate of reaction of ethyl arenesulfonates with ethoxide ion in ethanol.³³ A qualitative trend of increasing reactivity with the acidity of the conjugate acid of the leaving group also holds for less similar systems, although no generally applicable quantitative system for specifying leaving-group ability has been established.

Table 4.6 lists estimated relative rates of solvolysis of 1-phenylethyl esters and halides in 80% aqueous ethanol at 75°C.³⁴ The reactivity of the leaving groups generally parallels their electron-accepting capacity. Trifluoroacetate, for example, is about 10⁶ time as reactive as acetate and *p*-nitrobenzenesulfonate is about 10 times more reactive than *p*-toluenesulfonate. The order of the halide leaving groups is I⁻ > Br⁻ > Cl⁻ ≫ F⁻. This order is opposite to that of electronegativity and is dominated by the strength of the bond to carbon, which increases from ~ 55 kcal for the C—I bond to ~ 110 kcal for the C—F bond (see Table 3.2).

Sulfonate esters are especially useful reactants in nucleophilic substitution reactions in synthesis. They have a high level of reactivity and can be prepared from alcohols by reactions that do not directly involve the carbon atom at which substitution is to be effected. The latter feature is particularly important in cases where the stereochemical and structural integrity of the reactant must be maintained. Trifluoromethanesulfonate (triflate) ion is an exceptionally reactive leaving group and can

³³. M. S. Morgan and L. H. Cretcher, *J. Am. Chem. Soc.*, **70**, 375 (1948).

³⁴. D. S. Noyce and J. A. Virgilio *J. Org. Chem.*, **37**, 2643 (1972).

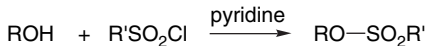
Table 4.6. Relative Solvolysis Rates of 1-Phenylethyl Esters and Halides^{a,b}

Leaving group	k_{rel}
CF_3SO_3^- (triflate)	1.4×10^8
<i>p</i> -Nitrobenzensulfonate (nosylate)	4.4×10^5
<i>p</i> -Toluenesulfonate (tosylate)	3.7×10^4
CH_3SO_3^- (mesylate)	3.0×10^4
I^-	91
Br^-	14
CF_3CO_2^-	2.1
Cl^-	1.0
F^-	9×10^{-6}
<i>p</i> -Nitrobenzoate	5.5×10^{-6}
CH_3CO_2^-	1.4×10^{-6}

a. From D. S. Noyce and J. A. Virgilio, *J. Org. Chem.*, **37**, 2643 (1972).

b. In 80% ethanol at 75°C.

be used for nucleophilic substitution reactions on unreactive substrates. Acetolysis of cyclopropyl triflate, for example, occurs 10^5 times faster than acetolysis of cyclopropyl tosylate.³⁵ Sulfonate esters are usually prepared by reaction of an alcohol with a sulfonyl halide in the presence of pyridine.



Tertiary alcohols are more difficult to convert to sulfonate esters and their high reactivity often makes them difficult to isolate.³⁶

It would be anticipated that the limiting S_N1 and S_N2 mechanisms would differ in their sensitivity to the nature of the leaving group. The ionization mechanism should exhibit a greater dependence on leaving-group ability because it requires cleavage of the bond to the leaving group without assistance by the nucleophile. Table 4.7 presents data on the variation of the relative leaving-group abilities of tosylate and bromide as a function of reactant structure. The dependence on structure is as expected, with smaller differences in reactivity between tosylate and bromide being observed for systems that react by the S_N2 mechanism. The largest differences are seen for tertiary systems, where nucleophilic participation is minimal.

Table 4.7. Tosylate/Bromide Rate Ratios for Solvolysis of RX in 80% Ethanol^a

R	$k_{\text{Tos}}/k_{\text{Br}}$
Methyl	11
Ethyl	10
Isopropyl	40
<i>t</i> -Butyl	4000
1-Adamantyl	9750

a. From J. L. Fry, C. J. Lancelot, L. K. M. Lam, J. M. Harris, R. C. Bingham, D. J. Raber, R. E. Hall, and P. v. R. Schleyer, *J. Am. Chem. Soc.*, **92**, 2539 (1970).³⁵. T. M. Su, W. F. Sliwinski, and P. v. R. Schleyer, *J. Am. Chem. Soc.*, **91**, 5386 (1969).³⁶. H. M. R. Hoffmann, *J. Chem. Soc.*, 6748 (1965).

Table 4.8. Relative Reactivity of Leaving Groups in S_N2 Substitution Reactions^a

Nucleophile	CH ₃ I	CH ₃ Br		CH ₃ OTs		
	MeOH	DMF	MeOH	DMF	MeOH	DMF
N ₃ ⁻	8.0 × 10 ⁻⁵	3.2	5.0 × 10 ⁻⁵	4.0 × 10 ⁻¹	5.0 × 10 ⁻⁴	5.0 × 10 ⁻²
NCS ⁻	5.0 × 10 ⁻⁴	8.0 × 10 ⁻²	2.5 × 10 ⁻⁴	1.3 × 10 ⁻²	1.3 × 10 ⁻⁴	8.0 × 10 ⁻⁴
NC ⁻	6.4 × 10 ⁻⁴	3.2 × 10 ²				
ArS ⁻	6.4 × 10 ⁻²	16			1.6 × 10 ⁻²	6.4 × 10 ⁻¹

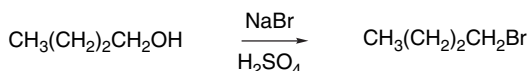
a. Bimolecular rate constants at 25°C. Data from the compilation of R. Alexander, E. C. F. Ko, A. J. Parker, and T. J. Broxton, *J. Am. Chem. Soc.*, **90**, 5049 (1968).

Leaving-group effects are diminished in S_N2 reactions, because the nucleophile assists in bond breaking. The mesylate/bromide ratio is compressed from 2 × 10³ (Table 4.6) to only about 10 for azide ion in methanol, as shown in Table 4.8. In the aprotic dipolar solvent DMF, the leaving-group order is I⁻ > Br⁻ > ⁻O₃SCH₃ for both azide and thiocyanate anions.

A poor leaving group can be made more reactive by coordination to an electrophile. Hydroxide is a very poor leaving group, so alcohols do not normally undergo direct nucleophilic substitution. It has been estimated that the reaction



is endothermic by 16 kcal/mol.³⁷ Since the activation energy for the reverse process is about 21 kcal/mol, the reaction would have an *E_a* of 37 kcal/mol. As predicted by this *E_a*, the reaction is too slow to detect at normal temperature, but it is greatly accelerated in acidic solution. Protonation of the hydroxy group provides the much better leaving group—water—which is about as good a leaving group as bromide ion. The practical result is that primary alcohols can be converted to alkyl bromides by heating with sodium bromide and sulfuric acid or with concentrated hydrobromic acid.



The reactivity of halides is increased by coordination with Lewis acids. For example, silver ion accelerates solvolysis of methyl and ethyl bromide in 80:20 ethanol water by more than 10³.³⁸ In Section 4.4.1, we will see that the powerful Lewis acids SbF₅ and SbCl₅ also assist in the ionization of halides.

4.2.4. Steric and Strain Effects on Substitution and Ionization Rates

The general trends of reactivity of primary, secondary, and tertiary systems have already been discussed. Reactions that proceed by the direct displacement mechanism are retarded by increased steric repulsions at the TS. This is the principal cause for the relative reactivity of methyl, ethyl, and *i*-propyl chloride, which are in the ratio 93:1:0.0076 toward iodide ion in acetone.³⁹ A statistical analysis of rate data for a

³⁷ R. A. Ogg, Jr., *Trans. Faraday Soc.*, **31**, 1385 (1935).

³⁸ L. C. Batman, K. A. Cooper, E. D. Hughes, and C. K. Ingold, *J. Chem. Soc.*, 925 (1940); J. Dostrovsky and E. D. Hughes, *J. Chem. Soc.*, 169 (1946); D. J. Pasto and K. Garves, *J. Org. Chem.*, **32**, 778 (1967).

³⁹ J. B. Conant and R. E. Hussey, *J. Am. Chem. Soc.*, **47**, 476 (1925).

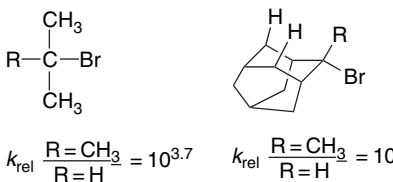
Table 4.9. Rate Constants for Nucleophilic Substitution of Primary Alkyl Bromides and Tosylates^a

$k \times 10^5$ for RCH_2-X^b	$\text{R} = \text{H}$	CH_3	CH_3CH_2	$(\text{CH}_3)_2\text{CH}$	$(\text{CH}_3)_3\text{C}$
$\text{RCH}_2\text{Br} + \text{LiCl}$, acetone, 25°C	600	9.9	6.4	1.5	2.6×10^{-4}
$\text{RCH}_2\text{I} + n\text{-Bu}_3\text{P}$, acetone, 35°C	26,000	154	64	4.9	
$\text{RCH}_2\text{Br} + \text{NaOCH}_3$, methanol	8140	906	335	67	
RCH_2OTs , acetic acid, 70°C^c	5.2×10^{-2}	4.4×10^{-2}		1.8×10^{-2}	4.2×10^{-3}

a. M. Charton, *J. Am. Chem. Soc.*, **97**, 3694 (1975).b. $M^{-1}\text{s}^{-1}$ c. pseudo-first order s^{-1}

number of sets of nucleophilic substitution reactions of substrates of the type RCH_2Y , where Y is a leaving group and R is H or alkyl, indicated that the steric effect of R is the dominant factor in determining rates.⁴⁰ Table 4.9 shows some of the data. The first three examples pertain to S_N2 reactions. Note that the fourth entry, involving solvolysis in acetic acid, shows a diminished sensitivity to steric effects. As acetic acid is a much weaker nucleophile than the other examples, the TS involves less nucleophilic participation.

In contrast to S_N2 reactions, rates of reactions involving TSs with cationic character increase with substitution. The relative rates of formolysis of alkyl bromides at 100°C are methyl, 0.58; ethyl, 1.00; *i*-propyl, 26.1; and *t*-butyl 10^8 .⁴¹ This order is clearly dominated by carbocation stability. The effect of substituting a methyl group for hydrogen depends on the extent of nucleophilic participation in the TS. A high CH_3/H rate ratio is expected if nucleophilic participation is weak and stabilization of the cationic nature of the TS is important. A low ratio is expected when nucleophilic participation is strong. The relative rate of acetolysis of *t*-butyl bromide to *i*-propyl bromide at 25°C is $10^{3.7}$, whereas that of 2-methyl-2-adamantyl bromide to 2-adamantyl bromide is $10^{8.1}$.⁴²

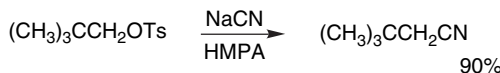


The reason the adamantyl system is much more sensitive to the CH_3 for H substitution is that its cage structure precludes solvent participation, whereas the *i*-propyl system allows much greater solvent participation. The electronic stabilizing effect of the methyl substituent is therefore more important in the adamantyl system.

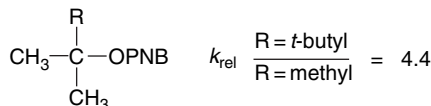
Neopentyl (2,2-dimethylpropyl) systems are resistant to nucleophilic substitution reactions. They are primary and do not form carbocation intermediates; moreover the *t*-butyl substituent hinders back-side displacement. The rate of reaction of neopentyl bromide with iodide ion is 470 times less than that of *n*-butyl bromide.⁴³ Under solvolysis conditions the neopentyl system usually reacts with rearrangement to the

40. M. Charton, *J. Am. Chem. Soc.*, **97**, 3694 (1975).41. L. C. Bateman and E. D. Hughes, *J. Chem. Soc.*, 1187 (1937); 945 (1940).42. J. L. Fry, J. M. Harris, R. C. Bingham, and P. v. R. Schleyer, *J. Am. Chem. Soc.*, **92**, 2540 (1970).43. P. D. Bartlett and L. J. Rosen, *J. Am. Chem. Soc.*, **64**, 543 (1942).

t-pentyl system, although use of good nucleophiles in polar aprotic solvents permits direct displacement to occur.⁴⁴



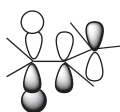
Steric effects of another kind become important in highly branched substrates, and ionization can be facilitated by relief of steric crowding in going from the tetrahedral ground state to the TS for ionization.⁴⁵ The relative hydrolysis rates in 80% aqueous acetone of *t*-butyl *p*-nitrobenzoate and 2,3,3-trimethyl-2-butyl *p*-nitrobenzoate are 1:4.4.



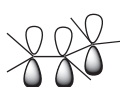
This effect has been called *B-strain* (back strain), and in this example only a modest rate enhancement is observed. As the size of the groups is increased, the effect on rate becomes larger. When all three of the groups in the above example are *t*-butyl, the solvolysis occurs 13,500 times faster than in *t*-butyl *p*-nitrobenzoate.⁴⁶

4.2.5. Effects of Conjugation on Reactivity

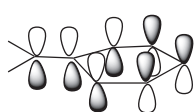
In addition to steric effects, there are other important substituent effects that influence both the rate and mechanism of nucleophilic substitution reactions. As we discussed on p. 302, the benzylic and allylic cations are stabilized by electron delocalization. It is therefore easy to understand why substitution reactions of the ionization type proceed more rapidly in these systems than in alkyl systems. Direct displacement reactions also take place particularly rapidly in benzylic and allylic systems; for example, allyl chloride is 33 times more reactive than ethyl chloride toward iodide ion in acetone.⁴⁷ These enhanced rates reflect stabilization of the $\text{S}_{\text{N}}2$ TS through overlap of the *p*-type orbital that develops at carbon.⁴⁸ The π systems of the allylic and benzylic groups provide extended conjugation. This conjugation can stabilize the TS, whether the substitution site has carbocation character and is electron poor or is electron rich as a result of a concerted $\text{S}_{\text{N}}2$ mechanism.



interaction of sp^2 hybridized substitution center with π LUMO



interaction of empty sp^2 orbital with π HOMO



interaction of empty sp^2 orbital of benzyl cation with HOMO aromatic π system

⁴⁴. B. Stephenson, G. Solladie, and H. S. Mosher, *J. Am. Chem. Soc.*, **94**, 4184 (1972).

⁴⁵. H. C. Brown, *Science*, **103**, 385 (1946); E. N. Peters and H. C. Brown, *J. Am. Chem. Soc.*, **97**, 2892 (1975).

⁴⁶. P. D. Bartlett and T. T. Tidwell, *J. Am. Chem. Soc.*, **90**, 4421 (1968).

⁴⁷. J. B. Conant and R. E. Hussey, *J. Am. Chem. Soc.*, **47**, 476 (1925).

⁴⁸. A. Streitwieser, Jr., *Solvolytic Displacement Reactions*, McGraw-Hill, New York, 1962, p. 13; F. Carrion and M. J. S. Dewar, *J. Am. Chem. Soc.*, **106**, 3531 (1984).

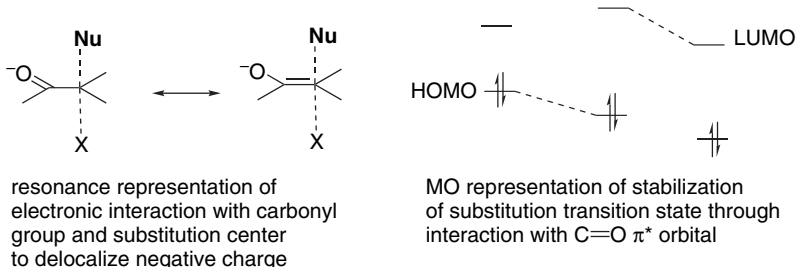
Table 4.10. Substituent Effects of α -EWG Substituents^a

Z	$Z-\text{CH}_2-\text{Cl}$	$+$	$\text{I}^- \longrightarrow Z-\text{CH}_2-\text{I}$
Z	Relative rate	Z	Relative rate
$\text{CH}_3\text{CH}_2\text{CH}_2$	1	PhC=O	3.2×10^4
PhSO_2	0.25	$\text{N}\equiv\text{C}$	3×10^3
$\text{CH}_3\text{C=O}$	3.5×10^4	$\text{C}_2\text{H}_5\text{OC=O}$	1.7×10^3

a. F. G. Bordwell and W. T. Branner, Jr., *J. Am. Chem. Soc.*, **86**, 4645 (1964).

Adjacent carbonyl groups also affect reactivity. Substitution by the ionization mechanism proceeds slowly on α -halo derivatives of ketones, aldehydes, acids, esters, nitriles, and related compounds. As discussed on p. 304, such substituents destabilize a carbocation intermediate, but substitution by the direct displacement mechanism proceeds especially readily in these systems. Table 4.10 indicates some representative relative rate accelerations.

Steric effects may be responsible for part of the observed acceleration, since an sp^2 carbon, such as in a carbonyl group, offers less steric resistance to the incoming nucleophile than an alkyl group. The major effect is believed to be electronic. The adjacent π LUMO of the carbonyl group can interact with the electron density that builds up at the pentacoordinate carbon in the TS. This can be described in resonance terminology as a contribution from an enolate-like structure to the TS. In MO terminology, the low-lying LUMO has a stabilizing interaction with the developing p orbital of the TS (see p. 394 for MO representations of the S_N2 transition state).⁴⁹



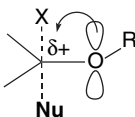
It should be noted that not all electron-attracting groups enhance reactivity. The sulfonyl and trifluoro groups, which cannot participate in this type of π conjugation, retard the rate of S_N2 substitution at an adjacent carbon.⁵⁰

The extent of the rate enhancement of adjacent substituents is dependent on the nature of the TS. The most important factor is the nature of the π -type orbital that develops at the trigonal bipyramidal carbon in the TS. If the carbon is cationic in character, electron donation from adjacent substituents becomes stabilizing. If bond formation at the TS is advanced, resulting in charge buildup at carbon, electron

⁴⁹. R. D. Bach, B. A. Coddens, and G. J. Wolber, *J. Org. Chem.*, **51**, 1030 (1986); F. Carrion and M. J. S. Dewar, *J. Am. Chem. Soc.*, **106**, 3531 (1984); S. S. Shaik, *J. Am. Chem. Soc.*, **105**, 4359 (1983); D. McLennan and A. Pross, *J. Chem. Soc., Perkin Trans.*, **2**, 981 (1984); T. I. Yousaf and E. S. Lewis, *J. Am. Chem. Soc.*, **109**, 6137 (1987).

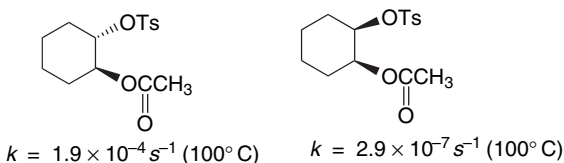
⁵⁰. F. G. Bordwell and W. T. Branner, Jr., *J. Am. Chem. Soc.*, **86**, 4645 (1964).

withdrawal is more stabilizing. Thus substituents such as carbonyl have their greatest effect on reactions with strong nucleophiles. Adjacent alkoxy substituents act as π donors and can stabilize S_N2 TSs that are cationic in character. Vinyl and phenyl groups can stabilize either type of TS, and allyl and benzyl systems show enhanced reactivity toward both strong and weak nucleophiles.⁵¹

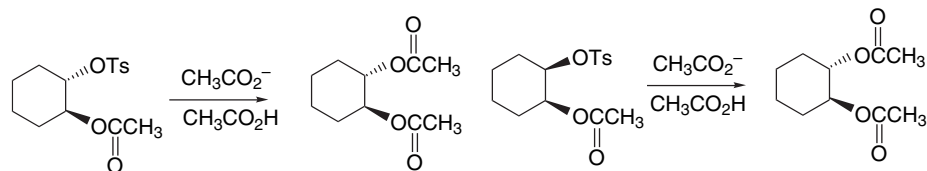


4.3. Neighboring-Group Participation

When a molecule that can react by nucleophilic substitution also contains a substituent group that can act as a nucleophile, it is often observed that the rate and stereochemistry of the nucleophilic substitution are strongly affected. The involvement of nearby nucleophilic substituents in a substitution process is called *neighboring-group participation*.⁵² A classic example of neighboring-group participation involves the solvolysis of compounds in which an acetoxy substituent is present next to the carbon that is undergoing nucleophilic substitution. For example, the rates of solvolysis of the *cis* and *trans* isomers of 2-acetoxycyclohexyl *p*-toluenesulfonate differ by a factor of about 670, the *trans* compound being more reactive.⁵³



Besides the pronounced difference in rate, the isomeric compounds reveal a striking difference in stereochemistry. The diacetate obtained from the *cis* isomer is the *trans* compound (inversion), whereas retention of configuration is observed for the *trans* isomer.



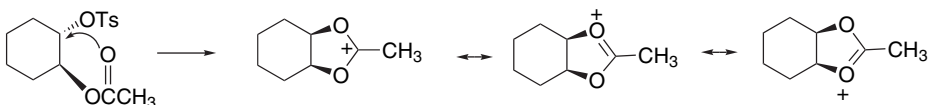
These results can be explained by the participation of the *trans* acetoxy group in the ionization process. The assistance provided by the acetoxy carbonyl group facilitates the ionization of the tosylate group, accounting for the rate enhancement. This kind of back-side participation by the adjacent acetoxy group is both sterically and

⁵¹ D. N. Kost and K. Aviram, *J. Am. Chem. Soc.*, **108**, 2006 (1986).

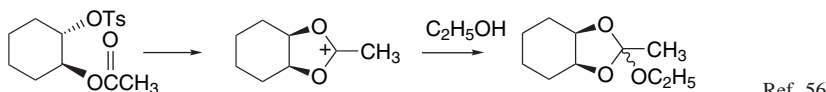
⁵² B. Capon, *Q. Rev. Chem. Soc.*, **18**, 45 (1964); B. Capon and S. P. McManus, *Neighboring Group Participation*, Plenum Press, New York, 1976.

⁵³ S. Winstein, E. Grunwald, R. E. Buckles, and C. Hanson, *J. Am. Chem. Soc.*, **70**, 816 (1948).

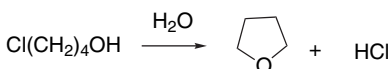
energetically favorable. The cation that is formed by participation is stabilized by both acetoxy oxygen atoms and is far more stable than a secondary carbocation. The resulting acetoxonium ion intermediate is subsequently opened by nucleophilic attack with inversion at either of the two equivalent carbons, leading to the observed *trans* product.⁵⁴



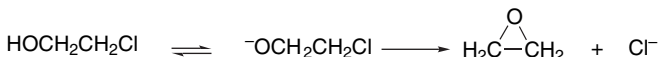
When enantiomerically pure *trans*-2-acetoxycyclohexyl tosylate is solvolyzed, the product is racemic *trans*-diacetate. This result is consistent with the proposed mechanism, because the acetoxonium intermediate is achiral and can only give rise to racemic material.⁵⁵ Additional evidence for this interpretation comes from the isolation of a cyclic orthoester when the solvolysis is carried out in ethanol, where the acetoxonium ion is captured by the solvent.



The hydroxy group can act as an intramolecular nucleophile. Solvolysis of 4-chlorobutanol in water gives tetrahydrofuran as the product.⁵⁷ The reaction is much faster than solvolysis of 3-chloropropanol under similar conditions. Participation in the latter case is less favorable because it involves formation of a strained four-membered ring.



The alkoxide ions formed by deprotonation in basic solution are even more effective nucleophiles. In ethanol containing sodium ethoxide, 2-chloroethanol reacts about 5000 times faster than ethyl chloride. The product is ethylene oxide, confirming the involvement of the oxygen atom as a nucleophile.



As would be expected, the effectiveness of neighboring-group participation depends on the ease with which the molecular geometry required for participation can be attained. The rate of cyclization of ω -hydroxyalkyl halides, for example, shows a strong dependence on the length of the chain separating the two groups. Some data are given in Table 4.11. The maximum rate occurs for the 4-hydroxybutyl system involving formation of a five-membered ring.

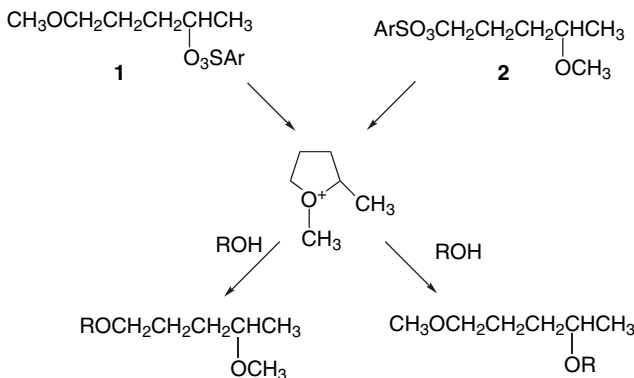
- ⁵⁴. S. Winstein, C. Hanson, and E. Grunwald, *J. Am. Chem. Soc.*, **70**, 812 (1948).
- ⁵⁵. S. Winstein, H. V. Hess, and R. E. Buckles, *J. Am. Chem. Soc.*, **64**, 2796 (1942).
- ⁵⁶. S. Winstein and R. E. Buckles, *J. Am. Chem. Soc.*, **65**, 613 (1943).
- ⁵⁷. H. W. Heine, A. D. Miller, W. H. Barton, and R. W. Greiner, *J. Am. Chem. Soc.*, **75**, 4778 (1953).

Table 4.11. Solvolysis Rates of ω -Chloro Alcohols^a

ω -Chloro alcohol	Approximate relative rate
$\text{Cl}(\text{CH}_2)_2\text{OH}$	2000
$\text{Cl}(\text{CH}_2)_3\text{OH}$	1
$\text{Cl}(\text{CH}_2)_4\text{OH}$	5700
$\text{Cl}(\text{CH}_2)_5\text{OH}$	20

a. B. Capon, *Q. Rev. Chem. Soc.*, **18**, 45 (1964); W. H. Richardson, C. M. Golino, R. H. Wachs, and M. B. Yelvington, *J. Org. Chem.*, **36**, 943 (1971).

Like the un-ionized hydroxy group, an alkoxy group is a weak nucleophile, but it can function as a neighboring nucleophile. For example, solvolysis of the isomeric *p*-bromobenzenesulfonate esters **1** and **2** leads to identical product mixtures, indicating the involvement of a common intermediate. This can occur by formation of a cyclic oxonium ion by intramolecular participation.⁵⁸



The occurrence of nucleophilic participation is also indicated by a rate enhancement. The maximum rate enhancement is observed when participation of a methoxy group occurs via a five-membered ring (see Table 4.12).

Table 4.13 provides data on two series of intramolecular nucleophilic substitution. One data set pertains to cyclization of ω -bromoalkylmalonate anions and the other

Table 4.12. Relative Solvolysis Rates of Some ω -Methoxyalkyl *p*-Bromobenzenesulfonates in Acetic Acid^a

$\text{CH}_3(\text{CH}_2)_2\text{OSO}_2\text{Ar}$	1.00
$\text{CH}_3\text{O}(\text{CH}_2)_2\text{OSO}_2\text{Ar}$	0.28
$\text{CH}_3\text{O}(\text{CH}_2)_3\text{OSO}_2\text{Ar}$	0.67
$\text{CH}_3\text{O}(\text{CH}_2)_4\text{OSO}_2\text{Ar}$	657
$\text{CH}_3\text{O}(\text{CH}_2)_5\text{OSO}_2\text{Ar}$	123
$\text{CH}_3\text{O}(\text{CH}_2)_6\text{OSO}_2\text{Ar}$	1.16

a. S. Winstein, E. Allred, R. Heck, and R. Glick, *Tetrahedron*, **3**, 1 (1958).

⁵⁸. E. L. Allred and S. Winstein, *J. Am. Chem. Soc.*, **89**, 3991 (1967).

Table 4.13. Relative Rates of Cyclization as a Function of Ring Size

Ring size	Lactonization of ω -bromo carboxylates ^a	ΔH^\ddagger (kcal/mol)	ΔS^\ddagger (eu)	Cyclization of ω -bromoalkylmalonates ^b
3	8.2×10^{-4}	22.0	-2.5	
4	0.92	17.7	-5.0	0.58
5	108	15.9	-5.5	833
6	1.00	17.2	-4.1	1.00
7	3.7×10^{-3}	17.4	-13.5	8.7×10^{-3}
8	3.8×10^{-5}	21.7	-9.2	1.5×10^{-4}
9	4.3×10^{-5}	20.3	-14.0	1.7×10^{-5}
10	1.3×10^{-4}	17.3	-20.7	1.4×10^{-6}
11	3.3×10^{-4}	16.4	-22.3	2.9×10^{-6}
12	4.1×10^{-4}	17.6	-18.0	4.0×10^{-4}
13	1.2×10^{-3}	15.3	-23.0	7.4×10^{-4}
17				2.9×10^{-3}
18	2.0×10^{-3}	15.2	-21.8	
21				4.3×10^{-3}
23	2.3×10^{-3}	14.5	-22.3	

a. C. Galli, G. Illuminati, L. Mandolini, and P. Tamborra, *J. Am. Chem. Soc.*, **99**, 2591 (1977); L. Mandolini, *J. Am. Chem. Soc.*, **100**, 550 (1978).

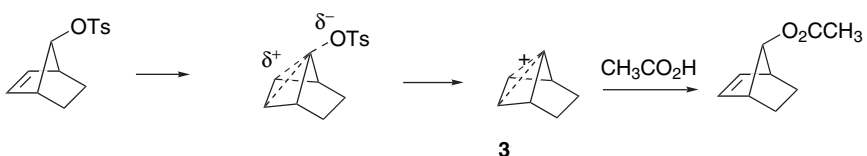
b. M. A. Casadei, C. Galli, and L. Mandolini, *J. Am. Chem. Soc.*, **106**, 1051 (1984).

to lactonization of ω -bromocarboxylates. Both reactions occur by direct displacement mechanisms. The dissection of the E_a of ring-closure reactions into enthalpy and entropy components shows some consistent features. The ΔH^\ddagger for formation of three- and four-membered rings is normally higher than for five- and six-membered rings, whereas ΔS^\ddagger is least negative for three-membered rings. The ΔS^\ddagger is comparable for four-, five-, and six-membered rings and then becomes more negative as the ring size increases above seven. The ΔH^\ddagger term reflects the strain that develops in the closure of three-membered rings, whereas the more negative entropy associated with larger rings indicates the decreased probability of encounter of the reaction centers as they get farther apart. Because of the combination of these two factors, the maximum rate is usually observed for the five- and six-membered rings.

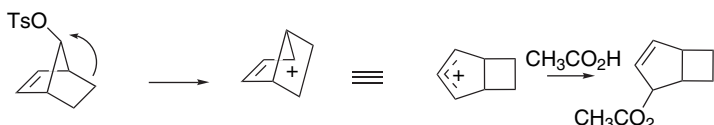
In general, any system that has a nucleophilic substituent situated properly for back-side displacement of a leaving group at another carbon atom of the molecule can be expected to display neighboring-group participation. The extent of the rate enhancement depends on how effectively the group acts as an internal nucleophile. The existence of participation may be immediately obvious from the structure of the product if a derivative of the cyclic intermediate is stable. In other cases, demonstration of kinetic acceleration or stereochemical consequences may provide the basis for identifying nucleophilic participation.

The π electrons of carbon-carbon double bonds can also become involved in nucleophilic substitution reactions. This participation can facilitate the ionization step if it leads to a carbocation having special stability. Solvolysis reactions of the *syn* and *anti* isomers of 7-norbornenyl tosylates provide some dramatic examples of the influence of participation by double bonds on reaction rates and stereochemistry. The *anti*-tosylate is more reactive by a factor of about 10^{11} than the saturated analog toward acetolysis. The reaction product, *anti*-7-acetoxy norbornene, is the product of *retention* of configuration. These results can be explained by participation of the π electrons of the double bond to give the ion **3**, which is stabilized by delocalization of the positive charge.⁵⁹

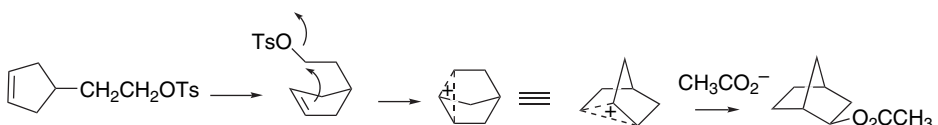
⁵⁹. S. Winstein, M. Shavatsky, C. Norton, and R. B. Woodward, *J. Am. Chem. Soc.*, **77**, 4183 (1955); S. Winstein and M. Shavatsky, *J. Am. Chem. Soc.*, **78**, 592 (1956); S. Winstein, A. H. Lewin, and K. C. Pande, *J. Am. Chem. Soc.*, **85**, 2324 (1963).



In contrast, the *syn* isomer, where the double bond is not in a position to participate in the ionization step, reacts 10^7 times slower than the *anti* isomer. The reaction product in this case is derived from a rearranged carbocation ion that is stabilized by virtue of being allylic.⁶⁰

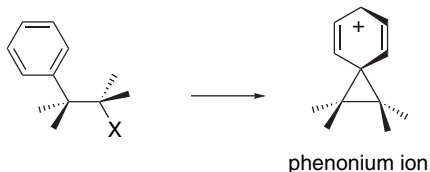


Participation of carbon-carbon double bonds in solvolysis reactions is revealed in some cases by isolation of products with new carbon-carbon σ bonds. A particularly significant case is the formation of the bicyclo[2.2.1]heptane ring during solvolysis of 2-cyclopent-3-enylethyl tosylate.⁶¹



In this case, the participation leads to the formation of the norbornyl cation, which is captured as the acetate. More is said about this important cation in Section 4.4.5.

A system in which the participation of aromatic π electron has been thoroughly probed is the “phenonium” ions, the species resulting from participation by a β -phenyl group.

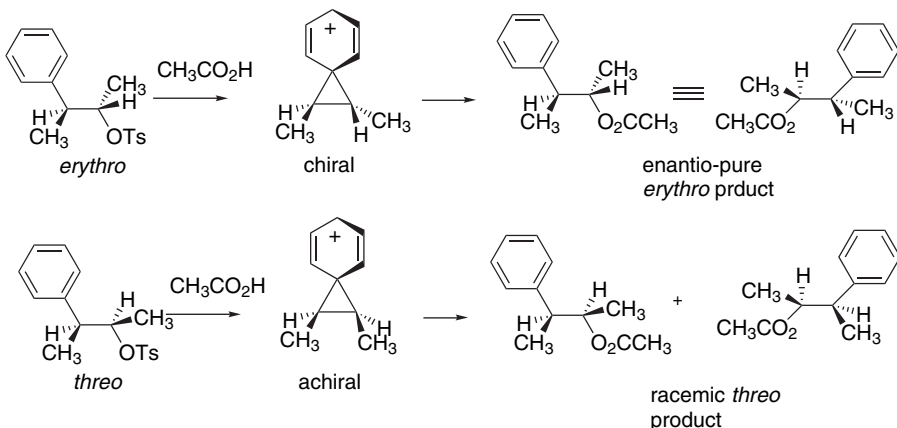


Such participation leads to a bridged carbocation with the positive charge delocalized into the aromatic ring. Evidence for this type of participation was first obtained by a study of the stereochemistry of solvolysis of 3-phenyl-2-butyl tosylates. The *erythro* isomer gave largely retention of configuration, a result that can be explained via a

⁶⁰. S. Winstein and E. T. Stafford, *J. Am. Chem. Soc.*, **79**, 505 (1957).

⁶¹. R. G. Lawton, *J. Am. Chem. Soc.*, **83**, 2399 (1961).

bridged ion intermediate. The *threo* isomer, where participation leads to an achiral intermediate, gave racemic *threo* product.⁶²



The relative importance of aryl participation is a function of the substituents on the ring. The extent of participation can be quantitatively measured by comparing the rate of direct displacement, k_s , with the rate of aryl-assisted solvolysis, designated k_Δ .⁶³ The relative contributions to individual solvolyses can be distinguished by taking advantage of the higher sensitivity to aryl substituent effects of the assisted mechanism. In systems with EWG substituents, the aryl ring does not participate effectively and only the process described by k_s contributes to the rate. Such compounds give a Hammett correlation with ρ values (-0.7 to -0.8) characteristic of a weak substituent effect. Compounds with ERG substituents deviate from the correlation line because of the aryl participation. The extent of reaction proceeding through the k_s process can be estimated from the correlation line for electron-withdrawing substituents.

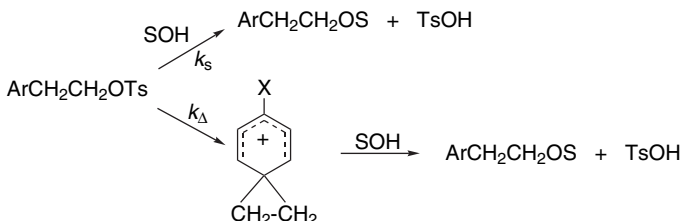


Table 4.14 gives data indicating the extent of aryl rearrangement for several substituents in different solvents. This method of analysis shows that the relative extent of participation of the β -phenyl groups is highly dependent on the solvent.⁶⁴ In solvents of good nucleophilicity (e.g., ethanol), the normal solvent displacement mechanism

⁶² D. J. Cram, *J. Am. Chem. Soc.*, **71**, 3863 (1949); **74**, 2129 (1952).

⁶³ A. Diaz, I. Lazdins, and S. Winstein, *J. Am. Chem. Soc.*, **90**, 6546 (1968).

⁶⁴ F. L. Schadt, III, C. J. Lancelot, and P. v. R. Schleyer, *J. Am. Chem. Soc.*, **100**, 228 (1978).

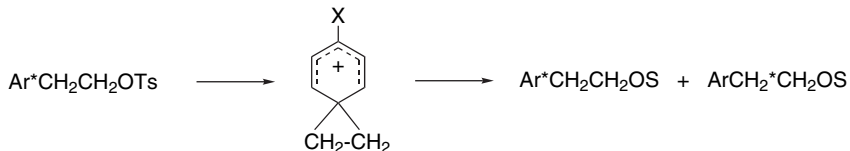
Table 4.14. Extent of Aryl Rearrangement in 2-Phenylethyl Tosylate Solvolysis

Substituent	Solvent		
	80% Ethanol ^a	Acetic acid ^b	Formic acid ^b
NO ₂	0	—	—
CF ₃	0	—	—
Cl	7	—	—
H	21	38	78
CH ₃	63	71	94
CH ₃ O	93	94	99

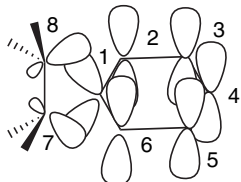
a. D. J. Raber, J. M. Harris, and P. v. R. Schleyer, *J. Am. Chem. Soc.*, **93**, 4829 (1971).

b. C. C. Lancelot and P. v. R. Schleyer, *J. Am. Chem. Soc.*, **91**, 4296 (1969).

makes a larger contribution. As solvent nucleophilicity decreases, the relative extent of aryl participation increases.



The bridged form of the β -phenylethyl cation can be observed in superacid media (see Section 4.4) and characterized by carbon and proton NMR spectra.⁶⁵ The bridged ion subsequently rearranges to the more stable α -methylbenzyl cation with E_a of about 13 kcal/mol. High-level MO and DFT calculations have been performed on the bridged ion. The bond length to C(1) from C(7) and C(8) is 1.625 Å, whereas the C(7)–C(8) bond length is 1.426 Å. The phenonium ion has a good deal of delocalization of the electron deficiency and the resulting positive charge into the cyclopropane ring.⁶⁶ This occurs by overlap of the cyclopropyl orbitals with the π system.



4.4. Structure and Reactions of Carbocation Intermediates

4.4.1. Structure and Stability of Carbocations

The critical step in the ionization mechanism for nucleophilic substitution is the generation of the carbocation intermediate. For this mechanism to operate, it is essential

⁶⁵. G. A. Olah, R. J. Spear, and D. A. Forsyth, *J. Am. Chem. Soc.*, **98**, 6284 (1976).

⁶⁶. S. Sieber and P. v. R. Schleyer, *J. Am. Chem. Soc.*, **115**, 6987 (1993); E. Del Rio, M. K. Menendez, R. Lopez, and T. L. Sordo, *J. Phys. Chem. A*, **104**, 5568 (2000); E. del Rio, M. I. Menendez, R. Lopez, and T. L. Sordo, *J. Am. Chem. Soc.*, **123**, 5064 (2001).

that the carbocation not be prohibitively high in energy. Carbocations are inherently high-energy species. The ionization of *t*-butyl chloride is endothermic by 153 kcal/mol in the gas phase.⁶⁷



An activation energy of this magnitude would lead to an unobservably slow reaction at normal temperature. Carbocation formation in solution is feasible because of solvation of the ions that are produced. It is also important to understand the effect structure and substituents have on carbocation stability. We introduced this subject in Section 3.4.1, where we emphasized inherent structural effects in the gas phase, but owing to the important role of solvation in ionization reactions, we have to consider carbocation stability in solution as well. A method that is applicable to highly stabilized cations is to determine the extent of carbocation formation from the parent alcohol in acidic solution. The triarylmethyl cations are stabilized by the conjugation that delocalizes the positive charge. In acidic solution, equilibrium is established between triarylcarbinols and the corresponding carbocation:



The relative stability of the carbocation can be expressed in terms of its $\text{p}K_{\text{R}^+}$, which is defined as

$$\text{p}K_{\text{R}^+} = \log \frac{[\text{R}^+]}{[\text{ROH}]} + H_{\text{R}}$$

where H_{R} is an acidity function defined for the medium.⁶⁸ In dilute aqueous solution, H_{R} is equivalent to pH, and $\text{p}K_{\text{R}^+}$ is equal to the pH at which the carbocation and alcohol are present in equal concentrations. The values shown in Table 4.15 were determined by measuring the extent of carbocation formation at several acidities and applying the definition of $\text{p}K_{\text{R}^+}$.

The $\text{p}K_{\text{R}^+}$ values allow for a comparison of the stability of relatively stable carbocations. The data in Table 4.15 show that ERG substituents on the aryl rings stabilize the carbocation (less negative $\text{p}K_{\text{R}^+}$), whereas EWGs such as nitro are destabilizing. This is as expected from the electron-deficient nature of carbocations. The diarylmethyl cations listed in Table 4.14 are 6–7 $\text{p}K_{\text{R}^+}$ units less stable than the corresponding triarylmethyl cations. This indicates that the additional aryl groups have a cumulative, although not necessarily additive, effect on the stability of the carbocation. Primary benzylic cations are generally not sufficiently stable for direct determination of $\text{p}K_{\text{R}^+}$ values. A value of ≤ 20 has been assigned to the benzyl cation based on rate measurements for the forward and reverse reactions.⁶⁹ A particularly stable benzylic ion, the 2,4,6-trimethylphenylmethyl cation has a $\text{p}K_{\text{R}^+}$ of -17.4 . *t*-Alkyl cations have $\text{p}K_{\text{R}^+}$ values around -15 .

Several very stable carbocations are included in the “Other Carbocations” part of Table 4.15. The tricyclopropylmethyl cation, for example, is more stable than the

⁶⁷ D. W. Berman, V. Anicich, and J. L. Beauchamp, *J. Am. Chem. Soc.*, **101**, 1239 (1979).

⁶⁸ N. C. Deno, J. J. Jaruzelski, and A. Schriesheim, *J. Am. Chem. Soc.*, **77**, 3044 (1955).

⁶⁹ T. L. Amyes, J. P. Richard, and M. Novak, *J. Am. Chem. Soc.*, **114**, 8032 (1992).

Table 4.15. Values of pK_{R^+} for Some Carbocations^a

Carbocation	pK_{R^+}	Carbocation	pK_{R^+}	SECTION 4.4
<i>A. Triarylmethyl</i>				<i>Structure and Reactions of Carbocation Intermediates</i>
Triphenyl	-6.63	4, 4', 4''-Tri(dimethylamino)phenyl	+9.36	
4, 4', 4''-Trimethyltriphenyl	-3.56	4, 4', 4''-Trichlorotriphenyl	-7.74	
4-Methoxytriphenyl	-3.40	4-Nitrotriphenyl	-9.15	
4, 4'-Dimethoxytriphenyl	-1.24	4, 4', 4''-Trinitrotriphenyl	-16.27	
4, 4', 4''-Trimethoxytriphenyl	+0.82			
<i>B. Diarylmethyl</i>				
Diphenyl	-13.3	2, 2', 4, 4', 6, 6'-Hexamethyldiphenyl	-6.6	
4, 4'-Dimethyldiphenyl	-10.4	4, 4'-Dichlorodiphenyl	-13.96	
4, 4'-Dimethoxydiphenyl	-5.71			
<i>C. Other Carbocations</i>				
Benzyl ^b	≤ -20	Triphenylcyclopropenyl ^e	+3.1	
t-Butyl ^c	-15.5	2,4,6-trimethylbenzyl	-17.4	
2-Phenyl-2-propyl ^b	-12.3	Trimethylcyclopropenyl ^f	+7.8	
Tropylium (Cycloheptatrienyl)	+4.7	Tricyclopropylcyclopropenyl ^g	+9.7	
Tricyclopropylmethyl ^d	-2.3			

a. Unless otherwise indicated, the pK_{R^+} values are taken from N. C. Deno, J. J. Jaruzelski, and A. Schriesheim, *J. Am. Chem. Soc.*, **77**, 3044 (1955); see also H. H. Freedman in *Carbonium Ions*, vol. IV, G. A. Olah and P. v. R. Schleyer, eds., Wiley-Interscience, New York, 1973, Chap. 28.

b. T. L. Amyes, J. P. Richard, and M. Novak, *J. Am. Chem. Soc.*, **114**, 8032 (1992).

c. R. H. Boyd, R. W. Taft, A. P. Wolf, and D. R. Christman, *J. Am. Chem. Soc.*, **82**, 4729 (1960); E. M. Arnett and T. C. Hofelich, *J. Am. Chem. Soc.*, **105**, 2889 (1983); D. D. M. Wayner, D. J. McPhee, and D. J. Griller, *J. Am. Chem. Soc.*, **110**, 132 (1988).

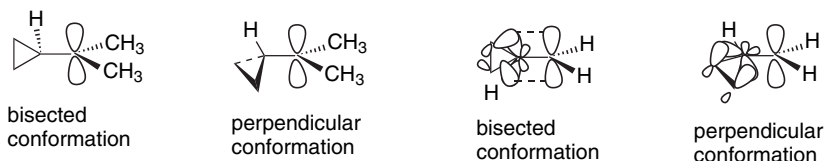
d. N. C. Deno, H. G. Richey, Jr., J. S. Liu, D. N. Lincoln, and J. O. Turner, *J. Am. Chem. Soc.*, **87**, 4533 (1965).

e. R. Breslow, H. Höver, and H. W. Chang, *J. Am. Chem. Soc.*, **84**, 3168 (1962); R. Breslow, J. Lockhart, and H. W. Chang, *J. Am. Chem. Soc.*, **83**, 2367 (1961).

f. J. Ciabattoni and E. C. Nathan, III, *Tetrahedron Lett.*, 4997 (1969).

g. K. Komatsu, I. Tomioka, and K. Okamoto, *Tetrahedron Lett.*, 947 (1980); R. A. Moss and R. C. Munjal, *Tetrahedron Lett.*, 1221 (1980).

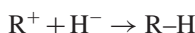
triphenylmethyl cation.⁷⁰ The stabilization of carbocations by cyclopropyl substituents results from the interaction of the cyclopropyl bonding orbitals with the vacant carbon p -orbital. The electrons in these orbitals are at relatively higher energy than normal σ -electrons and are therefore particularly effective in interacting with the vacant p -orbital of the carbocation. This interaction imposes a stereoelectronic preference for the bisected conformation of the cyclopropylmethyl cation in comparison to the perpendicular conformation. Only the bisected conformation aligns the cyclopropyl C–C orbitals for effective overlap.



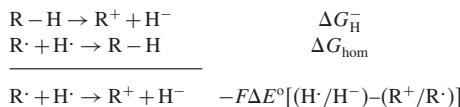
As discussed in Section 3.4.1, carbocation stability can also be expressed in terms of *hydride affinity*. Hydride affinity values based on solution measurements can be

⁷⁰. For reviews of cyclopropylmethyl cation see H. G. Richey, Jr., in *Carbonium Ions*, Vol. III, G. A. Olah and P. v. R. Schleyer, eds., Wiley-Interscience, New York, 1972, Chap. 25; G. A. Olah, V. Reddy, and G. K. S. Prakash, *Chem. Rev.*, **92**, 69 (1992); G. A. Olah, V. Reddy, and G. K. S. Prakash, *Chemistry of the Cyclopropyl Group*, Part 2, Z. Rappoport, ed., Wiley, Chichester, 1995, pp. 813–859.

derived from thermodynamic cycles that relate pK_a and electrochemical potentials. The hydride affinity, $-\Delta G$, for the reaction



is a measure of carbocation stability. This quantity can be related to an electrochemical potential by summation with the energy for hydrogen atom removal, i.e., the homolytic bond dissociation energy.



so

$$\Delta G_{\text{H}^-} = \Delta G_{\text{hom}} - -F\Delta E^\circ[(\text{H}\cdot/\text{H}^-) - (\text{R}^+/\text{R}\cdot)]$$

where $(\text{H}\cdot/\text{H}^-)$ and $(\text{R}^+/\text{R}\cdot)$ are one-electron oxidation potentials for H^- and $\text{R}\cdot$.⁷¹ The former potential is about -0.55 V in DMSO. Measurement of $(\text{R}^+/\text{R}\cdot)$ can be accomplished by cyclic voltammetry for relatively stable carbocations and by other methods for less stable cations. The values obtained range from 83 kcal/mol for the aromatic tropylium ion to 130 kcal/mol for a benzylic cation destabilized by a EWG substituents. Some of these data are included in Table 4.16. Note that these values are considerably smaller than the corresponding gas phase values, which range from 200 kcal/mol for tropylium ion to 239 kcal/mol for the benzyl cation, although the difference in stability is quite similar. This is the result of solvent stabilization.

It is possible to obtain thermodynamic data for the ionization of alkyl chlorides by reaction with SbF_5 , a strong Lewis acid, in the nonnucleophilic solvent SO_2ClF .⁷² The solvation energies of the carbocations in this medium are small and do not differ much from one another, which makes comparison of nonisomeric systems reasonable. As long as subsequent reactions of the carbocation can be avoided, the thermodynamic characteristics of the ionization reactions provide a measure of the relative ease of carbocation formation in solution. There is good correlation between these data and the

Table 4.16. Solution Hydride Affinity of Some Carbocations^a

Carbocation	ΔH (kcal/mol)	ΔH_{gas} (kcal/mol)
Tropylium ion	83	200 ^b
Ph_3C^+	96	215
$\text{Ph}_2\text{C}^+\text{H}$	105	222
PhCH_2^+	118	238
$p\text{-CH}_3\text{OC}_6\text{H}_4\text{CH}_2^+$	106	227
$p\text{-NCC}_6\text{H}_4\text{CH}_2^+$	122	247

a. J.-P. Cheng, K. L. Handoo, and V. D. Parker, *J. Am. Chem. Soc.*, **115**, 2655 (1993).
b. See Table 3.10.

⁷¹. J.-P. Cheng, K. L. Handoo, and V. D. Parker, *J. Am. Chem. Soc.*, **115**, 2655 (1993).

⁷². E. M. Arnett and N. J. Pienta, *J. Am. Chem. Soc.*, **102**, 3329 (1980); E. M. Arnett and T. C. Hofelich, *J. Am. Chem. Soc.*, **105**, 2889 (1983).

SECTION 4.4

Structure and Reactions
of Carbocation
Intermediates

gas phase data, in terms of both the stability order and the energy differences between the carbocations. A plot of the ionization enthalpy and gas phase hydride affinity gives a line of slope 1.63 with a correlation coefficient of 0.973. This result is in agreement with the expectation that the gas phase stability would be more sensitive to structure than the solution phase stability. The energy gap between tertiary and secondary ions is about 17 kcal/mol in the gas phase and about 9.5 kcal/mole in the SO_2ClF solution. An independent measurement of the energy difference between secondary and tertiary cations in solution is available from calorimetric measurement of the ΔH of isomerization of the *sec*-butyl cation to the *tert*-butyl cation. This value has been found to be 14.5 kcal/mol in SO_2ClF solution.⁷³ An MP2/6-31G* computation finds a difference of 14.8 kcal.⁷⁴ Some representative data are given in Table 4.17. These data give some basis for comparison of the stability of secondary and tertiary alkyl carbocations with aryl-substituted ions. Note also that the solution data also show that cyclopropyl groups are very stabilizing toward carbocations.

The increase in carbocation stability with additional alkyl substitution is one of the most important and general trends in organic chemistry. This stability relationship is fundamental to understanding many aspects of reactivity, especially nucleophilic substitution. Hyperconjugation is the principal mechanism by which alkyl substituents stabilize carbocations. There is considerable evidence of the importance of hyperconjugation on the structure of carbocations, including NMR data, crystallographic data, and computational studies. The *tert*-butyl cation has been studied by each method. The NMR results indicate shortening of the C–C bonds, as would be predicted by hyperconjugation.⁷⁵ The crystal structure gives a value of 1.44 Å.⁷⁶ A computational study at the MP2/6-31G** level shows a slight elongation of the C–H bonds aligned with the *p* orbital, and the C–C–H bond angles are slightly reduced (Figure 4.8).⁷⁷

Levy has performed NPA, Mulliken, AIM, and CHELPG charge analyses on the *iso*-propyl, *sec*-butyl, and *tert*-butyl cations using MP2/6-31G*-level computations.⁷⁴ As mentioned briefly in Section 3.4.1, the trivalent carbon atom in *tert*-butyl cation

Table 4.17. ΔH for Ionization of Chlorides and Alcohols in SO_2ClF

Reactant	ΔH (kcal/mol)	
	X=Cl	X=OH
$(\text{CH}_3)_2\text{CH}-\text{X}$	−15	
$\text{Ph}_2\text{C}(\text{CH}_3)-\text{X}$	−16	
$(\text{CH}_3)_3\text{C}-\text{X}$	−25	−35
$\text{PhC}(\text{CH}_3)_2-\text{X}$	−30	−40
$\text{Ph}_2\text{C}(\text{CH}_3)-\text{X}$		−37.5
$\text{Ph}_3\text{C}-\text{X}$		−49
$(\text{---})_3\text{C}-\text{X}$		−59

a. Data from E. M. Arnett and T. C. Hofelich, *J. Am. Chem. Soc.*, **105**, 2889 (1983).

⁷³. E. W. Bittner, E. M. Arnett, and M. Saunders, *J. Am. Chem. Soc.*, **98**, 3734 (1976).

⁷⁴. J. B. Levy, *Struct. Chem.*, **10**, 121 (1999).

⁷⁵. C. S. Yannoni, R. D. Kendrick, P. C. Myhre, D. C. Bebout, and B. L. Petersen, *J. Am. Chem. Soc.*, **111**, 6440 (1989).

⁷⁶. S. Hollenstein and T. Laube, *J. Am. Chem. Soc.*, **115**, 7240 (1993).

⁷⁷. S. Sieber, P. Buzek, P. v. R. Schleyer, W. Koch, and J. W. d. M. Carneiro, *J. Am. Chem. Soc.*, **115**, 259 (1993).

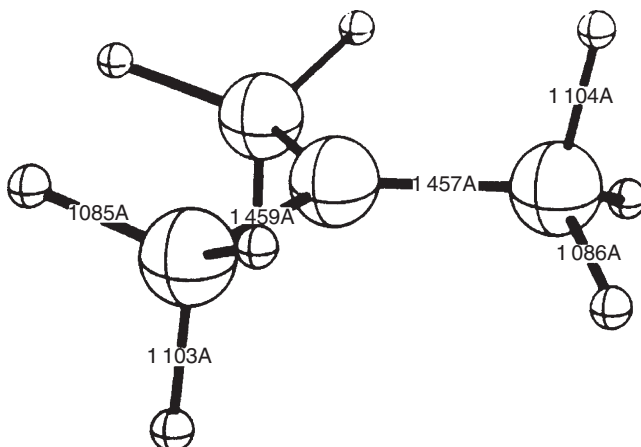
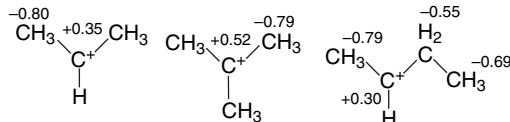
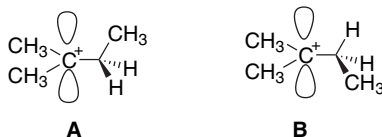


Fig. 4.8. MP2/6-31G** optimized structure of *t*-butyl cation with three hydrogens aligned with the *p* orbital. Reproduced from *J. Am. Chem. Soc.* **115**, 259 (1993), by permission of the American Chemical Society.

is found to be more positive than the carbon in the secondary ions. The adjacent carbons bear negative charges, as a result of electron donation from hydrogen. The charges on hydrogen range from +0.26 to +0.38, averaging +0.32 in the *tert*-butyl cation, according to the NPA analysis. This is consistent with the representation of the stabilizing effect in terms of hyperconjugation. This analysis also suggests that a significant part of the stabilization of the *tert*-butyl cation comes from the favorable electrostatic consequence of alternating positive and negative charges.



The 2-methyl-2-butyl cation provides the opportunity to compare C–C and C–H hyperconjugation. At the MP4/6-31G** level of calculation, little energy difference is found between structures **A** and **B**, which differ in alignment of CH₃ or H with the empty *p* orbital.⁷⁸ Structure **A**, however, gives a much closer approximation to the observed ¹³C chemical shift and thus seems to be preferred. The calculations also indicate a lengthening of the C(3)–C(4) bond (to 1.58 Å) and a contraction of the C(2)–C(3)–C(4) bond angle to 101.5°, both of which are consistent with C–C hyperconjugation.



A particularly interesting example of the effect of hyperconjugation is found in the 1-methylcyclohexyl carbocation. The NMR spectrum of this cation reveals the presence

⁷⁸ P. v. R. Schleyer, J. W. de Carneiro, W. Koch, and D. A. Forsyth, *J. Am. Chem. Soc.*, **113**, 3990 (1991).

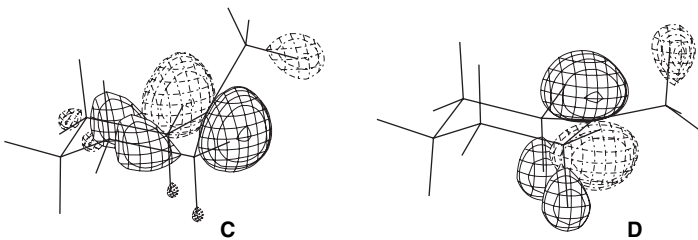
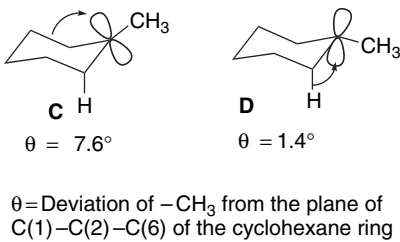


Fig. 4.9. Distribution of LUMO orbitals of isomeric 1-methylcyclohexyl cations showing dominant C–C (**C**) and C–H (**D**) hyperconjugation. Reproduced from *J. Am. Chem. Soc.*, **118**, 3761 (1996), by permission of the American Chemical Society.

of two isomeric cations that are separated by a small barrier. Investigation of the NMR chemical shifts using the MP2-GIAO method points to an axial and equatorial isomer of nearly equal energy. B3LYP/6-31G* calculations indicate an energy difference of about 0.6 kcal and suggest that the (nearly planar) TS is about 0.9 kcal above the minimum energy structure.⁷⁹ The cationic carbon is slightly pyramidalized toward the C–C or C–H bonds involved in hyperconjugation. The reason for the pyramidalization is better alignment with the C–C and C–H bonds that provide hyperconjugative stabilization. The hyperconjugation is also indicated by the differing shapes of the LUMO orbitals for the isomeric ions shown in Figure 4.9.



θ =Deviation of $-\text{CH}_3$ from the plane of
 $\text{C}(1)-\text{C}(2)-\text{C}(6)$ of the cyclohexane ring

The 1-adamantyl carbocation provides another example of C–C hyperconjugation. The $\text{C}\alpha$ - $\text{C}\beta$ bond is shortened by 0.06 Å in the crystal structure.⁸⁰ The NMR spectrum also shows characteristics of delocalization of the positive charge. A computational study also indicates delocalization of the positive charge.⁸¹



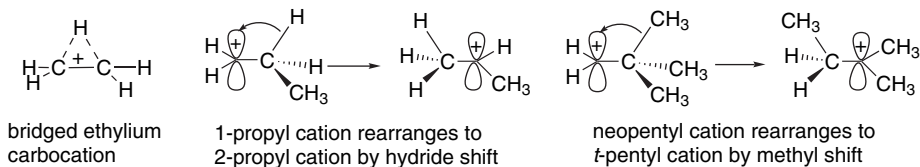
It is important to note the relationship of C–H and C–C hyperconjugation to the *reactivity* as well as the *structure* of carbocations. Hyperconjugation represents electron sharing with an empty orbital and can lead to structural changes or

⁷⁹. A. Rauk, T. S. Sorenson, C. Maerker, J. W. d. M. Carneiro, S. Sieber, and P. v. R. Schleyer, *J. Am. Chem. Soc.*, **118**, 3761 (1996); A. Rauk, T. S. Sorenson, and P. v. R. Schleyer, *J. Chem. Soc., Perkin Trans. 2*, 869 (2001).

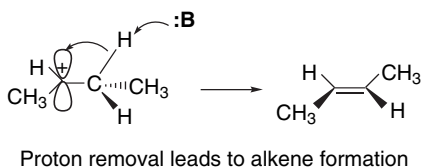
⁸⁰. T. Laube, *Angew. Chem. Intl. Ed. Engl.*, **25**, 349 (1986); T. Laube and E. Schaller, *Acta Crystallog. B*, **B51**, 177 (1995).

⁸¹. G. A. Olah, G. K. S. Prakash, J. G. Shih, V. V. Krishnamurthy, G. D. Mateescu, G. Liang, G. Sipos, V. Buss, T. M. Gund, and P. v. R. Schleyer, *J. Am. Chem. Soc.*, **107**, 2764 (1985).

reactions. If the electron density is substantially shared between the two atoms, the structure is *bridged*. If the electron sharing results in a shift of the donor group, *rearrangement* occurs. As we saw in Section 3.4.1, the ethyl cation is bridged. Larger primary cations rearrange to more stable carbocations; for example, the 1-propyl cation rearranges to the 2-propyl cation and a neopentyl cation rearranges to a *t*-pentyl cation. These rearrangements are the culmination of electron donation by formation of a new bond.



Hyperconjugation also makes carbocations susceptible to proton removal, as occurs in elimination reactions. The weakened C–H bond and increased positive charge make hydrogen susceptible to removal as a proton. When we study elimination reactions in Section 5.10, we will find that there is a preference for the removal of the proton from the most highly substituted carbon, which is the one that is most engaged in hyperconjugation.

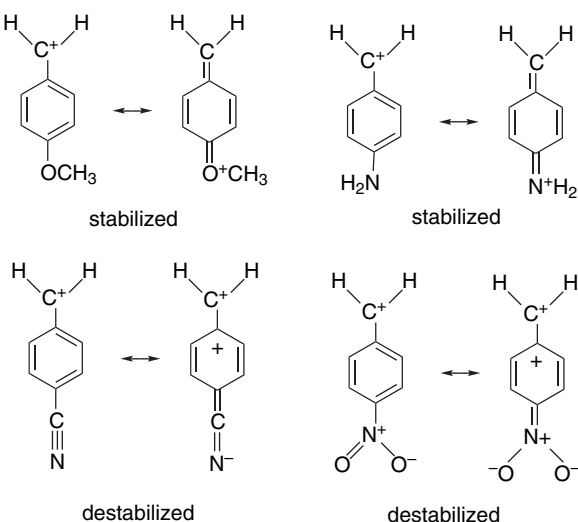


Within any given series of carbocations, substituents affect stability in predictable ways. ERG substituents stabilize carbocations, whereas EWG substituents destabilize them. Careful attention must be paid to both resonance and polar effects. The resonance effect is very strong for substituents directly on the cationic carbon. Benzylic cations are strongly stabilized by resonance interactions with the aromatic ring. Substituent effects can be correlated by the Yukawa-Tsuno equation.⁸² For example, gas phase chloride ion affinities correlate with the Yukawa-Tsuno equation with $\rho = -14.0$ and $r^+ = 1.29$, indicating a strong resonance interaction.⁸³ A molecular orbital calculation estimating the stabilization was done using STO-3G-level basis functions. The electron-donating *p*-amino and *p*-methoxy groups were found to stabilize a benzyl cation by 26 and 14 kcal/mol, respectively. On the other hand, electron-attracting groups such as *p*-cyano and *p*-nitro were destabilizing by 12 and 20 kcal/mol, respectively.⁸⁴

⁸². Y. Tsuno and M. Fujio, *Chem. Soc. Rev.*, **25**, 129 (1996).

⁸³. M. Mishima, K. Arima, H. Inoue, S. Usui, M. Fujio, and Y. Tsuno, *Bull. Chem. Soc. Jpn.*, **68**, 3199 (1995).

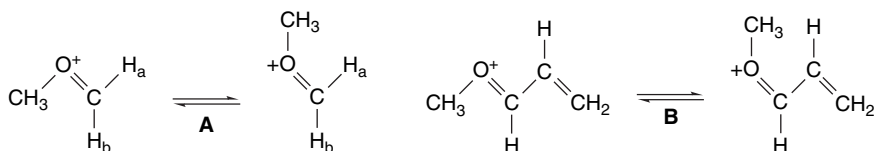
⁸⁴. W. J. Hehre, M. Taagepera, R. W. Taft, and R. D. Topsom, *J. Am. Chem. Soc.*, **103**, 1344 (1981).



Adjacent atoms with one or more unshared pairs of electrons strongly stabilize a carbocation. Table 3.11 (p. 304) indicates the stabilization of the methyl cation by such substituents. Alkoxy and dialkylamino groups are important examples of this effect.



Although these structures have a positive charge on a more electronegative atom, they benefit from an additional bond that satisfies the octet requirement of the tricoordinate carbon. These “carbocations” are best represented by the doubly bonded resonance structures. One indication of the strong participation of adjacent oxygen substituents is the existence of a barrier to rotation about the C–O bonds in this type of carbocation.



The barrier in A is about 14 kcal/mole (ΔG^*) as measured by NMR coalescence of the nonidentical vinyl protons.⁸⁵ The gas phase barrier is calculated by MO methods to be 26 kcal/mol. The observed barrier for B is 19 kcal/mol.^{86,87}

Even halogen substituents stabilize carbocations as a result of resonance donation from the halogen electron pairs. A fluorine or chlorine substituent is nearly as stabilizing as a methyl group in the gas phase.⁸⁸



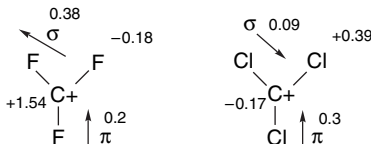
⁸⁵ D. Cremer, J. Gauss, R. F. Childs, and C. Blackburn, *J. Am. Chem. Soc.*, **107**, 2435 (1985).

⁸⁶ R. F. Childs and M. E. Hagar, *Can. J. Chem.*, **58**, 1788 (1980).

⁸⁷ There is another mechanism for equilibration of the cation pairs $\text{A}_1 \rightleftharpoons \text{A}_2$ and $\text{B}_1 \rightleftharpoons \text{B}_2$, namely inversion at oxygen. However, the observed barrier represents at least the *minimum* for the C=O rotational barrier and therefore demonstrates that the C–O bond has double-bond character.

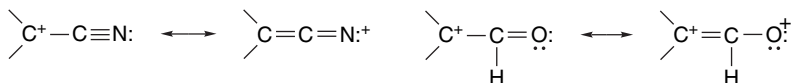
⁸⁸ C. H. Reynolds, *J. Am. Chem. Soc.*, **114**, 8676 (1992).

An NPA analysis has been performed on F_3C^+ and Cl_3C^+ .⁸⁹ According to this analysis, chlorine is a slightly better π donor than fluorine, and fluorine's polar effect is, of course, stronger. The net result is that the carbon in F_3C^+ is much more positive than the carbon in Cl_3C^+ . Note that even the Cl σ electrons are slightly shifted to the sp^2 carbon. According to this analysis, the positive charge in Cl_3C^+ is carried entirely by the chlorines, whereas in F_3C^+ the positive charge resides entirely on carbon.



Electron-withdrawing groups that are substituted directly on the cationic site are destabilizing. Table 4.18 gives an indication of the relative retardation of the rate of ionization and the calculated destabilization for several substituents.

The trifluoromethyl group, which exerts a powerful polar effect, is strongly destabilizing both on the basis of the kinetic data and the MO calculations. The cyano and formyl groups are less so. In fact, the destabilization of these groups is considerably less than would be predicted on the basis of their polar substituent constants. Both the cyano and formyl groups can act as π donors, even though the effect is to place partial positive charge and electron deficiency on nitrogen and oxygen atoms, respectively.



These resonance structures are the nitrogen and oxygen analogs of the allyl cation. The effect of this π delocalization is to attenuate the polar destabilization by these substituents.⁹⁰ These interactions are reflected in MO energies, bond lengths, and charge distributions calculated for such cations⁹¹ (review Section 3.4.1).

Table 4.18. Destabilization of 2-Substituted *i*-Propyl Cation by EWG Substituents

Z	Solvolytic rate relative to Z = H	Destabilization HF/4-31G (kcal/mol)
CN	$\sim 10^{-3a}$	9.9 ^b
CF ₃	$\sim 10^{-3c}$	37.3 ^b
CH=O	—	6.1 ^b

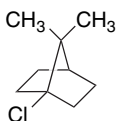
a. P. G. Gassman and J. J. Talley, *J. Am. Chem. Soc.*, **102**, 1214 (1980).

b. M. N. Paddon-Row, C. Santiago, and K. N. Houk, *J. Am. Chem. Soc.*, **102**, 6561 (1980).

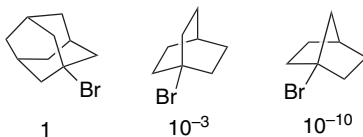
c. K. M. Koshy and T. T. Tidwell, *J. Am. Chem. Soc.*, **102**, 1216 (1980).

- ⁸⁹ G. Frenking, S. Fau, C. M. Marchand, and H. Gruetzmacher, *J. Am. Chem. Soc.*, **119**, 6648 (2000).
⁹⁰ T. T. Tidwell, *Angew. Chem. Int. Ed. Engl.*, **23**, 20 (1984); P. G. Gassman and T. T. Tidwell, *Acc. Chem. Res.*, **16**, 279 (1983); J. L. Holmes and P. M. Mayer, *J. Phys. Chem.*, **99**, 1366 (1995); J. L. Holmes, F. P. Lossing, and P. M. Mayer, *Chem. Phys. Lett.*, **212**, 134 (1993).
⁹¹ D. A. Dixon, P. A. Charlier, and P. G. Gassman, *J. Am. Chem. Soc.*, **102**, 3957 (1980); M. N. Paddon-Row, C. Santiago, and K. N. Houk, *J. Am. Chem. Soc.*, **102**, 6561 (1980); D. A. Dixon, R. A. Eades, R. Frey, P. G. Gassman, M. L. Hendewerk, M. N. Paddon-Row, and K. N. Houk, *J. Am. Chem. Soc.*, **106**, 3885 (1984); X. Creary, Y.-X. Wang, and Z. Jiang, *J. Am. Chem. Soc.*, **117**, 3044 (1995).

Up to this point, we have considered only carbocations in which the cationic carbons are sp^2 hybridized and planar. When this hybridization cannot be achieved, carbocations are of higher energy. In a classic experiment, Bartlett and Knox demonstrated that the tertiary chloride 1-chloroapocamphane was inert to nucleophilic substitution.⁹² Starting material was recovered unchanged even after refluxing for 48 h in ethanolic silver nitrate. The unreactivity of this compound is attributed to the structure of the bicyclic system, which prevents rehybridization to a planar sp^2 carbon. Back-side nucleophilic solvent participation is also precluded because of the bridgehead location of the C–Cl bond.



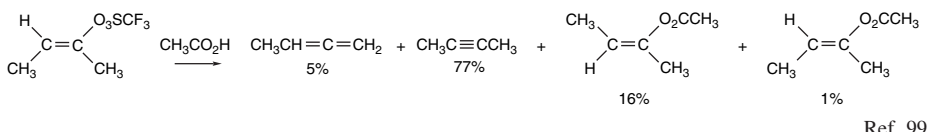
The apocamphyl structure is particularly rigid, and bridgehead carbocations become accessible in more flexible structures. The relative solvolysis rates of the bridgehead bromides 1-bromoadamantane, 1-bromobicyclo[2.2.2]octane, and 1-bromobicyclo[2.2.1]heptane illustrate this trend. The relative rates for solvolysis in 80% ethanol at 25 °C are shown.⁹³



The relative reactivity of tertiary bridgehead systems toward solvolysis is well correlated with the increase in strain that results from conversion of the ring structure to a carbocation, as calculated by molecular mechanics.⁹⁴ This result implies that the increased energy associated with a nonplanar carbocation is proportional to the strain energy present in the ground state reactant. The solvolysis rates also correlate with bridgehead cation stability measured by gas phase hydride affinity and MP2/6-311G** MO calculations.⁹⁵

Alkenyl carbocations in which the cationic carbon is sp hybridized are about 15 kcal higher in energy than similar cations in which the cationic center is sp^2 (see Figure 3.18).⁹⁶ This is because of the higher electronegativity of the orbital with increasing s -character. The intermediacy of substituted vinyl cations in solvolysis reactions has been demonstrated, but direct observation has not been possible for simple vinyl cations.⁹⁷ Most examples of solvolytic generation of vinyl cations involve very reactive leaving groups, especially trifluoromethanesulfonate (triflates). Typical products include alenes, alkynes, and vinyl esters.⁹⁸

- ⁹². P. D. Bartlett and L. H. Knox, *J. Am. Chem. Soc.*, **61**, 3184 (1939).
- ⁹³. For a review of bridgehead carbocations see R. C. Fort, Jr., in *Carbonium Ions*, Vol. IV, G. A. Olah and P. v. R. Schleyer, eds., Wiley-Interscience, New York, 1973, Chap. 32.
- ⁹⁴. T. W. Bentley and K. Roberts, *J. Org. Chem.*, **50**, 5852 (1985); R. C. Bingham and P. v. R. Schleyer, *J. Am. Chem. Soc.*, **93**, 3189 (1971); P. Müller and J. Mareda, *Helv. Chim. Acta*, **70**, 1017 (1987); P. Müller, J. Mareda, and D. Milin, *J. Phys. Org. Chem.*, **8**, 507 (1995).
- ⁹⁵. E. W. Della and W. K. Janowski, *J. Org. Chem.*, **60**, 7756 (1995); J. L. M. Abboud, O. Castano, E. W. Della, M. Herreros, P. Muller, R. Notario, and J.-C. Rossier, *J. Am. Chem. Soc.*, **119**, 2262 (1997).
- ⁹⁶. V. D. Nefedov, E. N. Sinotova, and V. P. Lebedev, *Russ. Chem. Rev.*, **61**, 283 (1992).
- ⁹⁷. H.-U. Siehl and M. Hanack, *J. Am. Chem. Soc.*, **102**, 2686 (1980).
- ⁹⁸. For reviews of vinyl cations, see Z. Rappoport in *Reactive Intermediates*, R. A. Abramovitch, ed., Vol. 3, Plenum Press, New York, 1983; *Dicoordinated Carbocations*, Z. Rappoport and P. J. Stang, eds., John Wiley & Sons, New York, 1997.



The phenyl cation is a very unstable cation, as is reflected by the high hydride affinity shown in Figure 3.18. In this case, the ring geometry resists rehybridization so the vacant orbital retains sp^2 character. Since the empty orbital is in the nodal plane of the ring, it receives no stabilization from the π electrons.

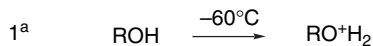


Phenyl cations are formed by thermal decomposition of aryl diazonium ions.¹⁰⁰ The cation is so reactive that under some circumstances it can recapture the nitrogen generated in the decomposition.¹⁰¹ Attempts to observe formation of phenyl cations by ionization of aryl triflates have only succeeded when especially stabilizing groups, such as trimethylsilyl groups are present at the 2- and 6-positions of the aromatic ring.¹⁰²

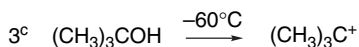
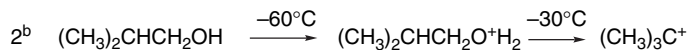
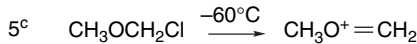
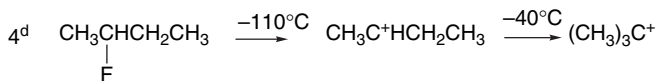
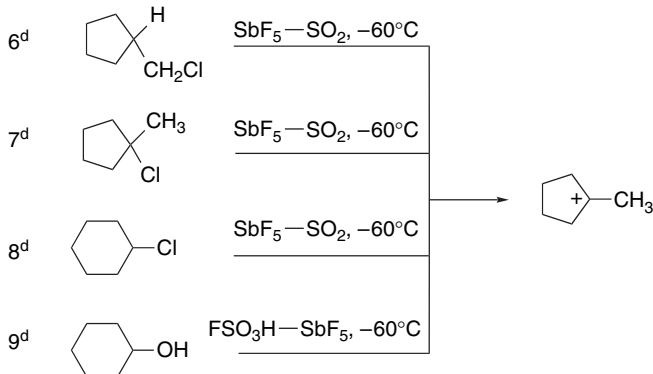
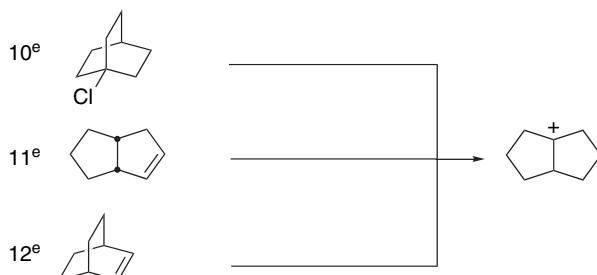
4.4.2. Direct Observation of Carbocations

A major advance in the study of carbocations occurred during the 1960s when methods for generation of carbocations in superacid media were developed. The term *superacid* refers to media of very high proton-donating capacity, e.g., more acidic than 100% sulfuric acid. A convenient medium for these studies is $\text{FSO}_3\text{H} - \text{SbF}_5 - \text{SO}_2$. The fluorosulfonic acid acts as a proton donor and antimony pentafluoride is a powerful Lewis acid that assists ionization. This particular combination has been dubbed “magic acid” because of its powerful protonating ability. The solution is essentially nonnucleophilic, so carbocation of even moderate stability can be generated and observed by NMR spectroscopy.¹⁰³ Some examples of these studies are given in Scheme 4.4. Alkyl halides and alcohols, depending on the structure of the alkyl group, react with magic acid and give rise to carbocations. Primary and secondary alcohols are protonated at -60°C , but do not ionize. Tertiary alcohols do ionize, giving rise to the corresponding cation. As the temperature is increased, carbocation formation also occurs from secondary alcohols. *sec*-Butyl alcohol ionizes with rearrangement to the

- ^{99.} R. H. Summerville, C. A. Senkler, P. v. R. Schleyer, T. E. Dueber, and P. J. Stang, *J. Am. Chem. Soc.*, **96**, 1100 (1974).
- ^{100.} C. G. Swain, J. E. Sheats, and K. G. Harbison, *J. Am. Chem. Soc.*, **97**, 783 (1975).
- ^{101.} R. G. Bergstrom, R. G. M. Landells, G. W. Wahl, Jr., and H. Zollinger, *J. Am. Chem. Soc.*, **98**, 3301 (1976).
- ^{102.} Y. Apeloig and D. Arad, *J. Am. Chem. Soc.*, **107**, 5285 (1985); Y. Himeshima, H. Kobayashi, and T. Sonoda, *J. Am. Chem. Soc.*, **107**, 5286 (1985).
- ^{103.} A review of the extensive studies of carbocations in superacid media is available in G. A. Olah, G. K. Surya Prakash, and J. Sommer, *Super Acids*, John Wiley & Sons, New York, 1985.

Scheme 4.4. Protonation, Ionization, and Rearrangement in Superacid**A. Alcohols in $\text{FSO}_3\text{H} - \text{SbF}_5 - \text{SO}_2$** 

R = methyl, ethyl, *n*-propyl, *i*-propyl, *n*-butyl, *s*-butyl,
n-amyl, *i*-amyl, neopentyl, *n*-hexyl, neohexyl

**B. Alkyl halides in antimony pentafluoride****C. Cyclopentyl and Cyclohexyl systems****D. Bicyclooctyl systems in $\text{SbF}_5 - \text{SO}_2\text{ClF}$, -78°C** 

a. G. A. Olah, J. Sommer, and E. Namanworth, *J. Am. Chem. Soc.*, **89**, 3576 (1967).

b. M. Saunders, F. L. Hagen, and J. Rosenfeld, *J. Am. Chem. Soc.*, **90**, 6882 (1968).

c. G. A. Olah and J. M. Bollinger, *J. Am. Chem. Soc.*, **89**, 2993 (1967).

d. G. A. Olah, J. M. Bollinger, C. A. Cupas, and J. Lukas, *J. Am. Chem. Soc.*, **89**, 2692 (1967).

e. G. A. Olah and G. Liang, *J. Am. Chem. Soc.*, **87**, 2998 (1965).

tert-butyl cation. At -30°C the protonated primary isomer, *iso*-butyl alcohol, ionizes, also forming the *tert*-butyl cation. Protonated *n*-butanol is stable to 0°C , at which point it, too, gives rise to the *t*-butyl cation. It is typically observed that ionizations in superacids give rise to the most stable of the isomeric carbocations that can be derived from the alkyl group. The *t*-butyl cation is generated from C₄ systems, whereas C₅ and C₆ alcohols give rise to the *t*-pentyl and *t*-hexyl ions, respectively. Some examples of these studies are given in Scheme 4.4. Entries 6 to 9 and 10 to 12 further illustrate the tendency for rearrangement to the most stable cation to occur. The tertiary 1-methylcyclopentyl cation is the only ion observed from a variety of five- and six-membered ring derivatives. The tertiary bicyclo[3.3.0]octyl cation is formed from all bicyclooctyl (C₈H₁₃⁺) precursors. The tendency to rearrange to the thermodynamically stable ions by multiple migrations is a consequence of the very low nucleophilicity of the solvent system. In the absence of nucleophilic capture by solvent, the carbocations undergo extensive skeletal rearrangement and accumulate as the most stable isomer.

Another important development in permitting structural conclusions from NMR studies on carbocations resulted from the use of theoretical computations of ¹³C and ¹H chemical shifts. Known as the MP2-GIAO method,¹⁰⁴ it has also been applied successfully to allylic, cyclopropylmethyl, and phenonium ions.¹⁰⁵

Carbocations can also be studied by X-ray crystallography.¹⁰⁶ Early studies involved strongly stabilized cations such as triphenylmethyl¹⁰⁷ and cyclopropylmethyl cations.¹⁰⁸ More recently, the structure of less stable ions, including the *t*-butyl cation, have been obtained.¹⁰⁹ The structure is planar with C–C bonds averaging 1.442 Å. This is substantially less than the *sp*²–*sp*³ bond length in neutral compounds, which is about 1.50 Å. This finding is consistent with C–H hyperconjugation, although the structure determination did not permit assignment of C–H bond lengths.

4.4.3. Competing Reactions of Carbocations

The product of a substitution reaction that follows the limiting S_N2 mechanism is determined by the identity of the nucleophile. The nucleophile replaces the leaving group and product mixtures are obtained only if there is competition from several nucleophiles. Product mixtures from ionization mechanisms are often more complex. For many carbocations there are two competing processes that lead to other products: *elimination* and *rearrangement*. We discuss rearrangements in the next section. Here we consider the competition between substitution and elimination under *solvolysis conditions*. We return to another aspect of this competition in Section 5.10, when base-mediated elimination is considered.

The fundamental nature of the substitution-versus-elimination competition is illustrated in Figure 4.10, which is applicable to carbocations such as tertiary alkyl and secondary benzylic that have lifetimes on the order of 10⁻¹² s⁻¹ in hydroxylic solvents (SOH). The carbocation is at a relatively high energy, with very small barriers to either solvent capture (*k_s*, substitution product) or proton loss (*k_e*, elimination product.) The

¹⁰⁴. J. Gauss, *J. Chem. Phys.*, **99**, 3629 (1993).

¹⁰⁵. P. v. R. Schleyer and C. Maerker, *Pure Appl. Chem.*, **67**, 755 (1995).

¹⁰⁶. T. Laube, *Acc. Chem. Res.*, **28**, 399 (1995).

¹⁰⁷. A. H. Gomes de Mesquita, C. H. MacGillavry, and K. Eriks, *Acta Cryst.* **18**, 437 (1965).

¹⁰⁸. R. F. Childs, R. Faggiani, C. J. L. Lock, M. Mahendran, and S. D. Zweep, *J. Am. Chem. Soc.*, **108**, 1692 (1986).

¹⁰⁹. S. Hollenstein and T. Laube, *J. Am. Chem. Soc.*, **115**, 7240 (1993).

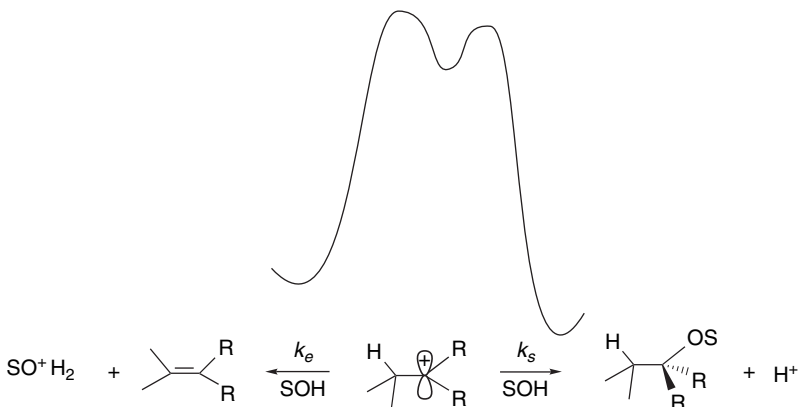
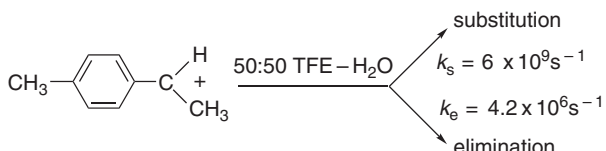


Fig. 4.10. Reaction energy profile illustrating competition between elimination and substitution by solvent for a *tert*-cation.

substitution reaction is more favorable in the thermodynamic sense, since the C–O bond is stronger than the π component of the double bond.

For both tertiary cations and secondary benzylic carbocation, the ratio of substitution to elimination is quite high. For example, for 1-(*p*-tolyl)ethyl cation in 50:50 TFE-water, the ratio is 1400.¹¹⁰ For the *tert*-butyl cation, the ratio is about 30 in water¹¹¹ and 60 in 50:50 TFE-water.¹¹² These ratios are on the order of 10^3 if account is taken of the need for solvent reorganization in the substitution process.¹¹³ The generalization is that *under solvolysis conditions, tert-alkyl and sec-benzyl carbocations prefer substitution to elimination.*



The origin of this preference has been considered by Richard and co-workers. One aspect of the puzzle can be seen by applying Hammond's postulate. Since the competing reactions have early transition states, it is unlikely that the difference in product stability governs the competition. Instead, the substitution process appears to have a smaller *intrinsic barrier* (in the context of the Marcus equation; see Section 3.2.4). The elimination reaction appears to have a barrier that is 3–4 kcal higher, at least for *sec*-benzylic systems.¹¹⁴ The structural basis of this difference has not been established, but it may be related to the fact that the elimination process has a bond-breaking component, whereas substitution requires only bond formation.

¹¹⁰ J. P. Richard and W. P. Jencks, *J. Am. Chem. Soc.*, **106**, 1373 (1984); J. P. Richard, T. L. Amyes, and K. B. Williams, *Pure Appl. Chem.*, **70**, 2007 (1998).

¹¹¹ I. Dostrovsky and F. S. Klein, *J. Chem. Soc.*, 791 (1955).

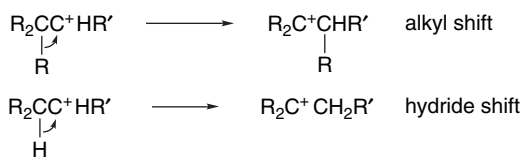
¹¹² M. M. Toteva and J. P. Richard, *Bioorg. Chem.*, **25**, 239 (1997).

¹¹³ M. M. Toteva and J. P. Richard, *J. Am. Chem. Soc.*, **118**, 11434 (1996).

¹¹⁴ J. P. Richard, *Tetrahedron*, **51**, 1535 (1995); J. P. Richard, T. L. Amyes, S.-S. Lin, A. M. C. O'Donoghue, M. M. Toteva, Y. Tsuji, and K. B. Williams, *Adv. Phys. Org. Chem.*, **35**, 67 (2000).

4.4.4. Mechanisms of Rearrangement of Carbocations

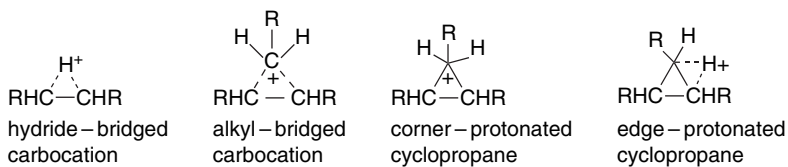
The discussions of the behavior of carbocation intermediates in superacid media and of neighboring-group participation have already provided examples of carbocation rearrangements. This is a characteristic feature of carbocations. Rearrangements can occur by shift of a hydrogen or an alkyl, alkenyl, or aryl group. Rearrangement creates a new carbocation with the positive charge located on the carbon atom from which the migration occurred. 1,2-Shifts are the most common type of rearrangement.¹¹⁵



A thermodynamic driving force exists for rearrangement in the direction of forming a more stable carbocation. Activation energies for migrations are small and it is not uncommon to observe overall rearrangements that involve individual steps that proceed from a more stable to a less stable species. Thus, while rearrangement of a tertiary to a secondary cation is endothermic by about 10 kcal/mol, this barrier is not prohibitive if the rearrangement can eventually lead to a more stable cation. Formation of primary cations by rearrangement is less likely to occur, since the primary ions are ~ 15 and ~ 25 kcal/mol higher in energy than secondary and tertiary cations, respectively. Rearrangements can occur through *bridged intermediates or transition structures* that are lower in energy than primary carbocations and comparable to secondary ions. The barriers for conversion to ions of greater (or equal) stability are very low and rearrangements occur very rapidly. For example, in superacid media at -160°C , the equilibration of the five methyl groups of the 2,3,3-trimethylbutyl cation by methyl shift is so fast that the barrier must be less than 5 kcal/mol.¹¹⁶



While many rearrangements can be formulated as a series of 1,2-shifts, both isotopic tracer studies and computational work have demonstrated the involvement of other species—bridged ions in which hydride or alkyl groups are partially bound to two other carbons. These can be transition structures for hydride and alkyl group shifts, but in some cases they may be intermediates. The alkyl-bridged structures can also be described as “corner-protonated” cyclopropanes, since if the bridging C–C bonds are considered to be fully formed, there is an “extra” proton on the bridging alkyl group. Another possible type of structure is called an “edge-protonated” cyclopropane. The carbon–carbon bonds are depicted as fully formed, with the “extra” proton associated with one of the “bent” bonds.



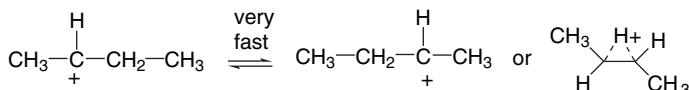
¹¹⁵. Reviews: V. G. Shubin, *Top. Current Chem.*, **116–117**, 267 (1984).

¹¹⁶. G. A. Olah and A. M. White, *J. Am. Chem. Soc.*, **91**, 5801 (1969).

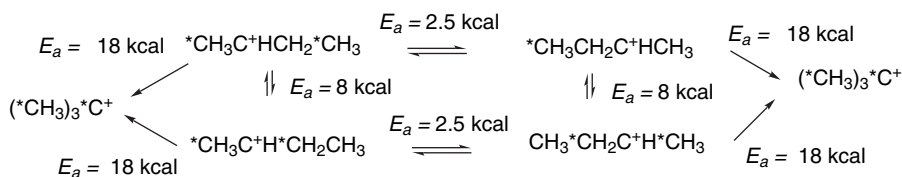
Theoretical calculations, structural studies under stable ion conditions, and product and mechanistic studies of reactions in solution have all been applied to understanding the nature of the intermediates involved in carbocation rearrangements. The energy surface for $C_3H_7^+$ in the gas phase has been calculated at the MP4/6-311G** level. The 1- and 2-propyl cations and corner- and edge-protonated cyclopropane structures were compared. The secondary carbocation was found to be the most stable structure.¹¹⁷ Hydrogen migration was found to occur through a process that involves the corner-protonated cyclopropane species. Similar conclusions were drawn at the G2 and B3LYP levels of calculation.¹¹⁸ Calculations that include an anion change the relative energy of the 1-propyl cation and the protonated cyclopropane. The 1-propyl cation becomes a stable structure in close proximity to an anion.¹¹⁹ Relative energies of $[C_3H_7]^+$ cations are shown below.

	$CH_3CH_2CH_2^+$	$CH_3C^+HCH_3$	\triangle^-H^+	
MP4/6-311*	+19.3	0	8.6	7.3
G2		0	8.2	7.2
B3LYP		0	16.0	12.2

The 2-butyl cation has been extensively investigated both computationally and experimentally. The 2-butyl cation can be observed under stable ion conditions. C(2) and C(3) are rapidly interconverted by a hydride shift. The NMR spectrum corresponds to a symmetrical species, which implies either a very rapid hydride shift or a symmetrical H-bridged structure. A maximum barrier of 2.5 kcal/mol for hydride shift can be assigned from the NMR data.¹²⁰



Scrambling of C(3) and C(4) [or C(1) and C(2)] occurs with an E_a of about 7–8 kcal/mol. The scrambling of C(3) and C(4) can occur via an edge-protonated intermediate. The rearrangement of 2-butyl cation to the *t*-butyl ion is rather slow, occurring with an E_a of 18 kcal/mol.¹²¹



¹¹⁷ W. Koch, B. Liu, and P. v. R. Schleyer, *J. Am. Chem. Soc.*, **111**, 3479 (1989).

¹¹⁸ M. V. Frash, V. B. Kazansky, A. M. Rigby, and P. A. van Santen, *J. Phys. Chem. B*, **101**, 5346 (1997).

¹¹⁹ D. Farcasiu and D. Hancu, *J. Am. Chem. Soc.*, **121**, 7173 (1999); D. Farcasiu and D. Hancu, *J. Phys. Chem. A*, **101**, 8695 (1997).

¹²⁰ M. Saunders and M. R. Kates, *J. Am. Chem. Soc.*, **100**, 7082 (1978).

¹²¹ D. M. Brouwer, *Recl. Trav. Chim. Pays-Bas*, **87**, 1435 (1968); D. M. Brouwer and H. Hogeveen, *Prog. Phys. Org. Chem.*, **9**, 179 (1972); M. Boronat, P. Viruela, and A. Corma, *J. Phys. Chem.*, **100**, 633 (1996).

There have been two extensive MO studies of the $C_4H_9^+$ species. The most stable structure is the *t*-butyl cation. At the MP4/6-311G** level, the H-bridged structure **A** was the next most stable structure and it was 2.3 kcal more stable than the open 2-butyl cation **D**.¹²² The methyl-bridged ion **B** is only slightly less stable. The structures were also calculated at the MP4/6-31G* level of theory.¹²³ The energies relative to the *t*-butyl cation are similar, although the methyl-bridged ion **B** is found to be slightly more stable than the hydride-bridged ion **A**. Relative energies of $[C_4H_9]^+$ cations are shown below in kcal/mol.

	A	B	C	D	E	F
MP4/6-311G*	13.4	13.8	21.9	15.7	33.0	0.0
MP4/6-31G**	12.8	12.0	20.5	32.6	0.0	

Along with the minimal barrier for hydride shift and the 18 kcal/mol 2-butyl to *t*-butyl rearrangement, these results give the energy profile shown in Figure 4.11, which

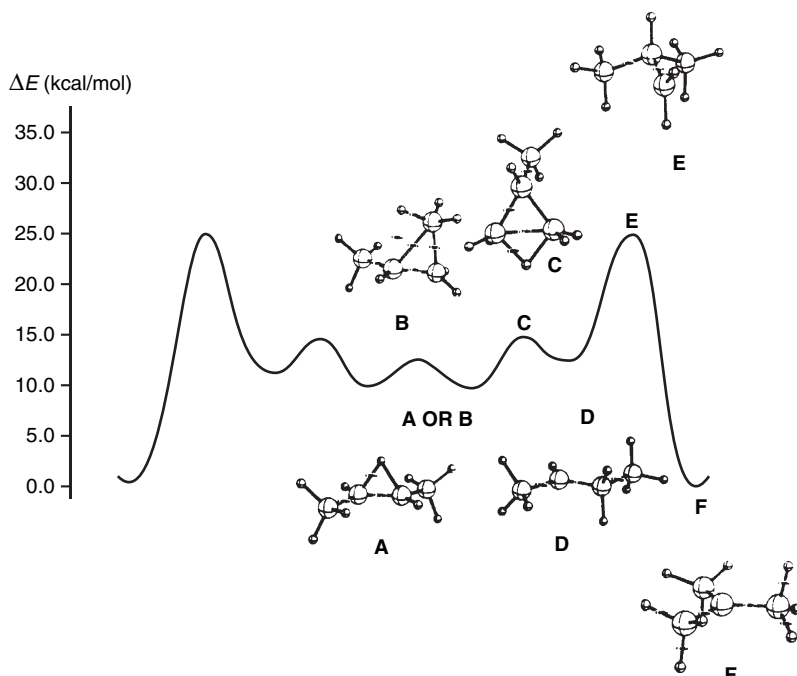
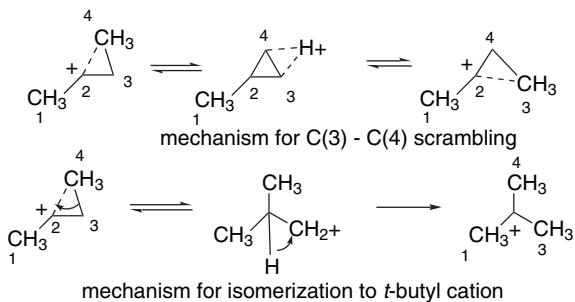


Fig. 4.11. Energy profile for the scrambling and rearrangement of $C_4H_9^+$ cation. (**A**) H-bridged; (**B**) methyl-bridged; (**C**) edge protonated methylcyclopropane; (**D**) classical secondary; (**E**) classical primary; (**F**) tertiary. Adapted from *J. Am. Chem. Soc.*, **112**, 4064 (1990); *J. Am. Chem. Soc.*, **115**, 259 (1993) and *J. Phys. Chem.*, **100**, 633 (1996), by permission of the American Chemical Society.

¹²² J. W. de M. Carneiro, P. v. R. Schleyer, W. Koch, and K. Raghavachari, *J. Am. Chem. Soc.*, **112**, 4064 (1990); S. Sieber, P. Buzek, P. v. R. Schleyer, W. Koch, and J. W. de M. Carneiro, *J. Am. Chem. Soc.*, **115**, 259 (1993).

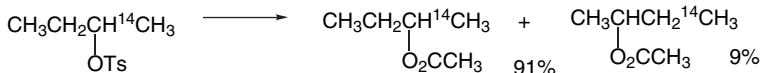
¹²³ M. Boronat, P. Viruela, and A. Corma, *J. Phys. Chem.*, **100**, 633 (1996).

pertains to the behavior of the carbocation *in the absence of a nucleophile*. This diagram indicates that the mechanism for C(3)–C(4) scrambling in the 2-butyl cation involves the edge-protonated cyclopropane intermediate. The primary cation is an intermediate in the isomerization to *t*-butyl ion, which explains the relatively slow rate of this process.

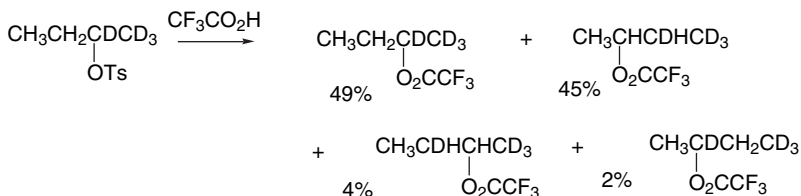


Visual models, additional information and exercises on C_4H_9 Carbocations can be found in the Digital Resource available at: Springer.com/carey-sundberg.

The occurrence and extent of rearrangement of the 2-butyl cation *during solvolysis* has been studied using isotopic labeling. When 2-butyl tosylate is solvolyzed in acetic acid, only 9% hydride shift occurs in the 2-butyl acetate that is isolated.¹²⁴ Thus, under these conditions most of the reaction proceeds by direct nucleophilic participation of the solvent.



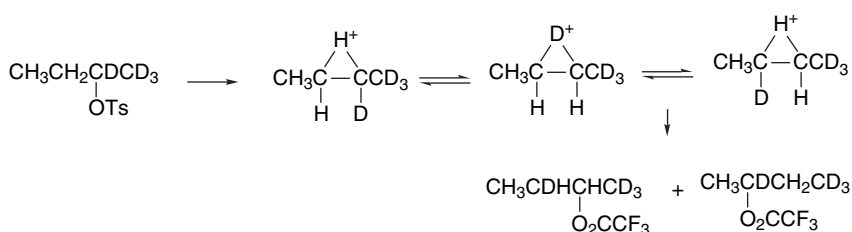
When 2-butyl tosylate is solvolyzed in the less nucleophilic trifluoroacetic acid (TFA), a different result emerges. The extent of migration approaches the 50% that would result from equilibration of the two secondary cations.¹²⁵



¹²⁴ J. D. Roberts, W. Bennett, R. E. McMahon, and E. W. Holroyd, Jr., *J. Am. Chem. Soc.*, **74**, 4283 (1952).

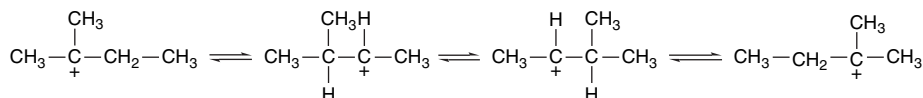
¹²⁵ J. J. Dannenberg, B. J. Goldberg, J. K. Barton, K. Dill, D. H. Weinwurzel, and M. O. Longas, *J. Am. Chem. Soc.*, **103**, 7764 (1981); J. J. Dannenberg, J. K. Barton, B. Bunch, B. J. Goldberg, and T. Kowalski, *J. Org. Chem.*, **48**, 4524 (1983); A. D. Allen, I. C. Ambridge, and T. T. Tidwell, *J. Org. Chem.*, **48**, 4527 (1983).

Two hydride shifts resulting in interchange of the C(2) and C(3) hydrogens can account for the two minor products.



Referring to Figure 4.11, we see that in acetic acid only a small portion of the reaction involves a carbocation. In TFA, the carbocation is formed, but only the H-migration process having an E_a of ~ 2.5 kcal competes with nucleophilic capture.

Both computational and solvolysis studies have also been done to characterize the $[\text{C}_5\text{H}_9]^+$ series of carbocations. The barrier to the hydride and methyl shifts that interconvert the methyl groups in the *t*-pentyl cation is 10–15 kcal/mol.¹²⁶ This rearrangement must pass through a secondary ion or related bridged species.



The solvolysis product of 3-methyl-2-butyl tosylate in TFA consists of 98.5% of the ester derived from the rearranged 2-methyl-2-butyl cation and 1.5% of the 3-methyl-2-butyl ester. Even the 1.5% of product retaining the 3-methyl-2-butyl structure has undergone some rearrangement.¹²⁷ The gas phase energies of possible intermediates have been calculated at several levels of theory.¹²⁸ Relative energies (kcal/mol) assigned to $[\text{C}_5\text{H}_9]^+$ cations are shown below.

MP2/6-31G*	11.7	7.2	0	34.1	17.8
B3P86	12.3	10.5	0	35.4	20.4
MP4/6-31G*	13.6	0		18.5	9.6 12.4

These results indicate an energy profile for the 3-methyl-2-butyl cation to 2-methyl-2-butyl cation rearrangement in which different rotamers of the open secondary cations are transition structures rather than intermediates, with the secondary cations represented as methyl-bridged C (corner-protonated cyclopropanes), as shown in Figure 4.12

The computational investigation of this system was extended to include the effect of a polar medium (dielectric constant = 39) and the effect of the proximity of anions

¹²⁶ M. Saunders and E. L. Hagen, *J. Am. Chem. Soc.*, **90**, 2436 (1968).

¹²⁷ D. Farcasiu, G. Marino, J. M. Harris, B. A. Hovanes, and C. S. Hsu, *J. Org. Chem.*, **59**, 154 (1994); D. Farcasiu, G. Marino, and C. S. Hsu, *J. Org. Chem.*, **59**, 163 (1994).

¹²⁸ M. Boronat, P. Viruela, and A. Corma, *J. Phys. Chem.*, **100**, 16514 (1996); D. Farcasiu and S. H. Norton, *J. Org. Chem.*, **62**, 5374 (1997).

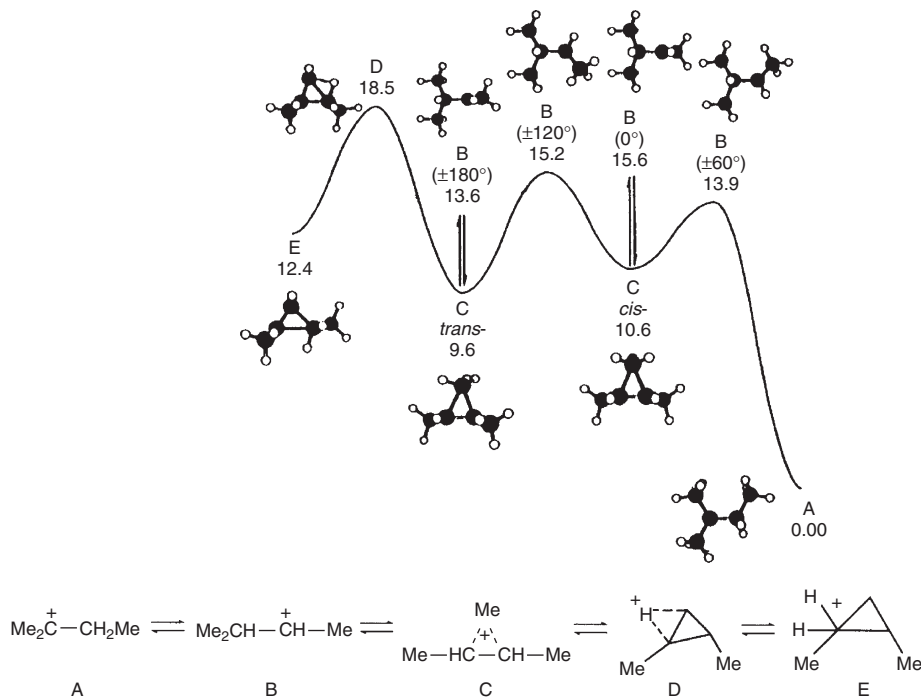
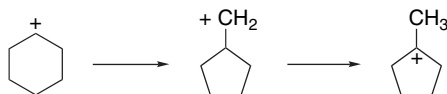


Fig. 4.12. Energy surface for the rearrangement of the 3-methyl-2-butyl cation to the 2-methyl-2-butyl cation. Reproduced from *J. Org. Chem.*, **62**, 5374 (1997), by permission of the American Chemical Society.

on the relative stability of ions **C** and **B**.¹²⁹ Whereas a polar medium reduced the energy of **B** relative to the gas phase results, the bridged ion **C** remained more stable than the secondary ion. The proximity of anions changed the situation more dramatically. Anions were modeled using $[\text{H-Li-H}]^-$ and $[\text{BH}_3\text{F}]^-$. At distances $< 3.3 \text{ \AA}$, the open secondary carbocation **B** is more stable. The energy difference depends on the location of the anion in relation to the cation. Orientations in which the anion approaches hydrogens on C(1) result in elimination to 3-methyl-1-butene, whereas approach to C(3) leads to 2-methyl-2-butene. These computational results present a picture of the elimination process similar to that in the previous section (page 439).

The ring contraction of a cyclohexyl cation to a methylcyclopentyl cation (see Entries 8 and 9 in Scheme 4.4) is thermodynamically favorable, but would require a substantial E_a if it proceeded through a primary cyclopentylmethyl cation.

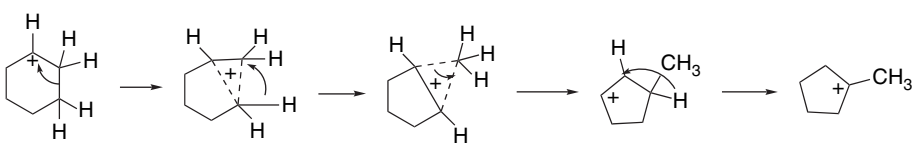


It is believed that a more correct description of the process involves migration through a pentacoordinate *protonated cyclopropane*, in which an alkyl group acts as a bridge in an electron-deficient carbocation structure. The cyclohexyl \rightarrow methylcyclopentyl rearrangement is postulated to occur by rearrangement between two such structures.¹³⁰

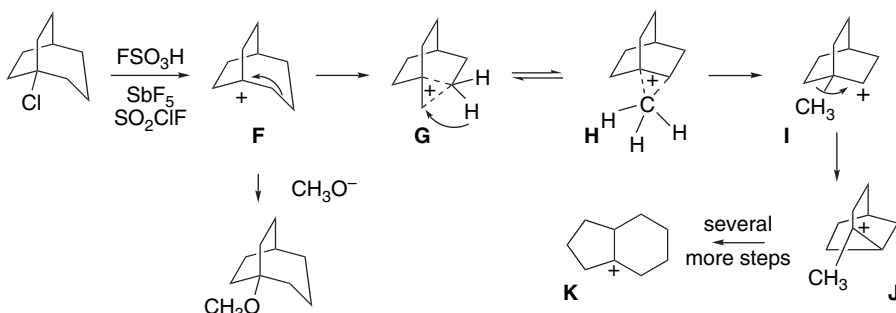
¹²⁹ D. Farcasiu, S. H. Norton, and D. Hancu, *J. Am. Chem. Soc.*, **122**, 668 (2000).

¹³⁰ M. Saunders, P. Vogel, E. L. Hagen, and J. Rosenfeld, *Acc. Chem. Res.*, **6**, 53 (1973).

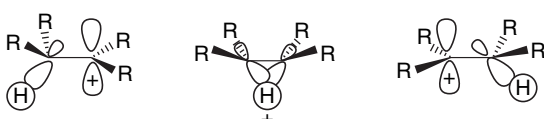
An E_a of 7.4 ± 1 kcal/mol for the rearrangement has been measured in the gas phase, which is consistent with the protonated cyclopropane mechanism.¹³¹



In some cases, NMR studies in superacid media have permitted the observation of successive intermediates in a series of rearrangements. An example is the series of $[C_9H_{15}]^+$ cations originating with the bridgehead ion **F**, generated by ionization of the corresponding chloride. Rearrangement eventually proceeds to the tertiary ion **K**. The bridgehead ion **F** is stable below $-75^\circ C$. The unarranged methyl ether is obtained if the solution is quenched with sodium methoxide in methanol at $-90^\circ C$. At about $-65^\circ C$, ion **F** rearranges to the tertiary ion **J**. This is believed to involve the methyl-bridged ion **H** as an intermediate. The tertiary ion **J** is stable below $-30^\circ C$ but above $-30^\circ C$, **K** is formed. This latter rearrangement involves a sequence of several steps, again including a methyl-bridged species.¹³² This multistep sequence terminating in the most stable $C_9H_{15}^+$ ion is typical of carbocations in superacid media. In the presence of nucleophilic anions or solvent, rearrangement usually does not proceed all the way to the most stable ion, because nucleophilic trapping captures one or more of the rearranged species.



The question of relative preference for rearrangement of different groups, which is sometimes referred to as “migratory aptitude,” is a complex one and there is no absolute order. In general, aryl groups and branched alkyl groups migrate in preference to unbranched alkyl groups, but as the barriers involved are low, selectivity is not high. Often the preferred migration involves the group that is best positioned from a stereoelectronic point of view. The preferred alignment of orbitals for a 1,2-hydride or alkyl shift involves coplanarity of the p -orbital at the carbocation ion center and the σ orbital of the migrating group.



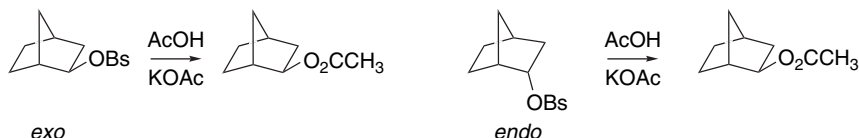
¹³¹. M. Attina, F. Cacace, and A. di Marzio, *J. Am. Chem. Soc.*, **111**, 6004 (1989).

¹³². G. A. Olah, G. Liang, J. R. Wiseman, and J. A. Chong, *J. Am. Chem. Soc.*, **94**, 4927 (1972).

The transition structure involves a three-center, two-electron bond and corresponds to a symmetrically bridged structure. As indicated above, the bridged structure may actually be an intermediate in some cases. The migration process can be concerted with the formation of the carbocation; that is, the migration can begin before the bond to the leaving group at the adjacent carbon atom is completely broken. The phenonium ion case discussed in Section 4.3 is one example. The ease of migration is also influenced by strain. In general, a shift that will reduce strain is favored.

4.4.5. Bridged (Nonclassical) Carbocations

In the discussion of carbocation rearrangements, we encountered examples of *bridged ions* that require expansion of bonding concepts beyond the two-center, two-electron bonds that suffice for most stable organic molecules. These bridged carbocations, involve delocalization of σ electrons and formation of three-center, two-electron bonds, and are sometimes called *nonclassical ions*. The recognition of the importance of bridged structures largely originated with a specific structure, the norbornyl cation, and the issue of whether its structure is classical or bridged.¹³³ The special properties of this intermediate were recognized on the basis of studies by Saul Winstein and his collaborators. The behavior of norbornyl systems in solvolytic displacement reactions was suggestive of neighboring-group participation by a saturated carbon-carbon bond. Evidence for both enhanced rate and unusual stereoselectivity was developed from the study of acetolysis of *exo*-2-norbornyl sulfonates. The acetolyses of both *exo*-2-norbornyl brosylate and *endo*-2-norbornyl brosylate produce exclusively *exo*-2-norbornyl brosylate. The *exo*-brosylate is more reactive than the *endo* isomer by a factor of 350.¹³⁴ Furthermore, enantiomerically pure *exo*-brosylate gives completely racemic *exo*-acetate, and the *endo*-brosylate gives acetate that is at least 93% racemic. These results suggest the involvement of an achiral species. Since the secondary norbornyl cation is chiral, it cannot account for the racemization.

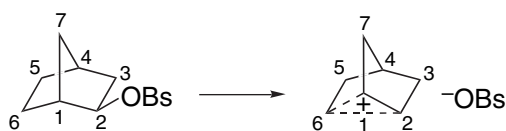


Both acetolyses were considered to proceed by way of a rate-determining formation of a carbocation. The rate of ionization of the *endo*-brosylate was considered normal, since its reactivity was comparable to that of cyclohexyl brosylate. Winstein

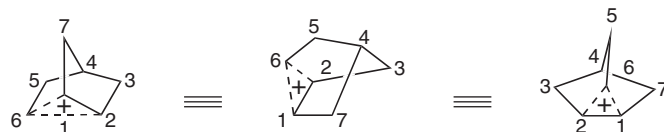
¹³³ H. C. Brown, *The Nonclassical Ion Problem*, Plenum Press, New York, 1977; H. C. Brown, *Tetrahedron*, **32**, 179 (1976); P. D. Bartlett, *Nonclassical Ions*, W. A. Benjamin, New York, 1965; S. Winstein, in *Carbonium Ions*, Vol. III, G. A. Olah and P. v. R. Schleyer, eds., Wiley-Interscience, New York, 1972, Chap. 22; G. D. Sargent, *ibid.*, Chap. 24; C. A. Grob, *Angew. Chem. Int. Ed. Engl.*, **21**, 87 (1982); G. M. Kramer and C. G. Scouten, *Adv. Carbocation Chem.*, **1**, 93 (1989).

¹³⁴ S. Winstein and D. S. Trifan, *J. Am. Chem. Soc.*, **71**, 2953 (1949); **74**, 1147, 1154 (1952); S. Winstein, E. Clippinger, R. Howe, and E. Vogelfanger, *J. Am. Chem. Soc.*, **87**, 376 (1965).

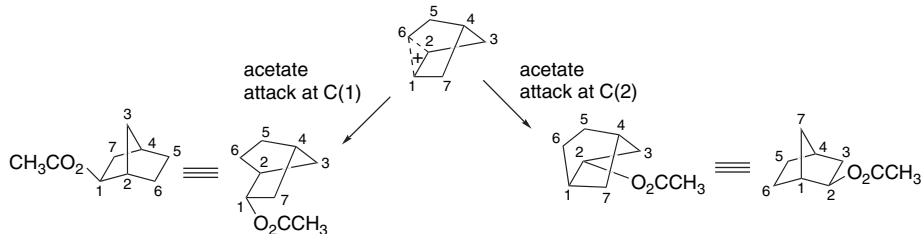
proposed that ionization of the *exo*-brosylate is *assisted* by the C(1)–C(6) bonding electrons and leads directly to the formation of a nonclassical ion as an intermediate.



This intermediate serves to explain the formation of racemic product, since it is achiral. The cation has a plane of symmetry passing through C(4), C(5), C(6), and the midpoint of the C(1)–C(2) bond. The plane of symmetry is seen more easily in an alternative, but equivalent, representation. Carbon 6, which bears two hydrogens, serves as the bridging atom in the cation.



Attack by acetate at C(1) or C(2) is equally likely and results in formation of equal amounts of the enantiomeric *exo*-acetates. The product is *exo* because reaction with acetate occurs from the direction opposite the bridging interaction. The bridged ion can be formed directly only from the *exo*-brosylate because it has the proper *anti* relationship between the C(1)–C(6) bond and the leaving group. The bridged ion can be formed from the *endo*-brosylate only after an unassisted ionization, which explains the rate difference between the *exo* and *endo* isomers.



The description of the nonclassical norbornyl cation developed by Winstein implied that the bridged ion is stabilized relative to a secondary ion by C–C σ bond delocalization. H. C. Brown put forward an alternative interpretation,¹³⁵ arguing that all the available data were consistent with describing the intermediate as a rapidly equilibrating classical secondary ion. The 1,2-shift that interconverts the two ions was presumed to be rapid, relative to capture of the nucleophile. Such a rapid rearrangement would account for the isolation of racemic product, and Brown suggested that the rapid migration would lead to preferential approach of the nucleophile from the *exo* direction.



¹³⁵ H. C. Brown, *The Transition State*, Chem. Soc. Spec. Publ., No. 16, 140 (1962); *Chem. Brit.*, 199 (1966); *Tetrahedron*, 32, 179 (1976).

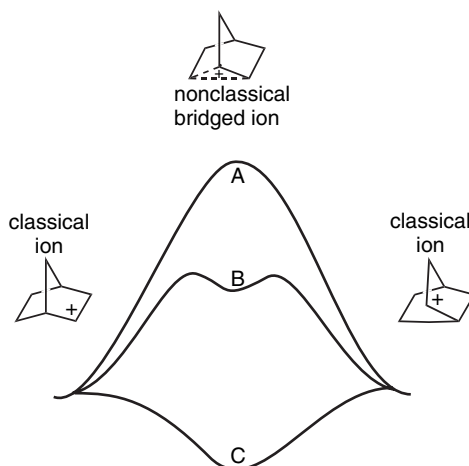


Fig. 4.13. Contrasting energy profiles for stable and unstable bridged norbornyl cation. (A) Bridged ion is a transition structure for rearrangement between classical structures. (B) Bridged ion is an intermediate in rearrangement of one classical structure to the other. (C) Bridged ion is the most stable structure.

The two alternative descriptions of the norbornyl cation were tested very extensively. In essence, the question that is raised has to do with the relative energy of the bridged structure. Is it lower in energy than the classical ion and therefore an *intermediate* to which the classical ion would collapse or is it a transition structure (or higher-energy intermediate) in the rapid isomerization of two classical structures? Figure 4.13 illustrates the energy profiles corresponding to the various possibilities.

When the techniques for direct observation of carbocations became available, the norbornyl cation was subjected to study by those methods. The norbornyl cation was generated in $\text{SbF}_5\text{-SO}_2\text{-SOF}_2$ and the temperature dependence of the proton magnetic resonance spectrum was examined.¹³⁶ Subsequently, the ^{13}C NMR spectrum was studied and the proton spectrum was determined at higher field strength. These studies excluded rapidly equilibrating classical ions as a description of the norbornyl cation under stable ion conditions.¹³⁷ The resonances observed in the ^{13}C spectrum were assigned. None of the signals appear near the position where the C(2) carbon of the classical secondary 2-propyl cation is found. Instead, the resonances for the norbornyl cation appear at relatively high field and are consistent with the bridged-ion structure.¹³⁸ Other NMR techniques were also applied to the problem and confirmed the conclusion that the spectra observed under stable ion conditions could not be the result of averaged spectra of two rapidly equilibrating ions.¹³⁹ It was also determined

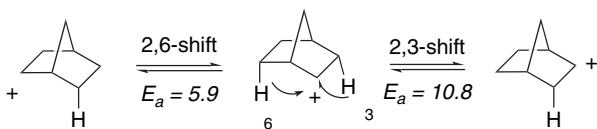
¹³⁶ P. v. R. Schleyer, W. E. Watts, R. C. Fort, Jr., M. B. Comisarow, and G. A. Olah, *J. Am. Chem. Soc.*, **86**, 5679 (1964); M. Saunders, P. v. R. Schleyer, and G. A. Olah, *J. Am. Chem. Soc.*, **86**, 5680 (1964).

¹³⁷ G. A. Olah, G. K. SuryaPrakash, M. Arvanaghi, and F. A. L. Anet, *J. Am. Chem. Soc.*, **104**, 7105 (1982).

¹³⁸ G. A. Olah, G. Liang, G. D. Mateescu, and J. L. Riemenschneider, *J. Am. Chem. Soc.*, **95**, 8698 (1973); G. A. Olah, *Acc. Chem. Res.*, **9**, 41 (1976).

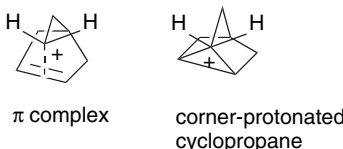
¹³⁹ C. S. Yannoni, V. Macho, and P. C. Myhre, *J. Am. Chem. Soc.*, **104**, 7105 (1982); M. Saunders and M. R. Kates, *J. Am. Chem. Soc.*, **102**, 6867 (1980); M. Saunders and M. R. Kates, *J. Am. Chem. Soc.*, **105**, 3571 (1983).

that 3,2- and 6,2-hydride shifts were occurring under stable ion conditions. Activation energies of 10.8 and 5.9 kcal/mol, respectively, were measured for these processes.



These results, which pertain to stable ion conditions, provide a strong case that the most stable structure for the norbornyl cation is the symmetrically bridged ion. How much stabilization does the bridging provide? An estimate based on molecular mechanics calculations and a thermodynamic cycle suggests a stabilization of about 6 ± 1 kcal/mol.¹⁴⁰ A gas phase value based on mass spectrometric measurements is 11 kcal/mol.¹⁴¹ Gas phase hydride affinity and chloride affinity data also show the norbornyl cation to be especially stable.¹⁴² MO calculations (MP2/6-31G*) give a bridged structure that is 13.6 kcal more stable than the classical secondary structure and predicts ^{13}C chemical shifts and coupling in agreement with the experimental results.¹⁴³ The C(1)–C(6)=C(2)–C(6) distance is found to be 1.832 Å by an MBPT(2)/DZP computation.¹⁴⁴ The difference in energy between the two structures is reduced only slightly when calculations include the effect of solvation, indicating that the bridged ion would be more stable than the classical ion, even in solution.¹⁴⁵ There is also good agreement between calculated and observed infrared spectra.¹⁴⁶

Werstiuk and Muchall computed the structure at the B3LYP and QCISD levels. The minimum energy structure was found to be a bridged ion with a C(1)–C(6) distance of 1.892 Å and a C(1)–C(2) distance of 1.389 Å (B3LYP/6-311+G(2d,2p)). They applied AIM concepts to a description of the structure.¹⁴⁷ This analysis resulted in the description of the norbornyl cation as a π complex, consistent with the relatively long C(1)–C(6) and C(2)–C(6) and short C(1)–C(2) distances indicated above. The bond critical points found by the AIM analysis show a T-configuration with the bond from C(6) intersecting with the C(1)–C(2) critical point. There is no bond path directly to C(1) or C(2). Carbon 6 is then best described as tetravalent, with the C(1)–C(2) double bond as the fourth ligand. These computations also examined the effect of bringing C(6) closer to C(1) and C(2) to form the more strongly bridged structure that would be implied by a corner-protonated cyclopropane representation.



- ¹⁴⁰. P. v. R. Schleyer and J. Chandrasekhar, *J. Org. Chem.*, **46**, 225 (1981).
- ¹⁴¹. M. C. Blanchette, J. L. Holmes, and F. P. Lossing, *J. Am. Chem. Soc.*, **109**, 1392 (1987).
- ¹⁴². R. B. Sharma, D. K. S. Sharma, K. Hiraoka, and P. Kebarle, *J. Am. Chem. Soc.*, **107**, 3747 (1985).
- ¹⁴³. P. v. R. Schleyer and S. Sieber, *Angew. Chem. Int. Ed. Engl.*, **32**, 1606 (1993).
- ¹⁴⁴. S. A. Perera and R. J. Bartlett, *J. Am. Chem. Soc.*, **118**, 7849 (1996).
- ¹⁴⁵. P. R. Schreiner, D. L. Severance, W. L. Jorgensen, P. v. R. Schleyer, and H. F. Schaefer, III, *J. Am. Chem. Soc.*, **117**, 2663 (1995).
- ¹⁴⁶. W. Koch, B. Liu, D. J. DeFrees, D. E. Sunko, and H. Vancik, *Angew. Chem. Int. Ed. Engl.*, **29**, 183 (1990).
- ¹⁴⁷. N. H. Werstiuk and H. M. Muchall, *J. Phys. Chem. A*, **104**, 2054 (2000); N. H. Werstiuk and H. M. Muchall, *Theochem*, **463**, 225 (1999).

The result is a structure that is 7.5 kcal/mol above the π complex. The π complex structure also gives better agreement with the experimental ^{13}C and ^1H NMR chemical shifts than the corner-protonated structure. The preference for the π complex structure persists in computations using a continuum solvent model. The picture that emerges from this analysis is of a primarily electrostatic attraction between a C(1)–C(2) double bond and a carbocation-like C(6).¹⁴⁸ Such a structure would be poised for nucleophilic attack *anti* to C(6), as is observed to occur.

Let us now return to the question of solvolysis and how it relates to the structure under stable ion conditions. To relate the structural data to solvolysis conditions, the primary issues that must be considered are the extent of solvent participation and the nature of solvation of the cationic intermediate. The extent of solvent participation has been probed by comparison of solvolysis characteristics in TFA with acetic acid. The *exo-endo* reactivity ratio in TFA is 1120, compared to 280 in acetic acid. While the *endo* isomer shows solvent sensitivity typical of normal secondary tosylates, the *exo* isomer reveals a reduced sensitivity. This result indicates that the TS for solvolysis of the *exo* isomer possesses a greater degree of charge dispersal, which is consistent with formation of a bridged structure. This fact, along with the rate enhancement of the *exo* isomer, indicates that the σ participation commences prior to ionization, and leads to the conclusion that bridging is a characteristic of the solvolysis TS, as well as of the stable ion structure.¹⁴⁹

Another line of evidence indicating that bridging is important in solvolysis comes from substituent effects for groups placed at C(4), C(5), C(6), and C(7) in the norbornyl system. The solvolysis rate is most strongly affected by C(6) substituents and the *exo* isomer is more sensitive to these substituents than the *endo* isomer. This implies that the TS for solvolysis is especially sensitive to C(6) substituents, as would be expected if the C(1)–C(6) bond participates in solvolysis.¹⁵⁰

Computation of the TS using ionization of the protonated *exo* and *endo* alcohols as a model has been done using B3LYP/6-311+G* calculations.¹⁵¹ The results confirm that participation occurs during the ionization process and is greater for the *exo* than the *endo* system. However, the stabilization resulting from the participation is considerably less than the full stabilization energy of the bridged carbocation. A difference of 3.7 kcal/mol is calculated between the *exo* and *endo* TSs. Figure 4.14 illustrates the relative energy relationships.

Many other cations besides the norbornyl cation have bridged structures.¹⁵² Scheme 4.5 shows some examples that have been characterized by structural studies or by evidence derived from solvolysis reactions. To assist in interpretation of the bridged structures, the bond representing the bridging electron pair is darkened in a corresponding classical structure. Not surprisingly, the borderline between classical and bridged structures is blurred. There are two fundamental factors that prevent an absolute division: (1) The energies of the two (or more) possible structures may

^{148.} N. H. Werstiuk, H. M. Muchall, and S. Noury, *J. Phys. Chem. A*, **104**, 11601 (2000).

^{149.} J. E. Nordlander, R. R. Gruetzmacher, W. J. Kelly, and S. P. Jindal, *J. Am. Chem. Soc.*, **96**, 181 (1974).

^{150.} F. Fuso, C. A. Grob, P. Sawlewicz, and G. W. Yao, *Helv. Chim. Acta*, **69**, 2098 (1986); P. Flury and C. A. Grob, *Helv. Chim. Acta*, **66**, 1971 (1983).

^{151.} P. R. Schreiner, P. v. R. Schleyer, and H. F. Schaefer, III, *J. Org. Chem.*, **62**, 4216 (1997).

^{152.} V. A. Barkhash, *Top. Current Chem.*, **115–117**, 1 (1984); G. A. Olah and G. K. SuryaPrakash, *Chem. Brit.*, **19**, 916 (1983).

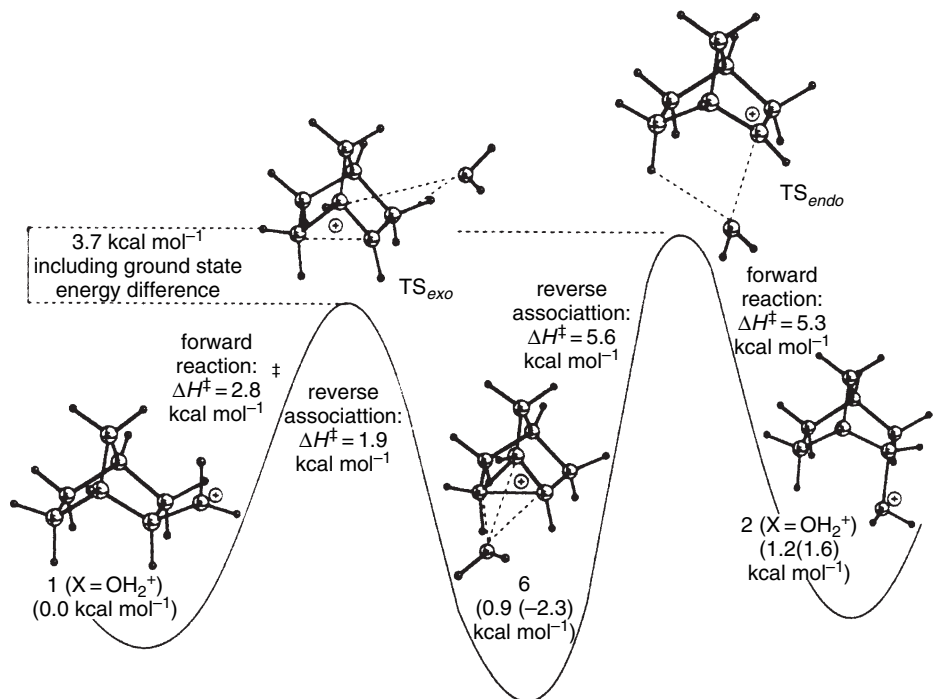
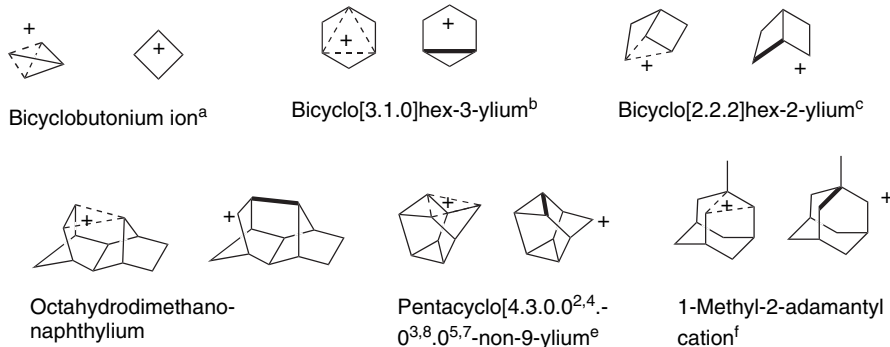


Fig. 4.14. Computational energy diagram (B3LYP/6-311+G*) for intermediates and transition states in ionization and rearrangement of protonated 2-norbornanol. Reproduced from *J. Org. Chem.*, **62**, 4216 (1997), by permission of the American Chemical Society.

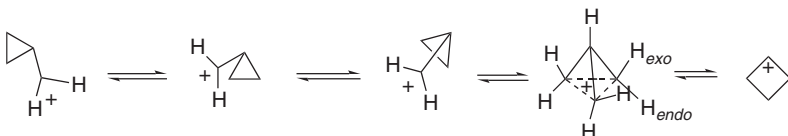
Scheme 4.5. Examples of Bridged Carbocations



- a. M. Saunders and H.-U. Siehl, *J. Am. Chem. Soc.*, **102**, 6868 (1980); J. S. Starat, J. D. Roberts, G. K. S. Prakash, D. J. Donovan, and G. A. Olah, *J. Am. Chem. Soc.*, **100**, 8016, 8018 (1978); W. Koch, B. Liu, and D. J. De Frees, *J. Am. Chem. Soc.*, **110**, 7325 (1988); M. Saunders, K. E. Laidig, K. B. Wiberg, and P. v. R. Schleyer, *J. Am. Chem. Soc.*, **110**, 7652 (1988); P. C. Myhre, G. C. Webb, and C. Y. Yannoni, *J. Am. Chem. Soc.*, **112**, 8992 (1990).
- b. G. A. Olah, G. K. S. Prakash, T. N. Rawdah, D. Whittaker, and J. C. Rees, *J. Am. Chem. Soc.*, **101**, 3935 (1979); K. J. Szabo, E. Kraka, and D. Cremer, *J. Org. Chem.*, **61**, 2783 (1996).
- c. R. N. McDonald and C. A. Curi, *J. Am. Chem. Soc.*, **101**, 7116, 7118 (1979).
- d. S. Winstein and R. L. Hansen, *Tetrahedron Lett.*, No. 25, 4 (1960).
- e. R. M. Coates and E. R. Fretz, *J. Am. Chem. Soc.*, **99**, 297 (1977); H. C. Brown and M. Ravindranathan, *J. Am. Chem. Soc.*, **99**, 299 (1977).
- f. J. E. Nordlander and J. E. Haky, *J. Am. Chem. Soc.*, **103**, 1518 (1981).

be so close as to prevent a clear distinction as to stability. (2) The molecule may adopt a geometry that is intermediate between a classical geometry and a symmetrical bridged structure. Computational studies (MP2/6-311G**) have been carried out on several nonclassical carbocations.¹⁵³ The results show structural features similar to the norbornyl cation, with relatively long ($\sim 1.8 \text{ \AA}$) bonds to the bridging carbon and a much shorter (1.39 \AA) bond between the bridged carbons. The bond path from the bridging carbon is directed between the two bridged carbons, with a bond order of ~ 0.48 , whereas the bridged bond order is ~ 1.2 .

The C_4H_7^+ cation shown as the first entry in Scheme 4.5 is a particularly interesting case. It can be described as a bridged structure that is isomeric with cyclopropylmethyl and cyclobutyl ions.



NMR studies show that all three methylene groups are equivalent, but the *exo* and *endo* sets of hydrogen do not exchange. The barrier for exchange among the three CH_2 groups is $< 2 \text{ kcal}$. MO calculations at the MP4SDTQ/6-31G* level indicate that both the cyclopropylmethyl and the bridged (bicyclobutonium) cations are energy minima, differing by only 0.26 kcal. The secondary cyclobutyl cation is about 12 kcal higher in energy.¹⁵⁴ The bridged structure is a tetracyclic cation in which each of the methylene groups is pentacoordinate.¹⁵⁵

To summarize, bridged structures are readily attainable intermediates or transition structures for many cations and are intimately involved in rearrangement processes. In some cases, such as the norbornyl cation, the bridged structure is the most stable one. As a broad generalization, tertiary cations are nearly always more stable than related bridged ions and therefore have classical structures. Primary carbocations can be expected to undergo rearrangement to more stable secondary or tertiary ions, with bridged ions being likely transition structures (or intermediates) on the rearrangement path. Recall that the ethylium ion, C_2H_5^+ , is an H-bridged structure in the gas phase. Unlike other primary carbocations, it cannot rearrange to a more stable secondary structures. The energy balance between classical secondary structures and bridged structures is close and depends on the individual system. Bridged structures are most likely to be stable where a strained bond can participate in bridging or where solvation of the positive charge is difficult. Because of poor solvation, bridged structures are particularly likely to be favored in superacid media and in the gas phase. In the cases examined so far, proximity to anions favors classical structures in relation to bridged structures.

¹⁵³ I. Alkorta, J. L. M. Abboud, E. Quintanilla, and J. Z. Davalos, *J. Phys. Org. Chem.*, **16**, 546 (2003).

¹⁵⁴ M. Saunders, K. E. Laidig, K. B. Wiberg, and P. v. R. Schleyer, *J. Am. Chem. Soc.*, **110**, 7652 (1988); S. Sieber, P. v. R. Schleyer, A. H. Otto, J. Gauss, F. Reichel, and D. Cremer, *J. Phys. Org. Chem.*, **6**, 445 (1993).

¹⁵⁵ For further discussion of this structure see R. F. W. Bader and K. E. Laidig, *Theochem*, **261**, 1 (1992).

Topic 4.1. The Role Carbocations and Carbonium Ions in Petroleum Processing

Petroleum refining is a basic industry in the modern world. The industry provides fuels for transportation, industrial energy, and residential heat, as well as petrochemicals for the manufacture of a wide range of products. The largest consumption of petroleum is for transportation fuels. The fundamental technology of petroleum refining involves distillation to remove nonvolatile materials and separate the hydrocarbons on the basis of boiling range. The gasoline b.p. range is approximately 30–200 °C, and the fuel oil range is 200–300 °C. There are also processes that modify the chemical composition, which include *cracking*, *hydrocracking*, and *catalytic reforming*. In cracking and hydrocracking, larger hydrocarbons are converted to hydrocarbons in the gasoline range; catalytic reforming involves isomerization to increase the fraction of branched chain, cyclic, and aromatic hydrocarbons in the gasoline product. The objective of catalytic reforming is to improve gasoline performance. One of the measures of performance is the *octane number*, which is a measure of the degree of engine knocking observed for a particular hydrocarbon or hydrocarbon mixture. The scale is calibrated with *n*-heptane as 0.0 and 2,2,4-trimethylpentane as 100.0. Table 4.19 shows some *research octane numbers* (RON) for the heptane and octane isomers. There is a second scale, *motor octane number* that is also used. Note that chain branching leads to improved octane numbers.

The chemical basis for engine performance is related to the rates of reaction of the peroxy radicals involved in the combustion process. Components with high octane numbers have relatively low rates of chain branching, which reduces the premature ignition that causes poor engine performance.¹⁵⁶ Engine performance can also be improved by gasoline additives. Tetraethyllead was used for this purpose for many years before it became apparent that the accumulating lead in the environment had many adverse consequences. Lead also interferes with the catalytic converters required

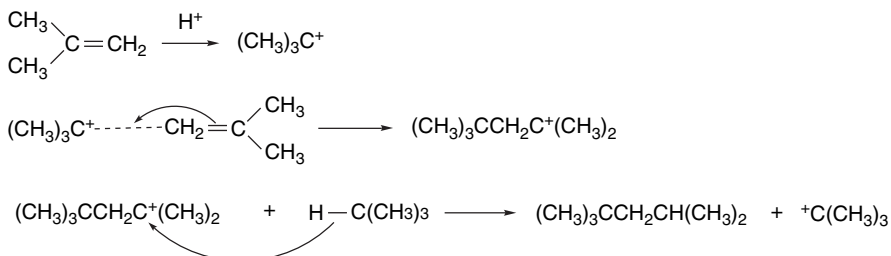
Table 4.19. Octane Numbers for Some Hydrocarbons

Heptanes	RON	Octanes	RON
<i>n</i> -Heptane	0.0	<i>n</i> -Octane	−19.0
2-Methylhexane	42.4	2-Methylheptane	21.7
3-Methylhexane	52.0	3-Methylheptane	36.8
3-Ethylpentane	65.0	4-Methylheptane	26.7
2,2-Dimethylpentane	92.8	3-Ethylhexane	33.5
2,3-Dimethylpentane	91.1	2,2-Dimethylhexane	72.5
2,4-Dimethylpentane	83.1	2,3-Dimethylhexane	71.5
3,3-Dimethylpentane	80.8	2,4-Dimethylhexane	65.2
2,2,3-Trimethylpentane	112.1	2,5-Dimethylhexane	55.5
		3,3-Dimethylhexane	75.5
		3,4-Dimethylhexane	76.3
		2-Methyl-3-ethylpentane	87.3
		3-Methyl-3-ethylpentane	80.8
		2,2,3-Trimethylpentane	109.6
		2,2,4-Trimethylpentane	100.0
		2,3,3-Trimethylpentane	106.1
		2,3,4-Trimethylpentane	102.7

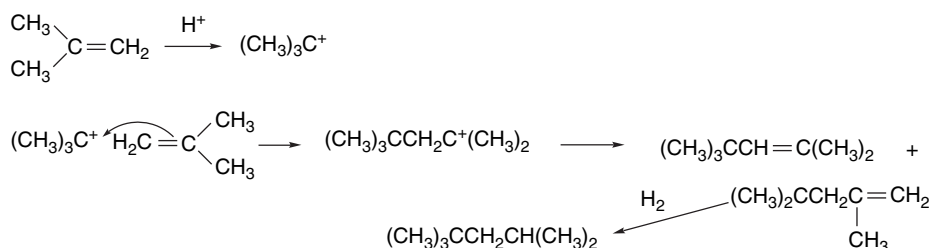
¹⁵⁶ C. Morley, *Combust. Sci. Technol.*, **55**, 115 (1987).

to reduce pollution from partial combustion. In the 1980s methyl *t*-butyl ether (MTBE) was introduced as a major antiknock component, but it was soon discovered that MTBE contaminated groundwater as a result of leakage and spillage.¹⁵⁷ It is being phased out as a gasoline performance enhancer.¹⁵⁸ As a result, new emphasis has been placed on catalytic reforming as a means of meeting engine performance requirements.

A possible replacement for MTBE is the mixture of branched C₈ hydrocarbons prepared by dimerization of C₄ compounds.¹⁵⁹ This is economically attractive since the C₄ compounds are by-products of other stages of petroleum refining. Isobutane and isobutene react with strong acid to give C₈ products.¹⁶⁰ The reaction involves intermolecular hydride transfers.



The same kind of product can be obtained by acid-catalyzed dimerization of isobutene, followed by hydrogenation.



The hydrocarbon mixtures formed by these processes have octane numbers ranging from 90 to 95.

Cracking, which is done at high temperatures (480–550 °C) in flow reactors with short contact times (seconds), converts high-boiling components of petroleum to hydrocarbons in the gasoline-boiling range. The catalysts are rapidly degraded and are regenerated by high-temperature (700 °C) exposure to air.¹⁶¹ The product mixture is complex but is enriched in hydrocarbons in the gasoline range. Low-boiling hydrocarbons such as methane and ethane are produced as by-products. Reactivity toward cracking increases with molecular weight and branching. Carbocations are intermediates in the cracking process, which leads to isomerizations.

¹⁵⁷ S. Fiorenza, M. P. Suarez, and H. S. Rifai, *J. Envir. Eng.*, **128**, 773 (2002); S. Erdal and B. D. Goldstein, *Ann. Rev. Energy Environ.*, **25**, 765 (2000).

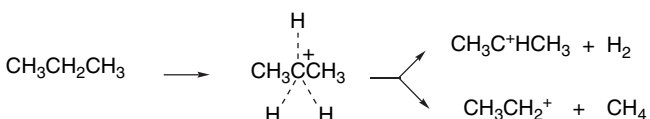
¹⁵⁸ A. K. Kolah, Q. Zhiwen, and S. M. Mahajani, *Chem. Innovation*, **31**, 15 (2001).

¹⁵⁹ J. M. Meister, S. M. B. Black, B. S. Muldoon, D. H. Wei, and C. M. Roesseler, *Hydrocarbon Process.*, **79**, 63 (2000).

¹⁶⁰ G. A. Olah, P. Batamack, D. Deffieux, B. Toeroek, Q. Wang, A. Molnar, and G. K. S. Prakash, *Appl. Catal. A*, **146**, 107 (1996).

¹⁶¹ Y. V. Kissin, *J. Catal.*, **126**, 600 (1990); Y. V. Kissin, *Catal. Rev.*, **43**, 85 (2001).

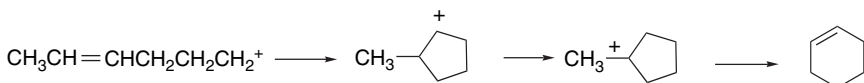
Cracking over acidic catalysts occurs through pentacovalent *carbonium ions*. The basic reactions are also observed with small hydrocarbons such as propane. Both the C–H and the C–C bond can be broken.



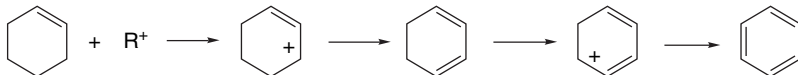
Alkenes are also formed and can react with trivalent carbocations to give alkylation products.



Intermediates with both a double bond and a carbocation can cyclize and rearrange.



Once cyclization has occurred, aromatization can occur through abstraction of hydride.



One process that occurs by these mechanisms, called the *Cyclar process*, uses a gallium-modified zeolite catalyst.¹⁶² The gallium increases the rate of the early cracking steps that generate alkenes. The Cyclar process can convert butane, propane, and ethane to mixtures of benzene, toluene, and the isomeric xylenes. The reactivity order is butane > propane > ethane.

Hydrocracking is used to convert high-boiling crude petroleum having a high content of nitrogen and sulfur and relatively low hydrogen content to material suitable for use as fuel.¹⁶³ Hydrocracking is also used in the processing of very heavy crude petroleum such as that obtained from tar sands and shale oil.¹⁶⁴ The chemical transformations include reductive removal of nitrogen and sulfur (forming ammonia and hydrogen sulfide) and cracking to smaller molecules. These processes are normally carried out in separate reaction chambers. The catalysts include transition metals capable of hydrogenation and zeolites that catalyze cracking. The final product composition can be influenced by reactor temperature and catalyst composition.

Reforming catalysts usually involve both transition metals, often platinum, and minerals, particularly zeolites modified with various metals; the zeolites are aluminum silicates. Depending on the exact structure, there are a number of anionic sites, which must be neutralized by metal cations or protons. The protonic forms are strongly acidic. The zeolites have distinctive pore sizes and are selective for certain molecular sizes or shapes.¹⁶⁵ For example, pore size can be a factor in determining the ratio of the *o*-, *m*-, and *p*-isomers of xylenes, with narrower pores favoring the last. Under normal

¹⁶² M. Guisnet, N. S. Gnepp, and F. Alario, *Appl. Catal. A*, **89**, 1 (1992).

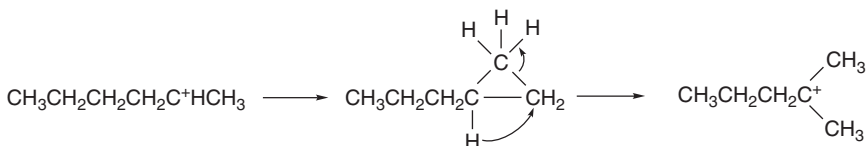
¹⁶³ J. W. Ward, *Fuel Proc. Technol.*, **35**, 55 (1993).

¹⁶⁴ J. F. Kriz, M. Ternan, and J. M. Denis, *J. Can. Pet. Technol.*, **22**, 29 (1983).

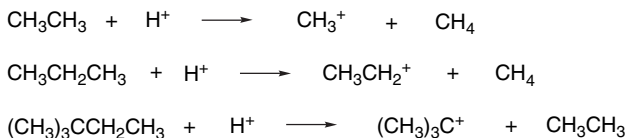
¹⁶⁵ C. R. Marcilly, *Top. Catal.*, **13**, 357 (2000).

operating conditions, the catalysts incorporate sulfur, which modifies the catalytic properties and tends to enhance rearrangement and aromatization.¹⁶⁶

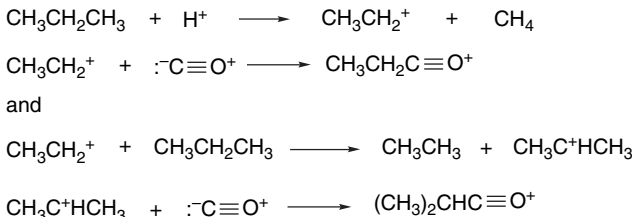
There is rapid interconversion of alkenes and carbocations over acidic zeolite catalysts, and the carbocations permit skeletal rearrangements and hydride transfer reactions. These reactions proceed in the direction of formation of more stable isomers.¹⁶¹ The rearrangements probably proceed through protonated cyclopropanes (see Section 4.4.4).



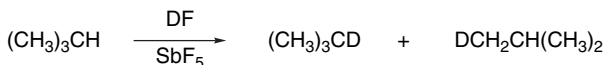
An important advance in understanding the mechanisms of reactions of alkanes with acidic catalysts resulted from study of the reactions of alkanes with superacids. This work demonstrated that both C–H and C–C bonds can be protonated, leading to fragmentation and formation of alkanes and carbocations.¹⁶⁷



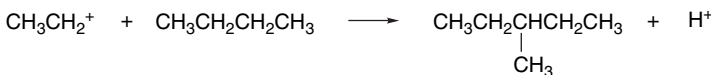
The reactions of propane and isobutene with HF-SbF₅ have been studied using C≡O to trap the carbocation intermediates.¹⁶⁸



The C–C bond of propane is more reactive than the C–H bonds, in accord with its lower bond strength. With isobutane, however, the reaction occurs with both the primary and tertiary C–H bonds, leading to hydrogen exchange.



The carbocation intermediates can also alkylate alkanes, leading to chain lengthening.

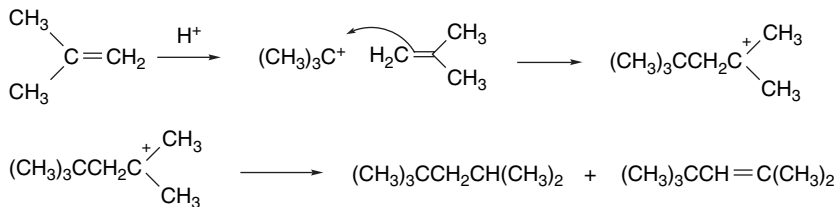


¹⁶⁶ P. G. Mennion and Z. Paal, *Ind. Eng. Chem. Res.*, **36**, 3282 (1997).

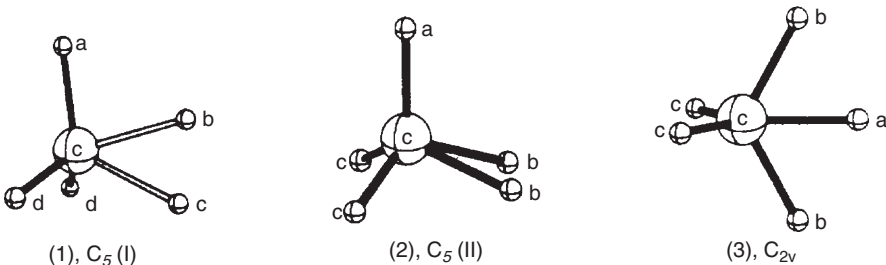
¹⁶⁷ G. A. Olah, Y. Halpern, J. Shen, and Y. K. Mo, *J. Am. Chem. Soc.*, **95**, 4960 (1973).

¹⁶⁸ J. Sommer and J. Bukala, *Acc. Chem. Res.*, **26**, 370 (1993).

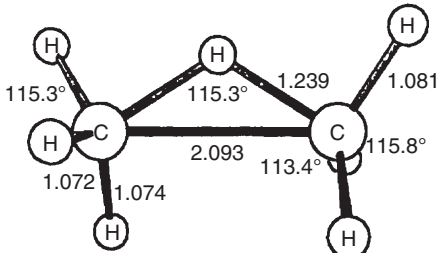
Similar reactions are observed over other strongly acidic catalysts, such as AlCl_3 and SbF_5 .¹⁶⁹ The acidic catalysts also promote dimerization and oligomerization of alkenes by mechanisms that are well known in the solution chemistry of carbocations.¹⁷⁰



The structure of pentacovalent carbonium ions has been investigated by ab initio MO (CCSD(T) methods. The CH_5^+ molecule is fluxional with facile conversion among closely related geometries.¹⁷¹



SD(Q)CI + DZP calculations find a bridged structure as the most stable form of C_2H_7^+ .



BLYP/6-311G** calculations have also been done on CH_5^+ and C_2H_7^+ .¹⁷²

Hydrocarbon protonations by catalysts have been modeled theoretically.¹⁷³ BLYP/6-31G** calculations suggest protonation of the C–C bonds, followed by collapse to alkane and alkene. The acidic catalyst site is regenerated by transfer of a proton to an adjacent oxygen. This model, which is summarized in Figure 4.15, undoubtedly oversimplifies the picture, but probably contains the fundamental aspects of the catalysis.

¹⁶⁹ G. A. Fuentes and B. C. Gates, *J. Catal.*, **76**, 440 (1982); G. A. Fuentes, J. V. Boegel, and B. C. Gates, *J. Catal.*, **78**, 436 (1982).

¹⁷⁰ J. P. G. Pater, P. A. Jacobs, and J. A. Martens, *J. Catal.*, **184**, 262 (1999).

¹⁷¹ P. R. Schreiner, S. J. Kim, H. F. Schaefer, III, and P. v. R. Schleyer, *J. Chem. Phys.*, **99**, 3716 (1993).

¹⁷² S. J. Collins and P. J. O'Malley, *Chem. Phys. Lett.*, **228**, 246 (1994).

¹⁷³ S. J. Collins and P. J. O'Malley, *J. Catal.*, **153**, 94 (1995); S. J. Collins and P. J. O'Malley, *Chem. Phys. Lett.*, **246**, 555 (1995).

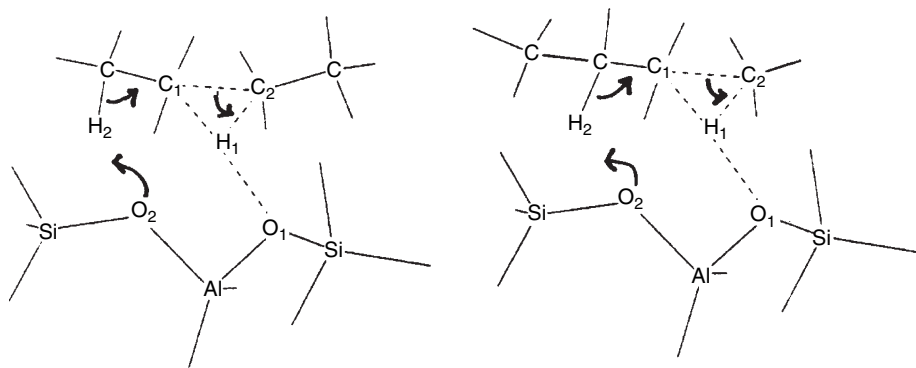


Fig. 4.15. Representation of C(2)-C(3) and C(1)-C(2) protonation and fragmentation to an alkane and alkene. Adapted from *Chem. Phys. Lett.*, **246**, 555 (1995).

General References

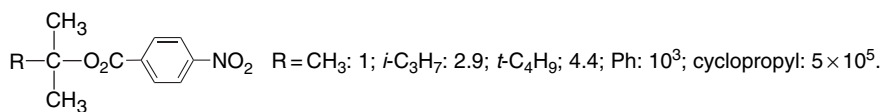
- S. P. McManus and C. U. Pittman, Jr., in *Organic Reaction Intermediates*, S. P. McManus, ed., Academic Press, New York, 1973, Chap. 4.
 G. A. Olah and P. v. R. Schleyer, eds., *Carbonium Ions*, Vols. I-IV, Wiley-Interscience, New York, 1968-1973.
 A. Streitwieser, Jr., *Solvolytic Displacement Reactions*, McGraw-Hill, New York, 1962.
 E. R. Thornton, *Solvolytic Mechanisms*, Ronald Press, New York, 1964.

Problems

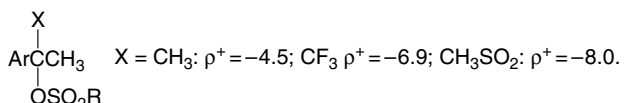
(References for these problems will be found on page 1159.)

4.1. Provide an explanation for the relative reactivity relationships revealed by the following data.

a. The relative rates of solvolysis in aqueous acetone of several tertiary *p*-nitrobenzoate esters:

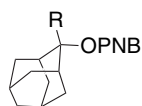


b. For solvolysis of *a*-substituted 1-aryl-1-ethyl sulfonates, the value of ρ^+ varies with the substituent.



c. The rates of solvolysis for a series of 2-alkyl-2-adamantyl *p*-nitrobenzoates in 80% aqueous acetone at 25 °C are: R=CH₃: $1.4 \times 10^{-10} \text{ s}^{-1}$;

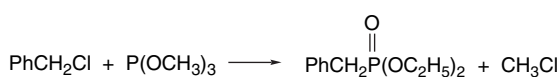
$\text{C}_2\text{H}_5 : 1.1 \times 10^{-9}\text{s}^{-1}$; $i\text{-C}_3\text{H}_7 : 5.0 \times 10^{-9}\text{s}^{-1}$; $t\text{-C}_4\text{H}_9 : 3.4 \times 10^{-5}\text{s}^{-1}$;
 $(\text{CH}_3)_3\text{CCH}_2 : 1.5 \times 10^{-9}\text{s}^{-1}$.



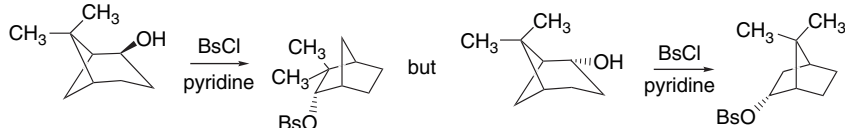
- d. The relative rates of methanolysis of a series of *w*-phenylthioalkyl chlorides depend on the chain length: $n = 1 : 3.3 \times 10^4$; $n = 2 : 1.5 \times 10^2$; $n = 3 : 1$; $n = 4 : 1.3 \times 10^2$; $n = 5 : 4.3$.

4.2. Suggest reasonable mechanisms for each of the following reactions. The starting materials are racemic, unless otherwise stated.

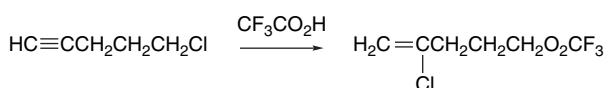
a.



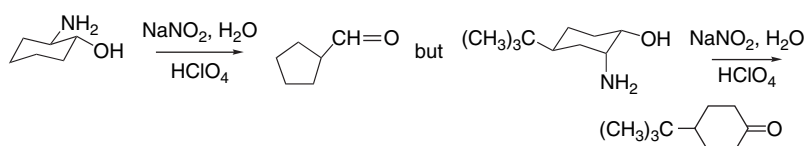
b.



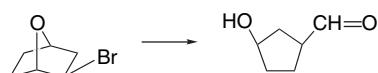
c.



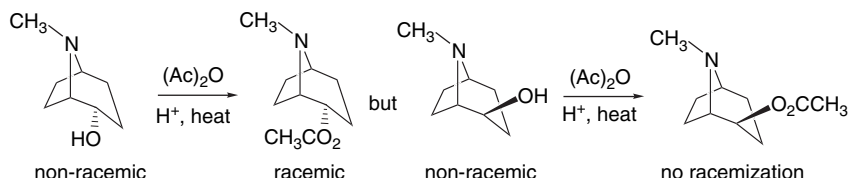
d.



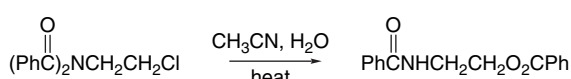
e.



f.



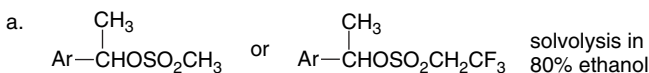
g.



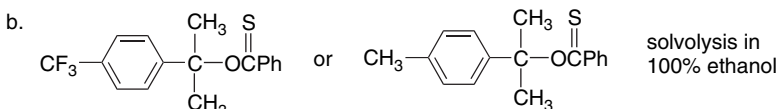
4.3. Which reaction in each pair would be expected to be faster? Explain.

461

PROBLEMS



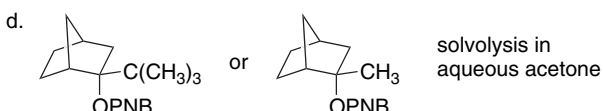
$\text{Ar} = 3, 5\text{-bis-(trifluoromethyl)phenyl}$



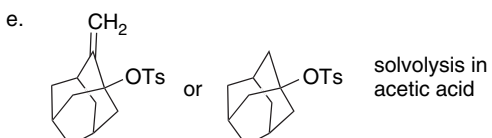
solvolytic in
100% ethanol



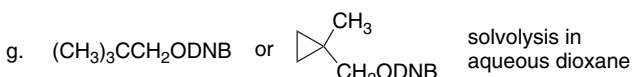
solvolytic in
acetic acid



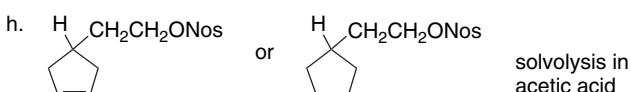
solvolytic in
aqueous acetone



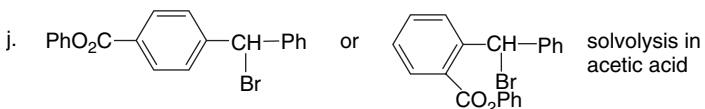
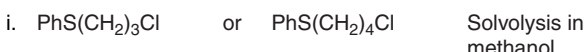
solvolytic in
acetic acid



solvolytic in
aqueous dioxane



solvolytic in
acetic acid



solvolytic in
acetic acid

4.4. The solvolysis of *2R,3S*-3-(4-methoxyphenyl)but-2-yl tosylate in acetic acid can be followed by several kinetic measurements: (a) rate of decrease of observed rotation (k_α); rate of release of the leaving group (k_t); and (c) when ^{18}O -labeled sulfonate is used, the rate of equilibration of the sulfonate oxygens in the reactant (k_{ex}). At 25 °C the rate constants are:

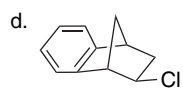
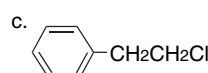
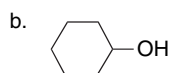
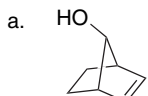
$$k_\alpha = 25.5 \times 10^{-6} \text{ s}^{-1}; k_t = 5.5 \times 10^{-6} \text{ s}^{-1}; k_{ex} = 17.2 \times 10^{-6} \text{ s}^{-1}$$

Indicate the nature of the process that is measured by each of these rate constants and devise an overall mechanism that includes each of these processes. Rationalize the order of the rates $k_\alpha > k_{ex} > k_t$.

- 4.5. Both *endo*- and *exo*-norbornyl brosylates react with $\text{R}_4\text{P}^+\text{N}_3^-$ (R is a long-chain alkyl) in toluene to give azides of inverted configuration. The yield from the *endo* and *exo* reactant is 95 and 80%, respectively. The remainder of the *exo* reactant is converted to nortricyclane (tricyclo[2.2.1.0^{2,6}]heptane.) The measured rates of azide formation are first order in both reactant and azide ion. The *endo* isomer reacts about twice as fast as the *exo* isomer. Both react considerably more slowly than cyclohexyl brosylate under the same conditions. No rearrangement of deuterium is observed when deuterium-labeled reactants are used. What conclusions about the mechanism of the substitution process can you draw from these results? How do the reaction conditions relate to the mechanism you have suggested? How is the nortricyclane formed?
- 4.6 The following observations have been made concerning the reaction of Z-1-phenyl-1,3-butadiene (**6-A**) and Z-4-phenyl-3-buten-2-ol (**6-B**) in 3–7 $\text{M}\text{H}_2\text{SO}_4$ and 0.5–3 MHClO_4
- Both compounds are converted to a mixture of the corresponding *E*-isomers with the rate governed by $\text{Rate} = k[\text{reactant}][\text{H}^+]$, where $[\text{H}^+]$ is measured by the H_0 acidity function.
 - The rate of isomerization of **6-A** is slower in deuterated ($\text{D}_2\text{SO}_4\text{-D}_2\text{O}$) media by a factor of 2 to 3. For **6-B**, the rate of isomerization is faster in by a factor of 2.5.
 - When ^{18}O -labeled **6-B** is used, the rate of loss of ^{18}O to the solvent is equal to the rate of isomerization.
 - The measured activation energies for **6-A** is $19.5 \pm 1 \text{ kcal/mol}$ and $22.9 \pm 0.7 \text{ kcal/mol}$ for **6-B**.

Write a mechanism that encompasses both isomerizations and is consistent with the information given.

- 4.7 Treatment of 2-(4-hydroxyphenyl)ethyl bromide with basic alumina produces a white solid, mp, 40–43 °C; IR 1640 cm⁻¹; UV_{max} 282 nm in H₂O; NMR two singlets of equal intensity at 1.69 and 6.44 ppm from TMS; anal: C 79.98% H, 6.71%. Suggest a possible structure for this product and explain how it could be formed.
- 4.8. In the discussion of the *syn*- and *anti*-norborn-2-en-7-yl tosylates (p. 422–423) it was pointed out that, relative to the saturated norborn-7-yl tosylate, the reactivities of the *syn* and *anti* isomers were 10^4 and 10^{11} , respectively. Whereas the *anti* isomer gives a product of retained configuration, the *syn* isomer gives a bicyclo[3.2.0]hept-2-enyl derivative. The high reactivity of the *anti* isomer was attributed to participation of the carbon-carbon bond. What explanation can you offer for the 10^4 acceleration of the *syn* isomer relative to the saturated system?
- 4.9. Indicate the structure of the final stable ion that would be formed from each of the following reactants in superacid media.



- 4.10. A series of ^{18}O -labeled sulfonate esters was studied to determine the extent of ^{18}O scrambling that accompanies solvolysis. The rate of ^{18}O exchange was compared with that of solvolysis and the results are shown below. Discuss the variation in the ratio $k_{\text{sol}} : k_{\text{exch}}$ and offer an explanation for the absence of exchange in the 3,3-dimethyl-2-butyl case.

R	k_{solv}	k_{exch}
i-propyl	3.6×10^{-5}	7.9×10^{-6}
cyclopentyl	3.8×10^{-3}	8.5×10^{-4}
2-adamantyl	1.5×10^{-3}	1.8×10^{-3}
3,3-dimethyl-2-butyl ^a	7.3×10^{-3}	Negligible

a. Solvolysis product is 2,3-dimethyl-2-butyl trifluoroacetate.

- 4.11. The relative stabilities of 1-phenylvinyl cations can be measured by determining the gas phase basicity of the corresponding alkynes. The table below gives data on free energy of protonation for substituted phenyethynes and phenylpropynes. These data give rise to the corresponding Yukawa-Tsuno relationships:

$$\text{For ArC}\equiv\text{CH} : \delta\Delta G^\circ = -14.1(\sigma^0 + 1.21\sigma_R^+)$$

$$\text{For ArC}\equiv\text{CCH}_3 : \delta\Delta G^\circ = -13.3(\sigma^0 + 1.12\sigma_R^+)$$

How do you interpret the values of ρ and r in these equations? Which system is more sensitive to the aryl substituents? How do you explain the difference in sensitivity? Sketch the resonance, polar, and hyperconjugative interactions that contribute to these substituent effects. What geometric constraints do these interactions place on the ions?

Substituent	$\delta\Delta G$ (kcal/mol)	
	Arylethyne	Arylpropyne
4-CH ₃ O	11.8	13.0
3-Cl-4-CH ₃ O	7.9	9.1
4-CH ₃	4.7	5.5
3-CH ₃	1.9	2.2
4-Cl	-0.5	0.1
3-F	-5.1	-5.6
3-Cl	-4.5	-5.1
3-CF ₃	-6.5	-6.6
3,5-diF	-8.4	
H	0	0

a. $\delta\Delta$ is the change in free energy relative to the unsubstituted compound.

- 4.12. Studies of the solvolysis of 1-phenylethyl chloride and its 4-substituted derivatives in aqueous trifluoroethanol containing azide anion provide information relative to the mechanism of nucleophilic substitution in this system.

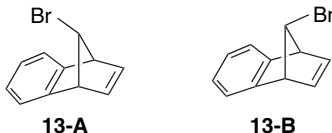
- a. The reaction rate is independent of the azide ion concentration for substituents that have σ^+ values more negative than -0.3 , but is first order in $[\text{N}_3^-]$ for substituents with σ^+ less negative than -0.08 .

- b. When other good nucleophiles, e.g., $\text{C}_3\text{H}_7\text{SH}$, are present, they can compete with azide ion. The reactants that are zero order in $[\text{N}_3^-]$ show little selectivity among competing nucleophiles.
- c. For reactants that solvolyze at rates independent of $[\text{N}_3^-]$, the ratio of 1-arylethyl azide to 1-arylethanol in the product increases as σ^+ of the substituent becomes more negative.
- d. The major product in reactions that are first order in $[\text{N}_3^-]$ are 1-arylethyl azides.

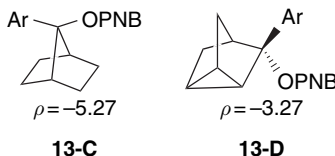
Consider these results in relation to the mechanism outlined in Figure 4.6 (p. 400). On the basis of the data given above, delineate the types of 1-arylethyl chlorides that react with azide ion according to those mechanistic types.

4.13. Offer a mechanistic interpretation of the following observations.

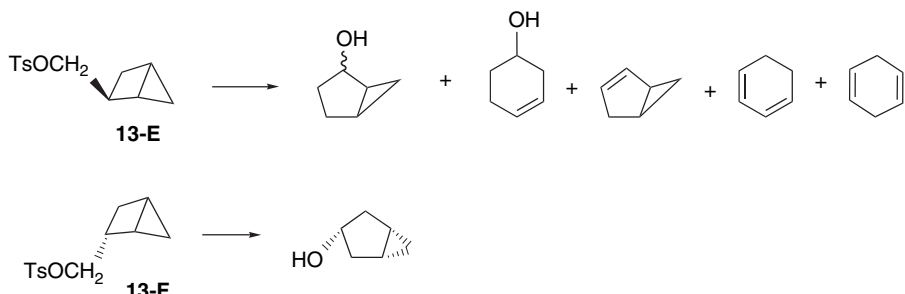
- a. Although there is a substantial difference in the rate at which **13-A** and **13-B** solvolyze (**13-A** reacts 4.4×10^4 times faster than **13-B** in acetic acid), both compounds give products of completely retained configuration.



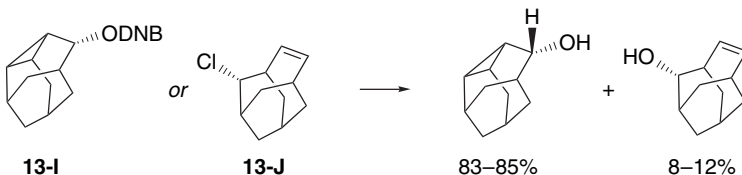
- b. The solvolysis of **13-C** is much more sensitive to aryl substituent effects than that of **13-D**.



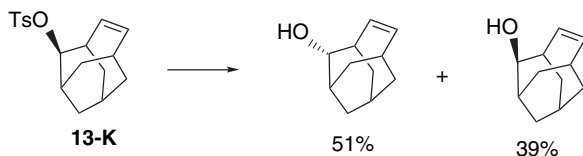
- c. Although stereoisomers **13-E** and **13-F** solvolyze in aqueous acetone at similar rates, the reaction products are quite different.



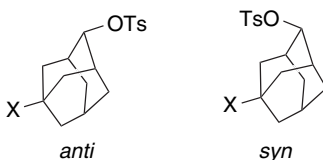
- d. Solvolysis of compounds **13-I** and **13-J** exhibits rate enhancement relative to a homoadamantane analog and gives product mixtures that are quite similar for both reactants.



On the other hand, compound **13-K** is less reactive than the saturated analog and gives a different product mixture.



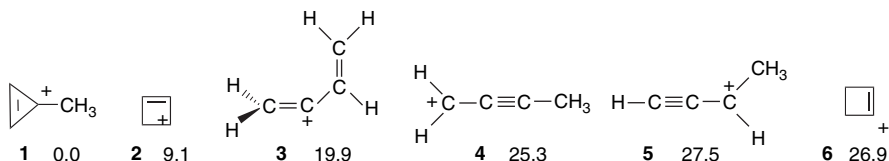
- e. The solvolysis of both stereoisomers of 5-fluoro- and 5-trimethylstannyl-2-adamantyl tosylate has been examined and the two have been compared. The relative rates and stereochemistry are summarized below.



X	<i>anti</i>		<i>syn</i>	
	Rate ^a	Stereochemistry	Rate	Stereochemistry
F	2.5×10^{-6}	4% net ret.	5×10^{-4}	100% ret.
$(\text{CH}_3)_3\text{Sn}$	10	100% ret.	15	63% net inv.

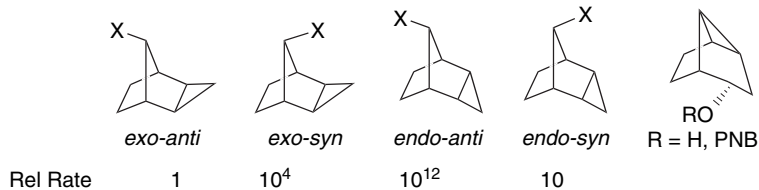
a. Rate is relative to unsubstituted system.

- 4.14. The six structures below are all found to be minima on the $[\text{C}_4\text{H}_5]^+$ energy surface. The relative energies from MP2/6-311G(*d,p*) calculations are shown in kcal/mol. Comment on the stabilizing features that are present in each of these cations.

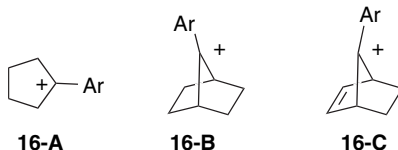


- 4.15. The rates of solvolysis of four stereoisomeric tricyclo[3.2.1.0^{2,4}]octan-8-yl systems have been determined. After accounting for leaving group and temperature, the relative rates are as shown. In aqueous dioxane, the *endo-anti* isomer

gives a product mixture consisting of the rearranged alcohol and the corresponding PNB ester (from leaving-group capture). The other isomers gave complex product mixtures that were not fully characterized. Explain the trend in rates and discuss the reason for the stereochemical outcome in the case of the *endo*-*anti* isomer.

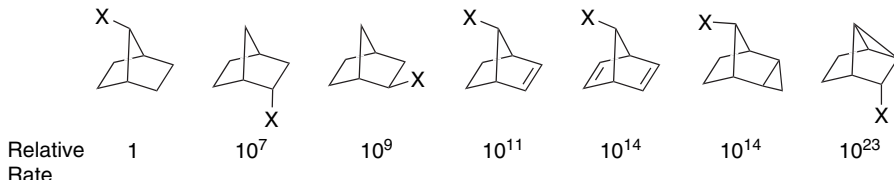


- 4.16. The ^{13}C -NMR chemical shift of the trivalent carbon is a sensitive indicator of carbocation structure. Generally, the greater the chemical shift value, the lower the electron density at the carbon. Data for three different cations with aryl substituents are given below. How do you explain the close similarity of the trend for the first two series and the opposite trend of the third?



Aryl substituent	Chemical shift (ppm)		
	16-A	16-B	16-C
3, 5-diCF ₃	287	283	73
4-CF ₃	284	278	81
H	272	264	109
4-CH ₃	262	252	165
4-OCH ₃	235	230	220

- 4.17. Relative rate data are available for a wide range of reactivities for rings related to the bicyclo[2.2.1]heptyl (norbornyl) system. Offer a discussion of the structural effects that are responsible for the observed relative rates.



- 4.18. Fujio and co-workers studied the reaction of pyridine with a wide range of 1-arylethyl bromides in acetonitrile. By careful analysis of the kinetic data, they were able to dissect each reaction into a first-order and a second-order component, as shown in the table below. The first-order components were correlated by a Yukawa-Tsuno equation: $\log k/k_o = 5.0(\sigma^\circ + 1.15\bar{\sigma}^+)$. The second-order component gave a curved plot, as shown in Figure 4.P18. Analyze the responses of the reaction to the aryl substituents in terms of transition state structures.

Substituent	$10^5 k_1 (\text{s}^{-1})$	$10^5 k_2 (\text{M}^{-1}\text{s}^{-1})$	Substituent	$10^5 k_1 (\text{s}^{-1})$	$10^5 k_2 (\text{M}^{-1}\text{s}^{-1})$
4-CH ₃ O	1660	2820	2-Naphthyl	0.28	11.6
4-CH ₃ S	103	215	3-CH ₃	0.055	7.29
4-C ₆ H ₅ O	41.5	119	H	0.032	5.54
3-Cl-4-CH ₃ O	21.2	79.0	4-Cl		4.37
2-Fluorenyl	18.3	59.5	3-Cl		2.085
3,4,5-tri-CH ₃	8.56	41.1	3-CF ₃		1.77
3,4-di-CH ₃	3.67	28.3	3-NO ₂		1.21
4-CH ₃	1.46	19.2	4-NO ₂		1.19
4-(CH ₃) ₃ C	0.82	15.2	3,5-di-CF ₃		0.651

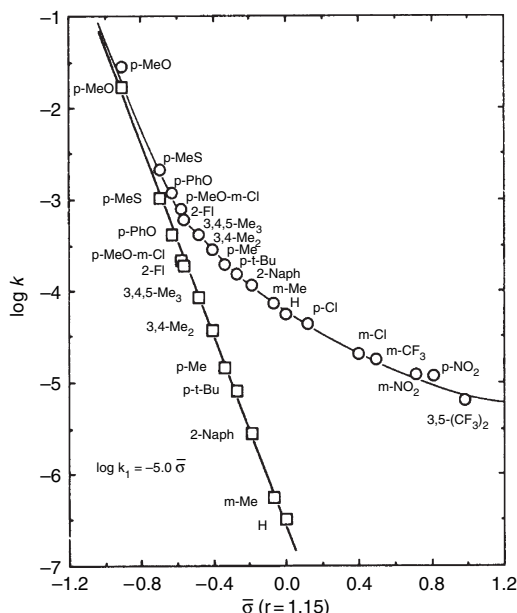
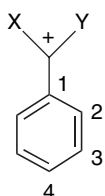


Fig. 4.P18. Substituent effects on the rates of reaction of pyridine with 1-arylethyl bromides in acetonitrile at 35°C. Squares are the first-order rates and open circles are the second-order rates. Reproduced from *Tetrahedron Lett.* **38**, 3243 (1997), by permission of Elsevier.

4.19 The Yukawa-Tsuno equation r values have been measured for the solvolysis reactions of substituted benzyl cations and α -substituted analogs. HF/6-31G* charges and bond orders have been calculated for the presumed cationic intermediates. Analyze the data for relationships between r and the structural parameters.



X,Y	H,H	CH ₃ , H	CH ₃ , CH ₃	CF ₃ , H
<i>r</i>	1.28	1.15	1.00	1.51
Mulliken Charge				
C(1)	-0.0024	-0.050	-0.068	-0.211
C(2)	+0.189	+0.164	+0.140	+0.053
C(3)	+0.051	+0.046	+0.043	+0.053
C(4)	+0.213	+0.190	+0.171	+0.233
Bond Order				
C(1)-C(7)	1.584	1.465	1.363	1.622
C(1)-C(2)	1.158	1.193	1.225	1.134
C(2)-C(3)	1.167	1.543	1.524	1.585
C(3)-C(4)	1.343	1.361	1.375	1.329

- 4.20. Reactions of substituted cumyl benzoates in 50:50 trifluoroethanol-water show no effect of $[\text{NaN}_3]$ on the rate of reaction between 0 and 0.5M for either EWG or ERG substituents. The product ratio, however, as shown in the figure, is highly dependent on the cumyl substituent. ERG substituents favor azide formation, whereas EWG groups result in more solvent capture. Formulate a reaction mechanism that is consistent with these observations.

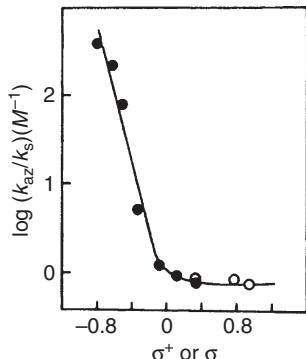
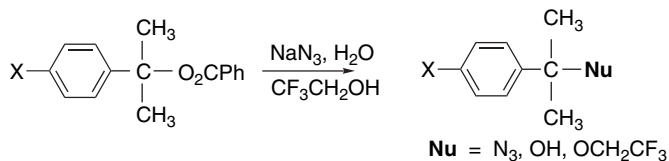


Fig. 4.P20. Log of product selectivity (k_{az}/k_s) M^{-1} versus σ^+ . Solid circles are substituted benzoate leaving groups and open circles are chloride. Reproduced from *J. Am. Chem. Soc.*, **113**, 5 871 (1991), by permission of the American Chemical Society.

4.21. The comparison of activation parameters for reactions in different solvents requires consideration of solvation differences of both the reactants and the transition states. The comparison can be done by using potential energy diagrams, such as that illustrated below for two different solvents A and B. It is possible to measure $\Delta H_{\text{transfer}}$ values, which correspond to the enthalpy change associated with transfer of a solute from one solvent to another.

— TS in A
 — TS in B
 reactants in A —
 reactants in B —

$\Delta H_{\text{transfer}}$ data for *n*-hexyl tosylate and several nucleophilic anions are given in Table 4.P1.21. In Table 4.P2.21, the activation parameters for S_N2 displacement reactions with *n*-hexyl tosylate are given. Use these data to construct a potential energy comparison for each of the nucleophiles. Use these diagrams to interpret the relative reactivity data given in Table 4.P3.21. Discuss the following aspects of the data.

- Why is Cl^- more reactive than Br^- in DMSO, whereas the reverse is true in methanol?
- Why does the rate of thiocyanate (SCN^-) ion change the least of the five nucleophiles on going from methanol to DMSO?
- Why does thiocyanate have the most negative entropy of activation?

Table 4.P1.21. Enthalpies of Transfer of Ions and *n*-Hexyl Tosylate From Methanol to DMSO at 25°C

Reactant	$\Delta H_{\text{transfer}}$ (kcal/mol)
<i>n</i> -C ₆ H ₁₃ OTs	-0.4
Cl ⁻	6.6
N ₃ ⁻	3.6
Br ⁻	2.3
NCS ⁻	1.0
I ⁻	-1.1

Table 4.P2.21. Activation Parameters for Nucleophilic Displacement Reactions of *n*-Hexyl Tosylate

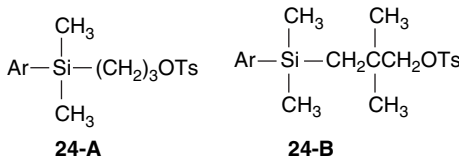
Nu : ⁻	Solvent	ΔH^\ddagger (kcal/mol)	ΔS^\ddagger (eu)	ΔG^\ddagger (kcal/mol)
Cl ⁻	MeOH	24.3	-4.2	25.5
	DMSO	20.2	-4.4	21.6
N ₃ ⁻	MeOH	21.2	-8.2	23.5
	DMSO	18.6	-7.8	21.0
Br ⁻	MeOH	22.9	-6.4	24.9
	DMSO	20.5	-5.6	22.0
NCS ⁻	MeOH	19.8	-15.8	24.2
	DMSO	20.0	-12.4	23.7
I ⁻	MeOH	22.4	-6.0	23.9
	DMSO	20.9	-5.8	22.8

Table 4.P3.21. Rates of Nucleophilic Substitution on *n*-Hexyl Tosylate^a

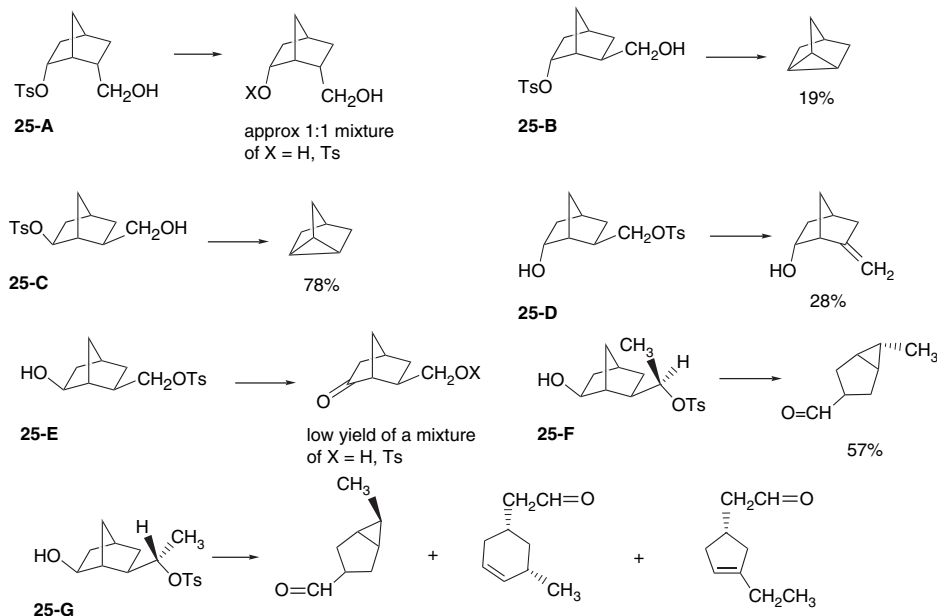
Nu : ⁻	Solvent	<i>k</i> (40 °C)	<i>k</i> (30 °C)	<i>k</i> (20 °C)
Cl ⁻	MeOH	0.0852	0.0226	0.00550
	DMSO	50.5	16.7	5.06
	MeOH	1.66	0.514	0.152
	DMSO	135	48.3	16.1
Br ⁻	MeOH	0.250	0.0721	0.0191
	DMSO	17.8	5.60	1.75
NCS ⁻	MeOH	0.481	0.165	0.0512
	DMSO	1.11	0.365	0.115
I ⁻	MeOH	0.956	0.275	0.0767
	DMSO	5.50	1.75	16.0 (50 °C)

a. $k_2 \times 10^4 M^{-1}s^{-1}$.

- d. Is there any correlation between softness (which is in the order I⁻ > SCN⁻ > N₃⁻ > Br⁻ > Cl⁻) and the effect of the solvent change on the rate of the reaction?
- 4.22. The Yukawa-Tsuno parameter r^+ has been measured for several solvolysis reactions. What relationship do you see among the properties of the reactants, the likely nature of the transition structures, and the observed value of r^+ ?
- a. Solvolysis of benzyl tosylates in acetic acid; $r^+ = 1.3$ compared to solvolysis of 1-aryl-2,2,2-trifluoroethyl tosylates in 80% aqueous acetone; $r^+ = 1.39$
 - b. Aryl-assisted solvolysis of 2-aryl-2-(trifluoromethyl)ethyl *m*-nitrobenzoates in 80% aqueous trifluoroethanol; $r^+ = 0.77$ compared to aryl-assisted solvolysis of 2-arylethyl tosylates; $r^+ = 0.6$
- 4.23. Comparison of several series of solvolysis reactions that proceed via carbocation intermediates revealed that an α -cyano substituent is rate retarding by a factor of about 10^{-3} . A β -cyano is even more rate retarding, with the difference being as much as 10^{-7} . Why are both α - and β -cyano rate retarding and why might the β -substituent have a stronger effect?
- 4.24. Several substituted propyl tosylates with γ -silicon groups have been studied. For the 2,2-dimethyl derivatives **24-B**, the solvolysis rates are 10^3 to 10^4 greater than for the nonsilyl analogs. The products are rearranged 1,1-dimethyl derivatives. The reaction shows modest sensitivity to substituents in the aryl group, correlating with a Hammett ρ value of -1.0 . When the parent system **24-A** (without the 2,2-dimethyl substituents) was studied in the nonnucleophilic solvent 97% TFE, cyclopropane was formed, ranging in yield from 0% with EWG (CF₃) to 100% with ERG (CH₃O). The Hammett correlation gave $\rho = -1.1$ for cyclopropane formation but no significant substituent effect for substitution. Describe a mechanism that is consistent with this information.



4.25. The reaction of several monotosylates derived from 6-hydroxy-2-(hydroxymethyl)norbornane were studied under conditions where alkoxide formation would be expected at the nontosylated hydroxy. Compounds **25-C** and **25-F** showed highly specific product formation, whereas the other compounds gave slower reactions and more complex product mixtures. Identify the structural features that make the observed pathways particularly favorable for **25-C** and **25-F**. Offer a mechanistic rationale for the formation of the products shown for the other reactants.



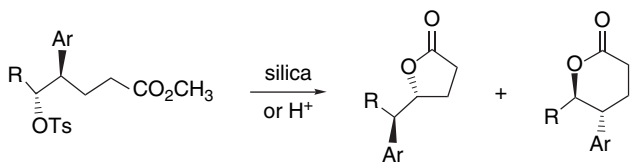
4.26. Table 4.P26 shows stabilization (+) and destabilization (−) of α -substituted ethyl and vinyl carbocations as determined by the isodesmic reactions shown below. Comment on the following trends in the data.

Table 4.P26. Stabilization of Ethyl and Vinyl Carbocations by α -Substituent

Substituent	$C_2H_5^+$	$CH_2=CH^+$	Substituent	$C_2H_5^+$	$CH_2=CH^+$
H	0.00	0.00	CN	−16.02	−11.71
CH_3	18.83	25.89	$CH=O$	−10.25	−4.51
CH_2Cl	5.59	12.90	F	6.95	−9.25
CH_2Br	8.66	14.00	Cl	9.83	11.17
CH_2OH	15.30	21.69	Br	9.52	12.70
CH_2CN	−2.10	4.76	I	13.32	20.53
CH_2CF_3	3.62	9.63	NH_2	64.96	53.69
CH_2F	4.98	10.89	OH	37.43	25.92
CF_3	−23.56	−16.41	SH	36.39	38.21
$CH_2=CH$	31.98	32.55	NO_2	−23.09	−25.44
$HC\equiv C$	18.17	25.64	$(CH_3)_3Si$	17.30	34.21
C_6H_5	36.77	54.10			
$c - C_3H_5$	42.97	47.06			



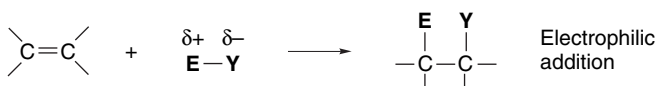
- a. The stabilization of vinyl cations tends to be somewhat larger than for the corresponding ethyl cation.
- b. F, OH, and NH₂ provide less stabilization of vinyl cations than of ethyl cations.
- c. CF₃ and CN are less destabilizing of vinyl cations than of ethyl cations.
- d. What factors dominate the effect of the CH₂-X substituents?
- e. Compare the π -donor and polar effects of the OH, NH₂, and SH substituents.
- 4.27. 4-Aryl-5-tosyloxyhexanoates are converted to mixtures of lactones when exposed to silica or heated with *p*-toluenesulfonic acid in various solvents. The aryl ring must have an EWG for the reaction to proceed. A similar reaction occurs with 4-aryl-5-tosyloxypentanoates, but in this case only γ -lactones are formed. Suggest a mechanism that accounts for both the observed regioselectivity and stereoselectivity and the requirement for an ERG on the aryl ring.



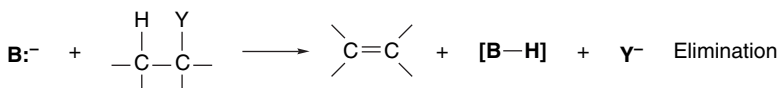
Polar Addition and Elimination Reactions

Introduction

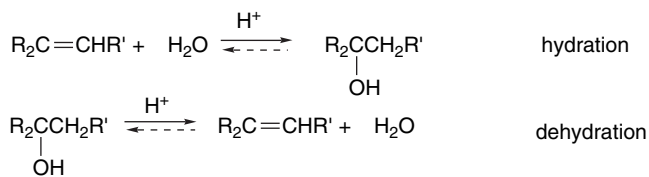
In this chapter, we discuss reactions that either add adjacent (*vicinal*) groups to a carbon-carbon double bond (*addition*) or remove two adjacent groups to form a new double bond (*elimination*). The discussion focuses on addition reactions that proceed by electrophilic polar (*heterolytic*) mechanisms. In subsequent chapters we discuss addition reactions that proceed by *radical* (*homolytic*), *nucleophilic*, and *concerted* mechanisms. The electrophiles discussed include protic acids, halogens, sulfenyl and selenenyl reagents, epoxidation reagents, and mercuric and related metal cations, as well as diborane and alkylboranes. We emphasize the relationship between the regio- and stereoselectivity of addition reactions and the reaction mechanism.



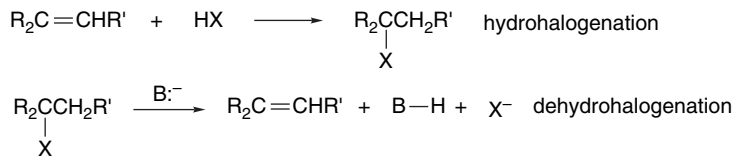
The discussion of elimination reactions considers the classical E2, E1, and E1cb eliminations that involve removal of a hydrogen and a leaving group. We focus on the kinetic and stereochemical characteristics of elimination reactions as key indicators of the reaction mechanism and examine how substituents influence the mechanism and product composition of the reactions, paying particular attention to the nature of transition structures in order to discern how substituent effects influence reactivity. We also briefly consider reactions involving trisubstituted silyl or stannyl groups. Thermal and concerted eliminations are discussed elsewhere.



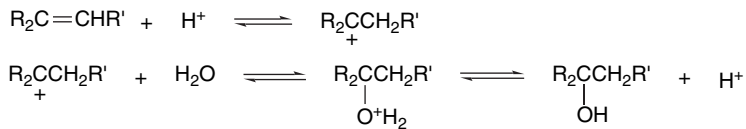
Addition and elimination processes are the formal reverse of one another, and in some cases the reaction can occur in either direction. For example, acid-catalyzed hydration of alkenes and dehydration of alcohols are both familiar reactions that constitute an addition-elimination pair.



Another familiar pair of addition-elimination reactions is hydrohalogenation and dehydrohalogenation, although these reactions are not reversible under normal conditions, because the addition occurs in acidic solution, whereas the elimination requires a base.



When reversible addition and elimination reactions are carried out under similar conditions, they follow the same mechanistic path, but in opposite directions. The *principle of microscopic reversibility* states that the mechanism of a reversible reaction is the same in the forward and reverse directions. The intermediates and transition structures involved in the addition process are the same as in the elimination reaction. Under these circumstances, mechanistic conclusions about the addition reaction are applicable to the elimination reaction and vice versa. The reversible acid-catalyzed reaction of alkenes with water is a good example. Two intermediates are involved: a carbocation and a protonated alcohol. The direction of the reaction is controlled by the conditions, which can be adjusted to favor either side of the equilibrium. Addition is favored in aqueous solution, whereas elimination can be driven forward by distilling the alkene from the reaction solution. The reaction energy diagram is shown in Figure 5.1.



Several limiting general mechanisms can be written for polar additions. Mechanism A involves prior dissociation of the electrophile and implies that a carbocation is generated that is free of the counterion Y^- at its formation. Mechanism B also involves a carbocation intermediate, but it is generated in the presence of an anion and exists initially as an ion pair. Depending on the mutual reactivity of the two ions, they might or might not become free of one another before combining to give product. Mechanism C leads to a bridged intermediate that undergoes addition by a second step in which the ring is opened by a nucleophile. Mechanism C implies stereospecific *anti* addition. Mechanisms A, B, and C are all $\text{Ad}_{\text{E}}2$ reactions; that

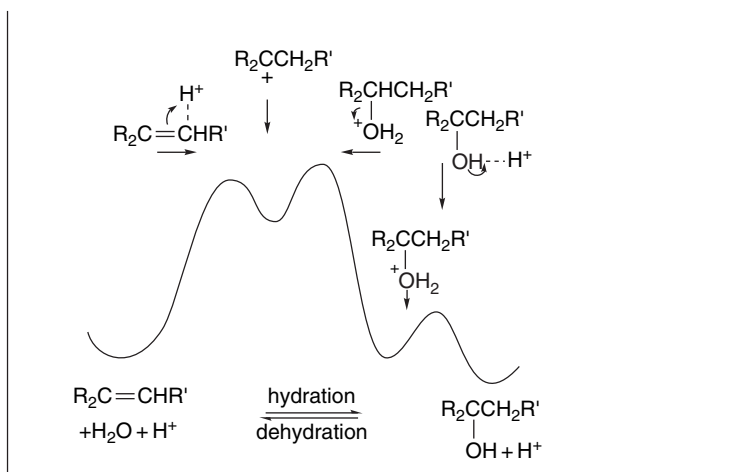
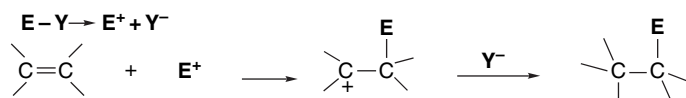


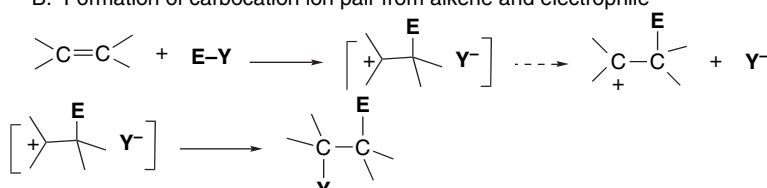
Fig. 5.1. Conceptual representation of the reversible reaction path for the hydration-dehydration reaction pair.

is, they are *bimolecular electrophilic additions*. Mechanism D is a process that has been observed for several electrophilic additions and implies concerted transfer of the electrophilic and nucleophilic components of the reagent from two separate molecules. It is a *termolecular electrophilic addition*, Ad_E3 , a mechanism that implies formation of a complex between one molecule of the reagent and the reactant and also is expected to result in *anti* addition. Each mechanism has two basic parts, the electrophilic interaction of the reagent with the alkene and a step involving reaction with a nucleophile. Either formation of the bond to the electrophile or nucleophilic capture of the cationic intermediate can be rate controlling. In mechanism D, the two stages are concurrent.

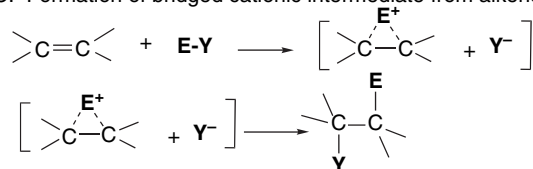
A. Prior dissociation of electrophile and formation of carbocation intermediate



B. Formation of carbocation ion pair from alkene and electrophile

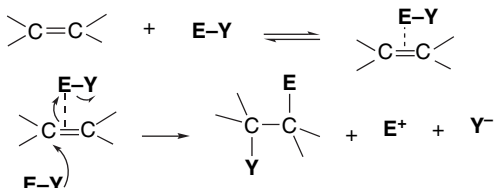


C. Formation of bridged cationic intermediate from alkene and electrophile



(Continued)

D. Concerted addition of electrophile and nucleophile in a termolecular reaction



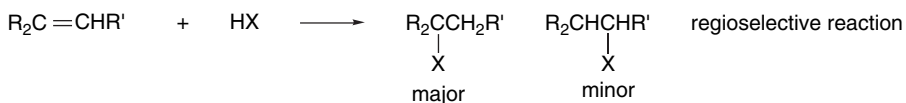
All of these mechanisms are related in that they involve electrophilic attack on the π bond of the alkene. Based on the electron distribution and electrostatic potential maps of alkenes (Section 1.4.5), the initial attack is expected to be perpendicular to the plane of the double bond and near the midpoint of the π bond. The mechanisms differ in the relative stability of the carbocation or bridged intermediates and in the timing of the bonding to the nucleophile. Mechanism A involves a prior dissociation of the electrophile, as would be the case in protonation by a strong acid. Mechanism B can occur if the carbocation is fairly stable and E^+ is a poor bridging group. The lifetime of the carbocation may be very short, in which case the ion pair would react faster than it dissociates. Mechanism C is an important general mechanism that involves bonding of E^+ to *both carbons of the alkene* and depends on the ability of the electrophile to function as a bridging group. Mechanism D avoids a cationic intermediate by concerted formation of the $\text{C}-\text{E}$ and $\text{C}-\text{Y}$ bonds.

The nature of the electrophilic reagent and the relative stabilities of the intermediates determine which mechanism operates. Because it is the hardest electrophile and has no free electrons for bridging, the proton is most likely to react via a carbocation mechanism. Similarly, reactions in which E^+ is the equivalent of F^+ are unlikely to proceed through bridged intermediates. Bridged intermediates become more important as the electrophile becomes softer (more polarizable). We will see, for example, that bridged halonium ions are involved in many bromination and chlorination reactions. Bridged intermediates are also important with sulfur and selenium electrophiles. Productive termolecular collisions are improbable, and mechanism D involves a prior complex of the alkene and electrophilic reagent. Examples of each of these mechanistic types will be encountered as specific reactions are considered in the sections that follow. The discussion focuses on a few reactions that have received the most detailed mechanistic study. Our goal is to see the common mechanistic features of electrophilic additions and recognize some of the specific characteristics of particular reagents.

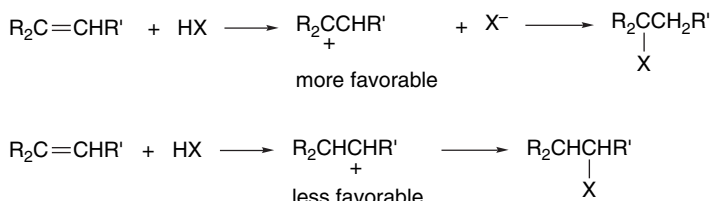
5.1. Addition of Hydrogen Halides to Alkenes

The addition of hydrogen halides to alkenes has been studied from a mechanistic perspective for many years. One of the first aspects of the mechanism to be established was its regioselectivity, that is, the direction of addition. A reaction is described as *regioselective* if an unsymmetrical alkene gives a predominance of one of the two isomeric addition products.¹

¹. A. Hassner, *J. Org. Chem.*, **33**, 2684 (1968).



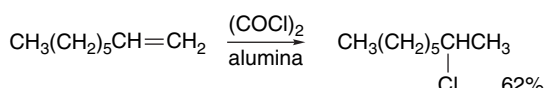
In the addition of hydrogen halides to alkenes, it is usually found that the nucleophilic halide ion becomes attached to the more-substituted carbon atom. This general observation is called *Markovnikov's rule*. The basis for this regioselectivity lies in the relative ability of the carbon atoms to accept positive charge. The addition of hydrogen halide is initiated by protonation of the alkene. The new C–H bond is formed from the π electrons of the carbon–carbon double bond. It is easy to see that if a carbocation is formed as an intermediate, the halide will be added to the more-substituted carbon, since protonation at the less-substituted carbon atom provides the more stable carbocation intermediate.



As is indicated when the mechanism is discussed in more detail, discrete carbocations are not always formed. Unsymmetrical alkenes nevertheless follow the Markovnikov rule, because the partial positive charge that develops is located predominantly at the carbon that is better able to accommodate an electron deficiency, which is the more-substituted one.

The regioselectivity of addition of hydrogen bromide to alkenes can be complicated if a free-radical chain addition occurs in competition with the ionic addition. The free-radical chain reaction is readily initiated by peroxidic impurities or by light and leads to the *anti* Markovnikov addition product. The mechanism of this reaction is considered more fully in Chapter 11. Conditions that minimize the competing radical addition include use of high-purity alkene and solvent, exclusion of light, and addition of a radical inhibitor.²

The order of reactivity of the hydrogen halides is HI > HBr > HCl, and reactions of simple alkenes with HCl are quite slow. The reaction occurs more readily in the presence of silica or alumina and convenient preparative methods that take advantage of this have been developed.³ In the presence of these adsorbents, HBr undergoes exclusively ionic addition. In addition to the gaseous hydrogen halides, liquid sources of hydrogen halide such as SOCl₂, (COCl)₂, (CH₃)₃SiCl, (CH₃)₃SiBr, and (CH₃)₃SiI can be used. The hydrogen halide is generated by reaction with water and/or hydroxy group on the adsorbent.



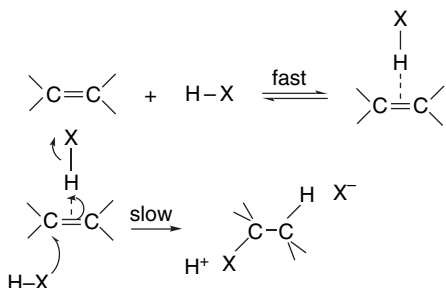
². D. J. Pasto, G. R. Meyer, and B. Lepeska, *J. Am. Chem. Soc.*, **96**, 1858 (1974).

³. P. J. Kropp, K. A. Daus, M. W. Tubergen, K. D. Kepler, V. P. Wilson, S. C. Craig, M. M. Baillargeon, and G. W. Breton, *J. Am. Chem. Soc.*, **115**, 3071 (1993).

Studies aimed at determining mechanistic details of hydrogen halide addition to alkenes have focused on the kinetics and stereochemistry of the reaction and on the effect of added nucleophiles. Kinetic studies often reveal rate expressions that indicate that more than one process contributes to the overall reaction rate. For addition of hydrogen bromide or hydrogen chloride to alkenes, an important contribution to the overall rate is often made by a third-order term.

$$\text{Rate} = k[\text{alkene}][\text{HX}]^2$$

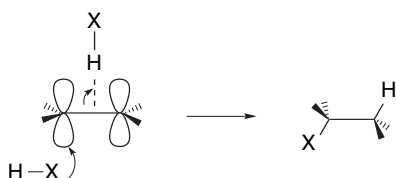
Among the cases in which this type of kinetics has been observed are the addition of HCl to 2-methyl-1-butene, 2-methyl-2-butene, 1-methylcyclopentene,⁴ and cyclohexene.⁵ The addition of HBr to cyclopentene also follows a third-order rate expression.² The TS associated with the third-order rate expression involves proton transfer to the alkene from one hydrogen halide molecule and capture of the halide ion from the second, and is an example of general mechanism D (Ad_{E3}). Reaction occurs through a complex formed by the alkene and hydrogen halide with the second hydrogen halide molecule.



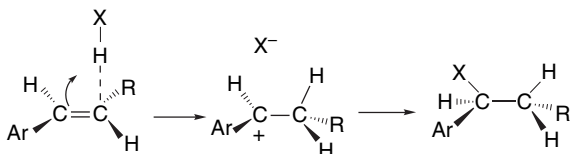
The stereochemistry of addition of hydrogen halides to unconjugated alkenes is usually *anti*. This is true for addition of HBr to 1,2-dimethylcyclohexene,⁶ cyclohexene,⁷ 1,2-dimethylcyclopentene,⁸ cyclopentene,² *Z*- and *E*-2-butene,² and 3-hexene,² among others. *Anti* stereochemistry is also dominant for addition of hydrogen chloride to 1,2-dimethylcyclohexene⁹ and 1-methylcyclopentene.⁴ Temperature and solvent can modify the stereochemistry, however. For example, although the addition of HCl to 1,2-dimethylcyclohexene is *anti* near room temperature, *syn* addition dominates at -78°C .¹⁰

Anti stereochemistry is consistent with a mechanism in which the alkene interacts simultaneously with a proton-donating hydrogen halide and a source of halide ion, either a second molecule of hydrogen halide or a free halide ion. The *anti* stereochemistry is consistent with the expectation that the attack of halide ion occurs from the opposite side of the π -bond to which the proton is delivered.

4. Y. Pocker, K. D. Stevens, and J. J. Champoux, *J. Am. Chem. Soc.*, **91**, 4199 (1969); Y. Pocker and K. D. Stevens, *J. Am. Chem. Soc.*, **91**, 4205 (1969).
5. R. C. Fahey, M. W. Monahan, and C. A. McPherson, *J. Am. Chem. Soc.*, **92**, 2810 (1970).
6. G. S. Hammond and T. D. Nevitt, *J. Am. Chem. Soc.*, **76**, 4121 (1954).
7. R. C. Fahey and R. A. Smith, *J. Am. Chem. Soc.*, **86**, 5035 (1964); R. C. Fahey, C. A. McPherson, and R. A. Smith, *J. Am. Chem. Soc.*, **96**, 4534 (1974).
8. G. S. Hammond and C. H. Collins, *J. Am. Chem. Soc.*, **82**, 4323 (1960).
9. R. C. Fahey and C. A. McPherson, *J. Am. Chem. Soc.*, **93**, 1445 (1971).
10. K. B. Becker and C. A. Grob, *Synthesis*, 789 (1973).

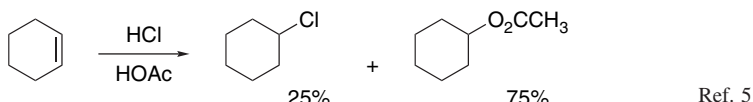
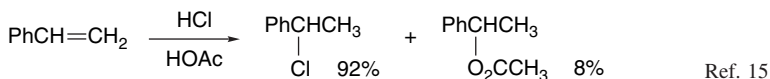


A change in the stereoselectivity is observed when the double bond is conjugated with a group that can stabilize a carbocation intermediate. Most of the specific cases involve an aryl substituent. Examples of alkenes that give primarily *syn* addition are *Z*- and *E*-1-phenylpropene,¹¹ *cis*- and *trans*- β -*t*-butylstyrene,¹² 1-phenyl-4-*t*-butylcyclohexene,¹³ and indene.¹⁴ The mechanism proposed for these reactions features an ion pair as the key intermediate. Owing to the greater stability of the benzylic carbocations formed in these reactions, concerted attack by halide ion is not required for protonation. If the ion pair formed by alkene protonation collapses to product faster than rotation takes place, *syn* addition occurs because the proton and halide ion are initially on the same face of the molecule.



Kinetic studies of the addition of hydrogen chloride to styrene support the conclusion than an ion pair mechanism operates. The reaction is first order in hydrogen chloride, indicating that only one molecule of hydrogen chloride participates in the rate-determining step.¹⁵

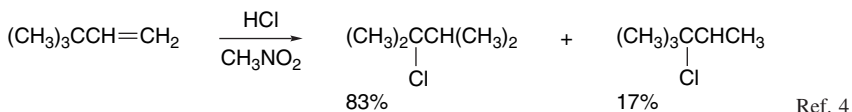
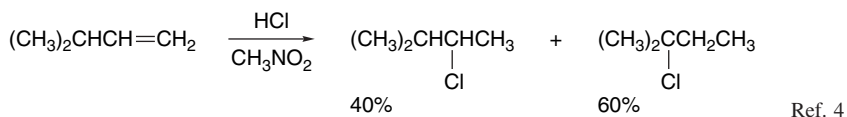
There is a competing reaction with solvent when hydrogen halide additions to alkenes are carried out in nucleophilic solvents.



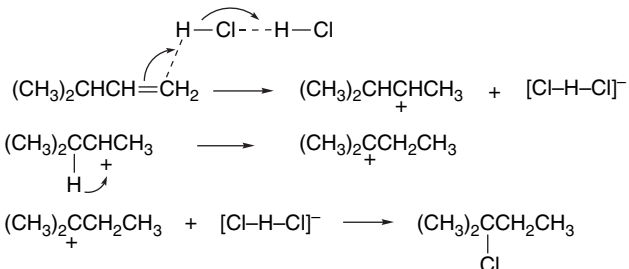
This result is consistent with the general mechanism for hydrogen halide additions. These products are formed because the solvent competes with halide ion as the nucleophilic component in the addition. Solvent addition can occur via a concerted mechanism or by capture of a carbocation intermediate. Addition of a halide salt increases the likelihood of capture of a carbocation intermediate by halide ion. The effect of added halide salt can be detected kinetically. For example, the presence of tetramethylammonium chloride increases the rate of addition of hydrogen chloride to cyclohexene.⁹ Similarly, lithium bromide increases the rate of addition of hydrogen bromide to cyclopentene.⁸

- ¹¹. M. J. S. Dewar and R. C. Fahey, *J. Am. Chem. Soc.*, **85**, 3645 (1963).
- ¹². R. J. Abraham and J. R. Monasterios, *J. Chem. Soc., Perkin Trans. 2*, 574 (1975).
- ¹³. K. D. Berlin, R. O. Lyerla, D. E. Gibbs, and J. P. Devlin, *J. Chem. Soc., Chem. Commun.*, 1246 (1970).
- ¹⁴. M. J. S. Dewar and R. C. Fahey, *J. Am. Chem. Soc.*, **85**, 2248 (1963).
- ¹⁵. R. C. Fahey and C. A. McPherson, *J. Am. Chem. Soc.*, **91**, 3865 (1969).

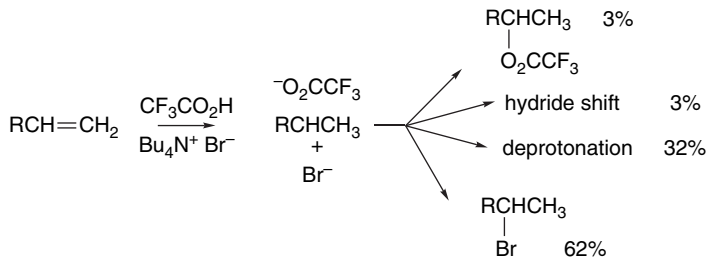
Skeletal rearrangements are possible in hydrogen halide additions if hydride or alkyl migration can give a more stable carbocation



Even though the rearrangements suggest that discrete carbocation intermediates are involved, these reactions frequently show kinetics consistent with the presence of at least two hydrogen chloride molecules in the rate-determining step. A termolecular mechanism in which the second hydrogen chloride molecule assists in the ionization of the electrophile has been suggested to account for this observation.⁴



Another possible mechanism involves halide-assisted protonation.¹⁶ The electrostatic effect of a halide anion can facilitate proton transfer. The key intermediate in this mechanism is an ion sandwich involving the acid anion and a halide ion. Bromide ion accelerates addition of HBr to 1-, 2-, and 4-octene in 20% TFA in CH₂Cl₂. In the same system, 3,3-dimethyl-1-butene shows substantial rearrangement, indicating formation of a carbocation intermediate. Even 1- and 2-octene show some evidence of rearrangement, as detected by hydride shifts. The fate of the 2-octyl cation under these conditions has been estimated.

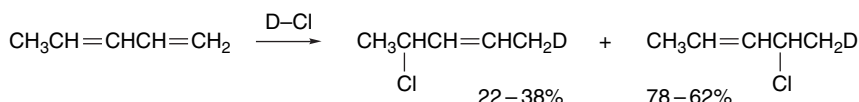


This behavior of the cationic intermediates generated by alkene protonation is consistent with the reactivity associated with carbocations generated by leaving-group

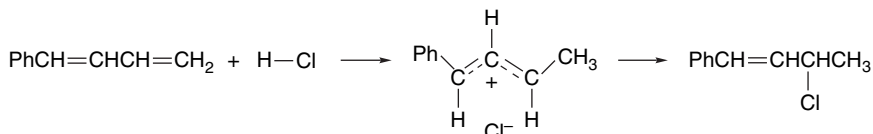
¹⁶ H. M. Weiss and K. M. Touchette, *J. Chem. Soc., Perkin Trans. 2*, 1517 (1998).

ionization, as discussed in Chapter 4. The prevalence of nucleophilic capture by Br^- over CF_3CO_2^- reflects relative nucleophilicity and is also dependent on Br^- concentration. Competing elimination is also consistent with the pattern of the solvolytic reactions.

The addition of hydrogen halides to dienes can result in either 1,2- or 1,4-addition. The extra stability of the allylic cation formed by proton transfer to a diene makes the ion pair mechanism more favorable. Nevertheless, a polar reaction medium is required.¹⁷ 1,3-Pentadiene, for example, gives a mixture of products favoring the 1,2-addition product by a ratio of from 1.5:1 to 3.4:1, depending on the temperature and solvent.¹⁸

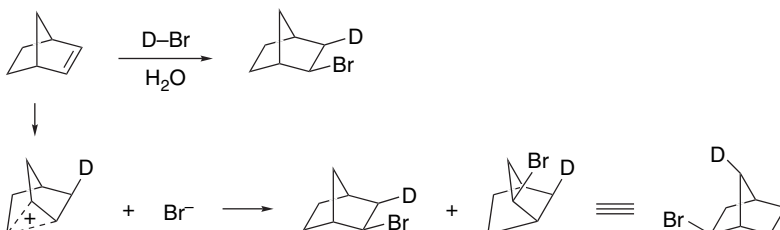


With 1-phenyl-1,3-butadiene, the addition of HCl is exclusively at the 3,4-double bond. This reflects the greater stability of this product, which retains styrene-type conjugation. Initial protonation at C(4) is favored by the fact that the resulting carbocation benefits from both allylic and benzylic stabilization.



The kinetics of this reaction are second order, as would be expected for the formation of a relatively stable carbocation by an $\text{Ad}_E 2$ mechanism.¹⁹

The additions of HCl or HBr to norbornene are interesting cases because such factors as the stability and facile rearrangement of the norbornyl cation come into consideration. (See Section 4.4.5 to review the properties of the 2-norbornyl cation.) Addition of deuterium bromide to norbornene gives *exo*-norbornyl bromide. Degradation to locate the deuterium atom shows that about half of the product is formed via the bridged norbornyl cation, which leads to deuterium at both the 3- and 7-positions.²⁰ The *exo* orientation of the bromine atom and the redistribution of the deuterium indicate the involvement of the bridged ion.



Similar studies have been carried out on the addition of HCl to norbornene.²¹ Again, the chloride is almost exclusively the *exo* isomer. The distribution of deuterium

¹⁷. L. M. Mascavage, H. Chi, S. La, and D. R. Dalton, *J. Org. Chem.*, **56**, 595 (1991).

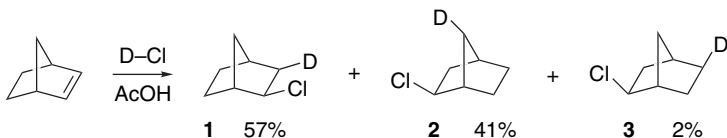
¹⁸. J. E. Nordlander, P. O. Owuor, and J. E. Haky, *J. Am. Chem. Soc.*, **101**, 1288 (1979).

¹⁹. K. Izawa, T. Okuyama, T. Sakagami, and T. Fueno, *J. Am. Chem. Soc.*, **95**, 6752 (1973).

²⁰. H. Kwart and J. L. Nyce, *J. Am. Chem. Soc.*, **86**, 2601 (1964).

²¹. J. K. Stille, F. M. Sonnenberg, and T. H. Kinstle, *J. Am. Chem. Soc.*, **88**, 4922 (1966).

in the product was determined by NMR. The fact that **1** and **2** are formed in unequal amounts excludes the possibility that the symmetrical bridged ion is the only intermediate.²²

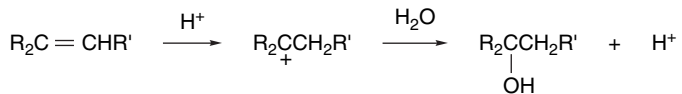


The excess of **1** over **2** indicates that some *syn* addition occurs by ion pair collapse before the bridged ion achieves symmetry with respect to the chloride ion. If the amount of **2** is taken as an indication of the extent of bridged ion involvement, one can conclude that 82% of the reaction proceeds through this intermediate, which must give equal amounts of **1** and **2**. Product **3** results from the C(6) → C(2) hydride shift that is known to occur in the 2-norbornyl cation with an activation energy of about 6 kcal/mol (see p. 450).

From these examples we see that the mechanistic and stereochemical details of hydrogen halide addition depend on the reactant structure. Alkenes that form relatively unstable carbocations are likely to react via a termolecular complex and exhibit *anti* stereospecificity. Alkenes that can form more stable cations can react via rate-determining protonation and the structure and stereochemistry of the product are determined by the specific properties of the cation.

5.2. Acid-Catalyzed Hydration and Related Addition Reactions

The formation of alcohols by acid-catalyzed addition of water to alkenes is a fundamental reaction in organic chemistry. At the most rudimentary mechanistic level, it can be viewed as involving a carbocation intermediate. The alkene is protonated and the carbocation then reacts with water.

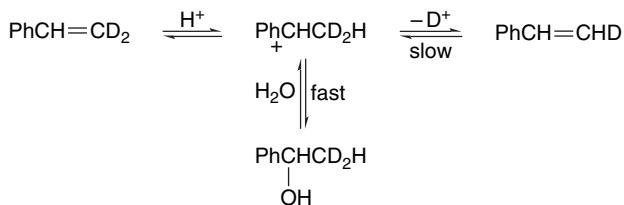


This mechanism explains the formation of the more highly substituted alcohol from unsymmetrical alkenes (Markovnikov's rule). A number of other points must be considered in order to provide a more complete picture of the mechanism. Is the protonation step reversible? Is there a discrete carbocation intermediate, or does the nucleophile become involved before proton transfer is complete? Can other reactions of the carbocation, such as rearrangement, compete with capture by water?

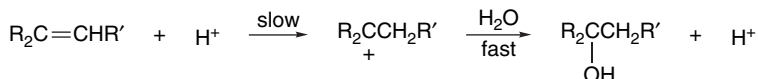
Much of the early mechanistic work on hydration reactions was done with conjugated alkenes, particularly styrenes. Owing to the stabilization provided by the phenyl group, this reaction involves a relatively stable carbocation. With styrenes, the rate of hydration is increased by ERG substituents and there is an excellent correlation

²² H. C. Brown and K.-T. Liu, *J. Am. Chem. Soc.*, **97**, 600 (1975).

with σ^+ .²³ A substantial solvent isotope effect $k_{\text{H}_2\text{O}}/k_{\text{D}_2\text{O}}$ equal to 2 to 4 is observed. Both of these observations are in accord with a rate-determining protonation to give a carbocation intermediate. Capture of the resulting cation by water is usually fast relative to deprotonation. This has been demonstrated by showing that in the early stages of hydration of styrene deuterated at C(2), there is no loss of deuterium from the unreacted alkene that is recovered by quenching the reaction. The preference for nucleophilic capture over elimination is also consistent with the competitive rate measurements under solvolysis conditions, described on p. 438–439. The overall process is reversible, however, and some styrene remains in equilibrium with the alcohol, so isotopic exchange eventually occurs.



Alkenes lacking phenyl substituents appear to react by a similar mechanism. Both the observation of general acid catalysis²⁴ and solvent isotope effect²⁵ are consistent with rate-limiting protonation of alkenes such as 2-methylpropene and 2,3-dimethyl-2-butene.



Relative rate data in aqueous sulfuric acid for a series of alkenes reveal that the reaction is strongly accelerated by alkyl substituents. This is as expected because alkyl groups both increase the electron density of the double bond and stabilize the carbocation intermediate. Table 5.1 gives some representative data. The $1 : 10^7 : 10^{12}$ relative rates for ethene, propene, and 2-methylpropene illustrate the dramatic rate enhancement by alkyl substituents. Note that styrene is intermediate between monoalkyl and dialkyl alkenes. These same reactions show solvent isotope effects consistent with the reaction proceeding through a rate-determining protonation.²⁶ Strained alkenes show enhanced reactivity toward acid-catalyzed hydration. *trans*-Cyclooctene is about 2500 times as reactive as the *cis* isomer,²⁷ which reflects the higher ground state energy of the strained alkene.

Other nucleophilic solvents can add to alkenes in the presence of strong acid catalysts. The mechanism is analogous to that for hydration, with the solvent replacing water as the nucleophile. Strong acids catalyze the addition of alcohols

²³ W. M. Schubert and J. R. Keefe, *J. Am. Chem. Soc.*, **94**, 559 (1972); W. M. Schubert and B. Lamm, *J. Am. Chem. Soc.*, **88**, 120 (1966); W. K. Chwang, P. Knittel, K. M. Koshy, and T. T. Tidwell, *J. Am. Chem. Soc.*, **99**, 3395 (1977).

24. A. J. Kresge, Y. Chiang, P. H. Fitzgerald, R. S. McDonald, and G. H. Schmid, *J. Am. Chem. Soc.*, **93**, 4907 (1971); H. Slebocza-Tilk and R. S. Brown, *J. Org. Chem.*, **61**, 8079 (1998).

²⁵. V. Gold and M. A. Kessick, *J. Chem. Soc.*, 6718 (1965).

²⁶. V. J. Nowlan and T. T. Tidwell, *Acc. Chem. Res.*, **10**, 252 (1977).

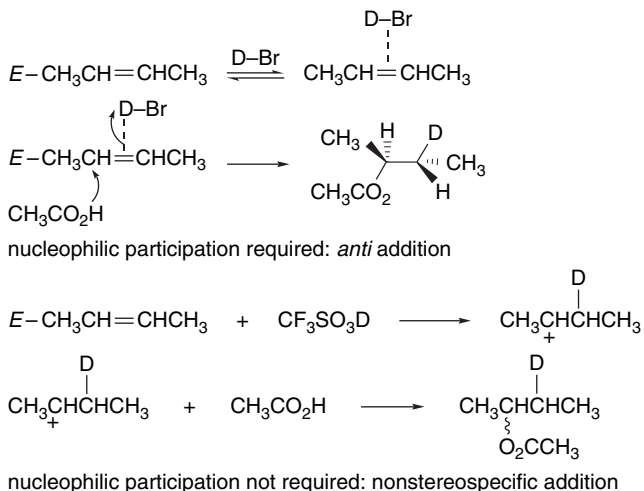
²⁷: X. Chiang and A. J. Kresge, *J. Am. Chem. Soc.*, **107**, 6363 (1985).

Table 5.1. Rates of Alkene Hydration in Aqueous Sulfuric Acid^a

Alkene	$k_2(M^{-1}s^{-1})$	k_{rel}
$\text{CH}_2=\text{CH}_2$	1.56×10^{-15}	1
$\text{CH}_3\text{CH}=\text{CH}_2$	2.38×10^{-8}	1.6×10^7
$\text{CH}_3(\text{CH}_2)_3\text{CH}=\text{CH}_2$	4.32×10^{-8}	3.0×10^7
$(\text{CH}_3)_2\text{C}=\text{CHCH}_3$	2.14×10^{-3}	1.5×10^{12}
$(\text{CH}_3)_2\text{C}=\text{CH}_2$	3.71×10^{-3}	2.5×10^{12}
$\text{PhCH}=\text{CH}_2$	2.4×10^{-6}	1.6×10^9

a. W. K. Chwang, V. J. Nowlan, and T. T. Tidwell, *J. Am. Chem. Soc.*, **99**, 7233 (1977).

to alkenes to give ethers, and the mechanistic studies that have been done indicate that the reaction closely parallels the hydration process.²⁸ The strongest acid catalysts probably react via discrete carbocation intermediates, whereas weaker acids may involve reaction of the solvent with an alkene-acid complex. In the addition of acetic acid to *Z*- or *E*-2-butene, the use of DBr as the catalyst results in stereospecific *anti* addition, whereas the stronger acid $\text{CF}_3\text{SO}_3\text{H}$ leads to loss of stereospecificity. This difference in stereochemistry can be explained by a stereospecific $\text{Ad}_{\text{E}}3$ mechanism in the case of DBr and an $\text{Ad}_{\text{E}}2$ mechanism in the case of $\text{CF}_3\text{SO}_3\text{D}$.²⁹ The dependence of stereochemistry on acid strength reflects the degree to which nucleophilic participation is required to complete proton transfer.



Trifluoroacetic acid adds to alkenes without the necessity of a stronger acid catalyst.³⁰ The mechanistic features of this reaction are similar to addition of water catalyzed by strong acids. For example, there is a substantial isotope effect when $\text{CF}_3\text{CO}_2\text{D}$ is used ($k_{\text{H}}/k_{\text{D}} = 4.33$)³¹ and the reaction rates of substituted styrenes are

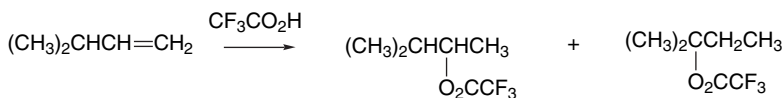
²⁸. N. C. Deno, F. A. Kish, and H. J. Peterson, *J. Am. Chem. Soc.*, **87**, 2157 (1965).

²⁹. D. J. Pasto and J. F. Gadberry, *J. Am. Chem. Soc.*, **100**, 1469 (1978).

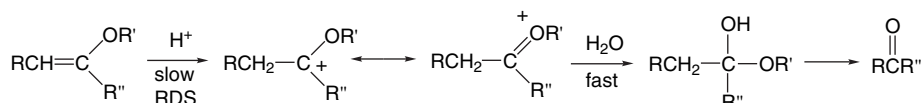
³⁰. P. E. Peterson and G. Allen, *J. Am. Chem. Soc.*, **85**, 3608 (1963); A. D. Allen and T. T. Tidwell, *J. Am. Chem. Soc.*, **104**, 3145 (1982).

³¹. J. J. Dannenberg, B. J. Goldberg, J. K. Barton, K. Dill, D. M. Weinwurzel, and M. O. Longas, *J. Am. Chem. Soc.*, **103**, 7764 (1981).

correlated with σ^+ .³² 2-Methyl-1-butene and 2-methyl-2-butene appear to react via the 2-methylbutyl cation, and 3-methyl-1-butene gives the products expected for a carbocation mechanism, including rearrangement. These results are consistent with rate-determining protonation.³³



The reactivity of carbon-carbon double bonds toward acid-catalyzed addition of water is greatly increased by ERG substituents. The reaction of vinyl ethers with water in acidic solution is an example that has been carefully studied. With these reactants, the initial addition products are unstable hemiacetals that decompose to a ketone and alcohol. Nevertheless, the protonation step is rate determining, and the kinetic results pertain to this step. The mechanistic features are similar to those for hydration of simple alkenes. Proton transfer is rate determining, as demonstrated by general acid catalysis and solvent isotope effect data.³⁴



5.3. Addition of Halogens

Alkene chlorinations and brominations are very general reactions, and mechanistic study of these reactions provides additional insight into the electrophilic addition reactions of alkenes.³⁵ Most of the studies have involved brominations, but chlorinations have also been examined. Much less detail is known about fluorination and iodination. The order of reactivity is $\text{F}_2 > \text{Cl}_2 > \text{Br}_2 > \text{I}_2$. The differences between chlorination and bromination indicate the trends for all the halogens, but these differences are much more pronounced for fluorination and iodination. Fluorination is strongly exothermic and difficult to control, whereas for iodine the reaction is easily reversible.

The initial step in bromination is the formation of a complex between the alkene and Br_2 . The existence of these relatively weak complexes has long been recognized. Their role as intermediates in the addition reaction has been established more recently.

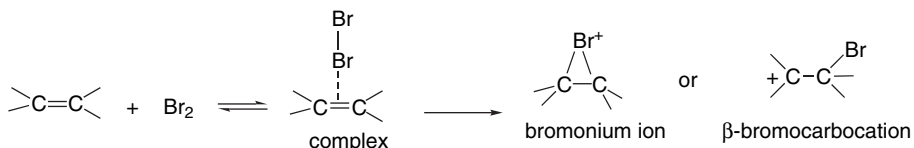
³² A. D. Allen, M. Rosenbaum, N. O. L. Seto, and T. T. Tidwell, *J. Org. Chem.*, **47**, 4234 (1982).

³³ D. Farcasiu, G. Marino, and C. S. Hsu, *J. Org. Chem.*, **59**, 163 (1994).

³⁴ A. J. Kresge and H. J. Chen, *J. Am. Chem. Soc.*, **94**, 2818 (1972); A. J. Kresge, D. S. Sagatys, and H. L. Chen, *J. Am. Chem. Soc.*, **99**, 7228 (1977).

³⁵ Reviews: D. P. de la Mare and R. Bolton, in *Electrophilic Additions to Unsaturated Systems*, 2nd Edition, Elsevier, New York, 1982, pp. 136–197; G. H. Schmidt and D. G. Garratt, in *The Chemistry of Double Bonded Functional Groups*, Supplement A, Part 2, S. Patai, ed., Wiley-Interscience, New York, 1977, Chap. 9; M.-F. Ruasse, *Adv. Phys. Org. Chem.*, **28**, 207 (1993); M.-F. Ruasse, *Industrial Chem. Library*, **7**, 100 (1995); R. S. Brown, *Industrial Chem. Library*, **7**, 113 (1995); G. Bellucci and R. Bianchini, *Industrial Chem. Library*, **7**, 128 (1995); R. S. Brown, *Acc. Chem. Res.*, **30**, 131 (1997).

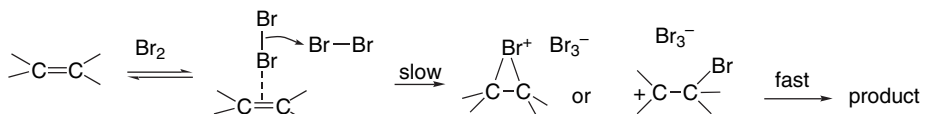
The formation of the complex can be observed spectroscopically, and they subsequently disappear at a rate corresponding to the formation of bromination product.^{36,37} The second step in bromination involves formation of an ionic intermediate, which can be either a bridged bromonium ion or a β -bromocarbocation. Whether a bridged intermediate or a carbocation is formed depends on the stability of the potential cation. Aliphatic systems normally react through the bridged intermediate but styrenes are borderline cases. When the phenyl ring has an ERG substituent, there is sufficient stabilization to permit carbocation formation, whereas EWGs favor the bridged intermediate.³⁸ Because this step involves formation of charged intermediates, it is strongly solvent dependent. Even a change from CCl_4 to 1,2-dichloroethane accelerates the reaction (with cyclohexene) by a factor of 10^5 .³⁹



The kinetics of bromination reactions are often complex, with at least three terms making contributions under given conditions.

$$\text{Rate} = k_1[\text{alkene}][\text{Br}_2] + k_2[\text{alkene}][\text{Br}_2]^2 + k_3[\text{alkene}][\text{Br}_2][\text{Br}^-]$$

In methanol, pseudo-second-order kinetics are observed when a high concentration of Br^- is present.⁴⁰ Under these conditions, the dominant contribution to the overall rate comes from the third term of the general expression. In nonpolar solvents, the observed rate is frequently described as a sum of the first two terms in the general expression.⁴¹ The mechanism of the third-order reaction is similar to the process that is first order in Br_2 , but with a second Br_2 molecule replacing solvent in the rate-determining conversion of the complex to an ion pair.



There are strong similarities in the second- and third-order reaction in terms of magnitude of ρ values and product distribution.^{41b} In fact, there is a quantitative correlation between the rate of the two reactions over a broad series of alkenes, which can be expressed as

$$\Delta G_3^\ddagger = \Delta G_2^\ddagger + \text{constant}$$

³⁶ S. Fukuzumi and J. K. Kochi, *J. Am. Chem. Soc.*, **104**, 7599 (1982).

³⁷ G. Bellucci, R. Bianchi, and R. Ambrosetti, *J. Am. Chem. Soc.*, **107**, 2464 (1985).

³⁸ M.-F. Ruasse, A. Argile, and J. E. Dubois, *J. Am. Chem. Soc.*, **100**, 7645 (1978).

³⁹ M.-F. Ruasse and S. Motallebi, *J. Phys. Org. Chem.*, **4**, 527 (1991).

⁴⁰ J.-E. Dubois and G. Mouvier, *Tetrahedron Lett.*, 1325 (1963); *Bull. Soc. Chim. Fr.*, 1426 (1968).

⁴¹ (a) G. Bellucci, R. Bianchi, R. A. Ambrosetti, and G. Ingrosso, *J. Org. Chem.*, **50**, 3313 (1985); G. Bellucci, G. Berti, R. Bianchini, G. Ingrosso, and R. Ambrosetti, *J. Am. Chem. Soc.*, **102**, 7480 (1980); (b) K. Yates, R. S. McDonald, and S. Shapiro, *J. Org. Chem.*, **38**, 2460 (1973); K. Yates and R. S. McDonald, *J. Org. Chem.*, **38**, 2465 (1973); (c) S. Fukuzumi and J. K. Kochi, *Int. J. Chem. Kinetics*, **15**, 249 (1983).

Table 5.2. Relative Reactivity of Alkenes toward Halogenation

Alkene	Relative reactivity			SECTION 5.3 <i>Addition of Halogens</i>
	Chlorination ^a	Bromination ^b	Bromination ^c	
Ethene		0.01	0.0045	
1-Butene	1.00	1.00	1.00	
3,3-Dimethyl-1-butene	1.15	0.27	1.81	
Z-2-Butene	63	27	173	
E-2-Butene	50	17.5	159	
2-Methylpropene	58	57	109	
2-Methyl-2-butene	1.1×10^4	1.38×10^4		
2,3-Dimethyl-2-butene	4.3×10^5	19.0×10^4		

a. M. L. Poutsma, *J. Am. Chem. Soc.*, **87**, 4285 (1965), in excess alkene.

b. J. E. Dubois and G. Mouvier, *Bull. Chim. Soc. Fr.*, 1426 (1968), in methanol.

c. A. Modro, G. H. Schmid, and K. Yates, *J. Org. Chem.*, **42**, 3673 (1977), in $\text{ClCH}_2\text{CH}_2\text{Cl}$.

where ΔG_3^\ddagger and ΔG_2^\ddagger are the free energies of activation for the third- and second-order processes, respectively.^{41c} These correlations suggest that the two mechanisms must be very similar.

Observed bromination rates are very sensitive to common impurities such as HBr^{42} and water, which can assist in formation of the bromonium ion.⁴³ It is likely that under normal preparative conditions, where these impurities are likely to be present, these catalytic mechanisms may dominate.

Chlorination generally exhibits second-order kinetics, first-order in both alkene and chlorine.⁴⁴ The relative reactivities of some alkenes toward chlorination and bromination are given in Table 5.2. The reaction rate increases with alkyl substitution, as would be expected for an electrophilic process. The magnitude of the rate increase is quite large, but not as large as for protonation. The relative reactivities are solvent dependent.⁴⁵ Quantitative interpretation of the solvent effect using the Winstein-Grunwald Y values indicates that the TS has a high degree of ionic character. The Hammett correlation for bromination of styrenes is best with σ^+ substituent constants, and gives $\rho = -4.8$.⁴⁶ All these features are in accord with an electrophilic mechanism.

Stereochemical studies provide additional information pertaining to the mechanism of halogenation. The results of numerous stereochemical studies can be generalized as follows: For brominations, *anti* addition is preferred for alkenes lacking substituent groups that can strongly stabilize a carbocation intermediate.⁴⁷ When the alkene is conjugated with an aryl group, the extent of *syn* addition increases and can become the dominant pathway. Chlorination is not as likely to be as stereospecific as bromination, but tends to follow the same pattern. Some specific results are given in Table 5.3.

⁴². C. J. A. Byrnell, R. G. Coombes, L. S. Hart, and M. C. Whiting, *J. Chem. Soc., Perkin Trans. 2*, 1079 (1983); L. S. Hart and M. C. Whiting, *J. Chem. Soc., Perkin Trans. 2*, 1087 (1983).

⁴³. V. V. Smirnov, A. N. Miroshnichenko, and M. I. Shilina, *Kinet. Catal.*, **31**, 482, 486 (1990).

⁴⁴. G. H. Schmid, A. Modro, and K. Yates, *J. Org. Chem.*, **42**, 871 (1977).

⁴⁵. F. Garnier and J.-E. Dubois, *Bull. Soc. Chim. Fr.*, 3797 (1968); F. Garnier, R. H. Donnay, and J.-E. Dubois, *J. Chem. Soc., Chem. Commun.*, 829 (1971); M.-F. Ruasse and J.-E. Dubois, *J. Am. Chem. Soc.*, **97**, 1977 (1975); A. Modro, G. H. Schmid, and K. Yates, *J. Org. Chem.*, **42**, 3673 (1977).

⁴⁶. K. Yates, R. S. McDonald, and S. A. Shapiro, *J. Org. Chem.*, **38**, 2460 (1973).

⁴⁷. J. R. Chretien, J.-D. Coudert, and M.-F. Ruasse, *J. Org. Chem.*, **58**, 1917 (1993).

Table 5.3. Stereochemistry of Alkene Halogenation

Alkene	Solvent	Ratio <i>anti:syn</i>
A. Bromination		
Z-2-Butene ^a	CH ₃ CO ₂ H	> 100 : 1
E-2-Butene ^a	CH ₃ CO ₂ H	> 100 : 1
Cyclohexene ^b	CCl ₄	Very large
Z-1-Phenylpropene ^c	CCl ₄	83:17
E-1-Phenylpropene ^c	CCl ₄	88:12
Z-2-Phenylbutene ^a	CH ₃ CO ₂ H	68:32
E-2-Phenylbutene ^a	CH ₃ CO ₂ H	63:37
<i>cis</i> -Stilbene ^d	CCl ₄	> 10 : 1
	CH ₃ NO ₂ ^d	1:9
B. Chlorination		
Z-2-Butene ^e	None	> 100 : 1
	CH ₃ CO ₂ H ^f	> 100 : 1
E-2-Butene ^e	None	> 100 : 1
	CH ₃ CO ₂ H ^f	> 100 : 1
Cyclohexene ^g	None	> 100 : 1
E-1-Phenylpropene ^f	CCl ₄	45:55
	CH ₃ CO ₂ H ^f	41:59
Z-1-Phenylpropene ^f	CCl ₄	32:68
	CH ₃ CO ₂ H ^f	22:78
<i>Cis</i> -Stilbene ^h	ClCH ₂ CH ₂ Cl	8:92
<i>Trans</i> -Stilbene ^h	ClCH ₂ CH ₂ Cl	35:65

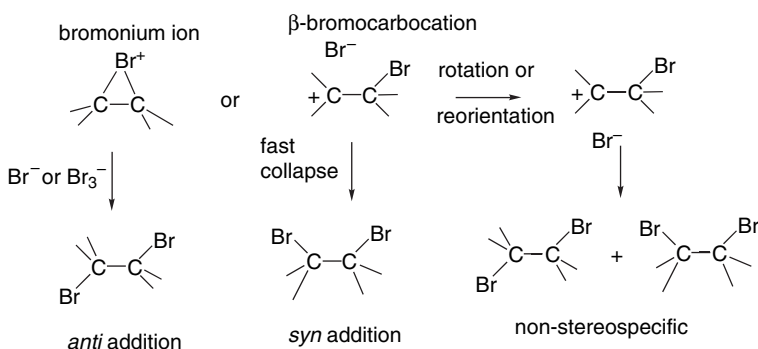
a. J. H. Rolston and K. Yates, *J. Am. Chem. Soc.*, **91**, 1469, 1477 (1969).b. S. Winstein, *J. Am. Chem. Soc.*, **64**, 2792 (1942).c. R. C. Fahey and H.-J. Schneider, *J. Am. Chem. Soc.*, **90**, 4429 (1968).d. R. E. Buckles, J. M. Bader, and R. L. Thurmaier, *J. Org. Chem.*, **27**, 4523 (1962).e. M. L. Poutsma, *J. Am. Chem. Soc.*, **87**, 2172 (1965).f. R. C. Fahey and C. Schubert, *J. Am. Chem. Soc.*, **87**, 5172 (1965).g. M. L. Poutsma, *J. Am. Chem. Soc.*, **87**, 2161 (1965).h. R. E. Buckles and D. F. Knaack, *J. Org. Chem.*, **25**, 20 (1960).

Interpretation of reaction stereochemistry has focused attention on the role played by bridged halonium ions. When the reaction with Br₂ involves a bromonium ion, the *anti* stereochemistry can be readily explained. Nucleophilic ring opening occurs by back-side attack at carbon, with rupture of one of the C–Br bonds, giving overall *anti* addition. On the other hand, a freely rotating open β-bromo carbocation can give both the *syn* and *anti* addition products. If the principal intermediate is an ion pair that collapses faster than rotation occurs about the C–C bond, *syn* addition can predominate. Other investigations, including kinetic isotope effect studies, are consistent with the bromonium ion mechanism for unconjugated alkenes, such as ethene,⁴⁸ 1-pentene,⁴⁹ and cyclohexene.⁵⁰

⁴⁸. T. Koerner, R. S. Brown, J. L. Gainsforth, and M. Klobukowski, *J. Am. Chem. Soc.*, **120**, 5628 (1998).

⁴⁹. S. R. Merrigan and D. A. Singleton, *Org. Lett.*, **1**, 327 (1999).

⁵⁰. H. Slebocka-Tilk, A. Neverov, S. Motallebi, R. S. Brown, O. Donini, J. L. Gainsforth, and M. Klobukowski, *J. Am. Chem. Soc.*, **120**, 2578 (1998).

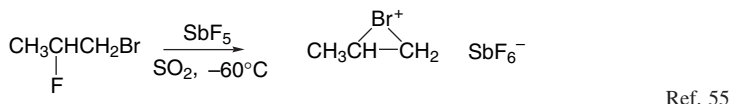


Substituent effects on stilbenes provide examples of the role of bridged ions versus nonbridged carbocation intermediates. In aprotic solvents, stilbene gives clean *anti* addition, but 4,4'-dimethoxystilbene gives a mixture of the *syn* and *anti* addition products indicating a carbocation intermediate.⁵¹

Nucleophilic solvents compete with bromide, but *anti* stereoselectivity is still observed, except when ERG substituents are present. It is proposed that *anti* stereoselectivity can result not only from a bridged ion intermediate, but also from very fast capture of a carbocation intermediate.⁵² Interpretation of the ratio of capture by competing nucleophiles has led to the estimate that the bromonium ion derived from cyclohexene has a lifetime on the order of 10⁻¹⁰ s in methanol, which is about 100 times longer than for secondary carbocations.⁵³

The stereochemistry of chlorination also can be explained in terms of bridged versus open cations as intermediates. Chlorine is a somewhat poorer bridging group than bromine because it is less polarizable and more resistant to becoming positively charged. Comparison of the data for *E*- and *Z*-1-phenylpropene in bromination and chlorination confirms this trend (see Table 5.3). Although *anti* addition is dominant for bromination, *syn* addition is slightly preferred for chlorination. Styrenes generally appear to react with chlorine via ion pair intermediates.⁵⁴

There is direct evidence for the existence of bromonium ions. The bromonium ion related to propene can be observed by NMR when 1-bromo-2-fluoropropane is subjected to superacid conditions.



A bromonium ion also is formed by electrophilic attack on 2,3-dimethyl-2-butene by a species that can generate a positive bromine.

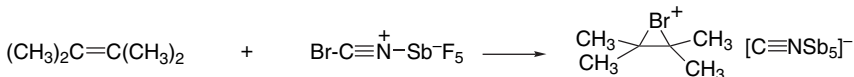
⁵¹ G. Bellucci, C. Chiappe, and G. Lo Moro, *J. Org. Chem.*, **62**, 3176 (1997).

⁵² M.-F. Ruasse, G. Lo Moro, B. Galland, R. Bianchini, C. Chiappe, and G. Bellucci, *J. Am. Chem. Soc.*, **119**, 12492 (1997).

⁵³ R. W. Nagorski and R. S. Brown, *J. Am. Chem. Soc.*, **114**, 7773 (1992).

⁵⁴ K. Yates and H. W. Leung, *J. Org. Chem.*, **45**, 1401 (1980).

⁵⁵ G. A. Olah, J. M. Bollinger, and J. Brinich, *J. Am. Chem. Soc.*, **90**, 2587 (1968).



Ref. 56

The highly hindered alkene adamantylideneadamantane forms a bromonium ion that crystallizes as a tribromide salt. This particular bromonium ion does not react further because of extreme steric hindrance to back-side approach by bromide ion.⁵⁷ Other very hindered alkenes allow observation of both the initial complex with Br₂ and the bromonium ion.⁵⁸ An X-ray crystal structure has confirmed the cyclic nature of the bromonium ion species (Figure 5.2).⁵⁹

Crystal structures have also been obtained for the corresponding chloronium and iodonium ions and for the bromonium ion with a triflate counterion.⁶⁰ Each of these structures is somewhat unsymmetrical, as shown by the dimensions below. The significance of this asymmetry is not entirely clear. It has been suggested that the bromonium ion geometry is affected by the counterion and it can be noted that the triflate salt is more symmetrical than the tribromide. On the other hand, the dimensions of the unsymmetrical chloronium ion, where the difference is considerably larger, has been taken as evidence that the bridging is inherently unsymmetrical.⁶¹ Note that the C–C bond lengthens considerably from the double-bond distance of 1.35 Å.

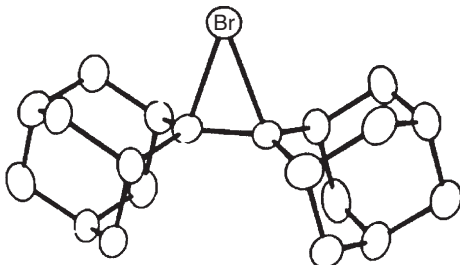
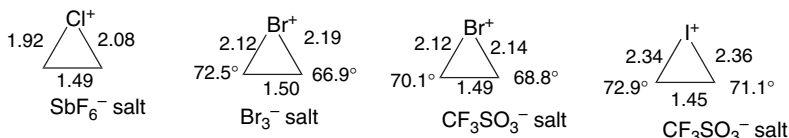
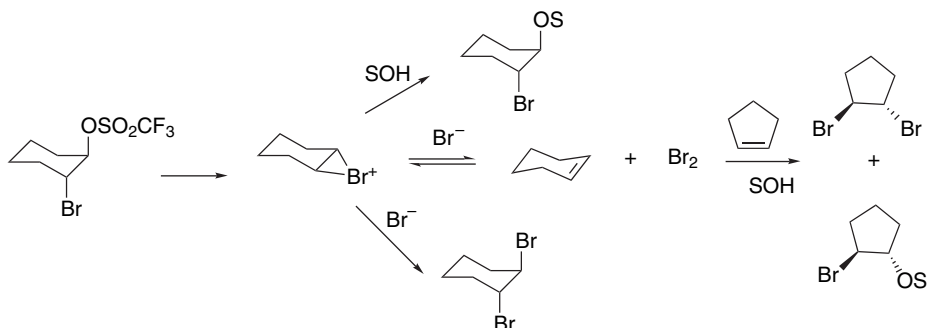


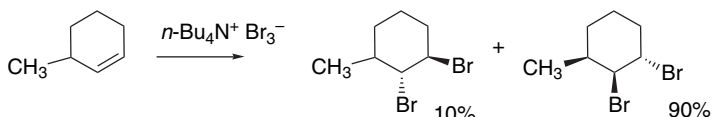
Fig. 5.2. X-ray crystal structure of the bromonium ion from adamantylideneadamantane. Reproduced from *J. Am. Chem. Soc.*, **107**, 4504 (1985), by permission of the American Chemical Society.

- ⁵⁶ G. A. Olah, P. Schilling, P. W. Westerman, and H. C. Lin, *J. Am. Chem. Soc.*, **96**, 3581 (1974).
- ⁵⁷ R. S. Brown, *Acc. Chem. Res.*, **30**, 131 (1997).
- ⁵⁸ G. Bellucci, R. Bianichini, C. Chiappe, F. Marioni, R. Ambrosetti, R. S. Brown, and H. Slebocka-Tilk, *J. Am. Chem. Soc.*, **111**, 2640 (1989); G. Bellucci, C. Chiappe, R. Bianchini, D. Lenoir, and R. Herges, *J. Am. Chem. Soc.*, **117**, 12001 (1995).
- ⁵⁹ H. Slebocka-Tilk, R. G. Ball, and R. S. Brown, *J. Am. Chem. Soc.*, **107**, 4504 (1985).
- ⁶⁰ R. S. Brown, R. W. Nagorski, A. J. Bennet, R. E. D. McClung, G. H. M. Aarts, M. Klobukowski, R. McDonald, and B. D. Santarisiero, *J. Am. Chem. Soc.*, **116**, 2448 (1994).
- ⁶¹ T. Mori, R. Rathore, S. V. Lindeman, and J. K. Kochi, *Chem. Commun.*, 1238 (1998); T. Mori and R. Rathore, *Chem. Commun.*, 927 (1998).

Another aspect of the mechanism is the reversibility of formation of the bromonium ion. Reversibility has been demonstrated for highly hindered alkenes,⁶² and attributed to a relatively slow rate of nucleophilic capture. However, even the bromonium ion from cyclohexene appears to be able to release Br₂ on reaction with Br⁻. The bromonium ion can be generated by neighboring-group participation by solvolysis of *trans*-2-bromocyclohexyl triflate. If cyclopentene, which is more reactive than cyclohexene, is included in the reaction mixture, bromination products from cyclopentene are formed. This indicates that free Br₂ is generated by reversal of bromonium ion formation.⁶³ Other examples of reversible bromonium ion formation have been found.⁶⁴

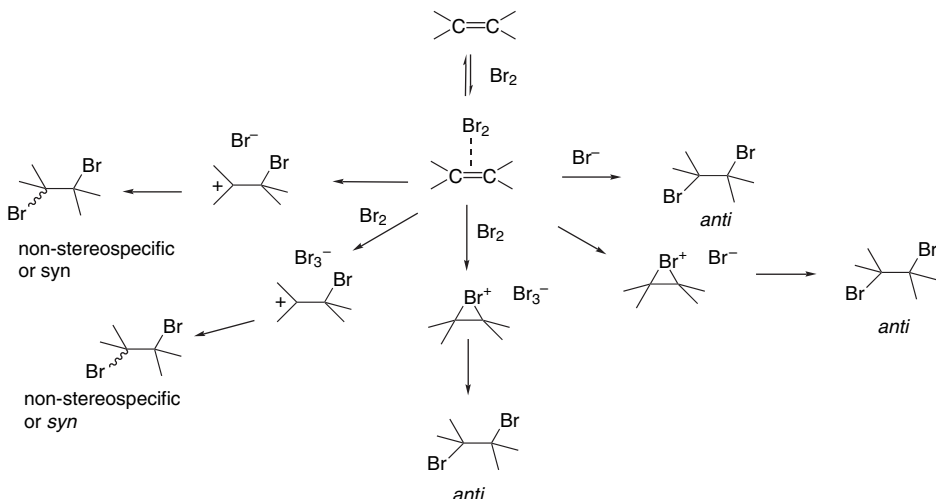


Bromination also can be carried out with reagents that supply bromine in the form of the Br₃⁻ anion. One such reagent is pyridinium bromide tribromide. Another is tetrabutylammonium tribromide.⁶⁵ These reagents are believed to react via the Br₂⁻-alkene complex and have a strong preference for *anti* addition.

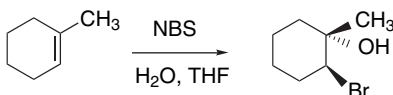


In summary, it appears that bromination usually involves a complex that collapses to an ion pair intermediate. The ionization generates charge separation and is assisted by solvent, acids, or a second molecule of bromine. The cation can be a β -carbocation, as in the case of styrenes, or a bromonium ion. Reactions that proceed through bromonium ions are stereospecific *anti* additions. Reactions that proceed through open carbocations can be *syn* selective or nonstereospecific.

- ⁶². R. S. Brown, H. Slebocka-Tilk, A. J. Bennet, G. Bellucci, R. Bianchini, and R. Ambrosetti, *J. Am. Chem. Soc.*, **112**, 6310 (1990); G. Bellucci, R. Bianchini, C. Chiappe, F. Marioni, R. Ambrosetti, R. S. Brown, and H. Slebocka-Tilk, *J. Am. Chem. Soc.*, **111**, 2640 (1989).
- ⁶³. C. Y. Zheng, H. Slebocka-Tilk, R. W. Nagorski, L. Alvarado, and R. S. Brown, *J. Org. Chem.*, **58**, 2122 (1993).
- ⁶⁴. R. Rodebaugh and B. Fraser-Reid, *Tetrahedron*, **52**, 7663 (1996).
- ⁶⁵. J. Berthelot and M. Fournier, *J. Chem. Educ.*, **63**, 1011 (1986); J. Berthelot, Y. Benamar, and C. Lange, *Tetrahedron Lett.*, **32**, 4135 (1991).

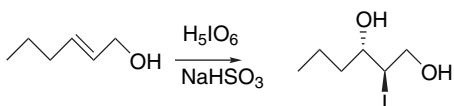


The cationic intermediates also can be captured by solvent. Halogenation with solvent capture is a synthetically important reaction, especially for the preparation of chlorohydrins and bromohydrins.⁶⁶ Chlorohydrins can be prepared using various sources of electrophilic chlorine. Chloroamine T is a convenient reagent for chlorohydrin formation.⁶⁷ Bromohydrins are prepared using NBS and an aqueous solvent mixture with acetone or THF. DMSO has also been recommended as a solvent.⁶⁸ These reactions are regioselective, with the nucleophile water introduced at the more-substituted position.



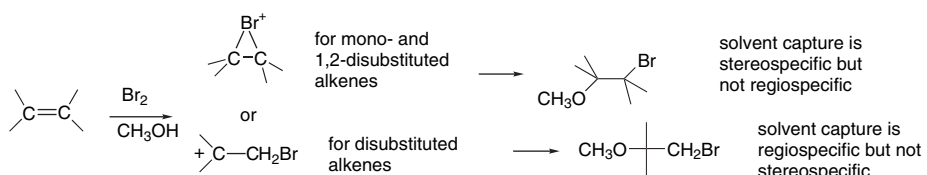
Ref. 69

Iodohydrins can be prepared using iodine or phenyliodonium di-trifluoroacetate.⁷⁰ Iodohydrins can be prepared in generally good yield and high *anti* stereoselectivity using H₅IO₆ and NaHSO₃.⁷¹ These reaction conditions generate hypoiodous acid. In the example shown below, the hydroxy group exerts a specific directing effect, favoring introduction of the hydroxyl at the more remote carbon.

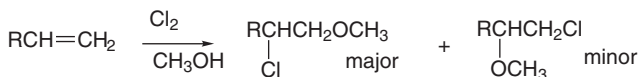


- ⁶⁶. J. Rodriguez and J. P. Dulcere, *Synthesis*, 1177 (1993).
- ⁶⁷. B. Damin, J. Garapon, and B. Sillion, *Synthesis*, 362 (1981).
- ⁶⁸. J. N. Kim, M. R. Kim, and E. K. Ryu, *Synth. Commun.*, **22**, 2521 (1992); V. L. Heasley, R. A. Skidgel, G. E. Heasley, and D. Strickland, *J. Org. Chem.*, **39**, 3953 (1974); D. R. Dalton, V. P. Dutta, and D. C. Jones, *J. Am. Chem. Soc.*, **90**, 5498 (1988).
- ⁶⁹. D. J. Porter, A. T. Stewart, and C. T. Wigal, *J. Chem. Educ.*, **72**, 1039 (1995).
- ⁷⁰. A. R. De Corso, B. Panunzi, and M. Tingoli, *Tetrahedron Lett.*, **42**, 7245 (2001).
- ⁷¹. H. Masuda, K. Takase, M. Nishio, A. Hasegawa, Y. Nishiyama, and Y. Ishii, *J. Org. Chem.*, **59**, 5550 (1994).

A study of several substituted alkenes in methanol developed some generalizations pertaining to the capture of bromonium ions by methanol.⁷² For both *E*- and *Z*-disubstituted alkenes, the addition of both methanol and Br^- was completely *anti* stereospecific. The reactions were also completely regioselective, in accordance with Markovnikov's rule, for disubstituted alkenes, *but not for monosubstituted alkenes*. The lack of high regioselectivity of the addition to monosubstituted alkenes can be interpreted as competitive addition of solvent at both the mono- and unsubstituted carbons of the bromonium ion. This competition reflects conflicting steric and electronic effects. Steric factors promote addition of the nucleophile at the unsubstituted position, whereas electronic factors have the opposite effect.

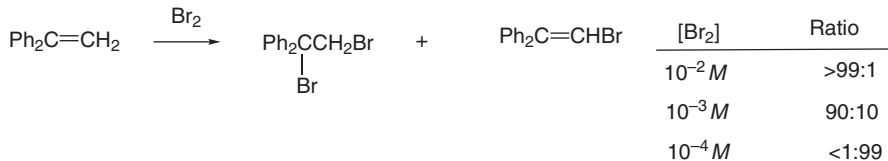


Similar results were obtained for chlorination of several of alkenes in methanol.⁷³ Whereas styrene gave only the Markovnikov product, propene, hexene, and similar alkenes gave more of the *anti* Markovnikov product. This result is indicative of strong bridging in the chloronium ion.



We say more about the regioselectivity of opening of halonium ions in Section 5.8, where we compare halonium ions with other intermediates in electrophilic addition reactions.

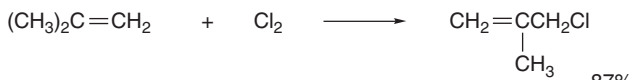
Some alkenes react with halogens to give substitution rather than addition. For example, with 1,1-diphenylethene, substitution is the main reaction at low bromine concentration. Substitution occurs when loss of a proton is faster than capture by bromide.



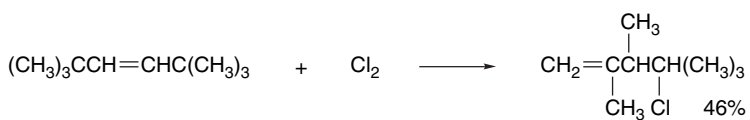
Similarly, in chlorination, loss of a proton can be a competitive reaction of the cationic intermediate. 2-Methylpropene and 2,3-dimethyl-2-butene give products of this type.

⁷² J. R. Chretien, J.-D. Coudert, and M.-F. Ruasse, *J. Org. Chem.*, **58**, 1917 (1993).

⁷³ K. Shinoda and K. Yasuda, *Bull. Chem. Soc. Jpn.*, **61**, 4393 (1988).



Alkyl migrations can also occur.



These reactions are characteristic of carbocation intermediates. Both proton loss and rearrangement are more likely in chlorination than in bromination because of the weaker bridging by chlorine.

There have been several computational investigations of bromonium and other halonium ions. These are gas phase studies and so do not account for the effect of solvent or counterions. In the gas phase, formation of the charged halonium ions from halogen and alkene is energetically prohibitive, and halonium ions are not usually found to be stable by these calculations. In an early study using PM3 and HF/3-21G calculations, bromonium ions were found to be unsymmetrical, with weaker bridging to the more stabilized carbocation.⁷⁶ Reynolds compared open and bridged $[\text{CH}_2\text{CH}_2\text{X}]^+$ and $[\text{CH}_3\text{CHCHXCH}_3]^+$ ions.⁷⁷ At the MP2/6-31G** level, the bridged haloethyl ion was favored slightly for $\text{X} = \text{F}$ and strongly for $\text{X} = \text{Cl}$ and Br . For the 3-halo-2-butyl ions, open structures were favored for F and Cl , but the bridged structure remained slightly favored for Br . The relative stabilities, as measured by hydride affinity are given below.

X	\triangle^+	$+$	$\begin{array}{c} \text{X}^+ \\ \diagup \\ \text{CH}_3 \end{array}$	$\begin{array}{c} \text{X} \\ \diagup \\ \text{CH}_3 \end{array}$
F	274.3	278.6	249.9	227.6
Cl	253.4	277.8	233.8	230.6
Br	239.9	270.8	221.6	225.0

Hydride affinity in kcal/mol

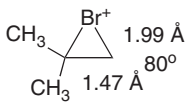
⁷⁴ M. L. Poutsma, *J. Am. Chem. Soc.*, **87**, 4285 (1965).

⁷⁵ R. C. Fahey, *J. Am. Chem. Soc.*, **88**, 4681 (1966).

⁷⁶ S. Yamabe and T. Minato, *Bull. Chem. Soc. Jpn.*, **66**, 3339 (1993).

⁷⁷ C. H. Reynolds, *J. Am. Chem. Soc.*, **114**, 8676 (1992).

The computed structure of bromonium ions from alkenes such as 2-methylpropene are highly dependent on the computational method used and inclusion of correlation is essential.⁷⁸ CISD/DZV calculations gave the following structural characteristics.

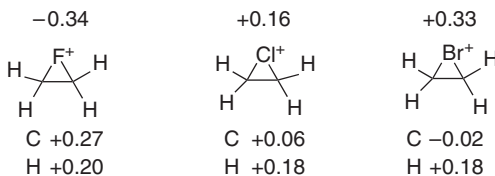


Another study gives some basis for comparison of the halogens.⁷⁹ QCISD(T)/6-311(d, p) calculations found the open carbocation to be the most stable for $[C_2H_4F]^+$ and $[C_2H_4Cl]^+$ but the bridged ion was more stable for $[C_2H_4Br]^+$. The differences were small for Cl and Br.

$+ \text{---} F$	F^+	$+ \text{---} \text{Cl}$	Cl^+	$+ \text{---} \text{Br}$	Br^+
0.0	27.7	0.0	3.3	2.4	0.0

Relative energy in kcal/mol of open and bridged $[C_2H_4X]^+$ ions

AIM charges for the bridged ions were as follows (MP2/6-311G(d, p)). Note the very different net charge for the different halogens.



MP2/6-311G(d, p) calculations favored open carbocations for the ions derived from cyclohexene. On the other hand, the bridged bromonium ion from cyclopentene was found to be stable relative to the open cation.

0.0	25.2	0.0	8.6	0.0	7.0	4.2	0.0

Relative stability of open and bridged cations in kcal/mol

Ref. 79

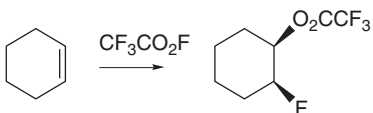
This result is in qualitative agreement with an NMR study under stable ion conditions that found that the bromonium ion from cyclopentene could be detected, but not the one from cyclohexene.⁸⁰ Broadly speaking, the computational results agree with the F < Cl < Br order in terms of bridging, but seem to underestimate the stability of the bridged ions, at least as compared to solution behavior.

⁷⁸. M. Klobukowski and R. S. Brown, *J. Org. Chem.*, **59**, 7156 (1994).

⁷⁹. R. Damrauer, M. D. Leavell, and C. M. Hadad, *J. Org. Chem.*, **63**, 9476 (1998).

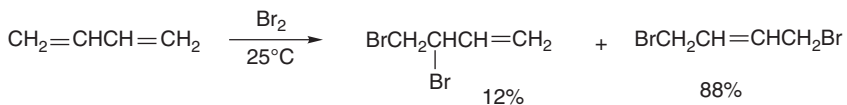
⁸⁰. G. K. S. Prakash, R. Aniszefeld, T. Hashimoto, J. W. Bausch, and G. A. Olah, *J. Am. Chem. Soc.*, **111**, 8726 (1989).

Much less detail is available concerning the mechanism of fluorination and iodination of alkenes. Elemental fluorine reacts violently with alkenes giving mixtures including products resulting from degradation of the carbon chain. Electrophilic additions of fluorine to alkenes can be achieved with xenon difluoride,⁸¹ electrophilic derivatives of fluorine,⁸² or by use of highly dilute elemental fluorine at low temperature.⁸³ Under the last conditions, *syn* stereochemistry is observed. The reaction is believed to proceed by rapid formation and then collapse of an β -fluorocarbocation-fluoride ion pair. Both from the stereochemical results and theoretical calculations,⁸⁴ it appears unlikely that a bridged fluoronium species is formed. Acetyl hypofluorite, which can be prepared by reaction of fluorine with sodium acetate at -75°C in halogenated solvents,⁸⁵ reacts with alkenes to give β -acetoxyalkyl fluorides.⁸⁶ The reaction gives predominantly *syn* addition, which is also consistent with rapid collapse of a β -fluorocarbocation-acetate ion pair.



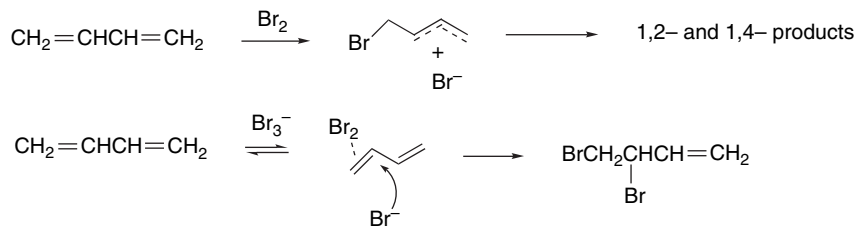
There have been relatively few mechanistic studies of the addition of iodine. One significant feature of iodination is that it is easily reversible, even in the presence of excess alkene.⁸⁷ The addition is stereospecifically *anti* but it is not entirely clear whether a polar or a radical mechanism is involved.⁸⁸

As with other electrophiles, halogenation can give 1,2- or 1,4-addition products from conjugated dienes. When molecular bromine is used as the brominating agent in chlorinated solvent, the 1,4-addition product dominates by $\sim 7:1$ in the case of butadiene.⁸⁹



The product distribution can be shifted to favor the 1,2-product by use of milder brominating agents such as the pyridine-bromine complex or the tribromide ion, Br_3^- . It is believed that molecular bromine reacts through a cationic intermediate, whereas

- ⁸¹ M. Zupan and A. Pollak, *J. Chem. Soc., Chem. Commun.*, 845 (1973); M. Zupan and A. Pollak, *Tetrahedron Lett.*, 1015 (1974).
- ⁸² For reviews of fluorinating agents, see A. Haas and M. Lieb, *Chimia*, **39**, 134 (1985); W. Dmowski, *J. Fluorine Chem.*, **32**, 255 (1986); H. Vyplel, *Chimia*, **39**, 134 (1985).
- ⁸³ S. Rozen and M. Brand, *J. Org. Chem.*, **51**, 3607 (1986); S. Rozen, *Acc. Chem. Res.*, **29**, 243 (1996).
- ⁸⁴ W. J. Hehre and P. C. Hiberty, *J. Am. Chem. Soc.*, **96**, 2665 (1974); T. Iwaoka, C. Kaneko, A. Shigihara, and H. Ichikawa, *J. Phys. Org. Chem.*, **6**, 195 (1993).
- ⁸⁵ O. Lerman, Y. Tov, D. Hebel, and S. Rozen, *J. Org. Chem.*, **49**, 806 (1984).
- ⁸⁶ S. Rozen, O. Lerman, M. Kol, and D. Hebel, *J. Org. Chem.*, **50**, 4753 (1985).
- ⁸⁷ P. W. Robertson, J. B. Butchers, R. A. Durham, W. B. Healy, J. K. Heyes, J. K. Johannesson, and D. A. Tait, *J. Chem. Soc.*, 2191 (1950).
- ⁸⁸ M. Zanger and J. L. Rabinowitz, *J. Org. Chem.*, **40**, 248 (1975); R. L. Ayres, C. J. Michejda, and E. P. Rack, *J. Am. Chem. Soc.*, **93**, 1389 (1971); P. S. Skell and R. R. Pavlis, *J. Am. Chem. Soc.*, **86**, 2956 (1964).
- ⁸⁹ G. Bellucci, G. Berti, R. Bianchini, G. Ingrosso, and K. Yates, *J. Org. Chem.*, **46**, 2315 (1981).

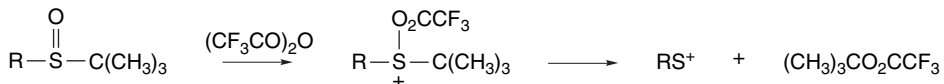


The stereochemistry of both chlorination and bromination of several cyclic and acyclic dienes has been determined. The results show that bromination is often stereospecifically *anti* for the 1,2-addition process, whereas *syn* addition is preferred for 1,4-addition. Comparable results for chlorination show much less stereospecificity.⁹⁰ It appears that chlorination proceeds primarily through ion pair intermediates, whereas in bromination a stereospecific *anti*-1,2-addition may compete with a process involving a carbocation intermediate. The latter can presumably give *syn* or *anti* product.

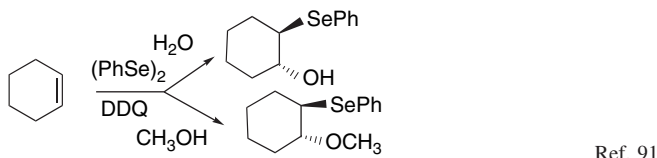
5.4. Sulfonylation and Selenenylation

Electrophilic derivatives of both sulfur and selenium can add to alkenes. A variety of such reagents have been developed and some are listed in Scheme 5.1. They are characterized by the formulas $\text{RS}-\text{X}$ and $\text{RSe}-\text{X}$, where X is a group that is more electronegative than sulfur or selenium. The reactivity of these reagents is sensitive to the nature of both the R and the X group.

Entry 4 is a special type of sulfonylation agent. The sulfoxide fragments after O-acylation, generating a sulphenyl electrophile.



Entries 12 to 14 are examples of oxidative generation of selenenylation reagents from diphenyldiselenide. These reagents can be used to effect hydroxy- and methoxyselenenylation.

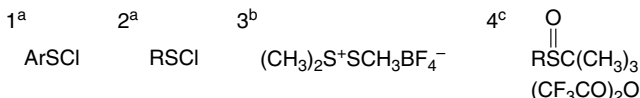


Entry 15 shows *N*-(phenylselenenyl)phthalimide, which is used frequently in synthetic processes.

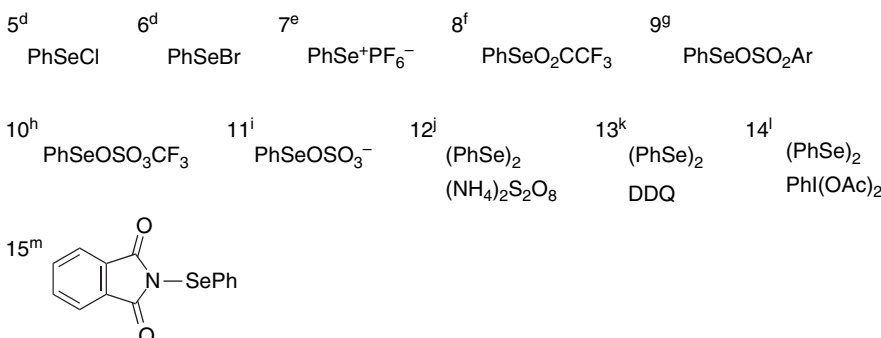
⁹⁰. G. E. Heasley, D. C. Hayes, G. R. McClung, D. K. Strickland, V. L. Heasley, P. D. Davis, D. M. Ingle, K. D. Rold, and T. L. Ungermann, *J. Org. Chem.*, **41**, 334 (1976).

⁹¹. M. Tiecco, L. Testaferri, A. Temperini, L. Bagnoli, F. Marini, and C. Santi, *Synlett*, 1767 (2001).

A. Sulfenylation Reagents



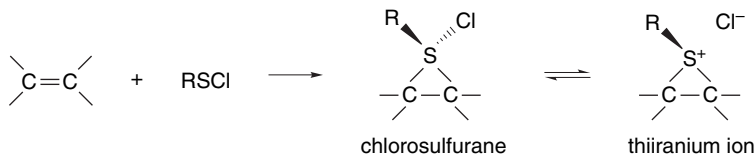
B. Selenenylation Reagents



- a. G. Capozzi, G. Modena, and L. Pasquato, in *The Chemistry of Sulphenic Acids and Their Derivatives*, S. Patai, editor, Wiley, Chichester, 1990, Chap. 10.
 - b. B. M. Trost, T. Shibata, and S. J. Martin, *J. Am. Chem. Soc.*, **104**, 3228 (1982).
 - c. M.-H. Brichard, M. Musick, Z. Janousek, and H. G. Viehe, *Synth. Commun.*, **20**, 2379 (1990).
 - d. K. B. Sharpless and R. F. Lauer, *J. Org. Chem.*, **39**, 429 (1974). e. W. P. Jackson, S. V. Ley, and A. J. Whittle, *J. Chem. Soc., Chem. Commun.*, 1173 (1980).
 - f. H. J. Reich, *J. Org. Chem.*, **39**, 428 (1974).
 - g. T. G. Back and K. R. Muralidharan, *J. Org. Chem.*, **58**, 2781 (1991).
 - h. S. Murata and T. Suzuki, *Tetrahedron Lett.*, **28**, 4297, 4415 (1987).
 - i. M. Tiecco, L. Testaferri, M. Tingoli, L. Bagnoli, and F. Marini, *J. Chem. Soc., Perkin Trans. 1*, 1989 (1993).
 - j. M. Tiecco, L. Testaferri, M. Tingoli, D. Chianelli, and D. Bartoli, *Tetrahedron Lett.*, **30**, 1417 (1989).
 - k. M. Tiecco, L. Testaferri, A. Temperini, L. Bagnoli, F. Marini, and C. Santi, *Synlett*, 1767 (2001).
 - l. M. Tingoli, M. Tiecco, L. Testaferri, and A. Temperini, *Synth. Commun.*, **28**, 1769 (1998).
 - m. K. C. Nicolaou, N. A. Petasis, and D. A. Claremon, *Tetrahedron*, **41**, 4835 (1985).

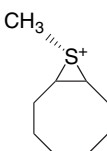
5.4.1. Sulfenylation

By analogy with halogenation, *thiiranium ions* can be intermediates in electrophilic sulfenylation. However, the corresponding tetravalent sulfur compounds, which are called *sulfuranes*, may also lie on the reaction path.⁹²

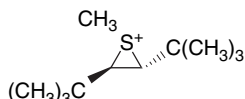


The sulfur atom is a stereogenic center in *both* the sulfurane and the thiiranium ion, and this may influence the stereochemistry of the reactions of stereoisomeric alkenes. Thiiranium ions can be prepared in various ways, and several have been characterized, such as the examples below.

⁹². M. Fachini, V. Lucchini, G. Modena, M. Pasi, and L. Pasquato, *J. Am. Chem. Soc.*, **121**, 3944 (1999).

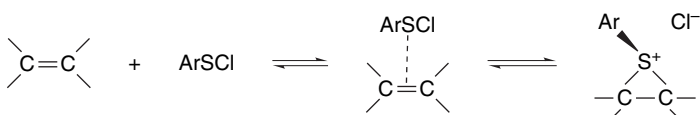


Ref. 93



Ref. 94

Perhaps the closest analog to the sulfenyl chlorides is chlorine, in the sense that both the electrophilic and nucleophilic component of the reagent are third-row elements. However, the sulfur is less electronegative and is a much better bridging element than chlorine. Although sulfenylation reagents are electrophilic in character, they are much less so than chlorine. The extent of rate acceleration from ethene to 2,3-dimethyl-2-butene is only 10^2 , as compared to 10^6 for chlorination and 10^7 for bromination (see Table 5.2). The sulfur substituent can influence reactivity. The initial complexation is expected to be favored by EWGs, but if the rate-determining step is ionization to the thiiranium ion, ERGs are favored.



As sulfur is less electronegative and more polarizable than chlorine, a strongly bridged intermediate, rather than an open carbocation, is expected for alkenes without ERG stabilization. Consistent with this expectation, sulfenylation is weakly regioselective and often shows a preference for *anti-Markovnikov addition*⁹⁵ as the result of steric factors. When bridging is strong, nucleophilic attack occurs at the less-substituted position. Table 5.4 gives some data for methyl- and phenyl-sulfenyl chloride. For bridged intermediates, the stereochemistry of addition is *anti*. Loss of stereospecificity with strong regioselectivity is observed when highly stabilizing ERG substituents are present on the alkene, as in 4-methoxyphenylstyrene.⁹⁶

Similar results have been observed for other sulfenyling reagents. The somewhat more electrophilic trifluoroethylsulfenyl group shows a shift toward Markovnikov regioselectivity but retains *anti* stereospecificity, indicating a bridged intermediate.⁹⁷

⁹³ D. J. Pettit and G. K. Helmkamp, *J. Org. Chem.*, **28**, 2932 (1963).

⁹⁴ V. Lucchini, G. Modena, and L. Pasquato, *J. Am. Chem. Soc.*, **113**, 6600 (1991); R. Destro, V. Lucchini, G. Modena, and L. Pasquato, *J. Org. Chem.*, **65**, 3367 (2000).

⁹⁵ W. H. Mueller and P. E. Butler, *J. Am. Chem. Soc.*, **88**, 2866 (1966).

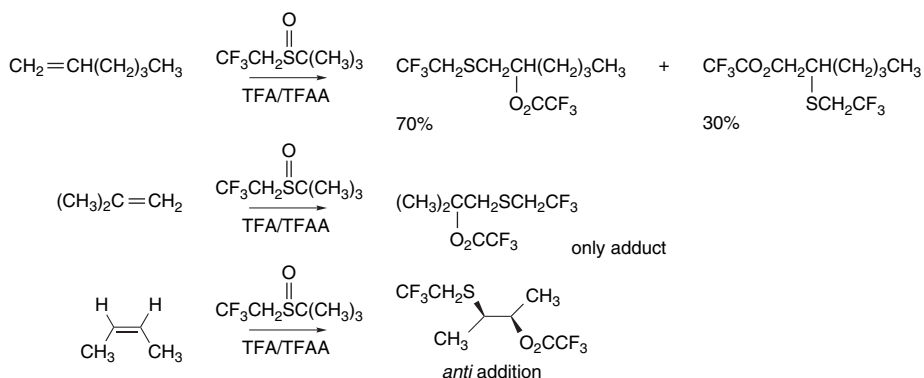
⁹⁶ G. H. Schmid and V. J. Nowlan, *J. Org. Chem.*, **37**, 3086 (1972); I. V. Bodrikov, A. V. Borisov, W. A. Smit, and A. I. Lutsenko, *Tetrahedron Lett.*, **25**, 4983 (1984).

⁹⁷ M. Redon, Z. Janousek, and H. G. Viehe, *Tetrahedron*, **53**, 15717 (1997).

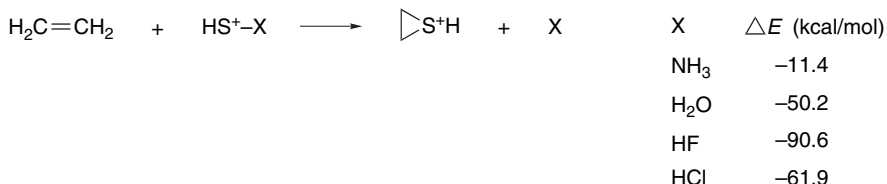
Table 5.4. Regiochemistry of Some Sulfenylation Reactions with Sulfenyl Chlorides

Alkene	Percent Markovnikov: <i>anti</i> -Markovnikov	
	CH ₃ SCl	PhSCl
Propene	18:82	32:68
3-Methylbutene	6:94	13:87
2-Methylpropene	20:80	
Styrene	98:2	

a. W. H. Mueller and P. E. Butler, *J. Am. Chem. Soc.*, **90**, 2075 (1968).



G2 computations have been used to model the reaction of sulfenyl electrophiles with alkenes.⁹⁸ The reactions were modeled by HS-X⁺, where X= FH, OH₂, NH₃, and ClH. The additions showed no gas phase barrier and the electrophile approaches the midpoint of the π bond. This is similar to halogenation. The overall exothermicity calculated for the reactions correlated with the leaving-group ability of HX.

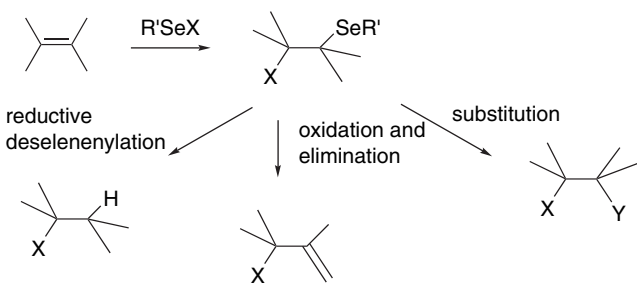


5.4.2. Selenenylation

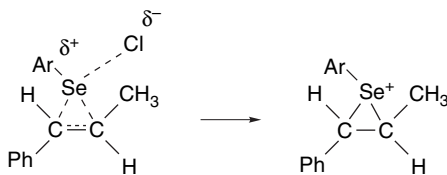
Electrophilic selenenylation has important synthetic applications. Much of the research emphasis has been on the development of convenient reagents.⁹⁹ The selenides, per se, are not usually the desired final product. Selenenylnyl substituents can be removed both reductively and oxidatively. In some cases, the selenenylnyl substituent

⁹⁸. T. I. Solling and L. Radom, *Chem. Eur. J.*, 1516 (2001).

⁹⁹. M. Tiecco, *Top. Curr. Chem.*, **208**, 7 (2000); T. G. Back, *Organoselenium Chemistry: A Practical Approach*, Oxford University Press, Oxford, 1999; C. Paulmier, *Selenium Reagents and Intermediates in Organic Chemistry*, Pergamon Press, Oxford, 1986; D. Liotta, *Organoselenium Chemistry*, Wiley, New York, 1987; S. Patai, ed., *The Chemistry of Organic Selenium and Tellurium Compounds*, Vols. 1 and 2, Wiley, New York, 1987.

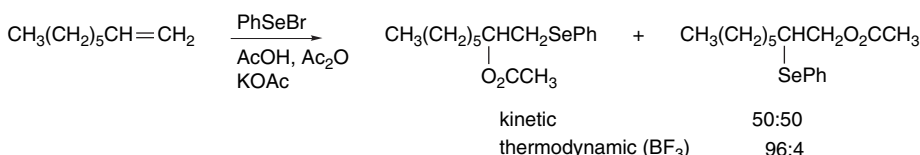


The various selenenylation reagents shown in Part B of Scheme 5.1 are characterized by an areneselenenyl group substituted by a leaving group. Some of the fundamental mechanistic aspects of selenenylation were established by studies of the reaction of *E*- and *Z*-1-phenylpropene with areneselenenyl chlorides.¹⁰⁰ The reaction is accelerated by an ERG in the arylselenenides. These data were interpreted in terms of a concerted addition, in which ionization of the Se–Cl bond leads C–Se bond formation. This accounts for the favorable effect of ERG substituents. Bridged seleniranium ions are considered to be intermediates.



As shown in Table 5.5, alkyl substitution enhances the reactivity of alkenes, but the effect is very small in comparison with halogenation (Table 5.2). Selenenylation seems to be particularly sensitive to steric effects. Note that a phenyl substituent is *rate retarding for selenenylation*. This may be due to both steric factors and alkene stabilization. The Hammett correlation with σ^+ gives a ρ value of -0.715 , also indicating only modest electron demand at the TS.¹⁰¹ Indeed, positive values of ρ have been observed in some cases.¹⁰²

Terminal alkenes show anti-Markovnikov regioselectivity, but rearrangement is facile.¹⁰³ The Markovnikov product is thermodynamically more stable (see Section 3.1.2.2).



Ref. 104

¹⁰⁰ G. H. Schmid and D. G. Garratt, *J. Org. Chem.*, **48**, 4169 (1983).

¹⁰¹ C. Brown and D. R. Hogg, *J. Chem. Soc. B*, 1262 (1968).

¹⁰² I. V. Bodrikov, A. V. Borisov, L. V. Chumakov, N. S. Zefirov, and W. A. Smit, *Tetrahedron Lett.*, **21**, 115 (1980).

¹⁰³ D. Liotta and G. Zima, *Tetrahedron Lett.*, 4977 (1978); P. T. Ho and R. J. Holt, *Can. J. Chem.*, **60**, 663 (1982); S. Raucher, *J. Org. Chem.*, **42**, 2950 (1977).

¹⁰⁴ L. Engman, *J. Org. Chem.*, **54**, 884 (1989).

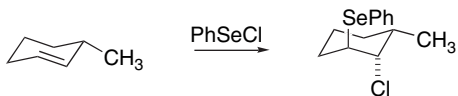
Table 5.5. Relative Reactivity of Some Alkenes toward 4-Chlorophenylsulfenyl Chloride and Phenylselenenylyl Chloride^a

Alkene	<i>p</i> -ClPhSCl <i>k</i> _{rel}	PhSeCl <i>k</i> _{rel}
Ethene	1.00	1.00
Propene	3.15	8.76
1-Butene	3.81	6.67
Z-2-Butene	20.6	3.75
<i>E</i> -2-Butene	6.67	2.08
Z-3-Hexene	54.8	5.24
<i>E</i> -3-Hexene	5.96	2.79
2-Methylpropene	8.46	6.76
2-Methyl-2-butene	46.5	3.76
2,3-Dimethyl-2-butene	119	2.46
Styrene	0.95	0.050
Z-1-Phenylpropene	0.66	0.010
<i>E</i> -1-Phenylpropene	1.82	0.016

a. G. H. Schmid and D. G. Garratt, in *The Chemistry of Double-Bonded Functional Groups, Supplement A, Part 2*, S. Patai, ed., Wiley, New York, 1977, Chap. 9.

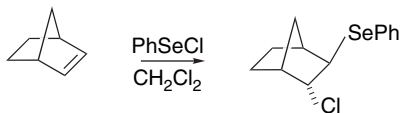
Styrene, on the other hand, is regioselective for the Markovnikov product, with the nucleophilic component bonding to the aryl-substituted carbon as the result of weakening of the bridging by the phenyl group.

Selenenylation is a stereospecific *anti* addition with acyclic alkenes.¹⁰⁵ Cyclohexenes undergo preferential diaxial addition.



Ref. 106

Norbornene gives highly stereoselective *exo-anti* addition, pointing to an *exo* bridged intermediate.



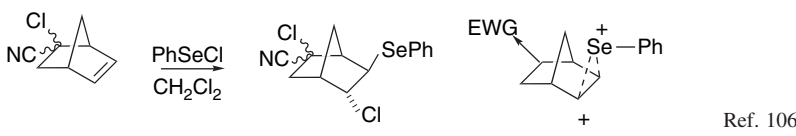
Ref. 107

The regiochemistry of addition to substituted norbornenes appears to be controlled by polar substituent effects.

¹⁰⁵. H. J. Reich, *J. Org. Chem.*, **39**, 428 (1974).

¹⁰⁶. D. Liotta, G. Zima, and M. Saindane, *J. Org. Chem.*, **47**, 1258 (1982).

¹⁰⁷. D. G. Garratt and A. Kabo, *Can. J. Chem.*, **58**, 1030 (1980).



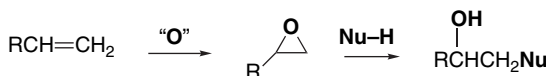
This regioselectivity is consistent with an unsymmetrically bridged seleniranium intermediate in which the more positive charge is remote from the EWG substituent. The directive effect is contrary to regiochemistry being dominated by the chloride ion approach, since chloride addition should be facilitated by the dipole of an EWG.

There has been some computational modeling of selenenylation reactions, particularly with regard to enantioselectivity of chiral reagents. The enantioselectivity is attributed to the relative ease of nucleophilic approach on the seleniranium ion intermediate, which is consistent with viewing the intermediate as being strongly bridged.¹⁰⁸ With styrene, a somewhat unsymmetrical bridging has been noted and the regiochemistry (Markovnikov) is attributed to the greater positive charge at C(1).¹⁰⁹

Broadly comparing sulfur and selenium electrophiles to the halogens, we see that they are *less electrophilic* and characterized by *more strongly bridged intermediates*. This is consistent with reduced sensitivity to electronic effects in alkenes (e.g., alkyl or aryl substituents) and an increased tendency to anti-Markovnikov regiochemistry. The strongly bridged intermediates favor *anti* stereochemistry.

5.5. Addition Reactions Involving Epoxides

Epoxidation is an electrophilic addition. It is closely analogous to halogenation, sulfenylation, and selenenylation in that the electrophilic attack results in the formation of a three-membered ring. In contrast to these reactions, however, the resulting epoxides are neutral and stable and normally can be isolated. The epoxides are susceptible to nucleophilic ring opening so the overall pattern results in the addition of OH⁺ and a nucleophile at the double bond. As the regiochemistry of the ring opening is usually controlled by the ease of nucleophilic approach, *the oxygen is introduced at the more-substituted carbon*. We concentrate on peroxidic epoxidation reagents in this chapter. Later, in Chapter 12 of Part B, transition metal-mediated epoxidations are also discussed.



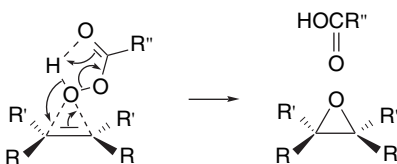
5.5.1. Epoxides from Alkenes and Peroxidic Reagents

The most widely used reagents for conversion of alkenes to epoxides are peroxy-carboxylic acids.¹¹⁰ *m*-Chloroperoxybenzoic acid¹¹¹ (MCPBA) is a common reagent.

- ^{108.} M. Spichty, G. Fragale, and T. Wirth, *J. Am. Chem. Soc.*, **122**, 10914 (2000); X. Wang, K. N. Houk, and M. Spichty, *J. Am. Chem. Soc.*, **121**, 8567 (1999).
- ^{109.} T. Wirth, G. Fragale, and M. Spichty, *J. Am. Chem. Soc.*, **120**, 3376 (1998).
- ^{110.} D. Swern, *Organic Peroxides*, Vol. II, Wiley-Interscience, New York, 1971, pp. 355–533; B. Plesnicar, in *Oxidation in Organic Chemistry*, Part C, W. Trahanovsky, ed., Academic Press, New York, 1978, pp. 211–253.
- ^{111.} R. N. McDonald, R. N. Steppel, and J. E. Dorsey, *Org. Synth.*, **50**, 15 (1970).

The magnesium salt of monoperoxyphthalic acid is an alternative.¹¹² Peroxyacetic acid, peroxybenzoic acid, and peroxytrifluoroacetic acid also are used frequently for epoxidation. All of the peroxycarboxylic acids are potentially explosive materials and require careful handling. Potassium hydrogen peroxysulfate, which is sold commercially as Oxone®,¹¹³ is a convenient reagent for epoxidations that can be done in aqueous solution.¹¹⁴

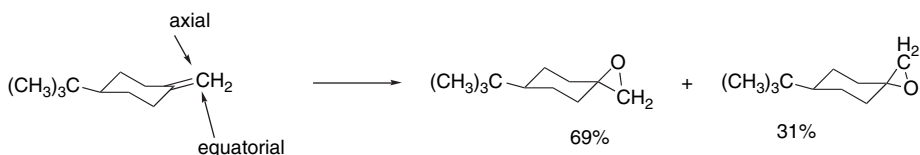
It has been demonstrated that no ionic intermediates are involved in the epoxidation of alkenes. The reaction rate is not very sensitive to solvent polarity.¹¹⁵ Stereospecific *syn* addition is consistently observed. The oxidation is considered to be a concerted process, as represented by the TS shown below. The plane including the peroxide bond is approximately perpendicular to the plane of the developing epoxide ring, so the oxygen being transferred is in a *spiro* position.



The rate of epoxidation of alkenes is increased by alkyl groups and other ERG substituents, and the reactivity of the peroxy acids is increased by EWG substituents.¹¹⁶ These structure-reactivity relationships demonstrate that the peroxy acid acts as an electrophile in the reaction. Low reactivity is exhibited by double bonds that are conjugated with strongly EWG substituents, and very reactive peroxy acids, such as trifluoroperoxyacetic acid, are required for oxidation of such compounds.¹¹⁷ Strain increases the reactivity of alkenes toward epoxidation. Norbornene is about twice as reactive as cyclopentene toward peroxyacetic acid.¹¹⁸ *trans*-Cyclooctene is 90 times more reactive than cyclohexene.¹¹⁹ Shea and Kim found a good correlation between relief of strain, as determined by MM calculations, and the epoxidation rate.¹²⁰ There is also a correlation with ionization potentials of the alkenes.¹²¹ Alkenes with aryl substituents are *less reactive* than unconjugated alkenes because of ground state stabilization and this is consistent with a lack of carbocation character in the TS.

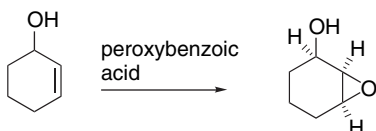
The stereoselectivity of epoxidation with peroxycarboxylic acids has been studied extensively.¹²² Addition of oxygen occurs preferentially from the less hindered side of nonpolar molecules. Norbornene, for example, gives a 96:4 *exo:endo* ratio.¹²³ In molecules where two potential modes of approach are not greatly different, a mixture

- ¹¹². P. Brougham, M. S. Cooper, D. A. Cummerson, H. Heaney, and N. Thompson, *Synthesis*, 1015 (1987).
- ¹¹³. Oxone is a registered trademark of E.I. du Pont de Nemours and company.
- ¹¹⁴. R. Bloch, J. Abecassis, and D. Hassan, *J. Org. Chem.*, **50**, 1544 (1985).
- ¹¹⁵. N. N. Schwartz and J. N. Blumbergs, *J. Org. Chem.*, **29**, 1976 (1964).
- ¹¹⁶. B. M. Lynch and K. H. Pausacker, *J. Chem. Soc.*, 1525 (1955).
- ¹¹⁷. W. D. Emmons and A. S. Pagano, *J. Am. Chem. Soc.*, **77**, 89 (1955).
- ¹¹⁸. J. Spanget-Larsen and R. Gleiter, *Tetrahedron Lett.*, **23**, 2435 (1982); C. Wipff and K. Morokuma, *Tetrahedron Lett.*, **21**, 4445 (1980).
- ¹¹⁹. K. J. Burgoine, S. G. Davies, M. J. Peagram, and G. H. Whitham, *J. Chem. Soc., Perkin Trans. I*, 2629 (1974).
- ¹²⁰. K. J. Shea and J. -S. Kim, *J. Am. Chem. Soc.*, **114**, 3044 (1992).
- ¹²¹. C. Kim, T. G. Traylor, and C. L. Perrin, *J. Am. Chem. Soc.*, **120**, 9513 (1998).
- ¹²². V. G. Dryuk and V. G. Kartsev, *Russ. Chem. Rev.*, **68**, 183 (1999).
- ¹²³. H. Kwart and T. Takeshita, *J. Org. Chem.*, **28**, 670 (1963).

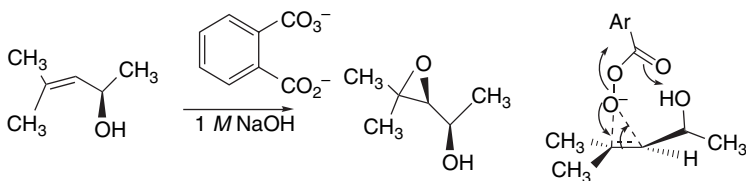


Several other conformationally biased methylenecyclohexanes have been examined and the small preference for axial attack is quite general, unless a substituent sterically encumbers one of the faces.¹²⁵

Hydroxy groups exert a directive effect on epoxidation and favor approach from the side of the double bond closest to the hydroxy group.¹²⁶ Hydrogen bonding between the hydroxy group and the peroxidic reagent evidently stabilizes the TS.



This is a strong directing effect that can exert stereochemical control even when steric effects are opposed. Other substituents capable of hydrogen bonding, in particular amides, also exert a *syn*-directive effect.¹²⁷ The hydroxy-directing effect also operates in alkaline epoxidation in aqueous solution.¹²⁸ Here the alcohol group can supply a hydrogen bond to assist the oxygen transfer.



The hydroxy-directing effect has been carefully studied with allylic alcohols.¹²⁹ The analysis begins with the reactant conformation, which is dominated by allylic strain.

¹²⁴ R. G. Carlson and N. S. Behn, *J. Org. Chem.*, **32**, 1363 (1967).

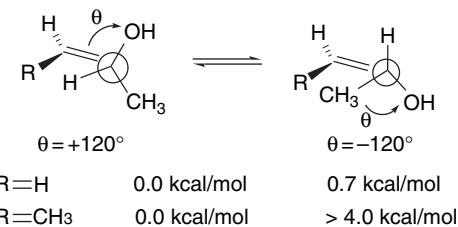
¹²⁵ A. Sevin and J. -N. Cense, *Bull. Chim. Soc. Fr.*, 964 (1974); E. Vedejs, W. H. Dent, III, J. T. Kendall, and P. A. Oliver, *J. Am. Chem. Soc.*, **118**, 3556 (1996).

¹²⁶ H. B. Henbest and R. A. L. Wilson, *J. Chem. Soc.*, 1958 (1957).

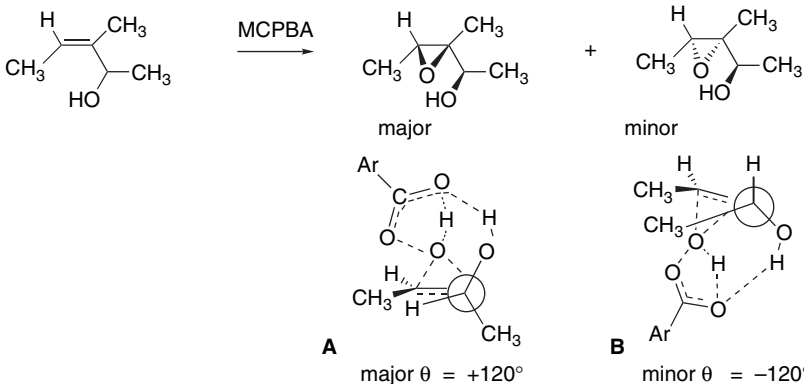
¹²⁷ F. Mohamadi and M. M. Spees, *Tetrahedron Lett.*, **30**, 1309 (1989); P. G. M. Wuts, A. R. Ritter, and L. E. Pruitt, *J. Org. Chem.*, **57**, 6696 (1992); A. Jenmalm, W. Berts, K. Luthman, I. Csoregh, and U. Hacksell, *J. Org. Chem.*, **60**, 1026 (1995); P. Kocovsky and I. Starý, *J. Org. Chem.*, **55**, 3236 (1990); A. Armstrong, P. A. Barsanti, P. A. Clarke, and A. Wood, *J. Chem. Soc., Perkin Trans., 1*, 1373 (1996).

¹²⁸ D. Ye, F. Finguelli, O. Piermattei, and F. Pizzo, *J. Org. Chem.*, **62**, 3748 (1997); I. Washington and K. N. Houk, *Org. Lett.*, **4**, 2661 (2002).

¹²⁹ W. Adam and T. Wirth, *Acc. Chem. Res.*, **32**, 703 (1999).

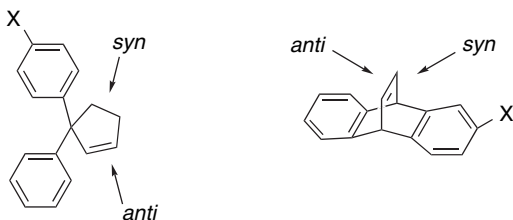


The epoxidation of goes through TGA, with 9:1 diastereoselectivity.¹³⁰



The preference is the result of the CH_3-CH_3 steric interaction that is present in TSB. The same stereoselectivity is exhibited by other reagents influenced by hydroxy-directing effects.¹³¹

There has been considerable interest in finding and interpreting electronic effects in sterically unbiased systems. (See Topic 2.4 for the application of this kind of study to ketones.) The results of two such studies are shown below. Generally, EWGs are *syn* directing, whereas ERGs are *anti* directing, but the effects are not very large.



X	<i>syn:anti</i>	X	<i>syn:anti</i>
NO_2	73:27	NO_2	77:23
Br	57:43	F	58:42
Cl	57:43	H	50:50
H	50:50	CH_3O	48:52
CH_3O	48:52		

Ref. 132

Ref. 133

¹³⁰ W. Adam and B. Nestler, *Tetrahedron Lett.*, **34**, 611 (1993).

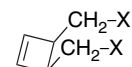
¹³¹ W. Adam, H.-G. Degen, and C. R. Saha-Moller, *J. Org. Chem.*, **64**, 1274 (1999).

¹³² R. L. Halterman and M. A. McEvoy, *Tetrahedron Lett.*, **33**, 753 (1992).

¹³³ T. Ohwada, I. Okamoto, N. Haga, and K. Shudo, *J. Org. Chem.*, **59**, 3975 (1994).

Whether these electronic effects have a stereoelectronic or an electrostatic origin is an open question. In either case, there would be a more favorable electronic environment *anti* to the ERG substituents and *syn* to the EWGs.

A related study of 3,4-disubstituted oxymethylcyclobutenes showed moderate *syn*-directive effects on MCPBA epoxidation.¹³⁴ In this case, the effect was attributed to interaction of the relatively electron-rich peroxide oxygens with the positively charged methylene hydrogens, but the electrostatic effect of the bond dipoles would be in the same direction.



X	<i>syn:anti</i>
H	55:45
OH	67:33
OCH ₃	62:38
O ₂ CCH ₃	72:28
OSO ₂ CH ₃	79:21
OSO ₂	70:30
(cyclic sulfite)	

There have been several computational studies of the peroxy acid–alkene reaction. The proposed spiro TS has been supported in these studies for alkenes that do not present insurmountable steric barriers. The spiro TS has been found for ethene (B3LYP/6-31G*),¹³⁵ propene and 2-methylpropene (QCISD/6-31G*),¹³⁶ and 2,3-dimethylbutene and norbornene (B3LYP/6-311+G(*d, p*)).¹³⁷ These computational studies also correctly predict the effect of substituents on the E_a and account for these effects in terms of less synchronous bond formation. This is illustrated by the calculated geometries and E_a (B3LYP/6-31G*) of the TS for ethene, propene, methoxyethene, 1,3-butadiene, and cyanoethene, as shown in Figure 5.3. Note that the TSs become somewhat unsymmetrical with ERG substituents, as in propene, methoxyethene, and butadiene. The TS for acrylonitrile with an EWG substituent is even more unsymmetrical and has a considerably shorter C(3)–O bond, which reflects the electronic influence of the cyano group. In this asynchronous TS, the nucleophilic character of the peroxidic oxygen toward the β -carbon is important. Note also that the E_a is increased considerably by the EWG.

Visual images and additional information available at: springer.com/cary-sundberg

Another useful epoxidizing agent is dimethyldioxirane (DMDO).¹³⁸ This reagent is generated by an *in situ* reaction of acetone and peroxymonosulfate in buffered aqueous solution. Distillation gives an $\sim 0.1\text{ M}$ solution of DMDO in acetone.¹³⁹

¹³⁴ M. Freccero, R. Gandolfi, and M. Sarzi-Amade, *Tetrahedron*, **55**, 11309 (1999).

¹³⁵ K. N. Houk, J. Liu, N. C. DeMello, and K. R. Condroski, *J. Am. Chem. Soc.*, **119**, 10147 (1997).

¹³⁶ R. D. Bach, M. N. Glukhovtsev, and C. Gonzalez, *J. Am. Chem. Soc.*, **120**, 9902 (1998).

¹³⁷ M. Freccero, R. Gandolfi, M. Sarzi-Amade, and A. Rastelli, *J. Org. Chem.*, **67**, 8519 (2002).

¹³⁸ R. W. Murray, *Chem. Rev.*, **89**, 1187 (1989); W. Adam and L. P. Hadjivarapoglou, *Topics Current Chem.*, **164**, 45 (1993); W. Adam, A. K. Smerz, and C. G. Zhao, *J. Prakt. Chem., Chem. Zeit.*, **339**, 295 (1997).

¹³⁹ R. W. Murray and R. Jeyaraman, *J. Org. Chem.*, **50**, 2847 (1985); W. Adam, J. Bialas, and L. Hadjivarapoglou, *Chem. Ber.*, **124**, 2377 (1991).

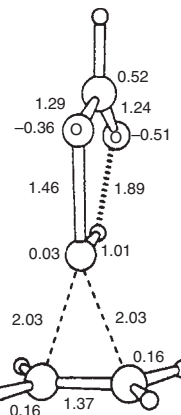
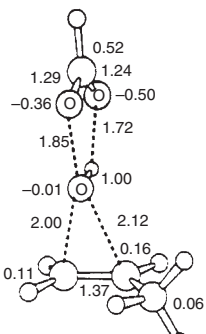
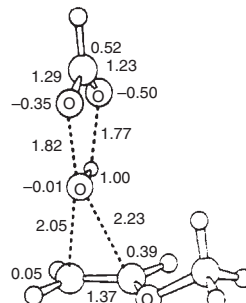
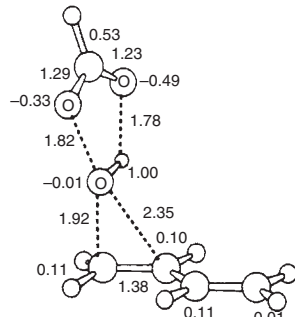
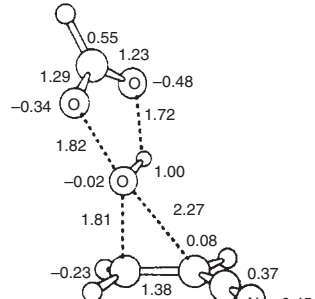
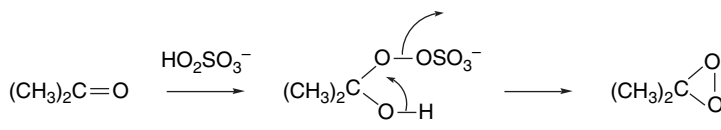
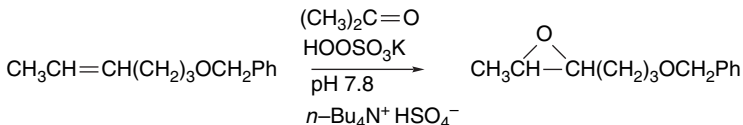
(a) $\Delta E_a = 14.1 \text{ kcal/mol}$ (b) $\Delta E_a = 12.0 \text{ kcal/mol}$ (c) $\Delta E_a = 8.5 \text{ kcal/mol}$ (d) $\Delta E_a = 11.7 \text{ kcal/mol}$ (e) $\Delta E_a = 17.3 \text{ kcal/mol}$

Fig. 5.3. Comparison of B3LYP/6-31G* TS structures and E_a for epoxidation by HCO_3H for: (a) ethene; (b) propene; (c) methoxyethene; (d) 1,3-butadiene, and (e) cyanoethene. Reproduced from *J. Am. Chem. Soc.*, **119**, 10147 (1997), by permission of the American Chemical Society.

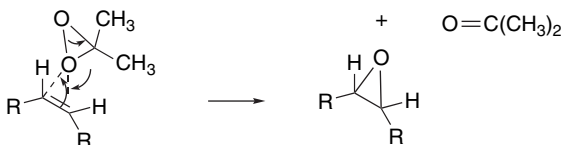


Higher concentrations of DMDO can be obtained by extraction of a 1:1 aqueous dilution of the distillate by CH_2Cl_2 , CHCl_3 , or CCl_4 .¹⁴⁰ Other improvements in convenience have been described,¹⁴¹ including in situ generation of DMDO under phase transfer conditions.¹⁴²

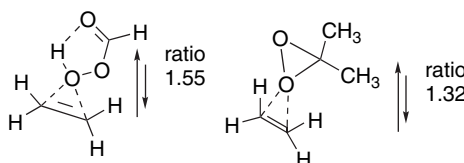


The yields and rates of oxidation by DMDO under these in situ conditions depend on pH and other reaction conditions.¹⁴³

Various computational models of the TS show that the reaction occurs by a concerted mechanism that is quite similar to that for peroxy acids.¹⁴⁴ Kinetics and isotope effects are consistent with this mechanism.¹⁴⁵



For example, the NPA charges for the DMDO and performic oxidations of ethene have been compared.¹⁴⁶ The ratio of the electrophilic interaction involving electron density transfer from the alkene to the O–O σ^* orbitals can be compared with the nucleophilic component involving back donation from the oxidant to the alkene π^* orbital. By this comparison, performic acid is somewhat more electrophilic.



¹⁴⁰ M. Gilbert, M. Ferrer, F. Sanchez-Baeza, and A. Messequer, *Tetrahedron*, **53**, 8643 (1997).

¹⁴¹ W. Adam, J. Bialoas, and L. Hadjiaropoglou, *Chem. Ber.*, **124**, 2377 (1991).

¹⁴² S. E. Denmark, D. C. Forbes, D. S. Hays, J. S. DePue, and R. G. Wilde, *J. Org. Chem.*, **60**, 1391 (1995).

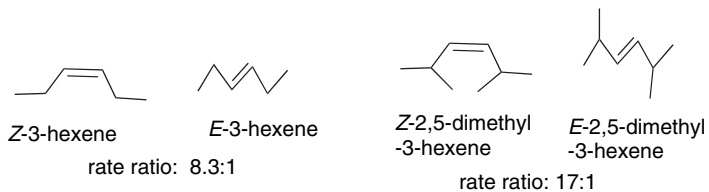
¹⁴³ M. Frohn, Z.-X. Wang, and Y. Shi, *J. Org. Chem.*, **63**, 6425 (1998); A. O'Connell, T. Smyth, and B. K. Hodnett, *J. Chem. Techn. Biotech.*, **72**, 60 (1998).

¹⁴⁴ R. D. Bach, M. N. Glukhovtsev, C. Gonzalez, M. Marquez, C. M. Estevez, A. G. Baboul, and H. Schlegel, *J. Phys. Chem.*, **101**, 6092 (1997); M. Freccero, R. Gandolfi, M. Sarzi-Amade, and A. Rastelli, *Tetrahedron*, **54**, 6123 (1998); J. Liu, K. N. Houk, A. Dinoi, C. Fusco, and R. Curci, *J. Org. Chem.*, **63**, 8565 (1998).

¹⁴⁵ W. Adam, R. Paredes, A. K. Smerz, and L. A. Veloza, *Liebigs Ann. Chem.*, 547 (1997); A. L. Baumstark, E. Michalenabaez, A. M. Navarro, and H. D. Banks, *Heterocycl. Commun.*, **3**, 393 (1997); Y. Angelis, X. J. Zhang, and M. Orfanopoulos, *Tetrahedron Lett.*, **37**, 5991 (1996).

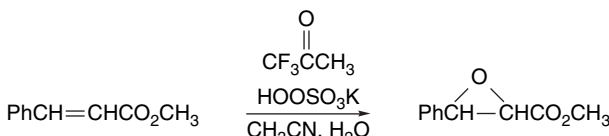
¹⁴⁶ D. V. Deubel, G. Frenking, H. M. Senn, and J. Sundermeyer, *J. Chem. Soc., Chem. Commun.*, 2469 (2000).

It has been suggested that the TS for DMDO oxidation of electron-poor alkenes, such as acrylonitrile, has a dominant nucleophilic component.¹⁴⁷ DMDO oxidations have a fairly high sensitivity to steric effect. The *Z*-isomers of alkenes are usually more reactive than the *E*-isomers because in the former case the reagent can avoid the alkyl groups.¹⁴⁸ We say more about this in Section 5.8.



Similarly to peroxycarboxylic acids, DMDO is subject to *cis* or *syn* stereoselectivity by hydroxy and other hydrogen-bonding functional groups.¹⁴⁹ The effect is strongest in nonpolar solvents. For other substituents, both steric and polar factors seem to have an influence, and several complex reactants have shown good stereoselectivity, although the precise origin of the stereoselectivity is not always evident.¹⁵⁰

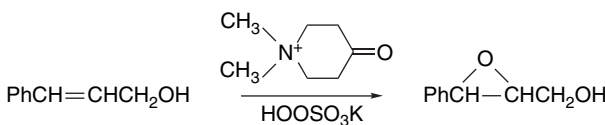
Other ketones apart from acetone can be used for *in situ* generation of dioxiranes by reaction with peroxyulfonate or another suitable peroxide. More electrophilic ketones give more reactive dioxiranes. 3-Methyl-3-trifluoromethylidioxirane is a more reactive analog of DMDO.¹⁵¹ This reagent, which can be generated *in situ* from 1,1,1-trifluoroacetone, is capable of oxidizing less reactive compounds such as methyl cinnamate.



Ref. 152

Hexafluoroacetone and hydrogen peroxide in buffered aqueous solution epoxidizes alkenes and allylic alcohols.¹⁵³ Other fluoroketones also function as epoxidation catalysts.^{154, 155} *N,N*-dialkylpiperidin-4-one salts are also good catalysts for

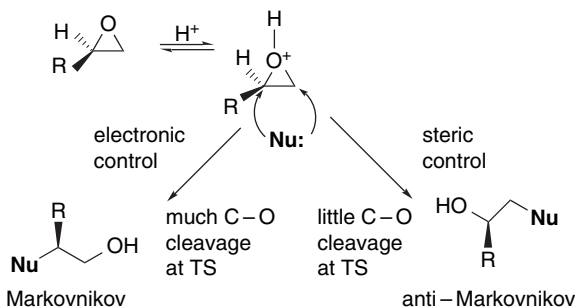
- ¹⁴⁷ D. V. Deubel, *J. Org. Chem.*, **66**, 3790 (2001).
- ¹⁴⁸ A. L. Baumstark and C. J. McCloskey, *Tetrahedron Lett.*, **28**, 3311 (1987); A. L. Baumstark and P. C. Vasquez, *J. Org. Chem.*, **53**, 3437 (1988).
- ¹⁴⁹ R. W. Murray, M. Singh, B. L. Williams, and H. M. Moncrieff, *J. Org. Chem.*, **61**, 1830 (1996); G. Asensio, C. Boix-Bernardini, C. Andreu, M. E. Gonzalez-Nunez, R. Mello, J. O. Edwards, and G. B. Carpenter, *J. Org. Chem.*, **64**, 4705 (1999).
- ¹⁵⁰ R. C. Cambie, A. C. Grimsdale, P. S. Rutledge, M. F. Walker, and A. D. Woodgate, *Austr. J. Chem.*, **44**, 1553 (1991); P. Boricelli and P. Lupattelli, *J. Org. Chem.*, **59**, 4304 (1994); R. Curci, A. Detomaso, T. Prencipe, and G. B. Carpenter, *J. Am. Chem. Soc.*, **116**, 8112 (1994); T. C. Henninger, M. Sabat, and R. J. Sundberg, *Tetrahedron*, **52**, 14403 (1996).
- ¹⁵¹ R. Mello, M. Fiorentino, O. Sciacovelli, and R. Curci, *J. Org. Chem.*, **53**, 3890 (1988).
- ¹⁵² D. Yang, M.-K. Wong, and Y.-C. Yip, *J. Org. Chem.*, **60**, 3887 (1995).
- ¹⁵³ R. P. Heggs and B. Ganem, *J. Am. Chem. Soc.*, **101**, 2484 (1979); A. J. Biloski, R. P. Hegge, and B. Ganem, *Synthesis*, 810 (1980); W. Adam, H.-G. Degen, and C. R. Saha-Moller, *J. Org. Chem.*, **64**, 1274 (1999).
- ¹⁵⁴ E. L. Grocock, B.A. Marples, and R. C. Toon, *Tetrahedron*, **56**, 989 (2000).
- ¹⁵⁵ J. Legros, B. Crousse, J. Bourdon, D. Bonnet-Delpont, and J.-P. Begue, *Tetrahedron Lett.*, **42**, 4463 (2001).



5.5.2. Subsequent Transformations of Epoxides

Epoxides are useful synthetic intermediates and the conversion of an alkene to an epoxide is often part of a more extensive overall transformation.¹⁵⁷ Advantage is taken of the reactivity of the epoxide ring to introduce additional functionality. As epoxide ring opening is usually stereospecific, such reactions can be used to establish stereochemical relationships between adjacent substituents. Such two- or three-step operations can achieve specific oxidative transformations of an alkene that might not be easily accomplished in a single step.

Ring opening of epoxides can be carried out under either acidic or basic conditions. The regiochemistry of the ring opening depends on whether steric or electronic factors are dominant. Base-catalyzed reactions in which the nucleophile provides the driving force for ring opening usually involve breaking the epoxide bond at the less-substituted carbon, since this is the position most accessible to nucleophilic attack (*steric factor dominates*).¹⁵⁸ The situation in acid-catalyzed reactions is more complicated. The bonding of a proton to the oxygen weakens the C–O bonds and facilitates rupture of the ring by weak nucleophiles. If the C–O bond is largely intact at the TS, the nucleophile will become attached to the less-substituted position for the same steric reasons that were cited for nucleophilic ring opening. If, on the other hand, C–O rupture is more complete when the TS is reached, the opposite orientation is observed. This results from the ability of the more-substituted carbon to stabilize the developing positive charge (*electronic factor dominates*). *Steric control corresponds to anti-Markovnikov regioselectivity, whereas electronic control leads to Markovnikov regioselectivity.*

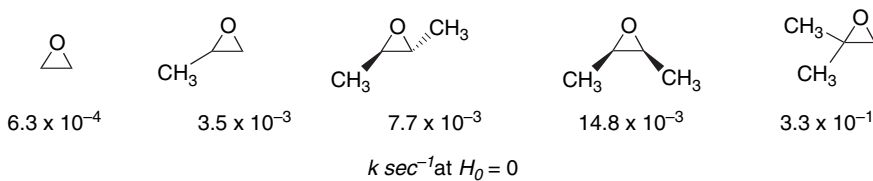


¹⁵⁶ S. E. Denmark, D. C. Forbes, D. S. Hays, J. S. DePue, and R. G. Wilde, *J. Org. Chem.*, **60**, 1391 (1995).

¹⁵⁷ J. G. Smith, *Synthesis*, 629 (1984).

¹⁵⁸ R. E. Parker and N. S. Isaacs, *Chem. Rev.*, **59**, 737 (1959).

These fundamental aspects of epoxide ring opening were established by kinetic and isotopic labeling studies.¹⁵⁹ The dominant role of bond cleavage in acidic hydrolysis is indicated by the increase in rates with additional substitution. Note in particular that the 2,2-dimethyl derivative is much more reactive than the *cis* and *trans* disubstituted derivative, as expected for an intermediate with carbocation character.



The pH-rate profiles of hydrolysis of 2-methyloxirane and 2,2-dimethyloxirane have been determined and interpreted.¹⁶⁰ The profile for 2,2-dimethyloxirane, shown in Figure 5.4, leads to the following rate constants for the acid-catalyzed, uncatalyzed, and base-catalyzed reactions.

$$k_{\text{H}^+} = 25.8 \pm 1.7 \text{ M}^{-1} \text{ s}^{-1}$$

$$k_{\text{H}_2\text{O}} = 2.19 \pm 10^{-6} \text{ M}^{-1} \text{ s}^{-1}$$

$$k_{-\text{OH}} = 1.95 \pm 10^{-4} \text{ M}^{-1} \text{ s}^{-1}$$

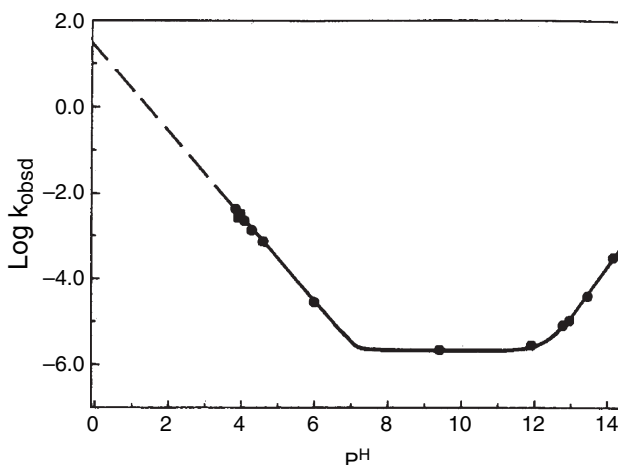
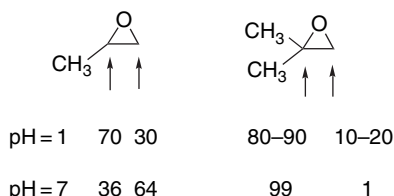


Fig. 5.4. pH-Rate profile for hydrolysis of 2,2-dimethyloxirane. Reproduced from *J. Am. Chem. Soc.*, **110**, 6492 (1988), by permission of the American Chemical Society.

¹⁵⁹. J. G. Pritchard and F. A. Long, *J. Am. Chem. Soc.*, **78**, 2667, 6008 (1956); F. A. Long, J. G. Pritchard, and F. E. Stafford, *J. Am. Chem. Soc.*, **79**, 2362 (1957).

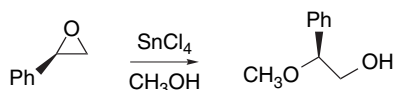
¹⁶⁰. Y. Pocker, B. P. Ronald, and K. W. Anderson, *J. Am. Chem. Soc.*, **110**, 6492 (1988).

Nucleophilic attack occurs at both the more-substituted and the less-substituted carbon, as determined by isotopic labeling.¹⁶¹

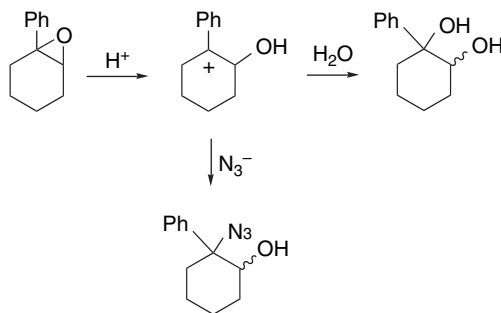


The opening of *cis*- and *trans*-2,3-dimethyloxirane in methanol or acetic acid is a stereospecific *anti* addition.¹⁶²

The presence of an aryl substituent favors cleavage of the benzylic C–O bond. The case of styrene oxide hydrolysis has been carefully examined. Under acidic conditions the bond breaking is exclusively at the benzylic position (electronic control). Under basic conditions, ring opening occurs at both epoxide carbons.¹⁶³ Styrene also undergoes highly regioselective ring opening in the presence of Lewis acids. For example, methanolysis is catalyzed by SnCl₄; it occurs with more than a 95% attack at the benzyl carbon and with high *inversion of configuration*.¹⁶⁴ Similar results are observed with BF₃.¹⁶⁵ The stereospecificity indicates a concerted nucleophilic opening of the complexed epoxide, with bond-weakening factors (electronic control) determining the regiochemistry.



In the case of epoxides of 1-arylhexene, there is direct evidence for a carbocation intermediate.¹⁶⁶ The hydrolysis product can be diverted by addition of azide ion as a competing nucleophile. As expected for a carbocation intermediate, both the *cis* and *trans* diols are formed.



¹⁶¹ F. A. Long and J. G. Pritchard, *J. Am. Chem. Soc.*, **78**, 2663, 2667 (1956); F. A. Long , J. G. Pritchard, and F. E. Stafford, *J. Am. Chem. Soc.*, **79**, 2362 (1957).

¹⁶² V. F. Shvets, N. N. Lebedev, and O. A. Tyukova, *Zh. Org. Khim.*, **7**, 1851 (1971).

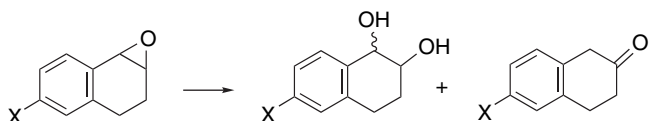
¹⁶³ B. Lin and D. L. Whalen, *J. Org. Chem.*, **59**, 1638 (1994); J. J. Blumenstein, V.C. Ukachukwu, R. S. Mohan, and D. L. Whalen, *J. Org. Chem.*, **58**, 924 (1993).

¹⁶⁴ C. Moberg, L. Rakos, and L. Tottie, *Tetrahedron Lett.*, **33**, 2191 (1992).

¹⁶⁵ Y. J. Liu, T. Y. Chu, and R. Engel, *Synth. Commun.*, **22**, 2367 (1992).

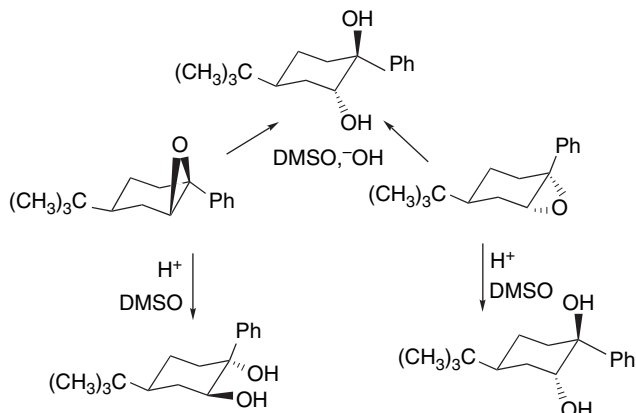
¹⁶⁶ L. Doan, K. Bradley, S. Gerdes, and D. L. Whalen, *J. Org. Chem.*, **64**, 6227 (1999).

Similarly, comparison of the epoxide of 1,2-dihydronaphthalene and its 6-methoxy analog provided interesting contrasts. The product was partitioned into the components formed by the acid-catalyzed and uncatalyzed mechanisms.¹⁶⁷ The unsubstituted compound gives the *trans* diol exclusively, indicating participation of the nucleophile in the ring opening. The 6-methoxy derivative gives a substantial amount of a rearrangement product and the diol is a mixture of the *cis* and *trans* stereoisomers. These differences indicate that the more stabilized carbocation has a significant lifetime.



X	<i>cis</i>	<i>trans</i>
H		
H ⁺ – catalyzed	6	94
uncatalyzed	0	100
CH ₃ O		
H ⁺ – catalyzed	81	19
uncatalyzed	17	7
		76

The conformationally biased *cis*- and *trans*-4-*t*-butyl derivatives were examined. The stereochemistry of both acid- and base-catalyzed reactions was investigated in 85:15 DMSO-H₂O. Under acidic conditions the epoxides give *anti* ring opening and the reaction is stereospecific. The base-catalyzed reactions involve *trans*-diaxial ring opening. The acid-catalyzed reactions occur by preferential opening of the benzylic bond with inversion.¹⁶⁸

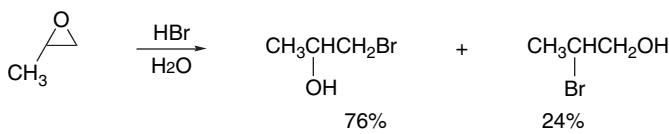


When saturated epoxides such as propylene oxide react with hydrogen halides, the dominant mode of reaction introduces halide at the less-substituted primary carbon (anti-Markovnikov).¹⁶⁹

¹⁶⁷ R. E. Gillilan, T. M. Pohl, and D. L. Whalen, *J. Am. Chem. Soc.*, **104**, 4481 (1982).

¹⁶⁸ G. Berti, B. Macchia, and F. Macchia, *Tetrahedron Lett.*, 3421 (1965).

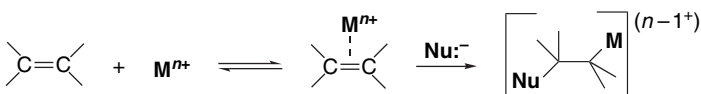
¹⁶⁹ C. A. Stewart and C. A. VanderWerf, *J. Am. Chem. Soc.*, **76**, 1259 (1954).



Substituents that further stabilize a carbocation intermediate lead to reversal of the mode of addition.¹⁷⁰ To summarize, because they are stable compounds, both the stereochemistry and regiochemistry of epoxides can be controlled by the reaction conditions. Ring opening that is dominated by the nucleophilic reagent is determined by steric access. Ring opening that is electrophilic in character introduces the nucleophile at the position that has the largest cationic character.

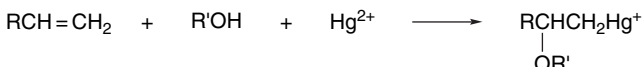
5.6. Electrophilic Additions Involving Metal Ions

Certain metal cations promote addition by electrophilic attack on alkenes. Addition is completed when a nucleophile adds to the alkene-cation complex. The nucleophile may be the solvent or a ligand from the metal ion's coordination sphere. The same process occurs for other transition metal cations, especially for Pd^{2+} , but the products often go on to react further. Synthetically important reactions involving Pd^{2+} are discussed in Section 8.2 of Part B. The mercuration products are stable, and this allows study of the addition reaction itself. We also consider reactions of the Ag^+ ion, which give complexes, but usually do not proceed to adducts.



5.6.1. Solvomercuration

The best characterized of these reactions involve the mercuric ion, Hg^{2+} , as the cation.¹⁷¹ The usual nucleophile is the solvent. The term *oxymercuration* is used to refer to reactions in which water or an alcohol acts as the nucleophile. The adducts can be isolated as halide salts, but in synthetic applications the mercury is often replaced by hydrogen (*oxymercuration reduction*; see below).



The reactivity of mercury salts is a function of both the solvent and the counterion.¹⁷² Mercuric chloride, for example, is unreactive and mercuric acetate is the most commonly used reagent, but the trifluoroacetate, trifluoromethanesulfonate, nitrate, or perchlorate salts are preferable in some applications.

¹⁷⁰ S. Winstein and L. L. Ingraham, *J. Am. Chem. Soc.*, **74**, 1160 (1952).

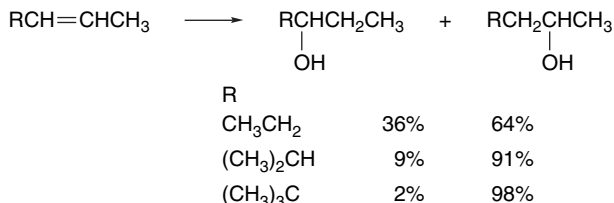
¹⁷¹ W. Kitching, *Organomet. Chem. Rev.*, **3**, 61 (1968); R. C. Larock, *Solvomercuration/Demercuration Reactions in Organic Synthesis*, Springer-Verlag, New York, 1986.

¹⁷² H. C. Brown, J. T. Kurek, M.-H. Rei, and K. L. Thompson, *J. Org. Chem.*, **49**, 2551 (1984).

The reactivity of different alkenes toward mercuration spans a considerable range and is governed by a combination of steric and electronic factors.¹⁷³ In contrast to protonation and halogenation reactions, the oxymercuration reaction is not always accelerated by alkyl substituents on the alkene. Dialkyl terminal alkenes are more reactive than monosubstituted ones, but internal disubstituted alkenes are less reactive. For example, 1-pentene is about ten times more reactive than *Z*-2-pentene and 40 times more reactive than *E*-2-pentene.¹⁷⁴ This reversal of reactivity is due to steric effects, which generally outweigh the normal electron-releasing effect of alkyl substituents.¹⁷⁵ The relative reactivity data for some pentene derivatives are given in Table 5.6.

As expected for an electrophilic reaction, the ρ values for oxymercuration of styrene (-3.16)¹⁷⁶ and α -methylstyrene (-3.12)¹⁷⁷ derivatives are negative. The positive deviation of the methoxy substituent, when treated by the Yukawa-Tsuno equation, is indicative of a modestly enhanced resonance component. The additional methyl substituent in α -methylstyrene is slightly activating and indicates that its electron-donating effect outweighs any adverse steric effect.

The addition of the nucleophile follows Markovnikov's rule and the regioselectivity of oxymercuration is ordinarily very high. Terminal alkenes are usually more than 99% regioselective and even disubstituted alkenes show significant regioselectivity, which is enhanced by steric effects.



Ref. 178

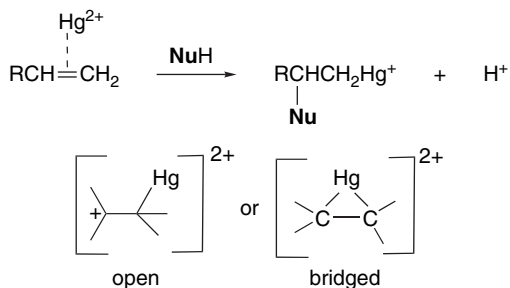
Table 5.6. Relative Reactivity of Some Alkenes in Oxymercuration

Alkene	Relative reactivity ^a
1-Pentene	6.6
2-Methyl-1-pentene	48
<i>Z</i> -2-Pentene	0.56
<i>E</i> -2-Pentene	0.17
2-Methyl-2-pentene	1.24
Cyclohexene	1.00

a. H. C. Brown and P. J. Geoghegan, Jr., *J. Org. Chem.*, **37**, 1937 (1972).

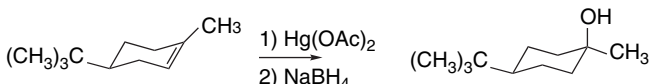
- ¹⁷³ H. C. Brown and P. J. Geoghegan, Jr., *J. Org. Chem.*, **37**, 1937 (1972); H. C. Brown, P. J. Geoghegan, Jr., G. J. Lynch, and J. T. Kurek, *J. Org. Chem.*, **37**, 1941 (1972); H. C. Brown, P. J. Geoghegan, Jr., and J. T. Kurek, *J. Org. Chem.*, **46**, 3810 (1981).
¹⁷⁴ H. C. Brown and P. J. Geoghegan, Jr., *J. Org. Chem.*, **37**, 1937 (1972).
¹⁷⁵ S. Fukuzumi and J. K. Kochi, *J. Am. Chem. Soc.*, **103**, 2783 (1981).
¹⁷⁶ A. Lewis and J. Azoro, *J. Org. Chem.*, **46**, 1764 (1981); A. Lewis, *J. Org. Chem.*, **49**, 4682 (1984).
¹⁷⁷ I. S. Hendricks and A. Lewis, *J. Org. Chem.*, **64**, 7342 (1999).
¹⁷⁸ H. C. Brown and J. P. Geoghegan, Jr., *J. Org. Chem.*, **35**, 1844 (1970).

In analogy with other electrophilic additions, the mechanism of the oxymercuration reaction can be discussed in terms of a cationic intermediate.¹⁷⁹ The cationic intermediate can be bridged (*mercurinium ion*) or open, depending on the structure of the particular alkene. The intermediates can be detected by NMR in nonnucleophilic solvents.¹⁸⁰ The addition is completed by attack of a nucleophile at the more positive carbon.

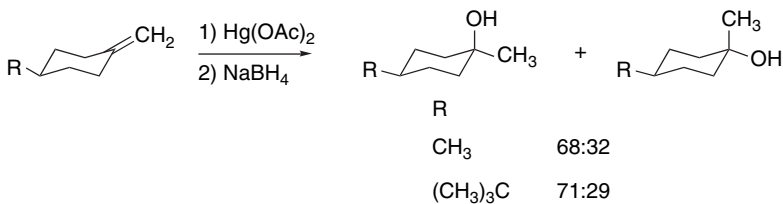


After the addition step is complete, the mercury is usually replaced by hydrogen, using a reducing agent. The net result is the addition of hydrogen and the nucleophile to the alkene, and the reaction is known as *oxymercuration reduction*. The regioselectivity is in the same sense as is observed for proton-initiated additions.¹⁸¹

Oxymercuration of unhindered alkenes is usually a stereospecific *anti* addition. This result is consistent with the involvement of a mercurinium ion intermediate that is opened by nucleophilic attack.¹⁸² Conformationally biased cyclic alkenes such as 4-*t*-butylcyclohexene and 4-*t*-butyl-1-methycyclohexene give exclusively the product of *anti*-diaxial addition.^{181,183}



Methylenecyclohexenes are not very stereoselective, showing a small preference for the axial alcohol, which corresponds to mercuration from the equatorial face.¹⁸⁴



^{179.} S. J. Cristol, J. S. Perry, Jr., and R. S. Beckley, *J. Org. Chem.*, **41**, 1912 (1976); D. J. Pasto and J. A. Gontarz, *J. Am. Chem. Soc.*, **93**, 6902 (1971).

^{180.} G. A. Olah and P. R. Clifford, *J. Am. Chem. Soc.*, **95**, 6067 (1973); G. A. Olah and S. H. Yu, *J. Org. Chem.*, **40**, 3638 (1975).

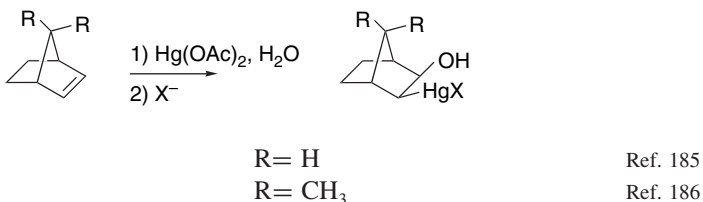
^{181.} H. C. Brown and P. J. Geoghegan, Jr., *J. Org. Chem.*, **35**, 1844 (1970); H. C. Brown, J. T. Kurek, M.-H. Rei, and K. L. Thompson, *J. Org. Chem.*, **49**, 2511 (1984); H. C. Brown, J. T. Kurek, M.-H. Rei, and K. L. Thompson, *J. Org. Chem.*, **50**, 1171 (1985).

^{182.} H. B. Vardhan and R. D. Bach, *J. Org. Chem.*, **57**, 4948 (1992).

^{183.} H. C. Brown, G. J. Lynch, W. J. Hammar, and L. C. Liu, *J. Org. Chem.*, **44**, 1910 (1979).

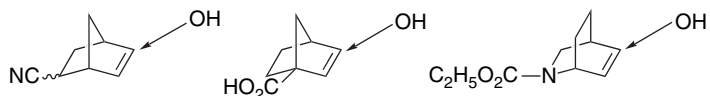
^{184.} Y. Senda, S. Kamiyama, and S. Imaizumi, *J. Chem. Soc., Perkin Trans. 1*, 530 (1978).

In contrast to the *anti* addition observed with acyclic and monocyclic alkenes, bicyclic alkenes frequently show *syn* addition. Norbornene gives exclusively *exo-syn* addition. Even 7,7-dimethylnorbornene gives the *exo-syn* product, in sharp contrast to the usual *endo*-directing effects of 7-substitution. These results are difficult to reconcile with a bridged mercurinium ion and suggest that intramolecular transfer of the nucleophile from mercury occurs. In norbornene derivatives, the competing *anti* addition is sterically restricted by the *endo* bridge.



Other bicyclic alkenes have been observed to give largely or exclusively *syn* addition.¹⁸⁷

Oxymercuration shows considerable sensitivity to polar substituents. Several early examples set the pattern, which is for the nucleophile to add at the carbon that is more remote from a polar EWG substituent.



Ref. 188

Ref. 188

Ref. 189

In considering the basis of this effect, Factor and Traylor¹⁸⁸ suggested that the EWGs “make the unsymmetrical TS having less positive charge near the substituted position the one of lowest energy.” Mayo and colleagues carried out a systematic study of the effect, including comparison of *exo* and *endo* substituents.¹⁹⁰ Some of the results of that study are shown below. The directive effect was found for both *exo* and *endo* substituents, but was somewhat stronger for *exo* groups.

A diagram of norbornene with substituents labeled: X at the bridgehead, 5 at the bridgehead position, and 6 at the adjacent position.

X	5:6 (<i>exo</i>)	5:6 (<i>endo</i>)
CH_2OTBS	1:1	1:1
CO_2CH_3	5:1	5:1
OH	6:1	3:1
OCH_2Ph	9:1	6:1
O_2CCH_3	14:1	9:1

¹⁸⁵ T. G. Traylor and A. W. Baker, *J. Am. Chem. Soc.*, **85**, 2746 (1963).

¹⁸⁶ H. C. Brown and J. H. Kawakami, *J. Am. Chem. Soc.*, **95**, 8665 (1973).

¹⁸⁷ T. N. Sokolova, V. R. Kartashov, O. V. Vasil'eva, and Y. K. Grishin, *Russ. Chem. Bull.*, **42**, 1583 (1993).

¹⁸⁸ A. Factor and T. G. Traylor, *J. Org. Chem.*, **33**, 2607 (1968).

¹⁸⁹ G. Krow, R. Rodebaugh, M. Grippi, and R. Carmosin, *Synth. Commun.*, **2**, 211 (1972).

¹⁹⁰ P. Mayo, G. Orlova, J. D. Goddard, and W. Tam, *J. Org. Chem.*, **66**, 5182 (2001).

These workers used B3PW91/LanL2DZ DFT calculations to probe the TS using $\text{Hg}(\text{O}_2\text{CH})_2$ as the reagent. Using ethene as the reactant, they found a symmetrical bridged structure to be a stable prereaction complex. The TS for addition is very unsymmetrical with partial bonding by one of the formate ligands. The TS for addition to norbornenes was somewhat looser and the addition corresponded to a four-center *syn* mechanism. These gas phase computations may bias the ethene TS toward *syn* addition by virtue of the attachment of the nucleophile to Hg^{2+} . However, the results with both ethene and norbornene suggest that there is no strong prohibition against a *syn* addition, in agreement with the experimental results.

The regioselectivity in substituted norbornenes is the result of polarization of the double bond, with the Hg^{2+} attacking the more negative carbon. The NPA charges calculated for the TS show that this polarization becomes much larger as the C–Hg bond is formed and the TS is approached. The substituent effect results from an initial polarization of the double bond that is enhanced as the TS is approached. Figure 5.5 shows the TS for C(5) and C(6) for the *endo* hydroxyl reactant. The ΔE^\ddagger for the two TSs differ by 1.6 kcal and in the direction of the observed preferred addition of Hg at C(6).

Visual models, additional information and exercises on Oxymercuration can be found in the Digital Resource available at: Springer.com/carey-sundberg.

The effect of remote polar substituents was also probed with substituted 7-methylenenorbornanes.¹⁹¹ The substituents are located in the *endo* position and cannot interact directly with the approaching reagent. Ester groups are strongly *syn*

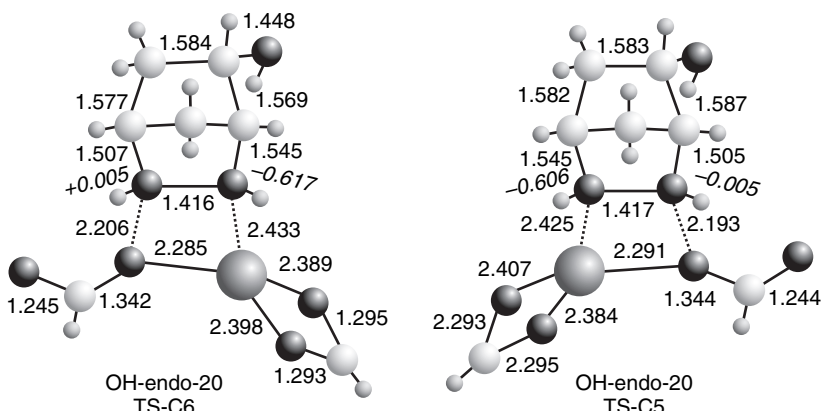
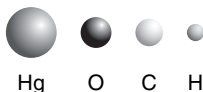
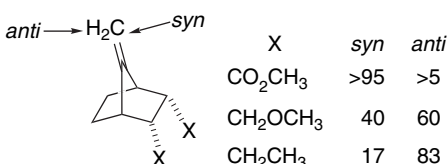


Fig. 5.5. Transition structures for C(6) and C(5) mercuration of the *endo* hydroxy derivative of norbornene. Italic numbers give the NPA charges at the reacting carbons. Reproduced from *J. Org. Chem.*, **66**, 5182 (2001), by permission of the American Chemical Society.

¹⁹¹ G. Mehta and F. A. Khan, *J. Chem. Soc., Chem. Commun.*, 18 (1991).

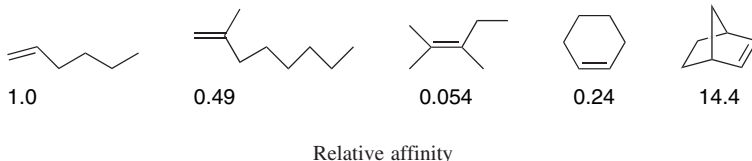
directing, whereas ethyl groups are *anti* directing. These results were attributed to differential polarization of the faces of the π bond (see Section 2.4). Similar, but much weaker, directive effects are seen for epoxidation and hydroboration.



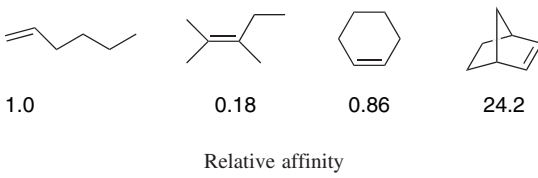
A broad mechanistic interpretation that can encompass most of these results suggests that the Hg^{2+} ion is rather loosely bound prior to the rate-determining nucleophilic addition. The bonding is weaker at the carbon best able to accommodate positive charge, resulting in Markovnikov regioselectivity. If there is little steric hindrance, *anti* addition of a nucleophile is preferred, but the *syn* mechanism is available. The *syn* mechanism, at least as modeled in the gas phase, seems to involve migration of a ligand from Hg^{2+} to carbon. It is *the nucleophilic capture that determines the regiochemistry and stereochemistry of the product*, since the mercuration step is reversible. It should also be noted that oxymercuration has a different electronic pattern from most of the other electrophilic additions in that the Hg-substituted carbon becomes *negatively charged* as bonding occurs (see Figure 5.5). This is also true in hydroboration, although less so, whereas halogenation, sulfenylation, and selenylation result in placing a more electronegative substituent on *both* carbons of the double bond.

5.6.2. Argentation—the Formation of Silver Complexes

Several analytical and separation techniques are based on the reversible formation of complexes between alkenes and Ag^+ ions.¹⁹² Analytical methods for terpenes, unsaturated acids and esters, and other unsaturated nonpolar compounds are based on the use of Ag^+ -impregnated materials for thin-layer (TLC) and high-pressure (HPLC) as well as gas-liquid (GLC) chromatography. GLC measurements done some years ago suggest that the affinity decreases with additional substituents, but increases with strain.¹⁹³



An NMR study in methanol showed a similar trend in relative stability of the Ag(I) complexes.¹⁹⁴



¹⁹² G. Dobson, W. W. Christie, and B. Nikolovadamyanova, *J. Chromatogr. B*, **671**, 197 (1995); C. M. Williams and L. N. Mander, *Tetrahedron*, **57**, 425 (2001).

¹⁹³ M. A. Muhs and F. T. Weiss, *J. Am. Chem. Soc.*, **84**, 4697 (1962).

¹⁹⁴ H. B. Varhan and R. D. Bach, *J. Org. Chem.*, **57**, 4948 (1992).

In contrast to Hg(II), Ag(I) does not normally induce intermolecular nucleophilic addition to alkenes. However, internal nucleophiles can sometimes be captured, leading to cyclization reactions.

The structure and stability of alkene-Ag⁺ complexes has also been examined by computation.¹⁹⁵ MP2/SBK(d) calculations indicate that three ethene molecules are accommodated at Ag⁺ with ΔE of -30 ± 3 kcal/mol, but subsequent ethenes are less strongly bound. The computations find stronger complexation with alkyl-substituted alkenes in the gas phase, which is in contrast to the trend in the solution stabilities. This might be the result of the greater importance of solvation in the liquid phase, whereas polarization might be the dominant factor in the gas phase.

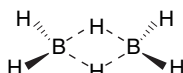
	Solution ^a	ΔE (gas phase) ^b kcal/mol
Ethene	1.32	-33.7
Propene	0.98	-36.6
Z-2-Butene	0.49	-38.0
E-2-Butene	0.27	-38.3
2-Methylpropene	0.16	-41.3
2,3-Dimethyl-2-butene	0.04	-43.5

a. T. A. van Beek and D. Suburtova, *Phytochem. Anal.*, **6**, 1 (1995).
A solution relative affinity value based on chromatographic measurements.

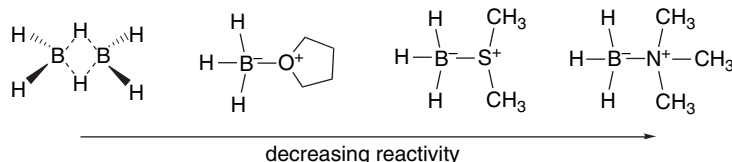
b. J. Kaneti, L. P. C. M. de Smet, R. Boom, H. Zuilhof, and E. J. R. Sudholter, *J. Phys. Chem. A*, **106**, 11197 (2002).

5.7. Synthesis and Reactions of Alkylboranes

Alkenes react with borane, BH₃, and a number of its derivatives to give synthetically useful alkylboranes. Borane is an electron-deficient molecule and in its pure form exists as a hydrogen-bridged dimer.



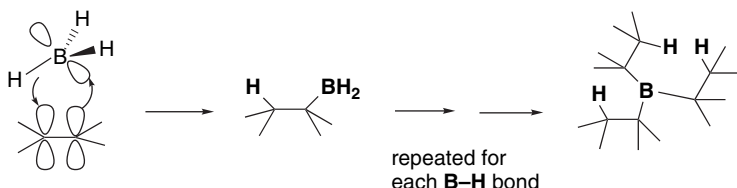
Borane reacts with electron pair donors to form Lewis acid-base complexes. The most common forms for use in synthesis are the THF and dimethyl sulfide complexes. Stronger bases, particularly amines, form less reactive adducts.



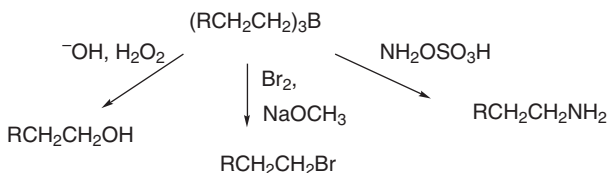
The addition of borane to alkenes is an electrophilic process, but it is concerted. The alkene donates electron density to the borane but a hydrogen shifts to carbon,

¹⁹⁵ J. Kaneti, L. C. P. M. de Smet, R. Boom, H. Zuilhof, and E. J. R. Sudholter, *J. Phys. Chem. A*, **106**, 11197 (2002).

resulting in an overall *syn* addition. In MO terms, the addition is viewed as taking place by interaction of the alkene π orbital with the vacant p orbital on boron, accompanied by concerted C–H bond formation by interaction with the empty π^* orbital.¹⁹⁶ Unhindered alkenes proceed to the trialkylborane stage by three successive additions.



As a result of a combination of steric and electronic factors, hydroboration is highly regioselective, with boron becoming bonded to the *less-substituted carbon*. The boron can eventually be replaced by hydroxy, carbonyl, amino, or halogen substituents. These reactions occur with retention of configuration. The overall transformations occur by *syn* addition with anti-Markovnikov regiochemistry.



5.7.1. Hydroboration

The synthetic applications of the hydroboration reaction are highly developed, largely through the work of H. C. Brown and his associates.¹⁹⁷ Hydroboration is one of the most widely applied of the alkene addition reactions for synthesis on a laboratory scale. Several aspects of the reaction are complementary to the reactions discussed earlier in this chapter. Hydroboration can be used to make alcohols and halides, and these reactions usually lead to the opposite (anti-Markovnikov) regiochemistry from reactions that proceed through cationic intermediates. Moreover, since there are no carbocation intermediates, there is no competition from rearrangement or elimination. The reactions are also stereospecific *syn* additions, as compared to the *anti* stereoselectivity for many reactions proceeding through cationic intermediates. On the basis of these contrasts, we might be inclined to think that hydroboration is fundamentally different from the other electrophilic addition reactions discussed in this chapter, but there are many similarities. At its outset, the hydroboration reaction involves an *electrophilic attack* on the π electrons of the alkene, just as is the case of the other reactions. The reaction is diverted to *syn* addition by the presence of the potentially

¹⁹⁶ D. J. Pasto, B. Lepeska, and T.-C. Cheng, *J. Am. Chem. Soc.*, **94**, 6083 (1972); P. R. Jones, *J. Org. Chem.*, **37**, 1886 (1972); S. Nagase, K. N. Ray, and K. Morokuma, *J. Am. Chem. Soc.*, **102**, 4536 (1980); X. Wang, Y. Li, Y.-D. Wu, M. N. Paddon-Row, N. G. Rondan, and K. N. Houk, *J. Org. Chem.*, **55**, 2601 (1990); N. J. R. van Eikema Hommes and P. v. R. Schleyer, *J. Org. Chem.*, **56**, 4074 (1991).

¹⁹⁷ G. Zweifel and H. C. Brown, *Org. React.*, **13**, 1 (1963); H. C. Brown, *Organic Synthesis via Boranes*, Wiley, New York, 1975; A. Pelter, K. Smith, and H. C. Brown, *Borane Reagents*, Academic Press, New York, 1988.

nucleophilic hydrogen on boron. As the electron-deficient boron bonds to one carbon, the hydrogen with two electrons shifts to the other carbon. The addition occurs through a four-center TS. Both the new C–B and C–H bonds are thus formed from the same side of the double bond.

Hydroboration is highly regioselective. The boron becomes bonded predominantly to the *less-substituted* carbon atom of the alkene. A combination of steric and electronic effects favors this orientation. Borane is an electrophilic reagent. The reaction with substituted styrenes exhibits a negative ρ value (-0.5).¹⁹⁸ Compared with bromination ($\rho^+ = -4.3$),¹⁹⁹ this is a weak substituent effect, but it does favor addition of the electrophilic boron at the more nucleophilic end of the double bond. In contrast to the case of addition of protic acids to alkenes, it is boron, not hydrogen, that is the more electrophilic atom. This electronic effect is reinforced by steric factors. Hydroboration is usually done under conditions in which the borane eventually reacts with three alkene molecules to give a trialkylborane. The second and third alkyl groups encounter severe steric repulsion if the boron is added at the internal carbon.

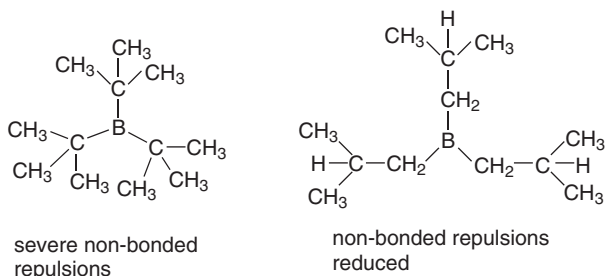


Table 5.7 provides some data on the regioselectivity of the addition of diborane and several of its derivatives to representative alkenes.

Table 5.7. Regioselectivity of Diborane and Derivatives toward Representative Alkenes

Hydroborating Reagent	Percent added at less-substituted carbon			
	1-Hexene	2-Methyl-1-Butene	4-Methyl-2-Pentene	Styrene
Diborane ^a	94	99	57	80
Chloroborane-dimethylsulfide ^b	99	99.5	—	98
Disiamylborane ^a	99	—	97	98
Thexyloborane ^c	94	—	66	95
Chlorothexylborane-dimethylsulfide ^d	99	99	97	99
9-Borabicyclo[3.3.1]nonane (9-BBN) ^e	99.9	99.8 ^f	99.8	98.5

a. G. Zweifel and H. C. Brown, *Org. React.*, **13**, 1 (1963).

b. H. C. Brown, N. Ravindran, and S. U. Kulkarni, *J. Org. Chem.*, **44**, 2417 (1969); H. C. Brown and U. S. Racherla, *J. Org. Chem.*, **51**, 895 (1986).

c. H. C. Brown and G. Zweifel, *J. Am. Chem. Soc.*, **82**, 4708 (1960).

d. H. C. Brown, J. A. Sikorski, S. U. Kulkarni, and H. D. Lee, *J. Org. Chem.* **45**, 4540 (1980).

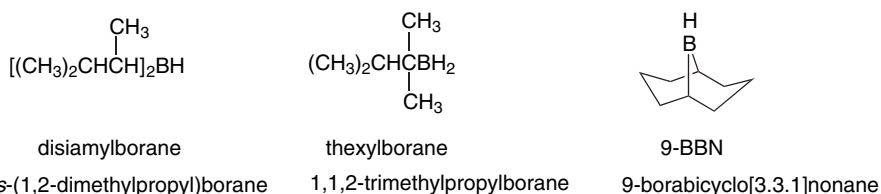
e. H. C. Brown, E. F. Knight, and C. G. Scouten, *J. Am. Chem. Soc.*, **96**, 7765 (1974).

f. Data for 2-methyl-1-pentene.

¹⁹⁸. L. C. Vishwakarma and A. Fry, *J. Org. Chem.*, **45**, 5306 (1980).

¹⁹⁹. J. A. Pincock and K. Yates, *Can. J. Chem.*, **48**, 2944 (1970).

Table 5.7 includes data for some mono- and dialkylboranes that show even higher regioselectivity than diborane itself. These derivatives are widely used in synthesis and are frequently referred to by the shortened names shown with the structures.



These reagents are prepared by hydroboration of the appropriate alkene, using control of stoichiometry to achieve the desired degree of alkylation. 9-BBN is prepared from 1,4-cyclooctadiene



As is true for most addition reactions, there is a preference for approach of the borane from the less hindered face of the double bond. Since diborane itself is a relatively small molecule, the stereoselectivity is not high for unhindered molecules. Table 5.8 gives some data comparing the direction of approach for three cyclic alkenes. The products in all cases result from *syn* addition, but the mixtures result from both the low regioselectivity and from addition to both faces of the double bond. Even 7,7-dimethylnorbornene shows only a modest preference for *endo* addition with diborane. The selectivity is much enhanced with the bulkier reagent 9-BBN.

The haloboranes BH_2Cl , BH_2Br , BHCl_2 , and BHBr_2 are also useful hydroborating reagents.²⁰⁰ These compounds are somewhat more regioselective than borane itself, but otherwise show similar reactivity. The halogen(s) can be replaced by hydride and a second hydroboration step can then be carried out. This allows for preparation of unsymmetrically substituted boranes.

Table 5.8. Stereoselectivity of Hydroboration with Cyclic Alkenes^a

Hydroboration Reagent	Product composition ^b							
	3-Methyl- cyclopentene			3-Methyl- cyclohexene			7,7-Dimethyl norbornene	
	<i>trans</i> -2	<i>cis</i> -3	<i>trans</i> -3	<i>cis</i> -2	<i>trans</i> -2	<i>cis</i> -3	<i>trans</i> -3	<i>exo</i>
Diborane	45		55	16	34	18	32	22 ^c
Disiamylborane	40		60	18	30	27	25	—
9-BBN	25	50	25	0	20	40	40	3
								97

a. Data from H. C. Brown, R. Liotta, and L. Brener, *J. Am. Chem. Soc.*, **99**, 3427 (1977), except where noted otherwise.

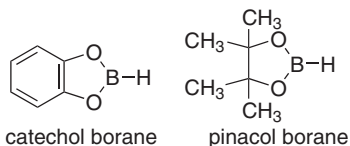
b. Product composition refers to the alcohols formed by subsequent oxidation.

c. H. C. Brown, J. H. Kawakami, and K.-T. Liu, *J. Am. Chem. Soc.*, **95**, 2209 (1973).

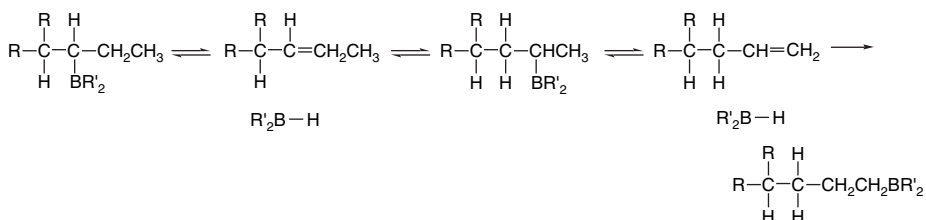
²⁰⁰ H. C. Brown and S. U. Kulkarni, *J. Organomet. Chem.*, **239**, 23 (1982).



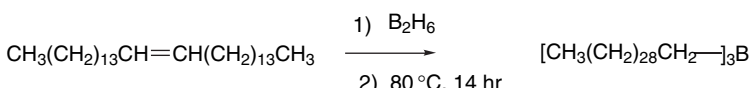
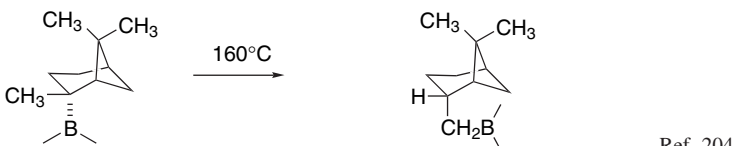
Catecholborane²⁰¹ and pinacolborane,²⁰² in which the boron has two oxygen substituents, are much less reactive hydroborating reagents than alkyl or haloboranes. The boron electron deficiency is attenuated by the oxygen atoms. Nevertheless, they are useful reagents for certain applications. The reactivity of catecholborane has been found to be substantially enhanced by addition of 10–20% of *N,N*-dimethylacetamide to CH₂Cl₂.²⁰³



Hydroboration is thermally reversible. At 160 °C and above, B–H moieties are eliminated from alkylboranes, but the equilibrium is still in favor of the addition products. This provides a mechanism for migration of the boron group along the carbon chain by a series of eliminations and additions.



Migration cannot occur past a quaternary carbon, however, since the required elimination is blocked. At equilibrium, the major trialkylborane is the least-substituted terminal isomer that is accessible, because it is the one that minimizes unfavorable steric interactions. The availability of the isomerization provides a means for *thermodynamic control* of the hydroboration reaction.



Ref. 205

²⁰¹ H. C. Brown and S. K. Gupta, *J. Am. Chem. Soc.*, **97**, 5249 (1975); H. C. Brown and J. Chandrasekharan, *J. Org. Chem.*, **48**, 5080 (1983).

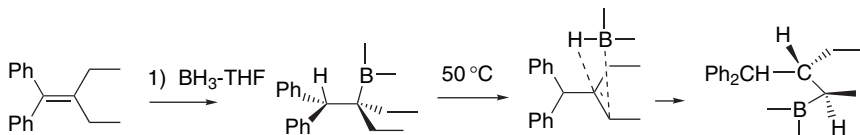
²⁰² C. E. Tucker, J. Davidson, and P. Knochel, *J. Org. Chem.*, **57**, 3482 (1992).

²⁰³ C. E. Garrett and G. C. Fu, *J. Org. Chem.*, **61**, 3224 (1996).

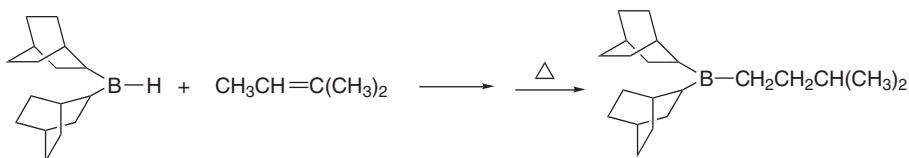
²⁰⁴ G. Zweifel and H. C. Brown, *J. Am. Chem. Soc.*, **86**, 393 (1964).

²⁰⁵ K. Maruyama, K. Terada, and Y. Yamamoto, *J. Org. Chem.*, **45**, 737 (1980).

Migrations are especially facile for *tetra*-substituted alkenes; they occur at 50–60°C and exhibit both regio- and stereoselectivity. The course of the reactions is dictated by the relative energy of the reversibly formed borane alkene complexes.²⁰⁶

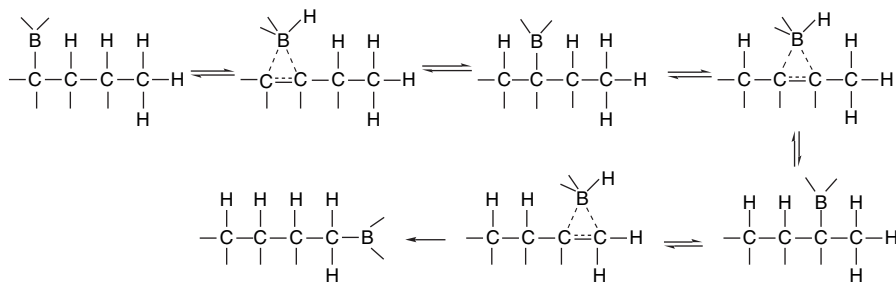


Unstrained bicyclic rings have little tendency to rearrange. *bis*-Bicyclo[2.2.2]octanylborane has been found to be particularly useful for formation and isomerization of monoalkyl derivatives.



Ref. 207

There is evidence that boron migration occurs *intramolecularly*.²⁰⁸ A TS that describes this process has been located computationally (Figure 5.6).²⁰⁹ It involves an electron-deficient π-complex about 20–25 kcal above the trialkylborane. These structures are analogous to the bridged carbocations in carbocation rearrangements. The boron can migrate to the end of the chain through a series of such structures.



5.7.2. Reactions of Organoboranes

Alkylboranes are very useful intermediates in organic synthesis. In this section we discuss methods by which the boron atom can be efficiently replaced by hydroxy,

²⁰⁶ L. O. Bromm, H. Laaziri, F. Lhermitte, K. Harms, and P. Knochel, *J. Am. Chem. Soc.*, **122**, 10218 (2000).

²⁰⁷ H. C. Brown and U. S. Racherla, *J. Am. Chem. Soc.*, **105**, 6506 (1983).

²⁰⁸ S. E. Wood and B. Rickborn, *J. Org. Chem.*, **48**, 555 (1983).

²⁰⁹ N. J. R. van Eikema Hommes and P. v. R. Schleyer, *J. Org. Chem.*, **56**, 4074 (1991).

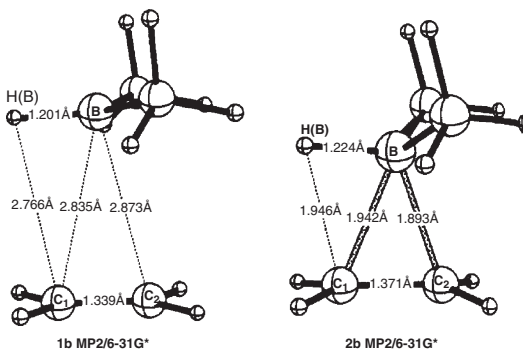
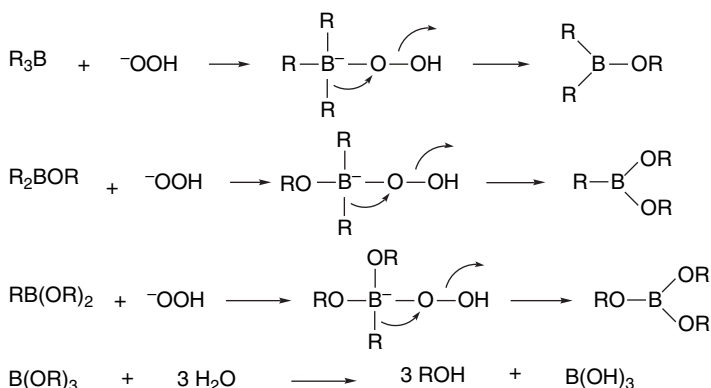


Fig. 5.6. Geometries (MP2/6-31G*) of (a) π complex and (b) transition state in reaction of ethene and dimethylborane. Reproduced from *J. Org. Chem.*, **56**, 4074 (1991), by permission of the American Chemical Society.

halogen, or amino groups. There are also important processes that use alkylboranes in the formation of new carbon-carbon bonds, and these reactions are discussed in Chapter 9 of Part B. The most widely used reaction of organoboranes is the oxidation to alcohols. Alkaline hydrogen peroxide is the reagent usually employed to effect the oxidation. The trialkylborane is converted to a trialkoxyborane (trialkyl borate) by a series of $B \rightarrow O$ migrations. The $R-O-B$ bonds are hydrolyzed in the alkaline aqueous solution, generating the alcohol. The mechanism is outlined below.



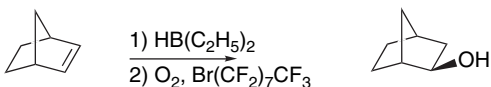
The stereochemical outcome is replacement of the $C-B$ bond by a $C-O$ bond with retention of configuration. In combination with the stereospecific *syn* hydroboration, this allows the structure and stereochemistry of the alcohols to be predicted with confidence. The preference for boronation at the less-substituted carbon of a double bond results in the alcohol being formed with regiochemistry that is complementary to that observed by direct hydration or oxymercuration, i.e., anti-Markovnikov.

Conditions that permit oxidation of organoboranes to alcohols using other oxidants, including molecular oxygen,²¹⁰ sodium peroxycarbonate,²¹¹ or amine

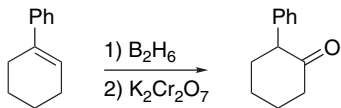
²¹⁰ H. C. Brown, M. M. Midland, and G. W. Kabalka, *J. Am. Chem. Soc.* **93**, 1024 (1971).

²¹¹ G. W. Kabalka, P. P. Wadgaonkar, and T. M. Shoup, *Tetrahedron Lett.*, **30**, 5103 (1989).

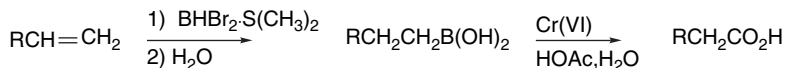
oxides²¹² have been developed. Oxone® has been recommended for oxidations done on a large scale.²¹³ The reaction with molecular oxygen is particularly effective in perfluoroalkane solvents.²¹⁴



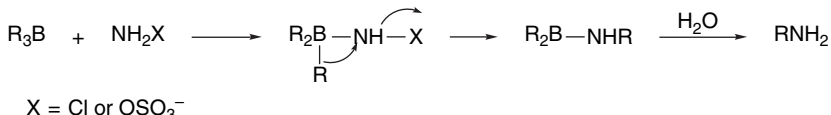
More vigorous oxidizing agents such as Cr(VI) reagents effect replacement of boron with oxidation to the carbonyl level.²¹⁵



An alternative procedure for oxidation to ketones involves treatment of the alkylborane with a quaternary ammonium perruthenate salt and an amine oxide.²¹⁶ Use of dibromoborane-dimethyl sulfide for hydroboration of terminal alkenes followed by hydrolysis and Cr(VI) oxidation gives carboxylic acids.²¹⁷



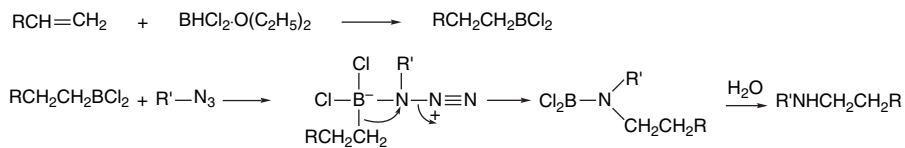
The boron atom can also be replaced by an amino group.²¹⁸ The reagents that effect this conversion are chloramine or hydroxylamine-*O*-sulfonic acid. The mechanisms of these reactions are very similar to that of the hydrogen peroxide oxidation of organoboranes. The nitrogen-containing reagent initially reacts as a nucleophile by adding at boron; then a B → N shift occurs with expulsion of chloride or sulfate. As in the oxidation, the migration step occurs with retention of configuration. The amine is freed from the borane by hydrolysis.



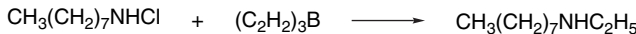
Secondary amines are formed by reaction of boranes with alkyl or aryl azides. The most efficient borane reagents are monoalkyldichloroboranes, which are generated by

- ²¹² G. W. Kabalka and H. C. Hedgecock, Jr., *J. Org. Chem.*, **40**, 1776 (1975); R. Koster and Y. Monta, *Justus Liebigs Ann. Chem.*, **704**, 70 (1967).
- ²¹³ D. H. B. Ripin, W. Cai, and S. T. Brenek, *Tetrahedron Lett.*, **41**, 5817 (2000).
- ²¹⁴ I. Klement and P. Knochel, *Synlett*, 1004 (1996).
- ²¹⁵ H. C. Brown and C. P. Garg, *J. Am. Chem. Soc.*, **83**, 2951 (1961); H. C. Brown, C. Rao, and S. Kulkarni, *J. Organomet. Chem.*, **172**, C20 (1979).
- ²¹⁶ M. H. Yates, *Tetrahedron Lett.*, **38**, 2813 (1997).
- ²¹⁷ H. C. Brown, S. V. Kulkarni, V. V. Khanna, V. D. Patil, and U. S. Racherla, *J. Org. Chem.*, **57**, 6173 (1992).
- ²¹⁸ M. W. Rathke, N. Inoue, K. R. Varma, and H. C. Brown, *J. Am. Chem. Soc.*, **88**, 2870 (1966); G. W. Kabalka, K. A. R. Sastry, G. W. McCollum, and H. Yoshioka, *J. Org. Chem.*, **46**, 4296 (1981).

the reaction of an alkene with $\text{BHCl}_2\cdot\text{Et}_2\text{O}$.²¹⁹ The entire sequence of steps and the mechanism of the final stages are summarized by the equation below.

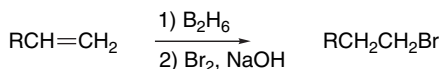


Secondary amines can also be made using the *N*-chloro derivatives of primary amines.²²⁰



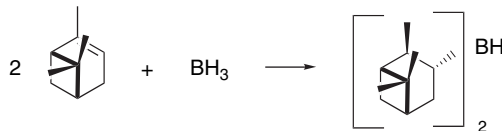
90%

Organoborane intermediates can also be used to synthesize alkyl halides. Replacement of boron by iodine is rapid in the presence of base.²²¹ The best yields are obtained using sodium methoxide in methanol.²²² If less basic conditions are desirable, the use of iodine monochloride and sodium acetate gives good yields.²²³ As is the case in hydroboration-oxidation, the regioselectivity of hydroboration-halogenation is opposite to that observed with direct ionic addition of hydrogen halides to alkenes. Terminal alkenes give primary halides.



5.7.3. Enantioselective Hydroboration

Several alkylboranes are available in enantiomerically enriched or pure form and they can be used to prepare enantiomerically enriched alcohols and other compounds from organoborane intermediates.²²⁴ The most thoroughly investigated of these boranes is *bis*-(isopinocampheyl)borane, $(\text{Ipc})_2\text{BH}$, which can be prepared in 100% enantiomeric purity from the readily available terpene α -pinene.²²⁵ Both enantiomers are available.



²¹⁹ H. C. Brown, M. M. Midland, and A. B. Levy, *J. Am. Chem. Soc.*, **95**, 2394 (1973).

²²⁰ G. W. Kabalka, G. W. McCollum, and S. A. Kunda, *J. Org. Chem.*, **49**, 1656 (1984).

²²¹ H. C. Brown, M. W. Rathke, and M. M. Rogic, *J. Am. Chem. Soc.*, **90**, 5038 (1968).

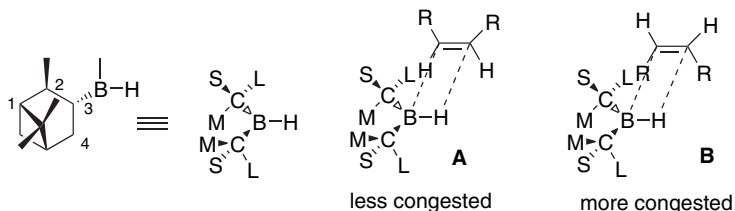
²²² N. R. De Lue and H. C. Brown, *Synthesis*, 114 (1976).

²²³ G. W. Kabalka and E. E. Gooch, III, *J. Org. Chem.*, **45**, 3578 (1980).

²²⁴ H. C. Brown and B. Singaram, *Acc. Chem. Res.*, **21**, 287 (1988); D. S. Matteson, *Acc. Chem. Res.*, **21**, 294 (1988).

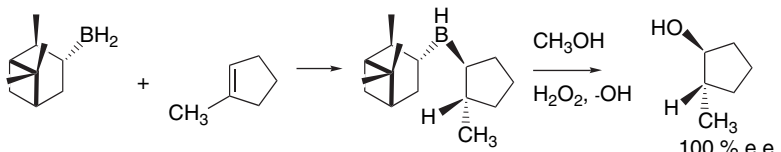
²²⁵ H. C. Brown, P. K. Jadhav, and A. K. Mandal, *Tetrahedron*, **37**, 3547 (1981); H. C. Brown and P. K. Jadhav, in *Asymmetric Synthesis*, Vol. 2, J. D. Morrison, ed., Academic Press, New York, 1983, Chap. 1.

(Ipc)₂BH adopts a conformation that minimizes steric interactions. This conformation can be represented schematically, where the S, M, and L substituents are, respectively, the 3-H, 4-CH₂, and 2-CHCH₃ groups of the carbocyclic structure. The steric environment at boron in this conformation is such that *Z*-alkenes encounter less steric encumbrance in TS A than in B.

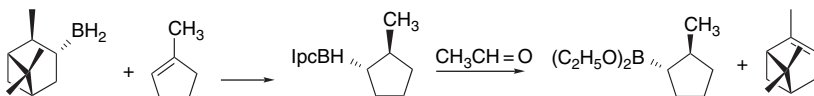


Z-2-Butene undergoes hydroboration with 98% enantioselectivity with (Ipc)₂BH.²²⁶ Other *Z*-disubstituted alkenes give good enantioselectivity (75–90%) but *E*-alkenes and simple cycloalkenes give low enantioselectivity (5–30%).²²⁷

Monoisopinocampheylborane (IpcBH₂) can be prepared in enantiomerically pure form by purification of its TMEDA adduct.²²⁸ When this monoalkylborane reacts with a prochiral alkene, one of the diastereomeric products is normally formed in excess and can be obtained in high enantiomeric purity by an appropriate separation.²²⁹ Oxidation of the borane then provides the enantiomerically enriched alcohol.



As direct oxidation also converts the original chiral terpene-derived group to an alcohol, it is not directly reusable as a chiral auxiliary. Although this is not a problem with inexpensive materials, the overall efficiency of generation of enantiomerically pure product is improved by procedures that can regenerate the original terpene. This can be done by heating the dialkylborane intermediate with acetaldehyde. The α -pinene is released and a diethoxyborane is produced.²³⁰ The usual oxidation conditions then convert this boronate ester to an alcohol.²³¹



²²⁶ H. C. Brown, M. C. Desai, and P. K. Jadhav, *J. Org. Chem.*, **47**, 5065 (1982).

²²⁷ H. C. Brown, P. K. Jadhav, and A. K. Mandal, *J. Org. Chem.*, **47**, 5074 (1982).

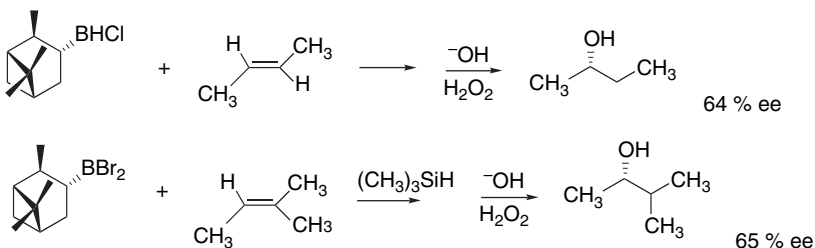
²²⁸ H. C. Brown, J. R. Schwier, and B. Singaram, *J. Org. Chem.*, **43**, 4395 (1978); H. C. Brown, A. K. Mandal, N. M. Yoon, B. Singaram, J. R. Schwier, and P. K. Jadhav, *J. Org. Chem.*, **47**, 5069 (1982).

²²⁹ H. C. Brown and B. Singaram, *J. Am. Chem. Soc.*, **106**, 1797 (1984); H. C. Brown, P. K. Jadhav, and A. K. Mandal, *J. Org. Chem.*, **47**, 5074 (1982).

²³⁰ H. C. Brown, B. Singaram, and T. E. Cole, *J. Am. Chem. Soc.*, **107**, 460 (1985); H. C. Brown, T. Imai, M. C. Desai, and B. Singaram, *J. Am. Chem. Soc.*, **107**, 4980 (1985).

²³¹ D. S. Matteson and K. M. Sadhu, *J. Am. Chem. Soc.*, **105**, 2077 (1983).

The corresponding haloboranes are also useful for enantioselective hydroboration. Isopinocampheylchloroborane can achieve 45–80% e.e. with representative alkenes.²³² The corresponding bromoborane achieves 65–85% enantioselectivity with simple alkenes when used at –78 °C.²³³



5.8. Comparison of Electrophilic Addition Reactions

In this section, we make some broad comparisons among the electrophilic addition reactions that have been discussed. We have presented data on substituent effects, regioselectivity, and stereochemistry for protonation, halogenation, sulfenylation and selenenylation, epoxidation, mercuration, and hydroboration. What general trends and insights can be gained by comparing these reactions? There have been several efforts at elucidating correlations among the different reactions. Fukuzumi and Kochi showed that when steric effects are considered in a quantitative way, there is a strong correlation between bromination and mercuration rates.²³⁴ Nelson and co-workers examined most of the reaction series and found correlations between the reactivity of various alkenes and the IP of the alkene. For some of these correlations, there were separate lines for mono-, di-, and trisubstituted alkenes, reflecting different steric environments.²³⁵ We take a similar but less detailed look at relative reactivity of several representative alkenes. Figure 5.7 is a graph of the relative reactivity (with ethene as the standard) for the various reactions. The log of the relative reactivity, as shown in Table 5.9, is plotted against alkene IP. A separate symbol is used for each reaction. The alkenes are in order of decreasing IP.

We make comparisons based on these data in very broad terms. Looking first at protonation, represented in Figure 5.7 by circles, we see that reactivity rises sharply with substitution from ethene to propene to 2-methylpropene, but 2-methyl-2-butene and 2,3-dimethyl-2-butene have rates roughly similar to 2-methylpropene. *The degree of substitution at the more-substituted carbon is the major factor in reactivity.* We can surmise from this trend that carbocation stability is the major factor in determining the protonation rates. Note also that styrene is *more reactive* than propene, again consistent with carbocation stability as the major influence on reactivity. In terms of the Hammond postulate, the carbocation is a good model of the TS because the protonation step is substantially *endothermic* and the TS is late.

²³² U. P. Dhotke, S. V. Kulkarni, and H. C. Brown, *J. Org. Chem.*, **61**, 5140 (1996).

²³³ U. P. Dhotke and H. C. Brown, *Tetrahedron Lett.*, **37**, 9021 (1996).

²³⁴ S. Fukuzumi and J. K. Kochi, *J. Am. Chem. Soc.*, **103**, 2783 (1981).

²³⁵ (a) D. J. Nelson and R. Soundararajan, *Tetrahedron Lett.*, **29**, 6207 (1988); (b) D. J. Nelson, P. J. Cooper, and R. Soundararajan, *J. Am. Chem. Soc.*, **111**, 1414 (1989); (c) D. J. Nelson, R. Li, and C. N. Brammer, *J. Org. Chem.*, **66**, 2422 (2001).

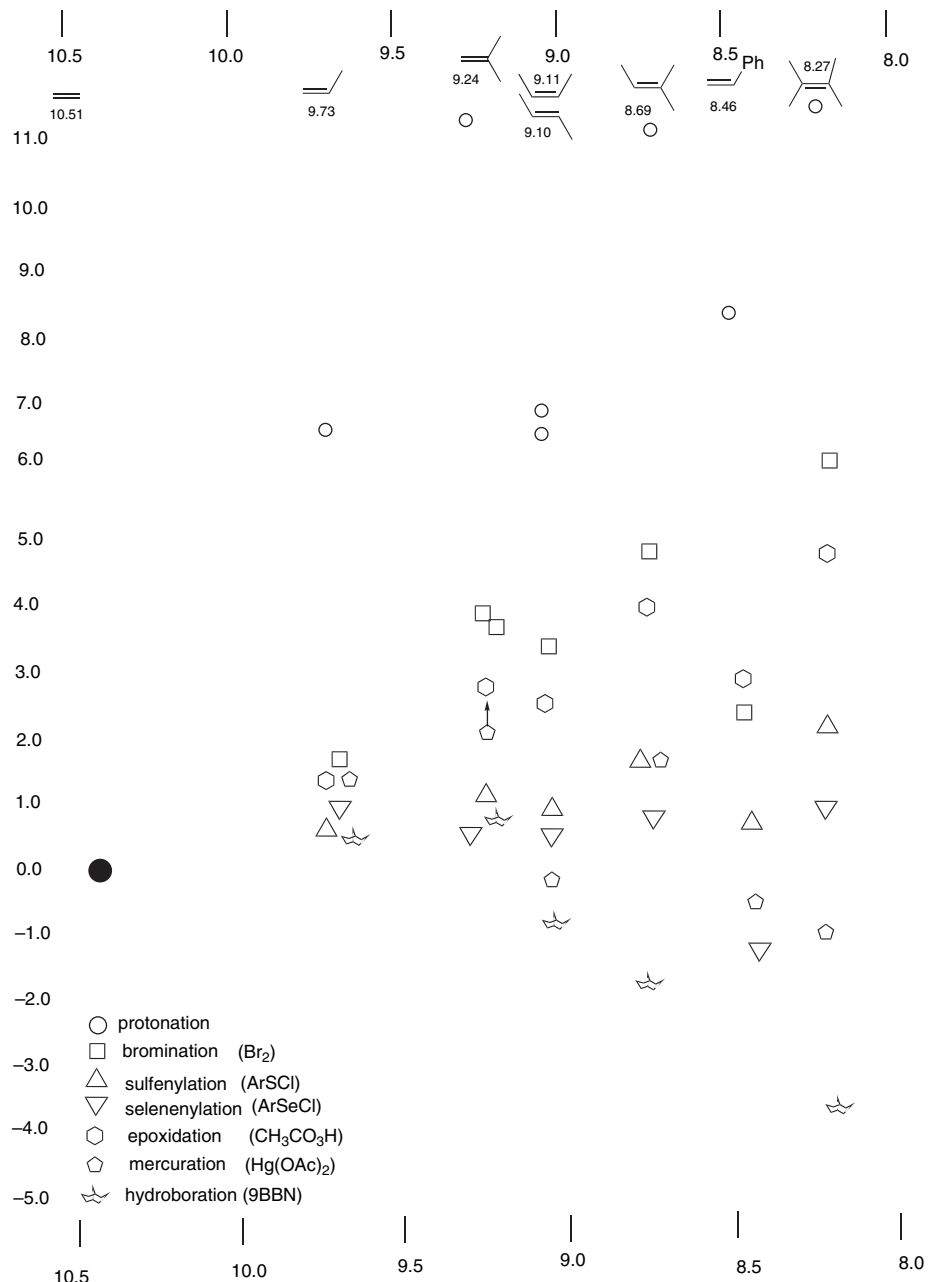


Fig. 5.7. Relationship between reactivity and IP for several alkenes.

Moving to bromination, represented by squares in the figure, we again see an increase of reactivity with alkyl substitution. Now, however, the *total number of substituents is important*. The rate continues to increase as substitution increases from ethene through 2,3-dimethyl-2-butene. This pattern is consistent with the more symmetrical (bridged) nature of the rate-determining TS. All of the substituents contribute to stabilization.

Table 5.9. Log of Relative Reactivity of Representative Alkenes.

Alkene	IP(ev) ^a	H ⁺ ^b	Br ₂ ^c	ArSeCl ^d	ArSeCl ^d	RCO ₃ H ^e	Hg ^{2+f}	9-BBN ^g	SECTION 5.8
Ethene	10.51	0	0	0	0	0	0	--	Comparison of Electrophilic Addition Reactions
Propene	9.73	6.2	1.8	0.50	0.94	1.3	1.3	0.3	
2-Methylpropene	9.24	11.5	3.7	0.93	0.83	2.5	>2	0.6	
Z-2-Butene	9.11	6.0	3.4	1.30	0.57	2.3	0.04	-1.0	
E-2-Butene	9.10	6.4	3.2	0.82	0.32	2.3	-0.5		
Z-3-Hexene	9.0 ^h							-1.2	
E-3-Hexene	9.0 ^h							-1.5	
Cyclohexene	8.95	7.5				2.8	0.0		
2-Methyl-2-butene	8.69	11.2	5.1	1.6	0.57	3.8	1.6	-2.0	
Styrene	8.46	8.2	2.4 ⁱ	-0.03	-1.3	2.7	-0.6		
2,3-Dimethyl-2-butene	8.27	11.3	6.0	2.1	0.39	4.8	-1.2	-4.2	

- a. D. R. Lide, ed., *Handbook of Chemistry and Physics*, 83rd Edition, CRC Press, Boca Raton, FL, 2002, Sec. 10.
 b. W. W. Chwang, V. J. Nowlan, and T. T. Tidwell, *J. Am. Chem. Soc.*, **99**, 7233 (1977); P. Knittel and T. T. Tidwell, *J. Am. Chem. Soc.*, **99**, 3408 (1977).
 c. J. E. Dubois and G. Mouvier, *Bull. Soc. Chim. Fr.*, 1426 (1968).
 d. G. H. Schmid and D. G. Garratt, in *The Chemistry of Double-Bonded Functional Groups*, Supplement A, Part 2, S. Patai, ed., Wiley, New York, 1977, Chap. 9.
 e. M. H. Khalil and W. Pritzkow, *J. Prakt. Chem.*, **315**, 58 (1973); The 2-butene data is for Z- and E-2-pentene.
 f. R. C. Larock, *Solvomercuration/Demercuration Reactions in Organic Synthesis*, Springer-Verlag, Berlin, 1986, pp. 86–87.
 g. D. J. Nelson, P. J. Cooper, and R. Soundararajan, *J. Am. Chem. Soc.*, **111**, 1414 (1989). The relative rates for ethene, propene and 2-methylpropene are not available. The relative rate of propene was taken as equal to that of 1-hexene and estimated as 0.5. The value listed for 2-methylpropene is that given for 2-methyl-2-pentene.
 h. Estimated from the tabulated value for the 2-hexene isomers.
 i. M.-F. Ruasse, J. E. Dubois, and A. Argile, *J. Org. Chem.*, **44**, 1173 (1979).

The most noteworthy feature of the sulfonylation and selenenylation rates (represented by the triangles) is their much diminished sensitivity to substitution. This reflects both smaller electron demand in the TS and increased sensitivity to steric factors. The relatively low rate of styrene toward selenenylation is somewhat of an anomaly, and may reflect both ground state stabilization and steric factors in the TS. The epoxidation data (CH₃CO₃H, hexagons) show a trend similar to bromination, but with a reduced slope. There is no evidence of a rate-retarding steric component. One indicator of a strong steric component is decreased reactivity of the *E*-isomer in an *E,Z*—disubstituted alkene pair, but the rates for the 2-butene isomers toward epoxidation are very similar (Table 5.9).

Mercuration exhibits a carbocation-like pattern, but with the superposition of a large steric effect. For unsubstituted terminal carbons, the rate increases from ethene to propene to 2-methylpropene. This trend also holds for internal alkenes, as 2-methyl-2-butene is more reactive than 2-butene. However, steric effects become dominant for 2,3-dimethylbutene. This incursion of steric effects in oxymercuration has long been recognized and is exemplified by the results of Nelson and co-workers, who found separate correlation lines for mono- and disubstituted alkenes.^{235b} Hydroboration by 9-BBN (structures) shows a different trend: steric effects are dominant and reactivity decreases with substitution. Similar trends apply to rates of addition of dibromoborane²³⁶ and diisiamylborane.²³⁷ The importance of steric factors is no doubt due in part to the relatively bulky nature of these boranes. However, it also reflects a decreased electron demand in the hydroboration TS.

²³⁶ H. C. Brown and J. Chandrasekharan, *J. Org. Chem.*, **48**, 644 (1983).

²³⁷ J. Chandrasekharan and H. C. Brown, *J. Org. Chem.*, **50**, 518 (1985).

An overall perspective of the data in Table 5.9 and Figure 5.7 can be gained by simply comparing the relative rates of ethene and 2,3-dimethyl-2-butene. These go from very large for protonation ($10^{11.4}$) to small ($10^{-4.2}$) for hydroboration by 9-BBN as the dominance of carbocation stability effects for protonation is replaced by dominant steric effects for hydroboration by 9-BBN.

Another useful perspective from which to compare the electrophilic addition reactions is to focus on structure of the TS and intermediates. Figure 5.8 arranges the

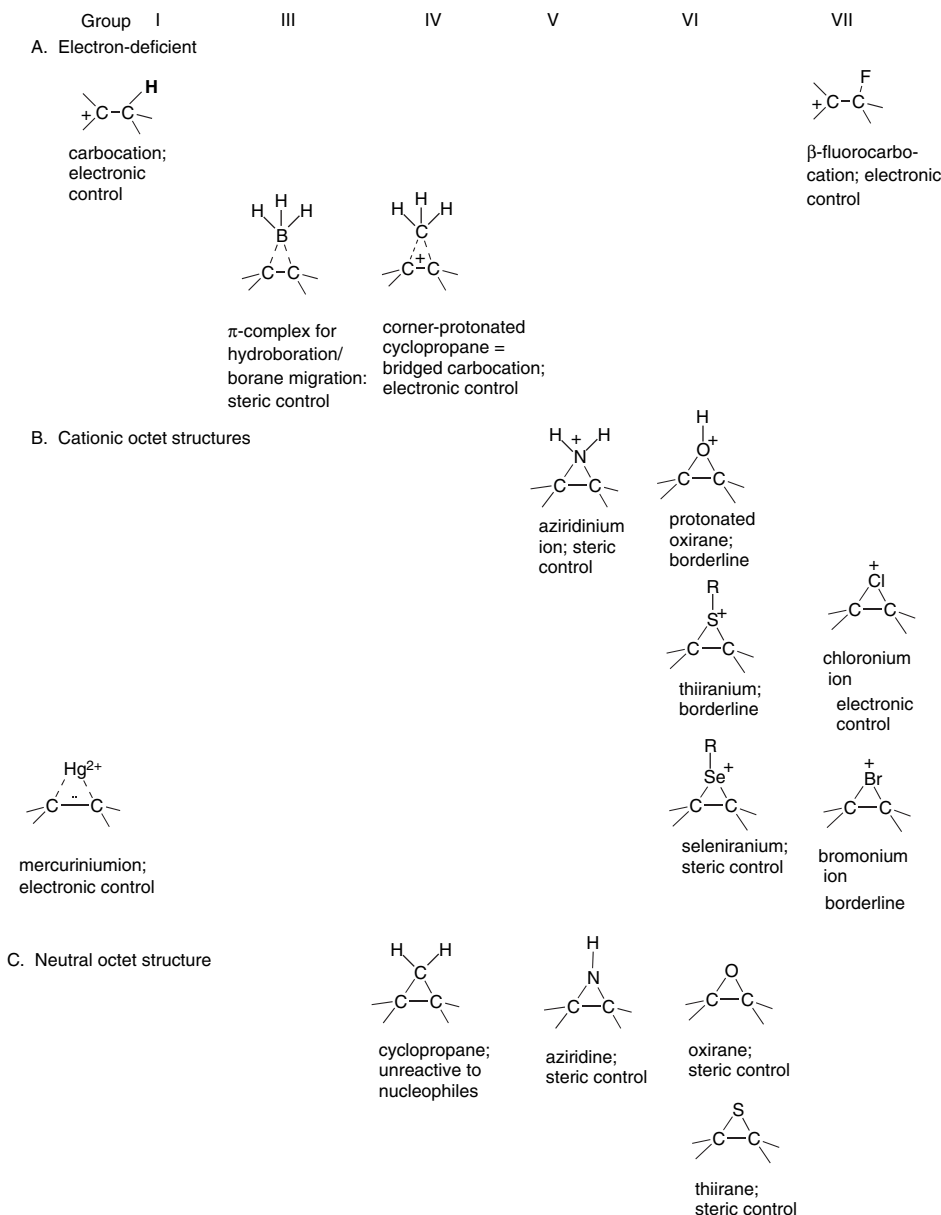
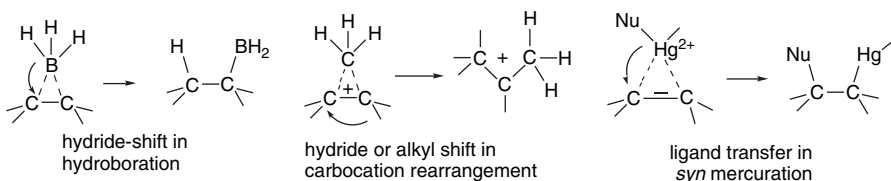


Fig. 5.8. Relationship between small ring structures and regiochemistry of addition reactions.

cationic and neutral species in relation to the periodic table. Some of these structures are stable products, others are reaction intermediates, and still other are transition structures. If the bridged and open versions of a species are comparable in energy, both are shown.

Taking the view that protonation of alkenes gives open carbocations, at least in solution, gives us a starting point for comparing the various addition reaction intermediates. From the discussion of carbocations in Chapter 4, we know the reactions that are characteristic of carbocations, namely nucleophilic capture, elimination of a proton, and rearrangement. These reactions are controlled by *electronic factors*, as illustrated by Markovnikov regioselectivity for nucleophile capture and Saytzeff regiochemistry for elimination. (see Section 4.4.3) The TSs for hydroboration and protonated cyclopropanes are related to open carbocations in being *electron deficient*. The hydroboration TS collapses by a hydride shift from boron to carbon that is driven by both electronegativity and steric factors. Corner-protonated cyclopropanes are converted to the carbocation best able to support positive charge. It is also clear from the mercuration reaction that a ligand transfer process is available when *anti-nucleophilic* addition is sterically hindered. The *syn* addition is similar to the hydride migration that occurs during hydroboration. The regiochemistry of the migration is dictated by electronic factors.



Moving to the right in the periodic table, aziridinium ions and protonated epoxides are no longer electron deficient, although they are electrophilic. Ring opening of aziridinium ions is normally controlled by *steric access*, because of the need for nucleophilic participation.²³⁸ The regioselectivity of solvo-fluorination, by contrast, is subject to electronic control and strictly follows Markovnikov's rule because of the carbocationic character of the species (see p. 496). An O-protonated or Lewis acid-activated oxirane is borderline, with instances of both Markovnikov and anti-Markovnikov ring opening (see Section 5.5.2).

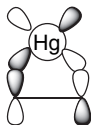
When we drop down to the next two rows of the periodic table, bridging becomes more important. For chloronium ions and bromonium ions (as in halohydrin formation; see p. 492), Markovnikov orientation (electronic control) usually prevails because the bridging bonds are relatively weak. However, the mixed regiochemistry of methoxybromination in methanol is an exception (see p. 493). For sulfenylation and selenenylation, the bridging bonds are stronger and anti-Markovnikov regiochemistry is frequently observed because nucleophilic engagement (steric access) is a critical feature for ring opening (see p. 499, 502). For the neutral small rings, cyclopropane is resistant to nucleophilic attack. Aziridines and epoxides are successively more reactive toward nucleophiles, but the regiochemistry is controlled by steric approach factors.

The proton that initiates acid-catalyzed addition processes is a hard acid and has no unshared electrons. It can form either a carbocation or a hydrogen-bridged cation. Both species are *electron deficient* and highly reactive. The formation of the cationic

²³⁸ C. M. Rayner, *Synlett*, 11 (1997).

intermediate is rate determining and nucleophilic capture is fast. The positive bromine in a bromonium ion intermediate is a softer electrophile and also has unshared electron pairs that permit a total of *four electrons* to participate in the bonding. The bromonium ion can be represented as having two covalent bonds to bromine and is *electrophilic* but not *electron deficient*. This results in a more strongly bridged and more stable species than is possible for the proton.

Where do mercuration reactions fit into this picture? A mercurinium ion has both similarities and differences, as compared with the intermediates that have been described for other electrophilic additions. The electrophile in oxymercuration reactions, ${}^+{\text{HgX}}$ or Hg^{2+} , is a soft Lewis acid and polarizes the π -electrons of an alkene to the extent that a three-center two-electron bond is formed between mercury and the two carbons of the double bond. However, there is also back bonding from $\text{Hg}^{2+}d$ orbitals to the alkene π^* orbital. There is weaker bridging in the mercurinium ion than in the three-center four-electron bonding of the bromonium ion.



Cremer and Kraka have provided another perspective on the nature of some the cyclic structures represented in Figure 5.9 by focusing on the bond paths for the three-membered ring.²³⁹ (See p. 63 to review the discussion of bond paths.) Neutral cyclopropane, aziridine, and oxirane rings are well described by the bent bond model, but the C–O bonds are somewhat less bent than those in cyclopropane. On the other hand, in protonated oxirane, the bonds begin to bend inward. For the bridged-fluorine species, there is no longer a ring; instead the structure is that of a π complex. (Remember, however, from p. 495 that a bridged fluoronium ion is unstable relative to the corresponding carbocation.) The differences in the nature of the bonds result from the relative ability of the bridging atom to donate electron density to the ring-forming orbitals, which is in the order $\text{CH}_2 > \text{NH} > \text{O} > \text{O}^+\text{H} > \text{F}^+$. These ideas are summarized in Figures 5.9.

5.9. Additions to Alkynes and Allenes

Reactions of alkynes with electrophiles are generally similar to those of alkenes. Since the HOMO of alkynes is also a π type orbital, it is not surprising that there is a good deal of similarity to the reactivity of alkenes.²⁴⁰ The fundamental questions about additions to alkynes include the following: How reactive are alkynes in comparison with alkenes? What is the stereochemistry of additions to alkynes? What is the regiochemistry of additions to alkynes? The important role of bridged ions in addition reactions of alkenes raises the question of whether similar species are involved with alkynes, where the bridged intermediates includes a double bond and would be expected to be substantially more strained.

²³⁹ D. Cremer and E. Kraka, *J. Am. Chem. Soc.*, **107**, 3800 (1985).

²⁴⁰ G. H. Schmid, *The Chemistry of the Carbon-Carbon Triple Bond*, Part. 1, S. Patai, ed., Wiley, New York, 1978, Chap. 3.

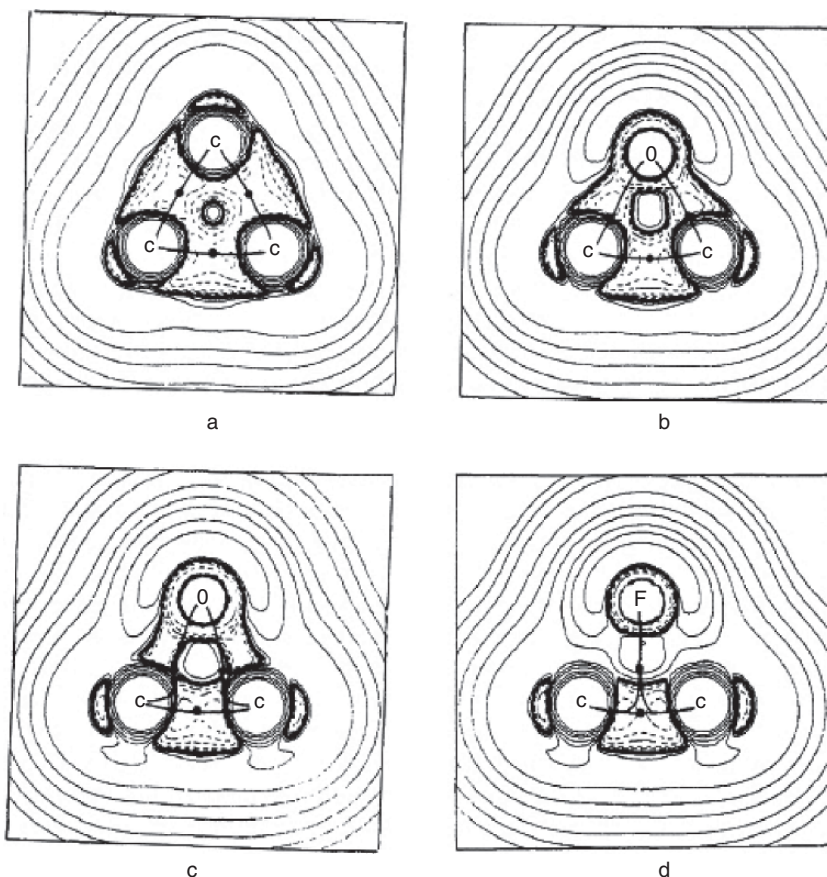
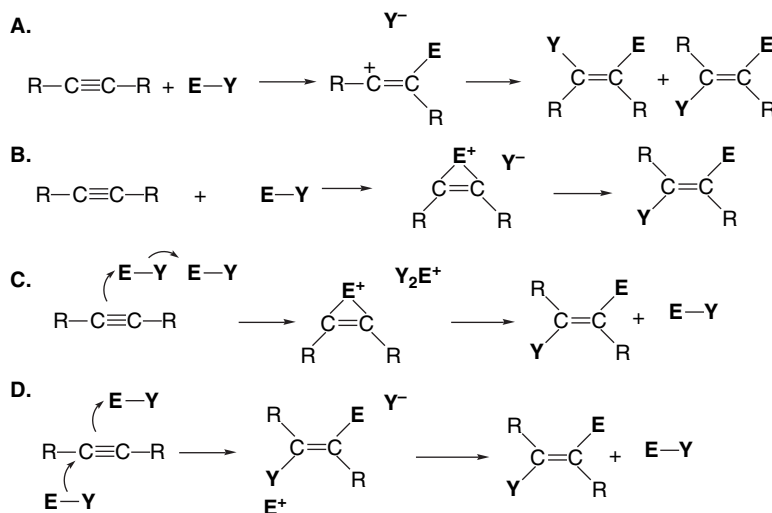


Fig. 5.9. Molecular graphs showing the Laplacian $-\nabla^2\rho(\mathbf{r})$ and bond paths. Bond paths are shown as solid lines and bond critical points as dots. Dashed contours show areas of electronic charge concentration and solid contours show regions of charge depletion. (a) cyclopropane, (b) oxirane, (c) protonated oxirane, and (d) fluorine-bridged cation. Reproduced from *J. Am. Chem. Soc.*, **107**, 3800 (1985), by permission of the American Chemical Society.



The basic mechanisms that are considered to be involved in electrophilic additions to alkynes are outlined below. The first, Mechanism A, involves a discrete vinyl cation. In general, this reaction will lead to a mixture of the two stereoisomeric addition products. Mechanisms **B** and **C** depict bridged intermediates formed without (**B**) or with (**C**) participation of a second electrophilic molecule. Mechanisms **B** and **C** should lead to *anti* addition. Mechanism **D** is a termolecular process that would be expected to be a stereospecific *anti* addition. Mechanisms **A** and **B** are of the Ad_E2 type, whereas **C** and **D** are classified as Ad_E3 . Each of these mechanisms may involve a prior complex formation between the alkyne and an electrophile.



In general, alkynes are somewhat less reactive than alkenes toward many electrophiles. A major reason for this difference in reactivity is the substantially higher energy of the vinyl cation intermediate that is formed by an electrophilic attack on an alkyne. It is estimated that vinyl cations are about 10 kcal/mol less stable than an alkyl cation with similar substitution (see p. 300). For additions that proceed through bridged intermediates, the alkynes are also less reactive because of additional strain in the intermediate. The differences in the rate of addition between alkenes and alkynes depends upon the specific electrophile and the reaction conditions.²⁴¹ Table 5.10 summarizes some specific rate comparisons. These results show large differences for bromination and chlorination but relatively small differences for protonation. The presence of a carbocation-stabilizing phenyl group reduces the difference for bromination and chlorination.

5.9.1. Hydrohalogenation and Hydration of Alkynes

Hydrogen chloride adds to aryl alkynes in acetic acid to give mixtures of α -chlorostyrenes and the corresponding vinyl acetate.²⁴² A vinyl cation, which is stabilized by the aryl substituent, is believed to be an intermediate. The ion pair formed by

Table 5.10. Relative Reactivity of Alkenes and Alkynes^a

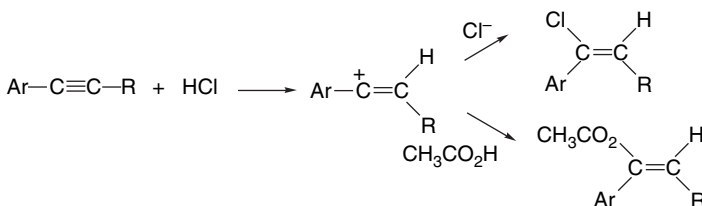
Alkene/alkyne pair	Bromination, HOAc	Chlorination, HOAc	Acid-catalyzed hydration
1-Hexene/1-hexyne	1.8×10^5	5.3×10^5	3.6
E-3-Hexene/3-hexyne	3.4×10^5	$\sim 1 \times 10^5$	16.6
Styrene/phenylethyne	2.6×10^3	7.2×10^2	0.65

a. From data tabulated in ref. 241.

²⁴¹ K. Yates, G. H. Schmid, T. W. Regulski, D. G. Garratt, H.-W. Leung, and R. McDonald, *J. Am. Chem. Soc.*, **95**, 160 (1973).

²⁴² R. C. Fahey and D.-J. Lee, *J. Am. Chem. Soc.*, **90**, 2124 (1968).

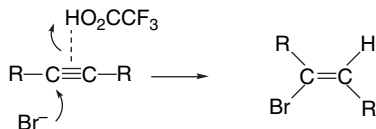
protonation can either collapse to give the vinyl halide or capture solvent to give the acetate. Aryl-substituted acetylenes give mainly the *syn* addition product.



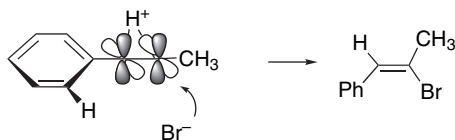
Alkyl-substituted acetylenes can react with HCl by either the Ad_E3 or the Ad_E2 mechanism. The Ad_E3 mechanism leads to *anti* addition. The preference for one or the other mechanism depends on the reactant structure and the reaction conditions. Added halide ion promotes the Ad_E3 mechanism and increases the overall rate of reaction.²⁴³ Reaction of 4-octyne with TFA in CH_2Cl_2 containing 0.1–1.0 M Br^- leads mainly to *Z*-4-bromo-4-octene by an *anti* addition. The presence of Br^- greatly accelerates the reaction as compared to reaction with TFA alone, indicating the involvement of the Br^- in the rate-determining protonation step.²⁴⁴



1-Octyne and 2-octyne also give more than 95% *anti* addition under these conditions. The reactions are formulated as concerted Ad_E3 processes, involving bromide attack on an alkene-acid complex.



Under these conditions, 1-arylalkynes react by a mixture of Ad_E2 and Ad_E3 mechanisms with the proportion of Ad_E3 reaction increasing with increasing bromide concentration and decreasing effective acidity.²⁴⁵ The Ad_E3 reaction of 1-phenylpropane gives the anti-Markovnikov product. This is believed to be due to a steric effect of the phenyl group.



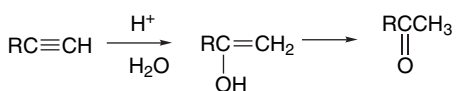
Compared to alkene additions carried out under similar conditions, there is less likely to be involvement of a cationic intermediate because of the higher energy of the vinyl cation (see Section 3.4.1).

²⁴³ R. C. Fahey, M. T. Payne, and D.-J. Lee, *J. Org. Chem.*, **39**, 1124 (1974).

²⁴⁴ H. M. Weiss and K. M. Touchette, *J. Chem. Soc., Perkin Trans. 2*, 1523 (1998).

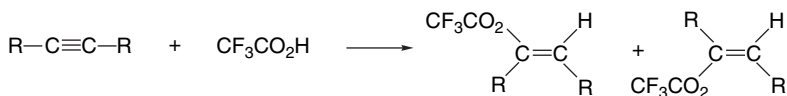
²⁴⁵ H. M. Weiss, K. M. Touchette, F. Andersen, and D. Iskhakov, *Org. Biomol. Chem.*, **1**, 2148 (2003); H. M. Weiss, K. M. Touchette, S. Angell, and J. Khan, *Org. Biomol. Chem.*, **1**, 2152 (2003).

Alkynes can be hydrated in concentrated aqueous acid solutions. The initial product is an enol, which isomerizes to the more stable ketone.



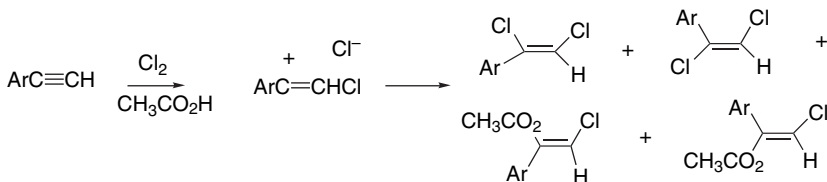
Alkynes are somewhat less reactive than alkenes. For example, 1-butene is 20 times more reactive than 1-butyne in 8.24 M H_2SO_4 .²⁴⁶ Alkyne reactivity increases with the addition of ERG substituents. Solvent isotope effects are indicative of a rate-determining protonation.²⁴⁷ These reactions are believed to proceed by rate-determining proton transfer to give a vinyl cation. Reactions proceeding through a vinyl cation would not be expected to be stereospecific, since the cation will adopt sp hybridization (see Section 3.4.1).

Alkynes react when heated with TFA to give addition products. Mixtures of *syn* and *anti* addition products are obtained.²⁴⁸ Similar addition reactions occur with trifluoromethanesulfonic acid.²⁴⁹ These reactions are analogous to acid-catalyzed hydration and proceed through a vinyl cation intermediate.



5.9.2. Halogenation of Alkynes

Alkynes undergo addition reactions with halogens. In the presence of excess halogen, tetrahaloalkanes are formed but mechanistic studies can be carried out with a limited amount of halogen so that the first addition step can be characterized. In general, halogenation of alkynes is slower than for the corresponding alkenes. We consider the reason for this later. The reaction shows typical characteristics of an electrophilic reaction. For example, the rates of chlorination of substituted phenylacetylenes are correlated by σ^+ with $\rho = -4.2$. In acetic acid, the reaction is overall second order, first order in both reactants. The addition is not very stereoselective and a considerable amount of solvent capture product is formed. All of these features are consistent with the reaction proceeding through a vinyl cation intermediate.²⁵⁰



²⁴⁶ A. D. Allen, Y. Chiang, A. J. Kresge, and T. T. Tidwell, *J. Org. Chem.*, **47**, 775 (1982).

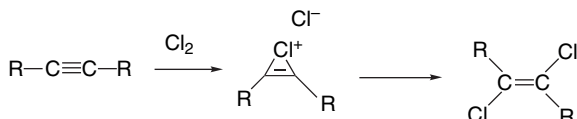
²⁴⁷ P. Cramer and T. T. Tidwell, *J. Org. Chem.*, **46**, 2683 (1981).

²⁴⁸ P. E. Peterson and J. E. Dudley, *J. Am. Chem. Soc.*, **88**, 4990 (1966); R. H. Summerville and P. v. R. Schleyer, *J. Am. Chem. Soc.*, **96**, 1110 (1974).

²⁴⁹ P. J. Stang and R. H. Summerville, *J. Am. Chem. Soc.*, **91**, 4600 (1969); R. H. Summerville, C. A. Senkler, P. v. R. Schleyer, T. E. Dueber, and P. J. Stang, *J. Am. Chem. Soc.*, **96**, 100 (1974); R. H. Summerville and P. v. R. Schleyer, *J. Am. Chem. Soc.*, **96**, 1110 (1974); G. I. Crisp and A. G. Meyer, *Synthesis*, 667 (1974).

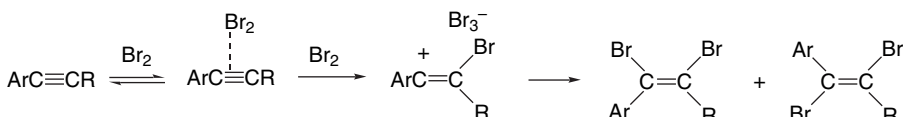
²⁵⁰ K. Yates and T. A. Go, *J. Org. Chem.*, **45**, 2377, 2385 (1980).

For alkyl-substituted alkynes, there is a difference in stereochemistry between mono- and disubstituted derivatives. The former give *syn* addition, whereas the latter react by *anti* addition. The disubstituted (internal) compounds are considerably (~ 100 times) more reactive than the monosubstituted (terminal) ones. This result suggests that the TS of the rate-determining step is stabilized by *both* alkyl substituents and points to a bridged structure. This interpretation is consistent with the *anti* stereochemistry of the reaction for internal alkynes.

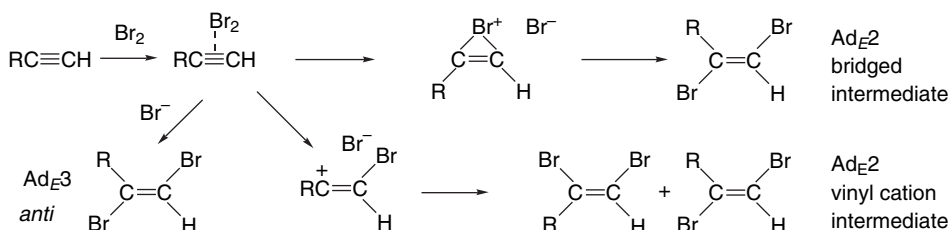


The monosubstituted intermediates do not seem to be effectively bridged, since *syn* addition predominates. A very short-lived vinyl cation appears to be the best description of the intermediate in this case.²⁵¹

The stereochemistry of bromination is usually *anti* for alkyl-substituted alkynes.²⁵² A series of substituted arylalkynes has been examined in dichloroethane.²⁵³ As with alkenes, a π -complex intermediate was observable. The ΔH for formation of the complex with 1-phenylpropane is about -3.0 kcal/mol . The overall kinetics are third order, as for an $\text{Ad}_{\text{E}3}$ mechanism. The rate-determining step is the reaction of Br_2 with the π complex to form a vinyl cation, and both *syn* and *anti* addition products are formed.



For the aryl-substituted alkynes, the reaction stereochemistry is sensitive to the aryl substitution. With EWG substituents (NO_2 , CN) the reaction becomes stereospecifically *anti* and the same is true for 2-hexyne, reflecting the diminished stability of the vinyl cation in these cases. Aryl-substituted alkynes can be shifted toward *anti* addition by including a bromide salt in the reaction medium. Under these conditions, a species preceding the vinyl cation must be intercepted by a bromide ion. This intermediate is presumably the complex of molecular bromine with the alkyne. An overall mechanistic summary is shown in the following equations.



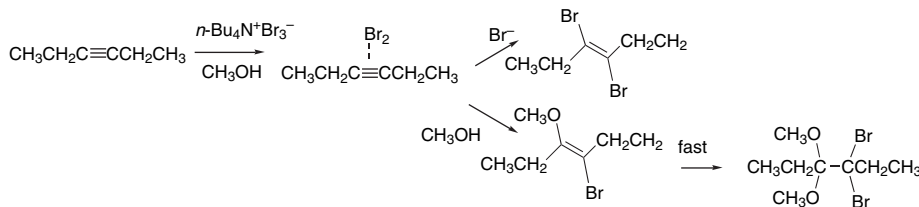
²⁵¹ K. Yates and T. A. Go, *J. Org. Chem.*, **45**, 2385 (1980).

²⁵² J. A. Pincock and K. Yates, *Can. J. Chem.*, **48**, 3332 (1970).

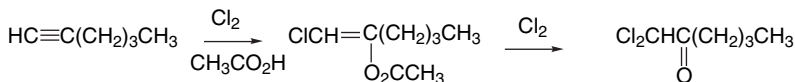
²⁵³ R. Bianchini, C. Chiappe, G. Lo Moro, D. Lenoir, P. Lemmen, and N. Goldberg, *Chem. Eur. J.*, 1570 (1999).

This scheme shows an alkyne-bromine complex as an intermediate in all alkyne brominations, which is analogous to the case of alkenes. The complex may dissociate to a vinyl cation when the cation is sufficiently stable, as is the case when there is an aryl substituent. It may collapse to a bridged bromonium ion or undergo reaction with a nucleophile. The latter is the dominant reaction for alkyl-substituted alkynes and leads to stereospecific *anti* addition. Reactions proceeding through vinyl cations are nonstereospecific.

As for alkenes, the alkyne-Br₂ complex can be intercepted by nucleophilic solvent. Alkynes react with *n*-Bu₄N⁺Br₃⁻ in methanol to give a mixture of dimethoxydibromo and *E*-dibromo products. A key aspect of this reaction is the high reactivity of the methoxybromo intermediate, which is more reactive than the starting material. Evidently, the dibromo intermediate is unreactive toward Br₃⁻.²⁵⁴



Chlorination of 1-hexyne in acetic acid gives mainly to 1,1-dichlorohexan-2-one via chlorination and deacetylation of the initial product, 2-acetoxy-1-chlorohexene.



The corresponding intermediate, *E*-3-acetoxy-4-chlorohexene can be isolated from 3-hexyne.²⁵⁵

The rates of bromination of a number of alkynes have been measured under conditions that permit comparison with the corresponding alkenes. The rate of bromination of styrene exceeds that of phenylacetylene by about 10³.²⁵⁶ For dialkylacetylene-disubstituted alkene comparisons, the ratios range from 10³ to 10⁷, being greatest in the least nucleophilic solvents.²⁵⁷ Bromination of alkyl-substituted alkynes shows rate enhancement by both alkyl substituents, and this indicates that the TS has bridged character.²⁵⁸ Remember (p. 512) that alkene bromination was similar in this respect. The lower reactivity of the alkynes is probably due to a combination of factors including greater strain in the bridged TS and reduced electron-donating capacity of alkynes. The IP of 2-butyne (9.6 eV), for example, is considerably higher than that of 2-butene (9.1 eV).

MP2/6-311+G** and B3LYP/6-311+G** computations have been used to compare the stability of the Br₂ complexes with ethene, ethyne, and allene. The computed

²⁵⁴ J. Berthelot, Y. Benammar, and B. Desmazieres, *Synth. Commun.*, **27**, 2865 (1997).

²⁵⁵ G. E. Heasley, C. Coddng, J. Sheehy, K. Gering, V. L. Heasley, D. F. Shellhamer, and T. Rempel, *J. Org. Chem.*, **50**, 1773 (1985).

²⁵⁶ M.-F. Ruasse and J.-E. Dubois, *J. Org. Chem.*, **42**, 2689 (1977).

²⁵⁷ K. Yates, G. H. Schmid, T. W. Regulski, D. G. Garratt, H.-W. Leung, and R. McDonald, *J. Am. Chem. Soc.*, **95**, 160 (1973); J. M. Kornprobst and J.-E. Dubois, *Tetrahedron Lett.*, 2203 (1974); G. Modena, F. Rivetti, and U. Tonellato, *J. Org. Chem.*, **43**, 1521 (1978).

²⁵⁸ G. H. Schmid, A. Modro, and K. Yates, *J. Org. Chem.*, **45**, 665 (1980).

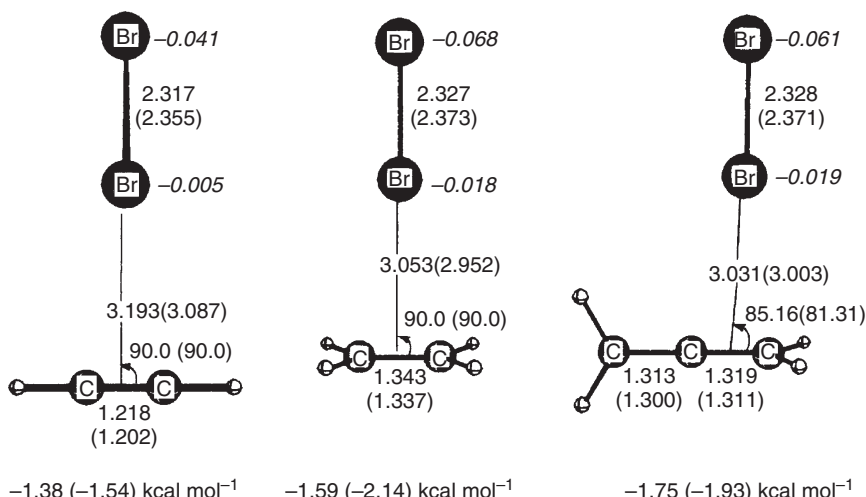
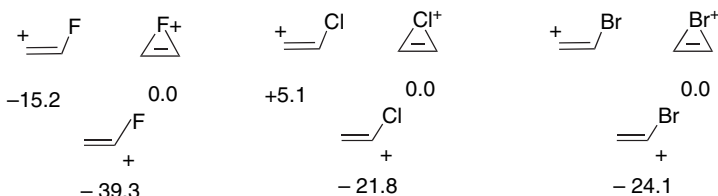


Fig. 5.10. Optimized structures and ΔE for formation of (a) ethyne-Br₂, (b) ethene-Br₂, and (c)allene-Br₂ complexes. Values of ΔE from MP2/6-311+G** and B3LYP/6-311G** (the latter in parentheses). Reproduced from *Chem. Eur. J.*, 967 (2002), by permission of Wiley-VCH.

structures and ΔE for formation of the complex are shown in Figure 5.10.²⁵⁹ The structures and energies are quite similar. This indicates that it is the formation of the cationic intermediate that is more difficult for alkynes.

Calculations comparing the open β -halovinyl and bridged cations have been reported using MP2/6-311G++(3d f ,3pd)- and B3LYP/6-31+G(d)-level computations.²⁶⁰ The bridged ions are found to be favored for chlorine and bromine but the open ion is favored for fluorine. The β -chloro and β -bromovinyl cations are found not to be minima. They rearrange to the much more stable α -halovinyl cations by a hydride shift. The bridged ions tend to be more strongly stabilized by solvation than the open ions. As was noted for the halonium ions derived from alkenes (p. 495), the charge on halogen is positive for Cl and Br, but negative for F.



When a methyl group is added, the vinyl cation is favored. The open cation was also favored for ions derived from 2-butyne.

Computational studies have also explored the issue of how the π complex is converted to the intermediate and several potential mechanisms have been described.²⁶¹

²⁵⁹. C. Chiappe, A. de Rubertis, H. Detert, D. Lenoir, C. S. Wannere, and P. v. R. Schleyer, *Chem. Eur. J.*, 967 (2002).

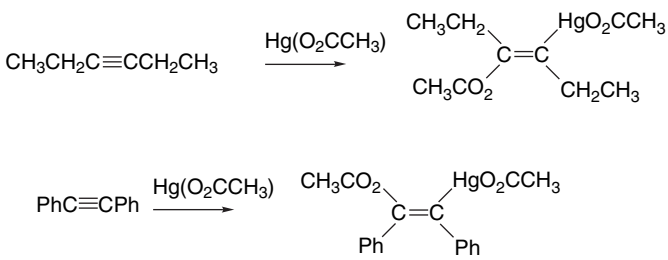
²⁶⁰. T. Okazaki and K. K. Laali, *J. Org. Chem.*, **70**, 9139 (2005).

²⁶¹. R. Herges, A. Papafilippopoulos, K. Hess, C. Chiappe, D. Lenoir, and H. Detert, *Angew. Chem. Int. Ed.*, **44**, 1412 (2005); M. Zabalov, S. S. Karlov, D. A. Le menovskii, and G. S. Zaitseva, *J. Org. Chem.*, **70**, 9175 (2005).

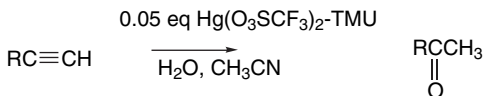
A salient result of these studies is that ionization is energetically prohibitive, at least in the gas phase. This finding is consistent with experimental studies that indicate strong acceleration in polar solvents or in the presence of acids that can facilitate ionization.

5.9.3. Mercuration of Alkynes

Alkynes react with mercuric acetate in acetic acid to give addition products. For 3-hexyne the product has *E*-stereochemistry but the *Z*-isomer is isolated from diphenylacetylene.²⁶² The kinetics of the addition reactions are first order in both alkyne and mercuric acetate.²⁶³



The most common synthetic application of mercury-catalyzed addition to alkynes is the conversion of alkynes to ketones. This reaction is carried out under aqueous conditions, where the addition intermediate undergoes protonation to regenerate Hg^{2+} . Mercuric triflate has been found to be a useful reagent for this reaction.²⁶⁴



5.9.4. Overview of Alkyne Additions

We can understand many of the general characteristics of electrophilic additions to alkynes by recognizing the possibility for both bridged ions and vinyl cations as intermediates. Reactions proceeding through vinyl cations are expected to be nonstereospecific, with the precise stereochemistry depending upon the lifetime of the vinyl cation and the identity and concentration of the potential nucleophiles. Stereospecific *anti* addition is expected from processes involving nucleophilic attack on either a bridged ion intermediate or an alkyne-electrophile complex. These general mechanisms also explain the relative reactivity of alkenes and alkynes in comparable addition processes. In general, reactions that proceed through vinyl cations, such as those involving rate-determining protonation, are only moderately slower for alkynes as compared to similar alkenes. This is attributed to the somewhat higher energy of vinyl cations compared to cations with sp^2 hybridization. It has been estimated that this difference for secondary ions is around 10–15 kcal/mol, a significant but not an

²⁶² R. D. Bach, R. A. Woodard, T. J. Anderson, and M. D. Glick, *J. Org. Chem.*, **47**, 3707 (1982).

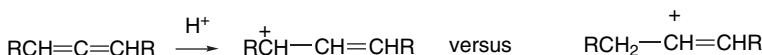
²⁶³ M. Bassetti and B. Floris, *J. Org. Chem.*, **51**, 4140 (1986).

²⁶⁴ M. Nishizawa, M. Skwarczynski, H. Imagawa, and T. Sugihara, *Chem. Lett.*, 12 (2002).

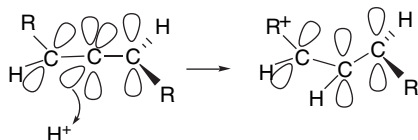
enormous difference,²⁶⁵ which is partially compensated by the higher ground state energy of the alkynes. Reactions that proceed through TSs leading to bridged intermediates typically show much greater rate retardation for the alkyne addition. Bromination is the best studied example of this type. The lower rate reflects the greater strain of bridged species in the case of alkynes. Bridged intermediates derived from alkynes must incorporate a double bond in the three-membered ring.²⁶⁶ The activation energies for additions to alkynes through bridged intermediates are thus substantially greater than for alkenes.

5.9.5. Additions to Allenes

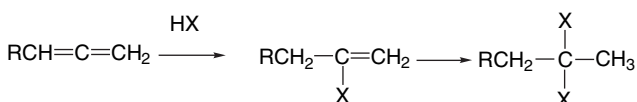
Electrophilic additions to allenes represent an interesting reaction type that is related to additions to both alkenes and alkynes.²⁶⁷ An allene could, for example, conceivably be protonated at either a terminal sp^2 carbon or the central sp carbon.



The allylic carbocation resulting from protonation of the center carbon might seem the obvious choice but, in fact, the kinetically favored protonation at a sp^2 carbon leads to the vinyl cation intermediate. The reason for this is stereoelectronic. The allene structure is nonplanar, so that a protonation of the center carbon leads to a twisted structure that lacks of allylic conjugation. This twisted cation is calculated to be about 36–38 kcal/mol higher in energy than the cation formed by protonation at a terminal carbon.²⁶⁸



Consistent with this generalization, addition of hydrogen halides to terminal allenes initially gives the vinyl halide; if the second double bond reacts, a geminal dihalide is formed.²⁶⁹ The regioselectivity of the second step is consistent with Markovnikov's rule because a halogen atom can stabilize a carbocation by resonance (see Section 3.4.1).



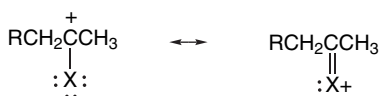
²⁶⁵ Z. Rappoport, in *Reactive Intermediates*, Vol. 3, R. A. Abramovitch, ed., Plenum Press, New York, 1985, Chap. 7; Y. Apeloig and T. Muller, in *Dicoordinated Carbocations*, Z. Rappoport and P. J. Stang, eds., John Wiley & Sons, New York, 1997, Chap. 2.

²⁶⁶ G. Melloni, G. Modena, and U. Tonellato, *Acc. Chem. Res.*, **8**, 227 (1981).

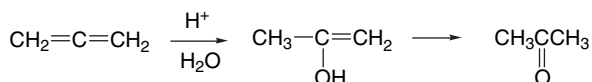
²⁶⁷ For a review of electrophilic additions to allenes, see W. Smadja, *Chem. Rev.*, **83**, 263 (1983).

²⁶⁸ K. B. Wiberg, C. M. Breneman, and T. J. Le Page, *J. Am. Chem. Soc.*, **112**, 61 (1990); A. Gobbi and G. Frenking, *J. Am. Chem. Soc.*, **116**, 9275 (1994).

²⁶⁹ T. L. Jacobs and R. N. Johnson, *J. Am. Chem. Soc.*, **82**, 6397 (1960); R. S. Charleston, C. K. Dalton, and S. R. Schraeder, *Tetrahedron Lett.*, 5147 (1969); K. Griesbaum, W. Naegle, and G. G. Wanless, *J. Am. Chem. Soc.*, **87**, 3151 (1965).

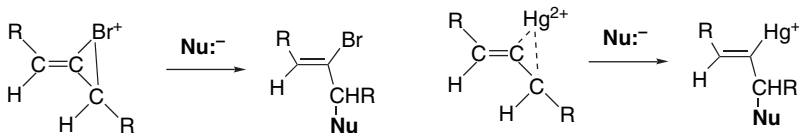


Strong acids in aqueous solution convert allenes to ketones via an enol intermediate. This process also involves protonation at a terminal carbon.



The kinetic features of this reaction, including the solvent isotope effect, are consistent with a rate-determining protonation to form a vinyl cation.²⁷⁰

Allenes react with other typical electrophiles such as the halogens and mercuric ion. In systems where bridged ion intermediates would be expected, nucleophilic capture generally occurs at the allylic position. This pattern is revealed, for example, in the products of solvent capture in halogen additions²⁷¹ and by the structures of mercurcation products.²⁷²



5.10. Elimination Reactions

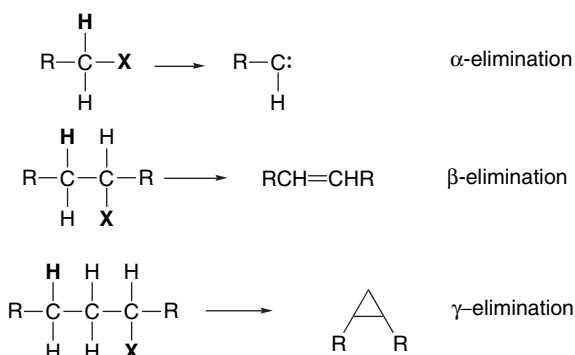
Elimination reactions involve the removal of another molecule from a reactant. In this section we focus on polar elimination reactions involving heterolytic bond breaking. A fundamental example involves deprotonation in conjunction with expulsion of a good leaving group, such as dehydrohalogenation. Elimination reactions can be classified according to the structural relationship between the proton and the leaving group. The products of α eliminations are unstable divalent carbon species called carbenes, which are discussed in Chapter 10 of Part B. Here attention is focused on β -elimination reactions that lead to formation of carbon-carbon double bonds.²⁷³

²⁷⁰ P. Cramer and T. T. Tidwell, *J. Org. Chem.*, **46**, 2683 (1981).

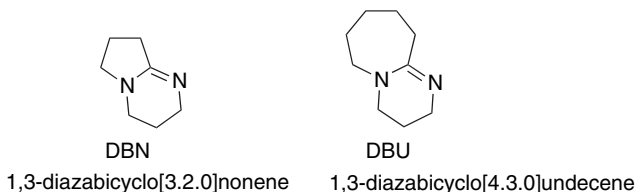
²⁷¹ H. G. Peer, *Recl. Trav. Chim. Pays-Bas*, **81**, 113 (1962); W. R. Dolbier, Jr., and B. H. Al-Sader, *Tetrahedron Lett.*, 2159 (1975).

²⁷² W. Waters and E. F. Kieter, *J. Am. Chem. Soc.*, **89**, 6261 (1967).

²⁷³ Reviews: J. R. Gandler, in *The Chemistry of Double-bonded Functional Groups*, S. Patai, ed., Wiley-Interscience, New York, 1989, Chap. 12; E. Baciocchi, in *Chemistry of Halides, Pseudo-Halides and Azides*, Part 2, S. Patai and Z. Rappoport, eds., Wiley-Interscience, New York, 1983, Chap. 23; W. H. Saunders, Jr., and A. F. Cockerill, *Mechanisms of Elimination Reactions*, Wiley, New York, 1973; D. J. McLennan, *Tetrahedron*, **31**, 2999 (1975).



Some representative examples of β -elimination reactions are given in Scheme 5.2. Entry 1 is a typical dehydrohalogenation that involves no issue of regioselectivity or stereoselectivity. With primary reactants, the main competing reaction is substitution. The base used in Entry 1 ($K^+ \cdot -O-t\text{-}Bu$) favors elimination over substitution, as compared with less branched alkoxides. Entry 2 illustrates the issues of regiochemistry and stereochemistry that can arise, even with a relatively simple reactant and also shows that substitution can compete with elimination in unhindered systems. Entry 3 shows the use of a very hindered alkoxide to favor the less-substituted product. The strong organic bases DBU²⁷⁴ and DBN²⁷⁵ can also effect dehydrohalogenation, as illustrated by Entry 4. These bases are particularly effective for reactants that are easily ionized, such as tertiary halides.



Entry 5 is a case in which the carbanion-stabilizing effect of a carbonyl group facilitates elimination by a relatively weak base and controls regiochemistry by favoring deprotonation of the α -carbon. Entries 6 and 7 are tosylate eliminations. Generally speaking, tosylates give a higher proportion of substitution than do halides.²⁷⁶ Entries 8 and 9 are examples of the *Hofmann elimination reaction*, which is a case where the relatively poor and bulky leaving group (trimethylamine) leads to a preference for formation of the less-substituted alkene (see Section 5.10.2).

In the sections that follow, we discuss the mechanisms of these and related reactions and explore the relationship between mechanism and regio-/stereoselectivity. We also look at some examples that illustrate how choice of reactant, reagent, and solvent can influence the outcome of the reaction.

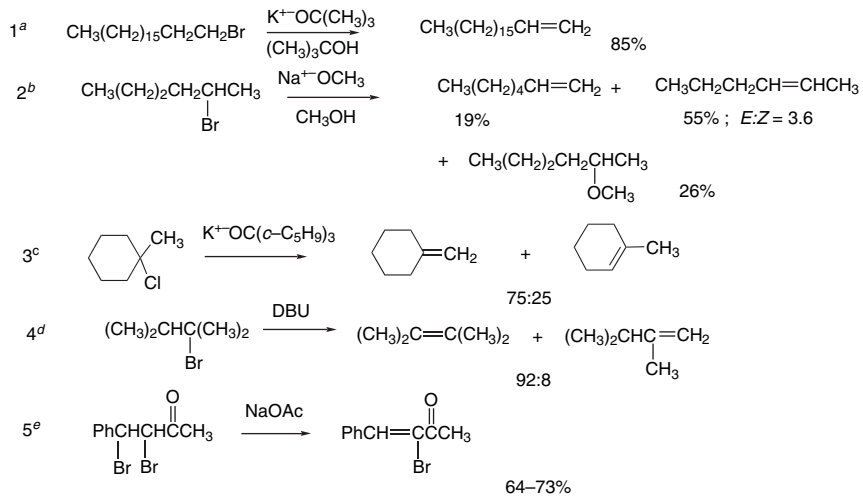
²⁷⁴ H. Oediger and F. Moeller, *Angew. Chem. Int. Ed. Engl.*, **6**, 76 (1967); P. Wolkoff, *J. Org. Chem.*, **47**, 1944 (1982).

²⁷⁵ H. Oediger, H. J. Kabbe, F. Moeller, and K. Eiter, *Chem. Ber.*, **99**, 2012 (1966).

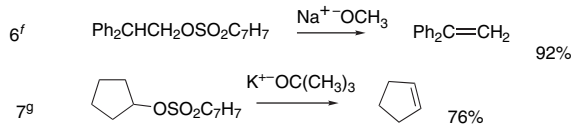
²⁷⁶ P. Veeravagu, R. T. Arnold, and E. W. Eigenmann, *J. Am. Chem. Soc.*, **86**, 3072 (1964).

Scheme 5.2. Representative β -Elimination Reactions

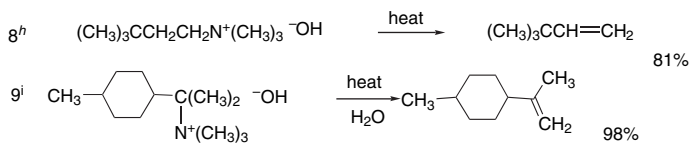
A. Dehydrohalogenation



B. Dehydrosulfonation



C. Eliminations of Quaternary Ammonium Hydroxides



a. P. Veeragu, R. T. Arnold, and E. W. Eigemann, *J. Am. Chem. Soc.*, **86**, 3072 (1964).

b. R. A. Bartsch and J. F. Bennett, *J. Am. Chem. Soc.*, **90**, 408 (1968).

c. S. A. Acharya and H. C. Brown, *J. Chem. Soc., Chem. Commun.*, 305 (1968).

d. P. Wolkoff, *J. Org. Chem.*, **47**, 1944 (1982).

e. N. H. Cromwell, D. J. Cram, and C. E. Harris, *Org. Synth.*, **III**, 125 (1953).

f. P. J. Hamrick, Jr., and C. R. Hauser, *J. Org. Chem.*, **26**, 4199 (1961).

g. C. H. Snyder and A. R. Soto, *J. Org. Chem.*, **29**, 742 (1964).

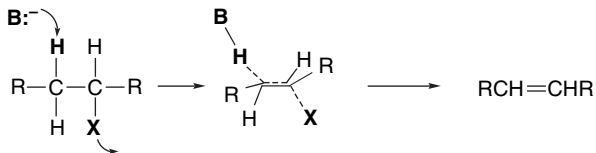
h. A. C. Cope and D. L. Ross, *J. Am. Chem. Soc.*, **83**, 3854 (1961).

i. L. C. King, L. A. Subuskey, and E. W. Stern, *J. Org. Chem.*, **21**, 1232 (1956).

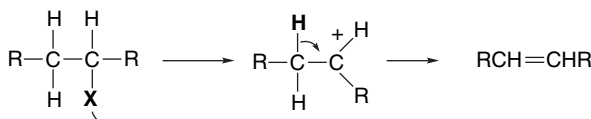
5.10.1. The E2, E1 and E1cb Mechanisms

The β -eliminations can be subdivided on the basis of the mechanisms involved. Three distinct limiting mechanisms are outlined below.

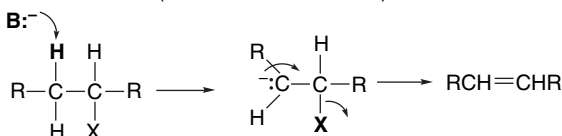
E2 Mechanism (concerted)



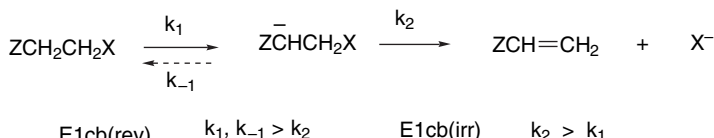
E1 Mechanism (carbocation intermediate)



E1cb Mechanism (carbanion intermediate)



The E2 mechanism involves a bimolecular TS in which removal of a proton β to the leaving group is concerted with departure of the leaving group. The rate-determining step in the E1 mechanism is the unimolecular ionization of the reactant to form a carbocation intermediate. This is the same process as the rate-determining step in the S_N1 mechanism. Elimination is completed by removal of a β -proton. The E1cb mechanism, like the E1, involves two steps, but the order is reversed. Deprotonation, forming a carbanion intermediate, precedes expulsion of the leaving group. E1cb mechanisms can be subdivided into $E1cb_{(irr)}$ and $E1cb_{(rev)}$, depending on whether the formation of the carbanion intermediate is or is not rate determining. If the anion is formed reversibly it may be possible to detect proton exchange with the solvent ($E1cb_{(rev)}$). This is not the case if formation of the carbanion is the rate-determining step ($E1cb_{(irr)}$).



The correlation of many features of β -elimination reactions is facilitated by recognition that these three mechanisms represent *variants of a continuum of mechanistic possibilities*. Many β -elimination reactions occur via mechanisms that are intermediate between the limiting mechanistic types. This idea, called the *variable E2 transition state theory*, is outlined in Figure 5.11.

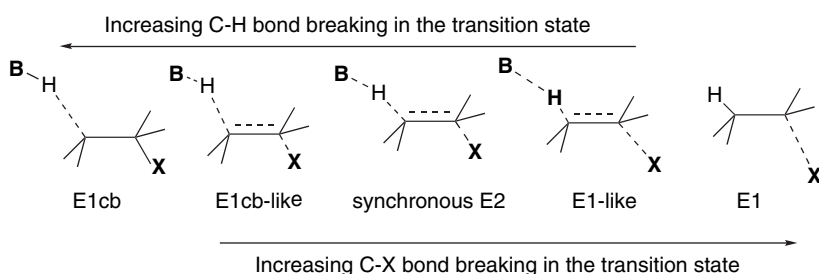
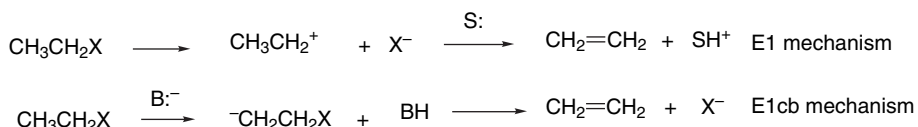


Fig. 5.11. Variable transition state theory of elimination reactions. J. F. Bunnett, *Angew. Chem. Int. Ed. Engl.*, **1**, 225 (1962); J. F. Bunnett, *Survey Prog. Chem.*, **5**, 53 (1969); W. H. Saunders, Jr., and A. F. Cockerill, *Mechanisms of Elimination Reactions*, John Wiley & Sons, New York, 1973, pp. 48–55; W. H. Saunders, Jr., *Acc. Chem. Res.*, **9**, 19 (1976).

The variable transition state theory allows discussion of reactions proceeding through TSs of intermediate character in terms of the limiting mechanistic types. These are called “E1cb-like” and “E1-like,” as illustrated in Figure 5.11. The most important factors to be considered are: (1) the nature of the leaving group, (2) electronic and steric effect of substituents in the reactant molecule, (3) the nature of the base, and (4) solvent effects.

The ideas embodied in the variable transition state theory of elimination reactions can be depicted in a two-dimensional potential energy diagram.²⁷⁷ If we consider the case of an ethyl halide, both stepwise reaction paths require the formation of high-energy intermediates. The E1 mechanism requires formation of a primary carbocation, whereas the E1cb proceeds via a carbanion intermediate.



In the absence of stabilizing substituent groups, both a primary carbocation and a primary carbanion are highly unstable intermediates. If we construct a reaction energy diagram in which progress of C–H bond breaking is one dimension, progress of C–X bond breaking is the second, and the energy of the reacting system is the third, we obtain a diagram such as the one in Figure 5.12. In Figure 5.12A only the two horizontal (bond-breaking) dimensions are shown. We see that the E1 mechanism corresponds to complete C–X cleavage before C–H cleavage begins, whereas the E1cb mechanism corresponds to complete C–H cleavage before C–X cleavage begins. In Figure 5.12B the energy dimension is added. The front-right and back-left corners correspond to the E1 and E1cb intermediates, respectively. Because of the high energy of both the E1 and E1cb intermediates, the lowest-energy path is the concerted E2 path, more or less diagonally across the energy surface. This pathway is of lower energy because the partially formed double bond provides some compensation for the energy required to break the C–H and C–X bonds and the high-energy intermediates are avoided.

The presence of a substituent on the ethyl group that stabilizes the carbocation intermediate lowers the right-front corner of the diagram, which corresponds

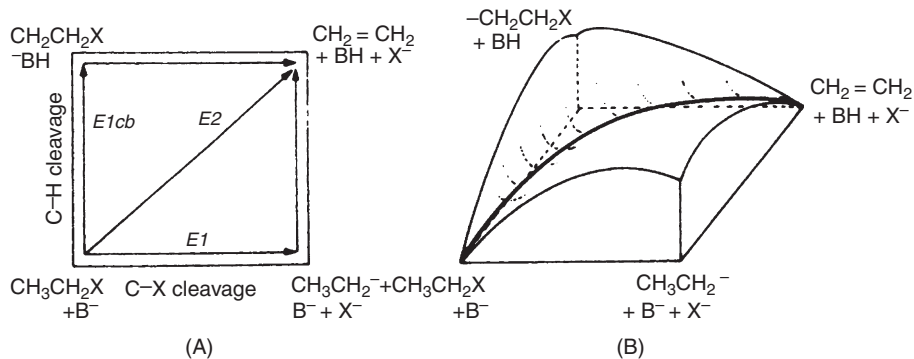


Fig. 5.12. Two-dimensional potential energy diagrams depicting E1, E2, and E1cb mechanisms.

²⁷⁷ R. A. More O’Ferrall, *J. Chem. Soc. B*, 274 (1970).

to the energy of the carbocation intermediate. Similarly, a substituent that stabilizes a carbanion intermediate lowers the back-left corner of the diagram. As a result, substituents that stabilize carbocation character move the E2 TS to a point that more closely resembles the E1 TS. A structural change that stabilizes carbanion character shifts the E2 TS to be more similar to the E1cb TS. In the E1-like TS, C–X bond cleavage is more advanced than C–H cleavage, whereas in the E1cb-like TS, the C–H bond breaking is more advanced. Figure 5.13 depicts these changes.

The variable transition state concept can be used to discuss specific structural effects that influence the possible mechanisms of elimination reactions. We have background that is pertinent to the structure-reactivity effects in E1 reactions from the discussion of S_N1 reactions in Chapter 4. Ionization is favored by: (1) electron-releasing groups that stabilize the positive charge in the carbocation intermediate; (2) readily ionized, i.e., “good,” leaving groups; and (3) solvents that facilitate ionization. The base plays no role in the rate-determining step in the E1 mechanism, but its identity cannot be ignored. After ionization, the cationic intermediate is subject to two competing reactions: nucleophilic capture (S_N1) or proton removal (E1). Remember from Section 4.4.3 (p. 437) that there is an inherent preference for substitution. The reaction can be diverted to elimination by bases. Stronger and harder bases favor the E1 path over the S_N1 path.

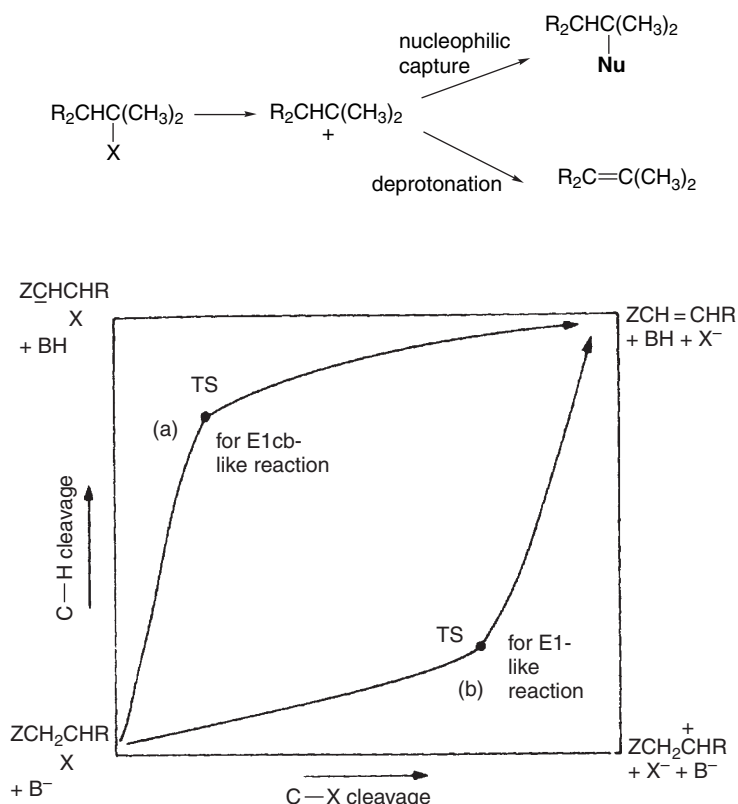


Fig. 5.13. Representation of changes in transition structure character in the E2 elimination reaction as a result of substituent effects: (a) substituent Z stabilizes carbanion character of E1cb-like TS; (b) substituent R stabilizes carbocation character of E1-like TS.

E2 reactions are distinguished from E1 reactions in that the base is present in the TS for the rate-determining step. The reactions therefore exhibit overall second-order kinetics. The precise nature of the TS is a function of variables such as the strength of the base, the identity of the leaving group, reactant structure, and the solvent. For example, an elimination reaction proceeding by an E2 TS will be moved in the E1cb direction by an increase in base strength or by a change to a poorer leaving group. On the other hand, a good leaving group in a highly ionizing solvent will result in an E2 TS that resembles an E1 process, with greater weakening of the bond to the leaving group. Reactions that proceed by the E1cb mechanism require substituents that can stabilize the carbanion intermediate. This mechanism is not observed with simple alkyl halides or sulfonates. It is more likely to be involved when the leaving group is β to a carbonyl, nitro, cyano, sulfinyl, or other carbanion-stabilizing group. Poorer leaving groups move the E2 TS in the E1cb direction, since they require greater buildup of negative charge at the β -carbon. Scheme 5.3 summarizes some of the characteristic features of the E1, E2, and E1cb mechanisms.

Scheme 5.4 shows some examples of reactions for which the mechanisms have been characterized. From these data, we can conclude that E1cb reactions generally require *both* carbanion stabilization and a relatively poor leaving group. For example, simple 2-arylethyl halides and tosylates react by the E2 mechanism and only when a *p*-nitro group is present is there clear evidence of an E1cb mechanism (Entry 1). Entry 2 illustrates one of the distinguishing characteristics of E2 reactions. Both the α - and β -carbons show isotope effects because rehybridization occurs at both carbons. Entry 3 illustrates some of the kinetic features that characterize E2 reactions. In addition to second-order kinetics, the concerted mechanism results in kinetic isotope effects at both the β -hydrogen and the leaving group. The substantial Br > Cl ratio also

Scheme 5.3. Distinguishing Features of Elimination Mechanisms

A. E1 Mechanism

First Order Kinetics: $\text{rate} = k[\text{RX}]$

LFER indicate cationic character of the TS

Strong dependence on leaving group

B. E2 Mechanism

Second Order Kinetics: $\text{rate} = k[\text{RX}][\text{base}]$

Leaving group effect is normally I > Br > Cl >> F because bond-breaking occurs in RDS.

Kinetic isotope effect for both β -C-H and leaving group.

Kinetic isotope effect for both α - and β -carbons.

C. E1cb(rev)

Second Order Kinetics: $\text{rate} = k[\text{RX}][\text{base}]$

Exchange of β -H with protic solvent

LFER indicate anionic character in TS

D. E1cb(irr)

Second Order Kinetics: $\text{rate} = k[\text{RX}][\text{base}]$

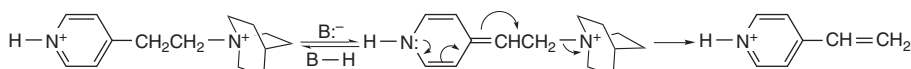
Leaving group effect may be F > Cl > Br > I, since C-X bond-breaking is not involved in RDS.

LFER indicates anionic character in TS

- 1.^a $\text{ArCH}_2\text{CH}_2\text{X} \xrightarrow[\text{DMSO, H}_2\text{O}]{\text{OH and buffer anions}} \text{ArCH}=\text{CH}_2$
 E2 for X = TsO^- , Br^- , and quinuclidinium, except for Ar = *p*-nitrophenyl and X = quinuclidinium: based on variation of sensitivity to base (Bronsted β) and LFER relationships.
- 2.^b $\text{ArCH}_2\text{CH}_2\text{N}^+(\text{CH}_3)_3 \xrightarrow{\text{NaOC}_2\text{H}_5} \text{ArCH}=\text{CH}_2$
 E2: based on $k^{12}\text{C}/k^{14}\text{C}$ isotope effects for both C(1) and C(2)
- 3.^c $\begin{array}{ccc} \text{PhCHCH}_2\text{Cl} & \xrightarrow[\text{EtOH, 75}^\circ\text{C}]{\text{NaOC}_2\text{H}_5} & \text{Ph} \\ | & & \diagup \\ \text{CH}_3 & & \text{CH}_3=\text{CH}_2 \end{array}$
 E2; based on $k^{35}\text{Cl}/k^{37}\text{Cl} = 1.0059$; $k_{\text{H}}/k_{\text{D}} = 5.37$, and $k_{\text{Br}}/k_{\text{Cl}} = 52$
- 4.^d $\text{O}_2\text{N}-\text{C}_6\text{H}_4-\text{CH}_2\text{CH}_2-\text{N}^+(\text{C}_6\text{H}_4-\text{X}) \xrightarrow{\text{KOH}} \text{O}_2\text{N}-\text{C}_6\text{H}_4-\text{CH}=\text{CH}_2$
 E1cb: based on kinetics and Bronsted dependence on substituent X; shifts from E1cb(irr) to E1cb(rev) as X becomes ERG
- 5.^e $\text{H}-\text{N}^+(\text{C}_6\text{H}_4-\text{CH}_2\text{CH}_2-\text{N}^+\text{C}_5\text{H}_5) \xrightarrow{\text{buffer}} \text{H}-\text{N}^+(\text{C}_6\text{H}_4-\text{CH}=\text{CH}_2)$
 E1cb(rev): based on observation of CH solvent exchange and solvent isotope effect
- 6.^f $\begin{array}{ccc} \text{Cl} & & \text{CH}_3 \\ | & & | \\ \text{C} & \xrightarrow[\text{(C}_2\text{H}_5)_3\text{N}]{\text{CH}_3\text{O}^-} & \text{CH}_3 \\ | & & | \\ \text{CH}_3 & & \text{CH}_3 \end{array}$
 E2: based on both CH and Cl kinetic isotope effects: $k_{\text{H}}/k_{\text{D}} = 7.1$ (CH_3O^-); 8.4 (($\text{C}_2\text{H}_5)_3\text{N}$)
 $k^{35}\text{Cl}/k^{37}\text{Cl} = 1.0086$ (CH_3O^-); 1.0101 (($\text{C}_2\text{H}_5)_3\text{N}$)
- 7.^g $\begin{array}{ccc} \text{CH}_2\text{OSO}_2\text{Ar} & \xrightarrow[\text{R}_3\text{N}]{\text{CH}_3\text{O}^- \text{ or }} & \text{CH}_2 \\ | & & | \\ \text{C}_6\text{H}_4-\text{C}_1\text{H}_4-\text{C}_6\text{H}_4 & & \text{C}_6\text{H}_4-\text{C}_1\text{H}_2-\text{C}_6\text{H}_4 \end{array}$
 E2 with transition to E1cb for ERG in Ar based on curved LFER (Hammett) relationships

- a. J. R. Gandler and W. P. Jencks, *J. Am. Chem. Soc.*, **104**, 1937 (1982).
 b. J. R. I. Eubanks, L. B. Sims, and A. Fry, *J. Am. Chem. Soc.*, **113**, 8821 (1991).
 c. H. F. Koch, D. McLennan, J. G. Koch, W. Tumas, B. Dobson, and N. H. Koch, *J. Am. Chem. Soc.*, **105**, 1930 (1983).
 d. J. W. Bunting and J. P. Kanter, *J. Am. Chem. Soc.*, **113**, 6950 (1991).
 e. S. Alunni, A. Conti and R. P. Errico, *J. Chem. Soc., Perkin Trans. II*, **2**, 453 (2000); S. Alunni, A. Conti, and R. P. Errico, *Res. Chem. Intermed.*, **27**, 635 (2001).
 f. J. S. Jia, J. Rudzinski, P. Paneth, and A. Thibblin, *J. Org. Chem.*, **67**, 177 (2002).
 g. F. G. Larkin, R. A. More O'Ferrall, and D. G. Murphy, *Coll Czech. Chem. Commun.*, **64**, 1833 (1999).

shows that the bond to the leaving group is involved in the rate-determining step. The pyridinium system in Entry 5 is an interesting case. Kinetic studies have shown that the reaction occurs through the *conjugate acid* of the reactant. The protonation of the pyridine ring enhances the acidity of the C–H bond. The reaction occurs with exchange, indicating that the proton removal is reversible.



The indenyl (Entry 6) and fluorenyl (Entry 7) ring systems have been studied carefully. Note that these are cases where (aromatic) anionic stabilization could potentially stabilize an anionic intermediate. However, the elimination reactions show E2 characteristics. The reaction in Entry 7 shifts to an E1cb mechanism if the leaving group is made less reactive.

Because of their crucial role in the ionization step, solvents have a profound effect on the rates of E1 reactions. These rates for a number of tertiary halides have been determined in a variety of solvents. For *t*-butyl chloride there are huge differences in the rates in water ($\log k = -1.54$), ethanol ($\log k = -7.07$), and diethyl ether ($\log k = -12.74$).²⁷⁸ Similarly, the rates of the E1 reaction of 1-methylcyclopentyl bromide range from $1 \times 10^{-3} \text{ s}^{-1}$ in methanol to $2 \times 10^{-9} \text{ s}^{-1}$ in hexane. Polar aprotic solvents such as DMSO ($k = 2 \times 10^{-4} \text{ s}^{-1}$) and acetonitrile ($k = 9 \times 10^{-5} \text{ s}^{-1}$) are also conducive for ionization.²⁷⁹ The solvent properties that are most important are polarity and the ability to assist leaving group ionization. These, of course, are the same features that favor S_N1 reactions, as we discussed in Section 3.8.

The details of the mechanism as well as the stereochemistry and regiochemistry also depend on the identity and degree of aggregation of the base. This is affected by variables such as the nature of the solvent, the cationic counterions, and the presence of coordinating ligands.²⁸⁰ Under given reaction conditions, there may be an equilibrium involving a number of different species, which, in turn, have different rates for inducing elimination. The nature of the TS in elimination reactions also controls the regiochemistry of β -elimination for compounds in which the double bond can be introduced at one of several positions. These effects are discussed in the next section.

5.10.2. Regiochemistry of Elimination Reactions

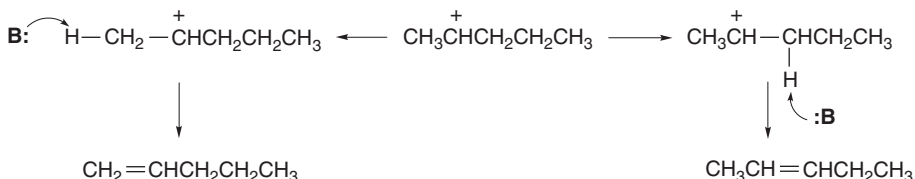
Useful generalizations and predictions regarding regioselectivity in elimination reactions can be drawn from the variable transition state theory. As we saw earlier in Figure 5.11, this theory proposes that the TSs in E2 reactions can vary over a mechanistic range between the E1 and E1cb extremes. When the base is present at the TS, the reaction will exhibit second-order kinetics and meet the other criteria of an E2 mechanism. There is no intermediate. The cleavage of the C–H and the C–X bonds is concerted, but not necessarily synchronous. The relative extent of the breaking of the two bonds at the TS may differ, depending on the nature of the leaving group X and the ease of removal of the β -hydrogen as a proton. If there are several nonequivalent β -hydrogens, competition among them determines which one is removed and the regiochemistry and stereochemistry of the reaction. If one compares E1 and E1cb eliminations, it is seen that quite different structural features govern the direction of elimination. The variable transition state theory suggests that E2 elimination proceeding through an “E1-like” TS will have the regiochemistry of E1 eliminations, whereas E2 eliminations proceeding through an “E1cb-like” TS will show regioselectivity similar to E1cb reactions. It is therefore instructive to consider these limiting mechanisms before discussing the E2 case.

²⁷⁸ M. H. Abraham, R. M. Doherty, M. J. Kamlet, J. M. Harris, and R. W. Taft, *J. Chem. Soc., Perkin Trans. 2*, 913 (1987).

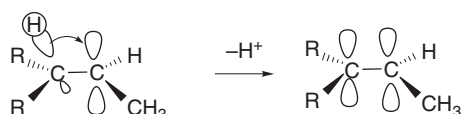
²⁷⁹ E. A. Ponomareva, I. V. Koshchii, T. L. Pervishko, and G. F. Dvorko, *Russ. J. Gen. Chem.*, **70**, 907 (2000).

²⁸⁰ R. A. Bartsch and J. Zavada, *Chem. Rev.*, **80**, 453 (1980).

In the E1 mechanism, the leaving group is completely ionized before C–H bond breaking occurs. The direction of the elimination therefore depends on the structure of the carbocation and the identity of the base involved in the proton transfer that follows C–X heterolysis. Because of the high energy of the carbocation intermediate, quite weak bases can effect proton removal. The solvent can serve this function. The counterion formed in the ionization step can also act as the proton acceptor.



The product composition of the alkenes formed in E1 elimination reaction usually favors the more-substituted alkene, and therefore the more stable one. This indicates that the energies of the *product-determining TSs parallel those of the isomeric alkenes*. However, since the activation energy for proton removal from a carbocation is low, the TS should resemble the carbocation intermediate much more than the alkene product (Hammond postulate; Section 3.3.2.2). In the carbocation there is hyperconjugation involving each β -hydrogen.²⁸¹ Since the hyperconjugation structures possess some double-bond character, the interaction with hydrogen is greatest at more highly substituted carbons; that is, there will be greater weakening of C–H bonds and more double-bond character at more highly substituted carbon atoms. This structural effect in the carbocation intermediate governs the direction of elimination and leads to the *preferential formation of the more highly substituted alkene*, as illustrated in Figure 5.14.



In the E1cb mechanism, the direction of elimination is governed by the *kinetic acidity* of the individual β -protons, which in turn is determined by the polar and

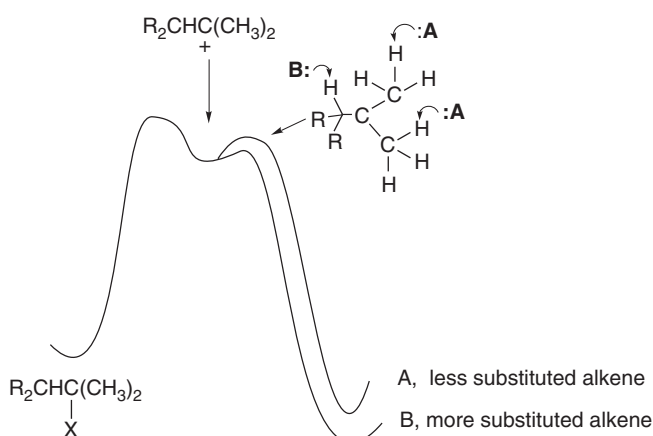


Fig. 5.14. Potential energy profile for product-determining step for E1 elimination.

²⁸¹ P. B. D. de la Mare, *Pure Appl. Chem.*, **56**, 1755 (1984).

resonance effects of adjacent substituents, and by the degree of steric hindrance to approach of base to the proton. Alkyl substituents tend to retard proton abstraction both electronically and sterically. Preferential proton abstraction from less-substituted carbons leads to the formation of the less-substituted alkene. Carbanion-stabilizing substituents control the regiochemistry of E1cb eliminations by favoring deprotonation at the most acidic carbon.

The preferred direction of elimination via the E2 mechanism depends on the precise nature of the TS. The two extreme TSs for the E2 elimination resemble the E1 and E1cb mechanisms in their orientational effects. At the “E1cb-like” end of the E2 range, a highly developed bond is present between the proton and the base. The leaving group remains tightly bound to carbon, and there is relatively little development of the carbon-carbon double bond. *When the TS of an E2 reaction has E1cb character, the direction of the elimination is governed by the ease of proton removal.* In this case, the less-substituted alkene usually dominates. At the “E1-like” end of the E2 spectrum, the TS is characterized by well-advanced cleavage of the C–X bond and a largely intact C–H bonds. An “E1-like” TS for E2 reactions leads to formation of the more highly substituted of the possible alkenes. In a more synchronous E2 reaction, the new double bond is substantially formed at the TS with partial rupture of both the C–H and C–X bonds. E2 eliminations usually give mainly the more-substituted alkene. This is because the TSs leading to the isomeric alkenes reflect the partial double-bond character and the greater stability of the more-substituted double bond. Concerted E2 reactions are also subject to the stereoelectronic requirement that the reacting C–H and C–X bond be antiperiplanar. This requirement makes reactant conformation a factor in determining the outcome of the reaction.

Prior to development of the mechanistic ideas outlined above, it was recognized by experience that some types of elimination reactions give the more substituted alkene as the major product. Such eliminations are said to follow the *Saytzeff rule*. This behavior is characteristic of E1 reactions and E2 reactions involving relatively good leaving groups, such as halides and sulfonates. These are now recognized as reactions in which C–X cleavage is well advanced in the TS. E2 reactions involving poor leaving groups, particularly those with quaternary ammonium salts, are said to follow the *Hofmann rule* and give primarily the less-substituted alkene. We now recognize that such reactions proceed through TSs with E1cb character.

The data recorded in Table 5.11 for the 2-hexyl system illustrate two general trends that have been recognized in other systems as well. First, poorer leaving groups favor elimination according to the Hofmann rule, as shown, for example, by the increasing amount of terminal olefin in the halogen series as the leaving group is changed from iodide to fluoride. Poorer leaving groups move the TS in the E1cb direction. A higher negative charge must build up on the β -carbon to induce loss of the leaving group. This charge increase is accomplished by more complete proton abstraction.

Comparison of the data for methoxide with those for *t*-butoxide in Table 5.11 illustrates a second general trend. Stronger bases favor formation of the less-substituted alkene.²⁸² A stronger base leads to an increase in the carbanion character at the TS and, thus, shifts it in the E1cb direction. A correlation between the strength of the

²⁸² (a) D. H. Froemsdorf and M. D. Robbins, *J. Am. Chem. Soc.*, **89**, 1737 (1967); I. N. Feit and W. H. Saunders, Jr., *J. Am. Chem. Soc.*, **92**, 5615 (1970); (b) R. A. Bartsch, G. M. Pruss, B. A. Bushaw, and K. E. Wiegers, *J. Am. Chem. Soc.*, **95**, 3405 (1973); (c) R. A. Bartsch, K. E. Wiegers, and D. M. Guritz, *J. Am. Chem. Soc.*, **96**, 430 (1974).

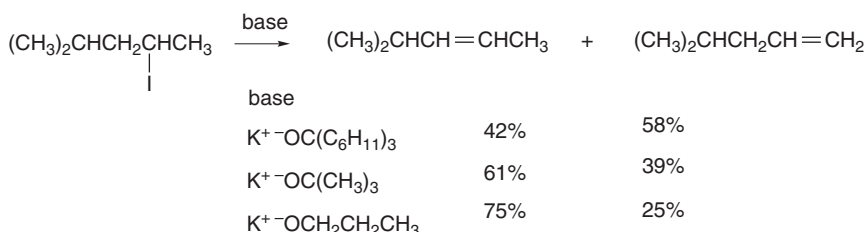
Table 5.11. Product Ratios for Some Elimination Reactions of 2-Hexyl Systems

Leaving group	Base/solvent	Product Composition		
		1-Hexene	E-2-Hexene	Z-2-Hexene
I	MeO ⁻ /MeOH	19	63	18
Cl	MeO ⁻ /MeOH	33	50	17
F	MeO ⁻ /MeOH	69	21	9
OSO ₂ C ₇ H ₇	MeO ⁻ /MeOH	33	44	23
I	t-BuO ⁻ /t-BuOH	78	15	7
Cl	t-BuO ⁻ /t-BuOH	91	5	4
F	t-BuO ⁻ /t-BuOH	97	2	1
OSO ₂ C ₇ H ₇	t-BuO ⁻ /t-BuOH	83	4	14

a. R. A. Bartsch and J. F. Bunnett, *J. Am. Chem. Soc.*, **91**, 1376 (1967).

base and the difference in ΔG^\ddagger for the formation of 1-butene versus 2-butene has been established.^{282b} Some of the data are given in Table 5.12.

The direction of elimination is also affected by steric effects, and if both the base and the reactant are highly branched, steric factors may lead to preferential removal of the less hindered hydrogen.²⁸³ Thus, when 4-methyl-2-pentyl iodide reacts with very hindered bases such as potassium tricyclohexylmethoxide, there is preferential formation of the terminal alkene. In this case, potassium t-butoxide favors the internal alkene, although by a smaller ratio than for less branched alkoxides.

**Table 5.12. Orientation of E2 Elimination as a Function of Base Strength**

Base (K ⁺ salt)	pK(DMSO)	Percent 1-butene	
		2-Iodobutane ^a	2-Butyl tosylate ^b
p-Nitrobenzoate	8.9	5.8	c
Benzoate	11.0	7.2	c
Acetate	11.6	7.4	c
Phenolate	16.4	11.4	30.6
Trifluoroethoxide	21.6	14.3	46.0
Methoxide	29.0	17.0	c
Ethoxide	29.8	17.1	56.0
t-Butoxide	32.2	20.7	58.5

a. R. A. Bartsch, G. M. Pruss, B. A. Bushaw, and K. E. Wiegers, *J. Am. Chem. Soc.*, **95**, 3405 (1973).

b. R. A. Bartsch, R. A. Read, D. T. Larsen, D. K. Roberts, K. J. Scott, and B. R. Cho, *J. Am. Chem. Soc.*, **101**, 1176 (1979).

c. Not reported.

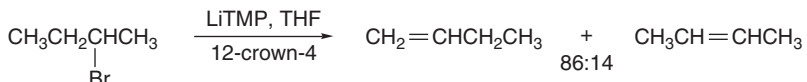
²⁸³. R. A. Bartsch, R. A. Read, D. T. Larsen, D. K. Roberts, K. J. Scott, and B. R. Cho, *J. Am. Chem. Soc.*, **101**, 1176 (1979).

Table 5.13. Orientation of Elimination from 2-Butyl Systems under E2 Conditions

Leaving group	Base/solvent	1-Butene (%)	2-Butene (%)
I ^a	PhCO ₂ ⁻ /DMSO	7	93
I ^a	C ₂ H ₅ O ⁻ /DMSO	17	83
I ^b	t-C ₄ H ₉ O ⁻ /DMSO	21	79
Br ^b	t-C ₄ H ₉ O ⁻ /DMSO	33	67
Cl ^b	t-C ₄ H ₉ O ⁻ /DMSO	43	57
Br ^c	C ₂ H ₅ O ⁻ /DMSO	19	81
OSO ₂ C ₇ H ₇ ^d	C ₂ H ₅ O ⁻ /DMSO	35	65
OSO ₂ C ₇ H ₇ ^d	t-C ₄ H ₉ O ⁻ /DMSO	61	39
S ⁺ (CH ₃) ₂ ^e	C ₂ H ₅ O ⁻ /DMSO	74	26
N ⁺ (CH ₃) ₃ ^f	OH ⁻	95	5

a. R. A. Bartsch, B. M. Pruss, B. A. Bushaw, and K. E. Wiegers, *J. Am. Chem. Soc.*, **95**, 3405 (1973).b. D. L. Griffith, D. L. Meges, and H. C. Brown, *J. Chem. Soc. Chem. Commun.*, 90 (1968).c. M. L. Dahr, E. D. Hughes, and C. K. Ingold, *J. Chem. Soc.*, 2058 (1948).d. D. H. Froemsdorf and M. D. Robbins, *J. Am. Chem. Soc.*, **89**, 1737 (1967).e. E. D. Hughes, C. K. Ingold, G. A. Maw, and L. I. Woolf, *J. Chem. Soc.*, 2077 (1948).f. A. C. Cope, N. A. LeBel, H.-H. Lee, and W. R. Moore, *J. Am. Chem. Soc.*, **79**, 4720 (1957).

Branched amide bases can also control the regiochemistry of elimination on the basis of steric effects. For example LiTMP favors formation of 1-butene from 2-bromobutane.

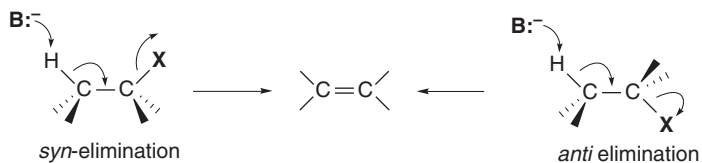


Ref. 284

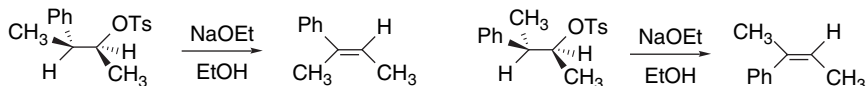
The leaving group also affects the amount of internal versus terminal alkene that is formed. The poorer the leaving group, the more E1cb-like the TS. This trend is illustrated for the case of the 2-butyl system by the data in Table 5.13. Positively charged leaving groups, such as in dimethylsulfonium and trimethylammonium salts, may also favor a more E1cb-like TS because their inductive and field effects increase the acidity of the β -protons.

5.10.3. Stereochemistry of E2 Elimination Reactions

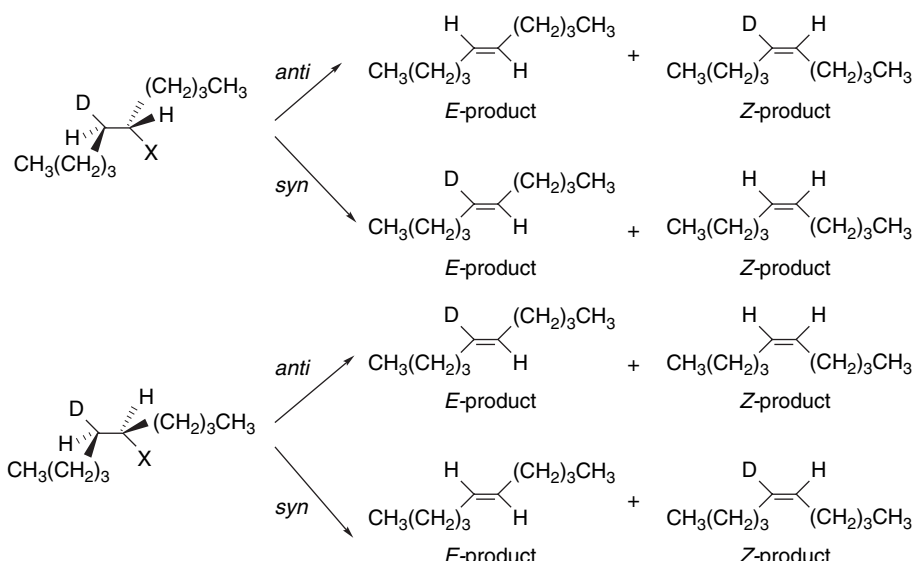
In this section we focus primarily on the stereochemistry of the concerted E2 mechanism. The most familiar examples are dehydrohalogenation and dehydrosulfonylation reactions effected by strong bases. In principle, elimination can proceed with either *syn* or *anti* stereochemistry. For acyclic systems, there is a preference for *anti* elimination, but this can be overridden if conformational factors favor a *syn* elimination. The *anti* TS maximizes orbital overlap and avoids the eclipsing that is present in the *syn* TS.

284. I. E. Kopka, M. A. Nowak, and M. W. Rathke, *Synth. Commun.*, **16**, 27 (1986).

In acyclic systems, the extent of *anti* versus *syn* elimination can be determined by use of either stereospecifically deuterated reactants or diastereomeric reactants that give different products by *syn* and *anti* elimination. The latter approach showed that elimination from 3-phenyl-2-butyl tosylate is a stereospecific *anti* process.²⁸⁵



The extent of *syn* elimination in 5-decyl systems was measured using diastereomeric deuterium-labeled substrates. Stereospecifically deuterated 5-substituted decane derivatives were prepared and subjected to various elimination conditions. By comparison of the amount of deuterium in the *E*- and *Z*-isomers of the product, it is possible to determine the extent of *syn* and *anti* elimination.²⁸⁶



Data obtained for three different leaving groups are shown in Table 5.14. The results demonstrate that *syn* elimination is extensive for quaternary ammonium salts. With better leaving groups, the extent of *syn* elimination is small in the polar solvent DMSO but quite significant in benzene. The factors that promote *syn* elimination are discussed below. Table 5.15 summarizes some data on *syn* versus *anti* elimination in other acyclic systems.

The general trend revealed by these and other data is that *anti* stereochemistry is normally preferred for reactions involving good leaving groups such as bromide and tosylate. With poorer leaving groups (e.g., fluoride, trimethylamine), *syn* elimination becomes important. The amount of *syn* elimination is small in the 2-butyl system, but it becomes a major pathway with 3-hexyl compounds and longer chains.

In cyclic systems, the extent of *anti* and *syn* elimination depends on ring size, among other factors. Cyclohexyl systems have a very strong preference for *anti* elimination via

²⁸⁵ W.-B. Chiao and W. H. Saunders, *J. Org. Chem.*, **45**, 1319 (1980).

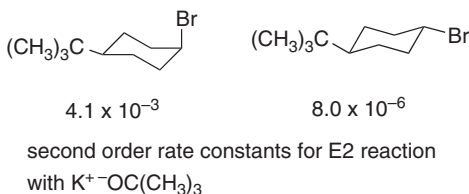
²⁸⁶ M. Pankova, M. Svoboda, and J. Zavada, *Tetrahedron Lett.*, 2465 (1972). The analysis of the data also requires that account be taken of (a) isotope effects and (b) formation of 4-decene. The method of analysis is described in detail by J. Sicher, J. Zavada, and M. Pankova, *Coll. Czech. Chem. Commun.*, **36**, 3140 (1971).

Table 5.14. Extent of *syn* Elimination as a Function of the Leaving Group in the 5-Decyl System^a

Leaving group	Percent <i>syn</i> elimination			
	E-product		Z-product	
DMSO	Benzene	DMSO	Benzene	
Cl	6	62	7	39
OTs	4	27	4	16
(CH ₃) ₃ N ⁺	93	92	76	84

a. M. Pankova, M. Svoboda, and J. Zavada, *Tetrahedron Lett.*, 2465 (1972); the base used was potassium *t*-butoxide.

conformations in which both the departing proton and the leaving group occupy axial positions. This orientation permits alignment of the orbitals so that concerted *anti* elimination can occur. For example, *cis*-4-*t*-butylcyclohexyl bromide undergoes E2 elimination at a rate about 500 times greater than the *trans* isomer because only the *cis* isomer permits *anti* elimination from the favored chair conformation.²⁸⁷



Other cyclic systems are not so selective. In the decomposition of *N,N,N*-trimethyl-cyclobutylammonium hydroxide, elimination is 90% *syn*.²⁸⁸ The cyclobutyl ring resists the conformation required for *anti* elimination. The more flexible five-membered ring analog undergoes about 50% *syn* elimination. Elimination from the

Table 5.15. Stereochemistry of E2 Elimination for Some Acyclic Systems

Reactant	Base/solvent	% anti	% syn
2-Bromobutane ^a	$\text{K}^+\text{-OC}(\text{CH}_3)_3/\text{t-BuOH}$	100	0
2-Butyl tosylate ^b	$\text{K}^+\text{-OC}(\text{CH}_3)_3/\text{t-BuOH}$	>98	<2
<i>N,N,N</i> -trimethyl-1-2-butylammonium ^c	$\text{K}^+\text{-OC}(\text{CH}_3)_3/\text{DMSO}$	100	0
3-Fluorohexane ^d	$\text{K}^+\text{-OC}(\text{CH}_3)_3/\text{t-BuOH}$	32	68
<i>N,N,N</i> -trimethyl-4-octylammonium ^e	$\text{K}^+\text{-OC}(\text{CH}_3)_3/\text{DMSO}$	24	76
5-Decyl tosylate ^f	$\text{K}^+\text{-OC}(\text{CH}_3)_3/\text{t-BuOH}$	93	7
5-Decyl chloride ^g	$\text{K}^+\text{-OC}(\text{CH}_3)_3/\text{benzene}$	62	38
5-Decyl fluoride ^g	$\text{K}^+\text{-OC}(\text{CH}_3)_3/\text{benzene}$	<20	>80
5-Decyl chloride ^g	$\text{K}^+\text{-OC}(\text{CH}_3)_3/\text{DMSO}$	93	7
5-Decyl fluoride ^g	$\text{K}^+\text{-OC}(\text{CH}_3)_3/\text{DMSO}$	80	20

a. R. A. Bartsch, *J. Am. Chem. Soc.*, **93**, 3683 (1971).

b. D. H. Froemsdorf, W. Dowd, W. A. Gifford, and S. Meyerson, *J. Chem. Soc., Chem. Commun.*, 449 (1968).

c. D. H. Froemsdorf, H. R. Pinnick, Jr., and S. Meyerson, *J. Chem. Soc., Chem. Commun.*, 1600 (1968).

d. J. K. Borchardt, J. C. Swanson, and W. H. Saunders, Jr., *J. Am. Chem. Soc.*, **96**, 3918 (1974).

e. J. Sicher, J. Zavada, and M. Pankova, *Collect. Czech. Chem. Commun.*, **36**, 3140 (1971).

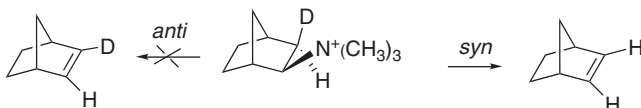
f. J. Zavada, M. Pankova, and J. Sicher, *J. Chem. Soc., Chem. Commun.*, 1145 (1968).

g. M. Pankova, M. Svoboda, and J. Zavada, *Tetrahedron Lett.*, 2465 (1972).

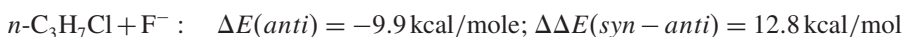
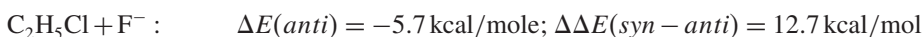
²⁸⁷ J. Zavada, J. Krupicka, and J. Sicher, *Coll. Czech. Chem. Commun.*, **33**, 1393 (1968).

²⁸⁸ M. P. Cooke, Jr., and J. L. Coke, *J. Am. Chem. Soc.*, **90**, 5556 (1968).

N,N,N-trimethylnorbornylammonium ion is exclusively *syn*.²⁸⁹ This is another case where the rigid ring prohibits attainment of an *anti*-elimination process. There is also a steric effect operating against removal of an *endo* proton, which is required for *anti* elimination. *Syn* elimination is especially prevalent in the medium-sized ring compounds.²⁹⁰



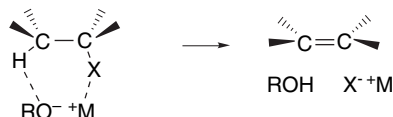
The energy difference between the *anti* and *syn* transition structures has been examined computationally using fluoride as the base and alkyl chlorides as the reactants. Simple primary and secondary chlorides show no barriers for *anti* elimination at the MP4SDQ/6-31+G** level. The *syn* TSs show positive barriers and the total difference between the *syn* and *anti* TSs is on the order of 13 kcal/mol.²⁹¹



The preferred TS for *syn* elimination is not periplanar, but rather has a torsion angle of about 30°. The *syn* TS has more E1cb character than the *anti*.

MP2/6-31+G** computations have been used to compare cyclopentyl and cyclohexyl systems.²⁹² As noted above, cyclohexyl systems have a much stronger preference for the *anti* stereochemistry.²⁹³ The optimum TSs are shown in Figure 5.15. Both the *anti* and *syn* TSs have negative barriers in the cyclopentyl system (−10.2 and −0.9 kcal/mol), whereas the *syn* system shows a positive barrier in the cyclohexyl system (−10.9 and +5.4 kcal/mol).

The factors that determine whether *syn* or *anti* elimination predominates are complex.²⁹⁴ One factor that is believed to be important is whether the base is free or present as an ion pair.²⁹⁵ The evidence suggests that an ion pair promotes *syn* elimination of anionic leaving groups. This effect can be explained by a TS in which the anion functions as a base and the cation assists in the departure of the leaving group.



This interpretation is in agreement with the solvent effect that is evident for the 5-decyl system data in Table 5.15. The extent of *syn* elimination is much higher in the nondissociating solvent benzene than in DMSO. The ion pair interpretation is also supported by the fact that addition of specific metal ion-complexing agents (crown

²⁸⁹ J. P. Coke and M. P. Cooke, *J. Am. Chem. Soc.*, **89**, 6701 (1967).

²⁹⁰ J. Sicher, *Angew. Chem. Int. Ed. Engl.*, **11**, 200 (1972).

²⁹¹ S. Gronert, *J. Am. Chem. Soc.*, **113**, 6041 (1991); *J. Am. Chem. Soc.*, **115**, 652 (1993).

²⁹² S. Gronert, *J. Org. Chem.*, **59**, 7046 (1994).

²⁹³ C. H. DePuy, G. F. Morris, J. S. Smith, and R. J. Smat, *J. Am. Chem. Soc.*, **87**, 2421 (1965).

²⁹⁴ R. A. Bartsch and J. Zavada, *Chem. Rev.*, **80**, 453 (1980).

²⁹⁵ R. A. Bartsch, G. M. Pruss, R. L. Buswell, and B. A. Bushaw, *Tetrahedron Lett.*, 2621 (1972); J. K. Borchardt, J. C. Swanson, and W. H. Saunders, Jr., *J. Am. Chem. Soc.*, **96**, 3918 (1974).

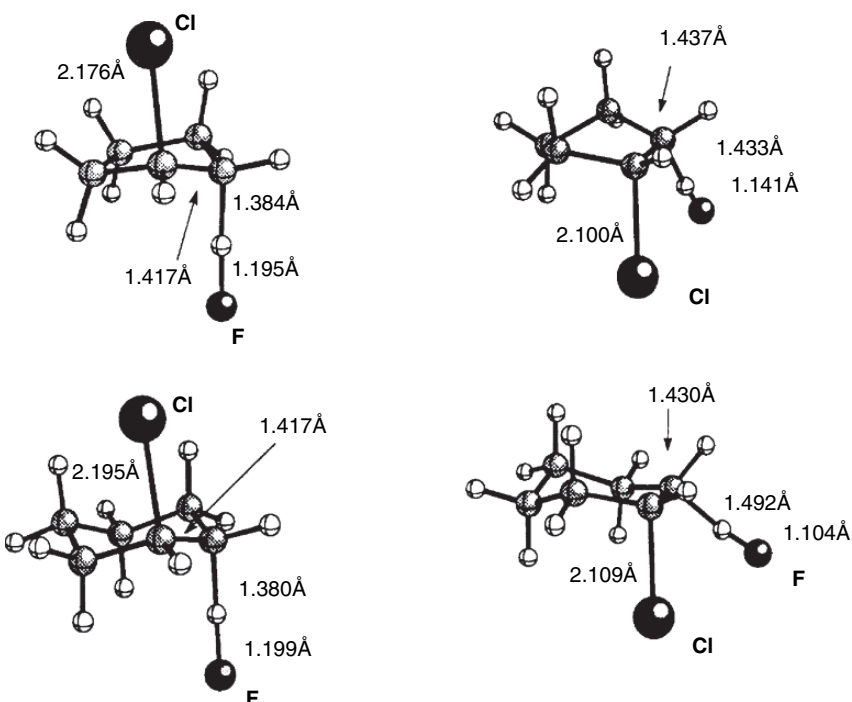


Fig. 5.15. *Anti* and *syn* transition states for fluoride-induced E2 elimination in (a) cyclopentyl and (b) cyclohexyl systems. Reproduced from *J. Org. Chem.*, **59**, 7046 (1994), by permission of the American Chemical Society.

ethers) that promote dissociation of the ion pair leads to diminished amounts of *syn* elimination.²⁹⁶ Another factor that affects the *syn:anti* ratio is the strength of the base. Strong bases exhibit a higher proportion of *syn* elimination.²⁹⁷

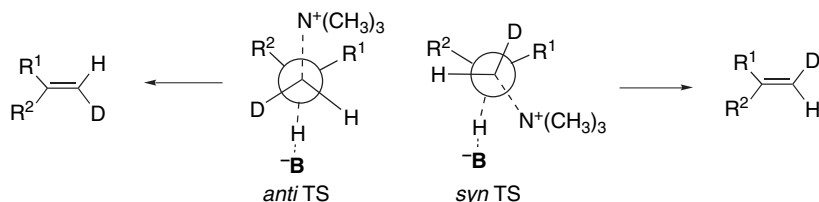
Steric and conformational effects also play a significant role in determining the *syn:anti* ratio. With *N*-(β,β -disubstituted-ethyl)-*N,N,N*-trimethylammonium ions, *syn* elimination is more prevalent when the β -substituents are aryl or branched. As the β -groups become less bulky, the amount of *syn* elimination decreases. This effect is illustrated by the data below.²⁹⁸

R^1	R^2	% <i>syn</i>	% <i>anti</i>
Ph	4-MeOPh	62	38
Ph	<i>i</i> -Pr	68	32
Ph	Me	26	74
<i>n</i> -Bu	H	<5	>95

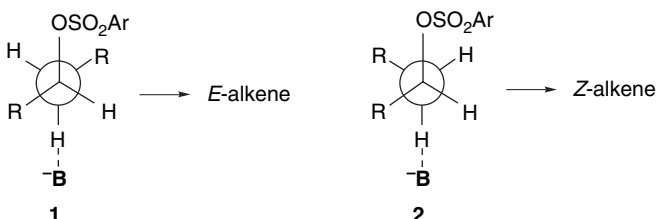
²⁹⁶ R. A. Bartsch, E. A. Mintz, and R. M. Parlman, *J. Am. Chem. Soc.*, **96**, 3918 (1974).

²⁹⁷ K. C. Brown and W. H. Saunders, Jr., *J. Am. Chem. Soc.*, **92**, 4292 (1970); D. S. Bailey and W. H. Saunders, Jr., *J. Am. Chem. Soc.*, **92**, 6904 (1970).

²⁹⁸ Y.-T. Tao and W. H. Saunders, Jr., *J. Am. Chem. Soc.*, **105**, 3183 (1983).



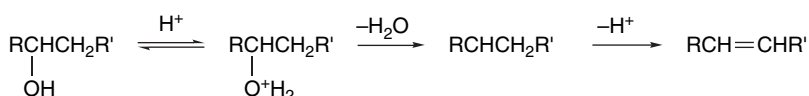
Another aspect of the stereochemistry of elimination reactions is the ratio of *E*-and *Z*-products. The proportion of *Z*-and *E*-isomers of disubstituted internal alkenes formed during elimination reactions depends on the identity of the leaving group. Halides usually give mainly the *E*-alkenes.²⁹⁹ Bulkier groups, particularly arenesulfonates, give higher proportions of the *Z*-alkene. Sometimes, more *Z*-isomer is formed than *E*-isomer. The preference for *E*-alkene probably reflects the unfavorable steric repulsions present in the E2 transition state leading to *Z*-alkene. High *Z*:*E* ratios are attributed to a second steric effect that becomes important only when the leaving group is large. The conformations leading to *E*-and *Z*-alkene by *anti* elimination are depicted below.



When the leaving group and base are both large, conformation **2** is favored because it permits the leaving group to occupy a position removed from the β -alkyl substituents, while also maintaining an *anti* relationship to the α -hydrogen. *Anti* elimination through a TS arising from conformation **2** gives *Z*-alkene.

5.10.4. Dehydration of Alcohols

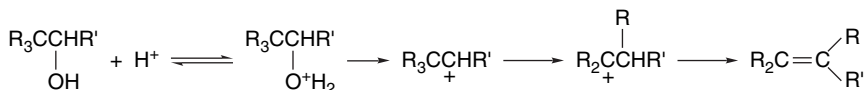
The dehydration of alcohols is an elimination reaction that takes place under acidic rather than basic conditions and involves an E1 mechanism.³⁰⁰ The function of the acidic reagent is to convert the hydroxy group to a better leaving group by protonation.



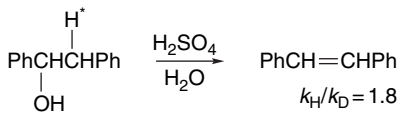
²⁹⁹. H. C. Brown and R. L. Kliminsch, *J. Am. Chem. Soc.*, **87**, 5517 (1965); I. N. Feit and W. H. Saunders, Jr., *J. Am. Chem. Soc.*, **92**, 1630 (1970).

³⁰⁰. D. V. Banthorpe, *Elimination Reactions*, Elsevier, New York, 1963, pp. 145–156.

This elimination reaction is the reverse of acid-catalyzed hydration, which was discussed in Section 5.2. Since a carbocation or closely related species is the intermediate, the elimination step is expected to favor the more-substituted alkene. The E1 mechanism also explains the trends in relative reactivity. Tertiary alcohols are the most reactive, and reactivity decreases going to secondary and primary alcohols. Also in accord with the E1 mechanism is the fact that rearranged products are found in cases where a carbocation intermediate would be expected to rearrange.



For some alcohols, exchange of the hydroxyl group with solvent competes with dehydration.³⁰¹ This exchange indicates that the carbocation can undergo S_N1 capture in competition with elimination. Under conditions where proton removal is rate determining, it would be expected that a significant isotope effect would be seen, which is, in fact, observed.

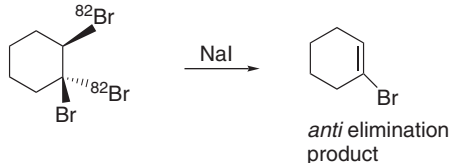


Ref. 302

5.10.5. Eliminations Reactions Not Involving C–H Bonds

The discussion of elimination processes thus far has focused on reactions that involve removal of a proton bound to a β -carbon, but it is the electrons in the C–H σ bond that are essential to the elimination process. Compounds bearing other substituents that can release electrons undergo β -eliminations. Many such reactions are known, and they are frequently stereospecific.

Vicinal dibromides can be debrominated by certain reducing agents, including iodide ion. The stereochemical course in the case of 1,1,2-tribromocyclohexane was determined using a ⁸²Br-labeled sample prepared by *anti* addition of ⁸²Br₂ to bromocyclohexene. Exclusive *anti* elimination gave unlabeled bromocyclohexene, whereas ⁸²Br-labeled product resulted from *syn* elimination. Debromination with sodium iodide was found to be cleanly an *anti* elimination.³⁰³

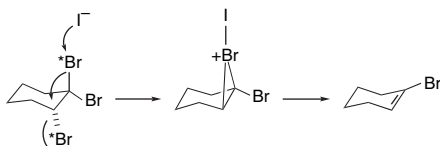


³⁰¹ C. A. Bunton and D. R. Llewellyn, *J. Chem. Soc.*, 3402 (1957); J. Manassen and F. S. Klein, *J. Chem. Soc.*, 4203 (1960).

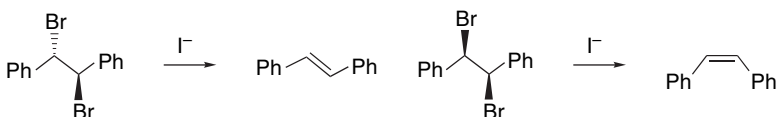
³⁰² D. S. Noyce, D. R. Hartter, and R. M. Pollack, *J. Am. Chem. Soc.*, **90**, 3791 (1968).

³⁰³ C. L. Stevens and J. A. Valicenti, *J. Am. Chem. Soc.*, **87**, 838 (1965).

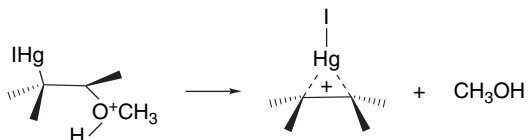
The iodide-induced reduction is essentially the reverse of a halogenation. Application of the principle of microscopic reversibility suggests that the reaction proceeds through a bridged intermediate.³⁰⁴



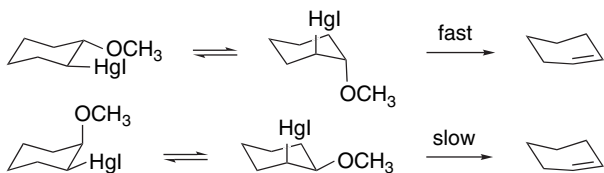
The rate-determining expulsion of bromide ion through a bridged intermediate requires an *anti* orientation of the two bromides. The nucleophilic attack of iodide at one bromide enhances its nucleophilicity and permits formation of the bridged ion. The stereochemical preference in noncyclic systems is also *anti*, as indicated by the fact that *meso*-stilbene dibromide yields *trans*-stilbene, whereas *d,l*-stilbene dibromide gives mainly *cis*-stilbene under these conditions.⁹⁴



Structures of type M–C–C–X in which M is a metal and X is a leaving group are very prone to elimination with formation of a double bond. One example is acid-catalyzed deoxymercuration.³⁰⁵ The β -oxyorganomercurials are more stable than similar reagents derived from more electropositive metals, but are much more reactive than simple alcohols. For example, $\text{CH}_3\text{CH}(\text{OH})\text{CH}_2\text{HgI}$ is converted to propene under acid-catalyzed conditions at a rate that is 10^{11} times greater than dehydration of 2-propanol under the same conditions. These reactions are believed to proceed through a bridged mercurinium ion by a mechanism that is the reverse of oxymercuration (see Section 5.6).



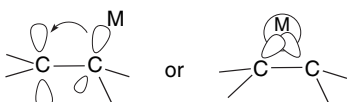
One of the pieces of evidence supporting this mechanism is the fact that the ΔH^\ddagger for deoxymercuration of *trans*-2-methoxycyclohexylmercuric iodide is about 8 kcal/mol less than for the *cis* isomer. Only the *trans* isomer can undergo elimination by an *anti* process through a chair conformation.



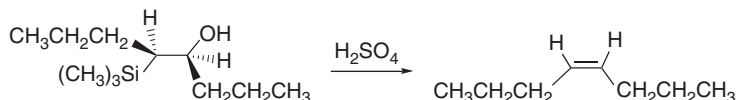
³⁰⁴. C. S. T. Lee, I. M. Mathai, and S. I. Miller, *J. Am. Chem. Soc.*, **92**, 4602 (1970).

³⁰⁵. M. M. Kreevoy and F. R. Kowitt, *J. Am. Chem. Soc.*, **82**, 739 (1960).

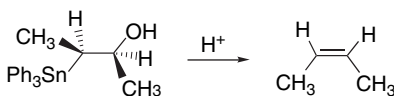
Comparing the rates of acid-catalyzed β -elimination of compounds of the type MCH_2CH_2OH yields the reactivity order for β -substituents $IHg \sim Ph_3Pb \sim Ph_3Sn > Ph_3Si > H$. The relative rates are within a factor of ten for the first three, but these are 10^6 greater than for Ph_3Si and 10^{11} greater than for a proton. There are two factors involved in these very large rate accelerations. One is bond energies. The relevant values are $Hg-C = 27 < Pb-C = 31 < Sn-C = 54 < Si-C = 60 < H-C = 96$ kcal/mol.³⁰⁶ The metal substituents also have a very strong stabilizing effect for carbocation character at the β -carbon. This stabilization can be pictured either as a orbital-orbital interaction in which the carbon-metal bond donates electron density to the adjacent *p* orbital, or as formation of a bridged species.



There are a number of synthetically valuable β -elimination processes involving organosilicon³⁰⁷ and organotin³⁰⁸ compounds. Treatment of β -hydroxyalkylsilanes or β -hydroxyalkylstannanes with acid results in stereospecific *anti* eliminations that are much more rapid than for compounds lacking the group IV substituent.

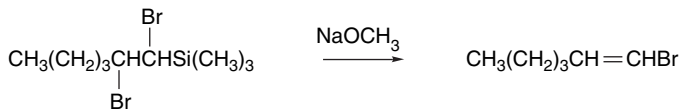


Ref. 309



Ref. 310

β -Halosilanes also undergo facile elimination when treated with methoxide ion.



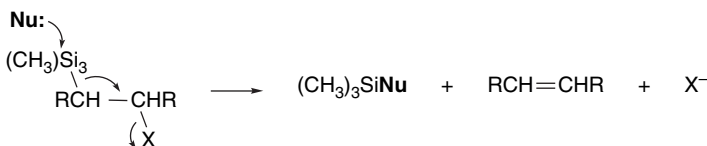
Ref. 311

- ³⁰⁶ D. D. Davis and H. M. Jococks, III, *J. Organomet. Chem.*, **206**, 33 (1981).
- ³⁰⁷ A. W. P. Jarvie, *Organomet. Chem. Rev. Sect. A*, **6**, 153 (1970); W. P. Weber, *Silicon Reagents for Organic Synthesis*, Springer-Verlag, Berlin, 1983; E. W. Colvin, *Silicon in Organic Synthesis*, Butterworths, London, 1981.
- ³⁰⁸ M. Pereyre, J.-P. Quintard, and A. Rahm, *Tin in Organic Synthesis*, Butterworths, London, 1987.
- ³⁰⁹ P. F. Hudrlick and D. Peterson, *J. Am. Chem. Soc.*, **97**, 1464 (1975).
- ³¹⁰ D. D. Davis and C. E. Gray, *J. Org. Chem.*, **35**, 1303 (1970).
- ³¹¹ A. W. P. Jarvie, A. Holt, and J. Thompson, *J. Chem. Soc. B*, 852 (1969); B. Miller and G. J. McGarvey, *J. Org. Chem.*, **43**, 4424 (1978).

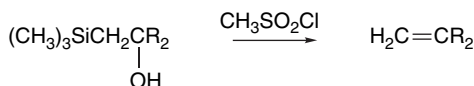


Ref. 312

These reactions proceed by alkoxide or fluoride attack at silicon that results in C–Si bond cleavage and elimination of the leaving group from the β -carbon. These reactions are stereospecific *anti* eliminations.

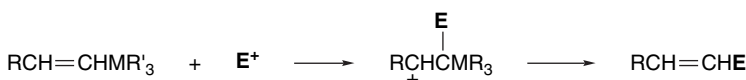


β -Elimination reactions of this type can also be effected by converting a β -hydroxy group to a better leaving group. For example, conversion of β -hydroxyalkylsilanes to the corresponding methanesulfonates leads to rapid elimination.³¹³



β -Trimethylsilylalkyl trifluoroacetates also undergo facile *anti* elimination.³¹⁴

The ability to promote β -elimination and the electron-donor capacity of the β -metalloid substituents can be exploited in a very useful way in synthetic chemistry.³¹⁵ Vinylstannanes and vinylsilanes react readily with electrophiles. The resulting intermediates then undergo elimination of the stannylic or silylic substituent, so that the net effect is replacement of the stannylic or silylic group by the electrophile. The silylic and stannylic substituents are crucial to these reactions in two ways. In the electrophilic addition step, they act as electron-releasing groups that promote addition and control the regiochemistry. A silylic or stannylic substituent strongly stabilizes carbocation character at the β -carbon atom and thus directs the electrophile to the α -carbon.



Computational investigations indicate that there is a ground state interaction between the alkene π orbital and the carbon-silicon bond that raises the energy of the π

³¹². P. Sieber, *Helv. Chim. Acta*, **60**, 2711 (1977).

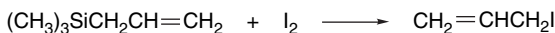
³¹³. F. A. Carey and J. R. Toler, *J. Org. Chem.*, **41**, 1966 (1976).

³¹⁴. M. F. Connell, B. Jousseanne, N. Noiret, and A. Saux, *J. Org. Chem.*, **59**, 1925 (1994).

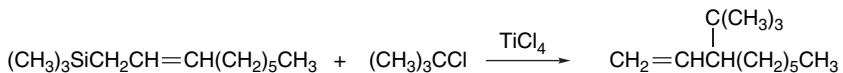
³¹⁵. T. H. Chan and I. Fleming, *Synthesis*, 761 (1979); I. Fleming, *Chem. Soc. Rev.*, **10**, 83 (1981).

HOMO and enhances reactivity.³¹⁶ MP3/6-31G* calculations indicate a stabilization of 38 kcal/mol, which is about the same as the value calculated for an α -methyl group.³¹⁷ Furthermore, this stereoelectronic interaction favors attack of the electrophile *anti* to the silyl substituent. The reaction is then completed by the elimination step in which the carbon-silicon or carbon-tin bond is broken.

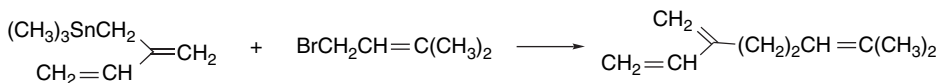
Allyl silanes and allyl stannanes are also reactive toward electrophiles and usually undergo a concerted elimination of the silyl substituent.



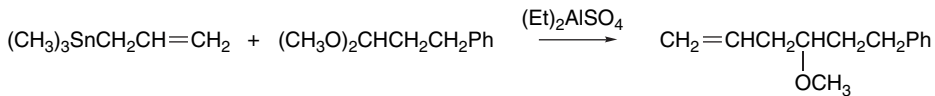
Ref. 318



Ref. 319

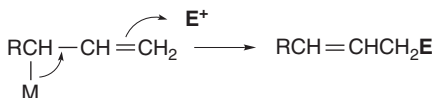


Ref. 320



Ref. 321

The common mechanistic pattern in these reactions involves electron release toward the developing electron deficiency on the C(2) of the double bond. Completion of the reaction involves loss of the electron-donating group and formation of the double bond. Further examples of these synthetically useful reactions can be found in Section 9.3 in Part B.



- ³¹⁶. S. D. Kahn, C. F. Pau, A. R. Chamberlin, and W. J. Hehre, *J. Am. Chem. Soc.*, **109**, 650 (1987).
- ³¹⁷. S. E. Wierschke, J. Chandrasekhar, and W. L. Jorgensen, *J. Am. Chem. Soc.*, **107**, 1496 (1985).
- ³¹⁸. D. Grafstein, *J. Am. Chem. Soc.*, **77**, 6650 (1955).
- ³¹⁹. I. Fleming and I. Paterson, *Synthesis*, 445 (1979).
- ³²⁰. J. P. Godschalx and J. K. Stille, *Tetrahedron Lett.*, **24**, 1905 (1983).
- ³²¹. A. Hosomi, H. Iguchi, M. Endo, and H. Sakurai, *Chem. Lett.*, 977 (1979).

- G. V. Boyd, in *The Chemistry of Triple-Bonded Functional Groups*, Supplement 2, S. Patai, ed., John Wiley & Sons, New York, 1994, Chap. 6.
- A. F. Cockerill and R. G. Harrison, *The Chemistry of Double-Bonded Functional Groups*, Part 1, S. Patai, ed., John Wiley & Sons, New York, 1977, Chap. 4.
- P. B. de la Mare and R. Bolton, *Electrophilic Additions to Unsaturated Systems*, 2nd Edition, Elsevier, New York, 1982.
- J. G. Gandler, in *The Chemistry of Double-Bonded Functional Groups*, Supplement A, Vol. 2, S. Patai, ed., John Wiley & Sons, New York, 1989, Chap. 12.
- G. H. Schmid, in *The Chemistry of Double-Bonded Functional Groups*, Supplement A, Vol. 2, S. Patai, ed., John Wiley & Sons, New York, 1989, Chap. 11.
- P. J. Stang and F. Diederich, eds., *Modern Acetylene Chemistry*, VCH Publishers, Weinheim, 1995.
- W. H. Saunders, Jr., and A. F. Cockerill, *Mechanisms of Elimination Reactions*, John Wiley & Sons, New York, 1973.

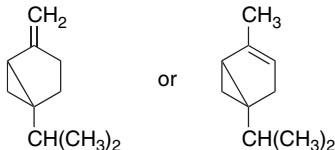
Problems

(References for these problems will be found on page 1160.)

5.1 Which compound of each pair will react faster with the specified reagent? Explain your answer.

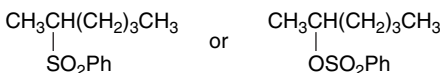
- 1-hexene or *E*-3-hexene with bromine in acetic acid.
- cis*- or *trans*-4-(*t*-butyl)cyclohexylmethyl bromide with $\text{KOC}(\text{CH}_3)_3$ in *t*-butyl alcohol.
- 2-phenylpropene or 4-(1-methylethenyl)benzoic acid with sulfuric acid in water.
-

d.



toward acid-catalyzed hydration.

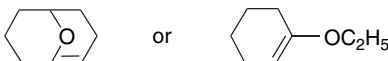
e.



with $\text{KOC}(\text{CH}_3)_3$ in *t*-butyl alcohol.

f. 4-bromophenylacetylene or 4-methylphenylacetylene with Cl_2 in acetic acid.

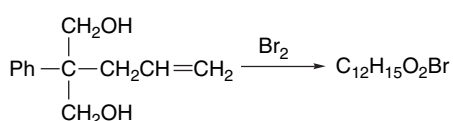
g.



toward acid-catalyzed hydration.

5.2. Predict the structure, including stereochemistry, of the product(s) expected for the following reactions. If more than one product is shown, indicate which is major and which is minor.

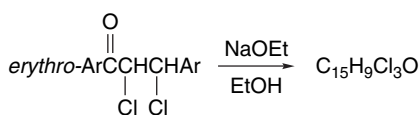
2



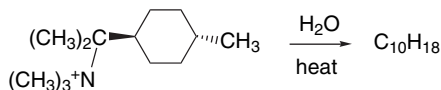
b.



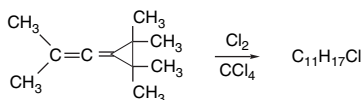
C₄



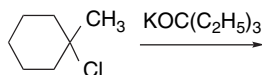
d.



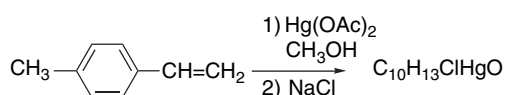
e.

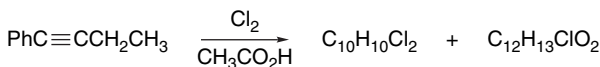


f.



g.



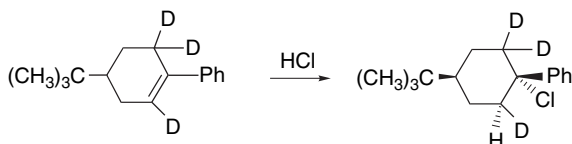


- 5.3. The reaction of the *cis* and *trans* isomers of *N,N,N*-trimethyl-(4-*t*-butylcyclohexyl)ammonium chloride with K⁺-O-*t*-Bu in *t*-butyl alcohol have been compared. The *cis* isomer gives 90% 4-*t*-butylcyclohexene and 10% *N,N*-dimethyl-(4-*t*-butylcyclohexyl)amine, whereas the *trans* isomer gives only the latter product in quantitative yield. Explain the different behavior of the two isomers.
- 5.4. For E2 eliminations in 2-phenylethyl systems with several different leaving groups, both the primary kinetic isotope effect and Hammett ρ have been determined. Deduce information about the nature and location (early, late) of the TS in the variable E2 spectrum. How does the identity of the leaving group affect the nature and location of the TS?

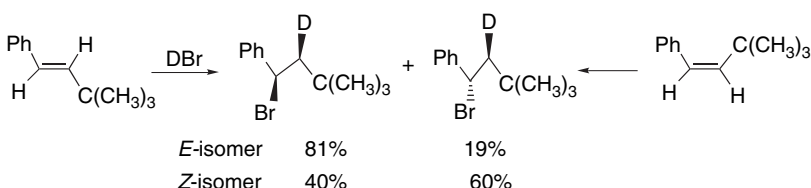
X	$k_{\text{H}}/k_{\text{D}}$	ρ
Br	7.11	2.1
OTs	5.66	2.3
⁺ S(CH ₃) ₂	5.07	2.7
⁺ N(CH ₃) ₃	2.98	3.7

- 5.5. Predict the effect on the 1-butene, *Z*-2-butene, and *E*-2-butene product ratio when the E2 elimination (KOEt, EtOH) of *erythro*-3-deutero-2-bromobutane is compared with 2-bromobutane. Which alkene(s) will increase in relative amount and which will decrease in relative amount? Explain the basis of your answer.
- 5.6. Arrange the following compounds in order of increasing rate of acid-catalyzed hydration: ethene, propene, 2-cyclopropylpropene, 2-methylpropene, 1-cyclopropyl-1-methoxyethene. Explain the basis of your answer.
- 5.7. Discuss the factors that are responsible for the regiochemistry and stereochemistry observed for the following reactions.

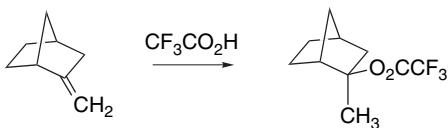
a.



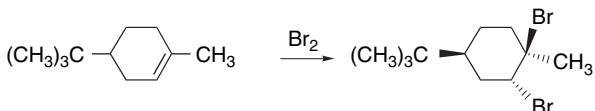
b.



c.

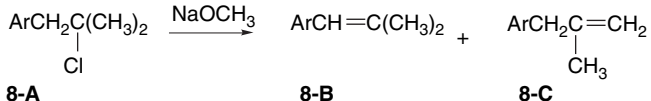


d.

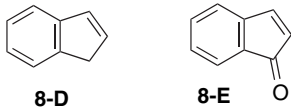


5.8. Explain the mechanistic basis of the following observations and discuss how the observation provides information about the reaction mechanism.

- a. When 1-aryl-2-methyl-2-propyl chlorides (**8-A**) react with NaOCH₃, roughly 1:1 mixtures of internal (**8-B**) and terminal alkene (**8-C**) are formed. By using the product ratios, the overall reaction rate can be dissected into the rates for formation of **8-B** and **8-C**. The rates are found to be substituent dependent for **8-B** ($\rho = +1.4$) but not for **8-C** ($\rho = -0.1 \pm 0.1$). All the reactions are second order, first order in reactant and first order in base.



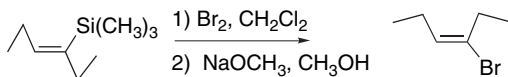
- b. When 1,3-pentadiene reacts with DCl, more *E*-4-chloro-5-deutero-2-pentene (60–75%) is formed than *E*-4-chloro-1-deutero-2-pentene (40–25%).
 c. When indene (**8-D**) is brominated in CCl₄, it gives some 15% *syn* addition, but indenone (**8-E**) gives only *anti* addition under these conditions. When the halogenation of indenone is carried out using Br–Cl, the product is *trans*-2-bromo-3-chloroindenone.



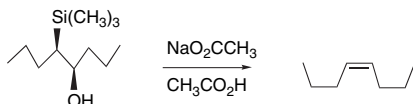
- d. The acid-catalyzed hydration of allene gives acetone, not allyl alcohol or propanal.
 e. In the addition of HCl to cyclohexene in acetic acid, the ratio of cyclohexyl acetate to cyclohexyl chloride drops significantly when tetramethylammonium chloride is added in increasing concentrations. The rate of the reaction is also accelerated. These effects are not observed with styrene.
 f. The ρ value for elimination of HF using K⁺–O-*t*-Bu from a series of 1-aryl-2-fluoroethanes increases from the mono- to di- and trifluoro derivatives, as indicated below.



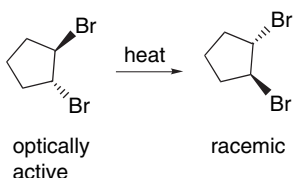
a.



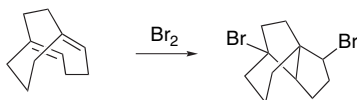
b.



c.

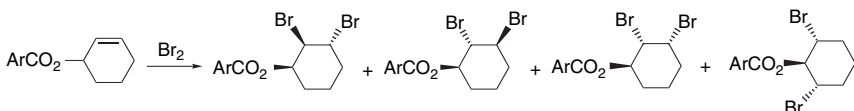


d.

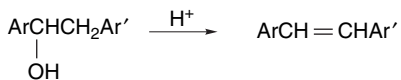


5.10. The rates of bromination of internal alkynes are roughly 100 times greater than the corresponding terminal alkynes. For hydration, however, the rates are less than 10 times greater for the disubstituted compounds. Account for this difference by comparison of the mechanisms for bromination and hydration.

5.11. The bromination of 3-aryloxyxyclohexenes gives rise to a mixture of stereoisomeric and regioisomeric products. The product composition for $\text{Ar} = \text{phenyl}$ is shown. Account for the formation of each of these products.



5.12. The Hammett correlation of the acid-catalyzed dehydration of 1,2-diaryl ethanols has been studied. The correlation resulting from substitution on both the 1- and 2-aryl rings is: $\log k = -3.78(\sigma_{\text{Ar}}^+ + 0.23\sigma_{\text{Ar}'}^-) - 3.18$. Rationalize the form of this correlation equation. What information does it give about the involvement of the Ar' ring in the rate-determining step of the reaction?

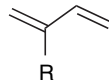


- 5.13. The addition of HCl to alkenes such as 2-methyl-1-butene and 2-methyl-2-butene in nitromethane follow a third-order rate expression:

$$\text{Rate} = k[\text{HCl}]^2[\text{alkene}]$$

It has also been established that there is no incorporation of deuterium into the reactant at 50% completion when DCl is used. Added tetraalkylammonium chloride retards the reaction, but the corresponding perchlorate salt does not. Propose a reaction mechanism that is consistent with these observations.

- 5.14. In the bromination of substituted styrenes, a $\rho\sigma^+$ plot is noticeably curved. If the extremes of the curve are taken to represent straight lines, the curve can be resolved into two Hammett relationships with $\rho = -2.8$ for EWG substituents and $\rho = -4.4$ for ERG substituents. The corresponding β -methylstyrenes give a similarly curved plot. The stereoselectivity of the reaction of the β -methylstyrenes is also dependent on the substituents. The reaction is stereospecifically *anti* for strong EWGs, but is only weakly stereoselective, e.g., 63% *anti*:37% *syn*, for methoxy. Discuss a possible mechanistic basis for the curved Hammett plots and the relationship to the observed stereochemistry.
- 5.15. The second-order rate constants and solvent kinetic isotope effects for acid-catalyzed hydration are given below for several 2-substituted 1,3-butadienes. The products are a mixture of 1,2- and 1,4-addition. What information do these data provide about the mechanism of the reaction?



R	$k_2(M^{-1}s^{-1})$	k_{H^+}/k_{D^+}
c-C ₃ H ₅	1.22×10^{-2}	1.2
CH ₃	3.19×10^{-5}	1.8
Cl	2.01×10^{-8}	1.4
H	3.96×10^{-8}	1.8
C ₂ H ₅ O	60	-

- 5.16. The reaction of both *E*- and *Z*-2-butene with acetic acid to give 2-butyl acetate is catalyzed by various strong acids. With DBr, DCl, and CH₃SO₃H in CH₃CO₂D, the reaction proceeds with largely (84 ± 2%) *anti* addition. If the reaction is stopped short of completion, there is no incorporation of deuterium into unreacted alkene, nor any interconversion of the *E*- and *Z*-isomers. When the catalyst is changed to CF₃SO₃H, the recovered butene shows small amounts of 1-butene and interconversion of the 2-butene stereoisomers. The stereoselectivity of the reaction drops to 60–70% *anti* addition. How can you account for the changes that occur when CF₃SO₃H is used as the catalyst, as compared with the other acids?
- 5.17. A comparison of rate and product composition of the products from reaction of *t*-butyl chloride with NaOCH₃ in methanol and methanol-DMSO mixtures has been reported. Some of the data are shown below. Interpret the changes in rates and product composition as the amount of DMSO in the solvent mixture is increased.

[NaOMe] <i>M</i>	100% MeOH			36.8% DMSO			64.2% DMSO		
	Rate <i>k</i> × 10 ⁴ s ⁻¹	Product comp.(%)		Rate <i>k</i> × 10 ⁴ s ⁻¹	Product comp.(%)		Rate <i>k</i> × 10 ⁴ s ⁻¹	Product comp.(%)	
		Ether	Alkene		Ether	Alkene		Ether	Alkene
0.00	2.15	73.8	26.2	0.81	50	50	0.24	24	76
0.20	2.40			1.52			5.3		
0.25	2.30	62.9	32.1						
0.30	2.26			1.90	10.5	89.5	10.3	0	100
0.40	2.36			2.65			17.5	0	100
0.50	2.56	58.6	41.4				24.2	0	100
0.70				4.11	1.1	98.9			
0.75	2.58	51.7	48.3						
0.80				4.59					
0.90	2.64			6.16	4.1	95.9			
1.00	2.74	52.2	47.8	6.81	3.8	96.2			

- 5.18 a. The gas phase basicity of substituted α -methyl styrenes follows the Yukawa-Tsuno equation with $r^+ = 1.0$. The corresponding r^+ for 1-phenylpropane is 1.12 and for phenylacetylene it is 1.21. How are these values related to the relative stability of the carbocations formed by protonation?

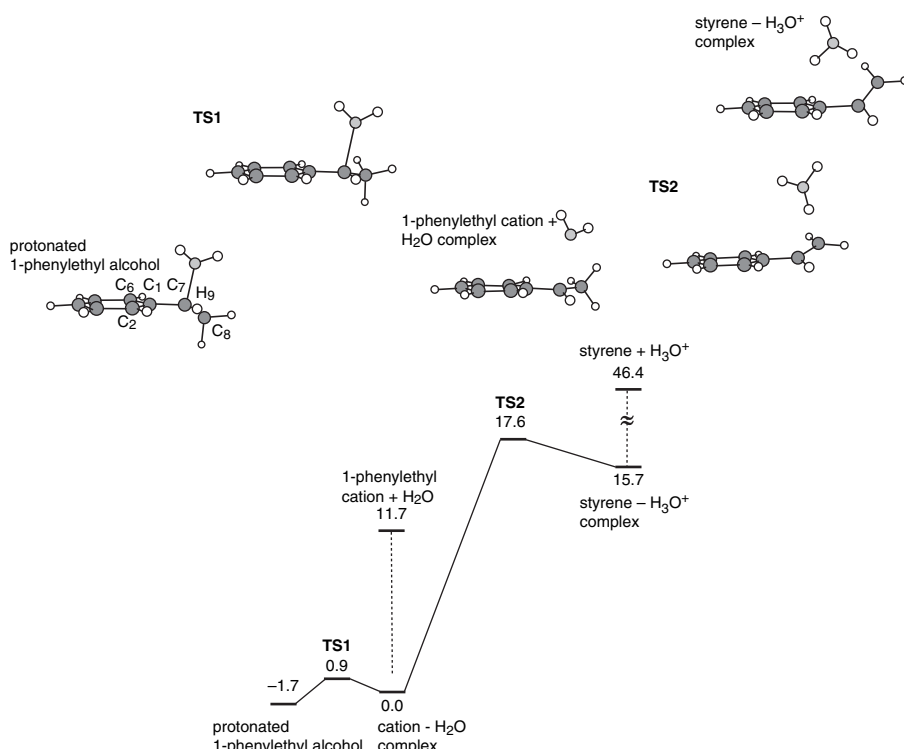


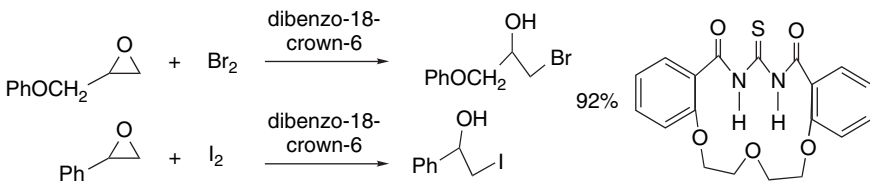
Fig. 5.P18b. Reaction profile for ionization and protonation routes to 1-phenylethyl cation. Relative energies are in kcal/mol. Reproduced from the *Bulletin of the Chemical Society of Japan.*, **71**, 2427 (1998).

Table 5.P18b. Selected Structural Parameters, Charge Densities, and Energies of Reactants and Transition States for Formation of a 1-Phenylethylium Ion

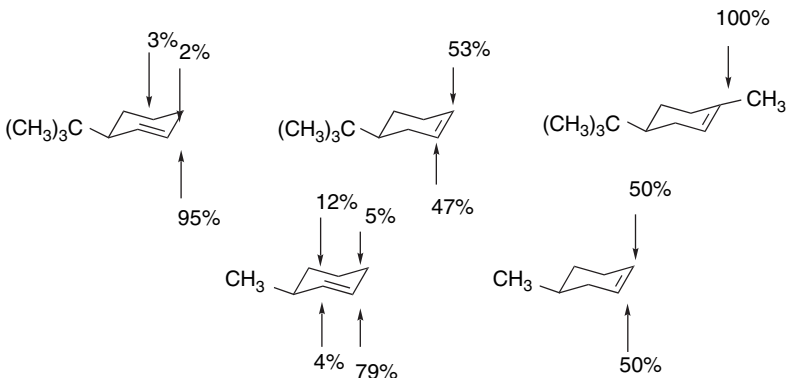
Bond length	Protonated Alcohol	TS1	Phenylethylium Cation-H ₂ O Complex	TS2	Styrene-H ₃ O ⁺ Complex	Styrene
C(1)–C(7)	1.474	1.420	1.395	1.457	1.478	1.472
C(7)–C(8)	1.500	1.481	1.469	1.367	1.353	1.343
C(7)–O	1.641	2.077	2.639			
C(8)–C(10)	1.093	1.091	1.098	1.608	2.118	
Charge on Ph	0.225	0.369	0.468	0.196	0.111	-0.002
Relative energy	-1.7	0.9	0.0	17.6	15.7	46.4

b. The acid-catalyzed hydration of styrene and the dissociation of protonated 1-phenylethanol provide alternative routes to the 1-phenylethylium cation. The resonance component (r^+) of the Yukawa-Tsuno equations are 0.70 and 1.15, respectively. The reactions have been modeled using MP2/6-31G* calculations and Figure 5.P18b gives the key results. Table 5.P18b lists some of the structural features of the reactants, TSs, and products. Interpret and discuss these results.

5.19. Crown ethers have been found to catalyze the ring opening of epoxides by I₂ and Br₂. The catalysts also improve the regioselectivity, favoring addition of the halide at the less-substituted position. A related structure (shown on the right) is an even better catalyst. Indicate a mechanism by which these catalytic effects can occur.

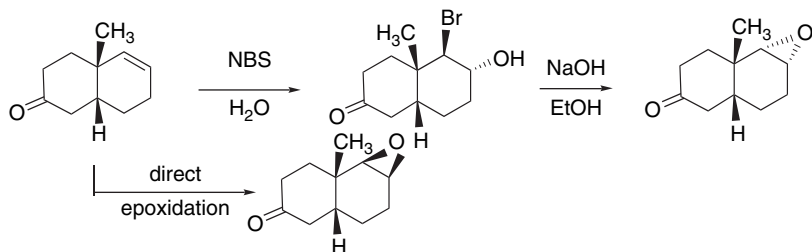


5.20. The chart below shows the regio- and stereoselectivity observed for oxymercuration reduction of some 3- and 4-alkylcyclohexenes. Provide an explanation for the product ratios in terms of the general mechanism for oxymercuration discussed in Section 5.6.1.

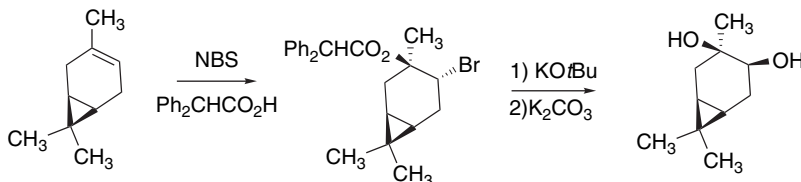


5.21. Solvohalogenation can be used to achieve both regio- and stereochemical control for synthetic purposes in alkene addition reactions. Some examples are shown below. Discuss the factors that lead to the observed regio- or stereochemical outcome.

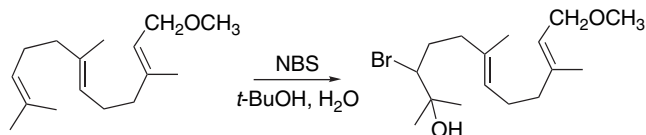
a. Control of the stereochemistry of an epoxide:



b. Formation of *cis*-diols:



c. Chemoselective functionalization of polyalkenes:



Carbanions and Other Carbon Nucleophiles

Introduction

This chapter is concerned with carbanions, which are the conjugate bases (in the Brønsted sense) formed by deprotonation at carbon atoms. Carbanions are very important in synthesis because they are good nucleophiles and formation of new carbon-carbon bonds often requires a nucleophilic carbon species. Carbanions vary widely in stability, depending on the hybridization of the carbon atom and the ability of substituent groups to stabilize the negative charge. In the absence of a stabilizing substituent, removal of a proton from a C–H bond is difficult. There has therefore been much effort devoted to study of the methods of generating carbanions and understanding substituent effects on stability and reactivity. Fundamental aspects of carbanion structure and stability were introduced in Section 3.4.2. In this chapter we first consider the measurement of hydrocarbon acidity. We then look briefly at the structure of organolithium compounds, which are important examples of carbanionic character in organometallic compounds. In Section 6.3 we study carbanions that are stabilized by functional groups, with emphasis on carbonyl compounds. In Section 6.4 the neutral nucleophilic enols and enamines are considered. Finally in Section 6.5 we look at some examples of carbanions as nucleophiles in S_N2 reactions.

6.1. Acidity of Hydrocarbons

In the discussion of the relative acidity of carboxylic acids in Chapter 1 (p. 53–54), the thermodynamic acidity, expressed as the acid dissociation constant in aqueous solution, was taken as the measure of acidity. Determining the dissociation constants of carboxylic acids in aqueous solution by measuring the titration curve with a pH-sensitive electrode is straightforward, but determination of the acidity of hydrocarbons is more difficult. As most are quite weak acids, very strong bases are required

to effect deprotonation. Water and alcohols are far more acidic than nearly all hydrocarbons and are unsuitable solvents for the generation of anions from hydrocarbons. Any strong base will deprotonate the solvent rather than the hydrocarbon. For synthetic purposes, aprotic solvents such as diethyl ether, THF, and DME are used, but for equilibrium measurements solvents that promote dissociation of ion pairs and ion clusters are preferred. Weakly acidic solvents such as dimethyl sulfoxide (DMSO) and cyclohexylamine are used in the preparation of strongly basic carbanions. The high polarity and cation-solvating ability of DMSO facilitates dissociation of ion pairs so that the equilibrium data refer to the solvated dissociated ions, rather than to ion aggregates.

The basicity of a base-solvent system can be specified by a basicity function H_- . The value of H_- corresponds essentially to the pH of strongly basic nonaqueous solutions. The larger the value of H_- , the greater the proton-abSTRACTING ability of the medium. The process of defining a basicity function is analogous to that described for acidity functions in Section 3.7.1.3. Use of a series of overlapping indicators permits assignment of H_- values to base-solvent systems, and allows pK 's to be determined over a range of 0–35 pK units.¹ The indicators employed include substituted anilines and arylmethanes that have significantly different electronic (UV–VIS) spectra in their neutral and anionic forms. Table 6.1 presents H_- values for some representative solvent-base systems.

The acidity of a hydrocarbon can be determined in an analogous way.² If the electronic spectra of the neutral and anionic forms are sufficiently different, the concentration of each can be determined directly in a solution of known H_- ; the equilibrium constant for



is related to pK_{RH} by the equation

$$pK_{\text{RH}} = H_- + \log \frac{[\text{RH}]}{[\text{R}^-]} \quad (6.1)$$

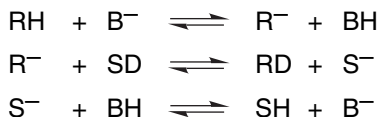
Table 6.1. Values of H_- for Some Representative Solvent-Base Systems

Solution	H_-^a
1 M KOH	14.0
5 M KOH	15.5
10 M KOH	17.0
1.0 M NaOMe in MeOH	17.0
5.0 M NaOMe in MeOH	19.0
0.01 M NaOMe in 1:1 DMSO-MeOH	15.0
0.01 M NaOMe in 10:1 DMSO-MeOH	18.0
0.01 M NaOEt in 20:1 DMSO-EtOH	21.0

a. Selected values from J. R. Jones, *The Ionization of Carbon Acids*, Academic Press, New York, 1973, Chap. 6, are rounded to the nearest 0.5 pH unit.

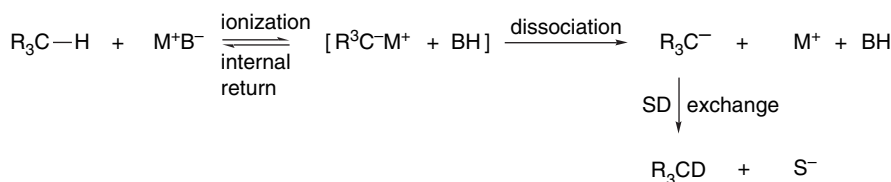
- We will restrict the use of pK_a to acid dissociation constants in aqueous solution. The designation pK refers to the acid dissociation constant under other conditions.
- D. Dolman and R. Stewart, *Can. J. Chem.*, **45**, 911 (1967); E. C. Steiner and J. M. Gilbert, *J. Am. Chem. Soc.*, **87**, 382 (1965); K. Bowden and R. Stewart, *Tetrahedron*, **21**, 261 (1965).

When the acidities of hydrocarbons are compared in terms of the relative stabilities of neutral and anionic forms, the appropriate data are *equilibrium* acidity measurements, which relate directly to the relative stability of the neutral and anionic species. For compounds with $pK > \sim 35$, it is difficult to obtain equilibrium data. In such cases, it may be possible to compare the *rates of deprotonation*, i.e., the *kinetic acidity*. These comparisons can be made between different protons in the same compound or between two different compounds by following an isotopic exchange. In the presence of a deuterated solvent, the rate of incorporation of deuterium is a measure of the rate of carbanion formation.³ Tritium (³H)-NMR spectroscopy is also a sensitive method for direct measurement of kinetic acidity.⁴



It has been found that there is often a correlation between the rate of proton abstraction (kinetic acidity) and the thermodynamic stability of the carbanion (thermodynamic acidity). Owing to this relationship, kinetic measurements can be used to extend scales of hydrocarbon acidities. These kinetic measurements have the advantage of not requiring the presence of a measurable concentration of the carbanion; instead, the relative ease of carbanion formation is judged by the rate at which exchange occurs. This method is applicable to weakly acidic hydrocarbons for which no suitable base will generate a measurable carbanion concentration.

The kinetic method of determining relative acidity suffers from one serious complication, however, which has to do with the fate of the ion pair that is formed immediately on abstraction of the proton.⁵ If the ion pair separates and diffuses rapidly into the solution, so that each deprotonation results in exchange, the exchange rate is an accurate measure of the rate of deprotonation. Under many conditions of solvent and base, however, an ion pair may return to reactants at a rate exceeding protonation of the carbanion by the solvent, a phenomenon known as *internal return*.



When there is internal return, a deprotonation event escapes detection because exchange does not occur. One experimental test for the occurrence of internal return is racemization at chiral carbanionic sites that takes place without exchange. Even racemization cannot be regarded as an absolute measure of the deprotonation rate because, under some conditions, hydrogen-deuteron exchange has been shown to occur with retention of configuration. Owing to these uncertainties about the fate of ion pairs, it is important

³ A. I. Shatenshtein, *Adv. Phys. Org. Chem.*, **1**, 155 (1963).

⁴ R. E. Dixon, P. G. Williams, M. Saljoughian, M. A. Long, and A. Streitwieser, *Magn. Res. Chem.*, **29**, 509 (1991); A. Streitwieser, L. Xie, P. Speers, and P. G. Williams, *Magn. Res. Chem.*, **36**, S 209 (1998).

⁵ W. T. Ford, E. W. Graham, and D. J. Cram, *J. Am. Chem. Soc.*, **89**, 4661 (1967); D. J. Cram, C. A. Kingsbury, and B. Rickborn, *J. Am. Chem. Soc.*, **83**, 3688 (1961).

that a linear relationship between exchange rates and equilibrium acidity be established for representative examples of the compounds under study. A satisfactory correlation provides a basis for using kinetic acidity data for compounds of that structural type.

The nature of the solvent in which the extent or rate of deprotonation is determined has a significant effect on the apparent acidity of the hydrocarbon. In general, the extent of ion aggregation is primarily a function of the ability of the solvent to solvate the ionic species. In THF, DME, and other ethers, there is usually extensive ion aggregation. In dipolar aprotic solvents, especially dimethyl sulfoxide, ion pairing is less significant.⁶ The identity of the cation also has a significant effect on the extent of ion pairing. Hard cations promote ion pairing and aggregation. Because of these factors, the numerical pK values are not absolute and are specific to the solvent and cation. Nevertheless, they provide a useful measure of relative acidity. The two solvents that have been used for most quantitative measurements on hydrocarbons are dimethyl sulfoxide and cyclohexylamine.

A series of hydrocarbons has been studied in cyclohexylamine, using cesium cyclohexylamide as base. For many of the compounds studied, spectroscopic measurements were used to determine the relative extent of deprotonation of two hydrocarbons and thus establish relative acidity.⁷ For other hydrocarbons, the acidity was derived by kinetic measurements. It was shown that the rate of tritium exchange for a series of related hydrocarbons is linearly related to the equilibrium acidities of these hydrocarbons in the solvent system. This method was used to extend the scale to hydrocarbons such as toluene for which the exchange rate, but not equilibrium data, can be obtained.⁸ Representative values of some hydrocarbons with pK values ranging from 16 to above 40 are given in Table 6.2. The pK values of a wide variety of organic compounds have been determined in DMSO,⁹ and some of these values are listed in Table 6.2 as well. It is not expected that these values will be numerically identical with those in other solvents, but for most compounds the same relative order of acidity is observed. For synthetic purposes, carbanions are usually generated in ether solvents, often THF or DME. There are relatively few quantitative data available on hydrocarbon acidity in such solvents. Table 6.2 contains a few entries for Cs^+ salts. The numerical values are scaled with reference to the pK of 9-phenylfluorene.¹⁰ The acidity trends are similar to those in cyclohexylamine and DMSO.

Some of the relative acidities in Table 6.2 can be easily understood. The order of decreasing acidity $\text{Ph}_3\text{CH} > \text{Ph}_2\text{CH}_2 > \text{PhCH}_3$, for example, reflects the ability of each successive phenyl group to stabilize the negative charge on carbon. This stabilization is a combination of both resonance and the polar EWG effect of the phenyl groups. The much greater acidity of fluorene relative to dibenzocycloheptatriene (Entries 5 and 6) is the result of the aromaticity of the cyclopentadienide ring in the anion of fluorene. Cyclopentadiene (Entry 9) is an exceptionally acidic hydrocarbon, comparable in acidity to simple alcohols, owing to the aromatic stabilization of the anion. Some more subtle effects are seen as well. Note that fusion of a benzene ring *decreases* the acidity

6. E. M. Arnett, T. C. Morarity, L. E. Small, J. P. Rudolph, and R. P. Quirk, *J. Am. Chem. Soc.*, **95**, 1492 (1973); T. E. Hogen-Esch and J. Smid, *J. Am. Chem. Soc.*, **88**, 307 (1966).
7. A. Streitwieser, Jr., J. R. Murdoch, G. Hafelinger, and C. J. Chang, *J. Am. Chem. Soc.*, **95**, 4248 (1973); A. Streitwieser, Jr., E. Ciuffarin, and J. H. Hammons, *J. Am. Chem. Soc.*, **89**, 63 (1967); A. Streitwieser, Jr., E. Juaristi, and L. L. Nebenzahl, in *Comprehensive Carbanion Chemistry*, Part A, E. Bunzel and T. Durst, ed., Elsevier, New York, 1980, Chap. 7.
8. A. Streitwieser, Jr., M. R. Granger, F. Mares, and R. A. Wolf, *J. Am. Chem. Soc.*, **95**, 4257 (1973).
9. F. G. Bordwell, *Acc. Chem. Res.*, **21**, 456 (1988).
10. D. A. Bors, M. J. Kaufman, and A. Streitwieser, Jr., *J. Am. Chem. Soc.*, **107**, 6975 (1985).

Table 6.2. Acidity of Some Hydrocarbons

Entry	Hydrocarbon	Cs^+ (CHA) ^a	Cs^+ (THF) ^b	K^+ (DMSO) ^c	SECTION 6.1 <i>Acidity of Hydrocarbons</i>
1	PhCH_2-H	41.2	40.9	43	
2		35.1	33.1		
3	$(\text{Ph}_2)\text{CH}-\text{H}$	33.4	33.3	32.3	
4	$(\text{Ph})_3\text{C}-\text{H}$	31.4	31.3	30.6	
5		31.2			
6		22.7	22.9	22.6	
7		19.9		20.1	
8		18.5	18.2	17.9	
9		16.6		18.1	

a. A Streitwieser, Jr., J. R. Murdoch, G. Hafelinger, and C. J. Chang, *J. Am. Chem. Soc.*, **93**, 4248 (1973); A. Streitwieser, Jr., E. Ciuffarin, and J. H. Hammons, *J. Am. Chem. Soc.*, **89**, 93 (1967); A. Streitwieser, Jr., and F. Guibe, *J. Am. Chem. Soc.*, **100**, 4523 (1978).

b. M. J. Kaufman, S. Gronert, and A. Streitwieser, *J. Am. Chem. Soc.*, **110**, 2829 (1988); A. Streitwieser, J. C. Ciula, J. A. Krom, and G. Thiele, *J. Org. Chem.*, **56**, 1074 (1991).

c. F. G. Bordwell, *Acc. Chem. Res.*, **21**, 456, 463 (1988).

of cyclopentadiene, as illustrated by comparing Entries 6, 7, and 9. (This relationship is considered in Problem 6.3)

Allylic conjugation stabilizes carbanions and pK values of 43 (in cyclohexylamine)¹¹ and 47–48 (in THF-HMPA)¹² were determined for propene. On the basis of exchange rates with cesium cyclohexylamide, cyclohexene and cycloheptene were found to have pK values of about 45 in cyclohexylamine.¹³ These data indicate that allylic positions have $pK \sim 45$. The hydrogens on the sp^2 carbons in benzene and ethene are more acidic than the hydrogens in saturated hydrocarbons. A pK of 45 has been estimated for benzene on the basis of extrapolation from a series of halogenated

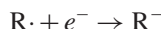
¹¹. D. W. Boerth and A. Streitwieser, Jr., *J. Am. Chem. Soc.*, **103**, 6443 (1981).

¹². B. Jaun, J. Schwarz, and R. Breslow, *J. Am. Chem. Soc.*, **102**, 5741 (1980).

¹³. A. Streitwieser, Jr., and D. W. Boerth, *J. Am. Chem. Soc.*, **100**, 755 (1978).

benzenes.¹⁴ Electrochemical measurements have been used to establish a lower limit of about 46 for the pK of ethene.¹²

For saturated hydrocarbons, exchange is too slow and reference points are so uncertain that determination of pK values by exchange measurements is not feasible. The most useful approach for obtaining pK data for such hydrocarbons involves making a measurement of the electrochemical potential for the reaction:



From this value and known C–H bond dissociation energies, we can calculate the pK values. Early application of these methods gave estimates of the pK of toluene of about 45 and of propene of about 48. Methane was estimated to have a pK in the range of 52–62.¹² Electrochemical measurements in DMF have given the results in Table 6.3.¹⁵ These measurements put the pK of methane at about 48, with benzylic and allylic stabilization leading to values of 39 and 38 for propene and toluene, respectively. These values are several units smaller than those determined by other methods. The electrochemical values overlap with the pK_{DMSO} scale for compounds such as diphenylmethane and triphenylmethane, and these values are also somewhat lower than those found by equilibrium studies.

Terminal alkynes are among the most acidic of the hydrocarbons. For example, in DMSO, phenylacetylene is found to have a pK near 26.5.¹⁶ In cyclohexylamine, the value is 23.2.¹⁷ An estimate of the pK in aqueous solution of 20 is based on a Brønsted relationship (see p. 348).¹⁸ The relatively high acidity of acetylenes is associated with the large degree of *s* character of the C–H bond. The *s* character is 50%, as opposed to 25% in sp^3 bonds. The electrons in orbitals with high *s* character experience decreased shielding from the nuclear charge. The carbon is therefore effectively *more electronegative*, as viewed from the proton sharing an *sp* hybrid orbital, and hydrogens on *sp* carbons exhibit greater acidity. (See Section 1.1.5 to review carbon hybridization-electronegativity relationships.) This same effect accounts for the relatively high acidity

Table 6.3. pK Values for Less Acidic Hydrocarbons

Hydrocarbon	$pK(\text{DMF})^{\text{a}}$
Methane	48
Ethane	51
Cyclopentane	49
Cyclohexane	49
Propene	38
Toluene	39
Diphenylmethane	31
Triphenylmethane	29

a. K. Daasbjerg, *Acta Chem. Scand.*, **49**, 878 (1995).

¹⁴. M. Stratakis, P. G. Wang, and A. Streitwieser, Jr., *J. Org. Chem.*, **61**, 3145 (1996).

¹⁵. K. Daasbjerg, *Acta Chem. Scand.*, **49**, 878 (1995).

¹⁶. F. G. Bordwell and W. S. Matthews, *J. Am. Chem. Soc.*, **96**, 1214 (1974).

¹⁷. A. Streitwieser, Jr., and D. M. E. Reuben, *J. Am. Chem. Soc.*, **93**, 1794 (1971).

¹⁸. D. B. Dahlberg, M. A. Kuzemko, Y. Chiang, A. J. Kresge, and M. F. Powell, *J. Am. Chem. Soc.*, **105**, 5387 (1983).

$$\text{p}K_a = 83.1 - 1.3(\%)s$$

The correlation can also be expressed in terms of the NMR coupling constant $J^{13}\text{C}-\text{H}$, which is related to hybridization.²⁰ These numerical relationships break down when applied to a wider range of molecules, where other factors contribute to carbanion stabilization.²¹

Knowledge of the structure of carbanions is important to understanding the stereochemistry of their reactions. Ab initio (HF/4-31G) calculations indicate a pyramidal geometry at carbon in the methyl and ethyl anions. The optimum H–C–H angle in these two carbanions is calculated to be 97°–100°. An interesting effect is found in that the proton affinity (basicity) of methyl anion decreases in a regular manner as the H–C–H angle is decreased.²² This increase in acidity with decreasing internuclear angle parallels the trend in small-ring compounds, in which the acidity of hydrogens is substantially greater than in compounds having tetrahedral geometry at carbon. Pyramidal geometry at carbanions can also be predicted on the basis of qualitative considerations of the orbital occupied by the unshared electron pair. In a planar carbanion, the lone pair would occupy a p orbital. In a pyramidal geometry, the orbital has more s character. Because the electron pair is of lower energy in an orbital with some s character, it is predicted that a pyramidal geometry will be favored. Qualitative VSEPR considerations also predict pyramidal geometry (see p. 7).

As was discussed in Section 3.8, measurements in the gas phase, which eliminate the effect of solvation, show structural trends that parallel measurements in solution but have much larger absolute energy differences. Table 6.4 gives some data for key hydrocarbons for the ΔH of proton dissociation. These data show a correspondence with

Table 6.4. Enthalpy of Proton Dissociation for Some Hydrocarbons (Gas Phase)^a

Hydrocarbon	$\Delta H(\text{kcal/mol})^{\text{a}}$
Methane	418.8
Ethene	407.5
Cyclopropane	411.5
Benzene	400.8
Toluene	381

a. S. T. Graul and R. R. Squires, *J. Am. Chem. Soc.*, **112**, 2517 (1990).

¹⁹. Z. B. Maksic and M. Eckert-Maksic, *Tetrahedron*, **25**, 5113 (1969); M. Randic and Z. Maksic, *Chem. Rev.*, **72**, 43 (1972).

²⁰. A. Streitwieser, Jr., R. A. Caldwell, and W. R. Young, *J. Am. Chem. Soc.*, **91**, 529 (1969); S. R. Kass and P. K. Chou, *J. Am. Chem. Soc.*, **110**, 7899 (1988); I. Alkorta and J. Elguero, *Tetrahedron*, **53**, 9741 (1997).

²¹. R. R. Sauers, *Tetrahedron*, **55**, 10013 (1999).

²². A. Streitwieser, Jr., and P. H. Owens, *Tetrahedron Lett.*, 5221 (1973); A. Streitwieser, Jr., P. H. Owens, R. A. Wolf, and J. E. Williams, Jr., *J. Am. Chem. Soc.*, **96**, 5448 (1974); E. D. Jemmis, V. Buss, P. v. R. Schleyer, and L. C. Allen, *J. Am. Chem. Soc.*, **98**, 6483 (1976).

hybridization and delocalization effects observed in solution. The very large heterolytic dissociation energies reflect both the inherent instability of the carbanions and the electrostatic attraction between the oppositely charged carbanion and proton. By way of comparison, enthalpy measurements in DMSO using $\text{K}^+ \cdot \text{O}-t\text{-Bu}$ or $\text{KCH}_2\text{SOCH}_3$ as base give values of -15.4 and -18.2 kcal/mol, respectively, for fluorene, a hydrocarbon with a pK of about 20 .²³

Aqueous phase acidity for a number of hydrocarbons has been computed theoretically. A continuum dielectric solvation model was used and B3LYP/6-311++G(*d, p*) and MP2/G2 computations were employed.²⁴ Some of the results are given in Table 6.5. There is good agreement with experimental estimates for most of the compounds, although cyclopropane is somewhat less acidic than anticipated.

Tupitsyn and co-workers dissected the energies of deprotonation into two factors—the C–H bond energy and the structural reorganization of the carbanion—by calculating the energy of the carbanion at the geometry of the reactant hydrocarbon and then calculating the energy of relaxation to the minimum energy structure using AM1 computations.²⁵ It was found that strained ring compounds were dominated by the first factor, whereas compounds such as propene and toluene that benefit from carbanion delocalization were dominated by the second term. Benzene has a very low relaxation energy, consistent with a carbanion localized in an sp^2 orbital. The broad general picture that emerges from this analysis is that there are two major factors that influence the acidity of hydrocarbons. One is the inherent characteristics of the C–H bond resulting from hybridization and strain and the other is anion stabilization, which depends on delocalization of the charge.

The stereochemistry observed in proton exchange reactions of carbanions is dependent on the conditions under which the anion is formed and trapped by proton transfer. The dependence on solvent, counterion, and base is the result of the importance of ion pairing effects. The base-catalyzed cleavage of **1** is illustrative. The anion of **1** is cleaved at elevated temperatures to 2-butanone and 2-phenyl-2-butyl anion, which under the conditions of the reaction is protonated by the solvent. Use of resolved

Table 6.5. Computed Aqueous pK Values for Some Hydrocarbons

Hydrocarbon	B3LYP	MP2/G2
Ethyne	24.7	25.1
Cyclopentadiene	17.8	19.1
Cyclopropane	52.2	52.3
Toluene	42.1	42.4
Ethane	53.8	55.0

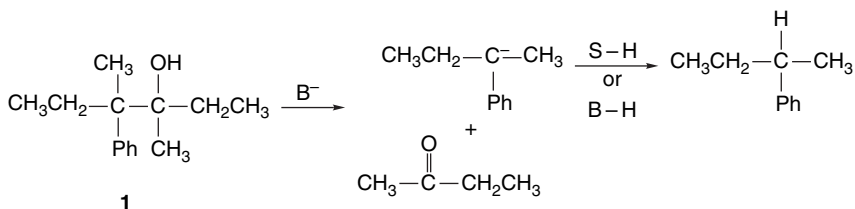
a. I. A. Topol, G. J. Tawa, R. A. Caldwell, M. A. Eisenstat, and S. K. Burt, *J. Phys. Chem. A*, **104**, 9619 (2000).

²³ E. M. Arnett and K. G. Venkatasubramanian, *J. Org. Chem.*, **48**, 1569 (1983).

²⁴ I. A. Topol, G. J. Tawa, R. A. Caldwell, M. A. Eisenstat, and S. K. Burt, *J. Phys. Chem. A*, **104**, 9619 (2000).

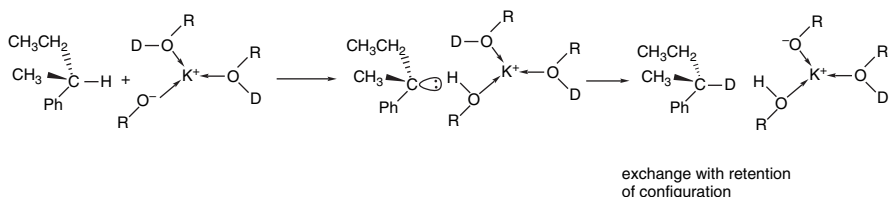
²⁵ I. F. Tupitsyn, A. S. Popov, and N. N. Zatsepina, *Russian J. Gen. Chem.*, **67**, 379 (1997).

1 allows the stereochemical features of the anion to be probed by measuring the enantiomeric purity of the 2-phenylbutane product.



Retention of configuration was observed in nonpolar solvents, while increasing amounts of inversion occurred as the proton-donating ability and the polarity of the solvent increased. Cleavage of **1** with potassium *t*-butoxide in benzene gave 2-phenylbutane with 93% net retention of configuration. The stereochemical course changed to 48% net inversion of configuration when potassium hydroxide in ethylene glycol was used. In DMSO using $\text{K}^+ \cdot \text{O-t-Bu}$ as base, completely racemic 2-phenylbutane was formed.²⁶ The retention in benzene presumably reflects a short lifetime for the carbanion in a tight ion pair. Under these conditions, the carbanion does not become symmetrically solvated before proton transfer from either the protonated base or the ketone. The solvent benzene is not an effective proton donor and the most likely proton source is *t*-butanol. In ethylene glycol, the solvent provides a good proton source and since net inversion is observed, the protonation must occur on an unsymmetrically solvated species that favors back-side protonation. The racemization that is observed in DMSO indicates that the carbanion has a sufficient lifetime to become symmetrically solvated. The stereochemistry observed in the three solvents is in good accord with their solvating properties. In benzene, reaction occurs primarily through ion pairs. Ethylene glycol provides a ready source of protons and fast proton transfer accounts for the observed inversion. DMSO promotes ion pair dissociation and equilibration, as indicated by the observed racemization.

The stereochemistry of hydrogen-deuterium exchange at the chiral carbon in 2-phenylbutane shows a similar trend. When potassium *t*-butoxide is used as the base, the exchange occurs with retention of configuration in *t*-butanol, but racemization occurs in DMSO.²⁷ The retention of configuration is visualized as occurring through an ion pair in which a solvent molecule coordinated to the metal ion acts as the proton donor. In DMSO, symmetrical solvation is achieved prior to protonation and there is complete racemization.

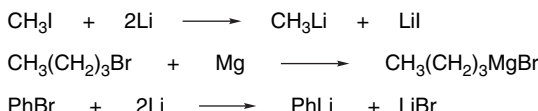


²⁶. D. J. Cram, A. Langemann, J. Allinger, and K. R. Kopecky, *J. Am. Chem. Soc.*, **81**, 5740 (1959).

²⁷. D. J. Cram, C. A. Kingsbury, and B. Rickborn, *J. Am. Chem. Soc.*, **83**, 3688 (1961).

6.2. Carbanion Character of Organometallic Compounds

The organometallic derivatives of lithium, magnesium, and other strongly electropositive metals have some of the properties expected for salts of carbanions. Owing to the low acidity of most hydrocarbons, organometallic compounds usually cannot be prepared by proton transfer reactions. Instead, the most general preparative methods start with the corresponding halogen compound.



There are other preparative methods, which are considered in Chapter 7 of Part B.

Organolithium compounds derived from saturated hydrocarbons are extremely strong bases and react rapidly with any molecule having an $-\text{OH}$, $-\text{NH}$, or $-\text{SH}$ group by proton transfer to form the hydrocarbon. Accurate pK values are not known, but range upward from the estimate of ~ 50 for methane. The order of basicity $\text{CH}_3\text{Li} < \text{CH}_3(\text{CH}_2)_3\text{Li} < (\text{CH}_3)_3\text{CLi}$ is due to the electron-releasing effect of alkyl substituents and is consistent with increasing reactivity in proton abstraction reactions in the order $\text{CH}_3\text{Li} < \text{CH}_3(\text{CH}_2)_3\text{Li} < (\text{CH}_3)_3\text{CLi}$. Phenyl-, methyl-, *n*-butyl-, and *t*-butyllithium are all stronger bases than the anions of the hydrocarbons listed in Table 6.2. Unlike proton transfers from oxygen, nitrogen, or sulfur, proton removal from carbon atoms is usually not a fast reaction. Thus, even though *t*-butyllithium is thermodynamically capable of deprotonating toluene, the reaction is quite slow. In part, the reason is that the organolithium compounds exist as tetramers, hexamers, and higher aggregates in hydrocarbon and ether solvents.²⁸

In solution, organolithium compounds exist as aggregates, with the degree of aggregation depending on the structure of the organic group and the solvent. The nature of the species present in solution can be studied by low-temperature NMR. *n*-Butyllithium in THF, for example, is present as a tetramer-dimer mixture.²⁹ The tetrameric species is dominant.



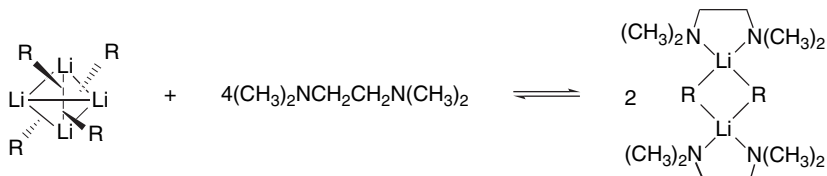
Tetrameric structures based on distorted cubic structures are also found for $(\text{CH}_3\text{Li})_4$ and $(\text{C}_2\text{H}_5\text{Li})_4$,³⁰ and they can be represented as tetrahedral of lithium ions with each face occupied by a carbanion ligand.



- ²⁸. G. Fraenkel, M. Henrichs, J. M. Hewitt, B. M. Su, and M. J. Geckle, *J. Am. Chem. Soc.*, **102**, 3345 (1980); G. Fraenkel, M. Henrichs, M. Hewitt, and B. M. Su, *J. Am. Chem. Soc.*, **106**, 255 (1984).
- ²⁹. D. Seebach, R. Hassig, and J. Gabriel, *Helv. Chim. Acta*, **66**, 308 (1983); J. F. McGarry and C. A. Ogle, *J. Am. Chem. Soc.*, **107**, 1805 (1984).
- ³⁰. E. Weiss and E. A. C. Lucken, *J. Organomet. Chem.*, **2**, 197 (1964); E. Weiss and G. Hencken, *J. Organomet. Chem.*, **21**, 265 (1970); H. Koester, D. Thoennes, and E. Weiss, *J. Organomet. Chem.*, **160**, 1 (1978); H. Dietrich, *Acta Crystallogr.*, **16**, 681 (1963); H. Dietrich, *J. Organomet. Chem.*, **205**, 291 (1981).

The THF solvate of lithium *t*-butylacetylidyne is another example of a tetrameric structure.³¹ In solutions of *n*-propyllithium in cyclopropane at 0°C, the hexamer is the main species, but higher aggregates are present at lower temperatures.²⁰

The reactivity of the organolithium compounds is increased by adding molecules capable of solvating the lithium cations. Tetramethylenediamine (TMEDA) is commonly used for organolithium reagents. This tertiary diamine can chelate lithium. The resulting complexes generally are able to effect deprotonation at accelerated rates.³² In the case of phenyllithium, NMR studies show that the compound is tetrameric in 1:2 ether-cyclohexane, but dimeric in 1:9 TMEDA-cyclohexane.³³



X-ray crystal structure determinations have been done on both dimeric and tetrameric structures. A dimeric structure crystallizes from hexane containing TMEDA.³⁴ This structure is shown in Figure 6.1a. A tetrameric structure incorporating four ether molecules forms from ether-hexane solution.³⁵ This structure is shown in Figure 6.1b. There is a good correspondence between the structures that crystallize and those indicated by the NMR studies.

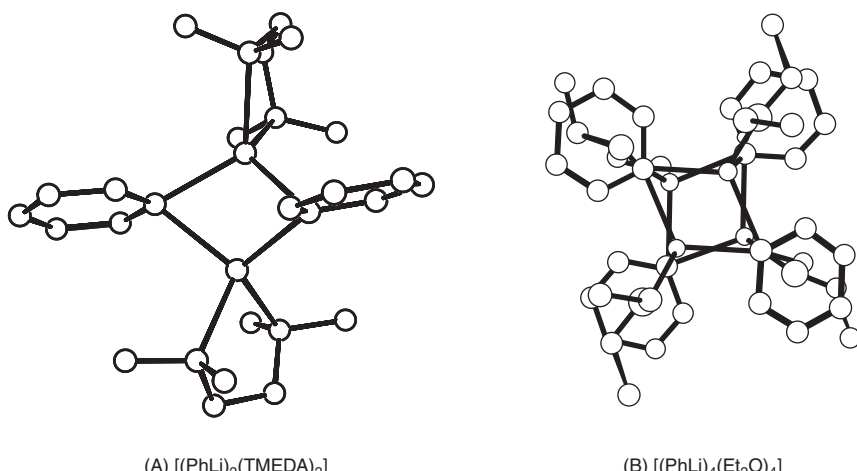


Fig. 6.1. Crystal structures of phenyllithium: (a) dimeric structure incorporating tetramethylethylenediamine; (b) tetrameric structure incorporating diethyl ether. Reproduced from *Chem. Ber.*, **111**, 3157 (1978) and *J. Am. Chem. Soc.*, **105**, 5320 (1983), by permission of Wiley-VCH and the American Chemical Society, respectively.

- ³¹ W. Neuberger, E. Weiss, and P. v. R. Schleyer, quoted in Ref. 37.
- ³² G. G. Eberhardt and W. A. Butte, *J. Org. Chem.*, **29**, 2928 (1964); R. West and P. C. Jones, *J. Am. Chem. Soc.*, **90**, 2656 (1968).
- ³³ L. M. Jackman and L. M. Scarmoutzos, *J. Am. Chem. Soc.*, **106**, 4627 (1984).
- ³⁴ D. Thoennes and E. Weiss, *Chem. Ber.*, **111**, 3157 (1978).
- ³⁵ H. Hope and P. P. Power, *J. Am. Chem. Soc.*, **105**, 5320 (1983).

Crystal structure determination has also been done on several complexes of *n*-butyllithium. A 4:1 *n*-BuLi:TMEDA complex is a tetramer accommodating two TMEDA molecules, which, rather than chelating a lithium, links the tetrameric units. The 2:2 *n*-BuLi:TMEDA complex has a structure similar to $[\text{PhLi}]_2 \cdot [\text{TMEDA}]_2$. Both 1:1 *n*-BuLi:THF and 1:1 *n*-BuLi:DME complexes are tetrameric with ether molecules coordinated at each lithium (Figure 6.2).³⁶ These and many other organolithium structures have been discussed in a review of this topic.³⁷

There has been extensive computational study of the structure of organolithium compounds.³⁸ The structures of the simple monolithium compounds are very similar to the corresponding hydrocarbons. The gas phase structure of monomeric methylolithium has been determined to be tetrahedral with an H–C–H bond angle of 106°.³⁹ These structural parameters are close to those calculated at the MP2/6-311G* level of theory.⁴⁰ Ethyllithium, and vinyllithium are also structurally similar to the corresponding

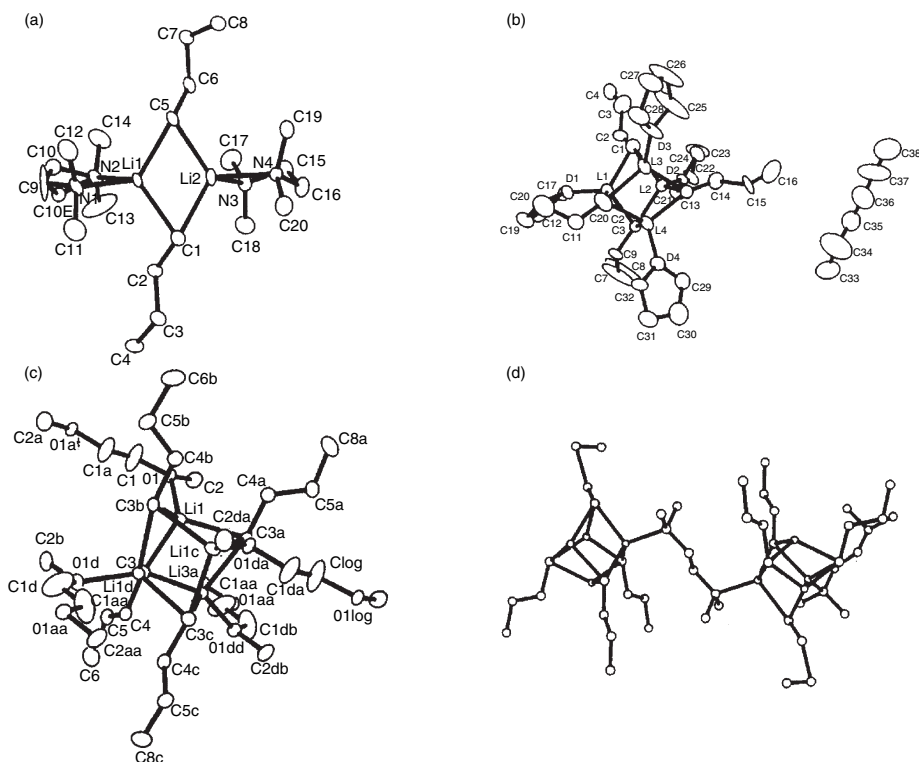


Fig. 6.2. Crystal structures of *n*-butyllithium: (a) $[(n\text{-BuLi}\cdot\text{TMEDA})_2]$; (b) $[(n\text{-BuLi}\cdot\text{THF})_4\text{hexane}]$; (c) $[(n\text{-BuLi}\cdot\text{DME})_4]$; (d) $[(n\text{-BuLi})_4\cdot\text{TMEDA}]$. Reproduced from *J. Am. Chem. Soc.*, **115**, 1568, 1573 (1993), by permission of the American Chemical Society.

- ³⁶ M. A. Nichols and P. G. Williard, *J. Am. Chem. Soc.*, **115**, 1568 (1993); N. D. R. Barnett, R. E. Mulvey, W. Clegg, and P. A. O'Neil, *J. Am. Chem. Soc.*, **115**, 1573 (1993).
- ³⁷ W. N. Setzer and P. v. R. Schleyer, *Adv. Organomet. Chem.*, **24**, 353 (1985).
- ³⁸ A. Streitwieser, S. M. Bachrach, A. Dorigo, and P. v. R. Schleyer, in *Lithium Chemistry*, A. M. Sapce and P. v. R. Schleyer, eds., Wiley, New York, 1995, pp. 1–43.
- ³⁹ D. B. Grotjahn, T. C. Pesch, J. Xin, and L. M. Ziurys, *J. Am. Chem. Soc.*, **119**, 12368 (1997).
- ⁴⁰ E. Kaufman, K. Raghavachari, A. E. Reed, and P. v. R. Schleyer, *Organometallics*, **7**, 1597 (1988).

hydrocarbon. This fact, along with the relatively high solubility of simple lithium compounds in nonpolar solvents, has given rise to the idea that the C–Li bond is largely covalent. However, AIM analysis of simple alkylolithium compounds indicates that the bonds are largely ionic. The charges on lithium in methyl- and vinylolithium are $+0.91e$ and $+0.92e$, respectively.⁴¹ The ionic character is also evident in the structure of allyl-lithium. The lithium is centered above the allyl anion, indicating an ionic structure.⁴² The good solubility in nonpolar solvents is perhaps due to the cluster-type structures, which place the organic groups on the periphery of the cluster.

The relative slowness of the abstraction of protons from carbon acids by organolithium reagents is probably also due to the compact character of the carbon-lithium clusters. Since the electrons associated with the carbanion are tightly associated with the cluster of lithium cations, some activation energy is required to break the bond before the carbanion can act as a base. This kinetic sluggishness of organometallic compounds as bases permits important reactions in which the organometallic species acts as a *nucleophile* in preference to functioning as a strong base. The addition reactions of organolithium and organomagnesium compounds to carbonyl groups in aldehydes, ketones, and esters are important examples. As will be seen in the next section, carbonyl compounds are much more acidic than hydrocarbons. Nevertheless, in most cases, the proton transfer reaction of organometallic reagents is *slower than nucleophilic attack at the carbonyl group*. It is this feature of the reactivity of organometallics that permits the very extensive use of organometallic compounds in organic synthesis. The reactions of organolithium and organomagnesium compounds with carbonyl compounds is discussed in a synthetic context in Chapter 7 of Part B.

6.3. Carbanions Stabilized by Functional Groups

Electron-withdrawing substituents cause very large increases in the acidity of C–H bonds. Among the functional groups that exert a strong stabilizing effect on carbanions are carbonyl, nitro, sulfonyl, and cyano. Both polar and resonance effects are involved in the ability of these functional groups to stabilize the negative charge. Perhaps the best basis for comparing these groups is the data on the various substituted methanes. Bordwell and co-workers determined the relative acidities of the substituted methanes with reference to aromatic hydrocarbon indicators in DMSO.⁴³ The data are given in Table 6.6, which established the ordering $\text{NO}_2 > \text{C}=\text{O} > \text{CO}_2\text{R} \sim \text{SO}_2 \sim \text{CN} > \text{CONR}_2$ for anion stabilization.

Carbanions derived from carbonyl compounds are often referred to as *enolates*, a name derived from the enol tautomer of carbonyl compounds. The resonance-stabilized enolate anion is the conjugate base of both the keto and enol forms of carbonyl compounds. The anions of nitro compounds are called *nitronates* and are also resonance stabilized. The stabilization of anions of sulfones is believed to be derived primarily from polar and polarization effects.

⁴¹ J. P. Richie and S. M. Bachrach, *J. Am. Chem. Soc.*, **109**, 5909 (1987).

⁴² T. Clark, C. Rohde, and P. v. R. Schleyer, *Organometallics*, **2**, 1344 (1983).

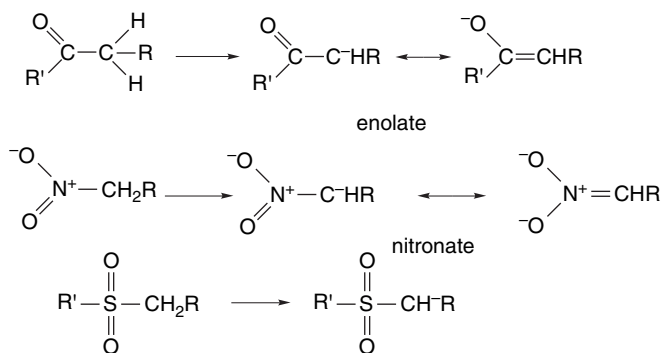
⁴³ F. G. Bordwell and W. S. Matthews, *J. Am. Chem. Soc.*, **96**, 1216 (1974); W. S. Matthews, J. E. Bares, J. E. Bartmess, F. G. Bordwell, F. J. Cornforth, G. E. Drucker, Z. Margolin, R. J. McCallum, G. J. McCollum, and N. R. Vanier, *J. Am. Chem. Soc.*, **97**, 7006 (1975).

Table 6.6. Equilibrium Acidities of Substituted Methanes in Dimethyl Sulfoxide^a

Compound	pK
CH ₃ NO ₂	17.2
CH ₃ COPh	24.7
CH ₃ COCH ₃	26.5
CH ₃ SO ₂ Ph	29.0
CH ₃ CO ₂ C ₂ H ₅	30.5 ^b
CH ₃ SO ₂ CH ₃	31.1
CH ₃ CN	31.3
CH ₃ CON(C ₂ H ₅) ₂	34.5 ^b

a. Except as noted otherwise, from W. S. Matthews, J. E. Barres, J. E. Bartness, F. G. Bordwell, F. J. Cornforth, G. E. Drucker, Z. Margolin, R. J. McCallum, G.J. McCollum, and N. R. Vanier, *J. Am. Chem. Soc.*, **97**, 7006 (1975).

b. F. G. Bordwell and H. E. Fried, *J. Org. Chem.*, **46**, 4327 (1981).



The presence of two EWGs further stabilizes the negative charge. Pentane-2,4-dione, for example, has a pK around 9 in water. Most β -diketones are sufficiently acidic that their carbanions can be generated using the conjugate bases of hydroxylic solvents such as water or alcohols, which have pK values of 15–20. Stronger bases are required for compounds that have a single stabilizing functional group. Alkali metal salts of ammonia or amines and sodium hydride are sufficiently strong bases to form carbanions from most ketones, aldehydes, and esters. The Li⁺ salt of diisopropylamine (LDA) is a popular strong base for use in synthetic procedures. It is prepared by reaction of *n*-BuLi with diisopropylamine. Lithium, sodium, and potassium salts of hexamethyldisilylamine (LiHMDS, NaHMDS, KHMDS) are also important.⁴⁴ The generation of carbanions stabilized by electron-attracting groups is very important from a synthetic point of view; the synthetic aspects of the chemistry of these carbanions is discussed in Chapters 1 and 2 of Part B. Table 6.7 gives experimental pK data for some representative compounds in DMSO.

There have been numerous studies of the rates of deprotonation of carbonyl compounds. These data are of interest not only because they define the relationship

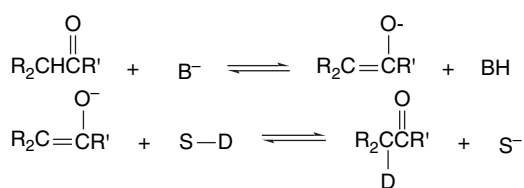
⁴⁴. T. L. Rathman, *Spec. Chem. Mag.*, **9**, 300 (1989).

Table 6.7. pK Values for Other Representative Compounds in DMSO^a

Ketones	pK	Esters	pK
	26.5		22.6
	24.7		21.4
	19.9		25.2
	18.7	Ketoesters	
	25.8		14.2
	26.4	Diesters	
	16.95		16.4
Diketones			7.3
	13.3	Nitroalkanes	
	13.35		17.2
	11.2		12.3
			16.0
			17.9

a. F. G. Bordwell, *Acc. Chem. Res.*, **21**, 456 (1988).

between thermodynamic and kinetic acidity for these compounds, but also because they are necessary for understanding mechanisms of reactions in which enolates are involved as intermediates. Rates of enolate formation can be measured conveniently by following isotopic exchange using either deuterium or tritium.



An older technique is to measure the rate of halogenation of the carbonyl compound. Ketones and aldehydes in their carbonyl forms do not react rapidly with the halogens but the enolate is rapidly attacked. The rate of halogenation is therefore a measure of the rate of deprotonation.

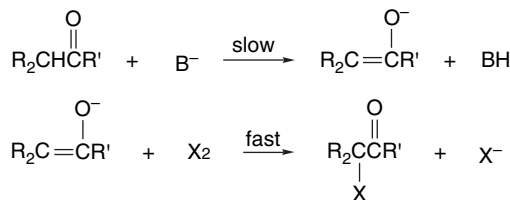


Table 6.8 gives data on the rates of deuteration of some alkyl ketones. From these data, the order of reactivity toward deprotonation is $\text{CH}_3 > \text{RCH}_2 > \text{R}_2\text{CH}$. Steric hindrance to the approach of the base is the major factor in establishing this order. The importance of steric effects can be seen by comparing the CH_2 group in 2-butanone with the more hindered CH_2 group in 4,4-dimethyl-2-pentanone. The two added methyl groups on the adjacent carbon decrease the rate of proton removal by a factor of about 100. The rather slow rate of exchange at the CH_3 group of 4,4-dimethyl-2-pentanone must also reflect a steric factor arising from the bulky nature of the neopentyl group. If bulky groups

Table 6.8. Relative Rates and E_a for Base-Catalyzed Deuteration of Some Ketones

Ketone	Relative Rate ^a	E_a ^b
$\text{CH}_3\text{CCH}_2-\text{H}$	100	11.9
$\text{CH}_3\overset{\text{O}}{\underset{\text{H}}{\text{C}}}(\text{CH}_3)\text{CH}_2\text{CH}_3$	41.5	12.1
$\text{H}-\text{CH}_2\overset{\text{O}}{\underset{\text{H}}{\text{C}}}(\text{CH}_2\text{CH}_3)\text{CH}_3$	45	
$\text{CH}_3\overset{\text{O}}{\underset{\text{H}}{\text{C}}}(\text{CH}_3)_2$	<0.1	
$\text{H}-\text{CH}_2\overset{\text{O}}{\underset{\text{H}}{\text{C}}}(\text{CH}_3)_2\text{CH}_3$	45	12.3
$\text{CH}_3\overset{\text{O}}{\underset{\text{H}}{\text{C}}}(\text{CH}_3)_3$	0.45	
$\text{H}-\text{CH}_2\overset{\text{O}}{\underset{\text{H}}{\text{C}}}(\text{CH}_3)_3\text{CH}_3$	5.1	

a. In aqueous solution with sodium carbonate as the base. The data of C. Rappe and W. H. Sachs, *J. Org. Chem.*, **32**, 4127 (1967), given on a per-group basis have been converted to a per-hydrogen basis.

b. CH_3O^- -catalyzed exchange in CH_3OD . T. Niya, M. Yukawa, H. Morishita, H. Ikeda, and Y. Goto, *Chem. Pharm. Bull.*, **39**, 2475 (1991).

interfere with effective solvation of the developing negative charge on oxygen, the rate of proton abstraction is reduced. The observed activation energies parallel the rates.⁴⁵

Structural effects on the rates of deprotonation of ketones have also been studied using very strong bases under conditions where complete conversion to the enolate occurs. In solvents such as THF or DME, bases such as LDA and KHMDS give solutions of the enolates that reflect the relative rates of removal of the different protons in the carbonyl compound (*kinetic control*). The least hindered proton is removed most rapidly under these conditions, so for unsymmetrical ketones the major enolate is the less-substituted one. Scheme 6.1 shows some representative data. Note that for many ketones, both *E*- and *Z*-enolates can be formed.

The equilibrium ratios of enolates for several ketone-enolate systems are also shown in Scheme 6.1. Equilibrium among the various enolates of a ketone can be established by the presence of an excess of the ketone, which permits reversible proton transfer. Equilibration is also favored by the presence of dissociating additives such as HMPA. As illustrated by most of the examples in Scheme 6.1, the kinetic enolate is formed by removal of the least hindered hydrogen. The composition of the equilibrium enolate mixture is usually more closely balanced than for kinetically

Scheme 6.1. Composition of Enolate Mixtures Formed under Kinetic and Thermodynamic Control^a

1		Kinetic (LDA 0 °C)		71%		13%		16%
2								99%
		Kinetic (KHMDS, -78 °C)		99%		1%		
		Thermodynamic (KH)		88%		12%		
3								
		Kinetic (LDA -78 °C)		100%		0%		0%
		Thermodynamic (KH, 20 °C)		42%		46%		12%
4b				<i>E</i>		<i>Z</i>		
		Kinetic LDA		40%		60%		
		LITMP		32%		68%		
		LiHMDS		2%		98%		
		LiNHC6H5Cl3		2%		98%		0
5								
		Kinetic (LDA 0 °C)		14%		86%		
		Thermodynamic (NaH)		2%		98%		
6								
		Kinetic (LDA, 0 °C)		99%		1%		
		Thermodynamic (NaH)		26%		74%		
7								
		Kinetic (Ph3CLi)		100%		0%		
		Thermodynamic (Ph3CK)		35%		65%		
8								
		Kinetic (Ph3CLi)		82%		18%		
		Thermodynamic (Ph3CK)		52%		48%		
9								
		Kinetic (LDA)		98%		2%		
		Thermodynamic (NaH)		50%		50%		

a. Selected from a more complete compilation by D. Caine, in *Carbon-Carbon Bond Formation*, R. L. Augustine, ed., Marcel Dekker, New York, 1979.

b. C. H. Heathcock, C. T. Buse, W. A. Kleschick, M. C. Pirrung, J. E. Sohn, and J. Lampe, *J. Org. Chem.*, **45**, 1066 (1980); L. Xie, K. van Landeghem, K. M. Isenberger, and C. Bernier, *J. Org. Chem.*, **68**, 641 (2003).

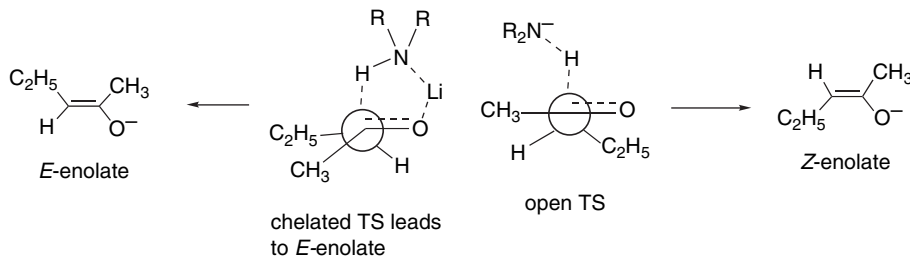
⁴⁵. T. Niiya, M. Yukawa, H. Morishita, H. Ikeda, and Y. Goto, *Chem. Pharm. Bull.*, **39**, 2475 (1991).

controlled conditions. In general, the more highly substituted enolate is the preferred isomer, but if the alkyl groups are sufficiently branched as to interfere with solvation of the enolate there are exceptions. This factor, along with CH_3/CH_3 repulsion, presumably accounts for the higher stability of the less-substituted enolate from 3-methyl-2-butanone (Entry 2). The acidifying effect of an adjacent phenyl group outweighs steric effects in the case of 1-phenyl-2-propanone, and as a result the conjugated enolate is favored by both kinetic and thermodynamic conditions (Entry 5).

The synthetic importance of the LDA and LiHMDS type of deprotonation has led to studies of enolate composition under various conditions. Deprotonation of 2-pentanone was examined with LDA in THF, with and without HMPA. C(1)-deprotonation was favored under both conditions, but the *Z:E* ratio for C(3) deprotonation was sensitive to the presence of HMPA (0.75 M).⁴⁶ More *Z*-enolate is formed when HMPA is present.

Conditions	Ratio C(1):C(3) deprotonation	Ratio <i>Z:E</i> for C(3) deprotonation
0°C, THF alone	7.9	0.20
−60°C, THF alone	7.1	0.15
0°C, THF – HMPA	8.0	1.0
−60°C, THF – HMPA	5.6	3.1

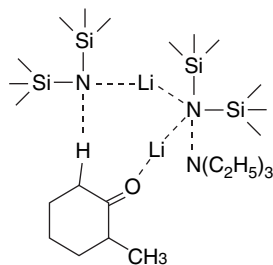
These and other related enolate ratios are interpreted in terms of a tight, reactant-like TS with Li chelation in THF and a looser TS in the presence of HMPA. The chelated TS favors the *E*-enolate, whereas the open TS favors the *Z*-enolate. The effect of the HMPA is to solvate the Li^+ ion, reducing the importance of Li^+ coordination with the carbonyl oxygen.⁴⁷



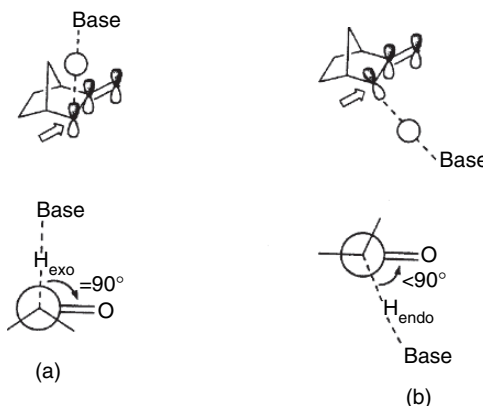
Very significant acceleration of the rate of deprotonation of 2-methylcyclohexanone by LiHMDS was observed when triethylamine was included in enolate-forming reactions in toluene. The rate enhancement is attributed to a TS containing LiHMDS dimer and triethylamine. This is an example of how modification of conditions can be used to affect rates and selectivity of deprotonation.

⁴⁶ L. Xie and W. H. Saunders, Jr., *J. Am. Chem. Soc.*, **113**, 3123 (1991).

⁴⁷ R. E. Ireland, R. H. Mueller, and A. K. Willard, *J. Am. Chem. Soc.*, **98**, 2868 (1972); R. E. Ireland, P. Wipf, and J. D. Armstrong, III, *J. Org. Chem.*, **56**, 650 (1991).



Structural effects on deprotonation rates have also been probed computationally.⁴⁸ In cyclic ketones, a stereoelectronic factor can be important in determining the rate of deprotonation. For the norbornanone ring, for example, the *exo* proton is more favorably aligned with the carbonyl group than the *endo* hydrogen. Computational investigation (B3LYP/6-31G*) of the TS for deprotonation by an OH⁻:H₂O complex found a difference of 3.8 kcal/mol favoring *exo* deprotonation.



A similar factor is found for deprotonation of cyclohexanone. There is a 2.8 kcal preference for removal of an axial proton because of the better stereoelectronic alignment and less torsional strain, as depicted in Figure 6.3.

Nitroalkanes show an interesting relationship between kinetic and thermodynamic acidity. Additional alkyl substituents on nitromethane retard the rate of proton removal, although the equilibrium is more favorable for the more highly substituted derivatives.⁴⁹ The alkyl groups have a strong stabilizing effect on the nitronate ion but unfavorable steric effects are dominant at the TS for proton removal. As a result, kinetic and thermodynamic acidity show opposite responses to alkyl substitution.

Nitroalkane	Kinetic acidity $k(M^{-1} \text{min}^{-1})$	Thermodynamic acidity (pK_a)
CH ₃ NO ₂	238	10.2
CH ₃ CH ₂ NO ₂	39.1	8.5
(CH ₃) ₂ CHNO ₂	2.08	7.7

⁴⁸. S. M. Behnam, S. E. Benham, K. Ando, N. S. Green, and K. N. Houk, *J. Org. Chem.*, **65**, 8970 (2000).

⁴⁹. F. G. Bordwell, W. J. Boyle, Jr., and K. C. Yee, *J. Am. Chem. Soc.*, **92**, 5926 (1970).

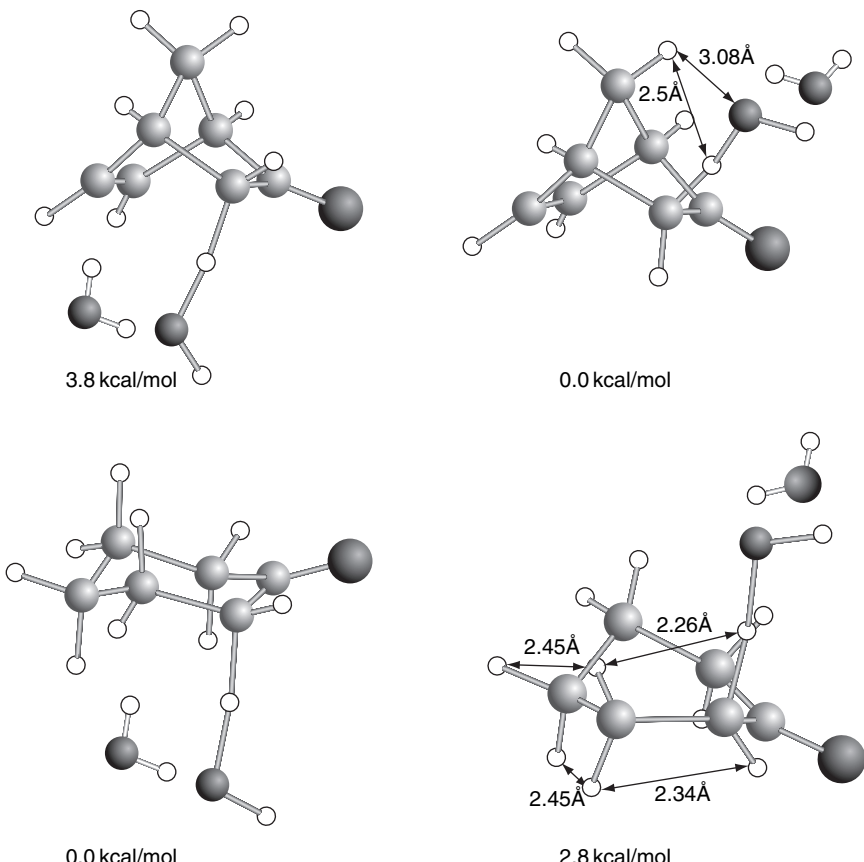


Fig. 6.3. Comparison of transition structures for deprotonation of 2-norbornanone (top) and cyclohexanone (bottom). In 2-norbornanone, *exo* protonation is favored by 3.8 kcal/mol. In cyclohexanone, axial deprotonation is favored by 2.8 kcal/mol. Reproduced from *J. Org. Chem.*, **65**, 8970 (2000), by permission of the American Chemical Society.

The cyano group is also effective at stabilizing negative charge on carbon. The minimal steric demands of the cyano group have made it possible to synthesize a number of hydrocarbon derivatives that are very highly substituted with cyano groups. Table 6.9 gives pK values for some of these compounds. As can be seen, the highly substituted derivatives are very strong acids.

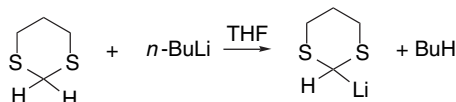
Table 6.9. Acidities of Some Cyanohydrocarbons^a

Compound	pK
CH_3CN	> 25
NCCH_2CN	11.2
$(\text{NC})_3\text{CH}$	-5.6
$(\text{NC})_2\text{C}=\text{C}(\text{CN})\text{CH}(\text{CN})_2$	< -8.5
Pentacyanocyclopentadiene	< -11.0

a. Selected from data in Tables 5.1 and 5.2 in J. R. Jones, *The Ionization of Carbon Acids*, Academic Press, New York, 1973, pp. 64,65.

Third-row elements, particularly phosphorus and sulfur, stabilize adjacent carbanions. The pK 's of some pertinent compounds are given in Table 6.10.

The conjugate base of 1,3-dithiane has proven valuable in synthetic applications as a nucleophile (Part B, Chap.3). The anion is generated by deprotonation using *n*-butyllithium.



The pK of 1,3-dithiane is 36.5 (Cs^+ ion pair in THF).⁵⁰ The value for 2-phenyl-1,3-dithiane is 30.5. There are several factors that can contribute to the anion-stabilizing effect of sulfur substituents. Bond dipole effects may contribute but cannot be the dominant factor since oxygen does not have a comparable stabilizing influence. Polarizability of sulfur can also stabilize the carbanion. Delocalization can be described as involving $3d$ orbitals on sulfur or hyperconjugation with the σ^* orbital of the C–S bond.⁵¹ An experimental study of the rates of deprotonation of phenylthionitromethane indicates that sulfur polarizability is the major factor.⁵² Whatever the structural basis, there is no question that thio substituents enhance the acidity of hydrogens on the adjacent carbons. The phenylthio group increases the acidity of hydrocarbons by at least 15 pK units. The effect is from 5–10 pK units in carbanions stabilized by other EWGs.⁵³

Table 6.10. Acidities of Some Compounds with Sulfur and Phosphorus Substituents

Compound	$pK(\text{DMSO})$
$\text{PhCH}_2\text{SPh}^{\text{a}}$	30.8
$\text{PhSO}_2\text{CH}_3^{\text{b}}$	29.0
$\text{PhSO}_2\text{CH}_2\text{Ph}^{\text{b}}$	23.4
$\text{PhCH}(\text{SPh})_2^{\text{a}}$	23.0
$(\text{PhS})_2\text{CH}_2^{\text{a}}$	38.0
$\text{PhSO}_2\text{CH}_2\text{SPh}^{\text{b}}$	20.3
$\text{PhSO}_2\text{CH}_2\text{PPh}_2^{\text{b}}$	20.2
$\text{C}_2\text{H}_5\text{O}_2\text{CCH}_2\text{PPh}_2^{\text{d}}$	9.2 ^c
$\text{PhCOCH}_2\text{PPh}_2^{\text{d}}$	6.0 ^c

a. F. G. Bordwell, J. E. Bares, J. E. Bartmess, G. E. Drucker, J. Gerhold, G. J. McCollum, M. Van Der Puy, N. R. Vanier, and W. S. Matthews, *J. Org. Chem.*, **42**, 326 (1977).

b. F. G. Bordwell, W. S. Matthews, and N. R. Vanier, *J. Am. Chem. Soc.*, **97**, 442 (1975).

c. In methanol.

d. A. J. Spezzale and K. W. Ratts, *J. Am. Chem. Soc.*, **85**, 2790 (1963).

⁵⁰. L. Xie, D. A. Bors, and A. Streitwieser, *J. Org. Chem.*, **57**, 4986 (1992).

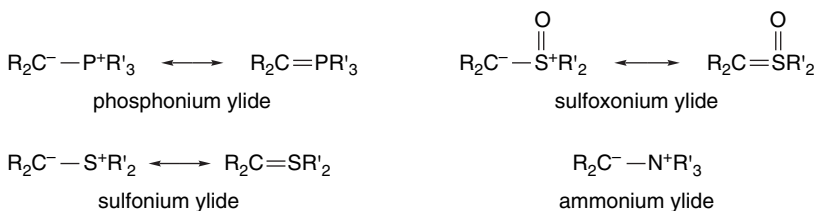
⁵¹. W. T. Borden, E. R. Davidson, N. H. Andersen, A. D. Deniston, and N. D. Epotis, *J. Am. Chem. Soc.*, **100**, 1604 (1978); A. Streitwieser, Jr., and S. P. Ewing, *J. Am. Chem. Soc.*, **97**, 190 (1975); A. Streitwieser, Jr., and J. E. Williams, Jr., *J. Am. Chem. Soc.*, **97**, 191 (1975); N. D. Epotis, R. L. Yates, F. Bernardi, and S. Wolfe, *J. Am. Chem. Soc.*, **98**, 5435 (1976); J.-M. Lehn and G. Wipff, *J. Am. Chem. Soc.*, **98**, 7498 (1976); D. A. Bors and A. Streitwieser, Jr., *J. Am. Chem. Soc.*, **108**, 1397 (1986).

⁵². C. F. Bernasconi and K. W. Kittredge, *J. Org. Chem.*, **63**, 1944 (1998).

⁵³. F. G. Bordwell, J. E. Bares, J. E. Bartmess, G. E. Drucker, J. Gerhold, G. J. McCollum, V. Van Der Puy, N. R. Vanier, and W. S. Matthews, *J. Org. Chem.*, **42**, 326 (1977); F. G. Bordwell, M. Van Der Puy, and N. R. Vanier, *J. Org. Chem.*, **41**, 1885 (1976).

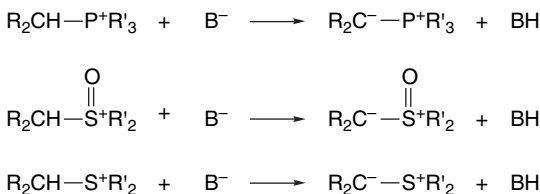
Trialkyl and triarylsilyl substituents have a modest carbanion-stabilizing effect that is attributed mainly to polarizability and is somewhat greater for the triarylsilyl substituents. This stabilization results in a reduced pK by 1 (trimethylsilyl) to 4 (triphenylsilyl) log units in fluorenes and 3 to 7.5, respectively, in sulfones.⁵⁴

Another important group of nucleophilic carbon species consists of the phosphorus and sulfur ylides. *Ylide* is the name given to molecules in which one of the contributing resonance structures has opposite charges on adjacent atoms when both atoms have octets of electrons. Since we are dealing with nucleophilic carbon species, our interest is in ylides with a negative charge on the carbon. These are of great synthetic importance, and their reactivity is considered in some detail in Chapter 2 of Part B. Here, we discuss the structures of some of the best-known ylides. The three groups of primary synthetic importance are phosphonium, sulfoxonium, and sulfonium ylides. Ylides of ammonium ions also have some synthetic significance.



The question of which resonance structure is the principal contributor has been a point of discussion. Since the uncharged *ylene* resonance structures have ten electrons at the phosphorus or sulfur atom, they imply participation of *d* orbitals on the heteroatoms. Such resonance structures are not possible for ammonium ylides. Structural studies indicate that the dipolar ylide structure is the main contributor.⁵⁵ The stabilizing effect of phosphonium and sulfonium substituents is primarily the result of dipolar and polarization effects.⁵⁶

The ylides are formed by deprotonation of the corresponding “onium salts.”



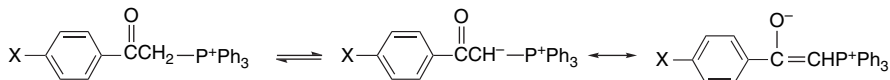
The stability of the ylide is increased by substituent groups that can stabilize the electron-rich carbon.⁵⁷ Phosphonium ions with acylmethyl substituents, for example,

⁵⁴. S. Zhang, X.-M. Zhang, and F. G. Bordwell, *J. Am. Chem. Soc.*, **117**, 602 (1995); A. Streitwieser, L. Xie, P. Wang, and S. M. Bachrach, *J. Org. Chem.*, **58**, 1778 (1993).

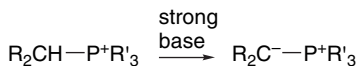
⁵⁵. H. Schmidbaur, W. Buchner, and D. Scheutzow, *Chem. Ber.*, **106**, 1251 (1973); D. G. Gilheany, in *The Chemistry of Organophosphorus Compounds*, F. R. Hartley, ed., Wiley, New York, 1994, pp. 1–44; S. M. Bachrach and C. I. Nitsche, in *The Chemistry of Organophosphorus Compounds*, F. R. Hartley, ed., Wiley, New York, 1994, pp. 273–302.

⁵⁶. X.-M. Zhang and F. G. Bordwell, *J. Am. Chem. Soc.*, **116**, 968 (1994).

⁵⁷. M. Schlosser, T. Jenny, and B. Schaub, *Heteroatom. Chem.*, **1**, 151 (1990).



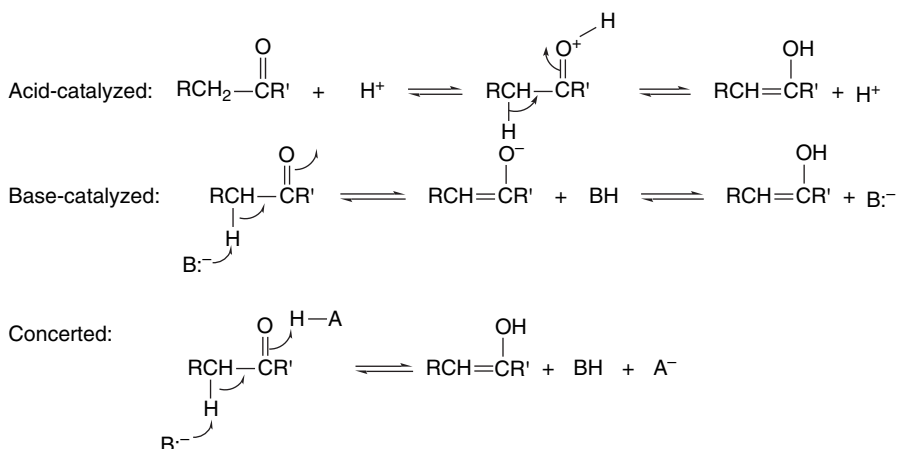
In the absence of the carbonyl or similar stabilizing group, the onium salts are less acidic. The pK_{DMSO} of methyltriphenylphosphonium ion is estimated to be 22. Strong bases such as amide ion or the anion of DMSO are required to deprotonate alkylphosphonium salts.



Similar considerations apply to the sulfoxonium and sulfonium ylides, which are formed by deprotonation of the corresponding positively charged sulfur-containing cations. The additional electronegative oxygen atom in the sulfoxonium salts stabilizes these ylides considerably, relative to the sulfonium ylides.⁵⁹

6.4. Enols and Enamines

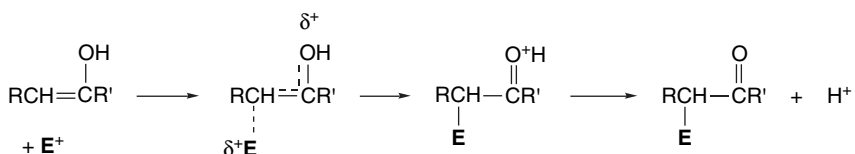
Carbonyl compounds can act as carbon nucleophiles in the presence of *acid catalysts*, as well as bases. The nucleophilic reactivity of carbonyl compounds in acidic solution is due to the presence of the *enol tautomer*. The equilibrium between carbonyl compounds and the corresponding enol can be acid- or base-catalyzed and can also occur by a concerted mechanism in which there is concurrent protonation and deprotonation. As we will see shortly, the equilibrium constant is quite small for monocarbonyl compounds, but the presence of the enol form permits reactions that do not occur from the carbonyl form.



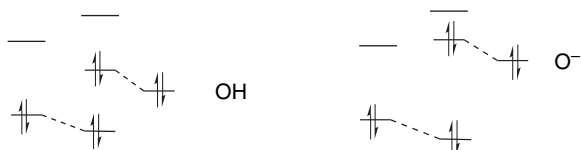
^{58.} S. Fliszar, R. F. Hudson, and G. Salvadori, *Helv. Chim. Acta*, **46**, 1580 (1963).

^{59.} E. J. Corey and M. Chaykovsky, *J. Am. Chem. Soc.*, **87**, 1353 (1965).

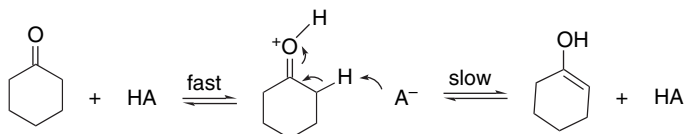
Like simple alkenes, enols are nucleophilic by virtue of their π electrons. Enols are much more reactive than simple alkenes, however, because the hydroxy group participates as an electron donor during the reaction process. The oxygen is deprotonated and the strong C=O bond is formed, providing a favorable energy contribution.



Enols are not as reactive as enolate anions, however. This lower reactivity reflects the presence of the additional proton in the enol, which decreases the electron density of the enol relative to the enolate. In MO terminology, the $-\text{OH}$ and $-\text{O}^-$ donor substituents both raise the energy of the $\pi\text{-HOMO}$, but the O^- group is the better donor.



A number of studies of the acid-catalyzed mechanism of enolization have been done, and the case of cyclohexanone is illustrative.⁶⁰ The reaction is catalyzed by various carboxylic acids and substituted ammonium ions. The effectiveness of these proton donors as catalysts correlates with their pK_a values. When plotted according to the Brønsted catalysis law (Section 3.6.1) the value of the slope α is 0.74. When deuterium or tritium is introduced in the α -position, there is a marked decrease in the rate of acid-catalyzed enolization: $k_{\text{H}}/k_{\text{D}} \sim 5$. This kinetic isotope effect indicates that the C–H bond cleavage is part of the rate-determining step. The generally accepted mechanism for acid-catalyzed enolization pictures the rate-determining step as deprotonation of the protonated ketone.



It is possible to measure the rate of enolization by isotopic exchange. NMR spectroscopy provides a very convenient method for following hydrogen-deuteron exchange. Data for several ketones are given in Table 6.11.

A point of contrast with the data for base-catalyzed removal of a proton (see Table 6.8) is the tendency for acid-catalyzed enolization to result in preferential formation of the *more-substituted enol*. For 2-butanone, the ratio of exchange at CH_2 to that at CH_3 is 4.2:1, after making the statistical correction for the number of hydrogens. The preference for acid-catalyzed enolization to give the more-substituted enol is the result of the stabilizing effect that alkyl groups have on carbon–carbon double bonds. To the extent that the TS resembles product,⁶¹ alkyl groups stabilize the

⁶⁰ G. E. Lienhard and T.-C. Wang, *J. Am. Chem. Soc.*, **91**, 1146 (1969).

⁶¹ C. G. Swain, E. C. Stivers, J. F. Reuwer, Jr., and L. J. Schaad, *J. Am. Chem. Soc.*, **80**, 5885 (1958).

Table 6.11. Relative Rates of Acid-Catalyzed Enolization of some Ketones^a

Ketone	Relative rate
	100
	220
	76
	171
	195
	80
	46
	105

a. In D₂O-dioxane with DCl catalyst. The data of C. Rappe and W. H. Sachs, *J. Org. Chem.*, **32**, 3700 (1967), given on a per group basis have been converted to a per-hydrogen basis.

more branched TS. There is an opposing steric effect that appears to be significant for 4,4-dimethyl-2-pentanone, in which the methylene group that is flanked by a *t*-butyl group is less reactive than the methyl group. The overall range of reactivity differences in acid-catalyzed exchange is much less than for base-catalyzed exchange, however (compare Tables 6.8 and 6.11). This is consistent with the C-deprotonation of the O-protonated compound having an earlier TS.

There are extensive data on the equilibrium constant for enolization. Table 6.12 gives data on the amount of enol present at equilibrium for some representative compounds. For simple aldehydes, the K_{enol} is in the range 10^{-4} to 10^{-5} . Ketones have *smaller* enol content, with K_{enol} around 10^{-8} . For esters and amides, where the carbonyl form is resonance stabilized, the K_{enol} drops to 10^{-20} . Somewhat surprisingly, 1-aryl substituents do not have a large effect on enol content, as in acetophenone, probably because there is conjugation in the ketone as well as in the enol. On the other hand, there is a large difference when the aryl group is β to the carbonyl, as in 2-indanone, which has a much higher enol content than 1-indanone.

The amount of enol present at equilibrium is influenced by other substituent groups. In the case of compounds containing a single ketone, aldehyde, or ester

Table 6.12. Equilibrium Constants for Enolization of Some Carbonyl Compounds

	Enolization equilibrium		$K_{\text{enol/keto}}$
1 ^b	$\text{CH}_3\text{CH}=\text{O} \rightleftharpoons \text{CH}_2=\text{CHOH}$		10^{-5}
2 ^c	$(\text{CH}_3)_2\text{CHCH}=\text{O} \rightleftharpoons (\text{CH}_3)_2\text{C}=\text{CHOH}$		1.4×10^{-4}
3 ^d	$\text{PhCH}_2\text{CH}=\text{O} \rightleftharpoons \text{PhCH}=\text{CHOH}$		8.5×10^{-4}
4 ^e	$\begin{array}{c} \text{O} \\ \parallel \\ \text{CH}_3\text{CCH}_3 \end{array} \rightleftharpoons \begin{array}{c} \text{OH} \\ \\ \text{CH}_2=\text{CCH}_3 \end{array}$		1.3×10^{-8}
5 ^e	$\begin{array}{c} \text{O} \\ \parallel \\ \text{CH}_3\text{CH}_2\text{CCH}_2\text{CH}_3 \end{array} \rightleftharpoons \begin{array}{c} \text{OH} \\ \\ \text{CH}_3\text{CH}=\text{CCH}_2\text{CH}_3 \end{array}$		3.7×10^{-8}
6 ^e	$(\text{CH}_3)_2\text{CHCCH}(\text{CH}_3)_2 \rightleftharpoons (\text{CH}_3)_2\text{C}=\text{CCH}(\text{CH}_3)_2$		3.0×10^{-8}
7 ^e	$\begin{array}{c} \text{O} \\ \parallel \\ \text{PhCCH}_3 \end{array} \rightleftharpoons \begin{array}{c} \text{OH} \\ \\ \text{PhC}=\text{CH}_2 \end{array}$		1.1×10^{-8}
8 ^e	$\begin{array}{c} \text{O} \\ \parallel \\ \text{PhCCH}(\text{CH}_3)_2 \end{array} \rightleftharpoons \begin{array}{c} \text{OH} \\ \\ \text{PhC}=\text{C}(\text{CH}_3)_2 \end{array}$		3.3×10^{-7}
9 ^e	$\begin{array}{c} \text{O} \\ \parallel \\ \text{Cyclopentanone} \end{array} \rightleftharpoons \begin{array}{c} \text{OH} \\ \\ \text{Cyclopentenol} \end{array}$		1.2×10^{-8}
10 ^e	$\begin{array}{c} \text{O} \\ \parallel \\ \text{Cyclohexanone} \end{array} \rightleftharpoons \begin{array}{c} \text{OH} \\ \\ \text{Cyclohexenol} \end{array}$		4.2×10^{-7}
11 ^f	$\begin{array}{c} \text{O} \\ \parallel \\ \text{CH}_3\text{COCH}_3 \end{array} \rightleftharpoons \begin{array}{c} \text{OH} \\ \\ \text{CH}_2=\text{COCH}_3 \end{array}$		3.2×10^{-19}
12 ^f	$\begin{array}{c} \text{O} \\ \parallel \\ \text{CH}_3\text{CNH}_2 \end{array} \rightleftharpoons \begin{array}{c} \text{OH} \\ \\ \text{CH}_2=\text{CNH}_2 \end{array}$		6.3×10^{-20}
13 ^g	$\begin{array}{c} \text{O} \\ \parallel \\ \text{Indanone} \end{array} \rightleftharpoons \begin{array}{c} \text{OH} \\ \\ \text{Indanol} \end{array}$		3.3×10^{-8}
14 ^h	$\begin{array}{c} \text{O} \\ \parallel \\ \text{Indanone} \end{array} \rightleftharpoons \begin{array}{c} \text{OH} \\ \\ \text{Indanol} \end{array}$		1.5×10^{-4}
15 ⁱ	$\begin{array}{c} \text{O} \\ \parallel \\ \text{CH}_3\text{CCH}_2\text{CCH}_3 \end{array} \rightleftharpoons \begin{array}{c} \text{OH} \\ \\ \text{CH}_3\text{C}=\text{CHCCH}_3 \end{array}$		$2.3 \times 10^{-1} (\text{H}_2\text{O})$
16 ^j	$\begin{array}{c} \text{O} \\ \parallel \\ \text{CH}_3\text{CCH}_2\text{CCH}_3 \end{array} \rightleftharpoons \begin{array}{c} \text{OH} \\ \\ \text{CH}_3\text{C}=\text{CHCCH}_3 \end{array}$		$29 (\text{CCl}_4)$
17 ⁱ	$\begin{array}{c} \text{O} \\ \parallel \\ \text{CH}_3\text{CCH}_2\text{COC}_2\text{H}_5 \end{array} \rightleftharpoons \begin{array}{c} \text{OH} \\ \\ \text{CH}_3\text{C}=\text{CHCOC}_2\text{H}_5 \end{array}$		$7 \times 10^{-2} (\text{H}_2\text{O})$
18 ⁱ	$\begin{array}{c} \text{O} \\ \parallel \\ \text{CH}_3\text{CCH}_2\text{COC}_2\text{H}_5 \end{array} \rightleftharpoons \begin{array}{c} \text{OH} \\ \\ \text{CH}_3\text{C}=\text{CHCOC}_2\text{H}_5 \end{array}$		$3 \times 10^{-1} (\text{CCl}_4)$
19 ⁱ	$\begin{array}{c} \text{O} \\ \parallel \\ \text{CH}_3\text{CCH}_2\text{CNH}_2 \end{array} \rightleftharpoons \begin{array}{c} \text{OH} \\ \\ \text{CH}_3\text{C}=\text{CHCNH}_2 \end{array}$		$1.3 (\text{H}_2\text{O})$

(Continued)

Table 6.12. (Continued)

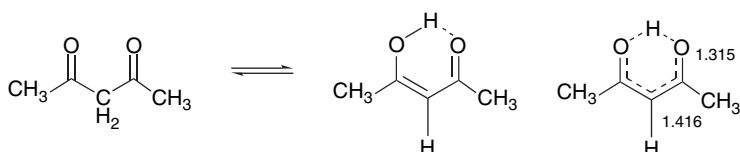
SECTION 6.4

Enols and Enamines

	Enolization equilibrium	<i>K</i> enol/keto
20 ^j		20 (H_2O) 0.05 (CHCl_3)
21 ^k	 76% 24%	> 50 (CCl_4)
22 ^l		5.4×10^{-2} (H_2O)

- a. In water unless otherwise noted.
b. J. P. Guthrie and P. A. Cullimore, *Can. J. Chem.*, **57**, 240 (1979).
c. Y. Chiang, A. J. Kresge, and P. A. Walsh, *J. Am. Chem. Soc.*, **108**, 6314 (1986).
d. Y. Chiang, A. J. Kresge, P. A. Walsh, and Y. Yin, *J. Chem. Soc., Chem. Commun.*, 869 (1989).
e. J. R. Keefe, A. J. Kresge, and N. P. Schepp, *J. Am. Chem. Soc.*, **112**, 4862 (1990).
f. J. P. Richard, G. Williams, A. M. C. O'Donoghue, and T. L. Amyes, *J. Am. Chem. Soc.*, **124**, 2957 (2002).
g. E. A. Jefferson, J. R. Keefe, and A. J. Kresge, *J. Chem. Soc. Perkin Trans. 2*, 2041 (1995).
h. J. R. Keefe, A. J. Kresge, and Y. Yin, *J. Am. Chem. Soc.*, **110**, 8201 (1988).
i. J. W. Bunting and J. P. Kanter, *J. Am. Chem. Soc.*, **115**, 11705 (1993).
j. S. G. Mills and P. Beak, *J. Org. Chem.*, **50**, 1216 (1985).
k. E. W. Garbisch, *J. Am. Chem. Soc.*, **85**, 1696 (1963).
l. J. A. Chang, A. J. Kresge, V. A. Nikolaev, and V. V. Popik, *J. Am. Chem. Soc.*, **125**, 6478 (2003).

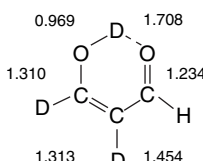
function, very little of the enol is present at equilibrium. When two such groups are close to one another, particularly if they are separated by a single carbon atom, the enol may be the major form. The enol forms of β -diketones and β -ketoesters are stabilized by intramolecular hydrogen bonds and by conjugation of the carbon-carbon double bond with the carbonyl group. The structural data given below for the enol form of 2,4-pentanedione were obtained by an electron diffraction study.⁶² In this case the data pertain to the time-averaged structure resulting from proton transfer between the two hydrogen-bonded oxygens.



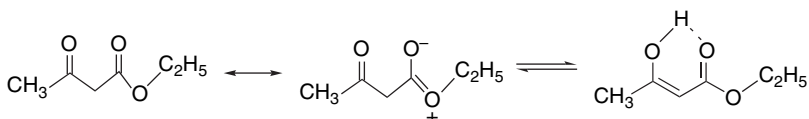
The simplest compound with this type of enolic structure is malonaldehyde. The structures determined by microwave spectroscopy on a deuterated analog have provided

⁶² A. H. Lowrey, C. George, P. D'Antonio, and J. Karle, *J. Am. Chem. Soc.*, **93**, 6399 (1971).

the bond length data shown below.⁶³ The barrier for shift of the enolic hydrogen (or deuterium) between the two oxygen atoms is about 4–5 kcal.⁶⁴

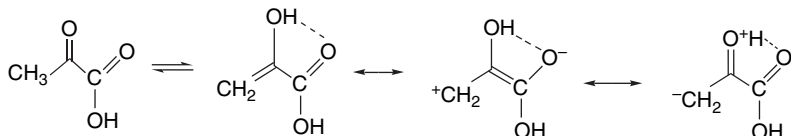


The extent of enolization at equilibrium is also solvent dependent.⁶⁵ The hydrogen-bonding capacity of the solvent is especially important. For example, for ethyl acetoacetate, the amount of enol is higher (15–30%) in nonpolar solvents such as carbon tetrachloride or benzene than in more polar solvents such as water or acetone (5% enol in acetone, 1% enol in water).⁶⁶ The strong intramolecular hydrogen bond in the enol form minimizes the molecular dipole by reducing the negative charge on the oxygen of the carbonyl group. In more polar solvents this stabilization is less important, and in protic solvents such as water, hydrogen bonding by the solvent is dominant.



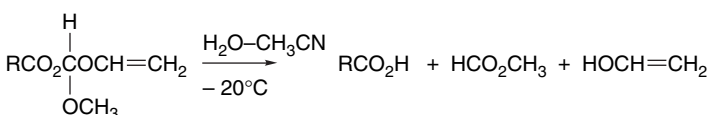
This relationship is reversed in compounds where intramolecular hydrogen bonding is not possible. (See the entry for 5,5-dimethylcyclohexane-1,3-dione in Table 6.12.)

α -Dicarbonyl compounds also have an enhanced tendency toward enolization, although it is not as pronounced as for β -dicarbonyl compounds. The K_{enol} for pyruvic acid is about 10^{-3} .⁶⁷ There is resonance stabilization between the enol double bond and the ester carbonyl as well as a contribution from hydrogen bonding.



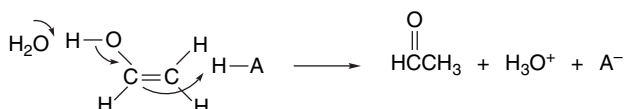
Enols of simple ketones can be generated in high concentrations as metastable species by special techniques.⁶⁸ Vinyl alcohol, the enol of acetaldehyde, can be generated by very careful hydrolysis of any of several ortho ester derivatives in which the group RCO_2^- is acetic acid or a chloroacetic acid.⁶⁹

- ⁶³. S. L. Baughcum, R. W. Duerst, W. F. Rowe, Z. Smith, and E. B. Wilson, *J. Am. Chem. Soc.*, **103**, 6296 (1981).
- ⁶⁴. S. L. Baughcum, Z. Smith, E. B. Wilson, and R. W. Duerst, *J. Am. Chem. Soc.*, **106**, 2260 (1984).
- ⁶⁵. J. Elmsley and N. J. Freeman, *J. Mol. Struct.*, **161**, 193 (1987); J. N. Spencer, E. S. Holcombe, M. R. Kirshenbaum, D. W. Firth, and P. B. Pinto, *Can. J. Chem.*, **60**, 1178 (1982).
- ⁶⁶. K. D. Grande and S. M. Rosenfeld, *J. Org. Chem.*, **45**, 1626 (1980); S. G. Mills and P. Beak, *J. Org. Chem.*, **50**, 1216 (1985).
- ⁶⁷. Y. Chiang, A. J. Kresge, and P. Pruszynski, *J. Am. Chem. Soc.*, **114**, 3103 (1992); J. Damitio, G. Smith, J. E. Meany, and Y. Pocker, *J. Am. Chem. Soc.*, **114**, 3081 (1992).
- ⁶⁸. B. Capon, B. Z. Guo, F. C. Kwok, A. F. Siddhanta, and C. Zucco, *Acc. Chem. Res.*, **21**, 135 (1988).
- ⁶⁹. B. Capon, D. S. Rycroft, T. W. Watson, and C. Zucco, *J. Am. Chem. Soc.*, **103**, 1761 (1981).

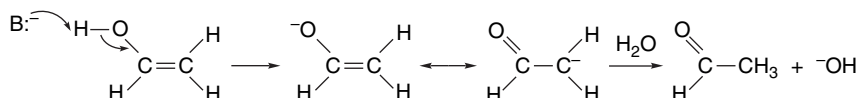


The enol can be observed by NMR and at -20°C has a half-life of several hours. At $+20^\circ\text{C}$ the half-life is only 10 min. The presence of bases causes very rapid isomerization to acetaldehyde via the enolate. Solvents have a significant effect on the lifetime of such unstable enols. Solvents such as DMF or DMSO, which are known to slow the rate of proton exchange by hydrogen bonding, increase the lifetime of unstable enols.⁷⁰

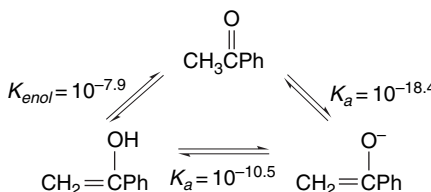
Solutions of unstable enols of simple ketones and aldehydes can also be generated in water by the addition of a solution of the enolate.⁷¹ The initial protonation takes place on oxygen, generating the enol, which is then ketonized at a rate that depends on the solution pH. The ketonization exhibits both acid and base catalysis.⁷² Acid catalysis involves C-protonation with concerted O-deprotonation. In agreement with expectation for a rate-determining proton transfer, the reaction shows general acid catalysis.



Base-catalyzed ketonization occurs by C-protonation of the enolate.

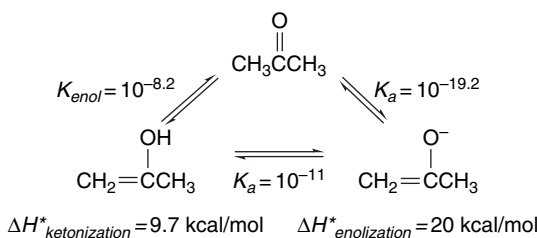


As would be expected on the basis of electronegativity arguments, enols are much more acidic than the corresponding keto form. It has been possible to determine the pK of the enol form of acetophenone as being 10.5 in water. The pK of the keto form is 18.4.⁷³ Since the enolate is the same for both equilibria, the difference in the pK values is equal to the enol \rightleftharpoons keto equilibrium constant, K_{enol} .



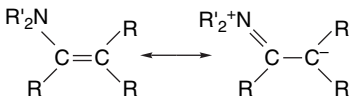
Similar measurements have been made for the equilibria involving acetone and its enol, 2-hydroxypropene.⁷⁴ In this case, the activation parameters were also determined and are shown below.⁷⁵

- ⁷⁰. E. A. Schmidt and H. M. R. Hoffmann, *J. Am. Chem. Soc.*, **94**, 7832 (1972).
- ⁷¹. Y. Chiang, A. J. Kresge, and P. A. Walsh, *J. Am. Chem. Soc.*, **104**, 6122 (1982); Y. Chiang, A. J. Kresge, and P. A. Walsh, *J. Am. Chem. Soc.*, **108**, 6314 (1986).
- ⁷². B. Capon and C. Zucco, *J. Am. Chem. Soc.*, **104**, 7567 (1982).
- ⁷³. Y. Chiang, A. J. Kresge, and J. Wirz, *J. Am. Chem. Soc.*, **106**, 6392 (1984).
- ⁷⁴. Y. Chiang, A. J. Kresge, Y. S. Tang, and J. Wirz, *J. Am. Chem. Soc.*, **106**, 460 (1984).
- ⁷⁵. Y. Chiang, A. J. Kresge, and N. P. Schepp, *J. Am. Chem. Soc.*, **111**, 3977 (1989).

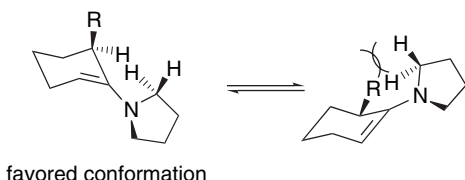


The accessibility of enols and enolates, respectively, in acidic and basic solutions of carbonyl compounds makes possible a wide range of reactions that depend on their nucleophilicity. These reactions are discussed in Chapter 7 and in Chapters 1 and 2 of Part B.

Amino substituents on a carbon-carbon double bond enhance the nucleophilicity of the β -carbon to an even greater extent than the hydroxy group in enols because of the greater electron-donating power of nitrogen. Such compounds are called *enamines*.⁷⁶



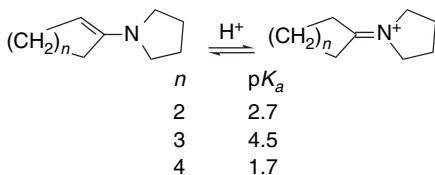
An interesting and useful property of enamines of 2-alkylcyclohexanone is the substantial preference for the less-substituted isomer to be formed. This tendency is especially pronounced for enamines derived from cyclic secondary amines such as pyrrolidine, a preference that can be traced to A^{1,3} allylic strain. In order to maximize conjugation between the nitrogen lone pair and the carbon-carbon double bond, the nitrogen substituent must be coplanar with the double bond. This creates a steric repulsion when the enamine bears a β -substituent and leads to a preference for the unsubstituted enamine. Because of the same preference for coplanarity in the enamine system, α -alkyl substituents adopt an axial conformation to minimize steric interaction with the amino group.



These steric factors are also indicated by the relative basicity of enamines derived from five-, six-, and seven-membered ketones.⁷⁷ The five- and seven-membered enamines

⁷⁶ A. G. Cook, *Enamines*, 2nd Edition, Marcel Dekker, New York, 1988, Chap. 1; Z. Rappoport, ed., *Chemistry of Enamines*, Wiley, Chichester, 1994.

⁷⁷ A. G. Cook, M. L. Absi, and V. F. Bowden, *J. Org. Chem.*, **60**, 3169 (1995).



The preparation of enamines is discussed in Chapter 7, and their application as carbon nucleophiles in synthesis is dealt with in Chapter 1 of Part B.

6.5. Carbanions as Nucleophiles in S_N2 Reactions

Carbanions are very useful intermediates in the formation of carbon-carbon bonds. This is true for both unstabilized structures found in organometallic reagents and stabilized structures such as enolates. Carbanions can participate as nucleophiles in both addition and substitution reactions. At this point we consider aspects of the reactions of carbanions as nucleophiles in reactions that proceed by the S_N2 mechanism. Other synthetic applications of carbanions are discussed more completely in Chapter 7 and in Chapters 1 and 2, Part B.

6.5.1. Substitution Reactions of Organometallic Reagents

Carbanions are classified as soft nucleophiles. They are expected to be good nucleophiles in S_N2 reactions and this is generally true. The reactions of aryl-, alkenyl-, and allyl lithium reagents with primary alkyl halides and tosylates appear to proceed by S_N2 mechanisms. Similar reactions occur between arylmagnesium halides (Grignard reagents) and alkyl sulfates and sulfonates. Some examples of these reactions are given in Scheme 6.2.

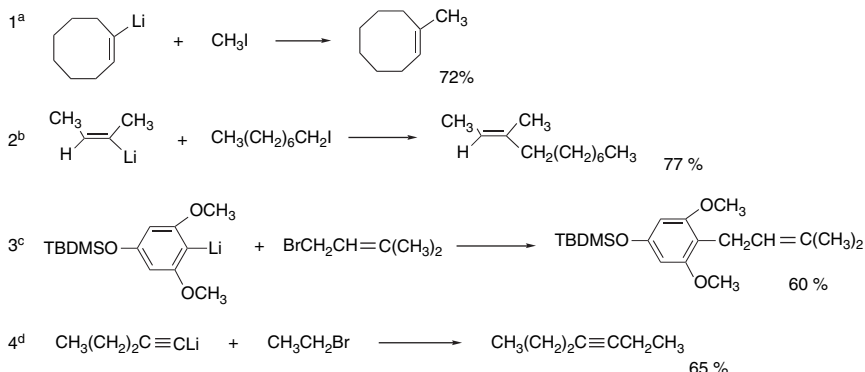
Note that all the examples in Scheme 6.2 involve either sp^2 or stabilized organometallic reagents. Evidence for an S_N2 -type mechanism in the reaction of allyl and benzyl lithium reagents has been obtained from stereochemical studies. With 2-bromobutane, both of these reagents react with complete inversion of configuration.⁷⁸ *n*-Butyllithium, however, gives largely racemic product, indicating that some competing process must also be occurring.⁷⁹ A general description of the mechanism for the reaction of organolithium compounds with alkyl halides must take account of the structure of the organometallic compound. It is known that halide anions are accommodated into typical organolithium cluster structures and can replace solvent molecules as ligands. A similar process in which the alkyl halide became complexed

^{78.} L. H. Sommer and W. D. Korte, *J. Org. Chem.*, **35**, 22 (1970).

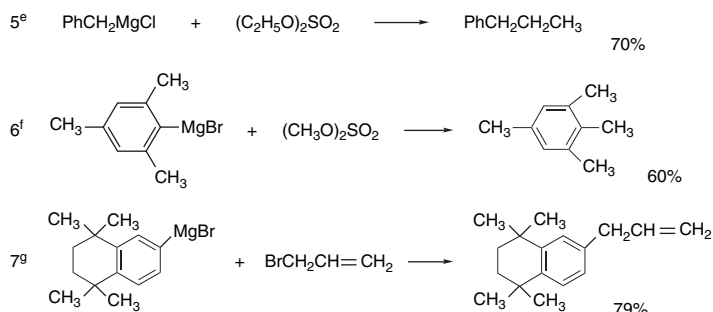
^{79.} H. D. Zook and R. N. Goldey, *J. Am. Chem. Soc.*, **75**, 3975 (1953).

Scheme 6.2. Alkylation Reactions of Some Organometallic Reagents

A. Organolithium Reagents

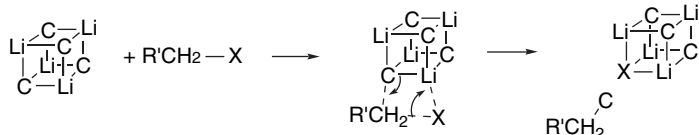


B. Organomagnesium reagents

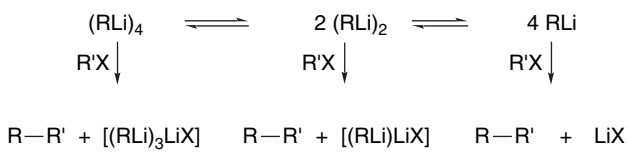


- a. H. Neumann and D. Seebach, *Chem. Ber.*, **111**, 2785 (1978).
 b. J. Millon, R. Lorne, and G. Linstrumelle, *Synthesis*, 434 (1975).
 c. T. L. Shih, M. J. Wyvatt, and H. Mrozik, *J. Org. Chem.*, **52**, 2029 (1987).
 d. A. J. Quillinan and F. Schienman, *Org. Synth.*, **58**, 1 (1978).
 e. H. Gilman and W. E. Catlin, *Org. Synth.*, **I**, 360 (1943).
 f. L. I. Smith, *Org. Synth.*, **II**, 360 (1943).
 g. J. Eustache, J. M. Bernardon, and B. Shroot, *Tetrahedron Lett.*, **28**, 4681 (1987).

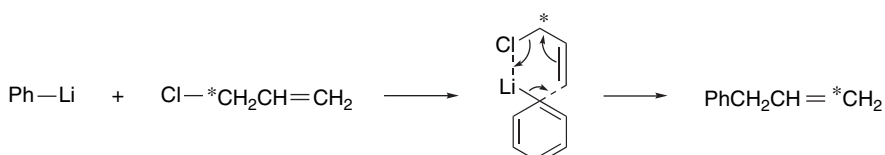
at lithium would provide an intermediate structure that could account for the subsequent alkylation. This process is represented below for a tetrameric structure, with the organic group simply represented by C.



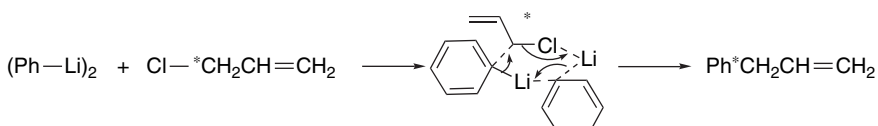
In general terms, the reactions of organolithium reagents with alkylating agents might occur at any of the aggregation stages present in solution and there could be reactivity differences among them. There has been little detailed mechanistic study that would distinguish among these possibilities.



The reaction of phenyllithium and allyl chloride using ^{14}C label reveals the occurrence of allylic transposition. About three-fourths of the product results from bond formation at C(3) rather than C(1), which can be accounted for by a cyclic mechanism.⁸⁰



The portion of the product formed by reaction at C(1) in allylic systems may form by direct substitution, but it has also been suggested that a cyclic TS involving an aryllithium dimer might be involved.



These mechanisms ascribe importance to the Lewis acid–Lewis base interaction between the allyl halide and the organolithium reagent. When substitution is complete, the halide ion is incorporated into the lithium cluster in place of one of the carbon ligands.

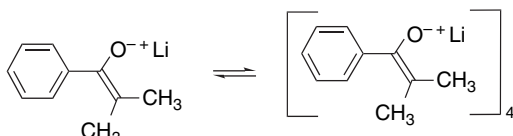
From a synthetic point of view, direct alkylation of lithium and magnesium organometallic compounds has been largely supplanted by transition metal–catalyzed processes. We discuss these reactions in Chapter 8 of Part B.

6.5.2. Substitution Reactions of Enolates

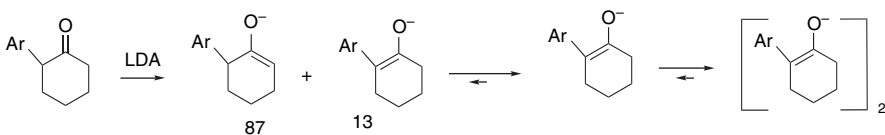
The alkylation reactions of enolate anions of both ketones and esters have been extensively utilized in synthesis. Both stable enolates, such as those derived from β -ketoesters, β -diketones, and malonate esters, as well as less stable enolates of monofunctional ketones, esters, nitriles, etc., are reactive. Many aspects of the relationships among reactivity, stereochemistry, and mechanism have been clarified. The starting point for the discussion of these reactions is the structure of the enolates. Studies of ketone enolates in solution indicate that both tetrameric and dimeric clusters can exist. THF, a solvent in which many synthetic reactions are performed, favors tetrameric structures for the lithium enolate of isobutyrophenone, for example.⁸¹

⁸⁰. R. M. Magid and J. G. Welch, *J. Am. Chem. Soc.*, **90**, 5211 (1968); R. M. Magid, E. C. Nieh, and R. D. Gandour, *J. Org. Chem.*, **36**, 2099 (1971).

⁸¹. L. M. Jackman and N. Szeverenyi, *J. Am. Chem. Soc.*, **99**, 4954 (1977); L. M. Jackman and B. C. Lange, *Tetrahedron*, **33**, 2737 (1977).



Detailed investigation of the degree of aggregation in solution has been applied to several alkyl aryl ketones.⁸² The lithium enolate of 4-(4-biphenyl)-2-methyl-1-propanone in THF exhibits a monomer-tetramer equilibrium.⁸³ The K_{eq} for tetramerization is estimated as $5 \times 10^8 M^3$, which corresponds to 1.3% of the enolate being present as the monomer. The kinetics of the alkylation reaction with benzyl bromide indicates that the *monomer is the reactive nucleophile*. Related studies were carried out with 2-(4-biphenyl)cyclohexanone. In this case, an initial 87:13 mixture of the regioisomeric enolates is completely converted to the conjugated enolate at equilibrium. There is an equilibrium between monomer and dimer, with $K_{eq} = 4.3 \times 10^3 M$. Again, the monomer is more reactive in the alkylation reaction. This is attributed to less electrostatic stabilization by a single Li^+ than by two or four in the aggregates.



$\text{Ar} = 4\text{-biphenyl}$

The structures of several lithium enolates of ketones have been determined by X-ray crystallography and reveal aggregated structures in which oxygen and lithium occupy alternating corners of distorted cubes. Figure 6.4 illustrates some of the observed structures. Figure 6.4a shows an unsolvated enolate of methyl *t*-butyl ketone (pinacolone).⁸⁴ The structures in Figures 6.4b and 6.4c are THF solvates of the enolates of methyl *t*-butyl ketone and cyclopentanone, respectively.⁸⁵ Each of these structures consists of clusters of four enolate anions and four lithium cations arranged with lithium and oxygen at alternating corners of a distorted cube. The structure in Figure 6.4d includes only two enolate anions. Four lithium ions are present, along with two di-*i*-propylamide ion. A significant feature of this structure is the coordination of the remote silyloxy oxygen atom to one of the lithium cations.⁸⁶ This is an example of the Lewis acid–Lewis base interactions that are frequently involved in organizing TS structure in the reactions of lithium enolates. A common feature of all four of the structures is the involvement of the enolate oxygen in multiple contacts with lithium cations in the cluster. An approaching electrophile will clearly be somewhat hindered from direct contact with oxygen in such structures, whereas the nucleophilic carbon is somewhat more exposed.

- ⁸². A. Streitwieser and D. Z.-R. Wang, *J. Am. Chem. Soc.*, **121**, 6213 (1999).
- ⁸³. A. Abbotto, S. S.-W. Leung, A. Streitwieser, and K. V. Kilway, *J. Am. Chem. Soc.*, **120**, 10807 (1998).
- ⁸⁴. P. G. Williard and G. B. Carpenter, *J. Am. Chem. Soc.*, **107**, 3345 (1985).
- ⁸⁵. R. Amstutz, W. B. Schweizer, D. Seebach, and J. D. Dunitz, *Helv. Chim. Acta*, **64**, 2617 (1981).
- ⁸⁶. P. G. Williard and M. J. Hintze, *J. Am. Chem. Soc.*, **109**, 5539 (1987).

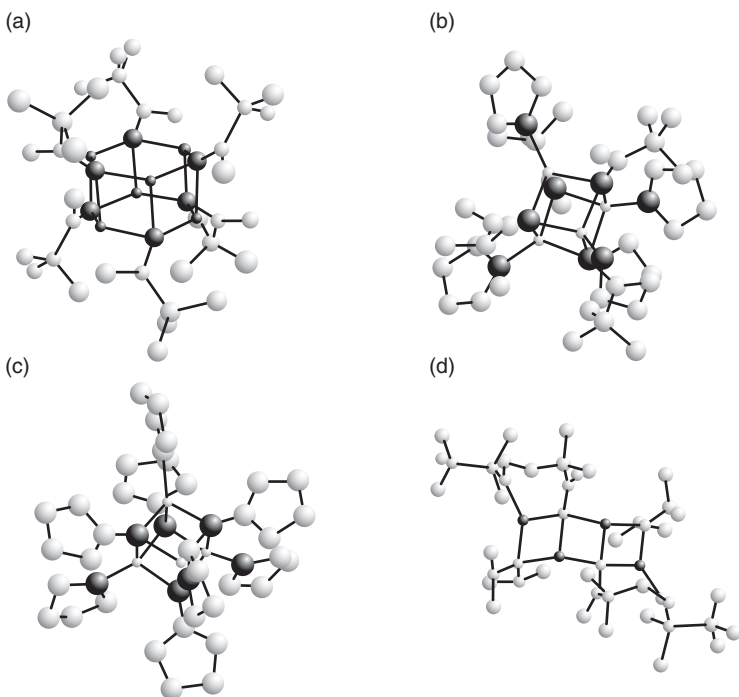


Fig. 6.4. Crystal structures of some enolates of ketones: (a) unsolvated hexameric enolate of methyl *t*-butyl ketone; (b) THF solvate of tetrameric enolate of methyl *t*-butyl ketone; (c) THF solvate of tetrameric enolate of cyclopentanone; and (d) dimeric enolate of 3,3-dimethyl-4-(*t*-butyldimethylsilyloxy)-2-pentanone. Adapted from *J. Am. Chem. Soc.*, **107**, 3345 (1985); *Helv. Chim. Acta*, **64**, 2617 (1981); *J. Am. Chem. Soc.*, **107**, 5403 (1985); and *J. Am. Chem. Soc.*, **109**, 5539 (1987), by permission of the American Chemical Society and Wiley-VCH.

Several ester enolates have also been examined by X-ray crystallography.⁸⁷ The enolates of *t*-butyl propionate and *t*-butyl 3-methylpropionate were obtained as TMEDA solvates of enolate dimers. Methyl 3,3-dimethylbutanoate was obtained as a THF-solvated tetramer.

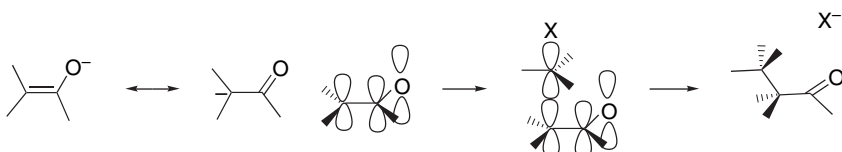
Most of the structural features of enolates are correctly modeled using B3LYP/6-31+G* computations with dimethyl ether as the solvent molecule.⁸⁸ Computational methods also indicate the stability of aggregated structures. Both ab initio and semiempirical calculations of the structure of the lithium enolate of methyl isobutyrate have been reported.⁸⁹ Although semiempirical PM3 calculations give adequate representations of the geometries of the aggregates, the energy values are not accurate. Dimeric and tetrameric structures give calculated ¹³C chemical shifts in agreement with the experimental values.

⁸⁷ D. Seebach, R. Amstutz, T. Laube, W. B. Schweizer, and J. D. Dunitz, *J. Am. Chem. Soc.*, **107**, 5403 (1985).

⁸⁸ A. Abbotto, A. Streitwieser, and P. v. R. Schleyer, *J. Am. Chem. Soc.*, **119**, 11255 (1997).

⁸⁹ H. Weiss, A. V. Yakimansky, and A. H. E. Mueller, *J. Am. Chem. Soc.*, **118**, 8897 (1996).

Because of the delocalized nature of enolates, an electrophile can attack either at oxygen or at carbon. Soft electrophiles prefer carbon and it is found experimentally that most alkyl halides react to give C-alkylation. Because of the π character of the HOMO of the anion, there is a stereoelectronic preference for attack of the electrophile approximately perpendicular to the plane of the enolate. The frontier orbital is ψ_2 with electron density mainly at O and C(2). The TS for an S_N2 alkylation of an enolate can be represented as below.



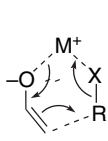
One of the general features of the reactivity of enolate anions is the sensitivity of both the reaction rate and the ratio of C versus O alkylation to the degree of aggregation of the enolate. For example, addition of HMPA frequently increases the rate of enolate alkylation reactions.⁹⁰ Use of a dipolar aprotic solvent such as DMF or DMSO in place of THF also leads to rate acceleration.⁹¹ These effects are attributed, at least in part, to dissociation of the enolate aggregates. Similar effects are observed when crown ethers or other cation-complexing agents are added to reaction mixtures.⁹² The order of enolate reactivity also depends on the metal cation that is present. The general order is $\text{BrMg} < \text{Li} < \text{Na} < \text{K}$, which is also in the order of greater dissociation of the enolate-cation ion pairs and ion aggregates. Carbon-13 chemical shift data provide an indication of electron density at the nucleophilic carbon in enolates. These shifts have been found to be both cation and solvent dependent. Apparent electron density is in the order $\text{K}^+ > \text{Na}^+ > \text{Li}^+$ and $\text{THF/HMPA} > \text{DME} > \text{THF} > \text{ether}$.⁹³ There is a good correlation with observed reactivity under the corresponding conditions.

The leaving group in the alkylating reagent has a major effect on whether C- or O-alkylation occurs. The C- versus O-alkylation ratio has been studied for the potassium salt of ethyl acetoacetate as a function of both solvent and leaving group.⁹⁴

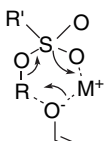
- ⁹⁰ L. M. Jackman and B. C. Lange, *J. Am. Chem. Soc.*, **103**, 4494 (1981); C. L. Liotta and T. C. Caruso, *Tetrahedron Lett.*, **26**, 1599 (1985).
- ⁹¹ H. D. Zook and J. A. Miller, *J. Org. Chem.*, **36**, 1112 (1971); H. E. Zaugg, J. F. Ratajczyk, J. E. Leonard, and A. D. Schaeffer, *J. Org. Chem.*, **37**, 2249 (1972); H. E. Zaugg, *J. Am. Chem. Soc.*, **83**, 837 (1961).
- ⁹² A. L. Kurts, S. M. Sakembaeva, J. P. Beletskaya, and O. A. Reutov, *Zh. Org. Khim. SSSR*, (Engl. Transl.), **10**, 1588 (1974).
- ⁹³ H. O. House, A. V. Prabhu, and W. V. Phillips, *J. Org. Chem.*, **41**, 1209 (1976).
- ⁹⁴ A. L. Kurts, A. Macias, N. K. Genkina, I. P. Beletskaya, and O. A. Reutov, *Dokl. Akad. Nauk, SSSR* (Engl. Transl.), **187**, 595 (1969); A. L. Kurts, N. K. Genkina, A. Macias, I. P. Beletskaya, and O. A. Reutov, *Tetrahedron*, **27**, 4777 (1971).

Leaving group X	Solvent	C:O ratio	Leaving group X	Solvent	C:O ratio
$\text{OSO}_2\text{OC}_2\text{H}_5$	THF	100:0	$\text{OSO}_2\text{C}_7\text{H}_7$	HMPA	12:88
$\text{OSO}_2\text{OC}_2\text{H}_5$	<i>t</i> -BuOH	100:0	Cl	HMPA	40:60
$\text{OSO}_2\text{OC}_2\text{H}_5$	EtOH	92:8	Br	HMPA	61:39
$\text{OSO}_2\text{OC}_2\text{H}_5$	CH_3CN	68:32	I	HMPA	87:13
$\text{OSO}_2\text{OC}_2\text{H}_5$	DMSO	30:70			
$\text{OSO}_2\text{OC}_2\text{H}_5$	DMF	21:79			
$\text{OSO}_2\text{OC}_2\text{H}_5$	HMPA	17:83			

These data show that a change from a hard leaving group (sulfonate, sulfate) to a softer leaving group (bromide, iodide) favors carbon alkylation. Another possible factor in C:O ratios may be the ability of sulfonates to form a six-membered cyclic TS for both modes of reaction, whereas halides can form such structures only for C-alkylation.⁸³



6-membered TS available
only for C-alkylation



6-membered TS available
for both C-and O-alkylation

The data for ethyl acetoacetate alkylation also show a shift from C-alkylation in THF and alcohols to dominant O-alkylation in DMSO, DMF, and HMPA. This reflects the more dissociated and weakly solvated state of the enolate in the aprotic dipolar solvents.

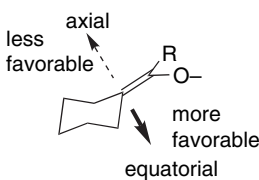
Another major influence on the C:O ratios is presumably the degree of aggregation. The reactivity at oxygen should be enhanced by dissociation since the electron density is less tightly associated with the cation. With the lithium enolate of acetophenone, for example, C-alkylation is the major product with methyl iodide but C-alkylation and O-alkylation occur to approximately equal extents with dimethyl sulfate. The C:O ratio is shifted more to O-alkylation by addition of HMPA or other cation-complexing agents. Thus, with four equivalents of HMPA the C:O ratio for methyl iodide drops from more than 200:1 to 10:1, whereas with dimethyl sulfate the C:O ratio changes from 1.2:1 to 0.2:1 when HMPA is added.⁹⁵

Steric and stereoelectronic effects control the direction of approach of an electrophile to the enolate. Electrophiles approach from the side of the enolate that is less hindered. Many examples of such effects have been observed.⁹⁶ In ketone and ester enolates that are exocyclic to a conformationally biased cyclohexane ring there is a small preference for the electrophile to approach from the equatorial

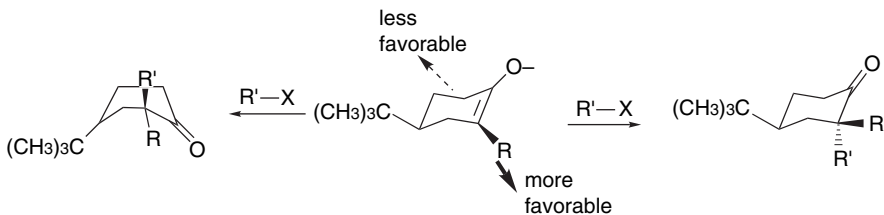
⁹⁵ L. M. Jackman and B. C. Lange, *J. Am. Chem. Soc.*, **103**, 4494 (1981).

⁹⁶ Reviews: D. A. Evans, in *Asymmetric Synthesis*, Vol. 3, J. D. Morrison, ed., Academic Press, New York, 1984, Chap. 1; D. Caine, in *Carbon-Carbon Bond Formation*, R. L. Augustine, ed., Marcel Dekker, New York, 1979.

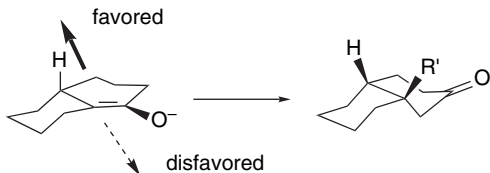
direction.⁹⁷ If the axial face is further hindered by the addition of a substituent, the selectivity is increased.



Endocyclic cyclohexanone enolates with 2-alkyl groups show a small preference (1:1–5:1) for approach of the electrophile from the direction that permits maintenance of the chair conformation.⁹⁸



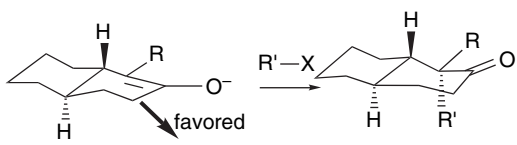
The 1(9)-enolate of 1-decalone exhibits a preference for alkylation to form a *cis* ring juncture.



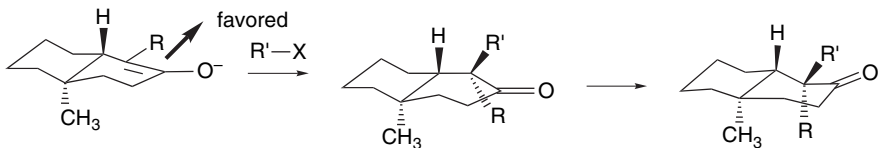
This is the result of a steric differentiation with the electrophile approaching from the side of the enolate occupied by the smaller hydrogen, rather than the ring methylene group at the C(10) position.

The 2(1)-enolate of *trans*-2-decalone is preferentially alkylated by an axial approach of the electrophile. The stereoselectivity is enhanced if there is an alkyl substituent at C(1). The factors operating in this case are similar to those described for 4-*t*-butylcyclohexanone. The *trans*-decalone framework is conformationally rigid. Axial attack from the lower face leads directly to the chair conformation of the product. The 1-alkyl group enhances this stereoselectivity because a steric interaction with the solvated enolate oxygen distorts the enolate in such a way as to favor the axial attack.⁹⁹

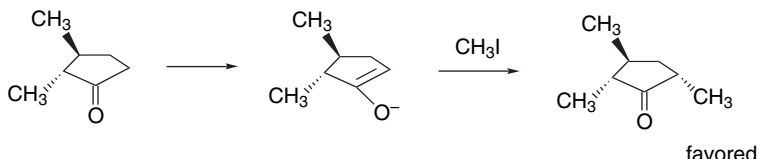
- ⁹⁷ A. P. Krapcho and E. A. Dundulis, *J. Org. Chem.*, **45**, 3236 (1980); H. O. House and T. M. Bare, *J. Org. Chem.*, **33**, 943 (1968).
- ⁹⁸ H. O. House, B. A. Tefertiller, and H. D. Olmstead, *J. Org. Chem.*, **33**, 935 (1968); H. O. House and M. J. Umen, *J. Org. Chem.*, **38**, 1000 (1973); J. M. Conia and P. Briet, *Bull. Soc. Chim. France*, 3881, 3886 (1966); C. Djerassi, J. Burakevich, J. W. Chamberlin, D. Elad, T. Toda, and G. Stork, *J. Am. Chem. Soc.*, **86**, 465 (1964); C. Agami, J. Levisalles, and B. Lo Cicero, *Tetrahedron*, **35**, 961 (1979).
- ⁹⁹ R. S. Mathews, S. S. Grigenti, and E. A. Folkers, *J. Chem. Soc., Chem. Commun.*, 708 (1970); P. Lansbury and G. E. DuBois, *Tetrahedron Lett.*, 3305 (1972).



The placement of an axial methyl group at C(10) in a 2(1)-decalone enolate introduces a 1,3-diaxial interaction with the approaching electrophile. The preferred alkylation product results from approach on the other side of the enolate.

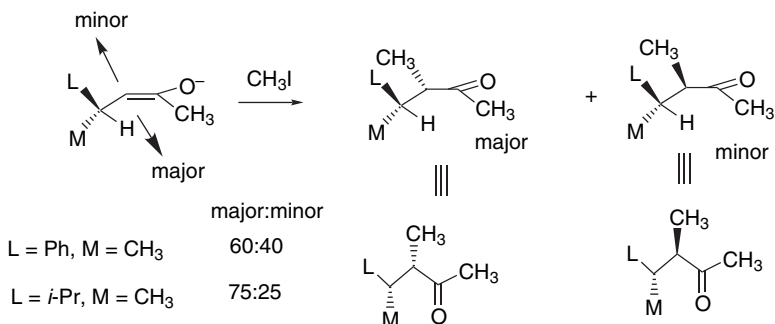


Houk and co-workers have emphasized the role of torsional effects in the stereoselectivity of enolate alkylation.¹⁰⁰ This analysis can explain the preference for C(5)-alkylation *syn* to the 2-methyl group in *trans*-2,3-dimethylcyclopentanone.



The *syn* TS is favored by about 1 kcal/mol, owing to reduced eclipsing, as illustrated in Figure 6.5. An experimental study using the kinetic enolate of 3-(*t*-butyl)-2-methylcyclopentanone in an alkylation reaction with benzyl iodide gave an 85:15 preference for the predicted *cis*-2,5-dimethyl derivative.

In acyclic systems, the enolate conformation comes into play. In unfunctionalized systems, alkylation usually takes place *anti* to the larger substituent, but with rather modest stereoselectivity.



Ref. 101

¹⁰⁰ K. Ando, N. S. Green, Y. Li, and K. N. Houk, *J. Am. Chem. Soc.*, **121**, 5334 (1999).

¹⁰¹ I. Fleming and J. J. Lewis, *J. Chem. Soc., Perkin Trans. 1*, 3257 (1992).

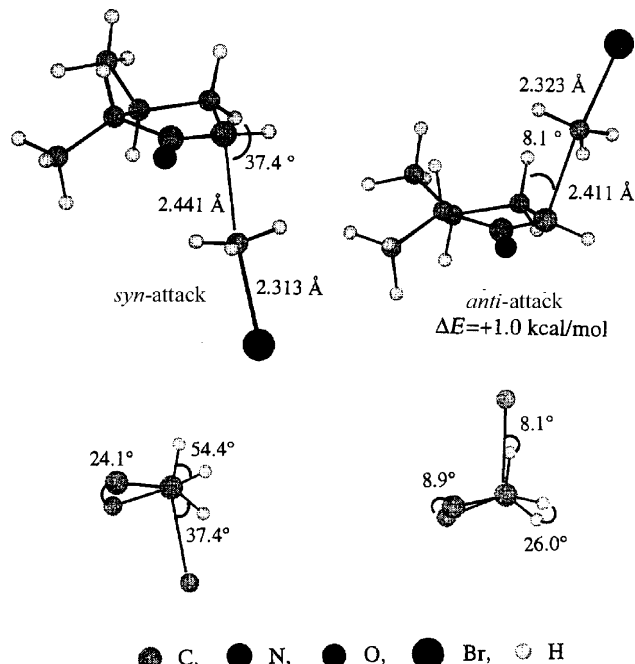
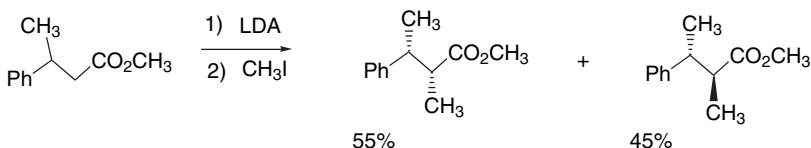
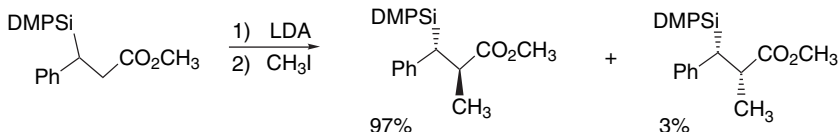


Fig. 6.5. Transition structures for *syn* and *anti* attack on the kinetic enolate of *trans*-2,3-dimethylcyclopentanone showing the staggered versus eclipsed nature of the newly forming bond. Reproduced from *J. Am. Chem. Soc.*, **121**, 5334 (1999), by permission of the American Chemical Society.

The enolate of the corresponding methyl ester gives a similar result.



When a silyl substituent is present, the reaction becomes much more selective.



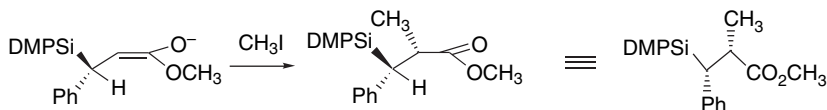
Ref. 102

¹⁰² R. A. N. C. Crump, I. Fleming, J. H. M. Hill, D. Parker, N. L. Reddy, and D. Waterson, *J. Chem. Soc., Perkin Trans. 2*, 3277 (1992).

This result is due to a dominant steric effect of the large silyl substituent.¹⁰³

619

PROBLEMS



In general, the stereoselectivity of enolate alkylation can be predicted and interpreted on the basis of the stereoelectronic requirement for an approximately perpendicular approach to the enolate with minimal torsional strain in combination and preference between the two faces on the basis of steric factors.

General References

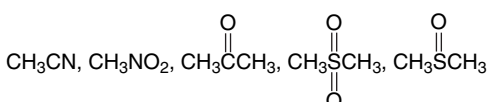
- E. Bunzel, *Carbanions: Mechanistic and Isotopic Aspects*, Elsevier, Amsterdam, 1975.
E. Bunzel and T. Durst, eds., *Comprehensive Carbanion Chemistry*, Elsevier, New York, 1981.
D. J. Cram, *Fundamentals of Carbanion Chemistry*, Academic Press, New York, 1965.
J. R. Jones, *The Ionization of Carbon Acids*, Academic Press, New York, 1973.
E. M. Kaiser and D. W. Slocum, in *Organic Reactive Intermediates*, S. P. McManus, ed., Academic Press, New York, 1973, Chap. 5.
Z. Rappoport, ed., *The Chemistry of Enols*, Wiley, New York, 1990.
M. Szwarc, *Ions and Ion Pairs in Organic Reactions*, Wiley, New York, 1972.
J. Toullec, *Adv. Phys. Org. Chem.*, **18**, 1 (1982).

Problems

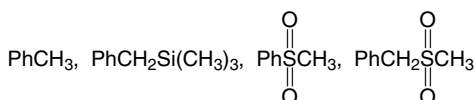
(References for these problems will be found on page 1161.)

6.1. Predict the order of increasing thermodynamic acidity in each series of compounds and explain the basis of your prediction.

- a. benzene, 1,4-cyclohexadiene, cyclopentadiene, cyclohexane
b.

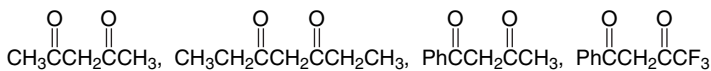


c.



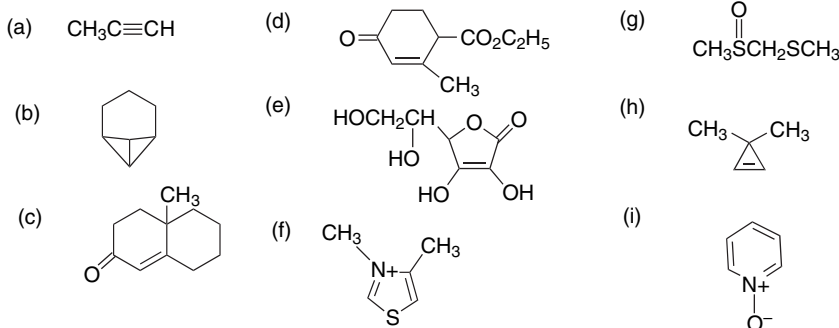
¹⁰³ I. Fleming, *J. Chem. Soc., Perkin Trans. 1*, 3363 (1992).

d.



- e. 9-(*m*-chlorophenyl)fluorene,
 9-phenylfluorene,
 9-(*p*-methylphenyl)fluorene.

6.2. Indicate the most acidic hydrogen in each of the following molecules. Explain your reasoning.

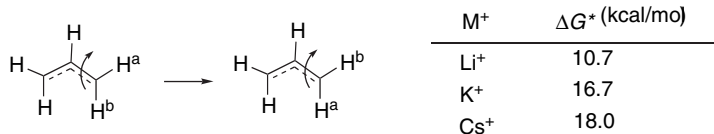


6.3. Offer an explanation for the following observations.

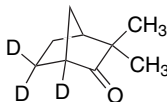
- Base-catalyzed exchange rates indicate that the hydrocarbon cubane is much more acidic than cyclobutane, and even more acidic than cyclopropane.
- Cyclopropyl phenyl ketone ($pK = 28.2$) is less acidic than acetophenone ($pK = 24.7$) and undergoes C–H exchange more slowly than phenyl *i*-propyl ketone, despite the fact that its most acidic hydrogen is located on a cyclopropyl ring.
- The order of acidity for cyclopentadiene, indene, and fluorene in DMSO is indicated below. The gas phase acidity is in the opposite direction, as measured by the proton affinity. Why does the fusion of benzene rings *decrease* the solution acidity relative to cyclopentadiene?

pK_{DMSO}	18.0	20.1
PA_{gas}	347.8	344.6

- d. The rotational barrier of the allyl anion in THF, as measured by NMR, is dependent on the identity of the cation present.



- 6.4 a. The relative rates of hydroxide ion-catalyzed deuterium exchange at C(3) have been measured for bicyclo[2.1.1]hexan-2-one, bicyclo[2.2.1]heptan-2-one, and bicyclo[2.2.2]octan-2-one. What factor(s) could account for the much smaller rate of exchange for bicyclo[2.1.1]hexan-2-one?
- b. Treatment of (+)-camphenilone with $\text{K}^+ \cdot \text{O}-t\text{-Bu}$ in *t*-BuOD at 185°C results in incorporation of D, as indicated below. Racemization occurs at the same rate. Suggest a mechanism that could account for these observations.

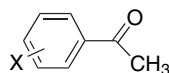


6.5. Using data from Tables 6.1 (p. 580) and 6.2 (p. 583), estimate the extent of deprotonation for each hydrocarbon-base combination below. Discuss the uncertainties that could affect the calculation.

- indene by 0.01 M NaOCH_3 in 1:1 DMSO- $\text{C}_2\text{H}_5\text{OH}$
 - fluorene by 0.01 M NaOC_2H_5 in 20:1 DMSO- $\text{C}_2\text{H}_5\text{OH}$
 - triphenylmethane by 5 M KOCH_3 in CH_3OH
- 6.6. The rates of removal of axial and equatorial protons from 4-*t*-butylcyclohexanone in NaOD/dioxane have been compared by an NMR technique. The rate of removal of an axial proton is 5.5 times faster than for an equatorial proton. How do you explain the difference?
- 6.7. The following table gives exchange rates in methanolic NaOCH_3 and $\text{p}K$ values for some hydrocarbons. Determine if there is a correlation between the kinetic and thermodynamic acidity.

Compound	k_{exchange} $M^{-1}\text{s}^{-1} (\times 10^4)$	$\text{p}K$
9-Phenylfluorene	173	18.5
Indene	50	19.9
3,4-Benzofluorene	90.3	19.75
1,2-Benzofluorene	31.9	20.3
2,3-Benzofluorene	2.15	23.5
Fluorene	3.95	22.7

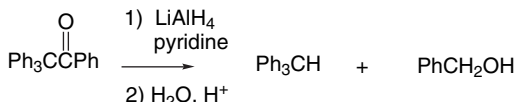
- 6.8. The acidity of various substituted acetophenones in DMSO is given below. Would you expect the ρ value to correlate best with σ , σ^+ , or σ^- ? Explain, considering each of the σ parameters explicitly. Do a plot of the $\text{p}K/\text{p}K_0$ values for each σ parameter.



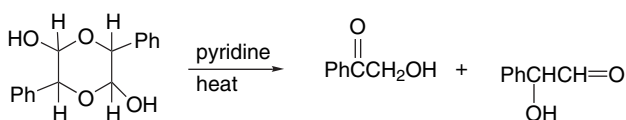
X	pK	X	pK	X	pK
<i>p</i> -(CH ₃) ₂ N	27.48	H	24.70	<i>m</i> -Cl	23.18
<i>p</i> -CH ₃ O	25.70	<i>p</i> -F	24.45	<i>m</i> -Br	23.19
<i>m</i> -(CH ₃) ₂ N	25.32	<i>m</i> -CH ₃ O	24.52	<i>m</i> -CF ₃	22.76
<i>p</i> -CH ₃	25.19	<i>p</i> -Br	23.81	<i>p</i> -CF ₃	22.69
<i>m</i> -CH ₃	24.95	<i>p</i> -Cl	23.78	<i>p</i> -CN	22.04
<i>p</i> -Ph	24.51	<i>m</i> -F	23.45		

6.9. Suggest mechanisms for the following reactions:

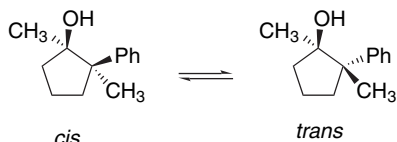
a.



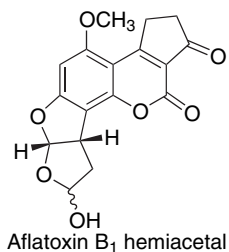
b.



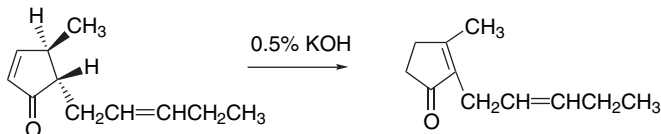
c. Treatment of the *cis* and *trans* isomers of 1,2-dimethyl-2-phenylcyclopentanol with 0.25 M NaCH₂SOCH₃ in DMSO leads to an 72:28 equilibrium mixture favoring the *trans* isomer.



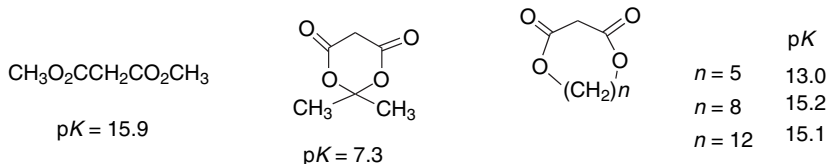
d. Aflatoxin B₁ hemiacetal racemizes readily in basic solution.



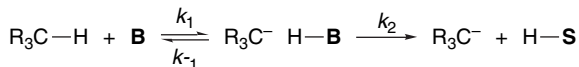
e. 4,5-Disubstituted cyclopent-2-enones can rearrange to 2,3-disubstituted cyclopent-2-enones in basic solution.



- 6.10. Meldrum's acid, $pK = 7.3$, is exceptionally acidic in comparison with acyclic analogs, such as dimethyl malonate ($pK = 15.9$). 5,5-Dimethyl-1,3-cyclohexadione is only moderately more acidic than pentane-2,4-dione. ($pK = 11.2$ versus 13.43). (All pK values in DMSO). It is found that the enhanced acidity of Meldrum's acid derivatives decreases as the ring size increases, with the larger ring compounds being similar in acidity to dimethyl malonate. Analyze the factors that contribute to the enhanced acidity of Meldrum's acid.



- 6.11. In some solvents, such as $\text{K}^+ \cdot \text{OR}-\text{DMSO}$, it can be shown that the *internal return* equilibrium characterized by k_1/k_{-1} is fast relative to the dissociation process characterized by k_2 . In this process, the base returns the proton to the carbanion faster than the proton donor exchanges with other molecules from solution. If internal return is important under a given set of conditions, how might that affect the correlation between observed kinetic and thermodynamic acidity? How can the occurrence of internal return be detected experimentally?

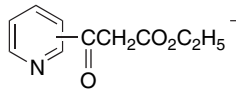


- 6.12. Discuss the following comparison of the enol content at equilibrium based on data given in Table 6.12. Discuss the reason for the differing enol content of the pairs of compounds in question.

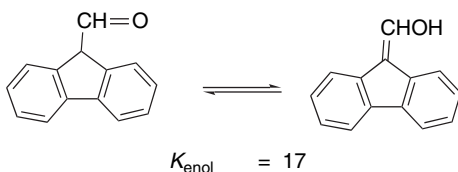
- Why does cyclohexanone have a somewhat higher enol content than cyclopentanone?
- Why do methyl acetate and acetamide have much lower enol content than acetone?
- Why does 2-indanone have a much higher enol content than 1-indanone?
- Why does 5,5-dimethyl-1,3-cyclohexa-1,3-dione have a higher enol content than acyclic diones such as acetylacetone, even though intramolecular hydrogen bonding is not possible?

- 6.13. Identify the structural factors that lead to the special stabilization of the enol form noted in each example.

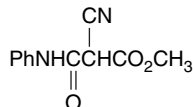
- The enol content of the 2-isomer of 3-(x-pyridyl)-3-oxopropanoate esters is higher than for the 3- and 4-isomers.

	position	K_{enol}
	2	0.86
	3	0.15
	4	0.19

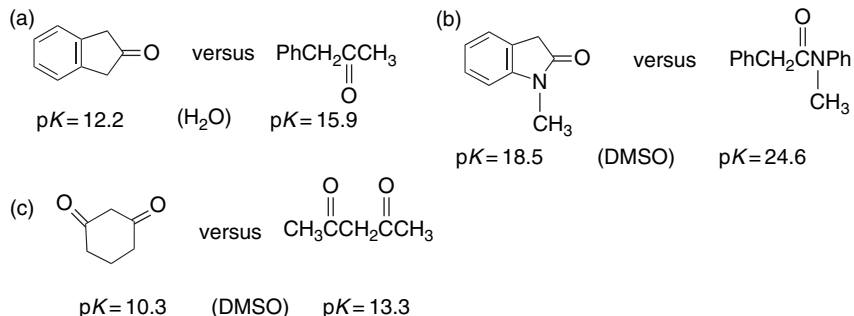
- b. The K_{enol} of 9-formylfluorene is 17, that is, the enol form is favored at equilibrium.



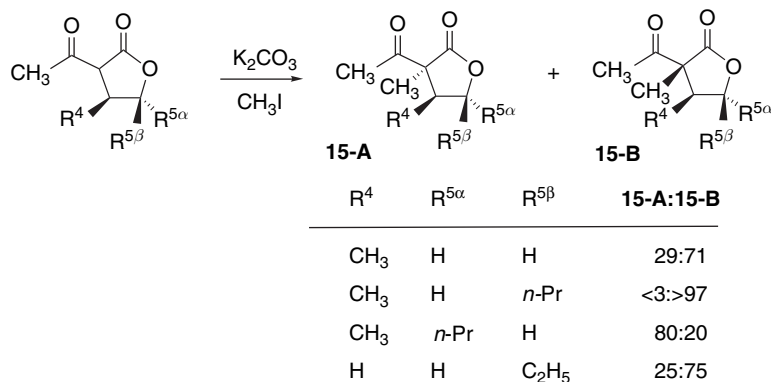
- c. Monoanilides of 2-cyanopropane-1,3-dicarboxyate monoesters exist in an enolic form in the solid state and in halogenated solvents.



- 6.14. Certain cyclic compounds exhibit enhanced acidity relative to acyclic models. Offer an explanation for the examples given below.

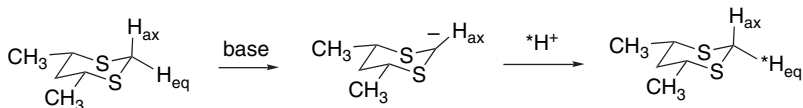


- 6.15. The stereoselectivity of alkylation of 3-acetylbutyrolactones is influenced by alkyl substituents at C(4) and C(5). Analyze possible conformations of the enolate and develop an explanation of the observed stereoselectivity.

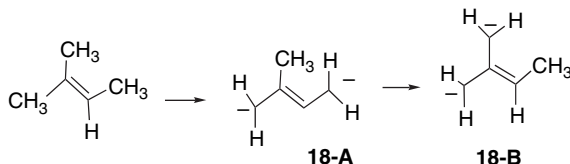


6.16. Metal ions such as Zn^{2+} , Ni^{2+} , and Cu^{2+} enhance the rate of general base-catalyzed enolization of 2-acetylpyridine by a several orders of magnitude. Account for this effect.

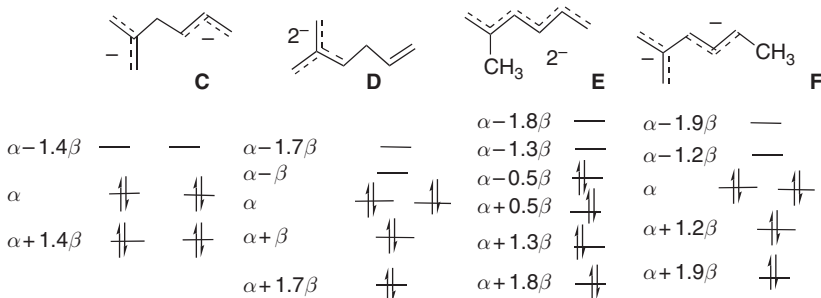
6.17. The C(2) equatorial hydrogen is selectively removed when 1,3-dithianes are deprotonated. Furthermore, if the resulting carbanion is protonated, there is a strong preference for equatorial protonation, even though it leads to the less stable axial orientation for the 2-substituent. Discuss the relevance of these observations to the structure of the sulfur-stabilized carbanion in MO terminology.



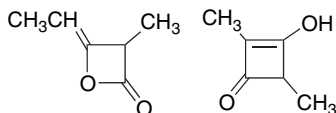
6.18. a. It is found that when 2-methyl-2-butene is converted to a dianion, it first gives the 2-methylbutadiene dianion **18-A**, but this is converted to the more stable anion **18-B**, which can be referred to as a “methyltrimethylenemethane” dianion. Does simple HMO theory offer an explanation for this result?



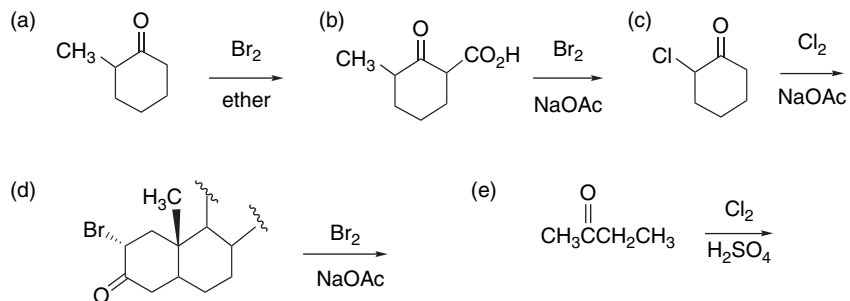
b. The HMO diagrams of several conceivable dianions that might be formed from double deprotonation of 2-methyl-1,5-hexadiene are given. On the basis of these diagrams, which dianion would be expected to be most stable?



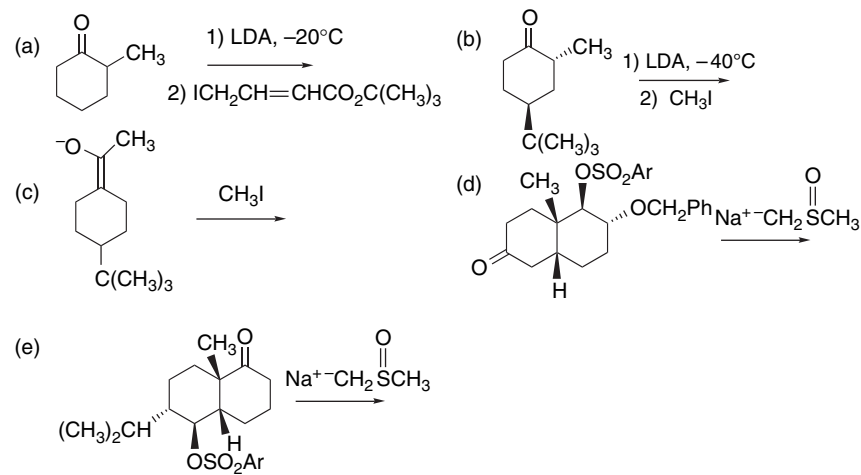
6.19. Which of the two possible structures for the dimer of methylketene is in best accord with the observed pK of 2.8? Explain.



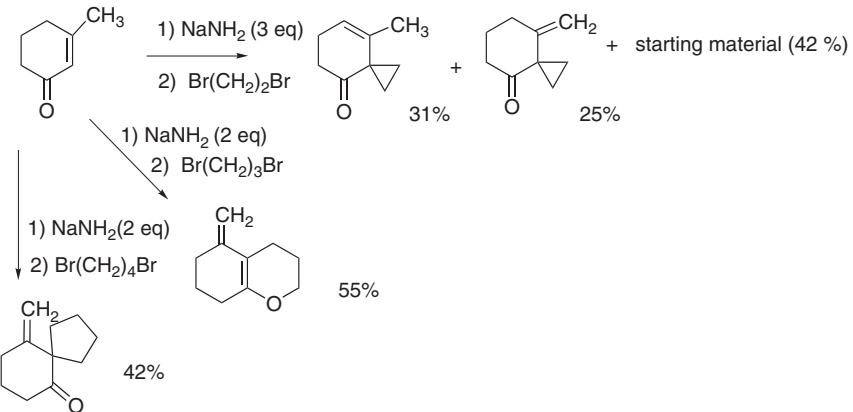
6.20. Predict the products of each of the following halogenation reactions.



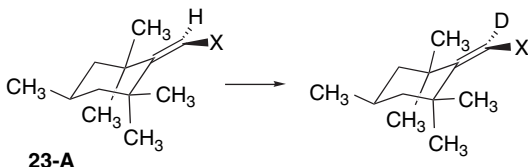
6.21. Predict the structure and stereochemistry of the products that would be obtained under the specified reaction conditions. Explain the basis of your prediction.



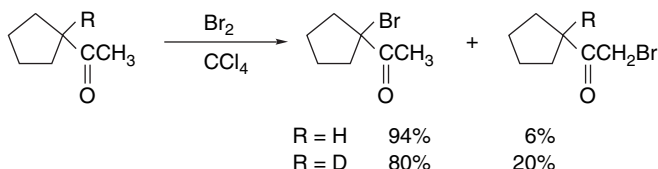
6.22. The alkylation of 3-methylcyclohex-2-enone with several dibromides led to the products shown below. Discuss the outcome of each reaction and suggest an explanation for the dependence of the product structure on the identity of the dihalide.



- 6.23. The stereochemistry of base-catalyzed deuterium exchange has been examined for **23-A**, where $X = \text{CN}$ and COPh . When $X = \text{CN}$, the exchange occurs with 99% retention of configuration, but with $X = \text{COPh}$, only about 30% net retention is observed. Explain these contrasting results.

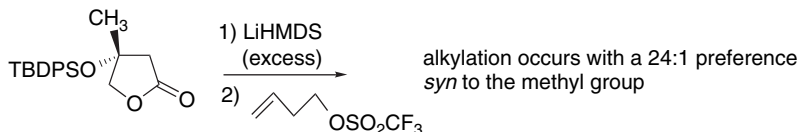


- 6.24. The distribution of α -bromoketones formed in the reaction of acetyl cyclopentane with bromine shows an altered product ratio when the 1-position of the ring is deuterated. Assuming that acid-catalyzed enolization is the rate-determining step in bromination, calculate the primary isotope effect.

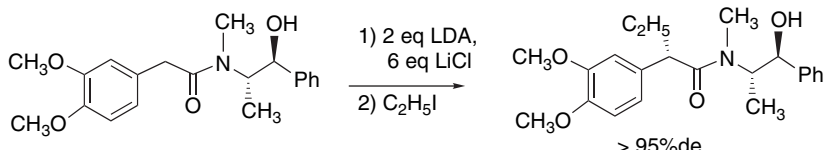


- 6.25. Analyze the mechanisms and transition structures for the following alkylation reactions in order to determine the factors that lead to the observed stereo-selectivity.

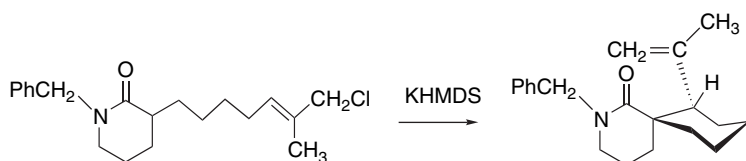
a.



b.



c.



6.26. Several dialkyl malate esters were alkylated with a benzylic bromide. The dimethyl and diethyl esters show a 8:1 and 9:1 selectivity for **26-A** (*si* face, respectively). The diastereoselectivities are shown for several more bulky esters. Figure 6.P26 gives the HF/6-31G* structures of the corresponding enolates. Explain the observed stereoselectivity on the basis of structural features present in these enolates.

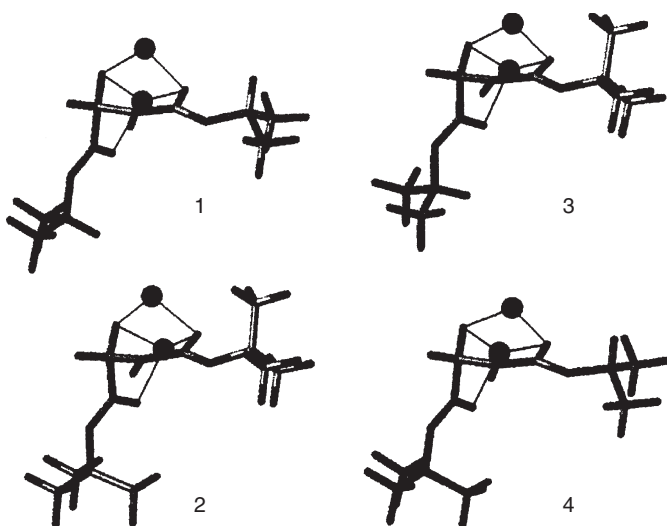
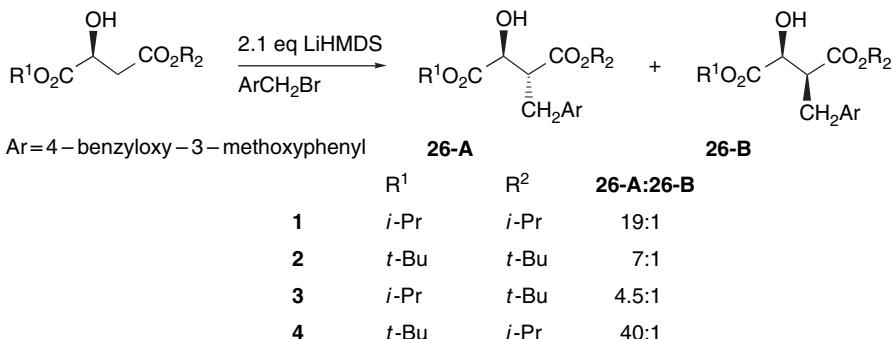


Fig. 6.P26. HF/6-31G* structures of enolates **1-4**. Reproduced from *Helv. Chim. Acta*, **85**, 4216 (2002), by permission of Wiley-VCH.